MODULATING TUMOR MICROENVIRONMENT USING COMBINATORIAL THERAPY

A Thesis submitted
In Partial Fulfillment of the Requirement
for the award of the Degree of

DOCTOR OF PHILOSOPHY

by

SMITA KUMARI
(2K18/PHD/BT/17)

Under the Supervision of

Prof. Pravir Kumar, PhD
Professor and Head, Department of Biotechnology
Dean, International Affairs
Delhi Technological University, Delhi

To the

FACULTY OF DEPARTMENT OF BIOTECHNOLOGY

DELHI TECHNOLOGICAL UNIVERSITY

(Formerly Delhi College of Engineering)
Shahbad Daulatpur, Main Bawana Road, Delhi-110042, India

September 2023

Copyright ©Delhi Technological University-2023
All rights reserved.

MODULATING TUMOR MICROENVIRONMENT USING COMBINATORIAL THERAPY

A Thesis submitted
In Partial Fulfillment of the Requirement
for the award of the Degree of

DOCTOR OF PHILOSOPHY

by

SMITA KUMARI
(2K18/PHD/BT/17)

Under the Supervision of

Prof. Pravir Kumar, PhD
Professor and Head, Department of Biotechnology
Dean, International Affairs
Delhi Technological University, Delhi

To the

FACULTY OF DEPARTMENT OF BIOTECHNOLOGY

DELHI TECHNOLOGICAL UNIVERSITY
(Formerly Delhi College of Engineering)
Shahbad Daulatpur, Main Bawana Road, Delhi-110042, India

September 2023

Dedicated
to
My
Family

DECLARATION

I hereby declare that the thesis entitled **"Modulating Tumor Microenvironment Using Combinatorial Therapy"** submitted by me, for the award of the degree of ***Doctor of Philosophy*** to **Delhi Technological University (Formerly DCE)** is a record of *bona fide* work carried out by me under the guidance of Prof. Pravir Kumar.

I further declare that the work reported in this thesis has not been submitted and will not be submitted, either in part or in full, for the award of any other degree or diploma in this Institute or any other Institute or University.

Name: Smita Kumari
Reg No: 2K18/PHDBT/17
Department of Biotechnology
Delhi Technological University (DTU)
Shahbad Daulatpur, Bawana Road, Delhi-110042
Place: New Delhi
Date: 15.09.2023

CERTIFICATE

This is to certify that the thesis entitled **"Modulating Tumor Microenvironment Using Combinatorial Therapy"** submitted by **Ms. Smita Kumari** to **Delhi Technological University (Formerly DCE)**, for the award of the degree of "Doctor of Philosophy" in Biotechnology is a record of *bona fide* work carried out by her. Smita Kumari has worked under my guidance and supervision and has fulfilled the requirements for the submission of this thesis, which to our knowledge has reached requisite standards.

The results contained in this thesis are original and have not been submitted to any other university or institute for the award of any degree or diploma.

Prof. Pravir Kumar, PhD
Professor and Head of Department
Dean, International Affairs
Department of Biotechnology
Delhi Technological University
Shahbad Daulatpur, Bawana Road, Delhi-110042
Place: New Delhi
Date: 15.09.2023

ABSTRACT

Glioblastoma multiforme (GBM) is an aggressive brain cancer with a poor prognosis. Currently, standard radiotherapy and chemotherapy is the only treatment option with adverse outcomes and low survival rate. Thus, advancements in the treatment of GBM are of utmost importance, which can be achieved in recent decades. However, despite having advancements in therapeutic strategies recurrence is inevitable, and the overall survival rate of patients is impossible to achieve. Currently, researchers across the globe target signaling events along with tumor microenvironment (TME) through different drug molecules to inhibit the progression of GBM, but clinically they failed to demonstrate much success. Additionally, the main therapeutic difficulties in treating hypoxia induced-(GBM) are toxicity of current treatments and resistance brought on by microenvironment. More effective therapeutic alternatives are urgently needed to reduce tumor lethality. Hence, we screened plant-based natural product panels intending to identify novel drugs without elevating drug resistance. We explored GEO for hypoxia GBM model and compared hypoxic genes to non-neoplastic brain cells. A total of 2429 differentially expressed genes expressed exclusively in hypoxia were identified. The functional enrichment analysis demonstrated genes associated with GBM, further PPI network was constructed, and biological pathways associated with them were explored. Seven webtools, including GEPIA2.0, TIMER2.0, TCGA-GBM, and GlioVis, were used to validate 32 hub genes discovered using Cytoscape tool in GBM patient samples. Four GBM-specific hypoxic hub genes-LYN, MMP9, PSMB9, and TIMP1-were connected to the TME using TIMER analysis. 11 promising hits demonstrated positive drug-likeness with non-toxic characteristics and successfully crossed blood-brain barrier and ADMET analysis. Top-ranking hits have stable intermolecular interactions with MMP9 protein, according to molecular docking, MD simulation, MM-PBSA, PCA, and DCCM analysis. Herein, we have

reported flavonoids: 7, 4'-dihydroxyflavan, (3R)-3-(4-Hydroxybenzyl)-6-hydroxy-8-methoxy-3,4-dihydro-2H-1-benzopyran, and 4'-hydroxy-7-methoxyflavan to inhibit MMP9, a novel hypoxia gene signature that could serve as promising predictors in various clinical applications, including GBM diagnosis, prognosis, and targeted therapy. Moreover, we highlighted the importance of BMP1, CTSB, LOX, LOXL1, PLOD1, MMP9, SERPINE1, and SERPING1 in GBM etiology. Further, we demonstrated the positive relationship between the E2 conjugating enzymes (Ube2E1, Ube2H, Ube2J2, Ube2C, Ube2J2, and Ube2S), E3 ligases (VHL and GNB2L1) and substrate (HIF1A). Additionally, we reported the novel HAT1-induced acetylation sites of Ube2S (K211) and Ube2H (K8, K52). Structural and functional characterization of Ube2S and Ube2H have identified their association with protein kinases. Lastly, our results found a putative therapeutic axis HAT1-Ube2S(K211)-GNB2L1-HIF1A and potential predictive biomarkers (CTSB, HAT1, Ube2H, VHL, and GNB2L1) that play a critical role in GBM pathogenesis. We also investigated the GEO dataset to compare the genes in the Peritumoral Brain Zone (PT) and tumor core (TC) with non-neoplastic brain cells to find significantly differentially expressed genes that are only involved in the growth of GBM tumor. Concurrently, protein targets of FDA-approved atypical antipsychotic drugs were examined. Through computational analysis and bioinformatics tools, we have found potential drug combinations for top-ranked atypical antipsychotic drugs and their associated significant cell cycle and calcium pathways. We quetiapine and clozapine as promising combination therapy. Molecular signatures connected to these pathways were CDK2, CCNA2, DRD4, GABRA5, CHRM1, ADRA1B, and HTR2A can act as biomarkers and therapeutic targets and have a significant impact on lowering the tumor burden and reducing pathogenesis of GBM.

ACKNOWLEDGEMENT

I am overwhelmed with gratitude as I complete my PhD thesis in Biotechnology. This monumental achievement would not have been possible without the unwavering support, encouragement, and love from numerous individuals who have touched my life in profound ways. I would like to express my heartfelt appreciation to:

First and foremost, I am thankful to almighty GOD for keeping me fit, healthy and energetic during entire course of my Ph.D. work.

I would like to thank to ***Prof. Jai Prakash Saini****, Vice chancellor, Delhi Technological University, Delhi for providing me with the opportunity to pursue my doctoral studies at this esteemed institute. Further, I express my gratitude to* ***Prof. Yogesh Singh****, former Vice chancellor Delhi Technological University, Delhi for providing me a conducive academic environment, the necessary facilities, resources, and infrastructure that facilitated the smooth execution of my research.*

With pleasure, I acknowledge my deep sense of gratitude to my guide and mentor ***Prof. Pravir Kumar****, Professor, DRC Chairman, Dean (International Affairs) and Head, Department of Biotechnology, Delhi Technological University, Delhi, for their enlightening guidance, intelligent approach, for their invaluable guidance, constant support, and unwavering belief in my abilities. Their expertise, enthusiasm, and commitment to excellence have been instrumental in shaping the direction of my research and enhancing my skills throughout this endeavor. I am truly grateful for their mentorship and the valuable lessons I have learned under their guidance. Here, I would also like to thanks* ***Prof. Jai Gopal Sharma****, former Head of the Department, Department of Biotechnology, for providing me the infrastructure and smooth functioning of official work.*

The constant guidance and encouragement received from ***Dr. Rashmi Ambasta****, CSIR Scientist, Delhi Technological University, Delhi, has been of crucial in shaping my research direction and enhancing the quality of my work. I am grateful for the valuable discussions, insightful feedback, and the freedom you granted me to explore new ideas.*

I wish to record my thanks and gratitude to my External DRC experts, ***Prof. Mukesh Kumar*** *(Scientist G, International Health Division, ICMR) and* ***Prof. S K Khare*** *(IIT Delhi) for their valuable guidance, critical and constructive discussion during this work.*

I would like to acknowledge the funding support provided by ***Department of Biotechnology, Government of India****. Their financial assistance was crucial in enabling me to carry out my*

research, attend conferences, and present my work to the scientific community.

I would like to thank my fellow researchers ***Dr. Rohan Gupta, Dr. Dia Advani****,* ***Rahul Tripathi****, and* ***Sudhanshu Sharma*** *for helping and encouraging me throughout my research. Moreover, I wish to thanks my juniors, namely* ***Mehar Sahu****,* ***Neetu Rani, Shefali and Shrutikriti*** *for their support during my research work. Their friendship, support, and shared aspirations have been instrumental in overcoming challenges and achieving our goals together. This would be incomplete without saying thanks to my senior* ***Dr. Dhiraj Kumar****, who have motivated me several times during my Ph.D. journey.*

My sincere gratitude goes to my colleagues ***Dr. Monideepa Roy, Dr. Aniruddha Sengupta, Dr. Sanghamitra Mylavarapu and Dr. Arindam Sarkar*** *who have been a constant source of motivation, intellectual stimulation, and support throughout my PhD journey. Their collaborative spirit, willingness to share knowledge, and insightful discussions have significantly contributed to the success of this work.*

I extend my appreciation to the ***Senior Management and technical staff Mr. C B Singh, Mr. Jitender and Mr. Lalit*** *of DTU, who help me to carry out all my official and administrative work smoothly during this tenure.*

Thanks are due to the wonderful friends ***Jwala, Eebha, Ramanpreet and Sravanti*** *in my life who were always on the stand by to bring me to positivity, hope and smiles when things didn't seem favoring and it seemed a far-fetched journey. Special mention to* ***Sandeep Yadav*** *being an integral part of my journey and for unwavering support and encouragement****.***

Lastly, I would to express my gratitude to my siblings ***Ankita Modi*** *and* ***Deepak Kumar Modi****, for their unwavering love, understanding, and always pushing me to reach higher and for celebrating every milestone with me.*

Finally, I want to dedicate this thesis to my parents, ***Sri Sachchidanand Modi*** *and* ***Mrs. Kusumlata Modi****, whose loving support has been my strongest inspiration. Their sacrifice allowed me to pursuit my dream and their belief in my abilities have been the driving force behind my perseverance and determination which made Ph.D. study completely painless.*

TABLE OF CONTENTS

LIST OF FIGURES

LIST OF TABLES

CHAPTER I

Introduction

CHAPTER I: Introduction

1.1. OVERVIEW

Glioblastoma multiforme (GBM) is defined as type IV brain cancer, which increases with the increase in age and exhibits a high prevalence rate in patients between 70-80 years old [1]. Further, the tumor microenvironment (TME) plays a pivotal role in tumor initiation and progression by creating a dynamic interaction with cancer cells. The TME consists of various cellular components, including endothelial cells, fibroblasts, pericytes, adipocytes, immune cells, cancer stem cells and vasculature, which provide a sustained environment for cancer cell proliferation [2]. The immunosuppressive GBM microenvironment is pro-angiogenic in nature, which have molecular and cellular heterogenicity, altered extracellular (pH and oxygen levels) and metabolic (glucose and lactate) components, and leads to therapeutic failure [3]. Mounting evidence highlighted the crucial role of various signaling pathways, such as the epidermal growth factor receptor (EGFR) pathway, Wnt/β-catenin signaling event, fibroblast growth factor receptor (FGFR) pathway, PI3K/AKT/mTOR cascade, and other in the progression and pathogenesis of GBM [4]. Recent multi-omics studies, including proteomics, transcriptomics, genomics, and metabolomics have discovered the critical role of post-translational modifications (PTMs) in the progression and pathogenesis of GBM. In addition, PTMs are critical regulators of chromatin architecture, gene expression, and TME, that play a crucial function in tumor development and progression. Moreover, studies have demonstrated that PTMs alter the oncogenic signaling events and offers a novel avenue in GBM therapeutics research through PTMs enzymes as potential biomarkers for drug targeting.

Further, standard treatment options involve chemotherapy, radiotherapy (RT), immunotherapy, and surgical resection, with low survival rates and high recurrence rates with adverse effects. Thus, there is utmost importance in developing novel therapeutic strategies to enhance the overall survival rate of GBM patients [5], [6]. Recent studies have emphasized the

implementation of advanced treatment strategies, such as adoptive cell therapy, gene therapy, viral and non-viral vectors-based therapy, RNAi therapy, photodynamic therapy (PDT), photothermal therapy (PTT), stem-cell-based therapy, drug repurposing, and vaccine therapy that exhibit promising primary outcomes in both experimental as well as clinical studies [7]–[10]. Thus, deciphering the mechanism of oncogenic signaling targets and TME biomarkers as therapeutic targets in GBM is of utmost importance.

1.2.MOTIVATION OF RESEARCH

- TME will play a critical role in the progression and pathogenesis of GBM through modulating signaling cascades.
- Targeting hypoxia microenvironmental condition and non-cellular secretory components of GBM microenvironment will enhance GBM therapeutics.
- Alteration in PTMs, namely acetylation and ubiquitination could enhance GBM progression and pathogenesis through modulating ubiquitin proteasome pathway.
- Conventional chemotherapy possesses several limitations, including resistance and toxicity, and thus, current therapeutic biomarkers failed to show effective treatment or diagnosis.
- Thus, there is a growing need to identify novel TME related biomarkers with site-specific acetylation and ubiquitination, which will reverse the GBM etiology.
- Combinatorial approach exhibits promising effects in reversing GBM progression. In addition, natural compound and antipsychotic drugs have potential to be act as promising therapeutic agent against GBM

1.3. AIM AND OBJECTIVES

1.3.1. AIM

- Modulating TME using combinatorial therapy.

1.3.2. OBJECTIVES

1. To identify the TME-based novel biomarkers in GBM therapeutics based on a multi-omics approach.
2. To elucidate the involvement of biomarkers on signaling events in GBM etiology.
3. To explore the possibilities of natural compound as potential therapeutic agent in GBM therapeutics.
4. To establish a connection between acetylation and ubiquitin proteasome signaling in TME
5. To dissect the molecular effect of combination therapy in GBM therapeutic through drug repurposing approach.

1.4. SUMMARY OF THE THESIS

The thesis is structured into six different chapters. Chapter 1 briefly discuss the motivation, rationale, aims, objectives, and overview of the current study. Further, chapter 2 introduces the etiology of the cancer and hallmarks of cancer association in respect to TME. We have especially focused on GBM and associated oncogenic signaling pathways. Additionally, chapter 2 reviews the TME and its component, including hypoxic microenvironment condition and non-cellular secretory components in respect to GBM. Moreover, we have also discussed about post-translation modifications (PTMs), such as acetylation and ubiquitination and its relevance in GBM pathogenesis. Further, we have briefly mentioned traditional and advance therapeutic approaches used for GBM therapeutics. In this chapter, we have also focused on TME as therapeutics markers and their mechanistic involvement in the progression and pathogenesis of GBM. We have elaborated the potential of natural compound as therapeutic drug against hypoxic-mediated GBM and relevance of combinatorial therapy in GBM

therapeutics. Chapter 3 is dedicated to the objective 1 *(To identify the TME-based novel biomarkers in GBM therapeutics based on a multi-omics approach*), objective 2 *(To elucidate the involvement of biomarkers on signaling events in GBM etiology)* and objective 3 *(To explore the possibilities of natural compound as potential therapeutic agent in GBM therapeutics)*, where hypoxic condition of GBM microenvironment has been studied to identify potential biomarkers of hypoxia (MMP9) in GBM cells lines with the help RNA sequencing datasets procured from GEO public database and their expression has been checked in GBM patients tumor samples data procured from TCGA datasets. Herein, we identified the HUB genes through protein-protein interaction (PPI) network. Further, NPACT database that contains plant-based natural compounds has been explored. We have applied ADMET analysis and blood-brain barrier (BBB) prediction to assess the pharmacokinetic and pharmacodynamic properties of the selected compounds. Moreover, molecular docking, Molecular dynamics (MD) simulation, Principal component analysis and others analysis of the shortlisted compounds were performed to select the best possible MMP9 inhibitor. The results supported that 3 flavonoids crosses BBB and have minimum toxicity and target MMP9 a hypoxic induced therapeutic marker in GBM. In chapter 4, we discussed objective 4 *(To establish a connection between acetylation and ubiquitin proteasome signaling in TME)* with aim to investigate another important TME components that is non cellular secretory components, including cytokines, chemokines, matrix modulating enzymes and growth factors involved in the pathogenesis of GBM. Herein, we integrated transcriptomics and proteomics expression data to find differential expressed genes in GBM. Additionally, K-M plot was studied to identified molecular markers their expression was linked to a poor prognosis in GBM patients, and found that common upregulated protein, hypoxia-inducible factor 1 alpha (HIF1A) linked with prognostic markers have been identified in GBM. In addition, associated E2 conjugating enzymes (E2s) and E3 ligase were explored and their correlation study was studied. The

identified overexpressed E2s were further analyzed to investigate the potential lysine residue for acetylation activity, along with the determination of the type of histone acetyltransferases (HATs) enzymes involved in the disease progression. Lastly, we have proposed two therapeutic axis including substrate, E2s and E3 ligases in GBM including HAT1-Ube2S(K211)-GNB2L1-HIF1A and HAT1-Ube2H(K8)-VHL-HIF1A. In addition, we have characterized proposed axis to find predictive biomarkers, associated protein kinases and association with top mutated genes in GBM. Further, we examined the biological pathways involved. Thus, till date, this is the first study to show that these two E2s along with novel acetylation lysine residues (Ube2S (K211) and Ube2H(K8) might act as therapeutic targets and can be explored further for designing inhibitor against them.

In chapter 5 of the thesis objective 5 *(To dissect the molecular effect of combination therapy in GBM therapeutic through drug repurposing approach)*, we recognize the potential inhibitor of anti-psychotic drug that may be involved in the reversal of GBM pathology. Herein, we investigated the Gene Expression Omnibus (GEO) dataset to compare the genes in the Peritumoral Brain Zone (PT) and tumor core (TC) with non-neoplastic brain cells to find significantly differentially expressed genes that are only involved in the growth of GBM tumor. Concurrently, protein targets of FDA-approved atypical antipsychotic drugs were examined. Through computational analysis and bioinformatics tools, we have found potential drug combinations for top-ranked atypical antipsychotic drugs and their associated significant cell cycle and calcium pathways. In this study, we have identified a putative drug combination therapy, namely Quetiapine and Clozapine as a promising therapeutic agent to reverse GBM. Molecular signatures connected to these pathways—CDK2, CCNA2, DRD4, GABRA5, CHRM1, ADRA1B, and HTR2A—can act as biomarkers and therapeutic targets and have a significant impact on lowering the tumor burden and reducing pathogenesis of GBM.

CHAPTER II

Review of Literature

CHAPTER II: Review of Literature

2. INTRODUCTION

GBM is the most prevalent and fatal brain tumor with a poor prognosis. The clinical prognosis is still lacking despite several approved therapies for GBM, including surgery, radiation, and chemotherapy [11]. The possible causes are the extensively invasive nature of GBM cells, the chemo- and radio-resistance, the high degree of vascularization, heterogeneity, and reduction of chemotherapeutic drugs effusion due to the BBB and heterogeneity of TME [12]. Mounting evidence highlighted the crucial role of various signaling pathways, such as the epidermal growth factor receptor (EGFR) pathway, Wnt/β-catenin signaling event, fibroblast growth factor receptor (FGFR) pathway, PI3K/AKT/mTOR cascade, and other in the progression and pathogenesis of GBM [4]. For example, Boso et al., 2019 demonstrated the potential involvement of HIF1A/Wnt signaling in neuronal differentiation of GBM stem cells, whereas, Portela et al., 2019 concluded that the Wnt pathway activates JNK/MMP signaling loop that enhanced GBM progression [13], [14]. Moreover, another crucial environmental condition known as hypoxia, which defined as lack of oxygen in tissue is one of hallmark of cancer including GBM. This impairs the availability of nutrients and promotes genetic instability because of an increase in the generation of reactive oxygen species (ROS) making it a crucial factor for tumorigenesis. As the master regulator orchestrating cellular responses to hypoxia, HIF1A plays an essential role in GBM aggressiveness [15]. Further, the extracellular matrix (ECM) structural proteins are among the non-cellular components of the TME that are released by tumor or stromal cells or extravasated from the intravascular compartments [16]. Additionally, ECM structural proteins impact the development of all blood cells and other cells that support the body's inflammatory and immunological reactions, which promote anti-cancer behaviour [17]. It has been suggested that non-cellular secreted components that constitute microenvironmental heterogeneity contain a variety of growth factors, cytokines,

chemokines, structural matrix, and matricellular proteins. These non-cellular components impacts to cancer survival and progression by providing autocrine and paracrine communication through growth signals, evading immune surveillance, drug resistance environment, metastatic and angiogenesis [16]. Thus, the ability of these secreted TME components to switch their actions from pro-cancer to anti-cancer has thus been thought of as a new approach in cancer therapies and drug resistance. The use of non-cellular secretory components as possible treatment targets and biomarker tools is now being investigated in several pre-clinical and clinical studies [18], [19]. Cytokine expression patterns in GBM are distinctive, and aberrations in cytokine expression have been linked to gliomagenesis. The complex cytokine network in the diverse microenvironment facilitates interactions between the tumor cells, healthy brain cells, immune cells, and stem cells within the heterogeneous milieu of the GBM [20].

Moreover, studies have shown that PTMs, namely methylation, acetylation, glycosylation, and ubiquitination of chemokines and cytokines, influence biological activities, inflammatory responses and inflammasome-dependent innate immune responses through modifying the protein stability, structure, and sequence [21], [22]. It is proactively controlled by HATs and histone deacetylases (HDACs) in homeostasis and is associated with several critical biological and cellular functions including transcription, migration, invasion, adhesion, DNA damage repair, and energy metabolism. Recent studies demonstrated that abnormally high histone acetylation levels could trigger chromatin-based mechanisms that promote tumorigenesis and malignant transformation. Further, it is interesting to note that most acetylated non-histone proteins are essential for immunological processes, tumorigenesis, and GBM cell growth [23]. Evidence have concluded that lysine acetylation modification affects the lysosomal clearance of specific substrates and proteasomal degradation by either inhibiting or enhancing polyubiquitination [24]. Additionally, studies have demonstrated that the UPS system degrades

HIF1A after interacting with von Hippel–Lindau protein (pVHL) under normoxia, mediating its ubiquitination. Likewise, acetylated retinoblastoma (Rb) recruits MDM2, an E3 ligase and mutation in its acetylation hotspots is linked with an increased risk of breast cancer [25]. Moreover, studying the mechanism and progression of GBM cells in the 2D culture model imposes various hurdles due to the absence of human microenvironment, and thus, the establishment of 3D model or organoid model was studied across the globe to extract the exact pathology of GBM [26].

Standard treatment options involve chemotherapy, radiotherapy (RT), immunotherapy, and surgical resection, with low survival rates and high recurrence rates with adverse effects. Thus, there is utmost importance in developing novel therapeutic strategies to enhance the overall survival rate of GBM patients [5], [6]. For instance, Yin et al., 2022 demonstrated that combined administration of ultrasmall Zirconium carbide nanodots and RT enhanced the therapeutic efficiency both *in vitro* and *in vivo* [27]. Herta et al., 2022 demonstrated that the Raman spectroscopy-enabled method effectively identifies tumor-infiltrated brains with higher sensitivity but lower specificity compared to the current standard of 5-aminolevulinic acid [28]. Recent studies emphasized the implementation of treatment strategies, such as adoptive cell therapy, gene therapy, viral and non-viral vectors-based therapy, RNAi therapy, PDT, PTT, stem-cell-based therapy, and vaccine therapy that exhibit promising primary outcomes in both experimental as well as clinical studies [7]–[10]. For Instance, Xu et al., 2022 concluded that targeted PDT of GBM cells induced by platelets marked the presence of DNA damage, reduced viability, and cell death [29]. Deciphering the mechanism of oncogenic signaling targets and TME biomarkers as therapeutic targets in GBM. Drug repositioning also referred to as "drug repurposing," is a current strategy for finding new treatments for GBM that involves using already-approved medications for other diseases. Clinical translation can be accelerated by using already FDA-approved drugs by eliminating or speeding up phases like chemical

optimization and toxicological analysis, which are essential to drug development. But in order to find compounds that can suppress GBM tumorigenesis, a screening procedure must be used to determine whether potential agents can cross the BBB [30].

2.1. CANCER DISEASES

Cancer is another word for a malignant tumor (a malignant neoplasm) is the uncontrolled growth of abnormal cells in the body [31]. It is a multifactorial disease and one of the leading causes of mortality worldwide. WHO estimates indicate that 9.6 million lives were lost to cancer in 2018, comprising 13% of all deaths. By 2030, the estimated number of deaths due to cancer is projected to rise to 13.1 million. The top cancers are breast (2.09 million cases), Lung (2.09 million cases), and Colorectal (1.80 million cases) [32]. One of the most aggressive cancers, GBM, is responsible for 14.5% of all central nervous system (CNS) tumors and 48.6% of aggressive CNS tumors. According to different reports, the incidence of GBM ranges from 3.19 cases per 100,000 people per year [33]. The etiology of the majority of human cancers are associated with a myriad of environmental causes, including physical, chemical, and biological factors. Various classes of chemical mutagens (alkylating agents, DNA intercalating agents, and deaminating agents) such as melphalan, benzidine, diethylstilbestrol, mediates base-analog and causes pyrimidines to shift, leading to mutagenesis in healthy cells. Studies also define the role of various infectious mutagens (bacteria and virus) that also interferes with the biological integrity of cells. Viruses of various modalities like the Epstein-Barr virus, Hepatitis B, and C elevates the cellular damage and are known to be linked with carcinogenesis. Epigenetic and genetic mechanisms are also known to be associated with the growth and development of various tumors [34]. Mutagens that interfere with the pathways associate with these mechanisms, such as differentiation, histone modifications, acetylation, methylation, etc., also degrades the DNA quality, causing cancer. Examples of these DNA-damaging carcinogens include mycotoxins, polycyclic aromatic hydrocarbons, forms DNA adducts. Studies that

govern the role of mutagens being the associator in the formation of DNA adducts are extensively described [35], [36]. Many studies have explored the therapeutic potential of natural compounds and phytochemical extracts in reducing the countereffects of these mutagens in various carcinomas [37]. Evident studies prescribe the role of environmental mutagens (endogenous and exogenous) in mediating inflammation-associated pathways. Dysregulation elements in these signaling like the nuclear factor-κB (NF-κB), signal transducer and activator of transcription 1 (STAT1), interferon regulatory factor 3 (IRF 3), and activation of caspases and bridging with mutagens, opens up a window how these mutagens guide inflammation, ultimately leading to cancer [38]. The release of various inflammatory cytokines like the IL-2, IL-10, and TNF-α and their secretions influence DNA-damage response and activation of pathways such as the JNK/STAT1, which can act as a therapeutic possibility targeting inflammation in cancer [39], [40]. In order to achieve stable, and functional DNA integrity, a certain DNA-repair mechanism comes (such as base-excision repair (BER), nucleotide-excision repair (NER), and mismatch repair) into action when struck by the effect of any exogenous and endogenous mutagens [41]. Deformity in the repair mechanism affects the cellular machinery that ultimately leads to the formation of an abnormal mass of cells, causing cancer. Therefore, targeting these repair mechanisms can be an asset to how these mutagens affect the cellular DNA and in the prevention of carcinomas. Another interesting character that comes into foreplay is hypoxia, being heterogeneous in nature, causes a metabolic shift in DNA stability by being linked with ROS generation causing oxidative stress and death of cells. HIF1A a major transcription factor in hypoxia, is also somewhere known to be linked to promoting carcinogenesis in healthy cells [42], [43]. Additionally, cancer has a high level of cellular, epigenetic, and genetic heterogeneity that complicates therapeutic methods and results in resistance [44]. For instance, Li et al., 2017 research demonstrated that drug resistance is universally but differentially induced by hypoxia. Additionally, hypoxia-

induced drug resistance and involvement with anticancer processes may be employed as possible biomarkers in the selection and development of chemotherapy drugs to enhance the treatment of hepatocellular carcinoma (HCC) [45]. Commonly used cancer therapies include chemotherapy, radiation therapy, combination therapies, nanomedicines, targeted therapy (including monoclonal antibody, antibody drug conjugates, small molecules inhibitors), stem cell therapy, ablation therapy (including thermal ablation, cryoablation, radiofrequency ablation), anti-angiogenic therapy, immunotherapy (antigen-TLR agonist fusion vaccines, anti-PD-1 monoclonal antibody), CAR T therapy, dendritic cell-based immunotherapy, hormone therapy, gene therapy (oncolytic virotherapy, gendicine, thymidine kinase (TK) gene delivery, RNA interference (RNAi), natural antioxidants (vitamins, polyphenols, and plant-derived bioactive compounds). Chemotherapy remains the most promising approach for treating cancer despite these advancements. Currently, drug resistance-related tumor invasion and metastasis account for 90% of chemotherapy failures. The understanding of oncogenes, and tumor suppressors, has broadened the field of innovative cancer therapies [46]. Current modern methods in oncology focus on the creating effective and safe treatment options, including several new technologies are currently under research in clinical trials, and some of them have already been approved (**Figure 2.1).**

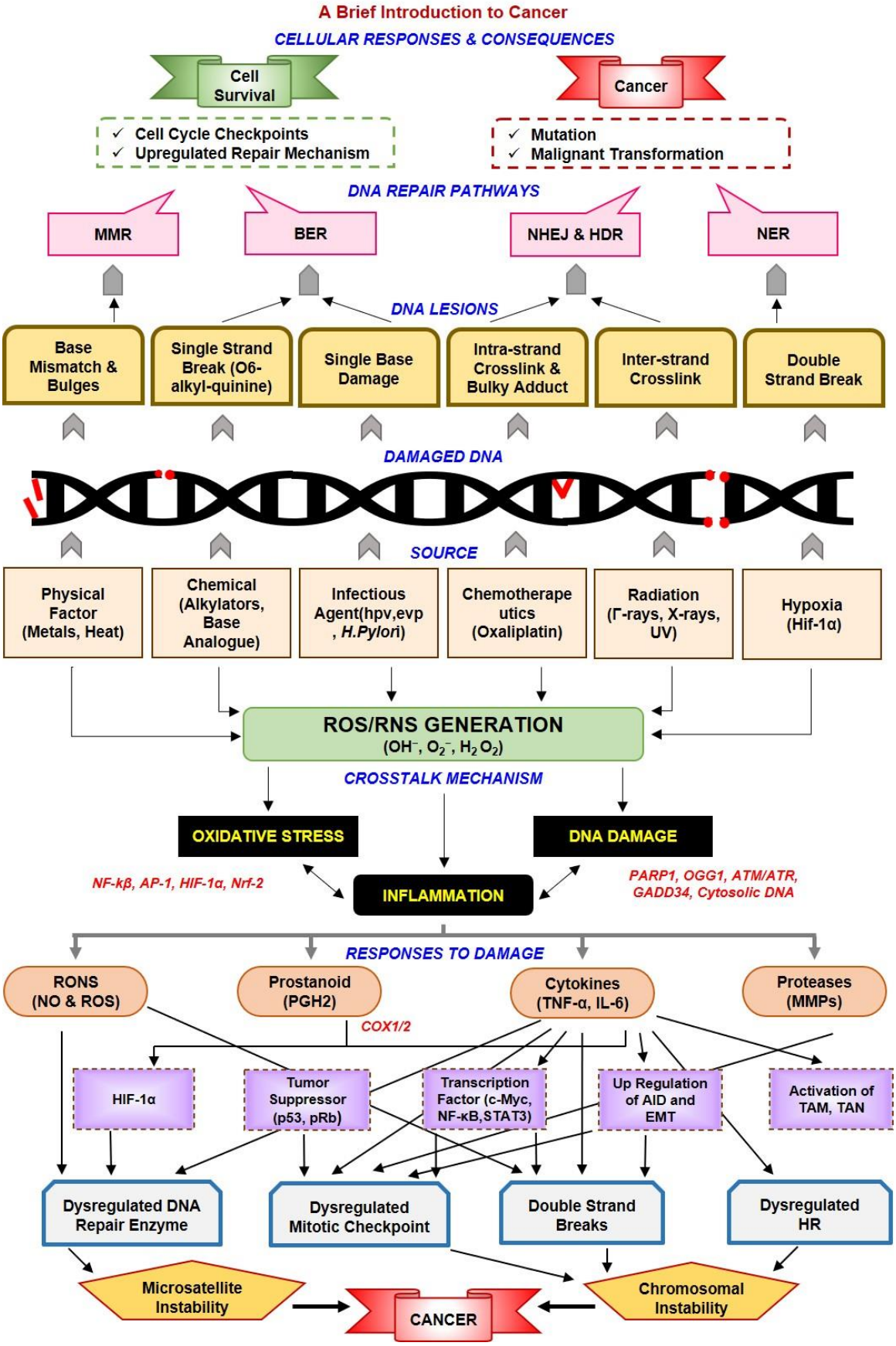

Figure 2.1: ***Model for Environmental Risk Factor, DNA Damage and Its Response in Biological Processes Linked to Cancer*****: Repetitive exposure of cells to intrinsic and extrinsic carcinogens may results into**

accumulation of free radicals such as ROS, which leads to oxidative stress and DNA damage and together all results into inflammation. These generate various growth factors (VEGF), cytokines (TGF-β, TNF-α, IL-6 etc.), transcription factors (c-Myc, NF-κβ, STAT3), HIF-1α. Elevation ROS upregulates the expression of MMPs through TGF β. Furthermore, ROS also mediate the expression of vimentin and VEGF which increases EMT (promotes cancer cell migration) and angiogenesis respectively. DNA damaging agents also generate a variety of lesions, such as mismatched nucleotides, base lesions, bulky (helix-distorting) adducts, SSBs, or DSBs which causes mutations, which have specific cellular consequences, including transformation or cell death. cellular events lead to genomic or microsatellite instability which causes cancer. The dysregulated DNA repair mechanism unable to recognize DNA lesion and which may subsequently lead to carcinogenesis. AID: Activation-induced cytidine deaminase.

2.2. HALLMARKS OF CANCER: PERSPECTIVE FOR THE TUMOR MICROENVIRONMENT

In 1863 Rudolf Virchow first proposed the link between chronic inflammation and tumorigenesis and observed that infiltrating leukocytes were a hallmark of tumors [47]. Hanahan and Weinberg, in their influential review, defined the hallmarks of cancer as a multistep process that includes biological functions such as sustaining proliferative signaling, evading growth suppression, resisting cell death, enabling replicative immortality, inducing angiogenesis, activating invasion/metastasis (henceforth termed Hallmarks I). A decade later, an updating review (hereafter termed Hallmarks II) added two emerging hallmarks: reprogramming energy metabolism and evading immune response, and two enabling traits: genome instability and mutation and tumor-promoting inflammation [48]. Here, we will discuss how each hallmark of cancer is related to TME **(Figure 2.2)**.

2.2.1. SUSTAINED PROLIFERATIVE SIGNALING

A recent exponential increase in our knowledge in oncology shed light on the role of TME in cancer progression and metastasis. Cancer cells use various distinct signaling pathways (such as TGF-β, Wnt, NOTCH, and HH) and reciprocal communication to efficiently recruit stromal cells, immune cells, and vascular cells in their vicinity, which, in turn, provides growth signals, intermediate metabolites, and a suitable environment for its progression as well as metastasis. This implies that TME does not act as a passer-by, but it proactively participates in tumor progression [49]. Infiltrating immune cells, inflammatory cells (chronic in nature and are enriched in Treg and mesenchymal stromal cells (MSC)) and stromal elements are

reprogrammed by the tumor to the pro-inflammatory mode favoring its survival. Antitumor functions of these infiltrates are downregulated because tumor-derived signals and activation of these immune cells in the TME are co-opted to promote tumor growth by sustained activation of the NF-κB pathway in the tumor milieu [50].

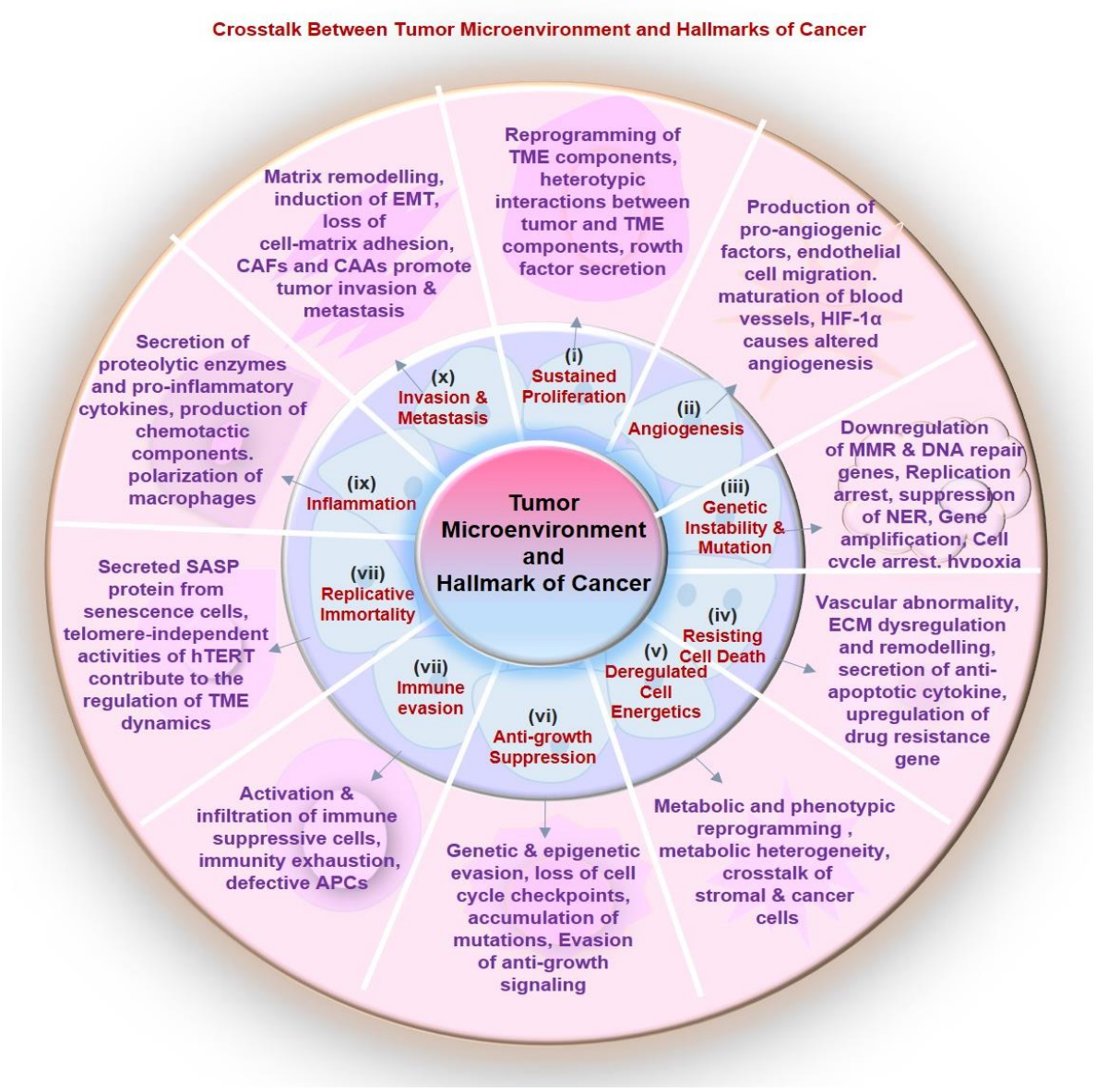

Figure 2.2: ***Role of TME in Modulating Different Hallmarks of Cancer. I) Sustained Proliferation is an Important Hallmark of Cancer*****: Various TME component cells undergo reprogramming and promote heterotypic interactions with tumor cells. The growth factors and cytokines secreted by TME cells assist growth and proliferation of tumor cells. ii) Angiogenesis is a popular hallmark of cancer progression where TME component cells release pro-angiogenic factors (VEGF, FGF, HIF-1α, TNF-β, Ang-1, Ang-2), chemokines, and cytokines which help in endothelial cell migration, proliferation, degradation of ECM, maturation of blood vessels and new blood vessel formation. iii) Genetic instability and mutational events are the important feature of cancer cells. In TME, downregulation of MMR genes, oxidative base damage, dysregulation of DNA repair genes, suppression of NER, gene amplification, cell cycle arrest, replication stress, ROS/RNS formation are the major events promoting genetic instability. iv) Cell death resistance is an important feature of cancer. Microenvironment components aids cancer cells to escape apoptosis by secretion of anti-apoptotic cytokines like IL-4, IL-6. Vascular abnormality, ECM dysfunction and remodeling**

leads to upregulation of gene responsible for apoptosis. v) Deregulated cellular energetics shown by cancer cells is promoted by metabolic and phenotypic reprogramming of stromal cells, oncogenic load, and cross talk with stromal cells (CAFs, endothelial cells, adipocytes, T-cells, and macrophages). vi) Anti-growth suppression is the protective mechanism adapted by cancer cells to acquire tumorigenicity. Various genetic (chromosomal deletion, mutation, loss of upstream and downstream effectors) and epigenetic (DNA methylation, histone methylation, and acetylation) mechanisms, loss of cell cycle checkpoints, evasion of anti-growth signaling, such as p53, PTEN, GDF15, IGF-1R, notch, hippo, in the TME are responsible for anti-growth mechanisms. vii) Immune evasion is one of the most important hallmarks shown by cancer cells. In the TME, tumor-associated antigen presentation is inhibited, secretion of immune suppressive cytokines, activation of immunosuppressive cells (MDSCs), suppression of T-cell mediated immunity, activation of immune checkpoint inhibition, and polarization of macrophages towards tumoricidal M1 phenotype are the major factors responsible for immune suppression. viii) Replicative immortality is another important hallmark of cancer cells. hTERT independent of telomere maintenance plays a pleiotropic role regulating various features of the TME such as angiogenesis, inflammation and immunosuppression, fibroblast activation, and maintenance of CSCs pluripotency. This contributes to the TME for promoting tumor invasion and metastasis ix). Inflammation is an important phenomenon exhibited by cancer cells promoted by secretion of proteolytic enzymes, inflammatory cytokines, pro-angiogenic mediators, chemotactic components such as CCL2, CCL5, CCL7, CXCL8, CXCL8, CXCL12, infiltration of inflammatory cells, and suppression of T-cell activity in TME. x). Invasion and metastasis are the crucial characteristic of cancer cells. TME components help cancer cells to metastasize by matrix remodeling, epithelial to mesenchymal transition (EMT), and by assisting tumor cell migration in the network of TME associated chemokines and cytokines. CAFs and Cancer associated adipocytes (CAAs) promotes tumor progression. CAAs promotes invasion and metastasis by secreting chemokines such as CCL2, CCL5, IL-1β, IL-6, VEGF. Moreover, CAAs preconditions TMEs by supporting anti-tumor immunity

2.2.2. TRIGGERING ANGIOGENESIS

Angiogenesis is the most important cancer hallmark because of its role in tumor progression and metastatic dissemination. Cells in tumor produce signals and endogenous factors in their microenvironment that promotes angiogenesis. TME, by secreting numerous pro-angiogenic and anti-angiogenic factors, has a modulating role in tumor vascularization. Since angiogenesis is essential for tumor metastasis and growth, site-specific micro environmental regulation of angiogenesis is one of the most important determinants of the organ preference of metastases [51]. VEGF, FGF, and platelet-derived growth factor (PDGF) are the three crucial protein-peptide families that have a role in promoting neovascularization and are known as angiogenic factors. Many cytokines such as TGF-β, Interferons (IFNs), Tumor necrosis factor-alpha (TNF-α), Interleukins (ILs) act in paracrine and autocrine fashion secreted by tumor cells in TME plays a critical role in regulating tumor angiogenesis [52]. The most prevalent immune/inflammatory cell type present in tumors is the tumor associate macrophages (TAMs). TAM plays an important role in angiogenesis, promoting cancer cells by secreting pro-angiogenic factors, including VEGF-A, EGF, PIGF, TGF-β, TNF-α, IL-1β, IL-8, CCL2, CXCL8, and CXCL12 [53]. Other important cells are mast cells recruited by VEGF, bFGF,

and TGF-β factor and produce MMPs such as MMP2 and 9, promoting angiogenesis by releasing VEGF and bFGF from the ECM. Thus, the tumor recruits mast cells from its surroundings and helps in forming new blood vessels and tumor progression in solid tumors [54], [55].

2.2.3. GENOME INSTABILITY AND MUTATION

Genomic integrity of cells is maintained through regulated DNA replication, DNA damage repair mechanisms, and cell-cycle checkpoints. Malignant tumors are associated with four types of genomic instabilities: chromosomal instability, intra-chromosomal instability, microsatellite instability, and epigenetic instability [56], [57]. Growing evidence has suggested that the TME itself constitutes a significant source of genetic instability [58]. This hypothesis is supported by somatic mutation theory, suggesting that mutation in DNA occurs because of genetic and environmental factors [59]. Telomere shortening, centrosome replication, DNA damage, and epigenetic modifications are the significant factors contributing to genomic instability [60]. Moreover, hypoxia has been proposed as a significant microenvironmental factor involved in genetic instability in solid tumors. Hypoxia in the TME mainly results from an imbalance between the oxygen supply and consumption rate [56]. A HIF1A transcription factor is the mediator of hypoxia signaling. The transcriptional and transcriptional changes in its activity alter DNA repair response by homologous and non-homologous recombination and mismatch repair. Furthermore, Radisky et al., 2005 mentioned ROS role, produced by inflammatory cells present in TME, in inducing genetic instability and EMT [61].

2.2.4. RESTING CELL DEATH/DEATH RESISTANCE

Programmed cell death, specifically apoptosis, is characterized by the cleavage of cell death-associated caspases and the mitochondrial release of pro-apoptotic proteins such as cytochrome c, with tight regulation of pro-and anti-apoptotic molecules, including those from the Bcl2 family [62], [63]. Tumor cells, in order to survive and proliferate, avoid different cell death

pathways, and they also evolve a variety of strategies to circumvent apoptosis. Amongst different classified cell death pathways by Nomenclature Committee on Cell Death (NCCD), apoptosis, necrosis/necroptosis and autophagy are mainly explored [64]. Microenvironment components help cancer cells to escape apoptosis. ECM undergoes continuous remodeling, and dysregulation of ECM molecules significantly affects cancer cell proliferation by inactivating pro-apoptotic molecules such as Bax and inducing expression of several anti-apoptotic genes, including Bcl2 [65]. Elevated levels of important cytokines are also considered, anti-apoptotic like IL-6 and IL-4 activate PI3 pathways, which results in increased phosphorylation of AKT, an important protein expressed in prostate cancer [66]–[68]. Similarly, IL-8 promotes migration, angiogenesis, and metastasis and is also implicated in the regulation of apoptosis in prostate, breast, and colon cancer [69], [70]. Weigel et al., 2014 have shown how insulin-like growth factor–binding proteins (IGFBPs) secreted by CAFs regulates anoikis, facilitating luminal filling in 3D cell culture and promote anchorage-independent growth in breast cancer cells [71].

2.2.5. DEREGULATING CELLULAR ENERGETICS

Deregulating cellular energetics is one of cancer's hallmarks, popularly known as metabolic reprogramming, a process in tumor cells [48], [72]. Even under normoxia conditions, tumor cells convert pyruvate into lactate without entering into the Krebs cycle, i.e., by aerobic glycolysis, which is known as the Warburg effect [73]. Components of the TME, such as stromal cell and immune cells (macrophages and tumor-infiltrating cells), increase lactate concentration within the TME. This increased lactate concentration, in turn leads to the acidification of the TME. This aids in tumor cell survival and proliferation, promotes angiogenesis, and alters immune infiltrating cells [74]. Lactate has an immunosuppressive role, as it affects proliferation and cytokine production of T cells, the cytotoxic role of natural killer cells (NK cells) and the cytolytic functions of $CD8^+$ T cells. As explored in a study, each cell

type in a particular cancer environment has unique metabolic demands that enable specific functions like immune, stromal, and cancer cells; they compete for nutrients to carry out biosynthesis and effector activities [75]. The TME is epitomized by deregulated metabolic properties, which include both Intrinsic features (e.g., a mutation in cancer cells like IDH1, IDH2, succinate dehydrogenase (SDH) complex, fumarate hydratase) and extrinsic features (e.g., oxygen and nutrient availability, pH) [76]–[78]. Several signaling pathways such as PI3K, mTOR, MAPK, HIF1A, and AMPK subscribes to the Warburg Effect and other cancer cells' metabolic phenotypes. Lactate secreted by tumor cells activates HIF1A in cancer cells, upregulates angiogenic signals, and stimulates an autocrine pro-angiogenic NF-κB/IL-8 pathway by inhibiting the oxygen-sensing prolyl hydroxylase 2 (PHD2). Further, it also turn-on receptor tyrosine kinases AXL, TIE2 and VEGFR-2 in a ligand-independent manner [79], [80].. This together results in establishing a long-lasting immunosuppressive environment in tumors, promote tumor cell proliferation, tumor cell survival, metastasis, and angiogenesis [81].

2.2.6. EVADING GROWTH SUPPRESSORS

The evasion of growth suppression is an essential hallmark of cancer and is an important characteristic of cancer cells. Cancer cells get away growth-inhibitory signals of p53, retinoblastoma protein (Rb), TGF-β, gap junctions and contact inhibition to promote tumorigenesis [82]. Various pathways that suppress tumor growth are dysregulated and mentioned as, i) The Rb pathway: downregulation of hyperphosphorylated Rb, inactivation of E2F and reduced activity of CDKs; ii) The p53 pathway: Upregulation of p53 expression; iii) PTEN pathway: Inhibition of PI3K-AKT and upregulation of PTEN; iv) NOTCH pathway: inhibition of notch signaling; v) Hippo signaling: Upregulation of the pathway by suppression of YAP/TEAD activity; vi) Inhibition of IGF-1R; vii) Activation of ARID1A and GDF 15. Chemokines promote infiltration and activation of host-derived inflammatory and stromal cells

that lead to a pro-tumorigenic microenvironment that is immunosuppressive along with vascular permissive [83]. Tumor cells are also known to upregulate autophagy mechanisms to survive micro-environmental stress, increase growth and aggressiveness and facilitate metastasis [84]. In the same context, it is known to suppress the proliferation of tumor cells. The mechanism used by autophagy to support cancer tumorigenesis includes suppressing activation of the p53 protein and maintaining the metabolic function of mitochondria [85], [86].

2.2.7. AVOIDING IMMUNE DESTRUCTION

Tumor cells are smart enough to adapt mechanisms to escape detection and destruction by the host's immune system. Each cancer behaves differently compared to others because some are inherently better at 'hiding' than others. For example, cancers, such as melanoma, bladder, and RCC, exhibit a lasting response and better efficacy to immunotherapy; however, breast cancer has not shown a durable response. The most probable mechanisms used by breast cancer cells to escape immune surveillance are, firstly, the expression of immune inhibitory co-stimulatory receptors (e.g., PD-1, CTLA-4, LAG-3), secondly the presence of tumor-derived immunosuppressive factors (e.g., TGF-β, IL-10, IDO), and lastly infiltration of suppressive immune cells (e.g., Tregs, MDSCs), TAMs and increase self-tolerance by regulating NK cells in the microenvironment. Numerous studies have shown that the host immune system has a critical dual role in promoting and suppressing tumor development by establishing a balance between immune recognition and tumor growth. Factors that tumor cells exploit to avoid immune response and embrace immune suppression in TME are infiltration of regulatory cells ($CD4^+CD25^+$ $FoxP3^+$, Tregs), defective antigen presentation (affecting MHC-I pathway, protein LMP2, LMP7, TAP, Tapasin), production of several immunosuppressive mediators such as VEGF, tumor gangliosides, receptor-binding cancer-associated surface antigen (RCAS1), IDO, arginase, and inhibitor of nuclear factor kappa-B kinase (IKK)2, differentiation and polarization of macrophage from cancer-promoting M2 type to cancer-

inhibiting M1 phenotype [87]. Infiltrated macrophages in most cancers are of the M2 phenotype, which release anti-inflammatory chemicals such IL-10, TGF-β, and arginase1, creating an immunosuppressive milieu for tumor growth. [88]. Tumor cells and some other cells (e.g., myeloid cells) in TME expressed PD-L1/2 inhibitory molecules on their surface and used them as a molecular shield to protect themselves from $CD8^+$ T cell activities [89], [90]. Studies have shown bone-derived mast cells could exert both immunostimulatory and immunosuppressive actions [91]. They are recruited at the tumor site by chemotactic factors (e.g., stem cell factor (SCF)) released by cancer cells. SCF-recruited mast cells establish a complicated relationship with another immune (including tumor-infiltrating immune cells) and tumor cells that create an immunosuppressive microenvironment altogether [92]. It has been proposed that stroma might be a barrier to antigen presentation and immune recognition, hindering immune recognition and destruction.

2.2.8. ENABLING REPLICATIVE IMMORTALITY

Cancer cells have the ability to replicate unlimitedly as compared to normal healthy cells. Hayflick Limit, named after scientist Leonard Hayflick discovered that normal cells have a limited capacity to divide, and after the loss of capacity to divide, cells reach an irreversible state of senescence [93]. Normal cells acquired senescence state by numerous stimuli, including intrinsic cellular processes like telomere impaired and gain of function of an oncogene and exogenous factors such as DNA damaging agents or oxidative environment. A plethora of experimental and clinical research data holds the concept that senescence response is important for preventing deregulated growth and malignant transformation. Faulty removal of senescent cells may lead to an unregulated stockpile of cancer. The senescence-associated secretory phenotype (SASP) aids in eliminating senescent cells by engaging immune cells but can potentially encourage the proliferation of tumor cells that are not stably growth arrested. NF-κB and C/EBPβ boost the expression of SASP factors, such as IL-6, IL-8, and IL-1β, acting

in an autocrine and paracrine manner to bring out a positive feedback loop increase SASP production [94]. For instance, Ruhland et al., 2016 mentioned that senescent stromal cells give rise to local inflammation and are involved in building an immunosuppressive microenvironment by accumulating MDSCs that limit $CD8^+$ T cell responses. This encourages immune-mediated tumor growth. SASP derived IL-6 cytokines play a role in inflammation, which mediates immunosuppression and tumor progression [95].

2.2.9. TUMOR PROMOTING INFLAMMATION

Cancer cells have the tremendous ability to seize inflammatory responses to promote their growth and survival. They manipulate immune cells within the complex TME that indirectly induce the production of various proteolytic enzymes, cytokines, chemokines and pro-angiogenic mediators. Dynamic crosstalk exists between cancer and inflammation as an inflammatory response plays a dual role in inhibiting or promoting cancer [96]. In the case of TME, the role of inflammation is type and level-dependent. Important underlying mechanism which mediate inflammation includes DNA mutation, infectious agents, epigenetic alterations, and impaired DNA repair [97]. A vicious cycle links DNA damage, and ROS production induces inflammation and vice versa, supporting a complex interplay between them [98]. Tumor modulates the inflammatory environment by producing inflammatory cytokines, such as TNF-α, TGF-β, IL-6, and IL-10. Pro-inflammatory cytokines favor the EMT process, and angiogenesis, VEGF, and IL-8 facilitate the latter. Further, anti-inflammatory cytokines, such as IL-10 and TGF-β, involves in evading the immune response. Other TME components, including TAM, TIL, CAF, DCs, MDSCs, T cells, mast cells, and NK cells, promote and maintain tumor growth and metastasis [52]. TAMs secrete a variety of chemotactic components such as CCL2, CCL5, CCL7, CXCL8 and CXCL12 and aid in maintaining immunosuppressive phenotype by inducing TAM to switch from a M1- to M2-polarized state. Inflammatory cytokines such as TNF-α, IFN-α, IL-12, and other ILs, increase the efficiency of NK cells in

combating the tumor load [99], [100]. A study by Balachander et al., 2018 showed that CAFs are valuable in understanding inflammatory responses in tumors as they play a vital role in NF-κB activation, production of pro-inflammatory cytokines, and upregulation of pro-inflammatory gene expression [101].

2.2.10. ACTIVATING INVASION AND METASTATIS

Tumor cell invasion and metastasis are two crucial characteristics of cancer, and it enables tumor cells to escape the primary site and colonize to the new secondary site in the new environment [48]. Development of carcinomas in the initial stages during metastasis occurs either due to gain of function of oncogenes and/or loss of function of tumor potential genes. The second step that allows tumor cells to invade includes expansion and invasion of basement membrane into surrounding tissue due to enhanced protease activity (for example, MMPs), increased cell mobility interaction with neighboring tissues (includes ECM/stromal cells), reduced integrity, cell-matrix adhesion (includes matrix–integrin interaction, cell-cell contacts (such as loss of E-cadherin-mediated cell-cell adhesion, loss of cell junction and tight junction) [102], [103]. As tumors grow, a bidirectional communication, dynamic and intricate network of interactions exists between tumor cells and other components of TME. The third step of invasion and metastasis includes invasion of cancer cells into the blood vessel mediated by upregulation of angiogenesis, the survival of cancer cells in circulation by immune evasion or suppression of immunosurveillance [103]. Tumor cells and/or other components of TME do this by the various mechanisms, which includes: secretion of angiogenesis-modulating enzymes, such as VEGF, thymidine phosphorylase that enhances the angiogenesis process [104]; recruitment of immune-suppressor cells, including TAM, mast cells, DCs, MDSCs and Tregs cells in response to activated cytokines (TGF-β, CXCL5-CXCR2) [105]. MDSCs and Treg cells infiltrate the developing tumor to disrupt immune surveillance and promote tumorigenesis via different mechanisms, including encouraging tumor vascularization,

interference of antigen presentation by DCs, repression of T and B cell proliferation and activation, or inhibition of NK cytotoxicity and M1 macrophage polarization [106]. TAM plays a vital role in tumor progression and metastasis as it is involved in stimulating angiogenesis (by VEGF secretion) and lymphangiogenesis, remodeling the ECM (by secreting MMPs), activating EMT transition, inducing immunosuppression. For example, macrophage-derived MMP9, pro-inflammatory cytokines (IL-1, TNF-α) promotes tumorigenesis and angiogenesis [107]. The fourth step includes invasion into secondary tissue by interaction and adaption to the new tissue microenvironment. Paget, an assistant surgeon, gave the 'seed and soil' theory of metastasis in 1889. He beautifully explained that metastasis is not a chance event. In contrast, a specific cancer cell (seed) from the primary site will only be established in a specific and preferred location (soil). Each cancer has an increased propensity to metastasis into one particular secondary location where the microenvironment plays a crucial role in regulating the growth of metastases [108].

2.3. BRAIN CANCER

There is a significant amount of morbidity and mortality in the United States due to brain and other CNS tumors, which are among the most lethal cancers. Between 2008 and 2017, the overall incidence rate of malignant brain tumors decreased by 0.8% annually, whereas, among children and adolescents, it ascended by 0.5% to 0.7% annually [11]. CNS malignancies make up approximately 3% of all cancers worldwide and are more prevalent in men than in women [109]. With an expected 30,000 new cases worldwide in 2020, brain tumors and other CNS cancers continue to pose a deadly threat to human health despite ongoing attempts to discover effective therapeutics [110]. Surgery, postoperative radiotherapy, and chemotherapy are all common general treatments for brain tumors, but they are often associated with serious side effects and a poor prognosis. Primary tumors, which grow and begin in the brain's CNS, are separated from secondary tumors, also known as metastases, which build from tumor cells in

other organs which include the lung, breast, gastrointestinal tract, etc., then spread to the nerve tissue [111]. According to WHO2021, classification has been shown in **Figure 2.3**. Additionally, the types, sizes, locations, grades, and general health of the patient all influence the therapy options for brain cancer. Surgery, radiation therapy, chemotherapy, targeted therapy, and immunotherapy are the main treatment techniques. Despite the fact that immuno treatment for brain tumors has had mixed results In clinical trials for the treatment of brain cancer, immune-based medicines such as immune checkpoint inhibitors are being investigated in order to improve the body's immune response against cancer cells [112]. Therapy for brain cancer has a number of difficulties and restrictions: i) The BBB, which prevents certain chemotherapy drugs from penetrating the brain tissue, reduces their efficacy, ii) Lack of efficient biomarkers (diagnostic, prognostic, and predictive markers) and therapeutic targets, acquired resistance to chemotherapy and radiation therapy, significant molecular and cellular heterogeneity, which may influence response to therapy and progression of the disease, iii) and the difficulty establishing animal models that accurately reflect human brain tumors are all factors that can make it difficult to deliver drugs to the tumor site. For preclinical testing of potential therapeutics, animal models that replicate the genetic and histological properties of brain tumors are crucial [113], iv) The degree of incision of the procedures needed and the scarcity of tissue samples make it difficult to obtain samples of brain tissues for research. This constraint may impede the cellular and molecular examination of brain cancer [114].

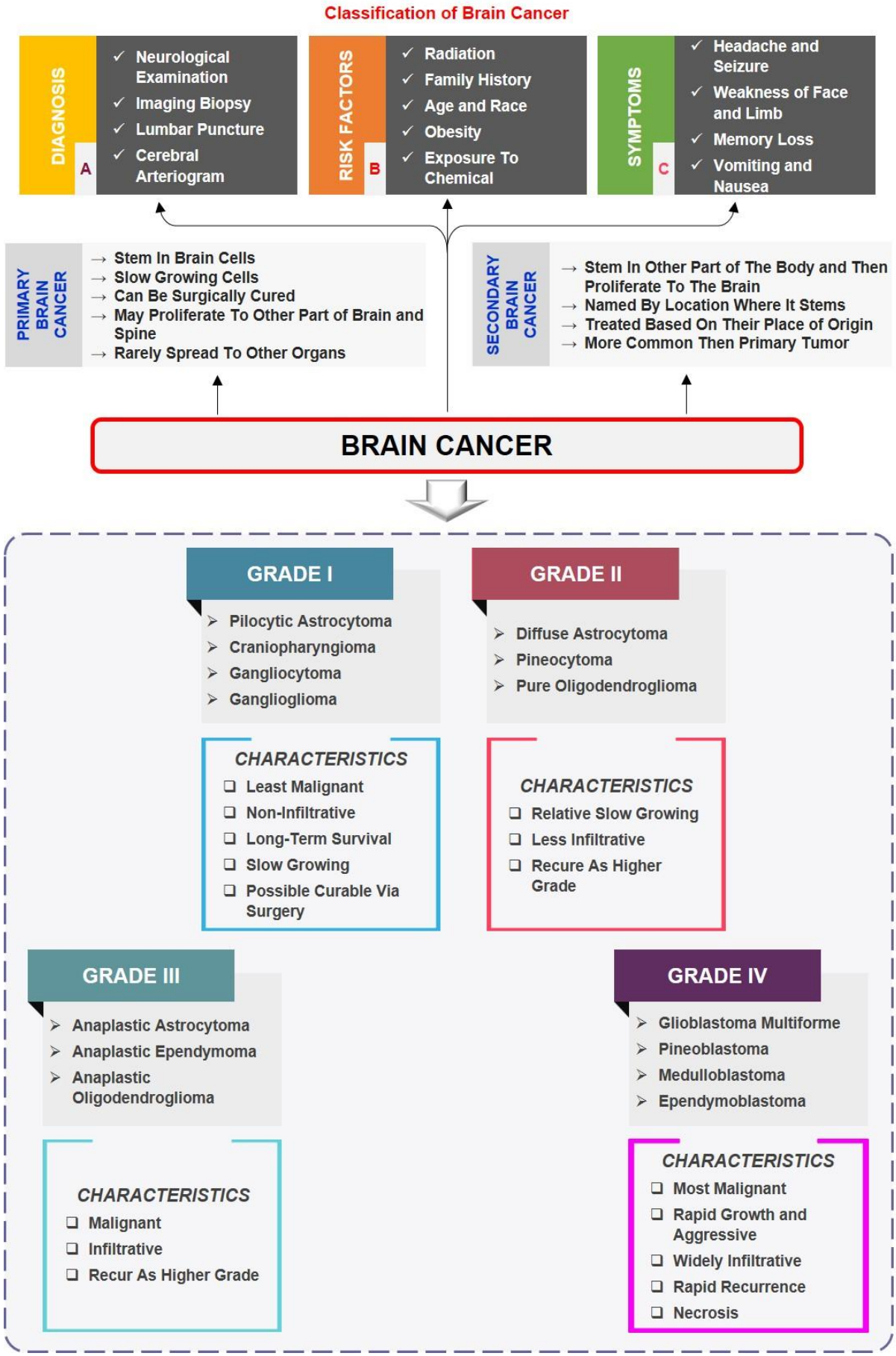
Classification of Brain Cancer
DIAGNOSIS
A
✓ Neurological Examination
✓ Imaging Biopsy
✓ Lumbar Puncture
✓ Cerebral Arteriogram
RISK FACTORS
B
✓ Radiation
✓ Family History
✓ Age and Race
✓ Obesity
✓ Exposure To Chemical
SYMPTOMS
C
✓ Headache and Seizure
✓ Weakness of Face and Limb
✓ Memory Loss
✓ Vomiting and Nausea
PRIMARY BRAIN CANCER
→ Stem In Brain Cells
→ Slow Growing Cells
→ Can Be Surgically Cured
→ May Proliferate To Other Part of Brain and Spine
→ Rarely Spread To Other Organs
SECONDARY BRAIN CANCER
→ Stem In Other Part of The Body and Then Proliferate To The Brain
→ Named By Location Where It Stems
→ Treated Based On Their Place of Origin
→ More Common Then Primary Tumor
BRAIN CANCER
GRADE I
➢ Pilocytic Astrocytoma
➢ Craniopharyngioma
➢ Gangliocytoma
➢ Ganglioglioma
CHARACTERISTICS
❑ Least Malignant
❑ Non-Infiltrative
❑ Long-Term Survival
❑ Slow Growing
❑ Possible Curable Via Surgery
GRADE II
➢ Diffuse Astrocytoma
➢ Pineocytoma
➢ Pure Oligodendroglioma
CHARACTERISTICS
❑ Relative Slow Growing
❑ Less Infiltrative
❑ Recure As Higher Grade
GRADE III
➢ Anaplastic Astrocytoma
➢ Anaplastic Ependymoma
➢ Anaplastic Oligodendroglioma
CHARACTERISTICS
❑ Malignant
❑ Infiltrative
❑ Recur As Higher Grade
GRADE IV
➢ Glioblastoma Multiforme
➢ Pineoblastoma
➢ Medulloblastoma
➢ Ependymoblastoma
CHARACTERISTICS
❑ Most Malignant
❑ Rapid Growth and Aggressive
❑ Widely Infiltrative
❑ Rapid Recurrence
❑ Necrosis

Figure 2.3: *WHO Classification of Brain Tumor Grades:* According to the WHO, brain tumors are graded according to their histological characteristics under a microscope, which is essentially used to determine if a tumor is benign or malignant. The brain tumor grading system was established by the World Health Organization (WHO). The symptoms of different forms of brain tumors vary depending on where the tumor is located, however, the symptoms indicated above are some of the potential ones.

2.3.1. GLIOBLASTOMA MULTIFORME

GBM is indicative by hypercellular anaplastic glioma cells with elevated mitotic activity, necrosis and microvascular proliferation. It is the most frequent primary CNS cancer, accounting for 45.2% of malignant CNS tumors and 55% of all gliomas [115]. Individuals aged 20-39 years experienced the most significant increases in survival, with 5-year survival increasing from 44% to 73%. In contrast, the failure to enhance survival in older age groups was primarily due to the inability to improve GBM therapy [11]. Currently, GBM is being treated with a combination of surgery, radiation therapy (RT), and chemotherapeutics (alkylating drug Temozolomide (TMZ) and antiangiogenic agent bevacizumab). Furthermore, novel treatments such as tumor-treating fields (TTFields) and immunotherapy offer promise for a better prognosis [116]. Despite these treatment options, GBM patients' overall survival and quality of life remain dismal. The plethora of research mentioned numerous obstacles to GBM treatment, including tumor heterogeneity, acidic microenvironment and immunosuppression, all of which are linked to the hypoxic environment to some degree [117]. Thus, there is utmost importance in developing novel therapeutic strategies to enhance the overall survival rate of GBM patients [5], [6]. For instance, Yin et al., 2022 demonstrated that combined administration of ultrasmall Zirconium carbide nanodots and RT enhanced the therapeutic efficiency both *in vitro* and *in vivo* [27]. Recent studies emphasized the implementation of treatment strategies, such as adoptive cell therapy, gene therapy, viral and non-viral vectors-based therapy, RNAi therapy, PDT, PTT, stem-cell-based therapy, and vaccine therapy that exhibit promising primary outcomes in both experimental as well as clinical studies [7]–[10]. For example, Abbott et al., 2021 employed retained display antibody platform to develop single-chain variable fragments that have the potential to recognize

epidermal growth factor receptor mutant variant III (EGFRvIII). The authors demonstrated that despite the higher affinity, GCT02 CAR T cells kill equivalently but secrete lower amounts of cytokine. In addition, GCT02-CAR T cells also mediate rapid and complete tumor elimination *in vivo* [118]. Thus, there is growing need to decipher the mechanism of oncogenic signaling targets and TME biomarkers as therapeutic targets in GBM (**Figure 2.4)**

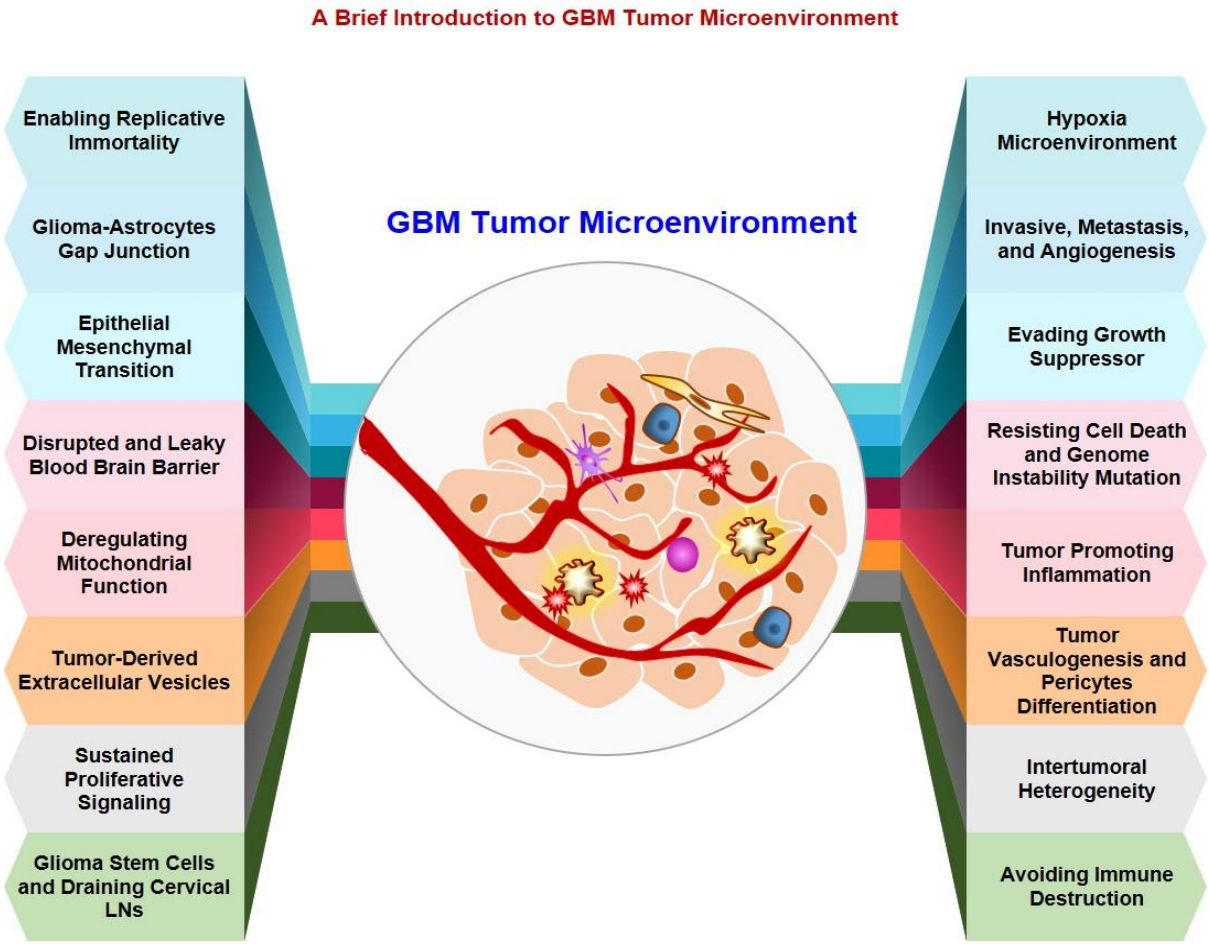

Figure 2.4: *A Brief Introduction to GBM Microenvironment*: The brain's glial cells can give rise to the aggressive brain tumor known as glioblastoma multiforme. A complex network comprised of multiple kinds of cell, involving tumor cells, immune cells, endothelial cells, vascular cells, and stromal cells, compose the GBM tumor microenvironment. These cells communicate with the ECM, which is an arrangement of proteins and compounds that gives tissues their structural support. The multifaceted and ever-changing GBM tumor microenvironment affects the growth, invasion, and therapeutic response of the tumor. Creating innovative and improved GBM strategies requires a thorough understanding of the manner in which tumor cells interact with the microenvironment surrounding them.

2.4. TUMOR MICROENVIRONMENT

Tumors are complex heterotypic tissues in which a non-transformed milieu influences the proliferation and advancement of transformed cells with which it shares space and time. The TME can be thought of as an ecosystem or community in which malignant cells live and grow

[31]. Growing evidence suggests that the TME can influence abnormal tissue function and play a crucial role in the progression of more advanced and refractory cancers [151]. Despite intense research in oncology, which has provided enormous insight, cancer continues to be a poorly understood disease. In earlier studies, cancer was viewed as a heterogeneous disease involving aberrant mutations in only tumor cells but it is now evident by intense research that their micro environmental composition also influences tumors. Since then, a plethora of studies have contributed to the characterization of the TME and understanding its crosstalk with tumor, which has further simplified the challenging task of treating cancer. It has been suggested that many environmental factors and oncogenic stimuli influence TME, affecting cancer cell metastasis in a dynamic process [106]. A dynamic bidirectional interaction exists between cancer cells and the host microenvironment, which involves a wide variety of components and a diverse range of mechanisms that are critical and support cancerous growth and spread [121], [122], and this communication leads to proliferation and metastasis [123]–[125]. Moreover, Pereira et al., 2015 mentioned the role of the lymph node microenvironment in cancer metastasis [126]. The role of the microenvironment in tumor development was initially proposed by Stephen Paget in the "seed and soil" hypothesis [108]. In solid tumors such as breast, head and neck, pancreatic, lung, brain, prostate, and cervix, DSB repair mechanisms get profoundly influenced by TME cellular and non-cellular factors including hypoxia, inflammation, genotoxic stress, cellular metabolism, and the immune system. The role of the TME and its relationship with DNA damage is emerging as an essential consideration in developing anti-cancer therapy that targets DNA repair-deficient cancer cells.

2.4.1. TUMOR MICROENVIRONMENT COMPONENTS

The TME consists of different cellular and non-cellular secreted components; the cellular components include tumor cells, fibroblasts or cancer-associated fibroblast (CAFs), MSC, pericytes, adipocytes, vasculature, lymphatic networks, myeloid population, MDSCs, immune

cells, and inflammatory cells. CAFs are the dominant cell type within the reactive stroma of tumors that secrete growth factors, such as hepatocyte growth factor (HGF), EGF, and cytokines like stromal cell-derived factor 1 (SDF-1) and IL-6 [127]. Exosomes containing microRNAs (miRNAs) (e.g., miR-155, miR-100, miR-222, miR-30a, and miR-146a) are secreted by chemotherapy-treated cancer cells and CAFs, that are known to mediate cancer resistance [128]. Recently, a growing number of publications show CAFs secrete IL-6 cytokines, a key player in molecular abnormality, chemoresistance, EMT and stem cell formation in various types of malignant cancer [129]. Similarly, adipose cells are the important component of the TME as they provide a highly inflammatory environment for cancer cell proliferation by secreting more than 50 cytokines, chemokines and various hormone-like growth-promoting factors. Like normal tissues, the TME has blood and lymphatic vascular networks as essential components for supplying oxygen and removing metabolic waste and carbon dioxide. These networks are characterized by sustained angiogenesis for making new blood vessels from the pre-existing ones [130]. Immune cells in TME include cells of adaptive immunity like dendritic cells (DCs), T lymphocytes, and effectors of innate immunity like NK cells, macrophages, and polymorphonuclear leukocytes. Moreover, tumor-infiltrating lymphocytes (TILs) comprising $CD3^+CD4^+$ and $CD3^+CD8^+$ T cells are also the major constituent of TME exclusive for tumor-associated antigens [131]. Besides, inflammatory cells in the TME either assist tumor progression by contributing to 'immune evasion' or resist tumor growth. Non-cellular components of TME include ECM, matrix remodeling enzymes, cytokines, chemokines, exosomes, growth factors, and inflammatory enzymes [16], [132]. The function of each component in TME and its role in tumor progression have been explained in **Table 2.1**. The ECM is the highly dynamic structural TME component comprising of various proteins, polysaccharides, proteoglycans (such as heparan sulphate proteoglycans, versican and hyaluronan) and glycoproteins (such as laminins, elastin, fibronectin and tenascins).

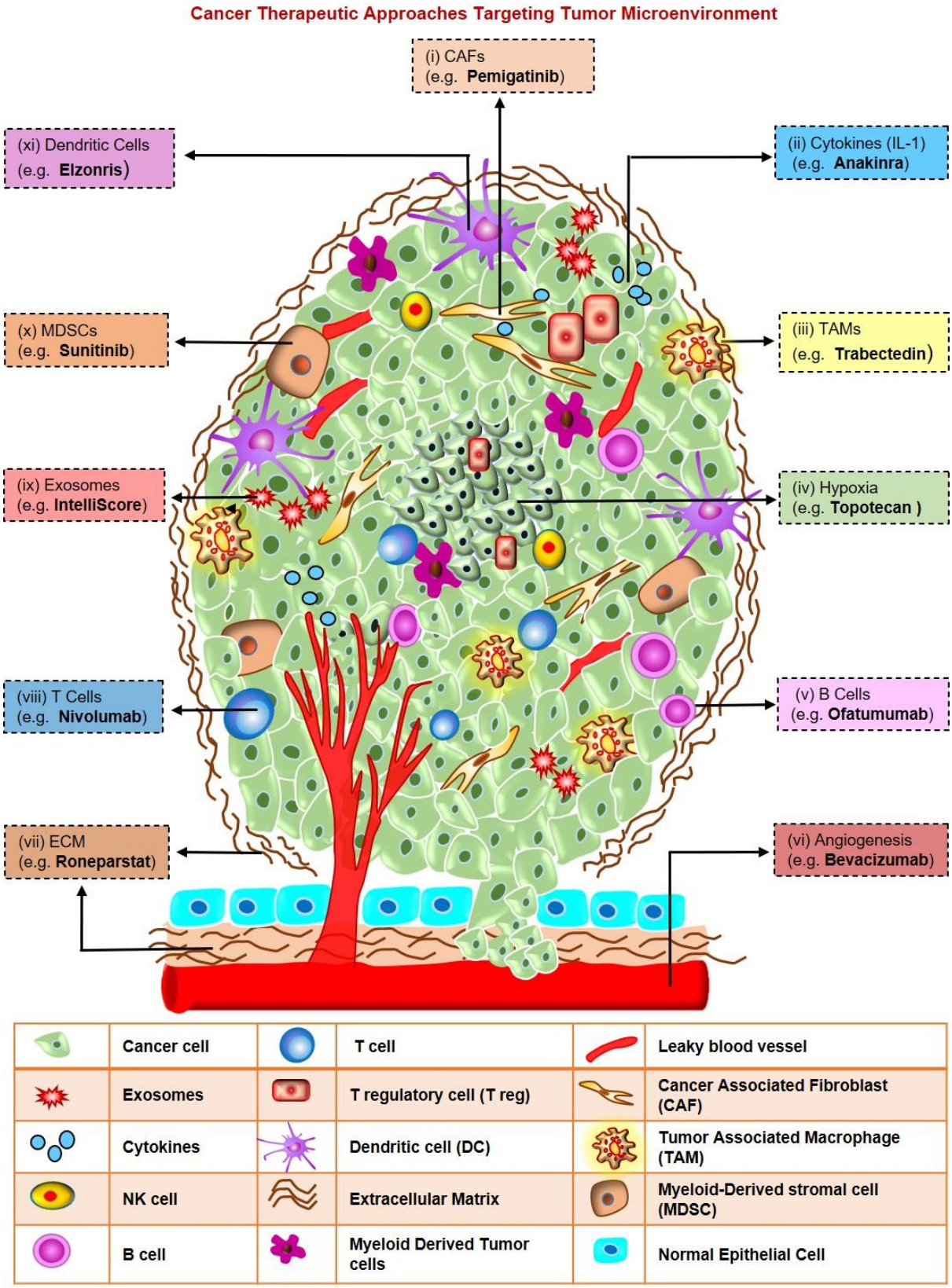

Figure 2.5: ***Approach Used to Target Tumor Microenvironment for Cancer Treatment:*** **Schematic illustration for heterogeneous and complex tumor microenvironment: i)** ***CAFs:*** **It promote angiogenesis via VEGF, CXCL12a and FGF-2 production, and modulate the immune response via macrophage infiltration and cell polarization. Pemigatinib, a potent inhibitor of fibroblast growth factor receptor (FGFR) types 1, 2, and 3 for the treatment of cholangiocarcinoma. ii)** ***Cytokines:*** **Anakinra an FDA approved IL-1 receptor antagonist (IL-1Ra) that inhibits pro-inflammatory cytokine IL-1. It is used in second line treatment of**

rheumatoid arthritis. It has also been used in combination with Nab-paclitaxel, Gemcitabine, and Cisplatin for Pancreatic cancer (NCT02550327). iii) R3Q9 *Tumor-associated macrophages (TAMs):* They are a key component of the tumor microenvironment, as they aid in metastasis and invasion by secreting matrix metalloproteinases, as well as promoting genetic instability. Trabectedin inhibits the G2 phase of the cell cycle, lowers TAM, and regulates the production of cytokines and angiogenic factors. iv) *Hypoxia*: Hypoxia-induced factor-1 governs the cellular response and inflammation inside the tumor microenvironment. FDA approved Topotecan, a medication that targets topoisomerase I and is known to block hypoxia-mediated HIF-1 activation. v) *B cells*: They play a role in humoral immunity. Ofatumumab is a human anti-CD20 human immunoglobulin G1 kappa (IgG1κ) monoclonal antibody that depletes B cells and used to treat non-Hodgkin's lymphoma, chronic lymphocytic leukemia. vi) EP20Q5 *Angiogenesis*: Tumor cells initiate angiogenesis, which results in the creation of chaotic branching structures. Bevacizumab is a humanized monoclonal antibody that prevents circulating VEGF from interacting with its receptors. vii) ECM: Collagen, elastin, fibronectin, hyaluronic acid, proteoglycans, and glycoproteins make up the ECM, which also contains several growth factors. Roneparstat being in Phase 1 is a heparinise inhibitor that EP20Q4 engages in degradation and remodelling of ECM and proven to be effective against the ECM. viii) *T cells:* They contribute in cell immunity. EP20Q3 Nivolumab is a fully human immunoglobulin G4 (IgG4) monoclonal antibody that binds to the PD-1 receptor and, by preventing its interaction with its ligands PD-L1 and PD-L2, it disrupts negative signaling to restore T-cell antitumor function. ix) *Exosome*s: Tumor cell-derived exosomes modulate the tumor microenvironment via paracrine signaling. ExoDx Prostate (IntelliScore), a urine exosome gene expression assay, is non-invasive test to determine elevated Prostate-Specific Antigen (PSA) for men. x)EP20Q1; EP20Q2 *Myeloid-derived suppressor cells (MDSCs)*: VEGF causes MDSCs activation. Activated MDSCs migrate to the tumor microenvironment, where they promote proliferation and vascularization while inhibiting the immune system. Sunitinib is a receptor tyrosine kinase inhibitor that targets and depletes MDSCs and Tregs in the peripheral blood, lowering their accumulation and reversing IFNγ suppression. xi) *Dendritic Cell*: Tumor microenvironment modulates dendritic cell to evade immune response by playing essential role in skewing tumor-specific cytotoxic T cells. Elzonris, recombinant human IL-3 and truncated diphtheria toxin (DT) fusion protein that block protein synthesis and used to treat Blastic plasmacytoid dendritic cell neoplasm (BPDCN).

Additionally, soluble factors, such as growth factors and other ECM-associated proteins bind to the ECM. In addition, receptors present on the cell surface binds with components of ECM and ECM-bound factors to regulate processes such as proliferation, migration, differentiation and apoptosis [133]. Due to the plasticity nature, ECM has been ascribing both pro-tumorigenic and anti-tumorigenic properties. ECM proteins are responsible for creating a barrier through which the drugs must pass in order to reach the cancer cells. Recent studies have revealed that ECM proteins, including collagen, laminin, hyaluron, POSTN, fibronectin, etc., are highly expressed by metastatic cells. Collagen is the most significant component of ECM as collagen processing enzymes are strongly expressed in TME. Collagen in combination with Elastin contributes to tumor rigidity it's palpability [134]. Nowadays, ECM is emerging as a critical player in malignant initiation, progression and chemoresistance. ECM continuously undergoes controlled remodelling. Specific enzymes that are responsible for ECM degradation, such as metalloproteinases (MMPs), mediate this process, which includes quantitative and qualitative changes in the ECM. MMPs are involved in nearly every significant stage of tumor

development, including tumor cell invasiveness and migration, metastasis, angiogenesis, immune surveillance escape, and apoptosis [135]. Chemokine families (namely, the C-, CC-, CXC- and CX_3C-chemokine families) are another important component, and they are produced by tumor cells as well as other TME cells, including immune cells and stromal cells. They directly and indirectly influence cancer progression, tumor immunity, and therapy outcomes [136]. Similarly, cytokines and exosomes influence TME [137] **(Figure 2.5)**.

Table 2.1: Components, Functions, and Classifications of TME [138]–[145]

CELL PLAYER	MAIN MARKER	FUNCTION	CLASSIFICATION	REFERENCE
Cancer-Associated Fibroblasts	**Human:** PDGF*; FAP*; FGFR*; α-SMA	▪ Modulate inflammation. ▪ Encourage proliferative signaling, angiogenesis and metastasis ▪ Participating in wound healing. ▪ Integrating collagen and protein to form the ECM fiber network. ▪ Evade immune destruction. ▪ Reprogram cellular metabolism. ▪ Stimulate genome instability and mutation ▪ CAFs can differentiate stimulation by ROS and TGF-β1-dependent and TGF-β1-independent mechanisms.	Pro-Tumorigenic; less known of Anti-tumorigenic	[138], [139], [146], [147]
Lymphatic Vessels	**Human:** VEGFR3; LYVE-1	▪ Upregulated VEGF-C induces enlargement of tumor-associated lymphatic vessels, increasing lymph flow and facilitating intravasation of cancer cells into the lymphatics. ▪ Overexpression of HGF induces lymphatic vessel hyperplasia and lymphatic metastasis. ▪ ET-1 induces Lymphatic Endothelial Cells (LECs) and Lymphatic Vessels to Grow and Invade. ▪ In TME, VEGFR-3 engagement by VEGF-C expands LECs (a process known as tumor-associated lymphangiogenesis).	Pro-Tumorigenic	[148]–[152]
Lymph Nodes	Prox1; VEGF-C	▪ Tumor overexpresses VEGF-C, which induces lymphangiogenesis and metastasis to regional lymph nodes. ▪ Lymph Nodes-LECs in TME is actively involved in immunological responses. ▪ The composition of the metastatic lymph node undergoes remodeling that influences the growth of cancer cells.	Pro-Tumorigenic	[126], [151], [153]
Bone Marrow	**BMDCs:** CD11c, CD80, CD86 and MHC II	▪ Cancer cell influences Bone marrow resident cells (osteoblasts, osteocytes, adipocyte, osteoclast, immune cells, endothelial cells, nerves). ▪ BMDCs in TME participate in tumorigenesis, tumor invasion and angiogenesis.	Pro-Tumorigenic	[154]–[156]
Spleen	CD11b, CD11c, F4/80, Gr-1, Ly6C, and Ly6G	▪ The spleen plays an important role in tumor progression in the tumor-bearing host. ▪ The spleen is a site of immune tolerance induction. ▪ The spleen is resident of several distinct populations of myeloid cells with varying immune functions, including neutrophils, eosinophils, monocytes, macrophages, and dendritic cells.	Pro-Tumorigenic	[157]–[159]
Thymus	**-**	▪ It is a central lymphoid organ for T cell development	Pro-Tumorigenic	[160]

		▪ Thymic function related to cancer development, relapse and anti-tumor immunity.		
Tumor Endothelial cells (TECs)	CD13/APN; CD54/ICAM-1; CD102/ICAM-2; CD144/VE-cadherin	▪ Alter TECs regulate tumor metastasis through biglycan secretion through activation of NF-κB and ERK signaling. ▪ TECs secret angiocrine factors such as IL-6, VEGF-A, bFGF. ▪ The balance between angiogenic activator and inhibitors regulates tumor angiogenesis.	Pro-Tumorigenic	[161]–[163]
Adipose cells	**Human:** AIs*; MBD6*	▪ Relating with inflammation. ▪ Recruiting immune cells. ▪ Assist vasculogenesis. ▪ Regulating the balance of systematic energy and metabolism ▪ Engage in metabolic symbiosis relationship with adjacent tumor cells.	Pro-Tumorigenic	[138], [139], [164]
Tumor associated macrophages (TAMs)	**Human:**CD11b+ CD68+ CSF1R+ CD163+ EMR1+ **Mouse:**CD11b+GR1 – CD68+ CSF1R+ F4/80+	▪ Activated M1 macrophages are pro-inflammatory and anti-tumorigenic and secrete TH1 cytokines. ▪ Activated M2 macrophages are anti-inflammatory and pro-tumorigenic and secrete TH2 cytokines. ▪ TAMs frequently exhibit an M2 phenotype; their presence in tumors supports angiogenesis and invasion.	Pro-Tumorigenic (M2); Anti-Tumorigenic (M1)	[106], [165]–[167]
Dendritic Cells (DCs)	**Human:**CD11c+ CD83+ CD123+ **Mouse:**CD11c+ CD83+ CD123+	▪ DCs are monocytic APCs that are derived from the bone marrow. ▪ DC-based vaccines induce both innate and adaptive immune responses to regress tumors and prevent relapse. ▪ Splenic DCs suppress T cell response via IDO expression.	Mainly tumor-inhibiting but TME is also known to turn into Pro-Tumorigenic	[168]–[170]
Tie2-expressing monocytes (TEMs)	**Human:**CD11b+ SCA1+ TIE2+ CD14+ CD16+ **Mouse:**CD11b+ GR1–SCA1+ TIE2+	▪ Tie2 is a receptor for the angiogenic growth factor angiopoietin. ▪ TEMs have a role during tumor angiogenesis through a paracrine signaling loop with angiopoietin-expressing endothelial cells.	Pro-Tumorigenic	[171], [172]
Neutrophils	**Human:**CD11b+ CD66b+ CD63+ **Mouse:**CD11b+ GR1+ 7/4+	▪ Most abundant circulating leukocytes in humans and are phenotypically plastic in nature. ▪ Similar to TAMs, neutrophils have been shown to context-dependent roles within the TME. ▪ Enhancement of angiogenesis and metastasis. ▪ Tumor-associated neutrophil is linked with poor prognosis.	Pro-Tumorigenic (N2); Anti-Tumorigenic (N1)	[173]–[177]
Mast cells	**Human:**CD11b– CD49d+ CD117+ CD203c+ **Mouse:**CD11b– CD49d+ CD117+ CD203c+	▪ Mast cells are best known for their role during allergies and autoimmunity. ▪ Mast cells are recruited to tumors, where they promote tumor angiogenesis. ▪ Promote remodeling of tissue by induction of changes in ECM composition.	Pro-Tumorigenic	[178], [179]
Myeloid-derived suppressor cells (MDSCs)	**Human:** *Monocytic:* CD11b+ CD33+ HLA-DR– CD14+ *Granulocytic:* CD14– CD15+ **Mouse:** *Monocytic:* CD11b+ GR1+ Ly6G–Ly6C+ *Granulocytic*: Ly6G+Ly6C	▪ Facilitate neovascularization (produce VEGF). ▪ Drive invasion & metastasis (produce MMPs). ▪ Supports malignant cells to colonize at metastatic niche. ▪ Immunosuppressive precursors of dendritic cells, macrophages and granulocytes. ▪ Disrupt tumor immunosurveillance by interfering with T cell activation, cytotoxic activity, antigen presentation and cell polarization. ▪ Differentiating into TAMs under hypoxic conditions.	Pro-Tumorigenic	[139], [180], [181]
Natural Killer (NK) cells	**Human:**CD56+CD16+ **Mouse:** CD335+NK1.1+	▪ Cytotoxic lymphocytes can kill stressed cells in the absence of antigen presentation. ▪ Detect and kill tumor cells through 'missing self-activation (loss of healthy cell markers)	Mainly Anti-Tumorigenic	[106], [182]

		or 'stress-induced' activation (gain of stressed cell markers).		
T Helper (TH) cells	**Human:**CD3+CD4+ **Mouse:**CD3+CD4+	▪ CD4+ TH cells can be divided into TH_1 and TH_2 lineages. ▪ TH_1 cells secrete pro-inflammatory cytokines and can be anti-tumorigenic. ▪ TH_2 cells secrete anti-inflammatory cytokines and can be pro-tumorigenic. ▪ The ratio of TH_1 to TH_2 cells in cancer correlates with tumor stage and grade.	Pro-Tumorigenic and Anti-Tumorigenic depend on stage and context	[106]
Regulatory T cells (T_{reg} cells)	**Human**:CD4+ CD25+ FOXP3+ CTLA-4+ CD45RA+ **Mouse**:CD4+CD25+ FOXP3+ CTLA-4+ CD103+	▪ Primarily pro-tumorigenic roles by suppressing immunosurveillance. ▪ Secreting cytokines such as IL-10, IL-35, TGF-β. ▪ High T_{regs} infiltration are linked with poor survival in various cancer types. ▪ Some T_{regs} secrete perforin & granzyme to direct kill cells. ▪ Synthesis & release cAMP to interfere with tumor cell metabolism.	Pro-Tumorigenic and Involved in tumor maintenance	[139], [183], [184]
T_C cells [CD8+ cytotoxic T cells (CTLs)]	**Human:**CD3+CD8+ **Mouse:** D3+CD8+	▪ Associated in the adaptive immune system. ▪ Especially recognize and kill cancer cells through perforin- and granzyme-mediated apoptosis.	Anti-Tumorigenic	[106]
B cells	**Human:**CD19+CD20+ **Mouse:** B220+CD19+CD22+	▪ Engaged in humoral immunity. ▪ Secreting pro-tumorigenic cytokines in TME and altering TH_1- to-TH_2 ratios. ▪ Involved in tumorigeneses.	Pro-Tumorigenic	[106], [185]
Extracellular vehicles (EVs) [Includes exosomes (30–100 nm), micro vesicles (100 nm–1 μm), and apoptotic bodies (500 nm–4 μm)]	**Exosomes:** tetraspanin family members (CD63, CD81, CD9), Tsg101, Alix, MHC molecules, HSP70; **Microvesicles**: PS, Integrins αIIbβ3 (CD41)) CD42b, and GPVI, selectin; **Apoptotic bodies:** Histone, fragmented DNA, PS hsa_circ_0000338**; miR-21, miR-196, let-7a, miR-1229 miR-23a, miR-141;	▪ Encapsulate biologically molecules (include proteins, miRNAs, cirRNA and lncRNAs) ▪ Involved in the bidirectional communication between tumor and TME. ▪ Regulating key signaling pathways, proliferation, drug resistance, and stemness. ▪ Reprogramming stromal cells to create a niche for survival. ▪ Tumor exosomes of CLL patients express tetraspanin, CD9, CD63, and CD37 markers and plasma-derived exosomes miRNA signature, including miR-29 family, miR-150, miR-155, and miR-223. ▪ Annexin A1 is a specific marker for classical microvesicles budding from the plasma membrane. ▪ Apoptotic bodies released by membrane blebbing and eventually engulfed by phagocytic cells and also promote intercellular communication by delivering their content into recipient cells	Pro-Tumorigenic; Anti-Tumorigenic	[140], [142], [186]–[191]
Extracellular Matrix	MMP-9, HSPGs circulating COL11A1, COMP, and COL10A1	▪ ECM components: fibrillar proteins such as collagen, elastin, fibronectin, & laminins, glycosaminoglycans (GAGs), proteoglycans (PGs), & other glycoproteins. ▪ Establishing the complex structural network. ▪ Manage cancer invasion and metastasis, angiogenesis. ▪ Involved in growth and proliferation signaling. ▪ Inhibiting cancer apoptosis. ▪ Produces heparanase enzyme that degrades HSPs (sugar moieties), this causes FGF release from ECM, making it accessible for tumor cells.	Pro-Tumorigenic	[144], [145]

***the targeting markers; **circular RNAs**

2.4.2. HYPOXIA-MEDIATED MICROENVIRONMENT

The hypoxia (a hallmark of cancer) is a sub-region in the TME along with nutrient deprivation, low extracellular pH, and high interstitial fluid pressure. The hypoxic condition arises when oxygen consumption by cells exceeds that of supply [192]. The hypoxic region is characterized as heterogeneous in nature, with regions of chronic and acute hypoxia, altered pH, and immune infiltration [193]. In a hypoxic TME (e.g., 0.2 to 1% O_2), tumor cells slowly adapt to hypoxic conditions where they continue to grow and proliferate with altered/amended cellular biology. In contrast, another microenvironment is known as permanent anoxic (e.g., close to 0% O_2). Tumor or normal cells are leading to cell death [194]. Hypoxia cells have defective DNA repair, increased mutation rate, and hypoxia has the capacity to accelerate genomic instability through increased chromosomal rearrangement and decreased centrosome function, increased unrepaired DSBs and replication errors, increased gene amplification, and inaugural of intra-chromosomal fragile sites [194]–[196]. The study by Kumareswaran et al., 2012 found that under hypoxia state, aberrant or compromised DNA-double strand break (DSB)repair of G1-associated DNA-DSBs as a potential factor responsible for increased genetic and/or chromosomal instability [197]. A consequence of hypoxia in causing genomic instability has been shown beautifully in **Figure 2.6.** One theory supports this hypoxia act on complexes I, II, and III of the Electron transport chain (ETC) in mitochondria which drive increased ROS production. ROS plays a pivotal role in stabilizing and activating HIF1A, which activates survival, proliferation, metastasis, and a tumor cell's metabolic changes [198]. ROS (being secondary messenger), hypoxia, and DNA damage contribute to the signaling cascade of receptors (e.g., members of the Toll-like receptors (TLRs) or Nucleotide-binding oligomerization domain (NOD)-like receptors (NLRs) that instigate pro-inflammatory innate immune response through an array of functionally diverse down-stream signaling elements (e.g., NF-κB, STAT1, IRF-3, and caspase-1 activation) [98] also cytokines such as IL6, STAT3, and TNF-α [199]. Hypoxia also induces replication arrest, which activates

DNA damage response through ATR- and ATM-mediated signaling thus leads to induction of p53-dependent apoptosis [200]. Moreover, studies also showed that hypoxia induces hypoxia-iNOS, which increases intracellular RNS and ROS free radicals' concentration, resulting in DNA damage with poor prognosis. Alteration in hypoxia affects DNA damage response pathways, including HR, NHEJ, miss-match repair (MMR), nucleotide excision repair (NER), base excision repair (BER), and the Fanconi anemia pathways [42], [201]. HIF1A is crucial for tumor adaption to hypoxic, and it is also a key prognostic tumor factor [202], [203]. Its overexpression has been linked with a poor disease outcome and increased patient mortality in various cancer such as bladder, brain, breast, cervix, colon, endometrium, lung, oropharynx, pancreas, skin, and stomach cancers [43], [204]–[206]. Loss of HIF1A control can enhance tumorigenesis and genomic instability via cooperation with oncogene c-Myc (c-Myc expression is downregulated in low-oxygen regions of solid tumors) [207], [208]. Recently a study by Riffle et al., 2017 mentioned the involvement of ATM kinase, but not ATR responsible for γ-H2AX formation (also known as DNA damage marker) in the hypoxic tumor spheroids, which mimic TME of A673 spheroids by hypoxia-induced phosphorylation of H2AX [209]. HIFs are the indispensable regulator of tumor inflammation. Indeed, hypoxic cells or cells growing in the hypoxic microenvironment acquire gene amplification, point mutations, and increased numbers of DNA strand breaks periodic hypoxia and reoxygenation cycle. These genetic changes cause further activation of oncogenes or inactivate tumor suppressor genes, resulting in a mutator phenotype [210]. GBM being a highly vascularized human tumor, and its microcirculation is poor, resulting in the hypoxia region inside the tumor. In TME unregulated cell proliferation in tumor (tumor size exceeds diameter of >1 mm) often surpass capacity of the preexisting blood capillaries to meet the oxygen demand [211]. This results in a condition known as hypoxia, which impairs the availability of nutrients and promotes genetic instability because of an increase in the generation of ROS making it a crucial factor for tumorigenesis. As the master regulator orchestrating cellular

responses to hypoxia plays an essential role in GBM aggressiveness [212]. Various chemotherapy drugs mainly focus on handling this HIF1 that connects to hypoxia and leads to tumor invasion and progression [204], [213]. For example, topoisomerase-1 inhibitors, such as Topotecan (FDA approved) are used as a second-line chemotherapy drug in malignancies such as NSCLC and ovarian carcinoma. Topotecan is majorly used in advanced solid carcinomas that express a high level of HIF1 [214]. Further, radiation exposure also triggers hypoxia that leads to the activation of an immune response via increased cytokines production, that further causes the recruitment of various immune cells [215].

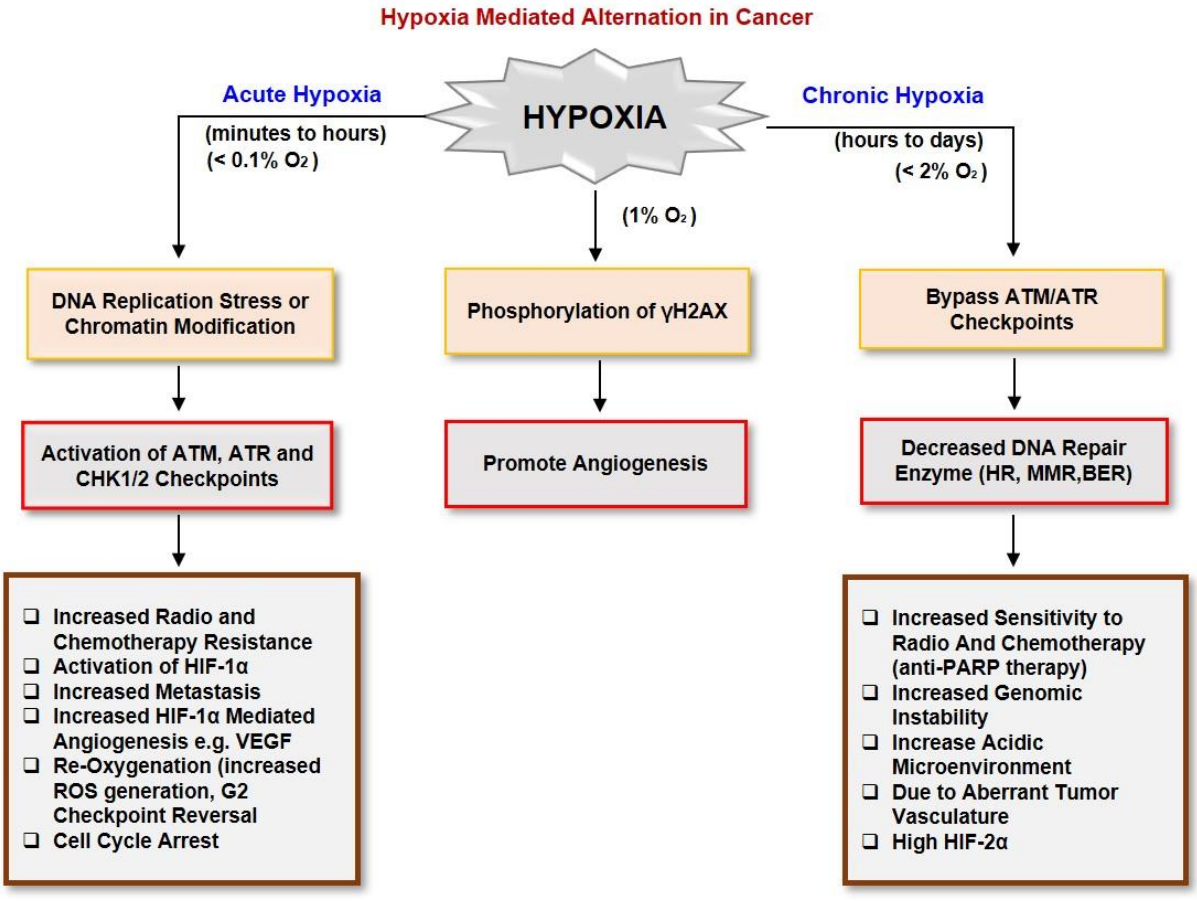

Figure 2.6: *Schematic of The Hypoxia-Mediated Genetic Instability and Alteration in Cancer*: Cancer cell exposed to acute hypoxia causes DNA damage or compromised DNA replication (also known as replication stress. which activate ATM–ATR-mediated cell cycle checkpoints to arrest the cell to repair any DNA damage caused by ROS. Due to impaired DNA repair enzyme or non-repaired DNA breaks causes genomic instability, which results in tumorigenesis. Further acute hypoxia causes activation and stabilisation of HIF-1α, promote angiogenesis and which results into radio and chemotherapy resistance. Whereas chronic hypoxia also gains genetic instability through decreased DNA repair enzymes, leading to increased mutation. It also upregulates expression of HIF-2α.

2.4.3. NON-CELLULAR SECRETORY COMPONENT

Non-cellular components of TME include ECM, matrix remodeling enzymes, cytokines, chemokines, exosomes, growth factors, and inflammatory enzymes [16], [132]. Chemokine families (namely, the C-, CC-, CXC- and CX_3C-chemokine families) are another important component, and they are produced by tumor cells as well as other TME cells, including immune cells and stromal cells. They directly and indirectly influence cancer progression, tumor immunity, and therapy outcomes [136]. Similarly, cytokines and exosomes influence TME [137]. Different cells present in TME, such as myeloid cells and fibroblasts and infiltrating cells, produce cytokines and growth factors such as TNF, EGF, IL-6, Wnt ligands. These growth factors may lead to chemoresistance as they are responsible for therapy efficiency used for treatment [216]. Recently, a growing number of publications show CAFs secrete IL-6 cytokines, a key player in molecular abnormality, chemoresistance, EMT and stem cell formation in various types of malignant cancer [129]. Many cytokines such as TGF-β, IFNs, TNF-α, ILs act in paracrine and autocrine fashion secreted by tumor cells in TME plays a critical role in regulating tumor angiogenesis [52]. Elevated levels of important cytokines are also considered, anti-apoptotic like IL-6 and IL-4 activate PI3K pathways, which results in increased phosphorylation of AKT, an important protein expressed in prostate cancer [66]–[68]. In breast cancer models, CAFs express MMPs that assist cancer cell growth, migration, adhesion and resistance to apoptosis by activating PI3K-Akt/PKB pathway and thus regulate ECM composition [217]. TAM produces various cytokines such as IL-10 and TGF-β in TME, which are involved in immunosuppression, weaken the activity of effector T cells, and inhibit DCs maturation [107]. Immune cells within the complex TME that indirectly induce the production of various proteolytic enzymes, cytokines, chemokines and pro-angiogenic mediators [96]. Alternatively, inflammatory cells also secrete cytokines (TNF-α) to induce O_2−accumulation in neighboring epithelial cells [166]. Tumor modulates the inflammatory

environment by producing inflammatory cytokines, such as TNF-α, TGF-β, IL-6, and IL-10. Pro-inflammatory cytokines favor the EMT process, and angiogenesis, VEGF, and IL-8 facilitate the latter [218]. Further, anti-inflammatory cytokines, such as IL-10 and TGF-β, involves in evading the immune response. Further, the multifunctional cytokine TGF-β is essential for immune responses, tissue wound healing, adult tissue homeostasis, and development. TGF-β signaling dysfunction has been linked to initiating and developing numerous tumor forms, including GBM, and maybe a therapeutic target [219]. Various cytokines, such as TNF and IL-1β, can alter the expression of transcription factors Twist and Slug involved in EMT [220], [221]. A study by Labelle and his colleague showed direct interaction of cancer cells with platelets, resulting in EMT and synergistically activating the TGF-β/Smad and NF-κB pathways in cancer cells, promoting invasion metastasis[222]. Dying cells release DAMPs such as ATP, calreticulin, and HMGB1, which stimulate immune-stimulatory cytokines and enhance the release of tumor neo-antigens which activate de novo anti-tumor T cell responses or may be responsible for immunosuppression [216]. Hypoxia condition leads to HMGB1 release encourages neutrophil recruitment, activation of DCs, and the release of pro-inflammatory cytokines, such as TNF-α and IL-6, from macrophages [223]. Extracellular secreted HMGB1 from cells encourage various cellular functions, including proliferation, inflammation, and angiogenesis, along with hampering host anti-cancer immunity, which together contributes to tumorigenesis [224]. Abundant published evidence suggests that pro-inflammatory cytokines such as TNF-α and IL-6 induce iNOS expression, leading to the formation of mutagenic DNA lesions and carcinogenesis under the inflammatory microenvironment [225]. TAMs secrete a variety of chemotactic components such as CCL2, CCL5, CCL7, CXCL8 and CXCL12 and aid in maintaining immunosuppressive phenotype by inducing TAM to switch from a M1- to M2-polarized state. NK cells are more effective at reducing the tumor burden when they are exposed to inflammatory cytokines like TNF-α, IFN-

α, IL-12, and other ILs [99], [100]. Yang et al., 2010 shown mast cells magnify inflammation along with immune suppression using the SCF/c-kit signaling pathway. Furthermore, mast cells support the suppressive function of MDSC by deploying them to the tumor site through the IL-17 pathway and stimulates IL-17 (a critical inflammatory cytokine) expression in MDSCs. Additionally, mast cells induce Treg infiltration and boost their suppressor function and parallelly induce IL-9 production by Treg; in turn, IL-9 promotes mast cells' pro-tumor effect in TME [226]. Besides immune cells, CAFs are also recognized to mediate cancer inflammation by releasing/producing cytokines and chemokines such as s IL-6, GM-CSF and MIP-3α, which aid in infiltration of inflammatory cells like macrophages monocytes and neutrophils to the tumor. A study by Jaiswal et al., 2020 reported that inflammatory cytokines (IL-1β, IFN-γ, and TNF-α) induce DNA damages and compromise DNA repair activity via a nitric oxide (NO)-dependent mechanism [227]. Moreover, pro-inflammatory cytokines energizing intracellular RONS production [228]. One of the important biological functions is to attune the activities of cytokines and chemokines [229], [230]. Nowadays, ECM is emerging as a critical player in malignant initiation, progression and chemoresistance. The ECM is constantly being modified and remodeled. This process, which involves both quantitative and qualitative alterations in the ECM, is mediated by certain enzymes that are in charge of ECM breakdown, such as metalloproteinases (MMPs). MMPs play a role in essentially every crucial phase during the formation of tumors, including immune surveillance escape, metastasis, angiogenesis, tumor cell invasion and migration, and apoptosis [135]. Furthermore, radiotherapy triggers multiple inflammatory cytokines (TNF-α, IL-1) followed by recruitment of various immune cells such as vascular cell adhesion molecule-1 (VCAM-1), ICAM1 and E-selectin. ROS production coordinated with NF-κB alters the TNF signaling leading to cellular stress, ultimately leading to death post-radiotherapy [231] **(Figure 2.7)**.

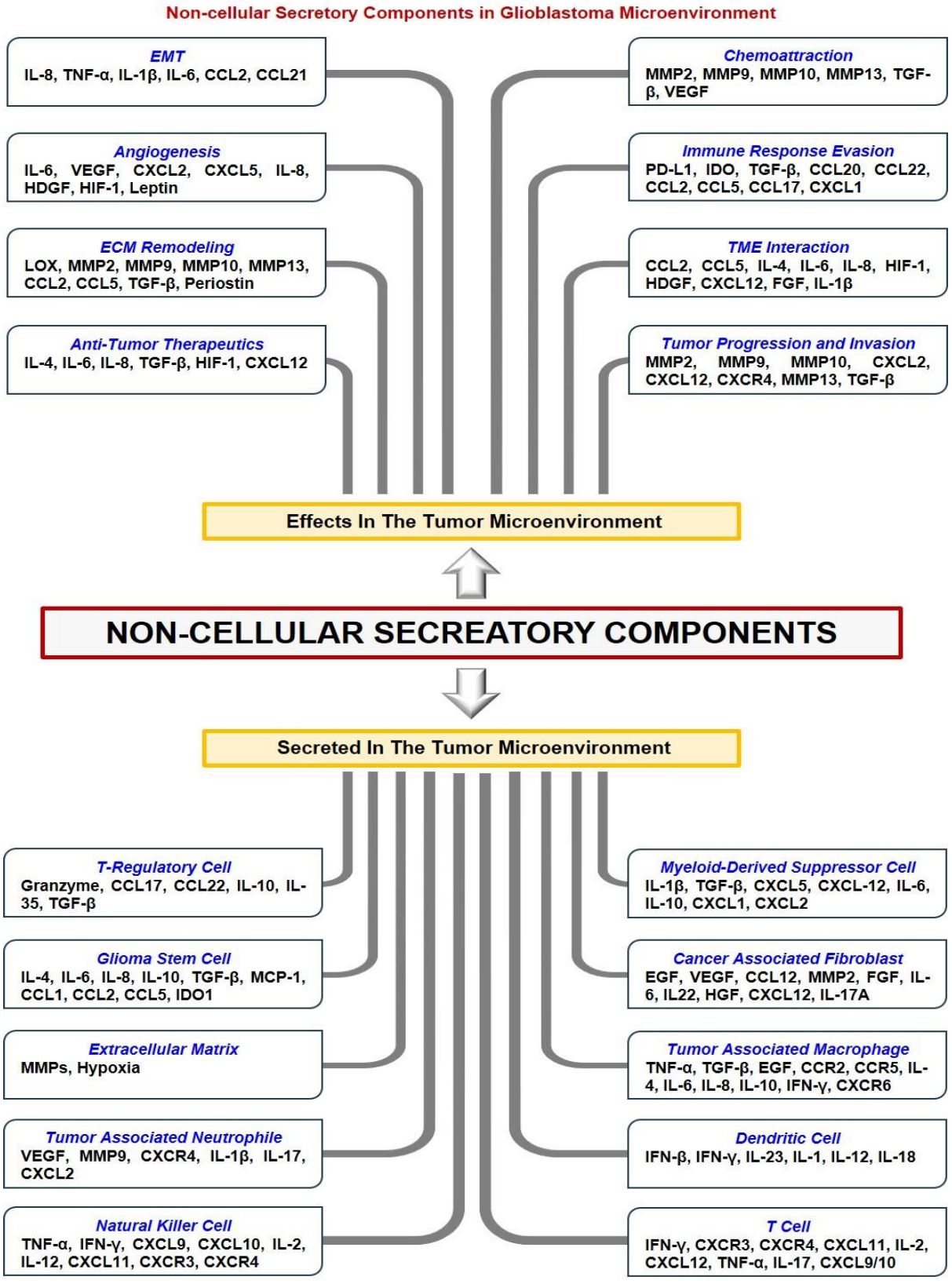

Figure 2.7*: Non-Cellular Secretory Components in Glioblastoma Microenvironment*: Non-cellular secretory components, including chemokines, cytokines, matrix modulating enzymes and growth factors secreted in microenvironment through various cells present in microenvironment such as immune cells, CAFs, Glioma stem cells, ECM matrix. These components participate in various important events such as EMT, angiogenesis, immune response, ECM remodelling, and regulates GBM proliferation and invasion.

Furthermore, the cellular (DNA damage response) DDR machinery also induces the release of pro-inflammatory cytokines within the TME. A study has shown that DNA damage causes the release of pro-inflammatory cytokines TNF-α and IL-6 [232]. Studies in DDR-deficient breast cancer cells have also shown enhanced production of chemokines CXCL10 and CCL5, creating a pro-inflammatory environment in cells [233]. STING pathway activation increases the transcriptional activity of type-I IFN and other cytokines after DNA damage [234].

2.5. POST-TRANSLATIONAL MODIFICATION AND GBM

PTMs are in actuality covalent alterations that take place after a transcript has been translated into a protein and that alter the structural makeup of already-existing proteins to enable participation in a variety of biological processes [235]. They play a critical part in the genesis and progression of tumors, malignant transformation, chromatin architecture, and transcription regulation [236] **(Figure 2.8)**. Various developing PTM types, functions, enzyme controllers, technologies for the study, and possible therapeutic targets. PTM enzymes are classified into three categories according to the functional specificity they perform; the "writers" are in charge of adding substrates, the "readers" identify changed proteins to start a signaling cascade downstream, and the "erasers" are best recognized for their removal of PTMs. Modifications of one or more kinds may occur at one location in the same protein. Similarly, to this, a modulator can play multiple roles. Based on their ability to activate or inhibit downstream signals, these PTMs may interact positively or negatively [237]. Indeed, the functional range of proteins has been substantially widened by the variety of PTMs, which is especially crucial for the immune detection of tumor therapy. Even though more than 300 PTMs have been discovered as a result of technological advancement, very few of them have functional study findings at the proteome level [238]. However, significant alterations in the respiratory chain and tricarboxylic acid cycle, the biogenesis of mitochondria and dynamics, oxidative stress regulation, and molecular signaling have occurred during the development, growth, and

survival of tumor cells.

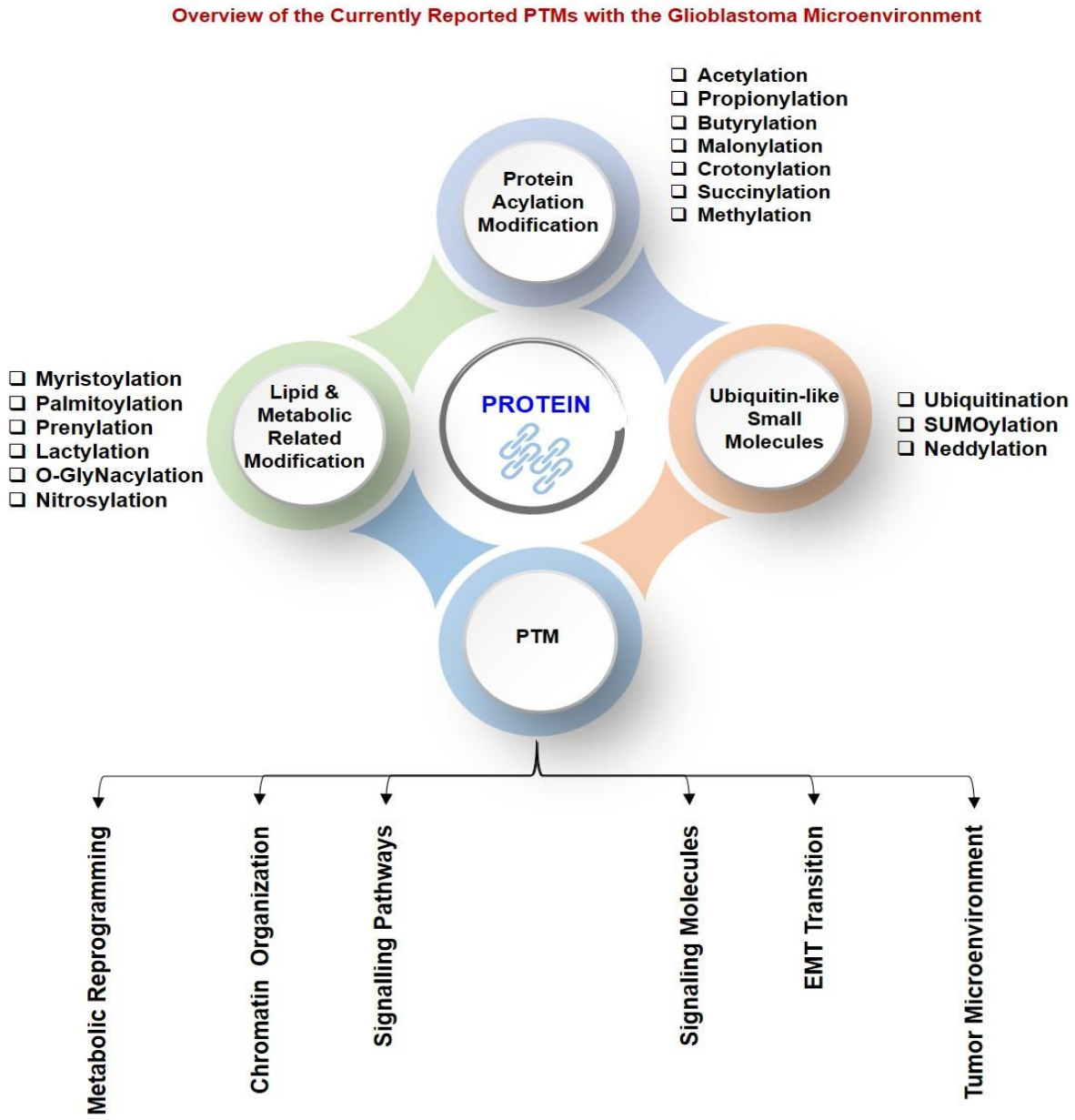

Figure 2.8: *Overview of the Currently Reported PTMs with the Glioblastoma Microenvironment*: It is classified into four main categories: protein acylation modification, lipid-related protein modification, metabolite-related protein modification, and ubiquitin-like small-molecule protein modification. Additionally, the biological impact associated with these PTMs on tumor cells in the glioblastoma microenvironment.

The PTMs of mitochondrial metabolic enzymes as well as signal molecules play an essential part in the reprogramming of mitochondrial metabolism [239]. On the other hand, the PTM of histone also controls chromatin organization and is essential for both dynamic and persistent modulation of the genome [240]. The newly reported PTMs can be classified into various groups, depending on the types of modified functional groups: protein acylation modification,

lipid-related protein modification, metabolite-related protein modification, and ubiquitin-like small-molecule protein modification. These are essential for chromatin organization, gene transcription, and other cellular processes [241].

2.5.1. LYSINE-INDUCED POST-TRANSLATIONAL MODICATIONS

Lysine (Lys, K) residues in proteins undergo a wide range of reversible PTMs, which can regulate enzyme activities, chromatin structure, PPIs, protein stability, and cellular localization. recently, a wide range of protein Lys acylations including propionylation (KPr), butylation (KBu), crotonylation (KCro), malonylation (KMal), succinylation (KSucc), glutarylation (KGlu), β-hydroxybutylation (KBhb), 2-hydroxyisobutyryation (KHib), lactylation (KLac), and benzoylation (KBz) have been reported although the functions of these PTMs are minimally characterized. In addition, acetylation (Kac), ubiquitination (KUb), ubiquitin-like PTMs such as SUMOylation (KSumo), NEDDylation (KNedd).

2.5.2. ACETLATION AND HDAC'S ENZYMES

The precursors of numerous biological macromolecules and significant metabolic stages in cells are acyl CoA compounds. The involvement of protein acylation modification has been gradually investigated as technology and research and development and level have advanced Several studies are concentrating on therapeutic techniques that target protein acetylation as a possible therapeutic strategy [242] **(Figure 2.9)**. Protein including histone and non-histone protein (E2F, p53, c-Myc, NF-Kb, STAT3, TFIIE, Rb, HIF1A, estrogen, and androgen receptor) acetylation is a reversible PTM refers to the transfer of the acetyl group from acetyl coenzyme to N-terminal (N-acetylation), the hydroxyl group at the serine or threonine terminal (O-acetylation) and lysine (K-acetylation) [242].

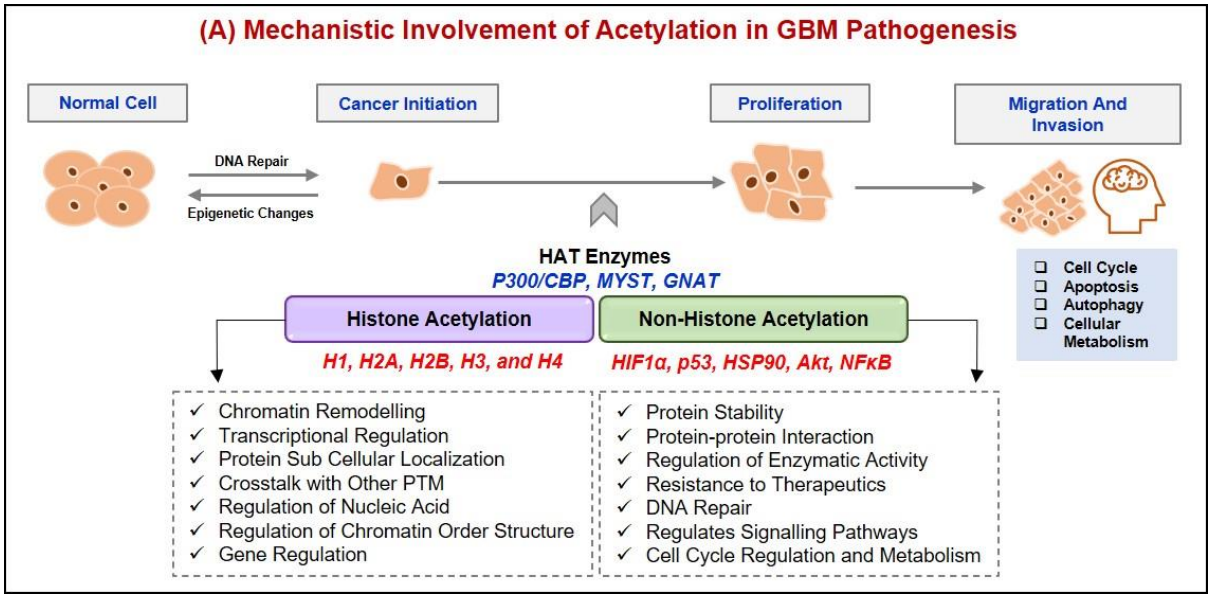

Figure 2.9: *The Role of Acetylation Modification in Glioblastoma Multiforme*: An acetyl group is added to lysine residues on histone proteins during acetylation, a reversible post-translational modification. Depending on the particular setting, acetylation alteration has been shown to have consequences in GBM that are either tumor-suppressive or tumor-promoting. The enzyme known as histone deacetylase (HDAC), which eliminates the acetyl groups from histones in order to result in gene silence and chromatin condensation, is one of the important players in acetylation control. The pathogenesis of GBM can also be influenced by the acetylation of non-histone proteins like transcription factors, co-regulators, and DNA repair proteins. For instance, GBM frequently exhibits dysregulation in the acetylation level of the tumor suppressor protein p53, a crucial regulator of cell cycle arrest and apoptosis. A complex part of GBM is played by acetylation modification. The abnormal regulation of histone and non-histone protein acetylation may influence the expression of genes, cell signaling networks, and mechanisms for DNA repair, eventually impacting the aggressive behavior and treatment response of GBM.

Protein acetylation is proactively controlled by HATs and HDACs in homeostasis and is associated with several critical biological and cellular functions including transcription, migration, invasion, adhesion, DNA damage repair, and energy metabolism **(Figure 2.10)**. This constitutes a significant molecular activity and is linked to a variety of diseases, including malignancies like GBM [243]. **Figure 2.11(A1) and Figure 2.11(A2)** showed expression of HDAC and HAT family in GBM respectively (Analysis was performed UCSC Xena webtool (total patient sample size, n=671) (http://xena.ucsc.edu/) [244]. **Table 2.2** summarizes acetylation involved in GBM. Histones' amino-terminal lysine residues receive acetyl groups from HATs (GNAT, MYST, and p300/CBP), creating an easy and accessible chromatin structure. HDACs eliminate these groups in the reverse direction, which causes chromatin to condense and transcription to be inhibited [245].

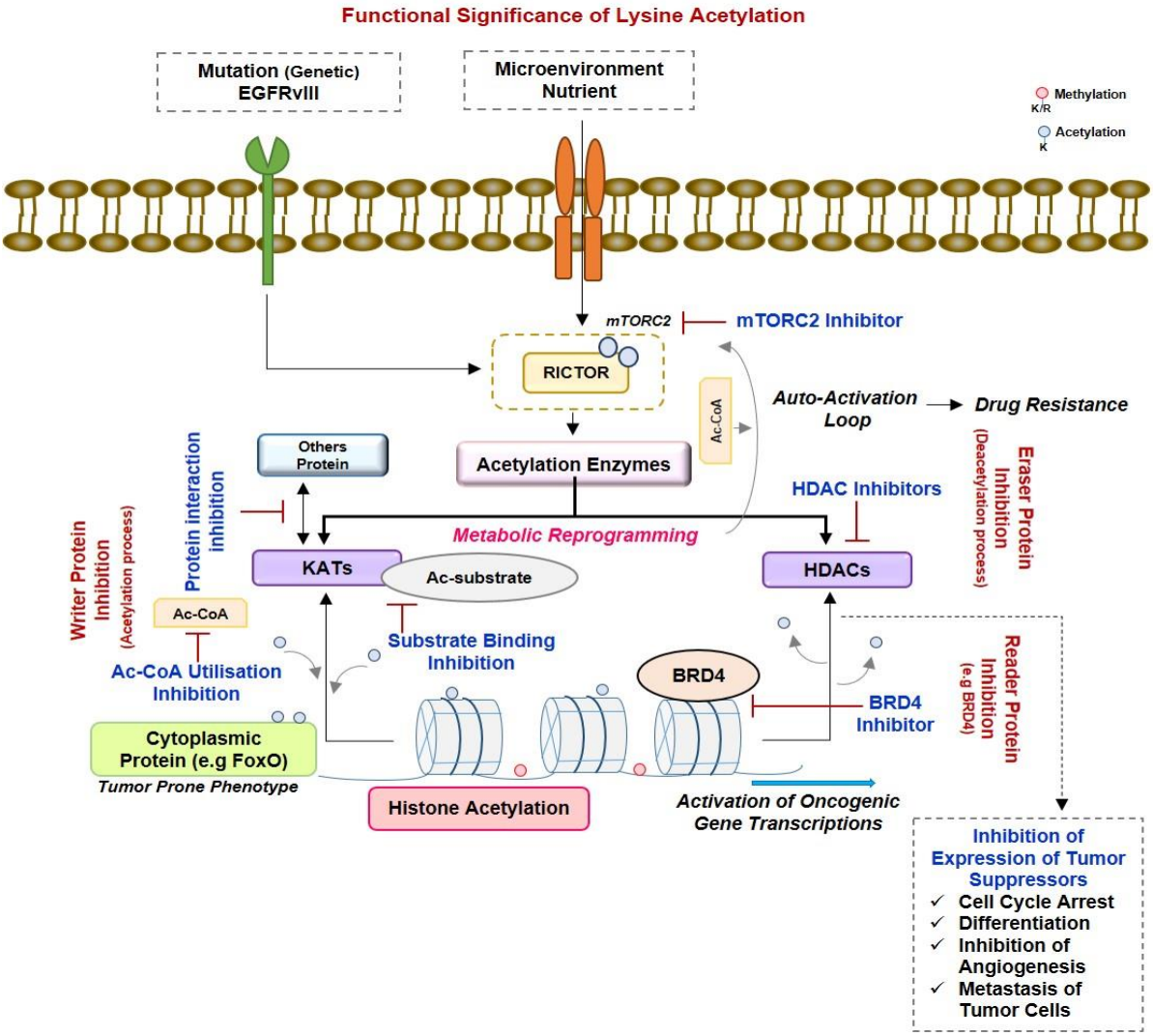

Figure 2.10: ***Potential Therapeutic Strategies to Target Protein Acetylation Systems:*** **mTORC2 as a strong acetylation driver in cancer. Genetic mutation including extrachromosomal DNA (ecDNA)-dependent EGFRvIII (epidermal growth factor receptor variant III) overexpression and nutrient in the microenvironment promote mTORC2 activity which facilitates protein acetylation including cytoplasmic protein (FoxO and Rictor) and nuclear histone protein. Inhibition of eraser protein or HDAC can eventually reactivate the expression of tumor suppressors, resulting in cell cycle arrest, apoptosis, differentiation, and inhibition of angiogenesis and metastasis in cancer cells. The use of HDAC inhibitors, in particular, to target acetylation processes, demonstrates promising as treatment strategy for this deadly brain tumor. mTORC2 is an integrator of protein acetylation systems, and targeted therapies against mTORC2 could be the next-generation therapeutic strategies to interfere with cancer-specific, acetylation-dependent metabolism and epigenetics.**

Here, in this section, we will focus on K-acetylation. For instance, a study by Hervas-corpion et al., 2023 demonstrated that K-acetylation was a crucially malfunctioning histone modification in GBM as contrasted with Lower-Grade Gliomas. In addition, transcriptomics sequencing analysis showed the cohort's K9 and K14, which had the least and maximum levels of acetylated H3, respectively, and were connected with the overall survival of patients [246]. A study by Feng et al. 2021 demonstrated that hypoxia causes PAK1 to become acetylated at

K420, which inhibits PAK1 dimerization and increases its activity, resulting in PAK1-mediated phosphorylation of ATG5 (autophagy-related 5) at the T101 residue and playing a crucial role in hypoxia-induced autophagy and promoting the incidence and growth of tumors [247]. In the same year, Tu et al.,2021 carried out a multi-omics analysis of K-acetylation regulators (LAR) in gliomas, and they found that LAR malfunction may help to partly describe the hypermutation condition of gliomas, which is associated with a poor prognosis. They learned that SIRT2 and EP300 were two tumor suppressors deleted in 19q deletion and 22q deletion incidents, respectively, and that HDAC1 oncogenes were removed in the 1p deletion event [248]. Another group found that in glioma-associated seizer, K-acetylation of disrupted ACAT2 and ACAA2 are implicated in metabolic processes such as the TCA cycle, oxidative phosphorylation, biosynthesis of amino acids, and fatty acid metabolism [249]. A plethora of studies shows the critical need of ensuring equilibrium between HAT and HDAC. Several studies have found a strong correlation between abnormal HDAC recruitment and treatment resistance in GBM malignancies [236]. For instance, by stimulating the transcription coactivator with PDZ-binding motif (TAZ), an oncogene and crucial downstream effector of the Hippo pathway, HDAC9 can enhance GBM proliferation and tumor development [250]. HDAC inhibitors (HDACi) have recently been recognized as innovative drugs to maintain this equilibrium, sparking a plethora of studies on it to develop more potent approaches to treating GBM and potentially reverse TMZ resistance. Using HDACi-based radiopharmaceuticals, such as [18F]FAHA and [18F]TFAHA, to identify patients who are likely to benefit with HDACi-targeted therapy [251]. The FDA has already authorised a number of HDACi, including Vorinostat, Belinostat, Romidepsin, Belinostat, Valproic acid, and Panobinostat [252]. HDACi have been intensively researched in GBM clinical trials due to the role that HDACs play in GBM. **Figure 2.11(B)** showed mechanistic involvement of HDACi in GBM.

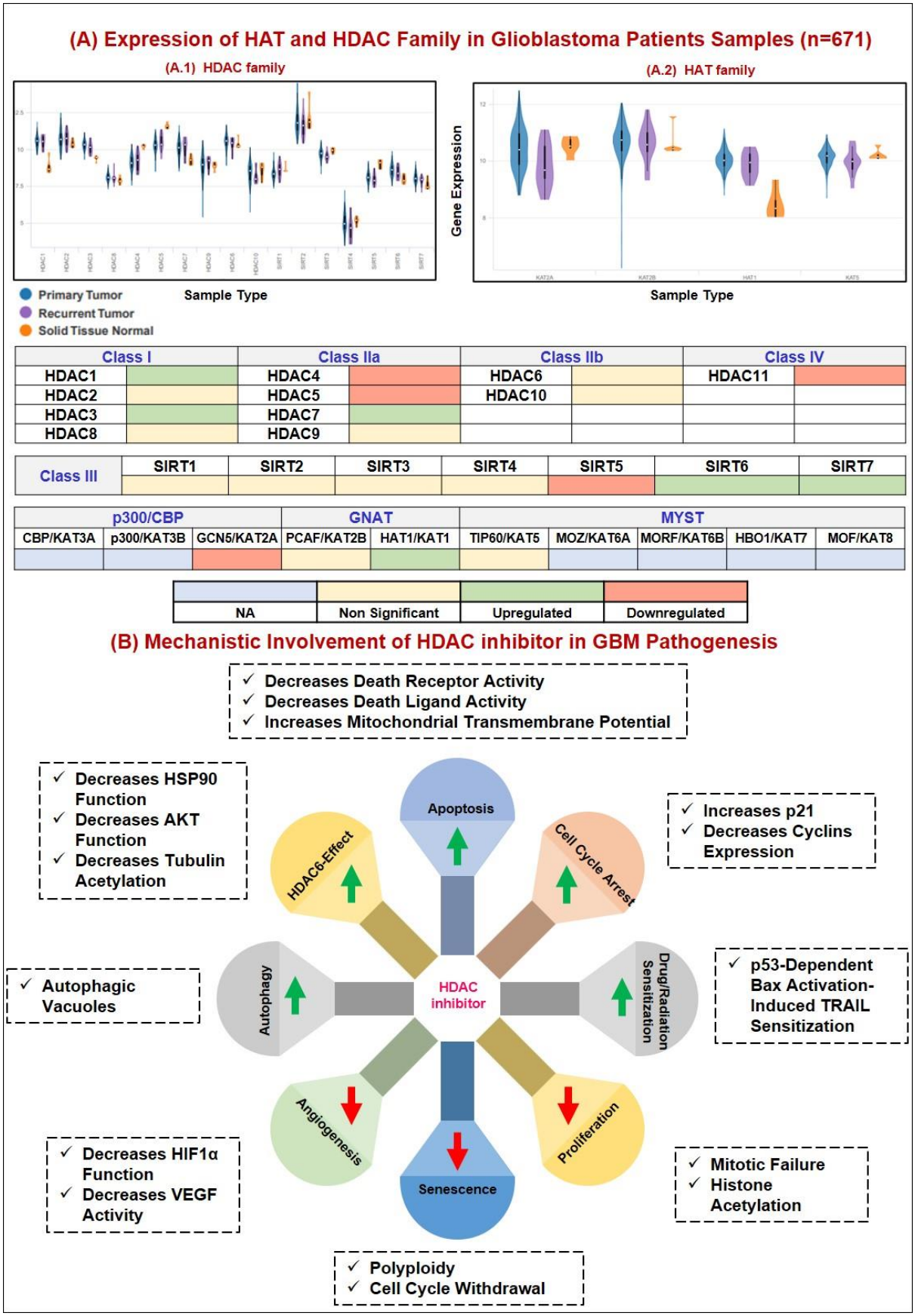

Figure 2.11: (A) Expression of HAT And HDAC Family in Glioblastoma Patient's Tumor Samples Procured from TCGA Glioblastoma Patient Genomics Dataset. Analysis was performed UCSC Xena webtool (total patient sample size, n=671) (http://xena.ucsc.edu/). (A.1) Violin plot showing expression of HDAC family in

GBM primary tumor and GBM recurrent tumor in comparison to solid normal tissue. (A.2) Violin plot showing expression of HAT family in GBM primary tumor and GBM recurrent tumor in comparison to solid normal tissue. Table showing Green: Upregulation, Red: Downregulation, Yellow: Non-significant, Grey: Not available. (B) Schematic Representation of Therapeutic Role of HDAC Inhibitor and Its Impact on Regulation of Anti-GBM Signaling Pathways. Green arrow: Upregulation; Red arrow: Downregulation.

The current data indicate that HDACi like Vorinostat, even when used in combination with chemotherapy, have no effect on OS. However, HDACi have unfavourable side effect profiles that continue to be a major barrier, in addition to concerns with efficacy.

Table 2.2: Acetylation as A Potential Lysine-Induced Post-Translational Modifications Involved in Glioblastoma Multiforme Progression and Pathogenesis

Experimental Model	HAT/HDAC Enzyme	Residues	Targets	Results	Signaling Involved	Reference
C6 glioma cells and U87MG cells	HDAC1, HDAC3	K9, K14	H3K9, H3K14	Combination of cAMP activator plus HDACi significantly repressed the tumor growth in a subcutaneous GSC-derived tumor model through increasing the histone acetylation status	cAMP signaling pathway	[253]
LN229, U87, and 293T cell lines	HAT1	K512 and K596	HIF2A	HAT1-dependent acetylation of HIF2A is vital to executing the hypoxia-induced cell survival and cancer stem cell growth, therefore proposing the HAT1-HIF2A axis as a potential therapeutic target	Hypoxia signaling cascade	[254]
U-87 MG, and T98G cells	HDAC4, HDAC5	___	SCNN1A	HDAC4/5 selective inhibitor LMK235 significantly reduced the viability and colony formation	Autophagy pathway	[255]
U87 and U251 cells	___	K601, K615, K631 and K685	STAT3	SHF selectively binds and inhibits acetylated STAT3 dimerization without affecting STAT3 phosphorylation or acetylation	STAT3 pathway	[256]
Primary GBM cells	CBP/p300	K27	H3K27Ac	Chromatin remodeling RBBP4/p300 complex in GBM cells and demonstrates that this complex regulates key survival genes	TWEAK pathway and cell death cascade	[257]
GBM Patients	HDAC1	K27	H3 and SLC30A3	Overexpression of HDAC1 resulted in a significant increase in DNA replication activity, a significant decline in apoptosis and cell cycle arrest in GBM cells	MAPK signaling pathway	[258]
The human GSCs lines TS543 and TS576	HDAC3	___	GLI1	The HDAC3i/BRD4i combination caused stronger tumor growth suppression than either drug alone	GLI1/IL6/STAT3 signaling axis	[259]
GBM patients	ELP3	K420	PAK1	Acetylation modification and kinase activity of PAK1 plays an instrumental role in hypoxia-induced autophagy initiation and maintaining GBM growth	Autophagy and hypoxia pathway	[247]
Human GBM cell lines U87MG and A172	HDAC6	___	Sp1	HDAC6 inhibitor with partial efficacy against HDAC1/2, induced G2/M arrest and senescence in both temozolomide-resistant cells and stemlike tumorspheres	HDAC/Sp1 axis	[260]
U87 and U251 human GBM cell lines	HDAC1, HDAC2	H2AZK4, H2AZK7, H3K27	USP11	EGFR-vIII mutation downregulates H2AZK4/7AC and H3K27AC, inhibiting USP11 expression though the PI3K/AKT-HDAC1/2 axis	PI3K/AKT-HDAC2 axis	[261]
LN229, U87, and A172 GBM cells	MYST1/KAT8	H4K16	CDK1, Cyclin A, Cyclin B1	MYST1 as a tumor promoter in GBM and an EGFR activator, and may be a potential drug target for GBM treatment	EGFR signaling	[262]
LN229, SF539, SF767, and U87MG cells	Sirtuin1	STAT3(K685), NF-κB(K310)	STAT3 and NF-κB	The acetylation and phosphorylation of p65 NF-κB and STAT3 in glioma cells were differentially affected by SRT2183	ER stress pathway	[263]

2.5.3. UBIQUITINATION AND E3 LIGASES

Along with the well-known PTMs for proteins like phosphorylation, methylation, ubiquitination, and SUMOylation, other common but understudied PTMs have received considerable attention in recent years. **Table 2.3** summarizes major lysine-induced PTMs involved in GBM progression and pathogenesis. A family of >700 proteins known as E3 ubiquitin ligases attach ubiquitin to target proteins, which triggers a variety of cellular reactions such as protein degradation, DNA repair, and pro-survival signaling. E3 ubiquitin ligases, which are crucial regulators in numerous areas of brain cancer development, control the selectivity in substrate labeling and chain elongation [264]. According to a recent study by Zhou et al., 2023 showed abnormal E3 ligase MAEA boosts stemness, decreased patient survival, growth, metastasis, and TMZ resistance by attacking prolyl hydroxylase domain 3 (PHD3) K159 to encourage their K48-linked polyubiquitination and depletion, hence improving the stability of HIF1A [265]. Another investigation revealed that the RNA-binding ubiquitin ligase MEX3A was significantly overexpressed in GBM samples. This enzyme binds to the tumor suppressor RIG-I and causes its ubiquitylation and proteasome-dependent degradation, which is important for differentiation, apoptosis, and innate immune response [266]. The findings of a study by Rimkush et al., 2022 demonstrated polyubiquitination caused by the E3 ubiquitin ligase NEDD4 is a unique procedure for tumor suppressor candidate 2 (TUSC2) clearance in GBM, and TUSC2 depletion accelerates GBM progression in particular by upregulating Bcl-xL [267]. In addition, the study by Vriend et al., 2022, found a significant deregulation of genes expression encoding E2s (Ube2C and Ube2S), E3 ligases (AURKA and TPX2) and their adaptors (CDC20), proteasome subunits, immunoproteasome subunits (PSMB8 and PSMB9) and DUBs (USP11, USP22, USP7, USP33, TNFAIP3) in GBM.

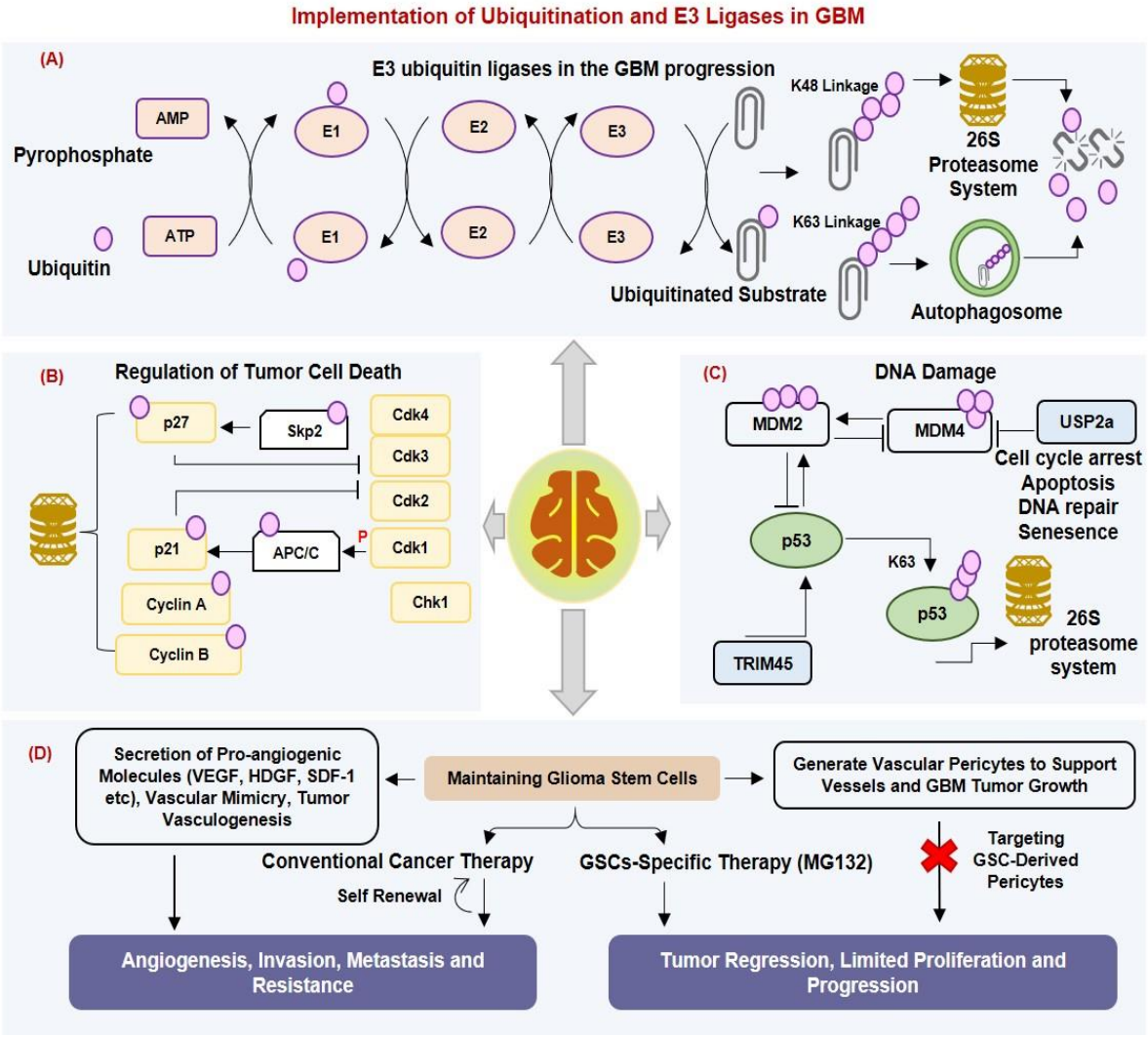

Figure 2.12: ***The Significance of E3 Ubiquitin Ligases in The Glioblastoma's Growth and Development*****: (A) A cascade of the ubiquitin ligases E1, E2, and E3 is used to bind ubiquitin to proteins. A protein's destiny after ubiquitin conjugation is determined by the precise lysine residues through which E3s attach ubiquitin. A family of four different E3 ligases namely RING, HECT, RBR, RCR performs the act of ligation. Ubiquitination pathways regulates various biological pathways such as (B) tumor cell death involving cyclin and CDKs, (C) p53 Regulation by the UPS in GBM and, (D) GSCs regulation secreted pro-angiogenesis molecules in microenvironment which results in angiogenesis, invasion, drug resistance and generate vascular pericytes. However, targeting GSCs-derived pericytes with aid in tumor regression, inhibit proliferation and progression.**

In GBM, the crucial dysregulated signaling pathways include Notch and Hippo pathways [268]. Ubiquitination and deubiquitination (DUB) play a role in the regulation of radioresistance and TMZ resistance in GBM. In GBM cells, the DUB and oncogene ubiquitin-specific protease 7 (USP7) is significantly expressed, and its suppression results in apoptosis. By specifically inhibiting USP7 with the novel inhibitor P5091, ARF4 (an anti-apoptotic factor) is made more ubiquitinated, which eventually causes GBM cells to die [269]. An

inventive tactic known as PROteolysis-TArgeting Chimera (PROTAC) makes use of the cell's own Ubiquitin-proteasome system (UPS). A ligand that attracts its target protein of interest (POI), a ligand particular to an E3 ubiquitin ligase enzyme, and a linker that joins these components make up each PROTAC molecule. When the PROTAC binds to the POI, the E3 is induced, leading to the POI's ubiquitylation-dependent proteasome destruction [270]. The PROTAC technology has so far been used in various human cancer clinical trials. In 2019, Zhao and Burgess examined the effectiveness of PROTACs based on the specific CDK4/6 inhibitors Palbociclib (Ibrance®,) and Ribociclib (Kisqali®) in GBM and breast cancer cell lines [271]. However according to Liu et al. in 2019, a recent study that took use of the capacity of the high-selective HDAC6 inhibitor J22352 to limit the growth of GBM tumors offered the first in vivo proof of the possibility of PROTACs as chemotherapeutic agents for GBM. As an outcome, the reduction in HDAC6 expression level greatly suppresses the formation of GBM tumors in U87MG cells, both in vitro and in vivo, by promoting autophagic cancer cell death and inducing immunosuppressive response [272] **(Figure 2.12)**.

Table 2.3: List of Major Lysine-Induced Post-Translational Modifications Involved in Glioblastoma Multiforme Progression and Pathogenesis

Modification	Experimental Model	Enzyme	Targets	Mechanism	Signaling Involved	Reference
Ubiquitination	U87 and T98G cells	USP4	___	USP4, as a potential novel oncogene, promotes GBM by activation of ERK pathway through regulating TGF-β	ERK pathway	[273]
	U251 and LN229 cells	UBA1	PERK, eIF2α, and IRE1α	UBA1 inhibition disrupts global protein ubiquitination in GBM cells, thereby inducing ER stress and UPR	PERK/ATF4 and IRE1α/XBP signaling axes	[274]
	A-172 and T98G GB cell lines	MEX3A	RIG-I	MEX3A binds RIG-I and induces its ubiquitylation and proteasome-dependent degradation	Cell Proliferation	[266]
	In vitro and *in vivo*	CBX3	PARK2 and STUB1	CSD domain of CBX3 interacted with PARK2 and regulated its ubiquitination to further reduce its protein level	EGFR Pathway	[275]
	In vivo	ANXA1	NEMO	SBSN activated NF-κB signaling by interacting with annexin A1, which further induced Lys63-linked and Met1-linear polyubiquitination of NF-κB essential modulator (NEMO)	NF-κB Signaling	[276]
	U251 cells	CUEDC2	TRIM21, GDNF	Abundant CREB involved in the binding to the GDNF promoter region contributes to GDNF high expression in	CREB signaling	[277]

				glioma cells		
	Hs683, T98G, DBTRG05MG, and U87MG GBM cell lines	USP6NL	EGFR	Controlling the USP6NL may offer an alternative, but efficient, therapeutic strategy for targeting and eradicating otherwise resistant and recurrent phenotypes of aggressive GBM cells	DNA repair pathway	[278]
	U251, A172, U87, and T98G	HECTD3	IRAK1, FOXA2, PRDX1	Overexpression of PRDX1 reverses the radiotherapy sensitization effect of IRAK1 depletion by diminishing autophagic cell death	IRAK1-PRDX1 axis	[279]
	T98G, U87 and U251 cells	UBE2D3	SHP-2, STAT3	UBE2D3 could promote the ubiquitination of SHP-2, which activated STAT3 pathway and promoted glioma proliferation as well as glycolysis	STAT3 signaling pathway	[280]
	Tumor tissues and patient-derived tumor cell lines	FBXO16	β-Trcp1, TCF4/LEF1	FBXO16 targets the nuclear β-catenin for degradation and inhibits TCF4/LEF1 dependent Wnt signaling pathway	Wnt signaling	[281]

2.6. ONCOGENIC SIGNALING TARGETS AND TUMOR MICROENVIRONMENT BIOMARKERS

2.6.1. ONCOGENIC SIGNALING EVENTS

The Wnt signaling pathway is associated with different stages of GBM due to its being involved in glioma genesis, TMZ and radioresistance (feedback by DNA repair genes), maintenance of GSCs (due to PLAGL2, FoxM1, Evi/Gpr177, and ASCL1 regulators), migration and invasion (upregulation of ZEB1, SNAIL, TWIST, SLUG, MMPs, and N-cadherin). Studies using transcriptomics data showed that β-catenin, Dvl3, and cyclin D1 were significantly higher in glioma specimens compared to non-tumor brain tissue, while studies using proteomics data showed that β-catenin, TCF4, LEF1, c-MYC, n-MYC, and cyclin D1 were significantly higher in glioma samples [282], [283]. Wnt's context-dependent activity and crucial part in maintaining the homeostasis of healthy tissues have led to the recognition of Wnt as a hallmark of therapeutic challenge [284]. Kouchi et al., 2017 have discovered (pro)renin receptor (PRR) plays a crucial part in the development of the GBM cell line (U251MG, U87MG, and T98G) by abnormal activation of the Wnt signaling pathway and has the ability to function as a therapeutic and prognostic marker [285]. Another small drug, SEN461, reduced the survival of cultured glioma cell lines and decreased the size of subcutaneously implanted xenograft tumors

by inhibiting the WNT/β-catenin pathway involving Axin stabilization and a process partially sensitive to tankyrase (TNKS) enzymes [286]. In phase, I/II research for patients with advanced cancer, including TNBC, NSCLC, Colorectal, and GBM (NCT02038699), the dopamine receptor D2 (DRD2) antagonist ONC201 significantly suppressed CSCs and repressed the expression of CSC-related genes in GBM tumors by inhibiting the Wnt signaling pathway [287].

Hedgehog (HH) signaling induced the transcription of a group of oncogenic proteins, such as Bmi1, Myc, and VEGFA, which aided proliferation, invasion, and angiogenesis. Many cancers, including GBM, are driven by tumorigenesis, which is caused by abnormal HH pathway activation [288]. SMO inhibition was beneficial in glioma lines that overexpressed Gli, suggesting that HH signaling is probably a driver in a subset GBMs. Wu et al., 2021 demonstrated that SMO-193a.a., a novel protein encoded by circular SMO, is essential for HH signaling, promotes the growth of GBM tumors, and represents a new target for the treatment of GBM [289]. LDE225 (25 µM), Shh inhibitors alone or in combo with Rapamycin (100 nM, mTOR inhibitor) exhibit additive impact in lowering cell viability of $CD133^{+}$ GSCs by encouraging the transition of LC3-I to LC3-II and stimulates autophagy through mTOR independent pathway which could potentially conquer chemoresistance in GBM [290]. In the C6 cell line, a different drug called Naringenin (114 g/ml, flavonoid) increased the expression of Sufu at the protein level while decreasing the transcription of Gli-1 and SMO [291]. Vismodegib (GDC-0449, SMO inhibitor), when combined it Robotnikinin (PTCH1 transmembrane antagonist), was more efficient in reducing proliferation, invasion, and migration in the U87MG cell line than when administered alone [292]. Similarly, Bureta et al., 2019 studied the synergistic effect of Vismodegib/ arsenic trioxide (HH pathway inhibitor) with TMZ to inhibit tumor growth in GBM pathogenesis [293]. For the first time, Linder et al., 2019 demonstrated that Arsenic Trioxide and (−)-Gossypol synergistically attack GSC-Like

cells by suppressing both HH and Notch Signaling [294]. An ongoing phase I/II clinical trial (NCT03466450) included 75 participants undergoing combination therapy, including Glasdegib (PF-04449913, SMO inhibitor). The HH route may also be a potential immunotherapy target for treating GBM. Nonetheless, it is still unclear how anti-PD-1 antibodies counteract GBM resistance by activating HH signaling. Despite the fact that the use of HH inhibitors in GBM hasn't been thoroughly studied, many studies have shown that using Hh inhibitors in addition to standard therapies can significantly boost efficacy and lower the occurrence of drug resistance [288].

Increasing data indicate that Notch signaling is extremely active in GSCs, where it delays differentiation and preserves stem-like characteristics, promoting the development of tumors and resistance to standard therapies. Notch was inhibited with the γ-secretase inhibitors DAPT, MRK-003, GSI-18, LLN1eCHO, L-685,458, Dibenzazepine, γ-secretase inhibitor X. α-secretase ADAM17 inhibitor including GW280264X, INCB3619, ADAM17 short hairpin RNA [295]. Alternative treatment options targeting the notch pathway were Arsenic Trioxide [296] (decreases expression of Notch 1-4), Niclosamide [297] (reduces NOTCH 1), Retinoic Acid (inhibition of neurosphere growth, decreased clonogenicity, and decreased CSCs markers), Resveratrol [298]. In GBM, miRNAs that Notch governs include miR-34a, miR-34a-5p, miR-34c-3p, miR-34c-5p, miRNA-181c (downregulated in GBM) and miR-148a, miR-31, miRNA-33a, miRNA-18a (upregulated in GBM) which impede their translation or cause their instability and degradation [299]. Further knowledge of this signaling system is required since failures in clinical trials with Notch inhibitors may be attributed to their contradictory effects on the tumor vs. the tumor vasculature [300]. Herrera-Rios et al., 2020 compared first-in-human tested Brontictuzumab antibody against Notch1 with MRK003. They found that Brontictuzumab treatment affects the Notch pathway by inhibiting transcription of Hes1/Hey1 genes and considerably decreasing cleaved Notch1 receptor protein quantity, hindering cellular

invasion in GSCs [301]. Clinical investigations focusing on Notch pathways in GBM are still being conducted. For instance, the Phase II clinical trials of RO4929097 for recurrent GBM demonstrate a 6-month PFS as well as a 50% reduction in the growth of neurospheres in fresh tissue [302]. For instance, Zhu et al., 2022 demonstrated that a biomimetic BBB-penetrating albumin nanosystem altered by a brain-targeting peptide was created for co-delivering a TGF-β receptor I inhibitor (LY2157299) and an mTOR inhibitor (Celastrol). The albumin nanosystem can suppress STAT3 signaling, which lowers TGF-1 production and triggers cell death, to target nAChRs that are overexpressed on both BBB and glioma cells and transform TAM to M1 phenotype [303] (**Figure 2.13)**

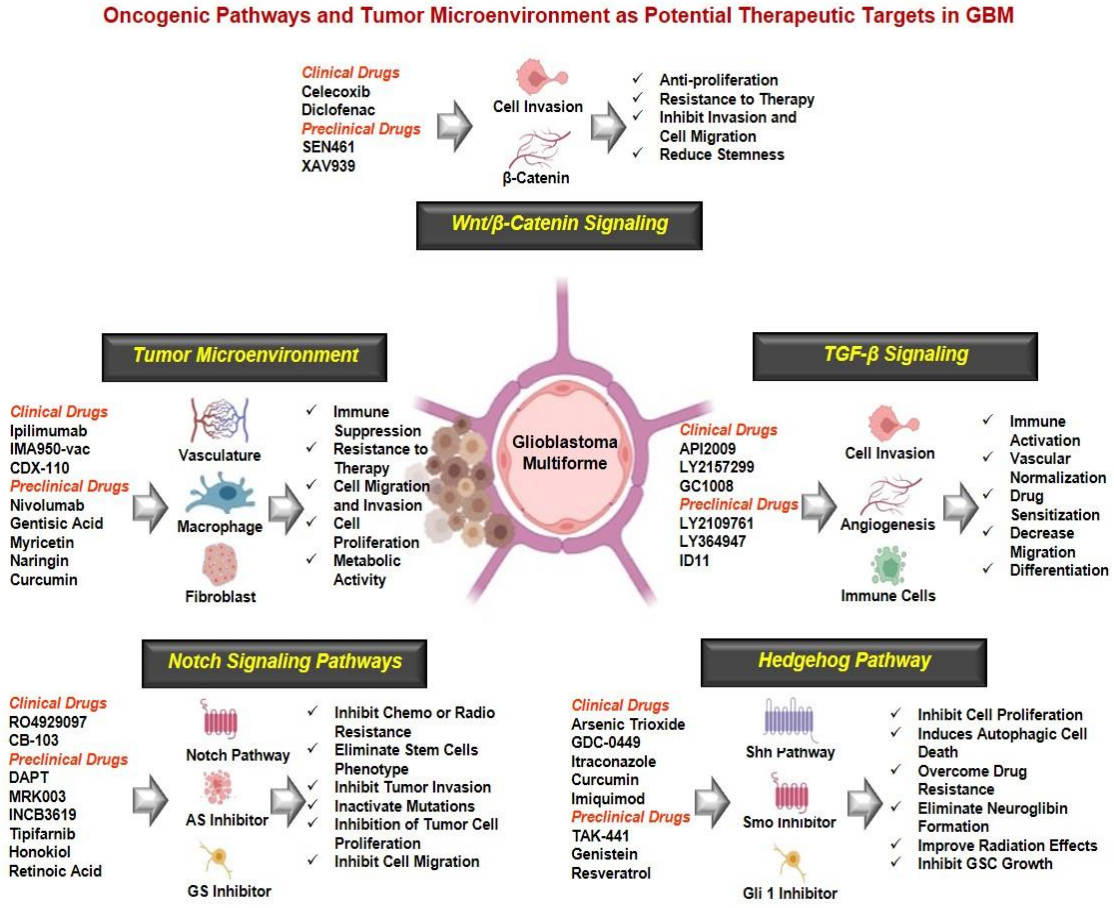

Figure 2.13: *Oncogenic Pathways and Tumor Microenvironment as Potential Therapeutic Targets in GBM:* studies have confirmed the involvement of several signaling pathways, namely Wnt/β-Catenin signaling, TGF-β signaling, Hedgehog pathway, and Notch signaling pathways in the pathogenesis and progression of GBM. Apart from signaling pathways, tumor microenvironment plays a critical role in GBM etiology through modulating cell migration, proliferation, and differentiation.

2.6.2. TUMOR MICROENVIRONMENT AS THERAPEUTICS MARKERS

The GBM microenvironment comprises immune cells, fibroblasts, endothelial cells, pericytes, GBM cells, GSCs, and ECM. The primary factor behind GBM's inadequate therapeutic impact is the TME [304]. Drug distribution via BBB crossing is one of the biggest challenges. In order to improve the effectiveness of drugs while minimizing their negative effects, cell-mediated drug delivery systems have been suggested as a potential technique in the cancer treatment process. Including the use of magnetic mesoporous silica NPs, liposomes, albumin NPs, and PLGA NPs, Hosseinalizadeh et al., 2022 employ neutrophils as Trojan horses for the delivery of drugs. Cytokines IL-8 activate neutrophils that show anticancer activity by developing neutrophil extracellular traps, allowing the concurrent release of NPs and delivery of chemotherapeutic drugs [305]. Besides, Li et al., 2021 constructed ZGO@TiO2@ALP-NEs, in which ZGO@TiO entraps paclitaxel and neutrophils to deliver anti-PD-1 antibodies. This can cross the BBB and move into tumor locations for enhanced and prolonged precision therapy, improving survival rates from 0% to 40% and providing long-term immuno-surveillance for tumor recurrence [306]. Another strategy is to use TAMs, which can be targeted in various ways, as possible therapeutic targets in the battle against GBM. By blocking the chemokine signaling that draws TAMs to the TME, one can interfere with the recruitment of TAMs to the tumor. A second approach is to boost anti-tumor immune responses by producing more TAMs with anti-tumor M1 characteristics. A third method minimizes the abundance of pro-tumor M2-like TAMs, which may enhance anti-tumor immune responses and ultimately slow tumor growth [307]. TAM expresses CSF1R, and BLZ-945, an inhibitor of this receptor, decreases M2 polarization, improving radiation effectiveness and reducing immune suppression in GBM [308]. Additional TAM-expressed markers like CD39, CD73, CD163, and CD204 may be exploited as therapeutic targets [307]. CAFs, the most prevalent cells in the tumor stroma, are a major cellular component of the TME and play a crucial role in

developing chemoresistance. CAFs also produce a significant tumor-promoting effect and physical barriers that prevent the delivery of nanomedicines by secreting pro-tumorigenic cytokines, increasing interstitial fluid pressure (IFP), and nonspecific internalization. Recent advancements in CAF-targeted nano-delivery methods increase the sensitivity of anti-tumor therapies by reversing malignancy, immunosuppression, or drug resistance in the TME [309], [310]. It is well-established that MDSCs contribute significantly to the immunosuppressive TME [311]. Research showed that cell surface markers such as CD33, CD15, CD11b, and CD66b are not great for the differentiation of these populations. Hence, the identification of transcription factors, including CCAAT/enhancer-binding protein (C/EBP), Rb and STAT3, as well as immune-regulatory substances such as arginase1 (Arg1), Nitric oxide (NO), and ROS should be taken into account [312]. The CCR2 antagonist, CCX872, reduced MDSCs and enhanced anti-PD-1 therapy in the GBM mouse model [313]. A promising therapeutic target is the macrophage inhibitory factor (MIF), also produced by glioma cells and regulates MDSC migration into the brain. Sulforaphane and Ibudilast, a MIF inhibitor, reduced the formation of MDSC and were toxic to glioma cells [311], [314]. To increase the synergistic benefits of radiation for brain cancer, Wu et al., 2019 created a zinc-doped iron oxide nanoparticle (NP) with a cationic polymer surface that can attack both tumor cells and the immunosuppressive TME [315]. Further, the recruitment of DCs cells to the brain and spinal cord through either afferent lymphatics or high endothelial venules. Current studies reveal a complicated interaction between DCs, microglia and macrophages, T-cells, and tumor cells in the TME, while the precise involvement of DCs in the context of GBM is still being clarified [316]. According to a study by Wang et al., 2020 exosomal LGALS9, produced by GBM cells, inhibits DC antigen presentation and cytotoxic T-cell activation in the cerebrospinal fluid (CSF), and that loss of this inhibitory action can result in long-lasting systemic antitumor immunity [317]. Active immunotherapy called DC vaccination (DCV) aims to trigger an

anticancer immune response. Hundreds of GBM patients have been vaccinated in numerous DCV trials, which have confirmed the vaccine's viability and safety [318]. Until this moment, no Phase III clinical trial for DC vaccines in GBM has successfully met its goals and effectively implemented clinical development and transformation. Targeting combination therapy methods will be a breakthrough in treating GBM with the DC vaccination [319].

2.6.3. MECHANISTIC INVOLVEMENT OF THERAPEUTICS TARGETS IN THE PROGRESSION AND PATHOGENESIS OF GBM

GBM molecular patterns can partially predict clinical results and treatment outcomes. Recent discoveries related to genetic and epigenetics markers have been discussed in the current review article. For example, isocitrate dehydrogenase (IDH) mutation (R132 for IDH1, R140 or R172 for IDH2) is a crucial and defining factor in glioma formation and development, and it may be a critical target for treatments [320], [321]. Another marker is STAT1, and research shows STAT1 transcribes SH2B adaptor protein 3 (SH2B3), predominantly expressed in GBM stem cells (GSCs), is significantly expressed in GBM and is associated with poor prognosis. The formation of xenograft tumors *in vivo* and the proliferation, migration, and self-renewal of GBM cells are all significantly hampered by targeting SH2B3 [322]. Another crucial factor is angiogenetic therapeutic indicators. Apart from VEGF, VEGFR, and neuronal markers NEFL, recently published studies have shown that human gliomas have significant levels of the novel angiogenic biomarker ELTD1. Anti-ELTD1 therapy dramatically improved survival, decreased tumor sizes, normalized the vasculature [323], [324]. In addition, major receptor tyrosine kinases (RTK) targets include VEGFR as well as the hepatocyte growth factor receptor (HGFR/MET), FGFR, platelet-derived growth factor receptor (PDGFR), and EGFR. Following the FDA's approval of Bevacizumab to target the VEGFR2 in adult patients with recurrent GBM, targeted therapy against RTKs (Afatinib, Sunitinib, PLB-1001, and Osimertinib) has emerged as a novel treatment option [325]. Moreover, metastasis, chemo- and

radio-resistance in GBM are connected to the loss of PTEN gene (therapeutic marker) activity. It is widely known that several epigenetic, transcriptional, and post-translational processes regulate PTEN's expression and function, pointing to the fact that PTEN is a crucial regulator of tumor sensitivity to various therapeutic modalities [326]. However, HDACi and DNA methyltransferase inhibitors have recently been utilized to treat malignancies, either separately or in combination, as part of epigenetic therapy. Many effective small drugs, such as 85P Mocetinostat (MGCD0103), Valproic Acid, SAHA, PXD101, and Beleodaq®, target HDAC, HATs enzymes, bromodomains and extra-terminal motif (BET) [327], [328]. Studies demonstrated that epigenetic reader proteins with BET domains were promising therapeutic targets in GBM. Jermakowicz et al., 2021 developed the novel BET inhibitor UM-002 (targets BRD4 bromodomain), which entered the brain and suppressed genes associated with cell cycle and invasion [329]. DNA methylation is another interesting therapeutic target. Li and colleagues 2019 further demonstrated that miR-148-3p suppressed proliferation, migration, and invasion of GBM by influencing the DNMT1-RUNX3 axis and the EMT (N-cadherin, vimentin, MMP2, and MMP9) in GBM [330]. However, Decitabine, a DNMT inhibitor, has been demonstrated to demethylate the STING promoter's cg16983159, turning on STING expression and activating the cGAS-STING signalling pathway, making GBM cells more susceptible to immunotherapies (converting ‘cold’ TME into ‘hot’ TME) [331]. Finally, ubiquitination governs apoptosis, GSCs, and the activation or inactivation of tumorigenic pathways in GBM. The ubiquitination pathways' molecular targets, Cul3, RNF41, TRIM8, CGIP, LZTR1, and PARK2, were intensively investigated in GBM. Several deubiquitinase, such as HAUSP, OTUB1, USP1, USP3-8, etc., are implicated in the development of tumors. Bortezomib, MG132, and Saquinavir, drugs with anti-glioma action by UPS targeting [332]. Fox et al., 2019 underlined the important protein SUMOylation plays in the pathobiology of GBM. E1 (SAE1), E2 (Ubc9), and E3 (PIAS1 and 3) components as well as a SUMO-specific

protease (SENP1) are potential therapeutic targets in GBM. Recently, it was discovered that topotecan inhibits global SUMOylation in GBM, which lowers levels of CDK6 and HIF1 and causes substantial alterations to cell cycle progression and metabolic activity [333]. Focusing on the genetics and epigenetics of GBM and the effects of its mutations has thus brought attention to various therapy modalities targeting therapeutic markers in combating GBM (**Figure 2.14**)

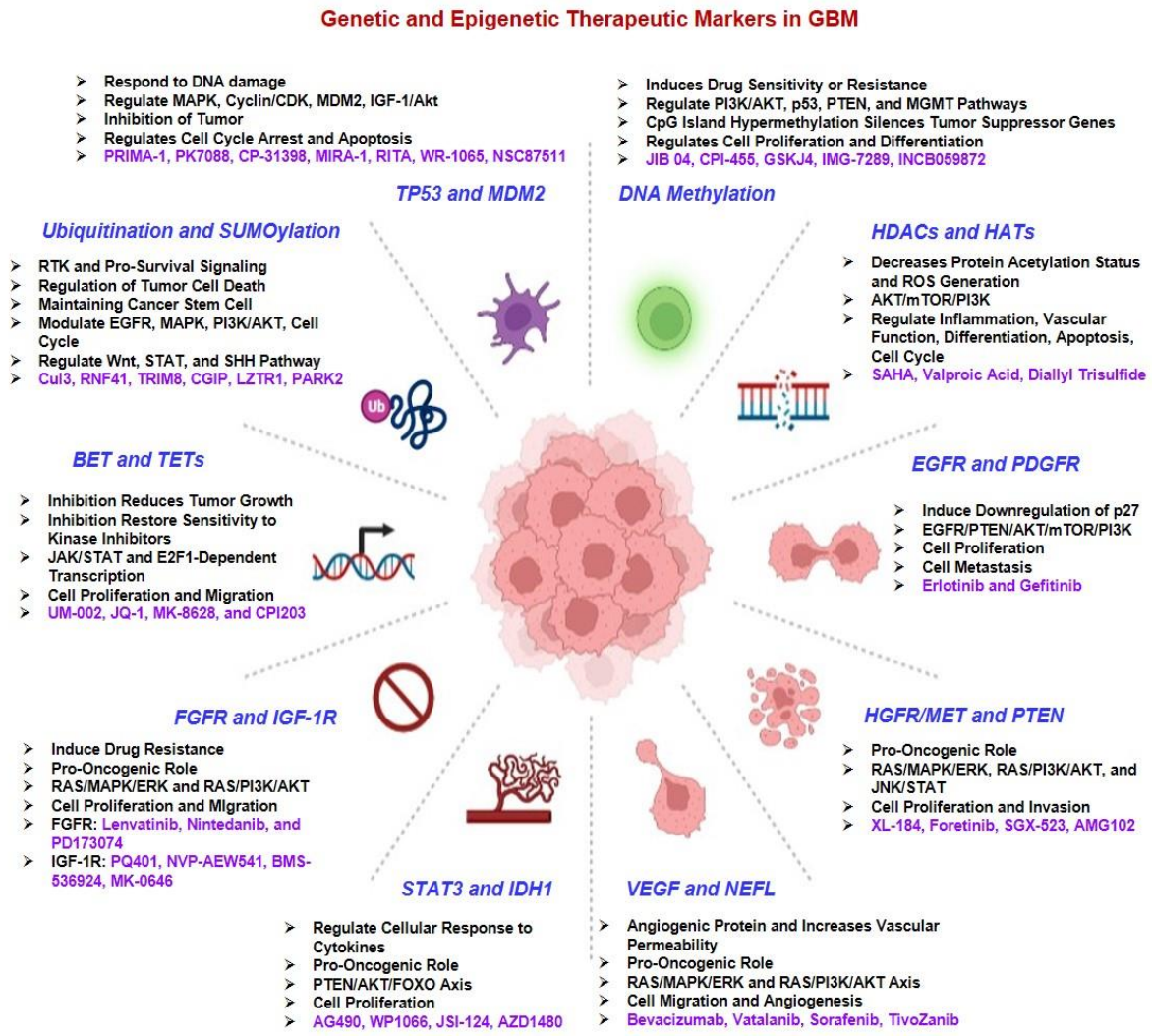

Figure 2.14: ***Genetic and Epigenetic Therapeutic Markers in GBM:*** **GBM is a multifactorial disease in which various genetic and epigenetic biomarkers have been implemented. For instance, STAT3, FGFR, PTEN, HGFR/MET, and IGF-1R involved in cell proliferation, whereas, VEGF, NEFL, and BETs are involved in cell migration. Likewise, EGFR and PDGFR causes cell proliferation and cell metastasis, which can be inhibited by the administration of erlotinib and gefitinib. Ubiquitination and acetylation are two prominent lysine-induced post-translational modifications that regulated various signaling events in the pathogenesis and progression of GBM. Histone deacetylases and histone acetyltransferase modulate cell cycle and apoptosis of GBM cells. DNA methylation is another epigenetic factor that regulates cell proliferation and differentiation through the modulation of PI3K/Akt and MGMT pathways**

2.7. GLIOBLASTOMA MULTIFORME'S THERAPEUTICS APPROACHES

Traditional approaches include surgery, targeted therapy, chemotherapy and radiotherapy (RT). GBM surgery aims to accomplish a "maximal safe resection" or remove the maximum amount of the tumor without permanently impairing brain function. Given that GBM can spread widely across several different brain regions, this strategy necessitates great neurosurgical competence [334]. Following brain glioma surgery, the extend of resection (EOR) is the most crucial prognostic factor. Several studies revealed that OS and PFS for GBM patients are favorably correlated with rising EOR [335]. Therapeutic approaches targeting EGFR pathway, PDGF pathways, MET pathway, The PI3K/AKT/mTOR pathway, Cell cycle regulation and apoptosis regulatory pathway, The p53 pathway, TERT promoter mutation, epigenetic regulation, angiogenesis, integrins. Thus, better knowledge of the molecular mechanisms behind GBM malignancy has resulted in the development of several biomarkers and drugs that target particular molecular mechanisms in malignant cells [336]. The development of chemotherapeutic drugs comes after determining the molecular targets and comprehending pathophysiology. Currently, GBM patients have access to four chemotherapy drugs: TMZ, Carmustine, Lomustine, and Cyclophosphamide (CPA) [337]. Currently, several potential drugs, including Alisertib, Disulfiram, Regorafenib, Sorafenib, Vorinostat, etc., are now being developed in various phases of clinical trials. Some clinical trials of major drugs and biologicals have been reviewed in articles [338]. Another important technique is RT. For patients under 70 years old, standard radiotherapy or external beam radiation (EBRT) is used. It is delivered in 1.8-2 Gy fractions daily, 5 days a week, continuously for 6 weeks, to a total dose of 54-60 Gy [339]. However, hypofractionated radiotherapy (HFRT) is advised for patients over the age of 70 years and those with a constrained prognosis due to poor prognostic characteristics. It employs a biologically equivalent dose of 40 Gy divided into 15 fractions of 2.67 Gy. This enhanced OS with lower rates of toxicity [340], [341]. The technical obstacles

related to conventional brachytherapy (means implantation of interstitial or intracavitary radioactive sources adjacent to the target tissue) are significantly reduced by embedding encapsulated ^{131}Cs radiation emitter seeds in collagen-based tiles [342]. In addition, emerging therapeutic approaches targeting GBM pathogenesis **(Figure 2.15)** includes immunotherapy, adoptive cell therapy, vaccine cell therapy, stem cell therapy, PDT, PTT, TFields, viral and non-viral vector-based therapy, CRISPR/Cas9 genome editing system, RNAi, targeted toxins, suicide gene therapy, Immunostimulatory gene therapy and oncolytic virotherapy, nanotechnology based targeted therapy. GBM is proficient at evading host immune surveillance. Using a patient's immune system as a tool, immunotherapies try to re-direct immune cells away from a tumor. Numerous immunotherapies, including immune checkpoint inhibitors (ICIs) and chimeric antigen receptor (CAR) T cell therapy, are now being researched as potential treatments for GBM. Such treatment has great success against aggressive tumors and less in brain cancer. In order to restore T cell function and anti-cancer activity, ICIs target T cell depletion by blocking immunological checkpoints PD-1 and CTLA-4 [343]. Adoptive T-cell transfer (ACT) includes tumor-infiltrate lymphocyte (TILs) transfer and genetically engineered T-cell transfer. It consists of re-infusing a patient of their own (autologous) or donor (allogenic) anti-tumor T-cells that are genetically modified to target tumor-associated antigens (TAAs) to attack receptors on the patient’s cancer cells. This increases the amount of specific T-cells a tumor encounters and guarantees that they are properly activated, making them less vulnerable to the intra-tumoral immunosuppressive milieu [344]. There is no FDA-approved T-cell treatment for GBM, unlike hematologic cancers. In a preliminary trial, it was shown that giving GBM patients autologous TIL with IL-2 was successful [345].

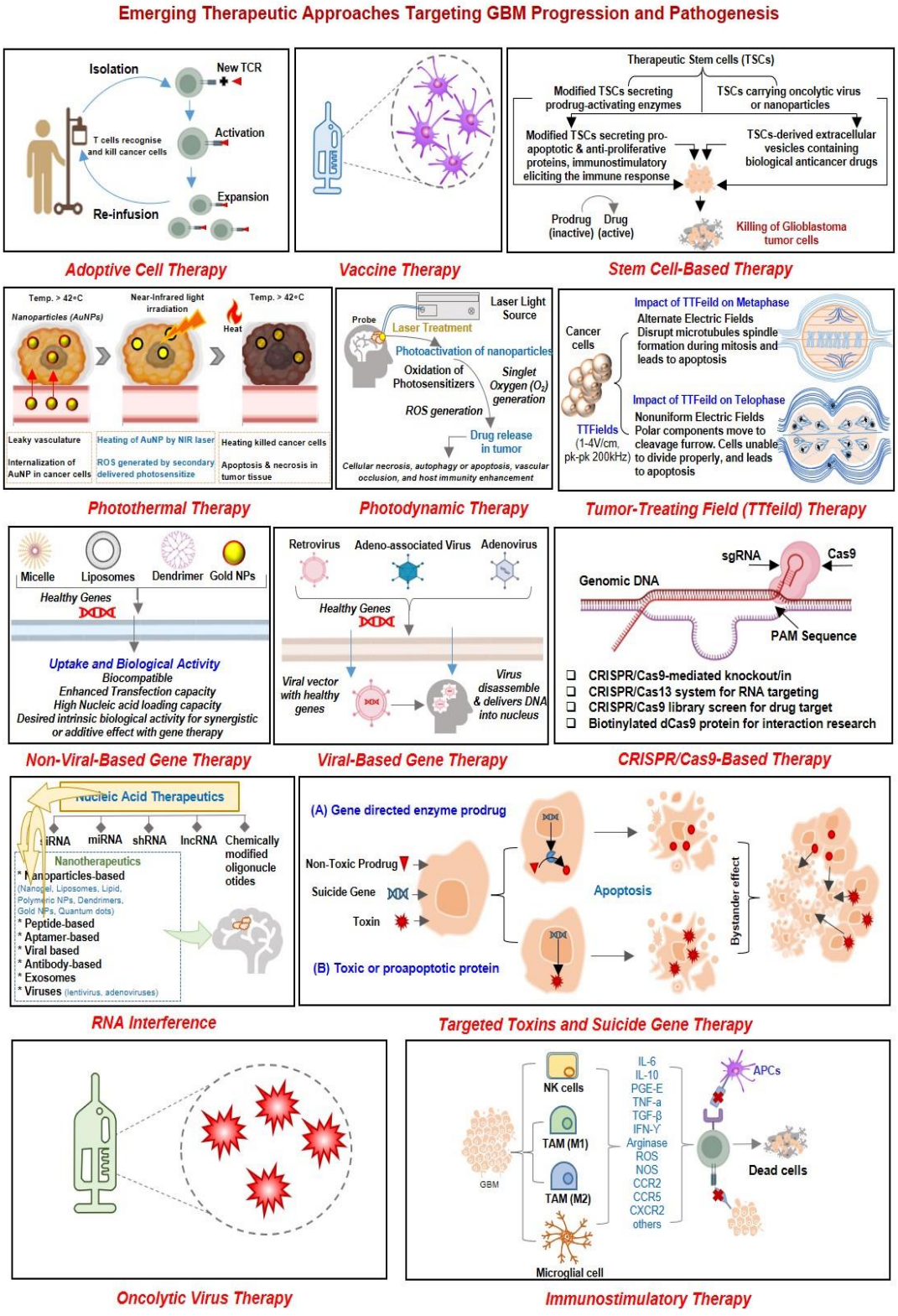

Figure 2.15: *Emerging Therapeutic Approaches Targeting GBM Progression and Pathogenesis*: Current treatment strategies in GBM includes chemotherapy, radiotherapy, immunotherapy, and surgical resection. However, despite having the rigorous amount of research, the survival rate is still imposing a huge challenge. Further, traditional therapeutic strategies come with a problem of adverse side effects. Thus, to overcome the challenges and hurdles in the traditional treatment strategies, scientists have developed various other therapeutic treatment approaches, namely adoptive cell therapy, stem-cell therapy, viral and non-viral gene therapy, tumor treating field, vaccine therapy, and others, which enhance the survival rate and prognosis rate.

CAR T cell research for GBM is intense: ongoing CAR T cell clinical trials in GBM, include EGFRvIII (NCT01454596, NCT05063682, NCT02209376, NCT02844062, and NCT03283631), ephrin type-A receptor 2 (EphA2) (NCT02575261, withdrawn), HER2 (NCT01109095, NCT03389230), IL-13Rα2 (NCT04510051, NCT05540873, NCT04003649, NCT02208362), and PD-L1 (NCT02937844) shown promising results. CAR T cell treatment is meant to be used in combination with other therapies because of the substantial tumor heterogeneity, immunoediting, and existence of a cold immunosuppressive microenvironment (with anti-PD-1 inhibitors, Pembrolizumab) [346].

Vaccines for GBM are an active immunotherapy method that can increase and modify immune responses against TAAs [347]. EGFRvIII, a mutant form of EGFR constitutively active and exclusively expressed in 50% of GBM, is the most thoroughly investigated TAAs [348]. In many clinical trials, the peptide vaccine Rindopepimut (CDX-110), which targets EGFRvIII, has been studied. Many studies demonstrate that GBM tumors initiated from GSCs are the root cause of cancer patients' resistance to treatments. GSC characteristics are upheld by the expression of the CSCs markers CD133, CD44, Oct4, Sox2, Nanog, and ALDH1A1, as well as by the signaling pathways mTOR, AKT, NOTCH1, and Wnt/β-catenin [349]. A viable, focused therapeutic option for GBM has recently been identified as PDT The photosensitizer (5-ALA, Porfimer sodium, Temoporfin, and Indocyanine green (ICG)) is activated by photoirradiation by transferring energy to the sensitizer, causing the excitation of molecular oxygen to a singlet or triplet state [350]. It is easier for 5-ALA (the most used photosensitizer) to diffuse into the tumor mass when the BBB is broken, which typically happens in the GBM microenvironment [8], [351], [352]. PTT is a non-invasive treatment using a photoabsorbing chemical (such as cyanine or porphyrin derivatives) that can accumulate at the tumor site in conjunction with an external NIR laser to irradiate the tumor topically or interstitially (via an optical fiber). After exposure to laser radiation, the PTA agent collects the light energy,

transforms it, and then releases it as heat, producing localized HT that results in partial or total tumor ablation. Viral vectors are employed to transfer therapeutic genes into target cells, where they can operate specifically against tumors, play an oncolytic role in gene delivery, and trigger a host immune response. Viral vectors used in GBM therapy, including retrovirus (HSV-TK, TOCA511); Lentivirus (shRNA-lentivirus, sh-SirT1 lentivirus, miRNA-100 lentivirus, GAS1-PTEN lentivirus); Adenovirus (ONYX-015), Delta-24); Herpes simplex virus (HSV1716, C134, G2017); Oncolytic virus (Pelareorep/REOLYSIN, TG6002, H-1PV, PVS-RIPO) [353]. In suicide gene therapy, retroviruses are primarily used to deliver the desired gene to the tumor location. For instance, Vocimagene amiretrorepvec (Toca 511), an experimental γ-retroviral replicating vector utilized in a multicenter, randomized clinical trial, enhanced patient survival after tumor excision for the first or second recurrence of GBM [354]. In addition, a prominent gene editing technique utilized in cancer research is the Clustered Regularly Interspaced Short Palindromic Repeats (CRISPR)/CRISPR associated (Cas) nuclease 9 (CRISPR/Cas9) system. It contributes to identifying new oncogenes that govern autophagy, angiogenesis, and invasion and are significant in developing GBM [355], [356]. Rodvolt et al., 2020, knockout the Unfolded Protein Response (UPR) genes ERN1, IGFBP3, and IGFBP5 in U251 cells using CRISPR/Cas9, which made the cells more vulnerable to cell death in response to 12 ADT, an ER stress-inducing drug [357]. Innovative multitarget modalities like RNAi are urgently needed. Small RNA oligonucleotides are used in RNAi-based therapeutics to control expression levels at the post-transcriptional mechanism [7]. Synthetic RNA oligonucleotides like siRNA, miRNA, shRNA and lncRNA have demonstrated potential as cutting-edge therapies. Even while RNAi therapy can be a valuable tool in the fight against cancer, especially for untreatable tumors like GBM, certain obstacles still stand in the way of realizing its full potential. To overcome this drawback, herein Liu et al., 2020 developed intelligent biomimetic nanotechnology-based RNAi that uses Angiopep-2 peptide-modified, immune-free

RBCm and charge conversational components to solve this disadvantage. This increased orthopedic GBM RNAi therapy's therapeutic effectiveness, increased patient survival rates, and reduced systemic adverse effects [358]. In addition, due to its anti-inflammatory, anti-oxidative, and neuroprotective properties, a novel nanomaterial called DNA tetrahedron has recently become a multipurpose treatment [359]. The goal of suicide gene therapy (SGT) is to introduce a gene that either code for a toxin or an enzyme that will make the target cell more susceptible to chemotherapy [360]. Solid tumors can be treated with SGT in two steps. A suicide gene, such as cytosine deaminase (CD), Herpes simplex virus 1 (HSV), or TKHSV-thymidine kinase (TK), is transduced into cancer cells in the first phase. This enzyme can catalyze the conversion of a prodrug into a harmful metabolite. The second stage entails administering the relevant prodrug, which, when catalyzed by the prodrug-converting enzyme, causes cell death. The nontoxic prodrug is changed through viral vectors into a toxic metabolite that kills tumor cells once the suicide gene is introduced into glioma cells [361]. Immunostimulatory gene therapy (IGT) aims to trigger tumor-specific lymphocyte death by stimulating DCs, T helper (Th-1) cells, and cytotoxic T lymphocytes (CTLs), shifting the continuing immunosuppression towards Th1 immunity. IGT aims to introduce genes that code for immunostimulatory proteins into the tumor site to promote tumor immunity. Drugs that block MDSCs, Tregs, or M2 macrophages should be combined with IGT. Preconditioning chemotherapy is frequently provided to reduce Tregs and MDSCs in patients receiving immunotherapy [362]. The tyrosine kinase inhibitor (TKI) sunitinib was created to target signaling in tumor cells, however, it was found that one of its modes of action was a direct inhibitory effect on MDSCs [363]. According to research by Hooren et al., 2021, systemic administration of immune-stimulatory agonistic CD40 antibodies in a glioma model causes the development of tertiary lymphoid structures related to T-cells with impaired function and compromises the response to ICIs [364]. Oncolytic virus (OVs) therapy is a very effective type

of cancer immunotherapy that uses genetically altered viruses to attack and destroy cancerous cells preferentially while sparing healthy cells. Lysis of tumor cells releases TAA, viral pathogen-associated molecular patterns (PAMPs), and DAMPs, which can be used by DCs and NK cells to quickly clear virus-infected cells, activating innate immunity, as well as uninfected tumor cells through bystander effects [365]. In addition, cytokines and proinflammatory cytokines activate APCs and enhance CTL infiltration, thus resulting in an adaptative immune response [366]. Additionally, methods are combined with OV therapy to greatly expand the therapeutic possibilities while minimizing their invasiveness and improving their accuracy.

2.7.1. IMPLEMENTATION OF NATURAL COMPOUNDS

Regardless of the fact that there have been few improvements in the progression of GBM therapies to boost patient survival, researchers and clinicians are indeed eager to study novel therapies and techniques for treating this disease [367]. Natural compounds and their structure analog have been the source of most medicines' active ingredients for various indications, including cancer [368]. Some widely used plant-derived natural compounds are etoposide, irinotecan, paclitaxel and vincristine; bacteria-derived anti-cancer therapeutics Mitomycin C and Actinomycin D; and marine-derived anti-cancer is Bleomycin [369]. Numerous studies suggest natural compounds are used as chemosensitizers (such as quercetin, resveratrol, withaferin A etc.), radiosensitizers (such as Tetrandrine, Zataria, Multiflora and Guduchi) and anti-proliferative (such as Curcumin, Oridonin, Rutin, Cucurbitacin), alkaloids and flavonoids agents [370], [371]. Identification of new drugs that can modify the BBB, decrease tumor growth, and prevent the development of recurring tumors is critical for improving overall patient prognosis. *In vitro* and/or *in vivo*, various natural compounds with well-established biological benefits have oncologic effects on GBM [372]. These include flavonoids, terpenoids, alkaloids, tannins, coumarins, curcuminoids, terpenes, lignans, natural steroids, and plant extracts [373]. Statistics show that over 60% of the approved anti-cancer agents are of

natural origin (natural compounds or synthetic compounds based on natural product models). Previous studies have also supported that multiple natural compounds have antitumor and apoptotic effects in TMZ and p53 resistance GBM cells. Various natural compounds such as Chrysin, Epigallocatechin-3-Gallate, Hispidulin, Rutin, And Silibinin were also used in combination with TMZ and other chemotherapeutic drugs due to their potential to act as chemosensitizers (such as Icariin, Quercetin), radiosensitizers (Zataria multiflora), inhibits proliferation (such as Zingiber officinale and Rhazya stricta) and migration and induces apoptosis (Baicalein) [370], [374], [375].

2.7.2. ANTIPSYCHOTIC DRUGS AS A PUTATIVE AGENTS AGAINST GBM

Indeed, a group of psychotropic medications known as antipsychotics is used to treat bipolar illness, psychosis, delirium, Huntington's disease, and Tourette syndrome. The classification of antipsychotics into typical or first-generation antipsychotics (FGAs) and atypical or second-generation antipsychotics (SGAs) is primarily determined by the likelihood that the patient would experience extrapyramidal symptoms (parkinsonism, dystonia) and tardive dyskinesia [376]. According to a literature review, SGAs outperformed FGAs in treating negative symptoms, mental hospitalization rate, and relapse-free survival. SGAs showed more remarkable persistence and commitment to treatment than FGAs. Studies have demonstrated the possible significance of antipsychotics in slowing the growth of GBM cells by obstructing each individual hallmark of cancer [377]. Antipsychotic medications have a long history of usage in a wide range of therapeutic psychological contexts, and they have moderate or low toxicities and well-known tolerability profiles. Hence, there are increasingly being explored for effectiveness in patients with various malignancies, including malignant brain tumors, due to their known safety and demonstrated ability to cross the BBB. Additionally, recent progress in medicine demonstrates the prevalence and benefit of combination therapy over monotherapy for minimizing disease pathogenesis. The anti-cancer agent TMZ frequently used to combat

GBM has earlier been utilized in combination with SGA or FGAs [378]. For instance, FGAs (Chlorpromazine) have already been used in combination therapy.

2.7.3. THE EMERGENCE OF COMBINATION THERAPIES: FOSTERS INNOVATION AND HOPE

Combination therapy is considered an essential and promising treatment method in various disease conditions, such as cancer, cardiovascular disease, and infectious diseases. Along with his colleagues, Emil Frei has given the concept of combination therapy using 6-mercaptopurine and Methotrexate to treat acute leukemia [379]. The rationale for using combinatorial treatment is to use more than one drug that may have different mechanisms of action, thereby decreasing the likelihood of developing acquired chemoresistance [380]. Combination therapy using multiple drugs or immunotherapies is an emerging treatment option to combat side effects associated with chemotherapeutic drugs. In some cases, combination therapies are found to be more effective. For instance, the combination of radiotherapy, chemotherapy and surgery is considered as the most standard treatment option for breast, ovarian, and lung and neck cancer [381]. Earlier combinational therapy targets different pathways within tumors, but now focus has also shifted towards an environment surrounding the tumor and aids tumor progression. In 2020, Durvalumab was approved by the FDA as a first-line treatment for patients with advanced-stage small-cell lung cancer in combination with etoposide and either Carboplatin or Cisplatin. [382]. In the same year, the FDA approved the use of two immunotherapy drugs Nivolumab and Ipilimumab, for patients with indications NSCLC, HCC and Mesothelioma [383]–[385]. A drug combination of Tafinlar (Dabrafenib) and Mekinist (Trametinib) gained FDA approval status to treat patients with BRAF V600–positive advanced or metastatic NSCLC. With this approval, BRAF V600E joins EGFR, ALK, and ROS-1 as the fourth actionable genetic biomarker in metastatic NSCLC. Recently, Fengxia et al., 2020 mentioned that a combination that includes Palbociclib (a cyclin-dependent kinase (CDK) 4/6 inhibitors)

and Human sulfatase-1 (HSulf-1) together exhibited a synergistic antitumor effect on Rb-positive TNBC. This also indicates HSulf-1 may be a potential therapeutic target for TNBC. Previously scientists have reported that HSulf-1 s a negative regulator of cyclin D1 and also emerging as a novel prognostic biomarker in Breast cancer. This is because enhanced HSulf-1 expression was also linked with increased progression-free survival and overall survival in patients with TNBC [386].

Advantages of using combinatorial therapy are enhanced efficacy (additive or synergistic); reduced chance of broad-spectrum chemoresistance by delaying the emergence of acquired resistance (combine therapeutic agents with different mechanisms of action); decreased toxicity (use of drugs with non-overlapping toxicities); hitting cancer more than one place, increase the opportunity to use lower doses of one or both drugs; reduced treatment duration and also address heterogeneous nature of tumors. Some drawbacks, such as drug interaction, can lead to side effects that could occur due to reactions between the medications; challenging to figure out the source of unwanted side effects [387]. These days' clinical trials evaluating a drug targeting only one TME component are rare, and hence numerous combinatorial therapies are approved and listed in **Table 2.4.**

Table 2.4: FDA approved Combinatorial Therapy targeting the Tumor microenvironment

S.NO	APPROVED DRUG COMBINATION	INDICATION	DRUG CLASS	FDA APPROVAL YEAR	REFERENCE
1	Opdivo (Nivolumab) and Yervoy (Ipilimumab)	Mesothelioma	**Nivolumab** (PD-1 inhibitor) ; **Ipilimumab** (CTLA-4 inhibitor)	2020	[385]
2	Opdivo (Nivolumab) and Yervoy (Ipilimumab)	HCC	**Nivolumab** (PD-1 inhibitor) ; **Ipilimumab** (CTLA-4 inhibitor)	2020	[384]
3	Opdivo (Nivolumab) and Yervoy (Ipilimumab)	Metastatic NSCLC (tumors express PD-L1 greater than or equal to 1%, as determined by FDA approved test)	**Nivolumab** (PD-1 inhibitor) ; **Ipilimumab** (CTLA-4 inhibitor)	2020	[383]
4	Imfinzi (Durvalumab) and Etoposide and Carboplatin/cisplatin	Extensive-stage small-cell lung cancer	**Imfinzi (**PD-L1 inhibitor) ; **Etoposide**(topoisomerase II inhibitor ; **Carboplatin** (alkylating agent)	2020	[382]
5	Encorafenib (BRAFTOVI) and Erbitux (Cetuximab)	Metastatic CRC (BRAF V600E mutation)	**Encorafenib** (BRAF inhibitor); **Cetuximab** (EGFR inhibitor)	2020	[388]

6	Neratinib (NERLYNX) and Capecitabine	Metastatic HER2+ Breast cancer	**Neratinib** (binds to and irreversibly inhibits EGFR, HER2,4 receptor)**;** **Capecitabine** (converted to fluorouracil (antimetabolite)	2020	[389]
7	Lynparza (Olaparib) and Avastin (Bevacizumab)	Advanced Ovarian cancer	**Olaparib** (inhibitor of PARP) enzymes**;** **Bevacizumab** (inhibits angiogenesis by targeting VEGF)	2020	[390]
8	Pemfexy (Pemetrexed for injection) and Cisplatin	Metastatic non-squamous	**Pemfexy™** (multitargeted antifolate)**;** **Cisplatin** (Alkylating agent Crosslink/damage DNA	2020	[391]
8	Pembrolizumab (KEYTRUDA) and Inlyta® (Axitinib)	Advanced RCC	**Inlyta®**(VEGFR-1,2,3 inhibitor) **Pembrolizumab** (PD-1 inhibitor)	2019	[392]
9	Lenvima (lenvatinib) and Keytruda (Pembrolizumab)	Advanced Endometrial carcinoma	**Lenvatinib** (RTK inhibitor of VEGFR1,2,3)**;** **Pembrolizumab** (PD-1 inhibitor)	2019	[393]
10	Avelumab (Bavencio) and Axitinib (Inlyta)	Advanced RCC	**Avelumab** (PD-L1 inhibitor) **;** **Inlyta®**(VEGFR-1,2,3 inhibitor)	2019	[394]
11	Polivy (Polatuzumab vedotin-piiq) and Bendamustine and Rituximab	Relapsed/refractory diffuse large B-cell lymphoma	**Polivy** (ADC binds CD79b found only on B cells**;** **Bendamustine** (alkylating agent)**;** **Rituximab** (engineered chimeric murine/human mAb directed against CD20 antigen found on the surface of normal and malignant B lymphocytes)	2019	[395]
12	Tecentriq (Atezolizumab) and Abraxane (Nab-paclitaxel) and Carboplatin	Nonsquamous NSCLC (Stage4)	**Atezolizumab** (PD-L1 inhibitor) **Abraxane** (antimicrotubule agent)**;** **Carboplatin** (alkylating agent)	2019	[396], [397]
13	Atezolizumab and Carboplatin and Etoposide	Extensive-stage small-cell lung cancer	**Atezolizumab** (PD-L1 inhibitor) **Etoposide** (topoisomerase II inhibitor)**;** **Carboplatin** (alkylating agent)	2019	[398]
14	Braftovi (Encorafenib) and Mektovi (Binimetinib) and Erbitux (Cetuximab)	Metastatic CRC (BRAF V600E mutation)	**Encorafenib** (BRAF inhibitor)**;** **Binimetinib** (MEK inhibitor)**;** **Cetuximab** (EGFR inhibitor)	2019	[399]
15	Atezolizumab and Abraxane (Nab-paclitaxel)	TNBC	**Atezolizumab** (PD-L1 inhibitor); **Abraxane** (anti-microtubule agent)	2018	[400]
16	Pembrolizumab (KEYTRUDA) and Pemetrexed and Platinum drug	Metastatic nonsquamous NSCLC	**Pembrolizumab** (PD-1 inhibitor)**;** **Premetrexed (**multitargeted antifolate)	2018	[401], [402]
17	Tecentriq (Atezolizumab); Bevacizumab; Paclitaxel and Carboplatin	Metastatic nonsquamous NSCLC	**Atezolizumab** (PD-L1 inhibitor) **Bevacizumab** (inhibits angiogenesis**;** **Carboplatin** (alkylating agent) **Paclitaxel** (mitotic inhibitor)	2018	[403]

18	Avastin (Bevacizumab) and Carboplatin and Paclitaxel	Epithelial ovarian, fallopian tubecancer	**Bevacizumab** (inhibits angiogenesis)**;** **Paclitaxel** (mitotic inhibitor)	2018	[404]
19	Imbruvica (Ibrutinib) and Rituxan (Rituximab)	Waldenström macroglobulinemia	**Ibrutinib** (binds permanently to a protein, Bruton's tyrosine kinase, that is important in B cells)**;** **Rituximab** (engineered chimeric murine/human monoclonal antibody directed against the CD20 antigen)	2018	[405]
20	Opdivo (Nivolumab) and Yervoy (Ipilimumab)	RCC	**Nivolumab** (PD-1 inhibitor)**;** **Ipilimumab** (CTLA-4 inhibitor)	2018	[406]
21	Opdivo (Nivolumab) and Yervoy (Ipilimumab)	MSI-H/dMMR metastatic CRC	**Nivolumab** (PD-1 inhibitor)**;** **Ipilimumab** (CTLA-4 inhibitor)	2018	[407]
22	Darzalex (Daratumumab) and Pomalyst (Pomalidomide) and Dexamethasone	Relapsed and/or refractory multiple myeloma	**Darzalex** (mAb that targets CD38+ multiple myeloma cells)**;** **Pomalyst** (inhibitor of COX2)**;** **Dexamethasone** (inhibit NF-κB and other inflammatory transcription factors	2017	[408]
23	Liposome contains Vyxeos (Daunorubicin) and Cytarabine	Therapy-related acute myeloid leukemia	**Daunorubicin** (anthracycline antitumor antibiotic); **Cytarabine** (pyrimidine nucleoside analog inhibits the synthesis of DNA)	2017	[409]
24	Arzerra (Ofatumumab) and Fludarabine and Cyclophosphamide	Relapsed chronic lymphocytic leukemia	**Ofatumumab** (anti-CD20 monoclonal antibody); **Fludarabine** (Adenosine deaminase inhibitor); **Cyclophosphamide** (alkylating nitrogen immunosuppressive agent)	2016	[410]
25	Tafinlar (Dabrafenib) and Mekinist (Trametinib)	Advanced or metastatic NSCLC (BRAF V600)	**Trametinib** (allosteric inhibitor of MEK1 and MEK2; **Dabrafenib** (inhibitor of BRAF (BRAF) protein)	2016	[411]
26	Opdivo (Nivolumab) and Yervoy (Ipilimumab)	Metastatic Melanoma (BRAF V600)	**Nivolumab** (PD-1 inhibitor); **Ipilimumab** (CTLA-4 inhibitor)	2015	[412]
27	Portrazza (Necitumumab) and Gemzar (Gemcitabine), and Cisplatin	Locally advanced or metastatic NSCLC	**Gemcitabine** (nucleoside analog of pyrimidines); **Necitumumab** (recombinant monoclonal IgG1 antibody; **Cisplatin** (Alkylating agent Crosslink/damage DNA	2015	[413]
28	Abraxane and Gemcitabine	Metastatic Pancreatic Cancer	**Abraxane**: Albumin-bound paclitaxel (anti-microtubule agent); **Gemcitabine** (nucleoside analog of pyrimidines);	2013	[414]
29	Temozolomide and radiation therapy	Glioblastoma multiforme	**Temozolomide:** DNA alkylating agent known to induce cell cycle arrest at G2/M phase	2005	[415]
30	Myocet and Cyclophosphamide	Metastatic Breast Cancer	**Myocet:** non-pegylated liposomal doxorubicin citrate; **Cyclophosphamide:** Alkylating agent of the nitrogen mustard type	2001	[416]

2.7.4. COMBINATORIAL THERAPY: ADVANCES THE GBM THERAPEUTIC RESEARCH

With recent development in molecular biology approaches and due to the lack of significant overall survival benefits, there is an utmost need for combinatorial strategies in GBM therapeutics (**Figure 2.16).** Mounting evidence has demonstrated that combining TMZ with other therapeutic drugs increases the therapeutic efficiency in patients with malignant glioma. For instance, the combination of TMZ either with Lomustine (100 mg/m^2), Ralimetinib (100 mg/kg), and Mebendazole (200 mg/kg) improves survival in patients with glioma with methylated MGMT promoter as compared to standard therapy of TMZ [417]–[419]. **Table 2.5** encompasses the list of combinatorial drugs administrated in GBM therapeutics. A clinical trial on 38 patients with recurrent GBM was administered with Macitentan (300 mg once a day) and Levetiracetam (2000 mg/day) that concluded the protective effect of repurposed drugs in combination with TMZ [420], [421]. Recently, Wang et al., 2021 demonstrated that treating GBM patients with Carelizumab, Anlotinib, and Oxitinib during RT increases the OS and PFS [422]. Likewise, Lustig et al., 2022 concluded that the combination of TMZ with Ko143, a non-toxic analog of fumitremorgin C, decreases IC_{50} of TMZ by 41.07% in the resistant phenotype and enhanced the inhibition rate of P-glycoprotein as compared to the treatment of TMZ alone [423]. Drug administration of a single drug is a crucial focus in GBM therapeutics, however, the combination of the drug with other therapies, such as radiotherapy and immunotherapy, increases its efficiency and overall survival rate. For instance, treatment of GBM patients with TMZ in combination with immunotherapy significantly enhanced the OS rate of patients at about 22 months [424]. A study conducted by Serra et al., 2022 reported that a combination of acriflavine, TMZ, and radiation significantly improved the OS rate in an intracranial rat gliosarcoma model [425]. Similarly, Momeny et al., 2021 concluded that Cediranib, a pan-inhibitor of VEGFR, inhibits cell proliferation rate and enhances therapeutic

sensitivity in GBM [426].

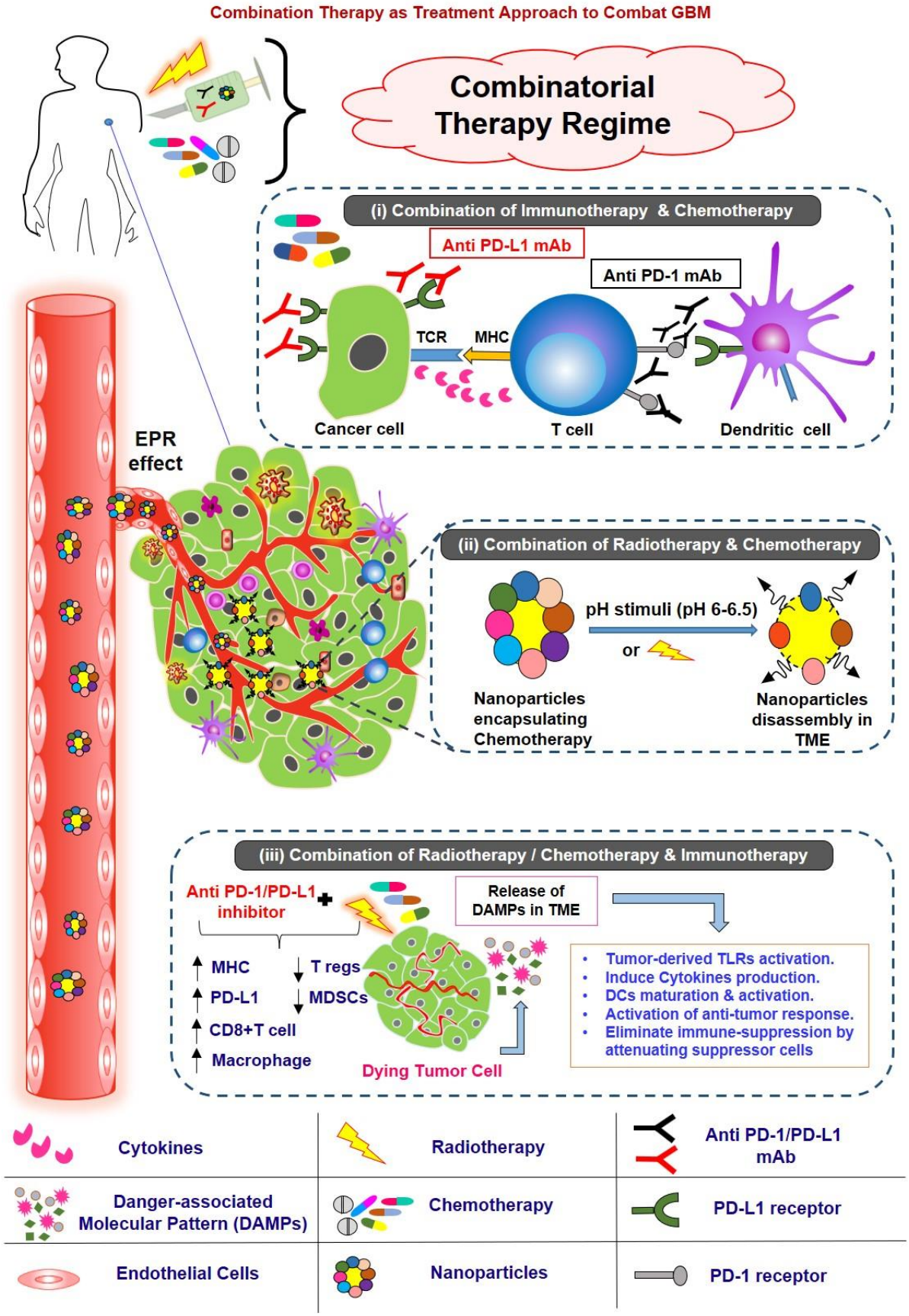

Figure 2.16: *Possible Combinatorial Approach to Treat Cancer*: *a) Mechanism of combination (immunotherapy with chemotherapy/immunotherapy)*: In cancer, there are enhanced expression of PD-L1 on tumor cell and APCs (such as DCs). PD-L1 specifically binds to its receptor, PD-1 on the surface of immune-related lymphocytes, (such as T cells, B cells, and myeloid cells). Breakdown of the PD-1/PD-L1 interaction by using anti-PDL1/anti-PD1 mAb (e.g Atezolizumab, Nivolumab) reactivates T cells activity and related immune responses. Novel combination strategies are combining checkpoint blockade with multiple therapies including traditional chemotherapy, PARP inhibitors, anti-VEGF agents, and anti-CTLA-4 antibodies (e.g Ipilimumab), likely targeting multiple mechanisms and overcoming resistance.b*) *Mechanism of combination (chemotherapy with radiotherapy):* TME-responsive Nanoparticle (such as liposomes, nano-shells, nanocapsules etc.) are capable of encapsulating more than one drug, which are capable of entering and accumulating more at tumor site due to leaky vasculature (because of enhanced EPR effects), and gets dissociate at tumor site due of change in pH (acidic pH ranging 6-6.9). For example, of gold nanocluster, a pH sensitive disrupts TME which enhance radiation therapy (e.g prostate cancer). Hollow mesoporous titanium dioxide nanoparticles are hypoxia induced nanoparticle creation via ultrasound irradiation. In brain cancer gold nanoparticles are used as Theranostics and drug release controlled by pH and disassembly mediated by Glutathione. Polymeric micelles usedfor the delivery of doxorubicin.c) *Mechanism of combination (immunotherapy with radiotherapy/Chemotherapy):* Chemotherapeutic drug e.g Gemcitabine, Doxorubicine, Paclitaxel etc) or Radiotherapy kill tumor cell directly by blocking dysregulated signaling pathways and it also induces immunogenic cell death (ICD) through release of DAMPs (includes secretion of HMGB1, ATP and translocation of calreticulin to cell surface). This collectively leads to activation of TLRs (specifically TLR4), activation of dendritic cells to induce tumor antigen specific T-cell responses and also decrease infiltration and accumulation of Tregs and MDSCs in the TME. Radiotherapy induces ICD and also causes DNA damage. Drug that can stop cancer cell's DNA repair mechanism could make radiotherapy more effective

Recently, the focus has been shifted towards identifying novel therapies for GBM, where a combination of drug-siRNA and drug-miRNA was the most promising approach. For example, a study conducted by Amini et al., 2021 showed that siRNA-mediated suppression of PIK3R3 activity inhibited cell proliferation and activated apoptosis by decreasing the IC_{50} value of Erlotinib [427]. Likewise, the combination of Sulforaphane and PNA-a15b increases the pro-apoptotic effects and inhibited cell proliferation through increasing the expression of caspase 3 and caspase 7 [428]. Setdi et al., 2022 tested a combination of fatty acids omega-3, 6, and 9 on mitochondria isolated from U87MG human glioma cells, where they reported that the combination significantly reduced the activity of succinate dehydrogenase and enhanced toxicity effects through mitochondria [429]. Likewise, a combination of Ulipristal-TMZ-hydroxyurea administration in the human U251 GBM cell line significantly reduced the cell proliferation and total antioxidant capacity. The study also concluded that the combination of three drugs reduced the expression of immunosuppressive and/or GBM-growth stimulating cytokines TGF-β, IL-10 and IL-17 while increasing the expression of GBM-growth suppressing cytokine IL-23 [430]. The combination of Chloroquine, Naringenin and Phloroglucinol synergistically potentiated the efficacy of TMZ on glioma *in vitro* and *in vivo*

through downregulation of Bcl-2 and VEGF [431]. On the same trend, the combination of epigenetic modifiers, namely BIX01294, DZNep, and Trichostatin A at low concentrations exhibited a synergistic effect on cell viability and cell proliferation [432]. Guo et al., 2022 reported the protective function of micheliolide- L-buthionine sulfoximine combination in GBM therapeutics through targeting redox and metabolic pathway [433]. BET proteins have been considered crucial epigenetic markers in GBM pathogenesis, where inhibition of BET through BETi in combination with TMZ induces increased levels of γ-H2AX, a proxy for DNA double-strand breaks [434]. Different other studies have demonstrated the positive effect of drug combinations, namely dabrafenib-trametinib, irinotecan-bevacizumab, and acridone derivatives-TMZ to overcome drug sensitivity and inhibit cell proliferation in GBM therapeutics [435]–[437]. Thus, the studies mentioned above have concluded the positive effect of combinatorial therapy against GBM pathogenesis and progression by inhibiting cell proliferation and migration.

Table 2.5: List of Combinatorial Drugs Administrated in GBM Therapeutics

Therapy 1	Therapy 2	Experimental Model	Dosage/IC_{50}	Target	Mechanism	Reference
Drug-Drug Combination						
Temozolomide	AZD3463	T98G GBM cells	Temozolomide: 1.54 mM AZD3463: 529 nM	PI3K/AKT signaling pathway	Causes the cell cycle arrest in distinct phases and induces apoptosis	[438]
Temozolomide	Resveratrol	Human LN-18 and LN-428 cell lines	Temozolomide: 750 µM Resveratrol: 75 µM	STAT3 signaling event	The combination significantly reduced the expression of the STAT3/Bcl-2/survivin signaling pathway	[439]
Temozolomide	Cedrol	DBTRG-05MG, RG2 cell lines, and CTX TNA2 rat astrocytes	Temozolomide: 206 µM and 5 mg/kg Cedrol: 112.4 µM and 75 mg/kg	MGMT, MDR1, and CD33	Resulted in consistently higher suppression of cell proliferation via regulation of the AKT and MAPK signaling pathways in GBM cells. Combination treatment induced cell cycle arrest at the G0/G1 phase	[440]
Dutasteride	Androgen receptor antagonists	U87 cell culture model	Dutasteride: 5 µM Cyproterone: 25 µM Flutamide: 50 µM	Androgen regulation	A combination of these drugs enhanced their inhibitory effects. The combination of dutasteride with flutamide was most effective at decreasing GBM cell proliferation	[441]
Polish propolis	Bacopa monnieri	T98G, LN-18, U87MG cell lines	NA	Necrosis and apoptosis pathway	The inhibitory effects on the viability and proliferation of the tested glioma cells observed after incubation with the combination of PPE and BcH were significantly stronger	[442]

Temozolomide	KC7F2	U87MG glioma cell line	Temozolomide: 100–500 μM KC7F2: 1–30 μM	HIF1A and HIF1β	Combined effect of the reduced effective dose of the TMZ alkylating agent and the effect was increased, and the effect of the combined therapy is assessed from a metabolic point of view and that it suppresses aerobic glycolysis	[443]
Gossypol	Phenformin	Sphere-cultured U87 and GBM TS (TS13-64)	Gossypol: 10 μM Phenformin: 10 μM	Autophagy pathway	Combination therapy with gossypol, phenformin, and TMZ induced a significant reduction in ATP levels, cell viability, stemness, and invasiveness compared to TMZ monotherapy and dual therapy with gossypol and phenformin	[444]
Dichloroacetate	Metformin	C57BL/6 mice GL-261 allograft model, Human U-87 MG (U-87) and murine GL-261 glioblastoma cell lines	Dichloroacetate: 20 mM Metformin: 10 mM	Apoptosis and necroptosis pathway	DCA and MET synergistically suppress the growth of glioblastoma cells *in vivo*	[445]
AZD6482	URMC-099	U87 MG, U118 MG, U138 MG, U343 MG, U373 MG, U251 MG, A172, LNZ308 and SKMG3 cell line model, normal human astrocytes cell line	AZD6482: 34.56 μM URMC-099: 4.57 μM	MLK3 and PI3Kβ	Combination of AZD6482 and URMC-099 effectively decreased glioblastoma xenograft growth in nude mice. Glioblastoma cells treated with this drug combination showed reduced phosphorylation of Akt and ERK and decreased protein expression of ROCK2 and Zyxin	[446]
MS-275	TAK-733/Trametinib	Human GB cell lines U87 and U251	MS-275: 1 μM TAK-733: 1 μM Trametinib: 1 μM	Histone H3, MAPK, p-MAPK	HDACi and MEKi alone at 1 μM significantly reduced the number of spheres formed	[447]
Cordycepin	Doxorubicin	LN229, U251 and T98G cells	Cordycepin: 80 μM Doxorubicin: 1 μM	EMT-related genes	Inhibits the growth and proliferation of LN-229 cells through various pathways. Combination inhibits cell invasion and migration by regulating the EMT switch of tumor cells	[448]
Temozolomide	Onalespib	Patient-derived glioma stem cell lines	Temozolomide: 10μM Onalespib: 0.4μM	HSP90 and GSCs	The combination of onalespib with radiation and TMZ extended survival in a zebra fish and a mouse xenograft model of GBM compared to the standard of care	[449]
Temozolomide	Anlotinib	A172, U87, and U251 human glioblastoma cell lines	Temozolomide: 100 μM Anlotinib: 2 μM	JAK2/STAT3 signaling pathway	Exerts anti-glioblastoma activity, possibly through the JAK2/STAT3/VEGFA signaling pathway.	[450]
Temozolomide	Taurine	U251 MG cell lines	Temozolomide: 375 μM Taurine: 12 mM	Cell cycle pathway	Exerts anticancer properties against U-251 MG manifested by the induction of G2/M arrest and apoptosis	[451]
Temozolomide	Menadione/ascorbate	GS9L cell transplants - intracranial model	NA	Mitochondrial superoxide	Causing redox alterations and oxidative stress only in the tumor.	[452]
Temozolomide	Bortezomib	T98G cells of human GBM	NA	MGMT	Combination of TMZ and CCNU with a proteasome inhibitor-bortezomib-significantly increases their ability to eradicate cells of a radioresistant GBM	[453]
Temozolomide	Valproic acid	GBM cell lines U87, DBTRG-05MG, U118MG, and LN229	Temozolomide: 3 mM Valproic acid: 2.5 mM	p53-PUMA apoptosis pathway	Survival benefit of a combined TMZ and VPA treatment in GBM patients is dependent on their p53 gene status	[454]

Acalabrutinib	Rapamycin	U87MG and LN229 cell lines	Acalabrutinib: 5 μM Rapamycin: 0.1 μM	SOX2, OCT4, CD133, KLF4, and NANOG	Rapamycin and Acalabrutinib effectively reduced the viability of gbm cell lines and exerted a synergistic antiproliferation effect, and reduced the tumorsphere-formation potential	[455]
Temozolomide	Celecoxib	LN229 and LN18 cell lines	Temozolomide: 250uM Celecoxib: 30uM	Cyclooxygenase-2	Combination therapy may inhibit cell proliferation, increases apoptosis, and increases the autophagy on LN229 and LN18	[456]
THTMP	T0510.3657	Mesenchymal cell lines derived from patients' tumors	THTMP: 50 μM T0510.3657: 10 μM	HSP27 and p53	Combination of THTMP + T0 profoundly increased the $[Ca2^{+}]i$, reactive oxygen species in a time-dependent manner, thus affecting MMP and leading to apoptosis	[457]
Temozolomide	Gefitinib	U87MG cell lines	Gefitinib: 11 μM Temozolomide: 100 μM	VEGF, MMP9, and MMP2	Indicates synergistic effects of GFI plus TMZ against glioma are mediated by the potentiated anti-angiogenesis	[458]
LY294002	Sorafenib	MOGGCCM and T98G cell lines	LY294002: 10 μM Sorafenib: 1 μM	PI3K and Raf	Combination of LY294002 and sorafenib was very efficient in apoptosis induction in glioma cells	[459]
Bevacizumab	Temsirolimus	Ex ovo CAM, Rat 9L or human U87 glioblastoma cells	Bevacizumab: 17 μg/ml Temsirolimus: 100 ng/ml	Angiogenesis and hypoxia signaling pathway	Combination therapy is effective even at concentrations further reduced 10-fold with a CI value of 2.42E-5, demonstrating high levels of synergy	[460]
Perampanel	Temozolomide	U87, U138, and A172 glioma cell lines	Perampanel: 150 μM Temozolomide: 300 μM	GluR2/3 receptor	Synergic effect causes apoptosis that inhibits the growth of the cells.	[461]
Arsenite	Gamabufotalin	Human glioblastoma cell lines U-87 and U-251	Arsenite: 3.3, 5, and 7.5 μM Gamabufotalin: 40, 60, and 90 nM	p38 MAPK	The results observed a synergistic cytotoxic effect of ASCII and gamabufotalin in glioblastoma cell line u-87 but not u-251	[462]
Ciclopirox	Bortezomib	Human glioblastoma cell lines U251, SF126, A172, and U118	Ciclopirox: 20 μM Bortezomib: 24 nM	JNK/p38 MAPK and NF-κB signaling	The combination of CPX and BTZ promotes apoptosis of GBM cells and inhibits GBM tumor growth *in vivo*	[463]
Temozolomide	ZSTK474	human GBM cells *in vitro* and *in vivo*	ZSTK474: 0.4 μM for SF295, 1.2 μM for U87 Temozolomide: 120 μM for SF295, 180 μM for U87	PI3K	The combination treatment led to significantly increased cell apoptosis and DNA double-strand breaks (DSBs)	[464]
Temozolomide	SB225002	Human umbilical vein endothelial cells (HUVECs)	SB225002: 0.03 μM Temozolomide: 10 μM	CXCR2 and VEGFR	Combination therapy induces downregulation of anti-apoptotic BCL2 and CXCR2 gene, and protein expression is altered differently by the combination therapy	[465]
Eicosapentaenoic acid	Cisplatin	DBTRG cells	Cisplatin: 25 μM Eicosapentaenoic acid: 30 μM	TRPM2 channel	Anticancer, apoptotic, and oxidant actions of CiSP were further increased via the activation of the TRPM2 channel in the DBTRGs by the treatment of EPA	[466]
Ascorbic acid	Menadione	U251 human glioblastoma cells	Ascorbic acid: 1 mM Menadione: 20 μM	AMPK/mTORC1/ULK1 pathway	Combined treatment induced strong cytoplasmic vacuolization and a significant decrease in cell density. Induces ROS- and mitochondrial depolarization-mediated necrotic cell death	[467]
Temozolomide	Metformin	LN229 cells	Temozolomide: 100 μM Metformin: 50 mM	MGMT and EMT pathway	The sensitivity of the TMZ-resistant GBM cell line to metformin might be mediated via the suppression of mitochondrial biogenesis, EMT, and MGMT expression	[468]
Melittin	Cisplatin	DBTRG-05MG cells	Cisplatin: 25 μM Melittin: 2.5 μg/ml	TRPM2	The treatment of MLT increased the anticancer, tumor cell death, apoptotic, and oxidant effects of CSP in the glioblastoma tumor	[469]

					cells via activating the TRPM2	
NBM-BMX	Temozolomide	GBM cell lines, U87, U87R, A172, and A172R	NBM-BMX: 10 μM Temozolomide: 50 μM	β-catenin/c-Myc/SOX2 Pathway and p53-Mediated MGMT pathway	BMX overcomes TMZ resistance by enhancing TMZ-mediated cytotoxic effect by downregulating the β-catenin/c-Myc/SOX2 signaling pathway and upregulating WT-p53 mediated MGMT inhibition	[470]
BH3-mimetics (ABT-263, WEHI-539, and S63845)	Chemotherapeutic drugs (Temozolomide, CCNU, and VCR)	GSC-ECLs	S63845: 0.1 μM WEHI-539: 1 μM Temozolomide: 250 μM CCNU: 20 μM VCR: 0.5 μM	NOXA pathway	Combination of BH3-mimetics targeting Bcl-xL with chemotherapeutic agents caused a marked increase in cell death and this sensitivity to Bcl-xL inhibition correlated with Noxa expression levels	[471]
Ruxolitinib	Temozolomide	U87MG, BCSC, and HBMEC cell lines	Ruxolitinib: 89.75 μM Temozolomide: 391.48 μM	WNT signaling pathway	The BBB-crossing agent ruxolitinib promises the potential to increase the efficacy of temozolomide in glioblastoma	[472]
Temozolomide	Etoposide	U87 MG cells	Temozolomide: Etoposide:	Oxidative stress, cell cycle, apoptosis, and autophagy signaling	Combined high-dose treatments of classical antineoplastic agents to sensitize tumors may trigger multi-drug resistance and inhibit maintenance treatment	[473]
Berbamine	Arcyriaflavin A	U87MG- and C6-derived GSCs	Arcyriaflavin A: 20 μM Berbamine: 10 μM	CaMKIIγ and CDK4	Promotes GSC apoptosis, downregulates CaMKIIγ-mediated growth signaling pathway	[474]
Matteucinol	Temozolomide	U251 cell line	Matteucinol: 28 μg/mL Temozolomide: 9.71 μg/ml	TNFR1	This combination selectively reduced cell viability in the tumor cell line (U-251 MG)	[475]
Letrozole	Temozolomide	patient-derived G76, BT142, G43, and G75 GBM lines	Letrozole: 40 nM Temozolomide: reduced by 8, 37, 240 and 640 folds in G76, BT-142, G43 and G75 cells, respectively	Apoptotic signaling pathways	LTZ increases DNA damage and synergistically enhances TMZ activity in TMZ-sensitive and TMZ-resistant GBM lines	[476]
Mebendazole	Temozolomide	U87 and U373 cells	Mebendazole: 0.2 μM Temozolomide: 50 μM	Cell cycle arrest	The combination of MBZ and CQ also showed an enhanced effect in TMZ-resistant glioblastoma cells	[477]
Cannabigerol (CBG)	Cannabidiol (CBD)	Human GB cell lines U87 and U373	CBG: 1.5 μM CBD: 5 μM	Apoptosis pathway	CBG similarly inhibited GBM invasion to CBD, and the TMZ	[478]
Osimertinib	Bevacizumab	GBM Patients	Osimertinib: 80 mg/day Bevacizumab: 15 mg/kg	STAT3 and PTEN	EGFR amplification plus EGFRvIII mutation	[479]
Temozolomide	Lonafarnib	GBM cells in multicellular tumor spheroid (MCTS) models	Lonafarnib: 5 μM Temozolomide: 100 μM	NESTIN, SOX2, CD133, NANOG, and OCT4	Expression of most of the stemness markers significantly increased in the LNF + TMZ treated condition as compared to the untreated condition	[480]

In addition, RT has been explored in combination with chemotherapy (TMZ) [481], immunotherapy (Nivolumab) [482], biologics (Bevacizumab) [483], natural compounds (Resveratrol) [484] etc., to improve efficacy and safety of GBM patients. Maloney et al., 2020 employed bioprint model to perform a proof-of-concept experiment to determine the efficacy of combination therapy, including multiple concentrations of Dacomitinib (an EGFR inhibitor)

and NSC59984 (p53 activator) along with the best methodology to quantify cell viability in complex systems. An antibody-drug combination called ABT-414 combines an anti-EGFR mAb with the tubulin inhibitor Monomethylauristatin F. GBM patient-derived xenograft models expressing wildtype EGFR or EGFRvIII showed cytotoxicity when treated with ABT-414 [485]. Cilengitide, a cyclic RGD pentapeptide, inhibits ligand binding and activation of αvβ3 and αvβ5 integrins and is used in combination with TMZ and RT against GBM [486]. However, the outcomes of numerous studies investigating the use of ICIs in glioma experimental models have been encouraging. Indeed, orthotopic GL261 tumors were eliminated by anti-PD-1 when administered in combination with TMZ and 44% when used alone. Tumor growth was not seen after rechallenge in mice treated with anti-PD-1 monotherapy, but it did occur in the combination group [343]. Recently Yang et al., 2021 demonstrated that dual targeting of IL-6 and CD40-sensitized GBM to ICBs, inhibits tumor growth and that the subsequent triple combination (anti-PD-1/anti-CTLA-4 + CD40 antibody, IL-6 antibody) dramatically increased survival and TILs as well as in IFN-secreting CD8 T cells [487]. Recent studies on CAR T cells have been focused on targeting TAA, including EphA2, EGFRvIII, CD70, HER2, and IL-13Rα [345]. CAR T cell research for GBM is intense: ongoing CAR T cell clinical trials in GBM include EGFRvIII (NCT01454596, NCT05063682, NCT02209376, NCT02844062, and NCT03283631), ephrin type-A receptor 2 (EphA2) (NCT02575261, withdrawn), HER2 (NCT01109095, NCT03389230), IL-13Rα2 (NCT04510051, NCT05540873, NCT04003649, NCT02208362), and PD-L1 (NCT02937844) shown promising results. CAR T cell treatment is meant to be used in combination with other therapies because of the substantial tumor heterogeneity, immunoediting, and existence of a cold immunosuppressive microenvironment (with anti-PD-1 inhibitors, Pembrolizumab) [346] instead of a single therapy. A phase I clinical trial (NCT03636477, NCT04006119) has 21 recurrent GBM patients showed Veledimex

regulatable IL-12 gene therapy dose-dependent efficacy in combination with Nivolumab and showed improved OS was 16.9 months [488].Moreover, the industrial illustration of TTFields is a product manufactured by Novocure called Optune®. Currently, there are several ongoing clinical trials in combination with chemotherapy (TMZ: NCT04474353, NCT03477110, NCT03705351, NCT04471844), biologics (NCT03223103), immunotherapy (NCT03430791) for new and recurrent GBM. In preclinical research and randomized phase III clinical studies, the benefits of TTFeilds in treating GBM have been shown to include non-invasive anti-tumor activity, enhanced therapeutic efficacy when combined with chemotherapy, and reduced systematic toxicity [489]. Additionally, some major systems and their combination with prodrugs used in suicide gene therapy in GBM were HSVtk/GCV system, CD/5-FC system, rabbit carboxylesterase (rCE)/irinotecan system, deoxycytidine kinase (dCK)/cytosine arabinoside (AraC) system [490]. **Table 2.6** discusses the emerging and traditional therapies-based drug combinations implemented in GBM therapeutics.

Table 2.6: List of Emerging and Traditional Therapies Used to Treat Pathogenesis and Progression of GBM

Therapy 1	Therapy 2	Experimental Model	Dosage/IC_{50}	Target	Mechanism	Reference
Immunotherapy-Based Combination						
Anti-PD-1	Anti-BTLA	C57BL/6 J mice were implanted with the murine glioma cell line GL261	Anti-PD-1: 600 µg Anti-BTLA: 1200 µg	CD4+ and CD8+ T cells	Combination of anti-BTLA and anti-PD-1 treatment increases the activation of CD4+ and CD8 + T cells and modulates the presence of Tregs in the brain and blood	[491]
Temozolomide	Interferon-gamma (IFN-ɣ)	Sprague-Dawley rats bearing intra-caudate nucleus (CN) culture medium	——	TLR-4, IL-10, and p-CREB	Combination therapy inhibited the growth of the tumor. Treatment groups alleviated tumor-induced anxiety-like behaviors and improved imbalance and memory impairment	[492]
PD-L1 antibody	LY2228820	C57BL/6 mice	LY2228820: 1 mg/kg/day PD-L1 antibody: 10 mg/kg/day	F4/80+/CD11b+	Combination therapy could be a treatment option for patients at the recurrence or chronic TMZ maintenance stages	[493]
IL-6	CD40	GL261 tumors	NA	Stat3/HIF1A axis	Combination of IL-6 inhibition with CD40 stimulation reverses Mϕ-mediated tumor immunosuppression, sensitizes tumors to checkpoint blockade, and extends animal survival in two syngeneic GBM models	[487]
Varlilumab	Nivolumab	175 GBM patients	Varlilumab: 3 mg/kg once every 2 weeks Nivolumab: 240 mg once every 2 weeks	PD1 and CD27	Varlilumab and nivolumab were well tolerated, without significant toxicity beyond that expected for each agent alone	[494]

Drug-Gene Therapy Combination						
Levetiracetam	Interferon-α	SKMG-4, U87, U373, and U251 cell line model	Interferon-α: 200 U/ml Levetiracetam: 40 μg/ml	NF-kB/p-NF-kB	Inhibited MGMT expression, activated pro-apoptosis molecules, and inhibit NF-kB phosphorylation	[495]
Temozolomide	IFN-ELP(V)	Female BALB/c nude mice	Temozolomide: 50 mg/kg/per mouse IFN-ELP(V): 53.47 pg/mL	IL-1β and IL-12	Resulting in dramatically improved pharmacokinetics and biodistribution, and thus inhibited GBM recurrence by stimulating antitumor immune response as compared to IFN	[496]
Bevacizumab	Ad-SGE-REIC	Human GBM cell lines U87ΔEGFR and U251MG	Bevacizumab: 0.1 mM Ad-SGE-REIC: MOI of 10	VEGF-A and Wnt signaling pathway	Cells treated with both bevacizumab and Ad-SGE-REIC and decreased β-catenin protein levels. Exerts anti-glioma effects by suppressing the angiogenesis and invasion of tumors	[497]
Drug-Adoptive Cell Therapy						
Cold atmospheric plasma	Temozolomide	U87MG	Temozolomide: 50 μM CAP: 180 s, 1 treatment	αvβ3 and αvβ5 cell surface integrin	CAP, in conjunction TMZ, increased DNA damage measured by the phosphorylation of H2AX and induced G2/M cell cycle arrest	[498]
Drug-Tumor Treating Fields						
Rapalink-1	Tumor treating fields	Glioblastoma neuro-spheres JHH520, SF188, BTSC233, NCH644, GBM1	NA	mTOR	Reduces cell growth	[499]
Drug-Radiotherapy						
A-96649	Iodine-131 beta-particles	U87MG cell lines	A-966492: 1 μM	DNA repair pathway	The results demonstrated that iodine-131, in combination with A-966492 and TPT, had marked effects on radio-sensitizing and can be used as a targeted radionuclide for targeting radiotherapy in combination with topoisomerase I and PARP inhibitors to enhance radiotherapy in clinics	[500]
AZD6738	Radiotherapy	MES-GBM/GSCs	AZD6738: 1.531 μM	STAT3 pathway	ARPC1B promoted MES phenotype maintenance and radiotherapy resistance by inhibiting TRIM21-mediated degradation of IFI16 and HuR, thereby activating the NF-κB and STAT3 signaling pathways, respectively	[501]
Drug-RNA Interference						
LB100	PRMT5 Depletion (siRNA)	Patient-derived primary GBM neurospheres (GBMNS)	LB100: 5 μM	MLKL	LB100 treatment combined with transient depletion of PRMT5 significantly decreased tumor size and prolonged survival	[502]
Fenofibrate	lncRNA HOTAIR	702 glioma patients' samples and human GBM cell lines U87 and U251	Fenofibrate: 100 μM	PPARα	Results suggest that HOTAIR can negatively regulate the expression of PPARα and that the combination of fenofibrate and si-HOTAIR treatment can significantly inhibit the progression of gliomas	[503]
Baicalin	Knockdown miR148a	Human glioblastoma multiforme T98G and U87MG cells	NA	Autophagy pathway	Significant reduction in cell viability and proliferation, the accumulation of subG1-phase cells and a reduced population of cells in the S and G2/M phases (only in the U87MG cell line), increased population of cells in the S phase in T98G cell line and apoptosis or necrosis induction and induction of autophagy for both cell lines	[504]
1-(3',4',5'-trimethoxyphenyl)-2-aryl-1H-	Anti-miR-10b-5p (lipofectamine	U251 GBM cell line	Anti-miR-10b-5p: 200 nM 1-(3',4',5'-	Caspase-3/7	Induces apoptosis and inhibits cell growth. Caused the highest level of accumulation of the cells	[505]

imidazole	RNAiMAX)		trimethoxyphenyl)-2-aryl-1H-imidazole: 0.25 μM		into the G2/M phase of the cell cycle	
Gene Therapy-Nanomaterial						
LPHNs-cRGD (CRISPR/Cas9)	FUS-MBs	NOD-SCID mice and T98G cells	NA	MGMT	LPHNs-cRGD could target GBM cells and mediate the transfection of pCas9/MGMT to downregulate the expression of MGMT, resulting in an increased sensitivity of GBM cells to TMZ. It inhibited tumor growth, and prolonged survival of tumor-bearing mice, with a high level of biosafety	[506]
Drug-Radiotherapy						
PBI-05204	Radiotherapy	U251, A172, U87MG and T98G cell lines and Female CD1-nu/nu mice (Xenograft model)	PBI-05204: 5.0 μg/ml Radiotherapy: 4 Gy	γH2AX, Ku70, pDNA-PKc	Reduced tumor progression evidenced by both subcutaneous as well as orthotopic implanted GBM tumors	[507]
Voxtalisib	Low-intensity pulsed ultrasound	GBMCSCs isolated from the human glioblastoma U87 MG cell line		PI3K/AKT/mTOR pathway	High doses of Vox+LIPUS inhibited mTOR and decreased the viability in both cell groups. Inhibiting mTOR-activated autophagy and LIPUS increased autophagy in GBM cells	[508]

2.7.5. REPURPOSING APPROACH IN GBM

The development and prosecution of novel anti-GBM drugs from bench to bedside can incur significant time and cost implications, and thus, drug-repurposing helps to overcome the obstacles imparted by *de novo* drug designing and development. Till now, various drug molecules, namely memantine, captopril (NCT02770378), metformin (NCT02780024), imipramine (NCT04863950), sertraline (NCT02770378), and others have been approved in clinical trials that target GBM-associated signaling pathways and molecules to treat GBM [509]. For example, the administration of Amitriptyline, Clomipramine, and Doxepin reduces cell proliferation and induces the autophagy pathway by inhibiting PI3K/Akt/mTOR signaling cascade. It also reduced cell stemness and invasive capacity, enhancing immunotherapy efficiency [510], [511]. Likewise, Aprepitant, an antiemetic drug, is used for chemotherapy through blocking substance-P activity and neurokinin-1 activation. A study demonstrated that the administration of Aprepitant inhibited GBM growth in a dose-dependent manner [512], [513]. Antibiotics, such as tetracyclines, macrolides, and antimycobacterial, were examined as

potential antineoplastics in GBM therapeutics through the regulation of mitochondrial biogenesis, oxidative stress, and energy requirements [514]–[516]. Recently, the potential of antiparasitic, antihypertensives and anti-inflammatory substances have been examined as potential antineoplastic agents against GBM. For instance, mebendazole inhibits VEGF2, which causes a decrease in tumor angiogenesis, microtubule formation, and microvascular density [517].

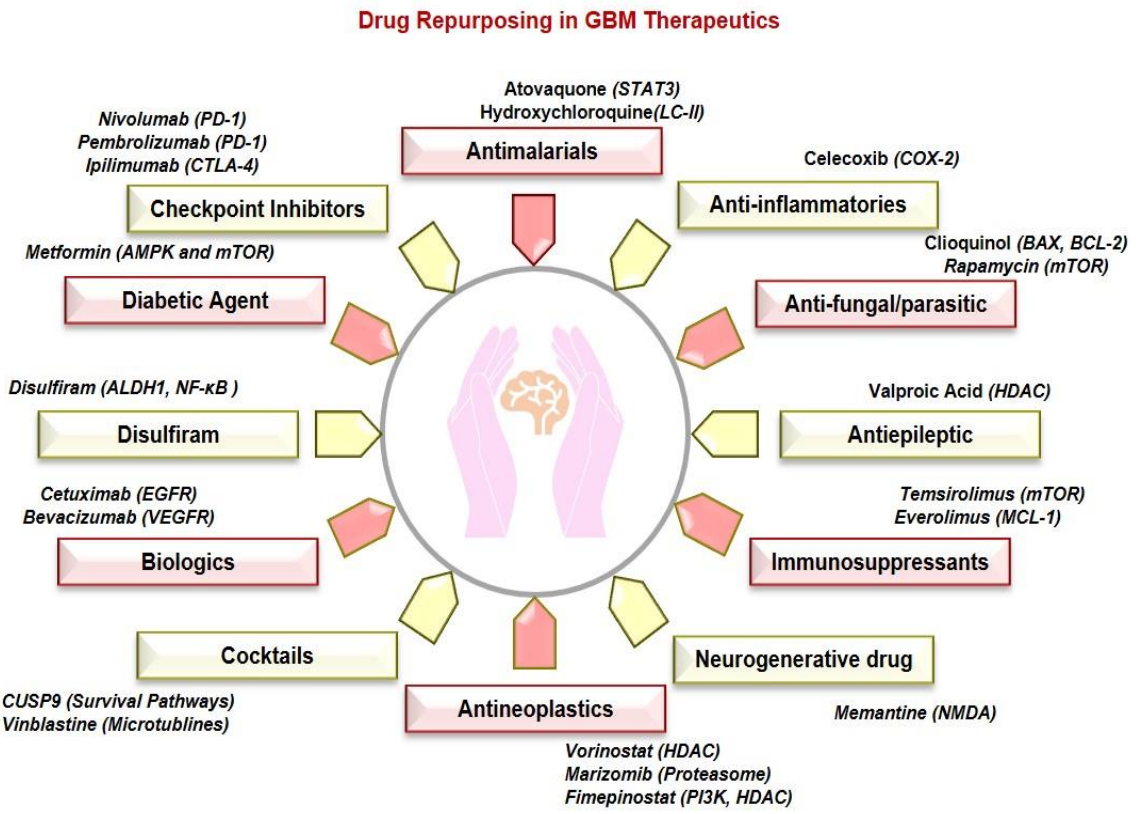

Figure 2.17: *Drug Repurposing in GBM Therapeutics*: Till date, several drugs have been repurposed for GBM, namely antimalarials, anti-inflammatory drugs, anti-fungal, anti-epileptic, neurodegenerative drugs, antineoplastics, anti-diabetic compounds, and others.

Applications of AI in drug repurposing for GBM therapeutics enhance the treatment facilities. For instance, Vargas-Toscano et al., 2020 demonstrated that a robotic workstation was programmed to perform a drug concentration to cell-growth analysis, which identified 22 potential therapeutic substances, and suggests the implication of neurotransmitter signal-modulating agents in GBM therapeutics [518]. Thus, further studies are required to extract the potential of AI/ML algorithms in drug repurposing for GBM therapeutics (**Figure 2.17)**.

CHAPTER III

Objective 1, Objective 2 and Objective 3

CHAPTER III

- ✓ **To identify the tumor microenvironment-based novel biomarkers in GBM therapeutics based on multi-omics approach.**
- ✓ **To elucidate the involvement of biomarkers on signaling events in GBM etiology.**
- ✓ **To explore the possibilities of natural compound as potential therapeutic agent in GBM therapeutics.**

3. INTRODUCTION

According to CBTRUS (Central Brain Tumor Registry of the United States), 2021 recent research, GBM, accounts for 48.6% of primary malignant brain tumors. Individuals aged 20-39 years experienced the most significant increases in survival, with 5-year survival increasing from 44% to 73%. In contrast, the failure to enhance survival in older age groups was primarily due to the inability to improve GBM therapy [11]. Currently, GBM is being treated with a combination of surgery, radiation therapy (RT), and chemotherapeutics (TMZ and antiangiogenic agent bevacizumab). Furthermore, novel treatments such as TTFields and immunotherapy offer promise for a better prognosis [116]. Despite these treatment options, GBM patients' overall survival and quality of life remain dismal. The plethora of research mentioned numerous obstacles to GBM treatment, including tumor heterogeneity, acidic microenvironment and immunosuppression, all of which are linked to the hypoxic environment to some degree [117]. GBM being a highly vascularized human tumor, and its microcirculation is poor, resulting in the hypoxia region inside the tumor. In TME unregulated cell proliferation in tumor (tumor size exceeds diameter of >1 mm) often surpass capacity of the preexisting blood capillaries to meet the oxygen demand [211]. This results in a condition known as hypoxia, which impairs the availability of nutrients and promotes genetic instability because of an increase in the generation of ROS making it a crucial factor for tumorigenesis. As the master regulator orchestrating cellular responses to hypoxia, hypoxia-inducible factor 1 (HIF1)

plays an essential role in GBM aggressiveness. This modulates the expression of angiogenic factors, such as VEGF, insulin-like growth factor II (IGF2) and PDGF, and several glucose and fatty acid metabolism factors, a tumor-immune microenvironment, stimulation of the EMT, suppressing apoptosis and promoting autophagy [519], [520]. In addition, hypoxia also serves as a niche environment for the aggregation of cancer stem cells (CSCs), which promote carcinogenesis and resistance. Tumor cells use a variety of strategies in response to hypoxia, including the expulsion of cytotoxic anticancer drug by ABC-transporters, manifesting a dormant state, and exhibiting pluripotency (stemness) traits, which can lead to the failure of existing therapy [521]. Studies showed that hypoxia promotes secretion of cytokines and chemokines which affects immunosurveillance by affecting $CD8^+$ T cells infiltration, disrupting the cytotoxicity of NK cells. In addition, hypoxic TAM reduce T cell responses and encourage tumor proliferation and angiogenesis [522], [523]. So, given hypoxia's critical role in intra-tumoral interactions, identifying targets that induce adaptation to the hypoxic niche is crucial for a better understanding of GBM origin, development, and treatment resistance [524]. Indeed, “hypoxia” is an essential driving force of GBM and could be used as a novel treatment tool [525].

Regardless of the fact that there have been few improvements in the progression of GBM therapies to boost patient survival, researchers and clinicians are indeed eager to study novel therapies and techniques for treating this disease [367]. Natural compounds and their structure analog have been the source of most medicines' active ingredients for various indications, including cancer [368]. Some widely used plant-derived natural compounds are etoposide, irinotecan, paclitaxel and vincristine; bacteria-derived anti-cancer therapeutics Mitomycin C and Actinomycin D; and marine-derived anti-cancer is Bleomycin [369]. Numerous studies suggest natural compounds are used as chemosensitizers (such as quercetin, resveratrol, withaferin A etc.), radiosensitizers (such as Tetrandrine, Zataria, Multiflora and Guduchi) and

anti-proliferative (such as Curcumin, Oridonin, Rutin, Cucurbitacin), alkaloids and flavonoids agents [370], [371]. Identification of new drugs that can modify the BBB, decrease tumor growth, and prevent the development of recurring tumors is critical for improving overall patient prognosis. *In vitro* and/or *in vivo*, various natural compounds with well-established biological benefits have oncologic effects on GBM [372]. These include flavonoids, terpenoids, alkaloids, tannins, coumarins, curcuminoids, terpenes, lignans, natural steroids, and plant extracts [373]. Statistics show that over 60% of the approved anti-cancer agents are of natural origin (natural compounds or synthetic compounds based on natural product models).

The present study conducted transcriptomic analysis between hypoxia and normoxia (in both normal non-neoplastic brain cells and GBM tumor cells) samples to screen differentially expressed genes (DEGs) related to hypoxia effects. Comprehensive bioinformatics and computational methodologies were used to identify hub genes (LYN, MMP9, PSMB9 and TIMP1) and significant modules and pathways related to TME. We found that matrix metalloproteinase 9 (MMP9) plays a vital role as a hypoxic gene signature, which has the potential to use as a biomarker. Numerous studies have also shown the dysregulation of MMP9 in the microenvironment associated with hypoxia and cancer [526]. MMP9 can cleave and remodel ECM proteins such as collagens and elastin involved in invasion, metastasis and angiogenesis [144]. MMP9 is produced *de novo* by monocytes and inflammatory macrophages, as well as most cancer cells, during stimulation induced by various extracellular signals present in TME, such as proinflammatory cytokines (such as TNF-α, IL-8, and IL-1β), and growth factors (such as TGF-β, PDGF, and bFGF), which can bind to their receptors and activate downstream signaling cascades involved in the activation of transcription factors including NF-κB, SP1, AP1, and HIF1A. This affects various downstream biological processes, including matrix degradation, remodeling, EMT, enhanced tumoral invasion, metastases, angiogenesis, inflammation, drug resistance etc.; hence, it acts as a challenging target for targeted therapy for

cancer [527]. Targeting TME has been a significant focus in recent years, and hence MMP inhibitors that will target a hypoxia condition in the microenvironment could be of great significance as a new antitumor agent. For this purpose, we have avail network pharmacology, structure-based drug design approaches such as molecular docking, MD simulation analysis and MM-PBSA approach to discover prospective classes of natural compounds with druggable and non-toxic properties from the plant-based natural compounds library. We identified eleven hits based on the particular interaction that satisfy the ADMET and LIPINSKI rule of five analyses, pass the toxicity profile, and have a significant affinity for the MMP9 binding site domain. The three best-docked compounds were further subjected to MDS for 50ns to understand protein-ligand complex stability. Previously also, researchers have explored the potential of alkaloids and flavonoids as anti-cancer treatments [528], [529]. Drugs, including natural compounds that target MMP9, have not been used in the clinical setting. Therefore, targeted MMP9 drugs must be screened for treating patients with GBM. Our results can potentially benefit from managing GBM malignancy caused by a hypoxia microenvironment. The findings of this study contribute to a better understanding of the role of the hypoxia microenvironment. **Figure 3.1** depicts the process of the methodologies used in this investigation.

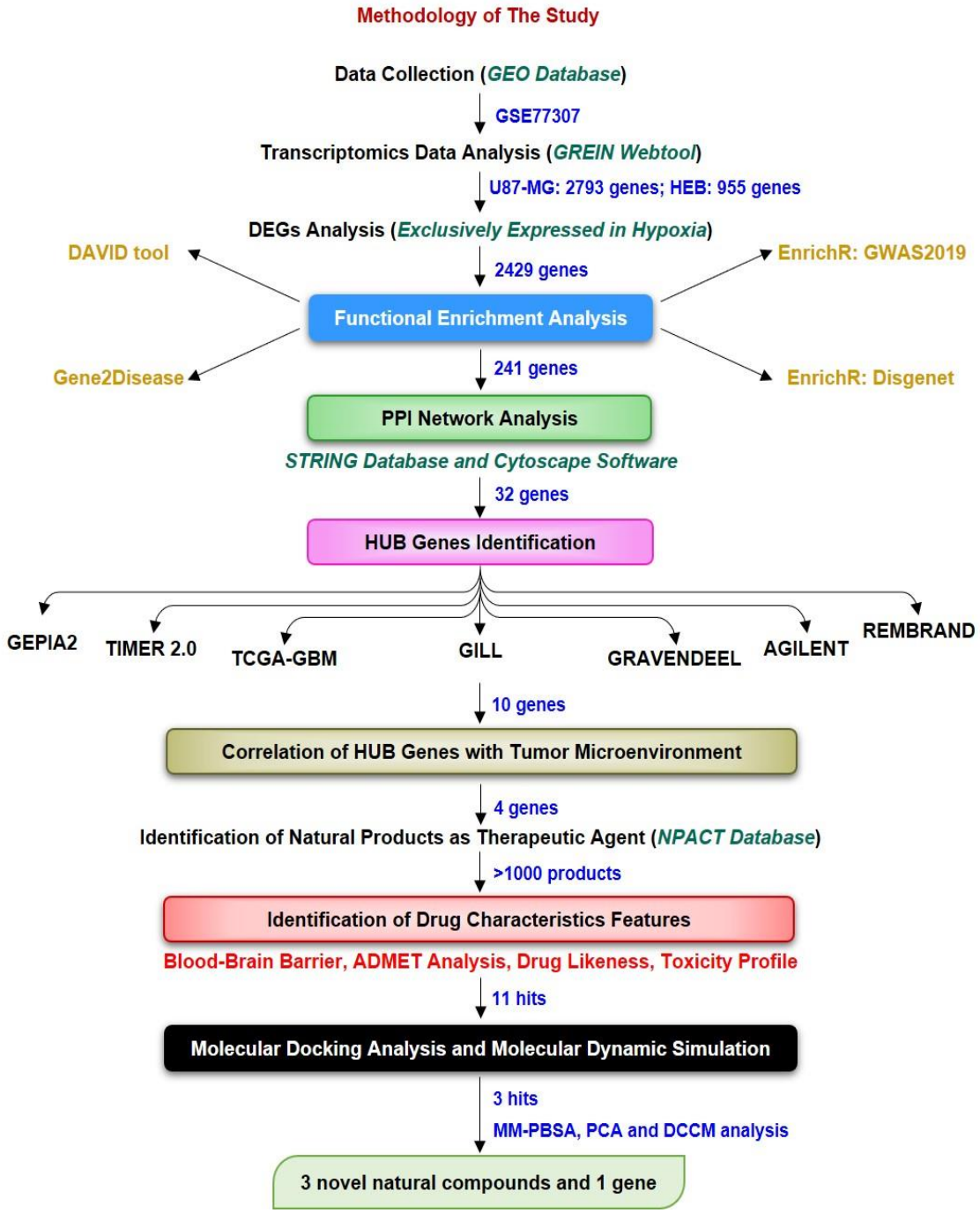

Figure 3.1: Workflow Scheme for Identification of Hypoxic Biomarkers and Novel Natural Compound (Target) Against GBM-Hypoxia Microenvironment.

3.1. MATERIAL AND METHODS

3.1.1. DATASET ACQUISITION AND PROCESSING

The NCBI-GEO (NCBI-GEO; https://www.ncbi.nlm.nih.gov/geo) database [530] is a publicly accessible library of next-generation sequencing, RNA sequencing, and microarray profiling was used to gather GBM and non-neoplastic brain tissue gene expression profiles from GEO

accession number, GSE77307. The transcriptome data in GSE77307 was derived from GPL11154, a platform using Illumina HiSeq 2000 (Homo sapiens). This included the three replicates of each U87-MG cell line as a human GBM cancer cell model and the human brain HEB cell line as a non-neoplastic brain cell model cultured in 21% Oxygen (normoxia) and 1% Oxygen (hypoxia) for transcriptional profiling. This dataset was chosen due to the availability of only one dataset in the database based on the filter (Glioblastoma; Hypoxia; TME) High-throughput functional transcriptomic expression data from GSE datasets was analyzed through GEO RNA-seq Experiments Interactive Navigator online server (GREIN; https://shiny.ilincs.org/grein) [531]. GREIN is provided by the backend compute pipeline for uniform processing of RNA-seq data and large numbers (>65000) of processed data sets.

3.1.2. ENRICHMENT ANALYSIS OF IDENTIFIED DEGS

Transcriptomics data analysis was performed using the GREIN web tool. DEGs were determined by comparing their expression levels in hypoxia (1% Oxygen) versus normoxia (21% Oxygen) in GBM cells, U87-MG and normal brain cells, HEB. Statistically significant DEGs were screened using cut-off filter criteria as unpaired t-test and p-value ≤ 0.05, false discovery rate (FDR) ≤ 0.05 and [Log Fold Change] ≥ 1.5. DEGs only exclusively expressed in hypoxia conditions were considered for further analysis. In addition, enrichment analysis of DEGs, including both upregulated and downregulated genes associated with GBM, was performed by utilizing different omics approaches such as the Database for Annotation, Visualization and Integrated Discovery (DAVID) functional annotation tool (https://david.ncifcrf.gov/) [532], gene set to diseases (GS2D) tool (http://cbdm.uni-mainz.de/geneset2diseases) [533], Enrichr-GWAS2019 and Enrichr-DisGeNET of Enrichr tool (https://amp.pharm.mssm.edu/Enrichr) [534], [535] to identify and prioritize the most significant genes associated with GBM. Furthermore, biological pathway and functional enrichment analysis of candidate DEGs and hub genes were determined through a freely

available software known as the FunRichr tool (version 3.1.3) (http://www.funrich.org/) [536] to identify biological pathways associated with them.

3.1.3. INTEGRATION OF PROTEIN-PROTEIN INTERACTION NETWORK AND HUB GENES IDENTIFICATION

The selected enriched genes were then examined for designing PPI using an online Search Tool for the Retrieval of Interacting Genes/Proteins (version 11.5) (STRING, https://string-db.org/) for Homo sapiens [537] that covers known and predicted interactions for different organisms. The experimentally significant interactions (with high confidence scores ≥ 0.700) were chosen to build a network model, while the others were excluded from the analysis. Cytoscape software (Version 3.8.1) (https://cytoscape.org/) [538] was implemented to analyze the PPI network and identify hub protein. To calculate topological parameters such as node degree (the number of connections to the hub in the PPI network) and betweenness (which corresponds to the centrality index of a particular node), we used the CentiScaPe plugin (Version 2.2). It denotes the shortest route between two nodes. Genes with higher values than the average score were chosen

3.1.4. HUB PROTEIN SHORTING AND VALIDATION

To verify and validate the expression of the shortlisted hub proteins, we have utilized both transcriptomics and genomics data from GBM patients. Different databases were explored for RNA sequencing data such as (GEPIA2.0, TIMER2.0, TCGA-GBM, GlioVis-GILL) and microarray data such as (GlioVis-REMBRANDT, GlioVis-AGILENT and GlioVis-Gravendeel) based on Cancer Genome Atlas (TCGA)-GBM [539]–[541]. GEPIA2.0 analyzed the RNA sequencing expression data of 9,736 cancers and 8,587 normal samples from the TCGA and GTEx projects using a standard processing pipeline. GlioVis is a user-friendly web tool that allows users to study brain tumor expression datasets through data visualization and analysis. GlioVis-GILL: Gill et al. conducted RNA-seq and histological examination on

radiographically labeled biopsies collected from different regions of GBM [542]. GlioVis-Repository of Molecular Brain Neoplasia Data (REMBRANDT), a cancer clinical genomics database and a web-based data mining and analysis platform, includes data produced from 874 glioma specimens with approximately 566 gene expression arrays and 834 copy number arrays generated through the Glioma Molecular Diagnostic Initiative [543]. In GlioVis-Gravendeel, gene expression profiling was carried out on a large cohort of glioma samples from all histologic subtypes and grades [544]. In TIMER2.0, Multiple immune deconvolution algorithms are used to assess the quantity of immunological infiltrates. Its Gene DE module allows users to investigate the differential expression of any gene of interest in tumors and surrounding normal tissues across all TCGA tumors. All hub genes significantly expressed in all seven patient GBM databases were chosen for subsequent research. Finally, shortlisted genes were again subjected to Tumor IMmune Estimation Resource (TIMER) (https://cistrome.shinyapps.io/timer) [545] analysis. Here, we utilized this database to link hub gene expression with tumor purity and estimate infiltration levels of six immune cell types (CD4+ T cells, CD8+ T cells, B cells, macrophages, neutrophils, and dendritic cells) in GBM datasets. This tool calculates immune infiltration based on immune subsets' preset characteristic gene matrix.

3.1.5. LOCALIZATION STUDY AND CONSTRUCTION OF TRANSCRIPTION FACTOR-GENE NETWORK

CELLO (http://cello.life.nctu.edu.tw/cello.html): subcellular localization predictor combines a two-level support vector machine (SVM) system and the homology search method-based tool to predict the subcellular localization of protein [546]. Identify regulatory Transcription factors (TFs) that control the expression of genes at the transcriptional level were obtained using the JASPAR database, containing curated and non-redundant experimentally defined TF binding sites [547]. The TF-gene interaction networks were constructed and analyzed with

NetworkAnalyst (version3.0) (https://www.networkanalyst.ca/) [548].

3.1.6. IDENTIFICATION OF NATURAL COMPOUNDS AND BLOOD-BRAIN PERMEABILITY PREDICTION

The plant-derived natural compounds with known anti-cancer bioactivity information were obtained from a literature survey through PubMed and the central resource Naturally Occurring Plant-based Anti-cancer Compound-Activity-Target database (NPACT, http://crdd.osdd.net/raghava/npact/) [549]. This database, which presently has 1574 compound entries, collects information on experimentally confirmed plant-derived natural compounds with anti-cancer action (*in vitro* and *in vivo*). We have chosen terpenoids (513 entries), flavonoids (329 entries), alkaloids (110 entries), polycyclic aromatic natural compounds (63 entries), aliphatic natural compounds (20 entries), tannin (6 entries). BBB obstructions make it difficult to create drugs to treat brain cancer. The BBB blocks the uptake of necessary therapeutic drugs into the brain. The epithelial-like tight connections seen in the brain capillary endothelium are the source of this characteristic. For the treatment of GBM, it is crucial to screen drugs that have the ability to cross the BBB [550]. While designing a drug for brain diseases, physicochemical properties and brain permeation properties should be optimized. In consideration of this challenge, we analyzed our candidate natural compounds for physicochemical properties using the SwissADME (http://www.swissadme.ch/) [551] analysis tool and CBLigand (version 0.90) online BBB predictor (https://www.cbligand.org/BBB/) [552].

3.1.7. PREDICTION OF MOLECULAR PROPERTIES AND DRUG TOXICITY

Each natural compounds molecular formula (MF), molecular weight (MW), hydrogen bond acceptor (HBA), hydrogen bond donor (HBD), logP value, and SMILES were retrieved using the PubChem chemical database (https://pubchem.ncbi.nlm.nih.gov/). The Lipinski rule of five was used to estimate the druggability of each phytocompound using the SMILES data of

individual compounds on the MolSoft web server (https://molsoft.com/mprop/) [553]. The server includes structural data such as MF, MW, HBA, HBD, and logP and a drug-likeness score prediction (DLS). The toxicity and pharmacokinetics of natural compounds with positive DLS were also predicted using the ADMETlab 2.0 (https://admetmesh.scbdd.com/) webserver [554].

3.1.8. MOLECULAR DOCKING STUDIES

Preparation of ligand*:* Based on the network analysis and pharmacology approach, 11 natural compounds, viz., 6 flavonoids, 3 alkaloids and 2 terpenoids, were qualified for all the criteria required for being used as a drug candidate. Thus, the three-dimensional (3D) structures of 11 natural compounds along with 2 reference drugs (one natural compound and one conventional standard molecule) were retrieved from the PubChem database (https://pubchem.ncbi.nlm.nih.gov/) in the structure data file (.sdf) format. These structures additionally went through the dock prep section of Discovery Studio Visualizer [555] (BIOVIA Discovery Studio Visualizer; https://discover.3ds.com/discovery-studio-visualizer-download) 2019. The conjugate gradients algorithm was used to minimize the ligand structures using the 'uff' forcefield [556]. The polar hydrogens and gastigers charges were added to the ligands to convert them into the ".pdbqt" format.

Preparation of protein: Based on network analysis and TIMER analysis the overexpressed MMP9 gene associated with TME that was prioritized for future investigation. The Research Collaboratory for Structural Bioinformatics (RCSB; https://www.rcsb.org/) protein data bank was used to retrieve the x-ray crystallographic structure of MMP9 (PDB: 4HMA). Further, the PrankWeb (https://prankweb.cz/) server based on P2Rank, a machine learning method, was used to retrive the information on target active site and binding pockets, and the ligand was docked within the predicted site. Functional characteristics of protein structures was validated using Ramachandran plot, ERRAT and VERIFY3D [557]–[559]. For a good quality model,

the ERRAT quality factor should be greater than 50, and the number of residues having a score ≥ 0.2 in the 3D/1D profile, as predicted by the VERIFY3D server, should be more than 80%.

Protein-ligand docking: All ligands were docked against protein using AutoDock vina 4.0 executed through POAP pipeline [560]. The intermolecular interaction compounds showing the least binding energy and maximum intermolecular interaction with active site residues were selected to visualize protein-ligand interactions using BIOVIA Discovery Studio Visualizer 2019 and further subjected for MD simulation.

3.1.9. MOLECULAR DYNAMICS (MD) SIMULATION OF BEST-DOCKED PROTEIN-LIGAND COMPLEX

In order infer the stability of docked complexes, we prioritized five complexes (3 test and 2 standard complexes) and subjected for all-atoms explicit MD simulation for 50ns production run using GROMACS version 2021.3 software package (GNU, General Public License; http://www.gromacs.org) [561]. The ligand and protein topology were generated using Amber ff99SB-ildn force field (https://ambermd. org/AmberTools.php) *via* antechamber x-leap tool. The system was solvated using TIP3P water model in an orthorhombic box with a boundary condition of 10.0 Å from the edges of the protein in all directions. The system was neutralized by adding necessary amounts of counter ions. The conjugate gradient approach was employed to obtain the near-global state least energy conformations after the steepest descent. Canonical (Constant temperature, constant volume, NVT) and isobaric (Constant temperature, constant pressure, NPT) equilibration was performed on the systems for 1 ns. A modified Berendsen thermostat method was used in NVT equilibration to keep both the volume and temperature constant (300 K). Similarly, a Parrinello-Rahman barostat was used during NPT equilibration to keep the pressure at 1 bar constant. The Particle Mesh Ewald approximation was used with a 1 nm cut-off to calculate the long-range electrostatic interactions, van der Waals interactions, and coulomb interactions. In order to control bond length, the LINCS algorithm (LINear

Constraint Solver algorithm) was utilized. The coordinates were recorded every two fs during each complex's production run of 50 ns. In-built GROMACS utilities were used to evaluate the generated trajectories, and other software packages were incorporated where necessary for more specialized analysis. MD trajectories were analysed to determine the c-alpha root mean square fluctuations (RMSF) and root mean square deviation (RSMD) of backbone and complex, protein radius of gyration (Rg), protein Solvent-accessible Surface Area (SASA) and the number of hydrogen bonds (NHB) between protein-ligand.

3.1.10. INVESTIGATION OF BINDING AFFINITY USING MOLECULAR MECHANICS POISSON–BOLTZMANN SURFACE AREA (MM-PBSA)

It is standard procedure to use the relative binding energy of a protein-ligand complex in MD simulations and thermodynamic calculations. MM-PBSA was performed by "g_mmpbsa" tool [562]. The total free energy of each of the three entities (ligand, protein receptor and complex) mentioned can be calculated by adding the potential energy of the molecular mechanics and the energy of solvation. Early research work [563], [564] was used to obtain parameter that was used to determine the binding energy.

Equation 1: Equation $\Delta G(\text{Binding}) = G(\text{Complex}) - G(\text{Protein}) - G(\text{Ligand})$

where “G (complex) is the total free energy of the ligand-protein complex, G(protein) and G(ligand) are total free energies of the isolated protein and ligand in the solvent, respectively. The binding energy was calculated over the stable trajectory observed between 50 ns using 50 representative snapshots.

3.1.11. PRINCIPAL COMPONENT AND DYNAMICS CROSS-CORRELATION MATRIX ANALYSIS

Principal component analysis (PCA) was used in the current work to analyze the main types of molecular motions utilizing MD trajectories. It is employed to study the eigenvectors, which are crucial to understanding the overall movements of proteins during ligand binding. The

"least square fit" to the reference structure is used to eliminate the molecule's translational and rotational mobility. The "time-dependent movements" that the components carry out in a specific vibrational mode are demonstrated by projecting the trajectory onto a particular eigenvector. The average of the projection's time signifies the involvement of atomic vibration components in this form of synchronized motion. Using the "g_covar" and "g_anaeig" tools, which are already included in the GROMACS software package, the PCA was performed by first creating the covariance matrix of the Cα -atoms of the protein and then diagonalizing it. The *xmgrace* tool was used to plot the graphs [565]–[567].

To determine if motion between atom pairs is correlated (positive or negative), the dynamic cross-correlation matrix (DCCM) measures the magnitude of all pairwise cross-correlation coefficients. Herein, we investigated each element of DCCM, where $C_{ij} = 1$, where in the case of positively correlated the fluctuations of atoms *i* and *j* have the same period and same phase, while $Cij = -1$ and $Cij = 0$, respectively, represent negatively or not correlated [568], [569].

3.1.12. STATISTICAL ANALYSIS

This study investigated the expression of hub genes in the GEPIA2.0 database and their connection with GBM using ANOVA. $|Log_2FoldChange|$ cutoff ≤ 1.5 and Q-value ≤ 0.05 were considered significant. Tukey's Honest Significant Difference (HSD) statistics were employed in the GlioVis database, where the p-value of the pairwise comparisons was used (***p≤0.001; **p≤0.01; *p≤0.05; ns, not significant). In TIMER2.0, the Wilcoxon test's statistical significance was indicated by the number of stars (***p≤0.001; **p≤0.01; *p≤0.05; ns, not significant). In the TIMER database analysis, a partial Spearman's correlation was applied. When |Rho| > 0.1, it indicated a correlation between the genes and immune cells. Significant data in biological and KEGG pathway enrichment were screened according to p-value ≤ 0.05 with students' t-test.

3.2. RESULTS

3.2.1. OMICS DATA MINING AND IDENTIFICATION OF DEGS IN GBMS HYPOXIA CONDITION

This study used the expression profile (GSE77307) from the NCBI-GEO database to identify DEGs exclusively expressed in hypoxia-induced GBM because targeting the hypoxic microenvironment could be a new tool for treatment [521]. Cells derived from GBM patient tumors and normal brain tissue were grown in hypoxic and normoxic conditions. GEO's raw RNA sequence (RNA-seq) data were processed and uploaded to GREIN using the GEO RNA-seq experiments processing (GREP2) pipeline. GREIN workflows with a graphical user interface (GUI) provide complete interpretation, visualization and analysis of processed datasets [570]. A normalized MA plot has been shown in **Annexure 1(A).** GBM cancer cell model (U87-MG) and the human non-neoplastic brain cell model (HEB) were analyzed separately by comparing hypoxia with normoxia conditions to find dysregulated genes in hypoxia conditions. Subsequently, Venn's analysis demonstrated the involvement of 364 genes that were common in hypoxia conditions in both cell lines. 591 and 2429 genes expressed exclusively in hypoxia conditions in HEB and U87-MG cell lines, respectively [571]. Among them, we were interested in 2429 hypoxia-related DEGs exclusively expressed in hypoxia conditions and hence were considered for further analysis **(Figure 3.2(A)).**

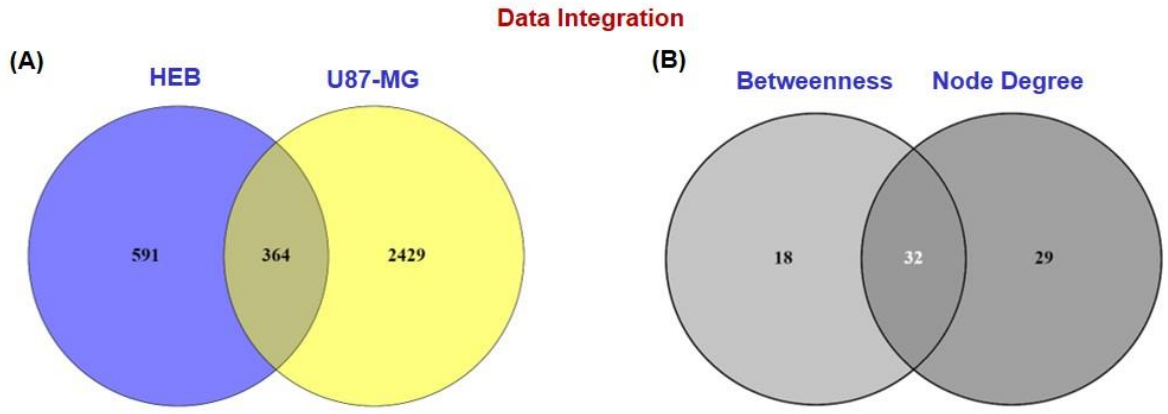

Figure 3.2: Interactive Venn Analysis: (A) Identification of DEGs in GBM-hypoxia microenvironment. A total 2429 altered DEGs exclusively expressed in hypoxia were identified from GSE77307 dataset using GREIN tool.The 'cross areas' are common DEGs in both cell lines. The cut-off criteria were p value≤0.05 and [log Fold Change] ≥ ±1.5. (B) A total of 32 hub genes among topology parameters (betweenness and degree) were identified from Cytoscape software. The 'cross areas' are common hub genes.

DAVID enrichment analysis of 2429 genes revealed that 30 genes have a significant association with GBM. In addition, G2SD enrichment (default cut-off parameter) showed 25 genes related to GBM. Similarly, GWAS-2019 and DisGeNET of Enrichr webtool enrichment analysis showed 3 and 242 genes linked with GBM, respectively. When we integrated the three enrichment analysis methods, a total of 241 GBM-related DEGs were documented, including 129 upregulated genes and 112 downregulated genes. **(Table 3.1).**

Table 3.1: List of Differentially Expressed Genes (DEGs) Exclusive Expressed in Hypoxia Condition in Glioblastoma Multiforme

129 Upregulated genes				112 Downregulated genes			
Gene	*Fold change*	*Gene*	*Fold change*	*Gene*	*Fold change*	*Gene*	*Fold change*
ABCB6	1.594	IGFBP5	4.937	ABCG2	-2.432	LYN	-2.247
ACKR3	3.375	IL1A	4.663	AIFM1	-1.845	MAP2K6	-2.69
ADGRB1	10.867	IL24	2.997	AIMP2	-1.65	MELK	-2.523
ADIPOQ	2.264	IL32	3.297	AKR1B10	-2.847	MKI67	-1.758
AGXT	2.537	IL6	3.459	AQP9	-2.14	MMP15	-1.877
ANGPT4	1.879	IRS2	1.963	AR	-2.118	MSH2	-1.643
ANGPTL6	3.868	ITGA6	2.382	ARHGEF26	-2.737	NCF2	-1.565
APOE	2.037	JAG2	2.005	ATAD3A	-1.628	NEU1	-2.229
AQP1	2.381	JUNB	1.777	ATR	-1.963	NMI	-2.054
ATF3	1.864	KCNH2	13.868	AURKA	-1.687	NOLC1	-1.989
BCL6	1.512	KCNJ3	2.315	AURKB	-1.982	NPAS3	-1.565
BMP7	1.759	KLF8	1.594	BATF2	-1.65	NTN4	-2.456
BRS3	4.442	L1CAM	4.383	BCL2	-2.275	OIP5	-1.841
CCL3	2.091	LRRFIP1	1.515	BEX1	-1.832	ORAI1	-1.752
CCL4	2.4	MARCKS	2.229	BMPR1B	-1.648	PAX6	-2.704
CCND2	4.128	MATK	1.766	BRCA1	-2.158	PBK	-1.85
CCR10	1.796	MMP9	2.144	BUB1B	-1.717	PCNA	-2.445
CDKN1B	1.572	MSI1	4.443	CASP1	-2.4	PKMYT1	-2.692
CDKN1C	5.597	MST1	1.682	CCL2	-1.976	PLAU	-4.532
CEBPD	1.781	NCAM1	1.762	CCNB1	-1.869	PLK1	-1.544
CHST15	8.202	NCR1	3.738	CD24	-2.632	PLK2	-2.004
CHSY1	1.596	NGF	3.011	CDC20	-2.102	PNO1	-1.594
CIC	1.629	PAX5	3.123	CDC25B	-1.904	PNP	-1.514
COL18A1	3.346	PDE4D	2.107	CDC42BPG	-2.018	POLE	-1.866
COL4A3	2.483	PDK3	1.86	CDH5	-3.748	PPARG	-2.047
CRISPLD2	2.004	PFKFB3	2.227	CDK15	-1.993	PRPS1	-1.948

CRYAB	2.071	PIWIL1	3.387	CDK2	-1.738	PSMB9	-2.096
CSF2	1.637	PLAGL1	1.526	CDS1	-2.265	RAD51	-2.532
CTNNA3	2.544	PLEK	1.817	CENPU	-2.946	RAVER2	-1.512
CYP2E1	1.608	PRKCB	7.352	CHAF1A	-2.07	RECQL4	-1.54
DBH	7.641	PROM1	1.747	COL4A1	-2.67	RFC4	-2.044
DCN	1.695	PRSS55	2.862	COX2	-1.573	SEMA3D	-2.442
DDR1	3.135	PTGS2	1.842	CPT1A	-1.749	SLC7A11	-2.733
DEPP1	4.692	PTPRU	2.062	CYB561	-2.009	SLC7A4	-1.588
DUOXA1	2.617	RARRES2	2.861	CYP19A1	-1.546	SMC1A	-1.706
EDN1	2.635	RCAN1	3.969	DKK1	-2.467	SOCS1	-1.896
EEF1A2	5.736	SALL2	5.194	DNMT1	-1.619	STAT1	-1.715
EFNB1	1.517	SIK1	1.537	E2F1	-2.624	SYT1	-1.569
EIF4EBP1	1.871	SIRPA	3.018	ELAVL2	-2.106	TACC3	-1.724
EPHA3	4.802	SLC16A8	2.634	EPHB2	-1.991	TACR1	-2.317
ETS1	2.261	SLC17A7	1.828	EPS8	-1.52	TLR4	-2.289
F3	4.345	SLC27A3	2.025	ERBB4	-2.665	TNFSF12	-2.762
FGF2	2.458	SLC2A14	3.989	EXO1	-3.654	TPX2	-1.827
FGFR4	2.542	SLC38A3	3.022	F2RL1	-4.432	TRPV2	-4.658
FLT1	2.519	SLC7A5	1.987	FABP5	-2.082	TTK	-1.651
FLT4	1.767	SPHKAP	4.615	FPR1	-1.998	TUSC3	-2.138
FOXP3	1.536	SREBF1	1.76	GABRA1	-2.007	UHRF1	-3.195
FZD4	1.562	SYT7	6.341	GCFC2	-1.624	--	--
GHRHR	4.442	TAF1L	1.747	HBEGF	-1.623	--	--
GLUL	3.058	TAT	1.537	HGF	-1.586	--	--
GNRH1	2.455	TERT	3.256	HNRNPA1P10	-5.698	--	--
GPM6B	2.706	TF	3.656	HSPA4	-1.608	--	--
GRIA1	2.324	TIMP1	1.647	IFIH1	-1.624	--	--
HES1	2.912	TIMP3	3.974	IL31RA	-1.927	--	--
HIC1	2.213	TNFAIP3	2.656	ITK	-2.238	--	--
HLA-A	2.2	TNFRSF19	1.559	JAG1	-1.727	--	--
HLA-C	3.219	TNFSF10	1.687	KBTBD7	-2.008	--	--
HNF1A	1.681	TNFSF13B	4.161	KCNH1	-2.339	--	--
HOXA11-AS	1.684	TNS1	2.736	KIF11	-1.779	--	--
HRG	3.083	TP73	4.984	KIF20B	-1.657	--	--
ICAM1	3.426	TREH	3.5	KITLG	-2.562	--	--
ID2	2.246	TYRP1	2.402	KPNA2	-1.601	--	--
IGF2BP1	1.906	WNK2	3.736	LAMC2	-2.477	--	--
IGFBP1	3.265	WNT3A	5.192	LRIG3	-3.287	--	--
		ZFP42	1.52	LRRC4	-3.02	--	--

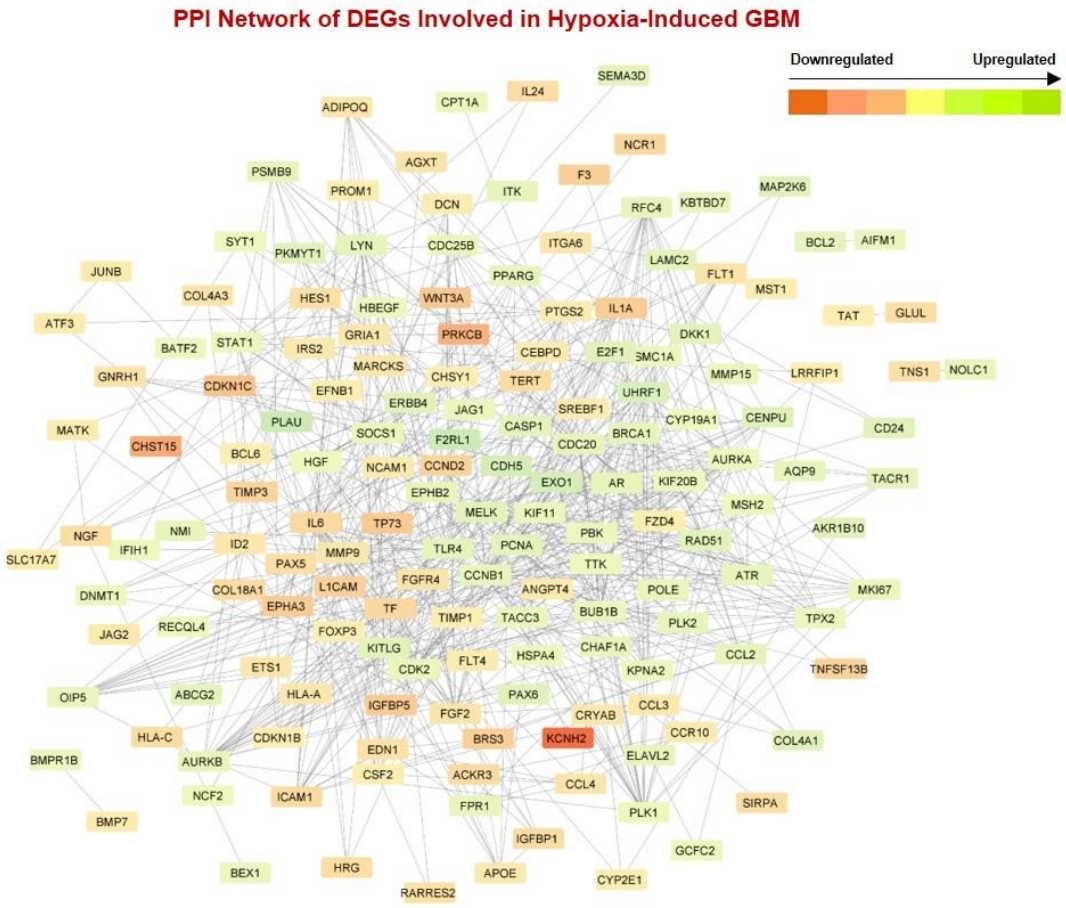

Figure 3.3: PPI Network Complex and Modular Analysis. Module 1: A total of 241 DEGs (129 upregulated genes and 112 downregulated genes) were filtered into the DEGs PPI network complex using STRING and Cytoscape software. It was composed of 163 nodes and 592 edges. DEGs: Differentially expressed genes; PPI: Protein-protein interaction; STRING: Search Tool for the Retrieval of Interacting Genes/Proteins database

3.2.2. PROTEIN-PROTEIN INTERACTION ANALYSIS AND EXPLORATION OF HUB SIGNATURES IN HYPOXIA-INDUCED GBM

With the help of the STRING database on Cytoscape software, we have evaluated the PPI network comprising 241 DEGs based on co-expression to explore the possibility of hub genes. The network consists of 163 nodes and 592 edges with a high confidence score of ≥ 0.700. Molecular signatures in the network were displayed based on their expression (green for up-regulation, red for down-regulation) and intensity based on fold change (Log Fold Change, value: -6 to +14). To evaluate the importance of nodes in the PPI network, the topological parameter, including degree centrality and betweenness centrality were calculated and utilized in the present study using the CentiScaPe plugin in Cytoscape software to find hub genes. We

observed degree with a range of 1 to 14 and betweenness with a range of 0 to 684. Using the online Venny 2.0 tool, we observed the exchange and generated a Venn plot between "degree and "betweenness" **(Figure 3.2(B)).** The 32 hub genes, a small number of critical nodes for the protein interactions in the PPI network, were chosen with a degree centrality > 7.00 (average value) and betweenness centrality > 342 (average value). PPI networks for DEGs and hub genes were shown in **Figure 3.3 and Figure 3.4,** respectively.

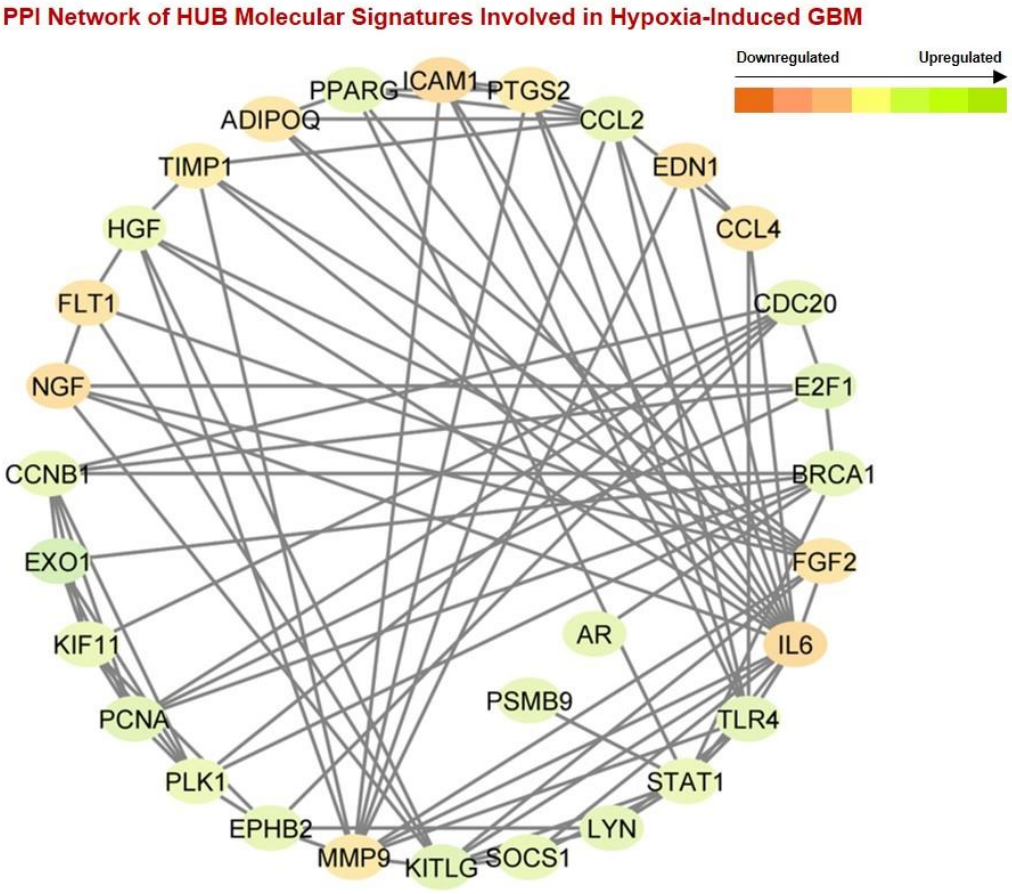

Figure 3.4: PPI Network Complex and Modular Analysis. Module 2 showed PPI network of 32 hub genes. Nodes in green signified upregulation and nodes in red signified downregulation. The colors from red to green represent the intensities of expression (log foldchange) where red represents downregulation and green represents upregulation.

3.2.3. VALIDATION OF HUB SIGNATURES IN GBM-PATIENTS

We conducted the expression analysis of all 32 HUB signatures using various online web servers for RNA sequencing data such as (GEPIA2.0, TIMER2.0, TCGA-GBM, and GlioVis-GILL) and microarray data such as (GlioVis-REMBRAND, GlioVis-AGILENT and GlioVis-Gravendeel). These web servers from the TCGA project provide extensive information

concerning GBM patients. The expression of all 32 genes was examined using the databases described above as described in **Table 3.2.** Based on selection criteria (***p≤0.001; **p≤0.01; *p≤0.05; ns, not significant), 10 genes out of 32 exhibited significant expression levels in both RNA and microarray databases of GBM patient samples. This also explains these 10 molecular signatures, namely BRCA1, CCNB1, CDC20, EXO1, KIF11, LYN, MMP9, PCNA, PSMB9, TIMP1 were expressed in GBM tumor samples**.** Molecular function of these signatures and its role in various malignancy has been briefly explained here. Breast Cancer Gene 1 (BRCA1) is a tumor suppressor protein that is essential for DNA damage repair, chromatin remodeling, and cell cycle regulation. Mutations in BRCA1 cause genetic changes, cancer, and a failure to repair DNA damage. Patients with BRCA1 germ line mutations have been associated with sporadic instances of GBM [572]. Cyclin B1 (CCNB1) and cell division cycle protein 20 (CDC20), both of which are associated with cell progression, demonstrated that their increased expression was substantially correlated with poor survival in GBM [573]. Exonuclease 1 (EXO1) is a member of the DNA damage repair enzyme family that is particularly active in homologous recombination (HR) and non-homologous end-joining (NHEJ) following DNA double strand breaks. It increases cell proliferation, invasion, and metastasis in glioma and HCC [574]. According to Liu et al, increased Kinesin family member 11 (KIF11) enhances cell cycle development and chemoresistance, negatively correlates with TP53 expression, and is a major cause of malignancy in GBM [575]. Lck/yes-related protein tyrosine kinase (LYN) showed a substantial positive connection with PD-L1, was connected to the control of carcinogenic genes, and was engaged in tumor mutation. In gliomas, LYN may serve as both a potential diagnostic and immunotherapy marker[576]. Likewise, the proliferative capacity of cells is impacted by high MMP9 expression in gliomas, which is also linked to patient survival rates [577]. Proteasome 20S Subunit Beta 9 (PSMB9), along with PSMB8 and PSMB10 genes that encode catalytic subunits of the immunoproteasome, was overexpressed in GBM and was

reported by Liu et al. as a novel biomarker for lower-grade glioma (LGG) prognosis and can be exploited as an immunotherapy target [578]. Similarly, a study by Smith et al, demonstrated that Proliferating Cell Nuclear Antigen (PCNA) a nuclear DNA replication and repair protein, has increased expression, poor prognosis in Pancreatic ductal adenocarcinoma [579]. Last but not least, tissue inhibitor of metalloproteinases-1 (TIMP-1) is known to control the proteolytic activity of the matrix metalloproteinases (MMPs) that break down ECM. High tumor TIMP-1 protein expression in GBM has been linked to Irinotecan resistance and anticipated to predict lower overall survival in GBM [580]. Thus, only 10 molecular signatures were selected for the further analysis that were significantly expressed in all seven patient GBM databases.

Table 3.2 *In Silico* Expression Analysis and Validation of All 32 HUB Signatures Using Various Databases Containing Data from GBM Patient Samples

Gene Name	RNA sequence dataset		Microarray datasets				
	GEPIA2	TIMER2.0	GlioVis				
			TCGA_GBM	GILL	REMBRANDT	AGILENT-4502a	Gravendeel
ADIPOQ							
AR							
BRCA1							
CCL2							
CCL4							
CCNB1							
CDC20							
E2F1							
EDN1							
EPHB2							
EXO1							
FGF2							
FLT1							
HGF							
ICAM1							
IL6							
KIF11							
KITLG							
LYN							
MMP9							
NCAM1							
NGF							
PCNA							
PLK1							
PPARG							
PSMB9							

PTGS2							
SOCS1							
STAT1							
TF							
TIMP1							
TLR4							
SAMPLE SIZE							
GBM TUMOR	163	156	75	153	219	489	159
NORMAL TISSUES	207	4	17	5	28	10	8

3.2.4. CORRELATION BETWEEN HUB SIGNATURES AND GBM TUMOR MICROENVIRONMENT

Here, in this study, to filter out molecular signatures involved in TME, we used the TIMER database to investigate the connection and correlation of 10 molecular signatures (BRCA1, CCNB1, CDC20, EXO1, KIF11, LYN, MMP9, PCNA, PSMB9, TIMP1) expression with tumor purity and immune cell infiltration in patients with hypoxia-induced GBM. Data has been compiled in **Figure 3.5(A).** In addition, we used GBM datasets to estimate the amounts of infiltration of six immune cell types (CD4+ T cells, CD8+ T cells, B cells, macrophages, neutrophils, and dendritic cells). Tumor purity normalized spearman correlation analyses revealed a positive and negative correlation expression of hub genes with B cells, CD4+ T cells, $CD8^+$ T cells, macrophages, neutrophils, and dendritic cells (DCs) in GBM cancer. After the inputs are successfully entered, scatterplots will be created and displayed, displaying the purity-corrected partial Spearman's rho value (ρ) and statistical significance. Genes with negative associations with tumor purity are highly expressed in TME, and positive associations are highly expressed in the tumor cells. Finally, we discovered four molecular signatures (LYN, MMP9, PSMB1 and TIMP1) with negative tumor purity, and it implicated in GBM's hypoxic microenvironment. **Figure 3.5(B)** illustrating scatterplot showing the relationship between LYN, MMP9, PSMB9, and TIMP1 gene expression and tumor purity and six key tumor infiltrating immune cell types in GBM. LYN expression shown positive correlation with B cells ($\rho = 0.28$, $p<0.001$), CD8+ T cells ($\rho = 0.23$, $p<0.001$), macrophages ($\rho = 0.24$, $p<0.001$),

neutrophils ($\rho = 0.39$, $p<0.001$), and DCs ($\rho = 0.49$, $p<0.001$) and negatively correlation with $CD8^+$ T Cell ($\rho = -0.35$, $p<0.001$) in GBM. MMP9 shows positive correlation with DCs ($\rho = 0.33$, $p<0.001$) and negatively correlation with CD8+ T Cell ($\rho = -0.18$, $p<0.001$). PSMB9 showed positive correlation with B cells ($\rho = 0.32$, $p<0.001$), macrophages ($\rho = 0.99$, $p<0.001$), neutrophils ($\rho = 0.15$, $p<0.001$), and DCs ($\rho = 0.22$, $p<0.001$) and negatively correlation with $CD8^+$ T Cell ($\rho = -0.21$, $p<0.001$). A study by Wang et al., showed that cancer derived MMP9 plays an crucial role in development of tolerogenic DCs which further affects Treg in case of laryngeal cancer [581]. Similarly, mounting evidence suggested that MMP9 was involved in cancer-related inflammation by proteolyzing extracellular signal proteins, primarily those belonging to the CXC (C-X-C motif) chemokine family. As a result, MMP9 is regarded as a key architect and organizer of the tumor immune microenvironment [582]. Lastly TIMP1 expression linked positively with DCs ($\rho = 0.54$, $p<0.001$) and negatively correlation with B cells ($\rho = -0.11$, $p<0.001$) and neutrophils ($\rho = -0.11$, $p<0.001$).

(A) Correlation Analysis of 10 HUB Molecular Signatures with GBM Tumor Microenvironment

Gene Name	Variable	Purity	B Cell	CD8+ T Cell	CD4+ T Cell	Macrophage	Neutrophil	Dendritic Cell
BRCA1	partial.correlation	0.312	-0.132	0.042	0.090	0.048	0.149	0.090
	p-value	0.000	0.007	0.396	0.066	0.327	0.002	0.065
CCNB1	partial.correlation	0.347	-0.069	0.011	-0.161	-0.069	-0.038	0.070
	p-value	0.000	0.159	0.823	0.001	0.161	0.441	0.154
CDC20	partial.correlation	0.413	-0.135	-0.056	-0.091	-0.073	-0.086	0.054
	p-value	0.000	0.006	0.257	0.062	0.136	0.078	0.267
EXO1	partial.correlation	0.487	-0.067	-0.059	-0.072	-0.052	-0.054	-0.022
	p-value	0.000	0.174	0.225	0.141	0.293	0.268	0.656
KIF11	partial.correlation	0.404	-0.098	-0.018	0.004	-0.008	0.058	0.073
	p-value	0.000	0.046	0.721	0.932	0.863	0.234	0.138
LYN	partial.correlation	-0.439	0.277	-0.358	0.232	0.241	0.399	0.500
	p-value	0.000	0.000	0.000	0.000	0.000	0.000	0.000
MMP9	partial.correlation	-0.173	-0.095	-0.186	-0.059	-0.086	0.037	0.333
	p-value	0.000	0.052	0.000	0.228	0.079	0.449	0.000
PCNA	partial.correlation	0.382	0.061	0.054	-0.108	-0.016	-0.028	0.077
	p-value	0.000	0.211	0.267	0.027	0.750	0.564	0.117
PSMB9	partial.correlation	-0.172	0.324	-0.214	-0.031	0.099	0.153	0.229
	p-value	0.000	0.000	0.000	0.527	0.042	0.002	0.000
TIMP1	partial.correlation	-0.392	-0.119	0.002	0.009	0.050	-0.120	0.547
	p-value	0.000	0.015	0.975	0.847	0.310	0.014	0.000

Spearman positive correlation (ρ>0, p<0.05) Spearman negative correlation (ρ<0, p<0.05)

(B) Correlation of 4 Molecular Signatures with Immune Infiltration in GBM

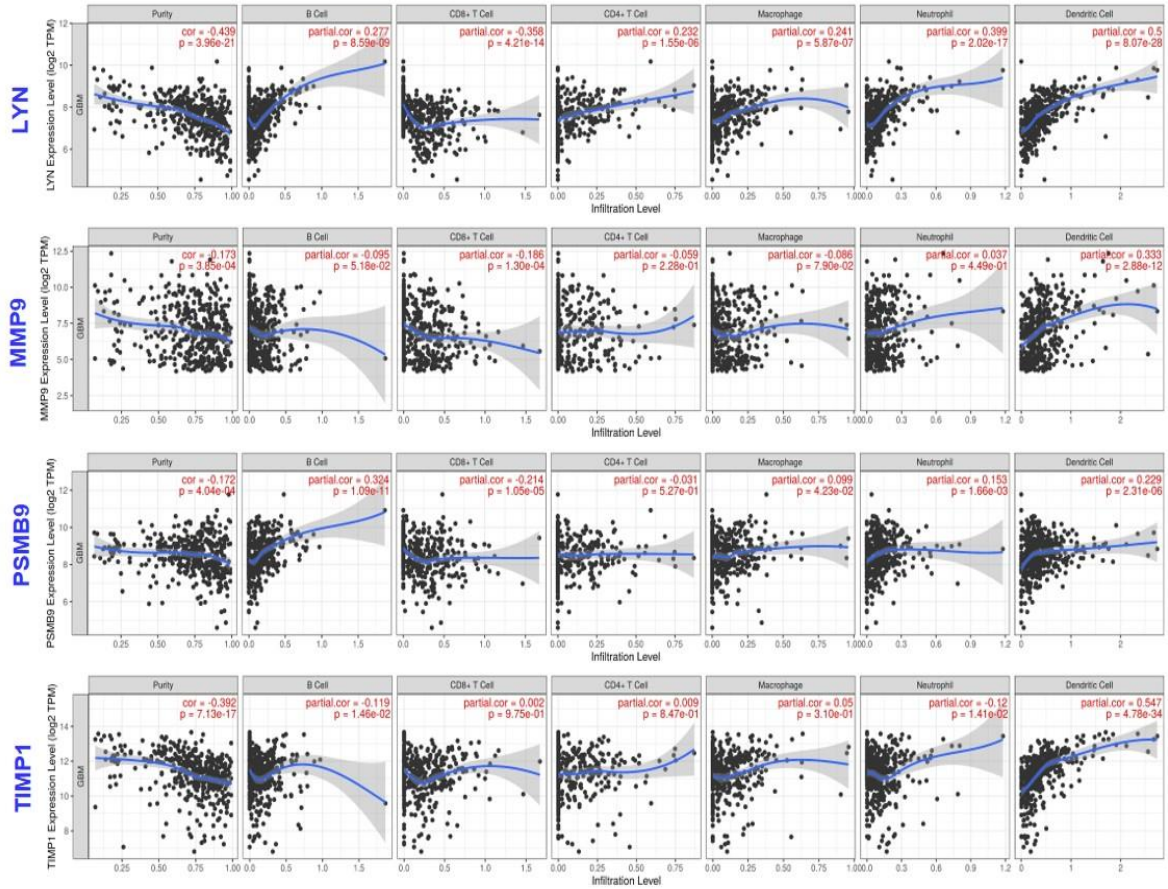

Figure 3.5: Correlation Analysis of 10 Validated Hub Genes with Tumor Microenvironment: (A) Figure showing correlation analysis of 10 validated hub genes in GBM patient's datasets with tumor purity and six tumor infiltrating immune cell (B-cells, CD8+ T cells, CD4+ T cells, Macrophages, Neutrophiles and Dendritic cells). Genes highlighted in blues showing negative tumor purity and hence shortlisted for further analysis. (B) Scatterplots from the TCGA-GBM dataset illustrating the relationship between LYN, MMP9, PSMB9, and TIMP1 gene expression and tumor purity and six key tumor infiltrating immune cell types in GBM. On the left-most panel, gene expression levels are compared to tumor purity, and genes that are highly expressed in the microenvironment are expected to have negative associations with tumor purity. In the TIMER database analysis, partial Spearman's correlation was applied. When |Rho, ρ| > 0.1 and P < 0.05, it indicated that there was a link between the genes and immune cells. In general, the smaller the Rho value is, the smoother the curve is; the larger the Rho value, the fuller the curve is; when Rho < 0.5, the curve is ellipse; when Rho = 0.5, the curve is parabola; when Rho > 0.5, the curve is hyperbola.

In contrast, BRCA1, CCNB1, CDC20, EXO1, KIF11, and PCNA showed positive correlations to tumor purity, attributed to their predominant expression and functions in tumor cells. Further, we identified the relationship between somatic cell number alteration (SCNA) and the presence of immune infiltrates of four genes **(Figure 3.6(A)).** Additionally, we have examined the connection between these molecular signatures and immune checkpoint inhibitors (ICIs), including PDCD1(PD1), CD274(PDL1), CTLA4, LAG-3 and HAVCR2 (TIM-3) **(Figure 3.6(B)).** According to data, the genes LYN, PSMB9, and TIMP1 were all positive correlation with ICIs except for LAG3, while TIMP1 was negatively correlated with LAG3. MMP9 only had a positive correlation with PD-1 and TIM-3. Therefore, we have discovered four molecular signatures, LYN, MMP9, PSMB9, and TIMP1, to target the microenvironment of GBM and to further research whether they are therapeutic targets or not. The study concluded that LYN and PSMB9 were downregulated in hypoxia-induced GBM with FC value of -2.247 and -2.096, whereas, MMP9 and TIMP1 were upregulated with Log_2 Fold Change value of 2.144 and 1.647, respectively. Thus, TIPM1 and MMP9 were selected for the identification of novel natural compounds in hypoxia-induced GBM therapeutics. However, TIMP1 lacks the approved control drug in terms of chemical compound, and hence discarded for further analysis. Thus, the current study aims to identify the novel natural compound against MMP9 in hypoxia-induced GBM

(A) Comparison of Tumor Infiltration Levels with Different Somatic Copy Number Alterations

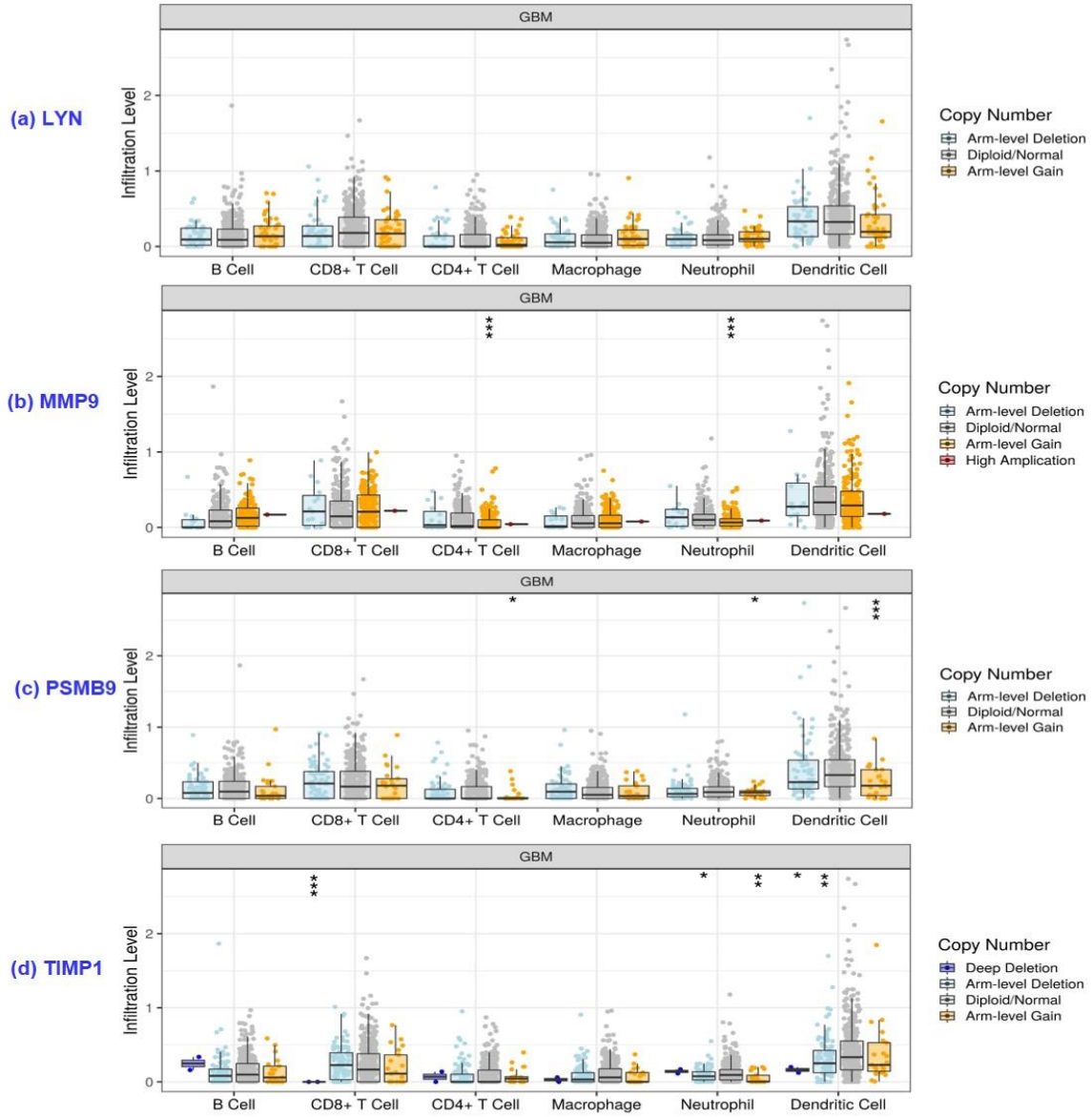

(B) Correlation Analysis of Molecular Signatures with Immune Checkpoint Inhibitors in GBM

Immune checkpoint inhibitor	PDCD1(PD1)	CD274(PDL1)	CTLA4	LAG-3	HAVCR2(TIM-3)
Biomarkers	Spearman Correlation Coefficient (ρ)				
LYN	0.39	0.4	0.46	0.088	0.77
MMP9	0.23	0.037	0.14	0.042	0.17
PSMB9	0.17	0.4	0.2	0.065	0.41
TIMP1	0.2	0.49	0.23	-0.16	0.32

Spearman positive correlation (ρ>0, p<0.05) | Spearman correlation (ρ> or<0, p>0.05) | Spearman negative correlation (ρ<0, p<0.05)

Figure 3.6: (A) The Comparison of Six Tumor Infiltration Levels (B-cells, CD8+ T cells, CD4+ T cells, Macrophages, Neutrophiles and Dendritic cells.), Among GBM with Different Somatic Copy Number Alterations for (a) LYN, (b) MMP9, (c) PSMB9, (d) TIMP1. (B) Correlation Analysis of Biomarkers with Immune Checkpoint Inhibitors including PDCD1, PDL1, CTLA4, LAG3 and TIM-3) in GBM partial Spearman's correlation was applied. When |Rho, ρ| > 0.1 and p < 0.05, it indicated that there was a link between the genes and immune checkpoint inhibitors. Color significance: Red = positive significant correlation (ρ>0; p value<0.05), Blue= negative significant correlation (ρ<0; p-value<0.05). Grey: non-significant correlation (p-value>0.05).

3.2.5. BIOLOGICAL PATHWAY ANALYSIS OF DEGS, HUB MOLECULAR SIGNATURES AND TME-RELATED SIGNATURES

Biological pathways analysis using FunRich software was performed on 241 DEGs, 32 hub genes and 4 genes involved in TME. As shown in **Figure 3.7(A)** DEGs involved in the top ten significant biological pathways were i) VEGF and VEGFR signaling, ii) Sphingosine 1-phosphate (S1P) pathways, iii) Glypican pathway, iv) ErbB receptor signaling pathway, v) Integrin family cell surface interactions, vi) TRAIL signaling pathway, vii) Plasma membrane (PM) estrogen receptor signaling, viii) Insulin Pathway, ix) Urokinase-type plasminogen activator (uPA) and uPAR-mediated signaling, x) Class I Phosphatidylinositol-3-kinase (PI3K) signaling. Similarly, analysis of 32 hubs genes enhanced in biological pathways were **(Figure 3.7(B))**: i) Glypican pathway, ii) Proteoglycan syndecan-mediated signaling, iii) VEGF and VEGFR signaling, iv) S1P pathway, v) Insulin Pathway, vi) uPA and uPAR-mediated signaling, vii) PDGFR-beta signaling, viii) ErbB1 signaling pathway, ix) Class I PI3K signaling, x) mTOR signaling pathway. In addition, we have also analyzed 4 shortlisted molecular signatures involved in TME in **Figure 3.7(C)** to understand the major pathways involved were i) Integrin-linked kinase (ILK) signaling, ii) Activating protein-1 (AP-1) transcription factor network, iii) CDC42 signaling events, iv) CXCR4-mediated signaling, v) Amb2 integrin signaling, vi) Lysophosphatidic acid (LPA) receptor-mediated. Biological pathways with p-value ≤ 0.05 and count > 2 were measured as statistically significant.

(A) Biological Pathway Analysis of DEGs

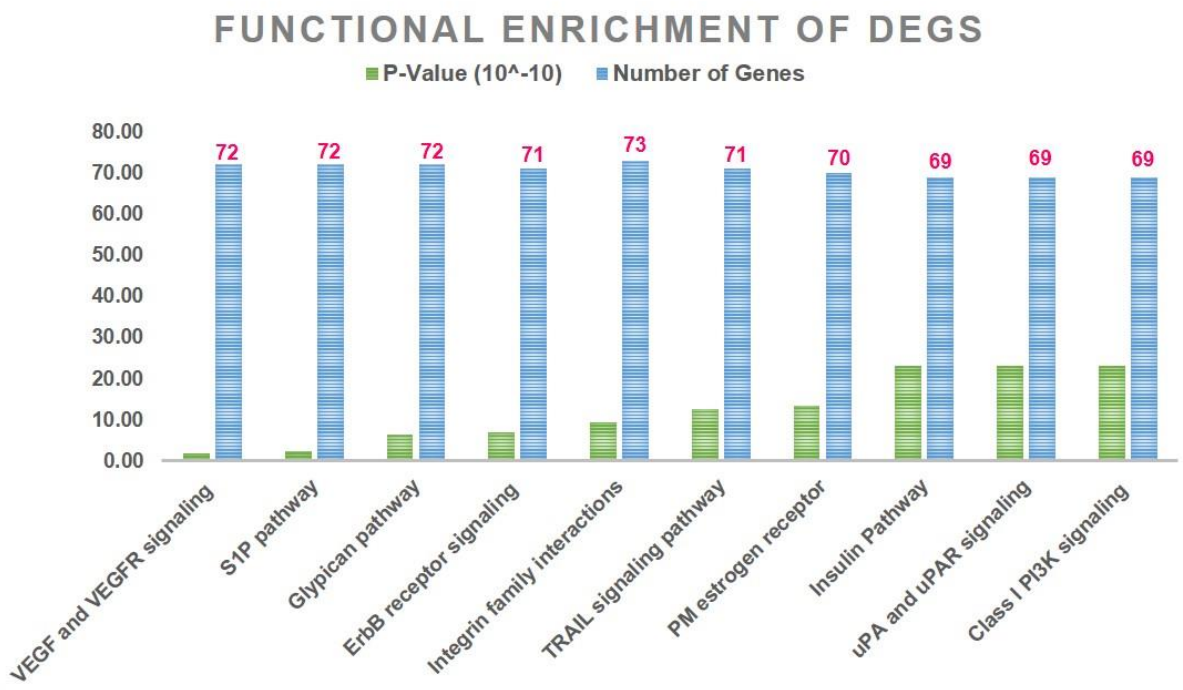

(B) Biological Pathway Analysis of 32 HUB Molecular Signatures

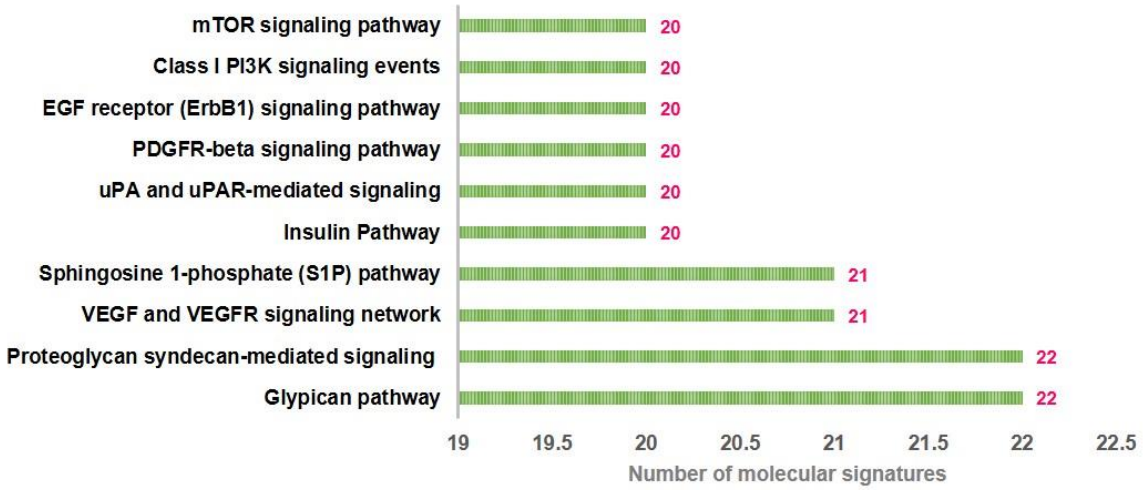

(C) Biological Pathway Analysis of TME Molecular Signatures

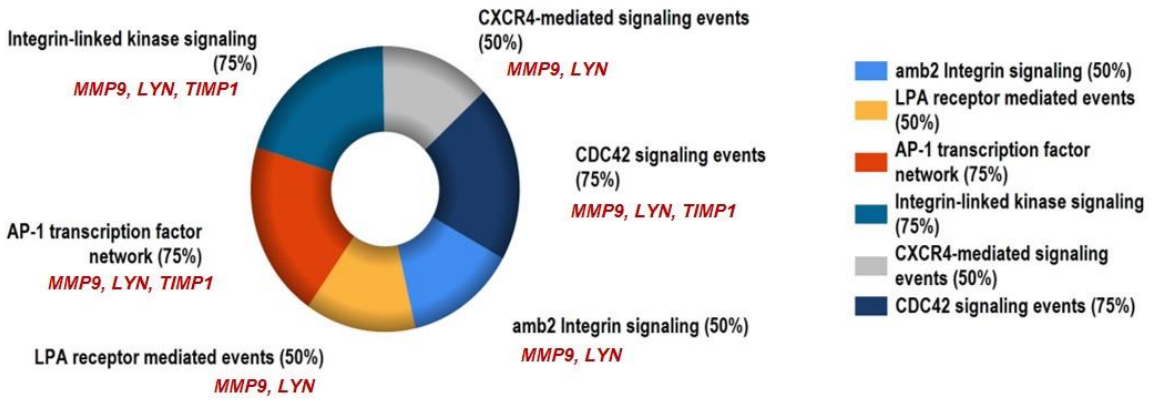

Figure 3.7: Significantly Enriched Biological Pathway Analysis: (A) Top ten significantly functional enriched biological pathways terms of 241 DEGs associated with hypoxia-GBM. (B) Top ten significantly functional enriched biological pathways terms of 32 hub signatures associated with hypoxia-GBM. (C) Top six enriched pathways of 4 molecular signatures (LYN, MMP9, PSMB9 and TIMP1) linked with GBM microenvironment. Functional and signaling pathway enrichment were conducted using KEGG pathway (http://www.genome.jp/kegg) and FunRich tool.

3.2.6. LOCALIZATION STUDY AND CONSTRUCTION OF TARGET SIGNATURE – REGULATORY TRANSCRIPTION FACTOR NETWORK

Based on the CELLO localization predictor, we have predicted the localization of 4 genes using their amino-acid protein sequences. Results showed that MMP9 and TIMP1 were majorly localized in extracellular space, followed by the plasma membrane. At the same time, LYN and PSMB9 were localized in Cytoplasm and chloroplast, respectively **(Figure 3.8).** Further, we have predicted target genes (LYN, PSMB9, MMP9 and TIMP1) related to Transcription factors (TFs) and their expression in GBM patient samples using JASPAR and GEPIA2.0 databases, respectively. The main transcription factor and its targets are listed in (**Annexure 1(B))** TIMP1, MMP9, and PSMB9 all share the Yin Yang 1 (YY1) TF with the highest degree (3) and betweenness (109.00), but the expression in the GBM patient sample is not statistically significant. In contrast, TIMP1 and PSMB9 shared the RELA (degree: 2; betweenness: 33.83), but TFAP2A and NFKB1 were elevated against PSMB9 with Log_2 Fold Change ≥ 1.4 (p-value ≤0.05) in GBM. However, TFs against the MMP9 gene were FOS, JUN, and TP53. These TFs were upregulated in GBM (Log_2 Fold change≥1.5, p-value ≤ 0.05), whereas STAT3 was only upregulated TF against the LYN gene. **Annexure 1(C)** demonstrate network showing associated transcription factor with molecular signatures in GBM.

Localization Study

Localization	CELLO Prediction: subCELlular LOcalization predictor											
	Extracellular	Plasma Membrane	Lysosomal	Mitochondrial	Nuclear	Cytoplasmic	Vacuole	Chloroplast	ER	Peroxisomal	Golgi	Cytoskeletal
MMP9	**2.82***	0.721	0.339	0.267	0.225	0.224	0.179	0.077	0.071	0.051	0.016	0.01
LYN	0.05	0.014	0.006	0.218	0.764	**3.542***	0.006	0.106	0.163	0.112	0.014	0.005
TIMP1	**4.44***	0.419	0.045	0.011	0.047	0.011	0.009	0.002	0.006	0.01	0.002	0.001
PSMB9	0.05	0.581	0.022	0.416	0.132	1.041	0.11	**2.453***	0.038	0.088	0.019	0.015

Figure 3.8: Localization Study Using Cello Predictor: Localization study of four molecular signatures MMP9, LYN, TIMP1 and PSMB9.

3.2.7. SCREENING OF NATURAL COMPOUNDS BASED ON BBB BARRIER AND ADMET ANALYSIS

We received plant-derived-naturals compounds from the NPACT database, including terpenoids, flavonoids, alkaloids, polycyclic aromatic natural compounds, aliphatic natural compounds, tannin, and PubMed database. We carried out BBB permeability of all-natural compounds using the SwissADME and CBLigand online tool with a cut-off value of 0.02, as we know that protein associated with GBM will be found in the particular region of the brain; thus, for a drug to be effective, it must pass the BBB [583]. In addition, these were checked for positive DLS based on drug-likeness score prediction [584]. Also, compounds were studied for Lipinski Rule (MW ≤500; logP≤5; HBA≤10; HBD≤5) and PAINS alert [585]. Sixty-five novel natural compounds had passed the criteria of BBB, Lipinski rule, PAINS and druglikness, which went under ADMET (absorption, distribution, metabolism, excretion, and toxicity) analysis [586]. ADMET analysis of nominated compounds was carried out to check the pharmacokinetics and pharmacodynamics properties. This server was selected to assess whether a ligand (drug) is hepatotoxic, nephrotoxic, arrhythmogenic, carcinogenic, or respiratory toxic because poor pharmacokinetics and toxicity of candidate compounds are the significant reasons for drug development failure. Our study predicts eighteen ADMET properties of selected compounds out of the 3 of absorption, 2 of distribution and excretion, 1 of metabolism and 10 toxicity properties.

For each compound to be an effective drug it must fulfill these parameters which have their own range values such as i) *Absorption*: Caco2 permeability > -5.15log cm/s, MDCK permeability (Papp) > $20X10^{-6}$ cm/s, intestinal absorption (HIA) >30%; ii) *Distribution*: Plasma protein binding (PPB) ≤ 90%, Volume Distribution (VD): 0.04-20l/kg; iii) *Metabolism*: CYP1A2 inhibitor a cytochrome P450 enzymes. Inhibitors of CYP1A2 will boost the medication's plasma concentrations, and in some situations, this will result in negative

consequences [587]; iv) *Excretion*: Clearance of a drug (CL) ≥ 5, the half-life of a drug ($T_{1/2}$): 0-0.3; v) *Toxicology*: human ether-a-go-go related gene (hERG Blockers), human hepatotoxicity (H-HT), Drug-induced liver injury (DILI), AMES Toxicity, Rat Oral Acute Toxicity, toxic dose threshold of chemicals in humans (FDAMDD), Skin Sensitization, Carcinogenicity, Eye Corrosion / Irritation, Respiratory Toxicity range between 0-0.3(---): excellent (green); 0.3-0.7(+)/(-): medium (yellow); 0.7-1.0(++): poor (red). Papp is extensively considered to be the *in vitro* point of reference for estimating the uptake efficiency of compounds into the body. Papp values of MDCK cell lines are also used to estimate the effect of the BBB. hERG- (Category 0) compounds had an IC_{50} > 10µM or < 50% inhibition at 10µM, whereas hERG + (Category 1) molecules will have opposite of this. The voltage-gated potassium channel encoded by hERG genes plays a key function in controlling the exchange of cardiac action potential and resting potential during cardiac depolarization and repolarization. Long QT syndrome (LQTS), arrhythmia, and Torsade de Pointes (TdP) are all possible side effects of hERG blocking and can result in palpitations, fainting, or even death.

Table 3.3 List of Identified Eleven Natural Compounds and Their Toxicity Profile

PubChem CID	**158280**	**185609**	**10424988**	**13886678**	**44479222**	**15549893**	**124256**	**162334**	**1548943**	**101477139**	**14313693**
Natural Compounds	7,4'-dihydroxyflavan	4'-hydroxy-7-methoxyflavan	4,4'-dihydroxy-2,6-dimethoxydihydrochalcone	7-Hydroxy-2',4'-dimethoxyisoflavanone	(3R)-3-(4-Hydroxybenzyl)-6-hydroxy-8-methoxy-3,4-dihydro-2H-1-benzopyran	4'-hydroxy-2,4-dimethoxydihydrochalcone	N-(4-hydroxyundecanoyl) anabasine	N-n-octanoyl nornicotine	8-Methyl-N-Vanillyl-6-Nonenamide	Multidione	Naviculol
Molecular formula	C15H14O3	C16H16O3	C17H18O5	C17H16O5	C17H18O4	C17H18O4	C21H34N2O2	C17H26N2O	C18H27NO3	C20H28O3	C15H26O
hERG Blockers	(---)	(--)	(---)	(---)	(--)	(--)	(---)	(---)	(---)	(---)	(---)
H-HT	(---)	(---)	(---)	(--)	(--)	(--)	(+)	(-)	(--)	(--)	(---)
DILI	(---)	(--)	(--)	(+)	(---)	(+)	(---)	(---)	(---)	(--)	(---)
AMES Toxicity	(-)	(+)	(---)	(+)	(---)	(--)	(---)	(---)	(---)	(---)	(---)
Rat Oral Acute Toxicity	(--)	(--)	(--)	(--)	(---)	(--)	(---)	(---)	(---)	(---)	(---)
FDAMDD	(+)	(+)	(-)	(+)	(++)	(-)	(+++)	(++)	(---)	(--)	(---)

Carcinogencity	(+)	(+)	(--)	(-)	(+)	(+)	(---)	(---)	(---)	(---)	(++)
Eye Corrosion	(+)	(---)	(---)	(---)	(---)	(---)	(---)	(---)	(---)	(---)	(---)
Eye Irritation	(+++)	(+++)	(+)	(---)	(++)	(++)	(---)	(---)	(---)	(+)	(+)
Respiratory Toxicity	(--)	(--)	(--)	(--)	(--)	(--)	(---)	(--)	(---)	(--)	(+)
Caco2 permeability (> -5.15log cm/s)	-4.691	-4.7	-4.695	-4.796	-4.663	-4.747	-4.68	-4.494	-4.476	-4.657	-4.205
MDCK Permeability (> 20X10-6 cm/s)	1.10E-05	1.40E-05	1.70E-05	3.40E-05	1.60E-05	2.10E-05	2.8E-05	1.90E-05	2.70E-05	2.10E-05	1.70E-05
Intestinal absorption	(---)	(---)	(---)	(---)	(---)	(---)	(---)	(---)	(---)	(---)	(---)
PPB (≤ 90%)	96.63%	97.48%	86.48%	98.13%	96.01%	91.47%	88.48%	86.43%	96.49%	98.34%	95.56%
VD (0.04-20L/kg)	1.111	1.194	0.595	0.55	1.044	0.574	0.956	0.867	1.098	0.316	1.553
CYP1A2 inhibitor	(+++)	(+++)	(+++)	(+++)	(+++)	(+++)	(---)	(-)	(++)	(-)	(--)
CL(≥ 5)	16.437	12.53	11.71	9.771	14.822	12.32	9.359	6.442	11.309	9.861	12.763
T1/2	0.757	0.335	0.914	0.384	0.813	0.818	0.3	0.281	0.892	0.465	0.22

Hepatotoxicity predicts the action of a compound on normal liver function. Furthermore, if the given compound is AMES positive, it will be considered mutagenic. Similarly, compound with positive carcinogenicity is due to their ability to damage the genome or disrupt cellular metabolic processes. Recently, respiratory toxicity has become the leading cause of drug withdrawal. Drug-induced respiratory toxicity is frequently underdiagnosed due to the lack of recognizable early signs or symptoms in commonly used drugs, resulting in severe morbidity and mortality. As a result, thorough monitoring and treating respiratory toxicity are critical [588], [589]. Our study indicates that all eleven predicted compounds, alkaloids (Pubchem CID:124256, 162334, 1548943); terpenoids (Pubchem CID: 101477139, 14313693) and flavonoids (Pubchem CID: 158280, 185609, 10424988, 13886678, 44479222, 15549893) fulfill the eligibility criteria and show favorable results**.** Therefore, we summarize in **Table 3.3** that all eleven natural compounds meet the ADMET criteria for being a novel compound to target GBM. The detailed methodology used to screen natural compounds were

shown in **Figure 3.9** and characteristics and physiochemical of natural compounds are mentioned in **Annexure 2.**

Figure 3.9: Detail Methodology Used to Filter Natural Compounds From NPACT Database

3.2.8. 7,4'-DIHYDROXYFLAVAN, (3R)-3-(4-HYDROXYBENZYL)-6-HYDROXY-8-METHOXY-3,4-DIHYDRO-2H-1-BENZOPYRAN) AND 4'-HYDROXY-7-METHOXYFLAVAN) AS PROMISING NATURAL FLAVONOIDS AGAINST MMP9: A MOLECULAR DOCKING APPROACH

To find effective drugs against the MMP9 gene, eleven natural compounds satisfied filter criteria, one reference drug, Captopril (FDA approved retrieved from the DrugBank database; https://www.drugbank.ca/) and one natural compound (Solasodine) from previous studies used [590], [591] were chosen. Autodock Vina 4.0 was used to perform blind molecular docking experiments of all prioritized natural compounds with MMP9 (PDB id: 4HMA) using default parameters.

Table 3.4: Binding Affinity and Binding Energy of 11 Natural Compounds and 2 Reference Drug

Group	Reference Drug		Experimental Natural Compounds										
PubChem CID	*442985*	*44093*	*158280*	*44479222*	*185609*	*13886678*	*101477139*	*10424988*	*124256*	*15549893*	*1548943*	*162334*	*14313693*
Class of compounds	*Alkaloid*	*Small molecules*	*Flavonoid*	*Flavonoid*	*Flavonoid*	*Flavonoid*	*Terpenoid*	*Flavonoid*	*Alkaloid*	*Flavonoid*	*Alkaloid*	*Alkaloid*	*Terpenoid*
Ligand Name	Solasodine	Captopril	7,4'-dihydroxyflavan	(3R)-3-(4-Hydroxybenzyl)-6-hydroxy-8-methoxy-3,4-dihydro-2H-1-benzopyran	4'-hydroxy-7-methoxyflavan	7-Hydroxy-2',4'-dimethoxyisoflavanone	Multidione	4,4'-dihydroxy-2,6-dimethoxydihydrochalcone	N-(4-hydroxyundecanoyl)anabasine	4'-hydroxy-2,4-dimethoxydihydrochalcone	8-Methyl-N-Vanillyl-6-Nonenamide	N-n-octanoylnornicotine	Naviculol
Total No. of interactions	15	14	17	17	16	16	17	16	22	15	17	14	9
No of interaction with active site residues	15	11	15	14	13	15	16	15	19	14	14	13	4
Binding Energy (kcal/mol)	-10.3	-6.6	-10.3	-10.3	-10	-8.5	-8.2	-8.2	-8.2	-8.2	-8.1	-7.1	-6.4
Conventional H-bond	HIS226	-	GLU241; ALA242	LEU188; HIS226	-	-	TYR248	HIS226	-	HIS226; GLN227; HIS236	GLN227; ARG249	TYR248	-
Carbon H-bond	-	ALA242	-	-	-	ALA189; HIS226	-	-	-	-	TYR245	PRO246	-

Van der waals	GLY186; ALA189; HIS190; ALA191; GLN227; HIS230; PRO246; MET247;	LEU188; VAL223; PRO240; GLU241; TYR245; MET247; ARG249; THR251	LEU188; HIS230; HIS236; PRO240; TYR245 PRO246; MET247; TYR251	ALA189; GLN227; GLU241; ALA242; TYR245; MET247; TYR248; ARG249; THR251; HIS257	HIS257; THR251; ALA242; LEU222; LEU188; GLN227; PRO246; MET247; TYR245; GLU241	LEU222; VAL223; GLN227; HIS236; LEU243; TYR245; PRO246 MET247; TYR 248; ARG249; THR251	ALA189; GLY186; LEU188; TYR218; LEU222; GLN227; ALA242; TYR245; PRO246; MET247; ARG249; HIS236	GLY186; LEU187; LEU222; VAL223; GLN227; LEU243; TYR245; PRO246; ARG249; THR251	GLY186; LEU187; ALA189; HIS190 ALA191; GLN227 GLU241; ALA242; TYR245; PRO246; MET247; ARG249; THR251	ALA189; LEU243; TYR245; MET247; TYR248; ARG249; THR251	ALA189; HIS230; GLU241; PRO246; MET247 TYR248; THR251; HIS257	GLY186; LEU187; ALA189; GLN227; HIS236; TYR245; LEU243; MET247;	GLY233; ASN262; GLY263; LEU267
Alkyl/PI-alkyl	TYR179; LEU187; LEU188; VAL223; HIS226; HIS236; TYR248	LEU222; PRO225; LEU243	LEU222; VAL223; HIS226; LEU243; TYR248; ARG249	LEU222; VAL223; HIS226 HIS236; PRO246	VAL223; HIS236; LEU243; TYR248; ARG249;	LEU187; LEU188	LEU187; VAL223; HIS; 226; LEU243	LEU188; HIS226; HIS230; HIS236; MET247	LEU188; LEU222; VAL223; HIS226; HIS230; HIS236; LEU243; TYR248; PRO255	LEU188; LEU222; HIS226; HIS230; HIS236; PRO246	LEU188; LEU222; VAL223; HIS236; LEU243; ARG249	LEU188; TYR218; VAL223 HIS226	PHE110; LEU234; HIS266
Pi cation	-	-	HIS226	-	HIS226	-	HIS226		-	-	HIS226	-	-
Pi-Pi Stacked	-	-	-	HIS226	-	HIS226	TYR248	TYR248	-	HIS226		-	-
Pi-sigma	HIS226	-	-	LEU188; LEU243	-	-	-	-	-	-	-	-	-
Pi-sulphur		HIS226; TYR248	-	-	-	-	-	-	-	-		-	-
Unfavorable donor-donor	-	-	GLN227	-	-	-	-	-	-	-	LEU188	-	ASP235

The docking or binding free energy screen the most effective chemicals and conformations. **Table 3.4** depicts the particular docking binding energy (-ΔG value (kcal/mol)) and details information regarding intermolecular interactions between ligands and proteins. In addition, we have predicted binding residues for ligand binding using the Prankweb tool. Pocket 1 with highest probability (0.99) was chosen whose residues for alpha chain was 179, 180, 186-193, 222, 223, 226, 227, 230, 233-238, 240, 242, 243, 245-249. The MMP9 3D structure revealed that 88.6% of the residues were in the highly favored region and 0.4% were in the disallowed region, respectively. Further structures were validated by ERRAT and VERIFY3D. The quality factor predicted by the ERRAT server for both alpha and beta chains of MMP9 was 76.17. VERIFY3D server predicted that 100% of residues had averaged a 3D-1D score ≥ 0.2, respectively. Moreover, the docking energy of reference drugs, Captopril and Solasodine were -6.6kcal/mol -10.3kcal/mol, respectively. Amongst eleven natural compounds, flavonoid 7,4'-

dihydroxyflavan) and (3R)-3-(4-Hydroxybenzyl)-6-hydroxy-8-methoxy-3,4-dihydro-2H-1-benzopyran) scored highest binding energy -10.3 kcal/mol with 2 H-bond interaction with GLU241, ALA242 and Leu188 and HIS226 respectively than both reference drug whereas 4'-hydroxy-7-methoxyflavan scored -10kcal/mol binding energy with no H-bond interaction. **Annexure 3** shows two-dimensional (2D) interaction diagrams for the docked complexes between MMP9 and ligand which includes all interactions such as H-bond and other interactions such as the van der walls force, pi-alkyl, pi-sigma etc. Shortlisted natural compounds' binding energy and H-bond interaction have been tabulated in detail in **Table 3.4.** Three natural compounds 7,4'-dihydroxyflavan and (3R)-3-(4-Hydroxybenzyl)-6-hydroxy-8-methoxy-3,4-dihydro-2H-1-benzopyran), and 4'-hydroxy-7-methoxyflavan) with scoring lowest binding energy and forming interaction with the active site was shortlisted for further studies along with Captopril and Solasodine. It was intriguing to note that all the best-identified natural compounds showed stable and conserved intermolecular interactions as demonstrated in **Figure 3.10.**

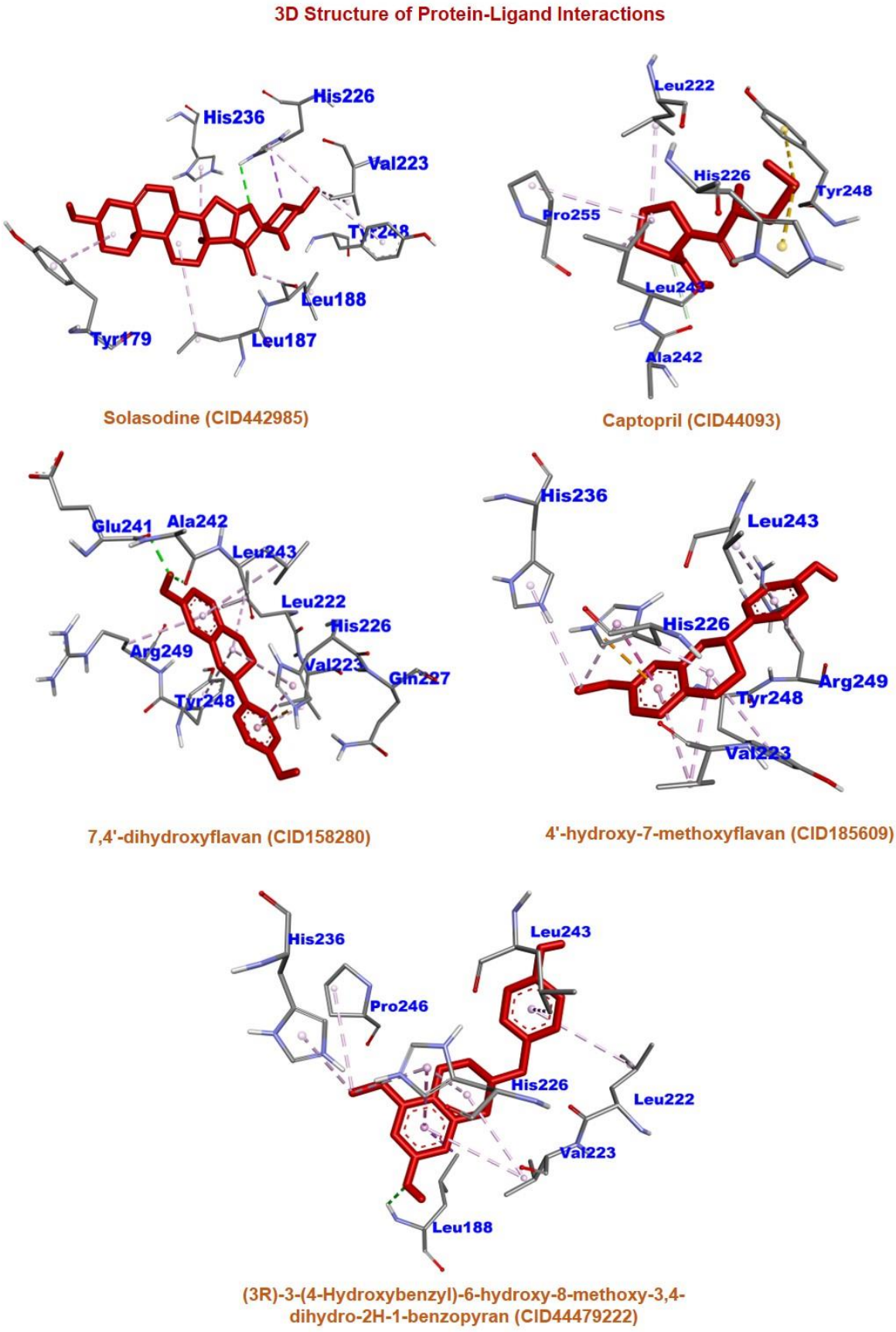

Figure 3.10: 3D-Dimensional Interaction Diagrams for The Docked Complexes Between MMP9 And Ligands Obtained in This Study

3.2.9. ASSESSMENT OF THE MOST PROMISING PROTEIN-LIGAND COMPLEX BY MD SIMULATION RUN

MD simulation (RMSD, RMSF, Rg, SASA) results of all mentioned protein-ligand complexes have been mentioned in **Figure 3.11** along with average score values of each parameter of three best-docked compounds and 2 reference drugs.

***Stability of MMP9-7,4'-dihydroxyflavan complex*:**

The time evolution of the Root Mean Square Deviation (RMSD) was determined to check the structural stability of the protein in complex ligands during the simulation. The average RMSD values for the backbone and complex were ~2.06 Å and ~2.62 Å, respectively. The complex slightly deviated as RMSD > ~3 Å between 19 ns and 24ns. At the binding site, a loop formed by the residues Pro240 and Arg249 that connects two helices displayed only slight residual fluctuations up to 0.9 Å. Flexible loops in the N-terminal region of the protein were extremely dynamic and exhibited RMSF > 2.5 Å. It was intriguing to observe that residues actively contributed to the stable interaction and exhibited significantly less fluctuation. The complex's overall average RMSF value was ~1.13 Å. The Rg value was determined for investigating the compactness and structural changes in the MMP9-7,4'-dihydroxyflavan complex. The root mean square distance of a protein atom in relation to the protein's center of mass is used to compute the Rg value of the protein. The average value of Rg for the complex is ~15.25 Å. The solvent-accessible surface area (SASA) was examined to study the protein compactness behavior. The initial and final surface area occupied by docked MMP9-7,4'-dihydroxyflavan complex is 91.40 nm^2 and 92.90 nm^2, respectively, with an average surface area of ~91.88 nm^2. This complex constructed two stable H-bonds, and both remained stagnant over the course of the simulations. The stable H-bond interactions were thought to be the primary factor that encouraged the stable complex formation. In addition, according to MM-PBSA calculation, the complex also demonstrated binding energy was -85.24 kJ/mol. Moreover, the residues that

contributed the most to the binding energy were found by computing the residue decomposition energy. The analysis suggested five residues, namely Leu222, Val223, Ala242, Met247, and Tyr248, contributed considerably to the creation of the stable complex. Most importantly, the residues Tyr248 showed significant contributions to the binding affinity by scoring the lowest contribution energy of -5.41 kJ/mol, followed by Leu222 (-4.71kJ/mol), Met247 (-3.96kJ/mol), Val223 (-2.67kJ/mol), Ala242 (-2.01kJ/mol). However, residues Gln241and Pro255 did not favor the interactions.

***Stability of MMP9-(3R)-3-(4-Hydroxybenzyl)-6-hydroxy-8-methoxy-3,4-dihydro-2H-1-benzopyran complex*:**

This complex showed consistent structural stability during the simulation run for 50 ns production run. Protein backbone and complex were found to have average RMSD values of ∼1.91 Å and ∼2.58 Å, respectively. The complex was a little unstable as RMSD > ∼3 Å between 33 and 37 ns and 39 to 47 ns, respectively. The maximum residual fluctuations in the N-terminal residues were >3.0 Å. However, the residues at the binding site from Leu222 to His230 (helix) and residues from Ala242 to Arg249 (loop), engaged in the stable and conserved non-bonded interactions, showed significantly much fewer variations of ∼0.5 Å and ∼1.13 Å, respectively. The complex has an average RMSF value of 1.13 Å. The average Rg value of 15.18 Å showed stable complex formation during the MD simulation by forming a compact structure. Meanwhile, the initial and final surface area employed by the complex was 92.17 nm^2 and 93.16 $nm^{2,}$ with the average SASA score of the complex being 92.15 nm^2. During the simulation, this complex created five H-bonds, of which four were stable. The estimated binding affinity of the compound to MMP9 protein was −94.16 kJ/mol. Additionally, the residues Leu188, Leu222, Val223, His226, and Tyr248 encouraged stable complex formation. Most importantly, decreasing order of binding affinity followed Leu222, Tyr248 and His226, Val223 and Leu188 with the lowest contribution energy of -5.74, -5.08, -4.58, -4.22 and -

3.40kJ/mol, respectively. However, the interactions weren't favored by the residues Gln227 and Arg249.

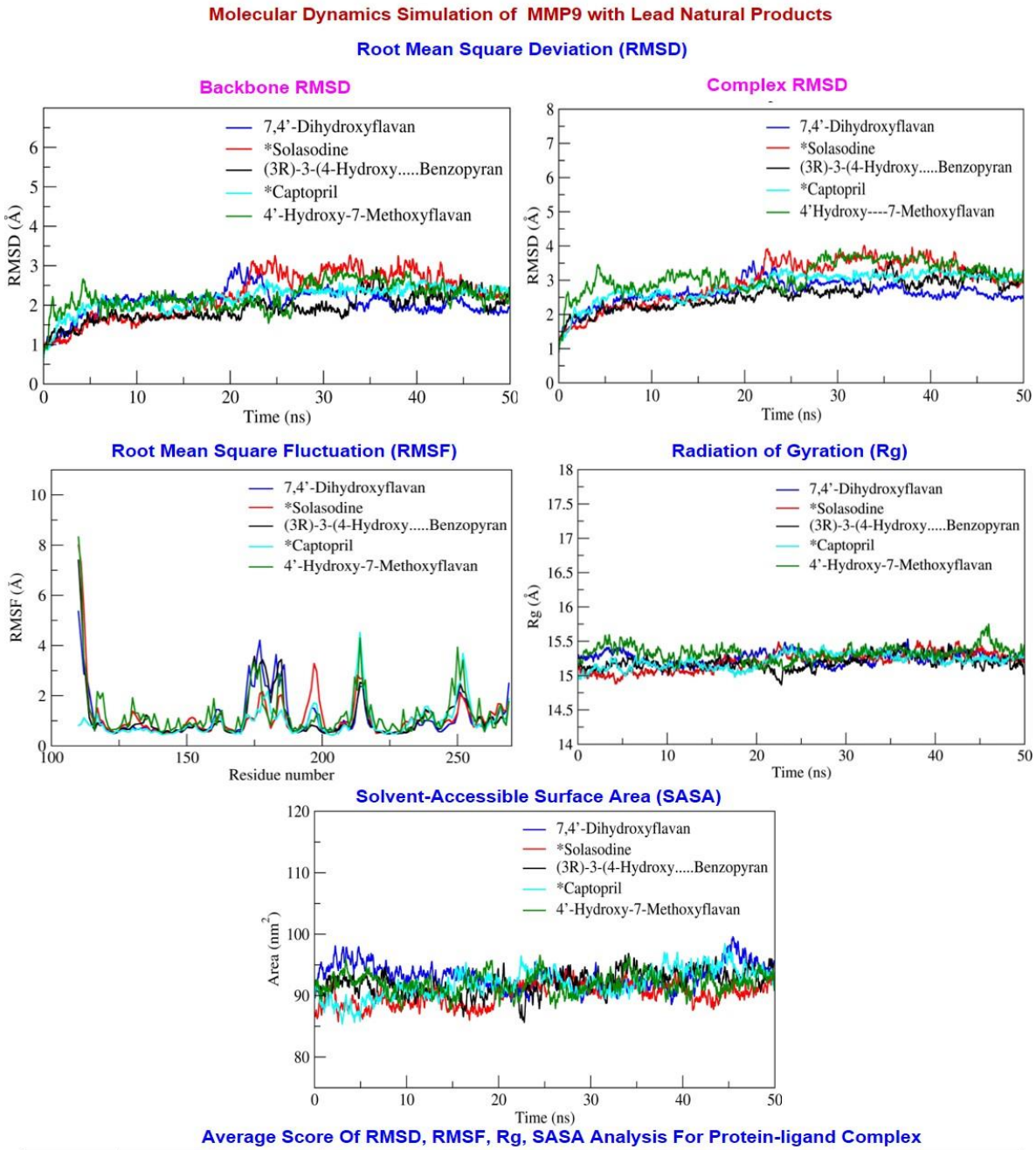

Average Score Of RMSD, RMSF, Rg, SASA Analysis For Protein-ligand Complex

Color Code	Category	PubChem CID	Ligand Name	RMSD (Å)		RMSF(Å)	Rg (Å)	SASA (nm^2)
				Backbone	Complex			
	Experimental	158280	7,4'-dihydroxyflavan	2.06	2.62	1.13	15.25	91.88
	Reference	442985	Solasodine	2.26	2.94	1.16	15.2	91.98
	Experimental	44479222	(3R)-3-(4-Hydroxybenzyl)-6-hydroxy-8-methoxy-3,4-dihydro-2H-1-benzopyran	1.91	2.58	1.13	15.18	92.15
	Reference	44093	Captopril	2.18	2.81	0.99	15.21	90.18
	Experimental	185609	4'-hydroxy-7-methoxyflavan	2.22	3.13	1.32	15.32	93.17

Figure 3.11: Molecular Dynamics (MD) Simulation Analysis of MMP9 Upon Binding of The Ligand as A Function of Time Throughout 50 ns. Graph Showing RMSD, RMSF And Radius of Gyration (Rg) For and SASA For MMP9 With Three Best-Docked Compounds And 2 Reference Drugs

***Stability of MMP9-185609 (4'-hydroxy-7-methoxyflavan) complexes*:**

The complex showed similar RMSD values of 50 ns and was stable. The complex's RMSD value ranged from 0.97Å to 3.39Å, whereas the backbone's RMSD value ranged from 0.85 to 2.5 Å. According to the residual fluctuations plotted for the Cα, binding pockets encompassing residues between Leu222 and Gly229 (helix) and Ala242 and Arg249 (loop) showed the establishment of stable non-bonded contacts in residues with lower fluctuations. Residues at N-terminal and residues adjacent to binding pockets, including Phe250 and Glu252, show higher residual fluctuation >3 Å due to increased local flexibility and ligand interaction observed during simulation. The overall average RMSF of the complex was 1.32 Å. Moreover, the Rg value demonstrated steady complex formation for 50 ns. In addition, the initial and final surface area occupied by complexes was 91.63 nm^2 and 96.49 $nm^{2,}$ with the average SASA score of complexes being 93.17 $nm^{2.}$ Two of the three H-bonds the complex created during the simulated period were consistent. The compound also had binding energy of about -78.44kJ/mol. Furthermore, the per-residue contribution energy showed six residues from the binding pocket: Leu188, Leu222, Val223, Leu243, Met247, and Tyr248—had a considerable impact on the creation of a stable complex. The residues Leu188, Leu222, Val223, Leu243, Met247, and Tyr248 from the binding pocket showed significant contributions to the binding affinity by scoring the least residue decomposition/contribution energy of -2.36, -4.25, -6.22, -3.44, -2.22 and -4.23 kJ/mol respectively. Arg249 residues do not favor the interaction.

***Stability of MMP9-Captopril and MMP9-Salosodine complexes*:**

MMP9-Captopril and MMP9-Salosodine complexes showed stable interaction during the simulation run. The average RMSD value of backbone and MMP9- Captopril complex was ∼2.18 Å and ∼2.81 Å, whereas the RMSD value with Solasodine was ∼2.26 Å and ∼2.94 Å. Moreover, the average RMSF value for the MMP9-captopril complex and MMP9 and MMP9-Salosodine were 0.99 Å and 1.16 Å, respectively. Solasodine causes the N-terminal to fluctuate

more than 3 Å, whereas Captopril did not cause this variation. Also, MMP9-Captopril and MMP9-Salosodine complexes have average Rg values of 15.21 Å and 15.2 Å, respectively. Meanwhile, MMP9-Captopril's initial and final surface areas were 88.85 nm2 and 91.54 nm^2, respectively, with an average SASA score of 90.18 nm^2. Comparatively, the MMP9-Salosodine complex had initial and final surface areas of 89.94nm^2 and 93.58 $nm^{2,}$ with an average SASA score of 91.98 nm^2. Moreover, out of three H-bonds formed, only two were stable during simulation for the Captopril complex and Solasodine complex. In addition, the complex showed the binding energy of MMP9-Captopril complexes and MMP9-Solasodine was -518.50kJ/mol and -588.15kJ/mol, respectively. Furthermore, The MMP9-Captopril complex also showed 10 residues from the binding pocket, including Asp201, Asp205, Asp206, Asp207, Glu208, Asp235, Glu241, Glu252, Asp259, and Asp260, significantly contributed to the stable complex formation. Likewise, twelve residues, Asp177, Asp182, Asp201, Asp205, Asp206, Glu208, Asp235, Glu241, Pro246, Glu252, Asp259, and Asp260, help create the stable MMP9-Solasodine complex.

Table 3.5: MM-PBSA Calculations of Top Hit Complexes' Binding Free Energy and Interaction Energies

Complex	MM-PBSA (KJ/mol)				
	ΔEVDW	**ΔEELE**	**ΔGSol**	**ΔGSurf**	**ΔGbind**
MMP9 - 7,4'-dihydroxyflavan	−167.19 ± 7.82	−14.98 ± 4.06	111.60 ± 9.88	−14.68 ± 0.78	−85.24 ± 11.81
MMP9 - Solasodine	−148.31 ± 11.20	−777.73 ± 18.62	353.45 ± 15.04	−15.55 ± 0.91	−588.15 ± 17.82
MMP9 - (3R)-3-(4-Hydroxybenzyl)-6-hydroxy-8-methoxy-3,4-dihydro-2H-1-benzopyran	−141.43 ± 13.78	−79.73 ± 8.29	142.50 ± 8.45	−15.49 ± 0.72	−94.16 ± 11.65
MMP9 - 4'-hydroxy-7-methoxyflavan	−154.50 ± 16.07	−27.86 ± 8.96	119.80 ± 20.33	−15.87 ± 0.90	−78.44 ± 16.16
MMP9 - Captopril	−83.65 ± 13.94	−622.30 ± 35.47	198.05 ± 38.01	−10.59 ± 1.54	−518.50 ± 22.39
ΔEVDW	Van der Waal energy	**ΔGSol**	Polar solvation energy	**ΔGSurf**	SASA energy
ΔEELE	Electrostatic energy	--	--	**ΔGbind**	Binding energy

Thus, data confirmed that the binding energy of MMP9 with ligands 7,4'-dihydroxyflavan, (3R)-3-(4-Hydroxybenzyl)-6-hydroxy-8-methoxy-3,4-dihydro-2H-1-benzopyran, and 4'-hydroxy-7-methoxyflavan were similar -10kcal/mol to reference drug Solasodine and better than Captopril. All three natural compounds, interact within the binding domain of the MMP9 pocket, and this interaction was stable for 50ns with less deviation and fluctuations. RMSD value difference between backbone and complex was <3 Å. RMSF, Rg and SASA also showed steady complex formation. The g_mmpbsa tool computed the binding affinity of the protein-ligand complex using the MM-PBSA method. The free energy (KJ/mol) contribution of lead hits and standard molecules in relation to their respective targets is summarized in **Table 3.5.** In addition, details description of total number of H-bond interactions between protein-ligand complex has been shown in **Annexure 4(A)** Similarly, contribution energy plot illustrates in **Annexure 4(B)** exhibits the importance of the binding pocket residues in stable complex formation.

3.2.10. PRINCIPAL COMPONENT AND DYNAMICS CROSS-CORRELATION MATRIX ANALYSIS OF COMPLEXES

We employ PCA analysis to explore the dynamics of protein-ligand conformation for five complexes (two complexes with reference drug and three complexes with natural compounds ligand) obtained from an MD simulation run of 50ns. A PCA produces a matrix of eigenvectors and a list of related eigenvalues, which together represent the principal components and amplitudes of the internal movements of a protein. The first two eigenvectors/principal components (eigenvector 1 and eigenvector 2) are used to calculate the concerted motions of the past 50 ns trajectory since they can best describe the majority of the internal movements within a protein. The first two eigenvectors' 2D projection as well as scatterplot shown in **Figure 3.12.** Captopril and Solasodine, two of the reference drugs employed in this study and directed at the MMP9 protein, were seen to have a greater range of conformations during the

simulations (shown as a red and aqua line, respectively, in **Figure 3.12 (A)**.

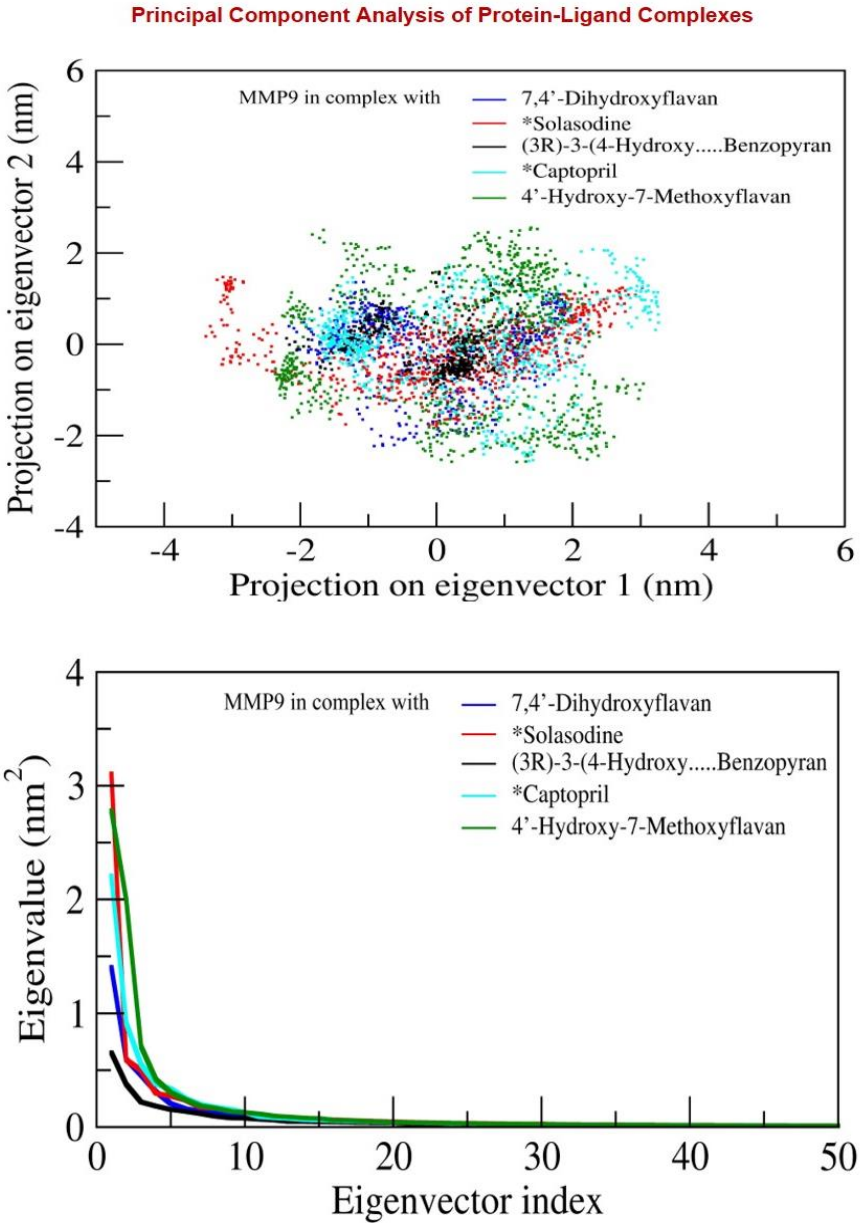

Figure 3.12: Principal Component Analysis (PCA) of MMP9-Ligand complexes. PCA of Protein-Ligand Complexes: In scatterplot the first two principal components (PC1, PC2) were plotted to analyze the collective motion of ligand bound protein complexes during the simulations. The dots with different colors (blue, red, black, aqua and green) represent collective motion of MMP9 residue after ligand binding. Dots with smaller regions represent the higher structural stability and conformation flexibility and vice versa. The collective motion of MMP9 in the presence of ligands is depicted in the second graph using projections of MD trajectories onto two eigenvectors corresponding to the first two principal components. The first 50 eigenvectors were plotted versus eigenvalue for 5 ligands including 3 hit natural compounds and 2 reference drugs. Color code used in scatterplot and Graph: Blue: 7,4'-dihydroxyflavan, Red: Solasodine, Black: (3R)-3-(4-Hydroxybenzyl)-6-hydroxy-8-methoxy-3,4-dihydro-2H-1-benzopyran), Aqua: Captopril, Green: 4'-hydroxy-7-methoxyflavan.

Moreover, during simulation, the shortlisted MMP9-targeting ligands 7,4'-dihydroxyflavan, (3R)-3-(4-Hydroxybenzyl)-6-hydroxy-8-methoxy-3,4-dihydro-2H-1-benzopyran and MMP9-4'-hydroxy-7-methoxyflavan displayed less diversity than the reference drug (shown in blue,

black and green lines, respectively). Both reference drugs demonstrated increased conformational flexibility with the maximum number of diverse conformations. Intriguingly, the MMP9 inhibitors 7,4'-dihydroxyflavan, (3R)-3-(4-Hydroxybenzyl)-6-hydroxy-8-methoxy-3,4-dihydro-2H-1-benzopyran and 4'-hydroxy-7-methoxyflavan took up substantially less conformational space than the captopril reference drug. In contrast, only 7,4'-dihydroxyflavan, (3R)-3-(4-Hydroxybenzyl)-6-hydroxy-8-methoxy-3,4-dihydro-2H-1-benzopyran performed better compared to the Solasodine reference drug as shown in scatterplot (less dispersed plot). Therefore, we suggest three lead-hit natural compounds could be more effective than reference drugs.

The dynamic cross-correlation (DCCM) of Cα atoms in complexes provides a deeper structural understanding of the collective motion of the ligand-binding regions. The coordinated residual motion of the Cα atoms in each of the simulated complexes is shown in **Figure 3.13.** Each residue exhibits a significant self-correlation with itself, as evidenced by the diagonal amber line. Scaling from amber to blue, respectively, is the strength of correlation (Cij = 1) and anticorrelation (Cij = -1). In complex MMP9-7,4'-dihydroxyflavan, the binding site residues show a positive correlation with the N-terminal domain of the MMP9. The scale of this correlation's amplitude goes from blue to amber color in smaller steps. Similarly, MMP9-MMP9- 4'-hydroxy-7-methoxyflavan also showed a positive correlation with higher amplitude near binding site residues 222 to 249. In contrast, complex MMP9-44479222 showed anticorrelation and its amplitude scaled from amber to blue color. The relevance of the active site residues in stabilizing the complexes was demonstrated by the coordinated motion displayed by the binding pocket residues spanning from 220 to 249 with the N-terminal region. The N-terminal residues of the MMP9 protein revealed a high association with the binding site residues of the reference ligands, such as Captopril and Solasodine. Comparing Captopril to the Solasodine ligand, the correlation magnitude was larger. The results showed that MMP9-

containing natural compounds complexes and the reference ligand exhibited similar correlations near binding residues. In light of this, the dynamic cross-correlation matrix displayed cooperative and anti-cooperative motion in the protein, indicating the conformational flexibility of the investigated complexes and stable connections mediated by non-cooperative motion on the opposite side, which triggered the opening and shutting of the binding pocket residues and enabled the stable complex formation during the MD simulation.

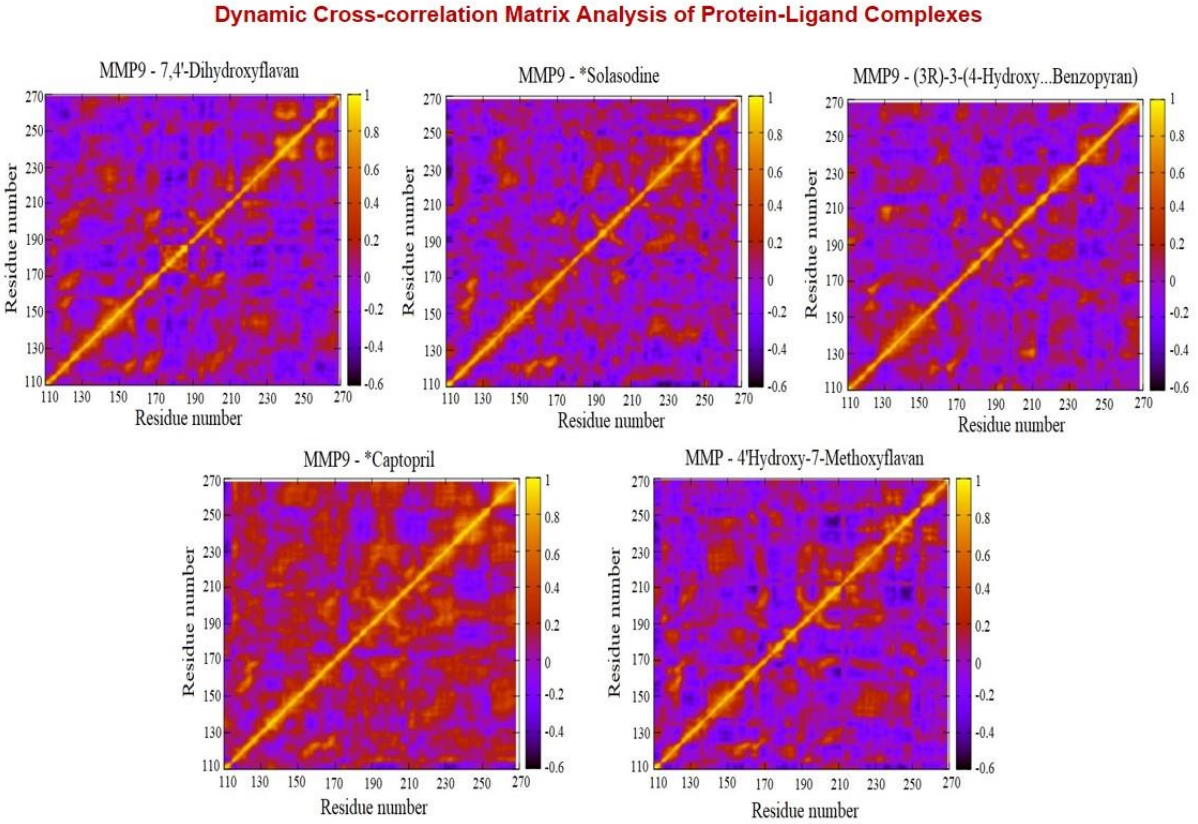

Figure 3.13: DCCM analysis of of MMP9-Ligand complexes. DCCM analysis of Cα atoms observed in complexes for 7,4'-dihydroxyflavan, Solasodine, (3R)-3-(4-Hydroxybenzyl)-6-hydroxy-8-methoxy-3,4-dihydro-2H-1-benzopyran), *Captopril*, 4'-hydroxy-7-methoxyflavan. The positive regions, colored amber, represent strongly correlated motions of Cα atoms (Cij = 1), whereas the negative regions, colored blue, represent anticorrelated motions (C*ij* = -1).

3.3. DISCUSSION

The present study analyzed hypoxic, a critical microenvironmental condition of GBM, to identify potential biomarkers and establish treatment strategies for GBM treatment. In recent years, TME gained the attention of researchers as it regulates tumor growth and significantly influences treatment response. Hypoxia condition and immune cell infiltration in TME promote and antagonize tumor growth. Herein, we identify hypoxia-related molecular signatures

involved in GBM pathogenesis. Based on functional enrichment analysis, we have found 32 HUB signatures whose expressions were validated through microarray and RNA sequence datasets obtained from TCGA datasets of GBM patients. Indeed, we subjected 10 shortlisted molecular signatures to RNA deconvolution-based TIMER analysis. From gene expression profiles, TIMER employs an algorithm to determine the abundance of tumor-infiltrating immune cells. The proportion of cancer cells in the tumor tissue is described as tumor purity (also known as tumor cell fraction), which indicates the characteristics of TME. Recent studies have shown that tumor purity is linked to a prognosis, mutation burden, and a robust immunological phenotype [592], [593]. Our results indicate LYN, MMP9, PSMB9 and TIMP1 were linked with the GBM microenvironment. Zhao et al., 2021 demonstrated a high expression of the PLOD family with negative tumor purity and high immune infiltration [594]. In our study, LYN was downregulated in the hypoxic condition in GBM. According to a study by Dai et al., 2019 hypoxia has little to no impact on the expression of phosphorylated LYN [595]. However, elevated MMP9 expression in hypoxic TME enhances DCs infiltration and reduces the infiltration of cytotoxic T cells ($CD8^+$ T cells) [596]. In contrast, increased CD8+ T-cell infiltration had been linked to a better predictive factor for long-term survival in Glioblastoma patients [597]. Additionally, PSMB8 and PSMB9 immunoproteasome subunits are overexpressed in melanoma cell lines, and their reduced expression is linked to a poor prognosis in non-small cell lung carcinoma [598]. Herein, in this study, reduced PSMB9 expression is linked to increased immune cell infiltration, with the exception of $CD8^+$ T cells. Our findings are backed up by the fact that all members of the TIMP family had significantly higher levels of expression in GBM [599]. TIMP1 expression levels in hypoxic-GBM are exclusively correlated with DCs infiltration and are inversely related to B cells and neutrophils. Consistent with our results, previous studies have also identified the four molecular signatures (LYN, TIMP1, MMP9, and PSMB9) as potential biomarkers associated with TME in GBM

and other cancers [600]–[602]. Herein, we briefly discussed the relevant pathways mentioned above by starting with the ILK pathway known to promote cell growth, cell cycle progression, and increase VEGF expression by stimulating HIF1A via a phosphatidylinositol 3-kinase (PI3K)–dependent activation [603]. Another significant pathway that is involved in the TME of GBM is the AP-1 transcription factor (dimeric in nature), which is made up of proteins from the Jun (c-Jun, JunB, and JunD) and Fos (c-Fos, FosB, Fra1, and Fra2) families. Studies have concluded that different triggers, such as inflammatory cytokines, stress inducers, or pathogens, activate the AP-1 transcription factor family, resulting in innate and adaptive immunity [604]. In addition, active CDC42 (Rho-GTPase) has been shown to facilitate glioma cell migration and invasion and regulate cell polarity [605]. In GBM, HIF1 and VEGF upregulate CXCR4, which is significant for angiogenesis and cell invasion [606]. Furthermore, another fascinating study showed that the interaction of microglia and GBM through the LPA pathway has important consequences for tumor progression. A deeper understanding of this interaction could lead to the development of new therapeutic techniques that target LPA as a possible GBM target [607]. Another study found that hypoxic TME stimulates invadopodia development (actin-rich protrusions of the plasma membrane that focus ECM breakdown through the secretion of MMPs), which are essential for metastasis [608]. In addition, our data showed that the localization of MMP9 was mainly extracellular region and FOS, JUN, and TP53 were only significantly overexpressed associated TFs in GBM patient's samples. MMP9 was overexpressed in different subtype of GBM including classical, mesenchymal, neural and proneural (**Figure 3.14(A))**. It also has potential to act as poor prognostic biomarkers (HR>1) as it shows significant disease-free survival (**Figure 3.14(B)**. This all together suggests the significance of targeting TME. LYN and PSMB9 being downregulated in hypoxic condition and due to unavailability of reported drug against TIMP1, these biomarkers were not explored in current study in identifying novel drug. Hence, MMP9 was selected for identifying natural

compounds as inhibitors in order to reduce GBM pathogenesis. MMP9, a member of the gelatinase family of MMPs that degrades and remodels ECM proteins, plays a vital role in cell migration and epithelial-mesenchymal transition (EMT), and angiogenesis [609]. Other TME components, such as non-malignant stromal cells, neutrophils, macrophages, and endothelial cells, release MMP9 in the microenvironment. MMPs are known to be induced by HIF1 [610], [611]. MMP inhibitors can diminish tumor cells' invasive and migratory abilities in cancer. MMP9 inhibitors were previously discovered using a computational technique, indicating that MMP9 is a targetable protein [612], [613]. Based on previous studies, we have selected Captopril and Solasodine as reference drugs against MMP9. Captopril as an MMP2 inhibitor for treating patients on continuous ambulatory peritoneal dialysis (CAPD) therapy [614]. Captopril inhibits MMP2 and MMP9 via chelating zinc ions at the enzyme's active site. It's also utilized alongside other medicines like Disulfiram and Nelfinavir as adjuvant therapy for GBM [615]. Moreover, it can inhibit MMP2 and MMP9, suspected of having a role in GBM metastasis and invasion, since it is an angiotensin-converting enzyme (ACE) inhibitor, which belongs to a family of metalloproteinases comparable to MMPs [616]. Similarly, Solasodine has been reported to inhibit MMP9 and induce cell apoptosis, particularly in human lung cancer. However, this drug's pharmacokinetics, safety, and effectiveness in clinical practice remain unclear [590], [617]. During identifying new agents for MMP9, we explored 6 classes of natural compounds, including Alkaloids, Flavonoids, Terpenoids, Aliphatic Compounds, Aromatic Compounds, and Tannins. Previous studies have also supported that multiple natural compounds have antitumor and apoptotic effects in TMZ and p53 resistance GBM cells. Various natural compounds such as Chrysin, Epigallocatechin-3-Gallate, Hispidulin, Rutin, And Silibinin were also used in combination with TMZ and other chemotherapeutic drugs due to their potential to act as chemosensitizers (such as Icariin, Quercetin), radiosensitizers (Zataria multiflora), inhibits proliferation (such as *Zingiber officinale* and *Rhazya stricta*) and

migration and induces apoptosis (Baicalein) [370], [374], [375]. However, these were checked for BBB permeability, druglikness, and LIPINSKI rules of 5 and performed ADMET analysis. We performed *in silico* molecular docking and MD simulation with MMP9 protein (alpha chain) using Autodock Vina 4.0 and GROMACS to evaluate the inhibitory effect of shortlisted drugs. Ramachandran Plot of MMP9 (PDB identifier: 4HMA) shown in **Figure 3.14(C)**. The binding affinity of ligands (drugs) was calculated and compared with reference drugs. In this instance, we have picked three best-docked compounds with binding energies comparable to Solasodine and better than Captopril for MD simulations. Stability should be taken into careful consideration during drug testing in addition to safety. The software's MD simulation module examined the stability of these MMP9-compound complexes in the natural environment. Further compounds interacted with targets with a minimum of at least 2 *H*-bond interactions. Numerous studies have been conducted in the past to implement molecular docking, MD simulations, and MM-PBSA assessment to record the drug transport variability, identify protein allosteric inhibition, consider the impact of chirality in selective enzyme inhibition, investigate the irreversible style of the receptors, and evaluate ligand-protein interactions. Similarly, this study examined the intermolecular contact stability of identified prospective lead compounds and standard molecules with their respective targets using classical MD simulation for 50 ns of MMP9 protein with ligands [618]. Subsequently, the efficacy of molecules' molecular interactions can be examined using structural analysis, such as RMSD and RMSF [619]. Results revealed that the binding energy of MMP9 with ligands 7,4'-dihydroxyflavan, (3R)-3-(4-Hydroxybenzyl)-6-hydroxy-8-methoxy-3,4-dihydro-2H-1-benzopyran, and 4'-hydroxy-7-methoxyflavan were similar -10kcal/mol to reference drug Solasodine and better than Captopril.

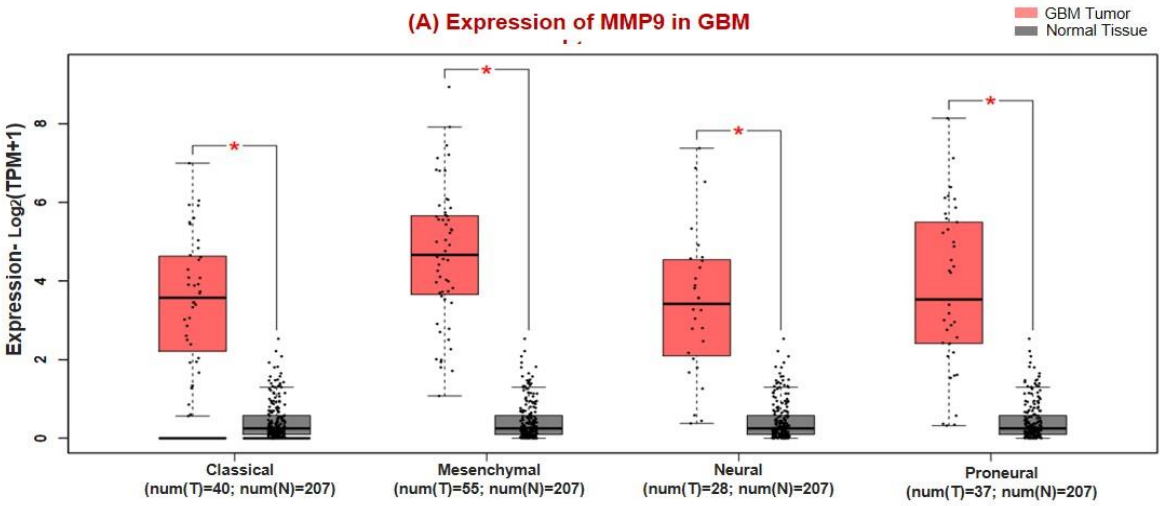

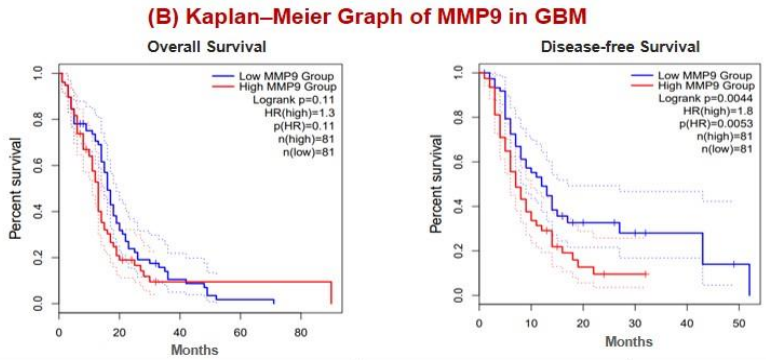

Parameter	Overall survival	Disease Free survival
Logrank- pvalue	0.11	0.0044
Hazard ratio,HR (high)	1.3	1.8
p-value of HR	0.11	0.0053
Prognostic marker	--	Poor prognostic marker

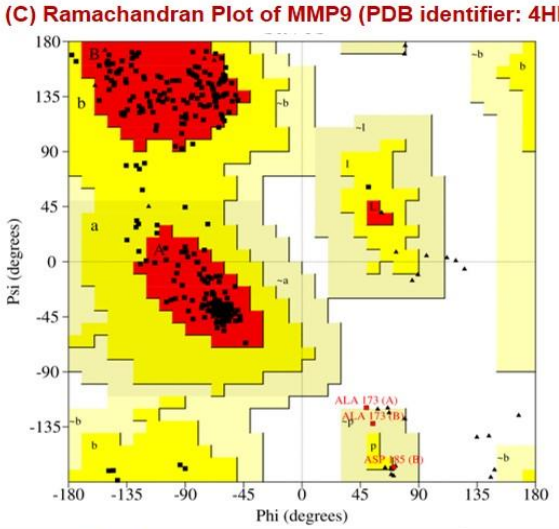

Results	MMP9
Residues in most favoured regions [A, B,L]	234 (88.6%)
Residues in additional allowed regions [a, b, l, p]	27 (10.2%)
Residues in generously allowed regions [~a, ~b, ~l, ~p]	2 (0.8%)
Residues in disallowed regions	1 (0.4%)

Figure 3.14: MMP9 Protein in Glioblastoma Multiforme: (A) mRNA expression in different subtype of GBM such as classical, mesenchymal, neural and proneural. (B) Kaplan-Meier Graph of MMP9 in GBM shows poor prognosis marker based on significant disease-free survival curve data (C)Ramachandran Plot of MMP9 (PDB identifier: 4HMA).

All three ligands, flavonoids in nature, interact within the binding domain of the MMP9 pocket, and this interaction was stable for 50ns with less deviation and fluctuations. RMSD value difference between backbone and complex was <3 Å. The MMP9-7, 4'-dihydroxyflavan complex findings suggest that five residues: Leu222, Val223, Ala242, Met247, and Tyr248, contributed significantly to the formation of the stable complex. Most importantly, the residues Tyr248 showed significant contributions to the binding affinity by scoring the lowest contribution energy of -5.41 kJ/mol. MMP9-(3R)-3-(4-Hydroxybenzyl)-6-hydroxy-8-methoxy-3,4-dihydro-2H-1-benzopyran had a 94.16 kJ/mol determining binding affinity. Leu188, Leu222, Val223, His226 and Tyr248 residues also facilitated stable compound formation. Leu222 scored the highest binding affinity of -5.74Kj/mol. Similarly, the binding energy of MMP9-4'-hydroxy-7-methoxyflavan was around 78.44 kJ/mol. The per-residue contribution energy also revealed that the formation of a stable complex was significantly influenced by six residues from the binding pocket: Leu188, Leu222, Val223, Leu243, Met247, and Tyr248. The binding affinity of the residue Met247 is -6.22 kJ/mol. Further, PCA analysis revealed that the MMP9-targeting ligands,4'-dihydroxyflavan, (3R)-3-(4-Hydroxybenzyl)-6-hydroxy-8-methoxy-3,4-dihydro-2H-1-benzopyran, and 4'-hydroxy-7-methoxyflavan had less diversity than the reference drug during the simulation run. Both reference drugs demonstrated increased conformational flexibility with the maximum number of diverse conformations. Interestingly, compared to the Captopril reference drug, the MMP9 inhibitors, 7, 4'-dihydroxyflavan, (3R)-3-(4-Hydroxybenzyl)-6-hydroxy-8-methoxy-3,4-dihydro-2H-1-benzopyran, and 4'-hydroxy-7-methoxyflavan used significantly less conformational space. Contrarily, only 7, 4'-dihydroxyflavan, (3R)-3-(4-Hydroxybenzyl)-6-hydroxy-8-methoxy-3,4-dihydro-2H-1-benzopyran, outperformed the Solasodine reference drug

Furthermore, 7, 4'-dihydroxyflavan, (3R)-3-(4-Hydroxybenzyl)-6-hydroxy-8-methoxy-3,4-dihydro-2H-1-benzopyran, and 4'-hydroxy-7-methoxyflavan showed positive correlations with

the N-terminal domain of proteins, while (3R)-3-(4-Hydroxybenzyl)-6-hydroxy-8-methoxy-3,4-dihydro-2H-1-benzopyran displayed an anticorrelation. As a result, we demonstrated how three lead flavonoids may be able to target MMP9 protein. The fact that 7, 4'-dihydroxyflavan was derived from the African forest tree *Guibourtia ehie* or *Shedua*, which has been utilized traditionally for tumor and wound healing, provided additional support for our findings in earlier investigations. It acts as a metabolite and shows anti-inflammatory and antioxidant effects in prostate cancer, breast cancer, and osteosarcoma by regulating Akt/Bad and MAPK signaling. In addition, (3R)-3-(4-Hydroxybenzyl)-6-hydroxy-8-methoxy-3,4-dihydro-2H-1-benzopyran was found in *Soymida febrifuge* (Indian-redwood). Its fruits are therapeutic and have been used to treat cervical and colon cancer [620]. Interestingly, a study by Sowmyya et al. discovered that extracts from these dried fruits contributed to the creation of silver nanoparticles by acting as reducing and stabilizing agents during the conversion of Ag^{+} to nano-silver [621]. The last compound, 4'-hydroxy-7-methoxyflavan, was derived from the orchid tree *Bauhinia divaricate* and was formerly used to treat skin and colon cancer. These three flavonoids will inhibit MMP9 and lower its overexpression brought on by hypoxia in GBM. As a result of these inhibitions, the downstream effects of MMP9 activation will be diminished, which will minimize the pathogenesis of GBM. Cell proliferation, invasion, angiogenesis, drug resistance, matrix remodeling, and immune cell infiltration are significant pathways that will be impacted. The infiltration of DCs cells in response to MMP9 overexpression was also demonstrated by our data, which also indicated a positive correlation with immune checkpoints like PD-1 and TIM-3. **Figure 3.15** illustrates the proposed mode of action for three novel flavonoids, including 7,4'-dihydroxyflavan (Pubchem CID 158280), (3R)-3-(4-Hydroxybenzyl)-6-hydroxy-8-methoxy-3,4-dihydro-2H-1-benzopyran (Pubchem CID 44479222), and 4'-hydroxy-7-methoxyflavan (Pubchem CID 185609). These will attenuate MMP9 activation's impact on GBM.

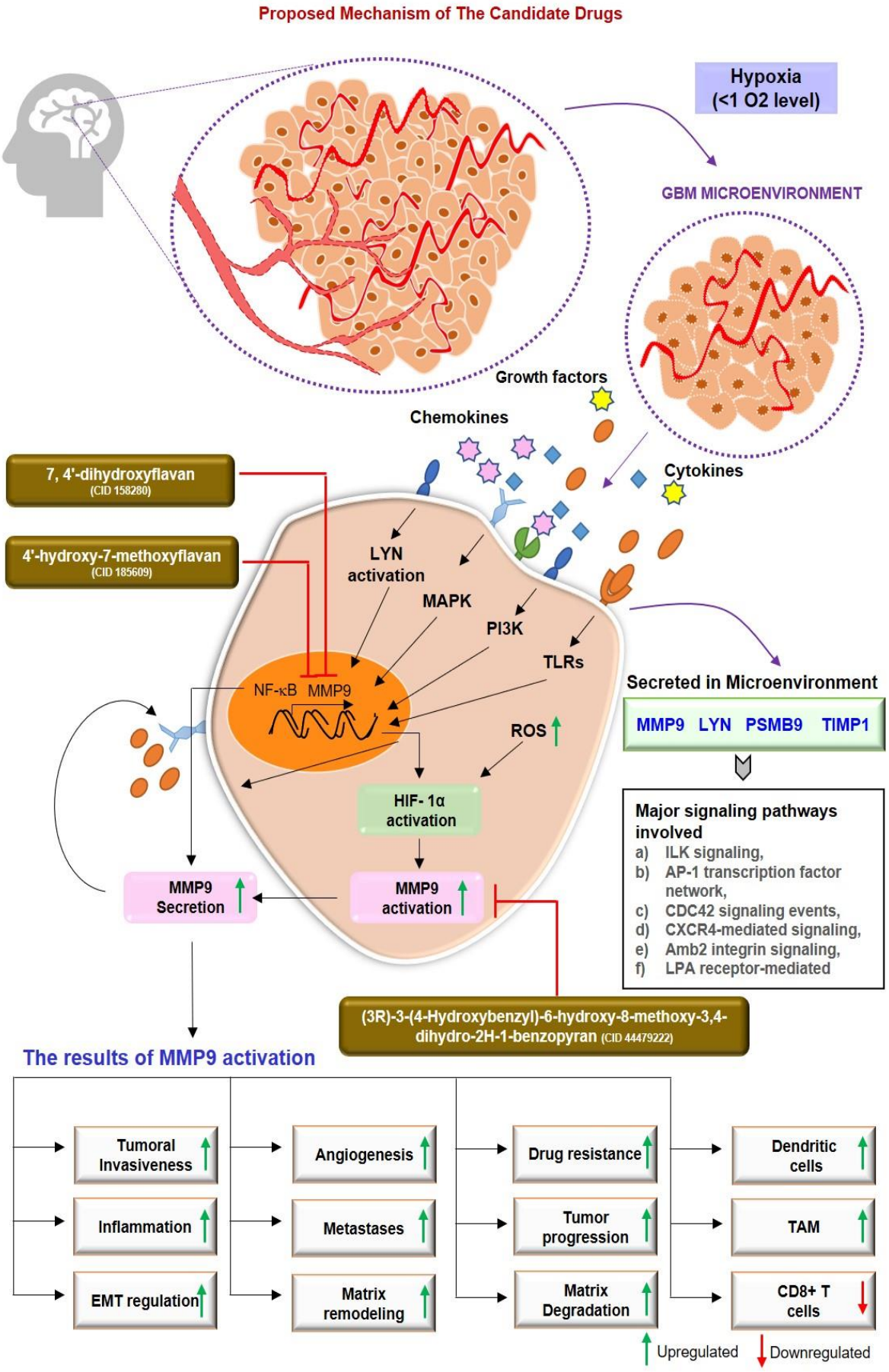
Proposed Mechanism of The Candidate Drugs
Hypoxia
(<1 O2 level)
GBM MICROENVIRONMENT
Growth factors
Chemokines
Cytokines
7, 4'-dihydroxyflavan
(CID 158280)
4'-hydroxy-7-methoxyflavan
(CID 185609)
LYN
activation
MAPK
PI3K
TLRs
NF-κB MMP9
ROS
HIF- 1α
activation
MMP9
Secretion
MMP9
activation
Secreted in Microenvironment
MMP9 LYN PSMB9 TIMP1
Major signaling pathways involved
a) ILK signaling,
b) AP-1 transcription factor network,
c) CDC42 signaling events,
d) CXCR4-mediated signaling,
e) Amb2 integrin signaling,
f) LPA receptor-mediated
(3R)-3-(4-Hydroxybenzyl)-6-hydroxy-8-methoxy-3,4-dihydro-2H-1-benzopyran (CID 44479222)
The results of MMP9 activation
Tumoral Invasiveness
Inflammation
EMT regulation
Angiogenesis
Metastases
Matrix remodeling
Drug resistance
Tumor progression
Matrix Degradation
Dendritic cells
TAM
CD8+ T cells
Upregulated
Downregulated

Figure 3.15: The Proposed Mechanism of Action of Candidate Flavonoids as Therapeutic Agent. The figure depicts the potential of novel inhibitors 7, 4'-dihydroxyflavan, (3R)-3-(4-Hydroxybenzyl)-6-hydroxy-8-methoxy-3,4-dihydro-2H-1-benzopyran, and 4'-hydroxy-7-methoxyflavan in suppressing GBM pathogenesis by interacting with MMP9 protein produced in a hypoxic environment condition. MMP9 is synthesized de novo during stimulation induced with cytokines by activating various signaling pathways such as NF-κB, HIF1, MAPK, PI3K etc. Cytokines (TNF-α, IL-8, and IL-1β) and growth factors (TGF-β, PDGF, and bFGF) bind to their receptors which regulate MMP9 activation and secretion. MMP9 is secreted by tumor cells, monocytes, inflammatory macrophages, and stromal cells in the extracellular environment. This affects various downstream biological processes, including matrix degradation, remodeling, EMT (enhanced tumoral invasion, metastases), angiogenesis, inflammation, drug resistance etc. Novel inhibitors 7, 4'-dihydroxyflavan, (3R)-3-(4-Hydroxybenzyl)-6-hydroxy-8-methoxy-3,4-dihydro-2H-1-benzopyran, and 4'-hydroxy-7-methoxyflavan binds to MMP9 and suppress its activation and thus reduces the expression and regulation of downstream process involved in GBM pathogenesis in the above figure. Our approaches to GBM treatment are being reoriented by focusing on these features of MMPs

3.4. CONCLUSIONS AND FUTURE PERSPECTIVES

Despite recent advancements in chemotherapy, radiotherapy, and immunotherapy, there is currently no satisfactory therapy for GBM in clinics due to many failure reasons, being toxicity of chemotherapy, failure of the drug to cross BBB, involvement of TME and less immune infiltration. For instance, immune checkpoint blockade targeting CD8+ T cells is ineffective for GBM [622]. There is an unmet need for novel approaches to treat GBM and other brain cancer. Here in our study, we have focused on a crucial TME parameter, i.e., hypoxia caused due to intense cell respiration, excessive nutrient consumption by tumor cells, and abnormal vasculature. However, hypoxia is a hallmark of brain tumors, and if and how hypoxia affects antitumor immunity in the brain remains unclear. Our findings shed light on MMP9's potential as a therapeutic target and a robust biomarker in GBM's hypoxic microenvironment. In **Figure 3.15**, it is illustrated that in response to cytokine-induced stimulation, MMP9 is synthesized from *de novo* by activating various signaling pathways including NF-κB, HIF1, MAPK, PI3K etc. Cytokines such as TNF-α, IL-8, and IL-1β and growth factors namely TGF-β, PDGF, and bFGF bind to their respective receptors, influence the activation and production of MMP9 This has an impact on a number of biological functions that come thereafter, such as drug resistance, remodeling of the matrix, EMT, increased tumoral invasion, metastases, angiogenesis, and remodeling. Previous studies supported our results where researchers have shown that MMP9, a zinc-dependent endopeptidase, was upregulated in glioma tissues, and its expression was

correlated with tumor grade and poor prognosis. Hypoxia condition increases protein expression of HIF1A, MMP2 and MMP9 in cancer [623] and regulates tight junction rearrangement, leading to vascular leakage in the brain [624]. The majority of the ECM components are substrates of MMPs. MMP-9 can cleave many ECM proteins to regulate ECM remodeling and affects the alteration of cell-cell and cell-ECM interactions. It can also cleave many plasma surface proteins to release them from the cell surface. It has been implicated in the invasion and also implicated in BBB opening as part of the neuroinflammatory response, metastasis through proliferation, vasculogenesis and angiogenesis [577]. MMP9 has been a potential biomarker for many cancers, including osteosarcoma, breast, cervical, ovarian, pancreatic, Giant Cell Tumor of Bone, and Non-Small Cell Lung Cancer [144]. Herein the current study, we have proposed MMP9 as a promising biomarker for hypoxic microenvironmental conditions in GBM. Other molecular signatures, such as LYN, PSMB9, and TIMP1, could be investigated further as druggable biomarkers or prognostic markers in addition to MMP9. Infiltration of immune cells such as neutrophils and DCs was linked to this gene's expression to varying degrees. This effect opens up new avenues for study into the MMP9 and GBM. A negative correlation with B cells, CD4+ T cells and CD8+ T cells support the failure of current immune checkpoint inhibitors.

The current study used *in silico* techniques such as compound-protein-pathway enrichment analysis, network pharmacology, molecular docking, MD simulation, MM-PBSA, PCA and DCCM investigations to identify a collection of druggable and non-toxic natural compounds from plants. The potential of natural compounds to be used as drugs was revealed by ADMET analysis of eleven novel hits. A chemical substance must have absorption, distribution, metabolism, excretion, and toxicity values to be utilized as a medication. Together results obtained showed flavonoids named 7,4'-dihydroxyflavan, (3R)-3-(4-Hydroxybenzyl)-6-hydroxy-8-methoxy-3,4-dihydro-2H-1-benzopyran and 4'-hydroxy-7-methoxyflavan as a

potential inhibitor of MMP9 produced from the hypoxic condition in GBM. These inhibitors have comparable or better results compared to reference drugs Solasodine and Captopril. Our results indicate that MMP9 and drug interaction are stable, and proposed novel flavonoids can inhibit or reduce MMP9 expression in hypoxia conditions, which will further affect downstream process involved in GBM pathogenesis. Hence, targeting an essential microenvironmental condition will improve therapeutic efficacy and expand the treatment drug library against GBM. Limiting to the present findings, we point out that the results presented in this work are based on processor simulations which need to be further validated with wet-lab experimental protocols.

In conclusion, the observations of this work suggest novel plant-based flavonoids inhibited the potential role of MMP9 as a biomarker factor and active MMP9 in GBM. Prior to synthesizing therapeutics, the results of this investigation could be helpful. Other natural compounds and plant-based natural compounds could be examined and studied to understand and explore whether they could be employed as future possibilities for GBM medicines. The results of this study are helpful for drug development. The findings may aid in the assisted screening of therapeutics for GBM. This study is novel in incorporating various computational methodologies for the virtual screening of natural compounds based on BBB, ADMET, PAINS, and Lipinski's rule. This study allows scientists to explore these molecules *in vitro* or *in vivo* as a medicinal approach. Although we have validated our results using different computational methodologies such as multiple-target validation, literature validation, TCGA databases (containing GBM samples data), cell culture, and animal model research will fill in the gaps. We identified the common residues via which the inhibitor can potentially bind to the target using bioinformatics tools and *in silico* studies. However, the molecular mechanism underlying the reduction of target expression needs only to be validated through *in vitro* experiments. New leads are being discovered in several ongoing studies using advanced

computational strategies and machine learning models to filter massive pharmaceutical libraries. The experimental screening strategy alone may not enhance lead productivity for the rapid development of viable medicines. Our findings will aid researchers in concentrating on TME components and their conditions in order to produce novel natural product-based anti-GBM therapies that address two major issues: toxicity and resistance and target a major microenvironmental condition: Hypoxia.

3.5. HIGHLIGHTS OF THE STUDY

- ✓ Multi-omics analysis identified LYN, MMP9, PSMB9, and TIMP1 as potential regulators of hypoxia-induced GBM.
- ✓ MMP9 as a novel biomarker correlated with tumor purity and immune filtration properties
- ✓ Three flavonoids, namely 7, 4'-dihydroxyflavan, (3R)-3-(4-Hydroxybenzyl)-6-hydroxy-8-methoxy-3,4-dihydro-2H-1-benzopyran, and 4'-hydroxy-7-methoxyflavan are potential inhibitors of MMP9 for GBM therapy.
- ✓ Identified compounds have a similar binding pattern compared to the reported MMP9 inhibitor, namely Captopril and Solasodine.
- ✓ PCA and DCCM analysis showed stable configuration, positive correlation, and less conformation diversity.
- ✓ Identified leads interacted strongly at the active site conforming to higher structural stability throughout the dynamic evolution of the complex.
- ✓ MM-PBSA analysis identified Tyr248, Leu222, as Val223 of MMP9 as the potential amino acid that interacts with therapeutic agents 7, 4'-dihydroxyflavan, (3R)-3-(4-Hydroxybenzyl)-6-hydroxy-8-methoxy-3,4-dihydro-2H-1-benzopyran, and 4'-hydroxy-7-methoxyflavan respectively.

CHAPTER IV

Objective 4

CHAPTER IV

✓ To establish a connection between acetylation and ubiquitin proteasome signaling in tumor microenvironment

4. INTRODUCTION

GBM is the most prevalent and fatal brain tumor with a poor prognosis. The clinical prognosis is still lacking despite several approved therapies for GBM, including surgery, radiation, and chemotherapy [11]. The possible causes are the extensively invasive nature of GBM cells, the chemo- and radio-resistance, the high degree of vascularization, heterogeneity, and reduction of chemotherapeutic drugs effusion due to the BBB, and heterogeneity of TME. Further, the ECM structural proteins are among the non-cellular components of the TME that are released by tumor or stromal cells or extravasated from the intravascular compartments other than cytokines, chemokines, and growth factors. [16]. Additionally, ECM structural proteins impact the development of all blood cells and other cells that support the body's inflammatory and immunological reactions, which promote anti-cancer behavior. [17]. The use of non-cellular secretory components as possible treatment targets and biomarker tools is now being investigated in several pre-clinical and clinical studies [18], [19]. Cytokine expression patterns in GBM are distinctive, and aberrations in cytokine expression have been linked to gliomagenesis. The complex cytokine network in the diverse microenvironment facilitates interactions between the tumor cells, healthy brain cells, immune cells, and stem cells within the heterogeneous milieu of the GBM [20]. In addition, chemokines recruit different immune cell populations in TME by binding with their receptors. For instance, microglia cells implicated in their recruitment at the site of inflammation possess elevated amounts of CCR1 expression. These affect tumor growth, metastasis, the transition from low to high-grade gliomas, and treatment outcomes [625]. Another study demonstrates that the recurrence of GBM pathogenicity occurs when neural stem cells crosstalk with microglial cells [626]. Moreover, studies have shown that PTMs, namely methylation, acetylation, glycosylation, and

ubiquitination of chemokines and cytokines, influence biological activities, inflammatory responses, and inflammasome-dependent innate immune responses through modifying the protein stability, structure, and sequence [21], [22]. A recent study by McCornack et al., (2023) discussed the significance of histone acetylation and methylation along with the consequences of targeted suppression of these enzymes by therapy in GBM [627]. Moreover, another study mentioned addressed the crucial role of histone acetylation in determining cell fate [253]. Further, the exploration of new therapeutic interventions requires a thorough understanding of pathways relevant to GBM [628]. Additionally, protein kinases serve a crucial role in the signaling processes that regulate the traits of malignant cells, thereby making them valuable targets for therapeutic intervention in the management of cancer through the uptake of glucose, signaling modulation, epigenetic modifications, and progression of the cell cycle [629]. Moreover, a variety of non-cellular secretory components of TME, including hormones, growth factors, chemokines, and cytokines bind to receptor tyrosine kinase and initiate downstream signaling, such as MAPK, PI3K/Ras that results in the proliferation and survival of tumor cells [630]. EGFR signaling crosstalk with other major oncogenic signaling cascades, such as PI3K/protein kinase B (Akt)/mTOR pathway and MAPK pathway [631]. However, in various cancers, protein kinase also controls TME and its constituent components. For example, in GBM tumor cells, IL-1β induces an HIF1A/IL-1β autocrine loop via activating Wnt-1 and RAS, which both contribute to the increase of HIF1A [632]. In contrast, IL-1β also stimulates the p38 MAPK-activated protein kinase 2-human antigen R (HuR), TLR-4, and other inflammatory-associated signaling pathways, which considerably enhance the levels of IL-6 and IL-8 in GBM tumor cells, eventually leading to an inflammatory TME in support of GBM invasion and growth [633]. In addition, cytokines, such as CCL5, was associated with intracellular calcium elevation. The activation of Akt and Ca^{2+}/calmodulin-dependent protein kinase II (CaMKII) in GBM cells controlled the migratory and invasive activities [634].

Further, Tyrosine kinase inhibitors (TKI) and other kinase inhibitors (such as SI113) alone or in combination with other drugs/therapy have the potential to manage GBM by overcoming limitations such as BBB penetration, adaptation to altered signaling pathways, and heterogeneity of GBM cells [630] [635].

Moreover, HATs, besides histones, acetylates a variety of non-histone substrates, and thus, referred to as lysine acetyltransferases that play an essential function in normal and malignant haematopoiesis [636]. Recent studies demonstrated that abnormally high histone acetylation levels could trigger chromatin-based mechanisms that promote tumorigenesis and malignant transformation. Further, it's interesting to note that most acetylated non-histone proteins are essential for immunological processes, tumorigenesis, and cancer cell growth [23]. Evidence that lysine acetylation modification affects the lysosomal clearance of specific substrates and proteasomal degradation by either inhibiting or enhancing polyubiquitination [24]. Additionally, studies have found that the UPS system degrades HIF1A after interacting with von Hippel–Lindau protein (pVHL) under normoxia, mediating its ubiquitination. For instance, Jeong et al. (2002) found that acetylation at specific lysine residues of HIF1A enhances its interaction with pVHL and its subsequent ubiquitination and degradation [637]. Likewise, acetylated retinoblastoma (Rb) recruits MDM2, an E3 ligase, and mutation in its acetylation hotspots is linked with an increased risk of breast cancer [25]. Acetylation has been studied extensively in proteosomes, Ub, E1, and E3 ligase, but few have in E2s. Hence, the current study was conducted to understand better how acetylation affects E2s, which will fill the gap between UPS and acetylation modification and its impact on microenvironmental secretory protein regulations. Herein, we aim to identify novel therapeutic targets in GBM, including HATs, E1, E2s, and E3 ligases and substrates, as well as possible acetylation sites on lysine residues of E2s.

Methodology of The Study

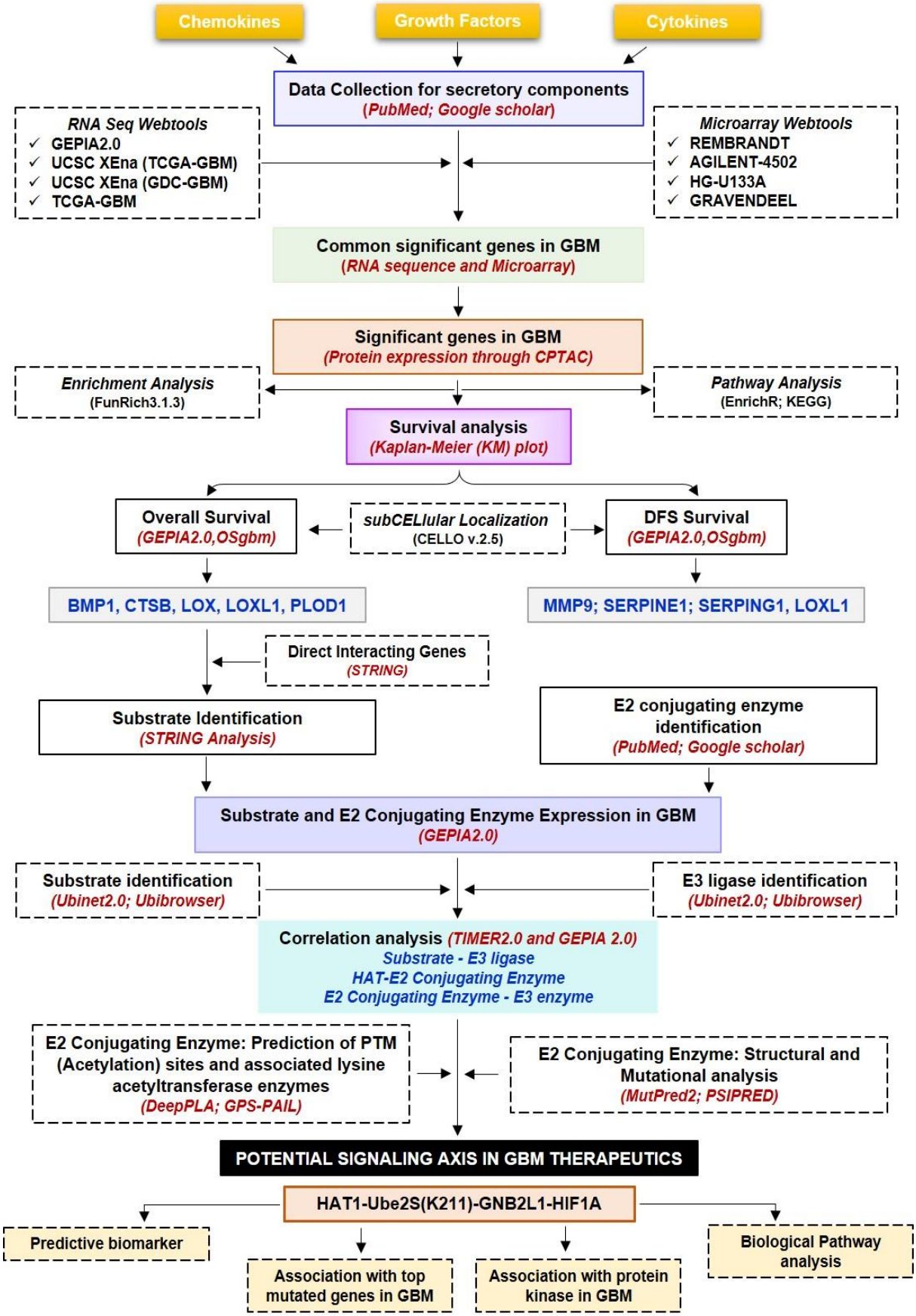

Figure 4.1: Methodology Used in The Current Study: Workflow and steps considered along with the datasets collected and processed to identify prognostic and predictive markers in GBM. The expression of non-cellular secretory components (cytokines, chemokines, and growth factors) was examined in GBM transcriptome and proteomic data before the Kaplain-Meir plot was used to find prognostic markers. In addition, a common protein has been found that is directly associated with prognostic indicators; of these, two have the ability to function as substrates in the UPS system, and only HIF1A was elevated in GBM. Additionally, putative E3 ligases and E2s that are linked to HIF1A have been found. Additionally, a correlation study was done between prognostic markers, HIF1A, E3 ligase, E2s, and HAT enzymes. Further, a potential acetylation site on the lysine residues of E2s was found. The figure highlights the involvement of the acetylation mechanism, E2 conjugating enzymes, and E3 ligase's finding novel therapeutic axis in GBM indication. Furthermore, a characterization investigation of the suggested treatment axis was carried out.

We also systematically investigate the prognostic and predictive relevance of non-cellular secretory elements, such as chemokines, cytokines, and growth factors in GBM, and offer a model for clinical diagnosis. In addition, we have also established the correlation between biomarkers and dysregulated protein kinases in GBM. For the first time, we have looked at the involvement of E2s and how PTM, particularly acetylation, affects these enzymes. In typically, researchers always target substrate or E3 ligase. **Figure 4.1** provides a quick overview of our analytical methodology, which adheres to the norms in bioinformatics investigations. We investigated the wide-ranging functions of non-cellular secretory components in the GBM microenvironment using the cancer genome atlas (TCGA) data. Hence, in-depth information about the expression of the whole family of secretory components and insights into the role of acetylation modification in UPS systems in GBM were provided by the study for the first time.

4.1. MATERIAL AND METHODS

4.1.1. DATA COLLECTION AND EXPRESSION PROFILING OF NON-CELLULAR SECRETORY COMPONENTS

The data for 306 non-cellular secretory components, including chemokines, cytokines, and growth factors, were extracted from PubMed, Google Scholar, and Scopus. Chemokines, cytokines, and growth factors were expressed differently in GBM patients when compared to normal tissue utilizing several web servers that included GBM patients' transcriptomics data such as RNA sequencing data [(Gene Expression Profiling Interactive Analysis (GEPIA2.0), UCSC Xena, GlioVis-TCGA] and microarray data [GlioVis-REMBRANDT, GlioVis-

AGILENT, GlioVis-HG-U133 and GlioVis-GRAVENDEEL] and proteomics data such as Osppc [244], [540], [541], [543], [544], [638]. GEPIA2.0 and UCSC XENA compare TCGA and GDC tumor samples with matched Genotype-Tissue Expression (GTEx) standard samples. Venn analysis was performed using Venny2.1 to identify common DEGs from transcriptomics (RNA sequences and microarray) and proteomics data (CPTAC).

4.1.2. GENE-SET ENRICHMENT AND PATHWAY ANALYSIS OF DIFFERENTIALLY REGULATED PROTEOMICS SIGNATURES

Functional enrichment analysis of the Kyoto Encyclopaedia of Genes (KEGG) pathways and gene ontologies (GOs) of candidate DEGs were determined through a FunRich tool (version 3.1.3) [536] and Enrichr server [534], [535]. These tools identify and prioritize the essential genes related to GBM, followed by exploring biological pathways linked with them. A p-value ≤ 0.05 was deemed significant for GO analysis and route analysis statistical evaluation, and the fold-enrichment value was considered.

Analysis of prognostic relevance of identified signatures and their subcellular localization:

To assess the prognostic relevance of DEGs, we performed Kaplan-Meier (KM) plots to examine the overall survival (OS) and disease-free survival (DFS) of the GBM cohorts through web servers such as GEPIA2.0 and OSgbm [639]. OSgbm web server includes 684 samples with transcriptome profiles and clinical information from TCGA, GEO, and Chinese Glioma Genome Atlas (CGGA). We used the median expression as the expression threshold to divide patient samples into high- and low-expression groups for survival analyses of differentially expressed genes between GBM cohorts, along with the hazard ratio (HR), 95% confidence interval (CI), and log-rank test p-value. The Cox proportional hazard regression model calculated all HRs based on a high vs. low comparison. In addition, CELLO v.2.5: subCELlular LOcalization predictor was used for predicting subcellular localization of biomarkers.

4.1.3. IDENTIFICATION OF POTENTIAL E2 CONJUGATING ENZYME, E3 LIGASE AND SUBSTRATE IN GBM

E2s data was assembled through the Ubiquitin and Ubiquitin-like Conjugation Database (UUCD) [640]. In addition, we collated human E3 ligase enzyme from four distinct sources UUCD databases, Database of Human E3 Ubiquitin Ligases, Cell Signaling Incorporated Database and UbiNet 2.0 [641] database. Moreover, to identify substrate associated with E3 ligase, we have explored STRING [537] webtool to perform PPIs based on experimental data and > 0.400 confidence score, UbiNeT2.0 and Ubibrowser 2.0 [642].

Correlation study between a substrate, E2 conjugating enzyme and E3 ligase:

Spearman's correlation coefficient approach was used to investigate the correlation between two proteins in GBM samples using two web tools, GEPIA2.0 and TIMER2.0 [539]. GEPIA2.0 provides pair-wise gene correlation analysis of a given set of TCGA and/or GTEx expression data. In addition, TIMER2.0 Modules examine associations between gene expression and tumor features in TCGA. We have also performed a purity adjustment. We have studied the correlation between i) biomarker substrate with E3 ligase and ii) E2s with E3 ligase and HAT enzymes. Proteins with significant positive correlation were selected for further studies.

4.1.4. PREDICTION OF LYSINE SIGNATURE FOR ACETYLATION AND ASSOCIATED HATS ENZYMES

Two PTM prediction webservers based on deep learning methods, such as Deep-PLA [643] and GPS-PAIL 2.0 [644], were used to predict acetylation sites on internal lysine residues along with seven HATs enzymes, including CREBBP, EP300, HAT1, KAT2A, KAT2B, KAT5 and KAT8. The technique predicts acetylation sites based on the idea that various HATs have unique sequence specificities for the substrate changes. GPS-PAIL trains a Group-Based Prediction System previously developed a method to create a computational model for each HAT enzyme.

4.1.5. STRUCTURAL ANALYSIS OF SELECTED E2 CONJUGATING ENZYME

Prediction of secondary structure*:* PTM affects the secondary structure of the protein, which governs its biological functions. PSIPRED: protein structure analysis workbench [645] was used to predict the structural selectivity of lysine acetylation sites. Subsequently, the relationship between the protein's secondary structure, fold recognition, and its corresponding acetylating sites was established. The output result was classified into three categories such as coiled, helix, and strand

Protein intrinsic disorder prediction: The FASTA sequence of the protein was procured from the Uniport [646] database. DISOPRED3 predicts structural order and disorder regions along with protein binding sites within disordered regions using a SVM that examines patterns of evolutionary sequence conservation, positional information and amino acid composition of putative disordered regions. As analyzed from the output, the extracted data were separated into two categories: ordered and disordered regions.

4.1.6. MUTATIONAL ANALYSIS OF LYSINE MODIFICATION

The functional impact of lysine mutations was investigated with the use of web applications such as PMut [647], SNAP2 [648], Polymorphism Phenotyping v2 (PolyPhen2) [649], and MutPred2 [650]. All these tools require protein sequences in the FASTA format and a list of amino acid substitutions. The output results were computed numerically, and the combined score of the four web tools was determined. If a mutation's confidence score is ≥ 2.5, referred to as a threshold value, the mutation is considered disease sensitive. The basic, charged lysine (K) residue was changed into glutamine (Q), leucine (L), glutamate (E), and arginine (R). Additionally, the software MutPred2 was employed to forecast the physical impact of a lysine mutation on acetylation. The impacted sites were divided into two groups based on whether neighboring sites gained or lost functionality.

4.1.7. CHARACTERIZATION OF THERAPEUTIC AXIS

ROC plotter: predictive marker identification: ROC plotter-an online ROC analysis tool [651], was employed to comprehend the association between gene expression and therapeutic response using transcriptomic level data from TCGA datasets of GBM and other cancer. This tool uses a JetSet probe to select the optimal microarray probe representing a gene. The package 'ROC' was used to calculate the area under the curve (AUC). The integrated database comprises 454 GBM patients from 3 independent datasets and 10 103 genes. Patients were categorized as responders/non-responders based on their survival status at 16 months post-surgery.

Expression response to top mutated gene in GBM: Literature was used to find the top 10 mutated genes in GBM. "Gene_Mutation" module of TIMER2.0 was used to compare the differential gene expression with different mutation statuses of top mutated genes (such as PTEN, TP53, EGFR, PIK3R1, PIK3CA, NF1, RB1, IDH1, PTPRD, and ERBB2) of GBM.

Correlation with protein kinase protein GBM: KinMap, a user-friendly web interface for human genome (the "kinome") was explored to retrieve 536 human protein kinase including eight typical groups (AGC, CAMK, CK1, CMGC, STE, TK, TKL, Other) and 13 atypical families [652]. Using the GEPIA2.0 tool, the expression of each kinase was examined in GBM patient tumor samples. Network analysis was employed to study correlation between the putative 'therapeutic axis' proteins and significantly dysregulated kinases.

4.1.8. STATISTICALLY ANALYSIS

In GEPIA2.0, we used the ANOVA statistical method for differential gene expression analysis, selected $\log_2(TPM + 1)$ transformed expression data for plotting, TCGA tumor compared to TCGA normal and GTEx normal for matched normal data in plotting, $|\log_2 FC|$ cut-off of 1.5, and a q-value cut-off of 0.05. For survival analysis, it uses the Mantel-Cox test for the hypothesis test. OSppc used Mann-Whitney Wilcoxon tests to calculate the significant

difference between proteomics data of tumors and adjacent normal tissues. In the TIMER2.0 database analysis, partial Spearman's correlation (ρ) was applied. When |Rho, ρ| > 0.1, it indicated a correlation between the genes and immune cells. Red color signifies: Positive correlation (p-value <0.05, ρ>0), blue color signifies: Negative correlation (p-value<0.05, ρ>0) and grey color signify: non-significant (p-value >0.05).

4.2. RESULTS AND DISCUSSION

4.2.1. EXPRESSION OF SECRETORY COMPONENTS IN GBM AND NORMAL TISSUE

The 306 non-cellular secretory components, including chemokines, cytokines, and growth-factor of TME, have been extracted from PubMed and Google Scholar. A total of 53 chemokines, including all 4 subfamilies CXC, CC, CX3C, and C [653], 253 cytokines and growth-factors including ILs, IFNs family, TNFs family, TGFs superfamily (BMP-like family, GDNFs family, TGF-β-like family), MMPs family, FGFs family, PDGFs family, VEGFs, TIMPs, prolactin, GCSFs, GMCSFs, were extracted. Firstly, we have studied the expression of chemokines, cytokines, and growth factors in GBM at transcriptomics and proteomics levels using a web tool based on TCGA data sets. RNA sequence data were analyzed using GEPIA2.0 (163 GBM tissue and 207 normal tissue, including GTEx normal tissue), UCSC Xena (154 GBM tissues and 5 Normal tissues), GlioVis-TCGA (156 GBM tissues and 4 Normal tissues), and microarray data were analyzed using GlioVis-REMBRANDT (225 GBM tissues and 28 Normal tissues), GlioVis-AGILENT (489 GBM and 10 normal tissues), GlioVis-HG-U133 (528 GBM tissues and 10 normal tissues), and GlioVis-GRAVENDEEL (117 GBM tissues and 8 normal tissues), and protein data from CPTAC, RPPA, and TCGA were analyzed using Osppc tool. We have used the Venny2.1.0 database to identify all non-cellular secreted components of TME that were significantly expressed in at least four RNA sequence data and microarray data. 73 genes were commonly expressed in RNA sequence and microarray data

(**Figure 4.2(A)).** Afterward, the protein expression of these 73 genes was checked. A total of 44 biomarkers has significantly dysregulated expression (log_2FC score ≥1.5 and p-value ≤0.05), out of which 41 were upregulated and 3 downregulated in patients with GBM compared with its normal tissues **(Figure 4.2(B)).**

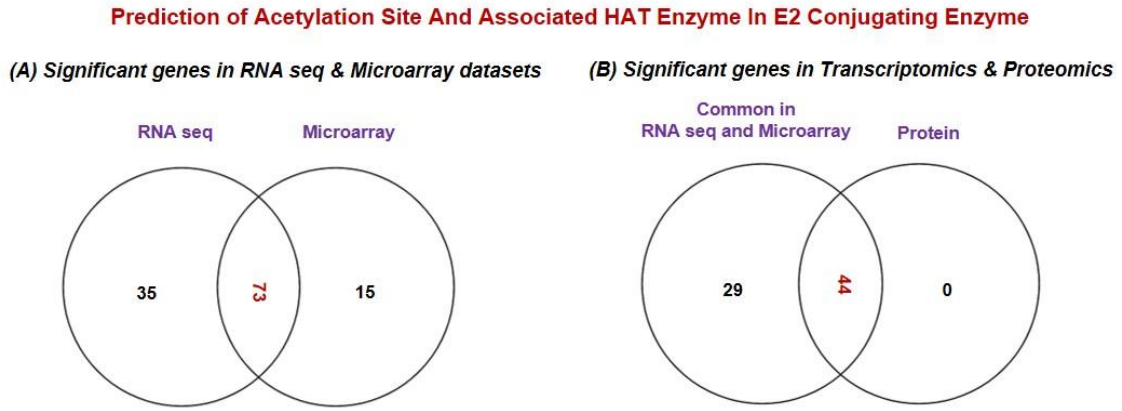

Figure 4.2: Data Sorting and Functional Enrichment of Significant Non-Cellular Secretory Biomarkers: (A) Venn diagram showing significant differentially expressed genes from transcriptomics data (RNAseq and Microarray) datasets. 73 genes overlap in RNA and microarray datasets (B) Venn diagram showing significant differentially expressed genes common in transcriptomics and proteomics datasets of GBM with the cut-off criteria of $|log_2FC| \geq 1.5$ and p-value≤ 0.05. 44 genes are common with protein datasets.

Thus, the details expression pattern of 306 secretory components has been tabulated in **Annexure 5,** and 44 shortlisted biomarkers were tabulated in **Table 4.1** (Description in **Annexure 6)**. Previous studies also support our observations. Out of 44, only 3 were chemokines in which CCL5 and CXCL16 were upregulated, whereas CX3CL1 was downregulated in GBM. A study by Dai et al., 2016 showed that CCL5 chemokines influence tumor progression through various mechanisms that directly affect cancer cell proliferation or indirectly regulate angiogenesis and recruitment of immune cells that promote tumor growth and metastasis [654], [655]. In addition to tumors, tumor-associated cells such as CAF, EC, MSC, MDSC, and TAM generate CXCL16 and influence tumor-associated cells in glial tumors [656], [657]. Cytokines and growth factors have a pleiotropic role in influencing various biological functions, including immune response, inflammation, and cell-to-cell communication. Studies on GBM provide evidence to support our observation of cytokines. For instance, Frei et al., 2015 demonstrated that TGFβ acts as a critical molecule implicated in

GBM malignancy [658]. Other studies show the importance of IL-18 in cell migration, which is fatal and untreatable, and the mechanism through which GBM cells release ECM proteins like fibronectin and vitronectin, in turn, causes the surrounding normal brain microglia to secrete more IL-18 [659], [660]. A comprehensive investigation of TIMPs in GBM by Han et al., 2021 revealed that TIMP3 indirectly controls MMPs signaling and ECM remodeling [599]. Multiple hormonal and non-hormonal growth-stimulating agents are also present in GBM and can function as biomarkers [661]. Recent research has also emphasized the critical role played by these secretory components in the pathogenesis of GBM and the creation of the immune milieu through immunological regulation, which inhibits anti-tumor responses and promotes the growth of tumors [662]. Thus, our results further confirm these previous findings.

Table 4.1: Transcriptomics and Proteomics Expression Analysis of Non-Cellular Secretary Components in GBM Patients Samples Compared with Normal Tissues

Webtools		RNA sequence datasets				Microarray datasets				Protein expression
		GEPIA 2.0	*UCSC XENA*		*GLIOVIS*	*GLIOVIS*		*TCGA_GBM*		*CPTAC*
		TCGA GBM_GTX	TCGA GBM	GDC TCGA GBA	TCGA RNA Sequence	REMBRANDT	GRAVENDEEL	HG-U133A	AGILENT -4502A	Osppc
Chemokine	CCL5									
	CX3CL1									
	CXCL16									
Cytokines and Growth factors	ANGPT2									
	BMP1									
	BMP7									
	COL1A1									
	COL1A2									
	COL3A1									
	COL4A1									
	COL4A2									
	COL5A1									
	COL5A2									
	CTSB									
	HIF1A									
	IL-18									
	LAMA4									
	LAMA5									
	LAMB1									
	LGALS3									
	LGALS9									
	LOX									
	LOXL1									
	LOXL3									

MMP14									
MMP17									
MMP2									
MMP9									
PLOD1									
PLOD2									
PLOD3									
PTGES2									
SDF2									
SDF4									
SERPINE1									
SERPING1									
SPP1									
TGFβ1									
TGFβ2									
TIMP1									
TIMP3									
TNFAIP6									
TNFRSF1B									
VEGFA									
Patient samples number used in the respective study									
TUMOR	163	154	155	156	225	117	528	489	153
N0N-TUMOR	207	5	5	4	28	8	10	10	—
Upregulated in GBM				p≤0.001		p≤0.01			p≤0.05
Downregulated in GBM				p≤0.001		p≤0.01			p≤0.05
Not significant in GBM			p>0.05						

4.2.2. FUNCTIONAL ENRICHMENT AND BIOLOGICAL PATHWAY ANALYSIS OF BIOMARKERS

We have performed functional enrichment analysis using the FunRich-functional enrichment analysis tool for (GO) and KEGG pathway enrichment analysis to investigate the role of 44 differential biomarkers in GBM. We selected only pathways that were involved in the pathogenesis of the GBM microenvironment and had a large number of genes with significant fold enrichment. We have also looked at how biomarkers are involved in the biological processes that lead to the pathology of GBM. According to the results of cellular components, the bulk of biomarkers is located in extracellular regions, the ECM, and extracellular vesicles (EVs). These data corroborate earlier findings that secretory components, which are located in the extracellular space of the microenvironment and have a variety of clinical implications, have the ability to function as biomarkers and potentially disrupt signaling pathways implicated

in tumorigenesis [18]. Cytokines are soluble factors released predominantly in soluble or EV-associated forms and are involved in cell-cell communications [663]. Molecular function analysis showed that the maximum number of biomarkers were engaged in structural components of ECM, cytokines and chemoattractant activities, integrin binding, growth-factors activities and PDGF binding. Chemokines act as chemoattraction, which binds to G protein-coupled seven transmembrane cell surface receptors (GPCRs) and thus activates a cascade of signaling G proteins, PI3K, protein kinase C, phospholipase C, RAS, and MAPKs to mediate immune cells migration, activation, cell chemotaxis, invasion, production of mediators promoting angiogenesis, and transactivation of EGFR [664]. Studies showed that the expression of specific integrins is upregulated in both tumor cells and stromal cells in a TME. Integrins receptors bind to specific secretory components from TME, which regulate ECM detachment, migration, invasion, proliferation and survival through PI3K-AKT signaling [665].

Biological process analysis showed top six processes were ECM organization, cell migration, inflammatory response, response to hypoxia, and angiogenesis. Additionally, we used the Enrichr tool to examine the KEGG Pathway 2021. We studied the biological pathway causing the pathology of GBM **(Figure 4.3).** According to the tool's combined score, the top 10 biological pathways were ECM-receptor interaction, proteoglycans in cancer, PI3K-Akt signaling pathway, HIF1 signaling pathway, TNF signaling pathway, cytokine-cytokine receptor interaction, lysine degradation, TGF-β signaling pathway, and Hippo signaling pathway. Previous studies have found that activation of the HIF1A pathway is a common feature of gliomas and may explain the intense vascular hyperplasia often seen in GBM [666], [667].

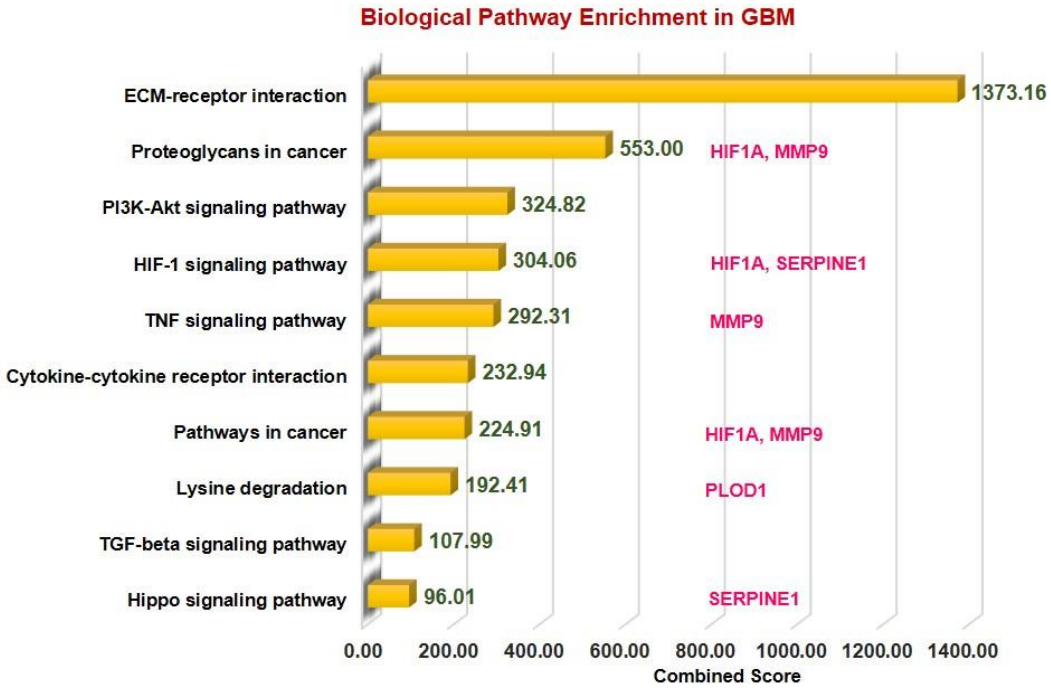

Figure 4.3: Functional Enrichment of Significant Non-Cellular Secretory Biomarkers: Biological Pathway Analysis Using KEGG Pathway: Among the top 10 biological pathways based on combined score* calculated by Enrichr tool are ECM-receptor, P13K-Akt, Hypoxia, TNF, TGF and Hippo pathways with p-value≤0.05 in GBM. *Combined score is computed by taking the log of the value from the Fisher-exact test and multiplying that by the z-score of the deviation from the expected rank.

Similarly, TNF signaling enhances invasion in GBM and upregulates MEK-ERK signaling, NF-κB1 and STAT expression [668]. In GBM, TNF secreted by the associated macrophages with the tumor encourages the activation of endothelial cells, which makes the patient resistant to anti-angiogenic treatments [669]. Similar to increased PI3K-AKT activation, it has a distinct function in tumor growth but does not cause resistance to treatment [670]. There is mounting evidence that Hippo signaling has a role in a number of cancers, including glioma, breast, lung, and colon cancer. The concept that this route might represent a potential target opening the door for alternative medicines is supported by the fact that it is less studied in GBM and engaged in tumorigenesis and metastasis [671]. Our pathways analysis results also line up with previous findings [665]. Herein, through the top-mentioned molecular functions and biological pathways, we have demonstrated that the majority of the shortlisted secretory biomarkers were localized in extracellular space and were critical for tumorigenesis, migration, and invasion in

the pathology of GBM. As a result, these signaling pathways have the potential to be further investigated in the context of GBM development and can be therapeutically addressed if we intend to target the GBM microenvironment in addition to the tumor cells. **Figure 4.4** demonstrate GO analysis of 44 biomarkers, respectively.

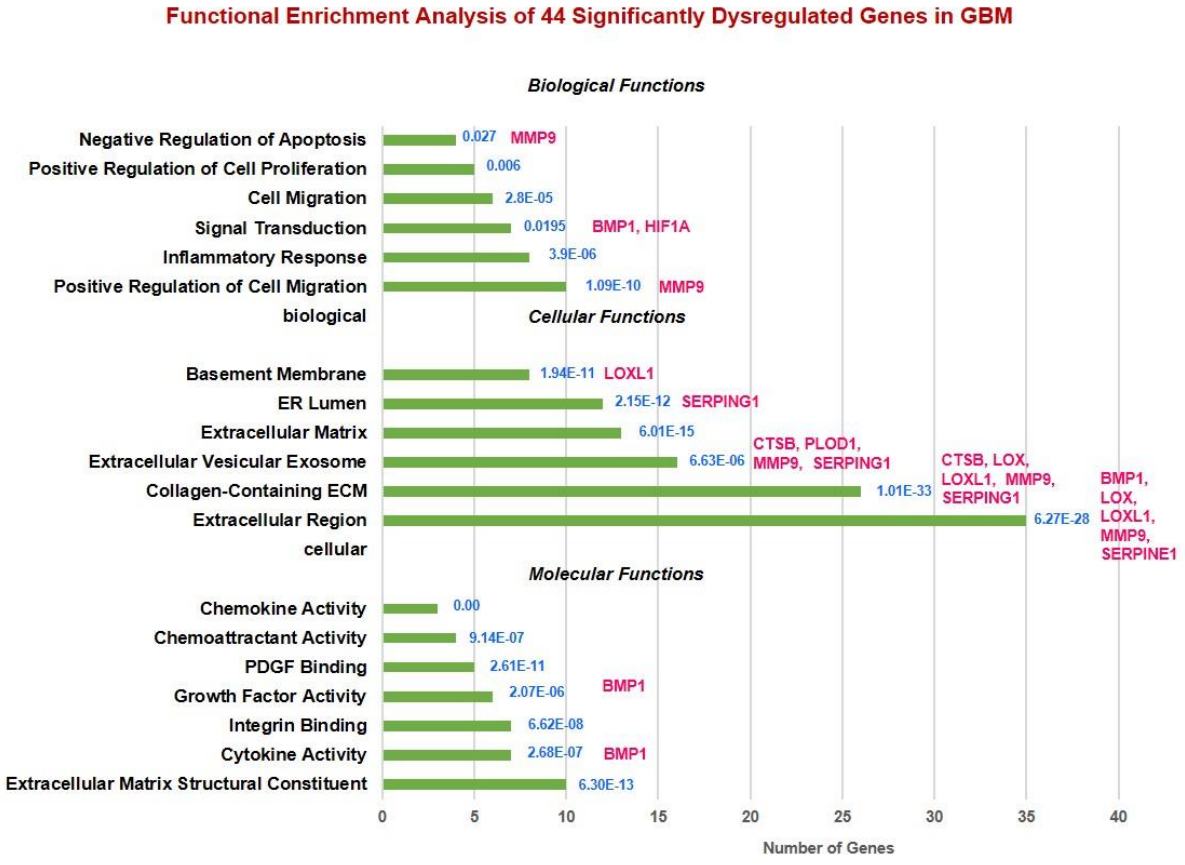

Figure 4.4: Functional Enrichment of Significant Non-Cellular Secretory Biomarkers: Gene Ontology (GO) Analysis contains three sub ontologies: molecular function, cellular components and biological process associated with 44 biomarkers. Molecular function and cellular components showed maximum numbers of biomarkers involved in ECM structural constitute and localized extracellular region. At the same time, top-ranked biological processes are ECM organization, cell migration, inflammation, response to hypoxia, signal transduction and angiogenesis. Blue text showing p-value of this analysis.

4.2.3. RELATIONSHIP BETWEEN BIOMARKERS AND SURVIVALS OF GBM PATIENTS

To evaluate the relation between 44 significantly differentially expressed genes and the prognosis of GBM patients, GEPIA2.0 and OSgbm web tools were used for plotting KM plots for OS and DFS analysis. These tools use GBM data from TCGA. The data was analyzed in KM plot where curves were stratified by median signal expression (high vs. low expression

group). The cox proportional HR and p-values are displayed on survival curves. A p-value ≤ 0.05 was considered statistically significant, HR>1 was considered a poor prognostic, and HR<1 was a good prognosis. **Figure 4.5(A)** and **Annexure 7** illustrate the strong association of overexpression of bone morphogenetic protein 1 (BMP1), cathepsin B (CTSB), lysyl oxidase (LOX), procollagen-lysine,2-oxoglutarate 5-dioxygenase 1 (PLOD1) with poor OS (HR >1 and p(HR) ≤ 0.05). CTSB proteases are essential in ECM degradation and are overexpressed in most human colon and other cancers. A recent study by Ma et al., 2022 also demonstrates that CTSB is a negative prognostic biomarker and biological pathway associated with immune suppression and inflammation in glioma [672]. Studies have demonstrated that CTSB regulates several forms of cell death, such as apoptosis, necroptosis, autophagy, pyroptosis, and ferroptosis, and is associated with radio-resistance, tissue invasion, and metastasis of GBM [673]**.** BMP1 (secreted metalloprotease of the astacin metalloproteinase family) recently emerged as a cancer-related protein in multiple cancer but is less explored in GBM. Signaling such as TGF-β involving BMP1 affects the proliferation and differentiation of glioma stem cells. According to the study by Xiao et al., 2019, increased expression of BMP1 reflects poor prognosis in clear cell renal cell carcinoma [674]. Similarly, we first time reported that BMP1 had poor OS in GBM patient samples. A study by Sachdeva et al., in 2019 showed that in the GBM microenvironment dysregulated BMP signaling via expression of p21 protein causes GSCs to enter a quiescent state, rather than developed into the differentiated astroglia cell [675]. In addition, a study showed that increased expression of LOX expression was strongly associated with the invasive features of malignant astrocytes. LOX is well recognized as secreted matrix-modifying enzyme. The key roles played by LOX include the regulation of gene expression, protein-lysine 6-oxidase activity, protein binding, and protein phosphorylation. It has an impact on cell cycle progression and apoptosis in GBM and can be exploited as a target for early detection and targeted treatment [676].

(A) Survival Analysis of GBM Patients By Kaplan-Meier Method

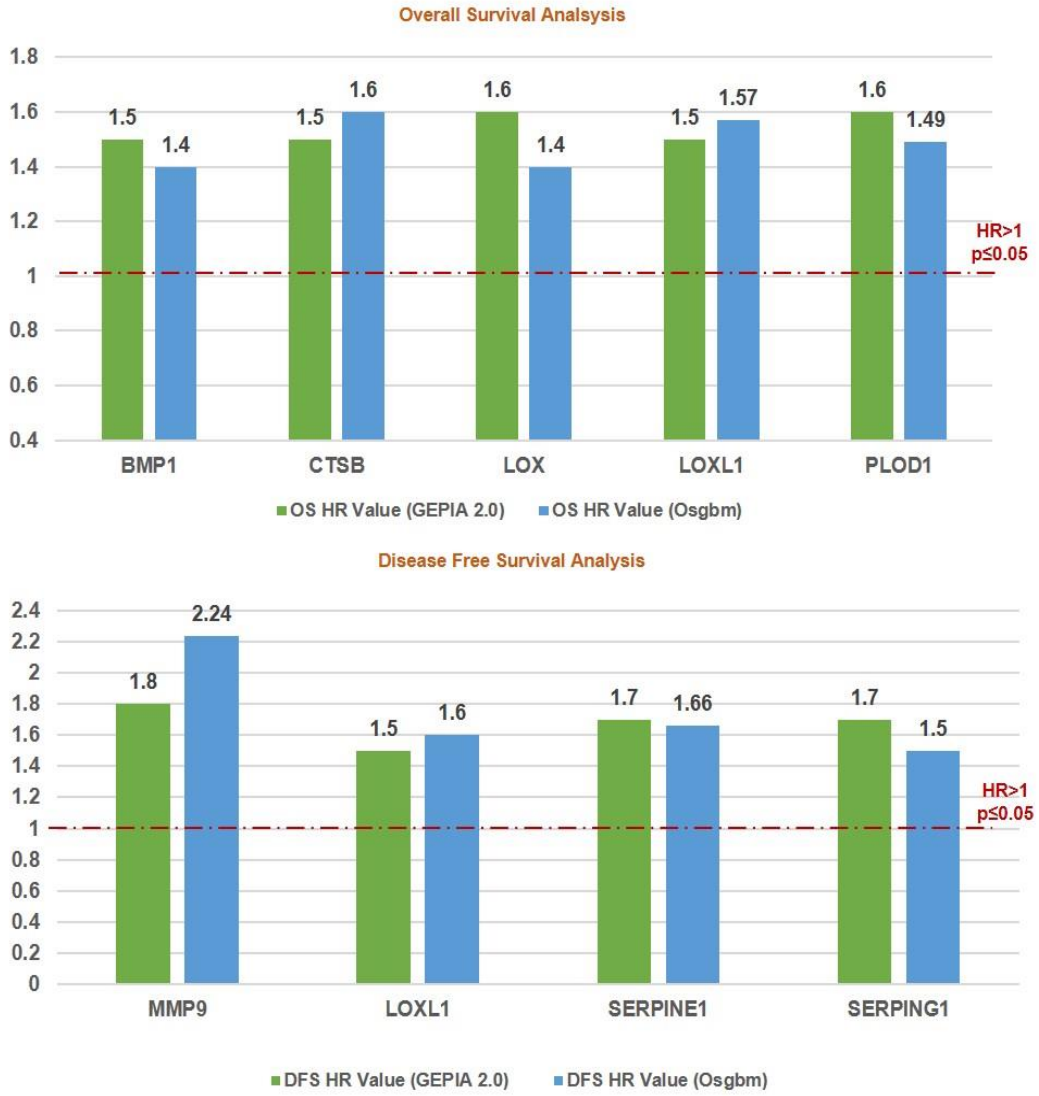

GEPIA2.0: Tumor = 163 GBM patients data; Osgbm: Tumor = 153 GBM patients data
p-value ≤ 0.05 and p(HR) value ≤ 0.05)

(B) Prediction of Protein Subcellular Localization

Analysis Report of CELLO v.2.5 Predictor						
Genes Name	**Extracellular**	**Cytoplasmic**	**Plasma Membrane**	**Mitochondrial**	**Lysosomal**	**Nuclear**
BMP1	**2.368***	0.759	0.358	0.079	0.094	1.079
CTSB	0.243	0.009	0.007	0.009	**4.630***	0.033
LOX	**3.140***	0.039	0.102	0.109	0.211	1.068
LOXL1	**2.194***	0.113	0.377	0.097	0.153	1.485
PLOD1	0.386	**1.836***	0.369	0.549	0.595	0.299
MMP9	**2.820***	0.224	0.721	0.267	0.339	0.225
SERPINE1	**2.101***	0.554	0.604	0.753	0.084	0.167
SERPING1	**2.377***	0.523	0.218	0.151	0.044	1.404

Figure 4.5: (A)Survival Analysis of GBM Patients by Kaplan-Meier Method: The Cox proportional Hazard ratio (HR) was plotted against prognostic markers. GEPIA and Osgbm perform overall survival (OS) or disease-free survival (DFS) analysis based on gene expression. It uses the Log-rank test and the Mantel-Cox test for the hypothesis test. Threshold HR value>1 signifies poor prognostic markers, and HR<1 represents good prognostic markers. Based on OS analysis over expression of BMP1, CTSB, LOX, LOXL1and PLOD1 and DFS overexpression of MMP9, LOXL1, SERPINE1 and SERPING1 were significantly associated with poor prognosis in GBM. Green bar color: Data from GEPIA2.0 webtool; Blue bar color: Data from Osgbm webtool. (B) Prediction of Protein Subcellular Localization by Cello Online Predictor: BMP1, LOX, LOXL1, MMP9, SERPINE1 and SERPING1 localized in majorly extracellular space. CTSB is majorly localized in lysosomes and PLOD1 in the cytoplasm, followed by extracellular space.

Li et al., 2021 showed that ECM-related gene LOX correlated with poor OS in glioma patients [677], including GBM [678] and gastric cancer [679]. Another investigation discovered a difference between Lysine oxidase-like 1 (LOXL1) and poor OS in GBM [680]. The antiapoptotic activity of LOXL1 is mediated via interactions with a variety of antiapoptotic modulators, including BAG2, and by Wnt/beta-catenin signaling [681]. Our finding revealed that the upregulation of LOXL1 was accompanied by both poor OS and DFS. Moreover, PLOD1 encourages cross-linking in ECM molecules, enabling ECM structural stability and maturation. In a study by Wang et al., 2020, increased PLOD1 expression in glioma was linked with a worse prognosis [682]. Significant overexpression of PLOD1 may encourage the growth and colony formation of U87MG cells by triggering the HSF1 signaling pathway [683] however, in hypoxic settings could stimulate invasiveness and the mesenchymal transition by inducing NF-κB signaling pathway [684]. Secondly, our data demonstrated the overexpression of Matrix metallopeptidase 9 (MMP9), Serpin Family E Member 1 (SERPINE1), and serine protease inhibitor family G1 (SERPING1) linked with poor DFS (HR>1 and p(HR)≤0.05) (**Figure 4.5) and Annexure 8.** Our finding supported previous studies that the overexpression of MMP9 indicates a poor prognosis in glioma [685]. In the microenvironment GBM-secreted factors influence increased human brain vascular endothelial cell migration as well as levels of MMP9 and CXCR4 which result in enhanced angiogenesis [686]. Indeed, Seker et al., 2019 research shows that poor patient survival in GBM is related to increased expression of SERPINE1 [687]. In hypoxic microenvironment condition, ROS promotes tumor progression, EMT in GBM through HIF1A-SERPINE1 signaling [688]. Shengmeng et al., 2018 found low

SERPING1 levels have been associated with poor DFS in prostate cancer [689]. In contrast, our study reported a higher level of SERPING1 linked with poor DFS/prognosis in GBM. These results showed that BMP1, CTSB, LOX, LOXL1, MMP9, SERPINE1, and SERPING1 are poor prognostic indicators in GBM since they had HR > 1 and p(HR) ≤ 0.05. Jia et al., 2018 also showed that SERPINE1 and SERPING1link with poor prognosis in GBM [690].

Moreover, we have also used CELLO v.2.5: subCELlular LOcalization predictor for finding the localization of identified prognostic markers. Results in **Figure 4.5(B)** showed that BMP1, LOX, LOXL1, MMP9, SERPINE1, and SERPING1 localized in extracellular space while PLOD1 localized majorly in cytoplasm followed by extracellular space and CTSB localized in lysosome followed by extracellular space. Studies have revealed a strong correlation between a protein's subcellular location and function. Sequencing similarity is helpful in predicting subcellular localization for sequences containing >30% sequence identity.

4.2.4. IDENTIFICATION OF HIF1A AS SUBSTRATE FROM DYSREGULATED BIOMARKERS AND ITS ASSOCIATED E3 LIGASE

To find the therapeutic axis to understand ubiquitination systems in GBM, we have focused on finding the possible substrate from the list of 44 differentially expressed biomarkers. We have used the STRING database to find the experimentally validated (confidence score>0.400) substrate and correspondence E3 ligase. The E3 ligase list was created by combining E3 ligase protein from four different sources: the Human E3 ligase database, CST, UUCD, and UbiNet 2.0. This list was used to make an individual PPI network with every 44 biomarkers in the STRING database. This study's results showed that BMP1, HIF1A, and TNFRSF1B are the biomarkers that also act as a substrate for E3 ligase and are involved in the Ubiquitination pathway. Results showed E3 ligase correspondence to substrate i) BMP1 was RMND5A, ii) HIF1A were EP300, GNB2L1, MDM2, PARK2, STUB1, TRAF6, VHL, FBXW7, SIAH1, SIAH2, iii) TNFRSF1B were TRAF1, TRAF2, ASB3, SMURF2. Subsequently, mRNA and

protein expression of these substrate and their corresponding E3 ligases were studied in GBM patients (**Table 4.2**). Based on the results, only substrate HIF1A and its E3 ligase von Hippel-Lindau (VHL) and GNB2L1 were dysregulated in GBM patients' samples both at transcriptomics and proteomics levels. Under the normoxic condition, HIF1A is ubiquitinated by VHL and E3 ligase for proteasome degradation in the cytoplasm. Once stabilized, HIF1A translocate to the nucleus, guided by a nuclear localization signal in its C-terminus [691], [692]. In contrast, Aga et al., 2014 demonstrated that endogenous HIF1A is detectable in exosomes [693] present in the microenvironment, and studies suggest that exosomes reflect the hypoxic status of glioma cells and mediate hypoxia-dependent activation of vascular cells during tumor development [694]. In addition, HIF1A initiates TNFα exosome-mediated secretion under hypoxic conditions [695]. In human glioblastoma cells, Bensaad et al., 2014 showed that HIF-1α was necessary to induce Fatty Acid Binding Protein 3 (FABP3) and FABP7, leading to lipid droplet accumulations [696]. According to reports, HIF1A is essential for the growth and development of GBM as well as for tumor cell migration, glucose absorption, angiogenesis, and chemoresistance. A plethora of research showed that hypoxia triggers glioma cells to release EVs with distinct functional proangiogenic cargo, including cytokines, growth factors, proteases, and miRNA to influence endothelial cells to promote angiogenesis, metabolic, and transcriptional signaling pathways such are the EGFR, PI3K/Akt and MAPK/ERK pathways. Hypoxia-stimulated glioma EVs promote tumor vascularization, pericyte vessel coverage, and cell proliferation, eventually reducing tumor hypoxia in the GBM microenvironment [697]. Hence, we have chosen HIF1A as substrate, VHL, and GNB2L1 (another gene name: RACK1) as an E3 ligase for further studies. Earlier investigations support our observation. Mutation in VHL genes causes renal cell carcinomas, pheochromocytomas, and cerebellar hemangioblastomas [698]. We were interested in exploring this interaction in GBM. However, based on experimental data, our analysis also proposed GNB2L1 interacting with HIF1A.

Earlier, this interaction was established in breast cancer [699]. Here we will discuss this in context with GBM.

Evidence from the literature suggests that the poor prognostic biomarkers LOX, BMP1, CTSB, LOXL1, PLOD1, MMP9, SERPINE1, and SERPING1 are related to the hypoxic microenvironment. First, there was a positive correlation between BMP1 and HIF1A and the malignant grade of astrocytoma, although there was no evidence of a direct or indirect association [674]. Additionally, Xiaofei et al., 2018 demonstrated that hypoxia upregulates CTSB and HIF1A in a fashion comparable to HepG2 cells. [700]. In several cancer types, including breast, head and neck, prostate, colon, and renal cell carcinomas, LOX controls HIF1A. The invasive and metastatic characteristics of hypoxic cancer cells, including astrocytoma, are caused by secreted LOX [701]. Under hypoxic conditions (<1% oxygen), LOX and LOXL1 promoted angiogenesis [702]. Recently, Wang et al., 2021 discovered that Hypoxia causes the overexpression of PLOD1, which, through NF-kB signaling, leads to the malignant phenotype of GBM [684]. HIF1A promotes the development of MMP9, which influences invasion in breast cancer by weakening the basement membrane and the ECM barrier. HIF1A is also implicated in the control of cell proliferation, growth factor release, and angiogenesis [703]. Furthermore, hypoxia-induced overproduction of ROS causes cancer to upregulate the SERPINE1 protein (protein that regulates cell adhesion), which controls cell adhesion in breast cancer [704]. In contrast, HIF2A, not HIF1A, controls the expression of SERPING1, which is linked to immunological infiltrations in glioblastoma [705]. Accordingly, we can state that HIF1A is a crucial biomarker that correlates with all cancer biomarkers that indicate a poor prognosis. As a result, we go forward with HIF1A and want to investigate its potential role in the therapeutic axis for treating GBM.

Table 4.2: Expression Analysis of Substrate and Its Associated E3 Ligase in GBM Patients Samples

Substrate (STRING, Ubibrowser2.0, Ubinet2.0)	E3 ligase (UUCD, CST, UbiNet2.0)	Combined score (STRING)	Expression in GBM	
			Gene Expression (GEPIA2.0)	Protein Expression (Osppm)
BMP1	RMND5A	0.483		
HIF1A	EP300	0.999		
	GNB2L1	0.998		
	MDM2	0.997		
	PARK2	0.762		
	STUB1	0.81		
	TRAF6	0.72		
	VHL	0.999		
	FBXW7	0.664		
	SIAH1	0.43		
	SIAH2	0.543		
TNFRSF1B	TRAF1	0.761		
	TRAF2	0.881		
	ASB3	0.485		
	SMURF2	0.57		
Sample size	Tumor tissues		163	153
	Normal tissues		207	--

4.2.5. IDENTIFICATION OF SIGNIFICANT E2 CONJUGATING ENZYME ASSOCIATED WITH VHL AND GNB2L1 IN GBM

Ubiquitin-conjugating enzymes (E2s) are the central players in the trio of enzymes responsible for the attachment of ubiquitin (Ub) to cellular proteins. It plays a more prominent role in ubiquitin signaling than a middleman. The UBC domain, a central catalytic domain in E2s, has about 150 amino acids. This domain adopts an α/β-fold typically with four α-helices and a four-stranded β-sheet. Important loop regions form part of the E3-binding site and the E2 active site. Several studies have suggested the dysregulation of E2 in multiple cancer. Understanding of E2s regulation is still emerging, and it is evident that E2s can be governed by various mechanisms [706]. Hence, we explore how E2s regulate and affect others, especially our shortlisted E3 ligases VHL and GNB2L1 and substrate HIF1A in GBM. We have extracted 36 E2s expressed in humans from previously published research.

In addition, we analyzed its expression at mRNA and protein levels in GBM patient samples with the help of the GEPIA2.0 and Osppc web applications (**Figure 4.6(A))**. We have found that at mRNA levels, 13 E2 conjugative enzymes were significantly (p-value ≤ 0.05, $\log_2$FC ≥ 1.5) dysregulated in GBM patient samples, including 11 upregulated (Ube2A, Ube2C, Ube2D2, Ube2D3, Ube2E1, Ube2H, Ube2J1, Ube2J2, Ube2L6, Ube2L6, Ube2N, Ube2S, Ube2T) and 1 downregulated (Ube2QL1). In addition, amongst 13 shortlisted enzymes, we found that protein levels of 7 were upregulated (Ube2A, Ube2C, Ube2E1, Ube2H, Ube2J1, Ube2H, Ube2J2, Ube2L6, Ube2S), 3 were downregulated (Ube2D2, Ube2J1, Ube2N), 2 were (Ube2D3, Ube2QL1) were not available in the database, and UBE2T were non-significant. Thus, based on both transcriptomics and proteomics expression data analysis, we moved further with 6 E2s named Ube2C, Ube2E1, Ube2H, Ube2J2, Ube2L6, Ube2S that were overexpressed in GBM. A study by Xiang et al., 2022, Ube2C serves as both an oncogene and a tumor suppressor gene, and its overexpression is crucial to the development of thyroid cancer [707]. Moreover, another study by Pan et al., 2021 demonstrates that Ube2D3 induces the ubiquitination of the SHP-2 protein, which in turn activates STAT3 signaling, promoting tumorigenesis and glycolysis in gliomas [708].

Further, we have also studied the correlation between E3 ligase with substrate and shortlisted E2s in GBM patient's samples using GEPIA2.0 (GBM tumor sample size, n=163) and TIMER2.0 (GBM tumor sample size, n=153). We have tabulated purity-adjusted partial Spearman's rho (ρ) value which gives the degree of their correlation in the form of a heatmap (**Figure 4.6(B))**. We have used spearman statistical analysis, and when $|\rho| > 0.1$, it indicated a correlation between the genes. Red color signifies: Positive correlation (p-value ≤0.05, ρ>0), blue color signifies: Negative correlation (p-value≤0.05, ρ>0) and grey color signify: non-significant (p-value>0.05). Results showed in GBM that both E3 ligase VHL and GNB2L1 were positively correlated with its substrate HIF1A. Moreover, VHL was positively correlated

with Ube2E1, Ube2H, and Ube2J2, whereas GNB2L1 was positively correlated with Ube2C, Ube2J2, and Ube2S.

Furthermore, to investigate the PTM (e.g., acetylation) that can modify lysine basic residues (lysine and/or arginine). Acetylation affects a large number of histone and non-histone proteins. Growing evidence suggests that reversible lysine acetylation of non-histone proteins regulates mRNA stability, protein localization and degradation, and protein-protein and protein–DNA interactions. The dynamic regulation of genes governing cellular proliferation, differentiation, and death depends largely on the recruitment of HATs and HDACs to the transcriptional machinery. Several oncogenes or tumor-suppressor genes produce many non-histone proteins specifically targeted by acetylation. These proteins have a direct role in carcinogenesis, tumor growth, and metastasis [709]. Researchers have found acetylation sites on Ub molecules and showed how acetylated Ub modulates E1 enzyme (Uba1) catalytic activity. On a similar note here, we explore the potential acetylation site on lysine residues and its impact on selected E2s such as Ube2E1, Ube2H, Ube2J2, Ube2C, and Ube2S in GBM [710]. In patients with anaplastic gliomas, a greater Ube2C expression was linked to mitotic cyclin degradation and a significantly reduced OS duration [711]. Additionally, Ube2S is controlled by the PTEN/Akt pathway and participates in DNA repair, particularly NHEJ-mediated DNA repair, which makes chemotherapeutic drugs more sensitive to GBM [332]. In a recent study, Shin et al. found a mutation (*de novo* missense variant) that resembles a variant found in a patient with neurodevelopmental abnormalities, induces irregular Ube2h function in zebrafish embryos, and results in abnormal brain development [712]. In addition, according to Lim and Joo, 2020, circulating Ube2H mRNA is potentially used to diagnose and treat Alzheimer's disease [713]. However, Ube2H has been studied in cancer, although there is little information about it in GBM [714].

(A) Expression Analysis of E2 Conjugating Enzymes in GBM

Category	Gene Name	RNA SEQ (TCGA-GBM)	Protein expression (CPTAC)
		GEPIA2.0	*Osppc*
E2 conjugating enzyme	Ube2A	*	*
	Ube2C	*	*
	Ube2D2	*	*
	Ube2D3	*	--
	Ube2E1	*	*
	Ube2H	*	*
	Ube2J1	*	*
	Ube2J2	*	*
	Ube2L6	*	*
	Ube2N	*	*
	Ube2QL1	*	--
	Ube2S	*	*
	Ube2T	*	ns

(B) Correlation Study Analysis

E3 ligase enzymes		VHL		GNB2L1/RACK1	
Substrate	Webtool	GEPIA2.0	TIMER2.0	GEPIA2.0	TIMER2.0
		Spearman's rho value (ρ)			
Substrate	*HIF1A*	0.27	0.176	0.2	0.081
E2 conjugating enzymes	*Ube2C*	0.31	0.138	0.53	0.4
	Ube2E1	0.33	0.279	0.19	0.122
	Ube2H	0.42	0.483	0.083	-0.033
	Ube2J2	0.42	0.303	0.53	0.335
	Ube2L6	-0.078	-0.209	-0.12	-0.177
	Ube2S	0.34	0.157	0.54	0.406

Substrate	HIF1A	
Prognostic Markers	GEPIA2.0	TIMER2.0
	Spearman's rho value (ρ)	
BMP1	0.33	0.231
CTSB	0.19	0.229
LOX	0.25	0.213
LOXL1	0.39	0.344
PLOD1	0.39	0.396
MMP9	0.11	0.056
SERPINE1	0.33	0.299
SERPING1	0.18	0.146

HATs enzymes	CREBBP		EP300		HAT1		KAT2A		KAT2B		KAT5	
Webtool	GEPIA2.0	TIMER2.0	GEPIA2.0	TIMER2.0	GEPIA2.0	TIMER2.0	GEPIA2.0	TIMER2.0	GEPIA2.0	TIMER2.0	GEPIA2.0	TIMER2.0
E2 conjugating Enzymes	Spearman's rho value (ρ)											
Ube2C	0.21	0.012	0.17	0.039	0.21	0.025	0.21	-0.082	-0.16	-0.391	0.23	-0.108
Ube2E1	0.03	-0.077	-0.042	-0.045	0.34	0.176	0.11	-0.126	0.26	0.144	0.21	0.006
Ube2H	0.66	0.668	0.64	0.062	0.38	0.403	0.22	0.138	0.36	0.292	0.38	0.288
Ube2J2	0.34	0.121	0.25	0.066	0.48	0.204	0.17	-0.079	0.13	-0.126	0.45	0.171
Ube2S	0.18	-0.032	0.18	0.045	0.15	0.19	0.2	-0.071	-0.027	-0.269	0.27	-0.068

Color code	
	Positive correlation (p<0.05, ρ>0)
	Negative correlation (p<0.05, ρ<0)
	Not significant (p>0.05)

(C) Gene And Protein Expression of HAT1 Enzyme in GBM

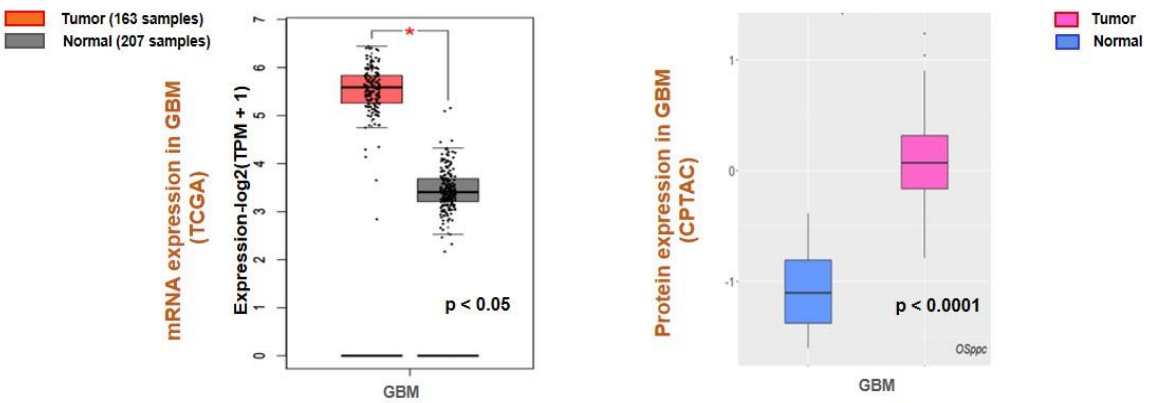

Figure 4.6: (A) Expression Analysis of E2 Conjugating Enzymes (E2s). Out of 35 reported E2 conjugating enzymes in humans, at the mRNA level, only 13 were dysregulated (including 12 up and 1 downregulated); at the protein level, 10 were dysregulated (including 7 upregulated and 3 downregulated). (B) Correlation Study Analysis: E3 ligase, VHL and GNB2L1 showed a significant positive correlation with substrate HIF1A and E2s. VHL showed a significant positive correlation between Ube2E1, Ube2H and Ube2J2, while GNB2L1 showed a positive correlation with Ube2C, Ube2J2 and Ube2S. In addition, HIF1A positively correlates with poor prognosis markers such as BMP1, CTSB, LOX, LOXL1, PLOD1 and SERPINE1. Heatmap 3 showed a significant correlation between HAT enzymes and E2s. Results showed that UBE2H positively correlates with CREBBP, EP300, HAT1, KAT2B, and KAT5. UBE2S with HAT1, Ube2J2 with HAT1 and KAT5, and Ube2C negatively correlate with KAT2B. (C) Gene and Protein Expression of HAT1 Enzymes In GBM: Box plot reveals that the significantly over-expression of HAT1 enzymes in GBM tumor samples as compared to normal sample both at mRNA and protein level. Expression data was collected from GEPIA2.0 and Osppc tool.

4.2.6. IDENTIFICATION OF POTENTIAL LYSINE (K) RESIDUES FOR ACETYLATION IN E2S AND PREDICTION OF ASSOCIATED HAT ENZYMES

Herein, we identified acetylation sites on lysine (K) residue of shortlisted E2s such as Ube2C, Ube2E1, Ube2H, Ube2J2, Ube2S and associated HATs enzymes, including CREBBP, EP300, HAT1, KAT2A, KAT2B, KAT5 and KAT8 with using deep learning methods such as Deep-PLA and GPS-PAIL. The total 'K' modification sites for Ube2C, Ube2E1, Ube2H, Ube2J2, and Ube2S are 12, 15, 13, 15 and 16, respectively. We have selected only those 'K' residues that fall under the filter (High confidence: DeepPLA: False positive rate (FPR) % <5 and GPS-PAIL score >1; Medium confidence: DeepPLA: FPR% <10 and GPS-PAIL score >1). The extracted acetylation sites were mapped to respective proteins. **Figure 4.7** and **Figure 4.8** illustrate all predicted acetylation site on 'K' residues and associated HATs enzymes. Our analysis observed potential acetylation 'K' residues that pass our filter criteria were Ube2C: K18, K33; Ube2E1 for K24, K31, K35, K43; Ube2H: K8, K52; Ube2J2: K7, K64, K88; Ube2S: K198, K205, K210, K211, K215, K216. Lacoursiere et al., 2022 have beautifully described the acetylation site in the UBC domain of 33 different E2s and its involvement in various cancer, including prostate cancer, gastric carcinoma, and leukemia. Mounting evidence from earlier studies has demonstrated acetylation sites for Ube2C (K18, leukemia), Ube2E1(K43, breast cancer), and Ube2H (K8, breast cancer) [715]. Our analysis has shown novel putative acetylation sites for E2s at lysine residues are Ube2C (K33); Ube2E1 (K24, K31, K35); Ube2H (K52); Ube2J2 (K7, K64, K88); Ube2S (K198, K205, K210, K211, K215, K216).

Further, we have identified associated HAT enzymes to E2s such as for a) Ube2C: EP300, HAT1 and KAT2B; b) Ube2E1: KAT2B, CREBBP, KAT2A and HAT1; c) Ube2H: HAT1; d) Ube2J2: HAT1, KAT5; e) Ube2S: HAT1, KAT2A, KAT2B and CREBBP. These E2 can be the potential substrate for HAT enzymes. Many additional HAT substrates have been discovered in the past as a result of acetylome research, and numerous non-histone HAT substrates, including AML1, AML1-ETO (AE), p53, c-Myc, NF-κB, cohesin, and tubulin, have been identified to be crucial for a variety of cellular functions [636]. Furthermore, the expression of these HAT enzymes was studied in GBM patient samples using GEPIA2.0 and OSppc tools. Analysis showed that HAT1 was upregulated while KAT2A was downregulated in GBM patient samples. Other HAT enzyme expressions, such as CREBBP, EP300, KAT2B, and KAT5, were insignificant. Hence, we moved with only upregulated HAT1 enzymes for further analysis. mRNA and protein expression data are shown in **Figure 4.6(C).**

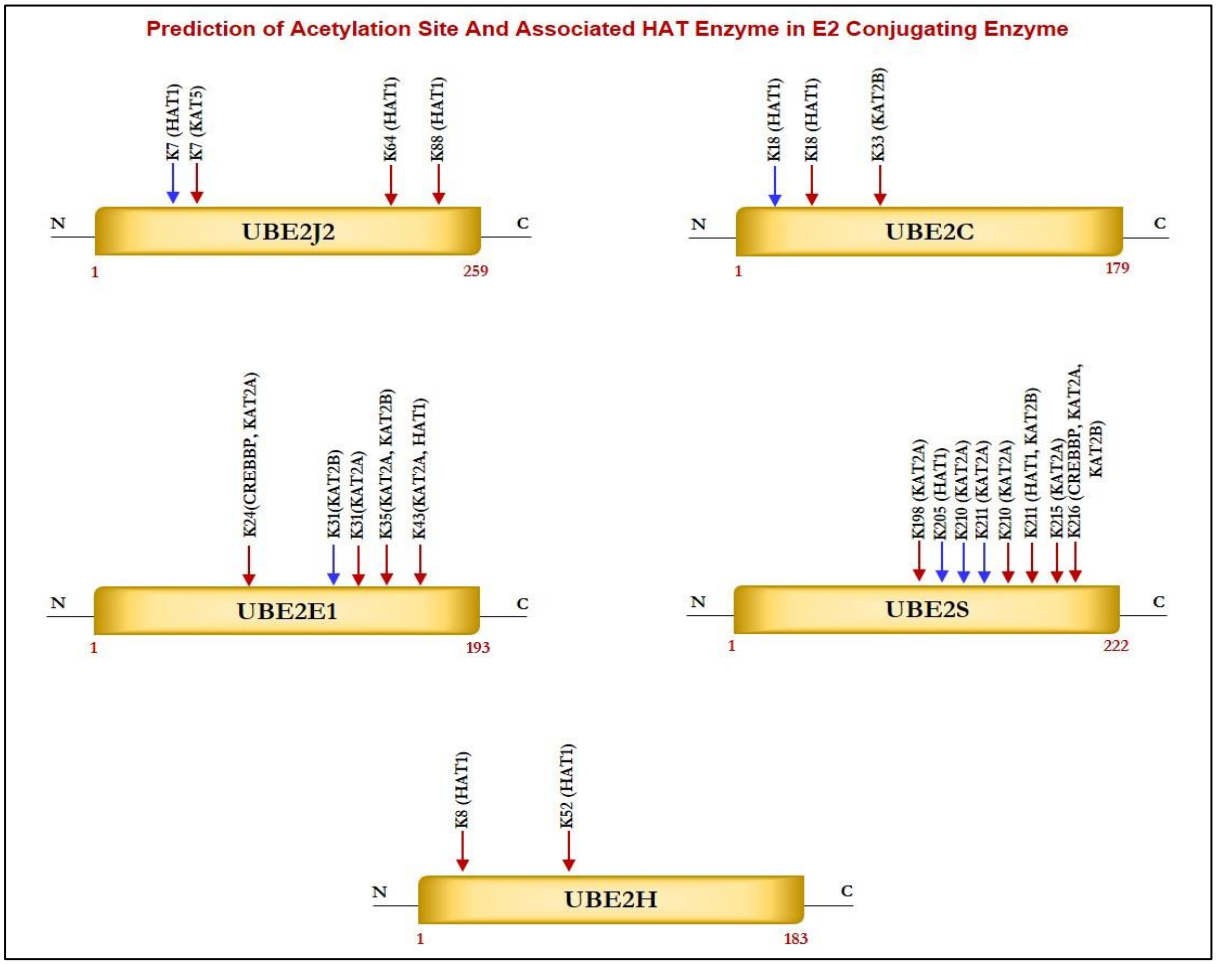

Figure 4.7: Prediction of Acetylation Site and Associated HAT Enzyme in E2 Conjugating Enzyme: Potential acetylation site on lysine residues of UBE2J2, UBE2C, UBE2E1, UBE2S, UBE2H and associated HAT enzymes were identified using DeepPLA and GPS-PAIL machine-learning based webtool. For UBE2C (K18, K33), UBE2E1(K24, K31, K35, K43), UBE2H (K8, K52), UBE2J2 (K7, K64, K88) and UBE2S (K198, K205, K210, K211, K215, K216).

4.2.7. STRUCTURAL CHARACTERIZATION AND IMPACT OF LYSINE MODIFICATION

Selected E2s Ube2C, Ube2E1, Ube2H, Ube2J2, and Ube2S have undergone structural characterization of the anticipated 'K' acetylation site as mutational investigation and its effect on disease susceptibility. Firstly, structure analysis of Ube2C, Ube2E1, Ube2H, Ube2J2, and Ube2S was performed**.** Our analysis demonstrated that Ube2E1 (3) and Ube2J2 (2) had a higher rate of acetylated 'K' sites falling in the coiled region, while Ube2S (6) and Ube2H (1) had a greater rate of these sites falling in helix region. Secondary structure analysis demonstrated the significance of the coiled structure in the PTM region compared to the helix and strand. Coiled areas govern protein interactions and aggregation propensity. Therefore mutations that damage coiled regions depress aggregation and protein activity, whereas mutations that improve coiled structure boost aggregation propensity [716]. Narasumani et al., 2018 demonstrated that PTMs preferred disordered regions compared to the ordered region, affecting their functions and interactions. Furthermore, the involvement of PTM in the disordered region influences disorder to order transition, thus altering the protein's stability and associated mechanisms. In the context of eukaryotic histones, the function of acetylation has been thoroughly investigated. Acetylation of disordered tail sections stimulates gene expression by removing inhibition [717]. However, not all PTMs prefer disordered regions [718], [719]. Hence, we predicted the distribution of predicted acetylation in protein intrinsic ordered and disordered regions using the machine-learning-based method DISOPRED3. Results indicated that the disordered area was more likely to include possible 'K' acetylation residues for all five E2s, Ube2C, Ube2E1, Ube2H, Ube2J2, and Ube2S, than the ordered region **(Figure 4.8).**

Prediction of Acetylation Site And Associated HAT Enzyme in E2 Conjugating Enzyme

Acetylation sites and associated HATs enzymes					Structural selectivity		
Sequence containing Lysine (K) amino acid	(K) residue Position	HATs Enzymes	DeepPLA (FPR% <10)	GPS-PAIL (score >1)	Structural Features	Region	Localisation
Ube2C (179aa)							
TSVAAARKGAEPSGG	18	EP300	2.86%	1.079	Coil	Disordered	Protein binding
TSVAAARKGAEPSGG	18	HAT1	10.34%	3.533	Coil	Disordered	Protein binding
AARGPVGKRLQQELM	33	KAT2B	5.32%	1.514	Helix	Ordered	Cytoplasmic
Ube2E1 (193aa)							
KETNTPKKKESKVSM	31	KAT2B	3.76%	1.862	Coil	Disordered	Protein binding
SSNQQTEKETNTPKK	24	CREBBP	7.62%	2.56	Coil	Disordered	Protein binding
SSNQQTEKETNTPKK	24	KAT2A	9.64%	1.087	Coil	Disordered	Protein binding
KETNTPKKKESKVSM	31	KAT2A	5.83%	1.101	Coil	Disordered	Protein binding
TPKKKESKVSMSKNS	35	KAT2A	6.28%	2.101	Coil	Disordered	Protein binding
TPKKKESKVSMSKNS	35	KAT2B	8.87%	2.459	Coil	Disordered	Protein binding
VSMSKNSKLLSTSAK	43	HAT1	8.28%	6.867	Helix	Disordered	Protein binding
VSMSKNSKLLSTSAK	43	KAT2A	5.83%	1.145	Helix	Disordered	Protein binding
Ube2H (183aa)							
MSSPSPGKRRMDTDV	8	HAT1	5.52%	9.867	Helix	Ordered	Cytoplasmic
PYEGGVWKVRVDLPD	52	HAT1	8.28%	1.333	Strand	Ordered	Cytoplasmic
Ube2J2 (259aa)							
-MSSTSSKRAPTTAT	7	HAT1	3.45%	7.933	Coil	Disordered	Protein binding
-MSSTSSKRAPTTAT	7	KAT5	6.51%	1.031	Coil	Disordered	Protein binding
EGGYYHGKLIFPREF	64	HAT1	8.28%	2	Strand	Ordered	Extracellular
ITPNGRFKCNTRLCL	88	HAT1	8.28%	6.133	Coil	Ordered	Extracellular
Ube2S (222aa)							
KHAGERDKKLAAKKK	205	HAT1	4.83%	4.333	Helix	Disordered	Cytoplasmic
RDKKLAAKKKTDKKR	210	KAT2A	0.00%	2.174	Helix	Disordered	Protein binding
DKKLAAKKKTDKKRA	211	KAT2A	0.67%	2.072	Helix	Disordered	Protein binding
AEGPMAKKHAGERDK	198	KAT2A	6.05%	1.029	Coil	Disordered	Cytoplasmic
RDKKLAAKKKTDKKR	210	KAT2B	2.90%	1.064	Helix	Disordered	Protein binding
DKKLAAKKKTDKKRA	211	HAT1	8.28%	1.067	Helix	Disordered	Protein binding
DKKLAAKKKTDKKRA	211	KAT2B	3.12%	1.028	Helix	Disordered	Protein binding
AAKKKTDKKRALRRL	215	KAT2A	1.79%	1.33	Helix	Disordered	Cytoplasmic
AKKKTDKKRALRRL-	216	CREBBP	7.87%	2.145	Helix	Disordered	Cytoplasmic
AKKKTDKKRALRRL-	216	KAT2A	2.24%	1.783	Helix	Disordered	Cytoplasmic
AKKKTDKKRALRRL-	216	KAT2B	8.17%	2.22	Helix	Disordered	Cytoplasmic

Figure 4.8: Detailed Prediction of Acetylation Site and Associated HAT Enzyme in E2 Conjugating Enzyme: Potential acetylation site on lysine residues of UBE2J2, UBE2C, UBE2E1, UBE2S, UBE2H and associated HAT enzymes were identified using DeepPLA and GPS-PAIL machine-learning based webtool. HAT enzymes associated with lysine residues are mentioned in the table. The lysine residue marked in blue color has a high confidence score: DeepPLA (FPR<5%) and GPS-PAIL (score>1), and the red color has a medium confidence score: DeepPLA (FPR<10%) and GPS-PAIL (score>1). In addition, structural analysis using PSIPRED and DISOPRED3 showed predicted lysine residue falls in coiled structure for UBE2C, UBE2E1, and UBE2J2 whereas, in helix structure for UBE2S. Moreover, our investigation showed acetylation occurs in disordered regions compared to ordered regions. FPR: False positive rate.

Furthermore, the localization of putative 'K' residue in the sequence has also been predicted; for example, the sequence containing K31 of Ube2E1 involves protein binding. Secondly, we have investigated the pathology of mutation (amino acid substitution) by substituting lysine (K) residue, which is a positively charged amino acid with each polar amino acid (glutamine, Q), non-polar (leucine, L), negatively charged (glutamate, E), and positively charged (arginine, R) through mutational analysis tools such as PMut, SNAP2, PolyPhen2 and Mutpred2. Our results observed that mutation at 'K' acetylation sites impacts disease susceptibility. For each tool, we have selected a score > 0.5. Each numerical prediction score value has been tabulated in **Table 4.3**.

Table 4.3: Impact of Amino Acid Substitution of "K" Putative Mutation to Either L, Q, R, Or E On Disease Susceptibility Predicted with The Help of Pmut, SNAP2, Polyphen2, and Mutpred2 tools

Substitution	Pmut	SNAP2	PolyPhen-2	MutPred2	Total Score
Ube2C					
K18L	0.74	1	0.005	0.772	2.517
K18Q	0.64	1	0.027	0.536	2.203
K18R	0.42	1	0.32	0.38	2.12
K18E	0.66	1	0.262	0.662	2.584
K33L	0.71	1	0.194	0.908	2.812
K33Q	0.59	1	0.003	0.804	2.397
K33R	0.25	1	0	0.681	1.931
K33E	0.59	1	0.049	0.868	2.507
Ube2E1					
K31L	0.49	1	0.037	0.156	1.683
K31Q	0.11	0	0.028	0.093	0.231
K31R	0.11	0	0	0.061	0.171
K31E	0.2	1	0	0.113	1.313
K24L	0.28	1	0.009	0.098	1.387
K24Q	0.09	0	0	0.066	0.156
K24R	0.09	0	0	0.044	0.134
K24E	0.11	0	0.002	0.079	0.191
K35L	0.58	1	0.09	0.196	1.866
K35Q	0.47	1	0.001	0.075	1.546
K35R	0.2	1	0	0.052	1.252
K35E	0.47	1	0.015	0.111	1.596
K43L	0.31	1	0.972	0.562	2.844
K43Q	0.2	0	0.924	0.368	1.492
K43R	0.12	1	0.007	0.211	1.338
K43E	0.35	1	0.896	0.369	2.615
Ube2H					
K8L	0.53	1	0.016	0.872	2.418
K8Q	0.51	1	0.437	0.758	2.705

K8R	0.26	1	0	0.661	1.921
K8E	0.39	1	0.354	0.831	2.575
K52L	0.63	1	0.82	0.943	3.393
K52Q	0.53	1	0.762	0.894	3.186
K52R	0.26	1	0.001	0.821	2.082
K52E	0.57	1	0.532	0.924	3.026
Ube2J2					
K7L	0.34	1	0.032	0.481	1.821
K7Q	0.37	0	0.897	0.266	1.533
K7R	0.19	0	0.868	0.205	0.395
K7E	0.33	1	0.020	0.346	1.676
K64L	0.62	1	1	0.704	3.324
K64Q	0.59	1	0.96	0.504	3.054
K64R	0.39	0	0.542	0.208	1.14
K64E	0.59	1	0.996	0.509	3.095
K88L	0.55	1	0.908	0.877	3.335
K88Q	0.48	1	0.071	0.704	2.255
K88R	0.46	1	0.009	0.538	2.007
K88E	0.52	1	0.503	0.812	2.835
Ube2S					
K198L	0.72	1	0.999	0.567	3.286
K198Q	0.45	1	0.997	0.285	2.732
K198R	0.4	1	0.996	0.186	2.582
K198E	0.44	1	0.779	0.383	2.602
K205L	0.36	1	0.133	0.529	2.022
K205Q	0.37	0	0.531	0.255	1.156
K205R	0.15	0	0.358	0.148	0.656
K205E	0.27	1	0.187	0.349	1.806
K210L	0.73	1	0.997	0.833	3.56
K210Q	0.52	1	0.999	0.559	3.078
K210R	0.29	1	0.996	0.39	2.676
K210E	0.45	1	0.996	0.686	3.132
K211L	0.68	1	0.997	0.683	3.36
K211Q	0.64	1	0.999	0.433	3.072
K211R	0.16	1	0.996	0.2	2.356
K211E	0.52	1	0.996	0.475	2.991
K215L	0.69	1	0.997	0.817	3.504
K215Q	0.7	0	0.999	0.576	2.275
K215R	0.48	0	0.996	0.365	1.841
K215E	0.79	1	0.996	0.664	3.45
K216L	0.88	1	0.997	0.859	3.736
K216Q	0.77	1	0.999	0.639	3.408
K216R	0.74	0	0.996	0.455	2.191
K216E	0.8	1	0.996	0.751	3.547

***For SNAP2= Probable Benign: Marked as "0"; Probable damage: Marked as "1"**
***For Pmut, MutPred2, and PolyPhen-2: Effect or Probable damage = >0.5 threshold**
***Gradient of the Green color showed Total confidence score (cumulative score of Pmut, SNAP2, MutPred2, and PolyPhen-2): Higher green color signifies a high confidence score.**

However, Ube2H (K52), Ube2J2 (K64, K88) and Ube2S (K198, K210, K211, K215, K216) exhibit higher confidence scores (cumulative confidence score value >2.5) on impact disease susceptibility. This signifies that a single amino acid substitution or mutation at identified 'K' residues leads to pathogenic and results in disease. Previous evidence also suggested that any mutation in these intrinsically disordered protein regions causes cancer [719]. Subsequently, we were interested in anticipating the molecular mechanism of pathogenicity due to mutation at the 'K' acetylation site through the Mutpred2 web application. **Table 4.4** demonstrates the functional impact of putative 'K' residue mutation on acetylation. The combined results depict

the role of putative 'K' mutation on other cellular functions. The results revealed that mutation in Ube2C (K33), Ube2H (K8), and Ube2S (K198, K205, K210, K211, K215 and K216) results in loss of acetylation on the same site. These findings confirm what we had already noticed. Thus, loss of acetylation with a mutation at K8 for Ube2H and at K198, K205, K210, K211, K215 and K216 for Ube2S signifies our predicted lysine residue is site acetylation, and any mutation will lead to disease. Other mechanisms, along with affected motifs, have been elaborated in **Table 4.4**. Moreover, selected disease-susceptible mutations were subjected to investigate their impact on protein structure stability. Mutation at Ube2C (K18) with (E), Ube2H (K8) with (R) and Ube2S (K210, K216) with (E) and (Q) leads to the gain of helix structure. This also signifies mutation at these acetylation sites will cause a topological change in the secondary structure.

Table 4.4: Physical Significance of E2 Conjugating Enzymes' Lysine (K) Residue Mutation Owing to A Single Amino Acid Substitution on Acetylation

Ube2C_HUMAN							
Lysin Residue	**Mutation substitution**	**Nature to mutation**	**Molecular mechanisms with p-values <= 0.05**	**MutPred2 Score**	**Probability**	**p-value**	**Affected PROSITE and ELM Motifs**
K18	Lys(K)-Leu(L)	Non-polar	Loss of Methylation at K18	0.772	0.49	1.10E-04	ELME000102
			Loss of Ubiquitylation at K18		0.34	4.40E-05	
			Loss of SUMOylation at K18		0.33	2.20E-03	
			Altered Disordered interface		0.28	4.00E-02	
			Loss of ADP-ribosylation at R17		0.23	2.00E-02	
			Loss of O-linked glycosylation at S23		0.13	4.00E-02	
	Lys(K)-Gln(Q)	Polar	Loss of Methylation at K18	0.536	0.49	1.10E-04	ELME000102
			Loss of Ubiquitylation at K18		0.34	4.40E-05	
			Loss of SUMOylation at K18		0.33	2.20E-03	
			Loss of ADP-ribosylation at R17		0.23	2.00E-02	
			Loss of O-linked glycosylation at S23		0.13	4.00E-02	
			Gain of Pyrrolidone carboxylic acid at K18		0.07	2.00E-02	
	Lys(K)-Glu(E)	Negatively	Loss of Methylation at K18	0.612	0.49	1.10E-04	ELME000102
			Loss of Ubiquitylation at K18		0.34	4.40E-05	
			Loss of SUMOylation at K18		0.33	2.20E-03	
			Loss of ADP-ribosylation at R17		0.24	2.00E-02	
			Loss of O-linked glycosylation at S23		0.13	4.00E-02	
			Gain of Helix		0.28	2.00E-02	
K33	Lys(K)-Leu(L)	Non-polar	Loss of Intrinsic disorder	0.908	0.41	2.00E-02	ELME000093, ELME000100, ELME000108,
			Loss of Acetylation at K33		0.23	2.00E-02	

			Loss of ADP-ribosylation at R28		0.21	3.00E-02	PS00009
			Loss of Methylation at K33		0.1	4.00E-02	
	Lys(K)-Gln(Q)	Polar	Loss of Acetylation at K33	0.804	0.23	2.00E-02	ELME000093, ELME000100, ELME000108, ELME000193, PS00009
			Loss of ADP-ribosylation at R28		0.21	3.00E-02	
			Loss of Methylation at K33		0.1	4.00E-02	
	Lys(K)-Arg(R)	Positively	Loss of Acetylation at K33	0.681	0.23	2.00E-02	ELME000012, ELME000093, ELME000100, ELME000102, ELME000108, PS00009
			Loss of ADP-ribosylation at R28		0.21	3.00E-02	
			Loss of Methylation at K33		0.1	5.00E-02	
	Lys(K)-Glu(E)	Negatively	Loss of Acetylation at K33	0.868	0.23	2.00E-02	ELME000093, ELME000100, ELME000108, ELME000193, PS00009
			Gain of ADP-ribosylation at R28		0.22	2.00E-02	
			Loss of Methylation at K33		0.1	4.40E-05	
Ube2E1_HUMAN							
K43	Lys(K)-Leu(L)	Non-polar	Altered Disordered interface	0.562	0.38	7.90E-03	ELME000053, ELME000173, ELME000333, ELME000335, ELME000336
			Loss of Ubiquitylation at K43		0.17	2.00E-02	
			Loss of Methylation at K40		0.09	5.00E-02	
Ube2H_HUMAN							
K8	Lys(K)-Leu(L)	Non-polar	Loss of Intrinsic disorder	0.827	0.47	1.00E-02	ELME000012, ELME000063, ELME000093, ELME000100, ELME000108, ELME000153, ELME000159, PS00009
			Altered Ordered interface		0.28	4.00E-02	
			Loss of B-factor		0.28	2.00E-02	
			Loss of Acetylation at K8		0.24	2.00E-02	
			Altered DNA binding		0.21	1.00E-02	
			Loss of Ubiquitylation at K8		0.18	2.00E-02	
			Loss of Methylation at K8		0.12	3.00E-02	
	Lys(K)-Gln(Q)	Polar	Loss of B-factor	0.758	0.26	4.00E-02	ELME000063, ELME000093, ELME000100, ELME000108, ELME000153, ELME000159, PS00009
			Loss of Acetylation at K8		0.24	2.00E-02	
			Altered DNA binding		0.2	2.00E-02	
			Loss of Ubiquitylation at K8		0.18	2.00E-02	
			Loss of Methylation at K8		0.12	3.00E-02	
	Lys(K)-Arg(R)	Positively	Gain of Helix	0.661	0.27	5.00E-02	ELME000012, ELME000061, ELME000063, ELME000093, ELME000100, ELME000108, ELME000153, ELME000159, PS00009
			Loss of Acetylation at K8		0.24	2.00E-02	
			Altered DNA binding		0.21	2.00E-02	
			Loss of Ubiquitylation at K8		0.18	2.00E-02	
			Loss of Methylation at K8		0.12	3.00E-02	
	Lys(K)-Glu(E)	Negatively	Loss of Acetylation at K8	0.831	0.24	2.00E-02	ELME000063, ELME000064, ELME000093, ELME000100, ELME000108, ELME000153, ELME000159, PS00006, PS00009
			Altered DNA binding		0.2	2.00E-02	
			Loss of Ubiquitylation at K8		0.18	2.00E-02	
			Loss of Methylation at K8		0.12	3.00E-02	
K52	Lys(K)-Leu(L)	Non-polar	Loss of Relative solvent accessibility	0.943	0.4	7.50E-04	ELME000047, ELME000155, ELME000333
			Altered Ordered interface		0.34	7.60E-03	
			Altered Transmembrane protein		0.29	1.90E-04	
			Altered Metal binding		0.28	6.40E-03	
			Loss of Allosteric site at W51		0.26	1.00E-02	

	Lys(K)-Gln(Q)	Polar	Loss of Relative solvent accessibility	0.894	0.39	1.00E-03	ELME000155
			Altered Metal binding		0.27	7.80E-03	
			Loss of Allosteric site at W51		0.27	8.90E-03	
			Altered Transmembrane protein		0.25	1.60E-03	
			Altered Ordered interface		0.25	2.00E-02	
	Lys(K)-Arg(R)	Positively	Loss of Relative solvent accessibility	0.821	0.33	4.10E-03	ELME000012, ELME000155
			Altered Ordered interface		0.29	3.00E-02	
			Altered Metal binding		0.27	8.80E-03	
			Altered Transmembrane protein		0.27	6.50E-04	
			Gain of Allosteric site at W51		0.26	7.80E-03	
	Lys(K)-Glu(E)	Negatively	Altered Ordered interface	0.924	0.29	3.00E-02	ELME000155
			Altered Transmembrane protein		0.28	6.60E-04	
			Loss of Relative solvent accessibility		0.28	2.00E-02	
			Loss of Allosteric site at W51		0.27	9.40E-03	
			Altered Metal binding		0.26	1.00E-02	
Ube2J2_HUMAN							
K64	Lys(K)-Leu(L)	Non-polar	Altered Transmembrane protein	0.704	0.3	1.50E-04	ELME000120, ELME000137, ELME000146, ELME000317
			Altered Metal binding		0.26	6.70E-03	
			Altered Ordered interface		0.25	0.02	
			Gain of Sulfation at Y60		0.02	0.02	
	Lys(K)-Gln(Q)	Polar	Altered Transmembrane protein	0.504	0.3	1.60E-04	ELME000137, ELME000146, ELME000163, ELME000317
			Altered Metal binding		0.25	8.20E-03	
			Altered Ordered interface		0.25	0.02	
			Gain of Sulfation at Y60		0.02	0.03	
	Lys(K)-Glu(E)	Negatively	Altered Transmembrane protein	0.59	0.31	1.20E-04	ELME000137, ELME000146, ELME000317
			Altered Metal binding		0.24	9.70E-03	
			Altered Ordered interface		0.24	4.00E-02	
			Gain of Sulfation at Y60		0.03	2.00E-02	
K88	Lys(K)-Leu(L)	Non-polar	Loss of Strand	0.538	0.26	4.00E-02	ELME000233, ELME000336
	Lys(K)-Gln(Q)	Polar	Gain of Strand	0.704	0.26	4.00E-02	ELME000233
	Lys(K)-Glu(E)	Negatively	Gain of Loop	0.812	0.29	1.00E-02	ELME000233
			Gain of Strand		0.26	4.00E-02	
Ube2S_HUMAN							
K198	Lys(K)-Leu(L)	Non-polar	Loss of Acetylation at K198	0.567	0.43	9.80E-04	None
			Loss of SUMOylation at K198		0.34	1.40E-03	
			Altered Disordered interface		0.36	8.90E-03	
			Gain of Ubiquitylation at K197		0.19	0.01	
			Loss of Methylation at K198		0.15	2.00E-02	
			Altered Coiled coil		0.14	3.00E-02	
K205	Lys(K)-Leu(L)	Non-polar	Loss of Acetylation at K205	0.529	0.58	3.60E-04	ELME000106, ELME000146
			Altered Disordered interface		0.39	7.30E-03	
			Altered Coiled coil		0.39	7.00E-03	
			Loss of SUMOylation at K205		0.32	2.30E-03	
			Loss of Methylation at K210		0.24	2.50E-03	
			Altered DNA binding		0.2	2.00E-02	
			Loss of Ubiquitylation at K205		0.17	0.02	

K210	Lys(K)-Leu(L)	Non-polar	Loss of Acetylation at K210	0.833	0.79	7.80E-05	ELME000008, PS00004
			Altered Coiled coil		0.51	6.90E-03	
			Altered Disordered interface		0.46	3.90E-03	
			Loss of Methylation at K210		0.41	1.80E-04	
			Loss of B-factor		0.31	5.30E-03	
			Altered DNA binding		0.3	2.70E-03	
			Loss of Helix		0.27	4.00E-02	
			Loss of SUMOylation at K210		0.24	0.01	
			Gain of Ubiquitylation at K205		0.16	0.03	
	Lys(K)-Gln(Q)	Polar	Loss of Acetylation at K210	0.559	0.79	7.80E-05	ELME000008, PS00004
			Loss of Methylation at K210		0.41	1.80E-04	
			Altered Disordered interface		0.38	7.60E-03	
			Altered Coiled coil		0.3	1.00E-02	
			Loss of B-factor		0.29	1.00E-02	
			Altered DNA binding		0.27	6.30E-03	
			Loss of SUMOylation at K210		0.24	0.01	
			Gain of Ubiquitylation at K205		0.16	0.03	
	Lys(K)-Glu(E)	Negatively	Loss of Acetylation at K210	0.686	0.79	7.80E-05	ELME000008, PS00004
			Altered Disordered interface		0.57	1.10E-03	
			Loss of Methylation at K210		0.41	1.80E-04	
			Altered Coiled coil		0.36	8.30E-03	
			Gain of Helix		0.28	2.00E-02	
			Loss of B-factor		0.27	2.00E-02	
			Altered DNA binding		0.27	5.30E-03	
			Gain of SUMOylation at K205		0.26	6.80E-03	
			Gain of Ubiquitylation at K205		0.18	0.02	
K211	Lys(K)-Leu(L)	Non-polar	Loss of Acetylation at K211	0.683	0.54	4.50E-04	ELME000008, PS00004
			Altered Coiled coil		0.53	4.00E-03	
			Loss of Methylation at K211		0.39	2.00E-04	
			Altered Disordered interface		0.38	6.70E-03	
			Loss of B-factor		0.33	2.90E-03	
			Loss of Helix		0.28	0.03	
			Altered DNA binding		0.28	4.90E-03	
			Loss of SUMOylation at K211		0.27	4.50E-03	
K215	Lys(K)-Leu(L)	Non-polar	Loss of Acetylation at K215	0.817	0.64	2.10E-04	ELME000008, PS00005
			Altered Coiled coil		0.61	3.00E-03	
			Altered DNA binding		0.37	6.00E-04	
			Altered Disordered interface		0.33	0.01	
			Loss of B-factor		0.31	6.40E-03	
			Loss of Helix		0.28	0.03	
			Loss of Methylation at K215		0.28	9.20E-04	
			Gain of SUMOylation at K211		0.21	0.03	
	Lys(K)-Gln(Q)	Polar	Loss of Acetylation at K215	0.576	0.64	2.10E-04	ELME000008, PS00005
			Altered Coiled coil		0.35	8.30E-03	
			Altered DNA binding		0.29	3.70E-03	

			Loss of B-factor		0.28	0.02	
			Gain of Helix		0.28	0.03	
			Loss of Methylation at K215		0.28	9.20E-04	
			Loss of SUMOylation at K215		0.2	0.03	
K216	Lys(K)-Leu(L)	Non-polar	Loss of Acetylation at K216	0.576	0.58	3.50E-04	ELME000008, ELME000052, ELME000100, ELME000108, ELME000146
			Altered Coiled coil		0.38	0.01	
			Loss of Methylation at K216		0.37	2.40E-04	
			Altered DNA binding		0.35	9.00E-04	
			Altered Disordered interface		0.3	0.02	
			Loss of B-factor		0.3	1.00E-02	
			Loss of Helix		0.28	0.03	
			Gain of SUMOylation at K212		0.2	0.03	
	Lys(K)-Gln(Q)	Polar	Loss of Acetylation at K216	0.639	0.58	3.50E-04	ELME000008, ELME000100, ELME000108, ELME000146
			Loss of Methylation at K216		0.37	2.40E-04	
			Altered Coiled coil		0.32	9.40E-03	
			Altered DNA binding		0.29	3.60E-03	
			Gain of Helix		0.28	0.03	
			Loss of B-factor		0.27	2.00E-02	
			Loss of SUMOylation at K211		0.2	0.03	
	Lys(K)-Glu(E)	Negatively	Loss of Acetylation at K216	0.751	0.58	3.50E-04	ELME000008, ELME000064, ELME000100, ELME000108, ELME000146, ELME000220, PS00006
			Loss of Methylation at K216		0.37	2.40E-04	
			Altered Coiled coil		0.32	9.50E-03	
			Altered DNA binding		0.31	2.10E-03	
			Gain of Helix		0.28	0.02	
			Loss of B-factor		0.26	4.00E-02	
			Gain of SUMOylation at K211		0.23	0.02	

*** The pathogenic score in the table indicates the likelihood that the amino acid substitution is pathogenic. A score threshold of 0.50 would indicate that a specific substitution is pathogenic**

4.2.8. PREDICTION OF THERAPEUTIC AXIS IN GBM PATHOLOGY

To comprehend how HIF1A biomarkers and their associated E3 ligases, as well as HAT enzymes and E2s, are involved, we have collated all of our research data. **Table 4.5** demonstrates the strategy for choosing the dysregulated final axis in GBM. It revealed that Ube2E1 (K43), Ube2H (K8, K52) were connected with VHL enzymes and Ube2C (K18, K33), Ube2S (K168, K210, K211, K215, K216) linked with GNB2L1, while Ube2J2 (K64, K88) was associated with both VHL and GNB2L1 enzymes. Only a few of the predicted acetylation sites K8 of Ube2H, K33 of Ube2C, K198, K210, K211, K215, and K216 of Ube2S were verified with the MutPred2 predictor outcome "loss of acetylation site" following a single amino acid substitution mutation. The GBM was examined for each E2s connection with the HATs

enzymes. Using the GEPIA2.0 program, the mRNA expression of each HATs enzyme was examined in a GBM patient sample. Out of all the enzymes, only HAT1 was connected to E2s at specific lysine residues. As a result, we suggested two novel pathways that may be therapeutic targets: HAT1-Ube2S(K211)-GNB2L1-HIF1A and HAT1-Ube2H(K8)-VHL-HIF1A. We anticipated a new route axis HAT1-Ube2S(K211)-GNB2L1-HIF1A implicated in the pathogenesis of GBM because K8 of Ube2H has already been identified in the literature [715]. Thus, we predicted a new route axis, HAT1-Ube2S(K211)-GNB2L1-HIF1A, implicated in the etiology of GBM. We have demonstrated that in this pathway, HAT1 acetylates E2s, Ube2S (a non-histone protein) at lysine residue K211 (near C-terminal), causing its overexpression. Numerous studies have demonstrated that non-histone protein acetylation is one of the critical factors influencing gene transcription. Alaei et al., 2018 found that the C-terminal acetylation of lysine modulates protein turnover and stability [720]. In contrast, early research showed that ubiquitin-mediated protein degradation could be stopped when the N-terminal-amino group is acetylated, and this degradation can happen to proteins with free-amino groups. Several signaling pathways along with the cell cycle can be regulated by protein acetylation [721]–[723]. Most HATs have a nucleus-specific location and operate as co-activators of transcription. The degradation of proteins is also connected to protein acetylation [724], [725]. Acetylation is a modification that can significantly modify a protein's function by changing its hydrophobicity, solubility, and surface characteristics. These changes may impact the protein's conformation and interactions with substrates, cofactors, and other macromolecules [726]. As a result, C-terminal acetylation controls lysine's ubiquitination and impacts its turnover. We postulated that acetylation of Ube2S at position 211, near the protein's C-terminus, promotes and regulates GNB2L1's protein turnover and ubiquitination modification. As a result of increased protein aggregation, the ability of GNB2L1 to ubiquitinate HIF1A is reduced, which further increases the expression level of the HIF1A

protein (prevents its degradation by the UPS system).

Table 4.5: Correlation and Expression Analysis of HAT Enzymes and Prediction of Therapeutic Axis In GBM

E3 ligase	E2 Conjugating Enzymes	Potential K Residue Position	Histone Acetyltransferases (HATs) Enzymes						Therapeutic Axis	Loss of Acetylation Site
		Confidence Score > 2.5	CREBBP	EP300	HAT1	KAT2A	KAT2B	KAT5		
VHL	UBE2E1	43	-	-	√	χ	-	-	HAT1-UBE2E1(K43)-VHL	No
	UBE2H	8	-	-	√	-	-	-	HAT1-UBE2H(K8)-VHL	Yes
		52	-	-	√	-	-	-	HAT1-UBE2H(K52)-VHL	No
	UBE2J2	64	-	-	√	-	-	-	HAT1-UBE2J2(K64)-VHL	No
		88	-	-	√	-	-	χ	HAT1-UBE2J2(K88)-VHL	No
GNB2L1	UBE2C	18	-	χ	√	-	-	-	HAT1-UBE2C(K18)-GNB2L1	No
	UBE2J2	33	-	-	-	-	χ	-	-	Yes
		64	-	-	√	-	-	-	HAT1-UBE2J2(K64)-GNB2L1	No
		88	-	-	√	-	-	χ	HAT1-UBE2J2(K88)-GNB2L1	No
	UBE2S	198	-	-	-	χ	-	-	-	Yes
		210	-	-	-	χ	-	-	-	Yes
		211	-	-	√	χ	χ	-	HAT1-UBE2S(K211)-GNB2L1	Yes
		215	-	-	-	χ	-	-	-	Yes
		216	χ	-	-	χ	χ	-	-	Yes

- **Lysine residues marked in blue are novel and have not been previously documented in the literature for acetylation modification in GBM patients.**
- **p-value≤0.05: significant; p-value>0.05; ns: not significant**
- **√: signifies HAT1 enzymes expression is upregulated, with the significant positive correlation between HAT1 and Ube2E1, Ube2H and Ube2C, Ube2J2, Ube2S**
- **χ: signifies KAT2A enzyme expression is downregulated, with a not significant association between KAT2A and Ube2E1, Ube2A**
- **χ: signifies CREBBP, EP300, KAT2B and KAT5 enzyme expression is not significant, with no significant association between CREBBP and Ube2S; EP300 and Ube2C; KAT2B and Ube2C, Ube2S; KAT5 and Ube2J2**
- **The pink rectangle box represents the first proposed therapeutic axis in GBM**
- **The brown rectangle box represents the second proposed therapeutic axis in GBM**

Overexpressed Ube2S is linked with increased GNB2L1 and elevated HIF1A substrate. As per earlier research, acetylation is essential for p53 activation because it prevents the ubiquitin E3 ligase Mdm2 from inhibiting its ability to bind p53 for ubiquitination and proteasomal destruction. According to the theory of inter-protein acetylation-ubiquitination crosstalk, acetylation of Mdm2 by p300/CBP may prevent p53 from being subsequently ubiquitinated,

increasing p53's stability and transcriptional activity [727]. Additionally, Sirt1's ubiquitination and degradation may control the acetylation status of the histones in the downstream region, which would further epigenetically restrict the expression of the autophagy gene and encourage the spread of colorectal cancer [728]. Further, this significantly correlates with the GBM biomarkers BMP1, CTSB, LOX, LOXL1, PLOD1, and SERPINE1. Critical biological pathways, such as canonical and noncanonical TGF signaling, are regulated by BMP1, LOX, and LOXL1. **Figure 4.9(A)** illustrates the putative therapeutic axis and its influence on biological pathways in GBM. According to studies, TGF signaling regulates VEGF expression through SMAD-dependent signaling, which is crucial for angiogenesis in GBM. It contributes to the pathophysiology of tumors by controlling tumor growth, maintaining GSCs, and suppressing anti-tumor immunity [675], [681], [729]. Besides this, extracellular secreted CTSB can modify the TME through various non-cellular components and degrade the ECM. Cathepsins are a crucial class of proteins that are involved in the growth and propagation of cancer since they also interfere with the cell-cell adhesion molecules which encourage cell invasion and metastasis [673]. Additionally, each contributes to the formation of collagen fibrils in the ECM. The normal brain contains minimal collagen, but it has been found that collagen gene expression is elevated in GBMs [730]. Moreover, LOX and LOXL1 isoforms are cleaved by BMP1-related proteases implies that these enzymes are matrix-oriented enzymes and possess strong binding with other ECM components including fibronectin, fibulin-4 and fibulin-5, and tropoelastin. In fact, research has revealed that inactivating the Lox and Loxl1 genes in mice models causes severe vascular problems because it disrupts the development of elastic fibers [731].

(A) Proposed Therapeutic Axis in GBM

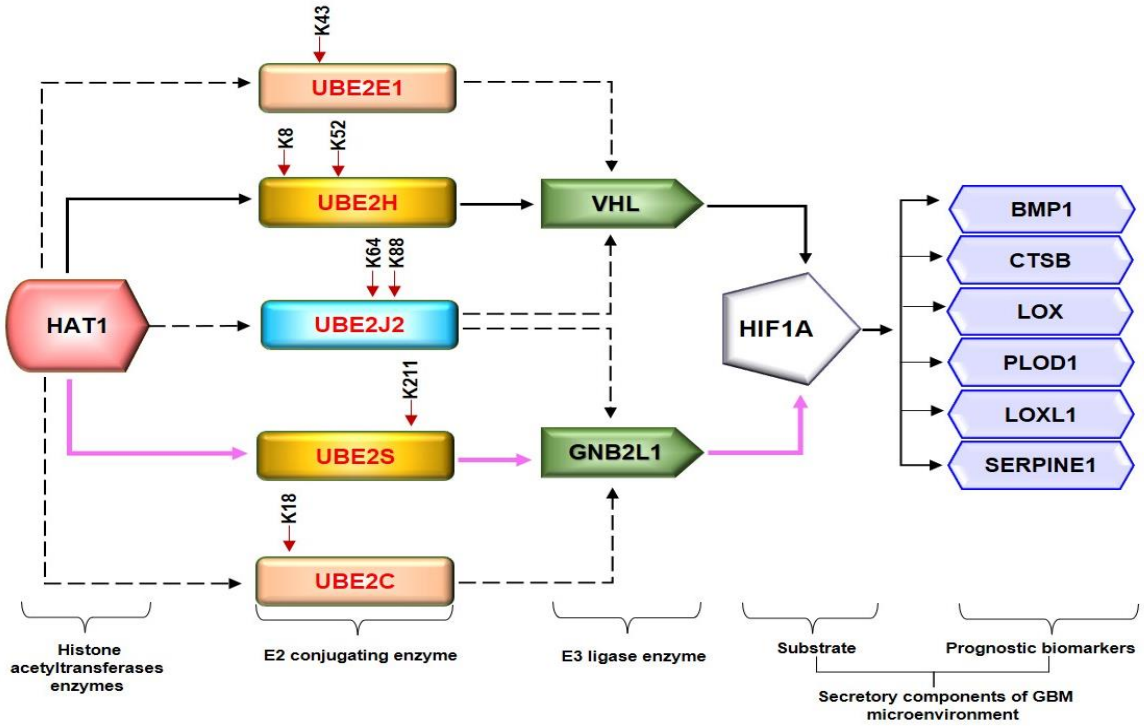

(B) Pathway Analysis of Therapeutic Axis Proteins in GBM

Pathways Involved in GBM	p-Value	Genes
Assembly of Collagen Fibrils	1.48E-07	BMP1, CTSB, LOX, LOXL1
ECM Organization	1.46E-06	BMP1, CTSB, LOX, LOXL1, PLOD1
TGF-β Signalling	2.07E-06	BMP1, LOX, LOXL1
Degradation Of The ECM	0.008	BMP1, CTSB
Interferon Gamma Response	0.010	HIF1A
VEGF, Hypoxia, & Angiogenesis	0.015	HIF1A
TNFR1 Signalling	0.016	GNB2L1
Trafficking & Processing Of Endosomal TLRs	0.025	CTSB
Ubiquitin Proteasome Pathway	0.044	Ube2S

Figure 4.9: (A) Proposed Therapeutic axis: Based on our findings, two axes were proposed. First, there was HAT1-UBE2S(K211)-GNB2L1-HIF1A-BMP1/CTSB/LOX/LOXL1/PLOD1/SERPINE1. In this process, HAT1 will acetylate lysine residues at the 211* positions of UBE2S conjugating enzymes. This increases transcription and upregulation, linked to GNB2L1, an E3 ligase that regulates HIF1A activity in GBM. HIF1A overexpression links with the identified poor prognosis markers BMP1, CTSB, LOX, LOXL1, PLOD1, and SERPINE1. A solid pink line represents this axis. Second, HAT1-Ube2H (K8, K52)-VHL-HIF1A-BMP1/CTSB/LOX/LOXL1/PLOD1/SERPINE1 is involved. HAT1 acetylates Lysine residues at K8 and K52* positions, and its overexpression has been linked to VHL, an E3 ligase, and HIF1A. This axis has been marked with a solid black line. Other therapeutic axes involving UBE2J2, UBE2E1 and VHL ligase, UBE2C and UBE2J2 and GNB2L1 ligase are possible, as illustrated in the figure with the dashed black line. * Signifies novel acetylation site on lysine residue. (B) Pathway Analysis of Therapeutic Axis's Protein Using the Enrichr Tool (Reactome, PANTHER, Wiki pathway database) showed genes involved in signaling pathways such as assembly of collagen fibrils, ECM organization, ECM degradation, Interferon-gamma response, hypoxia and angiogenesis, TNF signaling and ubiquitin-proteasome pathway.

Figure 4.9(B) depicts the study of different biological pathways of biomarkers associated with the proposed treatment axis in GBM. According to our findings, these expected axes in GBM may be targeted in GBM patient samples, which show that all proteins and enzymes associated with these pathways are noticeably enhanced at both the transcriptional and proteomic levels. Furthermore, they significantly connect with the appropriate partner proteins in GBM. So, we identified strategies that may be used to block the development of GBM.

4.2.9. CHARACTERIZATION OF PUTATIVE BIOMARKERS INVOLVED IN PROPOSED THERAPEUTIC AXIS IN GBM

Predictive markers response to GBM treatment

Despite advances in the molecular characterization of GBM, only a handful of predictive biomarkers exist with limited clinical relevance. We embraced the receiver operator characteristic (ROC) plotter webtool to link with protein expression amongst our proposed therapeutic axis in GBM tumor samples with therapies including TMZ, any chemotherapy, Angiogenesis inhibitor (including Vatalanib, Vandetanib, Thalidomide, Bevacizumab) and topoisomerase inhibitors (including Irinotecan, Topotecan, Etoposide, Teniposide). For each protein, HAT1, Ube2E1, Ube2H, Ube2J2, Ube2S, Ube2C, VHL, GNB2L1, HIF1A, BMP1, CTSB, LOX, LOXL1, PLOD1 and SERPINE1, the expression was compared between responders and non-responder's patients' data with a Mann–Whitney U-test and area under curve (AUC). In response to TMZ, we discovered enhanced expression of CTSB (AUC = 0.648) and VHL (AUC=0.667). In response to TMZ and chemotherapy, it was shown that the expression of Ube2H (AUC=0.635, 0.627 respectively) and HAT1 (AUC=0.576, 0.599 respectively) had decreased.

Expression of Proteins with Drug Treatment in GBM Patients Samples

Temozolomide (TMZ)

- Total: 319 GBM patients
- Non-responder: 154 GBM patients
- Responder: 165 GBM patients

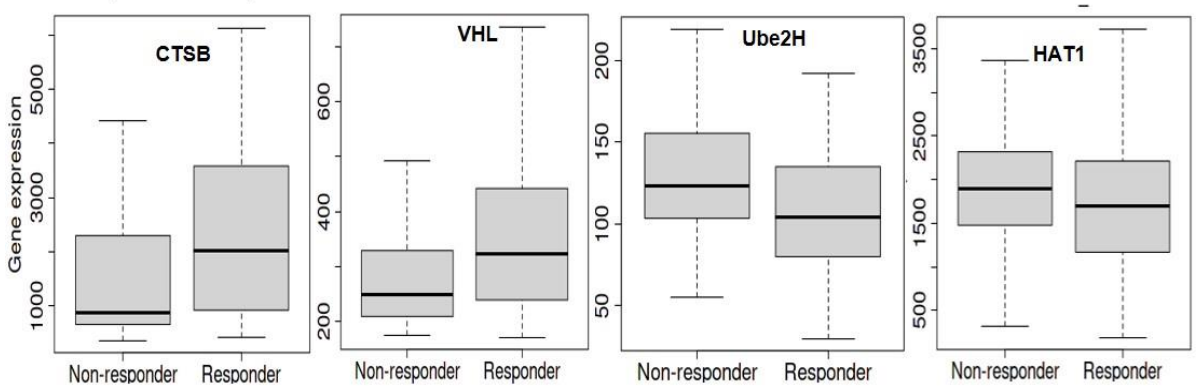

CTSB & VHL Upregulated in TMZ Responder Patients

Ube2H & HAT1 Downregulated in TMZ Responder Patients

Any Chemotherapy

- Total: 454 patients
- Non-responder: 231 patients
- Responder: 223 patients

Angiogenesis Inhibitors

- Total: 71 GBM patients
- Non-responder: 30 GBM patients
- Responder: 41 GBM patients

Topoisomerase Inhibitors

- Total: 62 GBM patients
- Non-responder: 16 GBM patients
- Responder: 46 GBM patients

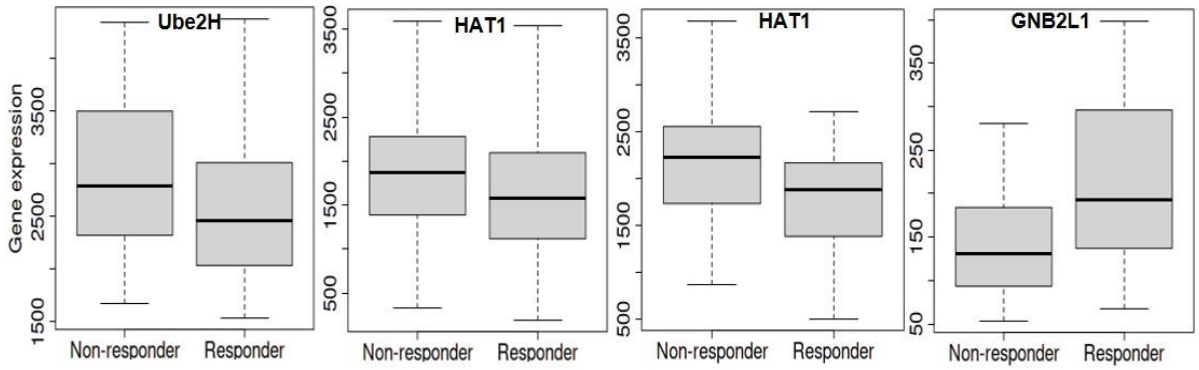

Ube2H and HAT1 Downregulated in Chemotherapy Responder Patients

HAT1 Downregulated in Angiogenesis Inhibitor Responder Patients

GNB2L1 Upregulated in Topoisomerase Inhibitor Responder Patients

Protein Name	Probe id	AUC	ROC (p-value)	Mann-Whitney test (p-value)	Fold change	Responder	Non-Responder
Temozolomide							
CTSB	227961_at*	0.648	8.00E-03	1.90E-02	1.5	55	35
Ube2H	226637_at*	0.635	1.20E-02	3.20E-02	1.3	55	35
VHL	1559227_s_at*	0.677	1.30E-03	5.00E-03	1.3	55	35
HAT1	203138_at	0.576	9.20E-03	2.00E-02	1.1	165	154
Any Chemotherapy							
Ube2H	222421_at*	0.627	3.30E-03	9.60E-04	1.1	87	59
HAT1	203138_at	0.599	1.00E-04	2.50E-04	1.1	223	231
Angiogenesis inhibitor (Vatalanib, Vandetanib, Thalidomide, Bevacizumab)							
HAT1	203138_at	0.677	5.30E-03	1.50E-02	1.2	41	30
Topoisomerase inhibitor (Irinotecan, Topotecan, Etoposide, Teniposide)							
GNB2L1	222034_at	0.683	1.30E-02	3.00E-02	1.4	46	16

Figure 4.10: Receiver Operating Characteristic (ROC) Curve for Biomarkers Involved in Therapeutic Expression in Glioblastoma Multiforme. AUC of time-dependent ROC curves verified the prognostic performance of the responder cohort after 16 months of treatment with Temozolomide (TMZ), chemotherapy, Angiogenesis and Topoisomerase Inhibitors. The therapeutic axis includes HAT1, E2 enzymes (Ube2H, Ube2S, Ube2E1, Ube2C, Ube2J2), E3 ligase (VHL, GNB2L1), Prognosis markers (BMP1, CTSB, LOX, LOXL1, PLOD1 and SERPINE1). (a) In the TMZ responder cohort: CTSB and VHL expression was upregulated, and Ube2H and HAT1 were downregulated. (b) Chemotherapy responder cohort: HAT1 and Ube2H were downregulated. (c) Angiogenesis inhibitor responder cohort: HAT1 downregulated (d) Topoisomerase Inhibitors responder cohort: GNB2L1 upregulated in the responder. Tables showing significant Area Under Curve (AUC) along with fold change expression between responder and non-responder patients to drug treatment.

Additionally, HAT1 expression was downregulated in angiogenesis inhibitor treatment responders (AUC=0.677). In addition, patients who responded well to topoisomerase inhibitor medication had increased expression of GBN2L1 (AUC=0.683). Hu et al. (2020) discovered YWHAB, PPAT, and NOL10 as novel biomarkers and validated their diagnostic and prognostic value for HCC, and Zhang et al. (2020) found ELANE, GPX4, GSDMD, and TIRAP as a prognosis marker in Endometrial Cancer using ROC plotter tool [732], [733]. Therefore, based on our findings, it can be concluded that CTSB, VHL, GNB2L1, Ube2H, and HAT1 have the potential to serve as candidates for predictive markers of response, provide a framework for preclinical investigations and perhaps improve patient classification for GBM in the future (**Figure 4.10**).

Correlation of therapeutic axis with top mutated genes in GBM

Here, we studied the differential expression of all proteins involved in the proposed therapeutic axis (HAT1, Ube2E1, Ube2H, Ube2J2, Ube2S, VHL, GNB2L1, HIF1A) along with prognostic biomarker (BMP1, CTSB, LOX, LOXL1, PLOD1, MMP9, SERPINE1, SERPING1) with top 10 genes mutated genes in GBM using "gene_module" tool of TIMER2.0 webserver. Research evidence suggests that the top 10 mutated genes in GBM are PTEN, TP53, EGFR, PIK3R1, PIK3CA, NF1, RB1, IDH1, PTPRD, and ERBB2 [734], [735].

Boxplot Showing Differential Prognostic Biomarker Expression with Different Mutation Status in GBM

Tumor: 148 GBM patients data (TCGA)

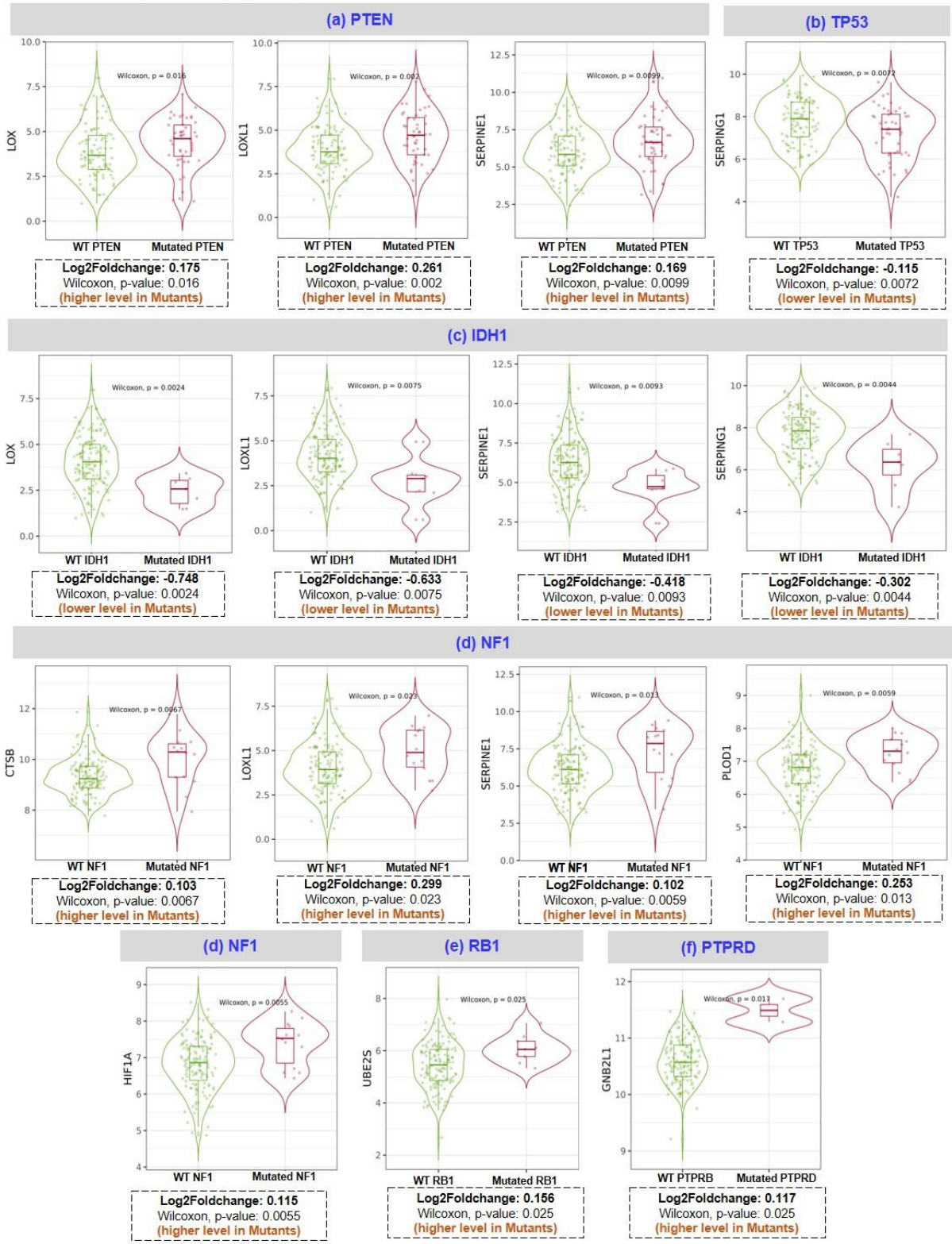

Mutation Type in GBM	*PTEN*	*TP53*	*IDH1*	*NF1*	*RB1*	*PTPRD*
% of Samples with Mutation	123/400	121/400	26/400	44/400	31/400	7/400

Figure 4.11: Differentiational Expression Analysis of Prognosis Biomarker with A Top Mutation In GBM. HAT1, E2 enzymes (Ube2H, Ube2S, Ube2E1, Ube2C, UbeJ2), E3 ligase (VHL, GNB2L1), Prognosis markers (BMP1, CTSB, LOX, LOXL1, PLOD1 and SERPING1) (a) PTEN mutation: LOX, LOXL1 and SERPINE1 were upregulated in GBM mutant group, (b) TP53 mutation: SERPING1 were downregulated in mutant GBM group, (c) IDH1 mutation: LOX, LOXL1, SERPINE1 and SERPING1 downregulated in the mutant group, (d) NF1 mutation: CTSB, LOXL1, SERPINE1, PLOD1 and HIF1A were upregulated in the mutant group. (e) RB1 mutation: UBE2S was upregulated, and (f) PTPRD: GNB2L1 was upregulated in the mutant group. PTPRD: Protein Tyrosine Phosphatase Receptor Type D; NF1: neurofibromin-1; RB1: Retinoblastoma gene; IDH1: isocitrate dehydrogenase 1 gene; PTEN: phosphatase and tensin homolog.

The incidence rate of each mutation in 400 GBM patient samples has been shown as PTEN (30.75%), TP53 (30.25%), EGFR (23.5%), NF1 (11%), PIK3CA (8.75%), PIK3R1 (8.5%), RB1 (7.75%), IDH1 (6.5%), PTPRD (1.75%), ERBB2 (1.25%). The expression of the interested protein was compared between GBM patients (n=148) with wild-type and mutant-type genes. We have observed that GBM patient samples having i) PTEN mutation have higher expression of LOX, LOXL1, SERPINE1 protein, ii) p53 mutation have decreased levels of SERPING1, iii) IDH1 mutation have decreased levels of LOX, LOXL1, SERPINE1 and SERPING1, iv) NF1 mutation have higher levels of CTSB, LOXL1, SERPINE1, PLOD1 and HIF1A, v) RB1 mutation have higher levels of Ube2S, vi) PTPRD mutation have higher levels of GNB2L1. **Figure 4.11** shows the boxplot of all significant biomarkers regulated with mutated genes in GBM.

Association with human protein kinases in GBM

We have studied the expression of 536 human protein kinases in GBM and showed that 71 kinases were upregulated and 46 kinases were downregulated. Using protein-protein network analysis, we have studied the interaction between biomarkers (BMP1, CTSB, LOX, LOXL1, PLOD1, SERPINE1) with dysregulated kinases. We have shown **(Figure 4.12(A))** i) LOX interacts with PDGFRA, KDR, TGFBR2, TGFBR1, ERBB2, EGFR; ii) SERPINE1 interacts with EGFR, ERBB2, KDR, TGFBR2, TGFBR1; iii) CTSB interact with EGFR, ERBB2, and iv) BMP1: ACVR1. In addition, we have discussed the PPI between E2s with kinases and showed that the proposed E2s Ube2S interact with 8 kinases including CDK2, AURKB, BUB1B, PLK1, NEK2, AURKA, CDK1, MAP3K1 whereas Ube2H interact only with TRIM28 kinases **(Figure 4.12(B)).**

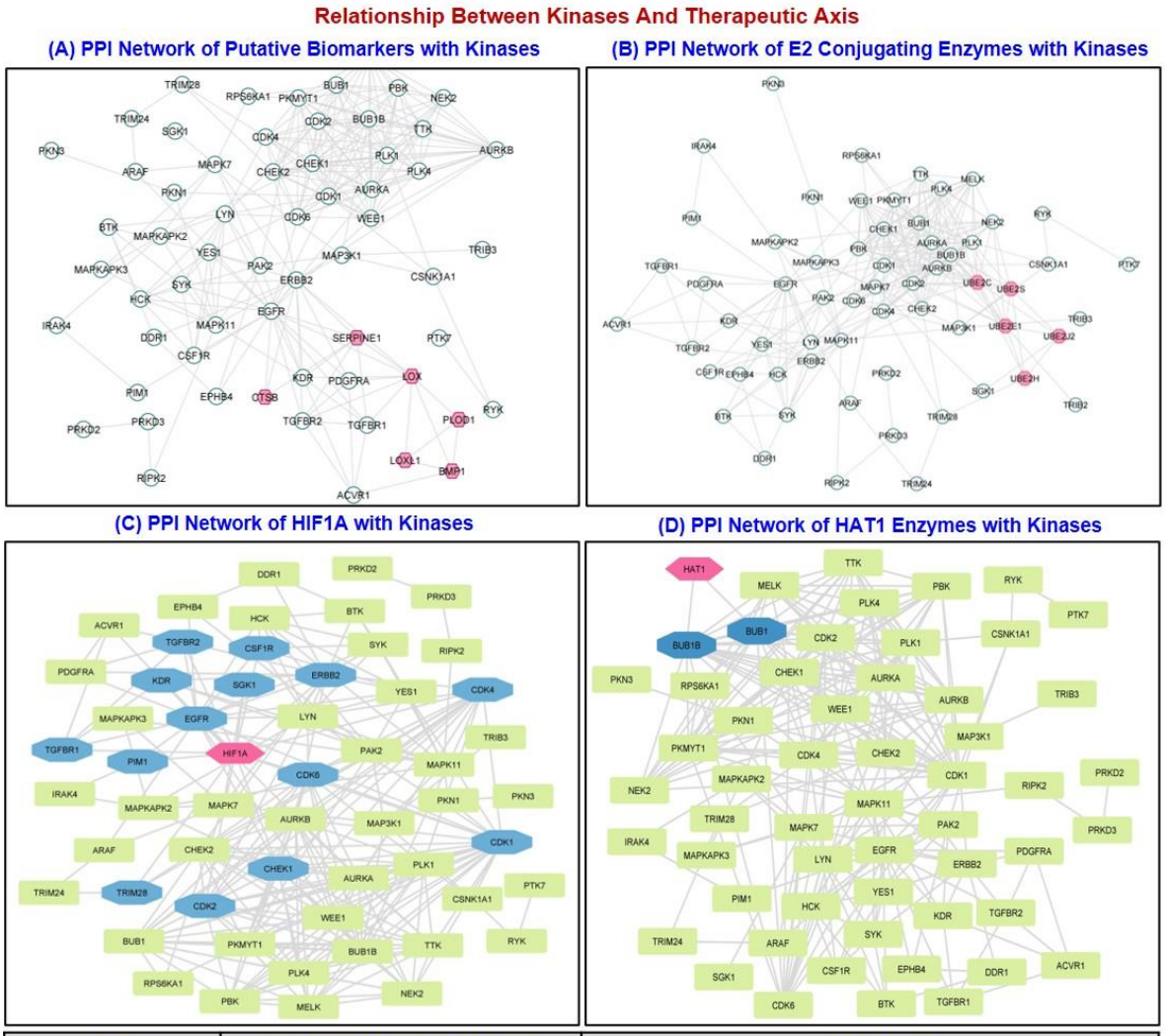

Biomarker	Total number of interacting Kinases	Protein Kinases
BMP1	1	ACVR1
CTSB	2	EGFR, ERBB2
LOX	6	PDGFRA, KDR, TGFBR2, TGFBR1, ERBB2, EGFR
LOXL1	0	--
SERPINE1	5	EGFR, ERBB2, KDR, TGFBR2, TGFBR1
PLOD1	0	--
E2 Enzymes	**Total number of interacting Kinases**	**Protein Kinases**
Ube2E1	8	CDK1, CDK2, AURKA, AURKB, BUB1B, PLK1, NEK2, TRIB2
Ube2H	1	TRIM28
Ube2J2	1	SGK1
Ube2S	8	CDK2, AURKB, BUB1B, PLK1, NEK2, AURKA, CDK1, MAP3K1
Ube2C	16	CDK4, CDK2, AURKB, BUB1B, PLK1, NEK2, MAPK7, AURKA, CDK1, PBK, CHEK1,TTK, PKMYT1, PLK4, MELK, BUB1
Therapeutic Markers	**Total number of interacting Kinases**	**Protein Kinases**
HAT1	2	BUB1, BUB1B
HIF1A	14	CHEK1, CDK2,TRIM28, CDK1, CDK6, PIM1, TGFBR1, EGFR, SGK1, KDR, TGFBR2, CSF1R, ERBB2, CDK4

Figure 4.12: Correlation of Dysregulated Protein Kinases (Upregulated In GBM) with Protein Involved in Proposed Therapeutic Axis. PPI network of kinases with (A) Putative biomarkers (BMP1, CTSB, LOX, LOXL1, PLOD1, SERPINE1); (B) E2s conjugating enzymes (Ube2S, Ube2H and others Ube2E1, Ube2C, Ube2J2); (C) HIF1A; (D) HAT1 enzymes.

Further the association of kinases with HIF1A biomarker and HAT1 enzymes. Results shows HIF1A interact with only BUB1 and BUB1B kinases whereas HAT1 enzymes interact with 14 kinases namely CHEK1, CDK1, CDK2, CDK4, CDK6, PIM1, TGFBR1, EGFR, SGK1, KDR, TGFBR2, CSF1R, ERBB2, and TRIM28 **(Figure 4.12(C, D)).** Here, we have briefly discussed the crucial role kinases play in the pathogenesis of GBM. For example, prior research confirmed that CDKs such as CDK2, 4, and 6 are stimulated in GBM which increases proliferation, radio, and chemoresistance; thus, inhibiting these will increase chemosensitivity to TMZ [736], [737]. Enhanced BUB1/BUB1B expression encourages growth and proliferation, whereas TRIM28 induces GBM cells to go into an autophagic phase and is associated with a bad prognosis for GBM patients [738], [739]. Additionally, AURKA inhibits FOXM1 ubiquitination and increases the development of GBM [740]. While ERBB2, a member of the EGF receptor family, regulates glioma cell proliferation, immunological response, and activation of downstream signaling cascades [741]. Other studies demonstrated that around 60% of initial GBMs have EGFR amplification, and 23% of classical tumors have a particular EGFR-III mutation, which makes them excellent candidates for therapeutic intervention. In contrast, a recent study investigated how EGFR functions as a tumor suppressor in EGFR-amplified GBM that is controlled by EGFR ligands [742], [743].

4.3. CONCLUSION

Together, our investigations offer fresh insights into the expression of secretory components and their prognostic significance in the pathogenesis of the GBM microenvironment. In GBM patient samples, 8 elevated biomarkers, such as BMP1, CTSB, LOX, LOXL1, PLOD1, MMP9, SERPINE1, and SERPING1, were linked to poor prognosis in patients, and only BMP1, HIF1A, and TNFRSF1B, have been identified as substrates involved in the ubiquitination process corresponding E3 ligases. Only E3 ligase VHL and GNB2L1 recognize HIF1A was highly expressed after mRNA and protein levels were analyzed for expression. Interestingly,

we found that the E2s Ube2C, Ube2E1, Ube2H, Ube2J2, Ube2L6, and Ube2S are highly expressed in GBM. After that, the correlation between E2s and VHL and GNB2L1 revealed a positive connection between VHL and Ube2E1, Ube2H, and Ube2J2 and GNB2L1 and Ube2C, Ube2J2, and Ube2S. Similarly, there was a significant association between VHL, and GNB2L1 with HIF1A. In addition, we have discovered all potential acetylation sites on the lysine residue of the E2s: UBE2C (12), Ube2E1 (15), Ube2H (13), Ube2J2 (15), and Ube2S (16). Only five E2s have confidence scores ≥ 2.5: K33 of Ube2C, K43 of Ube2E1, K8 and K52 of Ube2H, K64 and K88 of Ube2J2, and K198, K210, K211, K215, and K216.

According to the mutational analysis results, the acetylation site is lost due to a mutation at K33 of Ube2C or K8 of Ube2H with Q, L, R, or L. The Ube2S mutation causes the lack of acetylation at the corresponding "K" residue at K198 and K211 with L; at K210 and K216 with L, Q, and E; and K215 with L and Q. We have also discovered HATs enzymes that attack acetylated lysine residues in E2s. In GBM patient samples, we found that HAT1 positively correlated with the Ube2E1, Ube2H, Ube2J2, and Ube2S enzymes. In contrast, there is no correlation between HAT1 and Ube2C in GBM patient samples. Our study revealed that only HAT1 is overexpressed in GBM patient samples among the eight HAT enzymes. HAT1's role as an oncogene is well known, and solid tumors, including esophageal, lung, liver, and pancreatic cancer, have been shown to overexpress the gene [744]. After analyzing and collating all of the data from the study, we identified two pathways, one of which targeted either of the proteins' components and the other, which was significantly active in GBM. HAT1-Ube2S(K211)-GNB2L1/HIF1A-BMP1/CTSB/LOX/LOXL1/PLOD1/SERPINE1 and HAT1-UbeH(K8)-VHL-HIF1A-BMP1/CTSB/LOX/LOXL1/PLOD1/SERPINE1 had high and medium confidence scores, respectively. HAT1 enzymes acetylate Ube2S's 211-position lysine residue, increasing GNB2L1's protein turnover while decreasing its ability to ubiquitinate its substrate HIF1A. This causes HIF1A to accumulate and overexpress itself in

GBM. Being a transcription factor, HIF1A also controls the expression of BMP1, CTSB, LOX, LOXL1, PLOD1, and SERPINE1 indicators of poor prognosis in GBM. Major biological processes regulated by our identified axis were hypoxia, angiogenesis, ECM structure and degradation, EMT, IFN response, and TGF and TNF signaling. These signaling processes are essential to the pathophysiology of GBM. Therefore, we could target these cellular processes and reduce tumor burden by focusing on our identified therapeutic axis. We have also discovered the predictive markers CTSB and VHL for TMZ therapy, GNB2L1 for topoisomerase inhibitor therapy, Ube2H and HAT1 for TMZ and chemotherapy. HAT1 is also a hazard to angiogenesis inhibitors. The top 10 mutations already identified in GBM have been used to study alterations in the expression level of our therapeutic axis. Our work sheds light on the potential to investigate the use of secretory microenvironmental components in focusing on the GBM microenvironment. We have also demonstrated the PPI between E2s with kinases and showed that the proposed E2s Ube2S interact with 8 kinases including CDK2, AURKB, BUB1B, PLK1, NEK2, AURKA, CDK1, MAP3K1 whereas Ube2H interact only with TRIM28 kinases. Thus, using computational and machine-learning-based tools and webservers to anticipate acetylation sites of E2s greatly facilitates the study of acetylation and saves valuable research time. More research and scientific studies are required to explore non-cellular components of the GBM microenvironment, PTM, especially acetylation, and E2s. However, the current study is accompanied by limitations, such as the small number of patient samples, *in vitro* and *in vivo* validation of biomarkers and acetylation sites, and lack of predictive biomarkers, substrates, and signaling molecules expression in GBM. Although, despite a computational study, the current study aims to bridge the gap between GBM, biomarkers, acetylation, and ubiquitination enzymes. The study opens the way for the researchers to validate the identified biomarkers in GBM therapeutics. Further, *in vitro* or *in vivo* validation of acetylating sites and ubiquitination factors (E3 ligases and E2 enzymes) through proteomic

studies will lead to enhanced GBM therapeutics, which might cause an increased overall survival rate. Additionally, validation of identified therapeutic axis will have the potential to reverse the GBM etiology or help in drug discovery and development.

4.4. LINKS FOR WEBTOOL, SOFTWARE USED FOR DATA ANALYSIS AND INTERPRETATION

The datasets presented in this study can be found in online repositories. The names of the repository/repositories can be found below: GEPIA2.0: (http://gepia.cancer-pku.cn/index.html); UCSC XENA: (https://xena.ucsc.edu/), GlioVis: (http://gliovis.bioinfo.cnio.es/), Osppc: (https://bioinfo.henu.edu.cn/Protein/OSppc.html), Venny2.1 (https://bioinfogp.cnb.csic.es/tools/venny/); FunRichr tool (http://www.funrich.org/); Enrichr (https://amp.pharm.mssm.edu/Enrichr); OSgbm (http://bioinfo.henu.edu.cn/GBM/GBMList.jsp.);

CELLO v.2.5 (http://cello.life.nctu.edu.tw/); UUCD (http://uucd.biocuckoo.org); Database of Human E3 Ubiquitin Ligases (https://esbl.nhlbi.nih.gov/Databases/KSBP2/Targets/Lists/E3-ligases/); Cell Signaling Incorporated Database (http://www.cellsignal.com/common/content/content.jsp?id=science-tables-ubiquitin);

UbiNet 2.0 (https://awi.cuhk.edu.cn/~ubinet/index.php); STRING (https://string-db.org/); Ubibrowser2.0 (http://ubibrowser.ncpsb.org.cn); TIMER2.0 (http://timer.cistrome.org/); Deep-PLA (http://deeppla.cancerbio.info); GPS-PAIL 2.0 (http://pail.biocuckoo.org/); PSIPRED (http://bioinf.cs.ucl.ac.uk/psipred/); Uniport (https://www.uniprot.org/); PMut (http://mmb.irbbarcelona.org/PMut/); SNAP2 (https://rostlab.org/services/snap/), PolyPhen2 (http://genetics.bwh.harvard.edu/pph2/), MutPred2 (http://mutpred.mutdb.org/index.html)**;** ROC Plotter: (https://www.rocplot.org/), KinMap (http://www.kinhub.org/kinmap/) .

4.5. HIGHLIGHTS OF THE STUDY

- ✓ BMP1, CTSB, LOX, LOXL1, PLOD1, MMP9, SERPINE1 and SERPING1 are linked with poor prognosis in GBM patients.
- ✓ CTSB, HAT1, Ube2H, VHL, and GNB2L1 are predictive markers for GBM therapies.
- ✓ The poor prognostic markers BMP1, CTSB, LOX, LOXL1, PLOD1 and SERPINE1 were positively linked with HIF1A.
- ✓ Ube2C (18, K33); Ube2E1 (K43); Ube2H (K8, K52); Ube2J2 (K64, K88); Ube2S (K198, K210, K211, K215, K216) as putative acetylated sites.
- ✓ Ube2H (K8, K52) and Ube2S (K211) are associated with overexpressed HAT1 enzymes in GBM.
- ✓ Acetylation sites lie in a disordered region of E2s.
- ✓ HAT1-Ube2S(K211)-GNB2L1-HIF1A-BMP1/CTSB/LOX/LOXL1/PLOD1/SERPINE1 as a novel therapeutic axis in GBM

CHAPTER V

Objective 5

CHAPTER V

✓ To dissect the molecular effect of combination therapy in GBM therapeutics through drug repurposing approach.

5. INTRODUCTION

The most prevalent and deadly form of brain cancer called GBM. Intra and inter-heterogeneity, drug resistance, and tumor recurrence were a few challenges with GBM, and despite rigorous therapeutics research survival rate of GBM patients remains low. Identification of novel biomarkers as well as potential therapeutic targets in GBM malignancies after extensive genomic and proteomic investigation is a current need. Surgical resection, radiation therapy, and chemotherapy are the current gold standard of care and typically increase survival. The prognosis for people with GBM remains grim despite significant efforts over the past few decades. Drug repositioning also referred to as "drug repurposing," is a current strategy for finding new treatments for GBM that involves using already-approved medications for other diseases. Clinical translation can be accelerated by using already FDA-approved drugs by eliminating or speeding up phases like chemical optimization and toxicological analysis, which are essential to drug development. But in order to find compounds that can suppress GBM tumorigenesis, a screening procedure must be used to determine whether potential agents can cross the BBB [30]. Indeed, a group of psychotropic medications known as antipsychotics is used to treat bipolar illness, psychosis, delirium, Huntington's disease, and Tourette syndrome. The classification of antipsychotics into typical or first-generation antipsychotics (FGAs) and atypical or second-generation antipsychotics (SGAs) is primarily determined by the likelihood that the patient would experience extrapyramidal symptoms (parkinsonism, dystonia) and tardive dyskinesia [376]. According to a literature review, SGAs outperformed FGAs in treating negative symptoms, mental hospitalization rate, and relapse-free survival. SGAs showed more remarkable persistence and commitment to treatment than FGAs. Studies have demonstrated the possible significance of antipsychotics in slowing the growth of GBM cells

by obstructing each individual hallmark of cancer [377]. Antipsychotic medications have a long history of usage in a wide range of therapeutic psychological contexts, and they have moderate or low toxicities and well-known tolerability profiles. Hence, there are increasingly being explored for effectiveness in patients with various malignancies, including malignant brain tumors, due to their known safety and demonstrated ability to cross the BBB and modulate neuronal activity [745]. Additionally, recent progress in medicine demonstrates the prevalence and benefit of combination therapy over monotherapy for minimizing disease pathogenesis. Numerous studies have recently shown the benefit of implementing combination therapy rather than monotherapy in various diseases, including cancer. Combinatorial therapy can address heterogeneity in GBM, target numerous pathways and therapeutic targets simultaneously, and perhaps circumvent the BBB barrier by using drugs that can pass through the BBB using different mechanisms. Additionally, it can offer a personalized strategy that is tailored to the particular tumor characteristics of each patient, such as specific genetic alterations or molecular profiles.

The anti-cancer agent TMZ, frequently used to combat GBM has earlier been utilized in combination with SGA or FGAs [378]. For instance, FGAs (Chlorpromazine) have already been used in combination therapy. Therefore, the current study aims to identify potential SGA combinations that could be used to minimize the pathogenesis of GBM. The Peritumoral Brain Zone (PT) and tumor core (TC) samples were compared to non-neoplastic brain tissue (control) samples in order to analyze the gene expression profiles of the DEGs. In order to comprehend interactions and the mechanisms of action held by combination therapy, DEGs were, in fact explored using STRING and KEGG analysis. Additionally, two SGA medications used together have the potential to target critical biological pathways that have been found to be implicated in the pathogenesis of GBM due to their mechanisms of action and mode of action. Hence, based on our research findings, psychiatric treatments with well-established

pharmacologic and safety characteristics may be repurposed as anticancer medicines, and has potential to synergetic effect and thus opening new alternatives for the treatment of GBM.

5.1. MATERIALS AND METHODS

5.1.1. IDENTIFICATION OF DEGS

GSE116520 dataset was extracted from online database, namely GEO datasets with a total of 42 samples. The dataset was normalized and processed using GEO2R (https://www.ncbi.nlm.nih.gov/geo/geo2r/), where statistically significant DEGs were screened based on $|\text{Log}_2$ Fold Change (FC)$| \geq 1$ and $p \leq 0.05$. Peritumoural Brain Zone (PT) and tumor core (TC) samples were compared with non-neoplastic brain tissue (control) samples to identify DEGs. A Venn diagram of DEGs was constructed using Venny 2.1 tool (https://bioinfogp.cnb.csic.es/tools/venny/) to find common DEGs between PT vs Control and TC vs Control.

5.1.2. SCREENING OF ATYPICAL DRUG AND THEIR TARGET PREDICTION

To repurpose the drugs against GBM, FDA-approved atypical antipsychotic drugs were retrieved from ChEMBL, Drugbank database and FDA website. Protein targets against each drug were identified at probability score of ≥ 0.09 using the SwissTargetPrediction webtool (http://www.swisstargetprediction.ch/). The basis for SwissTargetPrediction is referred to as the "similarity principle," which usually indicates that two similar compounds are likely to have comparable properties. This approach assesses potential side effects, anticipates off-targets, and determines the possibility of repurposing molecules with therapeutic value in order to predict the probable macromolecular targets for a small molecule that is assumed to be bioactive. Pa (probability "to be active") and Pi (probability "to be inactive"). Moreover, Gene ID of each predicted protein target was extracted from the protein information database, namely UniProt.

5.1.3. RANKING OF DRUGS

Each drug was ranked based on a literature review supporting GBM, the number of targets predicted by SwissTargetPrediction, and the number of common genes between DEGs and drug targets

5.1.4. IDENTIFICATION OF DRUG COMBINATION

Drug combinations were made from the top ranked 5 shortlisted drugs. Each drug was paired with the remaining drugs. Thus, total 10 drug combinations were identified, where each drug, in combination, was studied for its biological functions.

5.1.5. VALIDATION OF SCREENED DRUG COMBINATIONS

Each drug in combination was checked for its biological spectrum using SMILES by querying at PASSonline at the logical activity (Pa) > pharmacological inactivity (Pi) (http://www.way2drug.com/passonline/). Before chemical synthesis and biological testing, this approach can qualitatively predict the biological activity of small molecules. The biological activity spectrum identifies a substance's "intrinsic" characteristic based only on its physical-chemical composition. Herein, drugs with high antineoplastic effects were selected for further analysis. Further common molecular signatures between both drugs and DEGs were studied for biological activities using STRING webtool (https://string-db.org/) and the KEGG database. Detailed Methodology was described in **Figure 5.1**.

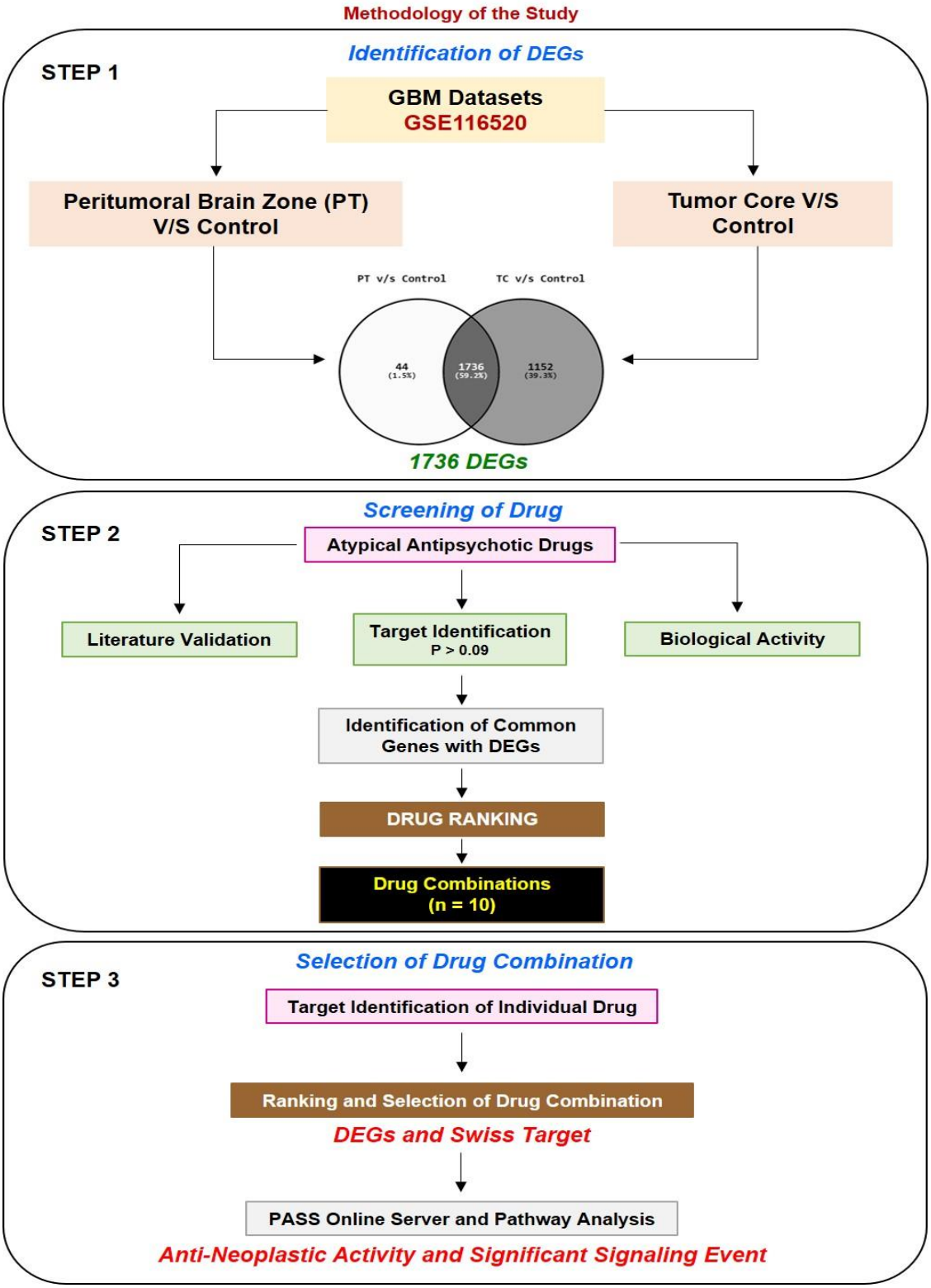

Figure 5.1: Methodology of The Current Study. Current study is majorly divided into three steps. STEP1 includes analysis of GSE116520 data sets procured from GEO database. Total RNA from the tumor core (TC), Peritumoural Brain Zone (PT) were compared with non-neoplastic brain tissue (control) to find common 1736 Differential expressed genes. In STEP 2 FDA-approved atypical antipsychotic drugs were retrieved from ChEMBL, Drugbank database and FDA website. Each drug's molecular targets and biological activity were examined, and then it was determined which targets it shared with DEGs. Drugs were ranked according to their most common targets. In STEP 3 combination were made and each combination were ranked based on common targets, anti-neoplastic activity and signaling pathways.

5.2. RESULT AND DISCUSSION

For GSE116520 transcriptomics data generated on Illumina HumanHT-12 V4.0 expression beadchip platform.

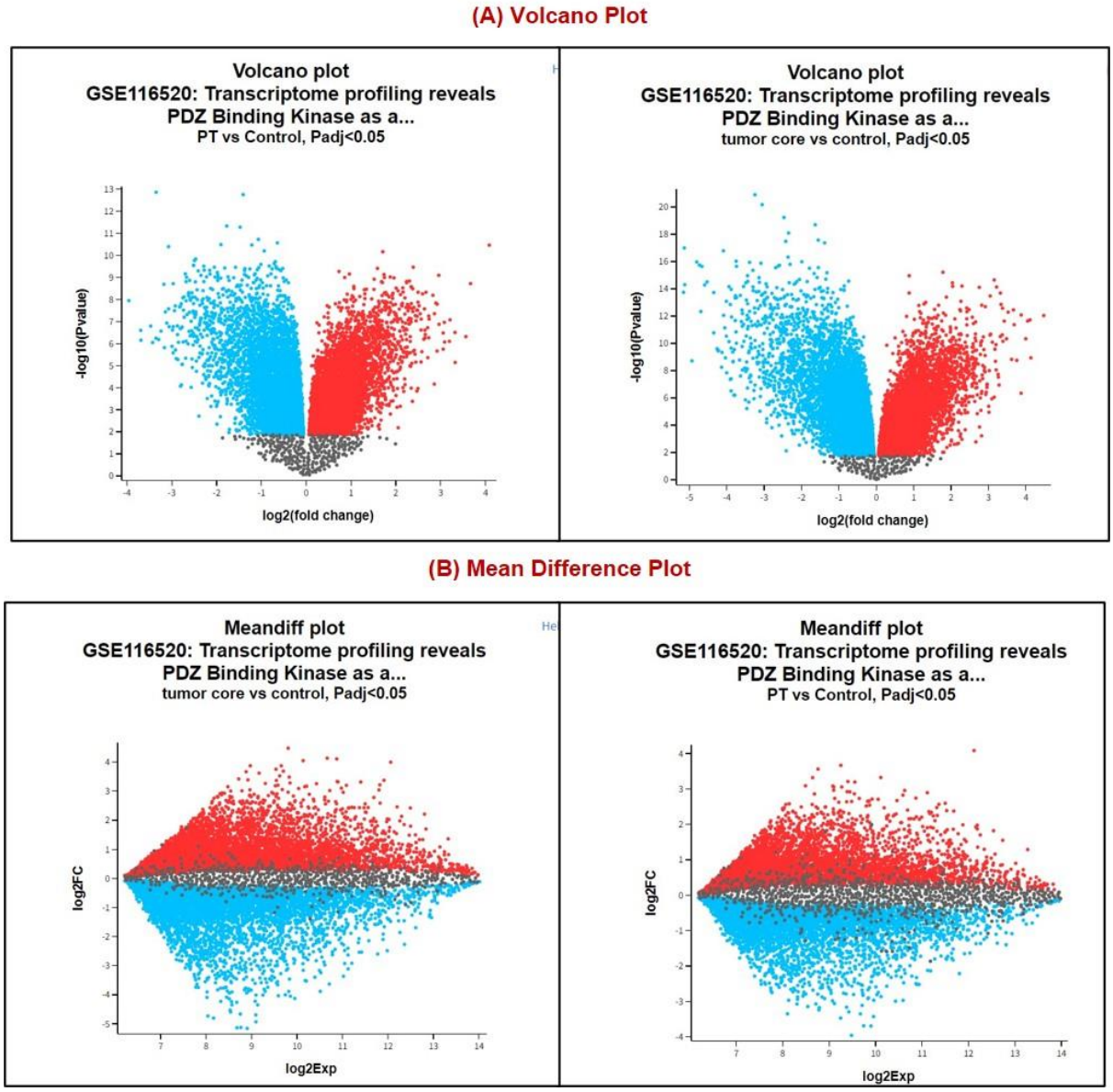

Figure 5.2: (A) Volcano Plot: For illustrating differentially expressed genes (DEGs), a volcano plot compares statistical significance (-log10 P value) to the magnitude of the change (log2 fold change). (B) A mean difference (MD) plot: An effective tool for identifying DEGs is the MD plot, which compares average log2 expression values to log2 fold change.

PT and TC samples were compared with control samples to identify the DEGs. **Figure 5.2** shows volcano plot displays statistical significance (-log10 P value) versus magnitude of change (FC) and is useful for visualizing differentially expressed genes. Highlighted genes

are significantly differentially expressed at a default adjusted p-value cutoff of 0.05 (red = upregulated, blue = downregulated). PT and TC have 17 samples and control have 8 samples from GBM WHO grade IV tumor tissues from adult patients. Total of 1780 DEGs were found to be significantly dysregulated in PT vs control and 2886 genes in TC vs control. A total list of common 1736 DEGs were identified, including 787 upregulated and 946 downregulated genes, between PT vs Control and TC vs control **(Figure 5.3)**.

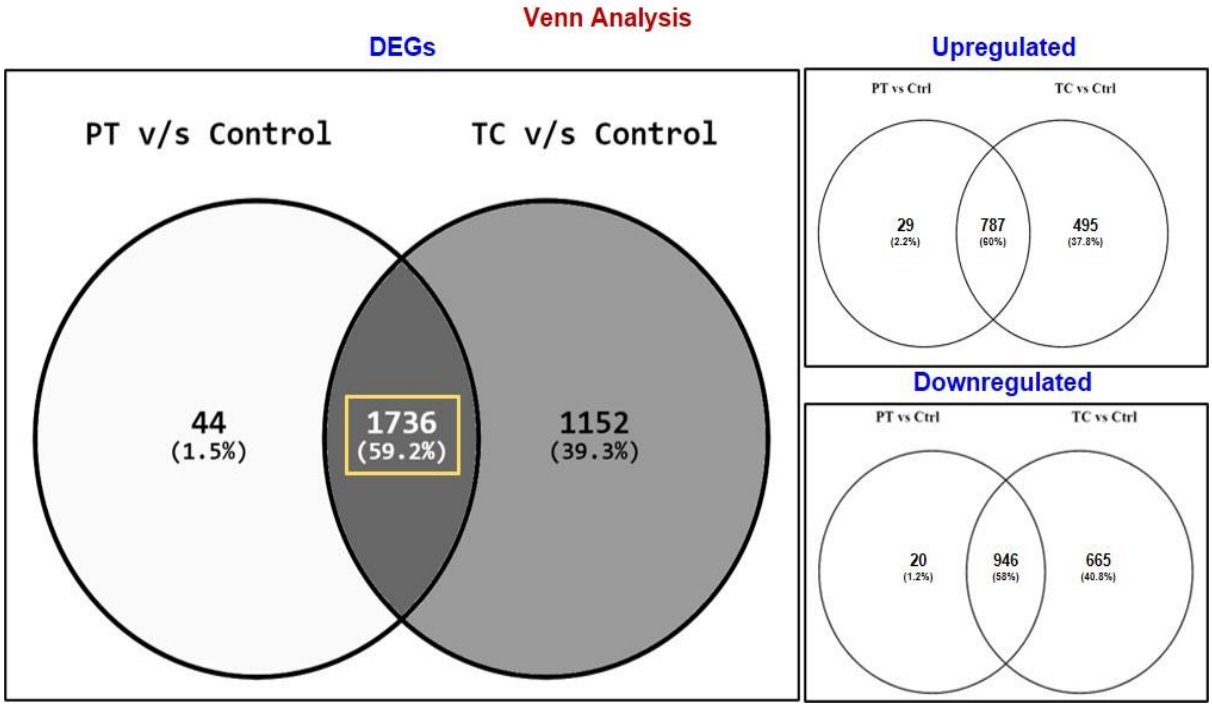

Figure 5.3: Venn Diagrams of Common Differentially Expressed Genes in Two Datasets, Constructed Using the Bioinformatics and Evolutionary Genomics Web Tool Venny. (A) Common UP genes in the two datasets. (B) Common DOWN genes in the two datasets. Blue represents the GSE13276 dataset and red represents the GSE116520 dataset. UP, upregulated; DOWN, downregulated.

The rationale for using common DEGs (1736 genes) for further study is to identify molecular signatures and associated biological pathways responsible for tumor progression and GBM recurrence. Targeting these key pathways with therapeutic agents will hold the potential to reduce GBM aggressiveness and aid patients with better efficacy and a minimum chance of recurrence. In addition, a total of 11 FDA-approved atypical antipsychotic drugs were used to repurpose in GBM **(Figure 5.4(A)).** The plethora of research evidence has shown that the

administration of antipsychotic drugs exhibits anticancer properties to combat brain cancer including GBM through various signaling events, namely PI3K/Akt pathway, AMPK/mTOR pathway, Wnt/β-catenin pathway, and others [746]. For instance, administration of an atypical antipsychotic drug, namely Clozapine inhibits the proliferation GBM human cells. Likewise, Aripiprazole inhibits migration and induces apoptosis of glioma cells U251 cells directly by inhibiting Src kinase [747].

(A) Shortlisting of Antipsychotic Drugs-Based on Target Frequency

Description	Number of Drugs	Molecular Signatures
FDA Approved Antipsychotic Drugs	11	Common 1736 DEGS (PT vs Control and TC vs Control)
Target Available (Probability score > 0.09)	9	
Total Drug Having Common Targets with DEGs	9	
Total Drug Having Common Targets (> 10 genes) with DEGs	7	

(B) Pairing Drug-Gene

Drug Name	Target Identified from SwissTarget Tool	Number of Targets Common with DEGs	Literature support in GBM	Reported Combination		
				Temozolomide	Marizomib	Panobinostat
OLANZAPINE	111	13	Yes	Yes	Yes	Yes
PALIPERIDONE	103	9	Yes	No	No	No
ARIPIPRAZOLE	100	15	Yes	Yes	Yes	Yes
LURASIDONE	101	16	No	No	No	No
RISPERIDONE	102	10	Yes	Yes	No	No
FLUOXETINE	42	5	Yes	Yes	No	No
ZIPRASIDONE	105	15	Yes	Yes	No	No
QUETIAPINE	109	22	Yes	Yes	No	No
CLOZAPINE	108	18	Yes	Yes	Yes	Yes
ILOPERIDONE	1	0	Yes	Yes	No	No

Figure 5.4. (A) Summary of Antipsychotic Drugs Shortlisted After Target Prediction Using Swisstarget Prediction Tool. (B) Summary Of Number of Targets Identified, Overlapped Genes with DEGs, And Already Reported Combination (Data Procured from Drugcombo Portal and Drugcombodb Portal)

Afterward, SwissTargetPrediction was employed to predict protein targets against each drug, and only 9 drugs qualified filter criteria (Probability score ≥ 0.09). Moreover, common molecular signatures were found between protein targets and DEGs. Amongst them, only 9 drugs have common genes, and 7 have more than 10 common target proteins, as described in **Figure 5.4(B)**. Each drug was ranked based on the highest number of common molecular signatures. Further, the biological spectrum of the top 5 drugs, such as Quetiapine, Clozapine, Aripiprazole, Olanzapine and Fluoxetine, was obtained from the PASSonline server using keywords such as antineoplastic, chemosensitizer and immunomodulator with Pa > Pi. Pa (probability "to be active") calculates the likelihood that the investigated compound belongs to the subclass of active compounds. According to PASS's high-confidence prediction, each compound should likely exhibit a specific biological action. Furthermore, the STRING database was used to create protein-protein networks and run KEGG pathway analysis on all common protein targets. In parallel, each shortlisted drug was paired with the remaining drugs to predict a combination therapeutic regime. A total of 10 combination regime was generated. Each combination regime was studied further for its biological activities **(Table 5.1)**. Common significant pathways ($p \leq 0.05$) between both drugs were chosen and studied further. Each drug combination was ranked based on the highest sharing pathways. Our analysis showed top 3 combinations were Quetiapine + Clozapine, Clozapine + Aripiprazole and Clozapine + Olanzapine, whereas other possible combinations were mentioned in **Figure 5.5**.

Table 5.1: The Biological Activity Spectrum of Antipsychotic Drugs

Drugs	Biological Activity							
	Chemosensitizer	Antineoplastic enhancer	Antineoplastic (GBM)	Antineoplastic (Brain Cancer)	Antineoplastic (Glioma)	Antineoplastic (Other Cancer)		Immunomodulator
	Pa (probability "to be active")							
QUETIAPINE	0.41	0.35	0.00	0.18	0.00	0.25	PC	0.31
CLOZAPINE	0.38	0.33	0.00	0.27	0.00	0.25	PC	0.00
ARIPIPRAZOLE	0.29	0.00	0.00	0.20	0.00	0.16	RC	0.22
OLANZAPINE	0.00	0.19	0.00	0.00	0.00	0.22	PC	0.00
PALIPERIDONE	0.00	0.00	0.00	0.00	0.00	0.29	MM	0.00
FLUOXETINE	0.00	0.00	0.18	0.00	0.13	0.00	__	0.00
LURASIDONE	0.00	0.00	0.00	0.00	0.00	0.00	__	0.00
ZIPRASIDONE	0.00	0.00	0.00	0.00	0.00	0.00	__	0.00
RISPERIDONE	0.00	0.00	0.00	0.00	0.00	0.00	__	0.22
ILOPERIDONE	0.00	0.00	0.00	0.00	0.00	0.15	UC	0.19
TEMOZOLOMIDE	0.00	0.849	0.00	0.00	0.00	0.20	OC	0.34
MARIZOMIB	0.387	0.957	0.00	0.00	0.00	0.67	NSCLC	0.00
PANOBINOSTAT	0.523	0.40	0.00	0.00	0.00	0.44	NSCLC	0.00

***Pa>Pi, Green color gradient showed the increasing value of Pi. PC: Pancreatic cancer; RC: Renal Cancer; MM: Multiple Myeloma; UC: Uterine Cancer; OC: Ovarian Cancer; NSCLC: Non-Small Cell Lung Cancer.**

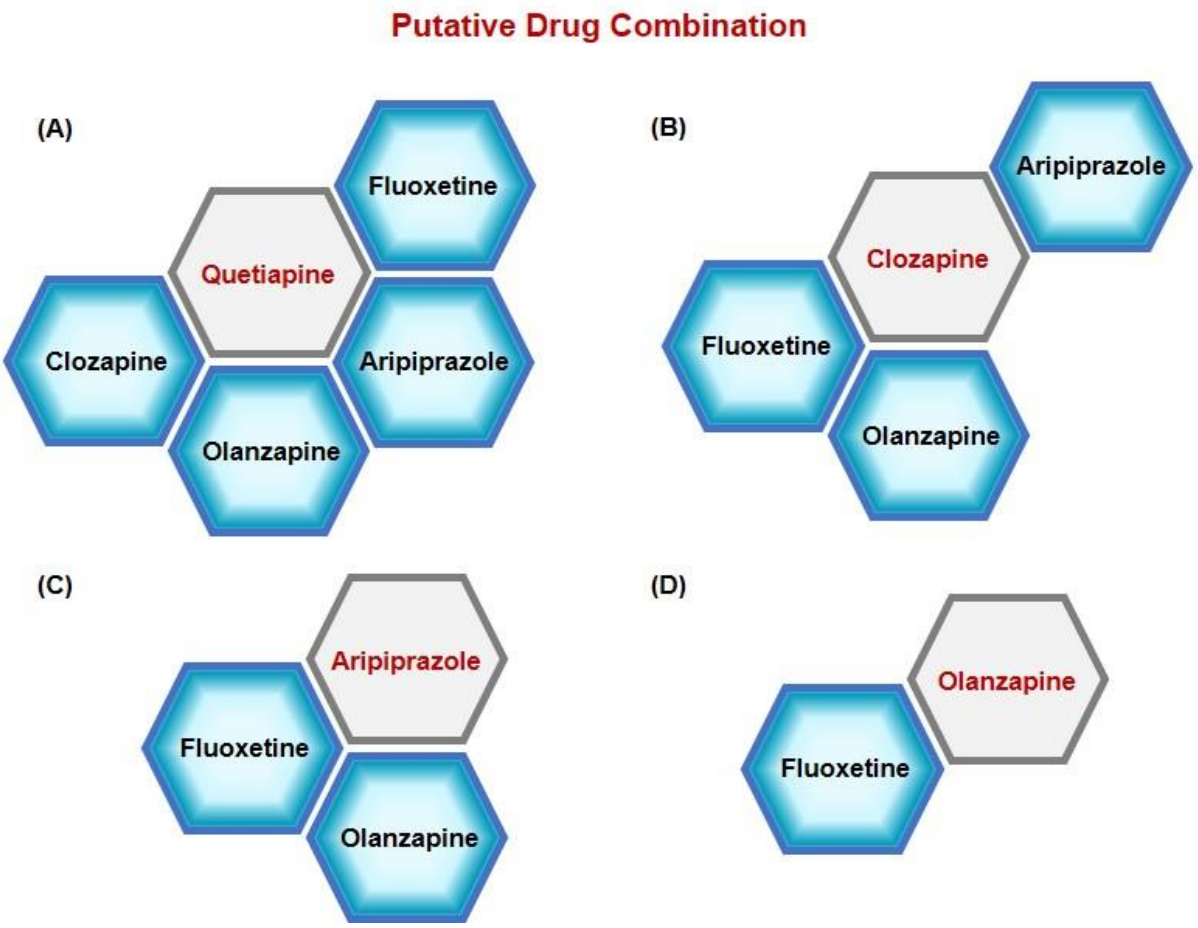

Figure 5.5: Ten Possible Combinations with Top 5 Drugs. (A) Combination with Quetiapine, (B) Combination with Clozapine, (C) Combination with Aripiprazole, (D) Combination with Olanzapine.

Further, pathway analysis showed that both drugs shared Neuroactive ligand-receptor interaction (DRD4, CHRM1, ADRA1B, GABRA5, HTR2A), calcium signaling cascade (CHRM1, ADRA1B, HTR2A) and cell cycle signaling (CDK2, CCNA2) as common genes. Plethora research showed that calcium (Ca^{2+}) is essential in the tumorigenesis, migration, EMT, invasion, metastasis, and vascularization. Hence, Ca^{2+} serves as a prospective treatment target in GBM. Additionally, overlapped target genes of each drug combination (Drug 1, Drug 2) and DEGs were referred to as "molecular signatures" **(Table 5.2).**

Table 5.2: List of Common Molecular Signatures in Proposed Drug Combinations

Drug Combinations	QUETIAPINE and CLOZAPINE	CLOZAPINE and ARIPIPRAZOLE	CLOZAPINE and OLANZAPINE
Molecular Signatures	ADRA1B	ADRA1B	ADRA1B
	APH1A	DRD4	APH1A
	CCNA2	HTR2A	CDK5R1
	CDK2	MAOB	CHRM1
	CHRM1	--	CHRM3
	DRD4	--	DRD4
	GABRA5	--	HTR2A
	HTR2A	--	KCNA5
	--	--	MAPK8

Molecular signature of toped ranked combination Quetiapine + Clozapine were ADRA1B, APH1A, CCNA2, CDK2, CHRM1, DRD4, GABRA5, HTR2A **(Figure 5.6)**. However, previous research evidences have indicated that the combination of our top-ranked drugs with TMZ, Marizomib and Panobinostat drugs was implemented in the GBM therapeutic. We have referred to two open-access databases, DrugComb Portal [748] and DrugComboDB [749], that integrate drug combination repositories from various sources and have been popularly used by researchers. Both comprehensive databases are devoted to gathering drug combinations from numerous sources, such as genetic information, HTS assay, PubMed, FDA-approved combinations, and failed combinations to assess their potential for efficacy for the management of cancer.

Top Ranked Drug Combination

Rank	Drug 1	Drug 2	Signaling Event	Molecular Signature
1	QUETIAPINE	CLOZAPINE	Calcium Signaling and Cell Cycle Pathway	CHRM1, ADRA1B, HTR2A, CDK2, CCNA2
2	CLOZAPINE	ARIPIPRAZOLE	Calcium Signaling Pathway	ADRA1B, HTR2A
3	CLOZAPINE	OLANZAPINE	Calcium Signaling Pathway	CHRM3, CHRM1, ADRA1B, HTR2A

Figure 5.6: Top Three Ranked Combinations: Biological Pathway Analysis Using STRING And KEGG Showed Common Pathways and Molecular Signatures Shared Between Drug 1 And Drug 2 And DEGs.

For instance, study have been concluded that administration of Quetiapine and TMZ exhibit combinatorial effect, which reduces the proliferation of GBM stem cells. Similarly, standalone treatment of Olanzapine inhibits the growth of GBM cells *in vitro*, and thus, promotes apoptosis, which enhances the antitumor activity of TMZ [750]. Thus, from the above study, it must be concluded that administration of anti-psychotic drugs could reverse the progression of GBM through initiation of apoptosis and reduction of GBM cell growth, and drug combination 1 showed synergetic effects along with immunomodulators.

***Limitation of current study*:** combination therapy prediction is based on computational algorithm and literature survey. However, predicted combination need to be checked experimental setting. In addition, various permutation and combination of different drug concentration need to be tried to find optimum dose concentration to get synergic outcome. The results of the current investigation may be utilized to design and perform subsequent studies, including preclinical tests, clinical trials, or translational research, to examine the therapeutic potential, safety, and effectiveness of the identified drug or drug combinations in particular cancer types or patient populations. Researchers working in the same field of repurposing anti-psychotic drugs as monotherapy or in combination to fight cancer can use the study results to design future studies.

5.3. RELEVANT WORK

Evidence for the therapeutic potential of anti-psychotic drugs, such as Chlorpromazine, Trifluoperazine, Pimozide, And Olanzapine, is growing in cancer including GBM [751]. For instance, the first atypical antipsychotic medicine, Clozapine, has been demonstrated to inhibit voltage-gated calcium channels and calmodulin (CaM) through the degradation of Akt protein, thereby decreasing the growth of U-87MG human glioma cells. Additionally, Quetiapine inhibits tumor growth when used alone by blocking RANKL (NFκB ligand) and when combined with the HMG-CoA reductase inhibitor Atorvastatin, its efficacy is enhanced [752],

[753]. In the past, it was normal practice to take multiple psychotropic drugs simultaneously to treat the behavioral and psychological dementia symptoms in Alzheimer's disease patients [754]. Thus, we wanted to use to study and explore benefit of both drugs in combating cancer specifically GBM. The rationale for combining different atypical anti-psychotic drugs is to perhaps increase their anti-tumor properties via synergistic interactions. However, it has not yet been thoroughly demonstrated if such combinations are safe and effective, particularly for GBM. Previously, treatment-resistant schizophrenia was treated with a combination of clozapine and other antipsychotic medications [755]. In addition, recent investigations have shown that Risperidone and Olanzapine are used in combination therapy for the management of schizophrenia [756]. As a result, there is currently data that suggests combining two atypical antipsychotics may be more effective than monotherapy, however, controlled studies have not been done [757]. Numerous evidence-based studies support the use of an *in-silico* method for personalized treatment using combination therapy regime development that predicts the interaction between two pharmaceuticals and a cell line utilizing genetic information, drug targets, and pharmacological data [11,12]. For instance, in BRAF mutant melanoma, Kaitlyn et al., have demonstrated wide computational strategy for determining synergistic combinations utilizing easily accessible single drug efficacy. [760]. However, this approach may be beneficial in identifying therapeutic synergy within a larger pool of potential drug combinations.

5.4. CONCLUSION

In this study, we have identified a putative drug combination therapy, namely Quetiapine and Clozapine as a promising therapeutic agent to reverse GBM through targeting crucial signaling pathways, such as neuroactive ligand-receptor interaction, calcium signaling and cell cycle. Moreover, molecular signatures that will be affected by identified combination were CDK2, CCNA2, DRD4, GABRA5, CHRM1, ADRA1B, and HTR2A. Targeting

identified signature will our identified combination therapy will altogether reduce tumor burden. However, clinical research can be done for the validation of the presented model, and other drugs should also be worked on to find their capability for the treatment of GBM.

Thus, combination therapy and pharmacological synergism show potential for targeted heterogeneous tumors like GBM and the associated tumor microenvironment. In order to maximize the anticancer potential of particular therapeutic modalities, future research should concentrate on identifying synergistic interactions between chemotherapy, repurposed drugs, radiation, and immunotherapy.

5.5. HIGHLIGHTS OF THE STUDY

- ✓ Molecular signature of toped ranked combination Quetiapine + Clozapine were ADRA1B, APH1A, CCNA2, CDK2, CHRM1, DRD4, GABRA5, HTR2A
- ✓ Putative drug combination therapy, namely Quetiapine and Clozapine as a promising therapeutic agent to reverse GBM
- ✓ Crucial signaling pathways, such as neuroactive ligand-receptor interaction, calcium signaling and cell cycle.

CHAPTER VI

Summary, Conclusion, and Future Perspectives

CHAPTER VI: SUMMARY, CONCLUSION, AND FUTURE PERSPECTIVES

Despite recent advancements in chemotherapy, radiotherapy, and immunotherapy, there is currently no satisfactory therapy for GBM in clinics due to many failure reasons, being toxicity of chemotherapy, failure of the drug to cross BBB, involvement of TME and less immune infiltration. Thus, there is an unmet need for novel approaches to treat GBM and other brain cancer. The motive of our study is to identify novel therapeutic compounds and targets in GBM. Here in our study, we have focused on a crucial TME parameter, i.e., hypoxia caused due to intense cell respiration, excessive nutrient consumption by tumor cells, and abnormal vasculature. However, hypoxia is a hallmark of brain tumors, and if and how hypoxia affects antitumor immunity in the brain remains unclear. Our findings shed light on MMP9's potential as a therapeutic target and a robust biomarker in GBM's hypoxic microenvironment. We have proposed MMP9 as a promising biomarker for hypoxic microenvironmental conditions in GBM. Other molecular signatures, such as LYN, PSMB9, and TIMP1, could be investigated further as druggable biomarkers or prognostic markers in addition to MMP9. Infiltration of immune cells such as neutrophils and DCs was linked to this gene's expression to varying degrees. This effect opens up new avenues for study into the MMP9 and GBM. A negative correlation with B cells, CD4+ T cells and CD8+ T cells support the failure of current immune checkpoint inhibitors. Moreover, the current study used *in silico* techniques such as compound-protein-pathway enrichment analysis, network pharmacology, molecular docking, MD simulation, MM-PBSA, PCA and DCCM investigations to identify a collection of druggable and non-toxic natural compounds. The potential of natural compounds to be used as drugs was revealed by ADMET analysis of eleven novel hits. A chemical substance must have absorption, distribution, metabolism, excretion, and toxicity values to be utilized as a medication. Together results obtained showed flavonoids named 7,4'-dihydroxyflavan, (3R)-3-(4-Hydroxybenzyl)-

6-hydroxy-8-methoxy-3,4-dihydro-2H-1-benzopyran and 4'-hydroxy-7-methoxyflavan as a potential inhibitor of MMP9 produced from the hypoxic condition in GBM. These inhibitors have comparable or better results compared to reference drugs Solasodine and Captopril. Our results indicate that MMP9 and drug interaction are stable, and proposed novel flavonoids can inhibit or reduce MMP9 expression in hypoxia conditions, which will further affect downstream process involved in GBM pathogenesis. Hence, targeting an essential microenvironmental condition will improve therapeutic efficacy and expand the treatment drug library against GBM. In summary, the observations of this work suggest novel plant-based flavonoids inhibited the potential role of MMP9 as a biomarker factor and active MMP9 in GBM. Prior to synthesizing therapeutics, the results of this investigation could be helpful. Other natural compounds and plant-based natural compounds could be examined and studied to understand and explore whether they could be employed as future possibilities for GBM medicines. The results of this study are helpful for drug development. The findings may aid in the assisted screening of therapeutics for GBM. This study is novel in incorporating various computational methodologies for the virtual screening of natural compounds based on BBB, ADMET, PAINS, and Lipinski's rule. This study allows scientists to explore these molecules *in vitro* or *in vivo* as a medicinal approach. Our findings will aid researchers in concentrating on TME components and their conditions in order to produce novel natural product-based anti-GBM therapies that address two major issues: toxicity and resistance and target a major microenvironmental condition: Hypoxia.

Additionally, our investigations offer fresh insights into the expression of secretory components and their prognostic significance in the pathogenesis of the GBM microenvironment. In GBM patient samples, 8 elevated biomarkers, such as BMP1, CTSB, LOX, LOXL1, PLOD1, MMP9, SERPINE1, and SERPING1, were linked to poor prognosis in patients, and only BMP1, HIF1A, and TNFRSF1B, have been identified as substrates

involved in the ubiquitination process corresponding E3 ligases. Only E3 ligase VHL and GNB2L1 recognize HIF1A was highly expressed after mRNA and protein levels were analyzed for expression. Interestingly, we found that the E2s Ube2C, Ube2E1, Ube2H, Ube2J2, Ube2L6, and Ube2S are highly expressed in GBM. After that, the correlation between E2s and VHL and GNB2L1 revealed a positive connection between VHL and Ube2E1, Ube2H, and Ube2J2 and GNB2L1 and Ube2C, Ube2J2, and Ube2S. Similarly, there was a significant association between VHL, and GNB2L1 with HIF1A. In addition, we have discovered all potential acetylation sites on the lysine residue of the E2s: UBE2C (12), Ube2E1 (15), Ube2H (13), Ube2J2 (15), and Ube2S (16). Only five E2s have confidence scores ≥ 2.5: K33 of Ube2C, K43 of Ube2E1, K8 and K52 of Ube2H, K64 and K88 of Ube2J2, and K198, K210, K211, K215, and K216. According to the mutational analysis results, the acetylation site is lost due to a mutation at K33 of Ube2C or K8 of Ube2H with Q, L, R, or L. The Ube2S mutation causes the lack of acetylation at the corresponding "K" residue at K198 and K211 with L; at K210 and K216 with L, Q, and E; and K215 with L and Q. We have also discovered HATs enzymes that attack acetylated lysine residues in E2s. In GBM patient samples, we found that HAT1 positively correlated with the Ube2E1, Ube2H, Ube2J2, and Ube2S enzymes. In contrast, there is no correlation between HAT1 and Ube2C in GBM patient samples. Our study revealed that only HAT1 is overexpressed in GBM patient samples among the eight HAT enzymes. After analyzing and collating all of the data from the study, we identified two pathways, one of which targeted either of the proteins' components and the other, which was significantly active in GBM.

HAT1-Ube2S(K211)-GNB2L1/HIF1A-BMP1/CTSB/LOX/LOXL1/PLOD1/SERPINE1 and HAT1-UbeH(K8)-VHL-HIF1A-BMP1/CTSB/LOX/LOXL1/PLOD1/SERPINE1 had high and medium confidence scores, respectively. HAT1 enzymes acetylate Ube2S's 211-position lysine residue, increasing GNB2L1's protein turnover while decreasing its ability to

ubiquitinate its substrate HIF1A. This causes HIF1A to accumulate and overexpress itself in GBM. Being a transcription factor, HIF1A also controls the expression of BMP1, CTSB, LOX, LOXL1, PLOD1, and SERPINE1 indicators of poor prognosis in GBM. Major biological processes regulated by our identified axis were hypoxia, angiogenesis, ECM structure and degradation, EMT, IFN response, and TGF and TNF signaling. These signaling processes are essential to the pathophysiology of GBM. Therefore, we could target these cellular processes and reduce tumor burden by focusing on our identified therapeutic axis. We have also discovered the predictive markers CTSB and VHL for TMZ therapy, GNB2L1 for topoisomerase inhibitor therapy, Ube2H and HAT1 for TMZ and chemotherapy. HAT1 is also a hazard to angiogenesis inhibitors. The top 10 mutations already identified in GBM have been used to study alterations in the expression level of our therapeutic axis. Our work sheds light on the potential to investigate the use of secretory microenvironmental components in focusing on the GBM microenvironment. We have also demonstrated the PPI between E2s with kinases and showed that the proposed E2s Ube2S interact with 8 kinases including CDK2, AURKB, BUB1B, PLK1, NEK2, AURKA, CDK1, MAP3K1 whereas Ube2H interact only with TRIM28 kinases. Thus, using computational and machine-learning-based tools and webservers to anticipate acetylation sites of E2s greatly facilitates the study of acetylation and saves valuable research time. More research and scientific studies are required to explore non-cellular components of the GBM microenvironment, PTM, especially acetylation, and E2s.

Moreover, we have identified a putative drug combination therapy, namely Quetiapine and Clozapine as a promising therapeutic agent to reverse GBM through targeting crucial signaling pathways, such as neuroactive ligand-receptor interaction, calcium signaling and cell cycle. Moreover, molecular signatures that will be affected by identified combination were CDK2, CCNA2, DRD4, GABRA5, CHRM1, ADRA1B, and HTR2A. Targeting identified signature will our identified combination therapy will altogether reduce tumor

burden. Thus, combination therapy and pharmacological synergism show potential for targeted heterogeneous tumors like GBM and the associated tumor microenvironment. In order to maximize the anticancer potential of particular therapeutic modalities, future research should concentrate on identifying synergistic interactions between chemotherapy, repurposed drugs, radiation, and immunotherapy.

Although, we have validated our results using different computational methodologies, such as multiple-target validation, literature validation, and TCGA databases (containing GBM samples data), but cell culture and animal model research will require to fill the research gaps. The molecular mechanism underlying the reduction of target expression needs only to be validated through *in vitro* experiments. Further, new leads are being discovered in several ongoing studies using advanced computational strategies and machine learning models to filter massive pharmaceutical libraries. However, the experimental screening strategy alone may not enhance lead productivity for the rapid development of viable medicines. Other limitations, such as the small number of patient samples, *in vitro* and *in vivo* validation of biomarkers and acetylation sites, and lack of predictive biomarkers, substrates, and signaling molecules expression in GBM should be rectified to harness the potential of natural compounds in GBM therapeutics. Similarly, despite a computational approach, the current study aims to bridge the gap between GBM, biomarkers, acetylation, and ubiquitination enzymes. Thus, *in vitro* or *in vivo* validation of acetylating sites and ubiquitination factors (E3 ligases and E2 enzymes) through proteomic studies will be required to enhance GBM therapeutics, which might cause an increased overall survival rate. Additionally, validation of identified therapeutic axis will have the potential to reverse the GBM etiology or help in drug discovery and development.

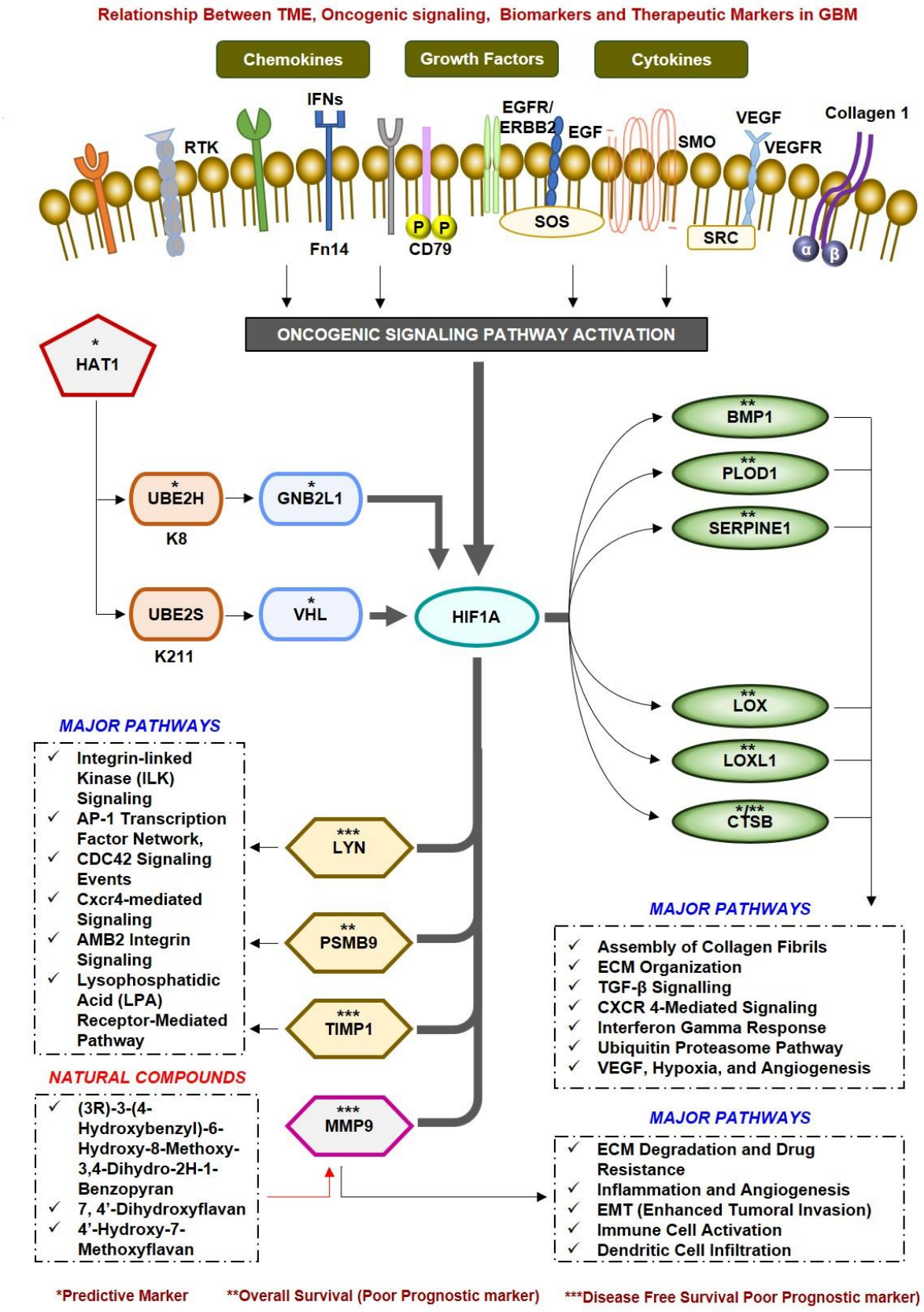

Figure 6.1: The Figure Demonstrates Our Study Key Finding That Shows the Relationship Between Tumor Microenvironment, Biomarkers and Therapeutic Markers In GBM.

ANNEXURE

(A) MA Normalization Plot of The Data

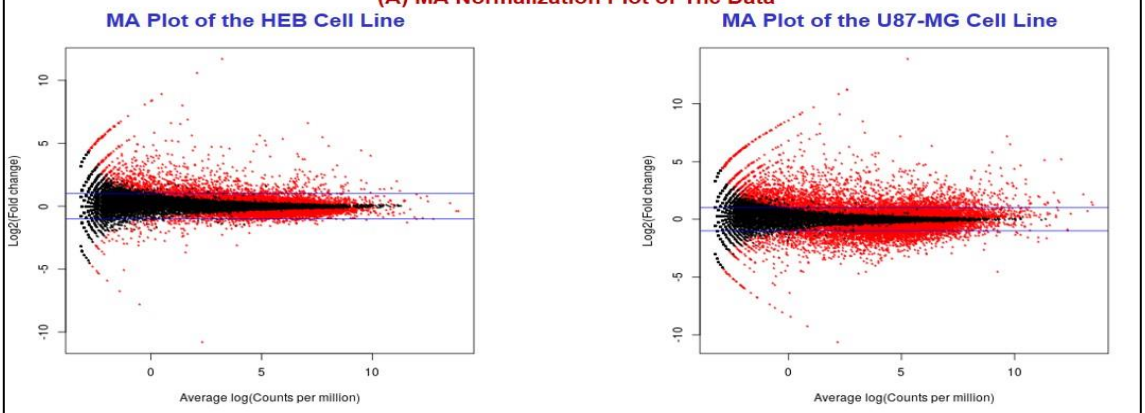

(B) Transcription Factor Associated with Molecular Signatures in GBM

Biomarkers	TFs	Degree	Betweenness	mRNA expression (GEPIA2.0)
TIMP1, MMP9, PSMB9	YY1	3	109.00	
TIMP1, LYN	JUND	2	65.58	
MMP9, LYN	SRF	2	51.67	
TIMP1, PSMB9	RELA	2	33.83	
TIMP1, MMP9	FOXC1	2	14.92	
TIMP1	NFIC	1	0	
	HNF4A	1	0	
	SREBF1	1	0	
MMP9	FOS	1	0	
	JUN	1	0	
	TP53	1	0	
PSMB9	BRCA1	1	0	
	CEBPB	1	0	
	CREB1	1	0	
	E2F1	1	0	
	TFAP2A	1	0	
	NFKB1	1	0	
	USF1	1	0	
LYN	PBX1	1	0	
	GATA2	1	0	
	POU2F2	1	0	
	STAT3	1	0	
	SOX10	1	0	

Upregulated in GBM tumor(|Log2FC| Cutoff:1.5; p<0.05)	
Upregulated in GBM tumor(|Log2FC| Cutoff:1.4; p<0.05)	
Not significant in GBM tumor	

GBM tumor samples	163
Normal tissue samples	207

(C) Network Showing Associated Transcription Factor With Molecular Signatures In GBM

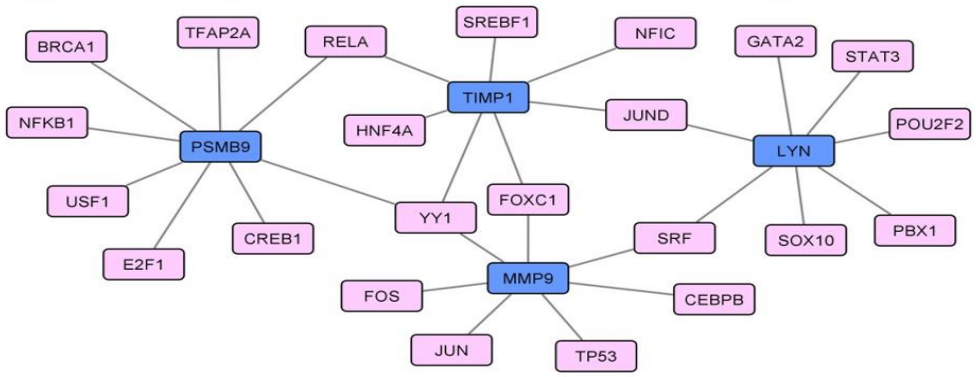

Annexure 1: (A) MA Plot: A Smear Plot Showing the Log of The Fold Changes on The Y-Axis Versus the Average of The Log of The CPM On the X-Axis. DEGs are marked in red and blue horizontal line indicates cut-off filter for LogFC) (Cut-off Log FC > ± 1.5) CPM: Count per million; DEGs: differentially expressed genes; LogFC: log foldchange. (B) Detail Methodology used to filter natural compounds from NPACT Database. (B) Transcription factors associated with molecular signatures (MMP9, LYN, TIMP1, PSMB9) calculated by JASPAR (using network analyst). B.1 shows common TFs shared by more than one biomarker based on degree and betweenness. In addition, expression levels in GBM have been calculated by GEPIA2.0. Green: logFc >1.5, p value<0.05; Light green: LogFc >1.4, p value<0.05; Grey: p value<0.05. (B) shows Network Showing Associated Transcription Factor with Molecular Signatures In GBM

Annexure 2: Physiochemical Properties of Eleven Hit Natural Compounds

PubChem Compound Id	SMILES	Molecular formula	Molecular weight (g/mol) (<500)	LogP (<5)	HBD* (<5)	HBA** (<10)	Lipinski Rule of 5	PAINS	BBB SWISSADME	BBB predictor (Cbligand)	BBB Score (>0.02)	Drug-likeness model score
158280	C1CC2=C(C=C(C=C2)O)OC1C3=CC=C(C=C3)O	C15H14O3	242.27	3.1	2	3	Yes	0 alert	Yes	Yes	4.56	0.47
185609	COC1=CC2=C(CCC(O2)C3=CC=C(C=C3)O)C=C1	C16H16O3	256.3	3.4	1	3	Yes	0 alert	Yes	Yes	4.99	0.77
10424988	COC1=CC(=CC(=C1CCC(=O)C2=CC=C(C=C2)O)OC)O	C17H18O5	302.32	2.7	2	5	Yes	0 alert	Yes	Yes	3.9	0.71
13886678	COC1=CC(=C(C=C1)C2COC3=C(C2=O)C=CC(=C3)O)OC	C17H16O5	300.3	2.7	1	5	Yes	0 alert	Yes	Yes	3.9	0.7
44479222	COC1=CC(=CC2=C1OCC(C2)CC3=CC=C(C=C3)O)O	C17H18O4	286.32	3.4	2	4	Yes	0 alert	Yes	Yes	4.26	0.41
15549893	COC1=CC(=C(C=C1)C(=O)CCC2=CC=C(C=C2)O)OC	C17H18O4	286.32	3.1	1	4	Yes	0 alert	Yes	Yes	4.33	0.41
124256	CCCCCCCC(CCC(=O)N1CCCCC1C2=CN=CC=C2)O	C21H34N2O2	346.5	4.1	1	3	Yes	0 alert	Yes	Yes	4.53	1
162334	CCCCCCCC(=O)N1CCCC1C2=CN=CC=C2	C17H26N2O	274.4	3.7	0	2	Yes	0 alert	Yes	Yes	4.94	0.33
1548943	CC(C)C=CCCCCC(=O)NCC1=CC(=C(C=C1)O)OC	C18H27NO3	305.4	3.6	2	3	Yes	0 alert	Yes	Yes	4.16	0.14
101477139	CC1=C(C=CC(=C1)C(=O)C(C)CC2C(C2(C)C)CCC(=O)C)O	C20H28O3	316.4	4	1	3	Yes	0 alert	Yes	Yes	4.24	0.56
14313693	CC1CCC2(C1(CCC(=CCO)C2C)C)C	C15H26O	222.37	3.8	1	1	Yes	0 alert	Yes	Yes	4.38	0.04

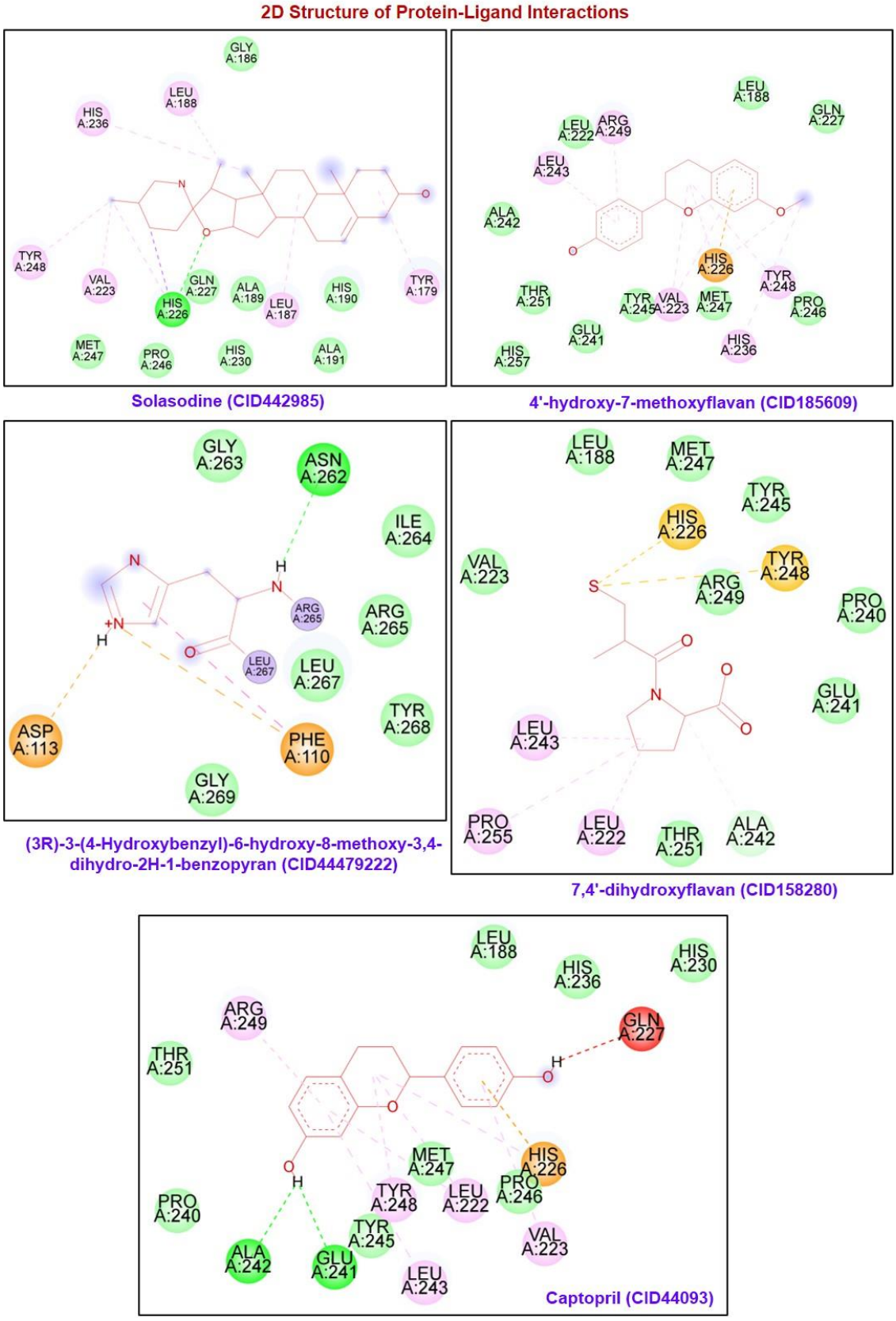

Annexure 3: Two-Dimensional Interaction Diagrams for The Docked Complexes Between MMP9 And Ligands Obtained In This Study. Legend color code: Dark Green: Conventional Hydrogen bond; Green: Van der waals; Light Green: Carbon hydrogen bond; Pink: Pi-Alkyl; Purple: Pi- Sigma; Dark-pink: Pi-Pi stacked

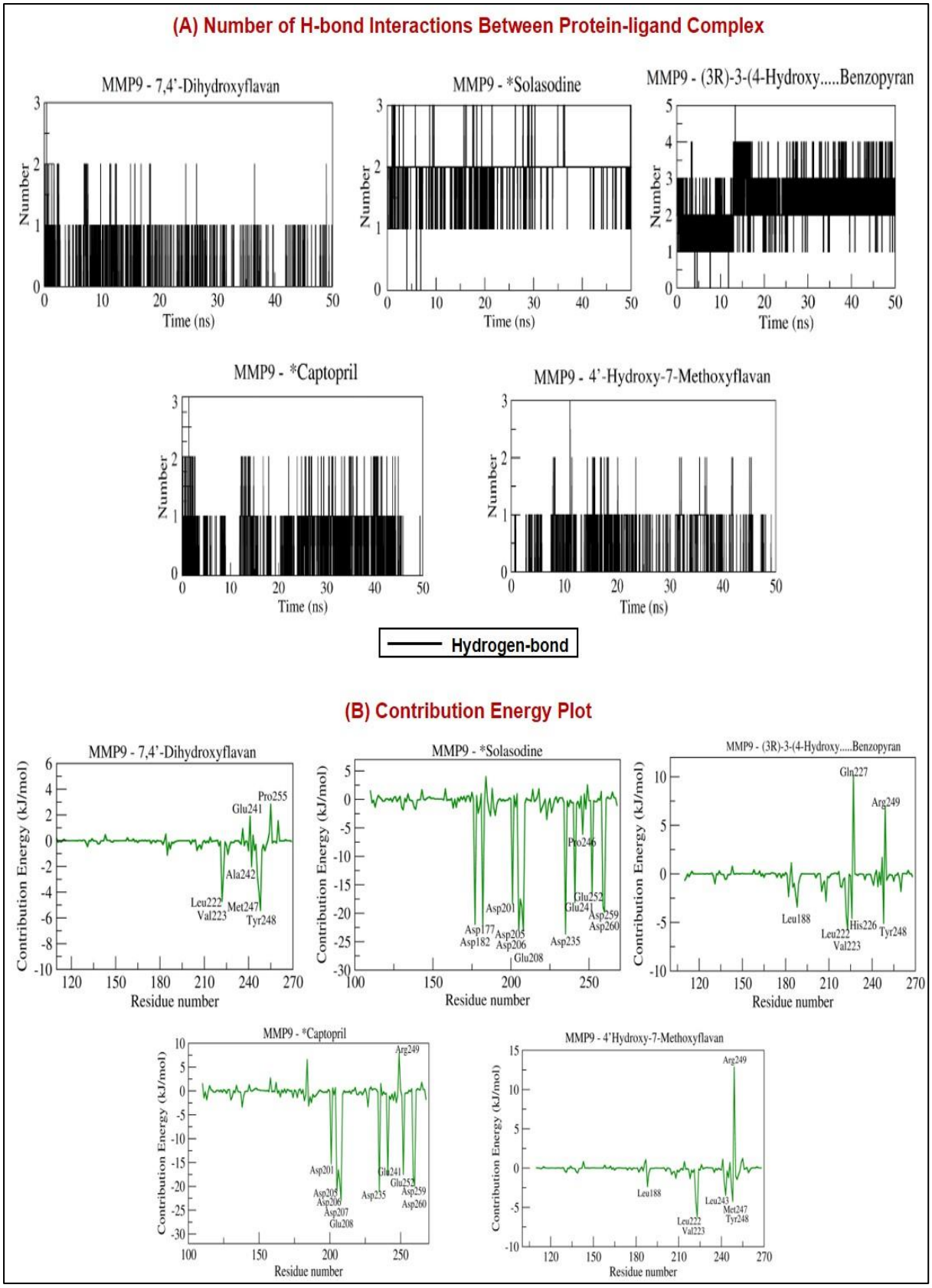

Annexure 4: (A) Number Of H-Bond Interactions Between Protein-Ligand Complex. (B) Contribution Energy Plot Highlighting the Importance of The Binding Pocket Residues In Stable Complex Formation.

Annexure 5: Expression Study of Non-Cellular Secretory Components of Tumor Microenvironment in Glioblastoma Multiforme

	Webtools	RNA Sequence datasets				Microarray datasets			
		GEPIA 2.0	*UCSC XENA*		*GLIOVIS*	*GLIOVIS*		*TCGA_GBM*	
		TCGA GBM_GTX	TCGA GBM	GDC TCGA GBA	TCGA RNA Sequence	REMBRANDT	GRAVENDEEL	HG-U133A	AGILENT-4502A
Chemokines	XCL1								
	CCL1								
	CCL11								
	CCL12								
	CCL13								
	CCL14								
	CCL15								
	CCL16								
	CCL17								
	CCL18								
	CCL19								
	CCL2								
	CCL20								
	CCL21								
	CCL22								
	CCL23								
	CCL24								
	CCL25								
	CCL26								
	CCL27								
	CCL28								
	CCL3								
	CCL3L1								
	CCL3L3								
	CCL4								
	CCL4L1								
	CCL4L2								
	CCL5								
	CCL6								
	CCL7								
	CCL8								
	CCL9/10								
	CX3CL1								
	CXCL1								
	CXCL10								
	CXCL11								
	CXCL12								
	CXCL13								
	CXCL14								
	CXCL15								
	CXCL16								
	CXCL17								
	CXCL2								
	CXCL22								
	CXCL3								
	CXCL4								
	CXCL4L1								
	CXCL5								
	CXCL6								
	CXCL7								
	CXCL8								
	CXCL9								
	XCL2								
	Activin								

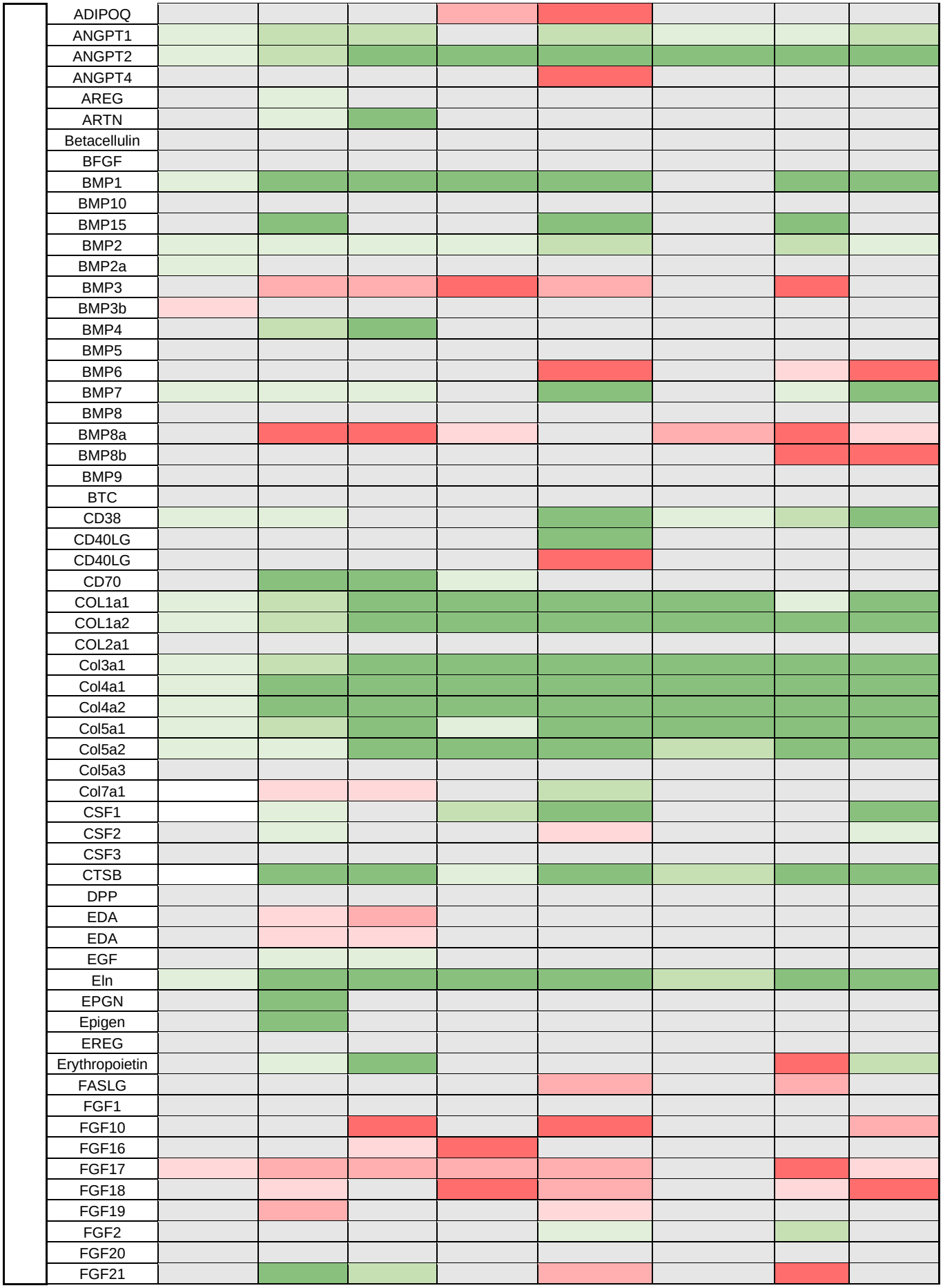
ADIPOQ
ANGPT1
ANGPT2
ANGPT4
AREG
ARTN
Betacellulin
BFGF
BMP1
BMP10
BMP15
BMP2
BMP2a
BMP3
BMP3b
BMP4
BMP5
BMP6
BMP7
BMP8
BMP8a
BMP8b
BMP9
BTC
CD38
CD40LG
CD40LG
CD70
COL1a1
COL1a2
COL2a1
Col3a1
Col4a1
Col4a2
Col5a1
Col5a2
Col5a3
Col7a1
CSF1
CSF2
CSF3
CTSB
DPP
EDA
EDA
EGF
Eln
EPGN
Epigen
EREG
Erythropoietin
FASLG
FGF1
FGF10
FGF16
FGF17
FGF18
FGF19
FGF2
FGF20
FGF21

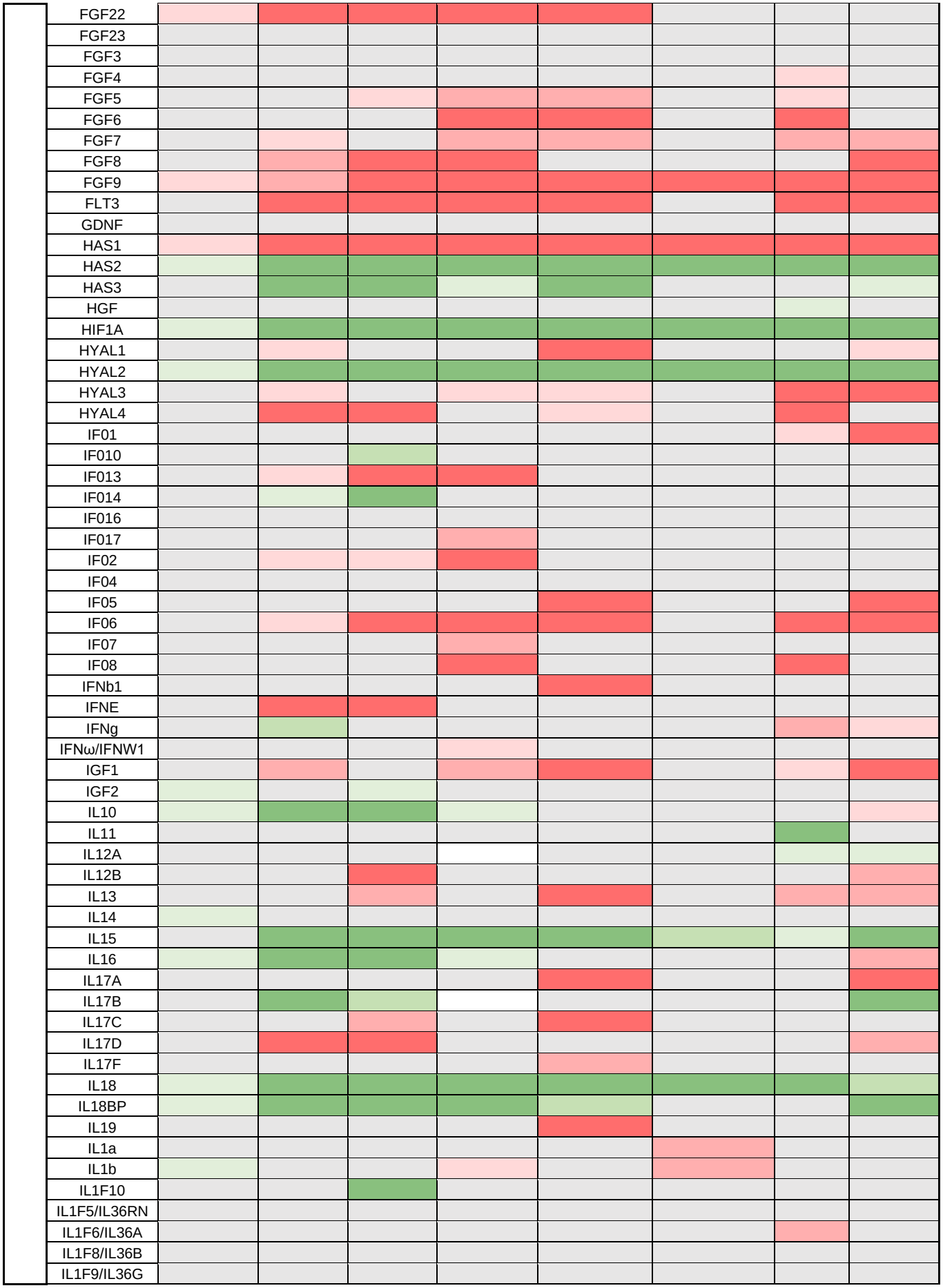
FGF22
FGF23
FGF3
FGF4
FGF5
FGF6
FGF7
FGF8
FGF9
FLT3
GDNF
HAS1
HAS2
HAS3
HGF
HIF1A
HYAL1
HYAL2
HYAL3
HYAL4
IF01
IF010
IF013
IF014
IF016
IF017
IF02
IF04
IF05
IF06
IF07
IF08
IFNb1
IFNE
IFNg
IFNω/IFNW1
IGF1
IGF2
IL10
IL11
IL12A
IL12B
IL13
IL14
IL15
IL16
IL17A
IL17B
IL17C
IL17D
IL17F
IL18
IL18BP
IL19
IL1a
IL1b
IL1F10
IL1F5/IL36RN
IL1F6/IL36A
IL1F8/IL36B
IL1F9/IL36G

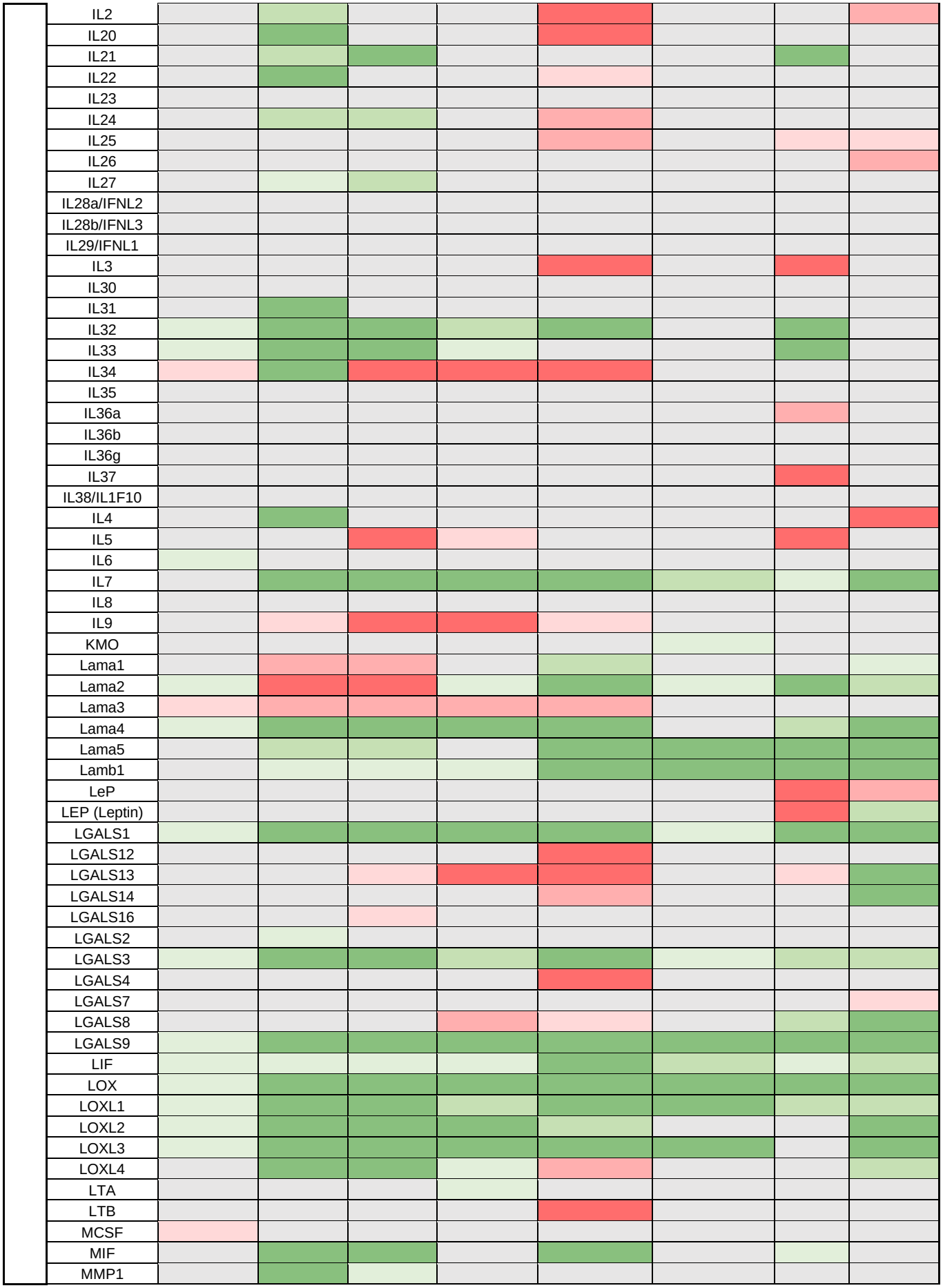
IL2
IL20
IL21
IL22
IL23
IL24
IL25
IL26
IL27
IL28a/IFNL2
IL28b/IFNL3
IL29/IFNL1
IL3
IL30
IL31
IL32
IL33
IL34
IL35
IL36a
IL36b
IL36g
IL37
IL38/IL1F10
IL4
IL5
IL6
IL7
IL8
IL9
KMO
Lama1
Lama2
Lama3
Lama4
Lama5
Lamb1
LeP
LEP (Leptin)
LGALS1
LGALS12
LGALS13
LGALS14
LGALS16
LGALS2
LGALS3
LGALS4
LGALS7
LGALS8
LGALS9
LIF
LOX
LOXL1
LOXL2
LOXL3
LOXL4
LTA
LTB
MCSF
MIF
MMP1

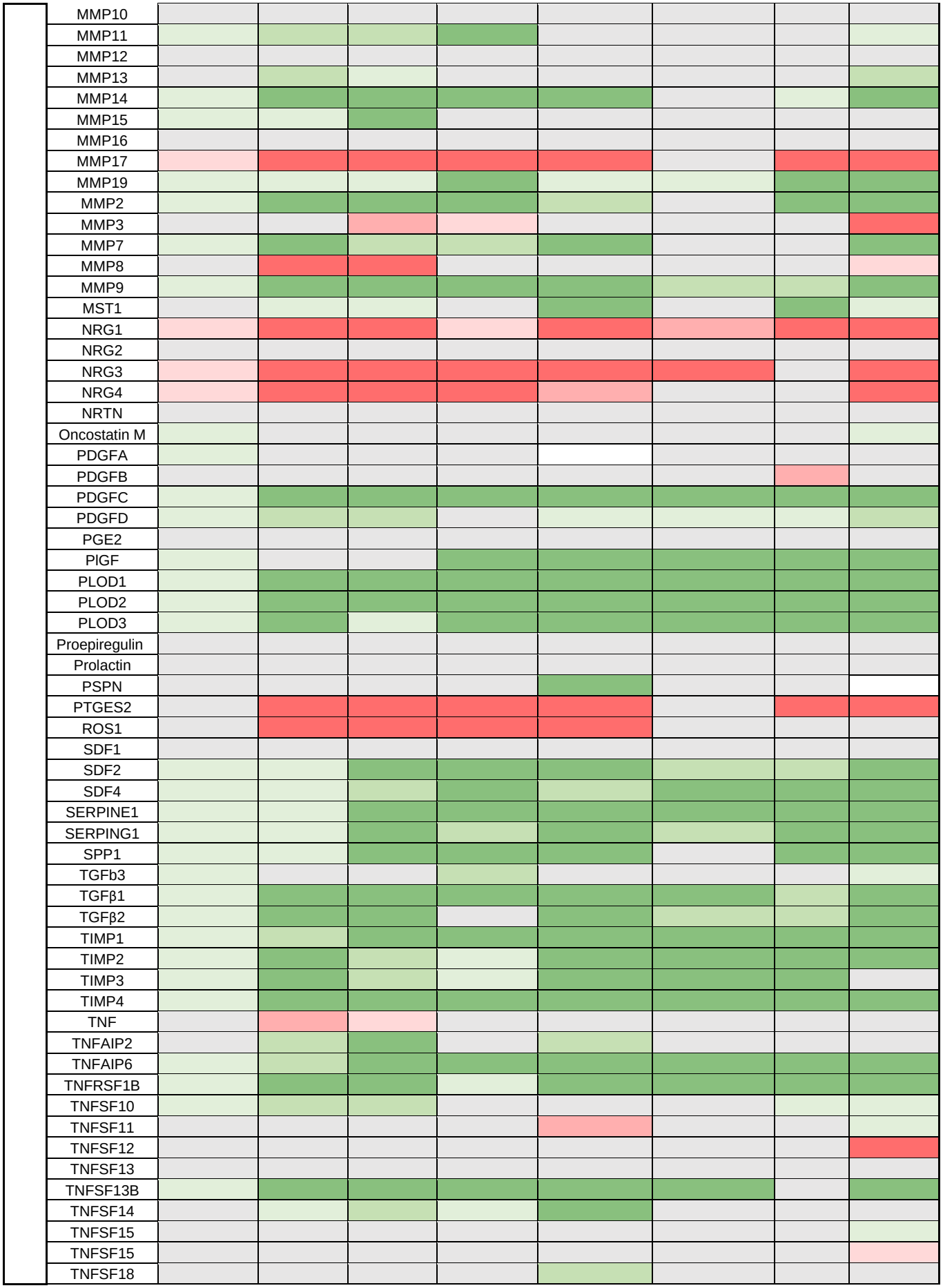
MMP10
MMP11
MMP12
MMP13
MMP14
MMP15
MMP16
MMP17
MMP19
MMP2
MMP3
MMP7
MMP8
MMP9
MST1
NRG1
NRG2
NRG3
NRG4
NRTN
Oncostatin M
PDGFA
PDGFB
PDGFC
PDGFD
PGE2
PlGF
PLOD1
PLOD2
PLOD3
Proepiregulin
Prolactin
PSPN
PTGES2
ROS1
SDF1
SDF2
SDF4
SERPINE1
SERPING1
SPP1
TGFb3
TGFβ1
TGFβ2
TIMP1
TIMP2
TIMP3
TIMP4
TNF
TNFAIP2
TNFAIP6
TNFRSF1B
TNFSF10
TNFSF11
TNFSF12
TNFSF13
TNFSF13B
TNFSF14
TNFSF15
TNFSF15
TNFSF18

	TNFSF2								
	TNFSF4								
	TNFSF8								
	TNFSF9								
	VEGFA								
	VEGFB								
	VEGFC								
	VEGFD								
Pateint samples number used in respective study									
TUMOR		163	154	155	156	225	117	528	489
N0N-TUMOR		207	5	5	4	28	8	10	10
Upregulated in GBM					**p<0.001**		**p<0.01**		**p<0.05**
Downregulated in GBM					**p<0.001**		**p<0.01**		**p<0.05**
Not significant									

Annexure 6: Description Of 44 Biomarkers Dysregulated in Glioblastoma Multiforme

Description of Genes	
Chemokines	
CCL5	C-C motif chemokine 5
CX3CL1	Fractalkine
CXCL16	C-X-C motif chemokine 16
Cytokines and Growth factors	
ANGPT2	Angiopoietin-2
BMP1	Bone morphogenetic protein 1
BMP7	Bone morphogenetic protein 7
COL1A1	Collagen alpha-1(I) chain
COL1A2	Collagen alpha-2(I) chain
COL3A1	Collagen alpha-1(III) chain
COL4A1	Collagen alpha-1(IV) chain
COL4A2	Collagen alpha-2(IV) chain
COL5A1	Collagen alpha-1(V) chain
COL5A2	Collagen alpha-2(V) chain
CTSB	Cathepsin B
HIF1A	Hypoxia-inducible factor 1-alpha
IL-18	Interleukin-18
LAMA4	Laminin subunit alpha-4
LAMA5	Laminin subunit alpha-5
LAMB1	Laminin subunit Beta-6
LGALS3	Galectin-3
LGALS9	Galectin-9
LOX	Protein-lysine 6-oxidase
LOXL1	Lysyl oxidase homolog 1
LOXL3	Lysyl oxidase homolog 3
MMP14	Matrix metalloproteinase-17
MMP17	Matrix metalloproteinase-15
MMP2	Matrix metalloproteinase-2
MMP9	Matrix metalloproteinase-9
PLOD1	Procollagen-lysine,2-oxoglutarate 5-dioxygenase 1
PLOD2	Procollagen-lysine,2-oxoglutarate 5-dioxygenase 2
PLOD3	Multifunctional procollagen lysine hydroxylase and glycosyltransferase LH3
PTGES2	Prostaglandin E synthase 2
SDF2	Stromal cell-derived factor 2
SDF4	45 kDa calcium-binding protein
SERPINE1	Plasminogen activator inhibitor 1
SERPING1	Plasma protease C1 inhibitor
SPP1	Osteopontin
TGFβ1	Transforming growth factor beta-1 proprotein
TGFβ2	Transforming growth factor beta-2 proprotein
TIMP1	Metalloproteinase inhibitor 1
TIMP3	Metalloproteinase inhibitor 3
TNFAIP6	Tumor necrosis factor-inducible gene 6 protein
TNFRSF1B	Tumor necrosis factor receptor superfamily member 1B
VEGFA	Vascular endothelial growth factor A

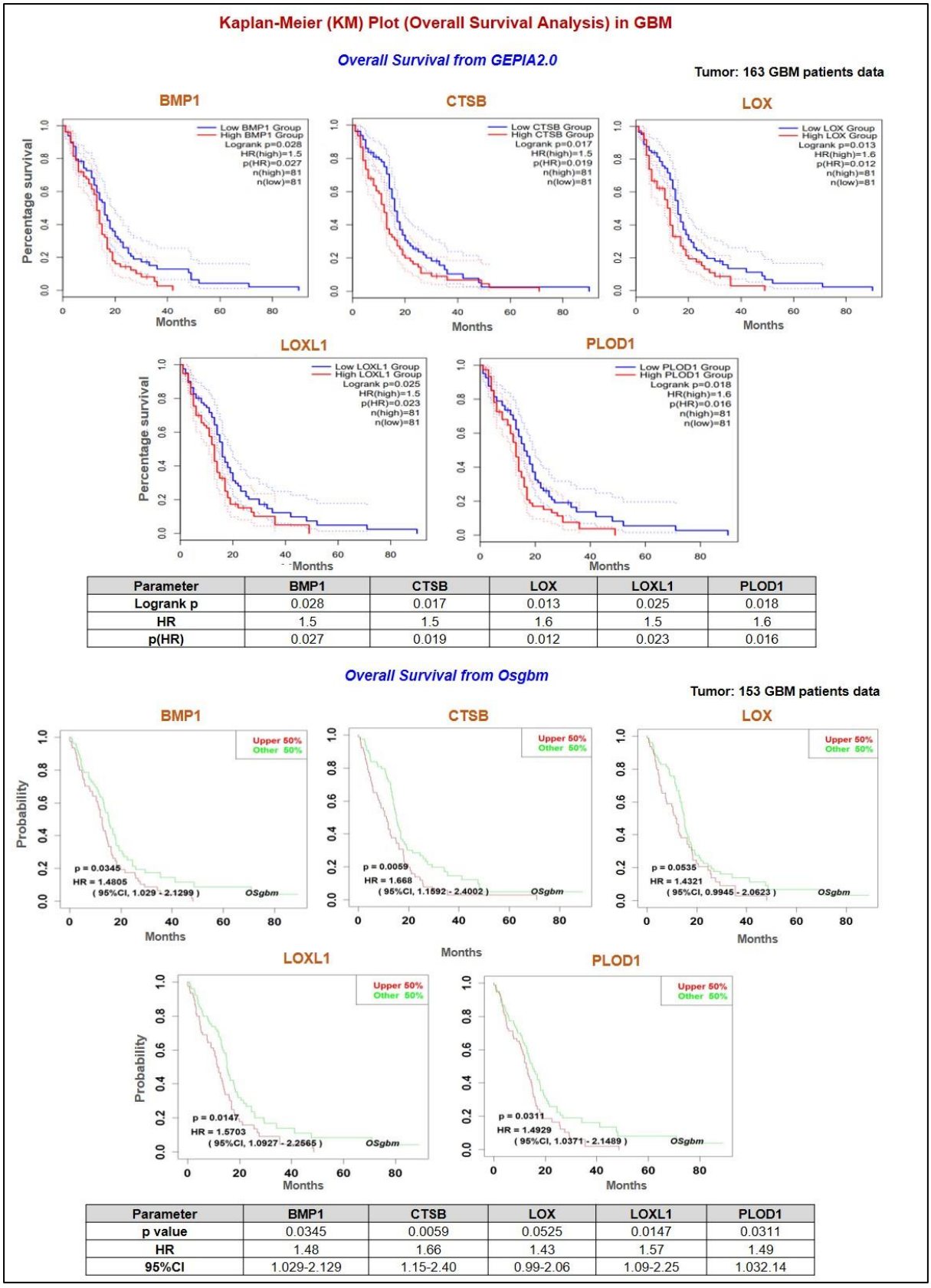

Parameter	BMP1	CTSB	LOX	LOXL1	PLOD1
Logrank p	0.028	0.017	0.013	0.025	0.018
HR	1.5	1.5	1.6	1.5	1.6
p(HR)	0.027	0.019	0.012	0.023	0.016

Parameter	BMP1	CTSB	LOX	LOXL1	PLOD1
p value	0.0345	0.0059	0.0525	0.0147	0.0311
HR	1.48	1.66	1.43	1.57	1.49
95%CI	1.029-2.129	1.15-2.40	0.99-2.06	1.09-2.25	1.032.14

Annexure 7: Kaplan-Meier (KM) Plot for Overall Survival (OS) In GBM Patient Samples from TCGA Datasets: OS time plotted through GEPIA2.0 and OSgbm between higher-expression-level and lower-expression-level tumors in GBM TCGA tumor types with shorter overall survival time and worse OS prognosis. Red line shows the cases with highly expressed biomarker and blue/green line is indicated for the cases with lowly expressed biomarker. HR: hazard ratio; p-value≤0.05.

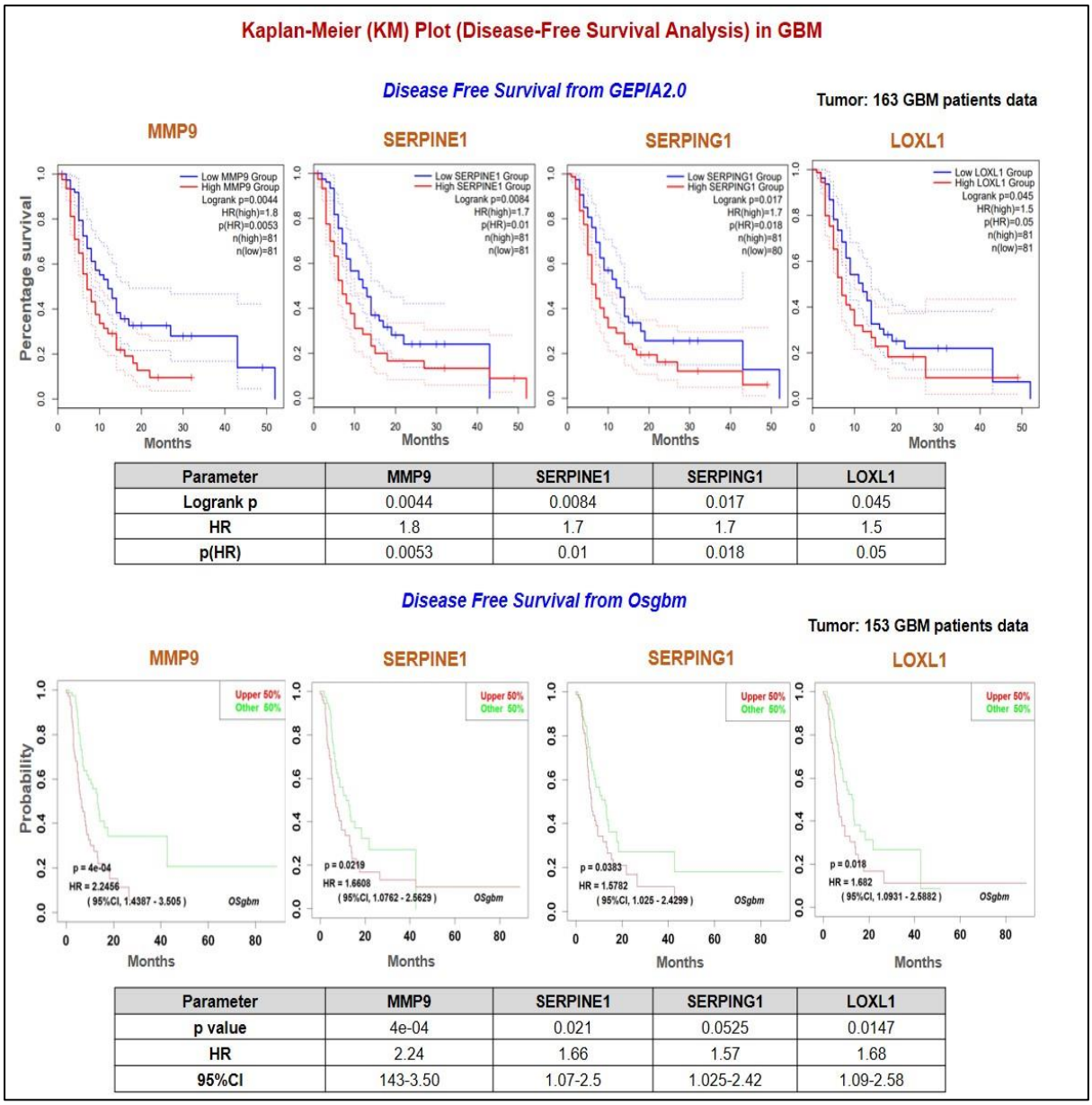

Parameter	MMP9	SERPINE1	SERPING1	LOXL1
Logrank p	0.0044	0.0084	0.017	0.045
HR	1.8	1.7	1.7	1.5
p(HR)	0.0053	0.01	0.018	0.05

Parameter	MMP9	SERPINE1	SERPING1	LOXL1
p value	4e-04	0.021	0.0525	0.0147
HR	2.24	1.66	1.57	1.68
95%CI	143-3.50	1.07-2.5	1.025-2.42	1.09-2.58

Annexure 8: Kaplan-Meier (KM) Plot for Disease Free Survival (DFS) In GBM Patient Samples from TCGA Datasets. (A) DFS time plotted through GEPIA2.0 and OSgbm between higher-expression-level and lower-expression-level tumor in the TCGA tumor types with worse prognosis. Red line shows the cases with highly expressed biomarker and blue/green line is indicated for the cases with lowly expressed biomarker. HR: hazard ratio, p-value<0.05.

REFERENCES

[1] F. Hanif, K. Muzaffar, K. Perveen, S. M. Malhi, and S. U. Simjee, "Glioblastoma Multiforme: A Review of its Epidemiology and Pathogenesis through Clinical Presentation and Treatment," *Asian Pac. J. Cancer Prev.*, vol. 18, no. 1, p. 3, 2017, doi: 10.22034/APJCP.2017.18.1.3.

[2] S. L. Perrin *et al.*, "Glioblastoma heterogeneity and the tumour microenvironment: implications for preclinical research and development of new treatments," *Biochem. Soc. Trans.*, vol. 47, no. 2, pp. 625–638, Apr. 2019, doi: 10.1042/BST20180444.

[3] V. K. Puduvalli, "Neuro-Oncology Advances emerging concepts," vol. 5, no. February, pp. 1–16, 2023.

[4] M. Khabibov *et al.*, "Signaling pathways and therapeutic approaches in glioblastoma multiforme (Review)," *Int. J. Oncol.*, vol. 60, no. 6, pp. 1–18, Jun. 2022, doi: 10.3892/IJO.2022.5359/HTML.

[5] E. N. Mathew, B. C. Berry, H. W. Yang, R. S. Carroll, and M. D. Johnson, "Delivering Therapeutics to Glioblastoma: Overcoming Biological Constraints," *Int. J. Mol. Sci.*, vol. 23, no. 3, Feb. 2022, doi: 10.3390/IJMS23031711.

[6] C. Fernandes *et al.*, "Current Standards of Care in Glioblastoma Therapy," *Glioblastoma*, pp. 197–241, Sep. 2017, doi: 10.15586/CODON.GLIOBLASTOMA.2017.CH11.

[7] E. L. Lozada-Delgado, N. Grafals-Ruiz, and P. E. Vivas-Mejía, "RNA interference for glioblastoma therapy: Innovation ladder from the bench to clinical trials," *Life Sci.*, vol. 188, pp. 26–36, Nov. 2017, doi: 10.1016/J.LFS.2017.08.027.

[8] S. W. Cramer and C. C. Chen, "Photodynamic Therapy for the Treatment of Glioblastoma," *Front. Surg.*, vol. 6, no. January, pp. 1–11, 2020, doi: 10.3389/fsurg.2019.00081.

[9] L. Wu *et al.*, "Delivery of therapeutic oligonucleotides in nanoscale," *Bioact. Mater.*, vol. 7, pp. 292–323, Jan. 2022, doi: 10.1016/J.BIOACTMAT.2021.05.038.

[10] L. Chen, W. Hong, W. Ren, T. Xu, Z. Qian, and Z. He, "Recent progress in targeted delivery vectors based on biomimetic nanoparticles," *Signal Transduct. Target. Ther. 2021 61*, vol. 6, no. 1, pp. 1–25, Jun. 2021, doi: 10.1038/s41392-021-00631-2.

[11] K. D. Miller *et al.*, "Brain and other central nervous system tumor statistics, 2021," *CA. Cancer J. Clin.*, vol. 71, no. 5, pp. 381–406, Sep. 2021, doi: 10.3322/CAAC.21693.

[12] N. A. Charles, E. C. Holland, R. Gilbertson, R. Glass, and H. Kettenmann, "The brain

tumor microenvironment," *Glia*, vol. 60, no. 3, pp. 502–514, 2012, doi: 10.1002/glia.21264.

[13] M. Portela *et al.*, "Glioblastoma cells vampirize WNT from neurons and trigger a JNK/MMP signaling loop that enhances glioblastoma progression and neurodegeneration," *PLOS Biol.*, vol. 17, no. 12, p. e3000545, 2019, doi: 10.1371/JOURNAL.PBIO.3000545.

[14] D. Boso *et al.*, "HIF-1α/Wnt signaling-dependent control of gene transcription regulates neuronal differentiation of glioblastoma stem cells," *Theranostics*, vol. 9, no. 17, p. 4860, 2019, doi: 10.7150/THNO.35882.

[15] J. H. Park and H. K. Lee, "Current Understanding of Hypoxia in Glioblastoma Multiforme and Its Response to Immunotherapy," *Cancers (Basel).*, vol. 14, no. 5, 2022, doi: 10.3390/cancers14051176.

[16] H. Patel, P. Nilendu, D. Jahagirdar, J. K. Pal, and N. K. Sharma, "Modulating secreted components of tumor microenvironment: A masterstroke in tumor therapeutics," *Cancer Biol. Ther.*, vol. 19, no. 1, pp. 3–12, Jan. 2018, doi: 10.1080/15384047.2017.1394538.

[17] R. Baghban *et al.*, "Tumor microenvironment complexity and therapeutic implications at a glance," *Cell Commun. Signal. 2020 181*, vol. 18, no. 1, pp. 1–19, Apr. 2020, doi: 10.1186/S12964-020-0530-4.

[18] C. Liu, D. Chu, K. Kalantar-Zadeh, J. George, H. A. Young, and G. Liu, "Cytokines: From Clinical Significance to Quantification," *Adv. Sci.*, vol. 8, no. 15, p. 2004433, Aug. 2021, doi: 10.1002/ADVS.202004433.

[19] J. A. Bridge, J. C. Lee, A. Daud, J. W. Wells, and J. A. Bluestone, "Cytokines, Chemokines, and Other Biomarkers of Response for Checkpoint Inhibitor Therapy in Skin Cancer," *Front. Med.*, vol. 5, no. DEC, p. 351, 2018, doi: 10.3389/FMED.2018.00351.

[20] V. F. Zhu, J. Yang, D. G. LeBrun, and M. Li, "Understanding the role of cytokines in Glioblastoma Multiforme pathogenesis," *Cancer Lett.*, vol. 316, no. 2, pp. 139–150, Mar. 2012, doi: 10.1016/J.CANLET.2011.11.001.

[21] J. Liu, C. Qian, and X. Cao, "Post-Translational Modification Control of Innate Immunity," *Immunity*, vol. 45, no. 1, pp. 15–30, Jul. 2016, doi: 10.1016/J.IMMUNI.2016.06.020.

[22] V. Vanheule, M. Metzemaekers, R. Janssens, S. Struyf, and P. Proost, "How post-translational modifications influence the biological activity of chemokines," *Cytokine*, vol. 109, pp. 29–51, Sep. 2018, doi: 10.1016/J.CYTO.2018.02.026.

[23] S. Spange, T. Wagner, T. Heinzel, and O. H. Krämer, “Acetylation of non-histone proteins modulates cellular signalling at multiple levels,” *Int. J. Biochem. Cell Biol.*, vol. 41, no. 1, pp. 185–198, Jan. 2009, doi: 10.1016/J.BIOCEL.2008.08.027.

[24] T. Narita, B. T. Weinert, and C. Choudhary, “Functions and mechanisms of non-histone protein acetylation,” *Nature Reviews Molecular Cell Biology*, vol. 20, no. 3. Nature Publishing Group, pp. 156–174, 01-Mar-2019, doi: 10.1038/s41580-018-0081-3.

[25] F. Ullah, N. Khurshid, Q. Fatimi, P. Loidl, and M. Saeed, “Mutations in the acetylation hotspots of Rbl2 are associated with increased risk of breast cancer,” *PLoS One*, vol. 17, no. 4, p. e0266196, Apr. 2022, doi: 10.1371/JOURNAL.PONE.0266196.

[26] E. Klein, A. C. Hau, A. Oudin, A. Golebiewska, and S. P. Niclou, “Glioblastoma Organoids: Pre-Clinical Applications and Challenges in the Context of Immunotherapy,” *Front. Oncol.*, vol. 10, no. December, pp. 1–18, 2020, doi: 10.3389/fonc.2020.604121.

[27] M. Yin *et al.*, “Ultrasmall zirconium carbide nanodots for synergistic photothermal-radiotherapy of glioma,” *Nanoscale*, vol. 14, no. 40, pp. 14935–14949, Oct. 2022, doi: 10.1039/D2NR04239H.

[28] J. Herta *et al.*, “Optimizing maximum resection of glioblastoma: Raman spectroscopy versus 5-aminolevulinic acid,” *J. Neurosurg.*, vol. 1, no. aop, pp. 1–10, Dec. 2022, doi: 10.3171/2022.11.JNS22693.

[29] H. Z. Xu *et al.*, “Targeted photodynamic therapy of glioblastoma mediated by platelets with photo-controlled release property,” *Biomaterials*, vol. 290, p. 121833, Nov. 2022, doi: 10.1016/J.BIOMATERIALS.2022.121833.

[30] S. K. Tan, A. Jermakowicz, A. K. Mookhtiar, C. B. Nemeroff, S. C. Schürer, and N. G. Ayad, “Drug Repositioning in Glioblastoma: A Pathway Perspective,” *Front. Pharmacol.*, vol. 9, no. MAR, p. 218, Mar. 2018, doi: 10.3389/FPHAR.2018.00218.

[31] D. Hanahan and R. A. Weinberg, “The hallmarks of cancer.,” *Cell*, vol. 100, no. 1, pp. 57–70, Jan. 2000, doi: 10.1016/s0092-8674(00)81683-9.

[32] World Health Organisation, “Cancer.” .

[33] J. Korbecki, K. Kojder, S. Grochans, A. M. Cybulska, and D. Simi, “Epidemiology of Glioblastoma Multiforme – Literature Review,” 2022.

[34] Y. Cheng *et al.*, “Targeting epigenetic regulators for cancer therapy: Mechanisms and advances in clinical trials,” *Signal Transduct. Target. Ther.*, vol. 4, no. 1, 2019, doi: 10.1038/s41392-019-0095-0.

[35] Y. Totsuka, M. Watanabe, and Y. Lin, “New horizons of DNA adductome for exploring

environmental causes of cancer," *Cancer Science*, vol. 112, no. 1. Blackwell Publishing Ltd, pp. 7–15, Jan-2021, doi: 10.1111/cas.14666.

[36] V. Arlt, M. Stiborova, C. Henderson, M. O.-C. Research, and undefined 2005, "Environmental pollutant and potent mutagen 3-nitrobenzanthrone forms DNA adducts after reduction by NAD (P) H: quinone oxidoreductase and conjugation by," *AACR*, 2005.

[37] M. Grover, T. Behl, T. V.-C. & Biodiversity, and undefined 2021, "Phytochemical Screening, Antioxidant Assay and Cytotoxic Profile for Different Extracts of Chrysopogon zizanioides Roots," *Wiley Online Libr.*, vol. 18, no. 8, Aug. 2021, doi: 10.1002/cbdv.202100012.

[38] M. M.-E. health and preventive and undefined 2018, "Inflammation and cancer," *environhealthprevmed …*.

[39] R. Sandhir, A. Halder, and A. Sunkaria, "Mitochondria as a centrally positioned hub in the innate immune response," *Biochimica et Biophysica Acta - Molecular Basis of Disease*. 2017, doi: 10.1016/j.bbadis.2016.10.020.

[40] A. Fadriquela, S. Sharma, T. T. Thi, R. Akter, and S. Goh, "Redox Effects of Molecular Hydrogen and Its Therapeutic Efficacy in the Treatment of Neurodegenerative Diseases. Processes 2021, 9, 308," *mdpi.com*, 2021, doi: 10.3390/pr9020308.

[41] N. Chatterjee and G. C. Walker, "Mechanisms of DNA damage, repair, and mutagenesis," *Environmental and Molecular Mutagenesis*, vol. 58, no. 5. John Wiley and Sons Inc., pp. 235–263, Jun-2017, doi: 10.1002/em.22087.

[42] A. R. Kaplan and P. M. Glazer, "Impact of hypoxia on DNA repair and genome integrity," *Mutagenesis*, vol. 35, no. 1, pp. 61–68, Feb. 2020, doi: 10.1093/mutage/gez019.

[43] J. C. Jun, A. Rathore, H. Younas, D. Gilkes, and V. Y. Polotsky, "Hypoxia-Inducible Factors and Cancer," *Current Sleep Medicine Reports*. 2017, doi: 10.1007/s40675-017-0062-7.

[44] T. Bin Emran *et al.*, "Multidrug Resistance in Cancer: Understanding Molecular Mechanisms, Immunoprevention and Therapeutic Approaches," *Front. Oncol.*, vol. 12, no. June, pp. 1–38, 2022, doi: 10.3389/fonc.2022.891652.

[45] J. Q. Li, X. Wu, L. Gan, X. L. Yang, and Z. H. Miao, "Hypoxia induces universal but differential drug resistance and impairs anticancer mechanisms of 5-fluorouracil in hepatoma cells," *Acta Pharmacol. Sin.*, vol. 38, no. 12, pp. 1642–1654, 2017, doi: 10.1038/aps.2017.79.

[46] B. Mansoori, A. Mohammadi, S. Davudian, S. Shirjang, and B. Baradaran, “The different mechanisms of cancer drug resistance: A brief review,” *Adv. Pharm. Bull.*, vol. 7, no. 3, pp. 339–348, 2017, doi: 10.15171/apb.2017.041.

[47] F. Balkwill and A. Mantovani, “Inflammation and cancer: Back to Virchow?,” *Lancet*. 2001, doi: 10.1016/S0140-6736(00)04046-0.

[48] D. Hanahan and R. A. Weinberg, “Hallmarks of cancer: The next generation,” *Cell*. 2011, doi: 10.1016/j.cell.2011.02.013.

[49] Y. Yuan, Y. C. Jiang, C. K. Sun, and Q. M. Chen, “Role of the tumor microenvironment in tumor progression and the clinical applications (Review),” *Oncology Reports*. 2016, doi: 10.3892/or.2016.4660.

[50] T. L. Whiteside, “The tumor microenvironment and its role in promoting tumor growth,” *Oncogene*. 2008, doi: 10.1038/onc.2008.271.

[51] Y. D. Jung *et al.*, “Role of the tumor microenvironment in mediating response to anti-angiogenic therapy,” *Cancer and Metastasis Reviews*. 2000, doi: 10.1023/A:1026510130114.

[52] G. Landskron, M. De La Fuente, P. Thuwajit, C. Thuwajit, and M. A. Hermoso, “Chronic inflammation and cytokines in the tumor microenvironment,” *Journal of Immunology Research*. 2014, doi: 10.1155/2014/149185.

[53] L. Q. Fu, W. L. Du, M. H. Cai, J. Y. Yao, Y. Y. Zhao, and X. Z. Mou, “The roles of tumor-associated macrophages in tumor angiogenesis and metastasis,” *Cellular Immunology*. 2020, doi: 10.1016/j.cellimm.2020.104119.

[54] D. Ribatti, A. Vacca, B. Nico, E. Crivellato, L. Roncali, and F. Dammacco, “The role of mast cells in tumour angiogenesis,” *British Journal of Haematology*. 2001, doi: 10.1046/j.1365-2141.2001.03202.x.

[55] C. Murdoch, M. Muthana, S. B. Coffelt, and C. E. Lewis, “The role of myeloid cells in the promotion of tumour angiogenesis,” *Nature Reviews Cancer*. 2008, doi: 10.1038/nrc2444.

[56] F. Gizem Sonugür and H. Akbulut, “The role of tumor microenvironment in genomic instability of malignant tumors,” *Front. Genet.*, 2019, doi: 10.3389/fgene.2019.01063.

[57] S. Negrini, V. G. Gorgoulis, and T. D. Halazonetis, “Genomic instability an evolving hallmark of cancer,” *Nature Reviews Molecular Cell Biology*. 2010, doi: 10.1038/nrm2858.

[58] R. S. Bindra and P. M. Glazer, “Genetic instability and the tumor microenvironment: Towards the concept of microenvironment-induced mutagenesis,” *Mutation Research* -

Fundamental and Molecular Mechanisms of Mutagenesis. 2005, doi: 10.1016/j.mrfmmm.2004.03.013.

[59] A. Palumbo, N. de Oliveira Meireles Da Costa, M. H. Bonamino, L. F. Ribeiro Pinto, and L. E. Nasciutti, "Genetic instability in the tumor microenvironment: A new look at an old neighbor," *Molecular Cancer*. 2015, doi: 10.1186/s12943-015-0409-y.

[60] L. R. Ferguson *et al.*, "Genomic instability in human cancer: Molecular insights and opportunities for therapeutic attack and prevention through diet and nutrition," *Seminars in Cancer Biology*. 2015, doi: 10.1016/j.semcancer.2015.03.005.

[61] D. C. Radisky *et al.*, "Rac1b and reactive oxygen species mediate MMP-3-induced EMT and genomic instability," *Nature*, 2005, doi: 10.1038/nature03688.

[62] S. Elmore, "Apoptosis: A Review of Programmed Cell Death," *Toxicologic Pathology*. 2007, doi: 10.1080/01926230701320337.

[63] J. M. Brown and L. D. Attardi, "The role of apoptosis in cancer development and treatment response," *Nat. Rev. Cancer*, 2005, doi: 10.1038/nrc1560.

[64] S. Grasso *et al.*, "Cell Death and Cancer, Novel Therapeutic Strategies," in *Apoptosis and Medicine*, 2012.

[65] M. W. Pickup, J. K. Mouw, and V. M. Weaver, "The extracellular matrix modulates the hallmarks of cancer," *EMBO Rep.*, 2014, doi: 10.15252/embr.201439246.

[66] G. J. Wise, V. K. Marella, G. Talluri, and D. Shirazian, "Cytokine variations in patients with hormone treated prostate cancer," *J. Urol.*, 2000, doi: 10.1016/s0022-5347(05)67289-8.

[67] S. O. Lee, W. Lou, M. Hou, S. A. Onate, and A. C. Gao, "Interleukin-4 enhances prostate-specific antigen expression by activation of the androgen receptor and Akt pathway," *Oncogene*, 2003, doi: 10.1038/sj.onc.1206735.

[68] T. D. K. Chung, J. J. Yu, T. A. Kong, M. T. Spiotto, and J. M. Lin, "Interleukin-6 activates phosphatidylinositol-3 kinase, which inhibits apoptosis in human prostate cancer cell lines," *Prostate*, 2000, doi: 10.1002/(SICI)1097-0045(20000101)42:1<1::AID-PROS1>3.0.CO;2-Y.

[69] C. Wilson, T. Wilson, P. G. Johnston, D. B. Longley, and D. J. J. Waugh, "Interleukin-8 signaling attenuates TRAIL- and chemotherapy-induced apoptosis through transcriptional regulation of c-FLIP in prostate cancer cells," *Mol. Cancer Ther.*, 2008, doi: 10.1158/1535-7163.MCT-08-0148.

[70] Z. Culig, "Cytokine disbalance in common human cancers," *Biochimica et Biophysica Acta - Molecular Cell Research*. 2011, doi: 10.1016/j.bbamcr.2010.12.010.

[71] K. J. Weigel *et al.*, "CAF-secreted IGFBPs regulate breast cancer cell anoikis," *Mol. Cancer Res.*, 2014, doi: 10.1158/1541-7786.MCR-14-0090.

[72] J. R. Cantor and D. M. Sabatini, "Cancer cell metabolism: One hallmark, many faces," *Cancer Discovery*. 2012, doi: 10.1158/2159-8290.CD-12-0345.

[73] O. Warburg, F. Wind, and E. Negelein, "The metabolism of tumors in the body," *J. Gen. Physiol.*, 1927, doi: 10.1085/jgp.8.6.519.

[74] P. Vaupel, "Metabolic microenvironment of tumor cells: A key factor in malignant progression," *Experimental Oncology*. 2010.

[75] T. Wang, G. Liu, and R. Wang, "The intercellular metabolic interplay between tumor and immune cells," *Frontiers in Immunology*, vol. 5, no. JUL. Frontiers Research Foundation, 2014, doi: 10.3389/fimmu.2014.00358.

[76] C. A. Lyssiotis and A. C. Kimmelman, "Metabolic Interactions in the Tumor Microenvironment," *Trends in Cell Biology*. 2017, doi: 10.1016/j.tcb.2017.06.003.

[77] M. G. Vander Heiden and R. J. DeBerardinis, "Understanding the Intersections between Metabolism and Cancer Biology," *Cell*. 2017, doi: 10.1016/j.cell.2016.12.039.

[78] C. Zhang, L. M. Moore, X. Li, W. K. A. Yung, and W. Zhang, "IDH1/2 mutations target a key hallmark of cancer by deregulating cellular metabolism in glioma," *Neuro-Oncology*. 2013, doi: 10.1093/neuonc/not087.

[79] B. Ghesquière, B. W. Wong, A. Kuchnio, and P. Carmeliet, "Metabolism of stromal and immune cells in health and disease," *Nature*. 2014, doi: 10.1038/nature13312.

[80] G. L. Semenza, "HIF-1 mediates metabolic responses to intratumoral hypoxia and oncogenic mutations," *Journal of Clinical Investigation*. 2013, doi: 10.1172/JCI67230.

[81] A. Ohta, "A metabolic immune checkpoint: Adenosine in Tumor Microenvironment," *Frontiers in Immunology*. 2016, doi: 10.3389/fimmu.2016.00109.

[82] R. Nahta *et al.*, "Mechanisms of environmental chemicals that enable the cancer hallmark of evasion of growth suppression," *Carcinogenesis*. 2015, doi: 10.1093/carcin/bgv028.

[83] L. Yang and M. Karin, "Roles of tumor suppressors in regulating tumor-associated inflammation," *Cell Death and Differentiation*. 2014, doi: 10.1038/cdd.2014.131.

[84] X. Li, S. He, and B. Ma, "Autophagy and autophagy-related proteins in cancer," *Molecular Cancer*. 2020, doi: 10.1186/s12943-020-1138-4.

[85] E. White, "the role for autophagy in cancer (White, 2015).pdf," *J. Clin. Invest.*, 2015.

[86] R. Mathew, V. Karantza-Wadsworth, and E. White, "Role of autophagy in cancer," *Nature Reviews Cancer*. 2007, doi: 10.1038/nrc2254.

[87] D. S. Vinay *et al.*, "Immune evasion in cancer: Mechanistic basis and therapeutic strategies," *Seminars in Cancer Biology*. 2015, doi: 10.1016/j.semcancer.2015.03.004.

[88] N. B. Hao, M. H. Lü, Y. H. Fan, Y. L. Cao, Z. R. Zhang, and S. M. Yang, "Macrophages in tumor microenvironments and the progression of tumors," *Clinical and Developmental Immunology*. 2012, doi: 10.1155/2012/948098.

[89] R. S. Herbst *et al.*, "Predictive correlates of response to the anti-PD-L1 antibody MPDL3280A in cancer patients," *Nature*, 2014, doi: 10.1038/nature14011.

[90] V. R. Juneja *et al.*, "PD-L1 on tumor cells is sufficient for immune evasion in immunogenic tumors and inhibits CD8 T cell cytotoxicity," *J. Exp. Med.*, 2017, doi: 10.1084/jem.20160801.

[91] C. Tkaczyk, I. Villa, R. Peroneta, … B. D.-J. of allergy and, and undefined 2000, "In vitro and in vivo immunostimulatory potential of bone marrow–derived mast cells on B- and T-lymphocyte activation," *Elsevier*.

[92] P. Yu, D. A. Rowley, Y. X. Fu, and H. Schreiber, "The role of stroma in immune recognition and destruction of well-established solid tumors," *Current Opinion in Immunology*. 2006, doi: 10.1016/j.coi.2006.01.004.

[93] L. Hayflick and P. S. Moorhead, "The serial cultivation of human diploid cell strains," *Exp. Cell Res.*, 1961, doi: 10.1016/0014-4827(61)90192-6.

[94] A. M. Battram, M. Bachiller, and B. Martín-Antonio, "Senescence in the development and response to cancer with immunotherapy: A double-edged sword," *International Journal of Molecular Sciences*. 2020, doi: 10.3390/ijms21124346.

[95] M. K. Ruhland *et al.*, "Stromal senescence establishes an immunosuppressive microenvironment that drives tumorigenesis," *Nat. Commun.*, 2016, doi: 10.1038/ncomms11762.

[96] E. Elinav, R. Nowarski, C. A. Thaiss, B. Hu, C. Jin, and R. A. Flavell, "Inflammation-induced cancer: Crosstalk between tumours, immune cells and microorganisms," *Nature Reviews Cancer*. 2013, doi: 10.1038/nrc3611.

[97] Q. Zhang, B. Zhu, and Y. Li, "Resolution of cancer-promoting inflammation: A new approach for anticancer therapy," *Frontiers in Immunology*. 2017, doi: 10.3389/fimmu.2017.00071.

[98] T. Pálmai-Pallag and C. Z. Bachrati, "Inflammation-induced DNA damage and damage-induced inflammation: A vicious cycle," *Microbes Infect.*, 2014, doi: 10.1016/j.micinf.2014.10.001.

[99] T. Hagemann *et al.*, "'Re-educating' tumor-associated macrophages by targeting NF-

κB," *J. Exp. Med.*, 2008, doi: 10.1084/jem.20080108.

[100] J. Wang, D. Li, H. Cang, and B. Guo, "Crosstalk between cancer and immune cells: Role of tumor-associated macrophages in the tumor microenvironment," *Cancer Medicine*. 2019, doi: 10.1002/cam4.2327.

[101] G. M. Balachander, P. M. Talukdar, M. Debnath, A. Rangarajan, and K. Chatterjee, "Inflammatory Role of Cancer-Associated Fibroblasts in Invasive Breast Tumors Revealed Using a Fibrous Polymer Scaffold," *ACS Appl. Mater. Interfaces*, 2018, doi: 10.1021/acsami.8b07609.

[102] T. Y. Na, L. Schecterson, A. M. Mendonsa, and B. M. Gumbiner, "The functional activity of E-cadherin controls tumor cell metastasis at multiple steps," *Proc. Natl. Acad. Sci. U. S. A.*, 2020, doi: 10.1073/pnas.1918167117.

[103] W. G. Jiang *et al.*, "Tissue invasion and metastasis: Molecular, biological and clinical perspectives," *Seminars in Cancer Biology*. 2015, doi: 10.1016/j.semcancer.2015.03.008.

[104] D. R. Bielenberg and B. R. Zetter, "The Contribution of Angiogenesis to the Process of Metastasis," *Cancer Journal (United States)*. 2015, doi: 10.1097/PPO.0000000000000138.

[105] D. Spano, C. Heck, P. De Antonellis, G. Christofori, and M. Zollo, "Molecular networks that regulate cancer metastasis," *Seminars in Cancer Biology*. 2012, doi: 10.1016/j.semcancer.2012.03.006.

[106] D. F. Quail and J. A. Joyce, "Microenvironmental regulation of tumor progression and metastasis," *Nature Medicine*. 2013, doi: 10.1038/nm.3394.

[107] H. Gonzalez, C. Hagerling, and Z. Werb, "Roles of the immune system in cancer: From tumor initiation to metastatic progression," *Genes and Development*. 2018, doi: 10.1101/GAD.314617.118.

[108] S. Paget, "THE DISTRIBUTION OF SECONDARY GROWTHS IN CANCER OF THE BREAST.," *Lancet*, 1889, doi: 10.1016/S0140-6736(00)49915-0.

[109] A. Carrano, J. J. Juarez, D. Incontri, A. Ibarra, and H. G. Cazares, "Sex-specific differences in glioblastoma," *Cells*, vol. 10, no. 7, pp. 1–22, 2021, doi: 10.3390/cells10071783.

[110] H. Sung *et al.*, "Global Cancer Statistics 2020: GLOBOCAN Estimates of Incidence and Mortality Worldwide for 36 Cancers in 185 Countries," *CA. Cancer J. Clin.*, vol. 71, no. 3, pp. 209–249, 2021, doi: 10.3322/caac.21660.

[111] A. Ardizzone *et al.*, "Role of Fibroblast Growth Factors Receptors (FGFRs) in Brain

Tumors, Focus on Astrocytoma and Glioblastoma," *Cancers (Basel).*, vol. 12, no. 12, pp. 1–22, Dec. 2020, doi: 10.3390/CANCERS12123825.

[112] S. H. Torp, O. Solheim, and A. J. Skjulsvik, "The WHO 2021 Classification of Central Nervous System tumours: a practical update on what neurosurgeons need to know—a minireview," *Acta Neurochir. (Wien).*, vol. 164, no. 9, pp. 2453–2464, 2022, doi: 10.1007/s00701-022-05301-y.

[113] P. C. Huszthy *et al.*, "Pitfalls and Perspectives," *Neuro. Oncol.*, vol. 14, no. 8, pp. 979–993, 2012.

[114] D. Hambardzumyan and G. Bergers, "Glioblastoma: Defining Tumor Niches," *Trends in Cancer*, vol. 1, no. 4, pp. 252–265, 2015, doi: 10.1016/j.trecan.2015.10.009.

[115] J. N. Cantrell *et al.*, "Progress Toward Long-Term Survivors of Glioblastoma," *Mayo Clin. Proc.*, vol. 94, no. 7, pp. 1278–1286, Jul. 2019, doi: 10.1016/J.MAYOCP.2018.11.031.

[116] S. S. Stylli, "Novel Treatment Strategies for Glioblastoma," *Cancers (Basel).*, vol. 12, no. 10, pp. 1–11, Oct. 2020, doi: 10.3390/CANCERS12102883.

[117] S. DeCordova *et al.*, "Molecular Heterogeneity and Immunosuppressive Microenvironment in Glioblastoma," *Front. Immunol.*, vol. 11, p. 1402, Jul. 2020, doi: 10.3389/FIMMU.2020.01402/BIBTEX.

[118] R. C. Abbott *et al.*, "Novel high-affinity EGFRvIII-specific chimeric antigen receptor T cells effectively eliminate human glioblastoma," *Clin. Transl. Immunol.*, vol. 10, no. 5, p. e1283, Jan. 2021, doi: 10.1002/CTI2.1283.

[119] R. Mroue and M. J. Bissell, "Three-dimensional cultures of mouse mammary epithelial cells," *Methods Mol. Biol.*, 2013, doi: 10.1007/978-1-62703-125-7_14.

[120] F. Chen *et al.*, "New horizons in tumor microenvironment biology: Challenges and opportunities," *BMC Med.*, vol. 13, no. 1, 2015, doi: 10.1186/s12916-015-0278-7.

[121] I. J. Fidler, "The organ microenvironment and cancer metastasis," *Differentiation*. 2002, doi: 10.1046/j.1432-0436.2002.700904.x.

[122] F. R. Balkwill, M. Capasso, and T. Hagemann, "The tumor microenvironment at a glance," *J. Cell Sci.*, vol. 125, no. 23, pp. 5591–5596, 2012, doi: 10.1242/jcs.116392.

[123] J. Zhu, L. Liang, Y. Jiao, and L. Liu, "Enhanced invasion of metastatic cancer cells via extracellular matrix interface," *PLoS One*, 2015, doi: 10.1371/journal.pone.0118058.

[124] J. Condeelis and J. W. Pollard, "Macrophages: Obligate partners for tumor cell migration, invasion, and metastasis," *Cell*. 2006, doi: 10.1016/j.cell.2006.01.007.

[125] Y. Jung *et al.*, "Recruitment of mesenchymal stem cells into prostate tumours promotes

metastasis," *Nat. Commun.*, 2013, doi: 10.1038/ncomms2766.

[126] E. R. Pereira, D. Jones, K. Jung, and T. P. Padera, "The lymph node microenvironment and its role in the progression of metastatic cancer," *Seminars in Cell and Developmental Biology*. 2015, doi: 10.1016/j.semcdb.2015.01.008.

[127] L. Tao, G. Huang, H. Song, Y. Chen, and L. Chen, "Cancer associated fibroblasts: An essential role in the tumor microenvironment (review)," *Oncology Letters*. 2017, doi: 10.3892/ol.2017.6497.

[128] Y. Jo, N. Choi, K. Kim, H. J. Koo, J. Choi, and H. N. Kim, "Chemoresistance of cancer cells: Requirements of tumor microenvironment-mimicking in vitro models in anti-cancer drug development," *Theranostics*, vol. 8, no. 19, pp. 5259–5275, 2018, doi: 10.7150/thno.29098.

[129] R. Bharti, G. Dey, and M. Mandal, "Cancer development, chemoresistance, epithelial to mesenchymal transition and stem cells: A snapshot of IL-6 mediated involvement," *Cancer Letters*. 2016, doi: 10.1016/j.canlet.2016.02.048.

[130] D. Hanahan and J. Folkman, "Patterns and emerging mechanisms of the angiogenic switch during tumorigenesis," *Cell*, vol. 86, no. 3. Cell Press, pp. 353–364, Aug-1996, doi: 10.1016/S0092-8674(00)80108-7.

[131] T. L. Whiteside, "The local tumor microenvironment," in *General Principles of Tumor Immunotherapy: Basic and Clinical Applications of Tumor Immunology*, Springer Netherlands, 2008, pp. 145–167.

[132] S. Tan *et al.*, "Exosomal miRNAs in tumor microenvironment," *Journal of Experimental and Clinical Cancer Research*, vol. 39, no. 1. BioMed Central Ltd., pp. 1–15, Apr-2020, doi: 10.1186/s13046-020-01570-6.

[133] J. F. Hastings, J. N. Skhinas, D. Fey, D. R. Croucher, and T. R. Cox, "The extracellular matrix as a key regulator of intracellular signalling networks," *British Journal of Pharmacology*, vol. 176, no. 1. John Wiley and Sons Inc., pp. 82–92, Jan-2019, doi: 10.1111/bph.14195.

[134] E. Henke, R. Nandigama, and S. Ergün, "Extracellular Matrix in the Tumor Microenvironment and Its Impact on Cancer Therapy," *Front. Mol. Biosci.*, vol. 6, no. January, pp. 1–24, 2020, doi: 10.3389/fmolb.2019.00160.

[135] A. Jabłońska-Trypuć, M. Matejczyk, and S. Rosochacki, "Matrix metalloproteinases (MMPs), the main extracellular matrix (ECM) enzymes in collagen degradation, as a target for anticancer drugs," *Journal of Enzyme Inhibition and Medicinal Chemistry*, vol. 31, no. S1. Taylor and Francis Ltd, pp. 177–183, Nov-2016, doi:

10.3109/14756366.2016.1161620.

[136] N. Nagarsheth, M. S. Wicha, and W. Zou, “Chemokines in the cancer microenvironment and their relevance in cancer immunotherapy,” *Nature Reviews Immunology*, vol. 17, no. 9. Nature Publishing Group, pp. 559–572, Sep-2017, doi: 10.1038/nri.2017.49.

[137] K. S. N. Atretkhany, M. S. Drutskaya, S. A. Nedospasov, S. I. Grivennikov, and D. V. Kuprash, “Chemokines, cytokines and exosomes help tumors to shape inflammatory microenvironment,” *Pharmacology and Therapeutics*, vol. 168. Elsevier Inc., pp. 98–112, Dec-2016, doi: 10.1016/j.pharmthera.2016.09.011.

[138] M. Wang *et al.*, “Role of tumor microenvironment in tumorigenesis,” *J. Cancer*, vol. 8, no. 5, pp. 761–773, 2017, doi: 10.7150/jca.17648.

[139] R. Wei, S. Liu, S. Zhang, L. Min, and S. Zhu, “Cellular and Extracellular Components in Tumor Microenvironment and Their Application in Early Diagnosis of Cancers,” *Anal. Cell. Pathol.*, vol. 2020, no. Figure 1, 2020, doi: 10.1155/2020/6283796.

[140] K. W. Hon, N. S. Ab-Mutalib, N. M. A. Abdullah, R. Jamal, and N. Abu, “Extracellular Vesicle-derived circular RNAs confers chemoresistance in Colorectal cancer,” *Sci. Rep.*, 2019, doi: 10.1038/s41598-019-53063-y.

[141] Y. Yoshioka, Y. Konishi, N. Kosaka, T. Katsuda, T. Kato, and T. Ochiya, “Comparative marker analysis of extracellular vesicles in different human cancer types,” *J. Extracell. Vesicles*, 2013, doi: 10.3402/jev.v2i0.20424.

[142] R. U. Takahashi, M. Prieto-Vila, A. Hironaka, and T. Ochiya, “The role of extracellular vesicle microRNAs in cancer biology,” *Clinical Chemistry and Laboratory Medicine*. 2017, doi: 10.1515/cclm-2016-0708.

[143] C. Tian *et al.*, “Cancer cell–derived matrisome proteins promote metastasis in pancreatic ductal adenocarcinoma,” *Cancer Res.*, 2020, doi: 10.1158/0008-5472.CAN-19-2578.

[144] H. Huang, “Matrix Metalloproteinase-9 (MMP-9) as a Cancer Biomarker and MMP-9 Biosensors: Recent Advances,” *Sensors (Basel).*, vol. 18, no. 10, Oct. 2018, doi: 10.3390/S18103249.

[145] M. Giussani *et al.*, “Extracellular matrix proteins as diagnostic markers of breast carcinoma,” *J. Cell. Physiol.*, 2018, doi: 10.1002/jcp.26513.

[146] Y. Yu, C. H. Xiao, L. D. Tan, Q. S. Wang, X. Q. Li, and Y. M. Feng, “Cancer-associated fibroblasts induce epithelial-mesenchymal transition of breast cancer cells through paracrine TGF-β signalling,” *Br. J. Cancer*, vol. 110, no. 3, pp. 724–732, Feb. 2014, doi: 10.1038/bjc.2013.768.

[147] “Tumor microenvironment: stromal and immune cells | Abcam.” .

[148] M. Skobe *et al.*, “Induction of tumor lymphangiogenesis by VEGF-C promotes breast cancer metastasis,” *Nat. Med.*, vol. 7, no. 2, pp. 192–198, 2001, doi: 10.1038/84643.

[149] F. Spinella *et al.*, “Endothelin-1 stimulates lymphatic endothelial cells and lymphatic vessels to grow and invade,” *Cancer Res.*, vol. 69, no. 6, pp. 2669–2676, Mar. 2009, doi: 10.1158/0008-5472.CAN-08-1879.

[150] K. Kajiya, S. Hirakawa, B. Ma, I. Drinnenberg, and M. Detmar, “Hepatocyte growth factor promotes lymphatic vessel formation and function,” *EMBO J.*, vol. 24, no. 16, pp. 2885–2895, Aug. 2005, doi: 10.1038/sj.emboj.7600763.

[151] T. Duong, P. Koopman, and M. Francois, “Tumor lymphangiogenesis as a potential therapeutic target,” *Journal of Oncology*. 2012, doi: 10.1155/2012/204946.

[152] L. Garnier, A. O. Gkountidi, and S. Hugues, “Tumor-associated lymphatic vessel features and immunomodulatory functions,” *Frontiers in Immunology*, vol. 10, no. APR. Frontiers Media S.A., 2019, doi: 10.3389/fimmu.2019.00720.

[153] R. C. Ji, “Lymph nodes and cancermetastasis: New perspectives on the role of intranodal lymphatic sinuses,” *International Journal of Molecular Sciences*, vol. 18, no. 1. MDPI AG, Jan-2017, doi: 10.3390/ijms18010051.

[154] Y. Shiozawa, “The Roles of Bone Marrow-Resident Cells as a Microenvironment for Bone Metastasis,” in *Advances in Experimental Medicine and Biology*, vol. 1226, Springer, 2020, pp. 57–72.

[155] I. Tirosh *et al.*, “Dissecting the multicellular ecosystem of metastatic melanoma by single-cell RNA-seq,” *Science (80-.).*, 2016, doi: 10.1126/science.aad0501.

[156] C. Anqi *et al.*, “Differentiation and roles of bone marrow-derived cells on the tumor microenvironment of oral squamous cell carcinoma,” *Oncol. Lett.*, vol. 18, no. 6, pp. 6628–6638, Dec. 2019, doi: 10.3892/ol.2019.11045.

[157] H. Yamagishi, T. Oka, I. Hashimoto, N. R. Pellis, and B. D. Kahan, “The role of the spleen in tumor bearing host: II. The influence of splenectomy in mice,” *Jpn. J. Surg.*, vol. 14, no. 1, pp. 72–77, Jan. 1984, doi: 10.1007/BF02469606.

[158] V. Bronte and M. J. Pittet, “The spleen in local and systemic regulation of immunity,” *Immunity*, vol. 39, no. 5. NIH Public Access, pp. 806–818, Nov-2013, doi: 10.1016/j.immuni.2013.10.010.

[159] S. Rose, A. Misharin, and H. Perlman, “A novel Ly6C/Ly6G-based strategy to analyze the mouse splenic myeloid compartment,” *Cytom. Part A*, vol. 81 A, no. 4, pp. 343–350, Apr. 2012, doi: 10.1002/cyto.a.22012.

[160] W. Wang, R. Thomas, O. Sizova, and D. M. Su, “Thymic Function Associated With

Cancer Development, Relapse, and Antitumor Immunity – A Mini-Review," *Frontiers in Immunology*, vol. 11. Frontiers Media S.A., Apr-2020, doi: 10.3389/fimmu.2020.00773.

[161] J. M. Butler, H. Kobayashi, and S. Rafii, "Instructive role of the vascular niche in promoting tumour growth and tissue repair by angiocrine factors," *Nature Reviews Cancer*, vol. 10, no. 2. Nat Rev Cancer, pp. 138–146, Feb-2010, doi: 10.1038/nrc2791.

[162] K. Hida, N. Maishi, D. A. Annan, and Y. Hida, "Contribution of tumor endothelial cells in cancer progression," *International Journal of Molecular Sciences*, vol. 19, no. 5. MDPI AG, May-2018, doi: 10.3390/ijms19051272.

[163] N. V. Goncharov *et al.*, "Markers of Endothelial Cells in Normal and Pathological Conditions," *Biochemistry (Moscow) Supplement Series A: Membrane and Cell Biology*, vol. 14, no. 3. Pleiades journals, pp. 167–183, Jul-2020, doi: 10.1134/S1990747819030140.

[164] S. J. Ioannides, P. L. Barlow, J. M. Elwood, and D. Porter, "Effect of obesity on aromatase inhibitor efficacy in postmenopausal, hormone receptor-positive breast cancer: a systematic review," *Breast Cancer Research and Treatment*, vol. 147, no. 2. Springer New York LLC, pp. 237–248, Sep-2014, doi: 10.1007/s10549-014-3091-7.

[165] Y. Lin, J. Xu, and H. Lan, "Tumor-associated macrophages in tumor metastasis: Biological roles and clinical therapeutic applications," *Journal of Hematology and Oncology*, vol. 12, no. 1. BioMed Central Ltd., pp. 1–16, Jul-2019, doi: 10.1186/s13045-019-0760-3.

[166] S. I. Grivennikov, F. R. Greten, and M. Karin, "Immunity, Inflammation, and Cancer," *Cell*. 2010, doi: 10.1016/j.cell.2010.01.025.

[167] C. Deligne and K. S. Midwood, "Macrophages and Extracellular Matrix in Breast Cancer: Partners in Crime or Protective Allies?," *Front. Oncol.*, vol. 11, p. 186, Feb. 2021, doi: 10.3389/FONC.2021.620773.

[168] B. Baban *et al.*, "A minor population of splenic dendritic cells expressing CD19 mediates IDO-dependent T cell suppression via type I IFN signaling following B7 ligation," *Int. Immunol.*, 2005, doi: 10.1093/intimm/dxh271.

[169] J. A. Cintolo, J. Datta, S. J. Mathew, and B. J. Czerniecki, "Dendritic cell-based vaccines: Barriers and opportunities," *Future Oncology*, vol. 8, no. 10. NIH Public Access, pp. 1273–1299, Oct-2012, doi: 10.2217/fon.12.125.

[170] W. Zhang *et al.*, "Bone marrow-derived inflammatory and steady state DCs are different in both functions and survival," *Cell. Immunol.*, vol. 331, pp. 100–109, Sep. 2018, doi:

10.1016/j.cellimm.2018.06.001.

[171] R. G. Akwii, M. S. Sajib, F. T. Zahra, and C. M. Mikelis, “Role of Angiopoietin-2 in Vascular Physiology and Pathophysiology,” *Cells*, vol. 8, no. 5, p. 471, May 2019, doi: 10.3390/cells8050471.

[172] Z. L. Zhang, Z. S. Liu, and Q. Sun, “Expression of angiopoietins, Tie2 and vascular endothelial growth factor in angiogenesis and progression of hepatocellular carcinoma,” *World J. Gastroenterol.*, vol. 12, no. 26, pp. 4241–4245, Jul. 2006, doi: 10.3748/wjg.v12.i26.4241.

[173] E. Uribe-Querol and C. Rosales, “Neutrophils in cancer: Two sides of the same coin,” *Journal of Immunology Research*, vol. 2015. Hindawi Publishing Corporation, 2015, doi: 10.1155/2015/983698.

[174] Y. W. Li *et al.*, “Intratumoral neutrophils: A poor prognostic factor for hepatocellular carcinoma following resection,” *J. Hepatol.*, vol. 54, no. 3, pp. 497–505, Mar. 2011, doi: 10.1016/j.jhep.2010.07.044.

[175] L. Wu and X. H. F. Zhang, “Tumor-Associated Neutrophils and Macrophages—Heterogenous but Not Chaotic,” *Frontiers in Immunology*, vol. 11. Frontiers Media S.A., Dec-2020, doi: 10.3389/fimmu.2020.553967.

[176] S. Cedrés *et al.*, “Neutrophil to lymphocyte ratio (NLR) as an indicator of poor prognosis in stage IV non-small cell lung cancer,” *Clin. Transl. Oncol.*, vol. 14, no. 11, pp. 864–869, Nov. 2012, doi: 10.1007/s12094-012-0872-5.

[177] B. Manfroi, J. Moreaux, C. Righini, F. Ghiringhelli, N. Sturm, and B. Huard, “Tumor-associated neutrophils correlate with poor prognosis in diffuse large B-cell lymphoma patients,” *Blood Cancer Journal*, vol. 8, no. 7. Nature Publishing Group, p. 66, Jul-2018, doi: 10.1038/s41408-018-0099-y.

[178] T. T. Maciel, I. C. Moura, and O. Hermine, “The role of mast cells in cancers,” *F1000Prime Rep.*, vol. 7, Jan. 2015, doi: 10.12703/P7-09.

[179] S. Maltby, K. Khazaie, and K. M. McNagny, “Mast cells in tumor growth: Angiogenesis, tissue remodelling and immune-modulation,” *Biochimica et Biophysica Acta - Reviews on Cancer*, vol. 1796, no. 1. NIH Public Access, pp. 19–26, Aug-2009, doi: 10.1016/j.bbcan.2009.02.001.

[180] D. I. Gabrilovich and S. Nagaraj, “Myeloid-derived suppressor cells as regulators of the immune system,” *Nature Reviews Immunology*. 2009, doi: 10.1038/nri2506.

[181] E. K. Vetsika, A. Koukos, and A. Kotsakis, “Myeloid-Derived Suppressor Cells: Major Figures that Shape the Immunosuppressive and Angiogenic Network in Cancer,” *Cells*,

vol. 8, no. 12. NLM (Medline), Dec-2019, doi: 10.3390/cells8121647.

[182] S. Paul and G. Lal, “The molecular mechanism of natural killer cells function and its importance in cancer immunotherapy,” *Frontiers in Immunology*, vol. 8, no. SEP. Frontiers Media S.A., p. 1, Sep-2017, doi: 10.3389/fimmu.2017.01124.

[183] C. Li, P. Jiang, S. Wei, X. Xu, and J. Wang, “Regulatory T cells in tumor microenvironment: New mechanisms, potential therapeutic strategies and future prospects,” *Molecular Cancer*, vol. 19, no. 1. BioMed Central, pp. 1–23, Jul-2020, doi: 10.1186/s12943-020-01234-1.

[184] A. Verma, R. Mathur, A. Farooque, V. Kaul, S. Gupta, and B. S. Dwarakanath, “T-regulatory cells in tumor progression and therapy,” *Cancer Management and Research*, vol. 11. Dove Medical Press Ltd, pp. 10731–10747, 2019, doi: 10.2147/CMAR.S228887.

[185] G. J. Yuen, E. Demissie, and S. Pillai, “B Lymphocytes and Cancer: A Love–Hate Relationship,” *Trends in Cancer*, vol. 2, no. 12. Cell Press, pp. 747–757, Dec-2016, doi: 10.1016/j.trecan.2016.10.010.

[186] B. Adem, P. F. Vieira, and S. A. Melo, “Decoding the Biology of Exosomes in Metastasis,” *Trends in Cancer*. 2020, doi: 10.1016/j.trecan.2019.11.007.

[187] A. Becker, B. K. Thakur, J. M. Weiss, H. S. Kim, H. Peinado, and D. Lyden, “Extracellular Vesicles in Cancer: Cell-to-Cell Mediators of Metastasis,” *Cancer Cell*, vol. 30, no. 6. Cell Press, pp. 836–848, Dec-2016, doi: 10.1016/j.ccell.2016.10.009.

[188] Y. Y. Yeh *et al.*, “Characterization of CLL exosomes reveals a distinct microRNA signature and enhanced secretion by activation of BCR signaling,” *Blood*, vol. 125, no. 21, pp. 3297–3305, 2015, doi: 10.1182/blood-2014-12-618470.

[189] A. Li, T. Zhang, M. Zheng, Y. Liu, and Z. Chen, “Exosomal proteins as potential markers of tumor diagnosis,” *Journal of Hematology and Oncology*, vol. 10, no. 1. BioMed Central Ltd., Dec-2017, doi: 10.1186/s13045-017-0542-8.

[190] M. Zarà *et al.*, “Biology and role of extracellular vesicles (Evs) in the pathogenesis of thrombosis,” *International Journal of Molecular Sciences*, vol. 20, no. 11. MDPI AG, Jun-2019, doi: 10.3390/ijms20112840.

[191] D. K. Jeppesen *et al.*, “Reassessment of Exosome Composition,” *Cell*, vol. 177, no. 2, pp. 428-445.e18, Apr. 2019, doi: 10.1016/j.cell.2019.02.029.

[192] P. Vaupel and L. Harrison, “Tumor Hypoxia: Causative Factors, Compensatory Mechanisms, and Cellular Response,” *Oncologist*, 2004, doi: 10.1634/theoncologist.9-90005-4.

[193] V. S. Hughes, J. M. Wiggins, and D. W. Siemann, “Tumor oxygenation and cancer therapy-then and now,” *British Journal of Radiology*. 2019, doi: 10.1259/bjr.20170955.

[194] K. R. Luoto, R. Kumareswaran, and R. G. Bristow, “Tumor hypoxia as a driving force in genetic instability,” *Genome Integrity*. 2013, doi: 10.1186/2041-9414-4-5.

[195] A. Coquelle, F. Toledo, S. Stern, A. Bieth, and M. Debatisse, “A new role for hypoxia in tumor progression: Induction of fragile site triggering genomic rearrangements and formation of complex DMs and HSRs,” *Mol. Cell*, 1998, doi: 10.1016/S1097-2765(00)80137-9.

[196] R. G. Bristow, “Hypoxia, DNA Repair, and Genetic Instability,” *AACR Educ. B.*, 2008, doi: 10.1158/aacr.edb-08-8388.

[197] R. Kumareswaran, O. Ludkovski, A. Meng, J. Sykes, M. Pintilie, and R. G. Bristow, “Chronic hypoxia compromises repair of DNA double-strand breaks to drive genetic instability,” *J. Cell Sci.*, vol. 125, no. 1, pp. 189–199, Jan. 2012, doi: 10.1242/jcs.092262.

[198] R. B. Hamanaka and N. S. Chandel, “Mitochondrial reactive oxygen species regulate hypoxic signaling,” *Current Opinion in Cell Biology*. 2009, doi: 10.1016/j.ceb.2009.08.005.

[199] D. Kidane *et al.*, “Interplay between DNA repair and inflammation, and the link to cancer,” *Critical Reviews in Biochemistry and Molecular Biology*. 2014, doi: 10.3109/10409238.2013.875514.

[200] M. Olcina, P. S. Lecane, and E. M. Hammond, “Targeting hypoxic cells through the DNA damage response,” *Clinical Cancer Research*. 2010, doi: 10.1158/1078-0432.CCR-10-0286.

[201] K. Begg and M. Tavassoli, “Inside the hypoxic tumour: reprogramming of the DDR and radioresistance,” *Cell Death Discovery*. 2020, doi: 10.1038/s41420-020-00311-0.

[202] S. Fukushima *et al.*, “Hypoxia-inducible factor 1 alpha is a poor prognostic factor and potential therapeutic target in malignant peripheral nerve sheath tumor,” *PLoS One*, 2017, doi: 10.1371/journal.pone.0178064.

[203] S. Han, T. Huang, F. Hou, L. Yao, X. Wang, and X. Wu, “The prognostic value of hypoxia-inducible factor-1α in advanced cancer survivors: a meta-analysis with trial sequential analysis,” *Ther. Adv. Med. Oncol.*, 2019, doi: 10.1177/1758835919875851.

[204] W. R. Wilson and M. P. Hay, “Targeting hypoxia in cancer therapy,” *Nature Reviews Cancer*. 2011, doi: 10.1038/nrc3064.

[205] G. L. Semenza, “Defining the role of hypoxia-inducible factor 1 in cancer biology and

therapeutics," *Oncogene*. 2010, doi: 10.1038/onc.2009.441.

[206] N. H. Barrak, M. A. Khajah, and Y. A. Luqmani, "Hypoxic environment may enhance migration/penetration of endocrine resistant MCF7- derived breast cancer cells through monolayers of other non-invasive cancer cells in vitro," *Sci. Rep.*, vol. 10, no. 1, pp. 1–14, Dec. 2020, doi: 10.1038/s41598-020-58055-x.

[207] Y. Li, X. X. Sun, D. Z. Qian, and M. S. Dai, "Molecular Crosstalk Between MYC and HIF in Cancer," *Frontiers in Cell and Developmental Biology*. 2020, doi: 10.3389/fcell.2020.590576.

[208] H. Okuyama, H. Endo, T. Akashika, K. Kato, and M. Inoue, "Downregulation of c-MYC protein levels contributes to cancer cell survival under dual deficiency of oxygen and glucose," *Cancer Res.*, 2010, doi: 10.1158/0008-5472.CAN-10-2720.

[209] S. Riffle, R. N. Pandey, M. Albert, and R. S. Hegde, "Linking hypoxia, DNA damage and proliferation in multicellular tumor spheroids," *BMC Cancer*, vol. 17, no. 1, p. 338, May 2017, doi: 10.1186/s12885-017-3319-0.

[210] N. Chan, C. Koch, and R. Bristow, "Tumor Hypoxia as a Modifier of DNA Strand Break and Cross-Link Repair," *Curr. Mol. Med.*, 2009, doi: 10.2174/156652409788167050.

[211] Y. Li, L. Zhao, and X. F. Li, "Hypoxia and the Tumor Microenvironment," *Technol. Cancer Res. Treat.*, vol. 20, 2021, doi: 10.1177/15330338211036304.

[212] N. Colwell *et al.*, "Hypoxia in the glioblastoma microenvironment: Shaping the phenotype of cancer stem-like cells," *Neuro. Oncol.*, vol. 19, no. 7, pp. 887–896, 2017, doi: 10.1093/neuonc/now258.

[213] T. Yu, B. Tang, and X. Sun, "Development of inhibitors targeting hypoxia-inducible factor 1 and 2 for cancer therapy," *Yonsei Medical Journal*. 2017, doi: 10.3349/ymj.2017.58.3.489.

[214] D. A.G. *et al.*, "A pilot trial of oral topotecan (TPT) in patients with refractory advanced solid neoplasms expressing HIF-1," *J. Clin. Oncol.*, 2010.

[215] X. F. Bai, J. Liu, O. Li, P. Zheng, and Y. Liu, "Antigenic drift as a mechanism for tumor evasion of destruction by cytolytic T lymphocytes," *J. Clin. Invest.*, 2003, doi: 10.1172/JCI17656.

[216] F. R. Greten and S. I. Grivennikov, "Inflammation and Cancer: Triggers, Mechanisms, and Consequences," *Immunity*. 2019, doi: 10.1016/j.immuni.2019.06.025.

[217] D. A. Senthebane *et al.*, "The role of tumor microenvironment in chemoresistance: To survive, keep your enemies closer," *Int. J. Mol. Sci.*, vol. 18, no. 7, 2017, doi: 10.3390/ijms18071586.

[218] A. Sistigu, F. Di Modugno, G. Manic, and P. Nisticò, "Deciphering the loop of epithelial-mesenchymal transition, inflammatory cytokines and cancer immunoediting," *Cytokine and Growth Factor Reviews*. 2017, doi: 10.1016/j.cytogfr.2017.05.008.

[219] J. L. Birch *et al.*, "Multifaceted transforming growth factor-beta (TGFβ) signalling in glioblastoma," *Cell. Signal.*, vol. 72, p. 109638, Aug. 2020, doi: 10.1016/J.CELLSIG.2020.109638.

[220] M. Ricciardi *et al.*, "Epithelial-to-mesenchymal transition (EMT) induced by inflammatory priming elicits mesenchymal stromal cell-like immune-modulatory properties in cancer cells," *Br. J. Cancer*, 2015, doi: 10.1038/bjc.2015.29.

[221] M. Suarez-Carmona, J. Lesage, D. Cataldo, and C. Gilles, "EMT and inflammation: inseparable actors of cancer progression," *Molecular Oncology*. 2017, doi: 10.1002/1878-0261.12095.

[222] M. Labelle, S. Begum, and R. O. Hynes, "Direct Signaling between Platelets and Cancer Cells Induces an Epithelial-Mesenchymal-Like Transition and Promotes Metastasis," *Cancer Cell*, 2011, doi: 10.1016/j.ccr.2011.09.009.

[223] G. Y, H. M, and Y. YM, "The Effect and Regulatory Mechanism of High Mobility Group Box-1 Protein on Immune Cells in Inflammatory Diseases," *Cells*, vol. 10, no. 5, Apr. 2021, doi: 10.3390/CELLS10051044.

[224] S. Wang and Y. Zhang, "HMGB1 in inflammation and cancer," *Journal of Hematology and Oncology*. 2020, doi: 10.1186/s13045-020-00950-x.

[225] O. Sokolova and M. Naumann, "Crosstalk between DNA damage and inflammation in the multiple steps of gastric carcinogenesis," in *Current Topics in Microbiology and Immunology*, 2019.

[226] Z. Yang *et al.*, "Mast cells mobilize myeloid-derived suppressor cells and Treg cells in tumor microenvironment via IL-17 pathway in murine hepatocarcinoma model," *PLoS One*, 2010, doi: 10.1371/journal.pone.0008922.

[227] M. Jaiswal, N. F. LaRusso, L. J. Burgart, and G. J. Gores, "Inflammatory cytokines induce DNA damage and inhibit DNA repair in cholangiocarcinoma cells by a nitric oxide-dependent mechanism," *Cancer Res.*, 2000.

[228] J. Kay, E. Thadhani, L. Samson, and B. Engelward, "Inflammation-induced DNA damage, mutations and cancer," *DNA Repair*. 2019, doi: 10.1016/j.dnarep.2019.102673.

[229] L. E. Collins and L. Troeberg, "Heparan sulfate as a regulator of inflammation and immunity," *Journal of Leukocyte Biology*. 2019, doi: 10.1002/JLB.3RU0618-246R.

[230] M. Xie and J. ping Li, "Heparan sulfate proteoglycan – A common receptor for diverse

cytokines," *Cell. Signal.*, 2019, doi: 10.1016/j.cellsig.2018.11.022.

[231] C. T. Viehl *et al.*, "Depletion of CD4+CD25+ regulatory T cells promotes a tumor-specific immune response in pancreas cancer-bearing mice," *Ann. Surg. Oncol.*, 2006, doi: 10.1245/s10434-006-9015-y.

[232] I. Karakasilioti *et al.*, "DNA damage triggers a chronic autoinflammatory response, leading to fat depletion in NER progeria," *Cell Metab.*, 2013, doi: 10.1016/j.cmet.2013.08.011.

[233] E. E. Parkes *et al.*, "Activation of STING-dependent innate immune signaling by s-phase-specific DNA damage in breast cancer," *J. Natl. Cancer Inst.*, 2017, doi: 10.1093/jnci/djw199.

[234] S. Grabosch *et al.*, "Cisplatin-induced immune modulation in ovarian cancer mouse models with distinct inflammation profiles," *Oncogene*, 2019, doi: 10.1038/s41388-018-0581-9.

[235] S. J. Serrano-Gomez, M. Maziveyi, and S. K. Alahari, "Regulation of epithelial-mesenchymal transition through epigenetic and post-translational modifications," *Mol. Cancer 2016 151*, vol. 15, no. 1, pp. 1–14, Feb. 2016, doi: 10.1186/S12943-016-0502-X.

[236] E. Kunadis, E. Lakiotaki, P. Korkolopoulou, and C. Piperi, "Targeting post-translational histone modifying enzymes in glioblastoma," *Pharmacol. Ther.*, vol. 220, p. 107721, Apr. 2021, doi: 10.1016/J.PHARMTHERA.2020.107721.

[237] Z. Wu, R. Huang, and L. Yuan, "Crosstalk of intracellular post-translational modifications in cancer," *Arch. Biochem. Biophys.*, vol. 676, Nov. 2019, doi: 10.1016/J.ABB.2019.108138.

[238] Y. Zhao and O. N. Jensen, "Modification-specific proteomics: Strategies for characterization of post-translational modifications using enrichment techniques," *Proteomics*, vol. 9, no. 20, p. 4632, Oct. 2009, doi: 10.1002/PMIC.200900398.

[239] Y. Peng, H. Liu, J. Liu, and J. Long, "Post-translational modifications on mitochondrial metabolic enzymes in cancer," *Free Radic. Biol. Med.*, vol. 179, pp. 11–23, Feb. 2022, doi: 10.1016/J.FREERADBIOMED.2021.12.264.

[240] B. C. Taylor and N. L. Young, "Combinations of histone post-translational modifications," *Biochem. J.*, vol. 478, no. 3, pp. 511–532, Feb. 2021, doi: 10.1042/BCJ20200170.

[241] J. E. Audia and R. M. Campbell, "Histone modifications and cancer," *Cold Spring Harb. Perspect. Biol.*, vol. 8, no. 4, pp. 1–31, 2016, doi: 10.1101/cshperspect.a019521.

[242] J. Yang, C. Song, and X. Zhan, “The role of protein acetylation in carcinogenesis and targeted drug discovery,” *Front. Endocrinol. (Lausanne).*, vol. 13, no. September, pp. 1–26, 2022, doi: 10.3389/fendo.2022.972312.

[243] J. V. Lee *et al.*, “Acetyl-CoA promotes glioblastoma cell adhesion and migration through Ca2+-NFAT signaling,” *Genes Dev.*, vol. 32, no. 7–8, pp. 497–511, Apr. 2018, doi: 10.1101/GAD.311027.117/-/DC1.

[244] M. J. Goldman *et al.*, “Visualizing and interpreting cancer genomics data via the Xena platform,” *Nat. Biotechnol. 2020 386*, vol. 38, no. 6, pp. 675–678, May 2020, doi: 10.1038/s41587-020-0546-8.

[245] R. Chen *et al.*, “The application of histone deacetylases inhibitors in glioblastoma,” *J. Exp. Clin. Cancer Res.*, vol. 39, no. 1, pp. 1–18, 2020, doi: 10.1186/s13046-020-01643-6.

[246] I. Hervás-Corpión *et al.*, “Defining a Correlative Transcriptional Signature Associated with Bulk Histone H3 Acetylation Levels in Adult Glioblastomas,” *Cells*, vol. 12, no. 3, p. 374, 2023, doi: 10.3390/cells12030374.

[247] X. Feng *et al.*, “Hypoxia-induced acetylation of PAK1 enhances autophagy and promotes brain tumorigenesis via phosphorylating ATG5,” *Autophagy*, vol. 17, no. 3, pp. 723–742, 2021, doi: 10.1080/15548627.2020.1731266.

[248] Z. Tu *et al.*, “Systematic and Multi-Omics Prognostic Analysis of Lysine Acetylation Regulators in Glioma,” *Front. Mol. Biosci.*, vol. 8, p. 49, Feb. 2021, doi: 10.3389/FMOLB.2021.587516/BIBTEX.

[249] Y. W. Xu *et al.*, “Acetylation Profiles in the Metabolic Process of Glioma-Associated Seizures,” *Front. Neurol.*, vol. 12, p. 1590, Oct. 2021, doi: 10.3389/FNEUR.2021.713293/BIBTEX.

[250] C. Yang, S. Croteau, and P. Hardy, “Histone deacetylase (HDAC) 9: versatile biological functions and emerging roles in human cancer,” *Cell. Oncol.*, vol. 44, no. 5, pp. 997–1017, 2021, doi: 10.1007/s13402-021-00626-9.

[251] L. Everix, E. N. Seane, T. Ebenhan, I. Goethals, and J. Bolcaen, “Introducing HDAC-Targeting Radiopharmaceuticals for Glioblastoma Imaging and Therapy,” *Pharmaceuticals*, vol. 16, no. 2, pp. 1–21, 2023, doi: 10.3390/ph16020227.

[252] A. D. Bondarev, M. M. Attwood, J. Jonsson, V. N. Chubarev, V. V. Tarasov, and H. B. Schiöth, “Recent developments of HDAC inhibitors: Emerging indications and novel molecules,” *Br. J. Clin. Pharmacol.*, vol. 87, no. 12, pp. 4577–4597, 2021, doi: 10.1111/bcp.14889.

[253] X. Liu *et al.*, "Differential regulation of H3K9/H3K14 acetylation by small molecules drives neuron-fate-induction of glioma cell," *Cell Death Dis.*, vol. 14, no. 2, Feb. 2023, doi: 10.1038/S41419-023-05611-8.

[254] N. Kumar, M. Mondal, B. P. Arathi, N. R. Sundaresan, and K. Somasundaram, "Histone acetyltransferase 1 (HAT1) acetylates hypoxia-inducible factor 2 alpha (HIF2A) to execute hypoxia response," *Biochim. Biophys. Acta - Gene Regul. Mech.*, vol. 1866, no. 1, p. 194900, Mar. 2023, doi: 10.1016/J.BBAGRM.2022.194900.

[255] H. H. Chang *et al.*, "A Selective Histone Deacetylase Inhibitor Induces Autophagy and Cell Death via SCNN1A Downregulation in Glioblastoma Cells," *Cancers (Basel).*, vol. 14, no. 18, p. 4537, Sep. 2022, doi: 10.3390/CANCERS14184537/S1.

[256] J. Wang *et al.*, "SHF Acts as a Novel Tumor Suppressor in Glioblastoma Multiforme by Disrupting STAT3 Dimerization," *Adv. Sci.*, vol. 9, no. 26, Sep. 2022, doi: 10.1002/ADVS.202200169.

[257] A. C. Mladek *et al.*, "RBBP4-p300 axis modulates expression of genes essential for cell survival and is a potential target for therapy in glioblastoma," *Neuro. Oncol.*, vol. 24, no. 8, p. 1261, Aug. 2022, doi: 10.1093/NEUONC/NOAC051.

[258] L. Zhang, Z. Liu, Y. Dong, and L. Kong, "Epigenetic targeting of SLC30A3 by HDAC1 is related to the malignant phenotype of glioblastoma," *IUBMB Life*, vol. 73, no. 5, pp. 784–799, May 2021, doi: 10.1002/IUB.2463.

[259] Q. Wang *et al.*, "A combination of BRD4 and HDAC3 inhibitors synergistically suppresses glioma stem cell growth by blocking GLI1/IL6/STAT3 signaling axis," *Mol. Cancer Ther.*, vol. 19, no. 12, pp. 2542–2553, Dec. 2020, doi: 10.1158/1535-7163.MCT-20-0037/87781/AM/A-COMBINATION-OF-BRD4-AND-HDAC3-INHIBITORS.

[260] W. Bin Yang *et al.*, "Increased activation of HDAC1/2/6 and Sp1 underlies therapeutic resistance and tumor growth in glioblastoma," *Neuro. Oncol.*, vol. 22, no. 10, p. 1439, Oct. 2020, doi: 10.1093/NEUONC/NOAA103.

[261] H. Zhao *et al.*, "EGFR-vIII downregulated H2AZK4/7AC though the PI3K/AKT-HDAC2 axis to regulate cell cycle progression," *Clin. Transl. Med.*, vol. 9, no. 1, Jan. 2020, doi: 10.1186/S40169-020-0260-7.

[262] Z. Dong *et al.*, "MYST1/KAT8 contributes to tumor progression by activating EGFR signaling in glioblastoma cells," *Cancer Med.*, vol. 8, no. 18, pp. 7793–7808, Dec. 2019, doi: 10.1002/CAM4.2639.

[263] T. Ye *et al.*, "Sirtuin1 activator SRT2183 suppresses glioma cell growth involving

activation of endoplasmic reticulum stress pathway," *BMC Cancer*, vol. 19, no. 1, p. 706, Jul. 2019, doi: 10.1186/S12885-019-5852-5.

[264] L. M. Humphreys, P. Smith, Z. Chen, S. Fouad, and V. D'Angiolella, "The role of E3 ubiquitin ligases in the development and progression of glioblastoma," *Cell Death Differ.*, vol. 28, no. 2, pp. 522–537, 2021, doi: 10.1038/s41418-020-00696-6.

[265] P. Zhou *et al.*, "E3 ligase MAEA-mediated ubiquitination and degradation of PHD3 promotes glioblastoma progression," *Oncogene 2023*, pp. 1–13, Mar. 2023, doi: 10.1038/s41388-023-02644-3.

[266] F. Bufalieri *et al.*, "The RNA-Binding Ubiquitin Ligase MEX3A Affects Glioblastoma Tumorigenesis by Inducing Ubiquitylation and Degradation of RIG-I," *Cancers 2020, Vol. 12, Page 321*, vol. 12, no. 2, p. 321, Jan. 2020, doi: 10.3390/CANCERS12020321.

[267] T. K. Rimkus *et al.*, "NEDD4 degrades TUSC2 to promote glioblastoma progression," *Cancer Lett.*, vol. 531, pp. 124–135, Apr. 2022, doi: 10.1016/J.CANLET.2022.01.029.

[268] J. Vriend and T. Klonisch, "Genes of the Ubiquitin Proteasome System Qualify as Differential Markers in Malignant Glioma of Astrocytic and Oligodendroglial Origin," *Cell. Mol. Neurobiol.*, no. 0123456789, 2022, doi: 10.1007/s10571-022-01261-0.

[269] T. Pan *et al.*, "USP7 inhibition induces apoptosis in glioblastoma by enhancing ubiquitination of ARF4," *Cancer Cell Int.*, vol. 21, no. 1, pp. 1–15, 2021, doi: 10.1186/s12935-021-02208-z.

[270] L. Lospinoso Severini, F. Bufalieri, P. Infante, and L. Di Marcotullio, "Proteolysis-Targeting Chimera (PROTAC): Is the Technology Looking at the Treatment of Brain Tumors?," *Front. Cell Dev. Biol.*, vol. 10, no. February, pp. 1–10, 2022, doi: 10.3389/fcell.2022.854352.

[271] B. Zhao and K. Burgess, "PROTACs suppression of CDK4/6, crucial kinases for cell cycle regulation in cancer," *Chem. Commun. (Camb).*, vol. 55, no. 18, pp. 2704–2707, 2019, doi: 10.1039/C9CC00163H.

[272] J. R. Liu, C. W. Yu, P. Y. Hung, L. W. Hsin, and J. W. Chern, "High-selective HDAC6 inhibitor promotes HDAC6 degradation following autophagy modulation and enhanced antitumor immunity in glioblastoma," *Biochem. Pharmacol.*, vol. 163, pp. 458–471, May 2019, doi: 10.1016/J.BCP.2019.03.023.

[273] Y. Zhou, P. Liang, W. Ji, Z. Yu, H. Chen, and L. Jiang, "Ubiquitin-specific protease 4 promotes glioblastoma multiforme via activating ERK pathway," *Onco. Targets. Ther.*, vol. 12, p. 1825, 2019, doi: 10.2147/OTT.S176582.

[274] G. Liu *et al.*, "GRP78 determines glioblastoma sensitivity to UBA1 inhibition-induced

UPR signaling and cell death," *Cell Death Dis. 2021 128*, vol. 12, no. 8, pp. 1–13, Jul. 2021, doi: 10.1038/s41419-021-04023-w.

[275] W. Peng *et al.*, "CBX3 accelerates the malignant progression of glioblastoma multiforme by stabilizing EGFR expression," *Oncogene 2022 4122*, vol. 41, no. 22, pp. 3051–3063, Apr. 2022, doi: 10.1038/s41388-022-02296-9.

[276] H. Chen *et al.*, "Extracellular vesicles-transferred SBSN drives glioma aggressiveness by activating NF-κB via ANXA1-dependent ubiquitination of NEMO," *Oncogene 2022 4149*, vol. 41, no. 49, pp. 5253–5265, Oct. 2022, doi: 10.1038/s41388-022-02520-6.

[277] X. F. Liu *et al.*, "Down-Regulated CUEDC2 Increases GDNF Expression by Stabilizing CREB Through Reducing Its Ubiquitination in Glioma," *Neurochem. Res.*, vol. 45, no. 12, pp. 2915–2925, Dec. 2020, doi: 10.1007/S11064-020-03140-W/FIGURES/5.

[278] I. C. Su *et al.*, "Ubiquitin-Specific Protease 6 n-Terminal-like Protein (USP6NL) and the Epidermal Growth Factor Receptor (EGFR) Signaling Axis Regulates Ubiquitin-Mediated DNA Repair and Temozolomide-Resistance in Glioblastoma," *Biomedicines*, vol. 10, no. 7, p. 1531, Jul. 2022, doi: 10.3390/BIOMEDICINES10071531/S1.

[279] J. Li *et al.*, "Radiation induces IRAK1 expression to promote radioresistance by suppressing autophagic cell death via decreasing the ubiquitination of PRDX1 in glioma cells," *Cell Death Dis. 2023 144*, vol. 14, no. 4, pp. 1–16, Apr. 2023, doi: 10.1038/s41419-023-05732-0.

[280] Z. Pan, J. Bao, L. Zhang, and S. Wei, "UBE2D3 Activates SHP-2 Ubiquitination to Promote Glycolysis and Proliferation of Glioma via Regulating STAT3 Signaling Pathway," *Front. Oncol.*, vol. 11, p. 2081, Jun. 2021, doi: 10.3389/FONC.2021.674286/BIBTEX.

[281] M. Khan, D. Muzumdar, and A. Shiras, "Attenuation of Tumor Suppressive Function of FBXO16 Ubiquitin Ligase Activates Wnt Signaling In Glioblastoma," *Neoplasia*, vol. 21, no. 1, pp. 106–116, Jan. 2019, doi: 10.1016/J.NEO.2018.11.005.

[282] C. Liu *et al.*, "Wnt/beta-Catenin pathway in human glioma: expression pattern and clinical/prognostic correlations," *Clin. Exp. Med.*, vol. 11, no. 2, pp. 105–112, Jun. 2011, doi: 10.1007/S10238-010-0110-9.

[283] Y. Lee, J. K. Lee, S. H. Ahn, J. Lee, and D. H. Nam, "WNT signaling in glioblastoma and therapeutic opportunities," *Lab. Investig. 2016 962*, vol. 96, no. 2, pp. 137–150, Dec. 2015, doi: 10.1038/labinvest.2015.140.

[284] M. Latour, N. G. Her, S. Kesari, and E. Nurmemmedov, "WNT Signaling as a Therapeutic Target for Glioblastoma," *Int. J. Mol. Sci.*, vol. 22, no. 16, Aug. 2021, doi:

10.3390/IJMS22168428.

[285] M. Kouchi, Y. Shibayama, D. Ogawa, K. Miyake, A. Nishiyama, and T. Tamiya, "(Pro)renin receptor is crucial for glioma development via the Wnt/b-catenin signaling pathway," *J. Neurosurg.*, vol. 127, no. 4, pp. 819–828, 2017, doi: 10.3171/2016.9.JNS16431.

[286] A. De Robertis *et al.*, "Identification and characterization of a small-molecule inhibitor of Wnt signaling in glioblastoma cells," *Mol. Cancer Ther.*, vol. 12, no. 7, pp. 1180–1189, 2013, doi: 10.1158/1535-7163.MCT-12-1176-T.

[287] I. Arrillaga-Romany *et al.*, "Biological activity of weekly ONC201 in adult recurrent glioblastoma patients," *Neuro. Oncol.*, vol. 22, no. 1, pp. 94–102, 2020, doi: 10.1093/NEUONC/NOZ164.

[288] H. Wang *et al.*, "Hedgehog signaling regulates the development and treatment of glioblastoma (Review)," *Oncol. Lett.*, vol. 24, no. 3, pp. 1–15, 2022, doi: 10.3892/ol.2022.13414.

[289] X. Wu *et al.*, "A novel protein encoded by circular SMO RNA is essential for Hedgehog signaling activation and glioblastoma tumorigenicity," *Genome Biol.*, vol. 22, no. 1, pp. 1–29, Dec. 2021, doi: 10.1186/S13059-020-02250-6/FIGURES/6.

[290] H. C. Hung, C. C. Liu, J. Y. Chuang, C. L. Su, and P. W. Gean, "Inhibition of Sonic Hedgehog Signaling Suppresses Glioma Stem-Like Cells Likely Through Inducing Autophagic Cell Death," *Front. Oncol.*, vol. 10, no. July, pp. 1–15, 2020, doi: 10.3389/fonc.2020.01233.

[291] M. L. Sargazi *et al.*, "Naringenin attenuates cell viability and migration of C6 glioblastoma cell line: a possible role of hedgehog signaling pathway," *Mol. Biol. Rep.*, vol. 48, no. 9, pp. 6413–6421, 2021, doi: 10.1007/s11033-021-06641-1.

[292] A. KARADAĞ and Y. BAŞBINAR, "Novel Approach to the Hedgehog Signaling Pathway: Combined Treatment of SMO and PTCH Inhibitors," *J. Basic Clin. Heal. Sci.*, vol. 1, no. 5, pp. 492–500, 2022, doi: 10.30621/jbachs.1193720.

[293] C. Bureta *et al.*, "Synergistic effect of arsenic trioxide, vismodegib and temozolomide on glioblastoma," *Oncol. Rep.*, vol. 41, no. 6, pp. 3404–3412, 2019, doi: 10.3892/or.2019.7100.

[294] B. Linder *et al.*, "Arsenic trioxide and (−)-gossypol synergistically target glioma stem-like cells via inhibition of hedgehog and notch signaling," *Cancers (Basel).*, vol. 11, no. 3, 2019, doi: 10.3390/cancers11030350.

[295] Z. Gersey *et al.*, "Therapeutic Targeting of the Notch Pathway in Glioblastoma

Multiforme," *World Neurosurg.*, vol. 131, pp. 252-263.e2, 2019, doi: 10.1016/j.wneu.2019.07.180.

[296] Y. Fang and Z. Zhang, "Arsenic trioxide as a novel anti-glioma drug: a review," *Cell. Mol. Biol. Lett.*, vol. 25, p. 44, 2020, doi: 10.1186/s11658-020-00236-7.

[297] H. C. Oh *et al.*, "Combined effects of niclosamide and temozolomide against human glioblastoma tumorspheres," *J. Cancer Res. Clin. Oncol.*, vol. 146, no. 11, pp. 2817–2828, 2020, doi: 10.1007/s00432-020-03330-7.

[298] F. Giordano, F. I. Montalto, M. L. Panno, S. Andò, and F. De Amicis, "A Notch inhibitor plus Resveratrol induced blockade of autophagy drives glioblastoma cell death by promoting a switch to apoptosis," *Am. J. Cancer Res.*, vol. 11, no. 12, pp. 5933–5950, 2021.

[299] R. Bazzoni and A. Bentivegna, "Role of Notch Signaling Pathway in Glioblastoma Pathogenesis," pp. 1–25, 2019, doi: 10.3390/cancers11030292.

[300] F. C. Kipper, M. W. Kieran, A. Thomas, and D. Panigrahy, "Notch signaling in malignant gliomas : supporting tumor growth and the vascular environment," *Cancer Metastasis Rev.*, pp. 737–747, 2022, doi: 10.1007/s10555-022-10041-7.

[301] D. Herrera-Rios *et al.*, "A computational guided, functional validation of a novel therapeutic antibody proposes Notch signaling as a clinical relevant and druggable target in glioma," *Sci. Rep.*, vol. 10, no. 1, pp. 1–12, 2020, doi: 10.1038/s41598-020-72480-y.

[302] D. M. Peereboom *et al.*, "A Phase II and Pharmacodynamic Trial of RO4929097 for Patients with Recurrent/Progressive Glioblastoma," *Neurosurgery*, vol. 88, no. 2, pp. 246–251, 2021, doi: 10.1093/neuros/nyaa412.

[303] S. Zhu *et al.*, "Brain-targeting biomimetic nanoparticles for codelivery of celastrol and LY2157299 for reversing glioma immunosuppression," *Int. J. Pharm.*, vol. 619, p. 121709, May 2022, doi: 10.1016/J.IJPHARM.2022.121709.

[304] D. F. Quail and J. A. Joyce, "The Microenvironmental Landscape of Brain Tumors," *Cancer Cell*, vol. 31, no. 3, pp. 326–341, 2017, doi: 10.1016/j.ccell.2017.02.009.

[305] H. Hosseinalizadeh, M. Mahmoodpour, Z. Razaghi Bahabadi, M. R. Hamblin, and H. Mirzaei, "Neutrophil mediated drug delivery for targeted glioblastoma therapy: A comprehensive review," *Biomed. Pharmacother.*, vol. 156, p. 113841, 2022, doi: 10.1016/j.biopha.2022.113841.

[306] Y. Li, X. Teng, Y. Wang, C. Yang, X. Yan, and J. Li, "Neutrophil Delivered Hollow Titania Covered Persistent Luminescent Nanosensitizer for Ultrosound Augmented Chemo/Immuno Glioblastoma Therapy," *Adv. Sci.*, vol. 8, no. 17, pp. 1–7, 2021, doi:

10.1002/advs.202004381.

[307] R. S. Andersen, A. Anand, D. S. L. Harwood, and B. W. Kristensen, “Tumor-associated microglia and macrophages in the glioblastoma microenvironment and their implications for therapy,” *Cancers (Basel).*, vol. 13, no. 17, pp. 1–26, 2021, doi: 10.3390/cancers13174255.

[308] M. F. Almahariq, T. J. Quinn, P. Kesarwani, S. Kant, C. R. Miller, and P. Chinnaiyan, “Inhibition of colony-stimulating factor-1 receptor enhances the efficacy of radiotherapy and reduces immune suppression in glioblastoma,” *In Vivo (Brooklyn).*, vol. 35, no. 1, pp. 119–129, 2021, doi: 10.21873/INVIVO.12239.

[309] B. C. Jena, C. K. Das, D. Bharadwaj, and M. Mandal, “Cancer associated fibroblast mediated chemoresistance: A paradigm shift in understanding the mechanism of tumor progression,” *Biochim. Biophys. Acta - Rev. Cancer*, vol. 1874, no. 2, p. 188416, 2020, doi: 10.1016/j.bbcan.2020.188416.

[310] J. Guo, H. Zeng, and Y. Chen, “Emerging Nano Drug Delivery Systems Targeting Cancer-Associated Fibroblasts for Improved Antitumor Effect and Tumor Drug Penetration,” *Mol. Pharm.*, vol. 17, no. 4, pp. 1028–1048, Apr. 2020, doi: 10.1021/ACS.MOLPHARMACEUT.0C00014/ASSET/IMAGES/MEDIUM/MP0C00014_0010.GIF.

[311] Y. Mi *et al.*, “The Emerging Role of Myeloid-Derived Suppressor Cells in the Glioma Immune Suppressive Microenvironment,” *Front. Immunol.*, vol. 11, no. April, pp. 1–11, 2020, doi: 10.3389/fimmu.2020.00737.

[312] M. Salemizadeh Parizi, F. Salemizadeh Parizi, S. Abdolhosseini, S. Vanaei, A. Manzouri, and F. Ebrahimzadeh, “Myeloid-derived suppressor cells (MDSCs) in brain cancer: challenges and therapeutic strategies,” *Inflammopharmacology*, vol. 29, no. 6, pp. 1613–1624, 2021, doi: 10.1007/s10787-021-00878-9.

[313] J. A. Flores-Toro *et al.*, “CCR2 inhibition reduces tumor myeloid cells and unmasks a checkpoint inhibitor effect to slow progression of resistant murine gliomas,” *Proc. Natl. Acad. Sci. U. S. A.*, vol. 117, no. 2, pp. 1129–1138, 2020, doi: 10.1073/pnas.1910856117.

[314] K. Bijangi-Vishehsaraei *et al.*, “Sulforaphane suppresses the growth of glioblastoma cells, glioblastoma stem cell-like spheroids, and tumor xenografts through multiple cell signaling pathways,” *J. Neurosurg.*, vol. 127, no. 6, pp. 1219–1230, 2017, doi: 10.3171/2016.8.JNS161197.

[315] C. Wu *et al.*, “Repolarization of myeloid derived suppressor cells via magnetic

nanoparticles to promote radiotherapy for glioma treatment," *Nanomedicine Nanotechnology, Biol. Med.*, vol. 16, pp. 126–137, Feb. 2019, doi: 10.1016/J.NANO.2018.11.015.

[316] S. Srivastava, C. Jackson, T. Kim, J. Choi, and M. Lim, "A Characterization of Dendritic Cells and Their Role in Immunotherapy in Glioblastoma: From Preclinical Studies to Clinical Trials," *Cancers 2019, Vol. 11, Page 537*, vol. 11, no. 4, p. 537, Apr. 2019, doi: 10.3390/CANCERS11040537.

[317] M. Wang, Y. Cai, Y. Peng, B. Xu, W. Hui, and Y. Jiang, "Exosomal LGALS9 in the cerebrospinal fluid of glioblastoma patients suppressed dendritic cell antigen presentation and cytotoxic T-cell immunity," *Cell Death Dis.*, vol. 11, no. 10, 2020, doi: 10.1038/s41419-020-03042-3.

[318] A. Datsi and R. V. Sorg, "Dendritic Cell Vaccination of Glioblastoma: Road to Success or Dead End," *Front. Immunol.*, vol. 12, no. November, pp. 1–28, 2021, doi: 10.3389/fimmu.2021.770390.

[319] L. Li, J. Zhou, X. Dong, Q. Liao, D. Zhou, and Y. Zhou, "Dendritic cell vaccines for glioblastoma fail to complete clinical translation: Bottlenecks and potential countermeasures," *Int. Immunopharmacol.*, vol. 109, p. 108929, Aug. 2022, doi: 10.1016/J.INTIMP.2022.108929.

[320] Z. Turkalp, J. Karamchandani, S. Das, S. Labatt Brain, K. Research Centre, and L. Ka Shing, "IDH Mutation in Glioma: New Insights and Promises for the Future," *JAMA Neurol.*, vol. 71, no. 10, pp. 1319–1325, Oct. 2014, doi: 10.1001/JAMANEUROL.2014.1205.

[321] S. Han *et al.*, "IDH mutation in glioma: molecular mechanisms and potential therapeutic targets," *Br. J. Cancer*, vol. 122, no. 11, pp. 1580–1589, 2020, doi: 10.1038/s41416-020-0814-x.

[322] S. Cai, J. X. Lu, Y. P. Wang, C. J. Shi, T. Yuan, and X. P. Wang, "SH2B3, Transcribed by STAT1, Promotes Glioblastoma Progression Through Transducing IL-6/gp130 Signaling to Activate STAT3 Signaling," *Front. Cell Dev. Biol.*, vol. 9, no. April, pp. 1–14, 2021, doi: 10.3389/fcell.2021.606527.

[323] M. Zalles *et al.*, "Optimized monoclonal antibody treatment against ELTD1 for GBM in a G55 xenograft mouse model," *J. Cell. Mol. Med.*, vol. 24, no. 2, pp. 1738–1749, Jan. 2020, doi: 10.1111/JCMM.14867.

[324] J. Ziegler *et al.*, "Targeting ELTD1, an angiogenesis marker for glioblastoma (GBM), also affects VEGFR2: molecular-targeted MRI assessment," *Am. J. Nucl. Med. Mol.*

Imaging, vol. 9, no. 1, p. 93, 2019.

[325] A. Qin, A. Musket, P. R. Musich, J. B. Schweitzer, and Q. Xie, "Receptor tyrosine kinases as druggable targets in glioblastoma: Do signaling pathways matter?," *Neuro-Oncology Adv.*, vol. 3, no. 1, pp. 1–12, 2021, doi: 10.1093/noajnl/vdab133.

[326] J. A. Benitez *et al.*, "PTEN regulates glioblastoma oncogenesis through chromatin-associated complexes of DAXX and histone H3.3," *Nat. Commun.*, vol. 8, no. May 2017, pp. 1–14, 2017, doi: 10.1038/ncomms15223.

[327] D. Wu, Y. Qiu, Y. Jiao, Z. Qiu, and D. Liu, "Small Molecules Targeting HATs, HDACs, and BRDs in Cancer Therapy," *Front. Oncol.*, vol. 10, no. November, pp. 1–14, 2020, doi: 10.3389/fonc.2020.560487.

[328] F. Khathayer, "85P Mocetinostat (MGCD0103) or MG0103 is an isotype-selective histone deacetylase (HDAC) inhibitor induce apoptosis and suppress tumor in glioblastoma cell lines C6 and T98G," *Ann. Oncol.*, vol. 33, p. S1409, Oct. 2022, doi: 10.1016/j.annonc.2022.09.086.

[329] A. M. Jermakowicz *et al.*, "The novel BET inhibitor UM-002 reduces glioblastoma cell proliferation and invasion," *Sci. Rep.*, vol. 11, no. 1, pp. 1–14, 2021, doi: 10.1038/s41598-021-02584-6.

[330] Y. Li *et al.*, "miR-148-3p Inhibits Growth of Glioblastoma Targeting DNA Methyltransferase-1 (DNMT1)," *Oncol. Res.*, vol. 27, no. 8, p. 911, Aug. 2019, doi: 10.3727/096504019X15516966905337.

[331] L. Qiu, Y. Meng, and J. Han, "STING cg16983159 methylation: a key factor for glioblastoma immunosuppression," *Signal Transduct. Target. Ther. 2022 71*, vol. 7, no. 1, pp. 1–3, Jul. 2022, doi: 10.1038/s41392-022-01093-w.

[332] S. Maksoud, "The role of the ubiquitin proteasome system in glioma: analysis emphasizing the main molecular players and therapeutic strategies identified in glioblastoma multiforme.," *Mol. Neurobiol.*, vol. 58, no. 7, p. 3252, Jul. 2021, doi: 10.1007/S12035-021-02339-4.

[333] B. M. Fox *et al.*, "SUMOylation in glioblastoma: A novel therapeutic target," *Int. J. Mol. Sci.*, vol. 20, no. 8, 2019, doi: 10.3390/ijms20081853.

[334] M. Lara-Velazquez *et al.*, "Advances in brain tumor surgery for glioblastoma in adults," *Brain Sci.*, vol. 7, no. 12, pp. 1–16, 2017, doi: 10.3390/brainsci7120166.

[335] D. Laurent *et al.*, "Impact of Extent of Resection on Incidence of Postoperative Complications in Patients With Glioblastoma," *Neurosurgery*, vol. 86, no. 5, pp. 625–630, May 2020, doi: 10.1093/NEUROS/NYZ313.

[336] S. Kumari, R. Gupta, R. K. Ambasta, and P. Kumar, “Multiple therapeutic approaches of glioblastoma multiforme: From terminal to therapy,” *Biochim. Biophys. Acta - Rev. Cancer*, vol. 1878, no. 4, p. 188913, 2023, doi: 10.1016/j.bbcan.2023.188913.

[337] H. Zhang, R. Wang, Y. Yu, J. Liu, T. Luo, and F. Fan, “Glioblastoma treatment modalities besides surgery,” *J. Cancer*, vol. 10, no. 20, pp. 4793–4806, 2019, doi: 10.7150/jca.32475.

[338] V. Rajaratnam, M. M. Islam, M. Yang, R. Slaby, H. M. Ramirez, and S. P. Mirza, “Glioblastoma : Pathogenesis and Current Status of,” *Cancers (Basel).*, vol. 12, no. 937, pp. 1–28, 2020.

[339] E. P. Sulman *et al.*, “Radiation therapy for glioblastoma: American Society of Clinical Oncology clinical practice guideline endorsement of the American Society for Radiation Oncology guideline,” *J. Clin. Oncol.*, vol. 35, no. 3, pp. 361–369, 2017, doi: 10.1200/JCO.2016.70.7562.

[340] P. Ciammella *et al.*, “Hypo-fractionated IMRT for patients with newly diagnosed glioblastoma multiforme: A 6 year single institutional experience,” *Clin. Neurol. Neurosurg.*, vol. 115, no. 9, pp. 1609–1614, 2013, doi: 10.1016/j.clineuro.2013.02.001.

[341] N. S. Floyd *et al.*, “Hypofractionated intensity-modulated radiotherapy for primary glioblastoma multiforme,” *Int. J. Radiat. Oncol. Biol. Phys.*, vol. 58, no. 3, pp. 721–726, 2004, doi: 10.1016/S0360-3016(03)01623-7.

[342] D. J. Gessler, C. Ferreira, K. Dusenbery, and C. C. Chen, “GammaTile®: Surgically targeted radiation therapy for glioblastomas,” *Futur. Oncol.*, vol. 16, no. 30, pp. 2445–2455, 2020, doi: 10.2217/fon-2020-0558.

[343] J. Park *et al.*, “Effect of combined anti-PD-1 and temozolomide therapy in glioblastoma,” *Oncoimmunology*, vol. 8, no. 1, Jan. 2018, doi: 10.1080/2162402X.2018.1525243.

[344] B. D. Choi *et al.*, “Immunotherapy for Glioblastoma : Adoptive T-cell Strategies,” vol. 25, no. 7, pp. 2042–2048, 2019, doi: 10.1158/1078-0432.CCR-18-1625.Immunotherapy.

[345] S. J. Bagley, A. S. Desai, G. P. Linette, C. H. June, and D. M. O’Rourke, “CAR T-cell therapy for glioblastoma: Recent clinical advances and future challenges,” *Neuro. Oncol.*, vol. 20, no. 11, pp. 1429–1438, 2018, doi: 10.1093/neuonc/noy032.

[346] E. A. Chong *et al.*, “PD-1 blockade modulates chimeric antigen receptor (CAR)-modified T cells: refueling the CAR,” *Blood*, vol. 129, no. 8, pp. 1039–1041, Feb. 2017, doi: 10.1182/BLOOD-2016-09-738245.

[347] M. Saxena, S. H. van der Burg, C. J. M. Melief, and N. Bhardwaj, “Therapeutic cancer vaccines,” *Nat. Rev. Cancer*, vol. 21, no. 6, pp. 360–378, Jun. 2021, doi: 10.1038/S41568-021-00346-0.

[348] M. Weller *et al.*, “Assessment and prognostic significance of the epidermal growth factor receptor vIII mutation in glioblastoma patients treated with concurrent and adjuvant temozolomide radiochemotherapy,” *Int. J. cancer*, vol. 134, no. 10, pp. 2437–2447, May 2014, doi: 10.1002/IJC.28576.

[349] A. R. Safa, M. R. Saadatzadeh, A. A. Cohen-Gadol, K. E. Pollok, and K. Bijangi-Vishehsaraei, “Emerging targets for glioblastoma stem cell therapy,” *J. Biomed. Res.*, vol. 30, no. 1, p. 19, 2016, doi: 10.7555/JBR.30.20150100.

[350] H. S. Kim and D. Y. Lee, “Nanomedicine in Clinical Photodynamic Therapy for the Treatment of Brain Tumors,” *Biomedicines*, vol. 10, no. 1, pp. 1–26, 2022, doi: 10.3390/biomedicines10010096.

[351] A. P. Michael, N. Nordmann, M. S. Zaghloul, and R. E. Kast, “5-Aminolevulinic acid radiodynamic therapy for treatment of high-grade gliomas,” *Horizons Cancer Res. Vol. 80*, vol. 80, no. 3, pp. 155–194, 2021, doi: 10.1007/s11060-019-03103-4.5-Aminolevulinic.

[352] E. S. Ara, A. V. Noghreiyan, and A. Sazgarnia, “Evaluation of photodynamic effect of Indocyanine green (ICG) on the colon and glioblastoma cancer cell lines pretreated by cold atmospheric plasma,” *Photodiagnosis Photodyn. Ther.*, vol. 35, p. 102408, Sep. 2021, doi: 10.1016/J.PDPDT.2021.102408.

[353] J. Li, W. Wang, J. Wang, Y. Cao, S. Wang, and J. Zhao, “Viral Gene Therapy for Glioblastoma Multiforme: A Promising Hope for the Current Dilemma,” *Front. Oncol.*, vol. 11, p. 1819, May 2021, doi: 10.3389/FONC.2021.678226/XML/NLM.

[354] T. F. Cloughesy *et al.*, “Effect of Vocimagene Amiretrorepvec in Combination With Flucytosine vs Standard of Care on Survival Following Tumor Resection in Patients With Recurrent High-Grade Glioma: A Randomized Clinical Trial,” *JAMA Oncol.*, vol. 6, no. 12, pp. 1939–1946, Dec. 2020, doi: 10.1001/JAMAONCOL.2020.3161.

[355] H. Yin, W. Xue, and D. G. Anderson, “CRISPR–Cas: a tool for cancer research and therapeutics,” *Nat. Rev. Clin. Oncol. 2019 165*, vol. 16, no. 5, pp. 281–295, Jan. 2019, doi: 10.1038/s41571-019-0166-8.

[356] X. Kang *et al.*, “Progresses, Challenges, and Prospects of CRISPR/Cas9 Gene-Editing in Glioma Studies,” pp. 1–15, 2023.

[357] J. J. Rodvold *et al.*, “IRE1α and IGF signaling predict resistance to an endoplasmic

reticulum stress-inducing drug in glioblastoma cells," *Sci. Rep.*, vol. 10, no. 1, pp. 1–12, 2020, doi: 10.1038/s41598-020-65320-6.

[358] Y. Liu *et al.*, "Charge Conversional Biomimetic Nanocomplexes as a Multifunctional Platform for Boosting Orthotopic Glioblastoma RNAi Therapy," *Nano Lett.*, vol. 20, no. 3, pp. 1637–1646, Mar. 2020, doi: 10.1021/ACS.NANOLETT.9B04683/SUPPL_FILE/NL9B04683_SI_001.PDF.

[359] Q. Zhang *et al.*, "Anti-inflammatory and Antioxidative Effects of Tetrahedral DNA Nanostructures via the Modulation of Macrophage Responses," *ACS Appl. Mater. Interfaces*, vol. 10, no. 4, pp. 3421–3430, Jan. 2018, doi: 10.1021/ACSAMI.7B17928.

[360] S. Saeb, J. Van Assche, T. Loustau, O. Rohr, C. Wallet, and C. Schwartz, "Suicide gene therapy in cancer and HIV-1 infection: An alternative to conventional treatments," *Biochem. Pharmacol.*, vol. 197, p. 114893, Mar. 2022, doi: 10.1016/J.BCP.2021.114893.

[361] A. J. Villatoro *et al.*, "Suicide gene therapy by canine mesenchymal stem cell transduced with thymidine kinase in a u-87 glioblastoma murine model: Secretory profile and antitumor activity," *PLoS One*, vol. 17, no. 2 February, pp. 1–16, 2022, doi: 10.1371/journal.pone.0264001.

[362] A. Loskog, "Immunostimulatory Gene Therapy Using Oncolytic Viruses as Vehicles," *Viruses*, vol. 7, no. 11, p. 5780, Nov. 2015, doi: 10.3390/V7112899.

[363] O. Draghiciu, H. W. Nijman, B. N. Hoogeboom, T. Meijerhof, and T. Daemen, "Sunitinib depletes myeloid-derived suppressor cells and synergizes with a cancer vaccine to enhance antigen-specific immune responses and tumor eradication," *Oncoimmunology*, vol. 4, no. 3, pp. 1–11, 2015, doi: 10.4161/2162402X.2014.989764.

[364] L. van Hooren *et al.*, "Agonistic CD40 therapy induces tertiary lymphoid structures but impairs responses to checkpoint blockade in glioma," *Nat. Commun.*, vol. 12, no. 1, 2021, doi: 10.1038/s41467-021-24347-7.

[365] T. Shi, X. Song, Y. Wang, F. Liu, and J. Wei, "Combining Oncolytic Viruses With Cancer Immunotherapy: Establishing a New Generation of Cancer Treatment," *Front. Immunol.*, vol. 11, Apr. 2020, doi: 10.3389/FIMMU.2020.00683.

[366] J. Zeng, X. Li, M. Sander, H. Zhang, G. Yan, and Y. Lin, "Oncolytic Viro-Immunotherapy: An Emerging Option in the Treatment of Gliomas," *Front. Immunol.*, vol. 12, Oct. 2021, doi: 10.3389/FIMMU.2021.721830.

[367] A. C. Tan, D. M. Ashley, G. Y. López, M. Malinzak, H. S. Friedman, and M. Khasraw, "Management of glioblastoma: State of the art and future directions," *CA. Cancer J.*

Clin., vol. 70, no. 4, pp. 299–312, Jul. 2020, doi: 10.3322/CAAC.21613.

[368] A. G. Atanasov *et al.*, "Natural products in drug discovery: advances and opportunities," *Nat. Rev. Drug Discov. 2021 203*, vol. 20, no. 3, pp. 200–216, Jan. 2021, doi: 10.1038/s41573-020-00114-z.

[369] M. Huang, J. J. Lu, and J. Ding, "Natural Products in Cancer Therapy: Past, Present and Future," *Nat. Products Bioprospect.*, vol. 11, no. 1, pp. 5–13, Feb. 2021, doi: 10.1007/S13659-020-00293-7/FIGURES/4.

[370] R. Vengoji, M. A. Macha, S. K. Batra, and N. A. Shonka, "Natural products: a hope for glioblastoma patients," *Oncotarget*, vol. 9, no. 31, p. 22194, Apr. 2018, doi: 10.18632/ONCOTARGET.25175.

[371] B. L. Santos *et al.*, "Flavonoids suppress human glioblastoma cell growth by inhibiting cell metabolism, migration, and by regulating extracellular matrix proteins and metalloproteinases expression," *Chem. Biol. Interact.*, vol. 242, pp. 123–138, Dec. 2015, doi: 10.1016/J.CBI.2015.07.014.

[372] M. Soukhtanloo *et al.*, "Natural products as promising targets in glioblastoma multiforme: a focus on NF-κB signaling pathway," *Pharmacol. Rep.*, vol. 72, no. 2, pp. 285–295, Apr. 2020, doi: 10.1007/S43440-020-00081-7.

[373] K. Zhai, M. Siddiqui, B. Abdellatif, A. Liskova, P. Kubatka, and D. Büsselberg, "Natural Compounds in Glioblastoma Therapy: Preclinical Insights, Mechanistic Pathways, and Outlook," *Cancers (Basel).*, vol. 13, no. 10, May 2021, doi: 10.3390/CANCERS13102317.

[374] G. Jiang, L. Zhang, J. Wang, and H. Zhou, "Animal Cells and Systems Baicalein induces the apoptosis of U251 glioblastoma cell lines via the NF-kB-p65-mediated mechanism Baicalein induces the apoptosis of U251 glioblastoma cell lines via the NF-kB-p65-mediated mechanism," 2016, doi: 10.1080/19768354.2016.1229216.

[375] K. Zhai, A. Mazurakova, L. Koklesova, P. Kubatka, and D. Büsselberg, "Flavonoids Synergistically Enhance the Anti-Glioblastoma Effects of Chemotherapeutic Drugs," *Biomolecules*, vol. 11, no. 12, Dec. 2021, doi: 10.3390/BIOM11121841.

[376] J. P. Zhang, J. A. Gallego, D. G. Robinson, A. K. Malhotra, J. M. Kane, and C. U. Correll, "Efficacy and safety of individual second-generation vs. first-generation antipsychotics in first-episode psychosis: a systematic review and meta-analysis," *Int. J. Neuropsychopharmacol.*, vol. 16, no. 6, pp. 1205–1218, Jul. 2013, doi: 10.1017/S1461145712001277.

[377] M. Persico *et al.*, "Tackling the Behavior of Cancer Cells: Molecular Bases for

Repurposing Antipsychotic Drugs in the Treatment of Glioblastoma," *Cells*, vol. 11, no. 2, 2022, doi: 10.3390/cells11020263.

[378] R. E. Kast, G. Karpel-Massler, and M. E. Halatsch, "Can the therapeutic effects of temozolomide be potentiated by stimulating AMP-activated protein kinase with olanzepine and metformin?," *Br. J. Pharmacol.*, vol. 164, no. 5, p. 1393, Nov. 2011, doi: 10.1111/J.1476-5381.2011.01320.X.

[379] E. FREI *et al.*, "A comparative study of two regimens of combination chemotherapy in acute leukemia.," *Blood*, 1958, doi: 10.1182/blood.v13.12.1126.1126.

[380] D. A. Yardley, "Drug Resistance and the Role of Combination Chemotherapy in Improving Patient Outcomes," *Int. J. Breast Cancer*, 2013, doi: 10.1155/2013/137414.

[381] P. A. Ascierto and F. M. Marincola, "Combination therapy: The next opportunity and challenge of medicine," *Journal of Translational Medicine*. 2011, doi: 10.1186/1479-5876-9-115.

[382] L. Paz-Ares *et al.*, "Durvalumab plus platinum–etoposide versus platinum–etoposide in first-line treatment of extensive-stage small-cell lung cancer (CASPIAN): a randomised, controlled, open-label, phase 3 trial," *Lancet*, 2019, doi: 10.1016/S0140-6736(19)32222-6.

[383] M. D. Hellmann *et al.*, "Nivolumab plus Ipilimumab in Advanced Non–Small-Cell Lung Cancer," *N. Engl. J. Med.*, 2019, doi: 10.1056/nejmoa1910231.

[384] T. Yau *et al.*, "Efficacy and Safety of Nivolumab plus Ipilimumab in Patients with Advanced Hepatocellular Carcinoma Previously Treated with Sorafenib: The CheckMate 040 Randomized Clinical Trial," *JAMA Oncol.*, 2020, doi: 10.1001/jamaoncol.2020.4564.

[385] A. Scherpereel *et al.*, "Nivolumab or nivolumab plus ipilimumab in patients with relapsed malignant pleural mesothelioma (IFCT-1501 MAPS2): a multicentre, open-label, randomised, non-comparative, phase 2 trial," *Lancet Oncol.*, 2019, doi: 10.1016/S1470-2045(18)30765-4.

[386] F. Chen, Z. Zhang, Y. Yu, Q. Liu, and F. Pu, "HSulf-1 and palbociclib exert synergistic antitumor effects on RB-positive triple-negative breast cancer," *Int. J. Oncol.*, 2020, doi: 10.3892/ijo.2020.5057.

[387] R. B. Mokhtari *et al.*, "Combination therapy in combating cancer," *Oncotarget*. 2017, doi: 10.18632/oncotarget.16723.

[388] US Food and Drug Administration, "FDA approves encorafenib in combination with cetuximab for metastatic colorectal cancer with a BRAF V600E mutation | FDA." .

[389] US Food and Drug Administration, “FDA approves neratinib for metastatic HER2-positive breast cancer | FDA.” .

[390] I. Ray-Coquard *et al.*, “Olaparib plus Bevacizumab as First-Line Maintenance in Ovarian Cancer,” *N. Engl. J. Med.*, 2019, doi: 10.1056/nejmoa1911361.

[391] “Eagle Pharmaceuticals, Inc. - Eagle Pharmaceuticals Receives Final FDA Approval for PEMFEXY™ (Pemetrexed for Injection).” .

[392] B. I. Rini *et al.*, “Pembrolizumab plus Axitinib versus Sunitinib for Advanced Renal-Cell Carcinoma,” *N. Engl. J. Med.*, 2019, doi: 10.1056/nejmoa1816714.

[393] V. Makker *et al.*, “Lenvatinib plus pembrolizumab in patients with advanced endometrial cancer: an interim analysis of a multicentre, open-label, single-arm, phase 2 trial,” *Lancet Oncol.*, 2019, doi: 10.1016/S1470-2045(19)30020-8.

[394] R. J. Motzer *et al.*, “Avelumab plus Axitinib versus Sunitinib for Advanced Renal-Cell Carcinoma,” *N. Engl. J. Med.*, 2019, doi: 10.1056/nejmoa1816047.

[395] US Food and Drug Administration, “FDA approves polatuzumab vedotin-piiq for diffuse large B-cell lymphoma | FDA.” .

[396] H. West *et al.*, “Atezolizumab in combination with carboplatin plus nab-paclitaxel chemotherapy compared with chemotherapy alone as first-line treatment for metastatic non-squamous non-small-cell lung cancer (IMpower130): a multicentre, randomised, open-label, phase 3 tria,” *Lancet Oncol.*, 2019, doi: 10.1016/S1470-2045(19)30167-6.

[397] US Food and Drug Administration, “FDA approves atezolizumab with nab-paclitaxel and carboplatin for metastatic NSCLC without EGFR/ALK aberrations | FDA.” .

[398] A. S. Mansfield *et al.*, “Safety and patient-reported outcomes of atezolizumab, carboplatin, and etoposide in extensive-stage small-cell lung cancer (IMpower133): a randomized phase I/III trial,” *Ann. Oncol.*, 2020, doi: 10.1016/j.annonc.2019.10.021.

[399] S. Kopetz *et al.*, “ Encorafenib, Binimetinib, and Cetuximab in BRAF V600E–Mutated Colorectal Cancer ,” *N. Engl. J. Med.*, 2019, doi: 10.1056/nejmoa1908075.

[400] P. Schmid *et al.*, “Atezolizumab and Nab-Paclitaxel in Advanced Triple-Negative Breast Cancer,” *N. Engl. J. Med.*, 2018, doi: 10.1056/nejmoa1809615.

[401] L. Gandhi *et al.*, “Pembrolizumab plus Chemotherapy in Metastatic Non–Small-Cell Lung Cancer,” *N. Engl. J. Med.*, 2018, doi: 10.1056/nejmoa1801005.

[402] US Food and Drug Administration, “FDA grants regular approval for pembrolizumab in combination with chemotherapy for first-line treatment of metastatic nonsquamous NSCLC | FDA.” .

[403] US Food and Drug Administration, “FDA approves atezolizumab with chemotherapy

and bevacizumab for first-line treatment of metastatic non-squamous NSCLC | FDA.” .

[404] US Food and Drug Administration, “FDA approves bevacizumab in combination with chemotherapy for ovarian cancer | FDA.” .

[405] Drugs.com, “FDA Approves Imbruvica (ibrutinib) Plus Rituximab for Patients with Waldenström’s Macroglobulinemia.” .

[406] US Food and Drug Administration, “FDA approves nivolumab plus ipilimumab combination for intermediate or poor-risk advanced renal cell carcinoma | FDA.” .

[407] M. J. Overman *et al.*, “Durable clinical benefit with nivolumab plus ipilimumab in DNA mismatch repair-deficient/microsatellite instability-high metastatic colorectal cancer,” *J. Clin. Oncol.*, 2018, doi: 10.1200/JCO.2017.76.9901.

[408] A. Chari *et al.*, “Daratumumab plus pomalidomide and dexamethasone in relapsed and/or refractory multiple myeloma,” *Blood*, 2017, doi: 10.1182/blood-2017-05-785246.

[409] A. C. Krauss *et al.*, “FDA approval summary: (daunorubicin and cytarabine) liposome for injection for the treatment of adults with high-risk acute myeloid leukemia,” *Clin. Cancer Res.*, 2019, doi: 10.1158/1078-0432.CCR-18-2990.

[410] T. Robak *et al.*, “Ofatumumab plus fludarabine and cyclophosphamide in relapsed chronic lymphocytic leukemia: results from the COMPLEMENT 2 trial,” *Leuk. Lymphoma*, 2017, doi: 10.1080/10428194.2016.1233536.

[411] “FDA Approves Tafinlar+Mekinist Combo for Melanoma,” *Oncol. Times*, 2016, doi: 10.1097/01.cot.0000480920.25709.4e.

[412] “Opdivo-Yervoy Combination Approved for Melanoma—First Combination-Immunotherapy Regimen for Cancer,” *Oncol. Times*, 2015, doi: 10.1097/01.cot.0000473604.35674.ee.

[413] “Portrazza (Necitumumab), an IgG1 Monoclonal Antibody, FDA Approved for Advanced Squamous Non–Small-Cell Lung Cancer.” .

[414] M. W. Saif, “U.S. food and drug administration approves paclitaxel protein-bound particles (Abraxane®) in combination with gemcitabine as first-line treatment of patients with metastatic pancreatic cancer,” *Journal of the Pancreas*. 2013, doi: 10.6092/1590-8577/2028.

[415] M. H. Cohen, J. R. Johnson, and R. Pazdur, “Food and drug administration drug approval summary: Temozolomide plus radiation therapy for the treatment of newly diagnosed glioblastoma multiforme,” *Clin. Cancer Res.*, 2005, doi: 10.1158/1078-0432.CCR-05-0722.

[416] G. Pillai, “Nanomedicines for Cancer Therapy: An Update of FDA Approved and Those under Various Stages of Development,” *SOJ Pharm. Pharm. Sci.*, 2014, doi: 10.15226/2374-6866/1/2/00109.

[417] U. Herrlinger *et al.*, “Lomustine-temozolomide combination therapy versus standard temozolomide therapy in patients with newly diagnosed glioblastoma with methylated MGMT promoter (CeTeG/NOA–09): a randomised, open-label, phase 3 trial,” *Lancet*, vol. 393, no. 10172, pp. 678–688, Feb. 2019, doi: 10.1016/S0140-6736(18)31791-4.

[418] J. Biau *et al.*, “Phase 1 trial of ralimetinib (LY2228820) with radiotherapy plus concomitant temozolomide in the treatment of newly diagnosed glioblastoma,” *Radiother. Oncol.*, vol. 154, pp. 227–234, Jan. 2021, doi: 10.1016/J.RADONC.2020.09.036.

[419] G. L. Gallia *et al.*, “Mebendazole and temozolomide in patients with newly diagnosed high-grade gliomas: results of a phase 1 clinical trial,” *Neuro-oncology Adv.*, vol. 3, no. 1, pp. 1–8, Jan. 2021, doi: 10.1093/NOAJNL/VDAA154.

[420] S. P. Weathers *et al.*, “Results of a phase I trial to assess the safety of macitentan in combination with temozolomide for the treatment of recurrent glioblastoma,” *Neuro-oncology Adv.*, vol. 3, no. 1, pp. 1–12, Jan. 2021, doi: 10.1093/NOAJNL/VDAB141.

[421] M. Sun *et al.*, “The efficacy of temozolomide combined with levetiracetam for glioblastoma (GBM) after surgery: a study protocol for a double-blinded and randomized controlled trial,” *Trials*, vol. 23, no. 1, Dec. 2022, doi: 10.1186/S13063-022-06168-1.

[422] Z. Wang, F. Du, Y. Ren, and W. Jiang, “Treatment of MGMT promoter unmethylated glioblastoma with PD-1 inhibitor combined with anti-angiogenesis and epidermal growth factor receptor tyrosine kinase inhibitor: a case report,” *Ann. Transl. Med.*, vol. 9, no. 19, pp. 1508–1508, Oct. 2021, doi: 10.21037/ATM-21-4625.

[423] S. D. Lustig, S. K. Kodali, S. L. Longo, S. Kundu, and M. S. Viapiano, “Ko143 Reverses MDR in Glioblastoma via Deactivating P-Glycoprotein, Sensitizing a Resistant Phenotype to TMZ Treatment,” *Anticancer Res.*, vol. 42, no. 2, pp. 723–730, Feb. 2022, doi: 10.21873/ANTICANRES.15530.

[424] S. W. Van Gool, J. Makalowski, M. Bitar, P. Van de Vliet, V. Schirrmacher, and W. Stuecker, “Synergy between TMZ and individualized multimodal immunotherapy to improve overall survival of IDH1 wild-type MGMT promoter-unmethylated GBM patients,” *Genes Immun.*, vol. 23, no. 8, p. 255, Dec. 2022, doi: 10.1038/S41435-022-00162-Y.

[425] R. Serra *et al.*, “Combined intracranial Acriflavine, temozolomide and radiation extends survival in a rat glioma model,” *Eur. J. Pharm. Biopharm.*, vol. 170, pp. 179–186, Jan. 2022, doi: 10.1016/J.EJPB.2021.12.011.

[426] M. Momeny *et al.*, “Cediranib, a pan-inhibitor of vascular endothelial growth factor receptors, inhibits proliferation and enhances therapeutic sensitivity in glioblastoma cells,” *Life Sci.*, vol. 287, p. 120100, Dec. 2021, doi: 10.1016/J.LFS.2021.120100.

[427] R. Amini, H. Karami, and M. Bayat, “Combination Therapy with PIK3R3-siRNA and EGFR-TKI Erlotinib Synergistically Suppresses Glioblastoma Cell Growth In Vitro,” *Asian Pac. J. Cancer Prev.*, vol. 22, no. 12, p. 3993, 2021, doi: 10.31557/APJCP.2021.22.12.3993.

[428] J. Gasparello *et al.*, “Treatment of Human Glioblastoma U251 Cells with Sulforaphane and a Peptide Nucleic Acid (PNA) Targeting miR-15b-5p: Synergistic Effects on Induction of Apoptosis,” *Molecules*, vol. 27, no. 4, Feb. 2022, doi: 10.3390/MOLECULES27041299.

[429] E. Seydi, H. Sadeghi, M. Ramezani, L. Mehrpouya, and J. Pourahmad, “Selective Toxicity Effect of Fatty Acids Omega-3, 6 and 9 Combination on Glioblastoma Neurons through their Mitochondria,” *Drug Res. (Stuttg).*, vol. 72, no. 2, pp. 94–99, Feb. 2022, doi: 10.1055/A-1640-8561/ID/R2021-08-2345-0036.

[430] M. A. ALTINOZ *et al.*, “Ulipristal-temozolomide-hydroxyurea combination for glioblastoma: in-vitro studies,” *J. Neurosurg. Sci.*, Jun. 2022, doi: 10.23736/S0390-5616.22.05718-6.

[431] S. Daisy Precilla, S. S. Kuduvalli, E. Angeline Praveena, S. Thangavel, and T. S. Anitha, “Integration of synthetic and natural derivatives revives the therapeutic potential of temozolomide against glioma- an in vitro and in vivo perspective,” *Life Sci.*, vol. 301, p. 120609, Jul. 2022, doi: 10.1016/J.LFS.2022.120609.

[432] A. R. Alexanian and A. Brannon, “Unique combinations of epigenetic modifiers synergistically impair the viability of the U87 glioblastoma cell line while exhibiting minor or moderate effects on normal stem cell growth,” *Med. Oncol.*, vol. 39, no. 5, pp. 1–5, May 2022, doi: 10.1007/S12032-022-01683-2/FIGURES/2.

[433] J. Guo *et al.*, “A rational foundation for micheliolide-based combination strategy by targeting redox and metabolic circuit in cancer cells,” *Biochem. Pharmacol.*, vol. 200, p. 115037, Jun. 2022, doi: 10.1016/J.BCP.2022.115037.

[434] A. Tancredi *et al.*, “BET protein inhibition sensitizes glioblastoma cells to temozolomide treatment by attenuating MGMT expression,” *Cell Death Dis.*, vol. 13,

no. 12, Dec. 2022, doi: 10.1038/S41419-022-05497-Y.

[435] G. Lu *et al.*, "Postmortem study of organ-specific toxicity in glioblastoma patients treated with a combination of temozolomide, irinotecan and bevacizumab," *J. Neurooncol.*, vol. 160, no. 1, pp. 221–231, Oct. 2022, doi: 10.1007/S11060-022-04144-Y/TABLES/3.

[436] G. Cerretti *et al.*, "Impressive response to dabrafenib and trametinib plus silybin in a heavily pretreated IDH wild-type glioblastoma patient with BRAFV600E -mutant and SOX2 amplification," *Anticancer. Drugs*, vol. 34, no. 1, pp. 190–193, Jan. 2023, doi: 10.1097/CAD.0000000000001376.

[437] M. Chakravarty, P. Ganguli, M. Murahari, R. R. Sarkar, G. J. Peters, and Y. C. Mayur, "Study of Combinatorial Drug Synergy of Novel Acridone Derivatives With Temozolomide Using in-silico and in-vitro Methods in the Treatment of Drug-Resistant Glioma," *Front. Oncol.*, vol. 11, p. 625899, Mar. 2021, doi: 10.3389/FONC.2021.625899/FULL.

[438] B. Goker Bagca, N. P. Ozates, A. Asik, H. O. Caglar, C. Gunduz, and C. Biray Avci, "Temozolomide treatment combined with AZD3463 shows synergistic effect in glioblastoma cells," *Biochem. Biophys. Res. Commun.*, vol. 533, no. 4, pp. 1497–1504, Dec. 2020, doi: 10.1016/J.BBRC.2020.10.058.

[439] Y. Liu, X. Song, M. Wu, J. Wu, and J. Liu, " Synergistic Effects of Resveratrol and Temozolomide Against Glioblastoma Cells: Underlying Mechanism and Therapeutic Implications ," *Cancer Manag. Res.*, vol. 12, pp. 8341–8354, Sep. 2020, doi: 10.2147/CMAR.S258584.

[440] K. F. Chang *et al.*, "Cedrol, a Sesquiterpene Alcohol, Enhances the Anticancer Efficacy of Temozolomide in Attenuating Drug Resistance via Regulation of the DNA Damage Response and MGMT Expression," *J. Nat. Prod.*, vol. 83, no. 10, pp. 3021–3029, Oct. 2020, doi: 10.1021/ACS.JNATPROD.0C00580/ASSET/IMAGES/LARGE/NP0C00580_0007.JPEG.

[441] M. Orozco, R. A. Valdez, L. Ramos, M. Cabeza, J. Segovia, and M. C. Romano, "Dutasteride combined with androgen receptor antagonists inhibit glioblastoma U87 cell metabolism, proliferation, and invasion capacity: Androgen regulation," *Steroids*, vol. 164, p. 108733, Dec. 2020, doi: 10.1016/J.STEROIDS.2020.108733.

[442] J. Moskwa *et al.*, "Chemical composition of Polish propolis and its antiproliferative effect in combination with Bacopa monnieri on glioblastoma cell lines," *Sci. Rep.*, vol.

10, no. 1, p. 21127, Dec. 2020, doi: 10.1038/S41598-020-78014-W.

[443] Z. Abbaszade, B. G. Bagca, and C. B. Avci, "Molecular biological investigation of temozolomide and KC7F2 combination in U87MG glioma cell line," *Gene*, vol. 776, p. 145445, Apr. 2021, doi: 10.1016/J.GENE.2021.145445.

[444] H. H. Park *et al.*, "Combinatorial Therapeutic Effect of Inhibitors of Aldehyde Dehydrogenase and Mitochondrial Complex I, and the Chemotherapeutic Drug, Temozolomide against Glioblastoma Tumorspheres," *Molecules*, vol. 26, no. 2, Jan. 2021, doi: 10.3390/MOLECULES26020282.

[445] L. Korsakova, J. A. Krasko, and E. Stankevicius, "Metabolic-targeted Combination Therapy With Dichloroacetate and Metformin Suppresses Glioblastoma Cell Line Growth In Vitro and In Vivo," *In Vivo (Brooklyn).*, vol. 35, no. 1, p. 341, Jan. 2021, doi: 10.21873/INVIVO.12265.

[446] H. fu Zhao *et al.*, "Synergism between the phosphatidylinositol 3-kinase p110β isoform inhibitor AZD6482 and the mixed lineage kinase 3 inhibitor URMC-099 on the blockade of glioblastoma cell motility and focal adhesion formation," *Cancer Cell Int.*, vol. 21, no. 1, Dec. 2021, doi: 10.1186/S12935-020-01728-4.

[447] E. I. Essien, T. P. Hofer, M. J. Atkinson, and N. Anastasov, "Combining HDAC and MEK Inhibitors with Radiation against Glioblastoma-Derived Spheres," *Cells*, vol. 11, no. 5, Mar. 2022, doi: 10.3390/CELLS11050775/S1.

[448] J. Chen *et al.*, "Exploring the mechanism of cordycepin combined with doxorubicin in treating glioblastoma based on network pharmacology and biological verification," *PeerJ*, vol. 10, Feb. 2022, doi: 10.7717/PEERJ.12942/SUPP-15.

[449] J. Xu *et al.*, "Disruption of DNA Repair and Survival Pathways through Heat Shock Protein inhibition by Onalespib to Sensitize Malignant Gliomas to Chemoradiation therapy," *Clin. Cancer Res.*, vol. 28, no. 9, p. 1979, May 2022, doi: 10.1158/1078-0432.CCR-20-0468.

[450] P. Xu, H. Wang, H. Pan, J. Chen, and C. Deng, "Anlotinib combined with temozolomide suppresses glioblastoma growth via mediation of JAK2/STAT3 signaling pathway," *Cancer Chemother. Pharmacol.*, vol. 89, no. 2, p. 183, Feb. 2022, doi: 10.1007/S00280-021-04380-5.

[451] T. Surarak, P. Chantree, and K. Sangpairoj, "Synergistic Effects of Taurine and Temozolomide Via Cell Proliferation Inhibition and Apoptotic Induction on U-251 MG Human Glioblastoma Cells," *Asian Pac. J. Cancer Prev.*, vol. 22, no. 12, p. 4001, 2021, doi: 10.31557/APJCP.2021.22.12.4001.

[452] A. Sumiyoshi *et al.*, "Pharmacological Strategy for Selective Targeting of Glioblastoma by Redox-active Combination Drug – Comparison With the Chemotherapeutic Standard-of-care Temozolomide," *Anticancer Res.*, vol. 41, no. 12, pp. 6067–6076, Dec. 2021, doi: 10.21873/ANTICANRES.15426.

[453] O. Pak, S. Zaitsev, V. Shevchenko, A. Sharma, H. S. Sharma, and I. Bryukhovetskiy, "Effectiveness of bortezomib and temozolomide for eradication of recurrent human glioblastoma cells, resistant to radiation," *Prog. Brain Res.*, vol. 266, pp. 195–209, Jan. 2021, doi: 10.1016/BS.PBR.2021.06.010.

[454] H. C. Tsai *et al.*, "Valproic Acid Enhanced Temozolomide-Induced Anticancer Activity in Human Glioma Through the p53–PUMA Apoptosis Pathway," *Front. Oncol.*, vol. 11, Oct. 2021, doi: 10.3389/FONC.2021.722754/FULL.

[455] Y. K. Su *et al.*, "Combined treatment with acalabrutinib and rapamycin inhibits glioma stem cells and promotes vascular normalization by downregulating btk/mtor/vegf signaling," *Pharmaceuticals*, vol. 14, no. 9, Sep. 2021, doi: 10.3390/PH14090876/S1.

[456] D. Yin *et al.*, "Celecoxib reverses the glioblastoma chemo-resistance to temozolomide through mitochondrial metabolism," *Aging (Albany NY)*, vol. 13, no. 17, p. 21268, Sep. 2021, doi: 10.18632/AGING.203443.

[457] P. Doan, P. Nguyen, A. Murugesan, N. R. Candeias, O. Yli-Harja, and M. Kandhavelu, "Alkylaminophenol and GPR17 agonist for glioblastoma therapy: A combinational approach for enhanced cell death activity," *Cells*, vol. 10, no. 8, Aug. 2021, doi: 10.3390/CELLS10081975/S1.

[458] A. Karami, M. Hossienpour, E. Mohammadi Noori, M. Rahpyma, K. Najafi, and A. Kiani, "Synergistic Effect of Gefitinib and Temozolomide on U87MG Glioblastoma Angiogenesis," *https://doi.org/10.1080/01635581.2021.1952441*, vol. 74, no. 4, pp. 1299–1307, 2021, doi: 10.1080/01635581.2021.1952441.

[459] A. Zając *et al.*, "LY294002 and sorafenib as inhibitors of intracellular survival pathways in the elimination of human glioma cells by programmed cell death," *Cell Tissue Res.*, vol. 386, no. 1, p. 17, Oct. 2021, doi: 10.1007/S00441-021-03481-0.

[460] M. I. Dorrell *et al.*, "A novel method of screening combinations of angiostatics identifies bevacizumab and temsirolimus as synergistic inhibitors of glioma-induced angiogenesis," *PLoS One*, vol. 16, no. 6, Jun. 2021, doi: 10.1371/JOURNAL.PONE.0252233.

[461] A. Salmaggi *et al.*, "Synergistic effect of perampanel and temozolomide in human glioma cell lines," *J. Pers. Med.*, vol. 11, no. 5, p. 390, May 2021, doi:

10.3390/JPM11050390/S1.

[462] B. Yuan *et al.*, "Cytotoxic Effects of Arsenite in Combination With Gamabufotalin Against Human Glioblastoma Cell Lines," *Front. Oncol.*, vol. 11, p. 628914, Mar. 2021, doi: 10.3389/FONC.2021.628914/FULL.

[463] Z. Su *et al.*, "Ciclopirox and bortezomib synergistically inhibits glioblastoma multiforme growth via simultaneously enhancing JNK/p38 MAPK and NF-κB signaling," *Cell Death Dis.*, vol. 12, no. 3, Mar. 2021, doi: 10.1038/S41419-021-03535-9.

[464] W. Jiao *et al.*, "ZSTK474 Sensitizes Glioblastoma to Temozolomide by Blocking Homologous Recombination Repair," *Biomed Res. Int.*, vol. 2022, 2022, doi: 10.1155/2022/8568528.

[465] R. M. Urbantat, C. Jelgersma, P. Vajkoczy, S. Brandenburg, and G. Acker, "Combining TMZ and SB225002 induces changes of CXCR2 and VEGFR signalling in primary human endothelial cells in vitro," *Oncol. Rep.*, vol. 48, no. 3, Sep. 2022, doi: 10.3892/OR.2022.8373.

[466] Ö. Öcal and M. Nazıroğlu, "Eicosapentaenoic acid enhanced apoptotic and oxidant effects of cisplatin via activation of TRPM2 channel in brain tumor cells," *Chem. Biol. Interact.*, vol. 359, p. 109914, May 2022, doi: 10.1016/J.CBI.2022.109914.

[467] A. Despotović *et al.*, "Combination of Ascorbic Acid and Menadione Induces Cytotoxic Autophagy in Human Glioblastoma Cells," *Oxid. Med. Cell. Longev.*, vol. 2022, 2022, doi: 10.1155/2022/2998132.

[468] S. W. Feng, P. C. Chang, H. Y. Chen, D. Y. Hueng, Y. F. Li, and S. M. Huang, "Exploring the Mechanism of Adjuvant Treatment of Glioblastoma Using Temozolomide and Metformin," *Int. J. Mol. Sci.*, vol. 23, no. 15, Aug. 2022, doi: 10.3390/IJMS23158171.

[469] K. Ertilav and M. Nazıroğlu, "Honey bee venom melittin increases the oxidant activity of cisplatin and kills human glioblastoma cells by stimulating the TRPM2 channel," *Toxicon*, vol. 222, p. 106993, Jan. 2023, doi: 10.1016/J.TOXICON.2022.106993.

[470] C. Y. Tsai *et al.*, "Nbm-bmx, an hdac8 inhibitor, overcomes temozolomide resistance in glioblastoma multiforme by downregulating the β-catenin/c-myc/sox2 pathway and upregulating p53-mediated mgmt inhibition," *Int. J. Mol. Sci.*, vol. 22, no. 11, p. 5907, Jun. 2021, doi: 10.3390/IJMS22115907/S1.

[471] M. B. Vera *et al.*, "Noxa and Mcl-1 expression influence the sensitivity to BH3-mimetics that target Bcl-xL in patient-derived glioma stem cells," *Sci. Rep.*, vol. 12, no. 1, Dec.

2022, doi: 10.1038/S41598-022-20910-4.

[472] B. Goker Bagca, N. P. Ozates, and C. Biray Avci, “Ruxolitinib enhances cytotoxic and apoptotic effects of temozolomide on glioblastoma cells by regulating WNT signaling pathway-related genes,” *Med. Oncol.*, vol. 40, no. 1, Jan. 2022, doi: 10.1007/S12032-022-01897-4.

[473] O. Doğanlar, Z. B. Doğanlar, S. Erdoğan, and E. Delen, “Antineoplastic multi-drug chemotherapy to sensitize tumors triggers multi-drug resistance and inhibits efficiency of maintenance treatment inglioblastoma cells,” *EXCLI J.*, vol. 22, p. 35, Jan. 2023, doi: 10.17179/EXCLI2022-5556.

[474] J. M. Han and H. J. Jung, “Synergistic Anticancer Effect of a Combination of Berbamine and Arcyriaflavin A against Glioblastoma Stem-like Cells,” *Molecules*, vol. 27, no. 22, Nov. 2022, doi: 10.3390/MOLECULES27227968/S1.

[475] J. B. Netto *et al.*, “Matteucinol combined with temozolomide inhibits glioblastoma proliferation, invasion, and progression: an in vitro, in silico, and in vivo study,” *Brazilian J. Med. Biol. Res.*, vol. 55, 2022, doi: 10.1590/1414-431X2022E12076.

[476] A. S. Karve *et al.*, “Potentiation of temozolomide activity against glioblastoma cells by aromatase inhibitor letrozole,” *Cancer Chemother. Pharmacol.*, vol. 90, no. 4, pp. 345–356, Oct. 2022, doi: 10.1007/S00280-022-04469-5/METRICS.

[477] S. Bin Jo, S. J. Sung, H. S. Choi, J. S. Park, Y. K. Hong, and Y. A. Joe, “Modulation of Autophagy is a Potential Strategy for Enhancing the Anti-Tumor Effect of Mebendazole in Glioblastoma Cells,” *Biomol. Ther. (Seoul).*, vol. 30, no. 6, p. 616, Nov. 2022, doi: 10.4062/BIOMOLTHER.2022.122.

[478] T. T. Lah *et al.*, “Cannabigerol Is a Potential Therapeutic Agent in a Novel Combined Therapy for Glioblastoma,” *Cells*, vol. 10, no. 2, pp. 1–22, Feb. 2021, doi: 10.3390/CELLS10020340.

[479] A. F. Cardona *et al.*, “Efficacy of osimertinib plus bevacizumab in glioblastoma patients with simultaneous EGFR amplification and EGFRvIII mutation,” *J. Neurooncol.*, vol. 154, pp. 353–364, 2021, doi: 10.1007/s11060-021-03834-3.

[480] P. S. Nakod, R. V. Kondapaneni, B. Edney, Y. Kim, and S. S. Rao, “The impact of temozolomide and lonafarnib on the stemness marker expression of glioblastoma cells in multicellular spheroids,” *Biotechnol. Prog.*, vol. 38, no. 5, p. e3284, Sep. 2022, doi: 10.1002/BTPR.3284.

[481] V. M. Lu, P. Kerezoudis, D. A. Brown, T. C. Burns, A. Quinones-Hinojosa, and K. L. Chaichana, “Hypofractionated versus standard radiation therapy in combination with

temozolomide for glioblastoma in the elderly: a meta-analysis," *J. Neurooncol.*, vol. 143, no. 2, pp. 177–185, 2019, doi: 10.1007/s11060-019-03155-6.

[482] A. Omuro *et al.*, "Radiotherapy combined with nivolumab or temozolomide for newly diagnosed glioblastoma with unmethylated MGMT promoter: An international randomized phase III trial," *Neuro. Oncol.*, vol. 25, no. 1, pp. 123–134, 2023, doi: 10.1093/neuonc/noac099.

[483] D. P. Kulinich *et al.*, "Radiotherapy versus combination radiotherapy-bevacizumab for the treatment of recurrent high-grade glioma: a systematic review," *Acta Neurochir. (Wien).*, vol. 163, no. 7, pp. 1921–1934, 2021, doi: 10.1007/s00701-021-04794-3.

[484] A. A. Arabzadeh, T. Mortezazadeh, T. Aryafar, E. Gharepapagh, M. Majdaeen, and B. Farhood, "Therapeutic potentials of resveratrol in combination with radiotherapy and chemotherapy during glioblastoma treatment: a mechanistic review," *Cancer Cell Int.*, vol. 21, no. 1, pp. 1–15, 2021, doi: 10.1186/s12935-021-02099-0.

[485] A. C. Phillips *et al.*, "ABT-414, an antibody-drug conjugate targeting a tumor-selective EGFR epitope," *Mol. Cancer Ther.*, vol. 15, no. 4, pp. 661–669, 2016, doi: 10.1158/1535-7163.MCT-15-0901.

[486] D. A. Reardon, B. Neyns, M. Weller, J. C. Tonn, L. B. Nabors, and R. Stupp, "Cilengitide: an RGD pentapeptide αvβ3 and αvβ5 integrin inhibitor in development for glioblastoma and other malignancies," *Future Oncol.*, vol. 7, no. 3, pp. 339–354, Mar. 2011, doi: 10.2217/FON.11.8.

[487] F. Yang *et al.*, "Synergistic immunotherapy of glioblastoma by dual targeting of IL-6 and CD40," *Nat. Commun.*, vol. 12, no. 1, Dec. 2021, doi: 10.1038/S41467-021-23832-3.

[488] E. A. Chiocca *et al.*, "Combined immunotherapy with controlled interleukin-12 gene therapy and immune checkpoint blockade in recurrent glioblastoma: An open-label, multi-institutional phase I trial," *Neuro. Oncol.*, vol. 24, no. 6, p. 951, Jun. 2022, doi: 10.1093/NEUONC/NOAB271.

[489] P. Zhu and J. J. Zhu, "Tumor treating fields: A novel and effective therapy for glioblastoma: Mechanism, efficacy, safety and future perspectives," *Chinese Clin. Oncol.*, vol. 6, no. 4, pp. 1–15, 2017, doi: 10.21037/cco.2017.06.29.

[490] R. Tamura, H. Miyoshi, K. Yoshida, H. Okano, and M. Toda, "Recent progress in the research of suicide gene therapy for malignant glioma," *Neurosurg. Rev. 2019 441*, vol. 44, no. 1, pp. 29–49, Nov. 2019, doi: 10.1007/S10143-019-01203-3.

[491] J. Choi *et al.*, "Combination checkpoint therapy with anti-PD-1 and anti-BTLA results

in a synergistic therapeutic effect against murine glioblastoma," *Oncoimmunology*, vol. 10, no. 1, 2021, doi: 10.1080/2162402X.2021.1956142.

[492] A. Moslemizadeh *et al.*, "Combination therapy with interferon-gamma as a potential therapeutic medicine in rat's glioblastoma: A multi-mechanism evaluation," *Life Sci.*, vol. 305, p. 120744, Sep. 2022, doi: 10.1016/J.LFS.2022.120744.

[493] W. Dang *et al.*, "Combination of p38 MAPK inhibitor with PD-L1 antibody effectively prolongs survivals of temozolomide-resistant glioma-bearing mice via reduction of infiltrating glioma-associated macrophages and PD-L1 expression on resident glioma-associated microglia," *Brain Tumor Pathol.*, vol. 38, no. 3, pp. 189–200, Jul. 2021, doi: 10.1007/S10014-021-00404-3/FIGURES/5.

[494] R. E. Sanborn *et al.*, "Original research: Safety, tolerability and efficacy of agonist anti-CD27 antibody (varlilumab) administered in combination with anti-PD-1 (nivolumab) in advanced solid tumors," *J. Immunother. Cancer*, vol. 10, no. 8, p. 5147, Aug. 2022, doi: 10.1136/JITC-2022-005147.

[495] X. R. Ni *et al.*, "Combination of levetiracetam and IFN-α increased temozolomide efficacy in MGMT-positive glioma," *Cancer Chemother. Pharmacol.*, vol. 86, no. 6, pp. 773–782, Dec. 2020, doi: 10.1007/S00280-020-04169-Y/FIGURES/5.

[496] P. Liang, G. Wang, X. Liu, Z. Wang, J. Wang, and W. Gao, "Spatiotemporal combination of thermosensitive polypeptide fused interferon and temozolomide for post-surgical glioblastoma immunochemotherapy," *Biomaterials*, vol. 264, p. 120447, Jan. 2021, doi: 10.1016/J.BIOMATERIALS.2020.120447.

[497] Y. Hattori *et al.*, "Combination of Ad-SGE-REIC and bevacizumab modulates glioma progression by suppressing tumor invasion and angiogenesis," *PLoS One*, vol. 17, no. 8, Aug. 2022, doi: 10.1371/JOURNAL.PONE.0273242.

[498] E. Gjika *et al.*, "Combination therapy of cold atmospheric plasma (CAP) with temozolomide in the treatment of U87MG glioblastoma cells," *Sci. Rep.*, vol. 10, no. 1, p. 16495, Dec. 2020, doi: 10.1038/S41598-020-73457-7.

[499] A. Vargas-Toscano *et al.*, "Rapalink-1 Targets Glioblastoma Stem Cells and Acts Synergistically with Tumor Treating Fields to Reduce Resistance against Temozolomide," *Cancers (Basel).*, vol. 12, no. 12, pp. 1–19, Dec. 2020, doi: 10.3390/CANCERS12123859.

[500] F. Koosha, S. Eynali, N. Eyvazzadeh, and M. A. Kamalabadi, "The effect of iodine-131 beta-particles in combination with A-966492 and Topotecan on radio-sensitization of glioblastoma: An in-vitro study," *Appl. Radiat. Isot.*, vol. 177, p. 109904, Nov. 2021,

doi: 10.1016/J.APRADISO.2021.109904.

[501] Z. Gao *et al.*, "ARPC1B promotes mesenchymal phenotype maintenance and radiotherapy resistance by blocking TRIM21-mediated degradation of IFI16 and HuR in glioma stem cells," *J. Exp. Clin. Cancer Res.*, vol. 41, no. 1, p. 323, Dec. 2022, doi: 10.1186/S13046-022-02526-8.

[502] Y. Otani *et al.*, "Inhibiting protein phosphatase 2A increases the antitumor effect of protein arginine methyltransferase 5 inhibition in models of glioblastoma," *Neuro. Oncol.*, vol. 23, no. 9, p. 1481, Sep. 2021, doi: 10.1093/NEUONC/NOAB014.

[503] W. Zhu *et al.*, "The lipid-lowering drug fenofibrate combined with si-HOTAIR can effectively inhibit the proliferation of gliomas," *BMC Cancer*, vol. 21, no. 1, Dec. 2021, doi: 10.1186/S12885-021-08417-Z.

[504] M. Paul-Samojedny *et al.*, "The combination of baicalin with knockdown of miR148a gene suppresses cell viability and proliferation and induces the apoptosis and autophagy of human glioblastoma multiforme T98G and U87MG cells," *Curr. Pharm. Biotechnol.*, vol. 23, Jun. 2022, doi: 10.2174/1389201023666220627144100.

[505] M. Zurlo, R. Romagnoli, P. Oliva, J. Gasparello, A. Finotti, and R. Gambari, "Synergistic Effects of A Combined Treatment of Glioblastoma U251 Cells with An Anti-miR-10b-5p Molecule and An AntiCancer Agent Based on 1-(3′,4′,5′-Trimethoxyphenyl)-2-Aryl-1H-Imidazole Scaffold," *Int. J. Mol. Sci.*, vol. 23, no. 11, Jun. 2022, doi: 10.3390/IJMS23115991/S1.

[506] Q. Yang, Y. Zhou, J. Chen, N. Huang, Z. Wang, and Y. Cheng, "Gene Therapy for Drug-Resistant Glioblastoma via Lipid-Polymer Hybrid Nanoparticles Combined with Focused Ultrasound," *Int. J. Nanomedicine*, vol. 16, p. 185, 2021, doi: 10.2147/IJN.S286221.

[507] A. Colapietro *et al.*, "The Botanical Drug PBI-05204, a Supercritical CO2 Extract of Nerium Oleander, Is Synergistic With Radiotherapy in Models of Human Glioblastoma," *Front. Pharmacol.*, vol. 13, p. 23, Mar. 2022, doi: 10.3389/FPHAR.2022.852941/FULL.

[508] I. Tutak, B. Ozdil, and A. Uysal, "Voxtalisib and low intensity pulsed ultrasound combinatorial effect on glioblastoma multiforme cancer stem cells via PI3K/AKT/mTOR," *Pathol. - Res. Pract.*, vol. 239, p. 154145, Nov. 2022, doi: 10.1016/J.PRP.2022.154145.

[509] S. Alomari *et al.*, "Drug Repurposing for Glioblastoma and Current Advances in Drug Delivery—A Comprehensive Review of the Literature," *Biomolecules*, vol. 11, no. 12,

p. 1870, Dec. 2021, doi: 10.3390/BIOM11121870.

[510] S. C. HIGGINS and G. J. PILKINGTON, “The In Vitro Effects of Tricyclic Drugs and Dexamethasone on Cellular Respiration of Malignant Glioma,” *Anticancer Res.*, vol. 30, no. 2, 2010.

[511] Y. Levkovitz, I. Gil-Ad, E. Zeldich, M. Dayag, and A. Weizman, “Differential induction of apoptosis by antidepressants in glioma and neuroblastoma cell lines: evidence for p-c-Jun, cytochrome c, and caspase-3 involvement,” *J. Mol. Neurosci.*, vol. 27, no. 1, pp. 029–042, 2005, doi: 10.1385/JMN:27:1:029.

[512] L. Patel and C. Lindley, “Aprepitant--a novel NK1-receptor antagonist,” *Expert Opin. Pharmacother.*, vol. 4, no. 12, pp. 2279–2296, 2003, doi: 10.1517/14656566.4.12.2279.

[513] M. Muñoz and R. Coveñas, “The Neurokinin-1 Receptor Antagonist Aprepitant: An Intelligent Bullet against Cancer?,” *Cancers (Basel).*, vol. 12, no. 9, pp. 1–22, Sep. 2020, doi: 10.3390/CANCERS12092682.

[514] Q. Tan *et al.*, “Induction of Mitochondrial Dysfunction and Oxidative Damage by Antibiotic Drug Doxycycline Enhances the Responsiveness of Glioblastoma to Chemotherapy,” *Med. Sci. Monit.*, vol. 23, pp. 4117–4125, Aug. 2017, doi: 10.12659/MSM.903245.

[515] R. Lamb *et al.*, “Antibiotics that target mitochondria effectively eradicate cancer stem cells, across multiple tumor types: treating cancer like an infectious disease,” *Oncotarget*, vol. 6, no. 7, pp. 4569–4584, 2015, doi: 10.18632/ONCOTARGET.3174.

[516] G. Karpel-Massler *et al.*, “Anti-glioma Activity of Dapsone and Its Enhancement by Synthetic Chemical Modification,” *Neurochem. Res.*, vol. 42, no. 12, pp. 3382–3389, Dec. 2017, doi: 10.1007/S11064-017-2378-6.

[517] A. R. Larsen *et al.*, “Repurposing the antihelmintic mebendazole as a hedgehog inhibitor,” *Mol. Cancer Ther.*, vol. 14, no. 1, p. 3, Jan. 2015, doi: 10.1158/1535-7163.MCT-14-0755-T.

[518] A. Vargas-Toscano *et al.*, “Robot technology identifies a Parkinsonian therapeutics repurpose to target stem cells of glioblastoma,” *CNS Oncol.*, vol. 9, no. 2, Jun. 2020, doi: 10.2217/CNS-2020-0004.

[519] W. J. Huang, W. W. Chen, and X. Zhang, “Glioblastoma multiforme: Effect of hypoxia and hypoxia inducible factors on therapeutic approaches (review),” *Oncol. Lett.*, vol. 12, no. 4, pp. 2283–2288, Oct. 2016, doi: 10.3892/OL.2016.4952/HTML.

[520] C. Velásquez *et al.*, “Hypoxia can induce migration of glioblastoma cells through a methylation-dependent control of ODZ1 gene expression,” *Front. Oncol.*, vol. 9, no.

SEP, p. 1036, Sep. 2019, doi: 10.3389/FONC.2019.01036/BIBTEX.

[521] A. Emami Nejad *et al.*, "The role of hypoxia in the tumor microenvironment and development of cancer stem cell: a novel approach to developing treatment," *Cancer Cell Int. 2021 211*, vol. 21, no. 1, pp. 1–26, Jan. 2021, doi: 10.1186/S12935-020-01719-5.

[522] X. Zheng *et al.*, "Mitochondrial fragmentation limits NK cell-based tumor immunosurveillance," *Nat. Immunol. 2019 2012*, vol. 20, no. 12, pp. 1656–1667, Oct. 2019, doi: 10.1038/s41590-019-0511-1.

[523] A. T. Henze and M. Mazzone, "The impact of hypoxia on tumor-associated macrophages," *J. Clin. Invest.*, vol. 126, no. 10, p. 3672, Oct. 2016, doi: 10.1172/JCI84427.

[524] A. Bronisz, E. Salińska, E. A. Chiocca, and J. Godlewski, "Hypoxic Roadmap of Glioblastoma-Learning about Directions and Distances in the Brain Tumor Environment," *Cancers (Basel).*, vol. 12, no. 5, May 2020, doi: 10.3390/CANCERS12051213.

[525] R. Kalkan, "Hypoxia Is the Driving Force Behind GBM and Could Be a New Tool in GBM Treatment," *Crit. Rev. Eukaryot. Gene Expr.*, vol. 25, no. 4, pp. 363–370, 2015, doi: 10.1615/CRITREVEUKARYOTGENEEXPR.2015015601.

[526] A. Pujada *et al.*, "Matrix metalloproteinase MMP9 maintains epithelial barrier function and preserves mucosal lining in colitis associated cancer," *Oncotarget*, 2017, doi: 10.18632/oncotarget.21841.

[527] K. Augoff, A. Hryniewicz-Jankowska, R. Tabola, and K. Stach, "MMP9: A Tough Target for Targeted Therapy for Cancer," *Cancers (Basel).*, vol. 14, no. 7, p. 1847, Apr. 2022, doi: 10.3390/CANCERS14071847.

[528] A. Atiq and I. Parhar, "Anti-neoplastic Potential of Flavonoids and Polysaccharide Phytochemicals in Glioblastoma," *Molecules*, vol. 25, no. 21, 2020, doi: 10.3390/molecules25214895.

[529] A. Mondal, A. Gandhi, C. Fimognari, A. G. Atanasov, and A. Bishayee, "Alkaloids for cancer prevention and therapy: Current progress and future perspectives," *Eur. J. Pharmacol.*, vol. 858, Sep. 2019, doi: 10.1016/J.EJPHAR.2019.172472.

[530] R. Edgar, M. Domrachev, and A. E. Lash, "Gene Expression Omnibus: NCBI gene expression and hybridization array data repository," *Nucleic Acids Res.*, vol. 30, no. 1, pp. 207–210, Jan. 2002, doi: 10.1093/NAR/30.1.207.

[531] N. Al Mahi, M. F. Najafabadi, M. Pilarczyk, M. Kouril, and M. Medvedovic, "GREIN:

An Interactive Web Platform for Re-analyzing GEO RNA-seq Data," *Sci. Reports 2019 91*, vol. 9, no. 1, pp. 1–9, May 2019, doi: 10.1038/s41598-019-43935-8.

[532] D. W. Huang, B. T. Sherman, and R. A. Lempicki, "Bioinformatics enrichment tools: paths toward the comprehensive functional analysis of large gene lists," *Nucleic Acids Res.*, vol. 37, no. 1, pp. 1–13, 2009, doi: 10.1093/NAR/GKN923.

[533] J. F. Fontaine and M. A. Andrade-Navarro, "Gene Set to Diseases (GS2D): disease enrichment analysis on human gene sets with literature data," *Genomics Comput. Biol.*, vol. 2, no. 1, pp. e33–e33, Oct. 2016, doi: 10.18547/GCB.2016.VOL2.ISS1.E33.

[534] M. V. Kuleshov *et al.*, "Enrichr: a comprehensive gene set enrichment analysis web server 2016 update," *Nucleic Acids Res.*, vol. 44, no. Web Server issue, p. W90, Jul. 2016, doi: 10.1093/NAR/GKW377.

[535] E. Y. Chen *et al.*, "Enrichr: Interactive and collaborative HTML5 gene list enrichment analysis tool," *BMC Bioinformatics*, vol. 14, no. 1, pp. 1–14, Apr. 2013, doi: 10.1186/1471-2105-14-128/FIGURES/3.

[536] M. Pathan *et al.*, "FunRich: An open access standalone functional enrichment and interaction network analysis tool," *Proteomics*, vol. 15, no. 15, pp. 2597–2601, Aug. 2015, doi: 10.1002/PMIC.201400515.

[537] D. Szklarczyk *et al.*, "The STRING database in 2021: customizable protein–protein networks, and functional characterization of user-uploaded gene/measurement sets," *Nucleic Acids Res.*, vol. 49, no. D1, pp. D605–D612, Jan. 2021, doi: 10.1093/NAR/GKAA1074.

[538] P. Shannon *et al.*, "Cytoscape: A Software Environment for Integrated Models of Biomolecular Interaction Networks," *Genome Res.*, vol. 13, no. 11, p. 2498, Nov. 2003, doi: 10.1101/GR.1239303.

[539] T. Li *et al.*, "TIMER2.0 for analysis of tumor-infiltrating immune cells," *Nucleic Acids Res.*, vol. 48, no. W1, pp. W509–W514, Jul. 2020, doi: 10.1093/NAR/GKAA407.

[540] R. L. Bowman, Q. Wang, A. Carro, R. G. W. Verhaak, and M. Squatrito, "GlioVis data portal for visualization and analysis of brain tumor expression datasets," *Neuro. Oncol.*, vol. 19, no. 1, pp. 139–141, Jan. 2017, doi: 10.1093/NEUONC/NOW247.

[541] Z. Tang, B. Kang, C. Li, T. Chen, and Z. Zhang, "GEPIA2: an enhanced web server for large-scale expression profiling and interactive analysis," *Nucleic Acids Res.*, vol. 47, no. W1, pp. W556–W560, Jul. 2019, doi: 10.1093/NAR/GKZ430.

[542] B. J. Gill *et al.*, "MRI-localized biopsies reveal subtype-specific differences in molecular and cellular composition at the margins of glioblastoma," *Proc. Natl. Acad. Sci. U. S.*

A., vol. 111, no. 34, pp. 12550–12555, Aug. 2014, doi: 10.1073/PNAS.1405839111/-/DCSUPPLEMENTAL/PNAS.1405839111.SAPP.PDF.

[543] S. Madhavan, J. C. Zenklusen, Y. Kotliarov, H. Sahni, H. A. Fine, and K. Buetow, "Rembrandt: helping personalized medicine become a reality through integrative translational research," *Mol. Cancer Res.*, vol. 7, no. 2, pp. 157–167, Feb. 2009, doi: 10.1158/1541-7786.MCR-08-0435.

[544] L. A. M. Gravendeel *et al.*, "Intrinsic gene expression profiles of gliomas are a better predictor of survival than histology," *Cancer Res.*, vol. 69, no. 23, pp. 9065–9072, Dec. 2009, doi: 10.1158/0008-5472.CAN-09-2307.

[545] T. Li *et al.*, "TIMER: A Web Server for Comprehensive Analysis of Tumor-Infiltrating Immune Cells," *Cancer Res.*, vol. 77, no. 21, pp. e108–e110, Nov. 2017, doi: 10.1158/0008-5472.CAN-17-0307.

[546] C. S. Yu, Y. C. Chen, C. H. Lu, and J. K. Hwang, "Prediction of protein subcellular localization," *Proteins Struct. Funct. Genet.*, 2006, doi: 10.1002/prot.21018.

[547] O. Fornes *et al.*, "JASPAR 2020: update of the open-access database of transcription factor binding profiles," *Nucleic Acids Res.*, vol. 48, no. D1, pp. D87–D92, Jan. 2020, doi: 10.1093/NAR/GKZ1001.

[548] G. Zhou, O. Soufan, J. Ewald, R. E. W. Hancock, N. Basu, and J. Xia, "NetworkAnalyst 3.0: a visual analytics platform for comprehensive gene expression profiling and meta-analysis," *Nucleic Acids Res.*, vol. 47, no. W1, pp. W234–W241, Jul. 2019, doi: 10.1093/NAR/GKZ240.

[549] M. Mangal, P. Sagar, H. Singh, G. P. S. Raghava, and S. M. Agarwal, "NPACT: Naturally Occurring Plant-based Anti-cancer Compound-Activity-Target database," *Nucleic Acids Res.*, vol. 41, no. Database issue, Jan. 2013, doi: 10.1093/NAR/GKS1047.

[550] E. Angeli, T. T. Nguyen, A. Janin, and G. Bousquet, "How to Make Anticancer Drugs Cross the Blood-Brain Barrier to Treat Brain Metastases," *Int. J. Mol. Sci.*, vol. 21, no. 1, Jan. 2019, doi: 10.3390/IJMS21010022.

[551] A. Daina, O. Michielin, and V. Zoete, "SwissADME: a free web tool to evaluate pharmacokinetics, drug-likeness and medicinal chemistry friendliness of small molecules," *Sci. Reports 2017 71*, vol. 7, no. 1, pp. 1–13, Mar. 2017, doi: 10.1038/srep42717.

[552] H. Liu *et al.*, "AlzPlatform: An Alzheimer's Disease Domain-Specific Chemogenomics Knowledgebase for Polypharmacology and Target Identification Research," *J. Chem. Inf. Model.*, vol. 54, no. 4, pp. 1050–1060, Apr. 2014, doi: 10.1021/CI500004H.

[553] “Molsoft L.L.C.: Drug-Likeness and molecular property prediction.” .

[554] G. Xiong *et al.*, “ADMETlab 2.0: an integrated online platform for accurate and comprehensive predictions of ADMET properties,” *Nucleic Acids Res.*, vol. 49, no. W1, pp. W5–W14, Jul. 2021, doi: 10.1093/NAR/GKAB255.

[555] “Free Download: BIOVIA Discovery Studio Visualizer - Dassault Systèmes.” .

[556] A. K. Rappé, C. J. Casewit, K. S. Colwell, W. A. Goddard, and W. M. Skiff, “UFF, a Full Periodic Table Force Field for Molecular Mechanics and Molecular Dynamics Simulations,” *J. Am. Chem. Soc.*, vol. 114, no. 25, pp. 10024–10035, Dec. 1992, doi: 10.1021/JA00051A040/SUPPL_FILE/JA00051A040_SI_001.PDF.

[557] R. J. Anderson, Z. Weng, R. K. Campbell, and X. Jiang, “Main-chain conformational tendencies of amino acids,” *Proteins*, vol. 60, no. 4, pp. 679–689, Sep. 2005, doi: 10.1002/PROT.20530.

[558] C. Colovos and T. O. Yeates, “Verification of protein structures: patterns of nonbonded atomic interactions,” *Protein Sci.*, vol. 2, no. 9, pp. 1511–1519, 1993, doi: 10.1002/PRO.5560020916.

[559] J. U. Bowie, R. Lüthy, and D. Eisenberg, “A method to identify protein sequences that fold into a known three-dimensional structure,” *Science*, vol. 253, no. 5016, pp. 164–170, 1991, doi: 10.1126/SCIENCE.1853201.

[560] A. Samdani and U. Vetrivel, “POAP: A GNU parallel based multithreaded pipeline of open babel and AutoDock suite for boosted high throughput virtual screening,” *Comput. Biol. Chem.*, vol. 74, pp. 39–48, Jun. 2018, doi: 10.1016/J.COMPBIOLCHEM.2018.02.012.

[561] D. Van Der Spoel, E. Lindahl, B. Hess, G. Groenhof, A. E. Mark, and H. J. C. Berendsen, “GROMACS: fast, flexible, and free,” *J. Comput. Chem.*, vol. 26, no. 16, pp. 1701–1718, Dec. 2005, doi: 10.1002/JCC.20291.

[562] R. Kumari, R. Kumar, and A. Lynn, “g_mmpbsa--a GROMACS tool for high-throughput MM-PBSA calculations,” *J. Chem. Inf. Model.*, vol. 54, no. 7, pp. 1951–1962, Jul. 2014, doi: 10.1021/CI500020M.

[563] V. V. Bhandare, B. V. Kumbhar, and A. Kunwar, “Differential binding affinity of tau repeat region R2 with neuronal-specific β-tubulin isotypes,” *Sci. Rep.*, vol. 9, no. 1, Dec. 2019, doi: 10.1038/S41598-019-47249-7.

[564] P. S. R. Dwivedi *et al.*, “System biology-based investigation of Silymarin to trace hepatoprotective effect,” *Comput. Biol. Med.*, vol. 142, no. September 2021, p. 105223, 2022, doi: 10.1016/j.compbiomed.2022.105223.

[565] L. Taidi, A. Maurady, and M. R. Britel, “Molecular docking study and molecular dynamic simulation of human cyclooxygenase-2 (COX-2) with selected eutypoids,” *https://doi.org/10.1080/07391102.2020.1823884*, vol. 40, no. 3, pp. 1189–1204, 2020, doi: 10.1080/07391102.2020.1823884.

[566] P. Khanal *et al.*, “Computational investigation of benzalacetophenone derivatives against SARS-CoV-2 as potential multi-target bioactive compounds,” *Comput. Biol. Med.*, vol. 146, p. 105668, Jul. 2022, doi: 10.1016/J.COMPBIOMED.2022.105668.

[567] V. V. Bhandare and A. Ramaswamy, “The proteinopathy of D169G and K263E mutants at the RNA Recognition Motif (RRM) domain of tar DNA-binding protein (tdp43) causing neurological disorders: A computational study,” *J. Biomol. Struct. Dyn.*, vol. 36, no. 4, pp. 1075–1093, 2018, doi: 10.1080/07391102.2017.1310670.

[568] G. E. Arnold and R. L. Ornstein, “Molecular dynamics study of time-correlated protein domain motions and molecular flexibility: Cytochrome P450BM-3,” *Biophys. J.*, vol. 73, no. 3, pp. 1147–1159, 1997, doi: 10.1016/S0006-3495(97)78147-5.

[569] P. Khanal *et al.*, “Integration of System Biology Tools to Investigate Huperzine A as an Anti-Alzheimer Agent,” *Front. Pharmacol.*, vol. 12, Dec. 2021, doi: 10.3389/FPHAR.2021.785964.

[570] N. Al Mahi, M. F. Najafabadi, M. Pilarczyk, M. Kouril, and M. Medvedovic, “GREIN: An Interactive Web Platform for Reanalyzing GEO RNA-seq Data,” *bioRxiv*, p. 326223, Oct. 2018, doi: 10.1101/326223.

[571] “Venny 2.1.0.” .

[572] M. Vassilakopoulou *et al.*, “BRCA1 Protein Expression Predicts Survival in Glioblastoma Patients from an NRG Oncology RTOG Cohort,” *Oncology*, vol. 99, no. 9, p. 580, 2021, doi: 10.1159/000516168.

[573] Y. Zhang, Q. Xia, and J. Lin, “Identification of the potential oncogenes in glioblastoma based on bioinformatic analysis and elucidation of the underlying mechanisms,” *Oncol. Rep.*, vol. 40, no. 2, pp. 715–725, Aug. 2018, doi: 10.3892/OR.2018.6483/HTML.

[574] G. Yang *et al.*, “EXO1 plays a carcinogenic role in hepatocellular carcinoma and is related to the regulation of FOXP3,” *J. Cancer*, vol. 11, no. 16, pp. 4917–4932, 2020, doi: 10.7150/jca.40673.

[575] B. Liu, G. Zhang, S. Cui, and G. Du, “Upregulation of KIF11 in TP53 Mutant Glioma Promotes Tumor Stemness and Drug Resistance,” *Cell. Mol. Neurobiol.*, vol. 42, no. 5, pp. 1477–1485, 2022, doi: 10.1007/s10571-020-01038-3.

[576] C. Jiang *et al.*, “Immune Characteristics of LYN in Tumor Microenvironment of

Gliomas," *Front. Cell Dev. Biol.*, vol. 9, no. February, pp. 1–15, 2022, doi: 10.3389/fcell.2021.760929.

[577] Q. Xue *et al.*, "High expression of MMP9 in glioma affects cell proliferation and is associated with patient survival rates," *Oncol. Lett.*, vol. 13, no. 3, p. 1325, Mar. 2017, doi: 10.3892/OL.2017.5567.

[578] J. Liu *et al.*, "Immune Characteristics and Prognosis Analysis of the Proteasome 20S Subunit Beta 9 in Lower-Grade Gliomas," *Front. Oncol.*, vol. 12, no. July, pp. 1–15, 2022, doi: 10.3389/fonc.2022.875131.

[579] S. J. Smith *et al.*, "Molecular Targeting of Cancer-Associated PCNA Interactions in Pancreatic Ductal Adenocarcinoma Using a Cell-Penetrating Peptide," *Mol. Ther. - Oncolytics*, vol. 17, no. June, pp. 250–256, 2020, doi: 10.1016/j.omto.2020.03.025.

[580] C. Aaberg-Jessen, L. Fogh, M. D. Sørensen, B. Halle, N. Brünner, and B. W. Kristensen, "Overexpression of TIMP-1 and Sensitivity to Topoisomerase Inhibitors in Glioblastoma Cell Lines," *Pathol. Oncol. Res.*, vol. 25, no. 1, pp. 59–69, 2019, doi: 10.1007/s12253-017-0312-5.

[581] B. Q. Wang, C. M. Zhang, W. Gao, X. F. Wang, H. L. Zhang, and P. C. Yang, "Cancer-derived matrix metalloproteinase-9 contributes to tumor tolerance," *J. Cancer Res. Clin. Oncol.*, vol. 137, no. 10, pp. 1525–1533, 2011, doi: 10.1007/s00432-011-1010-4.

[582] V. Juric *et al.*, "MMP-9 inhibition promotes anti-tumor immunity through disruption of biochemical and physical barriers to T-cell trafficking to tumors," *PLoS One*, vol. 13, no. 11, pp. 1–21, 2018, doi: 10.1371/journal.pone.0207255.

[583] O. Van Tellingen, B. Yetkin-Arik, M. C. De Gooijer, P. Wesseling, T. Wurdinger, and H. E. De Vries, "Overcoming the blood-brain tumor barrier for effective glioblastoma treatment," *Drug Resist. Updat.*, vol. 19, pp. 1–12, Mar. 2015, doi: 10.1016/J.DRUP.2015.02.002.

[584] O. Ursu, A. Rayan, A. Goldblum, and T. I. Oprea, "Understanding drug-likeness," *Wiley Interdiscip. Rev. Comput. Mol. Sci.*, vol. 1, no. 5, pp. 760–781, Sep. 2011, doi: 10.1002/WCMS.52.

[585] Z. Y. Yang *et al.*, "Benchmarking the mechanisms of frequent hitters: limitation of PAINS alerts," *Drug Discov. Today*, vol. 26, no. 6, pp. 1353–1358, Jun. 2021, doi: 10.1016/J.DRUDIS.2021.02.003.

[586] L. Guan *et al.*, "ADMET-score – a comprehensive scoring function for evaluation of chemical drug-likeness," *Medchemcomm*, vol. 10, no. 1, p. 148, 2019, doi: 10.1039/C8MD00472B.

[587] R. Zhu, L. Hu, H. Li, J. Su, Z. Cao, and W. Zhang, "Novel Natural Inhibitors of CYP1A2 Identified by in Silico and in Vitro Screening," *Int. J. Mol. Sci.*, vol. 12, no. 5, p. 3250, May 2011, doi: 10.3390/IJMS12053250.

[588] N. A. Durán-Iturbide, B. I. Díaz-Eufracio, and J. L. Medina-Franco, "In Silico ADME/Tox Profiling of Natural Products: A Focus on BIOFACQUIM," *ACS Omega*, vol. 5, no. 26, pp. 16076–16084, Jul. 2020, doi: 10.1021/ACSOMEGA.0C01581/SUPPL_FILE/AO0C01581_SI_001.PDF.

[589] T. Lei *et al.*, "ADMET Evaluation in Drug Discovery. Part 17: Development of Quantitative and Qualitative Prediction Models for Chemical-Induced Respiratory Toxicity," *Mol. Pharm.*, vol. 14, no. 7, pp. 2407–2421, 2017, doi: 10.1021/acs.molpharmaceut.7b00317.

[590] K. H. Shen, J. H. Hung, C. W. Chang, Y. T. Weng, M. J. Wu, and P. S. Chen, "Solasodine inhibits invasion of human lung cancer cell through downregulation of miR-21 and MMPs expression," *Chem. Biol. Interact.*, vol. 268, pp. 129–135, Apr. 2017, doi: 10.1016/J.CBI.2017.03.005.

[591] N. Liu *et al.*, "Computational study of effective matrix metalloproteinase 9 (MMP9) targeting natural inhibitors.," *Aging (Albany. NY).*, vol. 13, no. 19, pp. 22867–22882, Oct. 2021, doi: 10.18632/AGING.203581.

[592] Y. Mao *et al.*, "Low tumor purity is associated with poor prognosis, heavy mutation burden, and intense immune phenotype in colon cancer," *Cancer Manag. Res.*, vol. 10, p. 3569, 2018, doi: 10.2147/CMAR.S171855.

[593] Z. Gong, J. Zhang, and W. Guo, "Tumor purity as a prognosis and immunotherapy relevant feature in gastric cancer," *Cancer Med.*, vol. 9, no. 23, pp. 9052–9063, Dec. 2020, doi: 10.1002/CAM4.3505.

[594] Y. Zhao, X. Zhang, and J. Yao, "Comprehensive analysis of PLOD family members in low-grade gliomas using bioinformatics methods," *PLoS One*, vol. 16, no. 1, Jan. 2021, doi: 10.1371/JOURNAL.PONE.0246097.

[595] Y. Dai and D. Siemann, "c-Src is required for hypoxia-induced metastasis-associated functions in prostate cancer cells," *Onco. Targets. Ther.*, vol. 12, p. 3519, 2019, doi: 10.2147/OTT.S201320.

[596] J.-H. Baek, C. Birchmeier, M. Zenke, and T. Hieronymus, "The HGF Receptor/Met Tyrosine Kinase Is a Key Regulator of Dendritic Cell Migration in Skin Immunity," *J. Immunol.*, vol. 189, no. 4, pp. 1699–1707, Aug. 2012, doi: 10.4049/JIMMUNOL.1200729.

[597] I. Yang *et al.*, "CD8+ T-Cell Infiltrate in Newly Diagnosed Glioblastoma is Associated with Long-Term Survival," *J. Clin. Neurosci.*, vol. 17, no. 11, p. 1381, Nov. 2010, doi: 10.1016/J.JOCN.2010.03.031.

[598] S. Kalaora *et al.*, "Immunoproteasome expression is associated with better prognosis and response to checkpoint therapies in melanoma," *Nat. Commun. 2020 111*, vol. 11, no. 1, pp. 1–12, Feb. 2020, doi: 10.1038/s41467-020-14639-9.

[599] J. Han, Y. Jing, F. Han, and P. Sun, "Comprehensive analysis of expression, prognosis and immune infiltration for TIMPs in glioblastoma," *BMC Neurol.*, vol. 21, no. 1, pp. 1–15, Dec. 2021, doi: 10.1186/S12883-021-02477-1/FIGURES/7.

[600] B. Xu, "Prediction and analysis of hub genes between glioblastoma and low-grade glioma using bioinformatics analysis," *Medicine (Baltimore).*, vol. 100, no. 3, p. e23513, Jan. 2021, doi: 10.1097/MD.0000000000023513.

[601] G. Tornillo *et al.*, "Dual Mechanisms of LYN Kinase Dysregulation Drive Aggressive Behavior in Breast Cancer Cells," *Cell Rep.*, vol. 25, no. 13, pp. 3674-3692.e10, Dec. 2018, doi: 10.1016/J.CELREP.2018.11.103.

[602] H. Liu, D. Chen, P. Liu, S. Xu, X. Lin, and R. Zeng, "Secondary analysis of existing microarray data reveals potential gene drivers of cutaneous squamous cell carcinoma," *J. Cell. Physiol.*, vol. 234, no. 9, pp. 15270–15278, 2019, doi: 10.1002/jcp.28172.

[603] L. A. Edwards *et al.*, "Suppression of VEGF secretion and changes in glioblastoma multiforme microenvironment by inhibition of integrin-linked kinase (ILK)," *Mol. Cancer Ther.*, vol. 7, no. 1, pp. 59–70, Jan. 2008, doi: 10.1158/1535-7163.MCT-07-0329.

[604] H. Gazon, B. Barbeau, J. M. Mesnard, and J. M. Peloponese, "Hijacking of the AP-1 signaling pathway during development of ATL," *Front. Microbiol.*, vol. 8, no. JAN, p. 2686, Jan. 2018, doi: 10.3389/FMICB.2017.02686/BIBTEX.

[605] H. Okura *et al.*, "A role for activated Cdc42 in glioblastoma multiforme invasion," *Oncotarget*, vol. 7, no. 35, p. 56958, 2016, doi: 10.18632/ONCOTARGET.10925.

[606] D. Zagzag *et al.*, "Hypoxia-inducible factor 1 and VEGF upregulate CXCR4 in glioblastoma: implications for angiogenesis and glioma cell invasion," *Lab. Investig. 2006 8612*, vol. 86, no. 12, pp. 1221–1232, Oct. 2006, doi: 10.1038/labinvest.3700482.

[607] R. F. Amaral, L. H. M. Geraldo, M. Einicker-Lamas, T. C. L. d. S. e Spohr, F. Mendes, and F. R. S. Lima, "Microglial lysophosphatidic acid promotes glioblastoma proliferation and migration via LPA1 receptor," *J. Neurochem.*, vol. 156, no. 4, pp. 499–512, Feb. 2021, doi: 10.1111/JNC.15097.

[608] K. Harper, R. R. Lavoie, M. Charbonneau, K. Brochu-Gaudreau, and C. M. Dubois, "The Hypoxic Tumor Microenvironment Promotes Invadopodia Formation and Metastasis through LPA1 Receptor and EGFR Cooperation," *Mol. Cancer Res.*, vol. 16, no. 10, pp. 1601–1613, Oct. 2018, doi: 10.1158/1541-7786.MCR-17-0649.

[609] S. Quintero-Fabián *et al.*, "Role of Matrix Metalloproteinases in Angiogenesis and Cancer," *Front. Oncol.*, vol. 9, p. 1370, Dec. 2019, doi: 10.3389/FONC.2019.01370/BIBTEX.

[610] K. Kessenbrock, V. Plaks, and Z. Werb, "Matrix Metalloproteinases: Regulators of the Tumor Microenvironment," *Cell*, vol. 141, no. 1, p. 52, 2010, doi: 10.1016/J.CELL.2010.03.015.

[611] V. Petrova, M. Annicchiarico-Petruzzelli, G. Melino, and I. Amelio, "The hypoxic tumour microenvironment," *Oncog. 2018 71*, vol. 7, no. 1, pp. 1–13, Jan. 2018, doi: 10.1038/s41389-017-0011-9.

[612] S. Jana and S. K. Singh, "Identification of selective MMP-9 inhibitors through multiple e-pharmacophore, ligand-based pharmacophore, molecular docking, and density functional theory approaches," *J. Biomol. Struct. Dyn.*, vol. 37, no. 4, pp. 944–965, 2019, doi: 10.1080/07391102.2018.1444510.

[613] D. Yamamoto, S. Takai, D. Jin, S. Inagaki, K. Tanaka, and M. Miyazaki, "Molecular mechanism of imidapril for cardiovascular protection via inhibition of MMP-9," *J. Mol. Cell. Cardiol.*, vol. 43, no. 6, pp. 670–676, Dec. 2007, doi: 10.1016/J.YJMCC.2007.08.002.

[614] D. Yamamoto, S. Takai, I. Hirahara, and E. Kusano, "Captopril directly inhibits matrix metalloproteinase-2 activity in continuous ambulatory peritoneal dialysis therapy," *Clin. Chim. Acta.*, vol. 411, no. 9–10, pp. 762–764, 2010, doi: 10.1016/J.CCA.2010.02.059.

[615] R. E. Kast and M. E. Halatsch, "Matrix Metalloproteinase-2 and -9 in Glioblastoma: A Trio of Old Drugs—Captopril, Disulfiram and Nelfinavir—Are Inhibitors with Potential as Adjunctive Treatments in Glioblastoma," *Arch. Med. Res.*, vol. 43, no. 3, pp. 243–247, Apr. 2012, doi: 10.1016/J.ARCMED.2012.04.005.

[616] S. Lastakchi, M. K. Olaloko, and C. McConville, "A Potential New Treatment for High-Grade Glioma: A Study Assessing Repurposed Drug Combinations against Patient-Derived High-Grade Glioma Cells," *Cancers 2022, Vol. 14, Page 2602*, vol. 14, no. 11, p. 2602, May 2022, doi: 10.3390/CANCERS14112602.

[617] Q. W. Jiang, M. W. Chen, K. J. Cheng, P. Z. Yu, X. Wei, and Z. Shi, "Therapeutic Potential of Steroidal Alkaloids in Cancer and Other Diseases," *Med. Res. Rev.*, vol. 36,

no. 1, pp. 119–143, Jan. 2016, doi: 10.1002/MED.21346.

[618] W. Xue *et al.*, "Computational identification of the binding mechanism of a triple reuptake inhibitor amitifadine for the treatment of major depressive disorder," *Phys. Chem. Chem. Phys.*, vol. 20, no. 9, pp. 6606–6616, 2018, doi: 10.1039/C7CP07869B.

[619] P. Khanal *et al.*, "Combination of system biology to probe the anti-viral activity of andrographolide and its derivative against COVID-19," *RSC Adv.*, vol. 11, no. 9, pp. 5065–5079, Jan. 2021, doi: 10.1039/D0RA10529E.

[620] S. Awale *et al.*, "Cytotoxic constituents of Soymida febrifuga from Myanmar," *J. Nat. Prod.*, vol. 72, no. 9, pp. 1631–1636, Sep. 2009, doi: 10.1021/NP9003323.

[621] T. Sowmyya and G. Vijaya Lakshmi, "Antimicrobial and Catalytic Potential of Soymida febrifuga Aqueous Fruit Extract-Engineered Silver Nanoparticles," *Bionanoscience*, vol. 8, no. 1, pp. 179–195, Mar. 2018, doi: 10.1007/S12668-017-0458-3/SCHEMES/4.

[622] M. Lim, Y. Xia, C. Bettegowda, and M. Weller, "Current state of immunotherapy for glioblastoma," *Nat. Rev. Clin. Oncol.*, vol. 15, no. 7, pp. 422–442, Jul. 2018, doi: 10.1038/S41571-018-0003-5.

[623] Y.-L. Lee, W.-E. Cheng, S.-C. Chen, C. Chen, and C.-M. Shih, "The effects of hypoxia on the expression of MMP-2, MMP-9 in human lung adenocarcinoma A549 cells," *Eur. Respir. J.*, vol. 44, no. Suppl 58, 2014.

[624] A. T. Bauer, H. F. Bürgers, T. Rabie, and H. H. Marti, "Matrix metalloproteinase-9 mediates hypoxia-induced vascular leakage in the brain via tight junction rearrangement," *J. Cereb. Blood Flow Metab. Off. J. Int. Soc. Cereb. Blood Flow Metab.*, vol. 30, no. 4, p. 837, Apr. 2010, doi: 10.1038/JCBFM.2009.248.

[625] N. Zeren *et al.*, "The Chemokine Receptor CCR1 Mediates Microglia Stimulated Glioma Invasion," *Int. J. Mol. Sci.*, vol. 24, no. 6, p. 5136, 2023, doi: 10.3390/ijms24065136.

[626] X. Dai *et al.*, "Crosstalk between microglia and neural stem cells influences the relapse of glioblastoma in GBM immunological microenvironment," *Clin. Immunol.*, vol. 251, Jun. 2023, doi: 10.1016/J.CLIM.2023.109333.

[627] C. McCornack, T. Woodiwiss, A. Hardi, H. Yano, and A. H. Kim, "The function of histone methylation and acetylation regulators in GBM pathophysiology," *Front. Oncol.*, vol. 13, no. May, pp. 1–18, 2023, doi: 10.3389/fonc.2023.1144184.

[628] D. Gallego-Perez *et al.*, "On-Chip Clonal Analysis of Glioma-Stem-Cell Motility and Therapy Resistance," *Nano Lett.*, vol. 16, no. 9, pp. 5326–5332, Sep. 2016, doi: 10.1021/ACS.NANOLETT.6B00902.

[629] K. Pang *et al.*, “Role of protein phosphorylation in cell signaling, disease, and the intervention therapy,” *MedComm*, vol. 3, no. 4, pp. 1–28, 2022, doi: 10.1002/mco2.175.

[630] O. Alexandru *et al.*, “Receptor tyrosine kinase targeting in glioblastoma: Performance, limitations and future approaches,” *Wspolczesna Onkol.*, vol. 24, no. 1, pp. 55–66, 2020, doi: 10.5114/wo.2020.94726.

[631] M. J. Ramaiah and K. R. Kumar, “mTOR-Rictor-EGFR axis in oncogenesis and diagnosis of glioblastoma multiforme,” *Mol. Biol. Rep.*, vol. 48, no. 5, pp. 4813–4835, 2021, doi: 10.1007/s11033-021-06462-2.

[632] N. Chen, C. Peng, and D. Li, “Epigenetic Underpinnings of Inflammation: A Key to Unlock the Tumor Microenvironment in Glioblastoma,” *Front. Immunol.*, vol. 13, no. April, pp. 1–11, 2022, doi: 10.3389/fimmu.2022.869307.

[633] F. M. S. Gurgis *et al.*, “The p38-MK2-HuR pathway potentiates EGFRvIII-IL-1β-driven IL-6 secretion in glioblastoma cells,” *Oncogene*, vol. 34, no. 22, pp. 2934–2942, May 2015, doi: 10.1038/ONC.2014.225.

[634] C. Yu-Ju Wu *et al.*, “CCL5 of glioma-associated microglia/macrophages regulates glioma migration and invasion via calcium-dependent matrix metalloproteinase 2,” *Neuro. Oncol.*, vol. 22, no. 2, pp. 253–266, 2020, doi: 10.1093/neuonc/noz189.

[635] G. Kim and Y. T. Ko, “Small molecule tyrosine kinase inhibitors in glioblastoma,” *Arch. Pharm. Res.*, vol. 43, no. 4, pp. 385–394, 2020, doi: 10.1007/s12272-020-01232-3.

[636] X. J. Sun, N. Man, Y. Tan, S. D. Nimer, and L. Wang, “The role of histone acetyltransferases in normal and malignant hematopoiesis,” *Front. Oncol.*, vol. 5, no. MAY, p. 108, 2015, doi: 10.3389/FONC.2015.00108/BIBTEX.

[637] J. W. Jeong *et al.*, “Regulation and destabilization of HIF-1alpha by ARD1-mediated acetylation,” *Cell*, vol. 111, no. 5, pp. 709–720, Nov. 2002, doi: 10.1016/S0092-8674(02)01085-1.

[638] “OSppc.” .

[639] H. Dong *et al.*, “OSgbm: An Online Consensus Survival Analysis Web Server for Glioblastoma,” *Front. Genet.*, vol. 10, Feb. 2020, doi: 10.3389/FGENE.2019.01378/FULL.

[640] T. Gao *et al.*, “UUCD: a family-based database of ubiquitin and ubiquitin-like conjugation,” *Nucleic Acids Res.*, vol. 41, no. D1, pp. D445–D451, Jan. 2013, doi: 10.1093/NAR/GKS1103.

[641] Z. Li *et al.*, “UbiNet 2.0: a verified, classified, annotated and updated database of E3 ubiquitin ligase–substrate interactions,” *Database J. Biol. Databases Curation*, vol.

2021, 2021, doi: 10.1093/DATABASE/BAAB010.

[642] X. Wang *et al.*, "UbiBrowser 2.0: a comprehensive resource for proteome-wide known and predicted ubiquitin ligase/deubiquitinase–substrate interactions in eukaryotic species," *Nucleic Acids Res.*, vol. 50, no. D1, p. D719, Jan. 2022, doi: 10.1093/NAR/GKAB962.

[643] K. Yu *et al.*, "Deep learning based prediction of reversible HAT/HDAC-specific lysine acetylation," *Brief. Bioinform.*, vol. 21, no. 5, pp. 1798–1805, Sep. 2020, doi: 10.1093/BIB/BBZ107.

[644] W. Deng *et al.*, "GPS-PAIL: prediction of lysine acetyltransferase-specific modification sites from protein sequences," *Sci. Reports 2016 61*, vol. 6, no. 1, pp. 1–10, Dec. 2016, doi: 10.1038/srep39787.

[645] D. W. A. Buchan and D. T. Jones, "The PSIPRED Protein Analysis Workbench: 20 years on," *Nucleic Acids Res.*, vol. 47, no. W1, pp. W402–W407, Jul. 2019, doi: 10.1093/NAR/GKZ297.

[646] A. Bateman *et al.*, "UniProt: the universal protein knowledgebase," *Nucleic Acids Res.*, vol. 45, no. D1, pp. D158–D169, Jan. 2017, doi: 10.1093/NAR/GKW1099.

[647] V. López-Ferrando, A. Gazzo, X. De La Cruz, M. Orozco, and J. L. Gelpí, "PMut: a web-based tool for the annotation of pathological variants on proteins, 2017 update," *Nucleic Acids Res.*, vol. 45, no. Web Server issue, p. W222, Jul. 2017, doi: 10.1093/NAR/GKX313.

[648] M. Hecht, Y. Bromberg, and B. Rost, "Better prediction of functional effects for sequence variants," *BMC Genomics*, vol. 16, no. 8, pp. 1–12, Jun. 2015, doi: 10.1186/1471-2164-16-S8-S1/FIGURES/4.

[649] I. A. Adzhubei *et al.*, "A method and server for predicting damaging missense mutations," *Nat. Methods*, vol. 7, no. 4, p. 248, Apr. 2010, doi: 10.1038/NMETH0410-248.

[650] V. Pejaver *et al.*, "Inferring the molecular and phenotypic impact of amino acid variants with MutPred2," *Nat. Commun. 2020 111*, vol. 11, no. 1, pp. 1–13, Nov. 2020, doi: 10.1038/s41467-020-19669-x.

[651] O. Menyhárt, J. T. Fekete, and B. Gyorffy, "Gene expression-based biomarkers designating glioblastomas resistant to multiple treatment strategies," *Carcinogenesis*, vol. 42, no. 6, pp. 804–813, Jun. 2021, doi: 10.1093/CARCIN/BGAB024.

[652] S. Eid, S. Turk, A. Volkamer, F. Rippmann, and S. Fulle, "Kinmap: A web-based tool for interactive navigation through human kinome data," *BMC Bioinformatics*, vol. 18,

no. 1, pp. 1–6, 2017, doi: 10.1186/s12859-016-1433-7.

[653] W. Gao *et al.*, "Systematic Analysis of Chemokines Reveals CCL18 is a Prognostic Biomarker in Glioblastoma," *J. Inflamm. Res.*, vol. 15, pp. 2731–2743, Apr. 2022, doi: 10.2147/JIR.S357787.

[654] G. P. Takacs, J. A. Flores-Toro, and J. K. Harrison, "Modulation of the chemokine/chemokine receptor axis as a novel approach for glioma therapy," *Pharmacol. Ther.*, vol. 222, Jun. 2021, doi: 10.1016/J.PHARMTHERA.2020.107790.

[655] Z. Dai *et al.*, "CXCL5 promotes the proliferation and migration of glioma cells in autocrine- and paracrine-dependent manners," *Oncol. Rep.*, vol. 36, no. 6, pp. 3303–3310, Dec. 2016, doi: 10.3892/OR.2016.5155/HTML.

[656] K. Hattermann, J. Held-Feindt, A. Ludwig, and R. Mentlein, "The CXCL16-CXCR6 chemokine axis in glial tumors," *J. Neuroimmunol.*, vol. 260, no. 1–2, pp. 47–54, 2013, doi: 10.1016/J.JNEUROIM.2013.04.006.

[657] J. Korbecki *et al.*, "The Role of CXCL16 in the Pathogenesis of Cancer and Other Diseases," *Int. J. Mol. Sci. 2021, Vol. 22, Page 3490*, vol. 22, no. 7, p. 3490, Mar. 2021, doi: 10.3390/IJMS22073490.

[658] K. Frei *et al.*, "Transforming growth factor-β pathway activity in glioblastoma," *Oncotarget*, vol. 6, no. 8, pp. 5963–5977, 2015, doi: 10.18632/ONCOTARGET.3467.

[659] W. L. Yeh, D. Y. Lu, H. C. Liou, and W. M. Fu, "A forward loop between glioma and microglia: glioma-derived extracellular matrix-activated microglia secrete IL-18 to enhance the migration of glioma cells," *J. Cell. Physiol.*, vol. 227, no. 2, pp. 558–568, Jan. 2012, doi: 10.1002/JCP.22746.

[660] R. E. Kast, "The role of interleukin-18 in glioblastoma pathology implies therapeutic potential of two old drugs—disulfiram and ritonavir," *Chin. J. Cancer*, vol. 34, no. 4, pp. 1–5, Apr. 2015, doi: 10.1186/S40880-015-0010-1/FIGURES/1.

[661] D. Dahlberg *et al.*, "Glioblastoma microenvironment contains multiple hormonal and non-hormonal growth-stimulating factors," *Fluids Barriers CNS 2022 191*, vol. 19, no. 1, pp. 1–11, Jun. 2022, doi: 10.1186/S12987-022-00333-Z.

[662] E. C. F. Yeo *et al.*, "The Role of Cytokines and Chemokines in Shaping the Immune Microenvironment of Glioblastoma: Implications for Immunotherapy," *Cells 2021, Vol. 10, Page 607*, vol. 10, no. 3, p. 607, Mar. 2021, doi: 10.3390/CELLS10030607.

[663] W. Fitzgerald, M. L. Freeman, M. M. Lederman, E. Vasilieva, R. Romero, and L. Margolis, "A System of Cytokines Encapsulated in ExtraCellular Vesicles," *Sci. Rep.*, vol. 8, no. 1, Dec. 2018, doi: 10.1038/S41598-018-27190-X.

[664] J. Zhou *et al.*, "The role of chemoattractant receptors in shaping the tumor microenvironment," *Biomed Res. Int.*, vol. 2014, 2014, doi: 10.1155/2014/751392.

[665] A. Ellert-Miklaszewska, K. Poleszak, M. Pasierbinska, and B. Kaminska, "Integrin Signaling in Glioma Pathogenesis: From Biology to Therapy," *Int. J. Mol. Sci.*, vol. 21, no. 3, Feb. 2020, doi: 10.3390/IJMS21030888.

[666] B. Kaur, F. W. Khwaja, E. A. Severson, S. L. Matheny, D. J. Brat, and E. G. Van Meir, "Hypoxia and the hypoxia-inducible-factor pathway in glioma growth and angiogenesis," *Neuro. Oncol.*, vol. 7, no. 2, p. 134, Apr. 2005, doi: 10.1215/S1152851704001115.

[667] M. Domènech, A. Hernández, A. Plaja, E. Martínez-balibrea, and C. Balañà, "Hypoxia: The cornerstone of glioblastoma," *Int. J. Mol. Sci.*, vol. 22, no. 22, 2021, doi: 10.3390/ijms222212608.

[668] P. Ramaswamy, K. Goswami, N. Dalavaikodihalli Nanjaiah, D. Srinivas, and C. Prasad, "TNF-α mediated MEK–ERK signaling in invasion with putative network involving NF-κB and STAT-6: a new perspective in glioma," *Cell Biol. Int.*, vol. 43, no. 11, pp. 1257–1266, Nov. 2019, doi: 10.1002/CBIN.11125.

[669] Q. Wei *et al.*, "TNFα secreted by glioma associated macrophages promotes endothelial activation and resistance against anti-angiogenic therapy," *Acta Neuropathol. Commun.*, vol. 9, no. 1, pp. 1–19, Dec. 2021, doi: 10.1186/S40478-021-01163-0/FIGURES/6.

[670] J. Langhans *et al.*, "The effects of PI3K-mediated signalling on glioblastoma cell behaviour," vol. 6, p. 398, 2017, doi: 10.1038/s41389-017-0004-8.

[671] K. Masliantsev, L. Karayan-tapon, and P. O. Guichet, "Hippo Signaling Pathway in Gliomas," *Cells*, vol. 10, no. 1, pp. 1–14, Jan. 2021, doi: 10.3390/CELLS10010184.

[672] K. Ma, X. Chen, W. Liu, S. Chen, C. Yang, and J. Yang, "CTSB is a negative prognostic biomarker and therapeutic target associated with immune cells infiltration and immunosuppression in gliomas," *Sci. Reports 2022 121*, vol. 12, no. 1, pp. 1–15, Mar. 2022, doi: 10.1038/s41598-022-08346-2.

[673] X. Ding, C. Zhang, H. Chen, M. Ren, and X. Liu, "Cathepsins Trigger Cell Death and Regulate Radioresistance in Glioblastoma," *Cells*, vol. 11, no. 24, 2022, doi: 10.3390/cells11244108.

[674] W. Xiao, X. Wang, T. Wang, and J. Xing, "Overexpression of BMP1 reflects poor prognosis in clear cell renal cell carcinoma," *Cancer Gene Ther. 2019 275*, vol. 27, no. 5, pp. 330–340, Jun. 2019, doi: 10.1038/s41417-019-0107-9.

[675] R. Sachdeva *et al.*, "BMP signaling mediates glioma stem cell quiescence and confers

treatment resistance in glioblastoma," *Sci. Rep.*, vol. 9, no. 1, pp. 1–14, 2019, doi: 10.1038/s41598-019-51270-1.

[676] Md. Shuyuan Zhang, MDa, b, Weiwei Zhang, B. , Bin Wu, MDa, b, Liang Xia, MDa, b, Liwen Li, MDa, b, Kai Jin, MDa, and Md. Yangfan Zou, MDa, b, Caixing Sun, "Hub gene target of glioblastoma," vol. 45, no. February, 2022.

[677] X. Li *et al.*, "A Novel Risk Score Model Based on Eleven Extracellular Matrix-Related Genes for Predicting Overall Survival of Glioma Patients," *J. Oncol.*, vol. 2022, 2022, doi: 10.1155/2022/4966820.

[678] Y. Tang, C. Qing, J. Wang, and Z. Zeng, "DNA Methylation-based Diagnostic and Prognostic Biomarkers for Glioblastoma," *Cell Transplant.*, vol. 29, Jun. 2020, doi: 10.1177/0963689720933241.

[679] J. Zhu *et al.*, "Expression of LOX Suggests Poor Prognosis in Gastric Cancer," *Front. Med.*, vol. 8, p. 718986, Sep. 2021, doi: 10.3389/FMED.2021.718986.

[680] Z. Liu *et al.*, "A Novel Six-mRNA Signature Predicts Survival of Patients With Glioblastoma Multiforme," *Front. Genet.*, vol. 12, p. 259, Mar. 2021, doi: 10.3389/FGENE.2021.634116/BIBTEX.

[681] H. Yu *et al.*, "LOXL1 confers antiapoptosis and promotes gliomagenesis through stabilizing BAG2," *Cell Death Differ.*, vol. 27, no. 11, pp. 3021–3036, 2020, doi: 10.1038/s41418-020-0558-4.

[682] H. Wang, W. Luo, and L. Dai, "Expression and Prognostic Role of PLOD1 in Malignant Glioma," *Onco. Targets. Ther.*, vol. 13, p. 13285, 2020, doi: 10.2147/OTT.S265866.

[683] B. Yuan, Y. Xu, and S. Zheng, "PLOD1 acts as a tumor promoter in glioma via activation of the HSF1 signaling pathway," *Mol. Cell. Biochem.*, vol. 477, no. 2, pp. 549–557, 2022, doi: 10.1007/s11010-021-04289-w.

[684] Z. Wang, Y. Shi, C. Ying, Y. Jiang, and J. Hu, "Hypoxia-induced PLOD1 overexpression contributes to the malignant phenotype of glioblastoma via NF-κB signaling," *Oncogene 2021 408*, vol. 40, no. 8, pp. 1458–1475, Jan. 2021, doi: 10.1038/s41388-020-01635-y.

[685] W. Zhou *et al.*, "Increased expression of MMP-2 and MMP-9 indicates poor prognosis in glioma recurrence," *Biomed. Pharmacother.*, vol. 118, p. 109369, Oct. 2019, doi: 10.1016/J.BIOPHA.2019.109369.

[686] L. V. De Oliveira Rosario, B. G. Da Rosa, T. L. Goncalves, D. I. L. Matias, C. Freitas, and V. P. Ferrer, "Glioblastoma factors increase the migration of human brain endothelial cells in vitro by increasing MMP-9/CXCR4 levels," *Anticancer Res.*, vol.

40, no. 5, pp. 2725–2737, 2020, doi: 10.21873/anticanres.14244.

[687] F. Seker *et al.*, "Identification of SERPINE1 as a Regulator of Glioblastoma Cell Dispersal with Transcriptome Profiling," doi: 10.3390/cancers11111651.

[688] L. Zhang *et al.*, "Hypoxia-induced ROS aggravate tumor progression through HIF-1α-SERPINE1 signaling in glioblastoma," *J. Zhejiang Univ. Sci. B*, vol. 24, no. 1, pp. 32–49, 2023, doi: 10.1631/jzus.B2200269.

[689] S. Peng *et al.*, "Decreased expression of serine protease inhibitor family G1 (SERPING1) in prostate cancer can help distinguish high-risk prostate cancer and predicts malignant progression," *Urol. Oncol. Semin. Orig. Investig.*, vol. 36, no. 8, pp. 366.e1-366.e9, Aug. 2018, doi: 10.1016/J.UROLONC.2018.05.021.

[690] D. Jia, S. Li, D. Li, H. Xue, D. Yang, and Y. Liu, "Mining TCGA database for genes of prognostic value in glioblastoma microenvironment," *Aging (Albany. NY).*, vol. 10, no. 4, pp. 592–605, Apr. 2018, doi: 10.18632/AGING.101415.

[691] K. Tanimoto, Y. Makino, T. Pereira, and L. Poellinger, "Mechanism of regulation of the hypoxia-inducible factor-1α by the von Hippel-Lindau tumor suppressor protein," *EMBO J.*, vol. 19, no. 16, p. 4298, Aug. 2000, doi: 10.1093/EMBOJ/19.16.4298.

[692] F. Yu, S. B. White, Q. Zhao, and F. S. Lee, "HIF-1α binding to VHL is regulated by stimulus-sensitive proline hydroxylation," *Proc. Natl. Acad. Sci. U. S. A.*, vol. 98, no. 17, pp. 9630–9635, Aug. 2001, doi: 10.1073/PNAS.181341498/ASSET/63417DF0-6CE8-4581-9F93-0A6F93CA33FD/ASSETS/GRAPHIC/PQ1813414004.JPEG.

[693] M. Aga *et al.*, "Exosomal HIF1α supports invasive potential of nasopharyngeal carcinoma-associated LMP1-positive exosomes," *Oncogene 2014 3337*, vol. 33, no. 37, pp. 4613–4622, Mar. 2014, doi: 10.1038/onc.2014.66.

[694] P. Kucharzewska *et al.*, "Exosomes reflect the hypoxic status of glioma cells and mediate hypoxia-dependent activation of vascular cells during tumor development," *Proc. Natl. Acad. Sci. U. S. A.*, vol. 110, no. 18, pp. 7312–7317, Apr. 2013, doi: 10.1073/PNAS.1220998110/SUPPL_FILE/SM01.WMV.

[695] X. Yu *et al.*, "Mechanism of TNF-α autocrine effects in hypoxic cardiomyocytes: Initiated by hypoxia inducible factor 1α, presented by exosomes," *J. Mol. Cell. Cardiol.*, vol. 53, no. 6, pp. 848–857, Dec. 2012, doi: 10.1016/J.YJMCC.2012.10.002.

[696] K. Bensaad *et al.*, "Fatty Acid Uptake and Lipid Storage Induced by HIF-1α Contribute to Cell Growth and Survival after Hypoxia-Reoxygenation," *Cell Rep.*, vol. 9, no. 1, pp. 349–365, Oct. 2014, doi: 10.1016/J.CELREP.2014.08.056.

[697] A. Yekula, A. Yekula, K. Muralidharan, K. Kang, B. S. Carter, and L. Balaj,

"Extracellular Vesicles in Glioblastoma Tumor Microenvironment," *Front. Immunol.*, vol. 10, p. 3137, Jan. 2020, doi: 10.3389/FIMMU.2019.03137/BIBTEX.

[698] E. Kim and S. Zschiedrich, "Renal cell carcinoma in von Hippel-Lindau disease-From tumor genetics to novel therapeutic strategies," *Front. Pediatr.*, vol. 6, p. 16, Feb. 2018, doi: 10.3389/FPED.2018.00016/BIBTEX.

[699] Z. Zhou *et al.*, "Human rhomboid family-1 suppresses oxygen-independent degradation of hypoxia-inducible factor-1a in breast cancer," *Cancer Res.*, vol. 74, no. 10, pp. 2719–2730, May 2014, doi: 10.1158/0008-5472.CAN-13-1027/657631/AM/HUMAN-RHOMBOID-FAMILY-1-RHBDF1-SUPPRESSES-OXYGEN.

[700] C. Xiaofei, L. Yanqing, Z. Dongkai, C. Dong, Z. Feng, and W. Weilin, "Identification of cathepsin B as a novel target of hypoxia-inducible factor-1-alpha in HepG2 cells," *Biochem. Biophys. Res. Commun.*, vol. 503, no. 2, pp. 1057–1062, Sep. 2018, doi: 10.1016/J.BBRC.2018.06.116.

[701] R. Da Silva, M. Uno, S. K. Nagahashi Marie, and S. M. Oba-Shinjo, "LOX Expression and Functional Analysis in Astrocytomas and Impact of IDH1 Mutation," *PLoS One*, vol. 10, no. 3, Mar. 2015, doi: 10.1371/JOURNAL.PONE.0119781.

[702] Q. Xie *et al.*, "Hypoxia triggers angiogenesis by increasing expression of LOX genes in 3-D culture of ASCs and ECs," *Exp. Cell Res.*, vol. 352, no. 1, pp. 157–163, Mar. 2017, doi: 10.1016/J.YEXCR.2017.02.011.

[703] J. Y. Choi, Y. S. Jang, S. Y. Min, and J. Y. Song, "Overexpression of MMP-9 and hif-1α in breast cancer cells under hypoxic conditions," *J. Breast Cancer*, vol. 14, no. 2, pp. 88–95, 2011, doi: 10.4048/jbc.2011.14.2.88.

[704] I. Azimi, R. M. Petersen, E. W. Thompson, S. J. Roberts-Thomson, and G. R. Monteith, "Hypoxia-induced reactive oxygen species mediate N-cadherin and SERPINE1 expression, EGFR signalling and motility in MDA-MB-468 breast cancer cells," *Sci. Rep.*, vol. 7, no. 1, Dec. 2017, doi: 10.1038/S41598-017-15474-7.

[705] K. Xiao *et al.*, "Prognostic value and immune cell infiltration of hypoxic phenotype-related gene signatures in glioblastoma microenvironment," *J. Cell. Mol. Med.*, vol. 24, no. 22, pp. 13235–13247, Nov. 2020, doi: 10.1111/JCMM.15939.

[706] M. D. Stewart, T. Ritterhoff, R. E. Klevit, and P. S. Brzovic, "E2 enzymes: more than just middle men," *Cell Res.*, vol. 26, no. 4, p. 423, Apr. 2016, doi: 10.1038/CR.2016.35.

[707] C. Xiang and H.-C. Yan, "ARTICLE Ubiquitin conjugating enzyme E2 C (UBE2C) may play a dual role involved in the progression of thyroid carcinoma," doi: 10.1038/s41420-022-00935-4.

[708] Z. Pan, J. Bao, L. Zhang, and S. Wei, "UBE2D3 Activates SHP-2 Ubiquitination to Promote Glycolysis and Proliferation of Glioma via Regulating STAT3 Signaling Pathway," *Front. Oncol.*, vol. 11, p. 2081, Jun. 2021, doi: 10.3389/FONC.2021.674286/BIBTEX.

[709] B. N. Singh, G. Zhang, Y. L. Hwa, J. Li, S. C. Dowdy, and S. W. Jiang, "Nonhistone protein acetylation as cancer therapy targets," *Expert Rev. Anticancer Ther.*, vol. 10, no. 6, p. 935, Jun. 2010, doi: 10.1586/ERA.10.62.

[710] R. E. Lacoursiere and G. S. Shaw, "Acetylated Ubiquitin Modulates the Catalytic Activity of the E1 Enzyme Uba1," 2021, doi: 10.1021/acs.biochem.1c00145.

[711] R. Ma, X. Kang, G. Zhang, F. Fang, Y. Du, and H. Lv, "High expression of UBE2C is associated with the aggressive progression and poor outcome of malignant glioma," *Oncol. Lett.*, vol. 11, no. 3, pp. 2300–2304, 2016, doi: 10.3892/ol.2016.4171.

[712] U. Shin *et al.*, "A heterozygous mutation in UBE2H in a patient with developmental delay leads to an aberrant brain development in zebrafish," *Hum. Genomics*, vol. 17, no. 1, p. 44, 2023, doi: 10.1186/s40246-023-00491-7.

[713] K. H. Lim and J. Y. Joo, "Predictive potential of circulating Ube2h mRNA as an E2 ubiquitin-conjugating enzyme for diagnosis or treatment of Alzheimer's disease," *Int. J. Mol. Sci.*, vol. 21, no. 9, 2020, doi: 10.3390/ijms21093398.

[714] H. Zuo, L. Chen, N. Li, and Q. Song, "Identification of a Ubiquitination-Related Gene Risk Model for Predicting Survival in Patients With Pancreatic Cancer," *Front. Genet.*, vol. 11, no. December, pp. 1–12, 2020, doi: 10.3389/fgene.2020.612196.

[715] R. E. Lacoursiere, D. Hadi, and G. S. Shaw, "Acetylation, Phosphorylation, Ubiquitination (Oh My!): Following Post-Translational Modifications on the Ubiquitin Road," *Biomolecules*, vol. 12, no. 3, Mar. 2022, doi: 10.3390/BIOM12030467.

[716] F. Fiumara, L. Fioriti, E. R. Kandel, and W. A. Hendrickson, "Essential role of coiled coils for aggregation and activity of Q/N-rich prions and PolyQ proteins," *Cell*, 2010, doi: 10.1016/j.cell.2010.11.042.

[717] D. G. Christensen *et al.*, "Mechanisms, detection, and relevance of protein acetylation in prokaryotes," *MBio*, vol. 10, no. 2, Mar. 2019, doi: 10.1128/MBIO.02708-18/ASSET/C3D9AAC6-21BC-4C7D-8C82-9A71AD882A69/ASSETS/GRAPHIC/MBIO.02708-18-F0004.JPEG.

[718] M. Narasumani and P. M. Harrison, "Discerning evolutionary trends in post-translational modification and the effect of intrinsic disorder: Analysis of methylation, acetylation and ubiquitination sites in human proteins," 2018, doi:

10.1371/journal.pcbi.1006349.

[719] B. Mészáros, B. Hajdu-soltész, A. Zeke, and Z. Dosztányi, "Mutations of Intrinsically Disordered Protein Regions Can Drive Cancer but Lack Therapeutic Strategies," *Biomolecules*, vol. 11, no. 3, pp. 1–22, Mar. 2021, doi: 10.3390/BIOM11030381.

[720] S. R. Alaei, C. K. Abrams, J. C. Bulinski, E. L. Hertzberg, and M. M. Freidin, "Acetylation of C-terminal lysines modulates protein turnover and stability of Connexin-32," *BMC Cell Biol.*, vol. 19, no. 1, pp. 1–15, Sep. 2018, doi: 10.1186/S12860-018-0173-0/FIGURES/7.

[721] C. S. Hwang, A. Shemorry, and A. Varshavsky, "N-Terminal Acetylation of Cellular Proteins Creates Specific Degradation Signals," *Science*, vol. 327, no. 5968, p. 973, Feb. 2010, doi: 10.1126/SCIENCE.1183147.

[722] S. Zhuang, "Regulation of STAT Signaling by Acetylation," *Cell. Signal.*, vol. 25, no. 9, p. 1924, Sep. 2013, doi: 10.1016/J.CELLSIG.2013.05.007.

[723] H. You *et al.*, "The interaction of canonical Wnt/β-catenin signaling with protein lysine acetylation," *Cell. Mol. Biol. Lett.*, vol. 27, no. 1, pp. 1–14, Dec. 2022, doi: 10.1186/S11658-021-00305-5/TABLES/2.

[724] A. Varshavsky, "N-degron and C-degron pathways of protein degradation," *Proc. Natl. Acad. Sci. U. S. A.*, vol. 116, no. 2, pp. 358–366, Jan. 2019, doi: 10.1073/PNAS.1816596116/SUPPL_FILE/PNAS.1816596116.SAPP.PDF.

[725] D. E. Sterner and S. L. Berger, "Acetylation of histones and transcription-related factors," *Microbiol. Mol. Biol. Rev.*, vol. 64, no. 2, pp. 435–459, Jun. 2000, doi: 10.1128/MMBR.64.2.435-459.2000.

[726] D. G. Christensen *et al.*, "Post-translational Protein Acetylation: An elegant mechanism for bacteria to dynamically regulate metabolic functions," *Front. Microbiol.*, vol. 10, no. JULY, p. 1604, 2019, doi: 10.3389/FMICB.2019.01604/BIBTEX.

[727] X. Wang, J. Taplick, N. Geva, and M. Oren, "Inhibition of p53 degradation by Mdm2 acetylation," *FEBS Lett.*, vol. 561, no. 1–3, pp. 195–201, Mar. 2004, doi: 10.1016/S0014-5793(04)00168-1.

[728] T. Shen *et al.*, "Ube2v1-mediated ubiquitination and degradation of Sirt1 promotes metastasis of colorectal cancer by epigenetically suppressing autophagy," *J. Hematol. Oncol.*, vol. 11, no. 1, pp. 1–16, 2018, doi: 10.1186/s13045-018-0638-9.

[729] B. Lin *et al.*, "Massively parallel signature sequencing and bioinformatics analysis identifies up-regulation of TGFBI and SOX4 in human glioblastoma," *PLoS One*, vol. 5, no. 4, 2010, doi: 10.1371/journal.pone.0010210.

[730] K. B. Pointer, P. A. Clark, A. B. Schroeder, M. Shahriar, K. W. Eliceiri, and J. S. Kuo, "Association of collagen architecture with glioblastoma patient survival," vol. 126, no. 6, pp. 1812–1821, 2017, doi: 10.3171/2016.6.JNS152797.Association.

[731] N. Yang, D. F. Cao, X. X. Yin, H. H. Zhou, and X. Y. Mao, "Lysyl oxidases: Emerging biomarkers and therapeutic targets for various diseases," *Biomed. Pharmacother.*, vol. 131, no. September, p. 110791, 2020, doi: 10.1016/j.biopha.2020.110791.

[732] X. Hu, M. Bao, J. Huang, L. Zhou, and S. Zheng, "Identification and Validation of Novel Biomarkers for Diagnosis and Prognosis of Hepatocellular Carcinoma," *Front. Oncol.*, vol. 10, Sep. 2020, doi: 10.3389/FONC.2020.541479.

[733] X. Zhang and Q. Yang, "A Pyroptosis-Related Gene Panel in Prognosis Prediction and Immune Microenvironment of Human Endometrial Cancer," *Front. Cell Dev. Biol.*, vol. 9, Oct. 2021, doi: 10.3389/FCELL.2021.705828/FULL.

[734] A. Liu, C. Hou, H. Chen, X. Zong, and P. Zong, "Genetics and Epigenetics of Glioblastoma: Applications and Overall Incidence of IDH1 Mutation," *Front. Oncol.*, vol. 6, no. JAN, p. 1, 2016, doi: 10.3389/FONC.2016.00016.

[735] M. Zhang, D. Yang, and B. Gold, "Origin of mutations in genes associated with human glioblastoma multiform cancer: random polymerase errors versus deamination," *Heliyon*, vol. 5, no. 3, p. 1265, Mar. 2019, doi: 10.1016/J.HELIYON.2019.E01265.

[736] J. Wang *et al.*, "Cyclin-dependent kinase 2 promotes tumor proliferation and induces radio resistance in glioblastoma," *Transl. Oncol.*, vol. 9, no. 6, pp. 548–556, 2016, doi: 10.1016/j.tranon.2016.08.007.

[737] Y. Cao, X. Li, S. Kong, S. Shang, and Y. Qi, "CDK4/6 inhibition suppresses tumour growth and enhances the effect of temozolomide in glioma cells," *J. Cell. Mol. Med.*, vol. 24, no. 9, pp. 5135–5145, 2020, doi: 10.1111/jcmm.15156.

[738] Z. Long, T. Wu, Q. Tian, L. A. Carlson, W. Wang, and G. Wu, "Expression and prognosis analyses of BUB1, BUB1B and BUB3 in human sarcoma," *Aging (Albany. NY).*, vol. 13, no. 9, pp. 12395–12408, 2021, doi: 10.18632/aging.202944.

[739] Y. Peng, M. Zhang, Z. Jiang, and Y. Jiang, "TRIM28 activates autophagy and promotes cell proliferation in glioblastoma," *Onco. Targets. Ther.*, vol. 12, pp. 397–404, 2019, doi: 10.2147/OTT.S188101.

[740] P. Zhang *et al.*, "POLE2 facilitates the malignant phenotypes of glioblastoma through promoting AURKA-mediated stabilization of FOXM1," *Cell Death Dis.*, vol. 13, no. 1, pp. 1–10, 2022, doi: 10.1038/s41419-021-04498-7.

[741] J. Mei, T. Wang, R. Xu, D. Chen, and Y. Zhang, "Clinical and molecular immune

characterization of ERBB2 in glioma," *Int. Immunopharmacol.*, vol. 94, p. 107499, May 2021, doi: 10.1016/J.INTIMP.2021.107499.

[742] H. Xu *et al.*, "Epidermal growth factor receptor in glioblastoma (Review)," *Oncol. Lett.*, vol. 14, no. 1, pp. 512–516, 2017, doi: 10.3892/ol.2017.6221.

[743] G. Guo *et al.*, *EGFR ligand shifts the role of EGFR from oncogene to tumour suppressor in EGFR-amplified glioblastoma by suppressing invasion through BIN3 upregulation*, vol. 24, no. 8. 2022.

[744] H. Wu *et al.*, "Overexpressed histone acetyltransferase 1 regulates cancer immunity by increasing programmed death-ligand 1 expression in pancreatic cancer," *J. Exp. Clin. Cancer Res.*, vol. 38, no. 1, pp. 1–12, Feb. 2019, doi: 10.1186/S13046-019-1044-Z/FIGURES/6.

[745] F. You *et al.*, "Drug repositioning: Using psychotropic drugs for the treatment of glioma," *Cancer Lett.*, vol. 527, pp. 140–149, 2022, doi: 10.1016/j.canlet.2021.12.014.

[746] C. Zhuo *et al.*, "Surprising Anticancer Activities of Psychiatric Medications: Old Drugs Offer New Hope for Patients With Brain Cancer," vol. 10, 2019, doi: 10.3389/fphar.2019.01262.

[747] M. S. Kim *et al.*, "Src is the primary target of aripiprazole, an atypical antipsychotic drug, in its anti-tumor action," *Oncotarget*, vol. 9, no. 5, pp. 5979–5992, 2018, doi: 10.18632/oncotarget.23192.

[748] B. Zagidullin *et al.*, "DrugComb: An integrative cancer drug combination data portal," *Nucleic Acids Res.*, vol. 47, no. W1, pp. W43–W51, 2019, doi: 10.1093/nar/gkz337.

[749] H. Liu, W. Zhang, B. Zou, J. Wang, Y. Deng, and L. Deng, "DrugCombDB: A comprehensive database of drug combinations toward the discovery of combinatorial therapy," *Nucleic Acids Res.*, 2020, doi: 10.1093/nar/gkz1007.

[750] G. Karpel-Massler *et al.*, "Olanzapine inhibits proliferation, migration and anchorage-independent growth in human glioblastoma cell lines and enhances temozolomide's antiproliferative effect," doi: 10.1007/s11060-014-1688-7.

[751] J. K. Lee, D. H. Nam, and J. Lee, "Repurposing antipsychotics as glioblastoma therapeutics: Potentials and challenges (Review)," *Oncol. Lett.*, vol. 11, no. 2, pp. 1281–1286, 2016, doi: 10.3892/ol.2016.4074.

[752] K. Bhat *et al.*, "Dopamine Receptor Antagonists, Radiation, and Cholesterol Biosynthesis in Mouse Models of Glioblastoma," *J. Natl. Cancer Inst.*, vol. 113, no. 8, pp. 1094–1104, 2021, doi: 10.1093/jnci/djab018.

[753] M. N. A. Kamarudin and I. Parhar, "Emerging therapeutic potential of anti-psychotic

drugs in the management of human glioma: A comprehensive review," *Oncotarget*, vol. 10, no. 39, pp. 3952–3977, 2019, doi: 10.18632/oncotarget.26994.

[754] K. Orsel *et al.*, "Psychotropic drugs use and psychotropic polypharmacy among persons with Alzheimer's disease," *Eur. Neuropsychopharmacol.*, vol. 28, no. 11, pp. 1260–1269, Nov. 2018, doi: 10.1016/J.EURONEURO.2018.04.005.

[755] S. Barber, U. Olotu, M. Corsi, and A. Cipriani, "Clozapine combined with different antipsychotic drugs for treatment-resistant schizophrenia," *Cochrane Database Syst. Rev.*, vol. 2017, no. 3, 2017, doi: 10.1002/14651858.CD006324.pub3.

[756] L. Yang and X. Qi, "Effect of olanzapine combined with risperidone in the treatment of schizophrenia and its influence on cognitive function," *Pakistan J. Med. Sci.*, vol. 37, no. 3, pp. 646–650, 2021, doi: 10.12669/pjms.37.3.3348.

[757] H. A. Nasrallah, J. Friedman, and J. Knight, "Combination therapy is here to stay," vol. 9, no. 5, pp. 11–12.

[758] M. Jeon, S. Kim, S. Park, H. Lee, and J. Kang, "In silico drug combination discovery for personalized cancer therapy," *BMC Syst. Biol.*, vol. 12, no. Suppl 2, 2018, doi: 10.1186/s12918-018-0546-1.

[759] T. Truong, P. Moscato, and N. Noman, "A Computational Approach for Designing Combination Therapy in Combating Glioblastoma," *2019 IEEE Congr. Evol. Comput. CEC 2019 - Proc.*, pp. 127–134, 2019, doi: 10.1109/CEC.2019.8790337.

[760] K. M. Gayvert, O. Aly, J. Platt, M. W. Bosenberg, D. F. Stern, and O. Elemento, "A Computational Approach for Identifying Synergistic Drug Combinations," *PLoS Comput. Biol.*, vol. 13, no. 1, pp. 1–11, 2017, doi: 10.1371/journal.pcbi.1005308.

LIST OF PUBLICATIONS

Cumulative Impact Factor

Cumulative impact factor of all publications	=	**66.76**
h-index and i-10 index	=	**6 and 5**
Cumulative citation index	=	**78**

PUBLICATIONS FROM THESIS

1. **Smita Kumari**, and Pravir Kumar, "Identification and characterization of putative biomarkers and therapeutic axis in Glioblastoma multiforme microenvironment ", Frontiers in Cell and Development Biology, DOI: https://doi.org/10.3389/fcell.2023.1236271. (2023) **IF: 6.081** (Frontiers).
2. **Smita Kumari** and Pravir Kumar, " Design and Computational Analysis of an MMP9 Inhibitor in Hypoxia-Induced Glioblastoma Multiforme ", *ACS Omega*, DOI: https://doi.org/10.1021/acsomega.3c00441. (2023) **IF: 4.132** (ACS).
3. **Smita Kumari**, and Pravir Kumar, "Identification of novel drug combination in Glioblastoma multiforme therapeutics through drug repurposing" IEEE-2023 International Conference on Emerging Techniques in Computational Intelligence (ICETCI) (2023).
4. **Smita Kumari**, Rohan Gupta, Rashmi K Ambasta, and Pravir Kumar, " Multiple therapeutic approaches of glioblastoma multiforme: From terminal to therapy", *Biochimica et Biophysica Acta (BBA)-Reviews on Cancer*, DOI: https://doi.org/10.1016/j.bbcan.2023.188913. (2023) **IF: 11.414** (Elsevier).
5. **Smita Kumari,** Dia Advani, Sudhanshu Sharma, Rashmi K Ambasta, and Pravir Kumar, "Combinatorial therapy in tumor microenvironment: where do we stand?", *Biochimica et Biophysica Acta (BBA)-Reviews on Cancer*, DOI: https://doi.org/10.1016/j.bbcan.2021.188585. (2021) **IF: 11.414** (Elsevier).
6. **Smita Kumari**, Sudhanshu Sharma, Dia Advani, Rashmi K Ambasta, and Pravir Kumar, "Unboxing the molecular modalities of mutagens in cancer", *Environmental Science and*

Pollution Research, DOI: https://doi.org/10.1007/s11356-021-16726-w. (2021) **IF: 5.190** (Springer Berlin Heidelberg).

OTHER PUBLICATIONS

1. Rohan Gupta, **Smita Kumari**, Anusha Senapati, Rashmi K Ambasta, and Pravir Kumar, " New era of artificial intelligence and machine learning-based detection, diagnosis, and therapeutics in Parkinson disease", *Ageing Research Reviews*, (*Accepted on 06.07.2023*) **IF: 13.01** (Elsevier).
2. Rohan Gupta, **Smita Kumari**, Rahul Tripathi, Rashmi K Ambasta, and Pravir Kumar, "Unwinding the modalities of necrosome activation and necroptosis machinery in neurological diseases", *Ageing Research Reviews*, DOI: https://doi.org/10.1016/j.arr.2023.101855.(2023) **IF: 13.01** (Elsevier).
3. Dia Advani, Sudhanshu Sharma, **Smita Kumari**, Rashmi K Ambasta, and Pravir Kumar, "Precision oncology, signaling, and anticancer agents in cancer therapeutics ", *Anti-Cancer Agents in Medicinal Chemistry*, DOI: https://doi.org/10.1016/bs.acc.2020.09.004. (2022) **IF: 2.527** (Bentham Science Publishers).

CONFERENCES AND PRESENTATIONS

S.No.	Paper Title (Year)	Authors Name	Title of the conference	Organizer of the conference	Date	National or International	Venue
1	Design and Computational Analysis of an MMP9 Inhibitor in Hypoxia-Induced Glioblastoma Multiforme (2021)	**Smita Kumari** and Pravir Kumar*	Neurodegeneration and Cognition-Recent Advances in Neurological Disease	SNCI	02.12.2021 to 04.12.2021	National	University of Hyderabad
2	Identification of potential biomarkers in GBM (2022)	**Smita Kumari** and Pravir Kumar*	Neurochemical Legacy of Neurological Disorders: Brainstorming of Novel Approaches	SNCI	09.03.2022	National	Jamia Hamdard, Delhi

3	Identification of novel drug combination in GBM therapeutics through Drug repurposing (2023)	**Smita Kumari** and Pravir Kumar*	Emerging Techniques in Computational Intelligence	IEEE	21.09.2023 to 23.09.2023	International	Mahindra University, Hyderabad

- Secured **consolation prize** for best oral presentation entitled "Identification of novel natural products-based MMP9 inhibitors against hypoxia-induced Glioblastoma Multiforme". In one day, symposium entitled "Neurochemical Legacy of Neurological Disorders: Brainstorming of Novel Approaches". Jamia Hamdard, Delhi (9th March 2023).
- Attended One Day International E-Symposium on Women in Science Organized by Delhi Technological University Held on February 11, 2021.

WORKSHOPS

- National workshop on "**Advance Research Techniques for Cellular and Molecular System in Neuroscience**", 08th to 14th December 2021, SNCI, Jamia Hamdard, Delhi, India.
- Advanced Course on Care, **Management of Laboratory Animals, and Experimental Techniques (LAE)** Organized by CSIR-Central Drug Research Institute, Lucknow, India Conducted from 06th to 24th September 2021.
- International e-Workshop on **Bioinformatics** sponsored by DTU, 14th to 18th December 2020, Department of Biotechnology, Delhi Technological University, Delhi, India.

SMITA KUMARI
Phone: +91-8468026284
E-Mail: smitamodi6@gmail.com

Corresponding Address:
Molecular Neuroscience and Functional Genomics Laboratory, Department of Biotechnology, Delhi Technological University, Shahbad Daulatpur, Bawana Road, Delhi: 110042

EDUCATIONAL BACKGROUND

2018-2023*	Delhi Technological University, Delhi, India	Ph.D.	Molecular Neuro-oncology, Biotechnology
2009-2013	Beant College of Engineering and Technology, Gurdaspur, Punjab, India	B.Tech	Biotechnology

Funding: Department of Biotechnology, Government of India, Ph.D. Scholarship

PERSONAL STATEMENT

My scientific research interests involve translation research and exploring the mechanism of action drugs and drug combinations in various cancer types, especially glioblastoma, colorectal, and breast cancer as a therapeutic approach. My academic training, research experience, teaching assistance, and scientific training experience have provided me with excellent background on multiple disciplines, such as computational biology, biomedical informatics, drug designing, drug discovery, proteomic studies, genetics, and molecular biology. After completing my graduation, I joined the Biotechnology industry to enhance my career. In the initial phase of my career, I worked with Invictus Oncology Private Limited, where I worked on different projects, such as the identification of novel biomarkers, the mechanism of immune system activation, and drug discovery and development. Afterward, in 2019, I shifted to Akamara Biomedicine Private Limited, where I focused on immune cell activation, biomarkers, prognostic markers studies, and *in vivo* drug discovery studies. To study cancer biology deeply I joined Delhi Technological University as a doctoral student under the supervision of Prof. Pravir Kumar, where I was able to implement my experience of tissue and cell culture, computational biology, bioinformatics tools, molecular biology, network, and structural biology in understanding the role of novel signaling molecules and pathways in the GBM tumorigenesis to target them as a putative drug target. In my doctoral training, I published several first-author papers in major journals, namely BBA- reviews on cancer, environmental science and pollution research, ageing research reviews, ACS omega, and others. In my recent publication, I concluded the importance of MMP9 as a putative therapeutic target in hypoxic GBM. I also aim to identify potential natural compounds against MMP9 through molecular docking and simulation studies. Further, we explore the function of non-cellular secretory molecules of the GBM microenvironment. Later on, we aim to identify potential E2 conjugating enzymes and their associated acetylation phenomenon in the GBM microenvironment. We also explore the possibility of atypical anti-psychotic drug combinations as a putative therapeutic agent in GBM pathogenesis through a drug-repurposing approach. In my doctoral training, I received a research excellence award in 2022 and 2023, organized by Delhi Technological University. In summary, my previous experience in the biotechnology industry and doctoral career provided me

the expertise in molecular biology techniques exposure and animal handling along with the understanding of drug discovery procedures through *in vitro* assays, bioinformatics, and computational techniques. For my postdoctoral training, I will continue to incorporate my previous expertise *in silico*, *in vitro*, and *in vivo* techniques to elucidate the novel pathways and molecular phenomena in the pathogenesis and progression of life-threatening diseases.

SKILLS AND EXPERTISE

COMPUTATIONAL BIOLOGY AND BIOINFORMATICS:
Molecular Docking, Virtual Screening, Bioinformatic Tools, Blast, Data Processing and Visualization, Sequence Alignment, GraphPad Prism, ImageJ, CytoScape, Bioinformatics web tool, Sequence Homology, Network Biology, Drug-target identification, TCGA-GDC data analysis, Protein-protein network biology, Functional enrichment analysis

MOLECULAR BIOLOGY:
In-vitro characterization: Mammalian Cell Culture, Handling of primary, suspension, and established cancer cell lines (TNBC, breast, ovarian, colorectal, lung, melanoma, prostate, cervical, liver, glioblastoma), Cryopreservation of heterogeneous cancer cell populations, Nucleic Acid and Protein Extraction, Nucleic Acid and Protein Quantification, SDS-Gel Electrophoresis, Horizontal Gel Electrophoresis,
In-vivo characterization studies: Animal Handling, Mice tissue harvest and downstream processing, Immunohistochemistry of paraffin-embedded and cryo-sections, Comparative Apoptosis analysis from in vivo samples using TUNEL staining and gene expression analysis, Immunofluorescent staining for immune-profiling of tumor sections
Gene expression studies: RT-PCR
Proteomics studies: ELISA, Dot blot, Western blot, Drug-Antibody Conjugates, Immunohistochemistry, Immunofluorescence, Immunoprecipitation
***Drug characterization and mechanism of action studies*:** TUNEL Staining, Drug Stability Studies, MTT Cytotoxic Assays, Transfection Assays, Drug stability studies,
In-house assay optimization to determine: Combinatorial index, Cellular uptake of compounds, Evaluation of DNA adduct formation, and co-localization studies using fluorescent imaging (IFC),
Immuno-oncology studies: Immune cell isolation from murine tissue using magnetic associated cell sorting, Immunofluorescent staining for immune (B-Cells and T-Cells), Immunofluorescent staining for immune-profiling of tumor sections, co-culture experiment.

POSITIONS, TRAINING, AND CERTIFICATIONS

Positions:

- **Senior Associate Research Scientist I (2020)**
  Akamara Biomedicine Private Limited, Delhi, India
  - ✓ Deciphering the novel key mechanism (B cell response) behind the anti-tumor immune response by the in-house novel supramolecular drug in Triple-negative breast cancer mouse model.
  - ✓ Involved in Biomarker and Prognostic marker studies
  - ✓ Maintain accurate, complete, and timely data in laboratory notebooks.
  - ✓ Member of the Institutional Biosafety Committee (IBSC).
- **Associate Research Scientist (2018-2019)**
  Akamara Biomedicine Private Limited, Delhi, India
  - ✓ Understanding the mechanism of Immune activation by the in-house supramolecular drug in various cancer models.

- ✓ Involved in the design, optimization, and execution (*in vitro*) studies to assess the immunological impact of oncology-related therapeutic agents on immune cells (B and T cells).
- ✓ Maintain accurate, complete, and timely data in laboratory notebooks.
- ✓ Member of the Institutional Biosafety Committee (IBSC).

- **Associate Research Scientist (2013-2018)**
  Invictus Oncology Private Limited, Delhi, India
  - ✓ Understanding mechanism of Immune activation by in-house supramolecular drug in Triple-negative breast cancer and lung cancer models.
  - ✓ Evaluating the efficacy of in-house supramolecular platinum/taxane anti-cancer therapeutics and ADC (antibody drug conjugate) through in vitro and in vivo studies in multiple cancer models.
  - ✓ Involved in design, optimization and execution (in vitro) studies to assess immunological impact of oncology-related therapeutic agents on immune cells.
  - ✓ Understanding the underlying mechanism of internalization of supramolecular therapeutics using florescent imaging.
  - ✓ Evaluating the efficacy of supramolecular MAP kinase inhibitor in different cancer models and deciphering the mechanism of action.
  - ✓ Application of microarray analysis for development of personalized chemotherapy by predicting optimum dosage schedule and therapeutic efficacies.

Teaching Assistant:

- **ANALYTICAL TECHNIQUES LABORATORY (MSBT107)**
  The subject focuses on techniques in genetic engineering, namely DNA and RNA isolation, DNA gel electrophoresis, RNA gel electrophoresis, and polymerase chain reaction (PCR).
- **GENOMICS AND PROTEOMICS LABORATORY (BT306)**
  The subject was taught to master students that focus on the techniques of proteomics and genomics studies, namely protein isolation and electrophoresis, immunofluorescence techniques, EMSA, DNA and RNA isolation, DNA gel electrophoresis, RNA gel electrophoresis, polymerase chain reaction (PCR), and others.

Training Experience

- One Month International Workshop on "Cancer Genomics & Bioinformatics", 3rd Edition, 18th to 14th July, 2022, Organized by DE<code> LIFE,
- National workshop on "Advance Research Techniques for Cellular and Molecular System in Neuroscience", 08th to 14th December 2021, SNCI, Jamia Hamdard, Delhi, India.
- Advanced Course on Care, Management of Laboratory Animals, and Experimental Techniques (LAE) Organized by CSIR-Central Drug Research Institute, Lucknow, India Conducted from 06th to 24th September 2021.
- International e-Workshop on Bioinformatics sponsored by DTU, 14th to 18th December 2020, Department of Biotechnology, Delhi Technological University, Delhi, India.

CONTRIBUTION TO SCIENCE

1. ***Early Career*:** My early career focuses design, optimization, and execution of all biological *in-vitro* and preclinical studies to understand the mechanism of action of in-house supramolecular drugs in various cancer models such as breast, lung, ovarian, colorectal cancer, and others. I got a chance to handle more than 10 mammalian cancer lines including immune and macrophage cells. In addition, deciphering the novel key mechanism (B cell response) behind the anti-tumor immune response by the in-house novel supramolecular drug in a Triple-negative breast cancer mouse model. Additionally, my research also

focused on the identification of biomarkers and other prognostic targets through data mining strategies using the GEO database and array express database. In addition, I have learned the way to work under pressure, prioritize, and solve logistical or organizational research problems.

2. ***Doctoral Career***: In my doctoral career, I focused to study brain cancer specifically the GBM microenvironment. I worked on the project entitled "Modulating tumor microenvironment using combinatorial therapy". I am interested to dissect the potential of combination therapy, and drug repurposing to broaden the forum of therapeutic strategies. we have explored and highlighted the role of TME in disease pathogenesis and the failure of current therapies. We have found the three flavonoids selectively target MMP9, a hypoxic molecular marker, for its therapeutic role in the treatment of Glioblastoma Multiforme. In addition, we have highlighted the crucial role of lysine-induced post-translational modification, especially acetylation of E2s conjugating enzymes, and dissected the potential novel therapeutic axis HAT1-UBE2S^{K211}-GNB2L1-HIF1A in the GBM that regulates extracellular structure, angiogenesis, hypoxia, and IFN and TGF signaling. We have identified novel lysine residues for acetylation UBE2H (K8, K52) and UBE2S (K211) are associated with overexpressed HAT1 enzymes in GBM

PUBLICATIONS AND PRESENTATIONS

Cumulative Impact Factor

Cumulative impact factor of all publications	=	**112.22**
h-index and i-10 index	=	**6 and 5**
Cumulative citation index	=	**126**

First Author Publications

7. **Smita Kumari**, and Pravir Kumar, "Identification and characterization of putative biomarkers and therapeutic axis in Glioblastoma multiforme microenvironment", *Frontiers in Cell and Development Biology*, DOI: https://doi.org/10.3389/fcell.2023.1236271. (2023) **IF: 6.08** (Frontiers).
8. **Smita Kumari**, and Pravir Kumar, " Design and Computational Analysis of an MMP9 Inhibitor in Hypoxia-Induced Glioblastoma Multiforme ", *ACS Omega*, DOI: https://doi.org/10.1021/acsomega.3c00441. (2023) **IF: 4.132** (ACS).
9. **Smita Kumari,** and Pravir Kumar, "Identification of novel drug combination in Glioblastoma multiforme therapeutics through drug repurposing" *IEEE-2023 International Conference on Emerging Techniques in Computational Intelligence* (ICETCI) (2023).
10. **Smita Kumari**, Rohan Gupta, Rashmi K Ambasta, and Pravir Kumar, " Multiple therapeutic approaches of glioblastoma multiforme: From terminal to therapy", *Biochimica et Biophysica Acta (BBA)-Reviews on Cancer*, DOI: https://doi.org/10.1016/j.bbcan.2023.188913. (2023) **IF: 11.414** (Elsevier).
11. **Smita Kumari**, Dia Advani, Sudhanshu Sharma, Rashmi K Ambasta, and Pravir Kumar, " Combinatorial therapy in tumor microenvironment: where do we stand?", *Biochimica et Biophysica Acta (BBA)-Reviews on Cancer*, DOI: https://doi.org/10.1016/j.bbcan.2021.188585. (2021) **IF: 11.414** (Elsevier).
12. **Smita Kumari**, Sudhanshu Sharma, Dia Advani, Rashmi K Ambasta, and Pravir Kumar, " Unboxing the molecular modalities of mutagens in cancer", *Environmental Science and Pollution Research*, DOI: https://doi.org/10.1007/s11356-021-16726-w. (2021) **IF: 5.190** (Springer Berlin Heidelberg).

Co-author Publications

1. Rohan Gupta, **Smita Kumari**, Anusha Senapati, Rashmi K Ambasta, and Pravir Kumar, "

New era of artificial intelligence and machine learning-based detection, diagnosis, and therapeutics in Parkinson disease", *Ageing Research Reviews* DOI: https://doi.org/10.1016/j.arr.2023.102013 (2023) **IF: 13.01** (Elsevier).

2. Rohan Gupta, **Smita Kumari**, Rahul Tripathi, Rashmi K Ambasta, and Pravir Kumar, "Unwinding the modalities of necrosome activation and necroptosis machinery in neurological diseases", *Ageing Research Reviews*, DOI: https://doi.org/10.1016/j.arr.2023.101855.(2023) **IF: 13.01** (Elsevier).
3. Dia Advani, Sudhanshu Sharma, **Smita Kumari**, Rashmi K Ambasta, and Pravir Kumar, " Precision oncology, signaling, and anticancer agents in cancer therapeutics ", *Anti-Cancer Agents in Medicinal Chemistry*, DOI: https://doi.org/10.1016/bs.acc.2020.09.004. (2022) **IF: 2.527** (Bentham Science Publishers).
4. Pradeep Kumar Dutta, **Smita Kumari**, Rupali Sharma, Gonela Vinay kumar, Hari Sankar Das, Sreejyothi P, Swagata Sil, Swadhin K. Mandal, Aniruddha Sengupta and Arindam Sarkar, " Phenalenyl based platinum anticancer compounds with superior efficacy: design, synthesis, characterization, and interaction with nuclear DNA", *New Journal of Chemistry*, DOI: https://doi.org/10.1039/D0NJ06229D. (2021) **IF: 3.925** (Royal Society of Chemistry).
5. Nimish Gupta, Aasif Ansari, Gaurao V Dhoke, Maheshwerreddy Chilamari, Jwala Sivaccumar, **Smita Kumari**, Snigdha Chatterjee, Ravinder Goyal, Pradip Kumar Dutta, Mallik Samarla, Madhumita Mukherjee, Arindam Sarkar, Swadhin K Mandal, Vishal Rai, Goutam Biswas, Aniruddha Sengupta, Sudip Roy, Monideepa Roy, Shiladitya Sengupta, "Computationally designed antibody–drug conjugates self-assembled via affinity ligands", *Nature Biomedical Engineering*, DOI: https://doi.org/10.1038/s41551-019-0470-8. (2019) **IF: 29.23** (Nature Publishing Group UK).
6. Sanghamitra Mylavarapu, Harsh Kumar, **Smita Kumari**, LS Sravanthi, Misti Jain, Aninda Basu, Manjusha Biswas, Sivaram VS Mylavarapu, Asmita Das, Monideepa Roy, " Activation of epithelial-mesenchymal transition and altered β-catenin signaling in a novel Indian colorectal carcinoma cell line", *Frontiers in Oncology*, DOI: https://doi.org/10.3389/fonc.2019.00054. (2019) **IF: 6.244** (Frontiers Media SA).
7. Pradeep Kumar Dutta, Rupali Sharma, **Smita Kumari**, Ravindra Dhar Dubey, Sujit Sarkar, Justin Paulraj, Gonela Vinaykumar, Manoj Pandey, L.Sravanti, Mallik Samarla, Hari Sankar Das, Yashpal, Heeralal B, Ravinder Goyal, Nimish Gupta, Swadhin K. Mandal, Aniruddha Sengupta and Arindam Sarkar, "A safe and efficacious Pt (II) anticancer prodrug: design, synthesis, *in vitro* efficacy, the role of carrier ligands and *in vivo* tumour growth inhibition", *Chemical Communications*, DOI: https://doi.org/10.1039/c8cc06586a. (2019) **IF: 6.065** (Royal Society of Chemistry).
8. Aniruddha Sengupta, Sanghamitra Mylavarapu, **Smita Kumari**, Samad Hossain, Nimish Gupta, Arindam Sarkar, Aasif Ansari, Thirumurthy Velpandian, Monideepa Roy, Shiladitya Sengupta, " IO-125: A novel supramolecular platinum chemotherapy for triple negative breast cancer", *Journal of Clinical Oncology*, DOI: https://doi.org/10.1200/jco.2015.33.28_suppl.153. (2015) (American Society of Clinical Oncology).

Presentations in National/International Conferences

- National Conference on "Neurodegeneration and Cognition-Recent Advances in Neurological Disease", 02nd to 04th December 2021, SNCI, University of Hyderabad, India.
- One Day International E-Symposium on Women in Science Organized by Delhi Technological University Held on February 11, 2021.
- Presented Poster on "Phenalenyl Based Pt(II) Compounds: Understanding mechanism of action through cellular localization" at International Congress of Cell Biology, 2018, Hyderabad India.
- Presented Poster on Development of novel supramolecular Taxane, Invictus Oncology

Private Limited, 2017, Delhi India.

Attended National/International Conferences

- Attended “Systems Oncology: integrated Approaches to understand and Cure Cancer” conference at Amrita Centre for Nanoscience & Molecular Medicine, held at the Cochin, India" on March 2017.
- Attended "3rd Annual Symposium: Using High-Quality Rodent Disease Models in Pharma R&D" held at Radisson Hotel, Chhattarpur, Delhi, India on 26th August 2016

REFERENCES

1. **Prof. Pravir Kumar, Ph.D.**
   Professor and Head, Department of Biotechnology
   Molecular Neuroscience and Functional Genomics Laboratory
   Dean International Affair, Delhi Technological University (Formerly Delhi College of Engineering)
   Room# FW4TF3, Mechanical Engineering Building
   Shahbad Daulatpur, Bawana Road, Delhi 110042; Phone: +91- 9818898622
   Email: pravirkumar@dtu.ac.in; kpravir@gmail.com
2. **Dr. Aniruddha Sengupta, Ph.D.**
   Deputy General Manger
   Partnerships and Portfolio Strategy
   Sun Pharma Advanced Research Company Ltd.
   Email: Aniruddha.Sengupta@sparcmail.com; anirudd.sengupta@gmail.com
   Phone: +91- 8800145050
3. **Dr. Sanghamitra Mylavarapu, Ph.D.**
   DST WOS-A Woman Scientist
   Regional Centre for Biotechnology
   NCR Biotech Science Cluster
   3rd Milestone, Faridabad Gurgaon Expressway
   Faridabad Haryana – 121001
   Email: sanghamitra.m@gmail.com
   Phone: +91-9999974203

DECLARATION

I hereby declare that the given above information is accurate to the best of my knowledge and belief and can be supported with reliable documents when needed.

Smita Kumari
Date: 15.09.2023
Place: New Delhi, India

turnitin

Similarity Report ID: oid:27535:39001127

PAPER NAME

Modulating Tumor Microenvironment Using Combinatorial Therapy

AUTHOR

Smita Kumari 2K18/PHD/BT/17

WORD COUNT

94627 Words

CHARACTER COUNT

541070 Characters

PAGE COUNT

332 Pages

FILE SIZE

11.8MB

SUBMISSION DATE

Jul 14, 2023 10:10 AM GMT+5:30

REPORT DATE

Jul 14, 2023 10:14 AM GMT+5:30

8% Overall Similarity

Smita

The combined total of all matches, including overlapping sources, for each database.

- 4% Internet database
- Crossref database
- 4% Submitted Works database
- 4% Publications database
- Crossref Posted Content database

Excluded from Similarity Report

- Bibliographic material
- Cited material
- Manually excluded sources
- Quoted material
- Small Matches (Less then 10 words)

26/07/2023

8% Overall Similarity

26/07/2023

Top sources found in the following databases:

- 4% Internet database
- Crossref database
- 4% Submitted Works database
- 4% Publications database
- Crossref Posted Content database

TOP SOURCES

The sources with the highest number of matches within the submission. Overlapping sources will not be displayed.

1	huggingface.co Internet	2%
2	Pukar Khanal, Vishal S. Patil, Vishwambhar V. Bhandare, Prarambh S.R... Crossref	<1%
3	Sharda University on 2021-04-23 Submitted works	<1%
4	Imperial College of Science, Technology and Medicine on 2019-04-13 Submitted works	<1%
5	Rohan Gupta, Pravir Kumar. "Computational Analysis Indicates That P... Crossref	<1%
6	ouci.dntb.gov.ua Internet	<1%
7	tel.archives-ouvertes.fr Internet	<1%
8	wjgnet.com Internet	<1%

9	Rohan Gupta, Rashmi K. Ambasta, Pravir Kumar. "Identification of nove... Crossref	<1%
10	Daniela F Quail, Johanna A Joyce. "Microenvironmental regulation of t... Crossref	<1%
11	Anusree DasNandy, Vishal S. Patil, Harsha V. Hegde, Darasaguppe R. H... Crossref	<1%
12	mdpi-res.com Internet	<1%
13	Vishal S. Patil, Darasaguppe R. Harish, Umashankar Vetrivel, Subarna ... Crossref posted content	<1%
14	Jayesh J Sheth, Riddhi Bhavsar, Aadhira Nair, Chandni Patel et al. "Iden... Crossref posted content	<1%
15	University of Warwick on 2016-10-03 Submitted works	<1%
16	PEC University of Technology on 2017-03-08 Submitted works	<1%
17	"Encyclopedia of Signaling Molecules", Springer Nature, 2018 Crossref	<1%
18	"Full SNO 2020 Abstracts PDF", Neuro-Oncology, 2020 Crossref	<1%
19	Basavaraj Vastrad, Chanabasayya Vastrad, Iranna Kottursheti. "Identifi... Crossref posted content	<1%
20	Dhiraj Kumar, Pravir Kumar. "Integrated Mechanism of Lysine 351, PAR... Crossref	<1%

21	frontiersin.org Internet	<1%
22	RuYi Qi, ZhiMing Huang. "Novel diagnostic, therapeutic, and prognostic... Crossref posted content	<1%
23	theses.hal.science Internet	<1%
24	"Handbook of Immunosenescence", Springer Science and Business Me... Crossref	<1%
25	Oral Roberts University on 2018-09-02 Submitted works	<1%
26	ess.washington.edu Internet	<1%
27	University of Sydney on 2019-07-02 Submitted works	<1%
28	Faheem Ahmed, Anupama Samantasinghar, Afaque Manzoor Soomro, ... Crossref	<1%
29	Amandeep Thakur, Chetna Faujdar, Ram Sharma, Sachin Sharma, Basa... Crossref	<1%
30	vital.seals.ac.za:8080 Internet	<1%
31	"Biomarkers of the Tumor Microenvironment", Springer Science and Bu... Crossref	<1%
32	Indian Institute of Technology IIT Palakkad on 2023-05-02 Submitted works	<1%

33	ueaeprints.uea.ac.uk Internet	<1%
34	Lebanese University on 2020-10-02 Submitted works	<1%
35	Rafael Costa Lima Maia, Howard Lopes Ribeiro Junior, Natália Gindri Fi... Crossref posted content	<1%
36	Jaypee University of Information Technology on 2022-05-14 Submitted works	<1%
37	Trinity College Dublin on 2022-02-24 Submitted works	<1%
38	"Encyclopedia of Cancer", Springer Nature, 2009 Crossref	<1%
39	Indian Institute of Technology Guwahati on 2023-05-22 Submitted works	<1%
40	University of Huddersfield on 2023-03-26 Submitted works	<1%
41	archiv.ub.uni-heidelberg.de Internet	<1%
42	ascopubs.org Internet	<1%
43	University of Patras on 2022-01-16 Submitted works	<1%
44	ebin.pub Internet	<1%

45	"Abstracts from the 23rd Annual Scientific Meeting and Education Day ... Crossref	<1%
46	openscience.ub.uni-mainz.de Internet	<1%
47	Bombay College of Pharmacy on 2022-10-03 Submitted works	<1%
48	Interaction of Immune and Cancer Cells, 2014. Crossref	<1%
49	University of Sheffield on 2022-06-30 Submitted works	<1%
50	Swagatama Mukherjee, Prakash P. Pillai. "Current insights on extracell... Crossref	<1%
51	Associatie K.U.Leuven on 2023-06-09 Submitted works	<1%
52	Marina Baretti, Nilofer S. Azad. "Epigenetic therapy and DNA damage r... Crossref	<1%
53	Medizinischen Universität Wien on 2021-02-12 Submitted works	<1%
54	Yang Yang, Jiayu Liang, Junjie Zhao, Xinyuan Wang et al. "The Multi-O... Crossref posted content	<1%
55	etda.libraries.psu.edu Internet	<1%
56	livrepository.liverpool.ac.uk Internet	<1%

57	Laureate Higher Education Group on 2013-11-01 Submitted works	<1%
58	Lebanese University on 2020-10-01 Submitted works	<1%
59	Qihong Liu, Peiling Zhao, Xiaoying Lin, Xinran Zhang, Wenrong Wang, J... Crossref posted content	<1%
60	Adrián Sanvicente, Cristina Díaz-Tejeiro, Cristina Nieto-Jiménez, Lucia ... Crossref posted content	<1%
61	University of Birmingham on 2022-01-20 Submitted works	<1%
62	spsl.nsc.ru Internet	<1%
63	"Immunotherapy", Springer Science and Business Media LLC, 2021 Crossref	<1%
64	Adrien Dufour, Cyril Kurilo, Jan B. Stöckl, Denis Laloë et al. "Cell specifi... Crossref posted content	<1%
65	Anna Nieborak, Saulius Lukauskas, Jordi Capellades, Patricia Heyn et ... Crossref	<1%
66	Yining Zhang, Kevin R. Hughes, Ravi M. Raghani, Jeffrey Ma, Sophia Or... Crossref	<1%
67	Zheng Chen, Shaohua Su, Min Yang, Fei Wang, Ming Chen. "Profiling an... Crossref posted content	<1%
68	d-nb.info Internet	<1%

69	"Biomarkers of the Tumor Microenvironment", Springer Science and Bu... Crossref	<1%
70	"Hypoxia in Cancer: Significance and Impact on Cancer Therapy", Sprin... Crossref	<1%
71	"New Therapies in Advanced Cutaneous Malignancies", Springer Scien... Crossref	<1%
72	Linyue Hai, Xuchen Cao, Chunhua Xiao. "Exploration of the Shared Gen... Crossref posted content	<1%
73	Mancheng Gong, Shengxing Feng, Dongsheng Zhou, Jinquan Luo, Tian... Crossref posted content	<1%
74	Ramin Ranjbarzadeh, Annalina Caputo, Erfan Babaee Tirkolaee, Saeid J... Crossref	<1%
75	University of Sheffield on 2016-08-15 Submitted works	<1%
76	University of Sydney on 2022-02-28 Submitted works	<1%
77	Yingli Zhu, Lili Wu, Jianfan Lin, Yufei Li, Xuelan Chen, Xizhen Wu, Yaqi ... Crossref posted content	<1%
78	Basavaraj Vastrad, Chanabasayya Vastrad. "Identification of differentia... Crossref posted content	<1%
79	Hao Zhou, Weijie Wang, Ruopeng Liang, Rongtao Zhu, Jiahui Cao, Chen... Crossref posted content	<1%
80	Leiden University on 2022-03-18 Submitted works	<1%

81	Universitat Politècnica de València on 2022-05-17 Submitted works	<1%
82	Universiteit van Amsterdam on 2023-07-03 Submitted works	<1%
83	University of Sydney on 2020-07-21 Submitted works	<1%
84	University of Sydney on 2023-06-30 Submitted works	<1%
85	dokumen.pub Internet	<1%
86	research-information.bris.ac.uk Internet	<1%

Excluded from Similarity Report

- Bibliographic material
- Cited material
- Manually excluded sources
- Quoted material
- Small Matches (Less then 10 words)

EXCLUDED SOURCES

Smita Kumari, Pravir Kumar. "Design and Computational Analysis of an MMP9... Crossref	18%
ncbi.nlm.nih.gov Internet	18%
Smita Kumari, Rohan Gupta, Rashmi K. Ambasta, Pravir Kumar. "Multiple ther... Crossref	12%
Smita Kumari, Dia Advani, Sudhanshu Sharma, Rashmi K. Ambasta, Pravir Ku... Crossref	11%
link.springer.com Internet	2%
Smita Kumari, Sudhanshu Sharma, Dia Advani, Akanksha Khosla, Pravir Kuma... Crossref	2%
dspace.dtu.ac.in:8080 Internet	1%
researchgate.net Internet	1%

Smita

There are Student's publications.

26/07/2023

ACS OMEGA

http://pubs.acs.org/journal/acsodf

Article

Design and Computational Analysis of an MMP9 Inhibitor in Hypoxia-Induced Glioblastoma Multiforme

Smita Kumari and Pravir Kumar*

Cite This: *ACS Omega* 2023, 8, 10565−10590

Read Online

ACCESS | Metrics & More | Article Recommendations | Supporting Information

ABSTRACT: The main therapeutic difficulties in treating hypoxia-induced glioblastoma multiforme (GBM) are toxicity of current treatments and the resistance brought on by the microenvironment. More effective therapeutic alternatives are urgently needed to reduce tumor lethality. Hence, we screened plant-based natural product panels intending to identify novel drugs without elevating drug resistance. We explored GEO for the hypoxia GBM model and compared hypoxic genes to non-neoplastic brain cells. A total of 2429 differentially expressed genes expressed exclusively in hypoxia were identified. The functional enrichment analysis demonstrated genes associated with GBM, further PPI network was constructed, and biological pathways associated with them were explored. Seven webtools, including GEPIA2.0, TIMER2.0, TCGA-GBM, and GlioVis, were used to validate 32 hub genes discovered using Cytoscape tool in GBM patient samples. Four GBM-specific hypoxic hub genes, LYN, MMP9, PSMB9, and TIMP1, were connected to the tumor microenvironment using TIMER analysis. 11 promising hits demonstrated positive drug-likeness with nontoxic characteristics and successfully crossed blood−brain barrier and ADMET analyses. Top-ranking hits have stable intermolecular interactions with the MMP9 protein according to molecular docking, MD simulation, MM-PBSA, PCA, and DCCM analyses. Herein, we have reported flavonoids, 7,4′-dihydroxyflavan, (3*R*)-3-(4-hydroxybenzyl)-6-hydroxy-8-methoxy-3,4-dihydro-2*H*-1-benzopyran, and 4′-hydroxy-7-methoxyflavan, to inhibit MMP9, a novel hypoxia gene signature that could serve as a promising predictor in various clinical applications, including GBM diagnosis, prognosis, and targeted therapy.

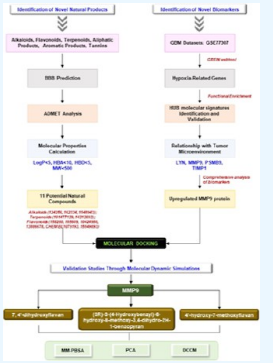

Downloaded via 117.97.226.178 on March 24, 2023 at 07:41:44 (UTC).
See https://pubs.acs.org/sharingguidelines for options on how to legitimately share published articles.

1. INTRODUCTION

According to CBTRUS (Central Brain Tumor Registry of the United States), 2021 recent research, glioblastoma multiforme (GBM) accounts for 48.6% of primary malignant brain tumors. Individuals aged 20−39 years experienced the most significant increases in survival, with 5 year survival increasing from 44 to 73%. In contrast, the failure to enhance survival in older age groups was primarily due to the inability to improve GBM therapy.[1] Currently, GBM is being treated with a combination of surgery, radiation therapy, and chemotherapeutics [alkylating drug temozolomide (TMZ) and antiangiogenic agent bevacizumab]. Furthermore, novel treatments such as tumor-treating fields and immunotherapy offer promise for a better prognosis.[2] Despite these treatment options, GBM patients' overall survival and quality of life remain dismal. The plethora of research mentioned numerous obstacles to GBM treatment, including tumor heterogeneity, acidic microenvironment, and immunosuppression, all of which are linked to the hypoxic environment to some degree.[3]

GBM, being a highly vascularized human tumor, its microcirculation is poor, resulting in the hypoxia region inside the tumor. In the tumor microenvironment (TME), unregulated cell proliferation in the tumor (tumor size exceeds the diameter of >1 mm) often surpasses the capacity of the pre-existing blood capillaries to meet the oxygen demand.[4] This results in a condition known as hypoxia, which impairs the availability of nutrients and promotes genetic instability because of an increase in the generation of reactive oxygen species making it a crucial factor for tumorigenesis. As the master regulator orchestrating cellular responses to hypoxia, hypoxia-inducible factor 1 (HIF-1) plays an essential role in GBM aggressiveness. This modulates the expression of angiogenic factors, such as vascular endothelial growth factor (VEGF), insulin-like growth factor II, and platelet-derived growth factor B (PDGF), and several glucose and fatty acid metabolism factors, the tumor-immune microenvironment, and stimulation of the epithelial−mesenchymal transition (EMT), suppressing apoptosis and promoting autophagy.[5,6] In addition, hypoxia also serves as a niche environment for the aggregation of cancer stem cells, which promotes carcinogenesis and resistance. Tumor cells use a variety of strategies in response to hypoxia, including the expulsion of cytotoxic anticancer drug by ABC-transporters, manifesting a dormant state and exhibiting pluripotency (stemness) traits, which can lead to the failure of existing therapy.[7] Studies showed that hypoxia promotes secretion of cytokines and chemokines which affects immunosurveillance by affecting CD8+ T cell infiltration and disrupting

Received: January 21, 2023
Accepted: February 28, 2023
Published: March 13, 2023

© 2023 The Authors. Published by American Chemical Society

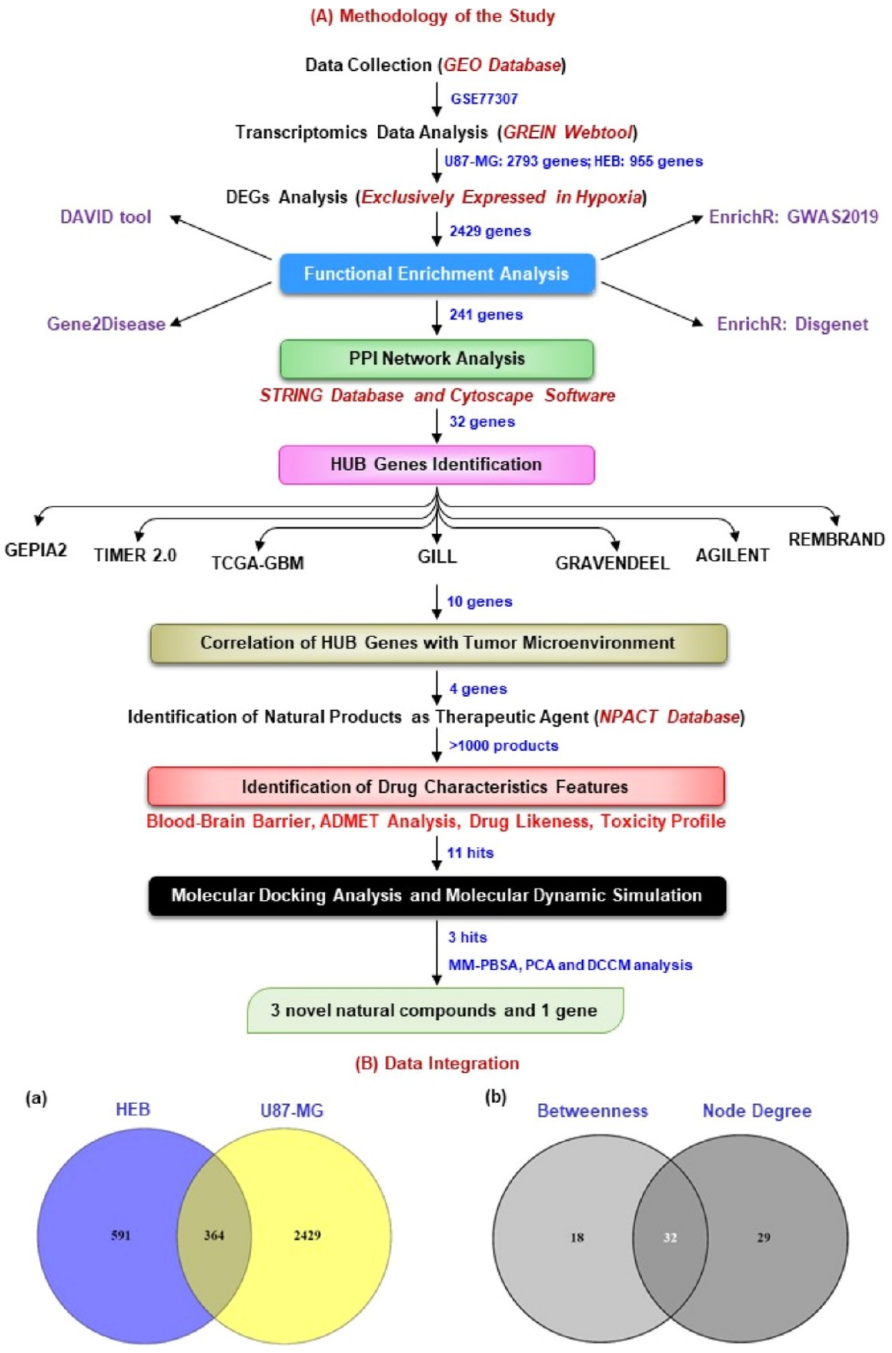

Figure 1. (A) Workflow scheme for identification of novel natural compounds (target) against GBM-hypoxia microenvironment. (B) Interactive Venn analysis: (a) identification of DEGs in the GBM-hypoxia microenvironment. A total of 2429 altered DEGs exclusively expressed in hypoxia were identified from the GSE77307 data set using the GREIN tool. The "cross areas" are common DEGs in both cell lines. The cutoff criteria were p value $\leq$ 0.05 and [log fold change] $\geq \pm 1.5$. (b) A total of 32 hub genes among topology parameters (betweenness and degree) were identified from Cytoscape software. The "cross areas" are common hub genes. HEB (purple): non-neoplastic brain cell; U87-MG (yellow): human GBM cell model.

the cytotoxicity of natural killer cells cells. In addition, hypoxic tumor-associated macrophages reduce T cell responses and encourage tumor proliferation and angiogenesis.[8,9] Another essential piece of research emphasizes the role of $\gamma\delta$ T cells as they do not require antigen presentation for activation compared to conventional T cells and are thus an excellent therapeutic target for brain tumors. This pathway is also mediated by hypoxia.[10] So, given hypoxia's critical role in intratumoral interactions, identifying targets that induce adaptation to the hypoxic niche is crucial for a better understanding of GBM origin, development, and treatment resistance.[11] Indeed, "hypoxia" is an essential driving force of GBM and could be used as a novel treatment tool.[12]

Regardless of the fact that there have been few improvements in the progression of GBM therapies to boost patient survival, researchers and clinicians are indeed eager to study novel therapies and techniques for treating this disease.[13] Natural compounds and their structure analogues have been the source of most medicines' active ingredients for various indications, including cancer.[14] Some widely used plant-derived natural compounds are etoposide, irinotecan, paclitaxel, and vincristine, bacteria-derived anti-cancer therapeutics are mitomycin C and

https://doi.org/10.1021/acsomega.3c00441
ACS Omega 2023, 8, 10565−10590

actinomycin D, and marine-derived anti-cancer therapeutics is bleomycin.[15] Numerous studies suggest that natural compounds are used as chemosensitizers (such as quercetin, resveratrol, withaferin A, etc.), radiosensitizers (such as tetrandrine, zataria, multiflora, and guduchi), and anti-proliferative (such as curcumin, oridonin, rutin, and cucurbitacin) alkaloids and flavonoid agents.[16,17] Identification of new drugs that can modify the BBB (blood−brain barrier), decrease the tumor growth, and prevent the development of recurring tumors is critical for improving overall patient prognosis. In vitro and/or in vivo, various natural compounds with well-established biological benefits have oncologic effects on GBM.[18] These include flavonoids, terpenoids, alkaloids, tannins, coumarins, curcuminoids, terpenes, lignans, natural steroids, and plant extracts.[19] Statistics show that over 60% of the approved anti-cancer agents are of natural origin (natural compounds or synthetic compounds based on natural product models).

The present study conducted transcriptomic analysis between hypoxia and normoxia (in both normal non-neoplastic brain cells and GBM tumor cells) samples to screen differentially expressed genes (DEGs) related to hypoxia effects. Comprehensive bioinformatics and computational methodologies were used to identify hub genes (LYN, MMP9, PSMB9, and TIMP1) and significant modules and pathways related to the TME. We found that matrix metalloproteinase 9 (MMP9) plays a vital role as a hypoxic gene signature, which has the potential to be used as a biomarker. Numerous studies have also shown the dysregulation of MMP9 in the microenvironment associated with hypoxia and cancer.[20] MMP9 can cleave and remodel extracellular matrix (ECM) proteins such as collagens and elastin involved in invasion, metastasis, and angiogenesis.[21] MMP9 is produced de novo by monocytes and inflammatory macrophages, as well as most cancer cells, during stimulation induced by various extracellular signals present in TME, such as proinflammatory cytokines (such as TNF-α, IL-8, and IL-1β) and growth factors (such as TGF-β, PDGF, and bFGF), which can bind to their receptors and activate downstream signaling cascades involved in the activation of transcription factors including NF-κB, SP1, AP1, and HIF-1α. This affects various downstream biological processes, including matrix degradation, remodeling, EMT, enhanced tumoral invasion, metastasis, angiogenesis, inflammation, drug resistance, and so forth; hence, it acts as a challenging target for targeted therapy for cancer.[22]

Targeting TME has been a significant focus in recent years, and hence MMP inhibitors that will target a hypoxia condition in the microenvironment could be of great significance as a new antitumor agent. For this purpose, we have availed network pharmacology, structure-based drug design approach such as molecular docking, molecular dynamics (MD) simulation analysis, and molecular mechanics Poisson−Boltzmann surface area (MM-PBSA) approach to discover prospective classes of natural compounds with druggable and nontoxic properties from the plant-based natural compounds library. We identified 11 hits based on the particular interaction that satisfy the ADMET and LIPINSKI rule of five analyses, pass the toxicity profile, and have a significant affinity for the MMP9 binding site domain. The three best-docked compounds were further subjected to MDS for 50 ns to understand protein−ligand complex stability. Previously also, researchers have explored the potential of alkaloids and flavonoids for anti-cancer treatments.[23,24] Drugs, including natural compounds that target MMP9, have not been used in the clinical setting. Therefore, targeted MMP9 drugs must be screened for treating patients with GBM. Our results can potentially benefit from managing GBM malignancy caused by a hypoxia microenvironment. The findings of this study contribute to a better understanding of the role of the hypoxia microenvironment. Figure 1A depicts the process of the methodologies used in this investigation.

2. MATERIALS AND METHODS

2.1. Data set Acquisition and Processing. The NCBI-Gene Expression Omnibus (NCBI-GEO; https://www.ncbi.nlm.nih.gov/geo) database[25] is a publicly accessible library of next-generation sequencing, RNA sequencing, and microarray profiling used to gather GBM and non-neoplastic brain tissue gene expression profiles from GEO accession number, GSE77307. The transcriptome data in GSE77307 were derived from GPL11154, a platform using Illumina HiSeq 2000 (*Homo sapiens*). This included three replicates of each U87-MG cell line as a human GBM cancer cell model and the human brain HEB cell line as a non-neoplastic brain cell model cultured in 21% oxygen (normoxia) and 1% oxygen (hypoxia) for transcriptional profiling. This data set was chosen due to the availability of only one data set in the database based on the filter (glioblastoma; hypoxiaTME). High-throughput functional transcriptomic expression data from GSE data sets were analyzed through GEO RNA-seq Experiments Interactive Navigator online server (GREIN; https://shiny.ilincs.org/grein).[26] GREIN is provided by the backend compute pipeline for uniform processing of RNA-seq data and large numbers (>65,000) of processed data sets.

2.2. Enrichment Analysis of Identified DEGs. Transcriptomics data analysis was performed using the GREIN web tool. DEGs were determined by comparing their expression levels in hypoxia (1% oxygen) versus normoxia (21% oxygen) in GBM cells, U87-MG, and normal brain cells, HEB. Statistically significant DEGs were screened using cutoff filter criteria such as unpaired t-test and p-value ≤ 0.05, false discovery rate ≤ 0.05, and [log fold change] ≥ 1.5. DEGs only exclusively expressed in hypoxia conditions were considered for further analysis. In addition, enrichment analysis of DEGs, including both upregulated and downregulated genes associated with GBM, was performed by utilizing different omics approaches such as the Database for Annotation, Visualization and Integrated Discovery (DAVID) functional annotation tool (https://david.ncifcrf.gov/),[27] gene set to diseases (GS2D) tool (http://cbdm.uni-mainz.de/geneset2diseases),[28] and Enrichr-GWAS2019 and Enrichr-DisGeNET of Enrichr tool (https://amp.pharm.mssm.edu/Enrichr)[29,30] to identify and prioritize the most significant genes associated with GBM. Furthermore, the biological pathway and functional enrichment analyses of candidate DEGs and hub genes were determined through a freely available software known as the FunRichr tool (version 3.1.3) (http://www.funrich.org/)[31] to identify the biological pathways associated with them.

2.3. Integration of Protein−Protein Interaction Network and Hub Genes Identification. The selected enriched genes were then examined for designing Protein−Protein Interaction (PPI) using an online Search Tool for the Retrieval of Interacting Genes/Proteins (version 11.5) (STRING, https://string-db.org/) for *H. sapiens*[32] that covers known and predicted interactions for different organisms. The experimentally significant interactions (with high confidence scores $\geq$ 0.700) were chosen to build a network model, while the others were excluded from the analysis. Cytoscape software (version

https://doi.org/10.1021/acsomega.3c00441
ACS Omega 2023, 8, 10565−10590

3.8.1) (https://cytoscape.org/)[33] was implemented to analyze the PPI network and identify the hub protein. To calculate the topological parameters such as the node degree (the number of connections to the hub in the PPI network) and betweenness (which corresponds to the centrality index of a particular node), we used the CentiScaPe plugin (version 2.2). It denotes the shortest route between two nodes. Genes with higher values than the average score were chosen.

2.4. Hub Protein Shorting and Validation. To verify and validate the expression of the shortlisted hub proteins, we have utilized both transcriptomics and genomics data from GBM patients. Different databases were explored for RNA sequencing data, such as GEPIA2.0, TIMER2.0, TCGA-GBM, and GlioVis-GILL, and microarray data, such as GlioVis-REMBRANDT, GlioVis-AGILENT, and GlioVis-Gravendeel based on Cancer Genome Atlas (TCGA)-GBM.[34−36] GEPIA2.0 analyzed the RNA sequencing expression data of 9736 cancers and 8587 normal samples from the TCGA and GTEx projects using a standard processing pipeline. GlioVis is a user-friendly web tool that allows users to study brain tumor expression data sets through data visualization and analysis. For GlioVis-GILL, Gill et al. conducted RNA-seq and histological examination on radiographically labeled biopsies collected from different regions of GBM.[37] GlioVis-Repository of Molecular Brain Neoplasia Data (REMBRANDT), a cancer clinical genomics database and a web-based data mining and analysis platform, includes data produced from 874 glioma specimens with approximately 566 gene expression arrays and 834 copy number arrays generated through the Glioma Molecular Diagnostic Initiative.[38] In GlioVis-Gravendeel, gene expression profiling was carried out on a large cohort of glioma samples from all histologic subtypes and grades.[39] In TIMER2.0, multiple immune deconvolution algorithms were used to assess the quantity of immunological infiltrates. Its Gene DE module allows users to investigate the differential expression of any gene of interest in tumors and surrounding normal tissues across all TCGA tumors. All hub genes significantly expressed in all seven patient GBM databases were chosen for subsequent research. Finally, shortlisted genes were again subjected to Tumor IMmune Estimation Resource (TIMER) (https://cistrome.shinyapps.io/timer)[40] analysis. Here, we utilized this database to link hub gene expression with tumor purity and estimate the infiltration levels of six immune cell types [CD4+ T cells, CD8+ T cells, B cells, macrophages, neutrophils, and dendritic cells (DCs)] in GBM data sets. This tool calculates immune infiltration based on immune subsets' preset characteristic gene matrix.

2.5. Localization Study and Construction of Transcription Factor-Gene Network. CELLO (http://cello.life.nctu.edu.tw/cello.html): subcellular localization predictor combines a two-level support vector machine system and the homology search method-based tool to predict the subcellular localization of the protein.[41] Regulatory transcription factors (TFs) that control the expression of genes at the transcriptional level were obtained using the JASPAR database, containing curated and nonredundant experimentally defined TF binding sites.[42] The TF-gene interaction networks were constructed and analyzed with NetworkAnalyst (version3.0) (https://www.networkanalyst.ca/).[43]

2.6. Identification of Natural Compounds and Blood−Brain Permeability Prediction. The plant-derived natural compounds with known anti-cancer bioactivity information were obtained from a literature survey through PubMed and the central resource Naturally Occurring Plant-based Anti-cancer Compound-Activity-Target database (NPACT, http://crdd.osdd.net/raghava/npact/).[44] This database, which presently has 1574 compound entries, collects information on experimentally confirmed plant-derived natural compounds with anticancer action (in vitro and in vivo). We have chosen terpenoids (513 entries), flavonoids (329 entries), alkaloids (110 entries), polycyclic aromatic natural compounds (63 entries), aliphatic natural compounds (20 entries), and tannin (6 entries).BBB obstructions make it difficult to create drugs to treat brain cancer. The BBB blocks the uptake of necessary therapeutic drugs into the brain. The epithelial-like tight connections seen in the brain capillary endothelium are the source of this characteristic. For the treatment of GBM, it is crucial to screen drugs that have the ability to cross the BBB.[45] While designing a drug for brain diseases, physicochemical properties and brain permeation properties should be optimized. In consideration of this challenge, we analyzed our candidate natural compounds for physicochemical properties using the SwissADME (http://www.swissadme.ch/)[46] analysis tool and the CBLigand (version 0.90) online BBB predictor (https://www.cbligand.org/BBB/).[47]

2.7. Prediction of Molecular Properties and Drug Toxicity. Each natural compound's molecular formula (MF), molecular weight (MW), hydrogen bond acceptor (HBA), hydrogen bond donor (HBD), log *P* value, and SMILES were retrieved using the PubChem chemical database (https://pubchem.ncbi.nlm.nih.gov/). The Lipinski rule of five was used to estimate the druggability of each phytocompound using the SMILES data of individual compounds on the MolSoft web server (https://molsoft.com/mprop/).[48] The server includes structural data such as MF, MW, HBA, HBD, and logP and a drug-likeness score prediction (DLS). The toxicity and pharmacokinetics of natural compounds with positive DLS were also predicted using the ADMETlab 2.0 (https://admetmesh.scbdd.com/) webserver.[49]

2.8. Molecular Docking Studies. *2.8.1. Preparation of Ligand.* Based on the network analysis and pharmacology approach, 11 natural compounds, viz., 6 flavonoids, 3 alkaloids, and 2 terpenoids, were qualified for all criteria required for being used as a drug candidate. Thus, the three-dimensional (3D) structures of 11 natural compounds along with 2 reference drugs (one natural compound and one conventional standard molecule) were retrieved from the PubChem database (https://pubchem.ncbi.nlm.nih.gov/) in the structure data file (.sdf) format. These structures additionally went through the dock prep section of Discovery Studio Visualizer[50] (BIOVIA Discovery Studio Visualizer; https://discover.3ds.com/discovery-studio-visualizer-download) 2019. The conjugate gradients algorithm was used to minimize the ligand structures using the "uff" forcefield.[51] The polar hydrogens and Gasteiger charges were added to the ligands to convert them into the ".pdbqt" format.

2.8.2. Preparation of Protein. Based on the network analysis and TIMER analysis, the overexpressed MMP9 gene associated with the TME was prioritized for future investigation. The Research Collaboratory for Structural Bioinformatics (RCSB; https://www.rcsb.org/) protein data bank was used to retrieve the X-ray crystallographic structure of MMP9 (PDB: 4HMA). Further, the PrankWeb (https://prankweb.cz/) server based on P2Rank, a machine learning method, was used to retrieve the information on the target active site and binding pockets, and the ligand was docked within the predicted site. Functional characteristics of protein structures were validated using

https://doi.org/10.1021/acsomega.3c00441
ACS Omega 2023, 8, 10565−10590

Ramachandran plot, ERRAT, and VERIFY3D.[52−54] For a good quality model, the ERRAT quality factor should be greater than 50, and the number of residues having a score ≥ 0.2 in the 3D/1D profile, as predicted by the VERIFY3D server, should be more than 80%.

2.8.3. Protein−Ligand Docking. All ligands were docked against protein using AutoDock vina 4.0 executed through the POAP pipeline.[55] The intermolecular interaction compounds showing the least binding energy and maximum intermolecular interaction with the active site residues were selected to visualize protein−ligand interactions using BIOVIA Discovery Studio Visualizer 2019 and further subjected for MD simulation.

2.9. MD Simulation of Best-Docked Protein−Ligand Complex. In order to infer the stability of docked complexes, we prioritized five complexes (three test and two standard complexes) and subjected to all-atoms explicit MD simulation for 50 ns production run using GROMACS version 2021.3 software package (GNU, General Public License; http://www.gromacs.org).[56] The ligand and protein topology were generated using Amber ff99SB-ildn force field (https://ambermd.org/AmberTools.php) via antechamber x-leap tool. The system was solvated using the TIP3P water model in an orthorhombic box with a boundary condition of 10.0 Å from the edges of the protein in all directions. The system was neutralized by adding necessary amounts of counterions. The conjugate gradient approach was employed to obtain the near-global state least-energy conformations after the steepest descent. Canonical (constant temperature, constant volume, *NVT*) and isobaric (constant temperature, constant pressure, *NPT*) equilibrations were performed on the systems for 1 ns. A modified Berendsen thermostat method was used in *NVT* equilibration to keep both the volume and temperature constant (300 K). Similarly, a Parrinello−Rahman barostat was used during *NPT* equilibration to keep the pressure at 1 bar constant. The particle mesh Ewald approximation was used with a 1 nm cutoff to calculate the long-range electrostatic interactions, van der Waals interactions, and coulomb interactions. In order to control the bond length, the LINCS algorithm (LINear Constraint Solver algorithm) was utilized. The coordinates were recorded every two fs during each complex's production run of 50 ns. In-built GROMACS utilities were used to evaluate the generated trajectories, and other software packages were incorporated where necessary for a more specialized analysis. MD trajectories were analyzed to determine the c-alpha root-mean-square fluctuation (RMSF) and root-mean-square deviation (RMSD) of the backbone and complex, the protein radius of gyration (R_g), the protein solvent-accessible surface area (SASA), and the number of hydrogen bonds between the protein and the ligand.

2.10. Investigation of Binding Affinity Using MM-PBSA. It is standard procedure to use the relative binding energy of a protein−ligand complex in MD simulations and thermodynamic calculations. MM-PBSA was performed by "g_mmpbsa" tool.[57] The total free energy of each of the three entities (ligand, protein receptor, and complex) mentioned can be calculated by adding the potential energy of the molecular mechanics and the energy of solvation. Early research work[58,59] was used to obtain the parameter that was used to determine the binding energy.

$$\Delta G_{(\text{binding})} = G_{(\text{complex})} - G_{(\text{protein})} - G_{(\text{ligand})} \quad (1)$$

where $G_{(\text{complex})}$ is the total free energy of the ligand−protein complex and $G_{(\text{protein})}$ and $G_{(\text{ligand})}$ are the total free energies of the isolated protein and ligand in the solvent, respectively.

The binding energy was calculated over the stable trajectory observed between 50 ns using 50 representative snapshots.

2.11. PCA and DCCM Analyses. Principal component analysis (PCA) was used in the current work to analyze the main types of molecular motions utilizing MD trajectories. It is employed to study the eigenvectors, which are crucial to understanding the overall movements of proteins during ligand binding. The "least square fit" to the reference structure is used to eliminate the molecule's translational and rotational mobilities. The "time-dependent movements" that the components carry out in a specific vibrational mode are demonstrated by projecting the trajectory onto a particular eigenvector. The average of the projection's time signifies the involvement of atomic vibration components in this form of synchronized motion. Using the "g_covar" and "g_anaeig" tools, which are already included in the GROMACS software package, the PCA was performed by first creating the covariance matrix of the Cα-atoms of the protein and then diagonalizing it. The *xmgrace* tool was used to plot the graphs.[60−62]

To determine if the motion between atom pairs is correlated (positive or negative), the dynamic cross-correlation matrix (DCCM) measures the magnitude of all pairwise cross-correlation coefficients. Herein, we investigated each element of DCCM, where C_{ij} = 1 representing the case of positively correlated fluctuations of atoms *i* and *j* have the same period and same phase, while C_{ij} = −1 and C_{ij} = 0, respectively, represent negatively or not correlated.[63,64]

2.12. Statistical Analysis. This study investigated the expression of hub genes in the GEPIA2.0 database and their connection with GBM using ANOVA. $|\log_2$ fold change$|$ cutoff ≤ 1.5 and *Q*-value ≤ 0.05 were considered significant. Tukey's Honest Significant Difference statistics were employed in the GlioVis database, where the *p*-value of the pairwise comparisons was used (***$p \le 0.001$; **$p \le 0.01$; *$p \le 0.05$; ns, not significant). In TIMER2.0, the Wilcoxon test's statistical significance was indicated by the number of stars (***$p \le 0.001$; **$p \le 0.01$; *$p \le 0.05$; ns, not significant). In the TIMER database analysis, a partial Spearman's correlation was applied. When $|\rho| > 0.1$, it indicated a correlation between the genes and immune cells. Significant data in the biological and KEGG pathway enrichment were screened according to *p*-value ≤ 0.05 with the Students' *t*-test.

3. RESULTS

3.1. Omics Data Mining and Identification of DEGs in GBM Hypoxia Condition. This study used the expression profile (GSE77307) from the NCBI-GEO database to identify DEGs exclusively expressed in hypoxia-induced GBM because targeting the hypoxic microenvironment could be a new tool for treatment.[7] Cells derived from GBM patient tumors and normal brain tissue were grown in hypoxic and normoxic conditions. GEO's raw RNA sequence (RNA-seq) data were processed and uploaded to GREIN using the GEO RNA-seq experiments processing (GREP2) pipeline. GREIN workflows with a graphical user interface provide complete interpretation, visualization, and analysis of processed data sets.[65] A normalized MA plot has been shown in Supporting Information Figure S1. GBM cancer cell model (U87-MG) and the human non-neoplastic brain cell model (HEB) were analyzed separately by comparing hypoxia with normoxia conditions to find dysregulated genes in hypoxia conditions. Subsequently, Venn's analysis demonstrated the involvement of 364 genes that were common in hypoxia conditions in both cell lines. 591 and 2429 genes

https://doi.org/10.1021/acsomega.3c00441
ACS Omega 2023, 8, 10565−10590

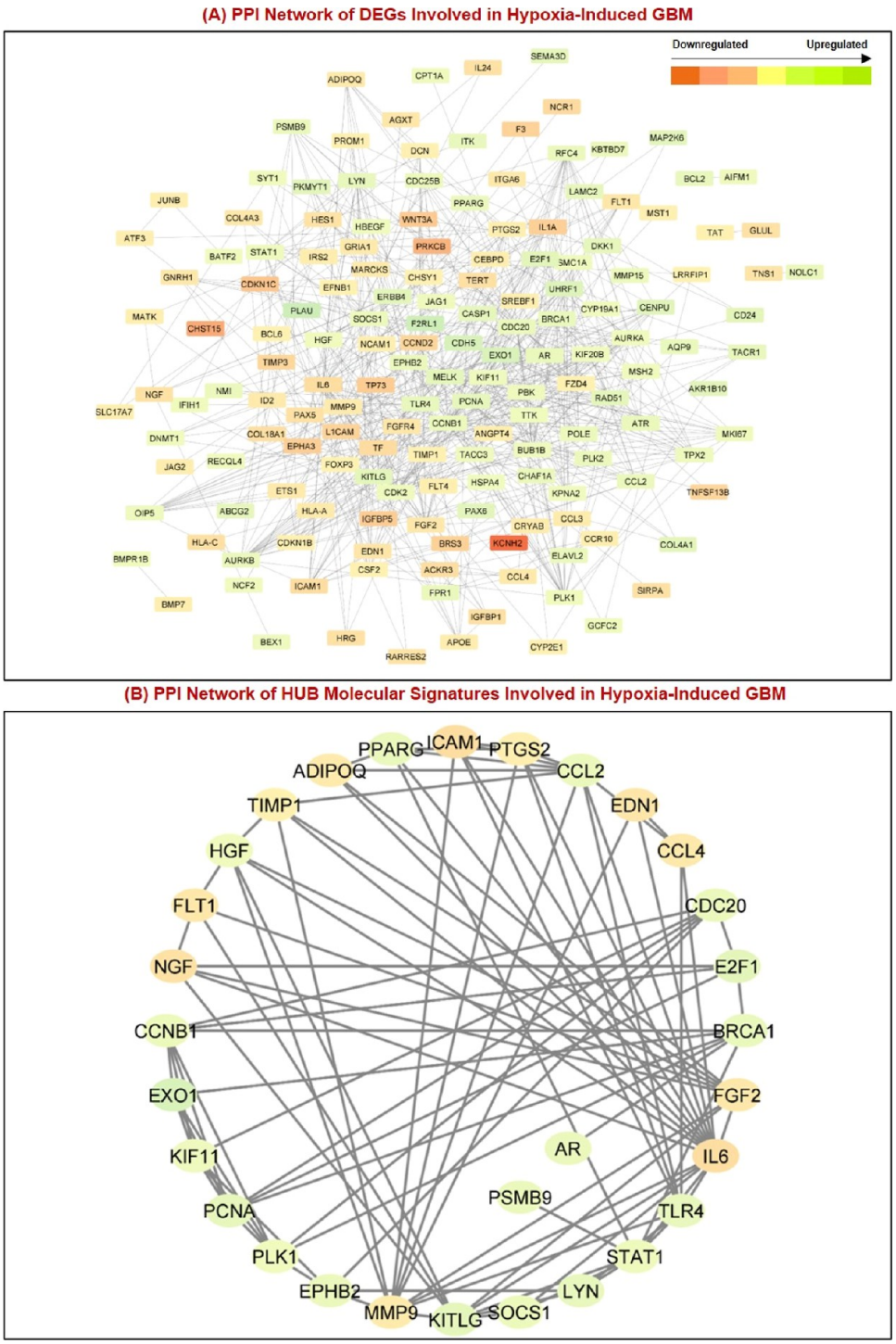

Figure 2. PPI network complex and modular analysis. (A) Module 1: a total of 241 DEGs (129 upregulated genes and 112 downregulated genes) were filtered into the DEG PPI network complex using STRING and Cytoscape software. It was composed of 163 nodes and 592 edges. (B) Module 2 showed a PPI network of 32 hub genes. Nodes in green signify upregulation and nodes in red signify downregulation. The colors from red to green represent the intensities of expression ($\log_2$ fold change, value: −6 to +14; cutoff value ±1.5), where red represents downregulation and green represents upregulation. In the presented figure, varying shades of red (from dark to light) show a decrease in the expression of downregulated genes, while shades of green (from light to dark) show increase in the expression of upregulated genes. Upregulated genes with $\log_2$ fold change $\geq$ 1.5 and downregulated genes with $\log_2$ fold change $\leq$ 1.5. STRING: Search Tool for the Retrieval of Interacting Genes/Proteins database.

expressed exclusively in hypoxia conditions in HEB and U87-MG cell lines, respectively.[66] Among them, we were interested in 2429 hypoxia-related DEGs exclusively expressed in hypoxia conditions and hence were considered for further analysis (Figure 1B,a). DAVID enrichment analysis of 2429 genes revealed that 30 genes have a significant association with GBM. In addition, G2SD enrichment (default cutoff parameter) showed 25 genes related to GBM. Similarly, GWAS-2019 and DisGeNET of Enrichr webtool enrichment analysis showed 3 and 242 genes linked with GBM, respectively. When we

https://doi.org/10.1021/acsomega.3c00441
ACS Omega 2023, 8, 10565−10590

Table 1. In Silico Expression Analysis and Validation of all 32 HUB Signatures Using Various Databases Containing Data from GBM Patient Samples[a]

Gene Name	RNA sequence dataset		Microarray datasets				
	GEPIA2	TIMER2.0	GlioVis				
			TCGA_GBM	GILL	REMBRANDT	AGILENT-4502a	Gravendeel
ADIPOQ							
AR							
BRCA1							
CCL2							
CCL4							
CCNB1							
CDC20							
E2F1							
EDN1							
EPHB2							
EXO1							
FGF2							
FLT1							
HGF							
ICAM1							
IL6							
KIF11							
KITLG							
LYN							
MMP9							
NGF							
PCNA							
PLK1							
PPARG							
PSMB9							
PTGS2							
SOCS1							
STAT1							
TF							
TIMP1							
TLR4							
SAMPLE SIZE							
GBM TUMOR	163	156	75	153	219	489	159
NORMAL TISSUES	207	4	17	5	28	10	8

[a]Dark green color = ***$p \leq 0.001$; medium green color = **$p \leq 0.01$; light green color = *$p \leq 0.05$; gray color = ns, not significant. In all seven GBM patient databases, including four RNA sequence data sets and three microarray data sets; the gene name printed in blue is among the top 10 hub genes that are significantly dysregulated.

https://doi.org/10.1021/acsomega.3c00441
ACS Omega 2023, 8, 10565−10590

(A) Correlation Analysis of 10 HUB Molecular Signatures with GBM Tumor Microenvironment

Gene Name	Variable	Purity	B Cell	CD8+ T Cell	CD4+ T Cell	Macrophage	Neutrophil	Dendritic Cell
BRCA1	partial.correlation	0.312	-0.132	0.042	0.090	0.048	0.149	0.090
	p-value	0.000	0.007	0.396	0.066	0.327	0.002	0.065
CCNB1	partial.correlation	0.347	-0.069	0.011	-0.161	-0.069	-0.038	0.070
	p-value	0.000	0.159	0.823	0.001	0.161	0.441	0.154
CDC20	partial.correlation	0.413	-0.135	-0.056	-0.091	-0.073	-0.086	0.054
	p-value	0.000	0.006	0.257	0.062	0.136	0.078	0.267
EXO1	partial.correlation	0.487	-0.067	-0.059	-0.072	-0.052	-0.054	-0.022
	p-value	0.000	0.174	0.225	0.141	0.293	0.268	0.656
KIF11	partial.correlation	0.404	-0.098	-0.018	0.004	-0.008	0.058	0.073
	p-value	0.000	0.046	0.721	0.932	0.863	0.234	0.138
LYN	partial.correlation	-0.439	0.277	-0.358	0.232	0.241	0.399	0.500
	p-value	0.000	0.000	0.000	0.000	0.000	0.000	0.000
MMP9	partial.correlation	-0.173	-0.095	-0.186	-0.059	-0.086	0.037	0.333
	p-value	0.000	0.052	0.000	0.228	0.079	0.449	0.000
PCNA	partial.correlation	0.382	0.061	0.054	-0.108	-0.016	-0.028	0.077
	p-value	0.000	0.211	0.267	0.027	0.750	0.564	0.117
PSMB9	partial.correlation	-0.172	0.324	-0.214	-0.031	0.099	0.153	0.229
	p-value	0.000	0.000	0.000	0.527	0.042	0.002	0.000
TIMP1	partial.correlation	-0.392	-0.119	0.002	0.009	0.050	-0.120	0.547
	p-value	0.000	0.015	0.975	0.847	0.310	0.014	0.000

Spearman positive correlation (ρ>0, p<0.05) Spearman negative correlation (ρ<0, p<0.05)

(B) Correlation Of 4 Molecular Signatures With Immune Infiltration in GBM

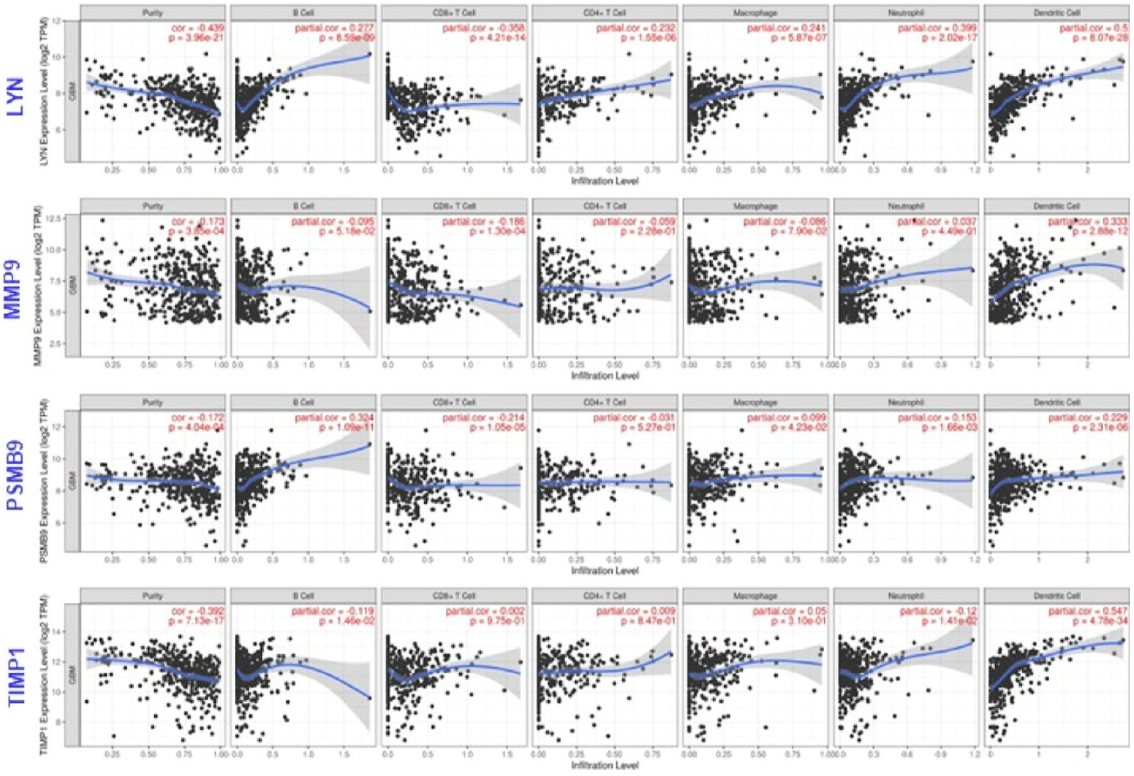

Figure 3. (A) Correlation analysis of 10 validated hub genes in GBM patient's data sets with tumor purity and six tumor infiltrating immune cells (B-cells, CD8+ T cells, CD4+ T cells, macrophages, neutrophiles, and DCs). Genes highlighted in blue show negative tumor purity and hence shortlisted for further analysis. (B) Scatterplots from the TCGA-GBM data set illustrating the relationship between LYN, MMP9, PSMB9, and TIMP1 gene expressions and tumor purity and six key tumor infiltrating immune cell types in GBM. On the left-most panel, gene expression levels are compared to tumor purity, and genes that are highly expressed in the microenvironment are expected to have negative associations with tumor purity. In the TIMER database analysis, partial Spearman's correlation was applied. When $|\rho| > 0.1$ and p-value ≤ 0.05, it indicated that there was a link between the genes and immune cells. In general, the smaller the ρ value, the smoother the curve; the larger the ρ value, the fuller the curve; when $\rho < 0.5$, the curve is ellipse; when $\rho = 0.5$, the curve is parabola; when $\rho \geq 0.5$, the curve is hyperbola.

https://doi.org/10.1021/acsomega.3c00441
ACS Omega 2023, 8, 10565−10590

integrated the 3 enrichment analysis methods, a total of 241 GBM-related DEGs were documented, including 129 upregulated genes and 112 downregulated genes (Supporting Information Table S1).

3.2. PPI Analysis and Exploration of HUB Signatures in Hypoxia-Induced GBM. With the help of the STRING database on Cytoscape software, we evaluated the PPI network comprising 241 DEGs based on coexpression to explore the possibility of hub genes. The network consists of 163 nodes and 592 edges with a high confidence score of ≥0.700. Molecular signatures in the network were displayed based on their expression (green for upregulation, red for downregulation) and intensity based on fold change (log fold change, value: −6 to +14). To evaluate the importance of nodes in the PPI network, the topological parameters, including degree centrality and betweenness centrality, were calculated and utilized in the present study using the CentiScaPe plugin in Cytoscape software to find hub genes. We observed degree with a range of 1−14 and betweenness with a range of 0−684. Using the online Venny 2.0 tool, we observed the exchange and generated a Venn plot between "degree" and "betweenness" (Figure 1B,b). The 32 hub genes, a small number of critical nodes for the protein interactions in the PPI network, were chosen with a degree centrality > 7.00 (average value) and betweenness centrality > 342 (average value). PPI networks for DEGs and hub genes are shown in Figure 2A,B, respectively.

3.3. Validation of HUB Signatures in GBM Patients. We conducted the expression analysis of all 32 HUB signatures using various online web servers for RNA sequencing data, such as GEPIA2.0, TIMER2.0, TCGA-GBM, and GlioVis-GILL, and microarray data, such as GlioVis-REMBRAND, GlioVis-AGILENT, and GlioVis-Gravendeel. These web servers from the TCGA project provide extensive information concerning GBM patients. The expression of all 32 genes was examined using the databases described above as described in Table 1. Based on the selection criteria (***$p \leq 0.001$; **$p \leq 0.01$; *$p \leq 0.05$; ns, not significant), 10 genes out of 32 exhibited significant expression levels in both RNA and microarray databases of GBM patient samples. This also explains that these 10 molecular signatures, namel,y BRCA1, CCNB1, CDC20, EXO1, KIF11, LYN, MMP9, PCNA, PSMB9, and TIMP1, were expressed in GBM tumor samples. Molecular function of these signatures and their role in various malignancies have been briefly explained here. Breast cancer gene 1 (BRCA1) is a tumor suppressor protein that is essential for DNA damage repair, chromatin remodeling, and cell cycle regulation. Mutations in BRCA1 cause genetic changes, cancer, and a failure to repair DNA damage. Patients with BRCA1 germ line mutations have been associated with sporadic instances of GBM.[67] Cyclin B1 (CCNB1) and cell division cycle protein 20 (CDC20), both of which are associated with cell progression, demonstrated that their increased expression was substantially correlated with poor survival in GBM.[68] Exonuclease 1 (EXO1) is a member of the DNA damage repair enzyme family that is particularly active in homologous recombination (HR) and nonhomologous end-joining following DNA double-strand breaks. It increases cell proliferation, invasion, and metastasis in glioma and hepatocellular carcinoma.[69] According to Liu et al., increased Kinesin family member 11 (KIF11) enhances cell cycle development and chemoresistance, negatively correlates with the TP53 expression, and is a major cause of malignancy in GBM.[70] Lck/yes-related protein tyrosine kinase (LYN) showed a substantial positive connection with PD-L1, was connected to the control of carcinogenic genes, and was engaged in tumor mutation. In gliomas, LYN may serve as both a potential diagnostic and immunotherapy marker.[71] Likewise, the proliferative capacity of cells is impacted by high MMP9 expression in gliomas, which is also linked to patient survival rates.[72] Proteasome 20S subunit beta 9 (PSMB9), along with PSMB8 and PSMB10 genes that encode catalytic subunits of the immunoproteasome, was overexpressed in GBM and was reported by Liu et al. as a novel biomarker for lower-grade glioma prognosis and can be exploited as an immunotherapy target.[73] Similarly, a study by Smith et al., demonstrated that proliferating cell nuclear antigen (PCNA), a nuclear DNA replication and repair protein, has increased expression and poor prognosis in pancreatic ductal adenocarcinoma.[74] Last but not least, tissue inhibitor of metalloproteinases-1 (TIMP-1) is known to control the proteolytic activity of the MMPs that break down the extracellular matrix. High tumor TIMP-1 protein expression in GBM has been linked to irinotecan resistance and anticipated to predict lower overall survival in GBM.[75]

Thus, only 10 molecular signatures were selected for further analysis, which were significantly expressed in all seven patient GBM databases.

3.4. Correlation between HUB Signatures and GBM TME. Here, in this study, to filter out molecular signatures involved in TME, we used the TIMER database to investigate the connection and correlation of 10 molecular signatures (BRCA1, CCNB1, CDC20, EXO1, KIF11, LYN, MMP9, PCNA, PSMB9, and TIMP1) expression with tumor purity and immune cell infiltration in patients with hypoxia-induced GBM. Data have been compiled in Figure 3A. In addition, we used GBM data sets to estimate the amounts of infiltration of six immune cell types [(CD4+ T cells, CD8+ T cells, B cells, macrophages, neutrophils, and DCs). Tumor purity normalized spearman correlation analyses revealed a positive and negative correlation expression of hub genes with B cells, CD4+ T cells, CD8+ T cells, macrophages, neutrophils, and DCs in GBM cancer. After the inputs are successfully entered, scatterplots will be created and displayed, displaying the purity-corrected partial Spearman's rho value (ρ) and statistical significance. Genes with negative associations with tumor purity are highly expressed in TME, and positive associations are highly expressed in the tumor cells. Finally, we discovered four molecular signatures (LYN, MMP9, PSMB1, and TIMP1) with negative tumor purity, and it implicated in the GBM's hypoxic microenvironment. Figure 3B illustrates the scatterplot showing the relationship between LYN, MMP9, PSMB9, and TIMP1 gene expressions and tumor purity and six key tumor-infiltrating immune cell types in GBM.

LYN expression shown positive correlation with B cells (ρ = 0.28, $p < 0.001$), CD8+ T cells (ρ = 0.23, $p < 0.001$), macrophages (ρ = 0.24, $p < 0.001$), neutrophils (ρ = 0.39, $p < 0.001$), and DCs (ρ = 0.49, $p < 0.001$) and negative correlation with $CD8^+$ T Cells (ρ = −0.35, $p < 0.001$) in GBM. MMP9 shows positive correlation with DCs (ρ = 0.33, $p < 0.001$) and negative correlation with CD8+ T Cells (ρ = −0.18, $p < 0.001$). PSMB9 showed positive correlation with B cells (ρ = 0.32, $p < 0.001$), macrophages (ρ = 0.99, $p < 0.001$), neutrophils (ρ = 0.15, $p < 0.001$), and DCs (ρ = 0.22, $p < 0.001$) and negative correlation with $CD8^+$ T Cells (ρ = −0.21, $p < 0.001$).

A study by Wang et al., showed that cancer-derived MMP9 plays a crucial role in the development of tolerogenic DCs which further affects regulatory T cells (T_{reg}) in the case of laryngeal cancer.[76] Similarly, mounting evidence suggested that MMP9

https://doi.org/10.1021/acsomega.3c00441
ACS Omega 2023, 8, 10565−10590

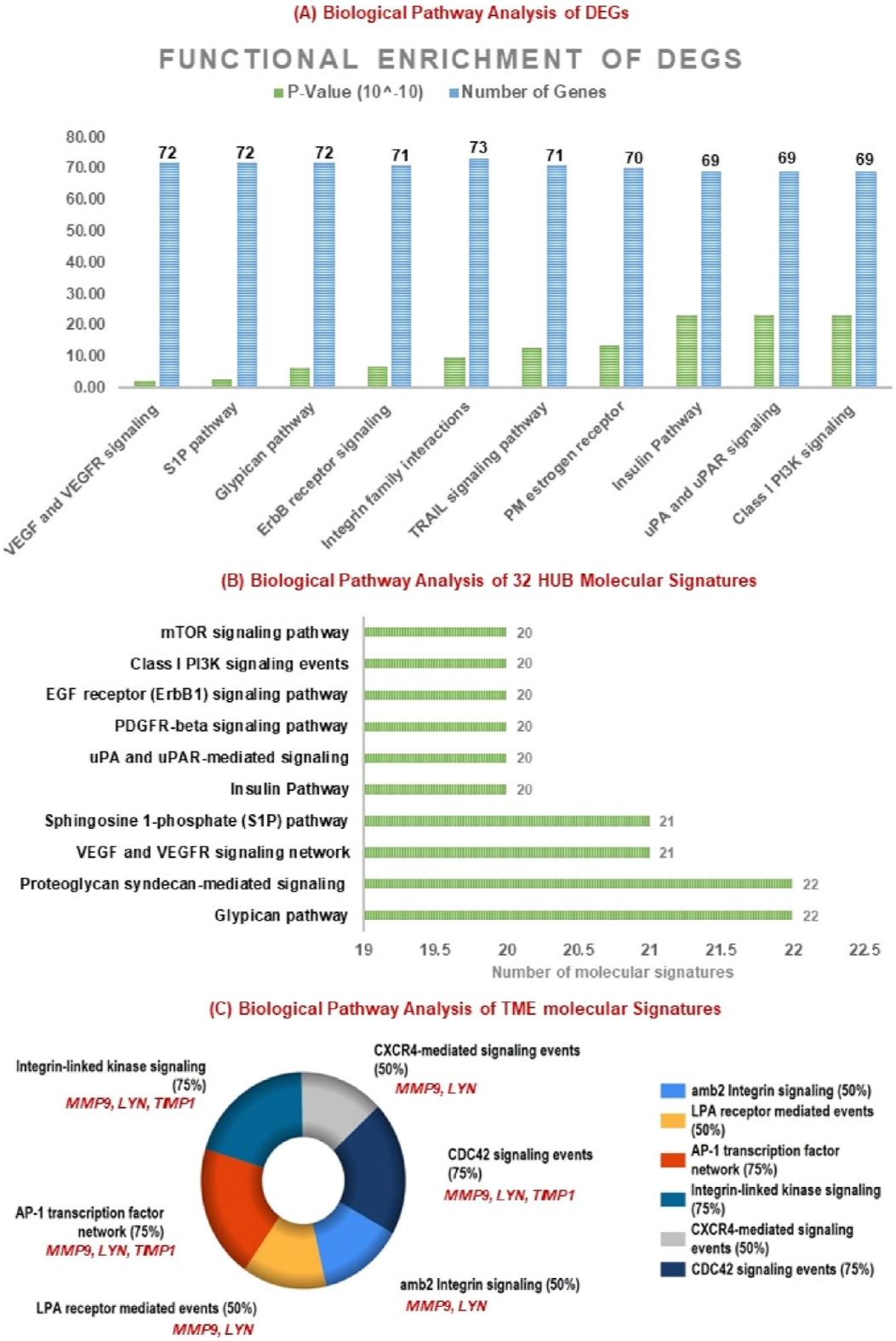

Figure 4. Significantly enriched biological pathway analysis: (A) Top 10 significantly functional enriched biological pathway terms of 241 DEGs associated with hypoxia-GBM. (B) Top 10 significantly functional enriched biological pathway terms of 32 hub signatures associated with hypoxia-GBM. (C) Top six enriched pathways of four molecular signatures (LYN, MMP9, PSMB9, and TIMP1) linked with the GBM microenvironment. Functional and signaling pathway enrichments were conducted using the KEGG pathway (http://www.genome.jp/kegg) and FunRich tool.

was involved in cancer-related inflammation by proteolyzing extracellular signal proteins, primarily those belonging to the CXC (C-X-C motif) chemokine family. As a result, MMP9 is regarded as a key architect and organizer of the tumor immune microenvironment.[77] Last TIMP1 expression linked positively with DCs ($\rho = 0.54$, $p < 0.001$) and negatively with B cells ($\rho = -0.11$, $p < 0.001$) and neutrophils ($\rho = -0.11$, $p < 0.001$). In contrast, BRCA1, CCNB1, CDC20, EXO1, KIF11, and PCNA

https://doi.org/10.1021/acsomega.3c00441
ACS Omega 2023, 8, 10565−10590

showed positive correlations with tumor purity, attributed to their predominant expression and functions in tumor cells. Further, we identified the relationship between somatic cell number alteration and the presence of immune infiltrates of four genes (Supporting Information Figure S2A). Additionally, we have examined the connection between these molecular signatures and immune checkpoint inhibitors (ICIs), including PDCD1(PD1), CD274(PDL1), CTLA4, LAG-3, and HAVCR2(TIM-3) (Supporting Information Figure S2B). According to data, the genes LYN, PSMB9, and TIMP1 were all positively correlated with ICIs except for LAG3, while TIMP1 was negatively correlated with LAG3. MMP9 only had positive correlation with PD1 and TIM-3.

Therefore, we have discovered four molecular signatures, LYN, MMP9, PSMB9, and TIMP1, to target the microenvironment of GBM and to further research whether they are therapeutic targets or not. The study concluded that LYN and PSMB9 were downregulated in hypoxia-induced GBM with $\log_2$ fold change values of −2.247 and −2.096, whereas MMP9 and TIMP1 were upregulated with $\log_2$ fold change values of 2.144 and 1.647, respectively. Thus, TIPM1 and MMP9 were selected for the identification of novel natural compounds in hypoxia-induced GBM therapeutics. However, TIMP1 lacks the approved control drug in terms of chemical compound and hence discarded for further analysis. Thus, the current study aims to identify the novel natural compound against MMP9 in hypoxia-induced GBM.

3.5. Biological Pathway Analysis of DEGs, HUB Molecular Signatures, and TME-Related Signatures. Biological pathway analysis using FunRich software was performed on 241 DEGs, 32 hub genes, and 4 genes involved in TME. As shown in Figure 4A, DEGs involved in the top 10 significant biological pathways were (a) VEGF and VEGFR signaling, (b) sphingosine 1-phosphate (S1P) pathways, (c) glypican pathway, (d) ErbB receptor signaling pathway, (e) integrin family cell surface interactions, (f) TRAIL signaling pathway, (g) plasma membrane estrogen receptor signaling, (h) insulin Pathway, (i) urokinase-type plasminogen activator (uPA) and uPAR-mediated signaling, and (j) class I phosphatidylinositol-3-kinase (PI3K) signaling. Similarly, analysis of 32 hub genes enhanced in biological pathways were (Figure 4B) (a) glypican pathway, (b) proteoglycan syndecan-mediated signaling, (c) VEGF and VEGFR signaling, (d) S1P pathway, (e) insulin pathway, (f) uPA and uPAR-mediated signaling, (g) PDGFR-beta signaling, (h) ErbB1 signaling pathway, (i) class I PI3K signaling, and (j) mTOR signaling pathway. In addition, we have also analyzed four shortlisted molecular signatures involved in TME in Figure 4C to understand the major pathways involved, which were (a) integrin-linked kinase (ILK) signaling, (b) activating protein-1 (AP-1) transcription factor network, (c) CDC42 signaling events, (d) CXCR4-mediated signaling, (e) Amb2 integrin signaling, and (f) lysophosphatidic acid (LPA) receptor-mediated. Biological pathways with p-value ≤ 0.05 and count > 2 were measured as statistically significant.

3.6. Localization Study and Construction of Target Signature−Regulatory Transcription Factor Network. Based on the CELLO localization predictor, we have predicted the localization of four genes using their amino acid protein sequences. Results showed that MMP9 and TIMP1 were majorly localized in the extracellular space, followed by the plasma membrane. At the same time, LYN and PSMB9 were localized in the cytoplasm and chloroplast, respectively (Supporting Information Figure S3A). Further, we have predicted target genes (LYN, PSMB9, MMP9, and TIMP1) related to TFs and their expression in GBM patient samples using JASPAR and GEPIA2.0 databases, respectively. The main transcription factor and its targets are listed in (Supporting Information Figure S3B.1). TIMP1, MMP9, and PSMB9 all share the Yin Yang 1 (YY1) TF with the highest degree (3) and betweenness (109.00), but the expression in the GBM patient sample is not statistically significant. In contrast, TIMP1 and PSMB9 shared the RELA (degree: 2; betweenness: 33.83), but TFAP2A and NFKB1 were elevated against PSMB9 with $\log_2$ fold change ≥ 1.4 (p-value ≤ 0.05) in GBM. However, TFs against the MMP9 gene were FOS, JUN, and TP53. These TFs were upregulated in GBM ($\log_2$ fold change ≥ 1.5, p-value ≤ 0.05), whereas STAT3 was only upregulated TF against the LYN gene. Supporting Information Figure S3B.2 demonstrates the network showing the associated transcription factor with molecular signatures in GBM.

3.7. Screening of Natural Compounds Based on BBB and ADMET Analyses. We received plant-derived naturals compounds from the NPACT database, including terpenoids, flavonoids, alkaloids, polycyclic aromatic natural compounds, aliphatic natural compounds, tannin, and PubMed database. We carried out BBB permeability of all-natural compounds using the SwissADME and CBLigand online tool with a cutoff value of 0.02 as we know that protein associated with GBM will be found in the particular region of the brain; thus, for a drug to be effective, it must pass the BBB.[78] In addition, these were checked for positive DLS based on drug-likeness score prediction.[79] Also, compounds were studied for Lipinski rule (MW ≤ 500; log P ≤ 5; HBA ≤ 10; HBD ≤ 5) and PAINS alert.[80] Sixty-five novel natural compounds had passed the criteria of BBB, Lipinski rule, PAINS, and drug-likeness, which went under ADMET (absorption, distribution, metabolism, excretion, and toxicity) analysis.[81] ADMET analysis of nominated compounds was carried out to check the pharmacokinetics and pharmacodynamics properties. This server was selected to assess whether a ligand (drug) is hepatotoxic, nephrotoxic, arrhythmogenic, carcinogenic, or respiratory toxic because poor pharmacokinetics and toxicity of candidate compounds are the significant reasons for drug development failure. Our study predicts 18 ADMET properties of selected compounds out of the 3 of absorption, 2 of distribution and excretion, 1 of metabolism, and 10 of toxicity properties.

For each compound to be an effective drug, it must fulfill these parameters which have their own range values such as (a) *Absorption*: Caco2 permeability > −5.15 log cm/s, MDCK permeability (Papp) > 20×10^{-6} cm/s, intestinal absorption > 30%; (b) *Distribution*: plasma protein binding ≤ 90%, volume distributionVD: 0.04−20 L/kg; (c) *Metabolism*: CYP1A2 inhibitor a cytochrome P450 enzymes. Inhibitors of CYP1A2 will boost the medication's plasma concentrations, and in some situations, this will result in negative consequences;[82] (d) *Excretion*: clearance of a drug ≥ 5, the half-life of a drug ($T_{1/2}$): 0−0.3; (e) *Toxicology*: human ether-a-go-go related gene (hERG blockers), human hepatotoxicity (H-HT), Drug-induced liver injury, AMES Toxicity, Rat Oral Acute Toxicity, toxic dose threshold of chemicals in humans (FDAMDD), skin sensitization, carcinogenicity, eye corrosion/irritation, and respiratory toxicity range between 0 and 0.3 (—): excellent (green); 0.3−0.7 (+)/(−): medium (yellow); 0.7−1.0 (++): poor (red).

https://doi.org/10.1021/acsomega.3c00441
ACS Omega 2023, 8, 10565−10590

Table 2. List of Identified 11 Natural Compounds and Their Toxicity Profiles[a]

PubChem CID	158280	185609	10424988	13886678	44479222	15549893	124256	162334	1548943	101477139	14313693
Natural Compounds	7,4'-dihydroxyflavan	4'-hydroxy-7-methoxyflavan	4,4'-dihydroxy-2,6-dimethoxydihydrochalcone	7-Hydroxy-2',4'-dimethoxyisoflavanone	(3R)-3-(4-Hydroxybenzyl)-6-hydroxy-8-methoxy-3,4-dihydro-2H-1-benzopyran	4'-hydroxy-2,4-dimethoxydihydrochalcone	N-(4-hydroxyundecanoyl)anabasine	N-n-octanoylnornicotine	8-Methyl-N-Vanillyl-6-Nonenamide	Multidione	Naviculol
Molecular formula	C15H14O3	C16H16O3	C17H18O5	C17H16O5	C17H18O4	C17H18O4	C21H34N2O2	C17H26N2O	C18H27NO3	C20H28O3	C15H26O
hERG Blockers	(---)	(--)	(---)	(---)	(--)	(--)	(---)	(---)	(---)	(---)	(---)
H-HT	(---)	(---)	(---)	(--)	(--)	(--)	(+)	(-)	(--)	(--)	(---)
DILI	(---)	(--)	(--)	(+)	(---)	(+)	(---)	(---)	(---)	(--)	(---)
AMES Toxicity	(-)	(+)	(---)	(+)	(---)	(--)	(---)	(---)	(---)	(---)	(---)
Rat Oral Acute Toxicity	(--)	(--)	(--)	(--)	(---)	(--)	(---)	(---)	(---)	(---)	(---)
FDAMDD	(+)	(+)	(-)	(+)	(++)	(-)	(+++)	(++)	(---)	(--)	(---)
Carcinogencity	(+)	(+)	(--)	(-)	(+)	(+)	(---)	(---)	(---)	(---)	(++)
Eye Corrosion	(+)	(---)	(---)	(---)	(---)	(---)	(---)	(---)	(---)	(---)	(---)
Eye Irritation	(+++)	(+++)	(+)	(---)	(++)	(++)	(---)	(---)	(---)	(+)	(+)
Respiratory Toxicity	(--)	(--)	(--)	(--)	(--)	(--)	(---)	(--)	(---)	(--)	(+)
Caco2 permeability (> -5.15log cm/s)	-4.691	-4.7	-4.695	-4.796	-4.663	-4.747	-4.68	-4.494	-4.476	-4.657	-4.205
MDCK Permeability (> 20X10-6 cm/s)	1.10E-05	1.40E-05	1.70E-05	3.40E-05	1.60E-05	2.10E-05	2.8E-05	1.90E-05	2.70E-05	2.10E-05	1.70E-05
Intestinal absorption	(---)	(---)	(---)	(---)	(---)	(---)	(---)	(---)	(---)	(---)	(---)
PPB (≤ 90%)	96.63%	97.48%	86.48%	98.13%	96.01%	91.47%	88.48%	86.43%	96.49%	98.34%	95.56%
VD (0.04-20L/kg)	1.111	1.194	0.595	0.55	1.044	0.574	0.956	0.867	1.098	0.316	1.553
CYP1A2 inhibitor	(+++)	(+++)	(+++)	(+++)	(+++)	(+++)	(---)	(-)	(++)	(-)	(--)
CL(≥ 5)	16.437	12.53	11.71	9.771	14.822	12.32	9.359	6.442	11.309	9.861	12.763
T1/2	0.757	0.335	0.914	0.384	0.813	0.818	0.3	0.281	0.892	0.465	0.22

[a]Color code: green/(—): signifies excellent with score range between 0 and 0.3; yellow/(+)/(−): signifies medium with score ranging between 0.3 and 0.7; red/(++/+++) signifies poor with score range between 0.7 and 1.0.

https://doi.org/10.1021/acsomega.3c00441
ACS Omega 2023, 8, 10565−10590

Papp is extensively considered to be the in vitro point of reference for estimating the uptake efficiency of compounds into the body. Papp values of MDCK cell lines were also used to estimate the effect of the BBB. hERG-(Category 0) compounds had an IC_{50} > 10 μM or <50% inhibition at 10 μM, whereas hERG + (Category 1) molecules will have the opposite of this. The voltage-gated potassium channel encoded by hERG genes plays a key function in controlling the exchange of cardiac action potential and resting potential during cardiac depolarization and repolarization. Long QT syndrome, arrhythmia, and Torsade de Pointes are all possible side effects of hERG blocking and can result in palpitations, fainting, or even death. Hepatotoxicity predicts the action of a compound on normal liver function. Furthermore, if the given compound is AMES positive, it will be considered mutagenic. Similarly, compounds have positive carcinogenicity because of their ability to damage the genome or disrupt the cellular metabolic processes. Recently, respiratory toxicity has become the leading cause of drug withdrawal. Drug-induced respiratory toxicity is frequently underdiagnosed due to the lack of recognizable early signs or symptoms in commonly used drugs, resulting in severe morbidity and mortality. As a result, thorough monitoring and treating respiratory toxicity are critical.[83,84] Our study indicates that all 11 predicted compounds, alkaloids (PubChem CID:124256, 162334, and 1548943), terpenoids (PubChem CID: 101477139 and 14313693), and flavonoids (PubChem CID: 158280, 185609, 10424988, 13886678, 44479222, and 15549893) fulfill the eligibility criteria and show favorable results. Therefore, we summarize in Table 2 that all 11 natural compounds meet the ADMET criteria for being a novel compound to target GBM. The detailed methodology used to screen natural compounds are shown in Supporting Information Figure S4, and the characteristics and physiochemical of natural compounds are mentioned in Supporting Information Table S2.

3.8. 7,4′-Dihydroxyflavan, (3*R*)-3-(4-Hydroxybenzyl)-6-hydroxy-8-methoxy-3,4-dihydro-2*H*-1-benzopyran), and 4′-Hydroxy-7-methoxyflavan) as Promising Natural Flavonoids Against MMP9: a Molecular Docking Approach. To find effective drugs against the MMP9 gene, 11 natural compounds satisfied the filter criteria, and one reference drug, Captopril (FDA approved retrieved from the DrugBank database; https://www.drugbank.ca/) and one natural compound (Solasodine) from previous studies[85,86] were chosen. Autodock Vina 4.0 was used to perform blind molecular docking experiments of all prioritized natural compounds with MMP9 (PDB id: 4HMA) using default parameters. The docking or binding free energy screens the most effective chemicals and conformations. Table 3 depicts the particular docking binding energy [$-\Delta G$ value (kcal/mol)] and the detailed information regarding intermolecular interactions between ligands and proteins. In addition, we have predicted the binding residues for ligand binding using the PrankWeb tool. Pocket 1 with highest probability (0.99) was chosen whose residues for alpha chain were 179, 180, 186−193, 222, 223, 226, 227, 230, 233−238, 240, 242, 243, and 245−249.

The MMP9 3D structure revealed that 88.6% of the residues were in the highly favored region and 0.4% were in the disallowed region respectively. Further structures were validated by ERRAT and VERIFY3D. The quality factor predicted by the ERRAT server for both alpha and beta chains of MMP9 was 76.17. VERIFY3D server predicted that 100% of residues had averaged a 3D−1D score ≥ 0.2respectively. Moreover, the docking energy of reference drugs, Captopril and Solasodine, were −6.6, −10.3 kcal/mol, respectively. Among 11 natural compounds, flavonoid 7,4′-dihydroxyflavan) and (3*R*)-3-(4-hydroxybenzyl)-6-hydroxy-8-methoxy-3,4-dihydro-2*H*-1-benzopyran) scored the highest binding energy −10.3 kcal/mol with 2 H-bond interaction with GLU241, ALA242, Leu188, and HIS226 than both the reference drugs, whereas 4′-hydroxy-7-methoxyflavan scored −10 kcal/mol binding energy with no H-bond interaction. Supporting Information Figure S5 shows two-

Table 3. Binding Affinity and Binding Energy of Prioritized Natural Compounds along with the Reference Drug

Group	Reference Drug		Experimental Natural Compounds										
PubChem CID	442985	44093	158280	44479222	185609	13886678	101477139	10424988	124256	15549893	1548943	162334	14313693
Class of compounds	Alkaloid	Small molecules	Flavonoid	Flavonoid	Flavonoid	Flavonoid	Terpenoid	Flavonoid	Alkaloid	Flavonoid	Alkaloid	Alkaloid	Terpenoid
Ligand Name	Solasodine	Captopril	7,4′-dihydroxy flavan	(3R)-3-(4-Hydroxybenzyl)-6-hydroxy-8-methoxy-3,4-dihydro-2H-1-benzopyran	4′-hydroxy-7-methoxyflavan	7-Hydroxy-2′,4′-dimethoxyisoflavanone	Multidiene	4,4′-dihydroxy-2,6-dimethoxydihydrochalcone	N-(4-hydroxyundecanoyl)anabasine	4′-hydroxy-2,4-dimethoxydihydrochalcone	8-Methyl-N-Vanillyl-6-Nonenamide	N-n-octanoylnorniccotine	Naviculol
Total No. of interactions	15	14	17	17	16	16	17	16	22	15	17	14	9
No of interaction with active site residues	15	11	15	14	13	15	16	15	19	14	14	13	4
Binding Energy (kcal/mol)	-10.3	-6.6	-10.3	-10.3	-10	-8.5	-8.2	-8.2	-8.2	-8.2	-8.1	-7.1	-6.4
Conventional H-bond	HIS226	-	GLU241; ALA242	LEU188; HIS226	-	-	TYR248	HIS226	-	HIS226; GLN227; HIS236	GLN227; ARG249	TYR248	-
Carbon H-bond	-	ALA242	-	-	-	ALA189; HIS226	-	-	-	-	TYR245	PRO246	-
Van der waals	GLY186; ALA189; HIS190; ALA191; GLN227; HIS230; PRO246; MET247;	LEU188; VAL223; PRO249; GLU241; TYR245; MET247; ARG249; THR251	LEU188; HIS230; HIS236; PRO240; TYR245 PRO246; MET247; TYR251	ALA189; GLN227; GLU241; ALA242; TYR245; MET247; TYR248; ARG249; THR251; HIS257	HIS257; THR251; ALA242; LEU222; LEU188; GLN227; PRO246; MET247; TYR245; GLU241	LEU222; VAL223; GLN227; HIS236; LEU243; TYR245 PRO246 MET247; TYR248; ARG249; THR251	ALA189; GLY186; LEU188; TYR218; LEU222; GLN227; ALA242; TYR245; PRO246; MET247; ARG249; HIS236	GLY186; LEU187; LEU222; VAL223; GLN227; LEU243; TYR245; PRO246; ARG249; THR251	GLY186; LEU187; ALA189; HIS190 ALA191; GLN227 GLU241; ALA242; TYR245; PRO246; MET247; ARG249; THR251	ALA189; LEU243; TYR245; MET247; TYR248; ARG249; THR251	ALA189; HIS230; GLU241; PRO246; MET247 TYR248; THR251; HIS257	GLY186; LEU187; ALA189; GLN227; HIS236; TYR245; LEU243; MET247;	GLY233; ASN262; GLY263; LEU267
Alkyl/Pi-alkyl	TYR179; LEU187; LEU188; VAL223; HIS226; HIS236; TYR248	LEU222; PRO225; LEU243	LEU222; VAL223; HIS226; LEU243; TYR248; ARG249	LEU222; VAL223; HIS226 HIS236 ; PRO246	VAL223; HIS236; LEU243; TYR248; ARG249;	LEU187; LEU188	LEU187; VAL223; HIS; 226; LEU243	LEU188; HIS226; HIS230; HIS236; MET247	LEU188; LEU222; VAL223; HIS226; HIS230; HIS236; LEU243; TYR248; PRO255	LEU188; LEU222; HIS226; HIS230; HIS236; PRO246	LEU188; LEU222; VAL223; HIS236; LEU243; ARG249	LEU188; TYR218; VAL223 HIS226	PHE110; LEU234; HIS266
Pi cation	-	-	HIS226	-	HIS226	-	HIS226		-	-	HIS226	-	-
Pi-Pi Stacked	-	-	-	HIS226	-	HIS226	TYR248	TYR248	-	HIS226		-	-
Pi-sigma	HIS226	-	-	LEU188; LEU243	-	-	-	-	-	-	-	-	-
Pi-sulphur		HIS226 ; TYR248	-	-	-	-	-	-	-	-		-	-
Unfavorable donor-donor	-	-	GLN227	-	-	-	-	-	-	-	LEU188	-	ASP235

https://doi.org/10.1021/acsomega.3c00441
ACS Omega 2023, 8, 10565−10590

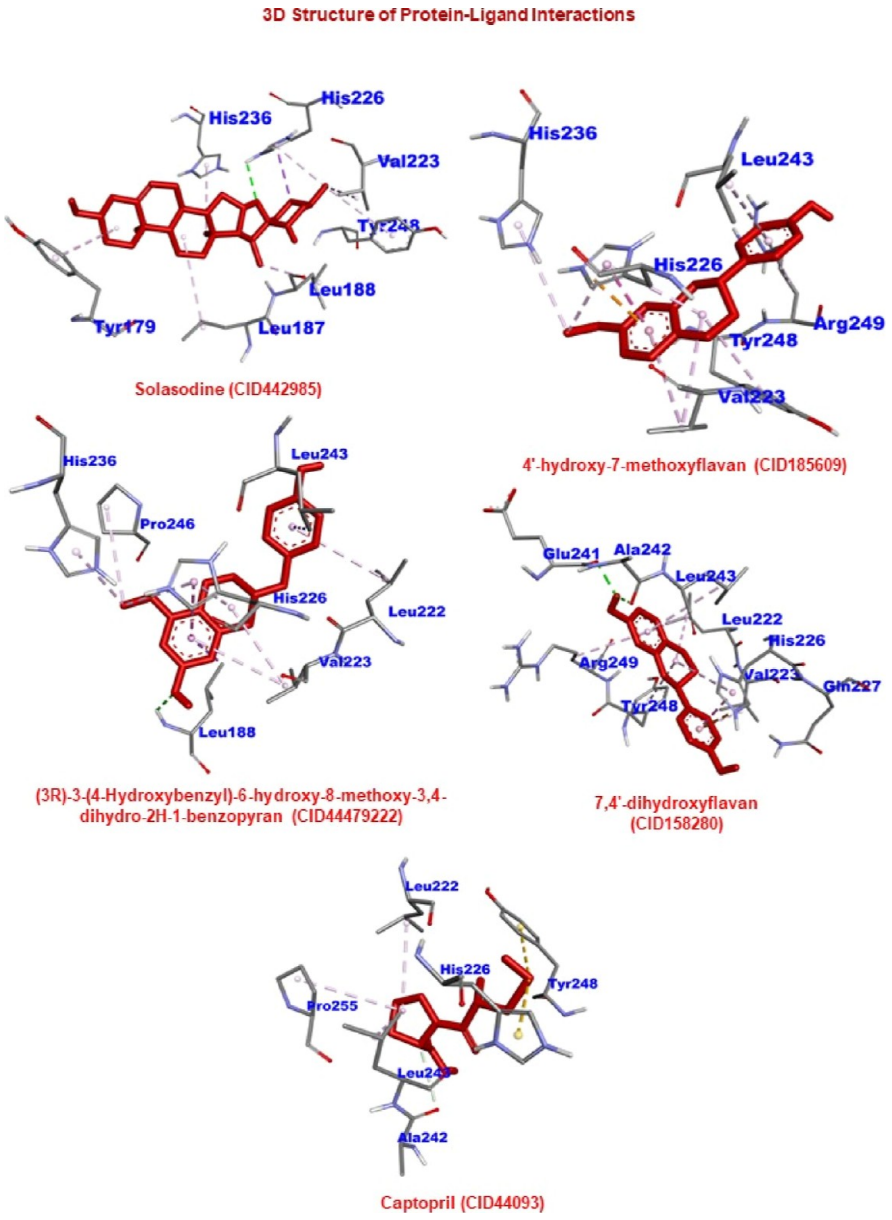

Figure 5. 3D interaction diagrams for the docked complexes between MMP9 and ligands obtained in this study.

dimensional (2D) interaction diagrams for the docked complexes between MMP9 and ligand which includes all interactions such as H-bond and other interactions such as the van der waals force, π-alkyl, π-sigma, and so forth. Shortlisted natural compounds' binding energy and H-bond interaction have been tabulated in detail in Table 3. Three natural compounds 7,4′-dihydroxyflavan and (3*R*)-3-(4-hydroxybenzyl)-6-hydroxy-8-methoxy-3,4-dihydro-2*H*-1-benzopyran), and 4′-hydroxy-7-methoxyflavan) scoring the lowest binding energy and forming interaction with the active site were shortlisted for further studies along with Captopril and Solasodine. It was intriguing to note that all best-identified natural compounds showed stable and conserved intermolecular interactions as demonstrated in Figure 5.

3.9. Assessment of the Most Promising Protein−Ligand Complex by MD Simulation Run. MD simulation (RMSD, RMSF, R_g, and SASA) results of all mentioned protein−ligand complexes have been mentioned in Figure 6 along with the average score values of each parameter of three best-docked compounds and two reference drugs.

3.9.1. Stability of MMP9-7,4′-Dihydroxyflavan Complex. The time evolution of the RMSD was determined to check the structural stability of the protein in complex ligands during the simulation. The average RMSD values for the backbone and complex were ∼2.06 and ∼2.62 Å, respectively. The complex slightly deviated as RMSD > ∼3 Å between 19 and 24 ns. At the binding site, a loop formed by the residues Pro240 and Arg249 that connects two helices displayed only slight residual fluctuations up to 0.9 Å. Flexible loops in the N-terminal region of the protein were extremely dynamic and exhibited RMSF > 2.5 Å. It was intriguing to observe that residues actively contributed to the stable interaction and exhibited significantly less fluctuation. The complex's overall average RMSF value was ∼1.13 Å. The R_g value was determined for investigating the compactness and structural changes in the MMP9-7,4′-dihydroxyflavan complex. The root-mean-square distance of a protein atom in relation to the protein's center of mass is used to

https://doi.org/10.1021/acsomega.3c00441
ACS Omega 2023, 8, 10565−10590

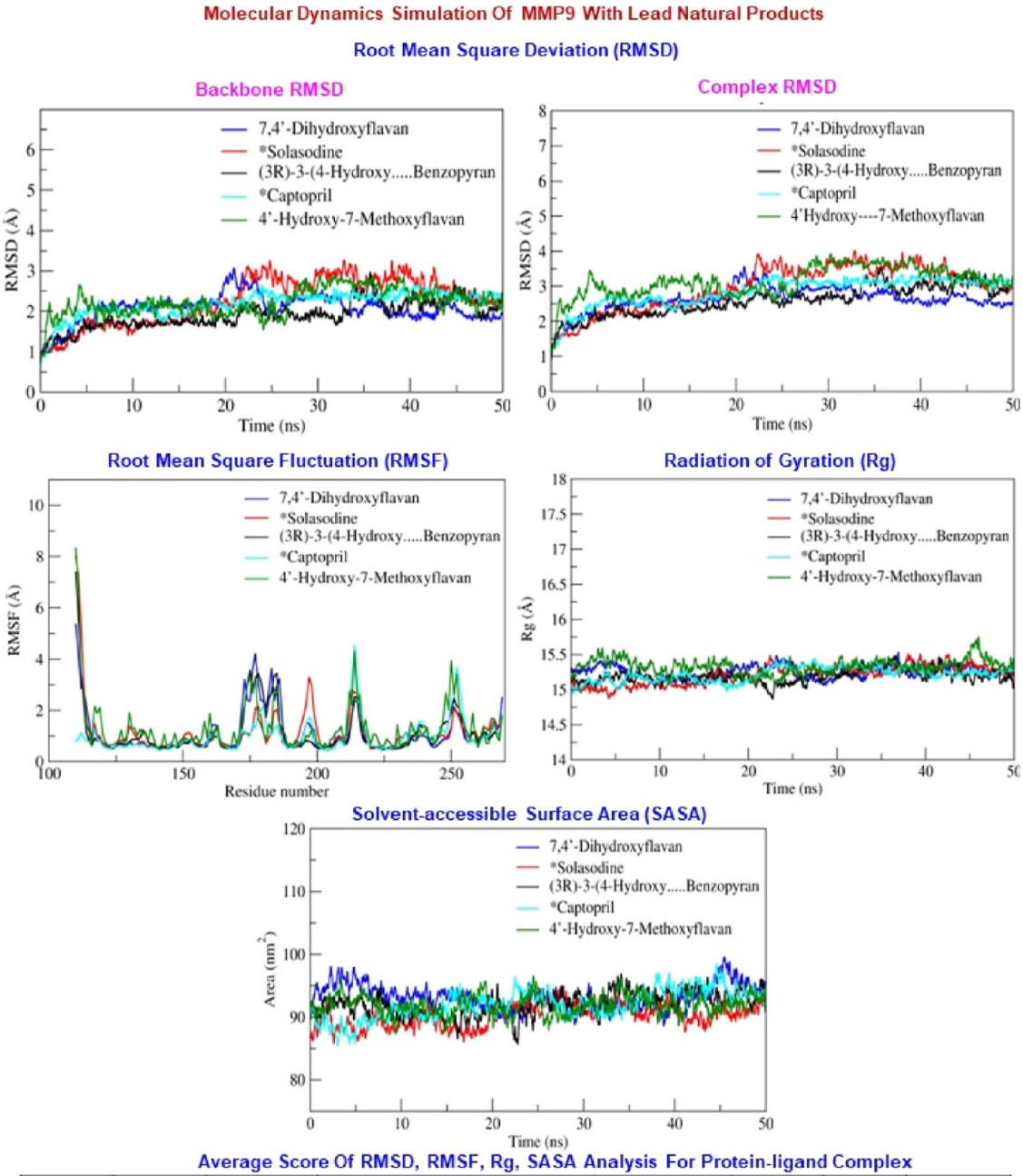

Average Score Of RMSD, RMSF, Rg, SASA Analysis For Protein-ligand Complex

Color Code	Category	PubChem CID	Ligand Name	RMSD (Å)		RMSF(Å)	Rg (Å)	SASA (nm^2)
				Backbone	Complex			
	Experimental	158280	7,4'-dihydroxyflavan	2.06	2.62	1.13	15.25	91.88
	Reference	442985	Solasodine	2.26	2.94	1.16	15.2	91.98
	Experimental	44479222	(3R)-3-(4-Hydroxybenzyl)-6-hydroxy-8-methoxy-3,4-dihydro-2H-1-benzopyran	1.91	2.58	1.13	15.18	92.15
	Reference	44093	Captopril	2.18	2.81	0.99	15.21	90.18
	Experimental	185609	4'-hydroxy-7-methoxyflavan	2.22	3.13	1.32	15.32	93.17

Figure 6. MD simulation analysis of MMP9 upon binding of the ligand as a function of time throughout 50 ns. Graph showing RMSD, RMSF, radius of gyration (R_g), and SASA for MMP9 with three best-docked compounds and two reference drugs.

compute the R_g value of the protein. The average value of R_g for the complex is ~15.25 Å. The SASA was examined to study the protein compactness behavior. The initial and final surface areas occupied by the docked MMP9-7,4′-dihydroxyflavan complex are 91.40 and 92.90 nm^2, respectively, with an average surface area of ~91.88 nm^2. This complex constructed two stable H-bonds, and both remained stagnant over the course of the simulations. The stable H-bond interactions were thought to be the primary factor that encouraged the stable complex formation. In addition, according to MM-PBSA calculation, the complex also demonstrated a binding energy of −85.24 kJ/mol. Moreover, the residues that contributed the most to the binding energy were found by computing the residue decomposition energy. The analysis suggested that five residues,

https://doi.org/10.1021/acsomega.3c00441
ACS Omega 2023, 8, 10565−10590

Table 4. MM-PBSA Calculations of Top Hit Complexes' Binding Free Energy and Interaction Energies[a]

complex	MM-PBSA (kJ/mol)				
	ΔE_{VDW}	ΔE_{ELE}	ΔG_{Sol}	ΔG_{Surf}	ΔG_{bind}
MMP9-7,4′-dihydroxyflavan	−167.19 ± 7.82	−14.98 ± 4.06	111.60 ± 9.88	−14.68 ± 0.78	−85.24 ± 11.81
MMP9-Solasodine	−148.31 ± 11.20	−777.73 ± 18.62	353.45 ± 15.04	−15.55 ± 0.91	−588.15 ± 17.82
MMP9-(3*R*)-3-(4-hydroxybenzyl)-6-hydroxy-8-methoxy-3,4-dihydro-2*H*-1-benzopyran	−141.43 ± 13.78	−79.73 ± 8.29	142.50 ± 8.45	−15.49 ± 0.72	−94.16 ± 11.65
MMP9-4′-hydroxy-7-methoxyflavan	−154.50 ± 16.07	−27.86 ± 8.96	119.80 ± 20.33	−15.87 ± 0.90	−78.44 ± 16.16
MMP9 - Captopril	−83.65 ± 13.94	−622.30 ± 35.47	198.05 ± 38.01	−10.59 ± 1.54	−518.50 ± 22.39

[a]ΔE_{VDW}—van der Waal energy, ΔE_{ELE}—electrostatic energy, ΔG_{Sol}—polar solvation energy, ΔG_{Surf}—SASA energy, and ΔG_{bind}—binding energy.

namely, Leu222, Val223, Ala242, Met247, and Tyr248, contributed considerably to the creation of the stable complex. Most importantly, the residue Tyr248 showed significant contributions to the binding affinity by scoring the lowest contribution energy of −5.41 kJ/mol, followed by Leu222 (−4.71 kJ/mol), Met247 (−3.96 kJ/mol), Val223 (−2.67 kJ/mol), and Ala242 (−2.01 kJ/mol). However, residues Gln241and Pro255 did not favor the interactions.

3.9.2. Stability of MMP9-(3R)-3-(4-Hydroxybenzyl)-6-hydroxy-8-methoxy-3,4-dihydro-2H-1-benzopyran Complex. This complex showed consistent structural stability during the simulation run for the 50 ns production run. Protein backbone and complex were found to have average RMSD values of ∼1.91 and ∼2.58 Å, respectively. The complex was a little unstable as RMSD > ∼3 Å between 33 and 37 ns and 39 to 47 ns. The maximum residual fluctuations in the N-terminal residues were >3.0 Å. However, the residues at the binding site from Leu222 to His230 (helix) and residues from Ala242 to Arg249 (loop) engaged in the stable and conserved nonbonded interactions and showed significantly much fewer variations of ∼0.5 and ∼1.13 Å, respectively. The complex has an average RMSF value of 1.13 Å. The average R_g value of 15.18 Å showed stable complex formation during the MD simulation by forming a compact structure. Meanwhile, the initial and final surface areas employed by the complex were 92.17 and 93.16 nm^2, with the average SASA score of the complex being 92.15 nm^2. During the simulation, this complex created five H-bonds, of which four were stable. The estimated binding affinity of the compound to MMP9 protein was −94.16 kJ/mol. Additionally, the residues Leu188, Leu222, Val223, His226, and Tyr248 encouraged stable complex formation. Most importantly, the decreasing order of binding affinity followed Leu222, Tyr248 and His226, Val223, and Leu188 with the lowest contribution energy of −5.74, −5.08, −4.58, −4.22, and −3.40 kJ/mol, respectively. However, the interactions were not favored by the residues Gln227 and Arg249.

3.9.3. Stability of MMP9-185609 (4′-Hydroxy-7-methoxyflavan) Complexes. The complex showed similar RMSD values of 50 ns and was stable. The complex's RMSD value ranged from 0.97 to 3.39 Å, whereas the backbone's RMSD value ranged from 0.85 to 2.5 Å. According to the residual fluctuations plotted for the Cα, binding pockets encompassing residues between Leu222 and Gly229 (helix) and Ala242 and Arg249 (loop) showed the establishment of stable nonbonded contacts in residues with lower fluctuations. Residues at the N-terminal and residues adjacent to binding pockets, including Phe250 and Glu252, show higher residual fluctuation >3 Å due to increased local flexibility and ligand interaction observed during simulation. The overall average RMSF of the complex was 1.32 Å. Moreover, the R_g value demonstrated steady complex formation for 50 ns. In addition, the initial and final surface areas occupied by complexes were 91.63 and 96.49 $nm^{2,}$ with the average SASA score of complexes being 93.17 nm^2. Two of the three H-bonds the complex created during the simulated period were consistent. The compound also had a binding energy of about −78.44 kJ/mol. Furthermore, the per-residue contribution energy showed six residues from the binding pocket, Leu188, Leu222, Val223, Leu243, Met247, and Tyr248, which had a considerable impact on the creation of a stable complex. The residues Leu188, Leu222, Val223, Leu243, Met247, and Tyr248 from the binding pocket showed significant contributions to the binding affinity by scoring the least residue decomposition/contribution energy of −2.36, −4.25, −6.22, −3.44, −2.22, and −4.23 kJ/mol, respectively. Arg249 residues do not favor the interaction.

3.9.4. Stability of MMP9-Captopril and MMP9-Solasodine Complexes. MMP9-Captopril and MMP9-Solasodine complexes showed stable interaction during the simulation run. The average RMSD value of the backbone and MMP9-Captopril complex was ∼2.18 and ∼2.81 Å, whereas the RMSD value with Solasodine was ∼2.26 and ∼2.94 Å. Moreover, the average RMSF values for the MMP9-Captopril complex and MMP9 and MMP9-Solasodine were 0.99 and 1.16 Å, respectively. Solasodine causes the N-terminal to fluctuate more than 3 Å, whereas Captopril did not cause this variation. Also, MMP9-Captopril and MMP9-Solasodine complexes have average R_g values of 15.21 and 15.2 Å, respectively. Meanwhile, MMP9-Captopril's initial and final surface areas were 88.85 and 91.54 nm^2, respectively, with an average SASA score of 90.18 nm^2. Comparatively, the MMP9-Solasodine complex had initial and final surface areas of 89.94 and 93.58 nm^2, with an average SASA score of 91.98 nm^2. Moreover, out of the three H-bonds formed, only two were stable during simulation for the Captopril complex and Solasodine complex. In addition, the the binding energy of MMP9-Captopril and MMP9-Solasodine was −518.50 and −588.15 kJ/mol, respectively. Furthermore, the MMP9-Captopril complex also showed 10 residues from the binding pocket, including Asp201, Asp205, Asp206, Asp207, Glu208, Asp235, Glu241, Glu252, Asp259, and Asp260, and significantly contributed to the stable complex formation. Likewise, 12residues, Asp177, Asp182, Asp201, Asp205, Asp206, Glu208, Asp235, Glu241, Pro246, Glu252, Asp259, and Asp260, helped create the stable MMP9-Solasodine complex.

Thus, data confirmed that the binding energies of MMP9 with ligands 7,4′-dihydroxyflavan, (3*R*)-3-(4-hydroxybenzyl)-6-hydroxy-8-methoxy-3,4-dihydro-2*H*-1-benzopyran, and 4′-hydroxy-7-methoxyflavan were similar (−10 kcal/mol) to that of the reference drug Solasodine and better than Captopril. All three natural compounds interact within the binding domain of the MMP9 pocket, and this interaction was stable for 50 ns with less deviation and fluctuations. The RMSD value difference

https://doi.org/10.1021/acsomega.3c00441
ACS Omega 2023, 8, 10565−10590

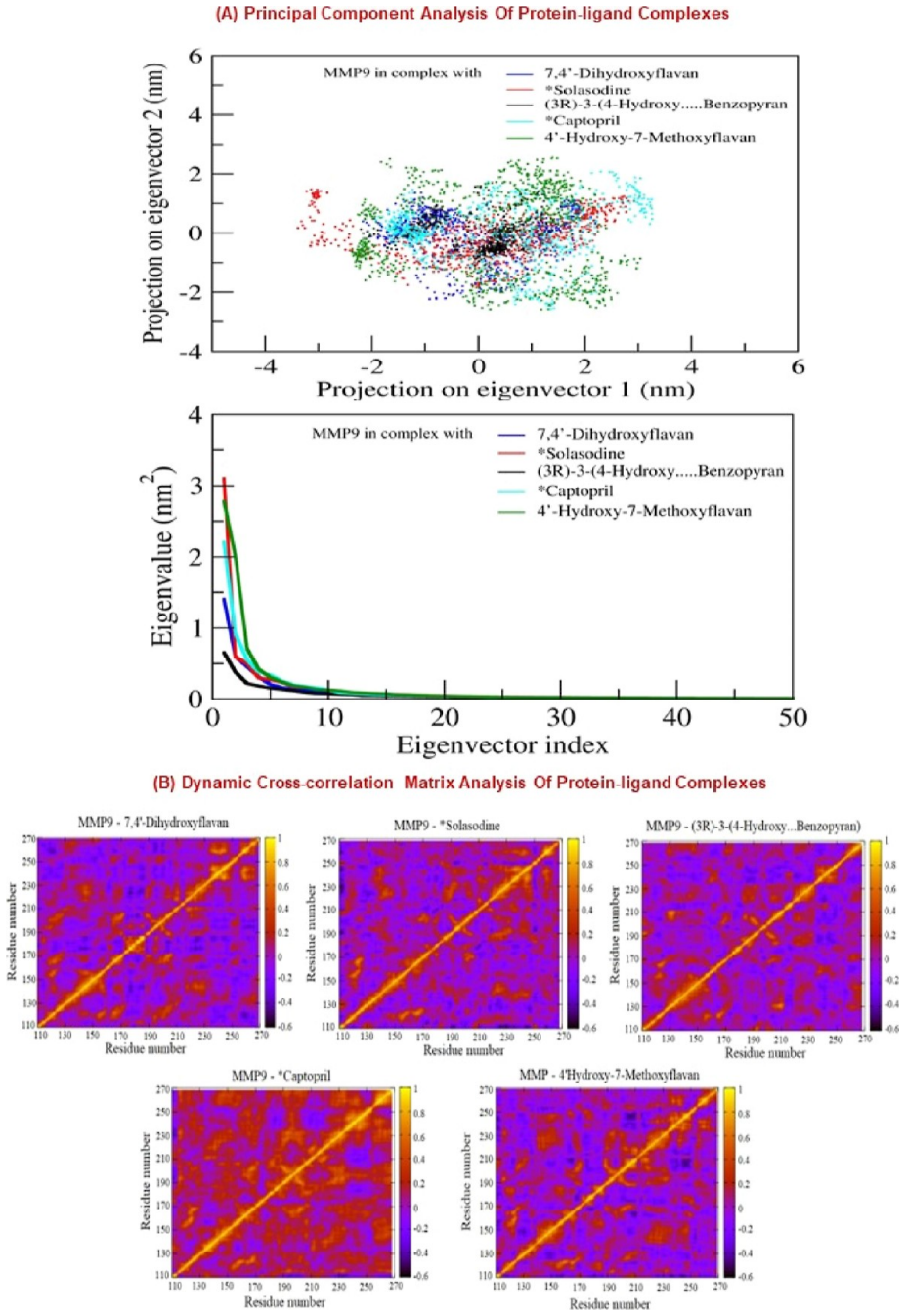

Figure 7. (A) PCA of protein−ligand complexes: In the scatterplot, the first two principal components (PC1, PC2) were plotted to analyze the collective motion of ligand-bound protein complexes during the simulations. The dots with different colors (blue, red, black, aqua, and green) represent the collective motion of MMP9 residue after ligand binding. Dots with smaller regions represent the higher structural stability and conformation flexibility and vice versa. The collective motion of MMP9 in the presence of ligands is depicted in the second graph using projections of MD trajectories onto two eigenvectors corresponding to the first two principal components. The first 50 eigenvectors were plotted versus eigenvalue for 5 ligands including 3 hit natural compounds and 2 reference drugs. Color code used in the scatterplot and graph: blue: 7,4′-dihydroxyflavan; red: Solasodine; black: (3*R*)-3-(4-hydroxybenzyl)-6-hydroxy-8-methoxy-3,4-dihydro-2*H*-1-benzopyran),;aqua: Captopril; Green: 4′-hydroxy-7-methoxy-flavan. (B) DCCM of Cα atoms observed in complexes for 7,4′-dihydroxyflavan, Solasodine, (3*R*)-3-(4-hydroxybenzyl)-6-hydroxy-8-methoxy-3,4-dihydro-2*H*-1-benzopyran), Captopril, and 4′-hydroxy-7-methoxyflavan. The positive regions, colored amber, represent strongly correlated motions of Cα atoms (C_{ij} = 1), whereas the negative regions, colored blue, represent anticorrelated motions (C_{ij} = −1).

between the backbone and the complex was <3 Å. RMSF, R_g, and SASA also showed steady complex formation.

The g_mmpbsa tool computed the binding affinity of the protein−ligand complex using the MM-PBSA method. The free energy (kJ/mol) contribution of lead hits and standard molecules in relation to their respective targets is summarized in Table 4. In addition, detailed description of the total number of H-bond interactions in the protein−ligand complex has been shown in Supporting Information Figure S6A. Similarly, the contribution energy plot illustrated in Supporting Information Figure S6B exhibits the importance of the binding pocket residues in stable complex formation.

https://doi.org/10.1021/acsomega.3c00441
ACS Omega 2023, 8, 10565−10590

3.10. PCA and DCCM Analysis of Complexes. We employ PCA analysis to explore the dynamics of protein−ligand conformation for five complexes (two complexes with the reference drug and three complexes with the natural compound ligand) obtained from an MD simulation run of 50 ns. A PCA produces a matrix of eigenvectors and a list of related eigenvalues, which together represent the principal components and amplitudes of the internal movements of a protein. The first two eigenvectors/principal components (eigenvector 1 and eigenvector 2) are used to calculate the concerted motions of the past 50 ns trajectory since they can best describe the majority of the internal movements within a protein. The first two eigenvectors' 2D projection as well as the scatterplot are shown in Figure 7A. Captopril and Solasodine, two of the reference drugs employed in this study and directed at the MMP9 protein, were seen to have a greater range of conformations during the simulations (shown as a red and aqua line, respectively, in Figure 7A. Moreover, during simulation, the shortlisted MMP9-targeting ligands 7,4′-dihydroxyflavan, (3*R*)-3-(4-hydroxybenzyl)-6-hydroxy-8-methoxy-3,4-dihydro-2*H*-1-benzopyran, and MMP9-4′-hydroxy-7-methoxyflavan displayed less diversity than the reference drug (shown in blue, black, and green lines, respectively). Both the reference drugs demonstrated increased conformational flexibility with the maximum number of diverse conformations. Intriguingly, the MMP9 inhibitors 7,4′-dihydroxyflavan, (3*R*)-3-(4-hydroxybenzyl)-6-hydroxy-8-methoxy-3,4-dihydro-2*H*-1-benzopyran, and 4′-hydroxy-7-methoxyflavan took up substantially less conformational space than the Captopril reference drug. In contrast, only 7,4′-dihydroxyflavan, (3*R*)-3-(4-hydroxybenzyl)-6-hydroxy-8-methoxy-3,4-dihydro-2*H*-1-benzopyran performed better compared to the Solasodine reference drug as shown in the scatterplot (less dispersed plot). Therefore, we suggest that three lead-hit natural compounds could be more effective than the reference drugs.

The DCCM of Cα atoms in complexes provides a deeper structural understanding of the collective motion of the ligand-binding regions. The coordinated residual motion of the Cα atoms in each of the simulated complexes is shown in Figure 7B. Each residue exhibits a significant self-correlation with itself, as evidenced by the diagonal amber line. Scaling from amber to blue, respectively, is the strength of correlation (C_{ij} = 1) and anticorrelation (C_{ij} = −1). In complex MMP9-7,4′-dihydroxyflavan, the binding site residues show a positive correlation with the N-terminal domain of the MMP9. The scale of this correlation's amplitude goes from blue to amber color in smaller steps. Similarly, MMP9-MMP9-4′-hydroxy-7-methoxyflavan also showed a positive correlation with higher amplitude near binding site residues 222−249. In contrast, complex MMP9-44479222 showed anticorrelation, and its amplitude scaled from amber to blue color. The relevance of the active site residues in stabilizing the complexes was demonstrated by the coordinated motion displayed by the binding pocket residues spanning from 220 to 249 with the N-terminal region. The N-terminal residues of the MMP9 protein revealed a high association with the binding site residues of the reference ligands, such as Captopril and Solasodine. Comparing Captopril to the Solasodine ligand, the correlation magnitude was larger. The results showed that MMP9-containing natural compounds complexes and the reference ligand exhibited similar correlations near binding residues. In light of this, the DCCM displayed cooperative and anticooperative motion in the protein, indicating the conformational flexibility of the investigated complexes and stable connections mediated by noncooperative motion on the opposite side, which triggered the opening and shutting of the binding pocket residues and enabled the stable complex formation during the MD simulation.

4. DISCUSSION

The present study analyzed hypoxia, a critical microenvironmental condition of GBM, to identify potential biomarkers and establish treatment strategies for GBM treatment. In recent years, TME gained the attention of researchers as it regulates tumor growth and significantly influences treatment response. Hypoxia condition and immune cell infiltration in TME promote and antagonize tumor growth. Herein, we identify hypoxia-related molecular signatures involved in GBM pathogenesis. Based on the functional enrichment analysis, we have found 32 HUB signatures whose expressions were validated through microarray and RNA sequence data sets obtained from TCGA data sets of GBM patients. Indeed, we subjected 10 shortlisted molecular signatures to the RNA deconvolution-based TIMER analysis. From the gene expression profiles, TIMER employs an algorithm to determine the abundance of tumor-infiltrating immune cells. The proportion of cancer cells in the tumor tissue is described as tumor purity (also known as tumor cell fraction), which indicates the characteristics of TME. Recent studies have shown that tumor purity is linked to prognosis, mutation burden, and a robust immunological phenotype.[87,88] Our results indicate that LYN, MMP9, PSMB9, and TIMP1 were linked with the GBM microenvironment. Zhao et al. demonstrated a high expression of the PLOD family with negative tumor purity and high immune infiltration.[89] In our study, LYN was downregulated in the hypoxic condition in GBM. According to a study by Dai and Siemann, hypoxia has little to no impact on the expression of phosphorylated LYN.[90] However, the elevated MMP9 expression in hypoxic TME enhances DC infiltration and reduces the infiltration of cytotoxic T cells (CD8+ T cells).[91] In contrast, increased CD8+ T-cell infiltration had been linked to a better predictive factor for long-term survival in glioblastoma patients.[92] Additionally, PSMB8 and PSMB9 immunoproteasome subunits are overexpressed in melanoma cell lines, and their reduced expression is linked to a poor prognosis in nonsmall-cell lung carcinoma.[93] Herein, in this study, the reduced PSMB9 expression is linked to increased immune cell infiltration, with the exception of CD8+ T cells. Our findings are backed up by the fact that all members of the TIMP family had significantly higher levels of expression in GBM.[94] TIMP1 expression levels in hypoxic-GBM are exclusively correlated with DC infiltration and are inversely related to B cells and neutrophils. Consistent with our results, previous studies have also identified the four molecular signatures (LYN, TIMP1, MMP9, and PSMB9) as potential biomarkers associated with TME in GBM and other cancers.[95−97] Herein, we briefly discussed the relevant pathways mentioned above by starting with the ILK pathway known to promote cell growth, cell cycle progression, and increase VEGF expression by stimulating HIF-1 via a phosphatidylinositol 3-kinase (PI3K)−dependent activation.[98] Another significant pathway that is involved in the TME of GBM is the AP-1 transcription factor (dimeric in nature), which is made up of proteins from the Jun (c-Jun, JunB, and JunD) and Fos (c-Fos, FosB, Fra1, and Fra2) families. Studies have concluded that different triggers, such as inflammatory cytokines, stress inducers, or pathogens, activate the AP-1 transcription factor family, resulting in innate and

https://doi.org/10.1021/acsomega.3c00441
ACS Omega 2023, 8, 10565−10590

adaptive immunities.[99] In addition, active CDC42 (ρ-GTPase) has been shown to facilitate glioma cell migration and invasion and regulate cell polarity.[100] In GBM, HIF-1 and VEGF upregulate CXCR4, which is significant for angiogenesis and cell invasion.[101] Furthermore, another fascinating study showed that the interaction of microglia and GBM through the LPA pathway has important consequences for tumor progression. A deeper understanding of this interaction could lead to the development of new therapeutic techniques that target LPA as a possible GBM target.[102] Another study found that hypoxic TME stimulates invadopodia development (actin-rich protrusions of the plasma membrane that focus ECM breakdown through the secretion of MMPs), which are essential for metastasis.[103] In addition, our data showed that the localization of MMP9 was mainly the extracellular region, and FOS, JUN, and TP53 were only significantly overexpressed associated TFs in GBM patient's samples. MMP9 was overexpressed in different subtypes of GBM including classical, mesenchymal, neural, and proneural (shown in Supporting Information Figure S7A). It also has the potential to act as a poor prognostic biomarker (HR > 1) as it shows significant disease-free survival (shown in Supporting Information Figure S7B). This all together suggests the significance of targeting TME. LYN and PSMB9 being downregulated in hypoxic condition, and due to unavailability of the reported drug against TIMP1, these biomarkers were not explored in the current study in identifying the novel drug. Hence, MMP9 was selected for identifying natural compounds as inhibitors in order to reduce GBM pathogenesis.

MMP9, a member of the gelatinase family of MMPs that degrades and remodels ECM proteins, plays a vital role in cell migration and EMT and angiogenesis.[104] Other TME components, such as nonmalignant stromal cells, neutrophils, macrophages, and endothelial cells, release MMP9 in the microenvironment. MMPs are known to be induced by HIF-1.[105,106] MMP inhibitors can diminish tumor cells' invasive and migratory abilities in cancer. MMP9 inhibitors were previously discovered using a computational technique, indicating that MMP9 is a targetable protein.[107,108] Based on previous studies, we have selected Captopril and Solasodine as reference drugs against MMP9. Captopril is an MMP2 inhibitor for treating patients on continuous ambulatory peritoneal dialysis therapy.[109] Captopril inhibits MMP2 and MMP9 via chelating zinc ions at the enzyme's active site. It also utilized alongside other medicines like Disulfiram and Nelfinavir as adjuvant therapy for GBM.[110] Moreover, it can inhibit MMP2 and MMP9, suspected of having a role in GBM metastasis and invasion, since it is an angiotensin-converting enzyme inhibitor, which belongs to a family of metalloproteinases comparable to MMPs.[111] Similarly, Solasodine has been reported to inhibit MMP9 and induce cell apoptosis, particularly in human lung cancer. However, this drug's pharmacokinetics, safety, and effectiveness in clinical practice remain unclear.[85,112]

During identifying new agents for MMP9, we explored six classes of natural compounds, including alkaloids, flavonoids, terpenoids, aliphatic compounds, aromatic compounds, and tannins. Previous studies have also supported that multiple natural compounds have antitumor and apoptotic effects in TMZ and p53 resistance GBM cells. Various natural compounds such as chrysin, epigallocatechin-3-gallate, hispidulin, rutin, and silibinin were also used in combination with TMZ and other chemotherapeutic drugs due to their potential to act as chemosensitizers (such as icariin and quercetin), radiosensitizers (*Zataria multiflora*), inhibits proliferation (such as *Zingiber officinale* and *Rhazya stricta*) and migration, and induces apoptosis (Baicalein).[16,113,114] However, these were checked for BBB permeability, druglikeness, and LIPINSKI rules of 5, and ADMET analysis was performed. We performed in silico molecular docking and MD simulations with MMP9 protein (alpha chain) using Autodock Vina 4.0 and GROMACS to evaluate the inhibitory effect of shortlisted drugs. Ramachandran plot of MMP9 (PDB identifier: 4HMA) is shown in Supporting Information Figure S7C. The binding affinity of ligands (drugs) was calculated and compared with reference drugs. In this instance, we have picked three best-docked compounds with binding energies comparable to Solasodine and better than Captopril for MD simulations. Stability should be taken into careful consideration during drug testing in addition to safety. The software's MD simulation module examined the stability of these MMP9-compound complexes in the natural environment. Further compounds interacted with targets with a minimum of at least 2 H-bond interactions. Numerous studies have been conducted in the past to implement molecular docking and MD simulations and MM-PBSA assessment to record drug transport variability, identify protein allosteric inhibition, consider the impact of chirality in selective enzyme inhibition, investigate the irreversible style of the receptors, and evaluate ligand−protein interactions. Similarly, this study examined the intermolecular contact stability of identified prospective lead compounds and standard molecules with their respective targets using classical MD simulation for 50 ns of MMP9 protein with ligands.[115] Subsequently, the efficacy of molecules' molecular interactions can be examined using structural analysis, such as RMSD and RMSF.[116] Results revealed that the binding energy of MMP9 with ligands 7,4′-dihydroxyflavan, (3*R*)-3-(4-hydroxybenzyl)-6-hydroxy-8-methoxy-3,4-dihydro-2*H*-1-benzopyran, and 4′-hydroxy-7-methoxyflavan was similar (−10 kcal/mol) to that of the reference drug Solasodine and better than Captopril. All three ligands, flavonoids in nature, interact within the binding domain of the MMP9 pocket, and this interaction was stable for 50 ns with less deviation and fluctuations. RMSD value difference between the backbone and complex was <3 Å. The MMP9-7,4′-dihydroxyflavan complex findings suggest that five residues, Leu222, Val223, Ala242, Met247, and Tyr248, contributed significantly to the formation of the stable complex. Most importantly, the residues Tyr248 showed significant contributions to the binding affinity by scoring the lowest contribution energy of −5.41 kJ/mol. MMP9-(3*R*)-3-(4-hydroxybenzyl)-6-hydroxy-8-methoxy-3,4-dihydro-2*H*-1-benzopyran had a 94.16 kJ/mol determining binding affinity. Leu188, Leu222, Val223, His226, and Tyr248 residues also facilitated stable compound formation. Leu222 scored the highest binding affinity of −5.74 kJ/mol. Similarly, the binding energy of MMP9-4′-hydroxy-7-methoxyflavan was around 78.44 kJ/mol. The per-residue contribution energy also revealed that the formation of a stable complex was significantly influenced by six residues from the binding pocket: Leu188, Leu222, Val223, Leu243, Met247, and Tyr248. The binding affinity of the residue Met247 is −6.22 kJ/mol. Further, PCA analysis revealed that the MMP9-targeting ligands, 4′-dihydroxyflavan, (3*R*)-3-(4-hydroxybenzyl)-6-hydroxy-8-methoxy-3,4-dihydro-2*H*-1-benzopyran, and 4′-hydroxy-7-methoxyflavan had less diversity than the reference drug during the simulation run. Both reference drugs demonstrated increased conformational flexibility with the maximum number of diverse conformations. Interestingly, compared to the Captopril reference drug, the MMP9 inhibitors, 7,4′-dihydroxy-

https://doi.org/10.1021/acsomega.3c00441
ACS Omega 2023, 8, 10565−10590

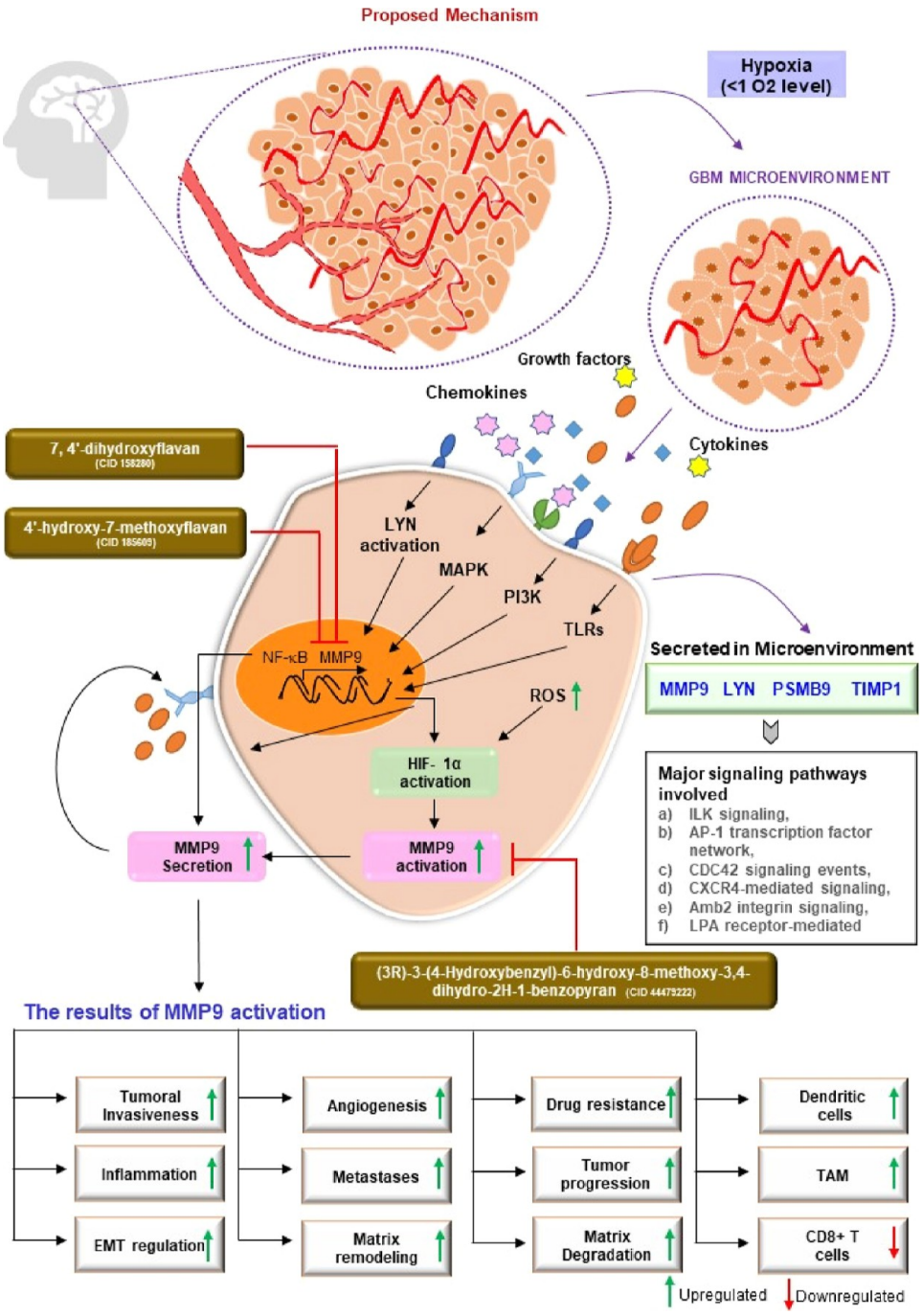

Figure 8. Potential of novel inhibitors 7,4′-dihydroxyflavan, (3*R*)-3-(4-hydroxybenzyl)-6-hydroxy-8-methoxy-3,4-dihydro-2*H*-1-benzopyran, and 4′-hydroxy-7-methoxyflavan in suppressing GBM pathogenesis by interacting with MMP9 protein produced in a hypoxic environment condition. MMP9 is synthesized de novo during stimulation induced with cytokines by activating various signaling pathways such as NF-κB, HIF-1, MAPK, PI3K, etc. Cytokines (TNF-α, IL-8, and IL-1β) and growth factors (TGF-β, PDGF, and bFGF) bind to their receptors which regulate MMP9 activation and secretion. MMP9 is secreted by tumor cells, monocytes, inflammatory macrophages, and stromal cells in the extracellular environment. This affects various downstream biological processes, including matrix degradation, remodeling, EMT (enhanced tumoral invasion, metastases), angiogenesis, inflammation, drug resistance, etc. Novel inhibitors 7,4′-dihydroxyflavan, (3*R*)-3-(4-hydroxybenzyl)-6-hydroxy-8-methoxy-3,4-dihydro-2*H*-1-benzopyran, and 4′-hydroxy-7-methoxyflavan bind to MMP9 and suppress its activation and thus reduce the expression and regulation of downstream process involved in GBM pathogenesis in the above figure. Our approaches to GBM treatment are being reoriented by focusing on these features of MMPs.

flavan, (3*R*)-3-(4-hydroxybenzyl)-6-hydroxy-8-methoxy-3,4-dihydro-2*H*-1-benzopyran, and 4′-hydroxy-7-methoxyflavan, used significantly less conformational space. Contrarily, only 7,4′-dihydroxyflavan and (3*R*)-3-(4-hydroxybenzyl)-6-hydroxy-8-methoxy-3,4-dihydro-2*H*-1-benzopyran outperformed the Solasodine reference drug.

Furthermore, 7,4′-dihydroxyflavan, (3*R*)-3-(4-hydroxybenzyl)-6-hydroxy-8-methoxy-3,4-dihydro-2*H*-1-benzopyran, and 4′-hydroxy-7-methoxyflavan showed positive correlations with

https://doi.org/10.1021/acsomega.3c00441
ACS Omega 2023, 8, 10565−10590

the N-terminal domain of proteins, while (3*R*)-3-(4-hydroxybenzyl)-6-hydroxy-8-methoxy-3,4-dihydro-2*H*-1-benzopyran displayed an anticorrelation. As a result, we demonstrated how three lead flavonoids may be able to target the MMP9 protein. The fact that 7,4′-dihydroxyflavan was derived from the African forest tree *Guibourtia ehie* or Shedua, which has been utilized traditionally for tumor and wound healing, provided additional support for our findings in earlier investigations. It acts as a metabolite and shows anti-inflammatory and antioxidant effects in prostate cancer, breast cancer, and osteosarcoma by regulating Akt/Bad and MAPK signaling. In addition, (3*R*)-3-(4-hydroxybenzyl)-6-hydroxy-8-methoxy-3,4-dihydro-2*H*-1-benzopyran was found in *Soymida febrifuge* (Indian-redwood). Its fruits are therapeutic and have been used to treat cervical and colon cancer.[117] Interestingly, a study by Sowmyya and Vijaya Lakshmi discovered that extracts from these dried fruits contributed to the creation of silver nanoparticles by acting as reducing and stabilizing agents during the conversion of Ag^+ to nano-silver.[118] The last compound, 4′-hydroxy-7-methoxyflavan, was derived from the orchid tree *Bauhinia divaricate* and was formerly used to treat skin and colon cancer. These three flavonoids will inhibit MMP9 and lower its overexpression brought on by hypoxia in GBM. As a result of these inhibitions, the downstream effects of MMP9 activation will be diminished, which will minimize the pathogenesis of GBM. Cell proliferation, invasion, angiogenesis, drug resistance, matrix remodeling, and immune cell infiltration are significant pathways that will be impacted. The infiltration of DCs in response to MMP9 overexpression was also demonstrated by our data, which also indicated a positive correlation with immune checkpoints like PD-1 and TIM-3. Figure 8 illustrates the proposed mode of action for three novel flavonoids, including 7,4′-dihydroxyflavan (PubChem CID 158280), (3*R*)-3-(4-hydroxybenzyl)-6-hydroxy-8-methoxy-3,4-dihydro-2*H*-1-benzopyran (PubChem CID 44479222), and 4′-hydroxy-7-methoxyflavan (PubChem CID 185609). These will attenuate MMP9 activation's impact on GBM.

5. CONCLUSIONS AND FUTURE PERSPECTIVES

Despite recent advancements in chemotherapy, radiotherapy, and immunotherapy, there is currently no satisfactory therapy for GBM in clinics due to many reasons, being toxicity of chemotherapy, failure of the drug to cross BBB, involvement of TME, and less immune infiltration. For instance, immune checkpoint blockade targeting CD8+ T cells is ineffective for GBM.[119] There is an unmet need for novel approaches to treat GBM and other brain cancers. Here in our study, we have focused on a crucial TME parameter, that is, hypoxia caused due to intense cell respiration, excessive nutrient consumption by tumor cells, and abnormal vasculature. However, hypoxia is a hallmark of brain tumors, and if and how hypoxia affects antitumor immunity in the brain remains unclear. Our findings shed light on the potential of MMP9 as a therapeutic target and a robust biomarker in GBM's hypoxic microenvironment. In Figure 8, it is illustrated that in response to cytokine-induced stimulation, MMP9 is synthesized de novo by activating various signaling pathways including NF-κB, HIF-1, MAPK, PI3K, and so forth. Cytokines such as TNF-α, IL-8, and IL-1β and growth factors namely TGF-β, PDGF, and bFGF bind to their respective receptors and influence the activation and production of MMP9. This has an impact on a number of biological functions that come thereafter, such as drug resistance, remodeling of the matrix, EMT, increased tumoral invasion, metastases, angiogenesis, and remodeling.

Previous studies supported our results where researchers have shown that MMP9, a zinc-dependent endopeptidase, was upregulated in glioma tissues, and its expression was correlated with tumor grade and poor prognosis. Hypoxia condition increases the protein expression of HIF-α, MMP2, and MMP9 in cancer[120] and regulates tight junction rearrangement, leading to vascular leakage in the brain.[121] Majority of the ECM components are substrates of MMPs. MMP-9 can cleave many ECM proteins to regulate ECM remodeling and affects the alteration of cell−cell and cell−ECM interactions. It can also cleave many plasma surface proteins to release them from the cell surface. It has been implicated in the invasion and also implicated in BBB opening as part of the neuroinflammatory response, metastasis through proliferation, vasculogenesis, and angiogenesis.[72] MMP9 has been a potential biomarker for many cancers, including osteosarcoma, breast, cervical, ovarian, and pancreatic, giant cell tumor of bone, and non-small cell lung cancer.[21] Herein the current study, we have proposed MMP9 as a promising biomarker for hypoxic microenvironmental conditions in GBM. Other molecular signatures, such as LYN, PSMB9, and TIMP1, could be investigated further as druggable biomarkers or prognostic markers in addition to MMP9. Infiltration of immune cells such as neutrophils and DCs was linked to this gene's expression to varying degrees. This effect opens up new avenues for study into MMP9 and GBM. A negative correlation with B cells, CD4+ T cells, and CD8+ T cells supports the failure of current immune checkpoint inhibitors.

The current study used in silico techniques such as compound-protein-pathway enrichment analysis, network pharmacology, molecular docking, MD simulation, MM-PBSA, PCA, and DCCM investigations to identify a collection of druggable and nontoxic natural compounds from plants. The potential of natural compounds to be used as drugs was revealed by ADMET analysis of 11 novel hits. A chemical substance must have absorption, distribution, metabolism, excretion, and toxicity values to be utilized as a medication. The results obtained showed flavonoids named 7,4′-dihydroxyflavan, (3*R*)-3-(4-hydroxybenzyl)-6-hydroxy-8-methoxy-3,4-dihydro-2*H*-1-benzopyran, and 4′-hydroxy-7-methoxyflavan as potential inhibitors of MMP9 produced from the hypoxic condition in GBM. These inhibitors have comparable or better results compared to reference drugs Solasodine and Captopril. Our results indicate that MMP9 and drug interaction are stable, and proposed novel flavonoids can inhibit or reduce MMP9 expression in hypoxia conditions, which will further affect the downstream process involved in GBM pathogenesis. Hence, targeting an essential microenvironmental condition will improve therapeutic efficacy and expand the treatment drug library against GBM. Limiting to the present findings, we point out that the results presented in this work are based on processor simulations which need to be further validated with wet-lab experimental protocols.

In conclusion, the observations of this work suggest novel plant-based flavonoids inhibited the potential role of MMP9 as a biomarker factor and active MMP9 in GBM. Prior to synthesizing therapeutics, the results of this investigation could be helpful. Other natural compounds and plant-based natural compounds could be examined and studied to understand and explore whether they could be employed as future possibilities for GBM medicines. The results of this study

https://doi.org/10.1021/acsomega.3c00441
ACS Omega 2023, 8, 10565−10590

are helpful for drug development. The findings may aid in the assisted screening of therapeutics for GBM. This study is novel in incorporating various computational methodologies for the virtual screening of natural compounds based on BBB, ADMET, PAINS, and Lipinski's rule. This study allows scientists to explore these molecules in vitro or in vivo as a medicinal approach. We have validated our results using different computational methodologies such as multiple-target validation, literature validation, TCGA databases (containing GBM samples data), cell culture, and animal model research which will fill in the gaps. We identified the common residues via which the inhibitor can potentially bind to the target using bioinformatics tools and in silico studies. However, the molecular mechanism underlying the reduction of target expression needs only to be validated through in vitro experiments. New leads are being discovered in several ongoing studies using advanced computational strategies and machine learning models to filter massive pharmaceutical libraries. The experimental screening strategy alone may not enhance lead productivity for the rapid development of viable medicines. Our findings will aid researchers in concentrating on TME components and their conditions in order to produce novel natural product-based anti-GBM therapies that address two major issues: toxicity and resistance and target of a major microenvironmental condition hypoxia.

■ ASSOCIATED CONTENT

Supporting Information

The Supporting Information is available free of charge at https://pubs.acs.org/doi/10.1021/acsomega.3c00441.

MA plot; list of DEGs; mutational and correlation analyses; localization and transcription factor analysis; screening of natural compounds; physiochemical properties; 2D docked structure; H-bond and contribution energy plot; and MMP9 characteristics (PDF)

■ AUTHOR INFORMATION

Corresponding Author

Pravir Kumar − *Molecular Neuroscience and Functional Genomics Laboratory, Department of Biotechnology, Delhi Technological University (Formerly DCE), Delhi 110042, India;* orcid.org/0000-0001-7444-2344; Phone: +91-9818898622; Email: pravirkumar@dtu.ac.in

Author

Smita Kumari − *Molecular Neuroscience and Functional Genomics Laboratory, Department of Biotechnology, Delhi Technological University (Formerly DCE), Delhi 110042, India*

Complete contact information is available at: https://pubs.acs.org/10.1021/acsomega.3c00441

Author Contributions

P.K. and S.K. conceived and designed the manuscript. S.K. collected, analyzed, and critically evaluated these data. S.K. prepared the figures and tables. P.K. and S.K. analyzed the entire data and wrote the manuscript.

Funding

S.K. has received Senior Research Fellowship (SRF) from the Department of Biotechnology (DBT), Govt. of India (Fellow ID: DBT/2019/DTU/1308).

Notes

The authors declare no competing financial interest.

■ ACKNOWLEDGMENTS

We would like to thank the senior management of Delhi Technological University (DTU) and the Department of Biotechnology (DBT), Government of India, for their constant support and financial assistance.

■ LIST OF ABBREVIATIONS

2D, 2-dimensional; 3D, 3-dimensional; Caco-2, colon adenocarcinoma cell lines; DCCM, domain cross-correlation matrix; DEGs, differentially regulated genes; DCs, dendritic cells; EPO, erythropoietin; GBM, glioblastoma multiforme; GEO, gene expression omnibus; GEPIA2.0, Gene Expression Profiling Interactive Analysis; GMQE, Global Model Quality Estimate; GS2D, gene set to diseases; HBA, hydrogen bond acceptor; HBD, hydrogen bond donor; H-bond, hydrogen bond; HIA, human intestinal absorption cells; HR, hazard ratio; KEGG, Kyoto Encyclopedia of Genes and Genomes; logCPM, $\log_2$-counts-per-millions; LYN, Lck/Yes-related novel protein tyrosine kinase; MB-PBSA, molecular mechanics Poisson−Boltzmann surface area; MD, molecular dynamics; MDCK, Madin−Darby canine kidney cells; MMP-9, matrix metalloproteinase 9; MW, molecular weight; PAINS, Pan Assay Interference Compounds; PCA, principal component analysis; PDGF, platelet-derived growth factor; PPI, protein−protein interaction; PSMB9, proteasome 20S subunit beta 9; RCSB, Research Collaboratory for Structural Bioinformatics; RMSD, root-mean-square deviation; RMSF, root-mean-square fluctuation; R_g, radiation of gyration; SASA, solvent accessible surface area; SMILES, Simplified Molecular-Input Line-Entry System; STRING, Search Tool for the Retrieval of Interacting Genes/Proteins; TFs, transcription factors; TIMP1, tissue inhibitor of metalloproteinases 1; TME, tumor microenvironment; TPM, transcript per million; vdw, van der Waal force; VEGF, vascular endothelial growth factor

■ REFERENCES

(1) Miller, K. D.; Ostrom, Q. T.; Kruchko, C.; Patil, N.; Tihan, T.; Cioffi, G.; Fuchs, H. E.; Waite, K. A.; Jemal, A.; Siegel, R. L.; Barnholtz-Sloan, J. S. Brain and Other Central Nervous System Tumor Statistics, 2021. *Ca -Cancer J. Clin.* **2021**, *71*, 381−406.

(2) Stylli, S. S. Novel Treatment Strategies for Glioblastoma. *Cancers* **2020**, *12*, 2883.

(3) DeCordova, S.; Shastri, A.; Tsolaki, A. G.; Yasmin, H.; Klein, L.; Singh, S. K.; Kishore, U. Molecular Heterogeneity and Immunosuppressive Microenvironment in Glioblastoma. *Front. Immunol.* **2020**, *11*, 1402.

(4) Li, Y.; Zhao, L.; Li, X. F. Hypoxia and the Tumor Microenvironment. *Technol. Cancer Res. Treat.* **2021**, *20*, 153303382110363.

(5) Huang, W. J.; Chen, W. W.; Zhang, X. Glioblastoma Multiforme: Effect of Hypoxia and Hypoxia Inducible Factors on Therapeutic Approaches (Review). *Oncol. Lett.* **2016**, *12*, 2283−2288.

(6) Velásquez, C.; Mansouri, S.; Gutiérrez, O.; Mamatjan, Y.; Mollinedo, P.; Karimi, S.; Singh, O.; Terán, N.; Martino, J.; Zadeh, G.; Fernández-Luna, J. L. Hypoxia Can Induce Migration of Glioblastoma Cells through a Methylation-Dependent Control of ODZ1 Gene Expression. *Front. Oncol.* **2019**, *9*, 1036.

(7) Emami Nejad, A.; Najafgholian, S.; Rostami, A.; Sistani, A.; Shojaeifar, S.; Esparvarinha, M.; Nedaeinia, R.; Haghjooy Javanmard, S.; Taherian, M.; Ahmadlou, M.; Salehi, R.; Sadeghi, B.; Manian, M. The Role of Hypoxia in the Tumor Microenvironment and Development of Cancer Stem Cell: A Novel Approach to Developing Treatment. *Cancer Cell Int.* **2021**, *21*, 62.

(8) Zheng, X.; Qian, Y.; Fu, B.; Jiao, D.; Jiang, Y.; Chen, P.; Shen, Y.; Zhang, H.; Sun, R.; Tian, Z.; Wei, H. Mitochondrial Fragmentation Limits NK Cell-Based Tumor Immunosurveillance. *Nat. Immunol.* **2019**, *20*, 1656−1667.
(9) Henze, A. T.; Mazzone, M. The Impact of Hypoxia on Tumor-Associated Macrophages. *J. Clin. Invest.* **2016**, *126*, 3672.
(10) Park, J. H.; Kim, H. J.; Kim, C. W.; Kim, H. C.; Jung, Y.; Lee, H. S.; Lee, Y.; Ju, Y. S.; Oh, J. E.; Park, S. H.; Lee, J. H.; Lee, S. K.; Lee, H. K. Tumor Hypoxia Represses Γδ T Cell-Mediated Antitumor Immunity against Brain Tumors. *Nat. Immunol.* **2021**, *22*, 336−346.
(11) Bronisz, A.; Salińska, E.; Chiocca, E. A.; Godlewski, J. Hypoxic Roadmap of Glioblastoma-Learning about Directions and Distances in the Brain Tumor Environment. *Cancers* **2020**, *12*, 1213.
(12) Kalkan, R. Hypoxia Is the Driving Force Behind GBM and Could Be a New Tool in GBM Treatment. *Crit. Rev. Eukaryot. Gene Expr.* **2015**, *25*, 363−369.
(13) Tan, A. C.; Ashley, D. M.; López, G. Y.; Malinzak, M.; Friedman, H. S.; Khasraw, M. Management of Glioblastoma: State of the Art and Future Directions. *Ca -Cancer J. Clin.* **2020**, *70*, 299−312.
(14) Atanasov, A. G.; Zotchev, S. B.; Dirsch, V. M.; Orhan, I. E.; Supuran, M.; Rollinger, J. M.; Barreca, D.; Weckwerth, W.; Bauer, R.; Bayer, E. A.; Majeed, M.; Bishayee, A.; Bochkov, V.; Bonn, G. K.; Braidy, N.; Bucar, F.; Cifuentes, A.; D'Onofrio, G.; Bodkin, M.; Diederich, M.; Dinkova-Kostova, A. T.; Efferth, T.; El Bairi, K.; Arkells, N.; Fan, T. P.; Fiebich, B. L.; Freissmuth, M.; Georgiev, M. I.; Gibbons, S.; Godfrey, K. M.; Gruber, C. W.; Heer, J.; Huber, L. A.; Ibanez, E.; Kijjoa, A.; Kiss, A. K.; Lu, A.; Macias, F. A.; Miller, M. J. S.; Mocan, A.; Müller, R.; Nicoletti, F.; Perry, G.; Pittalà, V.; Rastrelli, L.; Ristow, M.; Russo, G. L.; Silva, A. S.; Schuster, D.; Sheridan, H.; Skalicka-Woźniak, K.; Skaltsounis, L.; Sobarzo-Sánchez, E.; Bredt, D. S.; Stuppner, H.; Sureda, A.; Tzvetkov, N. T.; Vacca, R. A.; Aggarwal, B. B.; Battino, M.; Giampieri, F.; Wink, M.; Wolfender, J. L.; Xiao, J.; Yeung, A. W. K.; Lizard, G.; Popp, M. A.; Heinrich, M.; Berindan-Neagoe, I.; Stadler, M.; Daglia, M.; Verpoorte, R.; Supuran, C. T. Natural Products in Drug Discovery: Advances and Opportunities. *Nat. Rev. Drug Discovery* **2021**, *20*, 200−216.
(15) Huang, M.; Lu, J. J.; Ding, J. Natural Products in Cancer Therapy: Past, Present and Future. *Nat. Prod. Bioprospect.* **2021**, *11*, 5−13.
(16) Vengoji, R.; Macha, M. A.; Batra, S. K.; Shonka, N. A. Natural Products: A Hope for Glioblastoma Patients. *Oncotarget* **2018**, *9*, 22194.
(17) Santos, B. L.; Oliveira, M. N.; Coelho, P. L. C.; Pitanga, B. P. S.; da Silva, A. B.; Adelita, T.; Silva, V. D. A.; Costa, M. D. F. D.; El-Bachá, R. S.; Tardy, M.; Chneiweiss, H.; Junier, M. P.; Moura-Neto, V.; Costa, S. L. Flavonoids Suppress Human Glioblastoma Cell Growth by Inhibiting Cell Metabolism, Migration, and by Regulating Extracellular Matrix Proteins and Metalloproteinases Expression. *Chem. Biol. Interact.* **2015**, *242*, 123−138.
(18) Soukhtanloo, M.; Mohtashami, E.; Maghrouni, A.; Mollazadeh, H.; Mousavi, S. H.; Roshan, M. K.; Tabatabaeizadeh, S. A.; Hosseini, A.; Vahedi, M. M.; Jalili-Nik, M.; Afshari, A. R. Natural Products as Promising Targets in Glioblastoma Multiforme: A Focus on NF-KB Signaling Pathway. *Pharmacol. Rep.* **2020**, *72*, 285−295.
(19) Zhai, K.; Siddiqui, M.; Abdellatif, B.; Liskova, A.; Kubatka, P.; Büsselberg, D. Natural Compounds in Glioblastoma Therapy: Preclinical Insights, Mechanistic Pathways, and Outlook. *Cancers* **2021**, *13*, 2317.
(20) Pujada, A.; Walter, L.; Patel, A.; Bui, T. A.; Zhang, Z.; Zhang, Y.; Denning, T. L.; Garg, P. Matrix Metalloproteinase MMP9 Maintains Epithelial Barrier Function and Preserves Mucosal Lining in Colitis Associated Cancer. *Oncotarget* **2017**, *8*, 94650.
(21) Huang, H. Matrix Metalloproteinase-9 (MMP-9) as a Cancer Biomarker and MMP-9 Biosensors: Recent Advances. *Sensors* **2018**, *18*, 3249.
(22) Augoff, K.; Hryniewicz-Jankowska, A.; Tabola, R.; Stach, K. MMP9: A Tough Target for Targeted Therapy for Cancer. *Cancers* **2022**, *14*, 1847.
(23) Atiq, A.; Parhar, I. Anti-Neoplastic Potential of Flavonoids and Polysaccharide Phytochemicals in Glioblastoma. *Molecules* **2020**, *25*, 4895.
(24) Mondal, A.; Gandhi, A.; Fimognari, C.; Atanasov, A. G.; Bishayee, A. Alkaloids for Cancer Prevention and Therapy: Current Progress and Future Perspectives. *Eur. J. Pharmacol.* **2019**, *858*, 172472.
(25) Edgar, R.; Domrachev, M.; Lash, A. E. Gene Expression Omnibus: NCBI Gene Expression and Hybridization Array Data Repository. *Nucleic Acids Res.* **2002**, *30*, 207−210.
(26) Mahi, N. A.; Najafabadi, M. F.; Pilarczyk, M.; Kouril, M.; Medvedovic, M. GREIN: An Interactive Web Platform for Re-Analyzing GEO RNA-Seq Data. *Sci. Rep.* **2019**, *9*, 7580.
(27) Huang, D. W.; Sherman, B. T.; Lempicki, R. A. Bioinformatics Enrichment Tools: Paths toward the Comprehensive Functional Analysis of Large Gene Lists. *Nucleic Acids Res.* **2009**, *37*, 1−13.
(28) Fontaine, J. F.; Andrade-Navarro, M. A. Gene Set to Diseases (GS2D): Disease Enrichment Analysis on Human Gene Sets with Literature Data. *Genomics Comput. Biol.* **2016**, *2*, No. e33.
(29) Kuleshov, M. V.; Jones, M. R.; Rouillard, A. D.; Fernandez, N. F.; Duan, Q.; Wang, Z.; Koplev, S.; Jenkins, S. L.; Jagodnik, K. M.; Lachmann, A.; McDermott, M. G.; Monteiro, C. D.; Gundersen, G. W.; Ma'ayan, A. Enrichr: a comprehensive gene set enrichment analysis web server 2016 update. *Nucleic Acids Res.* **2016**, *44*, W90−W97.
(30) Chen, E. Y.; Tan, C. M.; Kou, Y.; Duan, Q.; Wang, Z.; Meirelles, G. V.; Clark, N. R.; Ma'ayan, A. Enrichr: Interactive and Collaborative HTML5 Gene List Enrichment Analysis Tool. *BMC Bioinf.* **2013**, *14*, 128.
(31) Pathan, M.; Keerthikumar, S.; Ang, C. S.; Gangoda, L.; Quek, C. Y. J.; Williamson, N. A.; Mouradov, D.; Sieber, O. M.; Simpson, R. J.; Salim, A.; Bacic, A.; Hill, A. F.; Stroud, D. A.; Ryan, M. T.; Agbinya, J. I.; Mariadason, J. M.; Burgess, A. W.; Mathivanan, S. FunRich: An Open Access Standalone Functional Enrichment and Interaction Network Analysis Tool. *Proteomics* **2015**, *15*, 2597−2601.
(32) Szklarczyk, D.; Gable, A. L.; Nastou, K. C.; Lyon, D.; Kirsch, R.; Pyysalo, S.; Doncheva, N. T.; Legeay, M.; Fang, T.; Bork, P.; Jensen, L. J.; von Mering, C. The STRING Database in 2021: Customizable Protein-Protein Networks, and Functional Characterization of User-Uploaded Gene/Measurement Sets. *Nucleic Acids Res.* **2021**, *49*, D605−D612.
(33) Shannon, P.; Markiel, A.; Ozier, O.; Baliga, N. S.; Wang, J. T.; Ramage, D.; Amin, N.; Schwikowski, B.; Ideker, T. Cytoscape: A Software Environment for Integrated Models of Biomolecular Interaction Networks. *Genome Res.* **2003**, *13*, 2498−2504.
(34) Li, T.; Fu, J.; Zeng, Z.; Cohen, D.; Li, J.; Chen, Q.; Li, B.; Liu, X. S. TIMER2.0 for Analysis of Tumor-Infiltrating Immune Cells. *Nucleic Acids Res.* **2020**, *48*, W509−W514.
(35) Bowman, R. L.; Wang, Q.; Carro, A.; Verhaak, R. G. W.; Squatrito, M. GlioVis Data Portal for Visualization and Analysis of Brain Tumor Expression Data sets. *Neuro Oncol.* **2017**, *19*, 139−141.
(36) Tang, Z.; Kang, B.; Li, C.; Chen, T.; Zhang, Z. GEPIA2: An Enhanced Web Server for Large-Scale Expression Profiling and Interactive Analysis. *Nucleic Acids Res.* **2019**, *47*, W556−W560.
(37) Gill, B. J.; Pisapia, D. J.; Malone, H. R.; Goldstein, H.; Lei, L.; Sonabend, A.; Yun, J.; Samanamud, J.; Sims, J. S.; Banu, M.; Dovas, A.; Teich, A. F.; Sheth, S. A.; McKhann, G. M.; Sisti, M. B.; Bruce, J. N.; Sims, P. A.; Canoll, P. MRI-Localized Biopsies Reveal Subtype-Specific Differences in Molecular and Cellular Composition at the Margins of Glioblastoma. *Proc. Natl. Acad. Sci. U.S.A.* **2014**, *111*, 12550−12555.
(38) Madhavan, S.; Zenklusen, J. C.; Kotliarov, Y.; Sahni, H.; Fine, H. A.; Buetow, K. Rembrandt: Helping Personalized Medicine Become a Reality through Integrative Translational Research. *Mol. Cancer Res.* **2009**, *7*, 157−167.
(39) Gravendeel, L. A. M.; Kouwenhoven, M. C. M.; Gevaert, O.; de Rooi, J. J.; Stubbs, A. P.; Duijm, J. E.; Daemen, A.; Bleeker, F. E.; Bralten, L. B. C.; Kloosterhof, N. K.; De Moor, B.; Eilers, P. H. C.; van der Spek, P. J.; Kros, J. M.; Sillevis Smitt, P. A. E.; van den Bent, M. J.; French, P. J. Intrinsic Gene Expression Profiles of Gliomas Are a Better Predictor of Survival than Histology. *Cancer Res.* **2009**, *69*, 9065−9072.

https://doi.org/10.1021/acsomega.3c00441
ACS Omega 2023, 8, 10565−10590

(40) Li, T.; Fan, J.; Wang, B.; Traugh, N.; Chen, Q.; Liu, J. S.; Li, B.; Liu, X. S. TIMER: A Web Server for Comprehensive Analysis of Tumor-Infiltrating Immune Cells. *Cancer Res.* **2017**, *77*, e108−e110.
(41) Yu, C. S.; Chen, Y. C.; Lu, C. H.; Hwang, J. K. Prediction of Protein Subcellular Localization. *Proteins: Struct., Funct., Bioinf.* **2006**, *64*, 643−651.
(42) Fornes, O.; Castro-Mondragon, J. A.; Khan, A.; van der Lee, R.; Zhang, X.; Richmond, P. A.; Modi, B. P.; Correard, S.; Gheorghe, M.; Baranašić, D.; Santana-Garcia, W.; Tan, G.; Chèneby, J.; Ballester, B.; Parcy, F.; Sandelin, A.; Lenhard, B.; Wasserman, W. W.; Mathelier, A. JASPAR 2020: Update of the Open-Access Database of Transcription Factor Binding Profiles. *Nucleic Acids Res.* **2020**, *48*, D87.
(43) Zhou, G.; Soufan, O.; Ewald, J.; Hancock, R. E. W.; Basu, N.; Xia, J. NetworkAnalyst 3.0: A Visual Analytics Platform for Comprehensive Gene Expression Profiling and Meta-Analysis. *Nucleic Acids Res.* **2019**, *47*, W234−W241.
(44) Mangal, M.; Sagar, P.; Singh, H.; Raghava, G. P. S.; Agarwal, S. M. NPACT: Naturally Occurring Plant-Based Anti-Cancer Compound-Activity-Target Database. *Nucleic Acids Res.* **2013**, *41*, D1124.
(45) Angeli, E.; Nguyen, T. T.; Janin, A.; Bousquet, G. How to Make Anticancer Drugs Cross the Blood-Brain Barrier to Treat Brain Metastases. *Int. J. Mol. Sci.* **2019**, *21*, 22.
(46) Daina, A.; Michielin, O.; Zoete, V. SwissADME: A Free Web Tool to Evaluate Pharmacokinetics, Drug-Likeness and Medicinal Chemistry Friendliness of Small Molecules. *Sci. Rep.* **2017**, *7*, 42717.
(47) Liu, H.; Wang, L.; Lv, M.; Pei, R.; Li, P.; Pei, Z.; Wang, Y.; Su, W.; Xie, X. Q. AlzPlatform: An Alzheimer's Disease Domain-Specific Chemogenomics Knowledgebase for Polypharmacology and Target Identification Research. *J. Chem. Inf. Model.* **2014**, *54*, 1050−1060.
(48) Molsoft L. L. C. Drug-Likeness and molecular property prediction. https://molsoft.com/mprop/ (accessed Dec 26, 2021).
(49) Xiong, G.; Wu, Z.; Yi, J.; Fu, L.; Yang, Z.; Hsieh, C.; Yin, M.; Zeng, X.; Wu, C.; Lu, A.; Chen, X.; Hou, T.; Cao, D. ADMETlab 2.0: An Integrated Online Platform for Accurate and Comprehensive Predictions of ADMET Properties. *Nucleic Acids Res.* **2021**, *49*, W5−W14.
(50) BIOVIA Discovery Studio Visualizer-Dassault Systèmes. https://discover.3ds.com/discovery-studio-visualizer-download (accessed Sep 11, 2022). Free Download.
(51) Rappe, A. K.; Casewit, C. J.; Colwell, K. S.; Goddard, W. A.; Skiff, W. M. UFF, a Full Periodic Table Force Field for Molecular Mechanics and Molecular Dynamics Simulations. *J. Am. Chem. Soc.* **1992**, *114*, 10024−10035.
(52) Anderson, R. J.; Weng, Z.; Campbell, R. K.; Jiang, X. Main-Chain Conformational Tendencies of Amino Acids. *Proteins* **2005**, *60*, 679−689.
(53) Colovos, C.; Yeates, T. O. Verification of Protein Structures: Patterns of Nonbonded Atomic Interactions. *Protein Sci.* **1993**, *2*, 1511−1519.
(54) Bowie, J. U.; Lüthy, R.; Eisenberg, D. A Method to Identify Protein Sequences That Fold into a Known Three-Dimensional Structure. *Science* **1991**, *253*, 164−170.
(55) Samdani, A.; Vetrivel, U. POAP: A GNU Parallel Based Multithreaded Pipeline of Open Babel and AutoDock Suite for Boosted High Throughput Virtual Screening. *Comput. Biol. Chem.* **2018**, *74*, 39−48.
(56) Van Der Spoel, D.; Lindahl, E.; Hess, B.; Groenhof, G.; Mark, A. E.; Berendsen, H. J. C. GROMACS: Fast, Flexible, and Free. *J. Comput. Chem.* **2005**, *26*, 1701−1718.
(57) Kumari, R.; Kumar, R.; Lynn, A. G_mmpbsa–a GROMACS Tool for High-Throughput MM-PBSA Calculations. *J. Chem. Inf. Model.* **2014**, *54*, 1951−1962.
(58) Bhandare, V. V.; Kumbhar, B. V.; Kunwar, A. Differential Binding Affinity of Tau Repeat Region R2 with Neuronal-Specific β-Tubulin Isotypes. *Sci. Rep.* **2019**, *9*, 10795.
(59) Dwivedi, P. S. R.; Patil, V. S.; Khanal, P.; Bhandare, V. V.; Gurav, S.; Harish, D. R.; Patil, B. M.; Roy, S. System Biology-Based Investigation of Silymarin to Trace Hepatoprotective Effect. *Comput. Biol. Med.* **2022**, *142*, 105223.
(60) Taidi, L.; Maurady, A.; Britel, M. R. Molecular Docking Study and Molecular Dynamic Simulation of Human Cyclooxygenase-2 (COX-2) with Selected Eutypoids. *J. Biomol. Struct. Dyn.* **2020**, *40*, 1189−1204.
(61) Khanal, P.; Patil, V. S.; Bhandare, V. V.; Dwivedi, P. S. R.; Shastry, C. S.; Patil, B. M.; Gurav, S. S.; Harish, D. R.; Roy, S. Computational Investigation of Benzalacetophenone Derivatives against SARS-CoV-2 as Potential Multi-Target Bioactive Compounds. *Comput. Biol. Med.* **2022**, *146*, 105668.
(62) Bhandare, V. V.; Ramaswamy, A. The Proteinopathy of D169G and K263E Mutants at the RNA Recognition Motif (RRM) Domain of Tar DNA-Binding Protein (Tdp43) Causing Neurological Disorders: A Computational Study. *J. Biomol. Struct. Dyn.* **2018**, *36*, 1075−1093.
(63) Arnold, G. E.; Ornstein, R. L. Molecular Dynamics Study of Time-Correlated Protein Domain Motions and Molecular Flexibility: Cytochrome P450BM-3. *Biophys. J.* **1997**, *73*, 1147−1159.
(64) Khanal, P.; Zargari, F.; Far, B. F.; Kumar, D.; R, M.; Mahdi, Y. K.; Jubair, N. K.; Saraf, S. K.; Bansal, P.; Singh, R.; Selvaraja, M.; Dey, Y. N. Integration of System Biology Tools to Investigate Huperzine A as an Anti-Alzheimer Agent. *Front. Pharmacol.* **2021**, *12*, 785964.
(65) Mahi, N. A.; Najafabadi, M. F.; Pilarczyk, M.; Kouril, M.; Medvedovic, M. GREIN: An Interactive Web Platform for Reanalyzing GEO RNA-Seq Data. *Sci. Rep.* **2019**, *9*, 7580.
(66) Venny 2.1.0. https://bioinfogp.cnb.csic.es/tools/venny/index.html (accessed Nov 29, 2021).
(67) Vassilakopoulou, M.; Won, M.; Curran, W. J.; Souhami, L.; Prados, M. D.; Langer, C. J.; Rimm, D. L.; Hanna, J. A.; Neumeister, V. M.; Melian, E.; Diaz, A. Z.; Atkins, J. N.; Komarnicky, L. T.; Schultz, C. J.; Howard, S. P.; Zhang, P.; Dicker, A. P.; Knisely, J. P. S. BRCA1 Protein Expression Predicts Survival in Glioblastoma Patients from an NRG Oncology RTOG Cohort. *Oncology* **2021**, *99*, 580.
(68) Zhang, Y.; Xia, Q.; Lin, J. Identification of the Potential Oncogenes in Glioblastoma Based on Bioinformatic Analysis and Elucidation of the Underlying Mechanisms. *Oncol. Rep.* **2018**, *40*, 715−725.
(69) Yang, G.; Dong, K.; Zhang, Z.; Zhang, E.; Liang, B.; Chen, X.; Huang, Z. EXO1 Plays a Carcinogenic Role in Hepatocellular Carcinoma and Is Related to the Regulation of FOXP3. *J. Cancer* **2020**, *11*, 4917−4932.
(70) Liu, B.; Zhang, G.; Cui, S.; Du, G. Upregulation of KIF11 in TP53 Mutant Glioma Promotes Tumor Stemness and Drug Resistance. *Cell. Mol. Neurobiol.* **2022**, *42*, 1477−1485.
(71) Jiang, C.; Zhang, H.; Wu, W.; Wang, Z.; Dai, Z.; Zhang, L.; Liu, Z.; Cheng, Q. Immune Characteristics of LYN in Tumor Microenvironment of Gliomas. *Front. Cell Dev. Biol.* **2022**, *9*, 760929.
(72) Xue, Q.; Cao, C.; Chen, X. Y.; Zhao, J.; Gao, L.; Li, S. Z.; Fei, Z. High Expression of MMP9 in Glioma Affects Cell Proliferation and Is Associated with Patient Survival Rates. *Oncol. Lett.* **2017**, *13*, 1325.
(73) Liu, J.; Yang, X.; Ji, Q.; Yang, L.; Li, J.; Long, X.; Ye, M.; Huang, K.; Zhu, X. Immune Characteristics and Prognosis Analysis of the Proteasome 20S Subunit Beta 9 in Lower-Grade Gliomas. *Front. Oncol.* **2022**, *12*, 875131.
(74) Smith, S. J.; Li, C. M.; Lingeman, R. G.; Hickey, R. J.; Liu, Y.; Malkas, L. H.; Raoof, M. Molecular Targeting of Cancer-Associated PCNA Interactions in Pancreatic Ductal Adenocarcinoma Using a Cell-Penetrating Peptide. *Mol. Ther. Oncolytics* **2020**, *17*, 250−256.
(75) Aaberg-Jessen, C.; Fogh, L.; Sørensen, M. D.; Halle, B.; Brünner, N.; Kristensen, B. W. Overexpression of TIMP-1 and Sensitivity to Topoisomerase Inhibitors in Glioblastoma Cell Lines. *Pathol. Oncol. Res.* **2019**, *25*, 59−69.
(76) Wang, B. Q.; Zhang, C. M.; Gao, W.; Wang, X. F.; Zhang, H. L.; Yang, P. C. Cancer-Derived Matrix Metalloproteinase-9 Contributes to Tumor Tolerance. *J. Cancer Res. Clin. Oncol.* **2011**, *137*, 1525−1533.
(77) Juric, V.; O'Sullivan, C.; Stefanutti, E.; Kovalenko, M.; Greenstein, A.; Barry-Hamilton, V.; Mikaelian, I.; Degenhardt, J.; Yue, P.; Smith, V.; Mikels-Vigdal, A. MMP-9 Inhibition Promotes Anti-Tumor Immunity through Disruption of Biochemical and Physical Barriers to T-Cell Trafficking to Tumors. *PLoS One* **2018**, *13*, No. e0207255.

https://doi.org/10.1021/acsomega.3c00441
ACS Omega 2023, 8, 10565−10590

(78) van Tellingen, O.; Yetkin-Arik, B.; de Gooijer, M. C.; Wesseling, P.; Wurdinger, T.; de Vries, H. E. Overcoming the Blood-Brain Tumor Barrier for Effective Glioblastoma Treatment. *Drug Resist. Updates* **2015**, *19*, 1−12.
(79) Ursu, O.; Rayan, A.; Goldblum, A.; Oprea, T. I. Understanding Drug-Likeness. *Wiley Interdiscip. Rev. Comput. Mol. Sci.* **2011**, *1*, 760−781.
(80) Yang, Z. Y.; Yang, Z. J.; He, J. H.; Lu, A. P.; Liu, S.; Hou, T. J.; Cao, D. S. Benchmarking the Mechanisms of Frequent Hitters: Limitation of PAINS Alerts. *Drug Discov. Today* **2021**, *26*, 1353−1358.
(81) Guan, L.; Yang, H.; Cai, Y.; Sun, L.; Di, P.; Li, W.; Liu, G.; Tang, Y. ADMET-Score − a Comprehensive Scoring Function for Evaluation of Chemical Drug-Likeness. *MedChemComm* **2019**, *10*, 148.
(82) Zhu, R.; Hu, L.; Li, H.; Su, J.; Cao, Z.; Zhang, W. Novel Natural Inhibitors of CYP1A2 Identified by in Silico and in Vitro Screening. *Int. J. Mol. Sci.* **2011**, *12*, 3250.
(83) Durán-Iturbide, N. A.; Díaz-Eufracio, B. I.; Medina-Franco, J. L. In Silico ADME/Tox Profiling of Natural Products: A Focus on BIOFACQUIM. *ACS Omega* **2020**, *5*, 16076−16084.
(84) Lei, T.; Chen, F.; Liu, H.; Sun, H.; Kang, Y.; Li, D.; Li, Y.; Hou, T. ADMET Evaluation in Drug Discovery. Part 17: Development of Quantitative and Qualitative Prediction Models for Chemical-Induced Respiratory Toxicity. *Mol. Pharm.* **2017**, *14*, 2407−2421.
(85) Shen, K. H.; Hung, J. H.; Chang, C. W.; Weng, Y. T.; Wu, M. J.; Chen, P. S. Solasodine Inhibits Invasion of Human Lung Cancer Cell through Downregulation of MiR-21 and MMPs Expression. *Chem. Biol. Interact.* **2017**, *268*, 129−135.
(86) Liu, N.; Wang, X.; Wu, H.; Lv, X.; Xie, H.; Guo, Z.; Wang, J.; Dou, G.; Zhang, C.; Sun, M. Computational Study of Effective Matrix Metalloproteinase 9 (MMP9) Targeting Natural Inhibitors. *Aging* **2021**, *13*, 22867−22882.
(87) Mao, Y.; Feng, Q.; Zheng, P.; Yang, L.; Liu, T.; Xu, Y.; Zhu, D.; Chang, W.; Ji, M.; Ren, L.; Wei, Y.; He, G.; Xu, J. Low Tumor Purity Is Associated with Poor Prognosis, Heavy Mutation Burden, and Intense Immune Phenotype in Colon Cancer. *Cancer Manage. Res.* **2018**, *10*, 3569.
(88) Gong, Z.; Zhang, J.; Guo, W. Tumor Purity as a Prognosis and Immunotherapy Relevant Feature in Gastric Cancer. *Cancer Med.* **2020**, *9*, 9052−9063.
(89) Zhao, Y.; Zhang, X.; Yao, J. Comprehensive Analysis of PLOD Family Members in Low-Grade Gliomas Using Bioinformatics Methods. *PLoS One* **2021**, *16*, No. e0246097.
(90) Dai, Y.; Siemann, D. C-Src Is Required for Hypoxia-Induced Metastasis-Associated Functions in Prostate Cancer Cells. *OncoTargets Ther.* **2019**, *12*, 3519.
(91) Baek, J.-H.; Birchmeier, C.; Zenke, M.; Hieronymus, T. The HGF Receptor/Met Tyrosine Kinase Is a Key Regulator of Dendritic Cell Migration in Skin Immunity. *J. Immunol.* **2012**, *189*, 1699−1707.
(92) Yang, I.; Tihan, T.; Han, S. J.; Wrensch, M. R.; Wiencke, J.; Sughrue, M. E.; Parsa, A. T. CD8+ T-Cell Infiltrate in Newly Diagnosed Glioblastoma Is Associated with Long-Term Survival. *J. Clin. Neurosci.* **2010**, *17*, 1381.
(93) Kalaora, S.; Lee, J. S.; Barnea, E.; Levy, R.; Greenberg, P.; Alon, M.; Yagel, G.; Bar Eli, G.; Oren, R.; Peri, A.; Patkar, S.; Bitton, L.; Rosenberg, S. A.; Lotem, M.; Levin, Y.; Admon, A.; Ruppin, E.; Samuels, Y. Immunoproteasome Expression Is Associated with Better Prognosis and Response to Checkpoint Therapies in Melanoma. *Nat. Commun.* **2020**, *11*, 896.
(94) Han, J.; Jing, Y.; Han, F.; Sun, P. Comprehensive Analysis of Expression, Prognosis and Immune Infiltration for TIMPs in Glioblastoma. *BMC Neurol.* **2021**, *21*, 447.
(95) Xu, B. Prediction and Analysis of Hub Genes between Glioblastoma and Low-Grade Glioma Using Bioinformatics Analysis. *Medicine* **2021**, *100*, No. e23513.
(96) Tornillo, G.; Knowlson, C.; Kendrick, H.; Cooke, J.; Mirza, H.; Aurrekoetxea-Rodríguez, I.; Vivanco, M. d. M.; Buckley, N. E.; Grigoriadis, A.; Smalley, M. J. Dual Mechanisms of LYN Kinase Dysregulation Drive Aggressive Behavior in Breast Cancer Cells. *Cell Rep.* **2018**, *25*, 3674−3692.
(97) Liu, H.; Chen, D.; Liu, P.; Xu, S.; Lin, X.; Zeng, R. Secondary Analysis of Existing Microarray Data Reveals Potential Gene Drivers of Cutaneous Squamous Cell Carcinoma. *J. Cell. Physiol.* **2019**, *234*, 15270−15278.
(98) Edwards, L. A.; Woo, J.; Huxham, L. A.; Verreault, M.; Dragowska, W. H.; Chiu, G.; Rajput, A.; Kyle, A. H.; Kalra, J.; Yapp, D.; Yan, H.; Minchinton, A. I.; Huntsman, D.; Daynard, T.; Waterhouse, D. N.; Thiessen, B.; Dedhar, S.; Bally, M. B. Suppression of VEGF Secretion and Changes in Glioblastoma Multiforme Microenvironment by Inhibition of Integrin-Linked Kinase (ILK). *Mol. Cancer Ther.* **2008**, *7*, 59−70.
(99) Gazon, H.; Barbeau, B.; Mesnard, J. M.; Peloponese, J. M. Hijacking of the AP-1 Signaling Pathway during Development of ATL. *Front. Microbiol.* **2018**, *8*, 2686.
(100) Okura, H.; Golbourn, B. J.; Shahzad, U.; Agnihotri, S.; Sabha, N.; Krieger, J. R.; Figueiredo, C. A.; Chalil, A.; Landon-Brace, N.; Riemenschneider, A.; Arai, H.; Smith, C. A.; Xu, S.; Kaluz, S.; Marcus, A. I.; Van Meir, E. G.; Rutka, J. T. A Role for Activated Cdc42 in Glioblastoma Multiforme Invasion. *Oncotarget* **2016**, *7*, 56958.
(101) Zagzag, D.; Lukyanov, Y.; Lan, L.; Ali, M. A.; Esencay, M.; Mendez, O.; Yee, H.; Voura, E. B.; Newcomb, E. W. Hypoxia-Inducible Factor 1 and VEGF Upregulate CXCR4 in Glioblastoma: Implications for Angiogenesis and Glioma Cell Invasion. *Lab. Invest.* **2006**, *86*, 1221−1232.
(102) Amaral, R. F.; Geraldo, L. H. M.; Einicker-Lamas, M.; e Spohr, T. C. L. d. S.; Mendes, F.; Lima, F. R. S. Microglial Lysophosphatidic Acid Promotes Glioblastoma Proliferation and Migration via LPA1 Receptor. *J. Neurochem.* **2021**, *156*, 499−512.
(103) Harper, K.; Lavoie, R. R.; Charbonneau, M.; Brochu-Gaudreau, K.; Dubois, C. M. The Hypoxic Tumor Microenvironment Promotes Invadopodia Formation and Metastasis through LPA1 Receptor and EGFR Cooperation. *Mol. Cancer Res.* **2018**, *16*, 1601−1613.
(104) Quintero-Fabián, S.; Arreola, R.; Becerril-Villanueva, E.; Torres-Romero, J. C.; Arana-Argáez, V.; Lara-Riegos, J.; Ramírez-Camacho, M. A.; Alvarez-Sánchez, M. E. Role of Matrix Metalloproteinases in Angiogenesis and Cancer. *Front. Oncol.* **2019**, *9*, 1370.
(105) Kessenbrock, K.; Plaks, V.; Werb, Z. Matrix Metalloproteinases: Regulators of the Tumor Microenvironment. *Cell* **2010**, *141*, 52.
(106) Petrova, V.; Annicchiarico-Petruzzelli, M.; Melino, G.; Amelio, I. The Hypoxic Tumour Microenvironment. *Oncogenesis* **2018**, *7*, 10.
(107) Jana, S.; Singh, S. K. Identification of Selective MMP-9 Inhibitors through Multiple e-Pharmacophore, Ligand-Based Pharmacophore, Molecular Docking, and Density Functional Theory Approaches. *J. Biomol. Struct. Dyn.* **2019**, *37*, 944−965.
(108) Yamamoto, D.; Takai, S.; Jin, D.; Inagaki, S.; Tanaka, K.; Miyazaki, M. Molecular Mechanism of Imidapril for Cardiovascular Protection via Inhibition of MMP-9. *J. Mol. Cell. Cardiol.* **2007**, *43*, 670−676.
(109) Yamamoto, D.; Takai, S.; Hirahara, I.; Kusano, E. Captopril Directly Inhibits Matrix Metalloproteinase-2 Activity in Continuous Ambulatory Peritoneal Dialysis Therapy. *Clin. Chim. Acta* **2010**, *411*, 762−764.
(110) Kast, R. E.; Halatsch, M. E. Matrix Metalloproteinase-2 and -9 in Glioblastoma: A Trio of Old Drugs—Captopril, Disulfiram and Nelfinavir—Are Inhibitors with Potential as Adjunctive Treatments in Glioblastoma. *Arch. Med. Res.* **2012**, *43*, 243−247.
(111) Lastakchi, S.; Olaloko, M. K.; McConville, C. A Potential New Treatment for High-Grade Glioma: A Study Assessing Repurposed Drug Combinations against Patient-Derived High-Grade Glioma Cells. *Cancers* **2022**, *14*, 2602.
(112) Jiang, Q. W.; Chen, M. W.; Cheng, K. J.; Yu, P. Z.; Wei, X.; Shi, Z. Therapeutic Potential of Steroidal Alkaloids in Cancer and Other Diseases. *Med. Res. Rev.* **2016**, *36*, 119−143.
(113) Jiang, G.; Zhang, L.; Wang, J.; Zhou, H. Baicalein Induces the Apoptosis of U251 Glioblastoma Cell Lines via the NF-KB-P65-Mediated Mechanism Baicalein Induces the Apoptosis of U251 Glioblastoma Cell Lines via the NF-KB-P65-Mediated Mechanism. *Anim. Cell Syst.* **2016**, *20*, 296.

https://doi.org/10.1021/acsomega.3c00441
ACS Omega 2023, 8, 10565−10590

(114) Zhai, K.; Mazurakova, A.; Koklesova, L.; Kubatka, P.; Büsselberg, D. Flavonoids Synergistically Enhance the Anti-Glioblastoma Effects of Chemotherapeutic Drugs. *Biomolecules* **2021**, *11*, 1841.
(115) Xue, W.; Wang, P.; Tu, G.; Yang, F.; Zheng, G.; Li, X.; Li, X.; Chen, Y.; Yao, X.; Zhu, F. Computational Identification of the Binding Mechanism of a Triple Reuptake Inhibitor Amitifadine for the Treatment of Major Depressive Disorder. *Phys. Chem. Chem. Phys.* **2018**, *20*, 6606−6616.
(116) Khanal, P.; Dey, Y. N.; Patil, R.; Chikhale, R.; Wanjari, M. M.; Gurav, S. S.; Patil, B. M.; Srivastava, B.; Gaidhani, S. N. Combination of System Biology to Probe the Anti-Viral Activity of Andrographolide and Its Derivative against COVID-19. *RSC Adv.* **2021**, *11*, 5065−5079.
(117) Awale, S.; Miyamoto, T.; Linn, T. Z.; Li, F.; Win, N. N.; Tezuka, Y.; Esumi, H.; Kadota, S. Cytotoxic Constituents of Soymida Febrifuga from Myanmar. *J. Nat. Prod.* **2009**, *72*, 1631−1636.
(118) Sowmyya, T.; Vijaya Lakshmi, G. Antimicrobial and Catalytic Potential of Soymida Febrifuga Aqueous Fruit Extract-Engineered Silver Nanoparticles. *Bionanoscience* **2018**, *8*, 179−195.
(119) Lim, M.; Xia, Y.; Bettegowda, C.; Weller, M. Current State of Immunotherapy for Glioblastoma. *Nat. Rev. Clin. Oncol.* **2018**, *15*, 422−442.
(120) Lee, Y.-L.; Cheng, W.-E.; Chen, S.-C.; Chen, C.; Shih, C.-M. The Effects of Hypoxia on the Expression of MMP-2, MMP-9 in Human Lung Adenocarcinoma A549 Cells. *Eur. Respir. J.* **2014**, *44*, P2699.
(121) Bauer, A. T.; Bürgers, H. F.; Rabie, T.; Marti, H. H. Matrix Metalloproteinase-9 Mediates Hypoxia-Induced Vascular Leakage in the Brain via Tight Junction Rearrangement. *J. Cerebr. Blood Flow Metabol.* **2010**, *30*, 837.

https://doi.org/10.1021/acsomega.3c00441
ACS Omega 2023, 8, 10565−10590

frontiers | Frontiers in Cell and Developmental Biology

TYPE Original Research
PUBLISHED 19 July 2023
DOI 10.3389/fcell.2023.1236271

Check for updates

OPEN ACCESS

EDITED BY
Saleha Anwar,
Jamia Hamdard University, India

REVIEWED BY
Manzar Alam,
University of Texas Southwestern Medical Center, United States
Rakesh Kumar,
Eunice Kennedy Shriver National Institute of Child Health and Human Development (NIH), United States

*CORRESPONDENCE
Pravir Kumar,
pravirkumar@dtu.ac.in

RECEIVED 07 June 2023
ACCEPTED 23 June 2023
PUBLISHED 19 July 2023

CITATION
Kumari S and Kumar P (2023), Identification and characterization of putative biomarkers and therapeutic axis in Glioblastoma multiforme microenvironment. *Front. Cell Dev. Biol.* 11:1236271. doi: 10.3389/fcell.2023.1236271

COPYRIGHT
© 2023 Kumari and Kumar. This is an open-access article distributed under the terms of the Creative Commons Attribution License (CC BY). The use, distribution or reproduction in other forums is permitted, provided the original author(s) and the copyright owner(s) are credited and that the original publication in this journal is cited, in accordance with accepted academic practice. No use, distribution or reproduction is permitted which does not comply with these terms.

Identification and characterization of putative biomarkers and therapeutic axis in Glioblastoma multiforme microenvironment

Smita Kumari and Pravir Kumar *

Molecular Neuroscience and Functional Genomics Laboratory, Department of Biotechnology, Delhi Technological University, Delhi, India

Non-cellular secretory components, including chemokines, cytokines, and growth factors in the tumor microenvironment, are often dysregulated, impacting tumorigenesis in Glioblastoma multiforme (GBM) microenvironment, where the prognostic significance of the current treatment remains unsatisfactory. Recent studies have demonstrated the potential of post-translational modifications (PTM) and their respective enzymes, such as acetylation and ubiquitination in GBM etiology through modulating signaling events. However, the relationship between non-cellular secretory components and post-translational modifications will create a research void in GBM therapeutics. Therefore, we aim to bridge the gap between non-cellular secretory components and PTM modifications through machine learning and computational biology approaches. Herein, we highlighted the importance of BMP1, CTSB, LOX, LOXL1, PLOD1, MMP9, SERPINE1, and SERPING1 in GBM etiology. Further, we demonstrated the positive relationship between the E2 conjugating enzymes (Ube2E1, Ube2H, Ube2J2, Ube2C, Ube2J2, and Ube2S), E3 ligases (VHL and GNB2L1) and substrate (HIF1A). Additionally, we reported the novel HAT1-induced acetylation sites of Ube2S (K211) and Ube2H (K8, K52). Structural and functional characterization of Ube2S (8) and Ube2H (1) have identified their association with protein kinases. Lastly, our results found a putative therapeutic axis HAT1-Ube2S(K211)-GNB2L1-HIF1A and potential predictive biomarkers (CTSB, HAT1, Ube2H, VHL, and GNB2L1) that play a critical role in GBM pathogenesis.

KEYWORDS

non-cellular secretory components, computational biology, E2 conjugating enzymes, acetylation, Glioblastoma multiforme, tumor microenvironment, protein kinases

Highlights

- BMP1, CTSB, LOX, LOXL1, PLOD1, MMP9, SERPINE1, and SERPING1 are linked with poor prognosis in GBM patients.
- CTSB, HAT1, Ube2H, VHL, and GNB2L1 are predictive markers for GBM therapies.
- The poor prognostic markers BMP1, CTSB, LOX, LOXL1, PLOD1, and SERPINE1 were positively linked with HIF1A.
- Ube2C (18, K33); Ube2E1 (K43); Ube2H (K8, K52); Ube2J2 (K64, K88); Ube2S (K198, K210, K211, K215, K216) as putative acetylated sites.
- Ube2H (K8, K52) and Ube2S (K211) are associated with overexpressed HAT1 enzymes in GBM.
- HAT1-Ube2S(K211)-GNB2L1-HIF1A-BMP1/CTSB/LOX/LOXL1/PLOD1/SERPINE1 as a novel therapeutic axis in GBM.

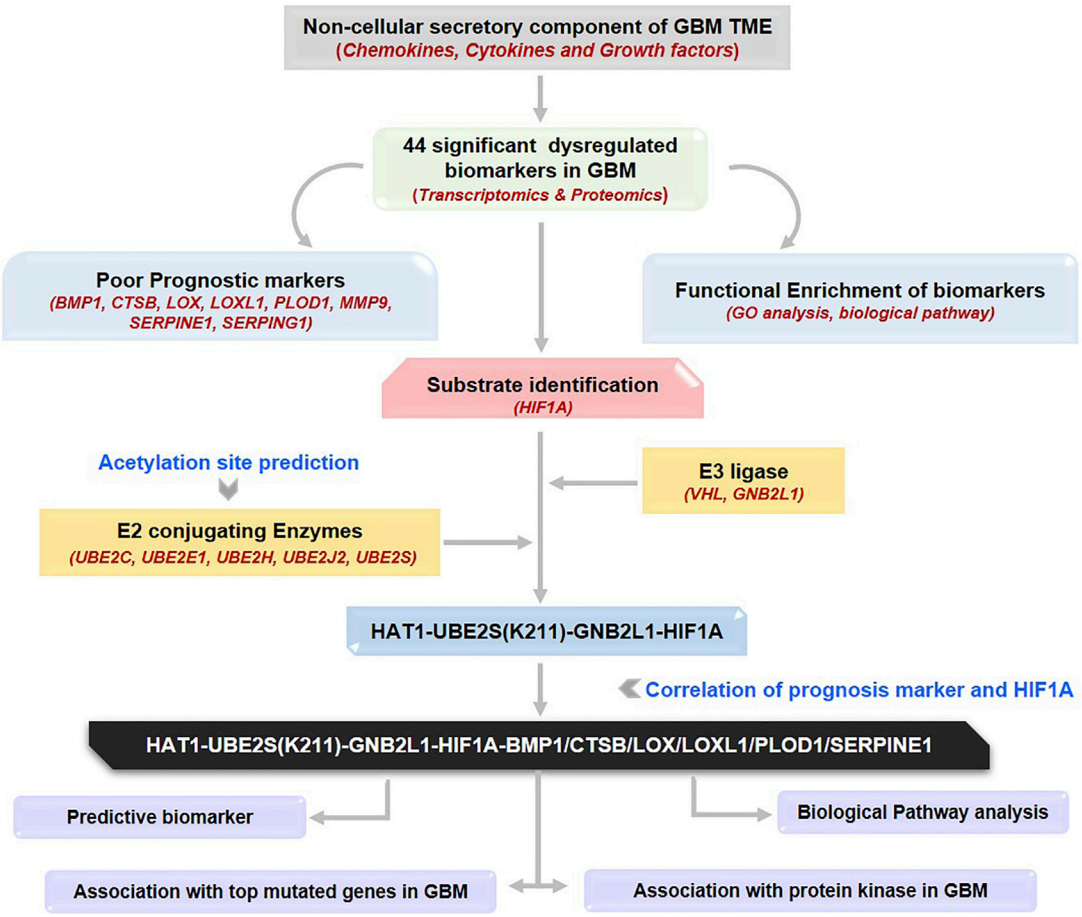

GRAPHICAL ABSTRACT
The workflow illustrates the process of identification of a novel therapeutic axis for targeting the GBM microenvironment. GBM: Glioblastoma multiforme, TME: Tumor microenvironment.

1 Introduction

Glioblastoma multiforme (*GBM*) is the most prevalent and fatal brain tumor with a poor prognosis. The clinical prognosis is still lacking despite several approved therapies for GBM, including surgery, radiation, and chemotherapy (Miller et al., 2021). The possible causes are the extensively invasive nature of GBM cells, the chemo- and radio-resistance, the high degree of vascularization, heterogeneity, and reduction of chemotherapeutic drugs effusion due to the blood-brain barrier (BBB), and heterogeneity of tumor microenvironment (TME). Further, the extracellular matrix (ECM) structural proteins are among the non-cellular components of the TME that are released by tumor or stromal cells or extravasated from the intravascular compartments other than cytokines, chemokines, and growth factors (Patel et al., 2018). Additionally, ECM structural proteins impact the development of all blood cells and other cells that support the body's inflammatory and immunological reactions, which promote anti-cancer behavior (Baghban et al., 2020). The use of non-cellular secretory components as possible treatment targets and biomarker tools is now being investigated in several pre-clinical and clinical studies (Bridge et al., 2018; Liu C. et al., 2021). Cytokine expression patterns in GBM are distinctive, and aberrations in cytokine expression have been linked to gliomagenesis. The complex cytokine network in the diverse microenvironment facilitates interactions between the tumor cells, healthy brain cells, immune cells, and stem cells within the heterogeneous milieu of the GBM (Zhu et al., 2012). In addition, chemokines recruit different immune cell populations in TME by binding with their receptors. For instance, microglia cells implicated in their recruitment at the site of inflammation possess elevated amounts of CCR1 expression. These affect tumor growth, metastasis, the transition from low to high-grade gliomas, and treatment outcomes (Zeren et al., 2023). Another study demonstrates that the recurrence of GBM pathogenicity occurs when neural stem cells crosstalk with microglial cells (Dai et al., 2023). Moreover, studies have shown that post-translational modifications (PTMs), namely, methylation, acetylation, glycosylation, and ubiquitination of chemokines and cytokines, influence biological activities, inflammatory responses, and inflammasome-dependent innate immune responses through modifying the protein stability, structure,

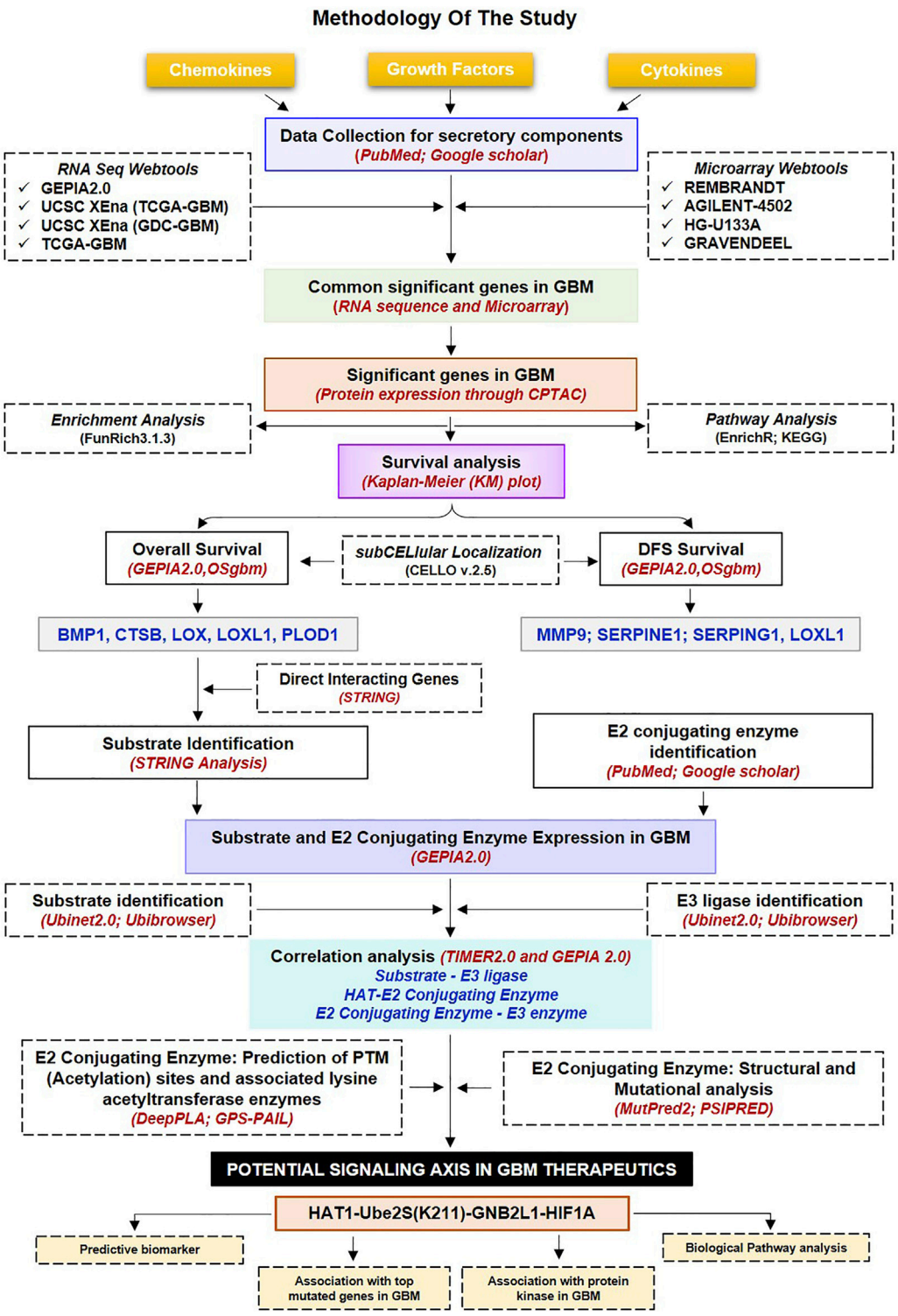

FIGURE 1
Methodology used in the current study: Workflow and steps considered along with the datasets collected and processed to identify prognostic and predictive markers in GBM. The expression of non-cellular secretory components (cytokines, chemokines, and growth factors) was examined in GBM transcriptome and proteomic data before the Kaplain-Meir plot was used to find prognostic markers. In addition, a common protein has been found that is directly associated with prognostic indicators; of these, two have the ability to function as substrates in the UPS system, and only HIF1A was elevated in GBM. Additionally, putative E3 ligases and E2s that are linked to HIF1A have been found. Additionally, a correlation study was done between prognostic markers, HIF1A, E3 ligase, E2s, and HAT enzymes. Further, a potential acetylation site on the lysine residues of E2s was found. The figure highlights the involvement of the acetylation mechanism, E2 conjugating enzymes, and E3 ligase's finding novel therapeutic axis in GBM indication. Furthermore, a characterisation investigation of the suggested treatment axis was carried out. GBM: Glioblastoma Multiforme; E2s E2 conjugating enzymes, UPS: Ubiquitin proteasome systems.

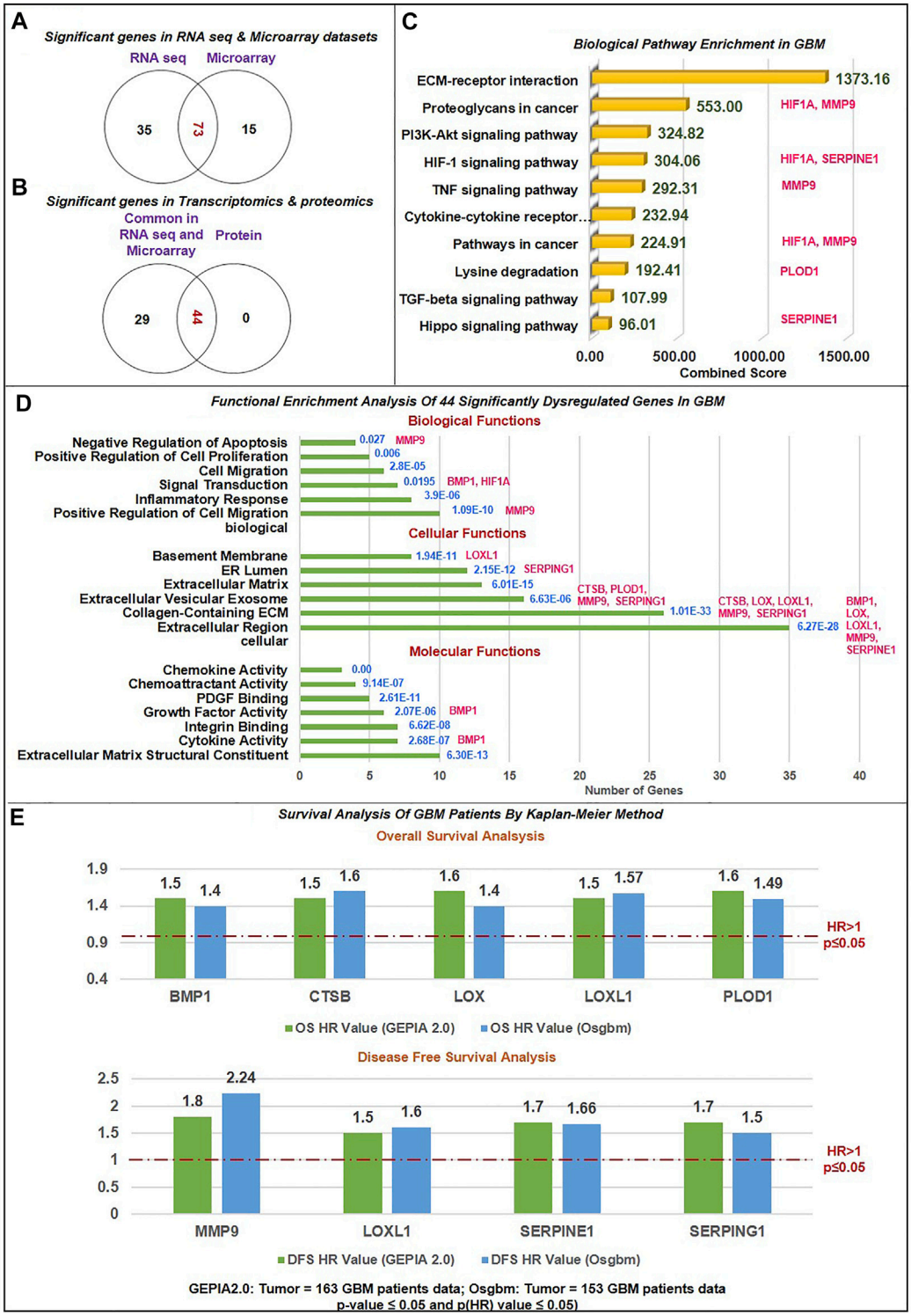

FIGURE 2
Data sorting and functional enrichment of significant non-cellular secretory biomarkers: **(A)** Venn diagram showing significant differentially expressed genes from transcriptomics data (RNAseq and Microarray) datasets. 73 genes overlap in RNA and microarray datasets **(B)** Venn diagram showing significant differentially expressed genes common in transcriptomics and proteomics datasets of GBM with the cut-off criteria of $|\log_2 FC| \geq 1.5$ and p-value≤ 0.05. 44 genes are common with protein datasets. **(C)** Biological pathway analysis using KEGG pathway: Among the top 10 biological pathways based on combined score* (written in green color) calculated by Enrichr tool are ECM-receptor, P13K-Akt, Hypoxia, TNF, TGF, and Hippo pathways with p-value≤ 0.05 in GBM. *Combined score is computed by taking the log of the value from the Fisher-exact test and multiplying that by the z-score of the deviation from the expected rank. Potential biomarkers identified in the current study have been mapped in front of each pathway. **(D)** Gene ontology (GO) analysis contains three sub-ontologies: molecular function, cellular components, and biological process associated with 44 biomarkers. Molecular function and cellular components showed maximum numbers of biomarkers involved in ECM structural constitute and

(*Continued*)

FIGURE 2 (Continued)
localized extracellular region. At the same time, top-ranked biological processes are extracellular matrix organization, cell migration, inflammation, response to hypoxia, signal transduction, and angiogenesis. Blue text showing the *p*-value of this analysis. Potential biomarkers identified in the current study have been mapped in front of each bar of the graph. **(E)** Survival Analysis of GBM Patients by Kaplan-Meier Method: The Cox proportional Hazard ratio (HR) was plotted against prognostic markers. GEPIA and Osgbm perform overall survival (OS) or disease-free survival (DFS) analysis based on gene expression. It uses the Log-rank test and the Mantel-Cox test for the hypothesis test. Threshold HR value > 1 signifies poor prognostic markers, and HR < 1 represents good prognostic markers. Based on OS analysis over expression of BMP1, CTSB, LOX, LOXL1and PLOD1 and DFS overexpression of MMP9, LOXL1, SERPINE1, and SERPING1 were significantly associated with poor prognosis in GBM. *Green bar color*: Data from GEPIA2.0 webtool; *Blue bar color*: Data from Osgbm webtool.

and sequence (Liu J. et al., 2016; Vanheule et al., 2018). A recent study by McCornack et al. (2023) discussed the significance of histone acetylation and methylation along with the consequences of targeted suppression of these enzymes by therapy in GBM (McCornack et al., 2023). Moreover, another study mentioned addressed the crucial role of histone acetylation in determining cell fate (Liu et al., 2023). Further, the exploration of new therapeutic interventions requires a thorough understanding of pathways relevant to GBM (Gallego-Perez et al., 2016). Additionally, protein kinases serve a crucial role in the signaling processes that regulate the traits of malignant cells, thereby making them valuable targets for therapeutic intervention in the management of cancer through the uptake of glucose, signaling modulation, epigenetic modifications, and progression of the cell cycle (Pang et al., 2022). Moreover, a variety of non-cellular secretory components of TME, including hormones, growth factors, chemokines, and cytokines bind to receptor tyrosine kinase and initiate downstream signaling, such as MAPK, PI3K/Ras that results in the proliferation and survival of tumor cells (Alexandru et al., 2020). EGFR signaling crosstalk with other major oncogenic signaling cascades, such as PI3K/protein kinase B (Akt)/mTOR pathway and MAPK pathway (Ramaiah and Kumar, 2021). However, in various cancers, protein kinase also controls TME and its constituent components. For example, in GBM tumor cells, IL-1β induces an HIF1A/IL-1β autocrine loop via activating Wnt-1 and RAS, which both contribute to the increase of HIF-1A (Chen et al., 2022). In contrast, IL-1β also stimulates the p38 MAPK-activated protein kinase 2-human antigen R (HuR), TLR-4, and other inflammatory-associated signaling pathways, which considerably enhance the levels of IL-6 and IL-8 in GBM tumor cells, eventually leading to an inflammatory TME in support of GBM invasion and growth (Gurgis et al., 2015). In addition, Cytokines, such as CCL5, was associated with intracellular calcium elevation. The activation of Akt and Ca^{2+}/calmodulin-dependent protein kinase II (CaMKII) in GBM cells controlled the migratory and invasive activities (Yu-Ju Wu et al., 2020). Further, Tyrosine kinase inhibitors (TKI) and other kinase inhibitors (such as SI113) alone or in combination with other drugs/therapy have the potential to manage GBM by overcoming limitations such as BBB penetration, adaptation to altered signaling pathways, and heterogeneity of GBM cells (Alexandru et al., 2020) (Kim and Ko, 2020).

Moreover, histone acetyltransferases (HATs), besides histones, acetylates a variety of non-histone substrates, and thus, referred to as lysine acetyltransferases that play an essential function in normal and malignant hematopoiesis (Sun et al., 2015). Recent studies demonstrated that abnormally high histone acetylation levels could trigger chromatin-based mechanisms that promote tumorigenesis and malignant transformation. Further, it is interesting to note that most acetylated non-histone proteins are essential for immunological processes, tumorigenesis, and cancer cell growth (Spange et al., 2009). Evidence that lysine acetylation modification affects the lysosomal clearance of specific substrates and proteasomal degradation by either inhibiting or enhancing polyubiquitination (Narita et al., 2019). Additionally, studies have found that the UPS system degrades HIF1A after interacting with von Hippel–Lindau protein (pVHL) under normoxia, mediating its ubiquitination. For instance, Jeong et al. (2002) found that acetylation at specific lysine residues of HIF1A enhances its interaction with pVHL and its subsequent ubiquitination and degradation (Jeong et al., 2002). Likewise, acetylated retinoblastoma (Rb) recruits MDM2, an E3 ligase, and mutation in its acetylation hotspots is linked with an increased risk of breast cancer (Ullah et al., 2022). Acetylation has been studied extensively in proteosomes, Ub, E1, and E3 ligase, but few have in E2s.

Hence, the current study was conducted to understand better how acetylation affects E2s, which will fill the gap between UPS and acetylation modification and its impact on microenvironmental secretory protein regulations. Herein, we aim to identify novel therapeutic targets in GBM, including HATs, E1, E2s, and E3 ligases and substrates, as well as possible acetylation sites on lysine residues of E2 conjugating enzymes (E2s). We also systematically investigate the prognostic and predictive relevance of non-cellular secretory elements, such as chemokines, cytokines, and growth factors in GBM, and offer a model for clinical diagnosis. In addition, we have also established the correlation between biomarkers and dysregulated protein kinases in GBM. For the first time, we have looked at the involvement of E2s and how PTM, particularly acetylation, affects these enzymes. In typically, researchers always target substrate or E3 ligase. Figure 1 provides a quick overview of our analytical methodology, which adheres to the norms in bioinformatics investigations. We investigated the wide-ranging functions of non-cellular secretory components in the GBM microenvironment using the cancer genome atlas (TCGA) data. Hence, in-depth information about the expression of the whole family of secretory components and insights into the

role of acetylation modification in UPS systems in GBM were provided by the study for the first time.

2 Material and methods

2.1 Data collection and expression profiling of non-cellular secretory components

The data for 306 non-cellular secretory components, including chemokines, cytokines, and growth factors, were extracted from PubMed, Google Scholar, and Scopus. Chemokines, cytokines, and growth factors were expressed differently in GBM patients when compared to normal tissue utilizing several web servers that included GBM patients' transcriptomics data such as RNA sequencing data [(Gene Expression Profiling Interactive Analysis (GEPIA2.0, http://gepia.cancer-pku.cn/index.html), UCSC Xena **R2Q6** (https://xena.ucsc.edu/), GlioVis-TCGA(http://gliovis.bioinfo.cnio.es/)] and microarray data [GlioVis-REMBRANDT, GlioVis-AGILENT, GlioVis-HG-U133, and GlioVis-GRAVENDEEL] and proteomics data such as Osppc (https://bioinfo.henu.edu.cn/Protein/OSppc.html) (Gravendeel et al., 2009; Madhavan et al., 2009; Bowman et al., 2017; Tang et al., 2019; Goldman et al., 2020; OSppc, 2022). GEPIA2.0 and UCSC XENA compare TCGA and GDC tumor samples with matched Genotype-Tissue Expression (GTEx) standard samples. Venn analysis was performed using Venny2.1 (https://bioinfogp.cnb.csic.es/tools/venny/) to identify common DEGs from transcriptomics (RNA sequences and microarray) and proteomics data (CPTAC).

2.2 Gene-set enrichment and pathway analysis of differentially regulated proteomics signatures

Functional enrichment analysis of the Kyoto Encyclopaedia of Genes (KEGG) pathways and gene ontologies (GOs) of candidate DEGs were determined through a FunRich tool (version 3.1.3) (http://www.funrich.org/) (Pathan et al., 2015) and Enrichr server (https://amp.pharm.mssm.edu/Enrichr) (Chen et al., 2013; Kuleshov et al., 2016). These tools identify and prioritize the essential genes related to GBM, followed by exploring biological pathways linked with them. A p-value ≤ 0.05 was deemed significant for GO analysis and route analysis statistical evaluation, and the fold-enrichment value was considered.

2.3 Analysis of prognostic relevance of identified signatures and their subcellular localization

To assess the prognostic relevance of DEGs, we performed Kaplan-Meier (KM) plots to examine the overall survival (OS) and disease-free survival (DFS) of the GBM cohorts through web servers such as GEPIA2.0 and OSgbm (http://bioinfo.henu.edu.cn/GBM/GBMList.jsp.) (Dong et al., 2020). OSgbm web server includes 684 samples with transcriptome profiles and clinical information from TCGA, Gene Expression Omnibus (GEO), and Chinese Glioma Genome Atlas (CGGA). We used the median expression as the expression threshold to divide patient samples into high- and low-expression groups for survival analyses of differentially expressed genes between GBM cohorts, along with the hazard ratio (HR), 95% confidence interval (CI), and log-rank test p-value. The Cox proportional hazard regression model calculated all HRs based on a high vs. low comparison. In addition, CELLO v.2.5: subCELlular LOcalization predictor (http://cello.life.nctu.edu.tw/) was used for predicting subcellular localization of biomarkers.

2.4 Identification of potential E2 conjugating enzyme, E3 Ligase, and substrate in GBM

E2s data was assembled through the Ubiquitin and Ubiquitin-like Conjugation Database (UUCD) (http://uucd.biocuckoo.org) (Gao et al., 2013). In addition, we collated human E3 ligase enzyme from four distinct sources UUCD databases, Database of Human E3 Ubiquitin Ligases (https://esbl.nhlbi.nih.gov/Databases/KSBP2/Targets/Lists/E3-ligases/), Cell Signaling Incorporated Database (http://www.cellsignal.com/common/content/content.jsp?id=science-tables-ubiquitin), and UbiNet 2.0 (https://awi.cuhk.edu.cn/~ubinet/index.php) (Li et al., 2021) database. Moreover, to identify substrate associated with E3 ligase, we have explored STRING (https://string-db.org/) (Szklarczyk et al., 2021) webtool to perform protein-protein interactions based on experimental data and >0.400 confidence score, UbiNeT2.0 and Ubibrowser 2.0 (http://ubibrowser.ncpsb.org.cn) (Wang et al., 2022).

2.5 Correlation study between a substrate, E2 conjugating enzyme, and E3 ligase

Spearman's correlation coefficient approach was used to investigate the correlation between two proteins in GBM samples using two web tools, GEPIA2.0 and TIMER2.0 (http://timer.cistrome.org/) (Li et al., 2020). GEPIA2.0 provides pair-wise gene correlation analysis of a given set of TCGA and/or GTEx expression data. In addition, TIMER2.0 Modules examine associations between gene expression and tumor features in TCGA. We have also performed a purity adjustment. We have studied the correlation between a) biomarker substrate with E3 ligase, and b) E2s with E3 ligase and HAT enzymes. Proteins with significant positive correlation were selected for further studies.

2.6 Prediction of Lysine signature for acetylation and associated HATs enzymes

Two PTM prediction webservers based on deep learning methods, such as Deep-PLA (http://deeppla.cancerbio.info) (Yu K. et al., 2020) and GPS-PAIL 2.0 (http://pail.biocuckoo.org/) (Deng et al., 2016), were used to predict acetylation sites on internal lysine residues along with seven HATs enzymes, including CREBBP, EP300, HAT1, KAT2A, KAT2B, KAT5 and KAT8. The technique predicts acetylation sites based on the idea

that various HATs have unique sequence specificities for the substrate changes. GPS-PAIL trains a Group-Based Prediction System previously developed method to create a computational model for each HAT enzyme.

2.7 Structural analysis of selected E2 conjugating enzyme

2.7.1 Prediction of secondary structure

PTM affects the secondary structure of the protein, which governs its biological functions. PSIPRED: protein structure analysis workbench (http://bioinf.cs.ucl.ac.uk/psipred/) (Buchan and Jones, 2019) was used to predict the structural selectivity of lysine acetylation sites. Subsequently, the relationship between the protein's secondary structure, fold recognition, and its corresponding acetylating sites was established. The output result was classified into three categories such as coiled, helix, and strand.

2.7.2 Protein intrinsic disorder prediction

The FASTA sequence of the protein was procured from the Uniport (https://www.uniprot.org/) (Bateman et al., 2017) database. DISOPRED3 (http://bioinf.cs.ucl.ac.uk/disopred) predicts structural order and disorder regions along with protein binding sites within disordered regions using a SVM that examines patterns of evolutionary sequence conservation, positional information, and amino acid composition of putative disordered regions. As analyzed from the output, the extracted data were separated into two categories: ordered and disordered regions.

2.8 Mutational analysis of Lysine modification

The functional impact of lysine mutations was investigated with the use of web applications such as PMut (http://mmb.irbbarcelona.org/PMut/) (López-Ferrando et al., 2017), SNAP2 (https://rostlab.org/services/snap/) (Hecht et al., 2015), Polymorphism Phenotyping v2 (PolyPhen2) (http://genetics.bwh.harvard.edu/pph2/) (Adzhubei et al., 2010), and MutPred2 (http://mutpred.mutdb.org/index.html) (Pejaver et al., 2020). All these tools require protein sequences in the FASTA format and a list of amino acid substitutions. The output results were computed numerically, and the combined score of the four web tools was determined. If a mutation's confidence score is ≥2.5, referred to as a threshold value, the mutation is considered disease sensitive. The basic, charged lysine (K) residue was changed into glutamine (Q), leucine (L), glutamate (E), and arginine (R). Additionally, the software MutPred2 was employed to forecast the physical impact of a lysine mutation on acetylation. The impacted sites were divided into two groups based on whether neighbouring sites gained or lost functionality.

2.9 Characterization of Therapeutic axis

2.9.1 ROC plotter: predictive marker identification

ROC plotter-an online ROC analysis tool (https://www.rocplot.org/) (Menyhárt et al., 2021), was employed to comprehend the association between gene expression and therapeutic response using transcriptomic level data from TCGA datasets of GBM and other cancer. This tool uses a JetSet probe to select the optimal microarray probe representing a gene. The package 'ROC' was used to calculate the area under the curve (AUC). The integrated database comprises 454 GBM patients from 3 independent datasets and 10103 genes. Patients were categorized as responders/non-responders based on their survival status at 16 months post-surgery.

2.9.2 Expression response to top mutated gene in GBM

Literature was used to find the top 10 mutated genes in GBM. "Gene_Mutation" module of TIMER2.0 was used to compare the differential gene expression with different mutation statuses of top mutated genes (such as PTEN, TP53, EGFR, PIK3R1, PIK3CA, NF1, RB1, IDH1, PTPRD, and ERBB2) of GBM.

2.9.3 Correlation with protein kinase protein GBM

KinMap, (http://www.kinhub.org/kinmap/), a user-friendly web interface for the human genome (the "kinome") was explored to retrieve 536 human protein kinases including eight typical groups (AGC, CAMK, CK1, CMGC, STE, TK, TKL, Other) and 13 atypical families (Eid et al., 2017). Using the GEPIA2.0 tool, the expression of each kinase was examined in GBM patient tumor samples. Network analysis was employed to study the correlation between the putative 'therapeutic axis' proteins and significantly dysregulated kinases.

2.10 Statistically analysis

In GEPIA2.0, we used the ANOVA statistical method for differential gene expression analysis, selected $\log_2$ (TPM +1) transformed expression data for plotting, TCGA tumor compared to TCGA normal and GTEx normal for matched normal data in plotting, $|\log_2 FC|$ cut-off of 1.5, and a q-value cut-off of 0.05. For survival analysis, it uses the Mantel-Cox test for the hypothesis test. OSppc used Mann-Whitney Wilcoxon tests to calculate the significant difference between proteomics data of tumors and adjacent normal tissues. In the TIMER2.0 database analysis, partial Spearman's correlation (ρ) was applied. When Rho, $\rho > 0.1$, it indicated a correlation between the genes and immune cells. Red color signifies: Positive correlation (p-value <0.05, $\rho > 0$), blue color signifies: Negative correlation (p-value<0.05, $\rho > 0$), and grey color signify: non-significant (p-value >0.05).

3 Results and discussion

3.1 Expression of secretory components in GBM and normal tissue

The 306 non-cellular secretory components, including chemokines, cytokines, and growth-factor of TME, have been extracted from PubMed and Google Scholar. A total of

53 chemokines, including all 4 subfamilies CXC, CC, CX3C, and C (Gao et al., 2022), 253 cytokines and growth-factors including ILs, IFNs family, TNFs family, TGFs superfamily (BMP-like family, GDNFs family, TGF-β-like family), MMPs family, FGFs family, PDGFs family, VEGFs, TIMPs, prolactin, GCSFs, GMCSFs, were extracted. Firstly, we have studied the expression of chemokines, cytokines, and growth factors in GBM at transcriptomics and proteomics levels using a web tool based on TCGA data sets. RNA sequence data were analyzed using GEPIA2.0 (163 GBM tissue and 207 normal tissue, including GTEx normal tissue), UCSC Xena (154 GBM tissues and 5 Normal tissues), GlioVis-TCGA (156 GBM tissues and 4 Normal tissues), and microarray data were analyzed using GlioVis-REMBRANDT (225 GBM tissues and 28 Normal tissues), GlioVis-AGILENT (489 GBM and 10 normal tissues), GlioVis-HG-U133 (528 GBM tissues and 10 normal tissues), and GlioVis-GRAVENDEEL (117 GBM tissues and 8 normal tissues), and protein data from CPTAC, RPPA, and TCGA were analyzed using Osppc tool. We have used the Venny2.1.0 database to identify all non-cellular secreted components of TME that were significantly expressed in at least four RNA sequence data and microarray data. 73 genes were commonly expressed in RNA sequence and microarray data (Figure 2A). Afterward, the protein expression of these 73 genes was checked. A total of 44 biomarkers has significantly dysregulated expression (log_2FC score ≥1.5 and p-value ≤0.05), out of which 41 were upregulated and 3 downregulated in patients with GBM compared with its normal tissues (Figure 2B). Thus, the details expression pattern of 306 secretory components has been tabulated in Supplementary Information Supplementary Table S1, and 44 shortlisted biomarkers were tabulated in Table 1 (Description in Supplementary Table S2. Previous studies also support our observations. Out of 44, only 3 were chemokines in which CCL5 and CXCL16 were upregulated, whereas CX3CL1 was downregulated in GBM. A study by Dai et al., 2016 showed that CCL5 chemokines influence tumor progression through various mechanisms that directly affect cancer cell proliferation or indirectly regulate angiogenesis and recruitment of immune cells that promote tumor growth and metastasis (Dai et al., 2016; Takacs et al., 2021). In addition to tumors, tumor-associated cells such as CAF, EC, MSC, MDSC, and TAM generate CXCL16 and influence tumor-associated cells in glial tumors (Hattermann et al., 2013; Korbecki et al., 2021). Cytokines and growth factors have a pleiotropic role in influencing various biological functions, including immune response, inflammation, and cell-to-cell communication. Studies on GBM provide evidence to support our observation of cytokines. For instance, Frei et al., 2015 demonstrated that TGFβ acts as a critical molecule implicated in GBM malignancy (Frei et al., 2015). Other studies show the importance of IL-18 in cell migration, which is fatal and untreatable, and the mechanism through which GBM cells release ECM proteins like fibronectin and vitronectin, in turn, causes the surrounding normal brain microglia to secrete more IL-18 (Yeh et al., 2012; Kast, 2015).

A comprehensive investigation of TIMPs in GBM by Han et al. revealed that TIMP3 indirectly controls MMPs signaling and ECM remodeling (Han et al., 2021). Multiple hormonal and non-hormonal growth-stimulating agents are also present in GBM and can function as biomarkers (Dahlberg et al., 2022). Recent research has also emphasized the critical role played by these secretory components in the pathogenesis of GBM and the creation of the immune milieu through immunological regulation, which inhibits anti-tumor responses and promotes the growth of tumors (Yeo et al., 2021). Thus, our results further confirm these previous findings.

3.2 Functional enrichment and biological pathway analysis of biomarkers

We have performed functional enrichment analysis using the FunRich-functional enrichment analysis tool for (GO) and KEGG pathway enrichment analysis to investigate the role of 44 differential biomarkers in GBM. We selected only pathways that were involved in the pathogenesis of the GBM microenvironment and had a large number of genes with significant fold enrichment. We have also looked at how biomarkers are involved in the biological processes that lead to the pathology of GBM. According to the results of cellular components, the bulk of biomarkers is located in extracellular regions, the ECM, and extracellular vesicles (EVs). These data corroborate earlier findings that secretory components, which are located in the extracellular space of the microenvironment and have a variety of clinical implications, have the ability to function as biomarkers and potentially disrupt signaling pathways implicated in tumorigenesis (Liu C. et al., 2021). Cytokines are soluble factors released predominantly in soluble or EV-associated forms and are involved in cell-cell communications (Fitzgerald et al., 2018). Molecular function analysis showed that the maximum number of biomarkers were engaged in structural components of ECM, cytokines and chemoattractant activities, integrin binding, growth-factors activities, and Platelet-derived growth factor binding. Chemokines act as chemoattraction, which binds to G protein-coupled seven transmembrane cell surface receptors (GPCRs) and thus activates a cascade of signaling G proteins, PI3K, protein kinase C, phospholipase C, RAS, and MAPKs to mediate immune cells migration, activation, cell chemotaxis, invasion, production of mediators promoting angiogenesis, and transactivation of EGFR (Zhou J. et al., 2014). Studies showed that the expression of specific integrins is upregulated in both tumor cells and stromal cells in a TME. Integrins receptors bind to specific secretory components from TME, which regulate ECM detachment, migration, invasion, proliferation, and survival through PI3K-AKT signaling (Ellert-Miklaszewska et al., 2020).

Biological process analysis showed top six processes were ECM organization, cell migration, inflammatory response, response to hypoxia, and angiogenesis. Additionally, we used the Enrichr tool to examine the KEGG Pathway 2021. We studied the biological pathway causing the pathology of GBM. According to the tool's combined score, the top 10 biological pathways were ECM-receptor interaction, proteoglycans in cancer, PI3K-Akt signaling pathway, HIF1 signaling pathway, TNF signaling pathway, cytokine-cytokine receptor interaction, lysine degradation, TGF-β signaling pathway, and Hippo signaling pathway. Previous studies have found that activation of the HIF1A pathway is a common feature of gliomas and may explain the intense vascular hyperplasia often seen in GBM (Kaur et al., 2005; Domènech et al., 2021).

Similarly, TNF signaling enhances invasion in GBM and upregulates MEK-ERK signaling, NF-κB1, and STAT expression

TABLE 1 Transcriptomics and proteomics expression analysis of non-cellular secretary components in GBM patients samples compared with normal tissues.

Webtools		RNA sequence datasets				Microarray datasets				Protein expression	Molecular function
		GEPIA 2.0	*UCSC XEna*		*GLIOVIS*	*GLIOVIS*		*TCGA_GBM*		*CPTAC*	
		TCGA GBM_GTX	TCGA GBM	GDC TCGA GBA	TCGA RNA sequence	REMBRANDT	GRAVENDEEL	HG-U133A	AGILENT-4502A	Osppc	
Chemokine	CCL5										The CCL5/CCR5 axis regulates the infiltration, and interactions with, mesenchymal stem cells, which constitute niches
	CX3CL1										encourage pro-tumorigenic effects, angiogenesis
	CXCL16										employs the CXCR6 receptor to trigger glial progenitor cells to migrate and invade
Cytokines and Growth factors	ANGPT2										a Tie2 antagonistic ligand has been linked with a poor outcome in GBM patients
	BMP1										oncogenic role and is implicated in the invasion of GBM cells
	BMP7										enhance transmigration, migration, and invasion of GBM cells
	COL1A1										important ECM component that encourages invasion and tumor growth
	COL1A2										increase GBM cell invasion and proliferation
	COL3A1										promotes EMT and immune infiltration
	COL4A1										boosted cancer-related pathways, including cell cycle control and the JAK/STAT signaling pathway
	COL4A2										correlates with immune cell infiltration
	COL5A1										enhances tumor immune tolerance, which has a negative prognosis
	COL5A2										The outcome of LGG is negatively impacted by COL5A2 overexpression
	CTSB										immunosuppression, immune cell infiltration, and poor prognostic indicators
	HIF1A										Under high HIF1A expression, T-cell exhaustion-related gene expression levels and immune cell numbers increased
	IL-18										IL-18 produced by microglia causes GBM cell movement and encourages centrifugal migration
	LAMA4										GBM selectively secreted protein in CSF
	LAMA5										stimulates VEGF activity, which reduces invasion but promotes tumor development by increasing GBM cell adhesion to blood arteries

(Continued on following page)

10.3389/fcell.2023.1236271

TABLE 1 (*Continued*) Transcriptomics and proteomics expression analysis of non-cellular secretary components in GBM patients samples compared with normal tissues.

Webtools		RNA sequence datasets				Microarray datasets				Protein expression	Molecular function
		GEPIA 2.0	*UCSC XEna*		*GLIOVIS*	*GLIOVIS*		*TCGA_GBM*		*CPTAC*	
		TCGA GBM_GTX	TCGA GBM	GDC TCGA GBA	TCGA RNA sequence	REMBRANDT	GRAVENDEEL	HG-U133A	AGILENT-4502A	Osppc	
	LAMB1										The ERK/c-Jun Axis-Mediated Upregulation of LAMB1 Enables Gastric Cancer Progression and Motility
	LGALS3										relates to tumor risk and prognosis and results in treatment resistance
	LGALS9										Exosomal LGALS9 from GBM cells controls the growth of tumors by preventing the presentation of DC antigens and the activation of cytotoxic T cells
	LOX										regulates the expression of MMP2,9 and is involved in the proliferation
	LOXL1										interact with several antiapoptosis modulators (BAG2) to display antiapoptotic action
	LOXL3										associated with genomic stability, cell proliferation, and metastasis in GBM
	MMP14										involved in radiosensitivity, cell migration, and invasion
	MMP17										tumorigenesis
	MMP2										degradation of IV collagen, an important marker in glioma genesis
	MMP9										by virtue of their proteolytic action, degrades gelatin, collagens IV, and V in the ECM
	PLOD1										Promotes tumor via HSF1 signaling pathway
	PLOD2										influences both tumor progression and the immune microenvironment
	PLOD3										promotes tumor progression and poor prognosis
	PTGES2										not much studied in GBM. In breast cancer: high expression has an immunomodulatory role
	SDF2										overexpressed in breast cancer
	SDF4										overexpresses in pancreatic cancer
	SERPINE1										Influence cell-substrate adhesion and directional movement of GBM cells through TGFβ signaling
	SERPING1										produced primarily by monocytes and works by blocking the traditional complement system pathway
	SPP1										high SPP1 expression promotes the GSCs properties and radiation resistance and is correlated with poor prognosis of GBM

(Continued on following page)

10.3389/fcell.2023.1236271

TABLE 1 (*Continued*) Transcriptomics and proteomics expression analysis of non-cellular secretary components in GBM patients samples compared with normal tissues.

Webtools		RNA sequence datasets				Microarray datasets				Protein expression	Molecular function
		GEPIA 2.0	*UCSC XEna*		*GLIOVIS*	*GLIOVIS*		*TCGA_GBM*		*CPTAC*	
		TCGA GBM_GTX	TCGA GBM	GDC TCGA GBA	TCGA RNA sequence	REMBRANDT	GRAVENDEEL	HG-U133A	AGILENT-4502A	Osppc	
	TGFβ1										modulates temozolomide resistance in GBM
	TGFβ2										promote EMT
	TIMP1										transcriptional factor Sp1 binds to the promoter of TIMP1 and triggers its expression and immune infiltration in GBM.
	TIMP3										high TIMP3 expression correlated with better overall survival (OS) and disease-specific survival (DSS) in GBM patient
	TNFAIP6										promotes invasion and metastasis
	TNFAIP6										promotes invasion and metastasis
	VEGFA										GSCs secrete the pro-angiogenic VEGF-A factor in extracellular vesicles
Patient samples number used in the respective study											
TUMOR		**163**	**154**	**155**	**156**	**225**	**117**	**528**	**489**	**153**	
N0N-TUMOR		**207**	**5**	**5**	**4**	**28**	**8**	**10**	**10**	__	
Upregulated in GBM					$p \leq 0.001$		$p \leq 0.001$			$p \leq 0.05$	
Downregulated in GBM					$p \leq 0.001$		$p \leq 0.001$			$p \leq 0.05$	
Not significant in GBM				**p > 0.05**							

10.3389/fcell.2023.1236271

(Ramaswamy et al., 2019). In GBM, TNF secreted by the associated macrophages with the tumor encourages the activation of endothelial cells, which makes the patient resistant to anti-angiogenic treatments (Wei et al., 2021). Similar to increased PI3K-AKT activation, it has a distinct function in tumor growth but does not cause resistance to treatment (Langhans et al., 2017). There is mounting evidence that Hippo signaling has a role in a number of cancers, including glioma, breast, lung, and colon cancer. The concept that this route might represent a potential target opening the door for alternative medicines is supported by the fact that it is less studied in GBM and engaged in tumorigenesis and metastasis (Masliantsev et al., 2021). Our pathways analysis results also line up with previous findings (Ellert-Miklaszewska et al., 2020). Herein, through the top-mentioned molecular functions and biological pathways, we have demonstrated that the majority of the shortlisted secretory biomarkers were localized in extracellular space and were critical for tumorigenesis, migration, and invasion in the pathology of GBM. As a result, these signaling pathways have the potential to be further investigated in the context of GBM development and can be therapeutically addressed if we intend to target the GBM microenvironment in addition to the tumor cells. Figures 2C,D demonstrate all biological pathways and GO analysis of 44 biomarkers, respectively.

3.3 Relationship between biomarkers and survivals of GBM patients

To evaluate the relation between 44 significantly differentially expressed genes and the prognosis of GBM patients, GEPIA2.0 and OSgbm web tools were used for plotting KM plots for OS and DFS analysis. These tools use GBM data from TCGA. The data was analyzed in KM plot where curves were stratified by median signal expression (high vs. low expression group). The cox proportional HR and *p*-values are displayed on survival curves. A *p*-value ≤0.05 was considered statistically significant, HR > 1 was considered a poor prognostic, and HR < 1 was a good prognosis. Figure 2E and Supplementary Figure S1 illustrate the strong association of overexpression of bone morphogenetic *protein* 1 (BMP1), cathepsin B (CTSB), lysyl oxidase (LOX), procollagen-lysine,2-oxoglutarate 5-dioxygenase 1 (PLOD1) with poor OS (HR > 1 and p (HR) ≤ 0.05). CTSB proteases are essential in ECM degradation and are overexpressed in most human colon and other cancers. A recent study by Ma et al. (2022) also demonstrates that CTSB is a negative prognostic biomarker and biological pathway associated with immune suppression and inflammation in glioma (Ma et al., 2022). Studies have demonstrated that CTSB regulates several forms of cell death, such as apoptosis, necroptosis, autophagy, pyroptosis, and ferroptosis, and is associated with radio-resistance, tissue invasion, and metastasis of GBM (Ding et al., 2022). BMP1 (secreted metalloprotease of the astacin metalloproteinase family) recently emerged as a cancer-related protein in multiple cancer but is less explored in GBM. Signaling such as TGFβ involving BMP1 affects the proliferation and differentiation of glioma stem cells. According to the study by Xiao et al. (2019), increased expression of BMP1 reflects poor prognosis in clear cell renal cell carcinoma (Xiao et al., 2019). Similarly, we first time reported that BMP1 had poor OS in GBM patient samples. A study by Sachdeva et al., in 2019 showed that in the GBM microenvironment dysregulated BMP signaling via expression of p21 protein causes GSCs to enter a quiescent state, rather than developed into the differentiated astroglia cell (Sachdeva et al., 2019). In addition, a study showed that increased expression of LOX expression was strongly associated with the invasive features of malignant astrocytes. LOX is well recognized as secreted matrix-modifying enzyme. The key roles played by LOX include the regulation of gene expression, protein-lysine 6-oxidase activity, protein binding, and protein phosphorylation. It has an impact on cell cycle progression and apoptosis in GBM and can be exploited as a target for early detection and targeted treatment (Zhang P. et al., 2022; Zhang S.et al., 2022). Li et al. (2021) showed that ECM-related gene LOX correlated with poor OS in glioma patients (Li et al., 2022), including GBM (Tang et al., 2020) and gastric cancer (Zhu et al., 2021). Another investigation discovered a difference between Lysine oxidase-like 1 (LOXL1) and poor OS in GBM (Liu Z. et al., 2021). The antiapoptotic activity of LOXL1 is mediated via interactions with a variety of antiapoptotic modulators, including BAG2, and by Wnt/beta-catenin signaling (Yu H. et al., 2020). Our finding revealed that the upregulation of LOXL1 was accompanied by both poor OS and DFS. Moreover, PLOD1 encourages cross-linking in ECM molecules, enabling ECM structural stability and maturation. In a study by Wang et al. (2020), increased PLOD1 expression in glioma was linked with a worse prognosis (Wang et al., 2020). Significant overexpression of PLOD1 may encourage the growth and colony formation of U87 cells by triggering the HSF1 signaling pathway (Yuan et al., 2022) however, in hypoxic settings could stimulate invasiveness and the mesenchymal transition by inducing NF-κB signaling pathway (Wang et al., 2021). Secondly, our data demonstrated the overexpression of Matrix metallopeptidase 9 (MMP9), Serpin Family E Member 1 (SERPINE1), and serine protease inhibitor family G1 (SERPING1) linked with poor DFS (HR > 1 and p (HR)≤0.05) (Figure 2E and Supplementary Figure S2A). Our finding supported previous studies that the overexpression of MMP9 indicates a poor prognosis in glioma (Zhou et al., 2019). In the microenvironment GBM-secreted factors influence increased human brain vascular endothelial cell migration as well as levels of MMP-9 and CXCR4 which result in enhanced angiogenesis (De Oliveira Rosario et al., 2020). Indeed, Seker et al. (2019) research shows that poor patient survival in GBM is related to increased expression of SERPINE1 (Seker et al., n. d.). In hypoxic microenvironment condition, ROS promotes tumor progression, EMT in GBM through HIF1A-SERPINE1 signaling (Zhang et al., 2023). In another study, it was found out that low SERPING1 levels have been associated with poor DFS in prostate cancer (Peng et al., 2018) In contrast, our study reported a higher level of SERPING1 linked with poor DFS/prognosis in GBM. These results showed that BMP1, CTSB, LOX, LOXL1, MMP9, SERPINE1, and SERPING1 are poor prognostic indicators in GBM since they had HR > 1 and p (HR) ≤ 0.05. Jia et al. (2018) also showed that SERPINE1 and SERPING1link with poor prognosis in GBM (Jia et al., 2018).

Moreover, we have also used CELLO v.2.5: subCELlular LOcalization predictor for finding the localization of identified prognostic markers. Results in Figure 3A showed that BMP1, LOX, LOXL1, MMP9, SERPINE1, and SERPING1 localized in

A *Prediction of Protein Subcellular Localization*

Analysis Report of CELLO v.2.5 Predictor						
Genes Name	Extracellular	Cytoplasmic	Plasma Membrane	Mitochondrial	Lysosomal	Nuclear
BMP1	**2.368***	0.759	0.358	0.079	0.094	1.079
CTSB	0.243	0.009	0.007	0.009	**4.630***	0.033
LOX	**3.140***	0.039	0.102	0.109	0.211	1.068
LOXL1	**2.194***	0.113	0.377	0.097	0.153	1.485
PLOD1	0.386	**1.836***	0.369	0.549	0.595	0.299
MMP9	**2.820***	0.224	0.721	0.267	0.339	0.225
SERPINE1	**2.101***	0.554	0.604	0.753	0.084	0.167
SERPING1	**2.377***	0.523	0.218	0.151	0.044	1.404

B *Expression Analysis of E2 Conjugating Enzymes In GBM*

Category	Gene Name	RNA SEQ (TCGA-GBM)	Protein expression (CPTAC)
		GEPIA2.0	*Osppc*
E2 conjugating enzyme	Ube2A	*	*
	Ube2C	*	*
	Ube2D2	*	*
	Ube2D3	*	--
	Ube2E1	*	*
	Ube2H	*	*
	Ube2J1	*	*
	Ube2J2	*	*
	Ube2L6	*	*
	Ube2N	*	*
	Ube2QL1	*	--
	Ube2S	*	*
	Ube2T	*	ns

C *Correlation Study Analysis*

E3 ligase enzymes		VHL		GNB2L1/RACK1	
Substrate	Webtool	GEPIA2.0	TIMER2.0	GEPIA2.0	TIMER2.0
		Spearman's rho value (ρ)			
	HIF1A	0.27	0.176	0.2	0.081
E2 conjugating enzymes	*Ube2C*	0.31	0.138	0.53	0.4
	Ube2E1	0.33	0.279	0.19	0.122
	Ube2H	0.42	0.483	0.083	-0.033
	Ube2J2	0.42	0.303	0.53	0.335
	Ube2L6	-0.078	-0.209	-0.12	-0.177
	Ube2S	0.34	0.157	0.54	0.406

Substrate	HIF1A	
Prognostic Markers	GEPIA2.0	TIMER2.0
	Spearman's rho value (ρ)	
BMP1	0.33	0.231
CTSB	0.19	0.229
LOX	0.25	0.213
LOXL1	0.39	0.344
PLOD1	0.39	0.396
MMP9	0.11	0.056
SERPINE1	0.33	0.299
SERPING1	0.18	0.146

HATs enzymes	CREBBP		EP300		HAT1		KAT2A		KAT2B		KAT5	
Webtool	GEPIA2.0	TIMER2.0	GEPIA2.0	TIMER2.0	GEPIA2.0	TIMER2.0	GEPIA2.0	TIMER2.0	GEPIA2.0	TIMER2.0	GEPIA2.0	TIMER2.0
E2 conjugating Enzymes	Spearman's rho value (ρ)											
Ube2C	0.21	0.012	0.17	0.039	0.21	0.025	0.21	-0.082	-0.16	-0.391	0.23	-0.108
Ube2E1	0.03	-0.077	-0.042	-0.045	0.34	0.176	0.11	-0.126	0.26	0.144	0.21	0.006
Ube2H	0.66	0.668	0.64	0.062	0.38	0.403	0.22	0.138	0.36	0.292	0.38	0.288
Ube2J2	0.34	0.121	0.25	0.066	0.48	0.204	0.17	-0.079	0.13	-0.126	0.45	0.171
Ube2S	0.18	-0.032	0.18	0.045	0.15	0.19	0.2	-0.071	-0.027	-0.269	0.27	-0.068

Color code	
	Positive correlation (p<0.05, ρ>0)
	Negative correlation (p<0.05, ρ<0)
	Not significant (p>0.05)

FIGURE 3
(A) Prediction of Protein subcellular localization by cello online predictor: BMP1, LOX, LOXL1, MMP9, SERPINE1, and SERPING1 localized in majorly extracellular space. CTSB is majorly localized in lysosomes and PLOD1 in the cytoplasm, followed by extracellular space. **(B)** Expression analysis of E2 conjugating Enzymes (E2s). Out of 35 reported E2s in humans, at the mRNA level, only 13 were dysregulated (including 12 up and 1 downregulated); at the protein level, 10 were dysregulated (including 7 upregulated and 3 downregulated). **(C)** Correlation study analysis: E3 ligase, VHL, and GNB2L1 showed a significant positive correlation with substrate HIF1A and E2s. VHL showed a significant positive correlation between Ube2E1, Ube2H, and Ube2J2, while GNB2L1 showed a positive correlation with Ube2C, Ube2J2, and Ube2S. In addition, HIF1A positively correlates with poor prognosis markers such as BMP1, CTSB, LOX, LOXL1, PLOD1, and SERPINE1. Heatmap 3 showed a significant correlation between HAT enzymes and E2s. Results showed that Ube2H positively correlates with CREBBP, EP300, HAT1, KAT2B, and KAT5. Ube2S with HAT1, Ube2J2 with HAT1 and KAT5, and Ube2C negatively correlate with KAT2B.

TABLE 2 Expression analysis of substrate and its associated E3 ligase in GBM patients samples.

Substrate (STRING, Ubibrowser2.0, Ubinet2.0)	E3 ligase (UUCD, CST, UbiNet2.0)	Combined score (STRING)	Expression in GBM	
			Gene expression (GEPIA2.0)	Protein expression (Osppm)
BMP1	RMND5A	0.483		
HIF1A	EP300	0.999		
	GNB2L1	0.998		
	MDM2	0.997		
	PARK2	0.762		
	STUB1	0.81		
	TRAF6	0.72		
	VHL	0.999		
	FBXW7	0.664		
	SIAH1	0.43		
	SIAH2	0.543		
TNFRSF1B	TRAF1	0.761		
	TRAF2	0.881		
	ASB3	0.485		
	SMURF2	0.57		
Sample size	Tumor tissues		163	153
	Normal tissues		207	–

*Green gradient signifies: significantly overexpressed in GBM, patient's samples ($p < 0.05$).
*Red gradient signifies: significantly downregulated in GBM, patient's samples ($p < 0.05$).
*Combined score calculated by STRING, webtool based on experimentally determined interaction data.

extracellular space while PLOD1 localized majorly in cytoplasm followed by extracellular space and CTSB localized in lysosome followed by extracellular space. Studies have revealed a strong correlation between a protein's subcellular location and function. Sequencing similarity is helpful in predicting subcellular localization for sequences containing >30% sequence identity.

3.4 Identification of HIF1A as the substrate from dysregulated biomarkers and its associated E3 ligase

To find the therapeutic axis to understand ubiquitination systems in GBM, we have focused on finding the possible substrate from the list of 44 differentially expressed biomarkers. We have used the STRING database to find the experimentally validated (confidence score>0.400) substrate and correspondence E3 ligase. The E3 ligase list was created by combining E3 ligase protein from four different sources: the Human E3 ligase database, CST, UUCD, and UbiNet 2.0. This list was used to make an individual PPI network with every 44 biomarkers in the STRING database. This study's results showed that BMP1, HIF1A, and TNFRSF1B are the biomarkers that also act as a substrate for E3 ligase and are involved in the Ubiquitination pathway. Results showed E3 ligase correspondence to substrate a) BMP1 was RMND5A, b) HIF1A were EP300, GNB2L1, MDM2, PARK2, STUB1, TRAF6, VHL, FBXW7, SIAH1, SIAH2, c) TNFRSF1B were TRAF1, TRAF2, ASB3, SMURF2. Subsequently, mRNA and protein expression of these substrate and their corresponding E3 ligases were studied in GBM patients (Table 2). Based on the results, only substrate HIF1A and its E3 ligase von Hippel-Lindau (VHL) and GNB2L1 were dysregulated in GBM patients' samples both at transcriptomics and proteomics levels. Under the normoxic condition, HIF1A is ubiquitinated by VHL and E3 ligase for proteasome degradation in the cytoplasm. Once stabilized, HIF1A translocate to the nucleus, guided by a nuclear localization signal in its C-terminus (Tanimoto et al., 2000; Yu et al., 2001).

In contrast, Aga et al. (2014) demonstrated that endogenous HIF1A is detectable in exosomes (Aga et al., 2014) present in the microenvironment, and studies suggest that exosomes reflect the hypoxic status of glioma cells and mediate hypoxia-dependent activation of vascular cells during tumor development (Kucharzewska et al., 2013). In addition, HIF1A initiates TNFα exosome-mediated secretion under hypoxic conditions (Yu et al.,

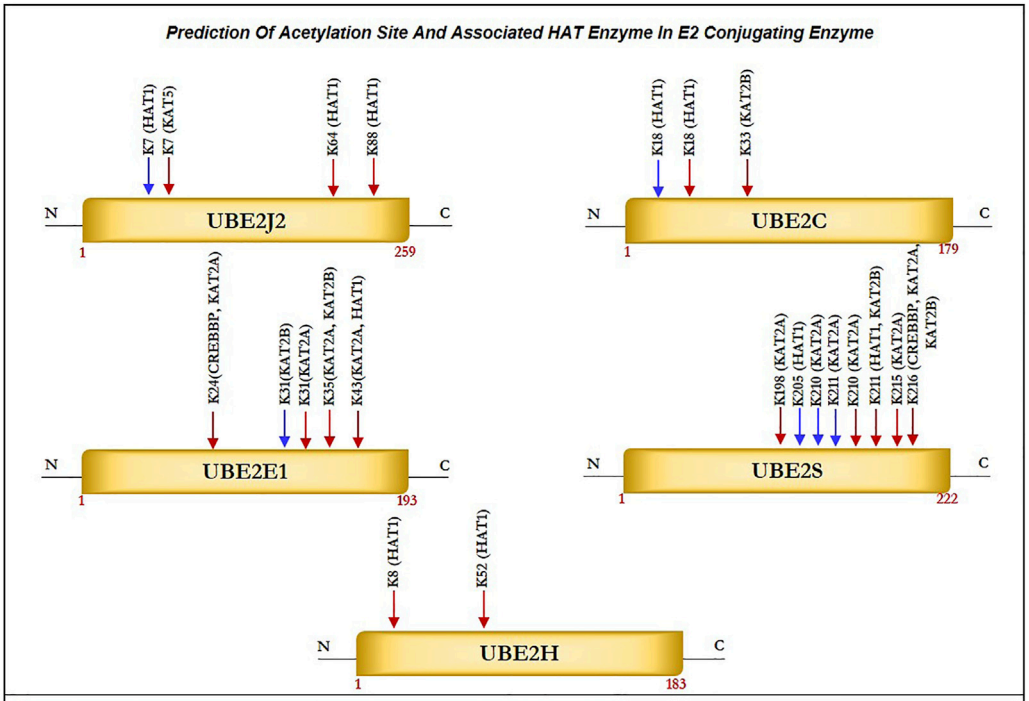

Acetylation sites and associated HATs enzymes					Structural selectivity		
Sequence containing Lysine (K) amino acid	(K) residue Position	HATs Enzymes	DeepPLA (FPR% <10)	GPS-PAIL (score >1)	Structural Features	Region	Localisation
Ube2C (179aa)							
TSVAAARKGAEPSGG	18	EP300	2.86%	1.079	Coil	Disordered	Protein binding
TSVAAARKGAEPSGG	18	HAT1	10.34%	3.533	Coil	Disordered	Protein binding
AARGPVGKRLQQELM	33	KAT2B	5.32%	1.514	Helix	Ordered	Cytoplasmic
Ube2E1 (193aa)							
KETNTPKKKESKVSM	31	KAT2B	3.76%	1.862	Coil	Disordered	Protein binding
SSNQQTEKETNTPKK	24	CREBBP	7.62%	2.56	Coil	Disordered	Protein binding
SSNQQTEKETNTPKK	24	KAT2A	9.64%	1.087	Coil	Disordered	Protein binding
KETNTPKKKESKVSM	31	KAT2A	5.83%	1.101	Coil	Disordered	Protein binding
TPKKKESKVSMSKNS	35	KAT2A	6.28%	2.101	Coil	Disordered	Protein binding
TPKKKESKVSMSKNS	35	KAT2B	8.87%	2.459	Coil	Disordered	Protein binding
VSMSKNSKLLSTSAK	43	HAT1	8.28%	6.867	Helix	Disordered	Protein binding
VSMSKNSKLLSTSAK	43	KAT2A	5.83%	1.145	Helix	Disordered	Protein binding
Ube2H (183aa)							
MSSPSPGKRRMDTDV	8	HAT1	5.52%	9.867	Helix	Ordered	Cytoplasmic
PYEGGVWKVRVDLPD	52	HAT1	8.28%	1.333	Strand	Ordered	Cytoplasmic
Ube2J2 (259aa)							
-MSSTSSKRAPTTAT	7	HAT1	3.45%	7.933	Coil	Disordered	Protein binding
-MSSTSSKRAPTTAT	7	KAT5	6.51%	1.031	Coil	Disordered	Protein binding
EGGYYHGKLIFPREF	64	HAT1	8.28%	2	Strand	Ordered	Extracellular
ITPNGRFKCNTRLCL	88	HAT1	8.28%	6.133	Coil	Ordered	Extracellular
Ube2S (222aa)							
KHAGERDKKLAAKKK	205	HAT1	4.83%	4.333	Helix	Disordered	Cytoplasmic
RDKKLAAKKKTDKKR	210	KAT2A	0.00%	2.174	Helix	Disordered	Protein binding
DKKLAAKKKTDKKRA	211	KAT2A	0.67%	2.072	Helix	Disordered	Protein binding
AEGPMAKKHAGERDK	198	KAT2A	6.05%	1.029	Coil	Disordered	Cytoplasmic
RDKKLAAKKKTDKKR	210	KAT2B	2.90%	1.064	Helix	Disordered	Protein binding
DKKLAAKKKTDKKRA	211	HAT1	8.28%	1.067	Helix	Disordered	Protein binding
DKKLAAKKKTDKKRA	211	KAT2B	3.12%	1.028	Helix	Disordered	Protein binding
AAKKKTDKKRALRRL	215	KAT2A	1.79%	1.33	Helix	Disordered	Cytoplasmic
AKKKTDKKRALRRL-	216	CREBBP	7.87%	2.145	Helix	Disordered	Cytoplasmic
AKKKTDKKRALRRL-	216	KAT2A	2.24%	1.783	Helix	Disordered	Cytoplasmic
AKKKTDKKRALRRL-	216	KAT2B	8.17%	2.22	Helix	Disordered	Cytoplasmic

FIGURE 4
Prediction of Acetylation Site and Associated HAT Enzyme in E2 Conjugating Enzyme: Potential acetylation site on lysine residues of Ube2J2, Ube2C, Ube2E1, Ube2S, Ube2H and associated HAT enzymes were identified using DeepPLA and GPS-PAIL machine-learning based webtool. For UBE2C (K18, K33), Ube2E1(K24, K31, K35, K43), Ube2H (K8, K52), Ube2J2 (K7, K64, K88) and Ube2S (K198, K205, K210, K211, K215, K216). HAT enzymes associated with lysine residues are mentioned in the table. The lysine residue marked in blue color has a high confidence score: DeepPLA (FPR<5%) and GPS-PAIL (score>1), and the red color has a medium confidence score: DeepPLA (FPR<10%) and GPS-PAIL (score>1). In addition, structural analysis using PSIPRED and DISOPRED3 showed predicted lysine residue falls in coiled structure for Ube2C, Ube2E1, and Ube2J2 whereas, in helix structure for Ube2S. Moreover, our investigation showed acetylation occurs in disordered regions compared to ordered regions. FPR: False positive rate.

TABLE 3 Impact of Amino Acid Substitution of "K" Putative Mutation to Either L, Q, R, Or E On Disease Susceptibility Predicted with The Help of Pmut, SNAP2, Polyphen2, and Mutpred2 tools.

Substitution	Pmut	SNAP2	PolyPhen-2	MutPred2	Total score
Ube2C					
K18L	0.74	1	0.005	0.772	2.517
K18Q	0.64	1	0.027	0.536	2.203
K18R	0.42	1	0.32	0.38	2.12
K18E	0.66	1	0.262	0.662	2.584
K33L	0.71	1	0.194	0.908	2.812
K33Q	0.59	1	0.003	0.804	2.397
K33R	0.25	1	0	0.681	1.931
K33E	0.59	1	0.049	0.868	2.507
Ube2E1					
K31L	0.49	1	0.037	0.156	1.683
K31Q	0.11	0	0.028	0.093	0.231
K31R	0.11	0	0	0.061	0.171
K31E	0.2	1	0	0.113	1.313
K24L	0.28	1	0.009	0.098	1.387
K24Q	0.09	0	0	0.066	0.156
K24R	0.09	0	0	0.044	0.134
K24E	0.11	0	0.002	0.079	0.191
K35L	0.58	1	0.09	0.196	1.866
K35Q	0.47	1	0.001	0.075	1.546
K35R	0.2	1	0	0.052	1.252
K35E	0.47	1	0.015	0.111	1.596
K43L	0.31	1	0.972	0.562	2.844
K43Q	0.2	0	0.924	0.368	1.492
K43R	0.12	1	0.007	0.211	1.338
K43E	0.35	1	0.896	0.369	2.615
Ube2H					
K8L	0.53	1	0.016	0.872	2.418
K8Q	0.51	1	0.437	0.758	2.705
K8R	0.26	1	0	0.661	1.921
K8E	0.39	1	0.354	0.831	2.575
K52L	0.63	1	0.82	0.943	3.393
K52Q	0.53	1	0.762	0.894	3.186
K52R	0.26	1	0.001	0.821	2.082
K52E	0.57	1	0.532	0.924	3.026
Ube2J2					
K7L	0.34	1	0.032	0.481	1.821
K7Q	0.37	0	0.897	0.266	1.533

(Continued on following page)

TABLE 3 (*Continued*) Impact of Amino Acid Substitution of "K" Putative Mutation to Either L, Q, R, Or E On Disease Susceptibility Predicted with The Help of Pmut, SNAP2, Polyphen2, and Mutpred2 tools.

Substitution	Pmut	SNAP2	PolyPhen-2	MutPred2	Total score
K7R	0.19	0	0.868	0.205	0.395
K7E	0.33	1	0.020	0.346	1.676
K64L	0.62	1	1	0.704	3.324
K64Q	0.59	1	0.96	0.504	3.054
K64R	0.39	0	0.542	0.208	1.14
K64E	0.59	1	0.996	0.509	3.095
K88L	0.55	1	0.908	0.877	3.335
K88Q	0.48	1	0.071	0.704	2.255
K88R	0.46	1	0.009	0.538	2.007
K88E	0.52	1	0.503	0.812	2.835
Ube2S					
K198L	0.72	1	0.999	0.567	3.286
K198Q	0.45	1	0.997	0.285	2.732
K198R	0.4	1	0.996	0.186	2.582
K198E	0.44	1	0.779	0.383	2.602
K205L	0.36	1	0.133	0.529	2.022
K205Q	0.37	0	0.531	0.255	1.156
K205R	0.15	0	0.358	0.148	0.656
K205E	0.27	1	0.187	0.349	1.806
K210L	0.73	1	0.997	0.833	3.56
K210Q	0.52	1	0.999	0.559	3.078
K210R	0.29	1	0.996	0.39	2.676
K210E	0.45	1	0.996	0.686	3.132
K211L	0.68	1	0.997	0.683	3.36
K211Q	0.64	1	0.999	0.433	3.072
K211R	0.16	1	0.996	0.2	2.356
K211E	0.52	1	0.996	0.475	2.991
K215L	0.69	1	0.997	0.817	3.504
K215Q	0.7	0	0.999	0.576	2.275
K215R	0.48	0	0.996	0.365	1.841
K215E	0.79	1	0.996	0.664	3.45
K216L	0.88	1	0.997	0.859	3.736
K216Q	0.77	1	0.999	0.639	3.408
K216R	0.74	0	0.996	0.455	2.191
K216E	0.8	1	0.996	0.751	3.547

*For SNAP2 = Probable Benign: Marked as "0"; Probable damage: Marked as "1".
*For Pmut, MutPred2, and PolyPhen-2: Effect or Probable damage = >0.5 threshold.
*Gradient of the Green color showed Total confidence score (cumulative score of Pmut, SNAP2, MutPred2, and PolyPhen-2): Higher green color signifies a high confidence score.

TABLE 4 Correlation and expression analysis of HAT enzymes and prediction of therapeutic axis In GBM.

E3 ligase	E2 conjugating enzymes	Potential K residue position	Histone acetyltransferases (HATs) enzymes						Therapeutic axis	Loss of acetylation site
		Confidence score >2.5	CREBBP	EP300	HAT1	KAT2A	KAT2B	KAT5		
VHL	UBE2E1	43	-	-	√	χ	-	-	HAT1-UBE2E1(K43)-VHL	No
	UBE2H	8	-	-	√	-	-	-	HAT1-UBE2H(K8)-VHL	Yes
		52	-	-	√	-	-	-	HAT1-UBE2H(K52)-VHL	No
	UBE2J2	64	-	-	√	-	-	-	HAT1-UBE2J2(K64)-VHL	No
		88	-	-	√	-	-	χ	HAT1-UBE2J2(K88)-VHL	No
GNB2L1	UBE2C	18	-	χ	√	-	-	-	HAT1-UBE2C(K18)-GNB2L1	No
		33	-	-	-	-	χ	-	-	Yes
	UBE2J2	64	-	-	√	-	-	-	HAT1-UBE2J2(K64)-GNB2L1	No
		88	-	-	√	-	-	χ	HAT1-UBE2J2(K88)-GNB2L1	No
	UBE2S	198	-	-	-	χ	-	-	-	Yes
		210	-	-	-	χ	-	-	-	Yes
		211	-	-	√	χ	χ	-	HAT1-UBE2S(K211)-GNB2L1	Yes
		215	-	-	-	χ	-	-	-	Yes
		216	χ	-	-	χ	χ	-	-	Yes

- Lysine residues marked in **blue are novel** and have not been previously documented in the literature for acetylation modification in GBM, patients.
- *p*-value≤0.05: significant; *p*-value>0.05; ns: not significant.
- √: signifies HAT1 enzymes expression is upregulated, with the significant positive correlation between HAT1 and Ube2E1, Ube2H and Ube2C, Ube2J2, Ube2S.
- χ: signifies KAT2A enzyme expression is downregulated, with a not significant association between KAT2A and Ube2E1, Ube2A.
- χ: signifies CREBBP, EP300, KAT2B, and KAT5 enzyme expression is not significant, with no significant association between CREBBP, and Ube2S; EP300 and Ube2C; KAT2B and Ube2C, Ube2S; KAT5 and Ube2J2.
- The pink rectangle box represents the first proposed therapeutic axis in GBM.
- The brown rectangle box represents the second proposed therapeutic axis in GBM.

2012). In human glioblastoma cells, Bensaad et al. showed that HIF-1α was necessary to induce Fatty Acid Binding Protein 3 (FABP3) and FABP7, leading to lipid droplet accumulations (Bensaad et al., 2014). According to reports, HIF1A is essential for the growth and development of GBM as well as for tumor cell migration, glucose absorption, angiogenesis, and chemoresistance. A plethora of research showed that hypoxia triggers glioma cells to release EVs with distinct functional proangiogenic cargo, including cytokines, growth factors, proteases, and miRNA to influence endothelial cells to promote angiogenesis, metabolic, and transcriptional signaling pathways such are the EGFR, PI3K/Akt and MAPK/ERK pathways. Hypoxia-stimulated glioma EVs promote tumor vascularization, pericyte vessel coverage, and cell proliferation, eventually reducing tumor hypoxia in the GBM microenvironment (Yekula et al., 2020). Hence, we have chosen HIF1A as substrate, VHL, and GNB2L1 (another gene name: RACK1) as an E3 ligase for further studies. Earlier investigations support our observation. Mutation in VHL genes causes renal cell carcinomas, pheochromocytomas, and cerebellar hemangioblastomas (Kim and Zschiedrich, 2018). We were interested in exploring this interaction in GBM. However, based on experimental data, our analysis also proposed GNB2L1 interacting with HIF1A. Earlier, this interaction was established in breast cancer (Zhou Z. et al., 2014). Here we will discuss this in context with GBM.

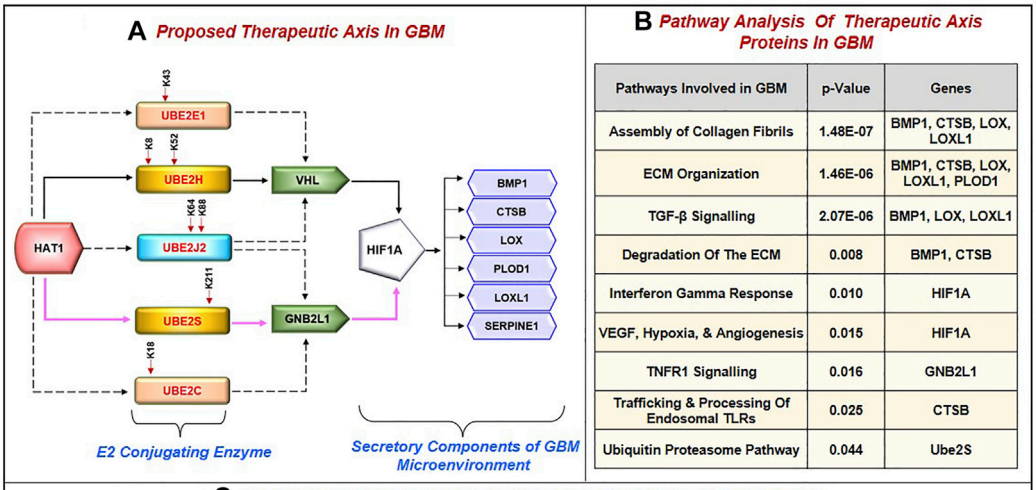

B *Pathway Analysis Of Therapeutic Axis Proteins In GBM*

Pathways Involved in GBM	p-Value	Genes
Assembly of Collagen Fibrils	1.48E-07	BMP1, CTSB, LOX, LOXL1
ECM Organization	1.46E-06	BMP1, CTSB, LOX, LOXL1, PLOD1
TGF-β Signalling	2.07E-06	BMP1, LOX, LOXL1
Degradation Of The ECM	0.008	BMP1, CTSB
Interferon Gamma Response	0.010	HIF1A
VEGF, Hypoxia, & Angiogenesis	0.015	HIF1A
TNFR1 Signalling	0.016	GNB2L1
Trafficking & Processing Of Endosomal TLRs	0.025	CTSB
Ubiquitin Proteasome Pathway	0.044	Ube2S

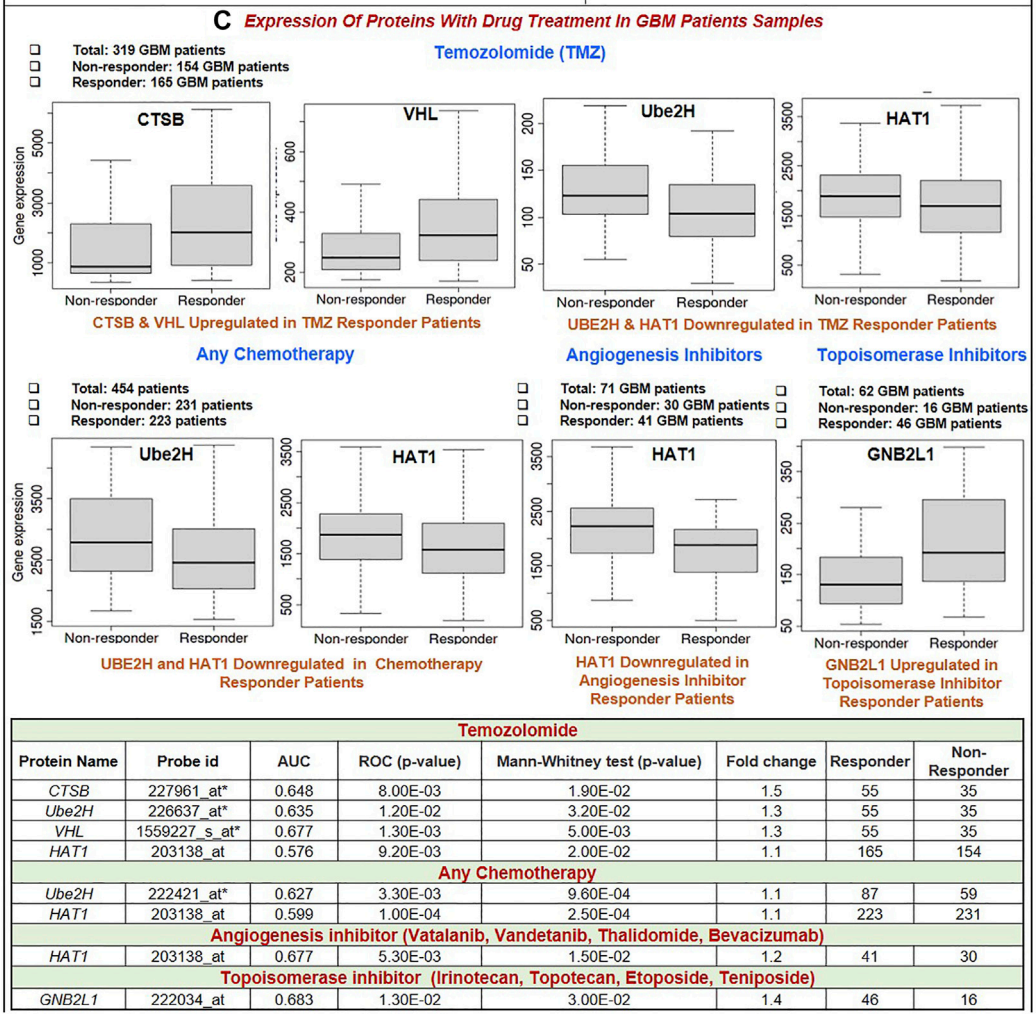

Protein Name	Probe id	AUC	ROC (p-value)	Mann-Whitney test (p-value)	Fold change	Responder	Non-Responder
Temozolomide							
CTSB	227961_at*	0.648	8.00E-03	1.90E-02	1.5	55	35
Ube2H	226637_at*	0.635	1.20E-02	3.20E-02	1.3	55	35
VHL	1559227_s_at*	0.677	1.30E-03	5.00E-03	1.3	55	35
HAT1	203138_at	0.576	9.20E-03	2.00E-02	1.1	165	154
Any Chemotherapy							
Ube2H	222421_at*	0.627	3.30E-03	9.60E-04	1.1	87	59
HAT1	203138_at	0.599	1.00E-04	2.50E-04	1.1	223	231
Angiogenesis inhibitor (Vatalanib, Vandetanib, Thalidomide, Bevacizumab)							
HAT1	203138_at	0.677	5.30E-03	1.50E-02	1.2	41	30
Topoisomerase inhibitor (Irinotecan, Topotecan, Etoposide, Teniposide)							
GNB2L1	222034_at	0.683	1.30E-02	3.00E-02	1.4	46	16

FIGURE 5
(A) Proposed Therapeutic axis: Based on our findings, two axes were proposed. First, there was HAT1-Ube2S(K211)-GNB2L1-HIF1A-BMP1/CTSB/LOX/LOXL1/PLOD1/SERPINE1. In this process, HAT1 will acetylate lysine residues at the 211* positions of Ube2S conjugating enzymes. This increases transcription and upregulation, linked to GNB2L1, an E3 ligase that regulates HIF1A activity in GBM. HIF1A overexpression links with the identified poor prognosis markers BMP1, CTSB, LOX, LOXL1, PLOD1, and SERPINE1. A solid pink colored line represents this axis. Second, HAT1-Ube2H(K8, K52)-VHL-HIF1A-BMP1/CTSB/LOX/LOXL1/PLOD1/SERPINE1 is involved. A solid black colored line represents this axis. HAT1 acetylates Lysine residues at K8 and K52* positions, and its overexpression has been linked to VHL, an E3 ligase, and HIF1A. This axis has been marked with a solid black line. Other therapeutic axes involving Ube2J2, Ube2E1 and VHL ligase, Ube2C and Ube2J2, and GNB2L1 ligase are possible, as illustrated in the figure with the dashed black line. * *Signifies novel acetylation site on lysine residue.* **(B)** Pathway analysis of the therapeutic axis's protein showed genes involved in signaling
(*Continued*)

FIGURE 5 (Continued)
pathways such as assembly of collagen fibrils, ECM organization, ECM degradation, Interferon-gamma response, hypoxia and angiogenesis, TNF signaling and ubiquitin-proteasome pathway. **(C)** Receiver operating characteristic (ROC) curve for biomarkers involved in therapeutic expression in Glioblastoma Multiforme. Area Under Curve (AUC) of time-dependent ROC curves verified the prognostic performance of the responder cohort after 16 months of treatment with Temozolomide (TMZ), chemotherapy, Angiogenesis, and Topoisomerase Inhibitors. The therapeutic axis includes HAT1, E2 enzymes (Ube2H, Ube2S, Ube2E1, Ube2C, Ube2J2), E3 ligase (VHL, GNB2L1), Prognosis markers (BMP1, CTSB, LOX, LOXL1, PLOD1 and SERPINE1). **(A)** In the TMZ responder cohort: CTSB and VHL expression was upregulated, and Ube2H and HAT1 were downregulated. **(B)** Chemotherapy responder cohort: HAT1 and Ube2H were downregulated. **(C)** Angiogenesis inhibitor responder cohort: HAT1 downregulated **(D)** Topoisomerase Inhibitors responder cohort: GNB2L1 upregulated in the responder. Tables show significant AUC and fold change expression between responder and non-responder patients to drug treatment.

Evidence from the literature suggests that the poor prognostic biomarkers LOX, BMP1, CTSB, LOXL1, PLOD1, MMP9, SERPINE1, and SERPING1 are related to the hypoxic microenvironment. First, there was a positive correlation between BMP1 and HIF1A and the malignant grade of astrocytoma, although there was no evidence of a direct or indirect association (Xiao et al., 2019). Additionally, Xiaofei et al. (2018) demonstrated that hypoxia upregulates CTSB and HIF1A in a fashion comparable to HepG2 cells. (Xiaofei et al., 2018). In several cancer types, including breast, head and neck, prostate, colon, and renal cell carcinomas, LOX controls HIF1A. The invasive and metastatic characteristics of hypoxic cancer cells, including astrocytoma, are caused by secreted LOX (Da Silva et al., 2015). Under hypoxic conditions (<1% oxygen), LOX and LOXL1 promoted angiogenesis (Xie et al., 2017). Recently, Wang et al. (2021) discovered that Hypoxia causes the overexpression of PLOD1, which, through NF-kB signaling, leads to the malignant phenotype of GBM (Wang et al., 2021). HIF1A promotes the development of MMP9, which influences invasion in breast cancer by weakening the basement membrane and the ECM barrier. HIF1A is also implicated in the control of cell proliferation, growth factor release, and angiogenesis (Choi et al., 2011). Furthermore, hypoxia-induced overproduction of reactive oxygen species (ROS) causes cancer to upregulate the SERPINE1 protein (protein that regulates cell adhesion), which controls cell adhesion in breast cancer (Azimi et al., 2017). In contrast, HIF2A, not HIF1A, controls the expression of SERPING1, which is linked to immunological infiltrations in glioblastoma (Xiao et al., 2020). Accordingly, we can state that HIF1A is a crucial biomarker that correlates with all cancer biomarkers that indicate a poor prognosis. As a result, we go forward with HIF1A and want to investigate its potential role in the therapeutic axis for treating GBM.

3.5 Identification of significant E2 conjugating enzyme associated with VHL and GNB2L1 in GBM

Ubiquitin-conjugating enzymes (E2s) are the central players in the trio of enzymes responsible for the attachment of ubiquitin (Ub) to cellular proteins. It plays a more prominent role in ubiquitin signaling than a middleman. The UBC domain, a central catalytic domain in E2s, has about 150 amino acids. This domain adopts an α/β-fold typically with four α-helices and a four-stranded β-sheet. Important loop regions form part of the E3-binding site and the E2 active site. Several studies have suggested the dysregulation of E2 in multiple cancer. Understanding of E2s regulation is still emerging, and it is evident that E2s can be governed by various mechanisms (Stewart et al., 2016). Hence, we explore how E2s regulate and affect others, especially our shortlisted E3 ligases VHL and GNB2L1 and substrate HIF1A in GBM. We have extracted 36 E2s expressed in humans from previously published research.

In addition, we analyzed its expression at mRNA and protein levels in GBM patient samples with the help of the GEPIA2.0 and Osppc web applications (Figure 3B). We have found that at mRNA levels, 13 E2 conjugative enzymes were significantly (p-value ≤0.05, $\log_2$FC ≥ 1.5) dysregulated in GBM patient samples, including 11 upregulated (Ube2A, Ube2C, Ube2D2, Ube2D3, Ube2E1, Ube2H, Ube2J1, Ube2J2, Ube2L6, Ube2L6, Ube2N, Ube2S, Ube2T) and 1 downregulated (Ube2QL1). In addition, amongst 13 shortlisted enzymes, we found that protein levels of 7 were upregulated (Ube2A, Ube2C, Ube2E1, Ube2H, Ube2J1, Ube2H, Ube2J2, Ube2L6, Ube2S), 3 were downregulated (Ube2D2, Ube2J1, Ube2N), 2 were (Ube2D3, Ube2QL1) were not available in the database, and UBE2T were non-significant. Thus, based on both transcriptomics and proteomics expression data analysis, we moved further with 6 E2s named Ube2C, Ube2E1, Ube2H, Ube2J2, Ube2L6, Ube2S that were overexpressed in GBM. A study by Xiang and Yan (2022), Ube2C serves as both an oncogene and a tumor suppressor gene, and its overexpression is crucial to the development of thyroid cancer (Xiang and Yan, n. d.). Moreover, another study by Pan et al. (2021) demonstrates that Ube2D3 induces the ubiquitination of the SHP-2 protein, which in turn activates STAT3 signaling, promoting tumorigenesis and glycolysis in gliomas (Pan et al., 2021).

Further, we have also studied the correlation between E3 ligase with substrate and shortlisted E2s in GBM patient's samples using GEPIA2.0 (GBM tumor sample size, n = 163) and TIMER2.0 (GBM tumor sample size, n = 153). We have tabulated purity-adjusted partial Spearman's rho (ρ) value which gives the degree of their correlation in the form of a heatmap (Figure 3C). We have used spearman statistical analysis, and when $|\rho| > 0.1$, it indicated a correlation between the genes. Red color signifies: Positive correlation (p-value ≤0.05, $\rho > 0$), blue color signifies: Negative correlation (p-value≤0.05, $\rho > 0$), and grey color signify: non-significant (p-value>0.05). Results showed in GBM that both E3 ligase VHL and GNB2L1 were positively correlated with its substrate HIF1A. Moreover, VHL was positively correlated with Ube2E1, Ube2H, and Ube2J2, whereas GNB2L1 was positively correlated with Ube2C, Ube2J2, and Ube2S.

Furthermore, to investigate the PTM (e.g., acetylation) that can modify lysine basic residues (lysine and/or arginine). Acetylation affects a large number of histone and non-histone proteins. Growing evidence suggests that reversible lysine acetylation of non-histone

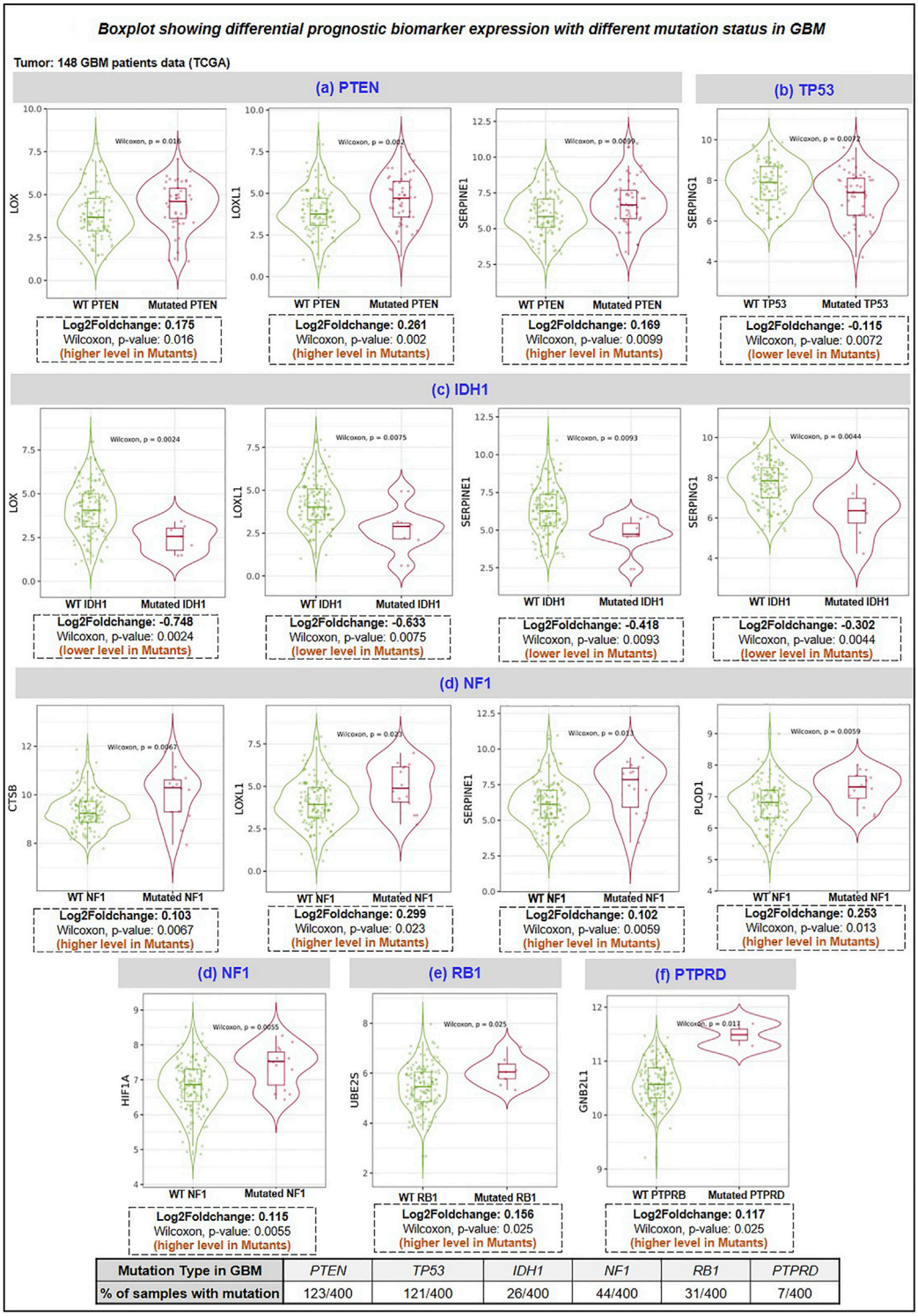

Mutation Type in GBM	*PTEN*	*TP53*	*IDH1*	*NF1*	*RB1*	*PTPRD*
% of samples with mutation	123/400	121/400	26/400	44/400	31/400	7/400

FIGURE 6
Differentiational expression analysis of prognosis biomarker with a top mutation in GBM. HAT1, E2 enzymes (Ube2H, Ube2S, Ube2E1, Ube2C, UbeJ2), E3 ligase (VHL, GNB2L1), Prognosis markers (BMP1, CTSB, LOX, LOXL1, PLOD1 and SERPING1) **(A)** PTEN mutation: LOX, LOXL1 and SERPINE1 were upregulated in GBM mutant group, **(B)** TP53 mutation: SERPING1 were downregulated in mutant GBM group, **(C)** IDH1 mutation: LOX, LOXL1, SERPINE1 and SERPING1 downregulated in the mutant group, **(D)** NF1 mutation: CTSB, LOXL1, SERPINE1, PLOD1 and HIF1A were upregulated in the mutant group. **(E)** RB1 mutation: Ube2S was upregulated, and **(F)** PTPRD: GNB2L1 was upregulated in the mutant group. PTPRD: Protein Tyrosine Phosphatase Receptor Type D; NF1: neurofibromin-1; RB1: Retinoblastoma gene; IDH1: isocitrate dehydrogenase 1 gene; PTEN: phosphatase and tensin homolog.

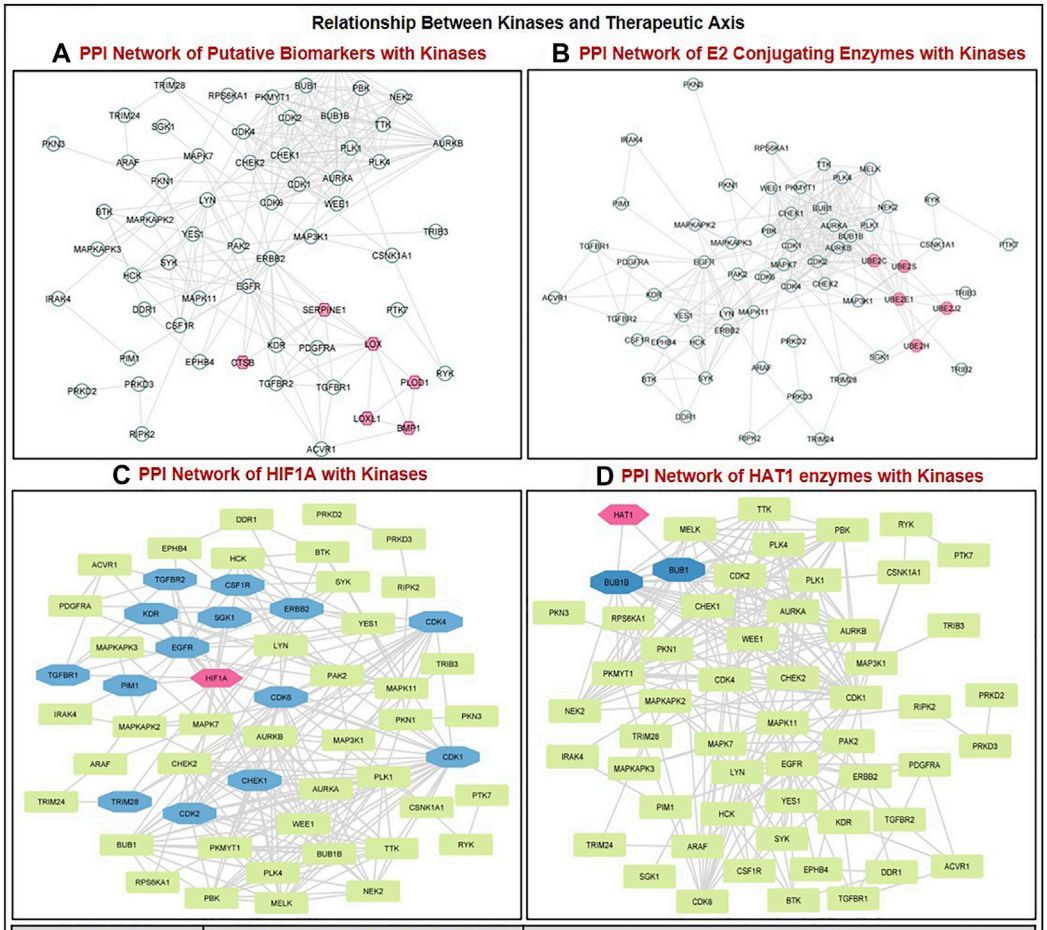

Biomarker	Total number of interacting Kinases	Protein Kinases
BMP1	1	ACVR1
CTSB	2	EGFR, ERBB2
LOX	6	PDGFRA, KDR, TGFBR2, TGFBR1, ERBB2, EGFR
LOXL1	0	--
SERPINE1	5	EGFR, ERBB2, KDR, TGFBR2, TGFBR1
PLOD1	0	--
E2 Enzymes	**Total number of interacting Kinases**	**Protein Kinases**
Ube2E1	8	CDK1, CDK2, AURKA, AURKB, BUB1B, PLK1, NEK2, TRIB2
Ube2H	1	TRIM28
Ube2J2	1	SGK1
Ube2S	8	CDK2, AURKB, BUB1B, PLK1, NEK2, AURKA, CDK1, MAP3K1
Ube2C	16	CDK4, CDK2, AURKB, BUB1B, PLK1, NEK2, MAPK7, AURKA, CDK1, PBK, CHEK1,TTK, PKMYT1, PLK4, MELK, BUB1
Therapeutic Markers	**Total number of interacting Kinases**	**Protein Kinases**
HAT1	2	BUB1, BUB1B
HIF1A	14	CHEK1, CDK2,TRIM28, CDK1, CDK6, PIM1, TGFBR1, EGFR, SGK1, KDR, TGFBR2, CSF1R, ERBB2, CDK4

FIGURE 7
Correlation of dysregulated protein kinases (upregulated in GBM patient tumor samples) with the proteins involved in the proposed therapeutic axis. PPI network of kinases with **(A)** Putative biomarkers (BMP1, CTSB, LOX, LOXL1, PLOD1, SERPINE1); **(B)** E2s conjugating enzymes (Ube2S, Ube2H, and others Ube2E1, Ube2C, Ube2J2); **(C)** HIF1A; **(D)** HAT1 enzymes. GBM: Glioblastoma multiforme; PPI: Protein-Protein Interaction.

proteins regulates mRNA stability, protein localization and degradation, and protein-protein and protein–DNA interactions. The dynamic regulation of genes governing cellular proliferation, differentiation, and death depends largely on the recruitment of HATs and histone deacetylases (HDACs) to the transcriptional machinery. Several oncogenes or tumor-suppressor genes produce

many non-histone proteins specifically targeted by acetylation. These proteins have a direct role in carcinogenesis, tumor growth, and metastasis (Singh et al., 2010). Researchers have found acetylation sites on Ub molecules and showed how acetylated Ub modulates E1 enzyme (Uba1) catalytic activity. On a similar note here, we explore the potential acetylation site on lysine residues and its impact on selected E2s such as Ube2E1, Ube2H, Ube2J2, Ube2C, and Ube2S in GBM (Lacoursiere and Shaw, 2021). Moreover, these E2s have in patients with anaplastic gliomas, a greater Ube2C expression was linked to mitotic cyclin degradation and a significantly reduced OS duration (Ma et al., 2016). Additionally, Ube2S is controlled by the PTEN/Akt pathway and participates in DNA repair, particularly NHEJ-mediated DNA repair, which makes chemotherapeutic drugs more sensitive to GBM (Maksoud, 2021). In a recent study, Shin et al. found a mutation (*de novo* missense variant) that resembles a variant found in a patient with neurodevelopmental abnormalities, induces irregular Ube2h function in zebrafish embryos, and results in abnormal brain development (Shin et al., 2023). In addition, according to Lim and Joo (2020), circulating Ube2H mRNA is potentially used to diagnose and treat Alzheimer's disease (Lim and Joo, 2020). However, Ube2H has been studied in cancer, although there is little information about it in GBM (Zuo et al., 2020).

3.6 Identification of potential lysine (K) residues for acetylation in E2s and prediction of associated HAT enzymes

Herein, we identified acetylation sites on lysine (K) residue of shortlisted E2s such as Ube2C, Ube2E1, Ube2H, Ube2J2, Ube2S and associated HATs enzymes, including CREBBP, EP300, HAT1, KAT2A, KAT2B, KAT5, and KAT8 with using deep learning methods such as Deep-PLA and GPS-PAIL. The total 'K' modification sites for Ube2C, Ube2E1, Ube2H, Ube2J2, and Ube2S are 12, 15, 13, 15, and 16, respectively. We have selected only those 'K' residues that fall under the filter (High confidence: DeepPLA: False positive rate (FPR) % <5 and GPS-PAIL score >1; Medium confidence: DeepPLA: FPR% <10 and GPS-PAIL score >1). The extracted acetylation sites were mapped to respective proteins. Figure 4 illustrate all predicted acetylation site on 'K' residues and associated HATs enzymes. Our analysis observed potential acetylation 'K' residues that pass our filter criteria were Ube2C: K18, K33; Ube2E1 for K24, K31, K35, K43; Ube2H: K8, K52; Ube2J2: K7, K64, K88; Ube2S: K198, K205, K210, K211, K215, K216. Lacoursiere et al. (2022) have beautifully described the acetylation site in the UBC domain of 33 different E2s and its involvement in various cancer, including prostate cancer, gastric carcinoma, and leukemia. Mounting evidence from earlier studies has demonstrated acetylation sites for Ube2C (K18, leukemia), Ube2E1(K43, breast cancer), and Ube2H (K8, breast cancer) (Lacoursiere et al., 2022). Our analysis has shown novel putative acetylation sites for E2s at lysine residues are Ube2C (K33); Ube2E1 (K24, K31, K35); Ube2H (K52); Ube2J2 (K7, K64, K88); Ube2S (K198, K205, K210, K211, K215, K216).

Further, we have identified associated HAT enzymes to E2s such as for a) Ube2C: EP300, HAT1 and KAT2B; b) Ube2E1: KAT2B, CREBBP, KAT2A and HAT1; c) Ube2H: HAT1; d) Ube2J2: HAT1, KAT5; e) Ube2S: HAT1, KAT2A, KAT2B and CREBBP. These E2 can be the potential substrate for HAT enzymes. Many additional HAT substrates have been discovered in the past as a result of acetylome research, and numerous non-histone HAT substrates, including AML1, AML1-ETO (AE), p53, c-Myc, NF-κB, cohesin, and tubulin, have been identified to be crucial for a variety of cellular functions (Sun et al., 2015). Furthermore, the expression of these HAT enzymes was studied in GBM patient samples using GEPIA2.0 and OSppc tools. Analysis showed that HAT1 was upregulated while KAT2A was downregulated in GBM patient samples. Other HAT enzyme expressions, such as CREBBP, EP300, KAT2B, and KAT5, were insignificant. Hence, we moved with only upregulated HAT1 enzymes for further analysis. mRNA and protein expression data are shown in Supplementary Figure S2B.

3.7 Structural characterization and impact of lysine modification

Selected E2s Ube2C, Ube2E1, Ube2H, Ube2J2, and Ube2S have undergone structural characterization of the anticipated 'K' acetylation site as mutational investigation and its effect on disease susceptibility. Firstly, structure analysis of Ube2C, Ube2E1, Ube2H, Ube2J2, and Ube2S was performed. Our analysis demonstrated that Ube2E1 (3) and Ube2J2 (2) had a higher rate of acetylated 'K' sites falling in the coiled region, while Ube2S (6) and Ube2H (1) had a greater rate of these sites falling in helix region. Secondary structure analysis demonstrated the significance of the coiled structure in the PTM region compared to the helix and strand. Coiled areas govern protein interactions and aggregation propensity. Therefore mutations that damage coiled regions depress aggregation and protein activity, whereas mutations that improve coiled structure boost aggregation propensity (Fiumara et al., 2010).

Narasumani and Harrison (2018) demonstrated that PTMs preferred disordered regions compared to the ordered region, affecting their functions and interactions. Furthermore, the involvement of PTM in the disordered region influences disorder to order transition, thus altering the protein's stability and associated mechanisms. In the context of eukaryotic histones, the function of acetylation has been thoroughly investigated. Acetylation of disordered tail sections stimulates gene expression by removing inhibition (Christensen et al., 2019a). However, not all PTMs prefer disordered regions (Narasumani and Harrison, 2018; Mészáros et al., 2021). Hence, we predicted the distribution of predicted acetylation in protein intrinsic ordered and disordered regions using the machine-learning-based method DISOPRED3. Results indicated that the disordered area was more likely to include possible 'K' acetylation residues for all five E2s, Ube2C, Ube2E1, Ube2H, Ube2J2, and Ube2S, than the ordered region. Furthermore, the localization of putative 'K' residue in the sequence has also been predicted; for example, the sequence containing K31 of Ube2E1 involves protein binding. Secondly, we have investigated the pathology of mutation (amino acid substitution) by substituting lysine (K) residue, which is a positively charged amino acid with each polar amino acid (glutamine, Q), non-polar (leucine, L),

negatively charged (glutamate, E), and positively charged (arginine, R) through mutational analysis tools such as PMut, SNAP2, PolyPhen2 and Mutpred2. Our results observed that mutation at 'K' acetylation sites impacts disease susceptibility. For each tool, we have selected a score >0.5. Each numerical prediction score value has been tabulated in Table 3. However, Ube2H (K52), Ube2J2 (K64, K88) and Ube2S (K198, K210, K211, K215, K216) exhibit higher confidence scores (cumulative confidence score value > 2.5) on impact disease susceptibility. This signifies that a single amino acid substitution or mutation at identified 'K' residues leads to pathogenic and results in disease. Previous evidence also suggested that any mutation in these intrinsically disordered protein regions causes cancer (Mészáros et al., 2021).

Subsequently, we were interested in anticipating the molecular mechanism of pathogenicity due to mutation at the 'K' acetylation site through the Mutpred2 web application. Supplementary Information Supplementary Table S3 demonstrates the functional impact of putative 'K' residue mutation on acetylation. The combined results depict the role of putative 'K' mutation on other cellular functions. The results revealed that mutation in Ube2C (K33), Ube2H (K8), and Ube2S (K198, K205, K210, K211, K215, and K216) results in loss of acetylation on the same site. These findings confirm what we had already noticed. Thus, loss of acetylation with a mutation at K8 for Ube2H and at K198, K205, K210, K211, K215, and K216 for Ube2S signifies our predicted lysine residue is site acetylation, and any mutation will lead to disease. Other mechanisms, along with affected motifs, have been elaborated in Supplementary Information Supplementary Table S3. Moreover, selected disease-susceptible mutations were subjected to investigate their impact on protein structure stability. Mutation at Ube2C (K18) with (E), Ube2H (K8) with (R) and Ube2S (K210, K216) with (E) and (Q) leads to the gain of helix structure. This also signifies mutation at these acetylation sites will cause a topological change in the secondary structure.

3.8 Prediction of therapeutic axis in GBM pathology

To comprehend how HIF1A biomarkers and their associated E3 ligases, as well as HAT enzymes and E2s, are involved, we have collated all of our research data. Table 4 demonstrates the strategy for choosing the dysregulated final axis in GBM. It revealed that Ube2E1 (K43), Ube2H (K8, K52) were connected with VHL enzymes and Ube2C (K18, K33), Ube2S (K168, K210, K211, K215, K216) linked with GNB2L1, while Ube2J2 (K64, K88) was associated with both VHL and GNB2L1 enzymes. Only a few of the predicted acetylation sites K8 of UBE2H, K33 of Ube2C, K198, K210, K211, K215, and K216 of Ube2S were verified with the MutPred2 predictor outcome "loss of acetylation site" following a single amino acid substitution mutation. The GBM was examined for each E2s connection with the HATs enzymes. Using the GEPIA2.0 program, the mRNA expression of each HATs enzyme was examined in a GBM patient sample. Out of all the enzymes, only HAT1 was connected to E2s at specific lysine residues. As a result, we suggested two novel pathways that may be therapeutic targets: HAT1-Ube2S(K211)-GNB2L1-HIF1A and HAT1-Ube2H(K8)-VHL-HIF1A. We anticipated a new route axis HAT1-Ube2S(K211)-GNB2L1-HIF1A implicated in the pathogenesis of GBM because K8 of Ube2H has already been identified in the literature (Lacoursiere et al., 2022). Thus, we predicted a new route axis, HAT1-Ube2S(K211)-GNB2L1-HIF1A, implicated in the etiology of GBM. We have demonstrated that in this pathway, HAT1 acetylates E2s, and Ube2S (a non-histone protein) at lysine residue K211 (near C-terminal), causing its overexpression. Numerous studies have demonstrated that non-histone protein acetylation is one of the critical factors influencing gene transcription. Alaei et al. (2018) found that the C-terminal acetylation of lysine modulates protein turnover and stability (Alaei et al., 2018). In contrast, early research showed that ubiquitin-mediated protein degradation could be stopped when the N-terminal-amino group is acetylated, and this degradation can happen to proteins with free-amino groups. Several signaling pathways along with the cell cycle can be regulated by protein acetylation (Hwang et al., 2010; Zhuang, 2013; You et al., 2022). Most HATs have a nucleus-specific location and operate as co-activators of transcription. The degradation of proteins is also connected to protein acetylation (Sterner and Berger, 2000; Varshavsky, 2019). Acetylation is a modification that can significantly modify a protein's function by changing its hydrophobicity, solubility, and surface characteristics. These changes may impact the protein's conformation and interactions with substrates, cofactors, and other macromolecules (Christensen et al., 2019b). As a result, C-terminal acetylation controls lysine's ubiquitination and impacts its turnover. We postulated that acetylation of Ube2S at position 211, near the protein's C-terminus, promotes and regulates GNB2L1's protein turnover and ubiquitination modification. As a result of increased protein aggregation, the ability of GNB2L1 to ubiquitinate HIF1A is reduced, which further increases the expression level of the HIF1A protein (prevents its degradation by the UPS system).

Overexpressed Ube2S is linked with increased GNB2L1 and elevated HIF1A substrate. As per earlier research, acetylation is essential for p53 activation because it prevents the ubiquitin E3 ligase Mdm2 from inhibiting its ability to bind p53 for ubiquitination and proteasomal destruction. According to the theory of inter-protein acetylation-ubiquitination crosstalk, acetylation of Mdm2 by p300/CBP may prevent p53 from being subsequently ubiquitinated, increasing p53's stability and transcriptional activity (Wang et al., 2004). Additionally, Sirt1's ubiquitination and degradation may control the acetylation status of the histones in the downstream region, which would further epigenetically restrict the expression of the autophagy gene and encourage the spread of colorectal cancer (Shen et al., 2018).

Further, this significantly correlates with the GBM biomarkers BMP1, CTSB, LOX, LOXL1, PLOD1, and SERPINE1. Critical biological pathways, such as canonical and noncanonical TGF signaling, are regulated by BMP1, LOX, and LOXL1. Figure 5A illustrates the putative therapeutic axis and its influence on biological pathways in GBM. According to studies, TGF signaling regulates VEGF expression through SMAD-dependent signaling, which is crucial for angiogenesis in GBM. It contributes to the pathophysiology of tumors by controlling tumor growth, maintaining GSCs, and suppressing anti-tumor immunity (Lin et al., 2010; Sachdeva et al., 2019; Yu H. et al., 2020). Besides this, extracellular secreted CTSB can modify the TME through various non-cellular components and

degrade the ECM. Cathepsins are a crucial class of proteins that are involved in the growth and propagation of cancer since they also interfere with the cell-cell adhesion molecules which encourage cell invasion and metastasis (Ding et al., 2022). Additionally, each contributes to the formation of collagen fibrils in the ECM. The normal brain contains minimal collagen, but it has been found that collagen gene expression is elevated in GBMs (Pointer et al., 2017). Moreover, LOX and LOXL1 isoforms are cleaved by BMP1-related proteases implies that these enzymes are matrix-oriented enzymes and possess strong binding with other ECM components including fibronectin, fibulin-4 and fibulin-5, and tropoelastin. In fact, research has revealed that inactivating the Lox and Loxl1 genes in mice models causes severe vascular problems because it disrupts the development of elastic fibers (Yang et al., 2020). Figure 5B depicts the study of different biological pathways of biomarkers associated with the proposed treatment axis in GBM. According to our findings, these expected axes in GBM may be targeted in GBM patient samples, which show that all proteins and enzymes associated with these pathways are noticeably enhanced at both the transcriptional and proteomic levels. Furthermore, they significantly connect with the appropriate partner proteins in GBM. So, we identified strategies that may be used to block the development of GBM.

3.9 Characterization of putative biomarkers involved in the proposed therapeutic axis in GBM

3.9.1 Predictive markers response to GBM treatment

Despite advances in the molecular characterization of GBM, only a handful of predictive biomarkers exist with limited clinical relevance. We embraced the receiver operator characteristic (ROC) plotter webtool to link with protein expression amongst our proposed therapeutic axis in GBM tumor samples with therapies including temozolomide (TMZ), chemotherapy, Angiogenesis inhibitor (including Vatalanib, Vandetanib, Thalidomide, Bevacizumab) and topoisomerase inhibitors (including Irinotecan, Topotecan, Etoposide, Teniposide). For each protein, HAT1, Ube2E1, Ube2H, Ube2J2, Ube2S, Ube2C, VHL, GNB2L1, HIF1A, BMP1, CTSB, LOX, LOXL1, PLOD1, and SERPINE1, the expression was compared between responders and non-responder's patients' data with a Mann–Whitney U-test and area under curve (AUC). In response to TMZ, we discovered the enhanced expression of CTSB (AUC = 0.648) and VHL (AUC = 0.667). In response to TMZ and chemotherapy, it was shown that the expression of Ube2H (AUC = 0.635, 0.627 respectively) and HAT1 (AUC = 0.576, 0.599 respectively) had decreased.

Additionally, HAT1 expression was downregulated in angiogenesis inhibitor treatment responders (AUC = 0.677). In addition, patients who responded well to topoisomerase inhibitor medication had increased expression of GBN2L1 (AUC = 0.683). Hu et al. (2020) discovered YWHAB, PPAT, and NOL10 as novel biomarkers and validated their diagnostic and prognostic value for Hepatocellular carcinoma, and Zhang et al. (2020) found ELANE, GPX4, GSDMD, and TIRAP as a prognosis marker in Endometrial Cancer using ROC plotter tool (Hu et al., 2020; Zhang and Yang, 2021). Therefore, based on our findings, it can be concluded that CTSB, VHL, GNB2L1, Ube2H, and HAT1 have the potential to serve as candidates for predictive markers of response, provide a framework for preclinical investigations and perhaps improve patient classification for GBM in the future (Figure 5C).

3.9.2 Correlation of therapeutic axis with top mutated genes in GBM

Here, we studied the differential expression of all proteins involved in the proposed therapeutic axis (HAT1, Ube2E1, Ube2H, Ube2J2, Ube2S, VHL, GNB2L1, HIF1A) along with prognostic biomarker (BMP1, CTSB, LOX, LOXL1, PLOD1, MMP9, SERPINE1, SERPING1) with top 10 genes mutated genes in GBM using "gene_module" tool of TIMER2.0 webserver. Research evidence suggests that the top 10 mutated genes in GBM are PTEN, TP53, EGFR, PIK3R1, PIK3CA, NF1, RB1, IDH1, PTPRD, and ERBB2 (Liu A. et al., 2016; Zhang et al., 2019). The incidence rate of each mutation in 400 GBM patient samples has been shown as PTEN (30.75%), TP53 (30.25%), EGFR (23.5%), NF1 (11%), PIK3CA (8.75%), PIK3R1 (8.5%), RB1 (7.75%), IDH1 (6.5%), PTPRD (1.75%), ERBB2 (1.25%). The expression of the interested protein was compared between GBM patients (n = 148) with wild-type and mutant-type genes. We have observed that GBM patient samples having a) PTEN mutation have higher expression of LOX, LOXL1, SERPINE1 protein, b) p53 mutation have decreased levels of SERPING1, c) IDH1 mutation have decreased levels of LOX, LOXL1, SERPINE1 and SERPING1, d) NF1 mutation have higher levels of CTSB, LOXL1, SERPINE1, PLOD1 and HIF1A, e) RB1 mutation have higher levels of Ube2S, f) PTPRD mutation have higher levels of GNB2L1. Figure 6 shows the boxplot of all significant biomarkers regulated with mutated genes in GBM.

3.9.3 Association with human protein kinases in GBM

We have studied the expression of 536 human protein kinases in GBM and showed that 71 kinases were upregulated and 46 kinases were downregulated. Using protein-protein network analysis, we have studied the interaction between biomarkers (BMP1, CTSB, LOX, LOXL1, PLOD1, SERPINE1) with dysregulated kinases. We have shown (Figure 7A) LOX interacts with PDGFRA, KDR, TGFBR2, TGFBR1, ERBB2, EGFR; b) SERPINE1 interacts with EGFR, ERBB2, KDR, TGFBR2, TGFBR1; c) CTSB interact with EGFR, ERBB2, and d) BMP1: ACVR1. In addition, we have discussed the protein-protein interaction (PPI) between E2s with kinases and showed that the proposed E2s Ube2S interact with 8 kinases including CDK2, AURKB, BUB1B, PLK1, NEK2, AURKA, CDK1, MAP3K1 whereas Ube2H interact only with TRIM28 kinases (Figure 7B). Further the association of kinases with HIF1A biomarker and HAT1 enzymes. Results shows HIF1A interact with only BUB1 and BUB1B kinases whereas HAT1 enzymes interact with 14 kinases, namely, CHEK1, CDK1, CDK2, CDK4, CDK6, PIM1, TGFBR1, EGFR, SGK1, KDR,

TGFBR2, CSF1R, ERBB2, and TRIM28 (Figures 7C,D**).** Here, we have briefly discussed the crucial role kinases play in the pathogenesis of GBM. For example, prior research confirmed that CDKs such as CDK2, 4, and 6 are stimulated in GBM which increases proliferation, radio, and chemoresistance; thus, inhibiting these will increase chemosensitivity to TMZ (Wang et al., 2016; Cao et al., 2020). Enhanced BUB1/BUB1B expression encourages growth and proliferation, whereas TRIM28 induces GBM cells to go into an autophagic phase and is associated with a bad prognosis for GBM patients (Peng et al., 2019; Long et al., 2021). Additionally, AURKA inhibits FOXM1 ubiquitination and increases the development of GBM (Zhang P. et al., 2022). While ERBB2, a member of the EGF receptor family, regulates glioma cell proliferation, immunological response, and activation of downstream signaling cascades (Mei et al., 2021). Other studies demonstrated that around 60% of initial GBMs have EGFR amplification, and 23% of classical tumors have a particular EGFR-III mutation, which makes them excellent candidates for therapeutic intervention. In contrast, a recent study investigated how EGFR functions as a tumor suppressor in EGFR-amplified GBM that is controlled by EGFR ligands (Xu et al., 2017; Guo et al., 2022).

4 Conclusion

Together, our investigations offer fresh insights into the expression of secretory components and their prognostic significance in the pathogenesis of the GBM microenvironment. In GBM patient samples, 8 elevated biomarkers, such as BMP1, CTSB, LOX, LOXL1, PLOD1, MMP9, SERPINE1, and SERPING1, were linked to poor prognosis in patients, and only BMP1, HIF1A, and TNFRSF1B, have been identified as substrates involved in the ubiquitination process corresponding E3 ligases. Only E3 ligase VHL and GNB2L1 recognize HIF1A was highly expressed after mRNA and protein levels were analyzed for expression. Interestingly, we found that the E2s Ube2C, Ube2E1, Ube2H, Ube2J2, Ube2L6, and Ube2S are highly expressed in GBM. After that, the correlation between E2s and VHL and GNB2L1 revealed a positive connection between VHL and Ube2E1, Ube2H, and Ube2J2 and GNB2L1 and Ube2C, Ube2J2, and Ube2S. Similarly, there was a significant association between VHL, and GNB2L1 with HIF1A. In addition, we have discovered all potential acetylation sites on the lysine residue of the E2s: UBE2C (12), Ube2E1 (15), Ube2H (13), Ube2J2 (15), and Ube2S (16). Only five E2s have confidence scores ≥2.5: K33 of Ube2C, K43 of Ube2E1, K8 and K52 of Ube2H, K64 and K88 of Ube2J2, and K198, K210, K211, K215, and K216.

According to the mutational analysis results, the acetylation site is lost due to a mutation at K33 of Ube2C or K8 of Ube2H with Q, L, R, or L. The Ube2S mutation causes the lack of acetylation at the corresponding "K" residue at K198 and K211 with L; at K210 and K216 with L, Q, and E; and K215 with L and Q. We have also discovered HATs enzymes that attack acetylated lysine residues in E2s. In GBM patient samples, we found that HAT1 positively correlated with the Ube2E1, Ube2H, Ube2J2, and Ube2S enzymes. In contrast, there is no correlation between HAT1 and Ube2C in GBM patient samples. Our study revealed that only HAT1 is overexpressed in GBM patient samples among the eight HAT enzymes. HAT1's role as an oncogene is well known, and solid tumors, including esophageal, lung, liver, and pancreatic cancer, have been shown to overexpress the gene (Wu et al., 2019). After analyzing and collating all of the data from the study, we identified two pathways, one of which targeted either of the proteins' components and the other, which was significantly active in GBM. HAT1-Ube2S(K211)-GNB2L1/HIF1A-BMP1/CTSB/LOX/LOXL1/PLOD1/SERPINE1 and HAT1-UbeH(K8)-VHL-HIF1A-BMP1/CTSB/LOX/LOXL1/PLOD1/SERPINE1 had high and medium confidence scores, respectively. HAT1 enzymes acetylate Ube2S's 211-position lysine residue, increasing GNB2L1's protein turnover while decreasing its ability to ubiquitinate its substrate HIF1A. This causes HIF1A to accumulate and overexpress itself in GBM. Being a transcription factor, HIF1A also controls the expression of BMP1, CTSB, LOX, LOXL1, PLOD1, and SERPINE1 indicators of poor prognosis in GBM. Major biological processes regulated by our identified axis were hypoxia, angiogenesis, ECM structure and degradation, EMT, IFN response, and TGF and TNF signaling. These signaling processes are essential to the pathophysiology of GBM. Therefore, we could target these cellular processes and reduce tumor burden by focusing on our identified therapeutic axis. We have also discovered the predictive markers CTSB and VHL for TMZ therapy, GNB2L1 for topoisomerase inhibitor therapy, Ube2H and HAT1 for TMZ and chemotherapy. HAT1 is also a hazard to angiogenesis inhibitors. The top 10 mutations already identified in GBM have been used to study alterations in the expression level of our therapeutic axis. Our work sheds light on the potential to investigate the use of secretory microenvironmental components in focusing on the GBM microenvironment. We have also demonstrated the protein-protein interaction between E2s with kinases and showed that the proposed E2s Ube2S interact with 8 kinases including CDK2, AURKB, BUB1B, PLK1, NEK2, AURKA, CDK1, MAP3K1 whereas Ube2H interact only with TRIM28 kinases. Thus, using computational and machine-learning-based tools and webservers to anticipate acetylation sites of E2s greatly facilitates the study of acetylation and saves valuable research time. More research and scientific studies are required to explore non-cellular components of the GBM microenvironment, PTM, especially acetylation, and E2s. However, the current study is accompanied by limitations, such as the small number of patient samples, *in vitro* and *in vivo* validation of biomarkers and acetylation sites, and lack of predictive biomarkers, substrates, and signaling molecules expression in GBM. Although, despite a computational study, the current study aims to bridge the gap between GBM, biomarkers, acetylation, and ubiquitination enzymes. The study opens the way for the researchers to validate the identified biomarkers in GBM therapeutics. Further, *in vitro* or *in vivo* validation of acetylating sites and ubiquitination factors (E3 ligases and E2 enzymes) through proteomic studies will lead to enhanced GBM therapeutics, which might cause an increased overall survival rate. Additionally, validation of identified therapeutic axis will have the potential to reverse the GBM etiology or help in drug discovery and development.

Data availability statement

The original contributions presented in the study are included in the article/Supplementary Material, further inquiries can be directed to the corresponding author.

Author contributions

PK and SK conceived and designed the manuscript. SK collected, analyzed, and critically evaluated these data. SK prepared the figures and tables. PK and SK analyzed the entire data and wrote the manuscript. All authors contributed to the article and approved the submitted version.

Funding

SK has received Senior Research Fellowship (SRF) from the Department of Biotechnology (DBT), Govt. of India (Fellow ID: DBT/2019/DTU/1308).

Acknowledgments

We would like to thank the senior management of Delhi Technological University (DTU) and the Department of Biotechnology (DBT), Government of India, for their constant support and financial assistance.

Conflict of interest

The authors declare that the research was conducted in the absence of any commercial or financial relationships that could be construed as a potential conflict of interest.

Publisher's note

All claims expressed in this article are solely those of the authors and do not necessarily represent those of their affiliated organizations, or those of the publisher, the editors and the reviewers. Any product that may be evaluated in this article, or claim that may be made by its manufacturer, is not guaranteed or endorsed by the publisher.

Supplementary material

The Supplementary Material for this article can be found online at: https://www.frontiersin.org/articles/10.3389/fcell.2023.1236271/full#supplementary-material

References

Adzhubei, I. A., Schmidt, S., Peshkin, L., Ramensky, V. E., Gerasimova, A., Bork, P., et al. (2010). A method and server for predicting damaging missense mutations. *Nat. Methods* 7, 248–249. doi:10.1038/NMETH0410-248

Aga, M., Bentz, G. L., Raffa, S., Torrisi, M. R., Kondo, S., Wakisaka, N., et al. (2014). Exosomal HIF1α supports invasive potential of nasopharyngeal carcinoma-associated LMP1-positive exosomes. *Oncogene* 33 (37), 4613–4622. doi:10.1038/onc.2014.66

Alaei, S. R., Abrams, C. K., Bulinski, J. C., Hertzberg, E. L., and Freidin, M. M. (2018). Acetylation of C-terminal lysines modulates protein turnover and stability of Connexin-32. *BMC Cell Biol.* 19, 22–15. doi:10.1186/s12860-018-0173-0

Alexandru, O., Horescu, C., Sevastre, A. S., Cioc, C. E., Baloi, C., Oprita, A., et al. (2020). Receptor tyrosine kinase targeting in glioblastoma: Performance, limitations and future approaches. *Wspolczesna Onkol.* 24, 55–66. doi:10.5114/wo.2020.94726

Azimi, I., Petersen, R. M., Thompson, E. W., Roberts-Thomson, S. J., and Monteith, G. R. (2017). Hypoxia-induced reactive oxygen species mediate N-cadherin and SERPINE1 expression, EGFR signalling and motility in MDA-MB-468 breast cancer cells. *Sci. Rep.* 7, 15140. doi:10.1038/S41598-017-15474-7

Baghban, R., Roshangar, L., Jahanban-Esfahlan, R., Seidi, K., Ebrahimi-Kalan, A., Jaymand, M., et al. (2020). Tumor microenvironment complexity and therapeutic implications at a glance. *Cell Commun. Signal.* 18, 59. doi:10.1186/S12964-020-0530-4

Bateman, A., Martin, M. J., O'Donovan, C., Magrane, M., Alpi, E., Antunes, R., et al. (2017). UniProt: The universal protein knowledgebase. *Nucleic Acids Res.* 45, D158–D169. doi:10.1093/NAR/GKW1099

Bensaad, K., Favaro, E., Lewis, C. A., Peck, B., Lord, S., Collins, J. M., et al. (2014). Fatty acid uptake and lipid storage induced by HIF-1α contribute to cell growth and survival after hypoxia-reoxygenation. *Cell Rep.* 9, 349–365. doi:10.1016/J.CELREP.2014.08.056

Bowman, R. L., Wang, Q., Carro, A., Verhaak, R. G. W., and Squatrito, M. (2017). GlioVis data portal for visualization and analysis of brain tumor expression datasets. *Neuro. Oncol.* 19, 139–141. doi:10.1093/NEUONC/NOW247

Bridge, J. A., Lee, J. C., Daud, A., Wells, J. W., and Bluestone, J. A. (2018). Cytokines, chemokines, and other biomarkers of response for checkpoint inhibitor therapy in skin cancer. *Front. Med.* 5, 351. doi:10.3389/FMED.2018.00351

Buchan, D. W. A., and Jones, D. T. (2019). The PSIPRED protein analysis workbench: 20 years on. *Nucleic Acids Res.* 47, W402–W407. doi:10.1093/NAR/GKZ297

Cao, Y., Li, X., Kong, S., Shang, S., and Qi, Y. (2020). CDK4/6 inhibition suppresses tumour growth and enhances the effect of temozolomide in glioma cells. *J. Cell. Mol. Med.* 24, 5135–5145. doi:10.1111/jcmm.15156

Chen, E. Y., Tan, C. M., Kou, Y., Duan, Q., Wang, Z., Meirelles, G. V., et al. (2013). Enrichr: Interactive and collaborative HTML5 gene list enrichment analysis tool. *BMC Bioinforma.* 14, 128–214. doi:10.1186/1471-2105-14-128

Chen, N., Peng, C., and Li, D. (2022). Epigenetic underpinnings of inflammation: A key to unlock the tumor microenvironment in glioblastoma. *Front. Immunol.* 13, 869307–869311. doi:10.3389/fimmu.2022.869307

Choi, J. Y., Jang, Y. S., Min, S. Y., and Song, J. Y. (2011). Overexpression of MMP-9 and hif-1α in breast cancer cells under hypoxic conditions. *J. Breast Cancer* 14, 88–95. doi:10.4048/jbc.2011.14.2.88

Christensen, D. G., Baumgartner, J. T., Xie, X., Jew, K. M., Basisty, N., Schilling, B., et al. (2019a). Mechanisms, detection, and relevance of protein acetylation in prokaryotes. *MBio* 10, e02708–e02718. doi:10.1128/mBio.02708-18

Christensen, D. G., Xie, X., Basisty, N., Byrnes, J., McSweeney, S., Schilling, B., et al. (2019b). Post-translational Protein Acetylation: An elegant mechanism for bacteria to dynamically regulate metabolic functions. *Front. Microbiol.* 10, 1604. doi:10.3389/fmicb.2019.01604

Da Silva, R., Uno, M., Nagahashi Marie, S. K., and Oba-Shinjo, S. M. (2015). LOX expression and functional analysis in astrocytomas and impact of IDH1 mutation. *PLoS One* 10, e0119781. doi:10.1371/JOURNAL.PONE.0119781

Dahlberg, D., Rummel, J., Distante, S., De Souza, G. A., Stensland, M. E., Mariussen, E., et al. (2022). Glioblastoma microenvironment contains multiple hormonal and non-hormonal growth-stimulating factors. *Fluids Barriers CNS* 19, 45–11. doi:10.1186/S12987-022-00333-Z

Dai, Z., Wu, J., Chen, F., Cheng, Q., Zhang, M., Wang, Y., et al. (2016). CXCL5 promotes the proliferation and migration of glioma cells in autocrine- and paracrine-dependent manners. *Oncol. Rep.* 36, 3303–3310. doi:10.3892/or.2016.5155

Dai, X., Ye, L., Li, H., Dong, X., Tian, H., Gao, P., et al. (2023). Crosstalk between microglia and neural stem cells influences the relapse of glioblastoma in GBM immunological microenvironment. *Clin. Immunol.* 251, 109333. doi:10.1016/J.CLIM.2023.109333

De Oliveira Rosario, L. V., Da Rosa, B. G., Goncalves, T. L., Matias, D. I. L., Freitas, C., and Ferrer, V. P. (2020). Glioblastoma factors increase the migration of human brain endothelial cells *in vitro* by increasing MMP-9/CXCR4 levels. *Anticancer Res.* 40, 2725–2737. doi:10.21873/anticanres.14244

Deng, W., Wang, C., Zhang, Y., Xu, Y., Zhang, S., Liu, Z., et al. (2016). GPS-PAIL: Prediction of lysine acetyltransferase-specific modification sites from protein sequences. *Sci. Rep.* 6, 39787–39810. doi:10.1038/srep39787

Ding, X., Zhang, C., Chen, H., Ren, M., and Liu, X. (2022). Cathepsins trigger cell death and regulate radioresistance in glioblastoma. *Cells* 11, 4108. doi:10.3390/cells11244108

Domènech, M., Hernández, A., Plaja, A., Martínez-balibrea, E., and Balañà, C. (2021). Hypoxia: The cornerstone of glioblastoma. *Int. J. Mol. Sci.* 22, 12608. doi:10.3390/ijms222212608

Dong, H., Wang, Q., Li, N., Lv, J., Ge, L., Yang, M., et al. (2020). OSgbm: An online consensus survival analysis web server for glioblastoma. *Front. Genet.* 10, 1378. doi:10.3389/fgene.2019.01378

Eid, S., Turk, S., Volkamer, A., Rippmann, F., and Fulle, S. (2017). Kinmap: A web-based tool for interactive navigation through human kinome data. *BMC Bioinforma.* 18, 16–6. doi:10.1186/s12859-016-1433-7

Ellert-Miklaszewska, A., Poleszak, K., Pasierbinska, M., and Kaminska, B. (2020). Integrin signaling in glioma pathogenesis: From biology to therapy. *Int. J. Mol. Sci.* 21, 888. doi:10.3390/IJMS21030888

Fitzgerald, W., Freeman, M. L., Lederman, M. M., Vasilieva, E., Romero, R., and Margolis, L. (2018). A system of cytokines encapsulated in ExtraCellular vesicles. *Sci. Rep.* 8, 8973. doi:10.1038/S41598-018-27190-X

Fiumara, F., Fioriti, L., Kandel, E. R., and Hendrickson, W. A. (2010). Essential role of coiled coils for aggregation and activity of Q/N-rich prions and PolyQ proteins. *Cell* 143, 1121–1135. doi:10.1016/J.CELL.2010.11.042

Frei, K., Gramatzki, D., Tritschler, I., Schroeder, J. J., Espinoza, L., Rushing, E. J., et al. (2015). Transforming growth factor-β pathway activity in glioblastoma. *Oncotarget* 6, 5963–5977. doi:10.18632/ONCOTARGET.3467

Gallego-Perez, D., Chang, L., Shi, J., Ma, J., Kim, S. H., Zhao, X., et al. (2016). On-chip clonal analysis of glioma-stem-cell motility and therapy resistance. *Nano Lett.* 16, 5326–5332. doi:10.1021/ACS.NANOLETT.6B00902

Gao, T., Liu, Z., Wang, Y., Cheng, H., Yang, Q., Guo, A., et al. (2013). UUCD: A family-based database of ubiquitin and ubiquitin-like conjugation. *Nucleic Acids Res.* 41, D445–D451. doi:10.1093/NAR/GKS1103

Gao, W., Li, Y., Zhang, T., Lu, J., Pan, J., Qi, Q., et al. (2022). Systematic analysis of chemokines reveals CCL18 is a prognostic biomarker in glioblastoma. *J. Inflamm. Res.* 15, 2731–2743. doi:10.2147/JIR.S357787

Goldman, M. J., Craft, B., Hastie, M., Repečka, K., McDade, F., Kamath, A., et al. (2020). Visualizing and interpreting cancer genomics data via the Xena platform. *Nat. Biotechnol.* 38, 675–678. doi:10.1038/s41587-020-0546-8

Gravendeel, L. A. M., Kouwenhoven, M. C. M., Gevaert, O., De Rooi, J. J., Stubbs, A. P., Duijm, J. E., et al. (2009). Intrinsic gene expression profiles of gliomas are a better predictor of survival than histology. *Cancer Res.* 69, 9065–9072. doi:10.1158/0008-5472.CAN-09-2307

Guo, G., Gong, K., Beckley, N., Zhang, Y., Yang, X., Chkheidze, R., et al. (2022). EGFR ligand shifts the role of EGFR from oncogene to tumour suppressor in EGFR-amplified glioblastoma by suppressing invasion through BIN3 upregulation. *Nat. Cell Biol.* 24 (8), 1291–1305. doi:10.1038/s41556-022-00962-4

Gurgis, F. M. S., Yeung, Y. T., Tang, M. X. M., Heng, B., Buckland, M., Ammit, A. J., et al. (2015). The p38-MK2-HuR pathway potentiates EGFRvIII-IL-1β-driven IL-6 secretion in glioblastoma cells. *Oncogene* 34, 2934–2942. doi:10.1038/ONC.2014.225

Han, J., Jing, Y., Han, F., and Sun, P. (2021). Comprehensive analysis of expression, prognosis and immune infiltration for TIMPs in glioblastoma. *BMC Neurol.* 21, 447–515. doi:10.1186/s12883-021-02477-1

Hattermann, K., Held-Feindt, J., Ludwig, A., and Mentlein, R. (2013). The CXCL16-CXCR6 chemokine axis in glial tumors. *J. Neuroimmunol.* 260, 47–54. doi:10.1016/J.JNEUROIM.2013.04.006

Hecht, M., Bromberg, Y., and Rost, B. (2015). Better prediction of functional effects for sequence variants. *BMC Genomics* 16, S1. doi:10.1186/1471-2164-16-S8-S1

Hu, X., Bao, M., Huang, J., Zhou, L., and Zheng, S. (2020). Identification and validation of novel biomarkers for diagnosis and prognosis of hepatocellular carcinoma. *Front. Oncol.* 10, 541479. doi:10.3389/FONC.2020.541479

Hwang, C. S., Shemorry, A., and Varshavsky, A. (2010). N-terminal acetylation of cellular proteins creates specific degradation signals. *Science* 327, 973–977. doi:10.1126/SCIENCE.1183147

Jeong, J. W., Bae, M. K., Ahn, M. Y., Kim, S. H., Sohn, T. K., Bae, M. H., et al. (2002). Regulation and destabilization of HIF-1alpha by ARD1-mediated acetylation. *Cell* 111, 709–720. doi:10.1016/S0092-8674(02)01085-1

Jia, D., Li, S., Li, D., Xue, H., Yang, D., and Liu, Y. (2018). Mining TCGA database for genes of prognostic value in glioblastoma microenvironment. *Aging (Albany. NY)* 10, 592–605. doi:10.18632/AGING.101415

Kast, R. E. (2015). The role of interleukin-18 in glioblastoma pathology implies therapeutic potential of two old drugs—Disulfiram and ritonavir. *Chin. J. Cancer* 34, 11–15. doi:10.1186/s40880-015-0010-1

Kaur, B., Khwaja, F. W., Severson, E. A., Matheny, S. L., Brat, D. J., and Van Meir, E. G. (2005). Hypoxia and the hypoxia-inducible-factor pathway in glioma growth and angiogenesis. *Neuro. Oncol.* 7, 134–153. doi:10.1215/S1152851704001115

Kim, G., and Ko, Y. T. (2020). Small molecule tyrosine kinase inhibitors in glioblastoma. *Arch. Pharm. Res.* 43, 385–394. doi:10.1007/s12272-020-01232-3

Kim, E., Zschiedrich, S., Kang, E. Y., and Seo, B. K. (2018). Value of transluminal attenuation gradient of stress CCTA for diagnosis of haemodynamically significant coronary artery stenosis using wide-area detector CT in patients with coronary artery disease: Comparison with stress perfusion CMR. *Front. Pediatr.* 6, 16–21. doi:10.5830/CVJA-2017-026

Korbecki, J., Bajdak-Rusinek, K., Kupnicka, P., Kapczuk, P., Simińska, D., Chlubek, D., et al. (2021). The role of CXCL16 in the pathogenesis of cancer and other diseases. *Int. J. Mol. Sci.* 22, 3490. doi:10.3390/IJMS22073490

Kucharzewska, P., Christianson, H. C., Welch, J. E., Svensson, K. J., Fredlund, E., Ringnér, M., et al. (2013). Exosomes reflect the hypoxic status of glioma cells and mediate hypoxia-dependent activation of vascular cells during tumor development. *Proc. Natl. Acad. Sci. U. S. A.* 110, 7312–7317. doi:10.1073/pnas.1220998110

Kuleshov, M. V., Jones, M. R., Rouillard, A. D., Fernandez, N. F., Duan, Q., Wang, Z., et al. (2016). Enrichr: A comprehensive gene set enrichment analysis web server 2016 update. *Nucleic Acids Res.* 44, W90–W97. doi:10.1093/NAR/GKW377

Lacoursiere, R. E., and Shaw, G. S. (2021). Acetylated ubiquitin modulates the catalytic activity of the E1 enzyme Uba1. *Biochemistry* 60 (16), 1276–1285. doi:10.1021/acs.biochem.1c00145

Lacoursiere, R. E., Hadi, D., and Shaw, G. S. (2022). Acetylation, phosphorylation, ubiquitination (oh my!): Following post-translational modifications on the ubiquitin Road. *Biomolecules* 12, 467. doi:10.3390/BIOM12030467

Langhans, J., Schneele, L., Trenkler, N., Von Bandemer, H., Nonnenmacher, L., Karpel-Massler, G., et al. (2017). The effects of PI3K-mediated signalling on glioblastoma cell behaviour. *Oncogenesis* 6, 398. doi:10.1038/s41389-017-0004-8

Li, T., Fu, J., Zeng, Z., Cohen, D., Li, J., Chen, Q., et al. (2020). TIMER2.0 for analysis of tumor-infiltrating immune cells. *Nucleic Acids Res.* 48, W509–W514. doi:10.1093/NAR/GKAA407

Li, Z., Chen, S., Jhong, J. H., Pang, Y., Huang, K. Y., Li, S., et al. (2021). UbiNet 2.0: A verified, classified, annotated and updated database of E3 ubiquitin ligase–substrate interactions. *Database J. Biol. Databases Curation* 2021, baab010. doi:10.1093/DATABASE/BAAB010

Li, X., Wang, Y., Wu, W., Xiang, J., Qi, L., Wang, N., et al. (2022). A novel risk score model based on eleven extracellular matrix-related genes for predicting overall survival of glioma patients. *J. Oncol.* 2022, 4966820. doi:10.1155/2022/4966820

Lim, K. H., and Joo, J. Y. (2020). Predictive potential of circulating Ube2h mRNA as an E2 ubiquitin-conjugating enzyme for diagnosis or treatment of Alzheimer's disease. *Int. J. Mol. Sci.* 21, 3398. doi:10.3390/ijms21093398

Lin, B., Madan, A., Yoon, J. G., Fang, X., Yan, X., Kim, T. K., et al. (2010). Massively parallel signature sequencing and bioinformatics analysis identifies up-regulation of TGFBI and SOX4 in human glioblastoma. *PLoS One* 5, e10210. doi:10.1371/journal.pone.0010210

Liu, A., Hou, C., Chen, H., Zong, X., and Zong, P. (2016a). Genetics and epigenetics of glioblastoma: Applications and overall incidence of IDH1 mutation. *Front. Oncol.* 6, 16. doi:10.3389/FONC.2016.00016

Liu, J., Qian, C., and Cao, X. (2016b). Post-translational modification control of innate immunity. *Immunity* 45, 15–30. doi:10.1016/J.IMMUNI.2016.06.020

Liu, C., Chu, D., Kalantar-Zadeh, K., George, J., Young, H. A., and Liu, G. (2021a). Cytokines: From clinical significance to quantification. *Adv. Sci.* 8, 2004433. doi:10.1002/ADVS.202004433

Liu, Z., Zhang, H., Hu, H., Cai, Z., Lu, C., Liang, Q., et al. (2021b). Electrical characterizations of planar Ga_2O_3 Schottky barrier diodes. *Front. Genet.* 12, 259. doi:10.3390/mi12030259

Liu, X., Guo, C., Leng, T., Fan, Z., Mai, J., Chen, J., et al. (2023). Differential regulation of H3K9/H3K14 acetylation by small molecules drives neuron-fate-induction of glioma cell. *Cell Death Dis.* 14, 142. doi:10.1038/s41419-023-05611-8

Long, Z., Wu, T., Tian, Q., Carlson, L. A., Wang, W., and Wu, G. (2021). Expression and prognosis analyses of BUB1, BUB1B and BUB3 in human sarcoma. *Aging (Albany. NY)* 13, 12395–12409. doi:10.18632/aging.202944

López-Ferrando, V., Gazzo, A., De La Cruz, X., Orozco, M., and Gelpí, J. L. (2017). PMut: A web-based tool for the annotation of pathological variants on proteins, 2017 update. *Nucleic Acids Res.* 45, W222–W228. doi:10.1093/NAR/GKX313

Ma, R., Kang, X., Zhang, G., Fang, F., Du, Y., and Lv, H. (2016). High expression of UBE2C is associated with the aggressive progression and poor outcome of malignant glioma. *Oncol. Lett.* 11, 2300–2304. doi:10.3892/ol.2016.4171

Ma, K., Chen, X., Liu, W., Chen, S., Yang, C., and Yang, J. (2022). CTSB is a negative prognostic biomarker and therapeutic target associated with immune cells infiltration and immunosuppression in gliomas. *Sci. Rep.* 12, 4295. doi:10.1038/s41598-022-08346-2

Madhavan, S., Zenklusen, J. C., Kotliarov, Y., Sahni, H., Fine, H. A., and Buetow, K. (2009). Rembrandt: Helping personalized medicine become a reality through integrative translational research. *Mol. Cancer Res.* 7, 157–167. doi:10.1158/1541-7786.MCR-08-0435

Maksoud, S. (2021). The role of the ubiquitin proteasome system in glioma: Analysis emphasizing the main molecular players and therapeutic strategies identified in glioblastoma multiforme. *Mol. Neurobiol.* 58, 3252–3269. doi:10.1007/S12035-021-02339-4

Masliantsev, K., Karayan-tapon, L., and Guichet, P. O. (2021). Hippo signaling pathway in gliomas. *Cells* 10, 184–214. doi:10.3390/CELLS10010184

McCornack, C., Woodiwiss, T., Hardi, A., Yano, H., and Kim, A. H. (2023). The function of histone methylation and acetylation regulators in GBM pathophysiology. *Front. Oncol.* 13, 1144184–1144218. doi:10.3389/fonc.2023.1144184

Mei, J., Wang, T., Xu, R., Chen, D., and Zhang, Y. (2021). Clinical and molecular immune characterization of ERBB2 in glioma. *Int. Immunopharmacol.* 94, 107499. doi:10.1016/J.INTIMP.2021.107499

Menyhárt, O., Fekete, J. T., and Gyorffy, B. (2021). Gene expression-based biomarkers designating glioblastomas resistant to multiple treatment strategies. *Carcinogenesis* 42, 804–813. doi:10.1093/CARCIN/BGAB024

Mészáros, B., Hajdu-soltész, B., Zeke, A., and Dosztányi, Z. (2021). Mutations of intrinsically disordered protein regions can drive cancer but lack therapeutic strategies. *Biomolecules* 11, 381–422. doi:10.3390/BIOM11030381

Miller, K. D., Ostrom, Q. T., Kruchko, C., Patil, N., Tihan, T., Cioffi, G., et al. (2021). Brain and other central nervous system tumor statistics, 2021. *Ca. Cancer J. Clin.* 71, 381–406. doi:10.3322/CAAC.21693

Narasumani, M., and Harrison, P. M. (2018). Discerning evolutionary trends in post-translational modification and the effect of intrinsic disorder: Analysis of methylation, acetylation and ubiquitination sites in human proteins. doi:10.1371/journal.pcbi.1006349

Narita, T., Weinert, B. T., and Choudhary, C. (2019). Functions and mechanisms of non-histone protein acetylation. *Nat. Rev. Mol. Cell Biol.* 20, 156–174. doi:10.1038/S41580-018-0081-3

OSppc (2022). OSppc: A web server for online survival analysis using proteome of pan-cancers. doi:10.1016/j.jprot.2022.104810

Pan, Z., Bao, J., Zhang, L., and Wei, S. (2021). UBE2D3 activates SHP-2 ubiquitination to promote glycolysis and proliferation of glioma via regulating STAT3 signaling pathway. *Front. Oncol.* 11, 2081. doi:10.3389/fonc.2021.674286

Pang, K., Wang, W., Qin, J. X., Shi, Z. D., Hao, L., Ma, Y. Y., et al. (2022). Role of protein phosphorylation in cell signaling, disease, and the intervention therapy. *MedComm* 3, 1755–e228. doi:10.1002/mco2.175

Patel, H., Nilendu, P., Jahagirdar, D., Pal, J. K., and Sharma, N. K. (2018). Modulating secreted components of tumor microenvironment: A masterstroke in tumor therapeutics. *Cancer Biol. Ther.* 19, 3–12. doi:10.1080/15384047.2017.1394538

Pathan, M., Keerthikumar, S., Ang, C. S., Gangoda, L., Quek, C. Y. J., Williamson, N. A., et al. (2015). FunRich: An open access standalone functional enrichment and interaction network analysis tool. *Proteomics* 15, 2597–2601. doi:10.1002/PMIC.201400515

Pejaver, V., Urresti, J., Lugo-Martinez, J., Pagel, K. A., Lin, G. N., Nam, H. J., et al. (2020). Inferring the molecular and phenotypic impact of amino acid variants with MutPred2. *Nat. Commun.* 11, 5918–6013. doi:10.1038/s41467-020-19669-x

Peng, S., Du, T., Wu, W., Chen, X., Lai, Y., Zhu, D., et al. (2018). Decreased expression of serine protease inhibitor family G1 (SERPING1) in prostate cancer can help distinguish high-risk prostate cancer and predicts malignant progression. *Urol. Oncol. Semin. Orig. Investig.* 36, 366.e1–366.e9. doi:10.1016/J.UROLONC.2018.05.021

Peng, Y., Zhang, M., Jiang, Z., and Jiang, Y. (2019). TRIM28 activates autophagy and promotes cell proliferation in glioblastoma. *Onco. Targets. Ther.* 12, 397–404. doi:10.2147/OTT.S188101

Pointer, K. B., Clark, P. A., Schroeder, A. B., Shahriar, M., Eliceiri, K. W., and Kuo, J. S. (2017). Association of collagen architecture with glioblastoma patient survival. *J. Neurosurg.* 126, 1812–1821. doi:10.3171/2016.6.JNS152797

Ramaiah, M. J., and Kumar, K. R. (2021). mTOR-Rictor-EGFR axis in oncogenesis and diagnosis of glioblastoma multiforme. *Mol. Biol. Rep.* 48, 4813–4835. doi:10.1007/s11033-021-06462-2

Ramaswamy, P., Goswami, K., Dalavaikodihalli Nanjaiah, N., Srinivas, D., and Prasad, C. (2019). TNF-α mediated MEK–ERK signaling in invasion with putative network involving NF-κB and STAT-6: A new perspective in glioma. *Cell Biol. Int.* 43, 1257–1266. doi:10.1002/CBIN.11125

Sachdeva, R., Wu, M., Johnson, K., Kim, H., Celebre, A., Shahzad, U., et al. (2019). BMP signaling mediates glioma stem cell quiescence and confers treatment resistance in glioblastoma. *Sci. Rep.* 9, 14569–14614. doi:10.1038/s41598-019-51270-1

Seker, F., Cingoz, A., Sur-Erdem, I., Erguder, N., Erkent, A., Uyulur, F., et al. (2019). Identification of SERPINE1 as a regulator of glioblastoma cell dispersal with transcriptome profiling. *Cancers(Basel).* 11, 1651. doi:10.3390/cancers11111651

Shen, T., Cai, L. D., Liu, Y. H., Li, S., Gan, W. J., Li, X. M., et al. (2018). Ube2v1-mediated ubiquitination and degradation of Sirt1 promotes metastasis of colorectal cancer by epigenetically suppressing autophagy. *J. Hematol. Oncol.* 11, 95–16. doi:10.1186/s13045-018-0638-9

Shin, U., Choi, Y., Ko, H. S., Myung, K., Lee, S., Cheon, C. K., et al. (2023). A heterozygous mutation in UBE2H in a patient with developmental delay leads to an aberrant brain development in zebrafish. *Hum. Genomics* 17, 44. doi:10.1186/s40246-023-00491-7

Singh, B. N., Zhang, G., Hwa, Y. L., Li, J., Dowdy, S. C., and Jiang, S. W. (2010). Nonhistone protein acetylation as cancer therapy targets. *Expert Rev. Anticancer Ther.* 10, 935–954. doi:10.1586/ERA.10.62

Spange, S., Wagner, T., Heinzel, T., and Krämer, O. H. (2009). Acetylation of non-histone proteins modulates cellular signalling at multiple levels. *Int. J. Biochem. Cell Biol.* 41, 185–198. doi:10.1016/J.BIOCEL.2008.08.027

Sterner, D. E., and Berger, S. L. (2000). Acetylation of histones and transcription-related factors. *Microbiol. Mol. Biol. Rev.* 64, 435–459. doi:10.1128/MMBR.64.2.435-459.2000

Stewart, M. D., Ritterhoff, T., Klevit, R. E., and Brzovic, P. S. (2016). E2 enzymes: More than just middle men. *Cell Res.* 26, 423–440. doi:10.1038/CR.2016.35

Sun, X. J., Man, N., Tan, Y., Nimer, S. D., and Wang, L. (2015). The role of histone acetyltransferases in normal and malignant hematopoiesis. *Front. Oncol.* 5, 108. doi:10.3389/fonc.2015.00108

Szklarczyk, D., Gable, A. L., Nastou, K. C., Lyon, D., Kirsch, R., Pyysalo, S., et al. (2021). The STRING database in 2021: Customizable protein–protein networks, and functional characterization of user-uploaded gene/measurement sets. *Nucleic Acids Res.* 49, D605–D612. doi:10.1093/NAR/GKAA1074

Takacs, G. P., Flores-Toro, J. A., and Harrison, J. K. (2021). Modulation of the chemokine/chemokine receptor axis as a novel approach for glioma therapy. *Pharmacol. Ther.* 222, 107790. doi:10.1016/J.PHARMTHERA.2020.107790

Tang, Z., Kang, B., Li, C., Chen, T., and Zhang, Z. (2019). GEPIA2: An enhanced web server for large-scale expression profiling and interactive analysis. *Nucleic Acids Res.* 47, W556–W560. doi:10.1093/NAR/GKZ430

Tang, Y., Qing, C., Wang, J., and Zeng, Z. (2020). DNA methylation-based diagnostic and prognostic biomarkers for glioblastoma. *Cell Transpl.* 29, 963689720933241. doi:10.1177/0963689720933241

Tanimoto, K., Makino, Y., Pereira, T., and Poellinger, L. (2000). Mechanism of regulation of the hypoxia-inducible factor-1 alpha by the von Hippel-Lindau tumor suppressor protein. *EMBO J.* 19, 4298–4309. doi:10.1093/EMBOJ/19.16.4298

Ullah, F., Khurshid, N., Fatimi, Q., Loidl, P., and Saeed, M. (2022). Mutations in the acetylation hotspots of Rbl2 are associated with increased risk of breast cancer. *PLoS One* 17, e0266196. doi:10.1371/JOURNAL.PONE.0266196

Vanheule, V., Metzemaekers, M., Janssens, R., Struyf, S., and Proost, P. (2018). How post-translational modifications influence the biological activity of chemokines. *Cytokine* 109, 29–51. doi:10.1016/J.CYTO.2018.02.026

Varshavsky, A. (2019). N-degron and C-degron pathways of protein degradation. *Proc. Natl. Acad. Sci. U. S. A.* 116, 358–366. doi:10.1073/pnas.1816596116

Wang, X., Taplick, J., Geva, N., and Oren, M. (2004). Inhibition of p53 degradation by Mdm2 acetylation. *FEBS Lett.* 561, 195–201. doi:10.1016/S0014-5793(04)00168-1

Wang, J., Yang, T., Xu, G., Liu, H., Ren, C., Xie, W., et al. (2016). Cyclin-dependent kinase 2 promotes tumor proliferation and induces radio resistance in glioblastoma. *Transl. Oncol.* 9, 548–556. doi:10.1016/j.tranon.2016.08.007

Wang, H., Luo, W., and Dai, L. (2020). Expression and prognostic role of PLOD1 in malignant glioma. *Onco. Targets. Ther.* 13, 13285–13297. doi:10.2147/OTT.S265866

Wang, Z., Shi, Y., Ying, C., Jiang, Y., and Hu, J. (2021). Hypoxia-induced PLOD1 overexpression contributes to the malignant phenotype of glioblastoma via NF-κB signaling. *Oncogene* 408, 1458–1475. doi:10.1038/s41388-020-01635-y

Wang, X., Li, Y., He, M., Kong, X., Jiang, P., Liu, X., et al. (2022). UbiBrowser 2.0: A comprehensive resource for proteome-wide known and predicted ubiquitin ligase/deubiquitinase–substrate interactions in eukaryotic species. *Nucleic Acids Res.* 50, D719–D728. doi:10.1093/NAR/GKAB962

Wei, Q., Singh, O., Ekinci, C., Gill, J., Li, M., Mamatjan, Y., et al. (2021). TNFα secreted by glioma associated macrophages promotes endothelial activation and resistance against anti-angiogenic therapy. *Acta Neuropathol. Commun.* 9, 1–19. doi:10.1186/S40478-021-01163-0/FIGURES/6

Wu, H., Fan, P., Zhao, J., Meng, Z., Wu, H., Wang, B., et al. (2019). Overexpressed histone acetyltransferase 1 regulates cancer immunity by increasing programmed death-ligand 1 expression in pancreatic cancer. *J. Exp. Clin. Cancer Res.* 38, 47–12. doi:10.1186/s13046-019-1044-z

Xiang, C., and Yan, H.-C. (2022). Ubiquitin conjugating enzyme E2 C (UBE2C) may play a dual role involved in the progression of thyroid carcinoma. *Cell Death Discov.* 8 (1), 130. doi:10.1038/s41420-022-00935-4

Xiao, W., Wang, X., Wang, T., and Xing, J. (2019). Overexpression of BMP1 reflects poor prognosis in clear cell renal cell carcinoma. *Cancer Gene Ther.* 27, 330–340. doi:10.1038/s41417-019-0107-9

Xiao, K., Tan, J., Yuan, J., Peng, G., Long, W., Su, J., et al. (2020). Prognostic value and immune cell infiltration of hypoxic phenotype-related gene signatures in glioblastoma microenvironment. *J. Cell. Mol. Med.* 24, 13235–13247. doi:10.1111/JCMM.15939

Xiaofei, C., Yanqing, L., Dongkai, Z., Dong, C., Feng, Z., and Weilin, W. (2018). Identification of cathepsin B as a novel target of hypoxia-inducible factor-1-alpha in HepG2 cells. *Biochem. Biophys. Res. Commun.* 503, 1057–1062. doi:10.1016/J.BBRC.2018.06.116

Xie, Q., Xie, J., Tian, T., Ma, Q., Zhang, Q., Zhu, B., et al. (2017). Hypoxia triggers angiogenesis by increasing expression of LOX genes in 3-D culture of ASCs and ECs. *Exp. Cell Res.* 352, 157–163. doi:10.1016/J.YEXCR.2017.02.011

Xu, H., Zong, H., Ma, C., Ming, X., Shang, M., Li, K., et al. (2017). Epidermal growth factor receptor in glioblastoma. *Oncol. Lett.* 14, 512–516. doi:10.3892/ol.2017.6221

Yang, N., Cao, D. F., Yin, X. X., Zhou, H. H., and Mao, X. Y. (2020). Lysyl oxidases: Emerging biomarkers and therapeutic targets for various diseases. *Biomed. Pharmacother.* 131, 110791. doi:10.1016/j.biopha.2020.110791

Yeh, W. L., Lu, D. Y., Liou, H. C., and Fu, W. M. (2012). A forward loop between glioma and microglia: Glioma-derived extracellular matrix-activated microglia secrete IL-18 to enhance the migration of glioma cells. *J. Cell. Physiol.* 227, 558–568. doi:10.1002/JCP.22746

Yekula, A., Yekula, A., Muralidharan, K., Kang, K., Carter, B. S., and Balaj, L. (2020). Extracellular vesicles in glioblastoma tumor microenvironment. *Front. Immunol.* 10, 3137. doi:10.3389/fimmu.2019.03137

Yeo, E. C. F., Brown, M. P., Gargett, T., Ebert, L. M., Beavis, P. A., Guimaraes, F. S. F., et al. (2021). The role of cytokines and chemokines in shaping the immune microenvironment of glioblastoma: Implications for immunotherapy. *Cells* 10, 607. doi:10.3390/CELLS10030607

You, H., Li, Q., Kong, D., Liu, X., Kong, F., Zheng, K., et al. (2022). Label compliance for ingredient verification: Regulations, approaches, and trends for testing botanical products marketed for "immune health" in the United States. *Cell. Mol. Biol. Lett.* 27, 1–20. doi:10.1080/10408398.2022.2124230

Yu, F., White, S. B., Zhao, Q., and Lee, F. S. (2001). HIF-1alpha binding to VHL is regulated by stimulus-sensitive proline hydroxylation. *Proc. Natl. Acad. Sci. U. S. A.* 98, 9630–9635. doi:10.1073/pnas.181341498

Yu, X., Deng, L., Wang, D., Li, N., Chen, X., Cheng, X., et al. (2012). Mechanism of TNF-α autocrine effects in hypoxic cardiomyocytes: Initiated by hypoxia inducible factor 1α, presented by exosomes. *J. Mol. Cell. Cardiol.* 53, 848–857. doi:10.1016/J.YJMCC.2012.10.002

Yu, H., Ding, J., Zhu, H., Jing, Y., Zhou, H., Tian, H., et al. (2020a). LOXL1 confers antiapoptosis and promotes gliomagenesis through stabilizing BAG2. *Cell Death Differ.* 27, 3021–3036. doi:10.1038/s41418-020-0558-4

Yu, K., Zhang, Q., Liu, Z., Du, Y., Gao, X., Zhao, Q., et al. (2020b). Deep learning based prediction of reversible HAT/HDAC-specific lysine acetylation. *Brief. Bioinform.* 21, 1798–1805. doi:10.1093/BIB/BBZ107

Yuan, B., Xu, Y., and Zheng, S. (2022). PLOD1 acts as a tumor promoter in glioma via activation of the HSF1 signaling pathway. *Mol. Cell. Biochem.* 477, 549–557. doi:10.1007/s11010-021-04289-w

Yu-Ju Wu, C., Chen, C. H., Lin, C. Y., Feng, L. Y., Lin, Y. C., Wei, K. C., et al. (2020). CCL5 of glioma-associated microglia/macrophages regulates glioma migration and invasion via calcium-dependent matrix metalloproteinase 2. *Neuro. Oncol.* 22, 253–266. doi:10.1093/neuonc/noz189

Zeren, N., Afzal, Z., Morgan, S., Marshall, G., Uppiliappan, M., Merritt, J., et al. (2023). The chemokine receptor CCR1 mediates microglia stimulated glioma invasion. *Int. J. Mol. Sci.* 24, 5136. doi:10.3390/ijms24065136

Zhang, X., and Yang, Q. (2021). A pyroptosis-related gene panel in prognosis prediction and immune microenvironment of human endometrial cancer. *Front. Cell Dev. Biol.* 9. doi:10.3389/fcell.2021.705828

Zhang, M., Yang, D., and Gold, B. (2019). Origin of mutations in genes associated with human glioblastoma multiform cancer: Random polymerase errors versus deamination. *Heliyon* 5, e01265. doi:10.1016/J.HELIYON.2019.E01265

Zhang, L., Cao, Y., Guo, X., Wang, X., Han, X., Kanwore, K., et al. (2023). Hypoxia-induced ROS aggravate tumor progression through HIF-1α-SERPINE1 signaling in glioblastoma. *J. Zhejiang Univ. Sci. B* 24, 32–49. doi:10.1631/jzus.B2200269

Zhang, P., Chen, X., Zhang, L. Y., Cao, D., Chen, Y., Guo, Z. Q., et al. (2022). POLE2 facilitates the malignant phenotypes of glioblastoma through promoting AURKA-mediated stabilization of FOXM1. *Cell Death Dis.* 13, 61–10. doi:10.1038/s41419-021-04498-7

Zhang, S., Zhong, Y., Wang, L., Yin, X., Li, Y., Liu, Y., et al. (2022). Anxiety, home blood pressure monitoring, and cardiovascular events among older hypertension patients during the COVID-19 pandemic. *Hypertens. Res.* 45, 856–865. doi:10.1038/s41440-022-00852-0,

Zhou, J., Xiang, Y., Yoshimura, T., Chen, K., Gong, W., Huang, J., et al. (2014a). The role of chemoattractant receptors in shaping the tumor microenvironment. *Biomed. Res. Int.* 2014, 751392. doi:10.1155/2014/751392

Zhou, Z., Liu, F., Zhang, Z. S., Shu, F., Zheng, Y., Fu, L., et al. (2014b). Human rhomboid family-1 suppresses oxygen-independent degradation of hypoxia-inducible factor-1a in breast cancer. *Cancer Res.* 74, 2719–2730. doi:10.1158/0008-5472.CAN-13-1027

Zhou, W., Yu, X., Sun, S., Zhang, X., Yang, W., Zhang, J., et al. (2019). Increased expression of MMP-2 and MMP-9 indicates poor prognosis in glioma recurrence. *Biomed. Pharmacother.* 118, 109369. doi:10.1016/J.BIOPHA.2019.109369

Zhu, V. F., Yang, J., LeBrun, D. G., and Li, M. (2012). Understanding the role of cytokines in Glioblastoma Multiforme pathogenesis. *Cancer Lett.* 316, 139–150. doi:10.1016/J.CANLET.2011.11.001

Zhu, J., Luo, C., Zhao, J., Zhu, X., Lin, K., Bu, F., et al. (2021). Expression of LOX suggests poor prognosis in gastric cancer. *Front. Med.* 8, 718986. doi:10.3389/FMED.2021.718986

Zhuang, S. (2013). Regulation of STAT signaling by acetylation. *Cell. Signal.* 25, 1924–1931. doi:10.1016/J.CELLSIG.2013.05.007

Zuo, H., Chen, L., Li, N., and Song, Q. (2020). Identification of a ubiquitination-related gene risk model for predicting survival in patients with pancreatic cancer. *Front. Genet.* 11, 612196–612212. doi:10.3389/fgene.2020.612196

Glossary

GBM	Glioblastoma Multiforme
E2s	E2 Conjugating Enzymes
BBB	Blood-Brain Barrier
TME	Tumor Microenvironment
ECM	Extracellular Matrix
PTMs	Post-Translational Modifications
HATs	Histone Acetyltransferases
UPP	Ubiquitin-Proteasome Pathway
Ub	Ubiquitin
UPS	Ubiquitin-Proteasome System
GEPIA2.0	Gene Expression Profiling Interactive Analysis
GTEx	Genotype-Tissue Expression
TCGA	The Cancer Genome Atlas
RPPAs	Reverse-Phase Protein Arrays
CPTAC	The National Cancer Institute's Clinical Proteomic Tumor Analysis Consortium
GO	Gene Ontologies
KEGG	Kyoto Encyclopaedia Of Genes
KM	Kaplan-Meier
OS	Overall Survival
DFS	Disease-Free Survival
GEO	Gene Expression Omnibus
HR	Hazard Ratio
CI	Confidence Interval
SVM	Support Vector Machines
UUCD	Ubiquitin And Ubiquitin-Like Conjugation Database
EVs	Extracellular Vesicles
BMP1	Bone Morphogenetic Protein
CTSB	Cathepsin B
LOX	Lysyl Oxidase
LOXL1	Lysine Oxidase Like 1
PLOD1	Procollagen-Lysine,2-Oxoglutarate 5-Dioxygenase 1; Matrix Metallopeptidase 9
SERPINE1	Serpin Family E Member 1
SERPING1	Serine Protease Inhibitor Family G1
VHL	Von Hippel-Lindau
FPR	False Positive Rate
ROC	Receiver Operator Characteristic
AUC	Area Under Curve
TMZ	Temozolomide
ROS	Reactive oxygen species

Identification of novel drug combination in Glioblastoma multiforme therapeutics through Drug Repurposing

Smita Kumari
Molecular Neuroscience and Functional Genomics Laboratory,
Dept. of Biotechnology
Delhi – 110042, India
smitamodi6@gmail.com

Pravir Kumar*
Molecular Neuroscience and Functional Genomics Laboratory,
Dept. of Biotechnology
Delhi Technological University
Delhi – 110042, India
pravirkumar@dtu.ac.in

***Abstract*- Glioblastoma multiforme is one of the leading causes of mortality worldwide. Tumor recurrence and resistance to conventional chemotherapy and radiation are a major setback for current treatment regime. The limitations in creating successful GBM therapeutics have been becoming more prominent. The growth and proliferation of tumors have recently been effectively inhibited by the introduction of numerous innovative chemotherapy medicines. But creating a novel medication takes time and money. Drug repurposing of existing medications to treat cancer is the best solution since it allows for a quicker and less expensive entry into clinical phase 3 trials in the event that successful preclinical research confirms the drugs' safety. The cornerstone of modern anticancer therapy is steadily evolving to be combination therapy. Additionally, antipsychotic drugs that are used to treat the symptoms of psychotic are known to involve in cancer therapeutics, and thus research have been focused to identify the anti-psychotic drugs as anti-cancer drugs through various approaches, including drug-repurposing.**

Herein, we investigated the Gene Expression Omnibus (GEO) dataset to compare the genes in the Peritumoral Brain Zone (PT) and tumor core (TC) with non-neoplastic brain cells to find significantly differentially expressed genes that are only involved in the growth of GBM tumor. Concurrently, protein targets of FDA-approved atypical antipsychotic drugs were examined. Through computational analysis and bioinformatics tools, we have found potential drug combinations for top-ranked atypical antipsychotic drugs and their associated significant cell cycle and calcium pathways. Molecular signatures connected to these pathways—CDK2, CCNA2, DRD4, GABRA5, CHRM1, ADRA1B, and HTR2A—can act as biomarkers and therapeutic targets and have a significant impact on lowering the tumor burden and reducing pathogenesis of GBM.

Keywords: Glioblastoma Multiforme; Recurrence, Atypical antipsychotic drug; combination therapy; computational analysis

I. INTRODUCTION

The most prevalent and deadly form of brain cancer is called glioblastoma multiforme (GBM). Intra and inter-heterogeneity, drug resistance, and tumor recurrence were a few challenges with GBM, and despite rigorous therapeutics research survival rate of GBM patients remains low. Identification of novel biomarkers as well as potential therapeutic targets in GBM malignancies after extensive genomic and proteomic investigation is a current need. Surgical resection, radiation therapy, and chemotherapy are the current gold standard of care and typically increase survival. The prognosis for people with GBM remains grim despite significant efforts over the past few decades. Drug repositioning also referred to as "drug repurposing," is a current strategy for finding new treatments for GBM that involves using already-approved medications for other diseases. Clinical translation can be accelerated by using already FDA-approved drugs by eliminating or speeding up phases like chemical optimization and toxicological analysis, which are essential to drug development. But in order to find compounds that can suppress GBM tumorigenesis, a screening procedure must be used to determine whether potential agents can cross the blood-brain barrier (BBB) [1]. Indeed, a group of psychotropic medications known as antipsychotics is used to treat bipolar illness, psychosis, delirium, Huntington's disease, and Tourette syndrome. The classification of antipsychotics into typical or first-generation antipsychotics (FGAs) and atypical or second-generation antipsychotics (SGAs) is primarily determined by the likelihood that the patient would experience extrapyramidal symptoms (parkinsonism, dystonia) and tardive dyskinesia [2]. According to a literature review, SGAs outperformed FGAs in treating negative symptoms, mental hospitalization rate, and relapse-free survival. SGAs showed more remarkable persistence and commitment to treatment than FGAs. Studies have demonstrated the possible significance of antipsychotics in slowing the growth of GBM cells by obstructing each individual hallmark of cancer [3]. Antipsychotic medications have a long history of usage in a wide range of therapeutic psychological contexts, and they have moderate or low toxicities and well-known tolerability profiles. Hence, there are increasingly being explored for effectiveness in patients with various malignancies, including malignant brain tumors, due to their known safety and demonstrated ability to cross the BBB and modulate neuronal activity [4]. Additionally, recent progress in medicine demonstrates the prevalence and benefit of combination therapy over monotherapy for minimizing disease pathogenesis. Numerous studies have recently shown the benefit of implementing combination therapy rather than monotherapy in various diseases, including cancer.

Combinatorial therapy can address heterogeneity in GBM, target numerous pathways and therapeutic targets simultaneously, and perhaps circumvent the BBB barrier by using drugs that can pass through the BBB using different mechanisms. Additionally, it can offer a personalized strategy that is tailored to the particular tumor characteristics of each patient, such as specific genetic alterations or molecular profiles.

The anti-cancer agent Temozolomide (TMZ, an alkylating chemotherapeutic agent) frequently used to combat GBM has earlier been utilized in combination with SGA or FGAs [5]. For instance, FGAs (Chlorpromazine) have already been used in combination therapy. Therefore, the current study aims to identify potential SGA combinations that could be used to minimize the pathogenesis of GBM. The Peritumoral Brain Zone (PT) and tumor core (TC) samples were compared to non-neoplastic brain tissue (control) samples in order to analyze the gene expression profiles of the DEGs. In order to comprehend interactions and the mechanisms of action held by combination therapy, DEGs were, in fact explored using STRING and KEGG analysis. Additionally, two SGA medications used together have the potential to target critical biological pathways that have been found to be implicated in the pathogenesis of GBM due to their mechanisms of action and mode of action. Hence, based on our research findings, psychiatric treatments with well-established pharmacologic and safety characteristics may be repurposed as anticancer medicines, and has potential to synergetic effect and thus opening new alternatives for the treatment of GBM.

II. RELEVANT WORK

Evidence for the therapeutic potential of anti-psychotic drugs, such as Chlorpromazine, Trifluoperazine, Pimozide, And Olanzapine, is growing in cancer including GBM [6]. For instance, the first atypical antipsychotic medicine, Clozapine, has been demonstrated to inhibit voltage-gated calcium channels and calmodulin (CaM) through the degradation of Akt protein, thereby decreasing the growth of U-87MG human glioma cells. Additionally, Quetiapine inhibits tumor growth when used alone by blocking RANKL (NFκB ligand) and when combined with the HMG-CoA reductase inhibitor Atorvastatin, its efficacy is enhanced [7,8]. In the past, it was normal practice to take multiple psychotropic drugs simultaneously to treat the behavioral and psychological dementia symptoms in Alzheimer's disease patients [9]. Thus, we wanted to use to study and explore benefit of both drugs in combating cancer specifically GBM. The rationale for combining different atypical anti-psychotic drugs is to perhaps increase their anti-tumor properties via synergistic interactions. However, it has not yet been thoroughly demonstrated if such combinations are safe and effective, particularly for GBM. Previously, treatment-resistant schizophrenia was treated with a combination of clozapine and other antipsychotic medications [10]. In addition, recent investigations have shown that Risperidone and Olanzapine are used in combination therapy for the management of schizophrenia [11]. As a result, there is currently data that suggests combining two atypical antipsychotics may be more effective than monotherapy, however, controlled studies have not been done [12]. Numerous evidence-based studies support the use of an *in-silico* method for personalized treatment using combination therapy regime development that predicts the interaction between two pharmaceuticals and a cell line utilizing genetic information, drug targets, and pharmacological data [11,12]. For instance, in BRAF mutant melanoma, Kaitlyn et al., have demonstrated wide computational strategy for determining synergistic combinations utilizing easily accessible single drug efficacy. [15]. However, this approach may be beneficial in identifying therapeutic synergy within a larger pool of potential drug combinations.

III. METHODOLOGY

A. Identification of DEGs

GSE116520 dataset was extracted from online database, namely GEO datasets with a total of 42 samples. The dataset was noirmalized and processed using GEO2R (https://www.ncbi.nlm.nih.gov/geo/geo2r/), where statistically significant DEGs were screened based on $|\log_2$ fold change (FC)$| \geq 1$ and $p \leq 0.05$. Peritumoural Brain Zone (PT) and tumor core (TC) samples were compared with non-neoplastic brain tissue (control) samples to identify DEGs. A Venn diagram of DEGs was constructed using Venny 2.1 tool (https://bioinfogp.cnb.csic.es/tools/venny/) to find common DEGs between PT vs Control and TC vs Control.

B. Screening of Atypical Antipsychotic Drugs and their target prediction

To repurpose the drugs against GBM, FDA-approved atypical antipsychotic drugs were retrieved from ChEMBL, Drugbank database and FDA website. Protein targets against each drug were identified at probability score of ≥ 0.09 using the SwissTargetPrediction webtool (http://www.swisstargetprediction.ch/). The basis for SwissTargetPrediction is referred to as the "similarity principle," which usually indicates that two similar compounds are likely to have comparable properties. This approach assesses potential side effects, anticipates off-targets, and determines the possibility of repurposing molecules with therapeutic value in order to predict the probable macromolecular targets for a small molecule that is assumed to be bioactive. Pa (probability "to be active") and Pi (probability "to be inactive"). Moreover, Gene ID of each predicted protein target was extracted from the protein information database, namely UniProt.

C. Ranking of Drugs

Each drug was ranked based on a literature review supporting GBM, the number of targets predicted by SwissTargetPrediction, and the number of common genes between DEGs and drug targets **(Fig. 1).**

D. Identification of Drug Combination

Drug combinations were made from the top ranked 5 shortlisted drugs. Each drug was paired with the remaining drugs. Thus, total 10 drug combinations were identified, where each drug, in combination, was studied for its biological functions.

E. Validation of Screened Drug Combinations

Each drug in combination was checked for its biological spectrum using SMILES by querying at

PASSonline at the logical activity (Pa) > pharmacological inactivity (Pi) (http://www.way2drug.com/passonline/). Before chemical synthesis and biological testing, this approach can qualitatively predict the biological activity of small molecules. The biological activity spectrum identifies a substance's "intrinsic" characteristic based only on its physical-chemical composition.. Herein, drugs with high antineoplastic effects were selected for further analysis. Further common molecular signatures between both drugs and DEGs were studied for biological activities using STRING webtool (https://string-db.org/) and the KEGG database. Detailed Methodology was described in **Fig. 1**.

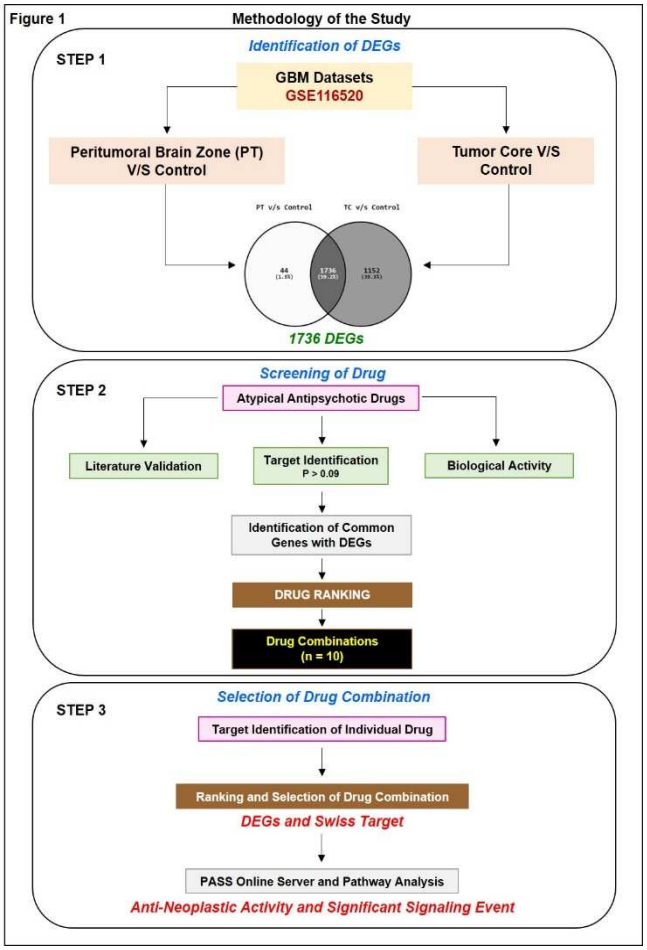

Fig. 1. Methodology of the current study.

IV. RESULTS AND DISCUSSION

For GSE116520 transcriptomics data generated on Illumina HumanHT-12 V4.0 expression beadchip platform. PT and TC samples were compared with control samples to identify the differentially expressed genes (DEGs). PT and TC have 17 samples and control have 8 samples from GBM WHO grade IV tumor tissues from adult patients. Total of 1780 DEGs were found to be significantly dysregulated in PT vs control and 2886 genes in TC vs control. A total list of common 1736 DEGs were identified, including 787 upregulated and 946 downregulated genes, between PT vs Control and TC vs control **(Fig. 2)**. The rationale for using common DEGs (1736 genes) for further study is to identify molecular signatures and associated biological pathways responsible for tumor progression and GBM recurrence. Targeting these key pathways with therapeutic agents will hold the potential to reduce GBM aggressiveness and aid patients with better efficacy and a minimum chance of recurrence. In addition, a total of 11 FDA-approved atypical antipsychotic drugs were used to repurpose in GBM. The plethora of research evidence has shown that the administration of antipsychotic drugs exhibits anticancer properties to combat brain cancer including GBM through various signaling events, namely PI3K/Akt pathway, AMPK/mTOR pathway, Wnt/β-catenin pathway, and others [16]. For instance, administration of a atypical antipsychotic drug, namely Clozapine inhibits the proliferation GBM human cells. Likewise, Aripiprazole inhibits migration and induces apoptosis of glioma cells U251 cells directly by inhibiting Src kinase [17].

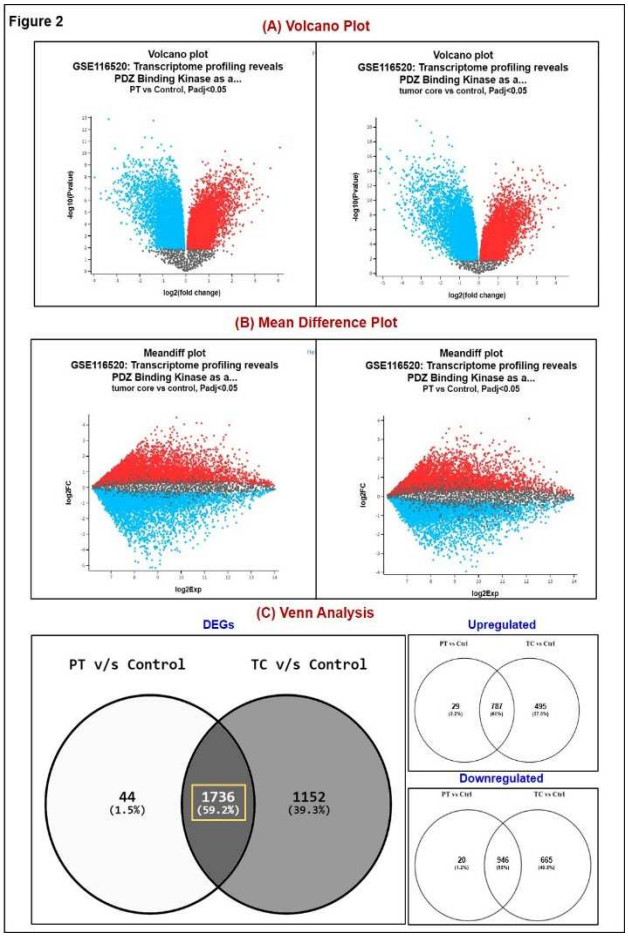

Fig. 2. (A) Volcano plot: For illustrating differentially expressed genes (DEGs), a volcano plot compares statistical significance (-log10 P value) to the magnitude of the change (log2 fold change). (B) A mean difference (MD) plot: An effective tool for identifying DEGs is the MD plot, which compares average log2 expression values to log2 fold change; (C) Venn diagrams of 1736 common DEGs, common 787 upregulated and 946 downregulated genes.*Blue color: downregulated genes; Red color: upregulated genes.

Afterward, SwissTargetPrediction was employed to predict protein targets against each drug, and only 9 drugs qualified filter criteria (Probability score ≥ 0.09). Moreover, common molecular signatures were found between protein targets and DEGs. Amongst them, only 9 drugs have common genes, and 7 have more than 10 common target proteins, as described in **Fig. 3(B)**. Each drug was ranked based on the highest number of common molecular signatures. Further, the biological spectrum of the top 5 drugs, such as Quetiapine, Clozapine, Aripiprazole, Olanzapine and Fluoxetine, was obtained from the PASSonline server using keywords such as

antineoplastic, chemosensitizer and immunomodulator with Pa > Pi. Pa (probability "to be active") calculates the likelihood that the investigated compound belongs to the subclass of active compounds. According to PASS's high-confidence prediction, each compound should likely exhibit a specific biological action. Furthermore, the STRING database was used to create protein-protein networks and run KEGG pathway analysis on all common protein targets. In parallel, each shortlisted drug was paired with the remaining drugs to predict a combination therapeutic regime. A total of 10 combination regime was generated. Each combination regime was studied further for its biological activities **(Table I)**. Common significant pathways ($p \leq 0.05$) between both drugs were chosen and studied further.

Table I. The Biological Activity Spectrum of antipsychotic drugs.

Drugs	Biological Activity							
	Chemosensitizer	Antineoplastic enhancer	Antineoplastic (GBM)	Antineoplastic (Brain Cancer)	Antineoplastic (Glioma)	Antineoplastic (Other Cancer)		Immunomodulator
	Pa (probability "to be active")							
QUETIAPINE	0.41	0.35	0.00	0.18	0.00	0.25	PC	0.31
CLOZAPINE	0.38	0.33	0.00	0.27	0.00	0.25	PC	0.00
ARIPIPRAZOLE	0.29	0.00	0.00	0.20	0.00	0.16	RC	0.22
OLANZAPINE	0.00	0.19	0.00	0.00	0.00	0.22	PC	0.00
PALIPERIDONE	0.00	0.00	0.00	0.00	0.00	0.29	MM	0.00
FLUOXETINE	0.00	0.00	0.18	0.00	0.13	0.00	—	0.00
LURASIDONE	0.00	0.00	0.00	0.00	0.00	0.00	—	0.00
ZIPRASIDONE	0.00	0.00	0.00	0.00	0.00	0.00	—	0.00
RISPERIDONE	0.00	0.00	0.00	0.00	0.00	0.00	—	0.22
ILOPERIDONE	0.00	0.00	0.00	0.00	0.00	0.15	UC	0.19
TEMOZOLOMIDE	0.00	0.849	0.00	0.00	0.00	0.20	OC	0.34
MARIZOMIB	0.387	0.957	0.00	0.00	0.00	0.67	NSCLC	0.00
PANOBINOSTAT	0.523	0.40	0.00	0.00	0.00	0.44	NSCLC	0.00

*Pa>Pi, Green color gradient showed the increasing value of Pi. PC: Pancreatic cancer; RC: Renal Cancer; MM: Multiple Myeloma; UC: Uterine Cancer; OC: Ovarian Cancer; NSCLC: Non-Small Cell Lung Cancer

Each drug combination was ranked based on the highest sharing pathways. Our analysis showed top 3 combinations were Quetiapine + Clozapine, Clozapine + Aripiprazole and Clozapine + Olanzapine, whereas other possible combinations were mentioned in **Fig. 3(C)**.

Figure 3

(A) Shortlisting of Antipsychotic Drugs-Based on Target Frequency

Description	Number of Drugs	Molecular Signatures
FDA Approved Antipsychotic Drugs	11	Common 1736 DEGS (PT vs Control and TC vs Control)
Target Available (Probability score > 0.09)	9	
Total Drug Having Common Targets with DEGs	9	
Total Drug Having Common Targets (> 10 genes) with DEGs	7	

(B) Pairing Drug-Gene

Drug Name	Target Identified from SwissTarget Tool	Number of Targets Common with DEGs	Literature support in GBM	Reported Combination		
				Temozolomide	Marizomib	Panobinostat
OLANZAPINE	111	13	Yes	Yes	Yes	Yes
PALIPERIDONE	103	9	Yes	No	No	No
ARIPIPRAZOLE	100	15	Yes	Yes	Yes	Yes
LURASIDONE	101	16	No	No	No	No
RISPERIDONE	102	10	Yes	Yes	No	No
FLUOXETINE	42	5	Yes	Yes	No	No
ZIPRASIDONE	105	15	Yes	Yes	No	No
QUETIAPINE	109	22	Yes	Yes	No	No
CLOZAPINE	108	18	Yes	Yes	Yes	Yes
ILOPERIDONE	1	0	Yes	Yes	No	No

(C) Putative Drug Combination

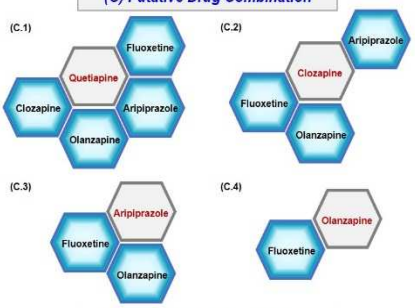

(D) Top Ranked Drug Combination

Rank	Drug 1	Drug 2	Signaling Event	Molecular Signature
1	QUETIAPINE	CLOZAPINE	Calcium Signaling and Cell Cycle Pathway	CHRM1, ADRA1B, HTR2A, CDK2, CCNA2
2	CLOZAPINE	ARIPIPRAZOLE	Calcium Signaling Pathway	ADRA1B, HTR2A
3	CLOZAPINE	OLANZAPINE	Calcium Signaling Pathway	CHRM3, CHRM1, ADRA1B, HTR2A

Fig. 3. (A) Summary of antipsychotic drugs shortlisted after target prediction using SWISSTarget Prediction tool. (B) Summary of number of targets identified, overlapped genes with DEGs, and already reported combination (data procured from DrugCombo Portal and DrugComboDB portal) (C) 10 possible combinations with top 5 drugs. (D) Biological Pathway analysis using STRING and KEGG showed common pathways and molecular signatures shared between Drug 1 and Drug 2 and DEGs.

Further, pathway analysis showed that both drugs shared Neuroactive ligand-receptor interaction (DRD4, CHRM1, ADRA1B, GABRA5, HTR2A), calcium signaling cascade (CHRM1, ADRA1B, HTR2A) and cell cycle signaling (CDK2, CCNA2) as common genes. Plethora research showed that calcium (Ca^{2+}) is essential in the tumorigenesis, migration, EMT, invasion, metastasis, and vascularization. Hence, Ca^{2+} serves as a prospective treatment target in GBM.

Table II. List of common molecular signatures in proposed drug combinations

Drug Combinations	QUETIAPINE and CLOZAPINE	CLOZAPINE and ARIPIPRAZOLE	CLOZAPINE and OLANZAPINE
Molecular Signatures	ADRA1B	ADRA1B	ADRA1B
	APH1A	DRD4	APH1A
	CCNA2	HTR2A	CDK5R1
	CDK2	MAOB	CHRM1
	CHRM1	--	CHRM3
	DRD4	--	DRD4
	GABRA5	--	HTR2A
	HTR2A	--	KCNA5
	--	--	MAPK8

Additionally, overlapped target genes of each drug combination (Drug 1, Drug 2) and DEGs were referred to as "molecular signatures". Molecular signature of toped ranked combination Quetiapine + Clozapine were ADRA1B, APH1A, CCNA2, CDK2, CHRM1, DRD4, GABRA5, HTR2A **(Fig. 3(D))**. However, previous research evidences have indicated that the combination of our top-ranked drugs with TMZ, Marizomib and Panobinostat drugs was implemented in the GBM therapeutic. We have referred to two open-access databases, DrugComb Portal [18] and DrugComboDB [19], that integrate drug combination repositories from various sources and have been popularly used by researchers. Both comprehensive databases are devoted to gathering drug combinations from numerous sources, such as genetic information, HTS assay, PubMed, FDA-approved combinations, and failed combinations to assess their potential for efficacy for the management of cancer.

For instance, study have been concluded that administration of Quetiapine and TMZ exhibit combinatorial effect, which reduces the proliferation of GBM stem cells. Similarly, standalone treatment of Olanzapine inhibits the growth of GBM cells *in vitro*, and thus, promotes apoptosis, which enhances the antitumor activity of TMZ [20]. Thus, from the above study, it must be concluded that administration of anti-psychotic drugs could reverse the progression of GBM through initiation of apoptosis and reduction of GBM cell growth, and drug combination 1 showed synergetic effects along with immunomodulators.

Limitation of current study: combination therapy prediction is based on computational algorithm and literature survey. However, predicted combination need to be checked experimental setting. In addition, various permutation and combination of different drug concentration need to be tried to find optimum dose concentration to get synergic outcome. The results of the current investigation may be utilized to design and perform subsequent studies, including preclinical tests, clinical trials, or translational research, to examine the therapeutic potential, safety, and effectiveness of the identified drug or drug combinations in particular cancer types or patient populations. Researchers working in the same field of repurposing anti-psychotic drugs as monotherapy or in combination to fight cancer can use the study results to design future studies.

IV. CONCLUSION

In this study, we have identified a putative drug combination therapy, namely Quetiapine and Clozapine as a promising therapeutic agent to reverse GBM through targeting crucial signaling pathways, such as neuroactive ligand-receptor interaction, calcium signaling and cell cycle. Moreover, molecular signatures that will be affected by identified combination were CDK2, CCNA2, DRD4, GABRA5, CHRM1, ADRA1B, and HTR2A. Targeting identified signature will our identified combination therapy will altogether reduce tumor burden. However, clinical research can be done for the validation of the presented model, and other drugs should also be worked on to find their capability for the treatment of GBM.

Thus, combination therapy and pharmacological synergism show potential for targeted heterogeneous tumors like GBM and the associated tumor microenvironment. In order to maximize the anticancer potential of particular therapeutic modalities, future research should concentrate on identifying synergistic interactions between chemotherapy, repurposed drugs, radiation, and immunotherapy

ACKNOWLEDGEMENT

We thank the biotechnology department of Delhi Technological University and the Department of Biotechnology (DBT), Govt OF India, for supporting this study.

REFERENCES

[1] Tan SK, Jermakowicz A, Mookhtiar AK, Nemeroff CB, Schürer SC, Ayad NG. Drug Repositioning in Glioblastoma: A Pathway Perspective. Front Pharmacol 2018;9. https://doi.org/10.3389/FPHAR.2018.00218.

[2] Zhang JP, Gallego JA, Robinson DG, Malhotra AK, Kane JM, Correll CU. Efficacy and safety of individual second-generation vs. first-generation antipsychotics in first-episode psychosis: a systematic review and meta-analysis. Int J Neuropsychopharmacol 2013;16:1205–18. https://doi.org/10.1017/S1461145712001277.

[3] Persico M, Abbruzzese C, Matteoni S, Matarrese P, Campana AM, Villani V, et al. Tackling the Behavior of Cancer Cells: Molecular Bases for Repurposing Antipsychotic Drugs in the Treatment of Glioblastoma. Cells 2022;11. https://doi.org/10.3390/cells11020263.

[4] You F, Zhang C, Liu X, Ji D, Zhang T, Yu R, et al. Drug repositioning: Using psychotropic drugs for the treatment of glioma. Cancer Lett 2022;527:140–9. https://doi.org/10.1016/j.canlet.2021.12.014.

[5] Kast RE, Karpel-Massler G, Halatsch ME. Can the therapeutic effects of temozolomide be potentiated by stimulating AMP-activated protein kinase with olanzepine and metformin? Br J Pharmacol 2011;164:1393. https://doi.org/10.1111/J.1476-5381.2011.01320.X.

[6] Lee JK, Nam DH, Lee J. Repurposing antipsychotics as glioblastoma therapeutics: Potentials and challenges (Review). Oncol Lett 2016;11:1281–6. https://doi.org/10.3892/ol.2016.4074.

[7] Bhat K, Saki M, Cheng F, He L, Zhang L, Ioannidis A, et al. Dopamine Receptor Antagonists, Radiation, and Cholesterol Biosynthesis in Mouse Models of

Glioblastoma. J Natl Cancer Inst 2021;113:1094–104. https://doi.org/10.1093/jnci/djab018.
[8] Kamarudin MNA, Parhar I. Emerging therapeutic potential of anti-psychotic drugs in the management of human glioma: A comprehensive review. Oncotarget 2019;10:3952–77. https://doi.org/10.18632/oncotarget.26994.
[9] Orsel K, Taipale H, Tolppanen AM, Koponen M, Tanskanen A, Tiihonen J, et al. Psychotropic drugs use and psychotropic polypharmacy among persons with Alzheimer's disease. Eur Neuropsychopharmacol 2018;28:1260–9. https://doi.org/10.1016/J.EURONEURO.2018.04.005.
[10] Barber S, Olotu U, Corsi M, Cipriani A. Clozapine combined with different antipsychotic drugs for treatment-resistant schizophrenia. Cochrane Database Syst Rev 2017;2017. https://doi.org/10.1002/14651858.CD006324.pub3.
[11] Yang L, Qi X. Effect of olanzapine combined with risperidone in the treatment of schizophrenia and its influence on cognitive function. Pakistan J Med Sci 2021;37:646–50. https://doi.org/10.12669/pjms.37.3.3348.
[12] Nasrallah HA, Friedman J, Knight J. Combination therapy is here to stay n.d.;9:11–2.
[13] Jeon M, Kim S, Park S, Lee H, Kang J. In silico drug combination discovery for personalized cancer therapy. BMC Syst Biol 2018;12. https://doi.org/10.1186/s12918-018-0546-1.
[14] Truong T, Moscato P, Noman N. A Computational Approach for Designing Combination Therapy in Combating Glioblastoma. 2019 IEEE Congr Evol Comput CEC 2019 - Proc 2019:127–34. https://doi.org/10.1109/CEC.2019.8790337.
[15] Gayvert KM, Aly O, Platt J, Bosenberg MW, Stern DF, Elemento O. A Computational Approach for Identifying Synergistic Drug Combinations. PLoS Comput Biol 2017;13:1–11. https://doi.org/10.1371/journal.pcbi.1005308.
[16] Zhuo C, Xun Z, Hou W, Ji F, Lin X, Tian H, et al. Surprising Anticancer Activities of Psychiatric Medications: Old Drugs Offer New Hope for Patients With Brain Cancer 2019;10. https://doi.org/10.3389/fphar.2019.01262.
[17] Kim MS, Yoo BC, Yang WS, Han SY, Jeong D, Song JM, et al. Src is the primary target of aripiprazole, an atypical antipsychotic drug, in its anti-tumor action. Oncotarget 2018;9:5979–92. https://doi.org/10.18632/oncotarget.23192.
[18] Zagidullin B, Aldahdooh J, Zheng S, Wang W, Wang Y, Saad J, et al. DrugComb: An integrative cancer drug combination data portal. Nucleic Acids Res 2019;47:W43–51. https://doi.org/10.1093/nar/gkz337.
[19] Liu H, Zhang W, Zou B, Wang J, Deng Y, Deng L. DrugCombDB: A comprehensive database of drug combinations toward the discovery of combinatorial therapy. Nucleic Acids Res 2020. https://doi.org/10.1093/nar/gkz1007.
[20] Karpel-Massler G, Richard •, Kast E, Westhoff M-A, Dwucet A, Welscher N, et al. Olanzapine inhibits proliferation, migration and anchorage-independent growth in human glioblastoma cell lines and enhances temozolomide's antiproliferative effect n.d. https://doi.org/10.1007/s11060-014-1688-7.

BBA - Reviews on Cancer 1876 (2021) 188585

Contents lists available at ScienceDirect

BBA - Reviews on Cancer

journal homepage: www.elsevier.com/locate/bbacan

Review

Combinatorial therapy in tumor microenvironment: Where do we stand?

Smita Kumari [a], Dia Advani [a], Sudhanshu Sharma [a], Rashmi K. Ambasta [a], Pravir Kumar [a,*]

[a] Molecular Neuroscience and Functional Genomics Laboratory, Delhi Technological University, Shahabad Daulatpur, Bawana Road, Delhi 110042

ARTICLE INFO

Keywords:
Tumor microenvironment
Combination therapy
Hallmarks
Chemoresistance
Targeted therapies

ABSTRACT

The tumor microenvironment plays a pivotal role in tumor initiation and progression by creating a dynamic interaction with cancer cells. The tumor microenvironment consists of various cellular components, including endothelial cells, fibroblasts, pericytes, adipocytes, immune cells, cancer stem cells and vasculature, which provide a sustained environment for cancer cell proliferation. Currently, targeting tumor microenvironment is increasingly being explored as a novel approach to improve cancer therapeutics, as it influences the growth and expansion of malignant cells in various ways. Despite continuous advancements in targeted therapies for cancer treatment, drug resistance, toxicity and immune escape mechanisms are the basis of treatment failure and cancer escape. Targeting tumor microenvironment efficiently with approved drugs and combination therapy is the solution to this enduring challenge that involves combining more than one treatment modality such as chemotherapy, surgery, radiotherapy, immunotherapy and nanotherapy that can effectively and synergistically target the critical pathways associated with disease pathogenesis. This review shed light on the composition of the tumor microenvironment, interaction of different components within tumor microenvironment with tumor cells and associated hallmarks, the current status of combinatorial therapies being developed, and various growing advancements. Furthermore, computational tools can also be used to monitor the significance and outcome of therapies being developed. We addressed the perceived barriers and regulatory hurdles in developing a combinatorial regimen and evaluated the present status of these therapies in the clinic. The accumulating depth

Abbreviation: 2D, Two dimensional culture; 3D, Three dimensional culture; ALL, Acute lymphoblastic leukemia; anti-GD2, anti-disialoganglioside; ARID1A, AT-Rich Interaction Domain 1A; ATP, Adenosine tri-phosphate; BPDCN, Blastic Plasmacytoid Dendritic Cell Neoplasm; CAFs, Cancer Associated Fibroblast; cAMP, Cyclic adenosine phosphate; COL11A1, Collagen 11a1; CCL2, C–C motif chemokine ligand 2; CCL5, C–C motif chemokine ligand 5; CCL7, Chemokine (C-C motif) ligand 7; COMP, Collagen oligomeric matrix protein; COL10A1, collagen 10a1; CRC, Colorectal Cancer; CML, Chronic myelogenous leukemia; CLL, Chronic lymphocytic leukemia; CTLA-4, Cytotoxic T-lymphocyte-associated protein 4; CSCs, Cancer Stem Cells; CXCL8, (C-X-C motif) ligand 8; CXCL12, C-X-C motif chemokine 12; DAMP, Damage-associated molecular pattern; DCs, Dendritic cells; EBRT, External beam radiotherapy; ECM, Extracellular matrix; EGF, Epidermal growth factor; EMT, Epithelial-to-mesenchymal transition; EPIC, Estimating the Proportions of Immune and Cancer cells; ERK, Extracellular signal-regulated kinase; ESTIMATE, Estimation of STromal and Immune cells in MAlignant Tumors using Expression data; FGF, Fibroblast growth factor; FGFR, Fibroblast growth factor Receptor; FH-SSL-Nav, Navitoclax -loaded nanoliposomes modified with peptide FH; FOXP3, Forkhead box P3; GD-15, Growth differentiation factor-15; GATK, Genome Analysis Toolkit; GISTs, Gastrointestinal Stromal Tumors; HCC, Hepatocellular carcinoma; H&N carcinoma, Head and Neck Carcinoma; HGF, Hepatocytes growth factor; Hh, Hedgehog; HIF-1α, hypoxia-inducible factor 1 alpha; HSPGs, Heparan sulfate proteoglycan; ICDs, Immunogenic cellular death; IDO, Indoleamine-pyrrole 2,3-dioxygenase; HLA, Human leukocyte antigen; IDH1, Isocitrate dehydrogenase 1; ILs, Interleukin; IFNs, Interferons; ImmuCellAI, Immune Cell Abundance Identifier; iPSC, Induced Pluripotent Stem Cells; JAK, Janus kinase; LAG 3, Lymphocyte-activation gene 3; lncRNA, Long non-coding RNAs; miRNA, microRNA; MAPK, Mitogen-activated protein kinase; MCC, Merkel cell carcinoma; MDSCs, Myeloid-derived suppressor cells; MET, Mesenchymal to epithelial transition; MSC, Mesenchymal stromal cells; mAb, monoclonal Antibody; MMPs, Matrix metalloproteinases; Nab, Nanoparticle Albumin Bound; NK cells, Natural Killer cells; NHGRI, National Human Genome Research Institute; NHL, Non-Hodgkin lymphoma; NOMID, Neonatal-Onset Multisystem Inflammatory Disease; NSCLC, Non small-cell lung carcinoma; NSG, Next generation Sequencing; OC, osteosarcoma cancer; PD-1, Programmed cell death protein 1; PD-L1, Programmed death-ligand 1; PDGF, Platelet-derived growth factor; PIGF, Placental growth factor; PKC, Protein kinase C; PI3K, Phosphatidylinositol 3-kinase; PSA, Prostate-Specific Antigen; RCC, Renal Cell Carcinoma; ROS, Reactive oxygen species; SASP, senescence-associated secretory phenotype; SDF-1, stromal cell-derived factor 1; SCLC, Small cell lung cancer; scRNAseq, single-cell RNA sequence; STAT, Signal transducer and activator of transcription; TAP, Transporter associated with antigen processing protein; TEMs, TIE2-exxpressing monocytes; TME, Tumor microenvironment; TGCT, Tenosynovial Giant Cell Tumor; TGF, Transforming growth factor; TNBC, Triple Negative Breast Cancer; TNF-α, Tumor necrosis factor alpha; TILs, Tumor-infiltrating lymphocytes; TIK, Tyrosine kinase Inhibitor; TSG101, Tumor susceptibility gene 101 protein; VEGF, Vascular endothelial growth factor; VEGF, Vascular endothelial growth factor Receptor; &, And.

* Corresponding author at: Department of Biotechnology, Molecular Neuroscience and Functional Genomics Laboratory, Delhi Technological University, Shahbad Daulatpur, Bawana Road, Delhi 110042; India Phone: +91- 9818898622

E-mail addresses: pravirkumar@dtu.ac.in, kpravir@gmail.com (P. Kumar).

https://doi.org/10.1016/j.bbcan.2021.188585
Received 22 February 2021; Received in revised form 28 May 2021; Accepted 23 June 2021
Available online 2 July 2021
0304-419X/© 2021 Elsevier B.V. All rights reserved.

of knowledge about the tumor microenvironment in cancer may facilitate further development of effective treatment modalities. This review presents the tumor microenvironment as a sweeping landscape for developing novel cancer therapies.

Table 1
Components, functions, and classifications of TME [37–44]

Cell player	Main marker	Function	Classification	Reference
Cancer-associated fibroblasts (CAFs)	**Human:** PDGF*; FAP*; FGFR*; α-SMA	▪ Modulate inflammation. ▪ Encourage proliferative signaling, angiogenesis and metastasis ▪ Participating in wound healing. ▪ Integrating collagen and protein to form the ECM fibre network. ▪ Evade immune destruction. ▪ Reprogram cellular metabolism. ▪ Stimulate genome instability and mutation ▪ CAFs can differentiate stimulation by ROS and TGF-β1-dependent and TGF-β1-independent mechanisms.	Pro-Tumorigenic; less known of Anti-tumorigenic	[37,38,45,46]
Lymphatic Vessels	**Human:** VEGFR3; LYVE-1	▪ Upregulated VEGF-C induces enlargement of tumor-associated lymphatic vessels, increasing lymph flow and facilitating intravasation of cancer cells into the lymphatics. ▪ Overexpression of HGF induces lymphatic vessel hyperplasia and lymphatic metastasis. ▪ ET-1 induces Lymphatic Endothelial Cells (LECs) and Lymphatic Vessels to Grow and Invade. ▪ In TME, VEGFR-3 engagement by VEGF-C expands LECs (a process known as tumor-associated lymphangiogenesis).	Pro-Tumorigenic	[47–51]
Lymph Nodes	Prox1; VEGF-C	▪ Tumor overexpresses VEGF-C, which induces lymphangiogenesis and metastasis to regional lymph nodes. ▪ Lymph Nodes-LECs in TME is actively involved in immunological responses. ▪ The composition of the metastatic lymph node undergoes remodeling that influences the growth of cancer cells.	Pro-Tumorigenic	[13,50,52]
Bone Marrow	**BMDCs:** CD11c, CD80, CD86 and MHC II	▪ Cancer cell influences Bone marrow resident cells (osteoblasts, osteocytes, adipocyte, osteoclast, immune cells, endothelial cells, nerves). ▪ BMDCs in TME participate in tumorigenesis, tumor invasion and angiogenesis.	Pro-Tumorigenic	[53–55]
Spleen	CD11b, CD11c, F4/80, Gr-1, Ly6C, and Ly6G	▪ The spleen plays an important role in tumor progression in the tumor-bearing host. ▪ The spleen is a site of immune tolerance induction. ▪ The spleen is resident of several distinct populations of myeloid cells with varying immune functions, including neutrophils, eosinophils, monocytes, macrophages, and dendritic cells.	Pro-Tumorigenic	[56–58]
Thymus	-	▪ It is a central lymphoid organ for T cell development ▪ Thymic function related to cancer development, relapse and anti-tumor immunity.	Pro-Tumorigenic	[59]
Tumor Endothelial cells (TECs)	CD13/APN; CD54/ICAM-1; CD102/ICAM-2; CD144/VE-cadherin	▪ Alter TECs regulate tumor metastasis through biglycan secretion through activation of NF-κB and ERK signaling. ▪ TECs secret angiocrine factors such as IL-6, VEGF-A, bFGF. ▪ The balance between angiogenic activator and inhibitors regulates tumor angiogenesis.	Pro-Tumorigenic	[60–62]
Adipose cells	**Human:** AIs*; MBD6*	▪ Relating with inflammation. ▪ Recruiting immune cells. ▪ Assist vasculogenesis. ▪ Regulating the balance of systematic energy and metabolism ▪ Engage in metabolic symbiosis relationship with adjacent tumor cells.	Pro-Tumorigenic	[37,38,63]
Tumor associated macrophages (TAMs)	**Human:**CD11b+ CD68+ CSF1R+ CD163+ EMR1+ **Mouse:**CD11b+GR1− CD68+ CSF1R+ F4/80+	▪ Activated M1 macrophages are pro-inflammatory and anti-tumorigenic and secrete TH1 cytokines. ▪ Activated M2 macrophages are anti-inflammatory and pro-tumorigenic and secrete TH2 cytokines. ▪ TAMs frequently exhibit an M2 phenotype; their presence in tumors supports angiogenesis and invasion. ▪ Upregulated inflammatory cytokines. e.g., TNF-β.	Pro-Tumorigenic (M2); Anti-Tumorigenic (M1)	[7,64–66]

(*continued on next page*)

Table 1 (*continued*)

Cell player	Main marker	Function	Classification	Reference
		▪ Increase ECM degradation.		
Dendritic Cells (DCs)	**Human:**CD11c+ CD83+ CD123+ **Mouse:**CD11c+ CD83+ CD123+	▪ DCs are monocytic APCs that are derived from the bone marrow. ▪ DC-based vaccines induce both innate and adaptive immune responses to regress tumors and prevent relapse. ▪ Splenic DCs suppress T cell response via IDO expression.	Mainly tumor-inhibiting but TME is also known to turn into Pro-Tumorigenic	[67–69]
Tie2-expressing monocytes (TEMs)	**Human:**CD11b+ SCA1+ TIE2+ CD14+ CD16+ **Mouse:**CD11b+ GR1–SCA1+ TIE2+	▪ Tie2 is a receptor for the angiogenic growth factor angiopoietin. ▪ TEMs have a role during tumor angiogenesis through a paracrine signaling loop with angiopoietin-expressing endothelial cells.	Pro-Tumorigenic	[70,71]
Neutrophils	**Human:**CD11b+ CD66b+ CD63+ **Mouse:**CD11b+ GR1+ 7/4+	▪ Most abundant circulating leukocytes in humans and are phenotypically plastic in nature. ▪ Similar to TAMs, neutrophils have been shown to context-dependent roles within the TME. ▪ Enhancement of angiogenesis and metastasis. ▪ Tumor-associated neutrophil is linked with poor prognosis. ▪ Neutrophil to lymphocyte ratio (NLR) measures poor prognosis in NSCLC.	Pro-Tumorigenic (N2); Anti-Tumorigenic (N1)	[72–76]
Mast cells	**Human:**CD11b– CD49d+ CD117+ CD203c+ **Mouse:**CD11b– CD49d+ CD117+ CD203c+	▪ Mast cells are best known for their role during allergies and autoimmunity. ▪ Mast cells are recruited to tumors, where they promote tumor angiogenesis. ▪ Promote remodeling of tissue by induction of changes in ECM composition.	Pro-Tumorigenic	[77,78]
Myeloid-derived suppressor cells (MDSCs)	**Human:** *Monocytic:* CD11b+ CD33+ HLA-DR– CD14+ *Granulocytic:* CD14– CD15+ **Mouse:** *Monocytic:* CD11b+ GR1+ Ly6G–Ly6C+ *Granulocytic*: Ly6G+Ly6C	▪ Facilitate neovascularization (produce VEGF). ▪ Drive invasion & metastasis (produce MMPs). ▪ Supports malignant cells to colonize at metastatic niche. ▪ Immunosuppressive precursors of dendritic cells, macrophages and granulocytes. ▪ Disrupt tumor immunosurveillance by interfering with T cell activation, cytotoxic activity, antigen presentation and cell polarization. ▪ Differentiating into TAMs under hypoxic conditions.	Pro-Tumorigenic	[38,79,80]
NK cells	**Human:**CD56+CD16+ **Mouse:** CD335+NK1.1+	▪ Cytotoxic lymphocytes can kill stressed cells in the absence of antigen presentation. ▪ Detect and kill tumor cells through 'missing self-activation (loss of healthy cell markers) or 'stress-induced' activation (gain of stressed cell markers).	Mainly Anti-Tumorigenic	[7,81]
T_H cells	**Human:**CD3+CD4+ **Mouse:**CD3+CD4+	▪ CD4+ TH cells can be divided into TH_1 and TH_2 lineages. ▪ TH_1 cells secrete pro-inflammatory cytokines and can be anti-tumorigenic. ▪ TH_2 cells secrete anti-inflammatory cytokines and can be pro-tumorigenic. ▪ The ratio of TH_1 to TH_2 cells in cancer correlates with tumor stage and grade.	Pro-Tumorigenic and Anti-Tumorigenic depend on stage and context	[7]
T_{reg} cells	**Human**:CD4+ CD25+ FOXP3+ CTLA-4+ CD45RA+ **Mouse**:CD4+CD25+ FOXP3+ CTLA-4+ CD103+	▪ Primarily pro-tumorigenic roles by suppressing immunosurveillance. ▪ Secreting cytokines such as IL-10, IL-35, TGF-β. ▪ High T_{regs} infiltration are linked with poor survival in various cancer types. ▪ Some T_{regs} secrete perforin & granzyme to direct kill cells. ▪ Synthesis & release cAMP to interfere with tumor cell metabolism.	Pro-Tumorigenic and Involved in tumor maintenance	[38,82,83]
T_C cells [CD8+ cytotoxic T cells (CTLs)]	**Human:**CD3+CD8+ **Mouse:** D3+CD8+	▪ Associated in the adaptive immune system. ▪ Especially recognize and kill cancer cells through perforin- and granzyme-mediated apoptosis.	Anti-Tumorigenic	[7]
B cells	**Human:**CD19+CD20+ **Mouse:** B220+CD19+CD22+	▪ Engaged in humoral immunity. ▪ Secreting pro-tumorigenic cytokines in TME and altering TH_1- to-TH_2 ratios. ▪ Involved in tumorigeneses.	Pro-Tumorigenic	[7,84]
Extracellular vehicles (EVs) [Includes exosomes (30–100 nm), micro vesicles (100 nm–1 μm), and apoptotic bodies (500 nm–4 μm)]	**Exosomes:** tetraspanin family members (CD63, CD81, CD9), Tsg101, Alix, MHC molecules, HSP70; **Microvesicles**: PS, Integrins αIIbβ3 (CD41)) CD42b, and GPVI, selectin; **Apoptotic bodies:** Histone, fragmented DNA, PS hsa_circ_0000338**; miR-21, miR-	▪ Encapsulate biologically molecules (include proteins, miRNAs, cirRNA and lncRNAs) ▪ Involved in the bidirectional communication between tumor and TME. ▪ Regulating key signaling pathways, proliferation, drug resistance, and stemness. ▪ Reprogramming stromal cells to create a niche for survival.	Pro-Tumorigenic; Anti-Tumorigenic	[39,41,85–90]

(*continued on next page*)

Table 1 (*continued*)

Cell player	Main marker	Function	Classification	Reference
	196, let-7a, miR-1229 miR-23a, miR-141;	▪ Tumor exosomes of CLL patients express tetraspanin, CD9, CD63, and CD37 markers and plasma-derived exosomes miRNA signature, including miR-29 family, miR-150, miR-155, and miR-223. ▪ Annexin A1 is a specific marker for classical microvesicles budding from the plasma membrane. ▪ Apoptotic bodies released by membrane blebbing and eventually engulfed by phagocytic cells and also promote intercellular communication by delivering their content into recipient cells		
Extracellular matrix (ECM)	MMP-9, HSPGs circulating COL11A1, COMP, and COL10A1	▪ ECM components: fibrillar proteins such as collagen, elastin, fibronectin, & laminins, glycosaminoglycans (GAGs), proteoglycans (PGs), & other glycoproteins. ▪ Establishing the complex structural network. ▪ Manage cancer invasion and metastasis, angiogenesis. ▪ Involved in growth and proliferation signaling. ▪ Inhibiting cancer apoptosis. ▪ Produces heparanase enzyme that degrades HSPs (sugar moieties), this causes FGF release from ECM, making it accessible for tumor cells.	Pro-Tumorigenic	[43,44]

*: the targeting markers; **: circular RNAs

Abbreviation:; AIs: Aromatase inhibitors; APCs: Antigen-presenting cells; α-SMA: alpha-smooth muscle actin; BDMC: Bone marrow derived cell; cAMP: Cyclic adenosine monophosphate; cirRNA: Circular RNA; COMP: Cartilage oligomeric matrix protein; COL11A1: collagen type XI α1; COL10A1: collagen type X α; CD163+ EMR1+: CD163+ EGF-like module-containing mucin-like hormone receptor-like 1; CD11b+GR1: CD11b+Granulocytes; CSF1R: Colony stimulating factor 1 receptor; ERK: extracellular signal-regulated kinase; ET-1: Endothelin 1; FAP: Fibroblast activation protein; FGFR: Fibroblast growth factor receptor; HGF: Hepatocyte growth factor; HSPs: Heat shock protein; ICAM-1: Intercellular adhesion molecule 1; ICAM-2: Intercellular adhesion molecule 2; IDO: Indoleamine-pyrrole 2,3-dioxygenase; LECs: Lymphatic Endothelial Cells; lncRNAs: Long non-coding RNAs; LYVE-1: Lymphatic vessel endothelial hyaluronan receptor 1; MBD6: Methyl-CpG-binding protein 6; MHC: major histocompatibility complex; miRNAs: microRNA MMPs: Matrix metalloproteinases; PDGF: Platelet-derived growth factor; Prox1: Prospero Homeobox 1; PS: phosphatidylserine; TIE2: TECs: Tumor endothelial cells; TGF-β1: Transforming growth factor beta 1; TNF-β: Tumor necrosis factor-beta; Tsg 101: tumor susceptibility gene 101 protein; VE-cadherin: Vascular endothelial-cadherin; VEGF-C: vascular endothelial growth factor; VEGFR3: Vascular Endothelial growth factor receptor 3.

1. Introduction

Cancer is another word for a malignant tumor (a malignant neoplasm) is the uncontrolled growth of abnormal cells in the body [1]. It is a multifactorial disease and one of the leading causes of mortality worldwide. WHO estimates indicate that 9.6 million lives were lost to cancer in 2018, comprising 13% of all mortality. By 2030, the estimated number of deaths due to cancer is projected to rise to 13.1 million. The top cancers are Lung (2.09 million cases), breast (2.09 million cases), and Colorectal (1.80 million cases) [2]. Low and middle-income countries bear approximately 70% burden of all deaths resulting from cancer in the world. Although the overall incidence of cancer in developing countries is less than that in developed nations, the mortality rates are comparable due to late diagnosis and lack of availability/affordability of treatment and care [3]. Tumors are complex heterotypic tissues in which a non-transformed milieu influences the proliferation and advancement of transformed cells with which it shares space and time. The tumor microenvironment (TME) can be thought of as an ecosystem or community in which malignant cells live and grow [1]. Growing evidence suggests that the TME can influence abnormal tissue function and play a crucial role in the progression of more advanced and refractory cancers [4,5]. Despite intense research in oncology, which has provided enormous insight, cancer continues to be a poorly understood disease. In earlier studies, cancer was viewed as a heterogeneous disease involving aberrant mutations in only tumor cells but it is now evident by intense research that their micro environmental composition also influences tumors. In 1863 Rudolf Virchow first proposed the link between chronic inflammation and tumorigenesis and observed that infiltrating leukocytes were a hallmark of tumors [6]. Since then, a plethora of studies have contributed to the characterization of the TME and understanding its crosstalk with tumor, which has further simplified the challenging task of treating cancer. It has been suggested that many environmental factors and oncogenic stimuli influence TME, affecting cancer cell metastasis in a dynamic process [7]. A dynamic bidirectional interaction exists between cancer cells and the host microenvironment, which involves a wide variety of components and a diverse range of mechanisms that are critical and support cancerous growth and spread [8,9], and this communication leads to proliferation and metastasis [10–12]. Moreover, Pereira et al. mentioned the role of the lymph node microenvironment in cancer metastasis [13]. The role of the microenvironment in tumor development was initially proposed by Stephen Paget in the "seed and soil" hypothesis. He suggested that metastatic cancer cells (seeds) interact with specific organ microenvironments (soil) to result in metastasis formation [14]. The aim of this review is to focus on characteristics of the TME that can be manipulated to design more effective cancer therapies and treatment strategies. Also, we describe the importance of targeting TME by putting more emphasis on combinatorial therapies.

1.1. Tumor microenvironment and its components

The TME consists of different cellular and non-cellular secreted components; the cellular components include tumor cells, fibroblasts or cancer-associated fibroblast (CAF), mesenchymal stromal cells (MSC), pericytes, adipocytes, vasculature, lymphatic networks, myeloid population, myeloid-derived suppressor cells (MDSC), immune cells, and inflammatory cells. CAFs are the dominant cell type within the reactive stroma of tumors that secrete growth factors, such as hepatocyte growth factor (HGF), epidermal growth factor (EGF), and cytokines like stromal cell-derived factor 1 (SDF-1) and IL-6 [15]. HGF-producing fibroblasts induce resistance to EGFR-tyrosine kinase inhibitors in lung cancer [16], and also, CAF stimulated with Cisplatin facilitates chemoresistance by activating the IL-11/IL-11R/STAT3 signaling pathway in lung cancer [17]. Exosomes containing microRNAs (miRNAs) (e.g., miR-155, miR-100, miR-222, miR-30a, and miR-146a) are secreted by chemotherapy-treated cancer cells and CAFs, that are known to mediate cancer

resistance [18]. Recently, a growing number of publications show CAFs secrete IL-6 cytokines, a key player in molecular abnormality, chemoresistance, EMT and stem cell formation in various types of malignant cancer [19]. Moreover, in primary prostate tumors, CAFs were found to produce SDF-1 that plays a major role in monocyte recruitment, tumor progression and immunosuppression [20]. Similarly, adipose cells are the important component of the TME as they provide a highly inflammatory environment for cancer cell proliferation by secreting more than 50 cytokines, chemokines and various hormone-like growth-promoting factors. Like normal tissues, the TME has blood and lymphatic vascular networks as essential components for supplying oxygen and removing metabolic waste and carbon dioxide. These networks are characterized by sustained angiogenesis for making new blood vessels from the pre-existing ones [21]. Immune cells in TME include cells of adaptive immunity like dendritic cells (DCs), T lymphocytes, and effectors of innate immunity like natural killer (NK) cells, macrophages, and polymorphonuclear leukocytes. Moreover, tumor-infiltrating lymphocytes (TILs) comprising $CD3^{+}CD4^{+}$ and $CD3^{+}CD8^{+}$ T cells are also the major constituent of TME exclusive for tumor-associated antigens [22]. Besides, inflammatory cells in the TME either assist tumor progression by contributing to 'immune evasion' or resist tumor growth.

Non-cellular components of TME include extracellular matrix (ECM), matrix remodeling enzymes, cytokines, chemokines, exosomes, growth factors, and inflammatory enzymes [23,24]. The function of each component in TME and its role in tumor progression have been explained in Table 1 The ECM is the highly dynamic structural TME component comprising of various proteins, polysaccharides, proteoglycans (such as heparan sulphate proteoglycans, versican and hyaluronan) and glycoproteins (such as laminins, elastin, fibronectin and tenascins). Soluble factors, such as growth factors and other ECM-associated proteins bind to the ECM. In addition, receptors present on the cell surface binds with components of ECM and ECM-bound factors to regulate processes such as proliferation, migration, differentiation and apoptosis [25]. Moreover, it provides a niche with distinct physical and biochemical properties for tumor cells and cancer stem cells and regulates their proliferation and differentiation. It has been explored that ECM components perform their functions in a time and tissue-specific manner and contribute to cancer stemness [26]. Due to the plasticity nature, ECM has been ascribing both pro-tumorigenic and anti-tumorigenic properties. ECM proteins are responsible for creating a barrier through which the drugs must pass in order to reach the cancer cells. Recent studies have revealed that ECM proteins, including collagen, laminin, hyaluron, POSTN, fibronectin, etc., are highly expressed by metastatic cells. Collagen is the most significant component of ECM as collagen processing enzymes are strongly expressed in TME. Collagen in combination with Elastin contributes to tumor rigidity it's palpability [27]. Another ECM component, Laminin-322, provides a specific microenvironment for directing tumor invasion and is found to be highly expressed in solid metastatic tumors [28]. Studies have shown that POSTN protein is responsible for the maintenance of cancer stem cells and metastasis. Similarly, Fibronectin is considered a biomarker for epithelial–mesenchymal transition (EMT) and promotes metastasis through the MAPK signaling pathway. Another important component of ECM is proteoglycans, which play a crucial role in tumor growth and metastasis. Proteoglycans influence tumor cell growth either through glycosaminoglycan (GAG) dependent or independent mechanism. For instance, the transmembrane chondroitin sulfate proteoglycan 4 (CSPG4) through the GAG-independent mechanism binds to growth factors and positively monitors cancer cell growth. On the contrary, Heparan Proteoglycans (HSPGs) interact with growth factors via a GAG-dependent mechanism [29]. Moreover, the interaction between HSPG and its ligand plays a significant role by modulating cellular proliferation, differentiation, adhesion, migration, apoptosis, angiogenesis, inflammation, invasion, and metastasis [29–31]. Studies show that deregulation of HSPGs results in malignancy, and depending on the type of cancer, HSPG-regulated FGF binding and receptor dimerization activates the signaling pathways, including MAPK/ERK, PI3K/AKT, JAK/STAT, Hh, Wnt signaling, transforming growth factor beta (TGF-β) family, FGF, HGF, VEGF and PKC pathways. One of the important biological functions is to attune the activities of cytokines and chemokines [32,33]. Nowadays, ECM is emerging as a critical player in malignant initiation, progression and chemoresistance. ECM continuously undergoes controlled remodelling. Specific enzymes that are responsible for ECM degradation, such as metalloproteinases (MMPs), mediate this process, which includes quantitative and qualitative changes in the ECM. MMPs are involved in nearly every significant stage of tumor development, including tumor cell invasiveness and migration, metastasis, angiogenesis, immune surveillance escape, and apoptosis[34]. Chemokine families (namely, the C-, CC-, CXC- and CX_3C-chemokine families) are another important component, and they are produced by tumor cells as well as other TME cells, including immune cells and stromal cells. They directly and indirectly influence cancer progression, tumor immunity, and therapy outcomes[35]. Similarly, cytokines and exosomes influence TME[36]

1.2. Role of epithelial-to-mesenchymal transition (EMT)

EMT, a crucial event in the cancer invasion process involving remodeling of cytoskeleton, is induced by the TME. EMT transitions and TME interactions synergize to direct cancer progression and also influence at all stages of metastasis. A dynamic series of interactions exists between structural, soluble, and changing cellular elements of the extracellular matrix and stromal tissue compartment [91]. An EMT is a primary process underlying the heterogeneity of carcinoma cells. Besides EMT, another important process, mesenchymal-to-epithelial transition (MET), also known as the reverse of EMT, is recognized as critical events that drive invasive and metastasis processes in cancer progression [92]. MET is a biological process in which the tumor cells with the mesenchymal phenotype transform to the epithelium phenotype. Thus, MET plays a crucial role in metastatic tumor formation. During EMT and MET, a two-way mutual communication exists between the host fibroblasts, extracellular matrix/basement membranes, and the immune cells [93]. Many researchers observed some loss of epithelial characteristics like apical-basis axis of polarity and cellular adherence with a gain of mesenchymal markers such as three-dimensional (3D) organization and increased motility. EMT helped in the progression from the normal epithelium to invasive carcinoma and the establishment of metastatic nodules in secondary organs [94]. Elisabetta Romeo and colleagues have beautifully summarized how EMT can occur in cancer cells in different conditions of TME, like (i) it can occur in response to stressors from the TME, such as hypoxia, a low pH, immune responses, mechanical stress, and antitumor drugs. These responses are mediated mainly by growth factors, chemokines and cytokines such as TGF-β. (ii) stressor-promoted epigenetic changes that induce heritable effects to allow for retention of the mesenchymal state even when the stressors are no longer present. (iii) independently activated signaling pathways due to the activation of oncogenic mutations or tumor-associated overexpression of pathway components [95]. Herein, the authors have shown that EMT and MET are not binary processes and, in few cases, EMT and MET are important. However, in some cases, EMT and MET play a permissive role by contributing to phenotype modulation that accelerates processes essential for tumor cells to invade and colonize into the secondary site.

1.3. Contributory role of TME in therapeutic resistance

Chemotherapy resistance occurs, when the patient develops tolerance to cancer therapy, either *de novo* or acquired. Resistance to cancer treatment is related to both the intrinsic and extrinsic properties (cellular or acellular parameters) of the TME [96]. Numerous studies have shown that cancer cells change their responsiveness to therapy by changing their interaction with the host microenvironment or their surroundings during treatment. As TME is quite complex, various

Table 2
Summary of "TME targeting" FDA approved repurposed anticancer drugs

Molecular target	Drug name	Mechanism of action	Indication	Clinical status	Reference
Cellular Component OF TME: Vasculature					
VEGF signaling					
VEGF	Bevacizumab	Humanised mAb against VEGF	Metastatic CRC, metastatic RCC, NSCLC, Glioblastoma	FDA approved	[102–105]
VEGFR	Ramucirumab	VEGFR2 Neutralizing Antibody and also impacts Tregs & CD8+ T cells in TME	CRC, HCC, NSCLC, Stomach adenocarcinoma	FDA approved	[106–108]
VEGFR	Sunitinib; Pazopanib	Small molecule RTK inhibitor of VEGFR1-3, PDGFR, c-kit	RCC, Pancreatic neuroendocrine tumors, Gastrointestinal stromal tumors; RCC	FDA approved	[105,109–111] ; [112]
VEGFR	Sorafenib	Small molecule, TKI of VEGFR2, PDGFR-b, RAF Increased immune cell infiltration	Advanced RCC, HCC	FDA approved	[105,113–115]
EGFR pathway					
EGFR	Erlotinib; Gefitinib	Small molecule, TKI of EGFR and suppresses recruitment of pericytes	NSCLC, Pancreatic cancer; NSCLC	FDA approved	[103,116,117] ; [103,118,119]
EGFR	Cetuximab; Panitumumab	mAb against EGFR	Metastatic CRC, H&N carcinoma; Metastatic CRC	FDA approved	[105] ; [120]
mTOR signaling					
Mtor	Everolimus	Small molecule, TKI against mTORC1 protein	Advanced RCC, CRC	FDA approved	[121,122]
PDGF signaling					
PDGFR	Imatinib	Small molecule, TKI against PDFR, c-KIT	CML, GISTs	FDA approved (PDGFR on pericytes)	[123,124]
Cellular Component of TME: Immune system					
Macrophages					
CSF-1R	Pexidartinib	Small molecule, TKI against CSF1/ CSF1R	Symptomatic TGCT	FDA approved	[125]
CSF-1R	Nilotinib	Small molecule, TKI against DDR, KIT, PDGFR, and CSF-1R	CML	FDA approved	[126]
NF-κB signaling and UPR signaling					
26S proteasome	Bortezomib	Inhibitor of 26S proteasome disrupting IkB degradation	Multiple Myeloma, Mantle cell lymphoma	FDA approved	[127,128]
Tumor-associated Macrophages (TAMs)					
TAMs	Trabectedin	G2 phase cell cycle arrest, Decreased TAMs, modulates cytokines and angiogenic factor production	Soft tissue sarcoma	European Commission and FDA approved	[129,130]
TAMs	Sorafenib	Small molecule, TKI, restore IL-12 secretion, IL-10 production suppression	Breast cancer	FDA approved	[131]
T cells					
PD-1	Pembrolizumab; Nivolumab	mAb against PD-1 receptor; prevent PD-L1 & PD-1 interaction	Melanoma, TNBC; Melanoma	FDA approved	[132] ; [133,134]
PD-L1	Atezolizumab; Durvalumab	mAb against PD-L1 prevent PD-1 and PD-L1 interaction	Advanced metastatic urothelial carcinoma NSCLC	FDA approved	[135] ; [136,137]
PD-L1	Avelumab	mAb against PD-L1, Triggers NK Cell-Mediated Cytotoxicity & Cytokine Production against TNBC	Urothelial carcinoma, Metastatic Merkel Cell Carcinoma, TNBC	FDA approved	[138,139]
CTLA-4	Ipilimumab	mAb against CTLA-4 that removes inhibitory signal & reduce T-cell activity	Melanoma	FDA approved	[140,141]
B cells					
CD20	Rituximab; Ofatumumab	mAb against CD20 expressed on B-cells	NHL; CLL	FDA approved	[142] ; [143]
Dendritic Cells					
CD123	Elzonris	Cytotoxin against CD123 expressing cells	BPDCN	FDA approved	STML-401-0114, NCT 02113982
Rho GTPase signaling	Paclitaxel (noncytotoxic dose)	The anti-mitotic drug, Attenuate the propagation of regulatory DCs	Lung Cancer	FDA approved	[144]
MDSCs					
STAT3	Sunitinib	RTK, Inhibit Stat3 in MDSCs, reduced tumor Tregs, downregulate angiogenic gene expression	Metastatic RCC, Pancreatic neuroendocrine tumor	FDA approved and Investigational	[145], [146], NCT00428597
STAT3	Axitinib	RTK, Downregulate STAT3 expression, reverse MDSC-mediated tumor-induced	Metastatic RCC	FDA approved	[147]

(*continued on next page*)

Table 2 (*continued*)

Molecular target	Drug name	Mechanism of action	Indication	Clinical status	Reference
		immunosuppression in spleens and tumor site			
Cellular Component of TME: Fibroblast					
FGFR2	Pemigatinib	Protein kinase inhibitor; blocking FGFR2	Cholangiocarcinoma (Cancer of Bile Ducts)	FDA approved	[148]
BCR-ABL, SRC family (SRC, LCK, YES, FYN), c-KIT, EPHA2, PDGFRβ	Dasatinib	TKI, reverse CAF to normal fibroblast	CML, ALL, Melanoma	FDA approved	[149]
Non-Cellular Component of TME: Targeting the ECM					
CMT-3 & COL-3	Incyclinide	Small molecule, CMT-3 and COL-3, MMPs inhibitor	Advanced solid tumors, recurrent high-grade astrocytoma	Investigational	NCT00004147, NCT00003721, NCT00001683NCT00020683
Heparanase	Roneparstat	Heparinase that participates in ECM degradation and remodeling and may be effective against the ECM	Multiple Myeloma	Phase 1	[150,151]
Non-Cellular Component of TME: Hypoxia Hypoxia-Inducible Factor (HIF)-1 signaling					
HIF-1α	Topotecan; Temsirolimus	Small molecule, inhibiting DNA topoisomerases I.	OC, NSCLC; RCC	FDA approved	[152] ; [153,154]
Hypoxia	Evofosfamide (TH-302)	Bio reductive prodrug of 2-nitroimidazole–based nitrogen Mustard	Multiple myeloma	Phase 1/2/3	[155]
HSP90	Tanespimycin In combination with Trastuzumab	Small molecule, HSP90 inhibitor	Metastatic Breast Cancer	Phase 2/3	[103,156]
Non-Cellular Component of TME: Cytokines					
Interleukin-1 (IL-1) receptor agonist	Anakinra	Protein-Based Therapies binding to the IL-1 receptor inhibit VEGF and other pro-angiogenic factors	**Rheumatoid arthritis, NOMID**	FDA approved	[157]
Non-Cellular Component of TME: Exosomes					
	ExoDx Prostate (IntelliScore)	Urine exosome gene expression assay for men with elevated PSA	Prostate Cancer	FDA approved	[158]
Small interference RNA (siRNA)	IExosomes	MSCs-derived exosomes with KrasG12D	Pancreatic cancer with KrasG12D mutation	Phase 1 NCT03608631	[159]
	Ipilimumab + Nivolumab	predictive value of circulating cell-free tumor DNA (ctDNA) and immune signature by exosome analysis via blood sample will be examined	Breast Cancer	Phase 2	NCT02892734
Interactions between tumor cells and their microenvironment					
RANK Ligand	Denosumab	mAb against RANK Ligand	Osteoporosis	FDA approved	[160,161]

Abbreviation: ALL: Acute lymphoblastic leukemia; BLK: B lymphocyte kinase; BPDCN: Blastic Plasmacytoid Dendritic Cell Neoplasm; CMT-3: Chemically modified tetracycline-3; CRC: Colorectal Cancer; CML: Chronic myelogenous leukemia; CLL: Chronic lymphocytic leukemia; CSF-1R: Colony-stimulating factor 1 receptor; CTLA-4: cytotoxic T-lymphocyte-associated protein 4; DCs: Dendritic cells; DDR: DNA damage response proteins ECM: Extracellular matrix; EGFR: Epidermal growth factor receptor; EPHA2: EPH Receptor A2; FDA: Food and Drug Administration; FGFR2: Fibroblast growth factor receptor 2; GISTs: Gastrointestinal Stromal Tumors; HCC: Hepatocellular carcinoma; H&N carcinoma: Head and Neck Carcinoma; HSP90: Heat shock protein 90; ILs: Interleukin; Lck: lymphocyte-specific protein tyrosine kinase; mAb: monoclonal Antibody; MCC: Merkel cell carcinoma; MDSCs: Myeloid-derived suppressor cells; MDSCs: Myeloid-derived suppressor cells; mTOR: Mammalian Target of Rapamycin; mTORC1: Mammalian target of Rapamycin complex 1; NK cells: Natural Killer cells; NF-κB: nuclear factor kappa-light-chain-enhancer of activated B cells; NHL: Non-Hodgkin lymphoma; NSCLC: Non small-cell lung carcinoma; NOMID: Neonatal-Onset Multisystem Inflammatory Disease; OC: osteosarcoma cancer; PD-1: Programmed cell death protein 1; PD-L1: Programmed death-ligand 1; PDGFR: Platelet-derived growth factor receptor; PDGFRβ: Platelet Derived Growth Factor Receptor Beta; RANK: Receptor activator of nuclear factor κ B; RAF: Rapidly Accelerated Fibrosarcoma gene (proto-oncogene serine/threonine-protein kinase); RCC: Renal Cell Carcinoma; RTK: Receptor tyrosine kinases; SCLC: Small cell lung cancer; STAT3 : Signal transducer and activator of transcription 3; TGCT: Tenosynovial Giant Cell Tumor; TKI: Tyrosine kinase Inhibitor; TME: Tumor microenvironment; TNBC: Triple Negative Breast Cancer; Tregs: Regulatory T cells; UPR: Unfolded protein response; VEGF: Vascular endothelial growth factor; VEGFR: Vascular endothelial growth factor Receptor.

components in the microenvironment in addition to cancer cells, the physical, chemical, and biological components, such as the ECM, interstitial flow, stromal cells, immune cells, vascular networks, and biochemical concentration gradients, are responsible for the failure of developing an effective drug or leads to the development of drug resistance [97]. Frequently, researchers overlook the environmental factors and utilize traditional two-dimensional (2D) culture techniques and models (e.g., monolayer cell culture) for drug discovery because of the ease of handling and reproducibility of results. 2D cultures do not wholly replicate cell-cell interaction, cell-ECM interaction like the three-dimensional (3D) organization of cells and ECM within tissues and organs. Also, cells growing in a monolayer in a 2D model have unlimited access to oxygen, nutrients, and signaling molecules from the culture medium, significantly different from 3D models (e.g., multicellular layers, spheroids, *ex vivo* cultures). However, this is one reason for the failure of many drugs in clinical trials because the results from traditional cell culture models exhibit significant differences from those of animal studies and human trials [18,98,99].

Herein, we attempt to bring the attention of all scientific readers by highlighting the importance of targeting TME and how it involves developing chemoresistance. It has been shown that TME has a dominating role in developing anticancer therapies, and efforts are being made to develop effective drugs extending from traditional chemotherapeutics to combination therapies for targeting various components of TME [100]. Several FDA-approved clinical drugs targeting tumor cells have repurposed for targeting TME components, and we have also summarized potential combined therapeutic approaches to improve drug efficacy and durability. Repurposed drugs have been summarized in Table 2 and also shown in Fig. 1. The advantage of repurposing drugs is to reduce costs, including the time and money involved in discovering and developing novel anti-cancer drugs. It also lowers the risk of failure of clinical trials involved in the process of approving novel drugs[101].

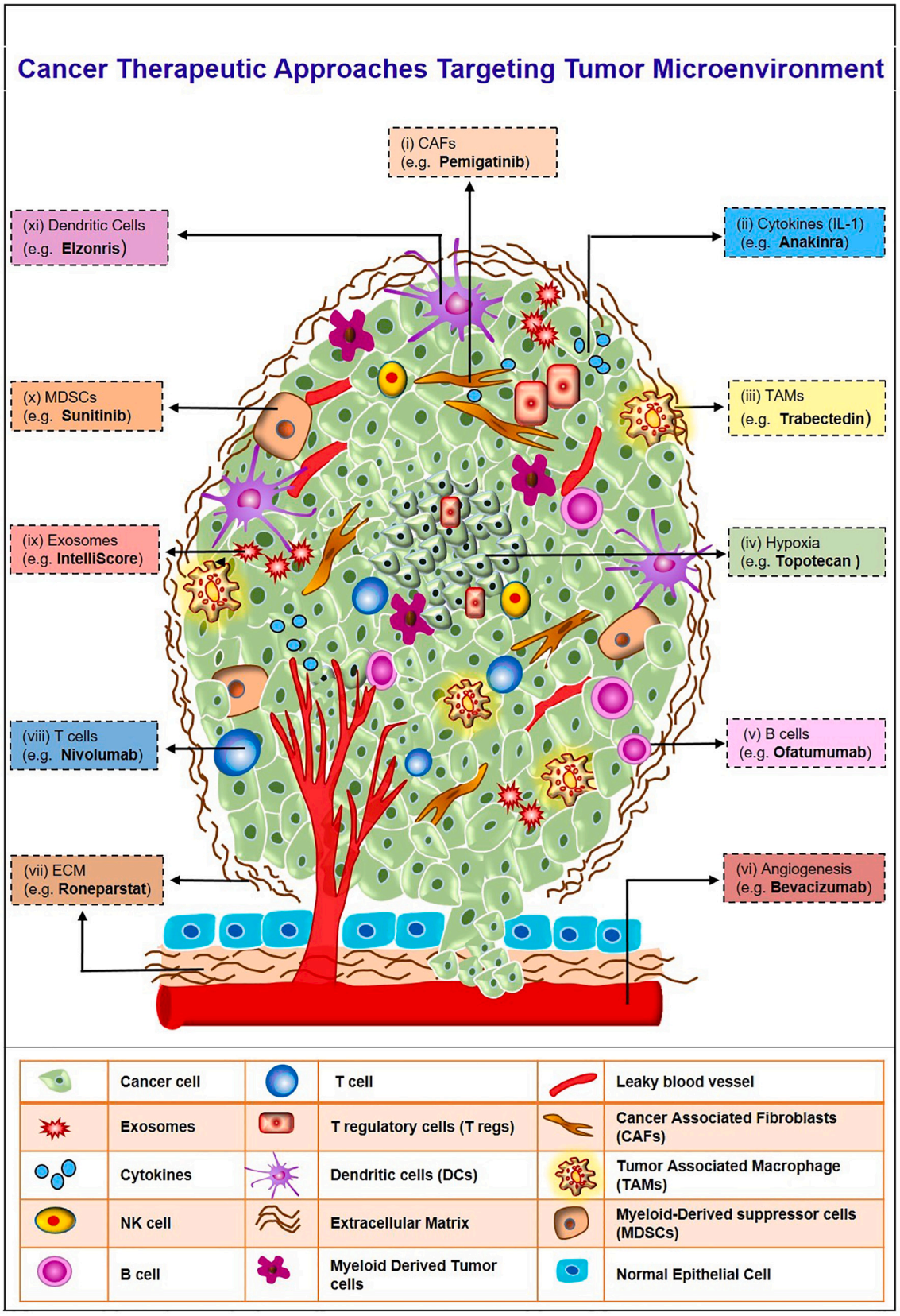

(caption on next page)

Fig. 1. *Approach used to target TME for cancer treatment:* Schematic illustration for heterogeneous and complex TME: (i) *Cancer-associated fibroblasts (CAFs):* They promote angiogenesis via VEGF, CXCL12a and FGF-2 production and modulate the immune response via macrophage infiltration and cell polarization. Pemigatinib is a potent inhibitor of fibroblast growth factor receptor (FGFR) types 1, 2, and 3 to treat cholangiocarcinoma. (ii) *Cytokines:* Anakinra, an FDA-approved IL-1 receptor antagonist (IL-1Ra), inhibits pro-inflammatory cytokine IL-1. It is used in the second-line treatment of rheumatoid arthritis. It has also been used in combination with Nab-paclitaxel, Gemcitabine, and Cisplatin for Pancreatic cancer (NCT02550327). (iii) TAMs*:* They are key component of the TME, as they aid in metastasis and invasion by secreting matrix metalloproteinases, as well as promoting genetic instability. Trabectedin inhibits the G2 phase of the cell cycle, lowers TAMs, and regulates the production of cytokines and angiogenic factors. (iv) *Hypoxia*: Hypoxia-induced factor-1 governs the cellular response and inflammation inside the TME. FDA approved Topotecan, a medication that targets topoisomerase I and is known to block hypoxia-mediated HIF-1 activation. (v) *B cells*: They play a role in humoral immunity. Ofatumumab is a human anti-CD20 human immunoglobulin G1 kappa (IgG1κ) mAb that depletes B cells and is used to treat non-Hodgkin's lymphoma, chronic lymphocytic leukemia. (vi) *Angiogenesis*: Tumor cells initiate angiogenesis, which results in the creation of chaotic branching structures. Bevacizumab is a humanized monoclonal antibody that prevents circulating VEGF from interacting with its receptors. (vii) Extracellular matrix (ECM): Collagen, elastin, fibronectin, hyaluronic acid, proteoglycans, and glycoproteins make up the ECM, which also contains several growth factors. Roneparstat being in Phase 1, is a heparinise inhibitor that engages in degradation and remodelling of ECM and proven to be effective against the ECM. (viii) *T cells:* They contribute to cell immunity. Nivolumab is a fully human immunoglobulin G4 (IgG4) mAb that binds to the PD-1 receptor and by preventing its interaction with its ligands PD-L1 and PD-L2, it disrupts negative signaling to restore T cell antitumor function. (ix) *Exosomes*: Tumor cell-derived exosomes modulate the TME via paracrine signaling. ExoDx Prostate (IntelliScore), a urine exosome gene expression assay, is a non-invasive test to determine elevated Prostate-Specific Antigen (PSA) for men. (x) *MDSCs*: VEGF causes MDSCs activation. Activated MDSCs migrate to the TME, where they promote proliferation and vascularization while inhibiting the immune system. Sunitinib is a receptor tyrosine kinase inhibitor that targets and depletes MDSCs and Tregs in the peripheral blood, lowering their accumulation and reversing IFNγ suppression. (xi) *Dendritic Cells*: TME modulates dendritic cells to evade the immune response by playing an essential role in skewing tumor-specific cytotoxic T cells. Elzonris, recombinant human IL-3 and truncated diphtheria toxin fusion protein block protein synthesis and treat Blastic plasmacytoid dendritic cell neoplasm (BPDCN). Abbreviation: mAb: monoclonal Antibody; CXCL12a: C-X-C Motif Chemokine Ligand 12a; FGF-2: Fibroblast growth factor 2; IFNγ: Interferon gamma; IL-1: Interleukin-1; MDSCs: Myeloid-derived suppressor cells; PD-L1: Programmed death-ligand 1; PD-L2: Programmed death-ligand 2; PD-1: Programmed cell death protein 1; TAM: Tumor-associated macrophages*;* TME: Tumor microenvironment; VEGF: Vascular endothelial growth factor.

We hypothesize that modulation of the TME with multi-directed therapy is an effective approach that can be successfully applied in clinics to treat cancer. This review aims to focus on characteristics of the TME that can be manipulated to design more effective cancer therapies and treatment strategies. Also, we describe the importance of targeting TME by putting more emphasis on combinatorial therapies.

2. The hallmarks of cancer: perspectives for the tumor microenvironment

Hanahan and Weinberg, in their influential review, defined the hallmarks of cancer as a multistep process that includes biological functions such as sustaining proliferative signaling, evading growth suppression, resisting cell death, enabling replicative immortality, inducing angiogenesis, activating invasion/metastasis (henceforth termed Hallmarks I). A decade later, an updating review (hereafter termed Hallmarks II) added two emerging hallmarks: reprogramming energy metabolism and evading immune response, and two enabling traits: genome instability and mutation and tumor-promoting inflammation [162]. Here, in this review, we will discuss how each hallmark of cancer is related to TME. The relation between each hallmark of cancer and TME, is depicted in Fig. 2.

2.1. Sustained proliferative signaling

A recent exponential increase in our knowledge in oncology shed light on the role of TME in cancer progression and metastasis. This provides researchers with novel approaches to target the TME for efficient anticancer therapy. Cancer cells use various distinct signaling pathways (such as TGF-β, Wnt, NOTCH, and Hh) and reciprocal communication to efficiently recruit stromal cells, immune cells, and vascular cells in their vicinity, which, in turn, provides growth signals, intermediate metabolites, and a suitable environment for its progression as well as metastasis. This implies that TME does not act as a passer-by, but it proactively participates in tumor progression [163]. Infiltrating immune cells, inflammatory cells (chronic in nature and are enriched in Treg and MSC) and stromal elements are reprogrammed by the tumor to the pro-inflammatory mode favoring its survival. Antitumor functions of these infiltrates are downregulated because tumor-derived signals and activation of these immune cells in the TME are co-opted to promote tumor growth by sustained activation of the NF-κB pathway in the tumor milieu [164]. K H Shain and team reviewed the vital role s TME in shaping B-cell malignancies' hallmarks. They have mentioned about recruitment and activation of TME-stromal cells along with other cells discussed above.

Activation of various signaling pathways in response to the stimulus generated from the tumor load occurs within the TME. This microenvironment further nurtures these abnormal cells in proliferation and metastasis. Hh-dependent signaling between epithelial cells and underlying mesenchymal or stromal cells regulates epithelial cell proliferation and survival by producing various signaling molecules. This signaling directly or indirectly enriches the TME facilitating tumor growth and progression by synthesizing signaling molecules. Moreover, Hh/GLI signaling has been explored in immune crosstalk and modulation [165]. In addition to this, Takabatake and his colleagues studied that Sonic Hedgehog Signaling promotes growth and invasion in TME of Oral Squamous Cell Carcinoma [166]. Another vital signaling studied is NOTCH signaling in regulating the crosstalk between the various compartments of the TME, which involves reciprocal juxtacrine and paracrine factors [167]. More importantly, a plethora of studies stipulates the critical role in development, cell proliferation, differentiation, and homeostasis and dysfunction of this pathway has been reported in various cancers such as breast, prostate, lung, colorectal, T-cell leukemia, as well as central nervous system (CNS) malignancies [168]. A recent study suggested that dysregulated Wnt signaling and its relationship with TME promotes tumor cells' proliferation and maintenance, including leukemia [169].

2.2. Triggering angiogenesis

Angiogenesis is the most important cancer hallmark because of its role in tumor progression and metastatic dissemination. Cells in tumor produce signals and endogenous factors in their microenvironment that promotes angiogenesis. TME, by secreting numerous pro-angiogenic and anti-angiogenic factors, has a modulating role in tumor vascularization. Since angiogenesis is essential for tumor metastasis and growth, site-specific micro environmental regulation of angiogenesis is one of the most important determinants of the organ preference of metastases [170]. VEGF, FGF, and platelet-derived growth factor (PDGF) are the three crucial protein-peptide families that have a role in promoting neovascularization and are known as angiogenic factors. Many cytokines such as TGF-β, Interferons (IFNs), Tumor necrosis factor-alpha (TNF-α), Interleukins (ILs) act in paracrine and autocrine fashion secreted by tumor cells in TME plays a critical role in regulating tumor angiogenesis [171]. In addition to angiogenic factors, recent studies shed light on non-coding RNAs' role in tumor angiogenesis. Long non-

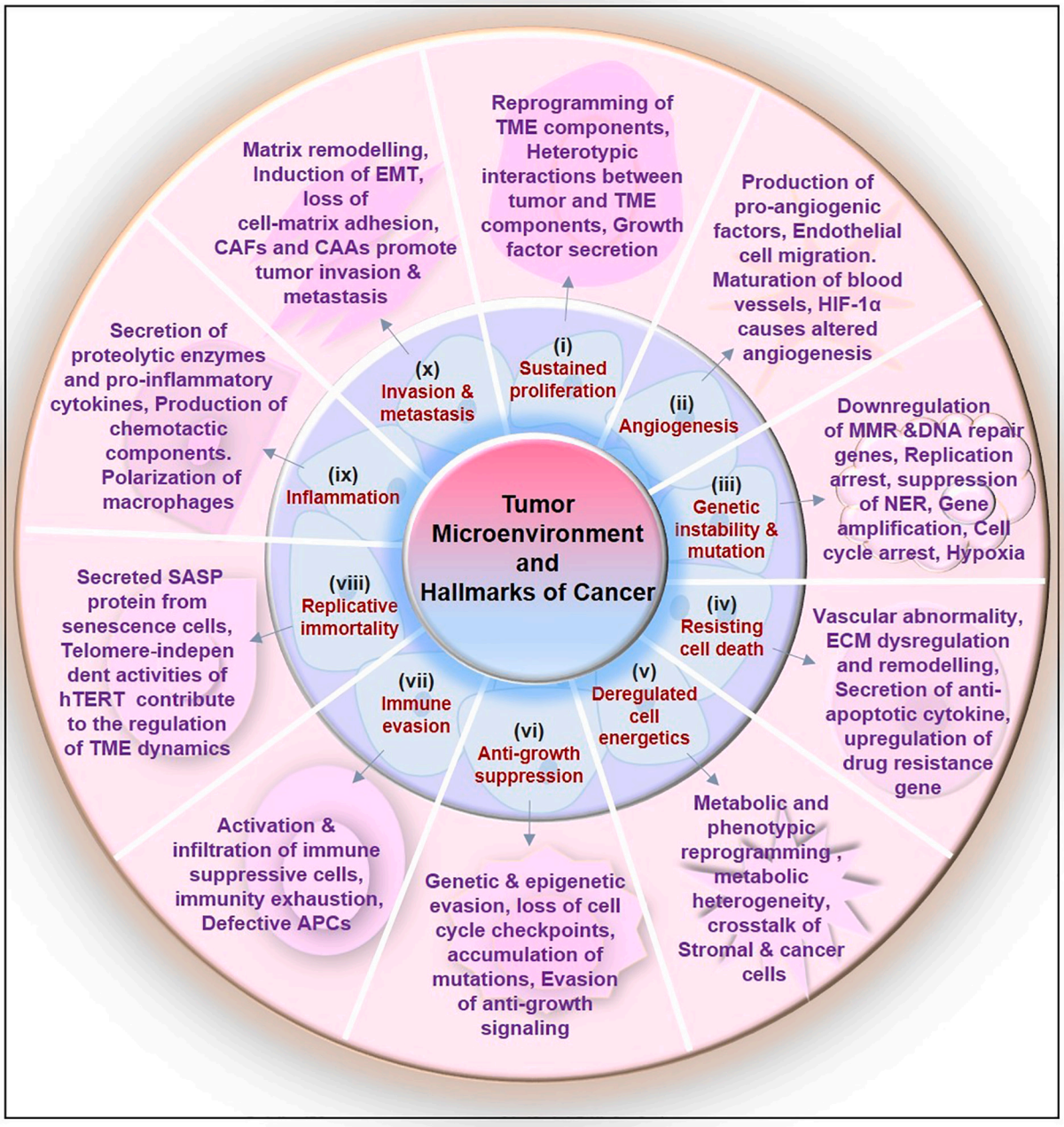

(caption on next page)

Fig. 2. *Role of TME in modulating different hallmarks of cancer.* (i) *Sustained proliferation* is an important hallmark of cancer. Various TME component cells undergo reprogramming and promote heterotypic interactions with tumor cells. The growth factors and cytokines secreted by TME cells assist the growth and proliferation of tumor cells. (ii) *Angiogenesis* is a popular hallmark of cancer progression where TME component cells release pro-angiogenic factors (VEGF, FGF, HIF-1α, TNF-β, Ang-1, Ang-2), chemokines, and cytokines which help in endothelial cell migration, proliferation, degradation of ECM, maturation of blood vessels and new blood vessel formation. (iii) *Genetic instability* and mutational events are the important feature of cancer cells. In TME, downregulation of MMR genes, oxidative base damage, dysregulation of DNA repair genes, suppression of NER, gene amplification, cell cycle arrest, replication stress, ROS/RNS formation are the major events promoting genetic instability. (iv) *Cell death resistance* is an important feature of cancer. Microenvironment components aid cancer cells to escape apoptosis by secretion of anti-apoptotic cytokines like IL-4, IL-6. Vascular abnormality, ECM dysfunction and remodelling leads to upregulation of gene responsible for apoptosis. (v) *Deregulated cellular* energetics shown by cancer cells is promoted by metabolic and phenotypic reprogramming of stromal cells, oncogenic load, and cross-talk with stromal cells (CAFs, endothelial cells, adipocytes, T cells, and macrophages). (vi) *Anti-growth suppression* is the protective mechanism adapted by cancer cells to acquire tumorigenicity. Various genetic (chromosomal deletion, mutation, loss of upstream and downstream effectors) and epigenetic (DNA methylation, histone methylation, and acetylation) mechanisms, loss of cell cycle checkpoints, evasion of anti-growth signaling such as p53, PTEN, GDF15, IGF-1R, notch, hippo, in the TME are responsible for anti-growth mechanisms. (vii) *Immune evasion* is one of the most important hallmarks shown by cancer cells. In the TME, tumor-associated antigen presentation is inhibited, secretion of immune suppressive cytokines, activation of immunosuppressive cells (e.g., MDSCs), and suppression of T cell-mediated immunity, activation of immune checkpoint inhibition, and polarisation of macrophages towards M2 (pro-tumorigenic) phenotype are the major factors responsible for immune suppression. (viii) *Replicative immortality* is another important hallmark of cancer cells. hTERT independent of telomere maintenance plays a pleiotropic role regulating various features of the TME such as angiogenesis, inflammation and immunosuppression, fibroblast activation, and maintenance of CSCs pluripotency. This contributes to the TME for promoting tumor invasion and metastasis. (ix) *Inflammation* is an important phenomenon exhibited by cancer cells promoted by secretion of proteolytic enzymes, inflammatory cytokines, pro-angiogenic mediators, chemotactic components such as CCL2, CCL5, CCL7, CXCL8, CXCL12, infiltration of inflammatory cells, and suppression of T-cell activity in TME. (x) *Invasion and metastasis* are the crucial characteristic of cancer cells. TME components help cancer cells metastasize by matrix remodelling, EMT, and by assisting tumor cell migration in the network of TME associated chemokines and cytokines. CAFs and CAAs promote tumor progression. CAAs promote invasion and metastasis by secreting chemokines such as CCL2, CCL5, IL-1β, IL-6, and VEGF. Moreover, CAAs preconditions TMEs by supporting anti-tumor immunity.

Abbreviation: &: and; Ang-1: Angiopoietin 1; Ang-2: Angiopoietin 2; APCs: Antigen-presenting cells; CAAs: Cancer-associated adipocytes; CCL2: C–C motif chemokine ligand 2; CCL5: C–C motif chemokine ligand 5; CCL7: Chemokine (C-C motif) ligand 7; CSCs: Cancer stem cells; CXCL8: (C-X-C motif) ligand 8; CXCL12: C-X-C motif chemokine 12; EMT: Epithelial to mesenchymal transition; ECM: Extracellular matrix; FGF: Fibroblast growth factors; GDF15: Growth differentiation factor 15; HIF-1α: Hypoxia-inducible factor 1-alpha; hTERT: Telomerase reverse transcriptase; IGF-1R: Insulin-like growth factor 1 receptor; IL: interleukin; MMR: Mismatch repair; NER: Nucleotide excision repair; PTEN: Phosphatase and tensin homolog; RNS: Reactive nitrogen species; ROS: Reactive oxygen species; TME: Tumor microenvironment; TNF-β: Tumor necrosis factor-beta; VEGF: Vascular endothelial growth factor.

coding RNAs (lncRNA) such as (i) lncRNA F630028O10Rik suppresses angiogenesis by inhibiting VEGF-A and by regulating miR-223-3p in lung tumor [172], ii) LncRNA UBE2CP3 increase VEGF-A expression by activating ERK/HIF-1α/VEGFA signaling in HCC, iii) LncRNA H19 targets miR-342 by Wnt5a/β-Catenin Pathway and also LncRNA TUG1 binds to miR-299 and upregulates VEGFA expression [173], have been explored for their angiogenic potential. In the last decade, miRNA has been studied in almost all human cancers as a master regulator of angiogenesis by targeting angiogenesis factors such as cytokines, metalloproteinases and growth factors, including VEGF, PDGF, FGF, EGF, HIF-1, as well as MAPK, PI3-kinase and TGF signaling pathways [174].

In melanoma, breast and prostate cancer, a correlation has been reported between MSCs and angiogenesis [175,176]. The most prevalent immune/inflammatory cell type present in tumors is the tumor associate macrophages (TAMs). TAM plays an important role in angiogenesis, promoting cancer cells by secreting pro-angiogenic factors, including VEGF-A, EGF, PlGF, TGF-β, TNF-α, IL-1β, IL-8, CCL2, CXCL8, and CXCL12 [177]. Other important cells are mast cells recruited by VEGF, bFGF, and TGF-β factor and produce MMPs such as MMP2 and 9, promoting angiogenesis by releasing VEGF and bFGF from the ECM. Thus, the tumor recruits mast cells from its surroundings and helps in forming new blood vessels and tumor progression in solid tumors [178,179]. Recently, Chung and co-workers investigated the interaction between stroma and tumor to understand how this interaction mediates resistance to anti-angiogenic therapy in multiple tumor models: lymphoma, lung and colon. They have shown that TH_{17} cells and their paracrine function in TME induces resistance and enhances tumor response to VEGF therapy.

2.3. Genome instability and mutation

Genomic integrity of cells is maintained through regulated DNA replication, DNA damage repair mechanisms, and cell-cycle checkpoints. Malignant tumors are associated with four types of genomic instabilities: chromosomal instability, intra-chromosomal instability, microsatellite instability, and epigenetic instability [180,181]. Growing evidence has suggested that the TME itself constitutes a significant source of genetic instability [182]. This hypothesis is supported by somatic mutation theory, suggesting that mutation in DNA occurs because of genetic and environmental factors [183]. Telomere shortening, centrosome replication, DNA damage, and epigenetic modifications are the significant factors contributing to genomic instability [184].

Moreover, hypoxia has been proposed as a significant microenvironmental factor involved in genetic instability in solid tumors. Hypoxia in the TME mainly results from an imbalance between the oxygen supply and consumption rate [180]. A HIF-1α transcription factor is the mediator of hypoxia signaling. The transcriptional and transcriptional changes in its activity alter DNA repair response by homologous and non-homologous recombination and mismatch repair. Furthermore, Radisky et al. mentioned Reactive oxygen species (ROS)'s role, produced by inflammatory cells present in TME, in inducing genetic instability and EMT [185].

2.4. Resisting cell death/death resistance

Programmed cell death, specifically apoptosis, is characterized by the cleavage of cell death-associated caspases and the mitochondrial release of pro-apoptotic proteins such as cytochrome c, with tight regulation of pro-and anti-apoptotic molecules, including those from the Bcl2 family [186,187]. Tumor cells, in order to survive and proliferate, avoid different cell death pathways, and they also evolve a variety of strategies to circumvent apoptosis. Amongst different classified cell death pathways by Nomenclature Committee on Cell Death (NCCD), apoptosis, necrosis/necroptosis and autophagy are mainly explored [188]. Microenvironment components help cancer cells to escape apoptosis. ECM undergoes continuous remodeling, and dysregulation of ECM molecules significantly affects cancer cell proliferation by inactivating pro-apoptotic molecules such as Bax and inducing expression of several anti-apoptotic genes, including Bcl2 [189]. Thus, along with his team, N Boudreau reported that ECM, but not fibronectin or collagen, suppresses apoptosis of mammary epithelial cells in tissue culture and *in vivo* through an integrin-dependent negative regulation of ICE expression[190]. IL-6 and NF-κB act as a crucial inducer for cancer in the inflammatory microenvironment by promoting cancer cell proliferation

and inhibiting apoptosis [191,192]. Elevated levels of important cytokines are also considered, anti-apoptotic like IL-6 and IL-4 activate phosphatidylinositol 3-kinase pathways, which results in increased phosphorylation of AKT, an important protein expressed in prostate cancer [193–195]. Similarly, IL-8 promotes migration, angiogenesis, and metastasis and is also implicated in the regulation of apoptosis in prostate, breast, and colon cancer [196,197]. Weigel et al. have shown how insulin-like growth factor–binding proteins (IGFBPs) secreted by CAFs regulates anoikis, facilitating luminal filling in 3D cell culture and promote anchorage-independent growth in breast cancer cells [198]. In breast cancer models, CAFs express matrix metalloproteinase (MMPs) that assist cancer cell growth, migration, adhesion and resistance to apoptosis by activating PI3K-Akt/PKB pathway and thus regulate ECM composition [199].

2.5. Deregulating cellular energetics

Deregulating cellular energetics is one of cancer's hallmarks, popularly known as metabolic reprogramming, a process in tumor cells [162,200]. Even under normoxia conditions, tumor cells convert pyruvate into lactate without entering into the Krebs cycle, i.e., by aerobic glycolysis, which is known as the Warburg effect [201]. Components of the TME, such as stromal cell and immune cells (macrophages and tumor-infiltrating cells), increase lactate concentration within the TME. This increased lactate concentration, in turn leads to the acidification of the TME. This aids in tumor cell survival and proliferation, promotes angiogenesis, and alters immune infiltrating cells [202]. Lactate has an immunosuppressive role, as it affects proliferation and cytokine production of T cells, the cytotoxic role of NK cells and the cytolytic functions of $CD8^+$ T cells. As explored in a study, each cell type in a particular cancer environment has unique metabolic demands that enable specific functions like immune, stromal, and cancer cells; they compete for nutrients to carry out biosynthesis and effector activities [203]. Transformed cancer cells accommodate collaborative metabolic interactions with other tumor cells. The TME is epitomized by deregulated metabolic properties, which include both Intrinsic features (e.g., a mutation in cancer cells like IDH1, IDH2, succinate dehydrogenase (SDH) complex, fumarate hydratase) and extrinsic features (e.g., oxygen and nutrient availability, pH) [204–206]. Several signaling pathways such as PI3K, mTOR, MAPK, HIF-1α, and AMPK subscribes to the Warburg Effect and other cancer cells' metabolic phenotypes. Lactate secreted by tumor cells activates HIF-1α in cancer cells, upregulates angiogenic signals, and stimulates an autocrine pro-angiogenic NF-κB/IL-8 pathway by inhibiting the oxygen-sensing prolyl hydroxylase 2 (PHD2).

Further, it also turn-on receptor tyrosine kinases AXL, TIE2 and VEGFR-2 in a ligand-independent manner [207,208]. Besides lactate, other metabolites such as adenosine are released within the TME. Adenosine inhibits immune cell function and provokes anti-inflammatory molecules by binding with adenosine receptors on various immune cells and immunoregulatory cells such as Treg cells, MDSCs, and M2-type macrophages. This together results in establishing a long-lasting immunosuppressive environment in tumors, promote tumor cell proliferation, tumor cell survival, metastasis, and angiogenesis [209].

2.6. Evading growth suppressors

The evasion of growth suppression is an essential hallmark of cancer and is an important characteristic of cancer cells. Cancer cells get away growth-inhibitory signals of p53, retinoblastoma protein (Rb), TGF-β, gap junctions and contact inhibition to promote tumorigenesis [210]. Various pathways that suppress tumor growth are dysregulated and mentioned as, (i) The Retinoblastoma (Rb) pathway: downregulation of hyperphosphorylated Rb, inactivation of E2F and reduced activity of CDKs; (ii) The p53 pathway: Upregulation of p53 expression; (iii) PTEN pathway: Inhibition of PI3K-AKT and upregulation of PTEN; (iv) NOTCH pathway: inhibition of notch signaling; (v) Hippo signaling: Upregulation of the pathway by suppression of YAP/TEAD activity; vi) Inhibition of IGF-1R; (vii) Activation of ARID1A and GDF 15. Chemokines promote infiltration and activation of host-derived inflammatory and stromal cells that lead to a pro-tumorigenic microenvironment that is immunosuppressive along with vascular permissive [211]. Tumor cells are also known to upregulate autophagy mechanisms to survive microenvironmental stress, increase growth and aggressiveness and facilitate metastasis [212]. In the same context, it's known to suppress the proliferation of tumor cells. The mechanism used by autophagy to support cancer tumorigenesis includes suppressing activation of the p53 protein and maintaining the metabolic function of mitochondria [213,214].

2.7. Avoiding immune destruction

Tumor cells are smart enough to adapt mechanisms to escape detection and destruction by the host's immune system. Each cancer behaves differently compared to others because some are inherently better at 'hiding' than others. For example, cancers, such as melanoma, bladder, and RCC, exhibit a lasting response and better efficacy to immunotherapy; however, breast cancer has not shown a durable response. The most probable mechanisms used by breast cancer cells to escape immune surveillance are, firstly, the expression of immune inhibitory co-stimulatory receptors (e.g., PD-1, CTLA-4, LAG-3), secondly the presence of tumor-derived immunosuppressive factors (e.g., TGF-β, IL-10, IDO), and lastly infiltration of suppressive immune cells (e.g., Tregs, MDSCs), TAMs and increase self-tolerance by regulating NK cells in the microenvironment. Numerous studies have shown that the host immune system has a critical dual role in promoting and suppressing tumor development by establishing a balance between immune recognition and tumor growth. Factors that tumor cells exploit to avoid immune response and embrace immune suppression in TME are infiltration of regulatory cells ($CD4^+CD25^+FoxP3^+$, Tregs), defective antigen presentation (affecting MHC-I pathway, protein LMP2, LMP7, TAP, Tapasin), production of several immunosuppressive mediators such as VEGF, tumor gangliosides, receptor-binding cancer-associated surface antigen (RCAS1), IDO, arginase, and inhibitor of nuclear factor kappa-B kinase (IKK)2, differentiation and polarization of macrophage from cancer-promoting M2 type to cancer-inhibiting M1 phenotype [215].

In most cancers, the infiltrated macrophages are considered to be of the M2 phenotype, and they secrete anti-inflammatory molecules, such as IL-10, TGF-β, and arginase1, which provides an immunosuppressive microenvironment for tumor growth [216]. Tumor cells and some other cells (e.g., myeloid cells) in TME expressed PD-L1/2 inhibitory molecules on their surface and used them as a molecular shield to protect themselves from $CD8^+$ T cell activities [217,218]. Moreover, tumor-derived TGF–β is known to escape immune attack via overproduction of IL-10 (suppressive cytokine), which drive the shift to pro-inflammatory T Helper 1 (TH_1) type to anti-inflammatory T Helper 2 (TH_2) type response (immune deviation, changing the Th1/Th2 balance) [219]. TAM produces various cytokines such as IL-10 and TGF-β in TME, which are involved in immunosuppression, weaken the activity of effector T cells, and inhibit DCs maturation [220]. DCs are bone marrow-derived cells that spread in almost all tissues in the human body. In this context, DeVito et al. mentioned how cancer cells use a mechanism to co-opt and tolerate local DC populations in TME [221]. Studies have shown bone-derived mast cells could exert both immunostimulatory and immunosuppressive actions [222]. They are recruited at the tumor site by chemotactic factors (e.g., stem cell factor (SCF)) released by cancer cells. SCF-recruited mast cells establish a complicated relationship with another immune (including tumor-infiltrating immune cells) and tumor cells that create an immunosuppressive microenvironment altogether. In addition to immune and tumor cell involvement in immune evasion, studies have also focused on the stromal microenvironment consisting of

a variety of non-malignant cells and ECM [223]. It has been proposed that stroma might be a barrier to antigen presentation and immune recognition, hindering immune recognition and destruction.

2.8. Enabling replicative immortality

Cancer cells have the ability to replicate unlimitedly as compared to normal healthy cells. Hayflick Limit, named after scientist Leonard Hayflick discovered that normal cells have a limited capacity to divide, and after the loss of capacity to divide, cells reach an irreversible state of senescence [224]. Normal cells acquired senescence state by numerous stimuli, including intrinsic cellular processes like telomere impaired and gain of function of an oncogene and exogenous factors such as DNA damaging agents or oxidative environment. A plethora of experimental and clinical research data holds the concept that senescence response is important for preventing deregulated growth and malignant transformation. Faulty removal of senescent cells may lead to an unregulated stockpile of cancer. The senescence-associated secretory phenotype (SASP) aids in eliminating senescent cells by engaging immune cells but can potentially encourage the proliferation of tumor cells that are not stably growth arrested. NF-κB and C/EBPβ boost the expression of SASP factors, such as IL-6, IL-8, and IL-1β, acting in an autocrine and paracrine manner to bring out a positive feedback loop increase SASP production [225]. For instance, Ruhland et al. mentioned that senescent stromal cells give rise to local inflammation and are involved in building an immunosuppressive microenvironment by accumulating MDSCs that limit $CD8^{+}$T-cell responses. This encourages immune-mediated tumor growth. SASP derived IL-6 cytokines play a role in inflammation, which mediates immunosuppression and tumor progression [226].

2.9. Tumor promoting inflammation

Cancer cells have the tremendous ability to seize inflammatory responses to promote their growth and survival. They manipulate Immune cells within the complex TME that indirectly induce the production of various proteolytic enzymes, cytokines, chemokines and pro-angiogenic mediators. Dynamic crosstalk exists between cancer and inflammation as an inflammatory response plays a dual role in inhibiting or promoting cancer [227]. In the case of TME, the role of inflammation is type and level-dependent. Important underlying mechanism s which mediate inflammation includes DNA mutation, infectious agents, epigenetic alterations, and impaired DNA repair [228]. A vicious cycle links DNA damage, and ROS production induces inflammation and vice versa, supporting a complex interplay between them [229]. Tumor modulates the inflammatory environment by producing inflammatory cytokines, such as TNF-α, TGF-β, IL-6, and IL-10. Pro-inflammatory cytokines favor the EMT process, and angiogenesis, VEGF, and IL-8 facilitate the latter. Further, anti-inflammatory cytokines, such as IL-10 and TGF-β, involves in evading the immune response. Other TME components, including TAM, TIL, CAF, DCs, MDSCs, T cells, mast cells, and NK cells, promote and maintain tumor growth and metastasis[171]. TAM represents the major inflammatory cell population that aids in maintaining inflammatory TME. TAMs secrete a variety of chemotactic components such as CCL2, CCL5, CCL7, CXCL8 and CXCL12 and aid in maintaining immunosuppressive phenotype by inducing TAM to switch from a M1- to M2-polarized state.

Inflammatory cytokines such as TNF-α, IFN-α, IL-12, and other ILs, increase the efficiency of NK cells in combating the tumor load [230,231]. Yang et al. shown mast cells magnify inflammation along with immune suppression using the SCF/c-kit signaling pathway. Furthermore, mast cells support the suppressive function of MDSC by deploying them to the tumor site through the IL-17 pathway and stimulates IL-17(a critical inflammatory cytokine) expression in MDSCs. Additionally, mast cells induce Treg infiltration and boost their suppressor function and parallelly induce IL-9 production by Treg; in turn, IL-9 promotes mast cells' pro-tumor effect in TME [232]. Besides immune cells, CAFs are also recognized to mediate cancer inflammation by releasing/producing cytokines and chemokines such as s IL-6, GM-CSF and MIP-3α, which aid in infiltration of inflammatory cells like macrophages monocytes and neutrophils to the tumor. A study by Balachander et al. showed that CAFs are valuable in understanding inflammatory responses in tumors as they play a vital role in NF-κB activation, production of pro-inflammatory cytokines, and upregulation of pro-inflammatory gene expression [233].

2.10. Activating invasion and metastasis

Tumor cell invasion and metastasis are two crucial characteristics of cancer, and it enables tumor cells to escape the primary site and colonize to the new secondary site in the new environment [162]. Development of carcinomas in the initial stages during metastasis occurs either due to gain of function of oncogenes and/or loss of function of tumor potential genes. The second step that allows tumor cells to invade includes expansion and invasion of basement membrane into surrounding tissue due to enhanced protease activity (for example, MMPs), increased cell mobility interaction with neighboring tissues (includes ECM/stromal cells), reduced integrity, cell-matrix adhesion (includes matrix–integrin interaction, cell-cell contacts (such as loss of E-cadherin-mediated cell-cell adhesion, loss of cell junction and tight junction) [234,235]. As tumors grow, a bidirectional communication, dynamic and intricate network of interactions exists between tumor cells and other components of TME. The third step of invasion and metastasis includes invasion of cancer cells into the blood vessel mediated by upregulation of angiogenesis, the survival of cancer cells in circulation by immune evasion or suppression of immunosurveillance [235].

Tumor cells and/or other components of TME do this by the various mechanisms, which includes: secretion of angiogenesis-modulating enzymes, such as VEGF, thymidine phosphorylase that enhances the angiogenesis process [236]; recruitment of immune-suppressor cells, including TAM, mast cells, DCs, MDSCs and Tregs cells in response to activated cytokines (e.g., TGF-β, CXCL5-CXCR2) [237]. MDSCs and Treg cells infiltrate the developing tumor to disrupt immune surveillance and promote tumorigenesis via different mechanisms, including encouraging tumor vascularization, interference of antigen presentation by DCs, repression of T and B cell proliferation and activation, or inhibition of NK cytotoxicity and M1 macrophage polarization [7]. TAM plays a vital role in tumor progression and metastasis as it is involved in stimulating angiogenesis (by VEGF secretion) and lymphangiogenesis, remodeling the ECM (by secreting MMPs), activating EMT transition, inducing immunosuppression. For example, macrophage-derived MMP9 promotes tumorigenesis and angiogenesis [220]. TAM produces pro-inflammatory cytokines (IL-1, TNF-α), which help in metastasis and enhances malignant cell invasiveness. The latter is due to TNF-α dependent MMP induction in the macrophages [238]. Numerous studies indicated that TAM accelerates tumor cell invasion via a paracrine signaling loop-mediated tumor-derived CSF-1 and macrophage-derived EGF in breast cancer and Glioblastoma [239,240]. The fourth step includes invasion into secondary tissue by interaction and adaption to the new tissue microenvironment. Paget, an assistant surgeon, gave the 'seed and soil' theory of metastasis in 1889. He beautifully explained that metastasis is not a chance event. In contrast, a specific cancer cell (seed) from the primary site will only be established in a specific and preferred location (soil). Each cancer has an increased propensity to metastasis into one particular secondary location where the microenvironment plays a crucial role in regulating the growth of metastases [14]. Recently, Zaghdoudi et al. studied the inactivation of focal adhesion kinase (FAK) protein activity in CAF, which turns down fibroblast migration/invasion, reduces ECM expression, and alters ECM track generation, adversely affecting M2 macrophage polarization and migration. As a result, they have reported FAK as an independent prognostic marker for disease-free and overall survival of a patient with pancreatic cancer [241].

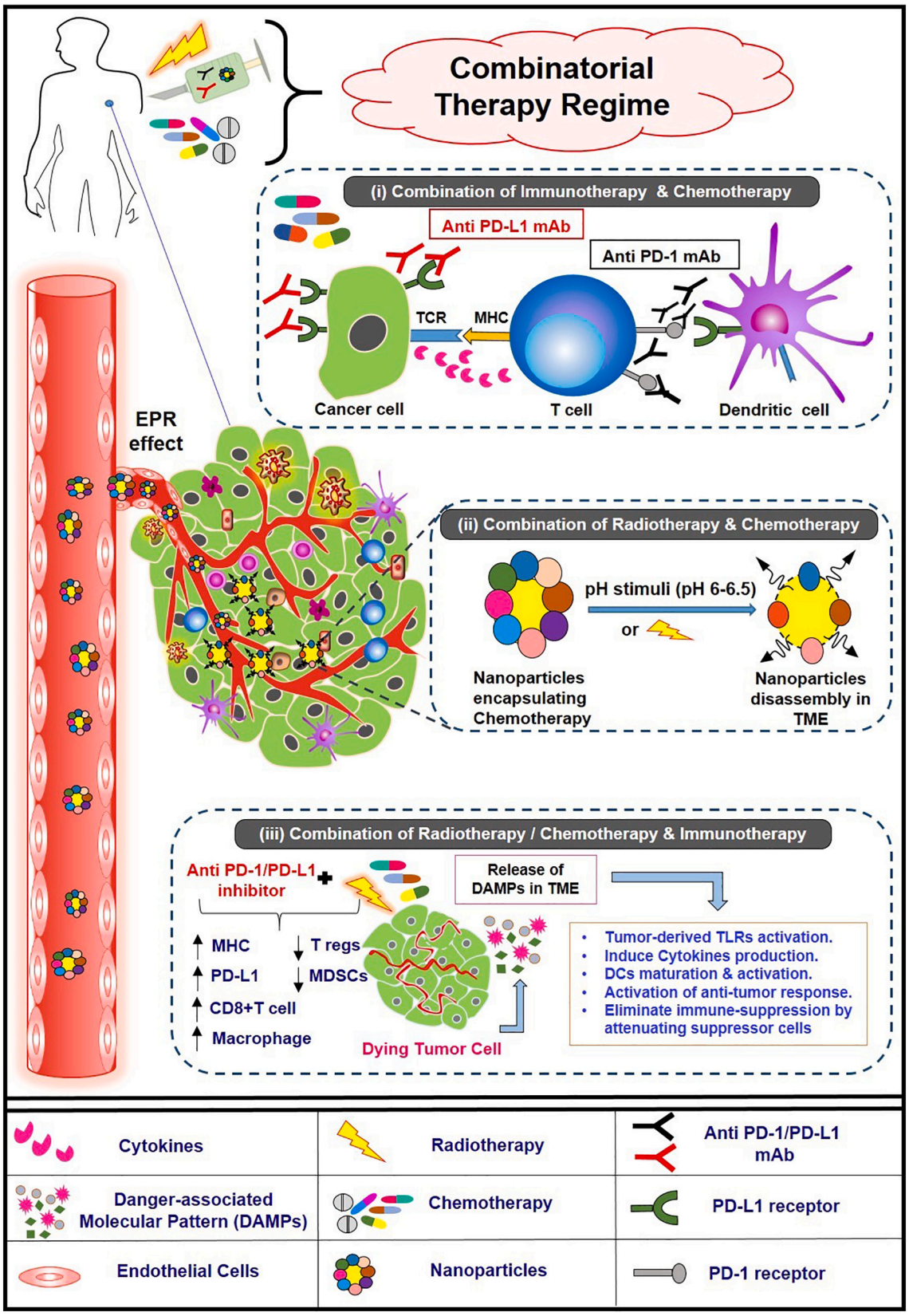

(caption on next page)

Fig. 3. *Possible combinatorial approach to treat cancer*: (i) *Mechanism of combination (immunotherapy with chemotherapy/immunotherapy)*: In cancer, there is an increase of expression of PD-L1 on tumor cells and APCs (such as DCs). PD-1 receptor is expressed on the surface of immune-related lymphocytes (such as T cells, B cells, and myeloid cells) and when it binds to its ligand PD-L1 on tumor cells leads to T cell exhaustion. Blockade of PD-1 (anti-PD-1 mAb, e.g., Nivolumab) or PD-L1 (anti-PD-L1 mAb, e.g., Atezolizumab) stimulates effector T cells to produce anti-tumor responses. Novel combination strategies are combining checkpoint blockade with multiple therapies, including traditional chemotherapy, PARP inhibitors, anti-VEGF agents, and anti-CTLA-4 antibodies (e.g., Ipilimumab), likely targeting multiple mechanisms and overcoming resistance. (ii) *Mechanism of combination (chemotherapy with radiotherapy):* TME-responsive Nanoparticles (such as liposomes, nanoshells, nanocapsules etc.) are capable of encapsulating more than one drug, which is capable of entering and accumulating more at the tumor site due to leaky vasculature (because of EPR effects), and gets dissociate at the tumor site in response to different TME stimuli such as abnormal pH (acidic pH range 6–6.5), hypoxia, enzymes, redox etc. For example, the disruption of TME by gold nanocluster (a pH-sensitive nanoparticle) enhances the effects of radiation therapy in prostate cancer. R3Q17 Hollow mesoporous titanium dioxide nanoparticle (HMTNP) is a hypoxia-sensitive nanoparticle that releases anti-cancer drugs when enter into hypoxic TME#. Gold nanoparticles (AuNPs) are used as theranostic* in the treatment of brain cancer, with release regulated by pH and disassembly mediated by glutathione. (iii) *Mechanism of combination (immunotherapy with radiotherapy/Chemotherapy):* Chemotherapeutic drug, e.g., Gemcitabine, Doxorubicin, Paclitaxel etc.) or Radiotherapy kills tumor cell directly by blocking dysregulated signaling pathways, and it also induces immunogenic cell death (ICD) through the release of DAMPs (including secretion of HMGB1, ATP and translocation of calreticulin to the cell surface). This collectively leads to activation of TLRs (specifically TLR4), activation of dendritic cells to induce tumor antigen-specific T-cell responses and decreased infiltration and accumulation of Tregs and MDSCs in the TME. Radiotherapy induces ICD and also causes DNA damage. Drugs that can stop cancer cell's DNA repair mechanism could make radiotherapy more effective.
APCs: Antigen-presenting cells; ATP: Adenosine tri-phosphate; CTLA-4: Cytotoxic T-lymphocyte-associated protein 4; DCs: Dendritic cells; EPR: Enhanced permeability and retention; HMGB1: High mobility group box protein 1; mAb: Monoclonal antibody; MDSCs: Myeloid-derived suppressor cells; MHC: major histocompatibility complex, PD-1: programmed death-1, PD-L1: programmed death-ligand 1, TCR: T cell receptor; TLRs: Toll-like receptors; TME: Tumor microenvironment; T regs: Regulatory T cells.
** AuNPs, as Theranostics refers to multifunctional AuNPs, may contain diagnostic and therapeutic functions that can be integrated into one system, thereby simultaneously facilitating diagnosis and therapy and monitoring therapeutic responses. # Ultrasound irradiation creates a hypoxic microenvironment when given in combination with HMTNP.*

3. The concept of combinatorial therapy: an armada of potential drugs combination in combating cancer

Combination therapy is considered an essential and promising treatment method in various disease conditions, such as cancer, cardiovascular disease, and infectious diseases. Along with his colleagues, Emil Frei has given the concept of combination therapy using 6-mercaptopurine and Methotrexate to treat acute leukemia [242]. The rationale for using combinatorial treatment is to use more than one drug that may have different mechanisms of action, thereby decreasing the likelihood of developing acquired chemoresistance [243]. Combination therapy using multiple drugs or immunotherapies is an emerging treatment option to combat side effects associated with chemotherapeutic drugs. In some cases, combination therapies are found to be more effective. For instance, the combination of radiotherapy, chemotherapy and surgery is considered as the most standard treatment option for breast, ovarian, and lung and neck cancer [244]. Earlier combinational therapy targets different pathways within tumors, but now focus has also shifted towards an environment surrounding the tumor and aids tumor progression. For instance, Mangiameli et al. sought combination therapy (using Lenalidomide and Sorafenib) targeting the TME as well as the tumor cells in a synergistic way to inhibit ocular melanoma[245]. Similarly, Kitano with his colleagues studied combinatorial therapy (Sunitinib and Everolimus) that modulates TME and impairs tumor growth in RCC [246]. Recently in 2020, FDA approved Durvalumab in combination with etoposide and either carboplatin or cisplatin as the first-line treatment of patients with extensive-stage small-cell lung cancer [247]. In the same year, the FDA approved the use of two immunotherapy drugs Nivolumab and Ipilimumab, for patients with indications NSCLC, HCC and Mesothelioma [248–250]. Liu et al. presented a comprehensive database, "DrugCombDB" allocated to drug combinations from various data sources such as HTS assays, FDA-approved and investigational combinatorial therapies, failed drug combination and PubMed literature. It contains the largest number combination to date.

A drug combination of Tafinlar (Dabrafenib) and Mekinist (Trametinib) gained FDA approval status to treat patients with BRAF V600–positive advanced or metastatic NSCLC. This approval makes BRAF V600E the fourth actionable genomic biomarker in metastatic NSCLC—along with EGFR, ALK and ROS-1. Along with this combination therapy Oncomine Dx Target Test, a next-generation sequencing (NGS) test, as a companion diagnostic kit, got approval, which detects the presence of BRAF, ROS-1, and EGFR gene mutations[251]. Combinatorial approaches to cancer treatment are shown in Fig. 3. Recently, Fengxia et al. mentioned that a combination that includes Palbociclib (a cyclin-dependent kinase (CDK) 4/6 inhibitors) and Human sulfatase-1 (HSulf-1) together exhibited a synergistic antitumor effect on retinoblastoma (RB)-positive TNBC. This also indicates HSulf-1 may be a potential therapeutic target for TNBC. Previously scientists have reported that HSulf-1 s a negative regulator of cyclin D1 and also emerging as a novel prognostic biomarker in Breast cancer. This is because enhanced HSulf-1 expression was also linked with increased progression-free survival and overall survival in patients with TNBC [252].

Advantages of using combinatorial therapy, which may include a combination of chemotherapy, antibodies, nanotherapy, etc. over single-drug chemotherapy, include: enhance efficacy (additive or synergistic); reduced chance of broad-spectrum chemoresistance by delaying the emergence of acquired resistance (combine therapeutic agents with different mechanisms of action); decreased toxicity (use of drugs with non-overlapping toxicities); hitting cancer more than one place, increase the opportunity to use lower doses of one or both drugs; reduced treatment duration and also address heterogeneous nature of tumors. Some drawbacks, such as drug interaction, can lead to side effects that could occur due to reactions between the medications; challenging to figure out the source of unwanted side effects [253]. These days' clinical trials evaluating a drug targeting only one TME component are rare, and hence numerous combinatorial therapies are approved and listed in Table 3.

ClinicalTrials.gov, the most comprehensive of the international clinical trial registries, offers a unique opportunity to see all drug combination trial treatments in one location. Many combination trials are still being tested for safety, efficacy, and toxicity in oncology, as outlined in Table 4 since studies show that drug combinations have the potential to enhance patient response, reduce the development of resistance, and minimize adverse effects. As a result, recognizing and understanding current combination trials is crucial for future clinical trials and preclinical study design. For example, Allen and co-workers investigated the mechanism by which anti-angiogenic therapy improves anti-PD-L1 treatment, especially by enhancing cytotoxic T cell infiltration due to the therapy's induction of intra-tumoral high endothelial venules. Moreover, they also hypothesized that the efficacy of anti-angiogenic therapy had been enhanced by anti-PD1 therapy in pancreatic and breast cancer models [283]. A KEYNOTE-021 trial combining Ipilimumab with Pembrolizumab in patients with NSCLC shows that this combination appears to be efficacious and associated with significant toxicity. A total of 51 patients were involved in this study, with 44 of them receiving a combination of Pembrolizumab 2 mg/kg and Ipilimumab 1 mg/kg. The objective response rate (ORR) was 30% (95% confidence interval (CI): 17%-45%), median progression-free

Table 3
FDA approved Combinatorial Therapy targeting the Tumor microenvironment

S. no	Approved drug combination	Indication	Drug class	FDA approval year	Reference
1	Opdivo (Nivolumab) and Yervoy (Ipilimumab)	Mesothelioma	**Nivolumab** (PD-1 inhibitor); **Ipilimumab** (CTLA-4 inhibitor)	2020	[250]
2	Opdivo (Nivolumab) and Yervoy (Ipilimumab)	HCC	**Nivolumab** (PD-1 inhibitor); **Ipilimumab** (CTLA-4 inhibitor)	2020	[249]
3	Opdivo (Nivolumab) and Yervoy (Ipilimumab)	Metastatic NSCLC (tumors express PD-L1 greater than or equal to 1%, as determined by FDA approved test)	**Nivolumab** (PD-1 inhibitor); **Ipilimumab** (CTLA-4 inhibitor)	2020	[248]
4	Imfinzi (Durvalumab) and Etoposide and Carboplatin/cisplatin	Extensive-stage small-cell lung cancer	**Imfinzi** (PD-L1 inhibitor); **Etoposide** (topoisomerase II inhibitor; **Carboplatin** (alkylating agent)	2020	[247]
5	Encorafenib (BRAFTOVI) and Erbitux (Cetuximab)	Metastatic CRC (BRAF V600E mutation)	**Encorafenib** (BRAF inhibitor); **Cetuximab** (EGFR inhibitor)	2020	[254]
6	Neratinib (NERLYNX) and Capecitabine	Metastatic HER2+ Breast cancer	**Neratinib** (binds to and irreversibly inhibits EGFR, HER2,4 receptor); **Capecitabine** (converted to fluorouracil (antimetabolite)	2020	[255]
7	Lynparza (Olaparib) and Avastin (Bevacizumab)	Advanced Ovarian cancer	**Olaparib** (inhibitor of PARP) enzymes; **Bevacizumab** (inhibits angiogenesis by targeting VEGF)	2020	[256]
8	Pemfexy (Pemetrexed for injection) and Cisplatin	Metastatic non-squamous	**Pemfexy™** (multitargeted antifolate); **Cisplatin** (Alkylating agent Crosslink/damage DNA	2020	[257]
8	Pembrolizumab (KEYTRUDA) and Inlyta® (Axitinib)	Advanced RCC	**Inlyta®**(VEGFR-1,2,3 inhibitor) **Pembrolizumab** (PD-1 inhibitor)	2019	[258]
9	Lenvima (lenvatinib) and Keytruda (Pembrolizumab)	Advanced Endometrial carcinoma	**Lenvatinib** (RTK inhibitor of VEGFR1,2,3); **Pembrolizumab** (PD-1 inhibitor)	2019	[259]
10	Avelumab (Bavencio) and Axitinib (Inlyta)	Advanced RCC	**Avelumab** (PD-L1 inhibitor); **Inlyta®**(VEGFR-1,2,3 inhibitor)	2019	[260]
11	Polivy (Polatuzumab vedotin-piiq) and Bendamustine and Rituximab	Relapsed/refractory diffuse large B-cell lymphoma	**Polivy** (ADC binds CD79b found only on B cells; **Bendamustine** (alkylating agent); **Rituximab** (engineered chimeric murine/human mAb directed against CD20 antigen found on the surface of normal and malignant B lymphocytes)	2019	[261]
12	Tecentriq (Atezolizumab) and Abraxane (Nab-paclitaxel) and Carboplatin	Nonsquamous NSCLC (Stage4)	**Atezolizumab** (PD-L1 inhibitor) **Abraxane** (antimicrotubule agent); **Carboplatin** (alkylating agent)	2019	[262,263]
13	Atezolizumab and Carboplatin and Etoposide	Extensive-stage small-cell lung cancer	**Atezolizumab** (PD-L1 inhibitor) **Etoposide** (topoisomerase II inhibitor); **Carboplatin** (alkylating agent)	2019	[264]
14	Braftovi (Encorafenib) and Mektovi (Binimetinib) and Erbitux (Cetuximab)	Metastatic CRC (BRAF V600E mutation)	**Encorafenib** (BRAF inhibitor); **Binimetinib** (MEK inhibitor); **Cetuximab** (EGFR inhibitor)	2019	[265]
15	Atezolizumab and Abraxane (Nab-paclitaxel)	TNBC	**Atezolizumab** (PD-L1 inhibitor); **Abraxane** (anti-microtubule agent)	2018	[266]
16	Pembrolizumab (KEYTRUDA) and Pemetrexed and Platinum drug	Metastatic nonsquamous NSCLC	**Pembrolizumab** (PD-1 inhibitor); **Premetrexed** (multitargeted antifolate)	2018	[267,268]
17	Tecentriq (Atezolizumab); Bevacizumab; Paclitaxel and Carboplatin	Metastatic non-squamous NSCLC	**Atezolizumab** (PD-L1 inhibitor) **Bevacizumab** (inhibits angiogenesis; **Carboplatin** (alkylating agent) **Paclitaxel** (mitotic inhibitor)	2018	[269]
18	Avastin (Bevacizumab) and Carboplatin and Paclitaxel	Epithelial ovarian, fallopian tubecancer	**Bevacizumab** (inhibits angiogenesis); **Paclitaxel** (mitotic inhibitor)	2018	[270]
19	Imbruvica (Ibrutinib) and Rituxan (Rituximab)	Waldenström macroglobulinemia	**Ibrutinib** (binds permanently to a protein, Bruton's tyrosine kinase, that is important in B cells); **Rituximab** (engineered chimeric murine/human monoclonal antibody directed against the CD20 antigen)	2018	[271]
20	Opdivo (Nivolumab) and Yervoy (Ipilimumab)	RCC	**Nivolumab** (PD-1 inhibitor); **Ipilimumab** (CTLA-4 inhibitor)	2018	[272]
21	Opdivo (Nivolumab) and Yervoy (Ipilimumab)	MSI-H/dMMR metastatic CRC	**Nivolumab** (PD-1 inhibitor); **Ipilimumab** (CTLA-4 inhibitor)	2018	[273]
22	Darzalex (Daratumumab) and Pomalyst (Pomalidomide) and Dexamethasone	Relapsed and/or refractory multiple myeloma	**Darzalex** (mAb that targets CD38+ multiple myeloma cells); **Pomalyst** (inhibitor of COX2); **Dexamethasone** (inhibit NF-κB and other inflammatory transcription factors	2017	[274]
23	Liposome contains Vyxeos (Daunorubicin) and Cytarabine	Therapy-related acute myeloid leukemia	**Daunorubicin** (anthracycline antitumor antibiotic); **Cytarabine** (pyrimidine nucleoside analog inhibits the synthesis of DNA)	2017	[275]
24	Arzerra (Ofatumumab) and Fludarabine and Cyclophosphamide	Relapsed chronic lymphocytic leukemia	**Ofatumumab** (anti-CD20 monoclonal antibody); **Fludarabine** (Adenosine deaminase inhibitor); **Cyclophosphamide** (alkylating nitrogen immunosuppressive agent)	2016	[276]
25	Tafinlar (Dabrafenib) and Mekinist (Trametinib)	Advanced or metastatic NSCLC (BRAF V600)	**Trametinib** (allosteric inhibitor of MEK1 and MEK2; **Dabrafenib** (inhibitor of BRAF (BRAF) protein)	2016	[277]
26	Opdivo (Nivolumab) and Yervoy (Ipilimumab)	Metastatic Melanoma (BRAF V600)	**Nivolumab** (PD-1 inhibitor); **Ipilimumab** (CTLA-4 inhibitor)	2015	[278]
27	Portrazza (Necitumumab) and Gemzar (Gemcitabine), and Cisplatin	Locally advanced or metastatic NSCLC	**Gemcitabine** (nucleoside analog of pyrimidines); **Necitumumab** (recombinant monoclonal IgG1 antibody; **Cisplatin** (Alkylating agent Crosslink/damage DNA	2015	[279]

(*continued on next page*)

Table 3 (*continued*)

S. no	Approved drug combination	Indication	Drug class	FDA approval year	Reference
28	Abraxane and Gemcitabine	Metastatic Pancreatic Cancer	**Abraxane**: Albumin-bound paclitaxel (anti-microtubule agent); **Gemcitabine** (nucleoside analog of pyrimidines);	2013	[280]
29	Temozolomide and radiation therapy	Glioblastoma multiforme	**Temozolomide:** DNA alkylating agent known to induce cell cycle arrest at G2/M phase	2005	[281]
30	Myocet and Cyclophosphamide	Metastatic Breast Cancer	**Myocet:** non-pegylated liposomal doxorubicin citrate; **Cyclophosphamide:** Alkylating agent of the nitrogen mustard type	2001	[282]

Abbreviation: ADC: Antibody-drug conjugate; CRC: Colorectal cancer; COX2: Cyclooxygenase 2; CTLA-4: Cytotoxic T-lymphocyte-associated protein 4; dMMR: DNA mismatch repair-deficient; EGFR: Epidermal growth factor receptor; HCC: Hepatocellular carcinoma; mAb: monoclonal antibody; MSI-H: Microsatellite instability-high; Nab-paclitaxel: Nanoparticle albumin-bound paclitaxel; NSCLC: Non-small-cell lung carcinoma; PARP: Poly ADP ribose polymerase; PD-1: Programmed cell death protein 1; PD-L1: Programmed death-ligand 1; RCC: Renal cell carcinoma; RTK: Receptor tyrosine kinases; TNBC: Triple-negative breast cancer; VEGFR: Vascular Endothelial Growth Factor receptor.

survival (PFS) was 4.1 (95% confidence interval: 1.4–5.8) months, and median overall survival was 10.9 (95% confidence interval: 6.1–23.7) months. Data indicates that heavily pretreated patients have antitumor activity. Antitumor activity was seen in highly pretreated patients, but it was linked to significant toxicity [284]. Similarly, Pembrolizumab offered in combination with Carboplatin plus Paclitaxel (Group A); Carboplatin, Paclitaxel, and Bevacizumab (Group B); and Carboplatin plus Pemetrexed (Group C) in a multicohort analysis (KEYNOTE-021) (Group C). Group C showed best antitumor activity (75% ORR, PFS of 10.2 months; 95% CI: 6.5–13.9)with manageable safety profile [285]. Another trial combines chemotherapy (Cisplatin or Paclitaxel) with radiotherapy (high-energy x-rays). The use of this combination before surgery in patients with esophageal cancer may destroy more tumor cells (NCT00003087). Other ongoing combination trails including different treatment regime and different therapies (such as chemotherapy, radiotherapy, surgery, nanotherapy and immunotherapy) gives hopes to patient for better treatment and provides scope for clinician and researchers for improvement to address drawbacks including excessive toxicity, low drug or therapy response, development of resistance to therapy, diversity of individual immune system and many more.

4. Strategies to modulate tumor microenvironment

4.1. The flagon of chemotherapeutics in the modulation of TME

Chemotherapy being a regime of cytotoxic drugs that potentially targets the tumor population of abnormal cellular metabolism remains the gold standard in the world of cancer therapeutics. These drugs are often given in combination with radiation or surgery, depending on the tumor specificity and staging, used for the treatment of various hematological and solid malignancies [286]. Tumor growth and development are contingent on TME thereby affecting the chemotherapeutic potential, leading to poor prognosis and decreased target efficiency [287]. Tumor progression in the early stages causes a metabolic shift and reprogramming in contents of TME comprising of immune cells (B and T cells, NK cells), stromal cells and rewriting of ECM, further leading to metastasis and formation of new vascularization [288], that is essential for tumor survival. Skilled mapping of TME changes during tumor growth and how it modulates the TME is essential as it can be useful to predict correct cytotoxic drugs or combinations of them so that the efficiency of these drugs can be significantly increased in combating various malignancies [163].

Selective targeting of various components within the TME such as ECM, the pericytes and the endothelial cells, differentiation of macrophages and their activation using diverse classes of cytotoxic drugs like the platinum-based regime, checkpoint inhibitors can be a more effective approach in dealing with tumor cells. Chemotherapy has been shown to be most effective when it induces a form of cell death called immunogenic cell death (ICD), which activates an anti-tumor immune response. Numerous damage-associated molecular patterns (DAMPs), including calreticulin (CALR), secreted ATP, annexin A1 (ANXA1), type I interferon, and high-mobility group box 1, are exposed and released during ICD (HMGB1). During ICD numerous DAMPs, including calreticulin (CALR), secreted ATP, annexin A1 (ANXA1), type I interferon, and high-mobility group box 1 (HMGB1), are exposed and released [289]. One of the pathways that get activated is type-I interferon signaling pathways in tumor cells, contributing to the downstream activation of host antitumor immunity [290]. This given scope combines chemotherapy and immunotherapy and employs different strategies for combination chemo-immunotherapy [291]. Gemcitabine is known to reduce the MDSCs population and interferon-gamma (which has an inhibitory role in immune response) [292]. Some chemotherapies show the dual role of cytotoxicity and immune activation, hence providing a rationale for developing combinations regime with immunotherapy. Combinatorial therapies effective in various clinical trials are used to handle various conditions such as hypoxia and acidosis generated in the TME. Examples include the use of gemcitabine and SLC0111 that is employed for targeting ductal malignancies of pancreatic origin (NCT03450018), use of Temozolomide and Acetazolamide as a therapeutic alliance in the treatment of grade IV gliomas within the brain (NCT03011671) [293]. Chemotherapeutic agents such as Cyclophosphamide, Doxorubicin and platinum-based drugs such as Oxaliplatin and Carboplatin show tumoral cell death (immunogenic in nature) and are known to induce a T-cell mediated anticancer effect. Modulation in ECM activity within the TME is also related to the up-regulation of MMPs, a significant intruder in cancer invasion and formation of cancer stem cells (CSCs), leading to poor survival and declined rate of prognosis in cancer patients [189,294,295]. Studies have shown that various inhibitors such as Incyclininde (also known as COL-3) is preferred for targeting these MMPs in advanced-stage carcinomas [296,297]. Hypoxia, another critical factor in TME, is regulated by HIF-1. Various chemotherapy drugs mainly focus on handling this HIF-1 that connects to hypoxia and leads to tumor invasion and progression [298,299]. For example, topoisomerase-1 inhibitors such as Topotecan (FDA approved) are used as a second-line chemotherapy drug in malignancies such as NSCLC and ovarian carcinoma. Topotecan is majorly used in advanced solid carcinomas that express a high level of HIF-1 [300]. Another guiding approach in handling TME is to target the endothelial cells that promote neo-vascularization in tumor cells. An example where Ipilimumab has been combined with carboplatin and paclitaxel in NSCLC, where both chemotherapies caused ICD production and stimulated immune response [301]. These chemotherapeutic agents, when administrated alone or in combination, can achieve a higher rate of success when talking about the modulation of TME in cancer.

4.2. Immunotherapy an exploratory tool in the modulation of TME

Conventional therapies also alter the immune system when

Table 4
List of ongoing clinical trials for combination therapy (from 2014 till present).

S. no	Regimen	Therapeutic combination	Current phase	Trial status	NCT number
1	Pembrolizumab + Epacadostat	Urothelial Cancer	Phase 3	Completed	NCT03361865
2	Pembrolizumab + Epacadostat + Platinum-based chemotherapy	Lung cancer	Phase 2	Completed	NCT03322566
3	Pembrolizumab + Epacadostat	Lung Cancer	Phase 2	Completed	NCT03322540
4	Pembrolizumab + Epacadostat +Oxaliplatin +5-Fluorouracil +Gemcitabine +nab-Paclitaxel +Carboplatin +Paclitaxel + Pemetrexed +Cyclophosphamide + Cisplatin	Advanced or Metastatic Solid tumor	Phase 1/2	Completed	NCT03085914
5	Pembrolizumab + Paclitaxel + Carboplatin	NSCLC	Phase 3	Active, not recruiting	NCT02775435
6	Carboplatin + Etoposide + Atezolizumab	SCLC	Phase 3	Active, not recruiting	NCT02763579
7	Niraparib + Pembrolizumab	TNBC, Ovarian Cancer, Metastatic and Advanced Breast Cancer, Fallopian Tube Cancer, Peritoneal Cancer	Phase 1/2	Active, not recruiting	NCT02657889
8	Pembrolizumab + Paclitaxel	SCLC	Phase 2	Completed	NCT02551432
9	Pembrolizumab +Cisplatin + 5-FU or Capecitabine	Gastric Adenocarcinoma	Phase 3	Active, not recruiting	NCT02494583
10	Avelumab +Axitinib (AG-013736)	RCC	Phase 1	Active, not recruiting	NCT02493751
11	Durvalumab +Tremelimumab	NSCLC	Phase 3	Active, not recruiting	NCT02453282
12	Atezolizumab in Combination with Carboplatin + Paclitaxel	Stage IV Squamous NSCLC	Phase 3	Active, not recruiting	NCT02367794
13	Atezolizumab in Combination with Carboplatin Plus (+) Nab-Paclitaxel	Stage IV Squamous NSCLC	Phase 3	Completed	NCT02367781
14	Durvalumab + Tremelimumab	Locally Advanced or Metastatic NSCLC	Phase 2	Active, not recruiting	NCT02352948
15	Cobimetinib + Atezolizumab + Paclitaxel	Breast Cancer	Phase 2	Active, not recruiting	NCT02322814
16	Ipilimumab + Paclitaxel + Carboplatin	NSCLC	Phase 3	Completed	NCT02279732
17	Nivolumab + Ipilimumab	Advanced or Metastatic RCC	Phase 3	Active, not recruiting	NCT02231749
18	Axitinib + Pembrolizumab (MK-3475)	RCC	Phase 1	Completed	NCT02133742
19	Arm A: Nivolumab + Gemcitabine + Cisplatin Arm B: Nivolumab + Pemetrexed + Cisplatin Arm C: Nivolumab + Paclitaxel + Carboplatin Arm H: Nivolumab + Ipilimumab	Stage IIIB/IV NSCLC	Phase 1	Active, not recruiting	NCT01454102
20	Nab-Paclitaxel + Nivolumab Nab-Paclitaxel + Gemcitabine + Nivolumab Nab-Paclitaxel, carboplatin and nivolumab Cycle 1 Nab-Paclitaxel + Nivolumab	Pancreatic Cancer Pancreatic Cancer NSCLC Breast Neoplasms	Phase 1	Completed	NCT02309177
21	Durvalumab + Epacadostat (INCB024360)	Advanced Solid Tumor	Phase 1/2	Completed	NCT02318277
22	Atezolizumab + Entinostat + Bevacizumab	Advanced RCC	Phase 1/2	Recruiting	NCT03024437
23	Capecitabine/bevacizumab + Atezolizumab	Metastatic CRC	Phase 2	Active, not recruiting	NCT02873195
25	Pembrolizumab + Paclitaxel + Carboplatin	NSCLC	Phase 1/2	Active, not recruiting	NCT02039674
26	Pembrolizumab + nab-paclitaxel (KNp) followed by Pembrolizumab + Doxorubicin + Cyclophosphamide	NSCLC	Phase 1	Completed	NCT02622074
27	Pembrolizumab 200 mg intravenously (IV) + Pemetrexed 500 mg/m^2 IV (with vitamin supplementation) + Cisplatin 75 mg/m^2 IV OR Carboplatin	NSCLC	Phase 3	Active, not recruiting	NCT02578680
28	Pembrolizumab + mFOLFOX6	CRC	Phase 2	Active, not recruiting	NCT02375672
29	Pembrolizumab +Cisplatin + 5-Fluorouracil (5-FU) or (Japan only) Capecitabine	Gastric Adenocarcinoma & Gastroesophageal Junction Adenocarcinoma	Phase 2	Active, not recruiting	NCT02335411
30	Nivolumab + Ipilimumab versus platinum-based chemotherapy + Nivolumab	Stage IIIB not amenable to radical treatment or stage IV or recurrent SCLC	Phase 2	Recruiting	NCT03823625
31	Pembrolizumab With or Without Carboplatin and Paclitaxel	Recurrent NSCLC	Phase 2	Active, not recruiting	NCT02581943
32	Atezolizumab + Vinorelbine	NSCLC	Phase 2	Active, not recruiting	NCT03801304
33	Avelumab + standard 1st line chemotherapy (Cisplatin or Carboplatin + Etoposide)	SCLC	Phase 2	Active, not recruiting	NCT03568097
34	Pembrolizumab (MK-3475) +Chemotherapy (Nab-paclitaxel, Paclitaxel, Gemcitabine, Carboplatin)	TNBC	Phase 3	Active, not recruiting	NCT02819518
35	Pembrolizumab (MK-3475) in Combination With Etoposide/Platinum (Cisplatin or Carboplatin)	SCLC	Phase 3	Active, not recruiting	NCT03066778
36	Pembrolizumab + Gemcitabine + Cisplatin	Bladder Cancer	Phase 2	Active, not recruiting	NCT02690558
37	Pembrolizumab + Cisplatin-based Chemotherapy	Penile Carcinoma	Phase 2	Recruiting	NCT04224740

(*continued on next page*)

Table 4 (*continued*)

S. no	Regimen	Therapeutic combination	Current phase	Trial status	NCT number
38	Nivolumab + XELOX (Oxaliplatin + Capecitabine)	Gastroesophageal Junction Cancer	Phase 3	Active, not recruiting	NCT02872116
39	Nivolumab + Cisplatin + Fluorouacil	Various Advanced Cancer	Phase 3	Active, not recruiting	NCT03143153
40	Nivolumab + Ipilimumab	Mesothelioma	Phase 3	Active, not recruiting	NCT02899299
41	Avelumab 10mg/kg with Carboplatin/Gemcitabine	Metastatic Urothelial Cancer	Phase 2	Active, not recruiting	NCT03390595
42	Atezolizumab + Nab-Paclitaxel	TNBC	Phase 3	Active, not recruiting	NCT02425891
43	Atezolizumab + Paclitaxel + Carboplatin Atezolizumab + Bevacizumab + Paclitaxel + Carboplatin	NSCLC	Phase 3	Completed	NCT02366143
44	Gemcitabine + Cisplatin + Nivolumab Nivolumab + Ipilimumab	Biliary Tract Neoplasms	Phase 2	Active, not recruiting	NCT03101566
45	Carboplatin + Abraxane +antiPD-L1	Invasive Ductal Breast Carcinoma	Phase 3	Active, not recruiting	NCT02620280
46	Paclitaxel +Durvalumab	Breast Cancer	Phase 1/2	Completed	NCT02628132
47	Durvalumab + Olaparib +/-Cediranib	Colorectal Neoplasms & Breast Neoplasms	Phase 1/2	Recruiting	NCT02484404
48	Gemcitabine +Cisplatin + Ipilimumab	Urothelial Carcinoma	Phase 2	Completed	NCT01524991
49	Pebrolizumab + QUADSHOT+ Radiotherapy	Head and Neck Cancer	Phase 2	Recruiting	NCT04373642
50	NBTXR3 activated by Brachytherapy & IMRT	Prostate Cancer	Phase 2	Recruiting	NCT02805894
51	DOTAP: Chol-TUSC2 + Erlotinib hydrochloride	NSCLC	Phase 2	Active, not recruiting	NCT01455389
52	CRLX101 + Enzalutamide	Prostate Cancer	Phase 2	Recruiting	NCT03531827
53	Nab-paclitaxel + Gemcitabine	Advanced Pancreatic Cancer	Phase 2	Recruiting	NCT03636308
54	EP0057(Nanoparticle Camptothecin) + Olaparib	Refractory SCLC	Phase 2	Recruiting	NCT02769962
55	NBTXR3 Crystalline Nanoparticles + Stereotactic Body Radiation Therapy	Liver Cancers	Phase 1/2	Active, not recruiting	NCT02721056
56	Phenelzine Sulfate + Nanoparticle albumin-bound paclitaxel	Advanced Breast Cancer	Phase 1	Completed	NCT03505528
57	Carboplatin -Nab Paclitaxel + HLX10	Stage IIIB/IIIC or IV NSCLC	Phase 3	Recruiting	NCT04033354
58	Polysiloxane Gd-Chelates based nanoparticles (AGuIX) + Cisplatin + EBRT + Uterovaginal brachytherapy	Gynecologic Cancer	Phase 1	Recruiting	NCT03308604
59	Radiotherapy + Nivolumab	Gastric Cancer	Phase 1/2	Active, not recruiting	NCT03453164
60	Carboplatin and Paclitaxel + Radiation Therapy	Endometrial Cancer	Phase 2	Recruiting	NCT03935256
61	Chemotherapy (Pemetrexed and cisplatin [or carboplatin]) + surgery + Radiation	Pleural Epithelioid Mesothelioma	Phase 3	Recruiting	NCT04158141
62	Surgery + Chemotherapy	Rectal Cancer Recurrent	Phase 3	Recruting	NCT04288999
63	Chemotherapy (FOLFIRINOX) + Radiation + Surgery	Rectal Cancer	Phase 2	Recruiting	NCT03879109
64	CHESS: Durvalumab + chemotherapy + stereotactic radiotherapy	NSCLC	Phase 2	Recruiting	NCT03965468
65	SBRT (Stereotactic Body Radiation Therapy) + Nivolumab/ Ipilimumab	RCC	Phase 2	Completed	NCT03065179
66	Olaparib + Durvalumab With Carboplatin, Etoposide, and/or Radiation Therapy	Stage Lung Small Cell Carcinoma	Phase1/2	Recruiting	NCT04728230
67	Camrelizumab+Radiotherapy	Esophageal Cancer	Phase 2	Recruiting	NCT04512417
68	Cisplatin + Pembrolizumab + Radiotherapy	Vulvar Cancer	Phase 2	Recruiting	NCT04430699
69	Sintilimab + Apatinib + Albumin-Bound Paclitaxel (Nab-Paclitaxel) +Carboplatin	Breast Cancer	Phase 2	Recruiting	NCT04722718
70	PD-1 inhibitor (Tislelizumab) + SOX (Tegafur + Oxaliplatin)	Adenocarcinoma of Gastroesophageal Junction	Phase 2	Recruiting	NCT04890392

Data acquired from the US National Library of Medicine (http://clinicaltrials.gov, accessed on 18th May 2021)
Abbreviation: 5-FU: Fluorouracil; NSCLC: Non-small cell Lung Cancer; Nab-Paclitaxel: Nanoparticle albumin-bound paclitaxel (Abraxane); RCC: Renal cell carcinoma; SCLC: Small cell lung Cancer; TNBC: Triple-negative cancer.

administrated to cancer patients, thereby making it immunocompromised. Immunotherapy, in a nutshell, are arbitrations that anchorages the immune system in combating various malignancies [302,303]. For immunotherapy to work effectively, it requires awaking the immune system, the evolution of effector cells and complete eradication of tumor cells. Modulating the TME to generate a better immunotherapy response is pillared on two therapeutic approaches (i) Direct immunomodulation targeting the tumor directly and (ii) Indirect immunomodulation that targets the microenvironment.

The immune system requires the active participation of various effector molecules such as cytokines, inflammatory barriers, T cell watch out, along with immune cells. Immunotherapeutic covers a whole ground of immune-modulating options, which includes checkpoint blockade antibodies, immune-stimulatory monoclonal antibodies [304], PRR agonists, cytokine targeting [305] and attacking chemokines [306]. Immune checkpoints such as CTLA-4 and PD-1 are known to erode the activity of T-cells, leading to the inhibition of anti-tumor efficiency within the immune system. Retarding the activity of these checkpoints and their ligands like PD-L1 have shown better efficiency in many clinical trials [307,308]. Studies have also shown that cancer patients with high expression rates of PD-L1 show a better response to anti PD therapies that are checkpoint blockers [309,310]. CTLA-4 combinations, along with these anti-PD therapies, increases the rate of stats, as seen in various clinical trials [311–313]. Targeting T-cell immunoglobulin and domain mucin-containing molecule-3 (TIM-3) with therapeutic combinations such as anti-PD-L1 and anti-CTLA-4 (Ipilimumab) have shown to be effective in various clinical trials [314,315]. Immunotherapy administrated in the form of tumor-targeting monoclonal antibodies (mAb) are the most studied form, and function to recognize the presence of an antigen on the tumor cells, binds to their receptors and then alter the signaling mechanism of these abnormal cells [316]. Some of these therapeutic options include VEGF targeting Bevacizumab [317], TNF

targeting Tigatuzumab [318]. Inducible T-cell co-stimulators (ITCS) monoclonal antibodies that are agonists are also in combination with anti-PD-L1 therapies used in the treatment of recurrent solid malignancies [319]. OX40 is known to be the enhancer of immunogenicity, which increases the T-cell stockpile and further enhances the microenvironment to immunity [320,321]. Oncolytic virus (the first approved FDA drug) has been found as the enhancer of the immune microenvironment [322]. Other strategies include the combination of ONCOS-102 and Cyclophosphamide, thereby overexpressing the pro-inflammatory system and hampers the microenvironment of immune-compromised cells [323]. Distortion of the ECM and its inhibition by excessive production enhances the nanoparticles. Therefore, immunotherapy strategies unwind a whole new set of opportunities in modulating the TME that can be used as a better therapeutic approach while dealing with cancer.

Researchers are focusing on cellular immunotherapies and exploring how these are changing the outlook for cancer patients. Adoptive cell therapy (ACT), also known as cellular immunotherapy, is a type of cancer treatment that employs the immune system's cells to combat the disease. Examples of ACT are Engineered T Cell Receptor (TCR) Therapy, Tumor-Infiltrating Lymphocyte (TIL) Therapy, Natural Killer (NK) Cell Therapy and Chimeric Antigen Receptor (CAR) T Cell Therapy [324–327]. We have concentrated on combination therapy in this article. Cell therapies are being tested in clinical trials for various cancer types, both alone and in combination with other treatments. Axicabtagene ciloleucel, Lisocabtagene maraleucel, Tisagenlecleucel, and Brexucabtagene autoleucel are CD19-targeting CAR T cell immunotherapies for lymphoma patients, and Idecabtagene vicleucel is a B-cell maturation antigen (BCMA)-targeting CAR T cell immunotherapy for advanced multiple myeloma patients.[328–332]. Interestingly, Chong et al. report a successful combination of CD19-CAR-T cells and PD-1 blocking antibody for the patient with refractory diffuse large B-cell lymphoma. Taking into account, combination therapies combining CAR-T cells and inhibitory receptors blockade come out as a new strategy for overcoming the tumor escape and strengthening CAR-T cells [333]. Moreover, Huye and colleagues exploit anti-tumor effects of rapamycin in combination with adoptive T cell therapy and designed a rapamycin-resistant CD19 second-generation CAR-T cell. They demonstrated that even in the presence of rapamycin, these CAR-T cells maintain mTOR signaling, proliferate, and exhibit effector function. Furthermore, they demonstrated greater antitumor activity in vitro against Burkitt's lymphoma, and pre-B ALL cell lines, implying that mTOR could enhance CAR-T cell functionality [334]. In TME, CAR-T cells are subjected to a slew of inhibitory signals that can impair their function. TME factors may influence both the fate of tumor-infiltrating CAR-T cells and the outcome of CAR-T cell-based therapies [335].

CAR-NK (CAR-T cell therapy) may be an alternative approach to circumventing the limitations of CAR-T cell therapy. This is because, unlike T cells, NK cells can kill tumor cells without the need for prior antigen priming, and their killing potential is not restricted by the target cell's expression of MHC molecules.[336]. Even at very low effector-to-target ratios, CAR-NK cells display quick and powerful anti-tumor cytotoxic action. An ongoing clinical investigation of FT500, an off-the-shelf, iPSC-derived NK cell product combined with an immune checkpoint inhibitor (ICI), is being conducted for patients with advanced solid tumor burden (NCT03841110). Another preclinical study found that activated NK cells, when combined with the anti-GD2 antibody Dinutuximab, improved neuroblastoma mouse survival after surgical resection. [337]. Sorafenib and Regorafenib, two multikinase inhibitors, are expected to synergistically impact when used in conjunction with NK cell therapy [338,339]. In addition, Li et al. investigated the use of NK cells in combination with chemotherapy (5-Fluorouracil or Oxaliplatin) in patients with locally advanced colon cancer. In the cohort study, the NK cell group had substantially higher five-year progression free survival (PFS) and overall survival (OS) rates as compared to the control group (51.1% versus 35%, P = 0.044; 72.5% versus 51.6%, P = 0.037, respectively). In patients with poorly differentiated carcinomas and low expression of human leukocyte antigen, the median PFS in the NK cell population are 23.5 months versus 12.1 months (P = 0.0475) and 33.1 months versus 18.5 months (P = 0.045), respectively [340]. Furthermore, Li et al. also looked at the overall results of combining CAR-NK and CAR-T cells as an anti-tumor therapy. They discovered that the NK plus T platform could leverage the advantages of both CAR-NK and CAR-T cells, allowing for both rapid and persistent killing while potentially limiting the toxicities associated with CAR-T cells, based on *in vitro* and *in vivo* experiments [341]. Despite their benefits, NK cells have a variety of limitation that may affect their efficacy including short lifespan in the absence of cytokine support, low cell counts that frequently necessitate ex vivo growth and activation, and, like other immune cells, sensitivity to the immunosuppressive TME, which could impair their trafficking and effector action, as shown in other immune cells. Overall, ACT has been safely administered and demonstrated great potential to enhance clinical outcomes in cancer patients.

4.3. TME modulation using radiotherapy as combating strategy in cancer

Radiotherapy seems to be one of the most effective therapies in dealing with cancer, acts by damaging the DNA within the cell. This form of cancer therapy is generally used in 50% of patients diagnosed with cancer and in the management of around 40% of patients undergoing other treatment regimens [342]. This radiotherapy-induced DNA damage generally creates an immune response within the dome of cancer cells [343]. When talking about the role of radiotherapy in modifying the cancer load by affecting the TME, radiobiology has not been so effective in promoting a suitable outcome. However, pre-clinical evidence suggests that radiotherapy in specific tumor models shows the increased invasion of cancer cells and metastasis, although no strong proof supports this myth [343]. Studies have also shown that radiation-exposed stromal might increase the tumor vascularization in COMMAD cells (cells exhibiting characteristics of normal mammary epithelial cells), led to increased tumor growth when impregnated in syngeneic hosts fat pads [344]. Therefore, radiotherapy's role on parameters such as activation of the immune response, hypoxia, and fibrosis within the TME, leading to therapy resistance or recurrence, needs in-depth knowledge to provide information on how this therapy can prevent or induce cancer localization and metastasis.

Radiation induces changes in endothelial cell function, including increased cellular permeabilization, apoptosis, and a loss of cell anchorage to the basal membrane [345,346]. Micro-vascularization also gets affected with increased radiation (8 to 16 Gy) in a dose-dependent manner, thereby depleting blood vessels [347]. Destruction of blood vessels is further enhanced by aggregation of platelets, forming microthrombus, and promoting adhesion of inflammatory cells within the perivascular space [348]. Prolong exposure to high radiation levels (15–20 Gy) has been shown to induce fibrosis, permanent damage to blood vessels and medical necrosis (necrosis of tissue) [349]. Radiation exposure also triggers hypoxia that leads to the activation of an immune response via increased cytokines production, that further causes the recruitment of various immune cells [350]. Studies have shown that radiation exposure to the tumor population reduced the invasive capability of tumor cells [351] and decreased motility of CAFs via increased expression of integrin following radiotherapy [352,353]. Radiation also leads to increased recruitment of circulating immune cells, elevated levels of antigen exposure, thereby affecting the immune channel of the TME and prompting the immune system for an adaptive response [354,355]. Post radiotherapy generation of inflammatory signals occurs via activation of various survival pathways, leading to the reactive innate immune response. In addition to these signals, radiotherapy triggers multiple inflammatory cytokines (TNF-α, IL-1) followed by recruitment of various immune cells such as vascular cell adhesion molecule-1 (VCAM-1), ICAM1 and E-selectin. ROS production

coordinated with NF-κB alters the TNF signaling leading to cellular stress, ultimately leading to death post-radiotherapy [355]. Intermediate doses of radiation cause DAMP-PRR to formulate cellular damage that promotes ICD in tumor cells. In some way, we can say that ICD acts to trigger an anti-cancer immune response [356]. Hence it is pertinent to state that ICD induced from radiotherapy in cancer cells is a complex phenomenon, and the immune response against TME when irradiated is somewhere neither completely immunosuppressive nor immune-stimulatory [357]. Further investigation of the radiotherapy mediated TME response is needed that may provide new light on developing an array of effective therapeutic strategies against cancer while keeping TME in the spotlight.

4.4. Nano-therapy a sting of hope in the era of TME modulation targeting cancer

Due to early resistance or inability to get precisely administered to the affected local area, a therapeutic regime such as chemotherapy or radiotherapy fails to induce or elicit a concrete response in cancer patients, resulting in metabolic damage in the tumor machinery [358]. This need to effectively deliver these drugs to the desired target site that can be favored with the combined action of nano-medicines that potentially targets the vascularization in TME, the ECM as conventional therapies fail from potential eradication, thereby generating a better immune response in tumor affected population. This efficiency of nanoparticles targeting the TME is also enhanced due to leaky tumor vasculature, also known as enhanced permeability and retention (EPR) effect and interstitial fluid pressure [359], leading to accumulation of nanoparticles in and around the tumor matrix. Targeting the nano-medicine to the tumor site depends on the extent of the EPR effect and the degree of vascularization and angiogenesis [360]. Poor vasculature within the tumor site ceases the ability of conventional therapies to induce a better response, thereby reducing the anticancer response [129]. TME-sensitive nanoparticles (nanocarriers) that target extracellular stimuli (interstitial fluid pressure, EPR) outperformed traditional or conventional stimuli-sensitive nanocarriers (focused on intracellular stimuli such as acidic endolysosomal compartments, reduced glutathione (GSH) of cytosol, and other harsh condition). Selective activation of nanocarriers through a change in their surface charge, charge conversion, ligand exposure, size conversion, drug release, nanocarrier disassembly, shell detachment, signal activation by pH change, radiation, within the TME increases the cellular attachment and efficiency of the nanoparticles [361].Various therapies targeting the tumor using nanoparticles enhance the drug concentration within the TME. One such study includes using a “nanocells” drug delivery system encapsulating combinations of Combretastatin and Doxorubicin that disrupt the tumor vascular machinery by altering the cytoskeleton structure of the affected cells. This was further preceded by the release of Doxorubicin from the inner core of the nanoparticle that overall increased the therapeutic potential along with reduced cytotoxicity [362]. A study by Chen et al. reported a novel tumor stroma-targeted nanoliposome system, FH-SSL-Nav, that targets CAFs to modulate TME and greatly enhance the tumor suppression tumor-targeted liposomal doxorubicin (7pep-SSL-DOX) [363].

Nanotherapy, when used in combination with other tumor-targeting therapies, showed more satisfactory results as compared to single targeting agents. Examples justifying this statement include using Poly(D, Llactide-co-glycolide) nanoparticles (~220 nm) coated with a LOX (lysyl oxidase) inhibitory antibody. This cancer nanotherapeutic inhibits the development of tumors originating from the mammary glands by binding to the ECM-modifying enzyme LOX and altering the ECM structure [364]. Another study concludes that the use of PLA (Poly-lactic acid) nanoparticles loaded with paclitaxel, when injected in mice affected with malignant gliomas, increased the survival rate by 70% [365]. IL-2, when incorporated with multi-lamellar vesicles of liposomes, decreased the rate of toxicity associated with hematology and increased the circulation of these inflammatory barriers in rats [366]. Intra-tumoral injections, when administrated in rats bearing B16 melanoma with TNF-α encapsulated polylactic acid microspheres (PLAM), resulted in complete eradication of tumor load, therefore, defining the therapeutic value of nanoparticles loaded with cytokines [367]. As CXCR4 is highly expressed in hepatocellular carcinoma, therefore, targeting CXCR4 with Sorafenib encapsulated with liposome in combination reduced the vascularization and the vessel density along with the declined rate of infiltration of TAM to the tumor site. Research also identified the role of gold-coated nanoparticles when dealing with doxorubicin sensitive and resistant colorectal cancer three-dimensional (3D) spheroids [368]. Apart from acting as therapeutic convection, these nanoparticles also show diagnostic prevalence. One such study highlights the use of gold nanoparticles conjugated with anti-GD2 (cancer-targeting antibodies), successfully tracked the GD2 expression in cancer cells, thereby helping in improving the tumor diagnostic in contrast to computed tomography (CT) [369]. Therefore, it is pertinent to say that nanoparticles mediated anti-tumor therapies targeting TME show better immunosuppressive effects when used in conjugating with other therapeutic regimes and have the potential to overcome this dreadful disease, cancer or malignant tumors.

4.5. Implication of surgery in TME

Surgery is one of several methods used for cancer treatment. Surgery aims to remove the tumor locally along with nearby tissue during an operation. The types vary depending on the surgery’s goal, the body part that needs surgery, the amount of tissue that needs to be removed, and, in some cases, the patient’s preferences. Several cancer treatments use surgical procedures: mastectomy of breast cancer, brain tumor by neurosurgery, prostatectomy for prostate cancer, kidney cancer, lung cancer, liver cancer, etc. Surgical techniques cannot fully remove cancer cells, and even a single cancer cell that is not visible will regrow into a new tumor and spread to other areas of the body [370].

In some cases, the treatment plan may use a combination of the treatment methods and surgery to have the maximum therapeutic outcome. The study by Zhao et al. showed that patients who underwent surgery followed by adjuvant therapy lived considerably longer than those who did not undergo adjuvant chemotherapy (median 84 months versus 31 months, p ¼ 0.043; 5-year survival rates 51.2% versus 43.8%, respectively) [371]. The most common treatment for ovarian carcinosarcoma (malignant mixed Mullerian tumor) is a combination of surgery, chemotherapy, and radiotherapy [372]. Also, Jung and colleagues compared two traditional treatment methods in Maxillary Sinus Cancer, and they found that patients who received a treatment regimen that included surgery, radiotherapy, and/or chemotherapy (SRCT) had greater progression-free survival (P =.043) and overall survival (P =.029) than those who received a treatment regimen that included concurrent chemoradiotherapy (CCRT) [373]. Nordlinger et al. also looked at the pros and cons of combining chemotherapy with or without targeted drugs with surgery in the treatment of CRC patients with liver metastases [374]. Moreover, Bakos and colleagues proposed a combination treatment strategy for solid tumors that protect against disease relapse. The use of perioperative immunotherapy in combination with standard-of-care surgery has proven to improve survival rates [375]. In the current era of effective immunotherapies and targeted therapies, there is the widespread use of Checkpoint inhibitors therapy, adoptive cell transfer (ACT) therapy and other investigational immunotherapies for many cancers. But due to limitations in immunotherapies, most patients either do not respond well or acquire a disease after the partial response. For these non-responder patients, local therapy, including surgery, ablation or stereotactic body radiotherapy (SBRT), may be useful for progression-free survival (PFS). The pattern of immunotherapy failure is associated with PFS after local therapy. Hence, extensive researches in this area have created a clear need to determine if and how surgery might best complement these newer treatments

Table 5
Computational and Artificial Intelligence-based Software and/or databases in healthcare

S. no	Software	Software's URL	Application	Developed BY	Reference
Flow Cytometry					
1	FlowJo	https://www.flowjo.com/	Used for Flow cytometry data analysis (cell cycle, immune cell profiling etc.)	Ashland, Oregon-based FlowJo LLC (a subsidiary of Becton Dickinson)	[421,422]
2	CYTOBANK and Cytobank community	https://www.cytobank.org/ https://community.cytobank.org/	Web-based application to analyze simultaneously multiple single-cell datasets from Flow cytometry	DVS Sciences Inc.	[389,423]
3	FlowRepository	https://flowrepository.org/	Web-based application for flow cytometry data repository Data can download, collected and annotated according to the MIFlowCyt standard (Uses object-oriented Ruby programming language)	International Society for Advancement of Cytometry (ISAC)	[389,424]
Immunochemistry Staining					
4	ImageJ	https://imagej.nih.gov/ij/download.html	Java based-open source Image processing program for scientific image processing which supports N-dimensional image data	NIH and LOCI, University of Wisconsin	[425,426]
5	CellProfiler	https://cellprofiler.org/	Open source for quantitative Image processing & Image analysis	Broad Institute, USA	[425,427]
6	DeepCell	https://deepcellbio.com/	AI-based technology for characterizing, identifying, and sorting cells without perturbation (deep learning models for large-scale cellular image analysis)	Dylan Bannon (Division of Biology and Bioengineering, California Institute of Technology)	[428,429]
Epigenetic Modification Analysis through RNA sequence data					
7	DESeq2	http://bioconductor.org/packages/DESeq2/	Methods for differential expression analysis of RNA-seq data using shrinkage estimators for dispersion and fold change.	Dr. Michael Love (Biostatistics Dept and Genetics Dept, UNC-Chapel Hill)	[399]
8	EdgeR	https://bioconductor.org/packages/edgeR/	Computational analysis tool for examining differential expression analysis of digital gene expression data from RNA-seq, ChIP-seq, CAGE, and SAGE data with biological replicates	Mark D. Robinson and Gordon K. Smyth (The University of Melbourne, Australia)	[430,431]
9	DiffBind	https://bioconductor.org/packages/DiffBind/	R Bioconductor package for identifying sites that are differentially enriched between two or more sample groups of ChIP-Seq data	Cancer Research Cambridge Research Institute, UK	[400,432]
10	MAnorm	http://manorm.readthedocs.io	A robust model for quantitative comparison of ChIP-Seq data sets that have a substantial number of peak regions in common and also reflect authentic biological differences	Shao Lab at CAS-MPG Partner Institute for Computational Biology, SIBS, CAS	[433] [434]
11	Minfi	https://bioconductor.org/packages/minfi/	Bioconductor package for analysis of DNA methylation data	-	[401,435]
12	BSMOOTH	http://rafalab.jhsph.edu/bsmooth	Open-source software for whole-genome bisulfite sequencing datasets (WGBS). Also, allow precise and accurate estimates of methylation profiles with low coverage of WGBS data	Rafael Irizarry at Harvard University (USA)	[436,437]
13	ENCODE	https://www.encodeproject.org/	Open access database that integrates multiple types of data and produces high-quality data in an integrative fashion. Launched to develop a comprehensive map of functional elements in the human genome	NHGRI USA as a follow-on to the Human Genome Project	[402,438]
14	NIH Roadmap Epigenomics Project	http://www.roadmapepigenomics.org/	Available through the GEO repository. Provides the largest collection of human epigenomes data (genome-wide epigenetic maps) for primary cells and tissues	National Institutes of Health (NIH)	[439]
15	BLUEPRINT-epigenome	http://www.blueprint-epigenome.eu/	Tool for functional genomics analysis on a defined set of primarily human samples from healthy and diseased individuals and to provide at least 100 reference epigenomes to the scientific community	Dr. Hendrik Stunnenberg Radboud University, Nijmegen, Netherlands	[440]
16	SEURAT	https://satijalab.org/seurat/	R toolkit designed for QC, analysis, and exploration of single-cell RNA-seq data	Satija Lab at The New York Genome Center, USA	[405,441,442]
17	scVI (Single-cell Variational Inference)	https://github.com/YosefLab/scvi-tools	Open-source software package for single-cell omics data analysis (single-cell RNA-seq data)	Romain Lopez, University of California, Berkeley, USA	[443,444]
18	Monocle2	http://cole-trapnell-lab.github.io/monocle-release/	Tool that tracks single-cell trajectories over pseudotime, Group and classify cells based on gene expression also find genes that vary between cell types and states, over trajectories, or in response to perturbations using statistically robust, flexible differential analysis (toolkit for single-cell RNA-Seq experiments)	Trapnell lab, University of Washington USA	[445]
19	SCIMPUTE	https://github.com/Vivianstats/scImpute	Tool for accurate and robust imputation of dropout values in scRNA-seq data	Dr.Wei Vivian Li & Dr. Jingyi Jessica Li, Department of Statistics, University of California, Los Angeles, USA	[406,446]
Enrichment Method					

(*continued on next page*)

Table 5 (*continued*)

S. no	Software	Software's URL	Application	Developed BY	Reference
20	ESTIMATE	https://sourceforge.net/projects/estimateproject/	Tool predicts stromal and immune score (infiltrating stromal/immune cells) to predict tumor intensity and purity using gene expression data	University of Texas, MD Anderson cancer center	[411,447]
21	xCell	https://xcell.ucsf.edu/	Web tool for estimating enrichment score for 64 different immune, stromal, and epithelial cell subsets	Butte lab, UCSF Medical Center at Mission Bay, San Francisco, USA	[448]
22	EPIC	http://epic.gfellerlab.org/	Tool with a unique collection of RNA-Seq reference gene expression profiles for estimating the proportions of different cell types from bulk gene expression data	Dr. David Gfellerlab, University of Lausanne, Switzerland	[413,449]
23	ImmuCellAI	https://bio.tools/ImmuCellAI	Method for gene set signature for precisely estimating the abundance of 24 immune cell types (including 18 T-cell subsets) from gene expression data	Department of Bioinformatics and Systems Biology, Huazhong University of Science and Technology, Wuhan China	[450,451]
24	TIMER- Cistrome	http://cistrome.org/TIMER/	Web resource for systematical evaluations of the clinical impact of different immune cells (present in TME) in diverse cancer types	Prof. X. Shirley Liu lab (Department of Biostatistics and Computational Biology at the Dana-Farber Cancer Institute	[452]
25	MCP-COUNTER; webMCP-counter	https://github.com/ebecht/MCPcounter	Web interface for quantification of 10 cell populations (8 immune populations, endothelial cells and fibroblasts) from transcriptomic profiles of human tissues	Etienne Becht team (Paris Descartes University) in collaboration of the CIT program with Catherine Sautès-Fridman and Hervé Fridman's lab	[453,454]
Deconvolution Method					
26	CIBERSORTX	https://cibersortx.stanford.edu/	Tool estimating cell-type proportions and computes the gene expression pattern from bulk transcriptomics data	Alizadeh Lab and Newman Lab, Stanford University School of Medicine, California, USA	[410,414,455,456]
27	IgBLAST	https://www.ncbi.nlm.nih.gov/igblast/	Tool to analyze nucleotide and protein sequences and allows searches against germline gene databases and other sequence databases simultaneously to minimize the chance of missing possibly the best matching germline V gene	NCBI	[417,457]
28	MiXCR	https://github.com/milaboratory/mixcr	Software for fast and accurate T- and B- cell receptor repertoire extraction. It provides a whole range of sequencing data sources (including TCR/BCR libraries, RNA-Seq, WGS, single-cell)	Shemyakin-Ovchinnikov Institute of bioorganic chemistry RAS, Moscow, Russia	[458]
29	GLIPH	https://github.com/immunoengineer/gliph	Tool clusters TCRs that are predicted to bind the same MHC-restricted peptide antigen and also provides predictions of which HLA-allele is presenting the antigen	Stanford University School of Medicine, Stanford, California USA	[418]
30	TraCeR	https://github.com/Teichlab/tracer	Tool for reconstructing the sequences of rearranged and expressed T cell receptor genes from single-cell RNA-seq data	Prof Sir Mike Stratton, Sanger Institute, UK	[459]
Bioinformatics Tool					
31	GATK	https://software.broadinstitute.org/gatk/	Tools for analyzing high-throughput sequencing data to identify single nucleotide tools for polymorphism based on Bayesian classifier	Broad Institute, Biomedical and genomic research center, Cambridge, and Massachusetts, USA	[460]
32	MuTect	https://software.broadinstitute.org/cancer/cga/mutect	Method for reliable and accurate identification of somatic point mutations in NSG data of cancer genomes	Broad Institute, Biomedical and genomic research center, Cambridge, Massachusetts, USA	[461]
33	POLYSOLVER	https://software.broadinstitute.org/cancer/cga/polysolver	Tool for HLA typing based on whole-exome sequencing (WES) data and infers alleles for the three major MHC class I (HLA-A, -B, -C) genes	Broad Institute of Harvard and MIT, USA	[462]
34	OptiType	https://github.com/FRED-2/OptiType	Fast HLA genotyping algorithm-based method on NSG data and provides an alternate novel source to HLA genotyping	Applied Bioinformatics, University of Tübingen, Germany	[463]
35	NETMHC	http://www.cbs.dtu.dk/services/NetMHC	Using artificial neural networks, it predicts peptide-MHC class I binding for any allele of known sequence	Agencia Nacional de Promoción Científica y Tecnológica, Argentina and NIH	[464]
36	MHCflurry	https://github.com/openvax/mhcflurry	Open source for MHC class I binding prediction	Python community	[465]
37	FRED-2	http://fred-2.github.io/	Python-based framework for computational immunomics (predicting framework for T cell epitope and vaccine design)	Applied Bioinformatics Group at Eberhard-Karls University Tübingen	[466]
38	NetTepi	http://www.cbs.dtu.dk/services/NetTepi/	Integrated based method for prediction of T cell epitopes by integrating three prediction types, peptide-MHC binding affinity, peptide-MHC stability and T cell propensity.	-	[467]
39	pVAC-SEQ	https://github.com/griffithlab/pVAC-Seq	An open-source tool for identifying cancer neoantigen	McDonnell Genome Institute, Washington University School of Medicine, St. Louis, MO, USA	[468,469]

Abbreviation: EPIC: Estimating the Proportions of Immune and Cancer cells; ESTIMATE: Estimation of STromal and Immune cells in MAlignant Tumors using Expression data; GATK: Genome Analysis Toolkit; GEO: Gene Expression Omnibus; GLIPH: Grouping of Lymphocyte Interactions by Paratope Hotspots; HLA: Human leukocyte antigen; ImmuCellAI: Immune Cell Abundance Identifier; MHC: Major histocompatibility complex NHGRI: National Human Genome Research Institute;

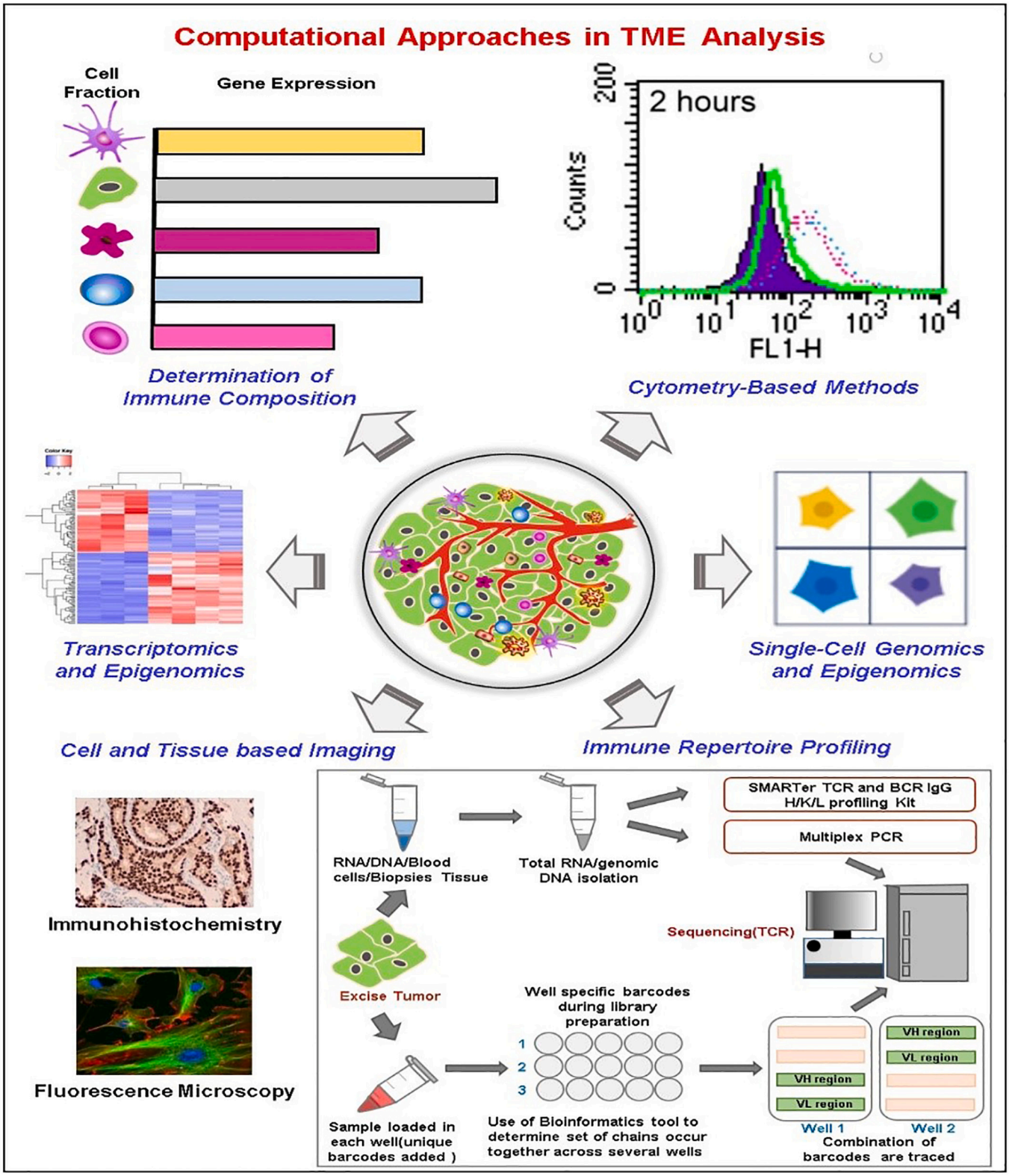

Fig. 4. Advancement in computational strategies and development of artificial intelligence in healthcare make it possible for cancer detection and diagnosis, where TME is no exception. There are many ways to target TME through computational strategies such as determination of immune composition, imaging, transcriptomics and epigenomics studies, cytometry-based methods, single-cell genomics and epigenomics studies, and immune repertoire profiling. Imaging consists of the analysis of immunohistochemistry and fluorescence microscopy results, whereas cytometry-based methods include analysis of flow-cytometry results through the application of artificial intelligence and machine learning. Determination of immune composition consists of determining gene expression of different types of cell fraction in a particular TME, such as immune cells and macrophages. Analysis of microarray and RNA-sequencing data through computational strategies, which can determine the gene expression of different genes in a TME, fall under single-cell genomics and epigenomics studies and transcriptomics and epigenomics studies. Immune repertoire profiling consists of applying artificial intelligence and machine learning in the determination of the VDJ combination. Abbreviation: BCR: B cell receptor; IgG: Immunoglobulin G; PCR: Polymerase chain reaction; TCR: T cell receptor; V(D)J: variable (V), diversity (D) and joining (J).

NSG: Next-generation Sequencing; pVAC-SEQ: personalized Variant Antigens by Cancer Sequencing; QC: Quality control; RNA-seq: RNA-sequencing; CHIP-Seq: Chromatin immunoprecipitation (ChIP) assays with sequencing; CAGE: Cap Analysis Gene Expression; SAGE: Serial Analysis of Gene Expression; scRNA: single-cell RNA: WGS: Whole-genome sequencing.

[376,377].

5. Challenges and future scope of using combinatorial therapy in cancer

Combination therapy has been felt most effective with regards to anti-tumor effects as it targets multiple pathways. Multiple drug combinations are used to target various ways to increase the chance of disease progression. Combination therapies can effectively target tumor heterogeneity and increase the therapeutic effectiveness of the treatments provided. Additionally, multiple drugs can also target drug resistance and contribute to killing cancer stem cells. Conventional chemotherapeutic drugs cannot target cancer stem cells. However, numerous agents used in combination therapies can overcome the likelihood of recurrence after remission. The fascinating advantage of combination therapy is the elimination of cancer stem cells. The chemotherapeutics are selective and cannot target cancer stem cells. The multiple agents used in combination therapies can target cancer stem cells and target cancer cell-specific characteristics such as self-renewal, differentiation, and invasiveness.

Studies have revealed several disadvantages of combination therapy in various cancers. Firstly, drug interaction is a major obstacle in delivering combination therapy to cancer patients. One drug can interrupt other drugs' metabolic activity used in combination, thus causes toxicity in the patient's body. Secondly, the multiple agents used in combination can generate additive side effects, and therapeutic dose assessment becomes difficult. Sometimes the side effects of two drugs are similar and can cause detrimental effects on a patient's life expectancy. Moreover, tumor cells may acquire multiple drug resistance (MDR) phenotype by overexpressing ATP dependent drug efflux pump, alteration in DNA repair mechanism and regulating cell death pathways.

Further, it will be challenging to figure out which drug is responsible for the observed side effects, and all the medications may need to be discontinued. For example, Berdeja et al. have reported multiple side effects, including heart failure and treatment-related death rose in multiple myeloma patients treated with a combination of Panobinostat and Carfilzomib [378]. The second challenging factor in adopting combination therapy is the testing of drugs that have not been licensed. Several scientific and regulatory hurdles hamper the potential application of drugs as licensable combination therapy. The next challenge is to control the drug ratios and dosage after administration in the patient body. It is extremely burdensome to regulate the co-administrated drugs' pharmacokinetics due to differences in their metabolism and uptake [379]. Another critical challenge is to provide scientific evidence and design of animal model studies to know the combinatorial approach's potential. For instance, Ascierto et al. have proposed guidelines to assess combinations used to treat melanoma [380]. Another challenge is the design of clinical trials for combination therapies. While designing a clinical trial, three factors must be considered: the requirement of preclinical studies, characteristics of individual drugs and patient population. The drug ratio and dose requirement need a single-arm phase 2 trial followed by a randomized phase II trial. Studies have suggested that a drug combination can directly be tested into phase 2 studies, despite being tested in a phase 1 study if *in vivo* studies have shown that both drugs can be given together without any toxicity compared to monotherapy [381].

Moreover, legal issues present a significant barrier in combination therapy development. Uncertainty about the commercial aspects, division of expenses and profits, and the unequal contribution of the collaborated partners, sponsorship and product liability are the significant concerns often cited as hurdles in developing combinatorial drug regimens. In the same line, regulatory problems cause an unnecessary delay in the combinatorial drug development process. The combination therapy must be superior to the monotherapy approach and demands extensive time and expense. The FDA currently does not have any regulatory policy to discriminate the adverse effects of a drug used in combination. It also has no authorized body for toxicity review and drug labelling for multi-agent drug development [382]. Therefore, all the challenges mentioned above should be addressed while designing a combinatorial approach to treat cancer.

6. Role of artificial intelligence in therapeutics concerning tumor microenvironment

Recent advancement in computational analysis and artificial intelligence advances our understating of TME. The TME associates immunological cells, stromal cells, and other cells that develop complex molecular data, which require sophisticated molecular computational analysis. Implementing these complex bioinformatics data and quantitative models to integrate and analyze is necessary to elucidate the molecular mechanism of TME and its pathological outcomes [383,384]. The artificial intelligence (AI) and computational biology in TME can be sub-divided into different parts such as cytometry-based method, imaging, bulk transcriptomics and epigenomics, single-cell transcriptomics and epigenomics, *in-silico* method for determining tissue composition, immune repertoire profiling, and neoantigen prediction [385,386]. Flow-cytometry is widely implemented in TME and has been used for the multivariant analysis of immune cells and single cells through monochrome-labeled antibodies and antigen interactions [387]. Fluorescence-activated cell sorting based on electrical charge can distinguish the immune subset in the TME, which can be used for further experiments [388]. Till now, two important public data repositories are available for flow cytometry data analysis- FlowJo and CYTOBANK. These data repositories can be used to perform different analyses, such as manual gating of cell populations [389]. However, manual gating in flow cytometry creates bias as it depends on the researcher. Thus, to minimize the bias, several methods have been developed for automated cell gating. Further, the researcher can perform immunochemistry staining or imaging, which yields consistent, quantitative measures, intensity, shape, and size [390]. To analyze such parameters, two publicly available software can be used, such as ImageJ [391] and CellProfiler [392]. Further, recent advances in NGS technologies, RNA sequence technology, and big data focus on the analysis of TME with bioinformatics tools and databases. These data applicable to studying TME and its associated interaction, classify immune cells and non-immune stromal cells and study the mechanistic role of genomics data [393–396]. Similarly, epigenetic modifications such as histone modification, RNA interference, and DNA methylation have been widely used in studying TME microenvironments, such as the association between genomic interaction, differential gene expression, pathway analysis, and identification biological themes [397,398]. Mounting evidence suggests that epigenetic modification modulates the phenotypic expression of immune cells and stromal cells induced by TME. For example, hypomethylation can increase genomic stability, whereas hypermethylation can deactivate tumor-causing genes. In order to achieve this, several computational analysis tools have been developed for epigenetic alteration analysis. For example, DESeq2 [399] is used for RNA-sequencing data analysis, whereas DiffBind [400] can be used to identify differential peak analysis. For the study DNA methylated region, Minfi, an R-based and t-test based algorithms have been developed [401]. To ease the bioinformatics analyses through a computational approach, several public databases such as ENCODE are prepared that store the epigenetic information [402]. Likewise, with bulk transcriptomics and epigenomics data, scientists move towards the computational analysis of single-cell

transcriptomics and epigenomics, which analyzes the complexity of single-cell and regulatory mechanisms between single cells. Emerging evidence demonstrates that Trishosh et al. [54] performed single-cell RNA sequence (scRNAseq) analysis on 4645 cells from 19 melanoma patients, whereas, Jerby-Arnon et al. [403] performed scRNAseq on 7186 cells from 33 melanoma tumors. These studies highlight the importance of investing in the association between immune cells and tumor cells for immunotherapy resistance. This evidence discovered several computational tools and databases to classify immune and tumor genes, assign cell types, and cluster cell types [404]. For example, SEURAT [405] and SCIMPUTE [406] are based on a probabilistic algorithm, graph-based algorithm, and non-linear reconstruction algorithm.

The major disadvantage of scRNAseq, cytometry-based analysis, transcriptomics and epigenomics is that they modulate the cellular phenotype of TME and distort cell representation. Another challenging task while using cytometry-based methods and scRNAseq data is that they often require fresh and frozen samples, difficult to obtain for diagnosis [407,408]. To overcome these challenges, computational approaches and artificial intelligence-based approaches have been developed, using the tissue sample directly from the bulk gene expression profiling. These methods are used to classify the tissue sample and allowing the user to quantify the TIL subset and their clinical aspects [409,410]. Further, *in silico* methods for determining tissue compositions are classified into two groups: enrichment method and deconvolution methods, both of which are based on the prior knowledge of marker genes. An adaptation of single-cell gene set enrichment analysis is used in the enrichment methods [411]. However, enrichment analysis techniques can only be useful to identify different pathways and gene sets that are differentially expressed in a tumor subset and cannot estimate the proportion of individual cell proportion [412].

Further, *in silico* methods do not rely on distinguishing cell subsets with overlapping molecular signatures. The latest advancement in the field led to the development of tools like EPIC [413], which employs RNA-seq data and other bulk gene expression data to estimate abundance and characterize immune cells and stromal cells. On the other hand, the deconvolution method relies on estimating cell-type proportions and computes the gene expression patterns from bulk transcriptomics data [414]. It implies both cellular abundance and cell-specificity from high throughput RNA-seq data without physical cell dissociation. Another important aspect of studying TME using computational approaches in immune profiling and neoantigen prediction [415,416]. T-cell receptors and B-cell receptors can identify an immense range of antigens through V(D)J recombination. Recent advancements enabled high-throughput sequencing through quantitative analysis of diverse immune repertoires. Early tools have been developed for immune repertoire profiling, such as IgBLAST [417] and GLIPH [418]. Similarly, neoantigen prediction involves three regulatory steps: identification of mutated proteins, HLA typing, and neoantigen-MHC binding affinity [419,420]. Bioinformatics tools for every step have been developed that have been outlined in Table 5. Altogether, decreasing the cost of high-throughput has generated a large amount of data, which transformed cancer and its associated environment. Although, computational methods based on artificial intelligence and deep learning techniques have been developed to address the big data problem. However, their reliability and accuracy are still a major concern, which needs to address. Scientists from different parts of the world working on immune biology, cancer biology, system biology, and data sciences are working towards exploiting the clinical relevance of computational approaches in TME. Fig. 4 describes progress in computational strategies and the development of artificial intelligence to study TME.

7. Conclusion

TME is an indispensable part of a tumor that contributes to many aspects of carcinogenesis and, therefore, is an essential and promising therapeutic target. This is because the behavior of tumors towards therapy is entirely different when they are alone (cells were grown in 2D culture) compared to where they have a surrounding microenvironment (grown in 3D culture or in the patient body). This TME greatly influences the expressed surface receptors on tumor cells, activated or silenced signaling pathways within tumor cells and will impact the therapeutic effect and response rate. Thus, targeting TME along with tumor provided hope for the patients who do not respond to therapy or develop chemoresistance. In this review, we have summarized the role and importance of targeting several different aspects of the TME with radiotherapy, chemotherapy, immunotherapy, nanotherapy to reduce tumor burden and the advantage of preferring combinatorial therapy over monotherapy. Cancer therapy and radiotherapy actions on the TME contribute to the success or failure of the treatment.

Further, the rapid advancement of nanotherapy and immunotherapy has revolutionized cancer therapy. Nanotherapy could be individualized/personalized according to the specific TME characteristics, including low pH, CAFs, and increased metalloproteinase expression. Immunotherapy positive response usually relies on dynamic bidirectional interactions between tumor cells and immunomodulators inside the TME. Monotherapy includes immune-checkpoint inhibitors as well as combining different immunotherapies and other treatments, including radiotherapy and other targeted therapies, and researchers hope that a larger population of patients will respond and for a longer duration. The combination therapy, which is considered a different combination of anticancer treatments, including different treatment regime dosing, has shown remarkable success in various cancers. The aim of using a combination approach over monotherapy is to expand the spectrum of patients responding to therapy, reduce toxicity by reducing doses, improve toxicity profile, and improve the quality of clinical responses (i.e., the extension of response duration, PFS, and OS). According to the current clinical trials, combinations of treatments appear to be the future. In the end, there is always a scope for new drug development targeting TME, but also based on the comprehensive knowledge and advancement in the current repertoire of anticancer therapy, the combination of therapy still holds the hope of addressing cancer treatment and aiding the patient. In the Future, understanding the mechanisms modulating TME may facilitate the design of novel anticancer treatment and may secure apparent success in cancer eradication.

Author's contribution

Conceived and designed by P.K. Materials collected and art work done by S.K., D.A., S.S, Critical evaluation and analysis of data done by R.K.A and PK. Manuscript written by S.K., D.A., S.S. R.K.A. and P.K. All authors read the manuscript and agreed to submit.

Declaration of Competing Interest

All authors have read the manuscript and declared no conflict or competing interests.

Acknowledgment

Authors would like to acknowledge Rohan Gupta for the expert opinion and inclusion of artificial intelligence and machine learning in this manuscript. We would like to thank the senior management of Delhi Technological University (DTU) and the Department of Biotechnology (DBT), Government of India, for their constant support and financial assistance.

References

[1] D. Hanahan, R.A. Weinberg, The hallmarks of cancer, Cell. 100 (2000) 57–70, https://doi.org/10.1016/s0092-8674(00)81683-9.

[2] World Health Organisation, Cancer. https://www.who.int/news-room/fact-sheets/detail/cancer, 2021. (Accessed 1 February 2021).
[3] A. Jemal, F. Bray, M.M. Center, J. Ferlay, E. Ward, D. Forman, Global cancer statistics.[Erratum appears in CA Cancer J Clin. 2011 Mar-Apr;61(2):134], CA, Cancer J. Clin. 68 (6) (2011) 394–424, https://doi.org/10.3322/caac.21609. , CA. Cancer J. Clin. (2011). Volume 61,Issue 2, Page no 69-90 DO1: https://doi.org/10.3322/caac.20107.
[4] R. Mroue, M.J. Bissell, Three-dimensional cultures of mouse mammary epithelial cells, Methods Mol. Biol. (2013), https://doi.org/10.1007/978-1-62703-125-7_14.
[5] F. Chen, X. Zhuang, L. Lin, P. Yu, Y. Wang, Y. Shi, G. Hu, Y. Sun, New horizons in tumor microenvironment biology: Challenges and opportunities, BMC Med. 13 (2015), https://doi.org/10.1186/s12916-015-0278-7.
[6] F. Balkwill, A. Mantovani, Inflammation and cancer: Back to Virchow? Lancet (2001) https://doi.org/10.1016/S0140-6736(00)04046-0.
[7] D.F. Quail, J.A. Joyce, Microenvironmental regulation of tumor progression and metastasis, Nat. Med. (2013), https://doi.org/10.1038/nm.3394.
[8] I.J. Fidler, The organ microenvironment and cancer metastasis, Differentiation (2002), https://doi.org/10.1046/j.1432-0436.2002.700904.x.
[9] F.R. Balkwill, M. Capasso, T. Hagemann, The tumor microenvironment at a glance, J. Cell Sci. 125 (2012) 5591–5596, https://doi.org/10.1242/jcs.116392.
[10] J. Zhu, L. Liang, Y. Jiao, L. Liu, Enhanced invasion of metastatic cancer cells via extracellular matrix interface, PLoS One (2015), https://doi.org/10.1371/journal.pone.0118058.
[11] J. Condeelis, J.W. Pollard, Macrophages: obligate partners for tumor cell migration, invasion, and metastasis, Cell (2006), https://doi.org/10.1016/j.cell.2006.01.007.
[12] Y. Jung, J.K. Kim, Y. Shiozawa, J. Wang, A. Mishra, J. Joseph, J.E. Berry, S. McGee, E. Lee, H. Sun, J. Wang, T. Jin, H. Zhang, J. Dai, P.H. Krebsbach, E. T. Keller, K.J. Pienta, R.S. Taichman, Recruitment of mesenchymal stem cells into prostate tumours promotes metastasis, Nat. Commun. (2013), https://doi.org/10.1038/ncomms2766.
[13] E.R. Pereira, D. Jones, K. Jung, T.P. Padera, The lymph node microenvironment and its role in the progression of metastatic cancer, Semin. Cell Dev. Biol. (2015), https://doi.org/10.1016/j.semcdb.2015.01.008.
[14] S. Paget, The distribution of secondary growths in cancer of the breast, Lancet (1889), https://doi.org/10.1016/S0140-6736(00)49915-0.
[15] L. Tao, G. Huang, H. Song, Y. Chen, L. Chen, Cancer associated fibroblasts: an essential role in the tumor microenvironment (review), Oncol. Lett. (2017), https://doi.org/10.3892/ol.2017.6497.
[16] W. Wang, Q. Li, T. Yamada, K. Matsumoto, I. Matsumoto, M. Oda, G. Watanabe, Y. Kayano, Y. Nishioka, S. Sone, S. Yano, Crosstalk to stromal fibroblasts induces resistance of lung cancer to epidermal growth factor receptor tyrosine kinase inhibitors, Clin. Cancer Res. (2009), https://doi.org/10.1158/1078-0432.CCR-09-1001.
[17] L. Tao, G. Huang, R. Wang, Y. Pan, Z. He, X. Chu, H. Song, L. Chen, Cancer-associated fibroblasts treated with cisplatin facilitates chemoresistance of lung adenocarcinoma through IL-11/IL-11R/STAT3 signaling pathway, Sci. Rep. (2016), https://doi.org/10.1038/srep38408.
[18] Y. Jo, N. Choi, K. Kim, H.J. Koo, J. Choi, H.N. Kim, Chemoresistance of cancer cells: requirements of tumor microenvironment-mimicking in vitro models in anti-cancer drug development, Theranostics. 8 (2018) 5259–5275, https://doi.org/10.7150/thno.29098.
[19] R. Bharti, G. Dey, M. Mandal, Cancer development, chemoresistance, epithelial to mesenchymal transition and stem cells: a snapshot of IL-6 mediated involvement, Cancer Lett. (2016), https://doi.org/10.1016/j.canlet.2016.02.048.
[20] L. Monteran, N. Erez, The dark side of fibroblasts: Cancer-associated fibroblasts as mediators of immunosuppression in the tumor microenvironment, Front. Immunol. (2019), https://doi.org/10.3389/fimmu.2019.01835.
[21] D. Hanahan, J. Folkman, Patterns and emerging mechanisms of the angiogenic switch during tumorigenesis, Cell. 86 (1996) 353–364, https://doi.org/10.1016/S0092-8674(00)80108-7.
[22] T.L. Whiteside, The local tumor microenvironment, in: Gen. Princ. Tumor Immunother. Basic Clin. Appl. Tumor Immunol., Springer Netherlands, 2008, pp. 145–167, https://doi.org/10.1007/978-1-4020-6087-8_7.
[23] S. Tan, L. Xia, P. Yi, Y. Han, L. Tang, Q. Pan, Y. Tian, S. Rao, L. Oyang, J. Liang, J. Lin, M. Su, Y. Shi, D. Cao, Y. Zhou, Q. Liao, Exosomal miRNAs in tumor microenvironment, J. Exp. Clin. Cancer Res. 39 (2020) 1–15, https://doi.org/10.1186/s13046-020-01570-6.
[24] H. Patel, P. Nilendu, D. Jahagirdar, J.K. Pal, N.K. Sharma, Modulating secreted components of tumor microenvironment: a masterstroke in tumor therapeutics, Cancer Biol. Ther. 19 (2018) 3–12, https://doi.org/10.1080/15384047.2017.1394538.
[25] J.F. Hastings, J.N. Skhinas, D. Fey, D.R. Croucher, T.R. Cox, The extracellular matrix as a key regulator of intracellular signalling networks, Br. J. Pharmacol. 176 (2019) 82–92, https://doi.org/10.1111/bph.14195.
[26] P. Lu, V.M. Weaver, Z. Werb, The extracellular matrix: a dynamic niche in cancer progression, J. Cell Biol. 196 (2012) 395–406, https://doi.org/10.1083/jcb.201102147.
[27] E. Henke, R. Nandigama, S. Ergün, Extracellular matrix in the tumor microenvironment and its impact on cancer therapy, Front. Mol. Biosci. 6 (2020) 1–24, https://doi.org/10.3389/fmolb.2019.00160.
[28] P. Rousselle, J.Y. Scoazec, Laminin 332 in cancer: when the extracellular matrix turns signals from cell anchorage to cell movement, Semin. Cancer Biol. 62 (2020) 149–165, https://doi.org/10.1016/j.semcancer.2019.09.026.
[29] T.D. Ahrens, S.R. Bang-Christensen, A.M. Jørgensen, C. Løppke, C.B. Spliid, N. T. Sand, T.M. Clausen, A. Salanti, M.O. Agerbæk, The role of proteoglycans in cancer metastasis and circulating tumor cell analysis, Front. Cell Dev. Biol 8 (2020), https://doi.org/10.3389/fcell.2020.00749.
[30] V. De Pasquale, L.M. Pavone, Heparan sulfate proteoglycan signaling in tumor microenvironment, Int. J. Mol. Sci. (2020), https://doi.org/10.3390/ijms21186588.
[31] A.D. Theocharis, N.K. Karamanos, Proteoglycans remodeling in cancer: underlying molecular mechanisms, Matrix Biol. (2019), https://doi.org/10.1016/j.matbio.2017.10.008.
[32] L.E. Collins, L. Troeberg, Heparan sulfate as a regulator of inflammation and immunity, J. Leukoc. Biol. (2019), https://doi.org/10.1002/JLB.3RU0618-246R.
[33] M. Xie, J. Ping Li, Heparan sulfate proteoglycan – a common receptor for diverse cytokines, Cell. Signal. (2019), https://doi.org/10.1016/j.cellsig.2018.11.022.
[34] A. Jabłońska-Trypuć, M. Matejczyk, S. Rosochacki, Matrix metalloproteinases (MMPs), the main extracellular matrix (ECM) enzymes in collagen degradation, as a target for anticancer drugs, J. Enzyme Inhib. Med. Chem. 31 (2016) 177–183, https://doi.org/10.3109/14756366.2016.1161620.
[35] N. Nagarsheth, M.S. Wicha, W. Zou, Chemokines in the cancer microenvironment and their relevance in cancer immunotherapy, Nat. Rev. Immunol. 17 (2017) 559–572, https://doi.org/10.1038/nri.2017.49.
[36] K.S.N. Atretkhany, M.S. Drutskaya, S.A. Nedospasov, S.I. Grivennikov, D. V. Kuprash, Chemokines, cytokines and exosomes help tumors to shape inflammatory microenvironment, Pharmacol. Ther. 168 (2016) 98–112, https://doi.org/10.1016/j.pharmthera.2016.09.011.
[37] M. Wang, J. Zhao, L. Zhang, F. Wei, Y. Lian, Y. Wu, Z. Gong, S. Zhang, J. Zhou, K. Cao, X. Li, W. Xiong, G. Li, Z. Zeng, C. Guo, Role of tumor microenvironment in tumorigenesis, J. Cancer 8 (2017) 761–773, https://doi.org/10.7150/jca.17648.
[38] R. Wei, S. Liu, S. Zhang, L. Min, S. Zhu, Cellular and extracellular components in tumor microenvironment and their application in early diagnosis of cancers, Anal. Cell. Pathol. 2020 (2020), https://doi.org/10.1155/2020/6283796.
[39] K.W. Hon, N.S. Ab-Mutalib, N.M.A. Abdullah, R. Jamal, N. Abu, Extracellular vesicle-derived circular RNAs confers chemoresistance in colorectal cancer, Sci. Rep. (2019), https://doi.org/10.1038/s41598-019-53063-y.
[40] Y. Yoshioka, Y. Konishi, N. Kosaka, T. Katsuda, T. Kato, T. Ochiya, Comparative marker analysis of extracellular vesicles in different human cancer types, J. Extracell. Vesicles (2013), https://doi.org/10.3402/jev.v2i0.20424.
[41] R.U. Takahashi, M. Prieto-Vila, A. Hironaka, T. Ochiya, The role of extracellular vesicle microRNAs in cancer biology, Clin. Chem. Lab. Med. (2017), https://doi.org/10.1515/cclm-2016-0708.
[42] C. Tian, D. Öhlund, S. Rickelt, T. Lidström, Y. Huang, L. Hao, R.T. Zhao, O. Franklin, S.N. Bhatia, D.A. Tuveson, R.O. Hynes, Cancer cell–derived matrisome proteins promote metastasis in pancreatic ductal adenocarcinoma, Cancer Res. (2020), https://doi.org/10.1158/0008-5472.CAN-19-2578.
[43] H. Huang, Matrix metalloproteinase-9 (MMP-9) as a cancer biomarker and MMP-9 biosensors: recent advances, Sensors (Switzerland) (2018), https://doi.org/10.3390/s18103249.
[44] M. Giussani, E. Landoni, G. Merlino, F. Turdo, S. Veneroni, B. Paolini, V. Cappelletti, R. Miceli, R. Orlandi, T. Triulzi, E. Tagliabue, Extracellular matrix proteins as diagnostic markers of breast carcinoma, J. Cell. Physiol. (2018), https://doi.org/10.1002/jcp.26513.
[45] Y. Yu, C.H. Xiao, L.D. Tan, Q.S. Wang, X.Q. Li, Y.M. Feng, Cancer-associated fibroblasts induce epithelial-mesenchymal transition of breast cancer cells through paracrine TGF-β signalling, Br. J. Cancer 110 (2014) 724–732, https://doi.org/10.1038/bjc.2013.768.
[46] Tumor microenvironment: stromal and immune cells, Abcam (2021). https://www.abcam.com/cancer/the-tumor-microenvironment-a-cellular-conspiracy. (Accessed 14 May 2021).
[47] M. Skobe, T. Hawighorst, D.G. Jackson, R. Prevo, L. Janes, P. Velasco, L. Riccardi, K. Alitalo, K. Claffey, M. Detmar, Induction of tumor lymphangiogenesis by VEGF-C promotes breast cancer metastasis, Nat. Med. 7 (2001) 192–198, https://doi.org/10.1038/84643.
[48] F. Spinella, E. Garrafa, V. Di Castro, L. Rosanò, M.R. Nicotra, A. Caruso, P. G. Natali, A. Bagnato, Endothelin-1 stimulates lymphatic endothelial cells and lymphatic vessels to grow and invade, Cancer Res. 69 (2009) 2669–2676, https://doi.org/10.1158/0008-5472.CAN-08-1879.
[49] K. Kajiya, S. Hirakawa, B. Ma, I. Drinnenberg, M. Detmar, Hepatocyte growth factor promotes lymphatic vessel formation and function, EMBO J. 24 (2005) 2885–2895, https://doi.org/10.1038/sj.emboj.7600763.
[50] T. Duong, P. Koopman, M. Francois, Tumor lymphangiogenesis as a potential therapeutic target, J. Oncol. (2012), https://doi.org/10.1155/2012/204946.
[51] L. Garnier, A.O. Gkountidi, S. Hugues, Tumor-associated lymphatic vessel features and immunomodulatory functions, Front. Immunol. 10 (2019), https://doi.org/10.3389/fimmu.2019.00720.
[52] R.C. Ji, Lymph nodes and cancermetastasis: New perspectives on the role of intranodal lymphatic sinuses, Int. J. Mol. Sci. 18 (2017), https://doi.org/10.3390/ijms18010051.
[53] Y. Shiozawa, The roles of bone marrow-resident cells as a microenvironment for bone metastasis, in: Adv. Exp. Med. Biol., Springer, 2020, pp. 57–72, https://doi.org/10.1007/978-3-030-36214-0_5.
[54] I. Tirosh, B. Izar, S.M. Prakadan, M.H. Wadsworth, D. Treacy, J.J. Trombetta, A. Rotem, C. Rodman, C. Lian, G. Murphy, M. Fallahi-Sichani, K. Dutton-Regester, J.R. Lin, O. Cohen, P. Shah, D. Lu, A.S. Genshaft, T.K. Hughes, C.G.K. Ziegler, S. W. Kazer, A. Gaillard, K.E. Kolb, A.C. Villani, C.M. Johannessen, A.Y. Andreev, E. M. Van Allen, M. Bertagnolli, P.K. Sorger, R.J. Sullivan, K.T. Flaherty, D. T. Frederick, J. Jané-Valbuena, C.H. Yoon, O. Rozenblatt-Rosen, A.K. Shalek,

A. Regev, L.A. Garraway, Dissecting the multicellular ecosystem of metastatic melanoma by single-cell RNA-seq, Science (80-.) (2016), https://doi.org/10.1126/science.aad0501.
[55] C. Anqi, K. Takabatake, H. Kawai, O.O. May Wathone, S. Yoshida, M. Fujii, H. Omori, S. Sukegawa, K. Nakano, H. Tsujigiwa, Z. Jinhua, H. Nagatsuka, Differentiation and roles of bone marrow-derived cells on the tumor microenvironment of oral squamous cell carcinoma, Oncol. Lett. 18 (2019) 6628–6638, https://doi.org/10.3892/ol.2019.11045.
[56] H. Yamagishi, T. Oka, I. Hashimoto, N.R. Pellis, B.D. Kahan, The role of the spleen in tumor bearing host: II. The influence of splenectomy in mice, Jpn. J. Surg 14 (1984) 72–77, https://doi.org/10.1007/BF02469606.
[57] V. Bronte, M.J. Pittet, The spleen in local and systemic regulation of immunity, Immunity. 39 (2013) 806–818, https://doi.org/10.1016/j.immuni.2013.10.010.
[58] S. Rose, A. Misharin, H. Perlman, A novel Ly6C/Ly6G-based strategy to analyze the mouse splenic myeloid compartment, Cytom. A. 81 (A) (2012) 343–350, https://doi.org/10.1002/cyto.a.22012.
[59] W. Wang, R. Thomas, O. Sizova, D.M. Su, Thymic function associated with cancer development, relapse, and antitumor immunity – a mini-review, Front. Immunol. 11 (2020), https://doi.org/10.3389/fimmu.2020.00773.
[60] J.M. Butler, H. Kobayashi, S. Rafii, Instructive role of the vascular niche in promoting tumour growth and tissue repair by angiocrine factors, Nat. Rev. Cancer 10 (2010) 138–146, https://doi.org/10.1038/nrc2791.
[61] K. Hida, N. Maishi, D.A. Annan, Y. Hida, Contribution of tumor endothelial cells in cancer progression, Int. J. Mol. Sci. 19 (2018), https://doi.org/10.3390/ijms19051272.
[62] N.V. Goncharov, P.I. Popova, P.P. Avdonin, I.V. Kudryavtsev, M.K. Serebryakova, E.A. Korf, P.V. Avdonin, Markers of endothelial cells in normal and pathological conditions, Biochem. Suppl. Ser. A Membr. Cell Biol. 14 (2020) 167–183, https://doi.org/10.1134/S1990747819030140.
[63] S.J. Ioannides, P.L. Barlow, J.M. Elwood, D. Porter, Effect of obesity on aromatase inhibitor efficacy in postmenopausal, hormone receptor-positive breast cancer: a systematic review, Breast Cancer Res. Treat. 147 (2014) 237–248, https://doi.org/10.1007/s10549-014-3091-7.
[64] Y. Lin, J. Xu, H. Lan, Tumor-associated macrophages in tumor metastasis: biological roles and clinical therapeutic applications, J. Hematol. Oncol. 12 (2019) 1–16, https://doi.org/10.1186/s13045-019-0760-3.
[65] S.I. Grivennikov, F.R. Greten, M. Karin, Immunity, inflammation, and cancer, Cell (2010), https://doi.org/10.1016/j.cell.2010.01.025.
[66] C. Deligne, K.S. Midwood, Macrophages and extracellular matrix in breast cancer: partners in crime or protective allies? Front. Oncol. 11 (2021) 186, https://doi.org/10.3389/FONC.2021.620773.
[67] B. Baban, A.M. Hansen, P.R. Chandler, A. Manlapat, A. Bingaman, D.J. Kahler, D. H. Munn, A.L. Mellor, A minor population of splenic dendritic cells expressing CD19 mediates IDO-dependent T cell suppression via type I IFN signaling following B7 ligation, Int. Immunol. (2005), https://doi.org/10.1093/intimm/dxh271.
[68] J.A. Cintolo, J. Datta, S.J. Mathew, B.J. Czerniecki, Dendritic cell-based vaccines: barriers and opportunities, Future Oncol. 8 (2012) 1273–1299, https://doi.org/10.2217/fon.12.125.
[69] W. Zhang, Y. Ding, L. Sun, Q. Hong, Y. Sun, L. Han, M. Zi, Y. Xu, Bone marrow-derived inflammatory and steady state DCs are different in both functions and survival, Cell. Immunol. 331 (2018) 100–109, https://doi.org/10.1016/j.cellimm.2018.06.001.
[70] R.G. Akwii, M.S. Sajib, F.T. Zahra, C.M. Mikelis, Role of angiopoietin-2 in vascular physiology and pathophysiology, Cells. 8 (2019) 471, https://doi.org/10.3390/cells8050471.
[71] Z.L. Zhang, Z.S. Liu, Q. Sun, Expression of angiopoietins, Tie2 and vascular endothelial growth factor in angiogenesis and progression of hepatocellular carcinoma, World J. Gastroenterol. 12 (2006) 4241–4245, https://doi.org/10.3748/wjg.v12.i26.4241.
[72] E. Uribe-Querol, C. Rosales, Neutrophils in cancer: two sides of the same coin, J Immunol Res 2015 (2015), https://doi.org/10.1155/2015/983698.
[73] Y.W. Li, S.J. Qiu, J. Fan, J. Zhou, Q. Gao, Y.S. Xiao, Y.F. Xu, Intratumoral neutrophils: a poor prognostic factor for hepatocellular carcinoma following resection, J. Hepatol. 54 (2011) 497–505, https://doi.org/10.1016/j.jhep.2010.07.044.
[74] L. Wu, X.H.F. Zhang, Tumor-associated neutrophils and macrophages—heterogenous but not chaotic, Front. Immunol. 11 (2020), https://doi.org/10.3389/fimmu.2020.553967.
[75] S. Cedrés, D. Torrejon, A. Martínez, P. Martinez, A. Navarro, E. Zamora, N. Mulet-Margalef, E. Felip, Neutrophil to lymphocyte ratio (NLR) as an indicator of poor prognosis in stage IV non-small cell lung cancer, Clin. Transl. Oncol. 14 (2012) 864–869, https://doi.org/10.1007/s12094-012-0872-5.
[76] B. Manfroi, J. Moreaux, C. Righini, F. Ghiringhelli, N. Sturm, B. Huard, Tumor-associated neutrophils correlate with poor prognosis in diffuse large B-cell lymphoma patients, Blood Cancer J. 8 (2018) 66, https://doi.org/10.1038/s41408-018-0099-y.
[77] T.T. Maciel, I.C. Moura, O. Hermine, The role of mast cells in cancers, F1000Prime Rep. 7 (2015), https://doi.org/10.12703/P7-09.
[78] S. Maltby, K. Khazaie, K.M. McNagny, Mast cells in tumor growth: Angiogenesis, tissue remodelling and immune-modulation, Biochim. Biophys. Acta - Rev. Cancer. 1796 (2009) 19–26, https://doi.org/10.1016/j.bbcan.2009.02.001.
[79] D.I. Gabrilovich, S. Nagaraj, Myeloid-derived suppressor cells as regulators of the immune system, Nat. Rev. Immunol. (2009), https://doi.org/10.1038/nri2506.
[80] E.K. Vetsika, A. Koukos, A. Kotsakis, Myeloid-derived suppressor cells: major figures that shape the immunosuppressive and angiogenic network in cancer, Cells 8 (2019), https://doi.org/10.3390/cells8121647.
[81] S. Paul, G. Lal, The molecular mechanism of natural killer cells function and its importance in cancer immunotherapy, Front. Immunol. 8 (2017) 1, https://doi.org/10.3389/fimmu.2017.01124.
[82] C. Li, P. Jiang, S. Wei, X. Xu, J. Wang, Regulatory T cells in tumor microenvironment: new mechanisms, potential therapeutic strategies and future prospects, Mol. Cancer 19 (2020) 1–23, https://doi.org/10.1186/s12943-020-01234-1.
[83] A. Verma, R. Mathur, A. Farooque, V. Kaul, S. Gupta, B.S. Dwarakanath, T-regulatory cells in tumor progression and therapy, Cancer Manag. Res. 11 (2019) 10731–10747, https://doi.org/10.2147/CMAR.S228887.
[84] G.J. Yuen, E. Demissie, S. Pillai, B lymphocytes and cancer: a love–hate relationship, Trends Cancer. 2 (2016) 747–757, https://doi.org/10.1016/j.trecan.2016.10.010.
[85] B. Adem, P.F. Vieira, S.A. Melo, Decoding the biology of exosomes in metastasis, Trends Cancer (2020), https://doi.org/10.1016/j.trecan.2019.11.007.
[86] A. Becker, B.K. Thakur, J.M. Weiss, H.S. Kim, H. Peinado, D. Lyden, Extracellular vesicles in cancer: cell-to-cell mediators of metastasis, Cancer Cell 30 (2016) 836–848, https://doi.org/10.1016/j.ccell.2016.10.009.
[87] Y.Y. Yeh, H.G. Ozer, A.M. Lehman, K. Maddocks, L. Yu, A.J. Johnson, J.C. Byrd, Characterization of CLL exosomes reveals a distinct microRNA signature and enhanced secretion by activation of BCR signaling, Blood. 125 (2015) 3297–3305, https://doi.org/10.1182/blood-2014-12-618470.
[88] A. Li, T. Zhang, M. Zheng, Y. Liu, Z. Chen, Exosomal proteins as potential markers of tumor diagnosis, J. Hematol. Oncol. 10 (2017), https://doi.org/10.1186/s13045-017-0542-8.
[89] M. Zarà, G.F. Guidetti, M. Camera, I. Canobbio, P. Amadio, M. Torti, E. Tremoli, S.S. Barbieri, Biology and role of extracellular vesicles (Evs) in the pathogenesis of thrombosis, Int. J. Mol. Sci. 20 (2019), https://doi.org/10.3390/ijms20112840.
[90] D.K. Jeppesen, A.M. Fenix, J.L. Franklin, J.N. Higginbotham, Q. Zhang, L. J. Zimmerman, D.C. Liebler, J. Ping, Q. Liu, R. Evans, W.H. Fissell, J.G. Patton, L. H. Rome, D.T. Burnette, R.J. Coffey, Reassessment of exosome composition, Cell 177 (2019), https://doi.org/10.1016/j.cell.2019.02.029, 428-445.e18.
[91] L.A. Shuman Moss, S. Jensen-Taubman, W.G. Stetler-Stevenson, Matrix metalloproteinases: Changing roles in tumor progression and metastasis, Am. J. Pathol. (2012), https://doi.org/10.1016/j.ajpath.2012.08.044.
[92] M. Takaishi, M. Tarutani, J. Takeda, S. Sano, Mesenchymal to epithelial transition induced by reprogramming factors attenuates the malignancy of cancer cells, PLoS One 11 (2016), e0156904, https://doi.org/10.1371/journal.pone.0156904.
[93] J.C. Tse, R. Kalluri, Mechanisms of metastasis: Epithelial-to-mesenchymal transition and contribution of tumor microenvironment, J. Cell. Biochem. 101 (2007) 816–829, https://doi.org/10.1002/jcb.21215.
[94] Y. Jing, Z. Han, S. Zhang, Y. Liu, L. Wei, Epithelial-mesenchymal Transition in tumor microenvironment, Cell Biosci (2011), https://doi.org/10.1186/2045-3701-1-29.
[95] E. Romeo, C.A. Caserta, C. Rumio, F. Marcucci, The vicious cross-talk between tumor cells with an EMT phenotype and cells of the immune system, Cells (2019), https://doi.org/10.3390/cells8050460.
[96] C. Laplagne, M. Domagala, A. Le Naour, C. Quemerais, D. Hamel, J.J. Fournié, B. Couderc, C. Bousquet, A. Ferrand, M. Poupot, Latest advances in targeting the tumor microenvironment for tumor suppression, Int. J. Mol. Sci. (2019), https://doi.org/10.3390/ijms20194719.
[97] O. Trédan, C.M. Galmarini, K. Patel, I.F. Tannock, Drug resistance and the solid tumor microenvironment, J. Natl. Cancer Inst. 99 (2007) 1441–1454, https://doi.org/10.1093/jnci/djm135.
[98] J. El-Ali, P.K. Sorger, K.F. Jensen, Cells on chips, Nature (2006), https://doi.org/10.1038/nature05063.
[99] E.R. Shamir, A.J. Ewald, Three-dimensional organotypic culture: experimental models of mammalian biology and disease, Nat. Rev. Mol. Cell Biol. (2014), https://doi.org/10.1038/nrm3873.
[100] C. Roma-Rodrigues, R. Mendes, P.V. Baptista, A.R. Fernandes, Targeting tumor microenvironment for cancer therapy, Int. J. Mol. Sci. 20 (2019), https://doi.org/10.3390/ijms20040840.
[101] M.Z. Jin, W.L. Jin, The updated landscape of tumor microenvironment and drug repurposing, Signal Transduct. Target. Ther (2020), https://doi.org/10.1038/s41392-020-00280-x.
[102] E. Cabebe, H. Wakelee, Role of anti-angiogenesis agents in treating NSCLC: focus on bevacizumab and VEGFR tyrosine kinase inhibitors, Curr. Treat. Options in Oncol. (2007), https://doi.org/10.1007/s11864-007-0022-4.
[103] H. Fang, Y.A. DeClerck, Targeting the tumor microenvironment: from understanding pathways to effective clinical trials, Cancer Res. (2013), https://doi.org/10.1158/0008-5472.CAN-13-0661.
[104] M.H. Cohen, Y.L. Shen, P. Keegan, R. Pazdur, FDA drug approval summary: Bevacizumab (Avastin®) as treatment of recurrent glioblastoma multiforme, Oncologist (2009), https://doi.org/10.1634/theoncologist.2009-0121.
[105] K. Podar, F. Fan, A. Schimming, D. Jaeger, Targeting the tumor microenvironment: focus on angiogenesis, J. Oncol. (2012), https://doi.org/10.1155/2012/281261.
[106] R.M. Poole, A. Vaidya, Ramucirumab: first global approval, Drugs (2014), https://doi.org/10.1007/s40265-014-0244-2.
[107] E. Larkins, B. Scepura, G.M. Blumenthal, E. Bloomquist, S. Tang, M. Biable, P. Kluetz, P. Keegan, R. Pazdur, U.S. Food and drug administration approval summary: Ramucirumab for the treatment of metastatic non-small cell lung

cancer following disease progression on or after platinum-based chemotherapy, Oncologist (2015), https://doi.org/10.1634/theoncologist.2015-0221.
[108] Y. Tada, Y. Togashi, D. Kotani, T. Kuwata, E. Sato, A. Kawazoe, T. Doi, H. Wada, H. Nishikawa, K. Shitara, Targeting VEGFR2 with Ramucirumab strongly impacts effector/ activated regulatory T cells and CD8+ T cells in the tumor microenvironment, J. Immunother. Cancer (2018), https://doi.org/10.1186/s40425-018-0403-1.
[109] E. Raymond, L. Dahan, J.L. Raoul, Y.J. Bang, I. Borbath, C. Lombard-Bohas, J. Valle, P. Metrakos, D. Smith, A. Vinik, J.S. Chen, D. Hörsch, P. Hammel, B. Wiedenmann, E. Van Cutsem, S. Patyna, D.R. Lu, C. Blanckmeister, R. Chao, P. Ruszniewski, Sunitinib malate for the treatment of pancreatic neuroendocrine tumors, N. Engl. J. Med. (2011), https://doi.org/10.1056/NEJMoa1003825.
[110] G.D. Demetri, A.T. van Oosterom, C.R. Garrett, M.E. Blackstein, M.H. Shah, J. Verweij, G. McArthur, I.R. Judson, M.C. Heinrich, J.A. Morgan, J. Desai, C. D. Fletcher, S. George, C.L. Bello, X. Huang, C.M. Baum, P.G. Casali, Efficacy and safety of sunitinib in patients with advanced gastrointestinal stromal tumour after failure of imatinib: a randomised controlled trial, Lancet (2006), https://doi.org/10.1016/S0140-6736(06)69446-4.
[111] K. Mittal, J. Ebos, B. Rini, Angiogenesis and the tumor microenvironment: vascular endothelial growth factor and beyond, Semin. Oncol. (2014), https://doi.org/10.1053/j.seminoncol.2014.02.007.
[112] J.E. Ward, W.M. Stadler, Pazopanib in renal cell carcinoma, Clin. Cancer Res. (2010), https://doi.org/10.1158/1078-0432.CCR-10-0728.
[113] L.C. Lu, Y.H. Lee, C.J. Chang, C.T. Shun, C.Y. Fang, Y.Y. Shao, T.H. Liu, A. L. Cheng, C.H. Hsu, Increased expression of programmed death-ligand 1 in infiltrating immune cells in hepatocellular carcinoma tissues after sorafenib treatment, Liver Cancer (2019), https://doi.org/10.1159/000489021.
[114] R.C. Kane, A.T. Farrell, H. Saber, S. Tang, G. Williams, J.M. Jee, C. Liang, B. Booth, N. Chidambaram, D. Morse, R. Sridhara, P. Garvey, R. Justice, R. Pazdur, Sorafenib for the treatment of advanced renal cell carcinoma, Clin. Cancer Res. (2006), https://doi.org/10.1158/1078-0432.CCR-06-1249.
[115] J.M. Llovet, S. Ricci, V. Mazzaferro, P. Hilgard, E. Gane, J.F. Blanc, A.C. De Oliveira, A. Santoro, J.L. Raoul, A. Forner, M. Schwartz, C. Porta, S. Zeuzem, L. Bolondi, T.F. Greten, P.R. Galle, J.F. Seitz, I. Borbath, D. Häussinger, T. Giannaris, M. Shan, M. Moscovici, D. Voliotis, J. Bruix, Sorafenib in advanced hepatocellular carcinoma, N. Engl. J. Med. (2008), https://doi.org/10.1056/NEJMoa0708857.
[116] R.K. Kelley, A.H. Ko, Erlotinib in the treatment of advanced pancreatic cancer, Biol. Targets Ther (2008), https://doi.org/10.2147/btt.s1832.
[117] M.H. Cohen, J.R. Johnson, Y. Chen, R. Sridhara, R. Pazdur, FDA drug approval summary: Erlotinib (Tarceva ®) tablets, Oncologist (2005), https://doi.org/10.1634/theoncologist.10-7-461.
[118] M.H. Cohen, G.A. Williams, R. Sridhara, G. Chen, R. Pazdur, FDA drug approval summary: Gefitinib (ZD1839) (Iressa ®) tablets, Oncologist (2003), https://doi.org/10.1634/theoncologist.8-4-303.
[119] E. Iivanainen, S. Lauttia, N. Zhang, D. Tvorogov, J. Kulmala, R. Grenman, P. Salven, K. Elenius, The EGFR inhibitor gefitinib suppresses recruitment of pericytes and bone marrow-derived perivascular cells into tumor vessels, Microvasc. Res. (2009), https://doi.org/10.1016/j.mvr.2009.06.010.
[120] L. Saltz, C. Easley, P. Kirkpatrick, Panitumumab, Nat. Rev. Drug Discov. (2006), https://doi.org/10.1038/nrd2204.
[121] R. Yuge, Y. Kitadai, K. Shinagawa, M. Onoyama, S. Tanaka, W. Yasui, K. Chayama, MTOR and PDGF pathway blockade inhibits liver metastasis of colorectal cancer by modulating the tumor microenvironment, Am. J. Pathol. (2015), https://doi.org/10.1016/j.ajpath.2014.10.014.
[122] L.C. Kim, R.S. Cook, J. Chen, MTORC1 and mTORC2 in cancer and the tumor microenvironment, Oncogene (2017), https://doi.org/10.1038/onc.2016.363.
[123] P.A. Kenny, G.Y. Lee, M.J. Bissell, Targeting the tumor microenvironment, Front. Biosci. (2007), https://doi.org/10.2741/2327.
[124] J. Ruan, M. Luo, C. Wang, L. Fan, S.N. Yang, M. Cardenas, H. Geng, J.P. Leonard, A. Melnick, L. Cerchietti, K.A. Hajjar, Imatinib disrupts lymphoma angiogenesis by targeting vascular pericytes, Blood (2013), https://doi.org/10.1182/blood-2013-03-490763.
[125] W.D. Tap, H. Gelderblom, E. Palmerini, J. Desai, S. Bauer, J.Y. Blay, T. Alcindor, K. Ganjoo, J. Martín-Broto, C.W. Ryan, D.M. Thomas, C. Peterfy, J.H. Healey, M. van de Sande, H.L. Gelhorn, D.E. Shuster, Q. Wang, A. Yver, H.H. Hsu, P.S. Lin, S. Tong-Starksen, S. Stacchiotti, A.J. Wagner, Pexidartinib versus placebo for advanced tenosynovial giant cell tumour (ENLIVEN): a randomised phase 3 trial, Lancet (2019), https://doi.org/10.1016/S0140-6736(19)30764-0.
[126] P.W. Manley, P. Drueckes, G. Fendrich, P. Furet, J. Liebetanz, G. Martiny-Baron, J. Mestan, J. Trappe, M. Wartmann, D. Fabbro, Extended kinase profile and properties of the protein kinase inhibitor nilotinib, Biochim. Biophys. Acta, Proteins Proteomics (2010), https://doi.org/10.1016/j.bbapap.2009.11.008.
[127] I. Gupta, K. Singh, N.K. Varshney, S. Khan, Delineating crosstalk mechanisms of the ubiquitin proteasome system that regulate apoptosis, Front. Cell Dev. Biol (2018), https://doi.org/10.3389/fcell.2018.00011.
[128] D. Vrábel, L. Pour, S. Ševčíková, The impact of NF-κB signaling on pathogenesis and current treatment strategies in multiple myeloma, Blood Rev. (2019), https://doi.org/10.1016/j.blre.2018.11.003.
[129] G. Germano, R. Frapolli, C. Belgiovine, A. Anselmo, S. Pesce, M. Liguori, E. Erba, S. Uboldi, M. Zucchetti, F. Pasqualini, M. Nebuloni, N. van Rooijen, R. Mortarini, L. Beltrame, S. Marchini, I. Fuso Nerini, R. Sanfilippo, P.G. Casali, S. Pilotti, C. M. Galmarini, A. Anichini, A. Mantovani, M. D'Incalci, P. Allavena, Role of macrophage targeting in the antitumor activity of trabectedin, Cancer Cell (2013), https://doi.org/10.1016/j.ccr.2013.01.008.
[130] M. D'Incalci, N. Badri, C.M. Galmarini, P. Allavena, Trabectedin, a drug acting on both cancer cells and the tumour microenvironment, Br. J. Cancer (2014), https://doi.org/10.1038/bjc.2014.149.
[131] J.P. Edwards, L.A. Emens, The multikinase inhibitor Sorafenib reverses the suppression of IL-12 and enhancement of IL-10 by PGE2 in murine macrophages, Int. Immunopharmacol. (2010), https://doi.org/10.1016/j.intimp.2010.07.002.
[132] M.K. Chuk, J.T. Chang, M.R. Theoret, E. Sampene, K. He, S.L. Weis, W.S. Helms, R. Jin, H. Li, J. Yu, H. Zhao, L. Zhao, M. Paciga, D. Schmiel, R. Rawat, P. Keegan, R. Pazdur, FDA Approval Summary: Accelerated Approval of Pembrolizumab for Second-Line Treatment of Metastatic Melanoma, Clin Cancer Res 23 (19) (2017 Oct 1) 5666–5670, https://doi.org/10.1158/1078-0432.CCR-16-0663.
[133] S.L. Topalian, M. Sznol, D.F. McDermott, H.M. Kluger, R.D. Carvajal, W. H. Sharfman, J.R. Brahmer, D.P. Lawrence, M.B. Atkins, J.D. Powderly, P. D. Leming, E.J. Lipson, I. Puzanov, D.C. Smith, J.M. Taube, J.M. Wigginton, G. D. Kollia, A. Gupta, D.M. Pardoll, J.A. Sosman, F.S. Hodi, Survival, durable tumor remission, and long-term safety in patients with advanced melanoma receiving nivolumab, J. Clin. Oncol. (2014), https://doi.org/10.1200/JCO.2013.53.0105.
[134] A.B. El-Khoueiry, B. Sangro, T. Yau, T.S. Crocenzi, M. Kudo, C. Hsu, T.Y. Kim, S. P. Choo, J. Trojan, T.H. Welling, T. Meyer, Y.K. Kang, W. Yeo, A. Chopra, J. Anderson, C. dela Cruz, L. Lang, J. Neely, H. Tang, H.B. Dastani, I. Melero, Nivolumab in patients with advanced hepatocellular carcinoma (CheckMate 040): an open-label, non-comparative, phase 1/2 dose escalation and expansion trial, Lancet (2017), https://doi.org/10.1016/S0140-6736(17)31046-2.
[135] L.A. Raedler, Tecentriq (Atezolizumab) first PD-L1 inhibitor approved for patients with advanced or metastatic urothelial carcinoma, Am. Heal. Drug Benefits 10 (2017). Eighth Annual Payers' Guide - Select Drug Profiles, Payers' Guide.
[136] C. Massard, M.S. Gordon, S. Sharma, S. Rafii, Z.A. Wainberg, J. Luke, T.J. Curiel, G. Colon-Otero, O. Hamid, R.E. Sanborn, P.H. O'Donnell, A. Drakaki, W. Tan, J. F. Kurland, M.C. Rebelatto, X. Jin, J.A. Blake-Haskins, A. Gupta, N.H. Segal, Safety and efficacy of durvalumab (MEDI4736), an anti-programmed cell death ligand-1 immune checkpoint inhibitor, in patients with advanced urothelial bladder cancer, J. Clin. Oncol. (2016), https://doi.org/10.1200/JCO.2016.67.9761.
[137] S.J. Antonia, A. Villegas, D. Daniel, D. Vicente, S. Murakami, R. Hui, T. Yokoi, A. Chiappori, K.H. Lee, M. De Wit, B.C. Cho, M. Bourhaba, X. Quantin, T. Tokito, T. Mekhail, D. Planchard, Y.C. Kim, C.S. Karapetis, S. Hiret, G. Ostoros, K. Kubota, J.E. Gray, L. Paz-Ares, J. De Castro Carpeño, C. Wadsworth, G. Melillo, H. Jiang, Y. Huang, P.A. Dennis, M. Özgüroğlu, Durvalumab after chemoradiotherapy in stage III non–small-cell lung cancer, N. Engl. J. Med. (2017), https://doi.org/10.1056/NEJMoa1709937.
[138] E.P. Juliá, A. Amante, M.B. Pampena, J. Mordoh, E.M. Levy, Avelumab, an IgG1 anti-PD-L1 immune checkpoint inhibitor, triggers NK cell-mediated cytotoxicity and cytokine production against triple negative breast cancer cells, Front. Immunol. (2018), https://doi.org/10.3389/fimmu.2018.02140.
[139] S.P. D'Angelo, J. Russell, C. Lebbé, B. Chmielowski, T. Gambichler, J.-J. Grob, F. Kiecker, G. Rabinowits, P. Terheyden, I. Zwiener, M. Bajars, M. Hennessy, H. L. Kaufman, Efficacy and safety of first-line Avelumab treatment in patients with stage IV metastatic merkel cell carcinoma, JAMA Oncol (2018), https://doi.org/10.1001/jamaoncol.2018.0077.
[140] C. Robert, L. Thomas, I. Bondarenko, S. O'Day, J. Weber, C. Garbe, C. Lebbe, J. F. Baurain, A. Testori, J.J. Grob, N. Davidson, J. Richards, M. Maio, A. Hauschild, W.H. Miller, P. Gascon, M. Lotem, K. Harmankaya, R. Ibrahim, S. Francis, T. T. Chen, R. Humphrey, A. Hoos, J.D. Wolchok, Ipilimumab plus dacarbazine for previously untreated metastatic melanoma, N. Engl. J. Med. (2011), https://doi.org/10.1056/NEJMoa1104621.
[141] E. Simeone, P.A. Ascierto, Anti-PD-1 and PD-L1 antibodies in metastatic melanoma, Melanoma Manag (2017), https://doi.org/10.2217/mmt-2017-0018.
[142] M.R. Smith, Rituximab (monoclonal anti-CD20 antibody): Mechanisms of action and resistance, Oncogene (2003), https://doi.org/10.1038/sj.onc.1206939.
[143] T. Robak, Ofatumumab, a human monoclonal antibody for lymphoid malignancies and autoimmune disorders, Curr. Opin. Mol. Ther. 10 (3) (2008) 294–309.
[144] H. Zhong, D.W. Gutkin, B. Han, Y. Ma, A.A. Keskinov, M.R. Shurin, G.V. Shurin, Origin and pharmacological modulation of tumor-associated regulatory dendritic cells, Int. J. Cancer (2014), https://doi.org/10.1002/ijc.28590.
[145] H. Xin, C. Zhang, A. Herrmann, Y. Du, R. Figlin, H. Yu, Sunitinib inhibition of Stat3 induces renal cell carcinoma tumor cell apoptosis and reduces immunosuppressive cells, Cancer Res. (2009), https://doi.org/10.1158/0008-5472.CAN-08-4323.
[146] J. Finke, J. Ko, B. Rini, P. Rayman, J. Ireland, P. Cohen, MDSC as a mechanism of tumor escape from sunitinib mediated anti-angiogenic therapy, Int. Immunopharmacol. (2011), https://doi.org/10.1016/j.intimp.2011.01.030.
[147] H. Yuan, P. Cai, Q. Li, W. Wang, Y. Sun, Q. Xu, Y. Gu, Axitinib augments antitumor activity in renal cell carcinoma via STAT3-dependent reversal of myeloid-derived suppressor cell accumulation, Biomed. Pharmacother. (2014), https://doi.org/10.1016/j.biopha.2014.07.002.
[148] P.C.C. Liu, H. Koblish, L. Wu, K. Bowman, S. Diamond, D. DiMatteo, Y. Zhang, M. Hansbury, M. Rupar, X. Wen, P. Collier, P. Feldman, R. Klabe, K.A. Burke, M. Soloviev, C. Gardiner, X. He, A. Volgina, M. Covington, B. Ruggeri, R. Wynn, T.C. Burn, P. Scherle, S. Yeleswaram, W. Yao, R. Huber, G. Hollis, INCB054828 (pemigatinib), a potent and selective inhibitor of fibroblast growth factor receptors 1, 2, and 3, displays activity against genetically defined tumor models, PLoS One (2020), https://doi.org/10.1371/journal.pone.0231877.
[149] S. Haubeiss, J.O. Schmid, T.E. Mürdter, M. Sonnenberg, G. Friedel, H. van der Kuip, W.E. Aulitzky, Dasatinib reverses Cancer-associated Fibroblasts (CAFs) from

primary Lung Carcinomas to a Phenotype comparable to that of normal Fibroblasts, Mol. Cancer (2010), https://doi.org/10.1186/1476-4598-9-168.
[150] A. Rossini, F. Zunino, G. Ruggiero, M. De Cesare, D. Cominetti, M. Tortoreto, C. Lanzi, G. Cassinelli, R. Zappasodi, C. Tripodo, A. Gulino, N. Zaffaroni, M. Di Nicola, Microenvironment modulation and enhancement of antilymphoma therapy by the heparanase inhibitor roneparstat, Hematol. Oncol. (2018), https://doi.org/10.1002/hon.2466.
[151] P. Barbieri, D. Paoletti, G. Giannini, R.D. Sanderson, A. Noseda, Roneparstat and heparanase inhibition: a new tool for cancer treat-ment, J. Pharmacol. Clin. Toxicol. 5 (2) (2017), 1071.
[152] Y.J. Choi, J.K. Rho, S.J. Lee, W.S. Jang, S.S. Lee, C.H. Kim, J.C. Lee, HIF-1α modulation by topoisomerase inhibitors in non-small cell lung cancer cell lines, J. Cancer Res. Clin. Oncol. (2009), https://doi.org/10.1007/s00432-009-0543-2.
[153] V.E. Kwitkowski, T.M. Prowell, A. Ibrahim, A.T. Farrell, R. Justice, S.S. Mitchell, R. Sridhara, R. Pazdur, FDA approval summary: temsirolimus as treatment for advanced renal cell carcinoma, Oncologist (2010), https://doi.org/10.1634/theoncologist.2009-0178.
[154] G.V. Thomas, C. Tran, I.K. Mellinghoff, D.S. Welsbie, E. Chan, B. Fueger, J. Czernin, C.L. Sawyers, Hypoxia-inducible factor determines sensitivity to inhibitors of mTOR in kidney cancer, Nat. Med. (2006), https://doi.org/10.1038/nm1337.
[155] J.P. Laubach, C.J. Liu, N.S. Raje, A.J. Yee, P. Armand, R.L. Schlossman, J. Rosenblatt, J. Hedlund, M. Martin, C. Reynolds, K.H. Shain, I. Zackon, L. Stampleman, P. Henrick, B. Rivotto, K.T.V. Hornburg, H.J. Dumke, S. Chuma, A. Savell, D.R. Handisides, S. Kroll, K.C. Anderson, P.G. Richardson, I. M. Ghobrial, A phase I/II study of evofosfamide, a hypoxia-activated prodrug with or without bortezomib in subjects with relapsed/ refractory multiple myeloma, Clin. Cancer Res. (2019), https://doi.org/10.1158/1078-0432.CCR-18-1325.
[156] S. Modi, A. Stopeck, H. Linden, D. Solit, S. Chandarlapaty, N. Rosen, G. D'Andrea, M. Dickler, M.E. Moynahan, S. Sugarman, W. Ma, S. Patil, L. Norton, A.L. Hannah, C. Hudis, HSP90 inhibition is effective in breast cancer: a phase II trial of tanespimycin (17-AAG) plus trastuzumab in patients with HER2-positive metastatic breast cancer progressing on trastuzumab, Clin Cancer Res 17 (15) (2011 Aug 1) 5132–5139, https://doi.org/10.1158/1078-0432.CCR-11-0072. PMID: 21558407. Epub 2011 May 10.
[157] M. Mertens, J.A. Singh, Anakinra for rheumatoid arthritis: a systematic review, J. Rheumatol. (2009), https://doi.org/10.3899/jrheum.090074.
[158] R. Tutrone, M.J. Donovan, P. Torkler, V. Tadigotla, T. McLain, M. Noerholm, J. Skog, J. McKiernan, Clinical utility of the exosome based ExoDx Prostate (IntelliScore) EPI test in men presenting for initial Biopsy with a PSA 2–10 ng/mL, Prostate Cancer Prostatic Dis. (2020), https://doi.org/10.1038/s41391-020-0237-z.
[159] C.A. Bradley, Pancreatic cancer: IExosomes target the "undruggable,", Nat. Rev. Cancer (2017) https://doi.org/10.1038/nrc.2017.54.
[160] P.D. Miller, Denosumab: anti-RANKL antibody, Curr. Osteoporos. Rep (2009), https://doi.org/10.1007/s11914-009-0004-5.
[161] C. Goessl, L. Katz, W.C. Dougall, P.J. Kostenuik, H.B. Zoog, A. Braun, R. Dansey, R.B. Wagman, The development of denosumab for the treatment of diseases of bone loss and cancer-induced bone destruction, Ann. N. Y. Acad. Sci. (2012), https://doi.org/10.1111/j.1749-6632.2012.06674.x.
[162] D. Hanahan, R.A. Weinberg, Hallmarks of cancer: the next generation, Cell (2011), https://doi.org/10.1016/j.cell.2011.02.013.
[163] Y. Yuan, Y.C. Jiang, C.K. Sun, Q.M. Chen, Role of the tumor microenvironment in tumor progression and the clinical applications (review), Oncol. Rep. (2016), https://doi.org/10.3892/or.2016.4660.
[164] T.L. Whiteside, The tumor microenvironment and its role in promoting tumor growth, Oncogene (2008), https://doi.org/10.1038/onc.2008.271.
[165] S. Grund-Gröschke, G. Stockmaier, F. Aberger, Hedgehog/GLI signaling in tumor immunity - New therapeutic opportunities and clinical implications, Cell Commun. Signal. (2019), https://doi.org/10.1186/s12964-019-0459-7.
[166] K. Takabatake, T. Shimo, J. Murakami, C. Anqi, H. Kawai, S. Yoshida, M.W. Oo, O. Haruka, S. Sukegawa, H. Tsujigiwa, K. Nakano, H. Nagatsuka, The role of sonic hedgehog signaling in the tumor microenvironment of oral squamous cell carcinoma, Int. J. Mol. Sci. (2019), https://doi.org/10.3390/ijms20225779.
[167] O. Meurette, P. Mehlen, Notch Signaling in the Tumor Microenvironment, Cancer Cell (2018), https://doi.org/10.1016/j.ccell.2018.07.009.
[168] A. Zlobin, J.C. Bloodworth, A.T. Baker, C. Osipo, Notch signaling pathway in carcinogenesis, Predict. Biomarkers Oncol. (2019), https://doi.org/10.1007/978-3-319-95228-4_17.
[169] Y. Ruan, H. Ogana, E. Gang, H.N. Kim, Y.M. Kim, Wnt signaling in the tumor microenvironment, Adv. Exp. Med. Biol. (2021), https://doi.org/10.1007/978-3-030-47189-7_7.
[170] Y.D. Jung, S.A. Ahmad, Y. Akagi, Y. Takahashi, W. Liu, N. Reinmuth, R. M. Shaheen, F. Fan, L.M. Ellis, Role of the tumor microenvironment in mediating response to anti-angiogenic therapy, Cancer Metastasis Rev. (2000), https://doi.org/10.1023/A:1026510130114.
[171] G. Landskron, M. De La Fuente, P. Thuwajit, C. Thuwajit, M.A. Hermoso, Chronic inflammation and cytokines in the tumor microenvironment, J. Immunol, Res, 2014, https://doi.org/10.1155/2014/149185.
[172] L. Qin, M. Zhong, D. Adah, L. Qin, X. Chen, C. Ma, Q. Fu, X. Zhu, Z. Li, N. Wang, Y. Chen, A novel tumour suppressor lncRNA F630028O10Rik inhibits lung cancer angiogenesis by regulating miR-223-3p, J. Cell. Mol. Med. (2020), https://doi.org/10.1111/jcmm.15044.
[173] X. Jiang, J. Wang, X. Deng, F. Xiong, S. Zhang, Z. Gong, X. Li, K. Cao, H. Deng, Y. He, Q. Liao, B. Xiang, M. Zhou, C. Guo, Z. Zeng, G. Li, X. Li, W. Xiong, The role of microenvironment in tumor angiogenesis, J. Exp. Clin. Cancer Res. (2020), https://doi.org/10.1186/s13046-020-01709-5.
[174] Y. Suárez, W.C. Sessa, MicroRNAs as novel regulators of angiogenesis, Circ. Res. (2009), https://doi.org/10.1161/CIRCRESAHA.108.191270.
[175] T. Zhang, W.Y.W. Lee, Y.F. Rui, T.Y. Cheng, X.H. Jiang, G. Li, Bone marrow-derived mesenchymal stem cells promote growth and angiogenesis of breast and prostate tumors, Stem Cell Res Ther (2013), https://doi.org/10.1186/scrt221.
[176] B. Sun, S. Zhang, C. Ni, D. Zhang, Y. Liu, W. Zhang, X. Zhao, C. Zhao, M. Shi, Correlation between melanoma angiogenesis and the mesenchymal stem cells and endothelial progenitor cells derived from bone marrow, Stem Cells Dev. (2005), https://doi.org/10.1089/scd.2005.14.292.
[177] L.Q. Fu, W.L. Du, M.H. Cai, J.Y. Yao, Y.Y. Zhao, X.Z. Mou, The roles of tumor-associated macrophages in tumor angiogenesis and metastasis, Cell. Immunol. (2020), https://doi.org/10.1016/j.cellimm.2020.104119.
[178] D. Ribatti, A. Vacca, B. Nico, E. Crivellato, L. Roncali, F. Dammacco, The role of mast cells in tumour angiogenesis, Br. J. Haematol. (2001), https://doi.org/10.1046/j.1365-2141.2001.03202.x.
[179] C. Murdoch, M. Muthana, S.B. Coffelt, C.E. Lewis, The role of myeloid cells in the promotion of tumour angiogenesis, Nat. Rev. Cancer (2008), https://doi.org/10.1038/nrc2444.
[180] F. Gizem Sonugür, H. Akbulut, The role of tumor microenvironment in genomic instability of malignant tumors, Front. Genet. (2019), https://doi.org/10.3389/fgene.2019.01063.
[181] S. Negrini, V.G. Gorgoulis, T.D. Halazonetis, Genomic instability an evolving hallmark of cancer, Nat. Rev. Mol. Cell Biol. (2010), https://doi.org/10.1038/nrm2858.
[182] R.S. Bindra, P.M. Glazer, Genetic instability and the tumor microenvironment: towards the concept of microenvironment-induced mutagenesis, Mutat. Res. - Fundam. Mol. Mech, Mutagen, 2005, https://doi.org/10.1016/j.mrfmmm.2004.03.013.
[183] A. Palumbo, N. de Oliveira Meireles Da Costa, M.H. Bonamino, L.F. Ribeiro Pinto, L.E. Nasciutti, Genetic instability in the tumor microenvironment: A new look at an old neighbor, Mol. Cancer (2015), https://doi.org/10.1186/s12943-015-0409-y.
[184] L.R. Ferguson, H. Chen, A.R. Collins, M. Connell, G. Damia, S. Dasgupta, M. Malhotra, A.K. Meeker, A. Amedei, A. Amin, S.S. Ashraf, K. Aquilano, A. S. Azmi, D. Bhakta, A. Bilsland, C.S. Boosani, S. Chen, M.R. Ciriolo, H. Fujii, G. Guha, D. Halicka, W.G. Helferich, W.N. Keith, S.I. Mohammed, E. Niccolai, X. Yang, K. Honoki, V.R. Parslow, S. Prakash, S. Rezazadeh, R.E. Shackelford, D. Sidransky, P.T. Tran, E.S. Yang, C.A. Maxwell, Genomic instability in human cancer: molecular insights and opportunities for therapeutic attack and prevention through diet and nutrition, Semin. Cancer Biol. (2015), https://doi.org/10.1016/j.semcancer.2015.03.005.
[185] D.C. Radisky, D.D. Levy, L.E. Littlepage, H. Liu, C.M. Nelson, J.E. Fata, D. Leake, E.L. Godden, D.G. Albertson, M.A. Nieto, Z. Werb, M.J. Bissell, Rac1b and reactive oxygen species mediate MMP-3-induced EMT and genomic instability, Nature (2005), https://doi.org/10.1038/nature03688.
[186] S. Elmore, Apoptosis: a review of programmed cell death, Toxicol. Pathol. (2007), https://doi.org/10.1080/01926230701320337.
[187] J.M. Brown, L.D. Attardi, The role of apoptosis in cancer development and treatment response, Nat. Rev. Cancer (2005), https://doi.org/10.1038/nrc1560.
[188] S. Grasso, M. Piedad, E. Carrasco-Garca, L. Mayor-Lpez, E. Tristante, L. Rocamora-Reverte, Ngeles Gmez-Martnez, P. Garca-Morales, J.A.M. Saceda, I. Martnez-Lacaci, Cell death and cancer, novel therapeutic strategies, Apoptosis Med. (2012), https://doi.org/10.5772/51285.
[189] M.W. Pickup, J.K. Mouw, V.M. Weaver, The extracellular matrix modulates the hallmarks of cancer, EMBO Rep. (2014), https://doi.org/10.15252/embr.201439246.
[190] N. Boudreau, C.J. Sympson, Z. Werb, M.J. Bissell, Suppression of ICE and apoptosis in mammary epithelial cells by extracellular matrix, Science (80-.) (1995), https://doi.org/10.1126/science.7531366.
[191] M. Karin, F.R. Greten, NF-κB: Linking inflammation and immunity to cancer development and progression, Nat. Rev. Immunol. (2005), https://doi.org/10.1038/nri1703.
[192] E. Pikarsky, R.M. Porat, I. Stein, R. Abramovitch, S. Amit, S. Kasem, E. Gutkovich-Pyest, S. Uriell-Shoval, E. Galun, Y. Ben-Neriah, NF-κB functions as a tumour promoter in inflammation-associated cancer, Nature (2004), https://doi.org/10.1038/nature02924.
[193] G.J. Wise, V.K. Marella, G. Talluri, D. Shirazian, Cytokine variations in patients with hormone treated prostate cancer, J. Urol. (2000), https://doi.org/10.1016/s0022-5347(05)67289-8.
[194] S.O. Lee, W. Lou, M. Hou, S.A. Onate, A.C. Gao, Interleukin-4 enhances prostate-specific antigen expression by activation of the androgen receptor and Akt pathway, Oncogene (2003), https://doi.org/10.1038/sj.onc.1206735.
[195] T.D.K. Chung, J.J. Yu, T.A. Kong, M.T. Spiotto, J.M. Lin, Interleukin-6 activates phosphatidylinositol-3 kinase, which inhibits apoptosis in human prostate cancer cell lines, Prostate (2000), https://doi.org/10.1002/(SICI)1097-0045(20000101)42:1<1::AID-PROS1>3.0.CO;2-Y.
[196] C. Wilson, T. Wilson, P.G. Johnston, D.B. Longley, D.J.J. Waugh, Interleukin-8 signaling attenuates TRAIL- and chemotherapy-induced apoptosis through transcriptional regulation of c-FLIP in prostate cancer cells, Mol. Cancer Ther. (2008), https://doi.org/10.1158/1535-7163.MCT-08-0148.
[197] Z. Culig, Cytokine disbalance in common human cancers, Biochim. Biophys. Acta - Mol, Cell Res, 2011, https://doi.org/10.1016/j.bbamcr.2010.12.010.
[198] K.J. Weigel, A. Jakimenko, B.A. Conti, S.E. Chapman, W.J. Kaliney, W.M. Leevy, M.M. Champion, Z.T. Schafer, CAF-secreted IGFBPs regulate breast cancer cell

anoikis, Mol. Cancer Res. (2014), https://doi.org/10.1158/1541-7786.MCR-14-0090.
[199] D.A. Senthebane, A. Rowe, N.E. Thomford, H. Shipanga, D. Munro, M.A.M. Al Mazeedi, H.A.M. Almazyadi, K. Kallmeyer, C. Dandara, M.S. Pepper, M.I. Parker, K. Dzobo, The role of tumor microenvironment in chemoresistance: to survive, keep your enemies closer, Int. J. Mol. Sci. 18 (2017), https://doi.org/10.3390/ijms18071586.
[200] J.R. Cantor, D.M. Sabatini, Cancer cell metabolism: one hallmark, many faces, Cancer Discov (2012), https://doi.org/10.1158/2159-8290.CD-12-0345.
[201] O. Warburg, F. Wind, E. Negelein, The metabolism of tumors in the body, J. Gen. Physiol. (1927), https://doi.org/10.1085/jgp.8.6.519.
[202] P. Vaupel, Metabolic microenvironment of tumor cells: a key factor in malignant progression, Exp. Oncol. 32 (3) (2010) 125–127.
[203] T. Wang, G. Liu, R. Wang, The intercellular metabolic interplay between tumor and immune cells, Front. Immunol. 5 (2014), https://doi.org/10.3389/fimmu.2014.00358.
[204] C.A. Lyssiotis, A.C. Kimmelman, Metabolic interactions in the tumor microenvironment, Trends Cell Biol. (2017), https://doi.org/10.1016/j.tcb.2017.06.003.
[205] M.G. Vander Heiden, R.J. DeBerardinis, Understanding the intersections between metabolism and cancer biology, Cell (2017), https://doi.org/10.1016/j.cell.2016.12.039.
[206] C. Zhang, L.M. Moore, X. Li, W.K.A. Yung, W. Zhang, IDH1/2 mutations target a key hallmark of cancer by deregulating cellular metabolism in glioma, Neuro-Oncology (2013), https://doi.org/10.1093/neuonc/not087.
[207] B. Ghesquière, B.W. Wong, A. Kuchnio, P. Carmeliet, Metabolism of stromal and immune cells in health and disease, Nature (2014), https://doi.org/10.1038/nature13312.
[208] G.L. Semenza, HIF-1 mediates metabolic responses to intratumoral hypoxia and oncogenic mutations, J. Clin. Invest. (2013), https://doi.org/10.1172/JCI67230.
[209] A. Ohta, A metabolic immune checkpoint: adenosine in tumor microenvironment, Front. Immunol. (2016), https://doi.org/10.3389/fimmu.2016.00109.
[210] R. Nahta, F. Al-Mulla, R. Al-Temaimi, A. Amedei, R. Andrade-Vieira, S. Bay, D. G. Brown, G.M. Calaf, R.C. Castellino, K.A. Cohen-Solal, A. Colacci, N. Cruickshanks, P. Dent, R. Di Fiore, S. Forte, G.S. Goldberg, R.A. Hamid, H. Krishnan, D.W. Laird, A. Lasfar, P.A. Marignani, L. Memeo, C. Mondello, C. C. Naus, R. Ponce-Cusi, J. Raju, D. Roy, R. Roy, E.P. Ryan, H.K. Salem, A. Ivana Scovassi, N. Singh, M. Vaccari, R. Vento, J. Vondráček, M. Wade, J. Woodrick, W.H. Bisson, Mechanisms of environmental chemicals that enable the cancer hallmark of evasion of growth suppression, Carcinogenesis (2015), https://doi.org/10.1093/carcin/bgv028.
[211] L. Yang, M. Karin, Roles of tumor suppressors in regulating tumor-associated inflammation, Cell Death Differ. (2014), https://doi.org/10.1038/cdd.2014.131.
[212] X. Li, S. He, B. Ma, Autophagy and autophagy-related proteins in cancer, Mol. Cancer (2020), https://doi.org/10.1186/s12943-020-1138-4.
[213] E. White, the role for autophagy in cancer (White, 2015).pdf, J. Clin. Invest. 125 (1) (2015) 42–46, https://doi.org/10.1172/JCI73941.
[214] R. Mathew, V. Karantza-Wadsworth, E. White, Role of autophagy in cancer, Nat. Rev. Cancer (2007), https://doi.org/10.1038/nrc2254.
[215] D.S. Vinay, E.P. Ryan, G. Pawelec, W.H. Talib, J. Stagg, E. Elkord, T. Lichtor, W. K. Decker, R.L. Whelan, H.M.C.S. Kumara, E. Signori, K. Honoki, A. G. Georgakilas, A. Amin, W.G. Helferich, C.S. Boosani, G. Guha, M.R. Ciriolo, S. Chen, S.I. Mohammed, A.S. Azmi, W.N. Keith, A. Bilsland, D. Bhakta, D. Halicka, H. Fujii, K. Aquilano, S.S. Ashraf, S. Nowsheen, X. Yang, B.K. Choi, B. S. Kwon, Immune evasion in cancer: mechanistic basis and therapeutic strategies, Semin. Cancer Biol. (2015), https://doi.org/10.1016/j.semcancer.2015.03.004.
[216] N.B. Hao, M.H. Lü, Y.H. Fan, Y.L. Cao, Z.R. Zhang, S.M. Yang, Macrophages in tumor microenvironments and the progression of tumors, Clin. Dev. Immunol. (2012), https://doi.org/10.1155/2012/948098.
[217] R.S. Herbst, J.C. Soria, M. Kowanetz, G.D. Fine, O. Hamid, M.S. Gordon, J. A. Sosman, D.F. McDermott, J.D. Powderly, S.N. Gettinger, H.E.K. Kohrt, L. Horn, D.P. Lawrence, S. Rost, M. Leabman, Y. Xiao, A. Mokatrin, H. Koeppen, P. S. Hegde, I. Mellman, D.S. Chen, F.S. Hodi, Predictive correlates of response to the anti-PD-L1 antibody MPDL3280A in cancer patients, Nature (2014), https://doi.org/10.1038/nature14011.
[218] V.R. Juneja, K.A. McGuire, R.T. Manguso, M.W. LaFleur, N. Collins, W. Nicholas Haining, G.J. Freeman, A.H. Sharpe, PD-L1 on tumor cells is sufficient for immune evasion in immunogenic tumors and inhibits CD8 T cell cytotoxicity, J. Exp. Med. (2017), https://doi.org/10.1084/jem.20160801.
[219] H. Maeda, A. Shiraishi, TGF-beta contributes to the shift toward Th2-type responses through direct and IL-10-mediated pathways in tumor-bearing mice, J. Immunol. 156 (1) (1996) 73–78.
[220] H. Gonzalez, C. Hagerling, Z. Werb, Roles of the immune system in cancer: From tumor initiation to metastatic progression, Genes Dev. (2018), https://doi.org/10.1101/GAD.314617.118.
[221] N.C. DeVito, M.P. Plebanek, B. Theivanthiran, B.A. Hanks, Role of tumor-mediated dendritic cell tolerization in immune evasion, Front. Immunol. (2019), https://doi.org/10.3389/fimmu.2019.02876.
[222] C. Tkaczyk, I. Villa, R. Peronet, B. David, S. Chouaib, S. Mécheri, In vitro and in vivo immunostimulatory potential of bone marrow-derived mast cells on B- and T-lymphocyte activation, J Allergy Clin Immunol. 105 (1) (2000) 134–142, https://doi.org/10.1016/s0091-6749(00)90188-x. PMID: 10629463.
[223] P. Yu, D.A. Rowley, Y.X. Fu, H. Schreiber, The role of stroma in immune recognition and destruction of well-established solid tumors, Curr. Opin. Immunol. (2006), https://doi.org/10.1016/j.coi.2006.01.004.
[224] L. Hayflick, P.S. Moorhead, The serial cultivation of human diploid cell strains, Exp. Cell Res. (1961), https://doi.org/10.1016/0014-4827(61)90192-6.
[225] A.M. Battram, M. Bachiller, B. Martín-Antonio, Senescence in the development and response to cancer with immunotherapy: a double-edged sword, Int. J. Mol. Sci. (2020), https://doi.org/10.3390/ijms21124346.
[226] M.K. Ruhland, A.J. Loza, A.H. Capietto, X. Luo, B.L. Knolhoff, K.C. Flanagan, B. A. Belt, E. Alspach, K. Leahy, J. Luo, A. Schaffer, J.R. Edwards, G. Longmore, R. Faccio, D.G. Denardo, S.A. Stewart, Stromal senescence establishes an immunosuppressive microenvironment that drives tumorigenesis, Nat. Commun. (2016), https://doi.org/10.1038/ncomms11762.
[227] E. Elinav, R. Nowarski, C.A. Thaiss, B. Hu, C. Jin, R.A. Flavell, Inflammation-induced cancer: crosstalk between tumours, immune cells and microorganisms, Nat. Rev. Cancer (2013), https://doi.org/10.1038/nrc3611.
[228] Q. Zhang, B. Zhu, Y. Li, Resolution of cancer-promoting inflammation: a new approach for anticancer therapy, Front. Immunol. (2017), https://doi.org/10.3389/fimmu.2017.00071.
[229] T. Pálmai-Pallag, C.Z. Bachrati, Inflammation-induced DNA damage and damage-induced inflammation: a vicious cycle, Microbes Infect. (2014), https://doi.org/10.1016/j.micinf.2014.10.001.
[230] T. Hagemann, T. Lawrence, I. McNeish, K.A. Charles, H. Kulbe, R.G. Thompson, S. C. Robinson, F.R. Balkwill, "Re-educating" tumor-associated macrophages by targeting NF-κB, J. Exp. Med. (2008), https://doi.org/10.1084/jem.20080108.
[231] J. Wang, D. Li, H. Cang, B. Guo, Crosstalk between cancer and immune cells: Role of tumor-associated macrophages in the tumor microenvironment, Cancer Med (2019), https://doi.org/10.1002/cam4.2327.
[232] Z. Yang, B. Zhang, D. Li, M. Lv, C. Huang, G.X. Shen, B. Huang, Mast cells mobilize myeloid-derived suppressor cells and Treg cells in tumor microenvironment via IL-17 pathway in murine hepatocarcinoma model, PLoS One (2010), https://doi.org/10.1371/journal.pone.0008922.
[233] G.M. Balachander, P.M. Talukdar, M. Debnath, A. Rangarajan, K. Chatterjee, Inflammatory role of cancer-associated fibroblasts in invasive breast tumors revealed using a fibrous polymer scaffold, ACS Appl. Mater. Interfaces (2018), https://doi.org/10.1021/acsami.8b07609.
[234] T.Y. Na, L. Schecterson, A.M. Mendonsa, B.M. Gumbiner, The functional activity of E-cadherin controls tumor cell metastasis at multiple steps, Proc. Natl. Acad. Sci. U. S. A. (2020), https://doi.org/10.1073/pnas.1918167117.
[235] W.G. Jiang, A.J. Sanders, M. Katoh, H. Ungefroren, F. Gieseler, M. Prince, S. K. Thompson, M. Zollo, D. Spano, P. Dhawan, D. Sliva, P.R. Subbarayan, M. Sarkar, K. Honoki, H. Fujii, A.G. Georgakilas, A. Amedei, E. Niccolai, A. Amin, S.S. Ashraf, L. Ye, W.G. Helferich, X. Yang, C.S. Boosani, G. Guha, M.R. Ciriolo, K. Aquilano, S. Chen, A.S. Azmi, W.N. Keith, A. Bilsland, D. Bhakta, D. Halicka, S. Nowsheen, F. Pantano, D. Santini, Tissue invasion and metastasis: Molecular, biological and clinical perspectives, Semin. Cancer Biol. (2015), https://doi.org/10.1016/j.semcancer.2015.03.008.
[236] D.R. Bielenberg, B.R. Zetter, The contribution of angiogenesis to the process of metastasis, Cancer J. (United States) (2015), https://doi.org/10.1097/PPO.0000000000000138.
[237] D. Spano, C. Heck, P. De Antonellis, G. Christofori, M. Zollo, Molecular networks that regulate cancer metastasis, Semin. Cancer Biol. (2012), https://doi.org/10.1016/j.semcancer.2012.03.006.
[238] A. Mantovani, T. Schioppa, C. Porta, P. Allavena, A. Sica, Role of tumor-associated macrophages in tumor progression and invasion, Cancer Metastasis Rev. (2006), https://doi.org/10.1007/s10555-006-9001-7.
[239] S.J. Coniglio, E. Eugenin, K. Dobrenis, E.R. Stanley, B.L. West, M.H. Symons, J. E. Segall, Microglial stimulation of glioblastoma invasion involves epidermal growth factor receptor (EGFR) and colony stimulating factor 1 receptor (CSF-1R) signaling, Mol. Med. (2012), https://doi.org/10.2119/molmed.2011.00217.
[240] S. Goswami, E. Sahai, J.B. Wyckoff, M. Cammer, D. Cox, F.J. Pixley, E.R. Stanley, J.E. Segall, J.S. Condeelis, Macrophages promote the invasion of breast carcinoma cells via a colony-stimulating factor-1/epidermal growth factor paracrine loop, Cancer Res. (2005), https://doi.org/10.1158/0008-5472.CAN-04-1853.
[241] S. Zaghdoudi, E. Decaup, I. Belhabib, R. Samain, S. Cassant-Sourdy, J. Rochotte, A. Brunel, D. Schlaepfer, J. Cros, C. Neuzillet, M. Strehaiano, A. Alard, R. Tomasini, V. Rajeeve, A. Perraud, M. Mathonnet, O.M. Pearce, Y. Martineau, S. Pyronnet, C. Bousquet, C. Jean, FAK activity in cancer-associated fibroblasts is a prognostic marker and a druggable key metastatic player in pancreatic cancer, EMBO Mol. Med (2020), https://doi.org/10.15252/emmm.202012010.
[242] E. Frei, J.F. Holland, M.A. Schneiderman, D. Pinkel, G. Selkirk, E.J. Freireich, R. T. Silver, G.L. Gold, W. Regelson, A comparative study of two regimens of combination chemotherapy in acute leukemia, Blood (1958), https://doi.org/10.1182/blood.v13.12.1126.1126.
[243] D.A. Yardley, Drug resistance and the role of combination chemotherapy in improving patient outcomes, Int. J. Breast Cancer (2013), https://doi.org/10.1155/2013/137414.
[244] P.A. Ascierto, F.M. Marincola, Combination therapy: the next opportunity and challenge of medicine, J. Transl. Med. (2011), https://doi.org/10.1186/1479-5876-9-115.
[245] D.P. Mangiameli, J.A. Blansfield, S. Kachala, D. Lorang, P.H. Schafer, G. W. Muller, D.I. Stirling, S.K. Libutti, Combination therapy targeting the tumor microenvironment is effective in a model of human ocular melanoma, J. Transl. Med. 5 (2007) 1–9, https://doi.org/10.1186/1479-5876-5-38.
[246] H. Kitano, Y. Kitadai, J. Teishima, R. Yuge, S. Shinmei, K. Goto, S. Inoue, T. Hayashi, K. Sentani, W. Yasui, A. Matsubara, Combination therapy using molecular-targeted drugs modulates tumor microenvironment and impairs tumor growth in renal cell carcinoma, Cancer Med (2017), https://doi.org/10.1002/cam4.1124.

[247] L. Paz-Ares, M. Dvorkin, Y. Chen, N. Reinmuth, K. Hotta, D. Trukhin, G. Statsenko, M.J. Hochmair, M. Özgüroğlu, J.H. Ji, O. Voitko, A. Poltoratskiy, S. Ponce, F. Verderame, L. Havel, I. Bondarenko, A. Kazarnowicz, G. Losonczy, N. V. Conev, J. Armstrong, N. Byrne, N. Shire, H. Jiang, J.W. Goldman, E. Batagelj, I. Casarini, A.V. Pastor, S.N. Sena, J.J. Zarba, O. Burghuber, S. Hartl, B. Lamprecht, M. Studnicka, L. Alberto Schlittler, F. Augusto Martinelli de Oliveira, A. Calabrich, G. Colagiovanni Girotto, P. Dos Reis, C. Fausto Nino Gorini, P. Rafael Martins De Marchi, C. Serodio da Rocha Baldotto, C. Sette, M. Zukin, A. Dudov, R. Ilieva, K. Koynov, R. Krasteva, I. Tonev, S. Valev, V. Venkova, M. Bi, C. Chen, Y. Chen, Z. Chen, J. Fang, J. Feng, Z. Han, J. Hu, Y. Hu, W. Li, Z. Liang, Z. Lin, R. Ma, S. Ma, K. Nan, Y. Shu, K. Wang, M. Wang, G. Wu, N. Yang, Z. Yang, H. Zhang, W. Zhang, J. Zhao, Y. Zhao, C. Zhou, J. Zhou, X. Zhou, V. Kolek, L. Koubkova, J. Roubec, J. Skrickova, M. Zemanova, C. Chouaid, W. Hilgers, H. Lena, D. Moro-Sibilot, G. Robinet, P.J. Souquet, J. Alt, H. Bischoff, C. Grohe, E. Laack, S. Lang, J. Panse, C. Schulz, K. Bogos, E. Csánky, A. Fülöp, Z. Horváth, J. Kósa, I. Laczó, G. Pajkos, Z. Pápai, Z. Pápai Székely, V. Sárosi, A. Somfay, É. Somogyiné Ezer, A. Telekes, J. Bar, M. Gottfried, N. I. Heching, A. Zer Kuch, R. Bartolucci, A.C. Bettini, A. Delmonte, M.C. Garassino, M. Minelli, F. Roila, S. Atagi, K. Azuma, H. Goto, K. Goto, Y. Hara, H. Hayashi, T. Hida, K. Kanazawa, S. Kanda, Y.H. Kim, S. Kuyama, T. Maeda, M. Morise, Y. Nakahara, M. Nishio, N. Nogami, I. Okamoto, H. Saito, M. Shinoda, S. Umemura, T. Yoshida, N. Claessens, R. Cornelissen, L. Heniks, J. Hiltermann, E. Smit, A. Staal van den Brekel, D. Kowalski, S. Mańdziuk, R. Mróz, M. Wojtukiewicz, T. Ciuleanu, D. Ganea, A. Ungureanu, A. Luft, V. Moiseenko, D. Sakaeva, A. Smolin, A. Vasilyev, L. Vladimirova, I. Anasina, J. Chovanec, P. Demo, R. Godal, P. Kasan, M. Stresko, M. Urda, E.K. Cho, J.H. Kim, S.W. Kim, G.W. Lee, J.S. Lee, K.H. Lee, K.H. Lee, Y.G. Lee, M. Amelia Insa Molla, M. Domine Gomez, J. Ignacio Delgado Mingorance, D. Isla Casado, M. Lopez Brea, M. Majem Tarruella, T. Morán Bueno, A. Navarro Mendivil, L. Paz-Ares Rodríguez, S. Ponce Aix, M. Rosario Garcia Campelo, G.C. Chang, Y.H. Chen, C.H. Chiu, T. C. Hsia, K.Y. Lee, C. Te Li, C.C. Wang, Y.F. Wei, S.Y. Wu, A. Alacacıoğlu, I. Çiçin, A. Demirkazik, M. Erman, T. Göksel, H. Adamchuk, O. Kolesnik, A. Kryzhanivska, Y. Ostapenko, S. Shevnia, Y. Shparyk, G. Ursol, N. Voitko, I. Vynnychenko, S. Babu, A. Chiang, W. Chua, S. Dakhil, A. Dowlati, B. Haque, R. Jamil, J. Knoble, S. Lakhanpal, K. Mi, P. Nikolinakos, S. Powell, H. Ross, E. Schaefer, J. Schneider, J. Spahr, D. Spigel, J. Stilwill, C. Sumey, M. Williamson, Durvalumab plus platinum–etoposide versus platinum–etoposide in first-line treatment of extensive-stage small-cell lung cancer (CASPIAN): a randomised, controlled, open-label, phase 3 trial, Lancet (2019), https://doi.org/10.1016/S0140-6736(19)32222-6.

[248] M.D. Hellmann, L. Paz-Ares, R. Bernabe Caro, B. Zurawski, S.-W. Kim, E. Carcereny Costa, K. Park, A. Alexandru, L. Lupinacci, E. de la Mora Jimenez, H. Sakai, I. Albert, A. Vergnenegre, S. Peters, K. Syrigos, F. Barlesi, M. Reck, H. Borghaei, J.R. Brahmer, K.J. O'Byrne, W.J. Geese, P. Bhagavatheeswaran, S. K. Rabindran, R.S. Kasinathan, F.E. Nathan, S.S. Ramalingam, Nivolumab plus ipilimumab in advanced non–small-cell lung cancer, N. Engl. J. Med. (2019), https://doi.org/10.1056/nejmoa1910231.

[249] T. Yau, Y.K. Kang, T.Y. Kim, A.B. El-Khoueiry, A. Santoro, B. Sangro, I. Melero, M. Kudo, M.M. Hou, A. Matilla, F. Tovoli, J.J. Knox, A. Ruth He, B.F. El-Rayes, M. Acosta-Rivera, H.Y. Lim, J. Neely, Y. Shen, T. Wisniewski, J. Anderson, C. Hsu, Efficacy and safety of nivolumab plus ipilimumab in patients with advanced hepatocellular carcinoma previously treated with sorafenib: the CheckMate 040 randomized clinical trial, JAMA Oncol (2020), https://doi.org/10.1001/jamaoncol.2020.4564.

[250] A. Scherpereel, J. Mazieres, L. Greillier, S. Lantuejoul, P. Dô, O. Bylicki, I. Monnet, R. Corre, C. Audigier-Valette, M. Locatelli-Sanchez, O. Molinier, F. Guisier, T. Urban, C. Ligeza-Poisson, D. Planchard, E. Amour, F. Morin, D. Moro-Sibilot, G. Zalcman, D. Debieuvre, S. Hiret, J. Cadranel, S. Fraboulet-Moreau, D. Carmier, Nivolumab or nivolumab plus ipilimumab in patients with relapsed malignant pleural mesothelioma (IFCT-1501 MAPS2): a multicentre, open-label, randomised, non-comparative, phase 2 trial, Lancet Oncol. (2019), https://doi.org/10.1016/S1470-2045(18)30765-4.

[251] T.M. Yu, C. Morrison, E.J. Gold, A. Tradonsky, A.J. Layton, Multiple biomarker testing tissue consumption and completion rates with single-gene tests and investigational use of oncomine Dx target test for advanced non–small-cell lung cancer: a single-center analysis, Clin. Lung Cancer. (2019), https://doi.org/10.1016/j.cllc.2018.08.010.

[252] F. Chen, Z. Zhang, Y. Yu, Q. Liu, F. Pu, HSulf-1 and palbociclib exert synergistic antitumor effects on RB-positive triple-negative breast cancer, Int. J. Oncol. (2020), https://doi.org/10.3892/ijo.2020.5057.

[253] R.B. Mokhtari, T.S. Homayouni, N. Baluch, E. Morgatskaya, S. Kumar, B. Das, H. Yeger, Combination therapy in combating cancer, Oncotarget (2017), https://doi.org/10.18632/oncotarget.16723.

[254] US Food and Drug Administration, FDA Approves Encorafenib in Combination with Cetuximab for Metastatic Colorectal Cancer with a BRAF V600E Mutation, FDA, 2020. https://www.fda.gov/drugs/resources-information-approved-drugs/fda-approves-encorafenib-combination-cetuximab-metastatic-colorectal-cancer-braf-v600e-mutation. (Accessed 4 September 2020).

[255] US Food and Drug Administration, FDA Approves Neratinib for Metastatic HER2-Positive Breast Cancer, FDA, 2021. https://www.fda.gov/drugs/resources-information-approved-drugs/fda-approves-neratinib-metastatic-her2-positive-breast-cancer. (Accessed 1 February 2021).

[256] I. Ray-Coquard, P. Pautier, S. Pignata, D. Pérol, A. González-Martín, R. Berger, K. Fujiwara, I. Vergote, N. Colombo, J. Mäenpää, F. Selle, J. Sehouli, D. Lorusso, E.M. Guerra Alía, A. Reinthaller, S. Nagao, C. Lefeuvre-Plesse, U. Canzler, G. Scambia, A. Lortholary, F. Marmé, P. Combe, N. de Gregorio, M. Rodrigues, P. Buderath, C. Dubot, A. Burges, B. You, E. Pujade-Lauraine, P. Harter, Olaparib plus bevacizumab as first-line maintenance in ovarian cancer, N. Engl. J. Med. (2019), https://doi.org/10.1056/nejmoa1911361.

[257] Eagle Pharmaceuticals, Inc, Eagle Pharmaceuticals Receives Final FDA Approval for PEMFEXY™ (Pemetrexed for Injection). https://investor.eagleus.com/press-releases/news-details/2020/Eagle-Pharmaceuticals-Receives-Final-FDA-Approval-for-PEMFEXY-Pemetrexed-for-Injection/default.aspx, 2020. (Accessed 10 February 2020).

[258] B.I. Rini, E.R. Plimack, V. Stus, R. Gafanov, R. Hawkins, D. Nosov, F. Pouliot, B. Alekseev, D. Soulières, B. Melichar, I. Vynnychenko, A. Kryzhanivska, I. Bondarenko, S.J. Azevedo, D. Borchiellini, C. Szczylik, M. Markus, R. S. McDermott, J. Bedke, S. Tartas, Y.-H. Chang, S. Tamada, Q. Shou, R.F. Perini, M. Chen, M.B. Atkins, T. Powles, Pembrolizumab plus Axitinib versus sunitinib for advanced renal-cell carcinoma, N. Engl. J. Med. (2019), https://doi.org/10.1056/nejmoa1816714.

[259] V. Makker, D. Rasco, N.J. Vogelzang, M.S. Brose, A.L. Cohn, J. Mier, C. Di Simone, D.M. Hyman, D.E. Stepan, C.E. Dutcus, E.V. Schmidt, M. Guo, P. Sachdev, R. Shumaker, C. Aghajanian, M. Taylor, Lenvatinib plus pembrolizumab in patients with advanced endometrial cancer: an interim analysis of a multicentre, open-label, single-arm, phase 2 trial, Lancet Oncol. (2019), https://doi.org/10.1016/S1470-2045(19)30020-8.

[260] R.J. Motzer, K. Penkov, J. Haanen, B. Rini, L. Albiges, M.T. Campbell, B. Venugopal, C. Kollmannsberger, S. Negrier, M. Uemura, J.L. Lee, A. Vasiliev, W.H. Miller, H. Gurney, M. Schmidinger, J. Larkin, M.B. Atkins, J. Bedke, B. Alekseev, J. Wang, M. Mariani, P.B. Robbins, A. Chudnovsky, C. Fowst, S. Hariharan, B. Huang, A. di Pietro, T.K. Choueiri, Avelumab plus Axitinib versus Sunitinib for Advanced Renal-Cell Carcinoma, N. Engl. J. Med. (2019), https://doi.org/10.1056/nejmoa1816047.

[261] US Food and Drug Administration, FDA Approves Polatuzumab Vedotin-piiq for Diffuse Large B-Cell Lymphoma, FDA, 2019. https://www.fda.gov/drugs/resources-information-approved-drugs/fda-approves-polatuzumab-vedotin-piiq-diffuse-large-b-cell-lymphoma. (Accessed 1 February 2019).

[262] H. West, M. McCleod, M. Hussein, A. Morabito, A. Rittmeyer, H.J. Conter, H. G. Kopp, D. Daniel, S. McCune, T. Mekhail, A. Zer, N. Reinmuth, A. Sadiq, A. Sandler, W. Lin, T. Ochi Lohmann, V. Archer, L. Wang, M. Kowanetz, F. Cappuzzo, Atezolizumab in combination with carboplatin plus nab-paclitaxel chemotherapy compared with chemotherapy alone as first-line treatment for metastatic non-squamous non-small-cell lung cancer (IMpower130): a multicentre, randomised, open-label, phase 3 tria, Lancet Oncol. (2019), https://doi.org/10.1016/S1470-2045(19)30167-6.

[263] U.S. Food, Drug Administration, FDA Approves Atezolizumab with Nab-Paclitaxel and Carboplatin for Metastatic NSCLC Without EGFR/ALK Aberrations, FDA, 2021. https://www.fda.gov/drugs/resources-information-approved-drugs/fda-approves-atezolizumab-nab-paclitaxel-and-carboplatin-metastatic-nsclc-without-egfralk. (Accessed 12 May 2019).

[264] A.S. Mansfield, A. Każarnowicz, N. Karaseva, A. Sánchez, R. De Boer, Z. Andric, M. Reck, S. Atagi, J.S. Lee, M. Garassino, S.V. Liu, L. Horn, X. Wen, C. Quach, W. Yu, F. Kabbinavar, S. Lam, S. Morris, R. Califano, Safety and patient-reported outcomes of atezolizumab, carboplatin, and etoposide in extensive-stage small-cell lung cancer (IMpower133): a randomized phase I/III trial, Ann. Oncol. (2020), https://doi.org/10.1016/j.annonc.2019.10.021.

[265] S. Kopetz, A. Grothey, R. Yaeger, E. Van Cutsem, J. Desai, T. Yoshino, H. Wasan, F. Ciardiello, F. Loupakis, Y.S. Hong, N. Steeghs, T.K. Guren, H.-T. Arkenau, P. Garcia-Alfonso, P. Pfeiffer, S. Orlov, S. Lonardi, E. Elez, T.-W. Kim, J.H. M. Schellens, C. Guo, A. Krishnan, J. Dekervel, V. Morris, A. Calvo Ferrandiz, L. S. Tarpgaard, M. Braun, A. Gollerkeri, C. Keir, K. Maharry, M. Pickard, J. Christy-Bittel, L. Anderson, V. Sandor, J. Tabernero, Encorafenib, Binimetinib, and Cetuximab in BRAF V600E–mutated colorectal cancer, N. Engl. J. Med. (2019), https://doi.org/10.1056/nejmoa1908075.

[266] P. Schmid, S. Adams, H.S. Rugo, A. Schneeweiss, C.H. Barrios, H. Iwata, V. Diéras, R. Hegg, S.-A. Im, G. Shaw Wright, V. Henschel, L. Molinero, S.Y. Chui, R. Funke, A. Husain, E.P. Winer, S. Loi, L.A. Emens, Atezolizumab and nab-paclitaxel in advanced triple-negative breast cancer, N. Engl. J. Med. (2018), https://doi.org/10.1056/nejmoa1809615.

[267] L. Gandhi, D. Rodríguez-Abreu, S. Gadgeel, E. Esteban, E. Felip, F. De Angelis, M. Domine, P. Clingan, M.J. Hochmair, S.F. Powell, S.Y.-S. Cheng, H.G. Bischoff, N. Peled, F. Grossi, R.R. Jennens, M. Reck, R. Hui, E.B. Garon, M. Boyer, B. Rubio-Viqueira, S. Novello, T. Kurata, J.E. Gray, J. Vida, Z. Wei, J. Yang, H. Raftopoulos, M.C. Pietanza, M.C. Garassino, Pembrolizumab plus chemotherapy in metastatic non–small-cell lung cancer, N. Engl. J. Med. (2018), https://doi.org/10.1056/nejmoa1801005.

[268] US Food and Drug Administration, FDA Grants Regular Approval for Pembrolizumab in Combination with Chemotherapy for First-Line Treatment of Metastatic Nonsquamous NSCLC, FDA, 2021. https://www.fda.gov/drugs/resources-information-approved-drugs/fda-grants-regular-approval-pembrolizumab-combination-chemotherapy-first-line-treatment-metastatic. (Accessed 20 August 2018).

[269] US Food and Drug Administration, FDA Approves Atezolizumab with Chemotherapy and Bevacizumab for First-Line Treatment of Metastatic Non-Squamous NSCLC, FDA, 2021. https://www.fda.gov/drugs/fda-approves-atezolizumab-chemotherapy-and-bevacizumab-first-line-treatment-metastatic-non-squamous. (Accessed 12 July 2018).

[270] US Food and Drug Administration, FDA Approves Bevacizumab in Combination with Chemotherapy for Ovarian Cancer, FDA, 2021. https://www.fda.gov/drugs/resources-information-approved-drugs/fda-approves-bevacizumab-combination-chemotherapy-ovarian-cancer. (Accessed 13 June 2018).

[271] Drugs.com, FDA Approves Imbruvica (ibrutinib) Plus Rituximab for Patients with Waldenström's Macroglobulinemia. https://www.drugs.com/newdrugs/fda-approves-imbruvica-ibrutinib-plus-rituximab-patients-waldenstr-m-s-macroglobulinemia-4812.html, 2021. (Accessed 14 September 2018).
[272] US Food and Drug Administration, FDA Approves Nivolumab Plus Ipilimumab Combination for Intermediate or Poor-Risk Advanced Renal Cell Carcinoma, FDA, 2021. https://www.fda.gov/drugs/resources-information-approved-drugs/fda-approves-nivolumab-plus-ipilimumab-combination-intermediate-or-poor-risk-advanced-renal-cell. (Accessed 16 April 2018).
[273] M.J. Overman, S. Lonardi, K.Y.M. Wong, H.J. Lenz, F. Gelsomino, M. Aglietta, M. A. Morse, E. Van Cutsem, R. McDermott, A. Hill, M.B. Sawyer, A. Hendlisz, B. Neyns, M. Svrcek, R.A. Moss, J.M. Ledeine, Z.A. Cao, S. Kamble, S. Kopetz, T. André, Durable clinical benefit with nivolumab plus ipilimumab in DNA mismatch repair-deficient/microsatellite instability-high metastatic colorectal cancer, J. Clin. Oncol. (2018), https://doi.org/10.1200/JCO.2017.76.9901.
[274] A. Chari, A. Suvannasankha, J.W. Fay, B. Arnulf, J.L. Kaufman, J. J. Ifthikharuddin, B.M. Weiss, A. Krishnan, S. Lentzsch, R. Comenzo, J. Wang, K. Nottage, C. Chiu, N.Z. Khokhar, T. Ahmadi, S. Lonial, Daratumumab plus pomalidomide and dexamethasone in relapsed and/or refractory multiple myeloma, Blood (2017), https://doi.org/10.1182/blood-2017-05-785246.
[275] A.C. Krauss, X. Gao, L. Li, M.L. Manning, P. Patel, W. Fu, K.G. Janoria, G. Gieser, D.A. Bateman, D. Przepiorka, Y.L. Shen, S.S. Shord, C.M. Sheth, A. Banerjee, J. Liu, K.B. Goldberg, A.T. Farrell, G.M. Blumenthal, R. Pazdur, FDA approval summary: (daunorubicin and cytarabine) liposome for injection for the treatment of adults with high-risk acute myeloid leukemia, Clin. Cancer Res. (2019), https://doi.org/10.1158/1078-0432.CCR-18-2990.
[276] T. Robak, K. Warzocha, K. Govind Babu, Y. Kulyaba, K. Kuliczkowski, K. Abdulkadyrov, J. Loscertales, I. Kryachok, J. Kłoczko, G. Rekhtman, W. Homenda, J.Z. Błoński, A. McKeown, M.M. Gorczyca, J.L. Carey, C.N. Chang, S. Lisby, I.V. Gupta, S. Grosicki, Ofatumumab plus fludarabine and cyclophosphamide in relapsed chronic lymphocytic leukemia: results from the COMPLEMENT 2 trial, Leuk. Lymphoma 58 (5) (2017) 1084–1093, https://doi.org/10.1080/10428194.2016.1233536.
[277] FDA approves Tafinlar+Mekinist combo for Melanoma, Oncol. Times (2016), https://doi.org/10.1097/01.cot.0000480920.25709.4e.
[278] Opdivo-Yervoy combination approved for Melanoma—first combination-immunotherapy regimen for cancer, Oncol. Times (2015), https://doi.org/10.1097/01.cot.0000473604.35674.ee.
[279] Portrazza (Necitumumab), an IgG1 Monoclonal Antibody, FDA Approved for Advanced Squamous Non–Small-Cell Lung Cancer. http://www.ahdbonline.com/articles/2115-portrazza-necitumumab-an-igg1-monoclonal-antibody-fda-approved-for-advanced-squamous-non-small-cell-lung-cancer, 2021. (Accessed 1 February 2021).
[280] M.W. Saif, U.S. food and drug administration approves paclitaxel protein-bound particles (Abraxane®) in combination with gemcitabine as first-line treatment of patients with metastatic pancreatic cancer, J. Pancreas (2013), https://doi.org/10.6092/1590-8577/2028.
[281] M.H. Cohen, J.R. Johnson, R. Pazdur, Food and drug administration drug approval summary: Temozolomide plus radiation therapy for the treatment of newly diagnosed glioblastoma multiforme, Clin. Cancer Res. (2005), https://doi.org/10.1158/1078-0432.CCR-05-0722.
[282] G. Pillai, Nanomedicines for cancer therapy: an update of FDA approved and those under various stages of development, SOJ Pharm. Pharm. Sci (2014), https://doi.org/10.15226/2374-6866/1/2/00109.
[283] E. Allen, A. Jabouille, L.B. Rivera, I. Lodewijckx, R. Missiaen, V. Steri, K. Feyen, J. Tawney, D. Hanahan, I.P. Michael, G. Bergers, Combined antiangiogenic and anti-PD-L1 therapy stimulates tumor immunity through HEV formation, Sci. Transl. Med. (2017), https://doi.org/10.1126/scitranslmed.aak9679.
[284] M.A. Gubens, L.V. Sequist, J.P. Stevenson, S.F. Powell, L.C. Villaruz, S. M. Gadgeel, C.J. Langer, A. Patnaik, H. Borghaei, S.I. Jalal, J. Fiore, S. Saraf, H. Raftopoulos, L. Gandhi, Pembrolizumab in combination with ipilimumab as second-line or later therapy for advanced non–small-cell lung cancer: KEYNOTE-021 cohorts D and H, Lung Cancer 130 (2019) 59–66, https://doi.org/10.1016/j.lungcan.2018.12.015.
[285] S.M. Gadgeel, J. Stevenson, C.J. Langer, L. Gandhi, H. Borghaei, A. Patnaik, L. C. Villaruz, M.A. Gubens, R.J. Hauke, J.C.-H. Yang, L.V. Sequist, R.D. Bachman, J. Y. Ge, H. Raftopoulos, V. Papadimitrakopoulou, Pembrolizumab (pembro) plus chemotherapy as front-line therapy for advanced NSCLC: KEYNOTE-021 cohorts A-C, J. Clin. Oncol. 34 (2016) 9016, https://doi.org/10.1200/jco.2016.34.15_suppl.9016.
[286] M. Björnmalm, K.J. Thurecht, M. Michael, A.M. Scott, F. Caruso, Bridging Bio-nano science and cancer nanomedicine, ACS Nano (2017), https://doi.org/10.1021/acsnano.7b04855.
[287] R.T. Netea-Maier, J.W.A. Smit, M.G. Netea, Metabolic changes in tumor cells and tumor-associated macrophages: a mutual relationship, Cancer Lett. (2018), https://doi.org/10.1016/j.canlet.2017.10.037.
[288] N. Willumsen, L.B. Thomsen, C.L. Bager, C. Jensen, M.A. Karsdal, Quantification of altered tissue turnover in a liquid biopsy: a proposed precision medicine tool to assess chronic inflammation and desmoplasia associated with a pro-cancerous niche and response to immuno-therapeutic anti-tumor modalities, Cancer Immunol. Immunother. (2018), https://doi.org/10.1007/s00262-017-2074-z.
[289] J. Fucikova, O. Kepp, L. Kasikova, G. Petroni, T. Yamazaki, P. Liu, L. Zhao, R. Spisek, G. Kroemer, L. Galluzzi, Detection of immunogenic cell death and its relevance for cancer therapy, Cell Death Dis. (2020), https://doi.org/10.1038/s41419-020-03221-2.
[290] A. Sistigu, T. Yamazaki, E. Vacchelli, K. Chaba, D.P. Enot, J. Adam, I. Vitale, A. Goubar, E.E. Baracco, C. Remédios, L. Fend, D. Hannani, L. Aymeric, Y. Ma, M. Niso-Santano, O. Kepp, J.L. Schultze, T. Tüting, F. Belardelli, L. Bracci, V. La Sorsa, G. Ziccheddu, P. Sestili, F. Urbani, M. Delorenzi, M. Lacroix-Triki, V. Quidville, R. Conforti, J.P. Spano, L. Pusztai, V. Poirier-Colame, S. Delaloge, F. Penault-Llorca, S. Ladoire, L. Arnould, J. Cyrta, M.C. Dessoliers, A. Eggermont, M.E. Bianchi, M. Pittet, C. Engblom, C. Pfirschke, X. Préville, G. Uzè, R. D. Schreiber, M.T. Chow, M.J. Smyth, E. Proietti, F. André, G. Kroemer, L. Zitvogel, Cancer cell–autonomous contribution of type I interferon signaling to the efficacy of chemotherapy, Nat. Med. (2014), https://doi.org/10.1038/nm.3708.
[291] J. Wu, D.J. Waxman, Immunogenic chemotherapy: Dose and schedule dependence and combination with immunotherapy, Cancer Lett. (2018), https://doi.org/10.1016/j.canlet.2018.01.050.
[292] L. Zitvogel, L. Galluzzi, M.J. Smyth, G. Kroemer, Mechanism of action of conventional and targeted anticancer therapies: reinstating immunosurveillance, Immunity. 39 (2013) 74–88, https://doi.org/10.1016/j.immuni.2013.06.014.
[293] E. Iessi, M. Logozzi, D. Mizzoni, R. Di Raimo, C.T. Supuran, S. Fais, Rethinking the combination of proton exchanger inhibitors in cancer therapy, Metabolites (2018), https://doi.org/10.3390/metabo8010002.
[294] A. Pujada, L. Walter, A. Patel, T.A. Bui, Z. Zhang, Y. Zhang, T.L. Denning, P. Garg, Matrix metalloproteinase MMP9 maintains epithelial barrier function and preserves mucosal lining in colitis associated cancer, Oncotarget (2017), https://doi.org/10.18632/oncotarget.21841.
[295] L. Hui, Y. Chen, Tumor microenvironment: Sanctuary of the devil, Cancer Lett. 368 (2015) 7–13, https://doi.org/10.1016/j.canlet.2015.07.039.
[296] Q.S.C. Chu, B. Forouzesh, S. Syed, M. Mita, G. Schwartz, J. Copper, J. Curtright, E. K. Rowinsky, A phase II and pharmacological study of the matrix metalloproteinase inhibitor (MMPI) COL-3 in patients with advanced soft tissue sarcomas, Investig. New Drugs (2007), https://doi.org/10.1007/s10637-006-9031-6.
[297] Y. Gu, M. Lee, J. Roemer, L. Musacchia, M. Golub, R. Simon, Inhibition of tumor cell invasiveness by chemically modified tetracyclines, Curr. Med. Chem. (2012), https://doi.org/10.2174/0929867013373642.
[298] W.R. Wilson, M.P. Hay, Targeting hypoxia in cancer therapy, Nat. Rev. Cancer (2011), https://doi.org/10.1038/nrc3064.
[299] T. Yu, B. Tang, X. Sun, Development of inhibitors targeting hypoxia-inducible factor 1 and 2 for cancer therapy, Yonsei Med. J. (2017), https://doi.org/10.3349/ymj.2017.58.3.489.
[300] A.G. Duffy, G. Melillo, B. Turkbey, D. Allen, P.L. Choyke, C. Chen, M. Raffeld, J. H. Doroshow, A. Murgo, S. Kummar, A pilot trial of oral topotecan (TPT) in patients with refractory advanced solid neoplasms expressing HIF-1α, Journal of Clinical Oncology 28 (15) (2010) e13518.
[301] T.J. Lynch, I. Bondarenko, A. Luft, P. Serwatowski, F. Barlesi, R. Chacko, M. Sebastian, J. Neal, H. Lu, J.M. Cuillerot, M. Reck, Ipilimumab in combination with paclitaxel and carboplatin as first-line treatment in stage IIIB/IV non-small-cell lung cancer: results from a randomized, double-blind, multicenter phase II study, J. Clin. Oncol. (2012), https://doi.org/10.1200/JCO.2011.38.4032.
[302] A.S. Cheung, D.J. Mooney, Engineered materials for cancer immunotherapy, Nano Today (2015), https://doi.org/10.1016/j.nantod.2015.06.007.
[303] I. Mellman, G. Coukos, G. Dranoff, Cancer immunotherapy comes of age, Nature (2011), https://doi.org/10.1038/nature10673.
[304] I. Melero, S. Hervas-Stubbs, M. Glennie, D.M. Pardoll, L. Chen, Immunostimulatory monoclonal antibodies for cancer therapy, Nat. Rev. Cancer (2007), https://doi.org/10.1038/nrc2051.
[305] S. Lee, K. Margolin, Cytokines in cancer immunotherapy, Cancers (Basel) (2011), https://doi.org/10.3390/cancers3043856.
[306] J.W. Griffith, C.L. Sokol, A.D. Luster, Chemokines and chemokine receptors: positioning cells for host defense and immunity, Annu. Rev. Immunol. (2014), https://doi.org/10.1146/annurev-immunol-032713-120145.
[307] S.L. Topalian, F.S. Hodi, J.R. Brahmer, S.N. Gettinger, D.C. Smith, D. F. McDermott, J.D. Powderly, R.D. Carvajal, J.A. Sosman, M.B. Atkins, P. D. Leming, D.R. Spigel, S.J. Antonia, L. Horn, C.G. Drake, D.M. Pardoll, L. Chen, W.H. Sharfman, R.A. Anders, J.M. Taube, T.L. McMiller, H. Xu, A.J. Korman, M. Jure-Kunkel, S. Agrawal, D. McDonald, G.D. Kollia, A. Gupta, J.M. Wigginton, M. Sznol, Safety, activity, and immune correlates of anti–PD-1 antibody in cancer, N. Engl. J. Med. (2012), https://doi.org/10.1056/nejmoa1200690.
[308] J.R. Brahmer, S.S. Tykodi, L.Q.M. Chow, W.J. Hwu, S.L. Topalian, P. Hwu, C. G. Drake, L.H. Camacho, J. Kauh, K. Odunsi, H.C. Pitot, O. Hamid, S. Bhatia, R. Martins, K. Eaton, S. Chen, T.M. Salay, S. Alaparthy, J.F. Grosso, A.J. Korman, S.M. Parker, S. Agrawal, S.M. Goldberg, D.M. Pardoll, A. Gupta, J.M. Wigginton, Safety and activity of anti-PD-L1 antibody in patients with advanced cancer, N. Engl. J. Med. (2012), https://doi.org/10.1056/NEJMoa1200694.
[309] M. Ai, M.A. Curran, Immune checkpoint combinations from mouse to man, Cancer Immunol. Immunother. (2015), https://doi.org/10.1007/s00262-014-1650-8.
[310] J.R. Brahmer, C.G. Drake, I. Wollner, J.D. Powderly, J. Picus, W.H. Sharfman, E. Stankevich, A. Pons, T.M. Salay, T.L. McMiller, M.M. Gilson, C. Wang, M. Selby, J.M. Taube, R. Anders, L. Chen, A.J. Korman, D.M. Pardoll, I. Lowy, S. L. Topalian, Phase I study of single-agent anti-programmed death-1 (MDX-1106) in refractory solid tumors: Safety, clinical activity, pharmacodynamics, and immunologic correlates, J. Clin. Oncol. (2010), https://doi.org/10.1200/JCO.2009.26.7609.
[311] J.D. Wolchok, H. Kluger, M.K. Callahan, M.A. Postow, N.A. Rizvi, A.M. Lesokhin, N.H. Segal, C.E. Ariyan, R.-A. Gordon, K. Reed, M.M. Burke, A. Caldwell, S. A. Kronenberg, B.U. Agunwamba, X. Zhang, I. Lowy, H.D. Inzunza, W. Feely, C.

E. Horak, Q. Hong, A.J. Korman, J.M. Wigginton, A. Gupta, M. Sznol, Nivolumab plus Ipilimumab in Advanced Melanoma, N. Engl. J. Med. (2013), https://doi.org/10.1056/nejmoa1302369.
[312] H.J. Hammers, E.R. Plimack, J.R. Infante, M.S. Ernstoff, B.I. Rini, D. F. McDermott, A.R.A. Razak, S.K. Pal, M.H. Voss, P. Sharma, C. K. Kollmannsberger, D.Y.C. Heng, J.L. Spratlin, Y. Shen, J.F. Kurland, P. Gagnier, A. Amin, Phase I study of nivolumab in combination with ipilimumab in metastatic renal cell carcinoma (mRCC), J. Clin. Oncol. (2014), https://doi.org/10.1200/jco.2014.32.15_suppl.4504.
[313] M.A. Postow, J. Chesney, A.C. Pavlick, C. Robert, K. Grossmann, D. McDermott, G.P. Linette, N. Meyer, J.K. Giguere, S.S. Agarwala, M. Shaheen, M.S. Ernstoff, D. Minor, A.K. Salama, M. Taylor, P.A. Ott, L.M. Rollin, C. Horak, P. Gagnier, J. D. Wolchok, F.S. Hodi, Nivolumab and Ipilimumab versus Ipilimumab in Untreated Melanoma, N. Engl. J. Med. (2015), https://doi.org/10.1056/nejmoa1414428.
[314] Y. Wolf, A.C. Anderson, V.K. Kuchroo, TIM3 comes of age as an inhibitory receptor, Nat. Rev. Immunol. (2020), https://doi.org/10.1038/s41577-019-0224-6.
[315] S.F. Ngiow, B. Von Scheidt, H. Akiba, H. Yagita, M.W.L. Teng, M.J. Smyth, Anti-TIM3 antibody promotes T cell IFN-γ-mediated antitumor immunity and suppresses established tumors, Cancer Res. (2011), https://doi.org/10.1158/0008-5472.CAN-11-0096.
[316] L.M. Weiner, R. Surana, S. Wang, Monoclonal antibodies: versatile platforms for cancer immunotherapy, Nat. Rev. Immunol. (2010), https://doi.org/10.1038/nri2744.
[317] M. Shibuya, Vascular endothelial growth factor (VEGF) and its receptor (VEGFR) signaling in angiogenesis: a crucial target for anti- and pro-angiogenic therapies, Genes Cancer (2011), https://doi.org/10.1177/1947601911423031.
[318] A. Forero-Torres, J. Shah, T. Wood, J. Posey, R. Carlisle, C. Copigneaux, F. Luo, S. Wojtowicz-Praga, I. Percent, M. Saleh, Phase I trial of weekly tigatuzumab, an agonistic humanized monoclonal antibody targeting death receptor 5 (DR5), Cancer Biother. Radiopharm. (2010), https://doi.org/10.1089/cbr.2009.0673.
[319] T.A. Yap, H.A. Burris, S. Kummar, G.S. Falchook, R.K. Pachynski, P. LoRusso, S. S. Tykodi, G.T. Gibney, J.F. Gainor, O.E. Rahma, T.Y. Seiwert, F. Meric-Bernstam, M.A. Blum Murphy, J.K. Litton, E.M.D. Hooper, H.A. Hirsch, C. Harvey, M. Clancy, T. McClure, M.K. Callahan, ICONIC: Biologic and clinical activity of first in class ICOS agonist antibody JTX-2011 +/- nivolumab (nivo) in patients (pts) with advanced cancers, J. Clin. Oncol. (2018), https://doi.org/10.1200/jco.2018.36.15_suppl.3000.
[320] D.A. Schaer, D. Hirschhorn-Cymerman, J.D. Wolchok, Targeting tumor-necrosis factor receptor pathways for tumor immunotherapy, J. Immunother, Cancer, 2014, https://doi.org/10.1186/2051-1426-2-7.
[321] D. Hirschhorn-Cymerman, G.A. Rizzuto, T. Merghoub, A.D. Cohen, F. Avogadri, A.M. Lesokhin, A.D. Weinberg, J.D. Wolchok, A.N. Houghton, OX40 engagement and chemotherapy combination provides potent antitumor immunity with concomitant regulatory T cell apoptosis, J. Exp. Med. (2009), https://doi.org/10.1084/jem.20082205.
[322] K.J. Harrington, I. Puzanov, J.R. Hecht, F.S. Hodi, Z. Szabo, S. Murugappan, H. L. Kaufman, Clinical development of talimogene laherparepvec (T-VEC): a modified herpes simplex virus type-1-derived oncolytic immunotherapy, Expert. Rev. Anticancer. Ther. (2015), https://doi.org/10.1586/14737140.2015.1115725.
[323] T. Ranki, S. Pesonen, A. Hemminki, K. Partanen, K. Kairemo, T. Alanko, J. Lundin, N. Linder, R. Turkki, A. Ristimäki, E. Jäger, J. Karbach, C. Wahle, M. Kankainen, C. Backman, M. von Euler, E. Haavisto, T. Hakonen, R. Heiskanen, M. Jaderberg, J. Juhila, P. Priha, L. Suoranta, L. Vassilev, A. Vuolanto, T. Joensuu, Phase I study with ONCOS-102 for the treatment of solid tumors - an evaluation of clinical response and exploratory analyses of immune markers, J. Immunother. Cancer (2016), https://doi.org/10.1186/s40425-016-0121-5.
[324] M.E. Dudley, J.R. Wunderlich, T.E. Shelton, J. Even, S.A. Rosenberg, Generation of tumor-infiltrating lymphocyte cultures for use in adoptive transfer therapy for melanoma patients, J. Immunother. 26 (2003) 332–342, https://doi.org/10.1097/00002371-200307000-00005.
[325] Y. Ping, C. Liu, Y. Zhang, REVIEW T-Cell Receptor-Engineered T Cells for Cancer Treatment: Current Status and Future Directions 9 (3) (2018) 254–266, https://doi.org/10.1007/s13238-016-0367-1.
[326] S. Feins, W. Kong, E.F. Williams, M.C. Milone, J.A. Fraietta, An introduction to chimeric antigen receptor (CAR) T-cell immunotherapy for human cancer, Am. J. Hematol. 94 (2019) S3–S9, https://doi.org/10.1002/ajh.25418.
[327] S. Oh, J.H. Lee, K. Kwack, S.W. Choi, Natural killer cell therapy: a new treatment paradigm for solid tumors, Cancers (Basel) 11 (2019) 1534, https://doi.org/10.3390/cancers11101534.
[328] M.W. Loretta Fala, Yescarta (Axicabtagene Ciloleucel) Second CAR T-Cell Therapy Approved for Patients with Certain Types of Large B-Cell Lymphoma. http://www.theoncologypharmacist.com/jhop-web-exclusives/fda-approvals-news-updates/17457-yescarta-axicabtagene-ciloleucel-second-car-t-cell-therapy-approved-for-patients-with-certain-types-of-large-b-cell-lymphoma, 2021. (Accessed 5 September 2018).
[329] BREYANZI (lisocabtagene maraleucel), FDA, 2021. https://www.fda.gov/vaccines-blood-biologics/cellular-gene-therapy-products/breyanzi-lisocabtagene-maraleucel. (Accessed 3 April 2021).
[330] M.C. O'Leary, X. Lu, Y. Huang, X. Lin, I. Mahmood, D. Przepiorka, D. Gavin, S. Lee, K. Liu, B. George, W. Bryan, M.R. Theoret, R. Pazdur, FDA approval summary: tisagenlecleucel for treatment of patients with relapsed or refractory b-cell precursor acute lymphoblastic leukemia, Clin. Cancer Res. (2019), https://doi.org/10.1158/1078-0432.CCR-18-2035.
[331] A. Mian, B.T. Hill, Brexucabtagene autoleucel for the treatment of relapsed/refractory mantle cell lymphoma, Expert. Opin. Biol. Ther. (2021), https://doi.org/10.1080/14712598.2021.1889510.
[332] A. Robinson, Idecabtagene Vicleucel (Abecma®), Oncol. Times. 43 (2021) 21, https://doi.org/10.1097/01.COT.0000753336.18581.7d.
[333] E.A. Chong, J.J. Melenhorst, S.F. Lacey, D.E. Ambrose, V. Gonzalez, B.L. Levine, C.H. June, S.J. Schuster, PD-1 blockade modulates chimeric antigen receptor (CAR)-modified T cells: refueling the CAR, Blood. 129 (2017) 1039–1041, https://doi.org/10.1182/blood-2016-09-738245.
[334] L.E. Huye, Y. Nakazawa, M.P. Patel, E. Yvon, J. Sun, B. Savoldo, M.H. Wilson, G. Dotti, C.M. Rooney, Combining mTor inhibitors with rapamycin-resistant T cells: a two-pronged approach to tumor elimination, Mol. Ther. 19 (2011) 2239–2248, https://doi.org/10.1038/mt.2011.179.
[335] A. Rodriguez-Garcia, A. Palazon, E. Noguera-Ortega, D.J. Powell, S. Guedan, CAR-T cells hit the tumor microenvironment: strategies to overcome tumor escape, Front. Immunol. 11 (2020) 1109, https://doi.org/10.3389/fimmu.2020.01109.
[336] G. Xie, H. Dong, Y. Liang, J.D. Ham, R. Rizwan, J. Chen, CAR-NK cells: a promising cellular immunotherapy for cancer, EBioMedicine. 59 (2020) 102975, https://doi.org/10.1016/j.ebiom.2020.102975.
[337] W.E. Barry, J.R. Jackson, G.E. Asuelime, H.W. Wu, J. Sun, Z. Wan, J. Malvar, M. A. Sheard, L. Wang, R.C. Seeger, E.S. Kim, Activated natural killer cells in combination with anti-GD2 antibody dinutuximab improve survival of mice after surgical resection of primary neuroblastoma, Clin. Cancer Res. 25 (2019) 325–333, https://doi.org/10.1158/1078-0432.CCR-18-1317.
[338] Q. Zhang, H. Zhang, J. Ding, H. Liu, H. Li, H. Li, M. Lu, Y. Miao, L. Li, J. Zheng, Combination therapy with EpCAM-CAR-NK-92 cells and regorafenib against human colorectal cancer models, J Immunol Res 2018 (2018), https://doi.org/10.1155/2018/4263520.
[339] F. Hosseinzadeh, J. Verdi, J. Ai, S. Hajighasemlou, I. Seyhoun, F. Parvizpour, F. Hosseinzadeh, A. Iranikhah, S. Shirian, Combinational immune? Cell therapy of natural killer cells and sorafenib for advanced hepatocellular carcinoma: a review, Cancer Cell Int. 18 (2018). doi:10.1186/s12935-018-0624-x.
[340] L. Li, W. Li, C. Wang, X. Yan, Y. Wang, C. Niu, X. Zhang, M. Li, H. Tian, C. Yao, H. Jin, F. Han, D. Xu, W. Han, D. Li, J. Cui, Adoptive transfer of natural killer cells in combination with chemotherapy improves outcomes of patients with locally advanced colon carcinoma, Cytotherapy. 20 (2018) 134–148, https://doi.org/10.1016/j.jcyt.2017.09.009.
[341] G. Li, X. Wu, I.H. Chan, J.B. Trager, Abstract 4235: a combination of CAR-NK and CAR-T cells results in rapid and persistent anti-tumor efficacy while reducing CAR-T cell mediated cytokine release and T-cell proliferation, in: Cancer Res, American Association for Cancer Research (AACR), 2020, p. 4235, https://doi.org/10.1158/1538-7445.am2020-4235.
[342] K.J. Harrington, L.J. Billingham, T.B. Brunner, N.G. Burnet, C.S. Chan, P. Hoskin, R.I. MacKay, T.S. Maughan, J. MacDougall, W.G. McKenna, C.M. Nutting, A. Oliver, R. Plummer, I.J. Stratford, T. Illidge, Guidelines for preclinical and early phase clinical assessment of novel radiosensitisers, Br. J. Cancer (2011), https://doi.org/10.1038/bjc.2011.240.
[343] A. Anusha, S. Kumar, S. Kaushik, A. Jyoti, Cancer immunotherapy, J. Pharm. Sci. Res (2017), https://doi.org/10.18203/issn.2456-3994.intjmolimmunooncol20183227.
[344] E. Héninger, T.E.G. Krueger, J.M. Lang, Augmenting antitumor immune responses with epigenetic modifying agents, Front. Immunol. (2015), https://doi.org/10.3389/fimmu.2015.00029.
[345] J. Šímová, V. Polláková, M. Indrová, R. Mikyšková, J. Bieblová, I. Štěpánek, J. Bubeník, M. Reiniš, Immunotherapy augments the effect of 5-azacytidine on HPV16-associated tumours with different MHC class I-expression status, Br. J. Cancer (2011), https://doi.org/10.1038/bjc.2011.428.
[346] M. Rao, N. Chinnasamy, J.A. Hong, Y. Zhang, M. Zhang, S. Xi, F. Liu, V. E. Marquez, R.A. Morgan, D.S. Schrump, Inhibition of histone lysine methylation enhances cancer-testis antigen expression in lung cancer cells: Implications for adoptive immunotherapy of cancer, Cancer Res. (2011), https://doi.org/10.1158/0008-5472.CAN-10-2442.
[347] A. Iannello, D.H. Raulet, Immune surveillance of unhealthy cells by natural killer cells, Cold Spring Harb. Symp. Quant. Biol. (2013), https://doi.org/10.1101/sqb.2013.78.020255.
[348] A.C. West, M.J. Smyth, R.W. Johnstone, The anticancer effects of HDAC inhibitors require the immune system, Oncoimmunology (2014), https://doi.org/10.4161/onci.27414.
[349] W. Zoul, V. Machelon, A. Coulomb-L'Hermin, J. Borvakz, F. Nome, T. Isaeva, S. Wei, R. Krzysieks, I. Durand-Gasselin, A. Gordon, T. Pustilnik, D.T. Curiel, P. Galanaud, F. Capron, D. Emilie, T.J. Curiel, Stromal-derived factor-1 in human tumors recruits and alters the function of plasmacytoid precursor dendritic cells, Nat. Med. (2001), https://doi.org/10.1038/nm1201-1339.
[350] X.F. Bai, J. Liu, O. Li, P. Zheng, Y. Liu, Antigenic drift as a mechanism for tumor evasion of destruction by cytolytic T lymphocytes, J. Clin. Invest. (2003), https://doi.org/10.1172/JCI17656.
[351] R.T. Prehn, J.M. Main, Immunity to methylcholanthrene-induced sarcomas, J. Natl. Cancer Inst. (1957), https://doi.org/10.1093/jnci/18.6.769.
[352] M. Burnet, Cancer-a biological approach I. The processes of control, Br. Med. J. (1957), https://doi.org/10.1136/bmj.1.5022.779.
[353] O. Stutman, Immunodepression and malignancy, Adv. Cancer Res. (1976), https://doi.org/10.1016/S0065-230X(08)60179-7.
[354] F. Ghiringhelli, C. Ménard, M. Terme, C. Flament, J. Taieb, N. Chaput, P.E. Puig, S. Novault, B. Escudier, E. Vivier, A. Lecesne, C. Robert, J.Y. Blay, J. Bernard, S. Caillat-Zucman, A. Freitas, T. Tursz, O. Wagner-Ballon, C. Capron,

W. Vainchencker, F. Martin, L. Zitvogel, CD4+CD25+ regulatory T cells inhibit natural killer cell functions in a transforming growth factor-β-dependent manner, J. Exp. Med. (2005), https://doi.org/10.1084/jem.20051511.
[355] C.T. Viehl, T.T. Moore, U.K. Liyanage, D.M. Frey, J.P. Ehlers, T.J. Eberlein, P. S. Goedegebuure, D.C. Linehan, Depletion of CD4+CD25+ regulatory T cells promotes a tumor-specific immune response in pancreas cancer-bearing mice, Ann. Surg. Oncol. (2006), https://doi.org/10.1245/s10434-006-9015-y.
[356] M.J. Maeurer, W.J. Storkus, J.M. Kirkwood, M.T. Lotze, New treatment options for patients with melanoma: review of melanoma-derived T-cell epitope-based peptide vaccines, Melanoma Res. (1996), https://doi.org/10.1097/00008390-199602000-00003.
[357] K. Palucka, J. Banchereau, Cancer immunotherapy via dendritic cells, Nat. Rev. Cancer (2012), https://doi.org/10.1038/nrc3258.
[358] A. Albini, M.B. Sporn, The tumour microenvironment as a target for chemoprevention, Nat. Rev. Cancer (2007), https://doi.org/10.1038/nrc2067.
[359] M. Kanapathipillai, A. Brock, D.E. Ingber, Nanoparticle targeting of anti-cancer drugs that alter intracellular signaling or influence the tumor microenvironment, Adv. Drug Deliv. Rev. (2014), https://doi.org/10.1016/j.addr.2014.05.005.
[360] R.K. Jain, Normalization of tumor vasculature: an emerging concept in antiangiogenic therapy, Science (80-.) (2005), https://doi.org/10.1126/science.1104819.
[361] H. Park, G. Saravanakumar, J. Kim, J. Lim, W.J. Kim, Tumor microenvironment sensitive nanocarriers for bioimaging and therapeutics, Adv. Healthc. Mater (2020), https://doi.org/10.1002/adhm.202000834.
[362] S. Sengupta, D. Eavarone, I. Capila, G. Zhao, N. Watson, T. Kiziltepe, R. Sasisekharan, Temporal targeting of tumour cells and neovasculature with a nanoscale delivery system, Nature (2005), https://doi.org/10.1038/nature03794.
[363] B. Chen, W. Dai, D. Mei, T. Liu, S. Li, B. He, B. He, L. Yuan, H. Zhang, X. Wang, Q. Zhang, Comprehensively priming the tumor microenvironment by cancer-associated fibroblast-targeted liposomes for combined therapy with cancer cell-targeted chemotherapeutic drug delivery system, J. Control. Release (2016), https://doi.org/10.1016/j.jconrel.2016.09.014.
[364] M. Kanapathipillai, A. Mammoto, T. Mammoto, J.H. Kang, E. Jiang, K. Ghosh, N. Korin, A. Gibbs, R. Mannix, D.E. Ingber, Inhibition of mammary tumor growth using lysyl oxidase-targeting nanoparticles to modify extracellular matrix, Nano Lett. (2012), https://doi.org/10.1021/nl301206p.
[365] B. Zhang, S. Shen, Z. Liao, W. Shi, Y. Wang, J. Zhao, Y. Hu, J. Yang, J. Chen, H. Mei, Y. Hu, Z. Pang, X. Jiang, Targeting fibronectins of glioma extracellular matrix by CLT1 peptide-conjugated nanoparticles, Biomaterials (2014), https://doi.org/10.1016/j.biomaterials.2014.01.046.
[366] P.M. Anderson, D. Hasz, L. Dickrell, S. Sencer, Interleukin-2 in liposomes: Increased intravenous potency and less pulmonary toxicity in the rat, Drug Dev. Res. (1992), https://doi.org/10.1002/ddr.430270103.
[367] A. Arora, G. Su, E. Mathiowitz, J. Reineke, A.E. Chang, M.S. Sabel, Neoadjuvant intratumoral cytokine-loaded microspheres are superior to postoperative autologous cellular vaccines in generating systemic anti-tumor immunity, J. Surg. Oncol. (2006), https://doi.org/10.1002/jso.20572.
[368] C. Roma-Rodrigues, I. Pombo, A.F.-I. journal of, undefined 2020, Hyperthermia Induced by Gold Nanoparticles and Visible Light Photothermy Combined with Chemotherapy to Tackle Doxorubicin Sensitive and Resistant Colorectal, Mdpi. Com, 2020.
[369] P. Jiao, M. Otto, Q. Geng, C. Li, F. Li, E.R. Butch, S.E. Snyder, H. Zhou, B. Yan, Enhancing both CT imaging and natural killer cell-mediated cancer cell killing by a GD2-targeting nanoconstruct, J. Mater. Chem. B (2016), https://doi.org/10.1039/c5tb02243f.
[370] J.J. Wang, K.F. Lei, F. Han, Tumor microenvironment: recent advances in various cancer treatments, Eur. Rev. Med. Pharmacol. Sci. 22 (2018) 3855–3864, https://doi.org/10.26355/eurrev-201806-15270.
[371] X. Zhao, B. Kallakury, J.J. Chahine, D. Hartmann, Y.W. Zhang, Y. Chen, H. Zhang, B. Zhang, C. Wang, G. Giaccone, Surgical resection of SCLC: prognostic factors and the tumor microenvironment, J. Thorac. Oncol. 14 (2019) 914–923, https://doi.org/10.1016/j.jtho.2019.01.019.
[372] T.S. Shylasree, A. Bryant, R. Athavale, Chemotherapy and/or radiotherapy in combination with surgery for ovarian carcinosarcoma, Cochrane Database Syst. Rev. 2013 (2013), https://doi.org/10.1002/14651858.CD006246.pub2.
[373] J.H. Kang, S.H. Cho, J. Pyeong Kim, K.M. Kang, K.S. Cho, W. Kim, Y. Mi Seol, S. Lee, H. Soo Park, W. Joo Hur, Y.J. Choi, S.Y. Oh, Treatment outcomes between concurrent chemoradiotherapy and combination of surgery, radiotherapy, and/or chemotherapy in stage III and IV maxillary sinus cancer: multi-institutional retrospective analysis, J. Oral Maxillofac. Surg. 70 (2012) 1717–1723, https://doi.org/10.1016/j.joms.2011.06.221.
[374] B. Nordlinger, E. Van Cutsem, T. Gruenberger, B. Glimelius, G. Poston, P. Rougie, A. Sobrero, M. Ychou, Combination of surgery and chemotherapy and the role of targeted agents in the treatment of patients with colorectal liver metastases: recommendations from an expert panel, Ann. Oncol. 20 (2009) 985–992, https://doi.org/10.1093/annonc/mdn735.
[375] O. Bakos, C. Lawson, S. Rouleau, L.H. Tai, Combining surgery and immunotherapy: turning an immunosuppressive effect into a therapeutic opportunity, J. Immunother. Cancer. 6 (2018) 1–11, https://doi.org/10.1186/s40425-018-0398-7.
[376] N.D. Klemen, M. Wang, P.L. Feingold, K. Cooper, S.N. Pavri, D. Han, F. C. Detterbeck, D.J. Boffa, S.A. Khan, K. Olino, J. Clune, S. Ariyan, R.R. Salem, S. A. Weiss, H.M. Kluger, M. Sznol, C. Cha, Patterns of failure after immunotherapy with checkpoint inhibitors predict durable progression-free survival after local therapy for metastatic melanoma, J. Immunother. Cancer (2019), https://doi.org/10.1186/s40425-019-0672-3.
[377] N.D. Klemen, M.L. Shindorf, R.M. Sherry, Role of surgery in combination with immunotherapy, Surg. Oncol. Clin. N. Am. 28 (2019) 481–487, https://doi.org/10.1016/j.soc.2019.02.011.
[378] J.G. Berdeja, L.L. Hart, J.R. Mace, E.R. Arrowsmith, J.H. Essell, R.S. Owera, J. D. Hainsworth, I.W. Flinn, Phase I/II study of the combination of panobinostat and carfilzomib in patients with relapsed/refractory multiple myeloma, Haematologica (2015), https://doi.org/10.3324/haematol.2014.119735.
[379] B.D. Liboiron, A.C. Louie, L.D. Mayer, Nanoscale complexes - a novel nanotechnology-based platform to optimize combination cancer therapies: Rational development & improved delivery using combiplex®, Drug Dev. Deliv 16 (1) (2016) 34–39.
[380] P.A. Ascierto, H.Z. Streicher, M. Sznol, Melanoma: a model for testing new agents in combination therapies, J. Transl. Med. (2010), https://doi.org/10.1186/1479-5876-8-38.
[381] R.W. Humphrey, L.M. Brockway-Lunardi, D.T. Bonk, K.M. Dohoney, J. H. Doroshow, S.J. Meech, M.J. Ratain, S.L. Topalian, D.M. Pardoll, Opportunities and challenges in the development of experimental drug combinations for cancer, J. Natl. Cancer Inst. (2011), https://doi.org/10.1093/jnci/djr246.
[382] A.D. Levinson, Cancer therapy reform, Science (80-.) (2010), https://doi.org/10.1126/science.1189749.
[383] D.J. Wooten, S.M. Groves, D.R. Tyson, Q. Liu, J.S. Lim, C.F. Lopez, J. Sage, V. Quaranta, Systems-level network modeling of Small Cell Lung Cancer subtypes identifies master regulators and destabilizers, BioRxiv (2018), https://doi.org/10.1101/506402.
[384] B. Li, E. Severson, J.C. Pignon, H. Zhao, T. Li, J. Novak, P. Jiang, H. Shen, J. C. Aster, S. Rodig, S. Signoretti, J.S. Liu, X.S. Liu, Comprehensive analyses of tumor immunity: implications for cancer immunotherapy, Genome Biol. (2016), https://doi.org/10.1186/s13059-016-1028-7.
[385] C.C. Liu, C.B. Steen, A.M. Newman, Computational approaches for characterizing the tumor immune microenvironment, Immunology (2019), https://doi.org/10.1111/imm.13101.
[386] M. Manoharan, N. Mandloi, S. Priyadarshini, A. Patil, R. Gupta, L. Iyer, R. Gupta, A. Chaudhuri, A computational approach identifies immunogenic features of prognosis in human cancers, Front. Immunol. (2018), https://doi.org/10.3389/fimmu.2018.03017.
[387] K. O'Neill, N. Aghaeepour, J. Špidlen, R. Brinkman, Flow cytometry bioinformatics, PLoS Comput. Biol. (2013), https://doi.org/10.1371/journal.pcbi.1003365.
[388] N. Aghaeepour, G. Finak, H. Hoos, T.R. Mosmann, R. Brinkman, R. Gottardo, R. H. Scheuermann, D. Dougall, A.H. Khodabakhshi, P. Mah, G. Obermoser, J. Spidlen, I. Taylor, S.A. Wuensch, J. Bramson, C. Eaves, A.P. Weng, E.S. Fortuno, K. Ho, T.R. Kollmann, W. Rogers, S. De Rosa, B. Dalai, A. Azad, A. Pothen, A. Brandes, H. Bretschneider, R. Bruggner, R. Finck, R. Jia, N. Zimmerman, M. Linderman, D. Dill, G. Nolan, C. Chan, F. El Khettabi, K. O'Neill, M. Chikina, Y. Ge, S. Sealfon, I. Sugár, A. Gupta, P. Shooshtari, H. Zare, P.L. De Jager, M. Jiang, J. Keilwagen, J.M. Maisog, G. Luta, A.A. Barbo, P. Májek, J. Vilček, T. Manninen, H. Huttunen, P. Ruusuvuori, M. Nykter, G.J. McLachlan, K. Wang, I. Naim, G. Sharma, R. Nikolic, S. Pyne, Y. Qian, P. Qiu, J. Quinn, A. Roth, P. Meyer, G. Stolovitzky, J. Saez-Rodriguez, R. Norel, M. Bhattacharjee, M. Biehl, P. Bucher, K. Bunte, B. Di Camillo, F. Sambo, T. Sanavia, E. Trifoglio, G. Toffolo, S.D. Slavica Dimitrieva, R. Dreos, G. Ambrosini, J. Grau, I. Grosse, S. Posch, N. Guex, M. Kursa, W. Rudnicki, B. Liu, M. Maienschein-Cline, P. Schneider, M. Seifert, M. Strickert, J.M.G. Vilar, Critical assessment of automated flow cytometry data analysis techniques, Nat. Methods (2013), https://doi.org/10.1038/NMETH.2365.
[389] D.R. Bandura, V.I. Baranov, O.I. Ornatsky, A. Antonov, R. Kinach, X. Lou, S. Pavlov, S. Vorobiev, J.E. Dick, S.D. Tanner, Mass cytometry: technique for real time single cell multitarget immunoassay based on inductively coupled plasma time-of-flight mass spectrometry, Anal. Chem. (2009), https://doi.org/10.1021/ac901049w.
[390] S. Di Cataldo, E. Ficarra, A. Acquaviva, E. Macii, Automated segmentation of tissue images for computerized IHC analysis, Comput. Methods Prog. Biomed. (2010), https://doi.org/10.1016/j.cmpb.2010.02.002.
[391] S.M. Hartig, Basic image analysis and manipulation in imageJ, Curr. Protoc. Mol, Biol, 2013, https://doi.org/10.1002/0471142727.mb1415s102.
[392] A.E. Carpenter, T.R. Jones, M.R. Lamprecht, C. Clarke, I.H. Kang, O. Friman, D. A. Guertin, J.H. Chang, R.A. Lindquist, J. Moffat, P. Golland, D.M. Sabatini, CellProfiler: image analysis software for identifying and quantifying cell phenotypes, Genome Biol. 7 (2006) R100, https://doi.org/10.1186/gb-2006-7-10-r100.
[393] R. Cristescu, R. Mogg, M. Ayers, A. Albright, E. Murphy, J. Yearley, X. Sher, X. Q. Liu, H. Lu, M. Nebozhyn, C. Zhang, J.K. Lunceford, A. Joe, J. Cheng, A. L. Webber, N. Ibrahim, E.R. Plimack, P.A. Ott, T.Y. Seiwert, A. Ribas, T. K. McClanahan, J.E. Tomassini, A. Loboda, D. Kaufman, Pan-tumor genomic biomarkers for PD-1 checkpoint blockade-based immunotherapy, Science (80-.) (2018), https://doi.org/10.1126/science.aar3593.
[394] P.L. Chen, W. Roh, A. Reuben, Z.A. Cooper, C.N. Spencer, P.A. Prieto, J.P. Miller, R.L. Bassett, V. Gopalakrishnan, K. Wani, M.P. De Macedo, J.L. Austin-Breneman, H. Jiang, Q. Chang, S.M. Reddy, W.S. Chen, M.T. Tetzlaff, R.J. Broaddus, M. A. Davies, J.E. Gershenwald, L. Haydu, A.J. Lazar, S.P. Patel, P. Hwu, W.J. Hwu, A. Diab, I.C. Glitza, S.E. Woodman, L.M. Vence, I.I. Wistuba, R.N. Amaria, L. N. Kwong, V. Prieto, R. Eric Davis, W. Ma, W.W. Overwijk, A.H. Sharpe, J. Hu, P. Andrew Futreal, J. Blando, P. Sharma, J.P. Allison, L. Chin, J.A. Wargo, Analysis of immune signatures in longitudinal tumor samples yields insight into

biomarkers of response and mechanisms of resistance to immune checkpoint blockade, Cancer Discov (2016), https://doi.org/10.1158/2159-8290.CD-15-1545.

[395] V. Thorsson, D.L. Gibbs, S.D. Brown, D. Wolf, D.S. Bortone, T.H. Ou Yang, E. Porta-Pardo, G.F. Gao, C.L. Plaisier, J.A. Eddy, E. Ziv, A.C. Culhane, E.O. Paull, I.K.A. Sivakumar, A.J. Gentles, R. Malhotra, F. Farshidfar, A. Colaprico, J. S. Parker, L.E. Mose, N.S. Vo, J. Liu, Y. Liu, J. Rader, V. Dhankani, S.M. Reynolds, R. Bowlby, A. Califano, A.D. Cherniack, D. Anastassiou, D. Bedognetti, A. Rao, K. Chen, A. Krasnitz, H. Hu, T.M. Malta, H. Noushmehr, C.S. Pedamallu, S. Bullman, A.I. Ojesina, A. Lamb, W. Zhou, H. Shen, T.K. Choueiri, J. N. Weinstein, J. Guinney, J. Saltz, R. Holt, C.E. Rabkin, S.J. Caesar-Johnson, J. A. Demchok, I. Felau, M. Kasapi, M.L. Ferguson, C.M. Hutter, H.J. Sofia, R. Tarnuzzer, Z. Wang, L. Yang, J.C. Zenklusen, J. (Julia) Zhang, S. Chudamani, J. Liu, L. Lolla, R. Naresh, T. Pihl, Q. Sun, Y. Wan, Y. Wu, J. Cho, T. DeFreitas, S. Frazer, N. Gehlenborg, G. Getz, D.I. Heiman, J. Kim, M.S. Lawrence, P. Lin, S. Meier, M.S. Noble, G. Saksena, D. Voet, H. Zhang, B. Bernard, N. Chambwe, V. Dhankani, T. Knijnenburg, R. Kramer, K. Leinonen, Y. Liu, M. Miller, S. Reynolds, I. Shmulevich, V. Thorsson, W. Zhang, R. Akbani, B.M. Broom, A. M. Hegde, Z. Ju, R.S. Kanchi, A. Korkut, J. Li, H. Liang, S. Ling, W. Liu, Y. Lu, G. B. Mills, K.S. Ng, A. Rao, M. Ryan, J. Wang, J.N. Weinstein, J. Zhang, A. Abeshouse, J. Armenia, D. Chakravarty, W.K. Chatila, I. de Bruijn, J. Gao, B. E. Gross, Z.J. Heins, R. Kundra, K. La, M. Ladanyi, A. Luna, M.G. Nissan, A. Ochoa, S.M. Phillips, E. Reznik, F. Sanchez-Vega, C. Sander, N. Schultz, R. Sheridan, S. O. Sumer, Y. Sun, B.S. Taylor, J. Wang, H. Zhang, P. Anur, M. Peto, P. Spellman, C. Benz, J.M. Stuart, C.K. Wong, C. Yau, D.N. Hayes, J.S. Parker, M.D. Wilkerson, A. Ally, M. Balasundaram, R. Bowlby, D. Brooks, R. Carlsen, E. Chuah, N. Dhalla, S.J.M. Jones, K. Kasaian, D. Lee, Y. Ma, M.A. Marra, M. Mayo, R.A. Moore, A. J. Mungall, K. Mungall, A.G. Robertson, S. Sadeghi, J.E. Schein, P. Sipahimalani, A. Tam, N. Thiessen, K. Tse, T. Wong, A.C. Berger, R. Beroukhim, A.D. Cherniack, C. Cibulskis, S.B. Gabriel, G. Ha, M. Meyerson, S.E. Schumacher, J. Shih, M. H. Kucherlapati, R.S. Kucherlapati, S. Baylin, L. Cope, L. Danilova, M. S. Bootwalla, P.H. Lai, D.T. Maglinte, D.J. Van Den Berg, D.J. Weisenberger, J. T. Auman, S. Balu, T. Bodenheimer, C. Fan, K.A. Hoadley, A.P. Hoyle, S. R. Jefferys, C.D. Jones, S. Meng, P.A. Mieczkowski, L.E. Mose, A.H. Perou, C. M. Perou, J. Roach, Y. Shi, J.V. Simons, T. Skelly, M.G. Soloway, D. Tan, U. Veluvolu, H. Fan, T. Hinoue, P.W. Laird, H. Shen, W. Zhou, M. Bellair, K. Chang, K. Covington, C.J. Creighton, H. Dinh, H.V. Doddapaneni, L. A. Donehower, J. Drummond, R.A. Gibbs, R. Glenn, W. Hale, Y. Han, J. Hu, V. Korchina, S. Lee, L. Lewis, W. Li, X. Liu, M. Morgan, D. Morton, D. Muzny, J. Santibanez, M. Sheth, E. Shinbrot, L. Wang, M. Wang, D.A. Wheeler, L. Xi, F. Zhao, J. Hess, E.L. Appelbaum, M. Bailey, M.G. Cordes, L. Ding, C.C. Fronick, L. A. Fulton, R.S. Fulton, C. Kandoth, E.R. Mardis, M.D. McLellan, C.A. Miller, H. K. Schmidt, R.K. Wilson, D. Crain, E. Curley, J. Gardner, K. Lau, D. Mallery, S. Morris, J. Paulauskis, R. Penny, C. Shelton, T. Shelton, M. Sherman, E. Thompson, P. Yena, J. Bowen, J.M. Gastier-Foster, M. Gerken, K.M. Leraas, T. M. Lichtenberg, N.C. Ramirez, L. Wise, E. Zmuda, N. Corcoran, T. Costello, C. Hovens, A.L. Carvalho, A.C. de Carvalho, J.H. Fregnani, A. Longatto-Filho, R. M. Reis, C. Scapulatempo-Neto, H.C.S. Silveira, D.O. Vidal, A. Burnette, J. Eschbacher, B. Hermes, A. Noss, R. Singh, M.L. Anderson, P.D. Castro, M. Ittmann, D. Huntsman, B. Kohl, X. Le, R. Thorp, C. Andry, E.R. Duffy, V. Lyadov, O. Paklina, G. Setdikova, A. Shabunin, M. Tavobilov, C. McPherson, R. Warnick, R. Berkowitz, D. Cramer, C. Feltmate, N. Horowitz, A. Kibel, M. Muto, C.P. Raut, A. Malykh, J.S. Barnholtz-Sloan, W. Barrett, K. Devine, J. Fulop, Q. T. Ostrom, K. Shimmel, Y. Wolinsky, A.E. Sloan, A. De Rose, F. Giuliante, M. Goodman, B.Y. Karlan, C.H. Hagedorn, J. Eckman, J. Harr, J. Myers, K. Tucker, L.A. Zach, B. Deyarmin, H. Hu, L. Kvecher, C. Larson, R.J. Mural, S. Somiari, A. Vicha, T. Zelinka, J. Bennett, M. Iacocca, B. Rabeno, P. Swanson, M. Latour, L. Lacombe, B. Têtu, A. Bergeron, M. McGraw, S.M. Staugaitis, J. Chabot, H. Hibshoosh, A. Sepulveda, T. Su, T. Wang, O. Potapova, O. Voronina, L. Desjardins, O. Mariani, S. Roman-Roman, X. Sastre, M.H. Stern, F. Cheng, S. Signoretti, A. Berchuck, D. Bigner, E. Lipp, J. Marks, S. McCall, R. McLendon, A. Secord, A. Sharp, M. Behera, D.J. Brat, A. Chen, K. Delman, S. Force, F. Khuri, K. Magliocca, S. Maithel, J.J. Olson, T. Owonikoko, A. Pickens, S. Ramalingam, D. M. Shin, G. Sica, E.G. Van Meir, H. Zhang, W. Eijckenboom, A. Gillis, E. Korpershoek, L. Looijenga, W. Oosterhuis, H. Stoop, K.E. van Kessel, E. C. Zwarthoff, C. Calatozzolo, L. Cuppini, S. Cuzzubbo, F. DiMeco, G. Finocchiaro, L. Mattei, A. Perin, B. Pollo, C. Chen, J. Houck, P. Lohavanichbutr, A. Hartmann, C. Stoehr, R. Stoehr, H. Taubert, S. Wach, B. Wullich, W. Kycler, D. Murawa, M. Wiznerowicz, K. Chung, W.J. Edenfield, J. Martin, E. Baudin, G. Bubley, R. Bueno, A. De Rienzo, W.G. Richards, S. Kalkanis, T. Mikkelsen, H. Noushmehr, L. Scarpace, N. Girard, M. Aymerich, E. Campo, E. Giné, A.L. Guillermo, N. Van Bang, P.T. Hanh, B.D. Phu, Y. Tang, H. Colman, K. Evason, P.R. Dottino, J. A. Martignetti, H. Gabra, H. Juhl, T. Akeredolu, S. Stepa, D. Hoon, K. Ahn, K. J. Kang, F. Beuschlein, A. Breggia, M. Birrer, D. Bell, M. Borad, A.H. Bryce, E. Castle, V. Chandan, J. Cheville, J.A. Copland, M. Farnell, T. Flotte, N. Giama, T. Ho, M. Kendrick, J.P. Kocher, K. Kopp, C. Moser, D. Nagorney, D. O'Brien, B. P. O'Neill, T. Patel, G. Petersen, F. Que, M. Rivera, L. Roberts, R. Smallridge, T. Smyrk, M. Stanton, R.H. Thompson, M. Torbenson, J.D. Yang, L. Zhang, F. Brimo, J.A. Ajani, A.M.A. Gonzalez, C. Behrens, J. Bondaruk, R. Broaddus, B. Czerniak, B. Esmaeli, J. Fujimoto, J. Gershenwald, C. Guo, A.J. Lazar, C. Logothetis, F. Meric-Bernstam, C. Moran, L. Ramondetta, D. Rice, A. Sood, P. Tamboli, T. Thompson, P. Troncoso, A. Tsao, I. Wistuba, C. Carter, L. Haydu, P. Hersey, V. Jakrot, H. Kakavand, R. Kefford, K. Lee, G. Long, G. Mann, M. Quinn, R. Saw, R. Scolyer, K. Shannon, A. Spillane, Onathan Stretch, M. Synott, J. Thompson, J. Wilmott, H. Al-Ahmadie, T.A. Chan, R. Ghossein, A. Gopalan, D.A. Levine, V. Reuter, S. Singer, B. Singh, N.V. Tien, T. Broudy, C. Mirsaidi, P. Nair, P. Drwiega, J. Miller, J. Smith, H. Zaren, J.W. Park, N. P. Hung, E. Kebebew, W.M. Linehan, A.R. Metwalli, K. Pacak, P.A. Pinto, M. Schiffman, L.S. Schmidt, C.D. Vocke, N. Wentzensen, R. Worrell, H. Yang, M. Moncrieff, C. Goparaju, J. Melamed, H. Pass, N. Botnariuc, I. Caraman, M. Cernat, I. Chemencedji, A. Clipca, S. Doruc, G. Gorincioi, S. Mura, M. Pirtac, I. Stancul, D. Tcaciuc, M. Albert, I. Alexopoulou, A. Arnaout, J. Bartlett, J. Engel, S. Gilbert, J. Parfitt, H. Sekhon, G. Thomas, D.M. Rassl, R.C. Rintoul, C. Bifulco, R. Tamakawa, W. Urba, N. Hayward, H. Timmers, A. Antenucci, F. Facciolo, G. Grazi, M. Marino, R. Merola, R. de Krijger, A.P. Gimenez-Roqueplo, A. Piché, S. Chevalier, G. McKercher, K. Birsoy, G. Barnett, C. Brewer, C. Farver, T. Naska, N.A. Pennell, D. Raymond, C. Schilero, K. Smolenski, F. Williams, C. Morrison, J. A. Borgia, M.J. Liptay, M. Pool, C.W. Seder, K. Junker, L. Omberg, M. Dinkin, G. Manikhas, D. Alvaro, M.C. Bragazzi, V. Cardinale, G. Carpino, E. Gaudio, D. Chesla, S. Cottingham, M. Dubina, F. Moiseenko, R. Dhanasekaran, K. F. Becker, K.P. Janssen, J. Slotta-Huspenina, M.H. Abdel-Rahman, D. Aziz, S. Bell, C.M. Cebulla, A. Davis, R. Duell, J.B. Elder, J. Hilty, B. Kumar, J. Lang, N. L. Lehman, R. Mandt, P. Nguyen, R. Pilarski, K. Rai, L. Schoenfield, K. Senecal, P. Wakely, P. Hansen, R. Lechan, J. Powers, A. Tischler, W.E. Grizzle, K.C. Sexton, A. Kastl, J. Henderson, S. Porten, J. Waldmann, M. Fassnacht, S.L. Asa, D. Schadendorf, M. Couce, M. Graefen, H. Huland, G. Sauter, T. Schlomm, R. Simon, P. Tennstedt, O. Olabode, M. Nelson, O. Bathe, P.R. Carroll, J.M. Chan, P. Disaia, P. Glenn, R.K. Kelley, C.N. Landen, J. Phillips, M. Prados, J. Simko, K. Smith-McCune, S. VandenBerg, K. Roggin, A. Fehrenbach, A. Kendler, S. Sifri, R. Steele, A. Jimeno, F. Carey, I. Forgie, M. Mannelli, M. Carney, B. Hernandez, B. Campos, C. Herold-Mende, C. Jungk, A. Unterberg, A. von Deimling, A. Bossler, J. Galbraith, L. Jacobus, M. Knudson, T. Knutson, D. Ma, M. Milhem, R. Sigmund, A.K. Godwin, R. Madan, H.G. Rosenthal, C. Adebamowo, S.N. Adebamowo, A. Boussioutas, D. Beer, T. Giordano, A.M. Mes-Masson, F. Saad, T. Bocklage, L. Landrum, R. Mannel, K. Moore, K. Moxley, R. Postier, J. Walker, R. Zuna, M. Feldman, F. Valdivieso, R. Dhir, J. Luketich, E.M.M. Pinero, M. Quintero-Aguilo, C.G. Carlotti, J.S. Dos Santos, R. Kemp, A. Sankarankuty, D. Tirapelli, J. Catto, K. Agnew, E. Swisher, J. Creaney, B. Robinson, C.S. Shelley, E. M. Godwin, S. Kendall, C. Shipman, C. Bradford, T. Carey, A. Haddad, J. Moyer, L. Peterson, M. Prince, L. Rozek, G. Wolf, R. Bowman, K.M. Fong, I. Yang, R. Korst, W.K. Rathmell, J.L. Fantacone-Campbell, J.A. Hooke, A.J. Kovatich, C. D. Shriver, J. DiPersio, B. Drake, R. Govindan, S. Heath, T. Ley, B. Van Tine, P. Westervelt, M.A. Rubin, J. Il Lee, N.D. Aredes, A. Mariamidze, J.S. Serody, E. G. Demicco, M.L. Disis, B.G. Vincent, Ilya Shmulevich, The immune landscape of cancer, Immunity (2018), https://doi.org/10.1016/j.immuni.2018.03.023.

[396] G. Kelsey, O. Stegle, W. Reik, Single-cell epigenomics: recording the past and predicting the future, Science (80-.) (2017), https://doi.org/10.1126/science.aan6826.

[397] N. Miyashita, M. Horie, H.I. Suzuki, M. Yoshihara, D. Djureinovic, J. Persson, H. Brunnström, C. Lindskog, H. Elfving, P. Micke, A. Saito, T. Nagase, An integrative analysis of transcriptome and epigenome features of ASCL1–positive lung adenocarcinomas, J. Thorac. Oncol. (2018), https://doi.org/10.1016/j.jtho.2018.07.096.

[398] K. Chaudhary, O.B. Poirion, L. Lu, L.X. Garmire, Deep learning–based multi-omics integration robustly predicts survival in liver cancer, Clin. Cancer Res. (2018), https://doi.org/10.1158/1078-0432.CCR-17-0853.

[399] M.I. Love, W. Huber, S. Anders, Moderated estimation of fold change and dispersion for RNA-seq data with DESeq2, Genome Biol. (2014), https://doi.org/10.1186/s13059-014-0550-8.

[400] C.S. Ross-Innes, R. Stark, A.E. Teschendorff, K.A. Holmes, H.R. Ali, M.J. Dunning, G.D. Brown, O. Gojis, I.O. Ellis, A.R. Green, S. Ali, S.F. Chin, C. Palmieri, C. Caldas, J.S. Carroll, Differential oestrogen receptor binding is associated with clinical outcome in breast cancer, Nature (2012), https://doi.org/10.1038/nature10730.

[401] M.J. Aryee, A.E. Jaffe, H. Corrada-Bravo, C. Ladd-Acosta, A.P. Feinberg, K. D. Hansen, R.A. Irizarry, Minfi: a flexible and comprehensive Bioconductor package for the analysis of Infinium DNA methylation microarrays, Bioinformatics (2014), https://doi.org/10.1093/bioinformatics/btu049.

[402] I. Dunham, A. Kundaje, S.F. Aldred, P.J. Collins, C.A. Davis, F. Doyle, C. B. Epstein, S. Frietze, J. Harrow, R. Kaul, J. Khatun, B.R. Lajoie, S.G. Landt, B. K. Lee, F. Pauli, K.R. Rosenbloom, P. Sabo, A. Safi, A. Sanyal, N. Shoresh, J. M. Simon, L. Song, N.D. Trinklein, R.C. Altshuler, E. Birney, J.B. Brown, C. Cheng, S. Djebali, X. Dong, J. Ernst, T.S. Furey, M. Gerstein, B. Giardine, M. Greven, R. C. Hardison, R.S. Harris, J. Herrero, M.M. Hoffman, S. Iyer, M. Kellis, P. Kheradpour, T. Lassmann, Q. Li, X. Lin, G.K. Marinov, A. Merkel, A. Mortazavi, S.C.J. Parker, T.E. Reddy, J. Rozowsky, F. Schlesinger, R.E. Thurman, J. Wang, L. D. Ward, T.W. Whitfield, S.P. Wilder, W. Wu, H.S. Xi, K.Y. Yip, J. Zhuang, B. E. Bernstein, E.D. Green, C. Gunter, M. Snyder, M.J. Pazin, R.F. Lowdon, L.A. L. Dillon, L.B. Adams, C.J. Kelly, J. Zhang, J.R. Wexler, P.J. Good, E.A. Feingold, G.E. Crawford, J. Dekker, L. Elnitski, P.J. Farnham, M.C. Giddings, T.R. Gingeras, R. Guigó, T.J. Hubbard, W.J. Kent, J.D. Lieb, E.H. Margulies, R.M. Myers, J. A. Stamatoyannopoulos, S.A. Tenenbaum, Z. Weng, K.P. White, B. Wold, Y. Yu, J. Wrobel, B.A. Risk, H.P. Gunawardena, H.C. Kuiper, C.W. Maier, L. Xie, X. Chen, T.S. Mikkelsen, S. Gillespie, A. Goren, O. Ram, X. Zhang, L. Wang, R. Issner, M. J. Coyne, T. Durham, M. Ku, T. Truong, M.L. Eaton, A. Dobin, A. Tanzer, J. Lagarde, W. Lin, C. Xue, B.A. Williams, C. Zaleski, M. Röder, F. Kokocinski, R. F. Abdelhamid, T. Alioto, I. Antoshechkin, M.T. Baer, P. Batut, I. Bell, K. Bell, S. Chakrabortty, J. Chrast, J. Curado, T. Derrien, J. Drenkow, E. Dumais, J. Dumais, R. Duttagupta, M. Fastuca, K. Fejes-Toth, P. Ferreira, S. Foissac, M. J. Fullwood, H. Gao, D. Gonzalez, A. Gordon, C. Howald, S. Jha, R. Johnson, P. Kapranov, B. King, C. Kingswood, G. Li, O.J. Luo, E. Park, J.B. Preall, K. Presaud, P. Ribeca, D. Robyr, X. Ruan, M. Sammeth, K.S. Sandhu, L. Schaeffer,

L.H. See, A. Shahab, J. Skancke, A.M. Suzuki, H. Takahashi, H. Tilgner, D. Trout, N. Walters, H. Wang, Y. Hayashizaki, A. Reymond, S.E. Antonarakis, G.J. Hannon, Y. Ruan, P. Carninci, C.A. Sloan, K. Learned, V.S. Malladi, M.C. Wong, G. P. Barber, M.S. Cline, T.R. Dreszer, S.G. Heitner, D. Karolchik, V.M. Kirkup, L. R. Meyer, J.C. Long, M. Maddren, B.J. Raney, L.L. Grasfeder, P.G. Giresi, A. Battenhouse, N.C. Sheffield, K.A. Showers, D. London, A.A. Bhinge, C. Shestak, M.R. Schaner, S.K. Kim, Z.Z. Zhang, P.A. Mieczkowski, J.O. Mieczkowska, Z. Liu, R.M. McDaniell, Y. Ni, N.U. Rashid, M.J. Kim, S. Adar, Z. Zhang, T. Wang, D. Winter, D. Keefe, V.R. Iyer, M. Zheng, P. Wang, J. Gertz, J. Vielmetter, E. C. Partridge, K.E. Varley, C. Gasper, A. Bansal, S. Pepke, P. Jain, H. Amrhein, K. M. Bowling, M. Anaya, M.K. Cross, M.A. Muratet, K.M. Newberry, K. McCue, A. S. Nesmith, K.I. Fisher-Aylor, B. Pusey, G. DeSalvo, S.L. Parker, S. Balasubramanian, N.S. Davis, S.K. Meadows, T. Eggleston, J.S. Newberry, S. E. Levy, D.M. Absher, W.H. Wong, M.J. Blow, A. Visel, L.A. Pennachio, H. M. Petrykowska, A. Abyzov, B. Aken, D. Barrell, G. Barson, A. Berry, A. Bignell, V. Boychenko, G. Bussotti, C. Davidson, G. Despacio-Reyes, M. Diekhans, I. Ezkurdia, A. Frankish, J. Gilbert, J.M. Gonzalez, E. Griffiths, R. Harte, D. A. Hendrix, T. Hunt, I. Jungreis, M. Kay, E. Khurana, J. Leng, M.F. Lin, J. Loveland, Z. Lu, D. Manthravadi, M. Mariotti, J. Mudge, G. Mukherjee, C. Notredame, B. Pei, J.M. Rodriguez, G. Saunders, A. Sboner, S. Searle, C. Sisu, C. Snow, C. Steward, E. Tapanari, M.L. Tress, M.J. Van Baren, S. Washietl, L. Wilming, A. Zadissa, Z. Zhang, M. Brent, D. Haussler, A. Valencia, N. Addleman, R.P. Alexander, R.K. Auerbach, S. Balasubramanian, K. Bettinger, N. Bhardwaj, A.P. Boyle, A.R. Cao, P. Cayting, A. Charos, Y. Cheng, C. Eastman, G. Euskirchen, J.D. Fleming, F. Grubert, L. Habegger, M. Hariharan, A. Harmanci, S. Iyengar, V.X. Jin, K.J. Karczewski, M. Kasowski, P. Lacroute, H. Lam, N. Lamarre-Vincent, J. Lian, M. Lindahl-Allen, R. Min, B. Miotto, H. Monahan, Z. Moqtaderi, X.J. Mu, H. O'Geen, Z. Ouyang, D. Patacsil, D. Raha, L. Ramirez, B. Reed, M. Shi, T. Slifer, H. Witt, L. Wu, X. Xu, K.K. Yan, X. Yang, K. Struhl, S. M. Weissman, L.O. Penalva, S. Karmakar, R.R. Bhanvadia, A. Choudhury, M. Domanus, L. Ma, J. Moran, A. Victorsen, T. Auer, L. Centanin, M. Eichenlaub, F. Gruhl, S. Heermann, B. Hoeckendorf, D. Inoue, T. Kellner, S. Kirchmaier, C. Mueller, R. Reinhardt, L. Schertel, S. Schneider, R. Sinn, B. Wittbrodt, J. Wittbrodt, G. Jain, G. Balasundaram, D.L. Bates, R. Byron, T.K. Canfield, M. J. Diegel, D. Dunn, A.K. Ebersol, T. Frum, K. Garg, E. Gist, R.S. Hansen, L. Boatman, E. Haugen, R. Humbert, A.K. Johnson, E.M. Johnson, T.V. Kutyavin, K. Lee, D. Lotakis, M.T. Maurano, S.J. Neph, F.V. Neri, E.D. Nguyen, H. Qu, A. P. Reynolds, V. Roach, E. Rynes, M.E. Sanchez, R.S. Sandstrom, A.O. Shafer, A. B. Stergachis, S. Thomas, B. Vernot, J. Vierstra, S. Vong, H. Wang, M.A. Weaver, Y. Yan, M. Zhang, J.M. Akey, M. Bender, M.O. Dorschner, M. Groudine, M. J. MacCoss, P. Navas, G. Stamatoyannopoulos, K. Beal, A. Brazma, P. Flicek, N. Johnson, M. Lukk, N.M. Luscombe, D. Sobral, J.M. Vaquerizas, S. Batzoglou, A. Sidow, N. Hussami, S. Kyriazopoulou-Panagiotopoulou, M.W. Libbrecht, M. A. Schaub, W. Miller, P.J. Bickel, B. Banfai, N.P. Boley, H. Huang, J.J. Li, W. S. Noble, J.A. Bilmes, O.J. Buske, A.D. Sahu, P.V. Kharchenko, P.J. Park, D. Baker, J. Taylor, L. Lochovsky, An integrated encyclopedia of DNA elements in the human genome, Nature (2012), https://doi.org/10.1038/nature11247.

[403] L. Jerby-Arnon, P. Shah, M.S. Cuoco, C. Rodman, M.J. Su, J.C. Melms, R. Leeson, A. Kanodia, S. Mei, J.R. Lin, S. Wang, B. Rabasha, D. Liu, G. Zhang, C. Margolais, O. Ashenberg, P.A. Ott, E.I. Buchbinder, R. Haq, F.S. Hodi, G.M. Boland, R. J. Sullivan, D.T. Frederick, B. Miao, T. Moll, K.T. Flaherty, M. Herlyn, R. W. Jenkins, R. Thummalapalli, M.S. Kowalczyk, I. Cañadas, B. Schilling, A.N. R. Cartwright, A.M. Luoma, S. Malu, P. Hwu, C. Bernatchez, M.A. Forget, D. A. Barbie, A.K. Shalek, I. Tirosh, P.K. Sorger, K. Wucherpfennig, E.M. Van Allen, D. Schadendorf, B.E. Johnson, A. Rotem, O. Rozenblatt-Rosen, L.A. Garraway, C. H. Yoon, B. Izar, A. Regev, A cancer cell program promotes T cell exclusion and resistance to checkpoint blockade, Cell (2018), https://doi.org/10.1016/j.cell.2018.09.006.

[404] B. Hwang, J.H. Lee, D. Bang, Single-cell RNA sequencing technologies and bioinformatics pipelines, Exp. Mol. Med. (2018), https://doi.org/10.1038/s12276-018-0071-8.

[405] A. Butler, P. Hoffman, P. Smibert, E. Papalexi, R. Satija, Integrating single-cell transcriptomic data across different conditions, technologies, and species, Nat. Biotechnol. (2018), https://doi.org/10.1038/nbt.4096.

[406] W.V. Li, J.J. Li, An accurate and robust imputation method scImpute for single-cell RNA-seq data, Nat. Commun. (2018), https://doi.org/10.1038/s41467-018-03405-7.

[407] D. van Dijk, R. Sharma, J. Nainys, K. Yim, P. Kathail, A.J. Carr, C. Burdziak, K. R. Moon, C.L. Chaffer, D. Pattabiraman, B. Bierie, L. Mazutis, G. Wolf, S. Krishnaswamy, D. Pe'er, Recovering gene interactions from single-cell data using data diffusion, Cell (2018), https://doi.org/10.1016/j.cell.2018.05.061.

[408] M.R. Corces, J.D. Buenrostro, B. Wu, P.G. Greenside, S.M. Chan, J.L. Koenig, M. P. Snyder, J.K. Pritchard, A. Kundaje, W.J. Greenleaf, R. Majeti, H.Y. Chang, Lineage-specific and single-cell chromatin accessibility charts human hematopoiesis and leukemia evolution, Nat. Genet. (2016), https://doi.org/10.1038/ng.3646.

[409] S.C. Van Den Brink, F. Sage, Á. Vértesy, B. Spanjaard, J. Peterson-Maduro, C. S. Baron, C. Robin, A. Van Oudenaarden, Single-cell sequencing reveals dissociation-induced gene expression in tissue subpopulations, Nat. Methods (2017), https://doi.org/10.1038/nmeth.4437.

[410] A.M. Newman, C.B. Steen, C.L. Liu, A.J. Gentles, A.A. Chaudhuri, F. Scherer, M. S. Khodadoust, M.S. Esfahani, B.A. Luca, D. Steiner, M. Diehn, A.A. Alizadeh, Determining cell type abundance and expression from bulk tissues with digital cytometry, Nat. Biotechnol. (2019), https://doi.org/10.1038/s41587-019-0114-2.

[411] K. Yoshihara, M. Shahmoradgoli, E. Martínez, R. Vegesna, H. Kim, W. Torres-Garcia, V. Treviño, H. Shen, P.W. Laird, D.A. Levine, S.L. Carter, G. Getz, K. Stemke-Hale, G.B. Mills, R.G.W. Verhaak, Inferring tumour purity and stromal and immune cell admixture from expression data, Nat. Commun. (2013), https://doi.org/10.1038/ncomms3612.

[412] S.S. Shen-Orr, R. Tibshirani, P. Khatri, D.L. Bodian, F. Staedtler, N.M. Perry, T. Hastie, M.M. Sarwal, M.M. Davis, A.J. Butte, Cell type-specific gene expression differences in complex tissues, Nat. Methods (2010), https://doi.org/10.1038/nmeth.1439.

[413] J. Racle, K. de Jonge, P. Baumgaertner, D.E. Speiser, D. Gfeller, Simultaneous enumeration of cancer and immune cell types from bulk tumor gene expression data, Elife (2017), https://doi.org/10.7554/eLife.26476.

[414] A.M. Newman, C.L. Liu, M.R. Green, A.J. Gentles, W. Feng, Y. Xu, C.D. Hoang, M. Diehn, A.A. Alizadeh, Robust enumeration of cell subsets from tissue expression profiles, Nat. Methods (2015), https://doi.org/10.1038/nmeth.3337.

[415] X. Liu, J. Wu, History, applications, and challenges of immune repertoire research, Cell Biol. Toxicol. (2018), https://doi.org/10.1007/s10565-018-9426-0.

[416] R.O. Emerson, A.M. Sherwood, M.J. Rieder, J. Guenthoer, D.W. Williamson, C. S. Carlson, C.W. Drescher, M. Tewari, J.H. Bielas, H.S. Robins, High-throughput sequencing of T-cell receptors reveals a homogeneous repertoire of tumour-infiltrating lymphocytes in ovarian cancer, J. Pathol. (2013), https://doi.org/10.1002/path.4260.

[417] J. Ye, N. Ma, T.L. Madden, J.M. Ostell, IgBLAST: an immunoglobulin variable domain sequence analysis tool, Nucleic Acids Res. (2013), https://doi.org/10.1093/nar/gkt382.

[418] J. Glanville, H. Huang, A. Nau, O. Hatton, L.E. Wagar, F. Rubelt, X. Ji, A. Han, S. M. Krams, C. Pettus, N. Haas, C.S.L. Arlehamn, A. Sette, S.D. Boyd, T.J. Scriba, O. M. Martinez, M.M. Davis, Identifying specificity groups in the T cell receptor repertoire, Nature (2017), https://doi.org/10.1038/nature22976.

[419] H. Hackl, P. Charoentong, F. Finotello, Z. Trajanoski, Computational genomics tools for dissecting tumour-immune cell interactions, Nat. Rev. Genet. (2016), https://doi.org/10.1038/nrg.2016.67.

[420] B. Mlecnik, F. Sanchez-Cabo, P. Charoentong, G. Bindea, F. Pagès, A. Berger, J. Galon, Z. Trajanoski, Data integration and exploration for the identification of molecular mechanisms in tumor-immune cells interaction, BMC Genomics (2010), https://doi.org/10.1186/1471-2164-11-S1-S7.

[421] H.S. Park, W.S. Kwon, S. Park, E. Jo, S.J. Lim, C.K. Lee, J.B. Lee, M. Jung, H. S. Kim, S.H. Beom, J.Y. Park, T.S. Kim, H.C. Chung, S.Y. Rha, Comprehensive immune profiling and immune-monitoring using body fluid of patients with metastatic gastric cancer, J. Immunother. Cancer. 7 (2019) 268, https://doi.org/10.1186/s40425-019-0708-8.

[422] Cell Cycle, Univariate | FlowJo Documentation - Just another WordPress site. https://docs.flowjo.com/flowjo/experiment-based-platforms/cell-cycle-univariate/, 2021. (Accessed 15 April 2021).

[423] DVS Sciences and Cytobank Announce Partnership to Analyze and Manage High-Parameter Mass Cytometry Data, Business Wire, 2012. https://www.businesswire.com/news/home/20120623005025/en/DVS-Sciences-and-Cytobank-announce-partnership-to-analyze-and-manage-high-parameter-mass-cytometry-data. (Accessed 15 April 2021).

[424] J. Spidlen, K. Breuer, C. Rosenberg, N. Kotecha, R.R. Brinkman, FlowRepository: a resource of annotated flow cytometry datasets associated with peer-reviewed publications, Cytom. A. 81A (2012) 727–731, https://doi.org/10.1002/cyto.a.22106.

[425] A.E. Carpenter, T.R. Jones, M.R. Lamprecht, C. Clarke, I.H. Kang, O. Friman, D. A. Guertin, J.H. Chang, R.A. Lindquist, J. Moffat, P. Golland, D.M. Sabatini, CellProfiler: image analysis software for identifying and quantifying cell phenotypes, Genome Biol. (2006), https://doi.org/10.1186/gb-2006-7-10-r100.

[426] C.T. Rueden, J. Schindelin, M.C. Hiner, B.E. DeZonia, A.E. Walter, E.T. Arena, K. W. Eliceiri, ImageJ2: ImageJ for the next generation of scientific image data, BMC Bioinformatics. 18 (2017) 529, https://doi.org/10.1186/s12859-017-1934-z.

[427] C. McQuin, A. Goodman, V. Chernyshev, L. Kamentsky, B.A. Cimini, K. W. Karhohs, M. Doan, L. Ding, S.M. Rafelski, D. Thirstrup, W. Wiegraebe, S. Singh, T. Becker, J.C. Caicedo, A.E. Carpenter, CellProfiler 3.0: next-generation image processing for biology, PLoS Biol. 16 (2018), https://doi.org/10.1371/journal.pbio.2005970 e2005970.

[428] D.A. Van Valen, T. Kudo, K.M. Lane, D.N. Macklin, N.T. Quach, M.M. DeFelice, I. Maayan, Y. Tanouchi, E.A. Ashley, M.W. Covert, Deep learning automates the quantitative analysis of individual cells in live-cell imaging experiments, PLoS Comput. Biol. (2016), https://doi.org/10.1371/journal.pcbi.1005177.

[429] D. Bannon, E. Moen, M. Schwartz, E. Borba, S. Cui, K. Huang, I. Camplisson, N. Koe, D. Kyme, T. Kudo, B. Chang, E. Pao, E. Osterman, W. Graf, D. Van Valen, Dynamic allocation of computational resources for deep learning-enabled cellular image analysis with Kubernetes, BioRxiv (2018) 505032, https://doi.org/10.1101/505032.

[430] M.D. Robinson, D.J. McCarthy, G.K. Smyth, edgeR: a Bioconductor package for differential expression analysis of digital gene expression data, Bioinformatics (2009), https://doi.org/10.1093/bioinformatics/btp616.

[431] M.D. Robinson, G.K. Smyth, Moderated statistical tests for assessing differences in tag abundance, Bioinformatics. 23 (2007) 2881–2887, https://doi.org/10.1093/bioinformatics/btm453.

[432] R. Stark, G. Brown, DiffBind : differential binding analysis of ChIP-Seq peak data, 2012.

[433] Z. Shao, Y. Zhang, G.C. Yuan, S.H. Orkin, D.J. Waxman, MAnorm: a robust model for quantitative comparison of ChIP-Seq data sets, Genome Biol. (2012), https://doi.org/10.1186/gb-2012-13-3-r16.

[434] M.D. Robinson, A. Kahraman, C.W. Law, H. Lindsay, M. Nowicka, L.M. Weber, X. Zhou, Statistical methods for detecting differentially methylated loci and regions, Front. Genet. (2014), https://doi.org/10.3389/fgene.2014.00324.
[435] Z. Wang, X.L. Wu, Y. Wang, A framework for analyzing DNA methylation data from Illumina Infinium HumanMethylation450 BeadChip, BMC Bioinformatics. 19 (2018) 115, https://doi.org/10.1186/s12859-018-2096-3.
[436] K.D. Hansen, B. Langmead, R.A. Irizarry, BSmooth: from whole genome bisulfite sequencing reads to differentially methylated regions, Genome Biol. (2012), https://doi.org/10.1186/gb-2012-13-10-R83.
[437] I. Huh, X. Wu, T. Park, S.V. Yi, Detecting differential DNA methylation from sequencing of bisulfite converted DNA of diverse species, Brief. Bioinform. 20 (2019) 33–46, https://doi.org/10.1093/bib/bbx077.
[438] National Human Genome Research Institute (NHGRI), National Institutes of Health (NIH). https://www.nih.gov/about-nih/what-we-do/nih-almanac/national-human-genome-research-institute-nhgri, 2021 (accessed April 18, 2021).
[439] Roadmap Epigenomics Consortium, A. Kundaje, W. Meuleman, J. Ernst, M. Bilenky, A. Yen, A. Heravi-Moussavi, P. Kheradpour, Z. Zhang, J. Wang, M. J. Ziller, V. Amin, J.W. Whitaker, M.D. Schultz, L.D. Ward, A. Sarkar, G. Quon, R. S. Sandstrom, M.L. Eaton, Y.C. Wu, A.R. Pfenning, X. Wang, M. Claussnitzer, Y. Liu, C. Coarfa, R.A. Harris, N. Shoresh, C.B. Epstein, E. Gjoneska, D. Leung, W. Xie, R.D. Hawkins, R. Lister, C. Hong, P. Gascard, A.J. Mungall, R. Moore, E. Chuah, A. Tam, T.K. Canfield, R.S. Hansen, R. Kaul, P.J. Sabo, M.S. Bansal, A. Carles, J.R. Dixon, K.H. Farh, S. Feizi, R. Karlic, A.R. Kim, A. Kulkarni, D. Li, R. Lowdon, G. Elliott, T.R. Mercer, S.J. Neph, V. Onuchic, P. Polak, N. Rajagopal, P. Ray, R.C. Sallari, K.T. Siebenthall, N.A. Sinnott-Armstrong, M. Stevens, R. E. Thurman, J. Wu, B. Zhang, X. Zhou, A.E. Beaudet, L.A. Boyer, P.L. De Jager, P. J. Farnham, S.J. Fisher, D. Haussler, S.J.M. Jones, W. Li, M.A. Marra, M. T. McManus, S. Sunyaev, J.A. Thomson, T.D. Tlsty, L.H. Tsai, W. Wang, R. A. Waterland, M.Q. Zhang, L.H. Chadwick, B.E. Bernstein, J.F. Costello, J. R. Ecker, M. Hirst, A. Meissner, A. Milosavljevic, B. Ren, J. A. Stamatoyannopoulos, T. Wang, M. Kellis, Integrative analysis of 111 reference human epigenomes, Nature (2015), https://doi.org/10.1038/nature14248.
[440] A cornucopia of advances in human epigenomics, Cell (2016), https://doi.org/10.1016/j.cell.2016.11.001.
[441] R. Satija, J.A. Farrell, D. Gennert, A.F. Schier, A. Regev, Spatial reconstruction of single-cell gene expression data, Nat. Biotechnol. 33 (2015) 495–502, https://doi.org/10.1038/nbt.3192.
[442] Tools for Single Cell Genomics • Seurat. https://satijalab.org/seurat/, 2021 (accessed April 18, 2021).
[443] R. Lopez, J. Regier, M.B. Cole, M.I. Jordan, N. Yosef, Deep generative modeling for single-cell transcriptomics, Nat. Methods (2018), https://doi.org/10.1038/s41592-018-0229-2.
[444] scvi · PyPI. https://pypi.org/project/scvi/, 2021 (accessed April 16, 2021).
[445] X. Qiu, Q. Mao, Y. Tang, L. Wang, R. Chawla, H.A. Pliner, C. Trapnell, Reversed graph embedding resolves complex single-cell trajectories, Nat. Methods (2017), https://doi.org/10.1038/nmeth.4402.
[446] M. Zand, J. Ruan, Network-based single-cell RNA-seq data imputation enhances cell type identification, Genes (Basel) 11 (2020), https://doi.org/10.3390/genes11040377.
[447] Z. Deng, J. Wang, B. Xu, Z. Jin, G. Wu, J. Zeng, M. Peng, Y. Guo, Z. Wen, Mining TCGA database for tumor microenvironment-related genes of prognostic value in hepatocellular carcinoma, Biomed. Res. Int. 2019 (2019), https://doi.org/10.1155/2019/2408348.
[448] D. Aran, Z. Hu, A.J. Butte, xCell: Digitally portraying the tissue cellular heterogeneity landscape, Genome Biol. (2017), https://doi.org/10.1186/s13059-017-1349-1.
[449] J. Racle, D. Gfeller, EPIC: a tool to estimate the proportions of different cell types from bulk gene expression data, in: Methods Mol. Biol, Humana Press Inc., 2020, pp. 233–248, https://doi.org/10.1007/978-1-0716-0327-7_17.
[450] Y. Miao, Q. Zhang, Q. Lei, M. Luo, G. Xie, H. Wang, A. Guo, ImmuCellAI: a unique method for comprehensive T-cell subsets abundance prediction and its application in cancer immunotherapy, Adv. Sci. 7 (2020) 1902880, https://doi.org/10.1002/advs.201902880.
[451] L.A. Hildebrand, C.J. Pierce, M. Dennis, M. Paracha, A. Maoz, Artificial intelligence for histology-based detection of microsatellite instability and prediction of response to immunotherapy in colorectal cancer, Cancers (Basel). 13 (2021) 1–24, https://doi.org/10.3390/cancers13030391.
[452] A.C. Berger, A. Korkut, R.S. Kanchi, A.M. Hegde, W. Lenoir, W. Liu, Y. Liu, H. Fan, H. Shen, V. Ravikumar, A. Rao, A. Schultz, X. Li, P. Sumazin, C. Williams, P. Mestdagh, P.H. Gunaratne, C. Yau, R. Bowlby, A.G. Robertson, D.G. Tiezzi, C. Wang, A.D. Cherniack, A.K. Godwin, N.M. Kuderer, J.S. Rader, R.E. Zuna, A. K. Sood, A.J. Lazar, A.I. Ojesina, C. Adebamowo, S.N. Adebamowo, K.A. Baggerly, T.W. Chen, H.S. Chiu, S. Lefever, L. Liu, K. MacKenzie, S. Orsulic, J. Roszik, C. S. Shelley, Q. Song, C.P. Vellano, N. Wentzensen, S.J. Caesar-Johnson, J. A. Demchok, I. Felau, M. Kasapi, M.L. Ferguson, C.M. Hutter, H.J. Sofia, R. Tarnuzzer, Z. Wang, L. Yang, J.C. Zenklusen, J. (Julia) Zhang, S. Chudamani, J. Liu, L. Lolla, R. Naresh, T. Pihl, Q. Sun, Y. Wan, Y. Wu, J. Cho, T. DeFreitas, S. Frazer, N. Gehlenborg, G. Getz, D.I. Heiman, J. Kim, M.S. Lawrence, P. Lin, S. Meier, M.S. Noble, G. Saksena, D. Voet, H. Zhang, B. Bernard, N. Chambwe, V. Dhankani, T. Knijnenburg, R. Kramer, K. Leinonen, M. Miller, S. Reynolds, I. Shmulevich, V. Thorsson, W. Zhang, R. Akbani, B.M. Broom, Z. Ju, J. Li, H. Liang, S. Ling, Y. Lu, G.B. Mills, K.S. Ng, M. Ryan, J. Wang, J.N. Weinstein, J. Zhang, A. Abeshouse, J. Armenia, D. Chakravarty, W.K. Chatila, I. de Bruijn, J. Gao, B.E. Gross, Z.J. Heins, R. Kundra, K. La, M. Ladanyi, A. Luna, M.G. Nissan, A. Ochoa, S.M. Phillips, E. Reznik, F. Sanchez-Vega, C. Sander, N. Schultz, R. Sheridan, S.O. Sumer, Y. Sun, B.S. Taylor, P. Anur, M. Peto, P. Spellman, C. Benz, J.M. Stuart, C.K. Wong, D.N. Hayes, J.S. Parker, M.D. Wilkerson, A. Ally, M. Balasundaram, D. Brooks, R. Carlsen, E. Chuah, N. Dhalla, R. Holt, S.J. M. Jones, K. Kasaian, D. Lee, Y. Ma, M.A. Marra, M. Mayo, R.A. Moore, A. J. Mungall, K. Mungall, S. Sadeghi, J.E. Schein, P. Sipahimalani, A. Tam, N. Thiessen, K. Tse, T. Wong, R. Beroukhim, C. Cibulskis, S.B. Gabriel, G.F. Gao, G. Ha, M. Meyerson, S.E. Schumacher, J. Shih, M.H. Kucherlapati, R. S. Kucherlapati, S. Baylin, L. Cope, L. Danilova, M.S. Bootwalla, P.H. Lai, D. T. Maglinte, D.J. Van Den Berg, D.J. Weisenberger, J.T. Auman, S. Balu, T. Bodenheimer, C. Fan, K.A. Hoadley, A.P. Hoyle, S.R. Jefferys, C.D. Jones, S. Meng, P.A. Mieczkowski, L.E. Mose, A.H. Perou, C.M. Perou, J. Roach, Y. Shi, J. V. Simons, T. Skelly, M.G. Soloway, D. Tan, U. Veluvolu, T. Hinoue, P.W. Laird, W. Zhou, M. Bellair, K. Chang, K. Covington, C.J. Creighton, H. Dinh, H. V. Doddapaneni, L.A. Donehower, J. Drummond, R.A. Gibbs, R. Glenn, W. Hale, Y. Han, J. Hu, V. Korchina, S. Lee, L. Lewis, W. Li, X. Liu, M. Morgan, D. Morton, D. Muzny, J. Santibanez, M. Sheth, E. Shinbrot, L. Wang, M. Wang, D.A. Wheeler, L. Xi, F. Zhao, J. Hess, E.L. Appelbaum, M. Bailey, M.G. Cordes, L. Ding, C. C. Fronick, L.A. Fulton, R.S. Fulton, C. Kandoth, E.R. Mardis, M.D. McLellan, C. A. Miller, H.K. Schmidt, R.K. Wilson, D. Crain, E. Curley, J. Gardner, K. Lau, D. Mallery, S. Morris, J. Paulauskis, R. Penny, C. Shelton, T. Shelton, M. Sherman, E. Thompson, P. Yena, J. Bowen, J.M. Gastier-Foster, M. Gerken, K.M. Leraas, T. M. Lichtenberg, N.C. Ramirez, L. Wise, E. Zmuda, N. Corcoran, T. Costello, C. Hovens, A.L. Carvalho, A.C. de Carvalho, J.H. Fregnani, A. Longatto-Filho, R. M. Reis, C. Scapulatempo-Neto, H.C.S. Silveira, D.O. Vidal, A. Burnette, J. Eschbacher, B. Hermes, A. Noss, R. Singh, M.L. Anderson, P.D. Castro, M. Ittmann, D. Huntsman, B. Kohl, X. Le, R. Thorp, C. Andry, E.R. Duffy, V. Lyadov, O. Paklina, G. Setdikova, A. Shabunin, M. Tavobilov, C. McPherson, R. Warnick, R. Berkowitz, D. Cramer, C. Feltmate, N. Horowitz, A. Kibel, M. Muto, C.P. Raut, A. Malykh, J.S. Barnholtz-Sloan, W. Barrett, K. Devine, J. Fulop, Q. T. Ostrom, K. Shimmel, Y. Wolinsky, A.E. Sloan, A. De Rose, F. Giuliante, M. Goodman, B.Y. Karlan, C.H. Hagedorn, J. Eckman, J. Harr, J. Myers, K. Tucker, L.A. Zach, B. Deyarmin, H. Hu, L. Kvecher, C. Larson, R.J. Mural, S. Somiari, A. Vicha, T. Zelinka, J. Bennett, M. Iacocca, B. Rabeno, P. Swanson, M. Latour, L. Lacombe, B. Têtu, A. Bergeron, M. McGraw, S.M. Staugaitis, J. Chabot, H. Hibshoosh, A. Sepulveda, T. Su, T. Wang, O. Potapova, O. Voronina, L. Desjardins, O. Mariani, S. Roman-Roman, X. Sastre, M.H. Stern, F. Cheng, S. Signoretti, A. Berchuck, D. Bigner, E. Lipp, J. Marks, S. McCall, R. McLendon, A. Secord, A. Sharp, M. Behera, D.J. Brat, A. Chen, K. Delman, S. Force, F. Khuri, K. Magliocca, S. Maithel, J.J. Olson, T. Owonikoko, A. Pickens, S. Ramalingam, D. M. Shin, G. Sica, E.G. Van Meir, W. Eijckenboom, A. Gillis, E. Korpershoek, L. Looijenga, W. Oosterhuis, H. Stoop, K.E. van Kessel, E.C. Zwarthoff, C. Calatozzolo, L. Cuppini, S. Cuzzubbo, F. DiMeco, G. Finocchiaro, L. Mattei, A. Perin, B. Pollo, C. Chen, J. Houck, P. Lohavanichbutr, A. Hartmann, C. Stoehr, R. Stoehr, H. Taubert, S. Wach, B. Wullich, W. Kycler, D. Murawa, M. Wiznerowicz, K. Chung, W.J. Edenfield, J. Martin, E. Baudin, G. Bubley, R. Bueno, A. De Rienzo, W.G. Richards, S. Kalkanis, T. Mikkelsen, H. Noushmehr, L. Scarpace, N. Girard, M. Aymerich, E. Campo, E. Giné, A.L. Guillermo, N. Van Bang, P.T. Hanh, B.D. Phu, Y. Tang, H. Colman, K. Evason, P.R. Dottino, J. A. Martignetti, H. Gabra, H. Juhl, T. Akeredolu, S. Stepa, D. Hoon, K. Ahn, K. J. Kang, F. Beuschlein, A. Breggia, M. Birrer, D. Bell, M. Borad, A.H. Bryce, E. Castle, V. Chandan, J. Cheville, J.A. Copland, M. Farnell, T. Flotte, N. Giama, T. Ho, M. Kendrick, J.P. Kocher, K. Kopp, C. Moser, D. Nagorney, D. O'Brien, B. P. O'Neill, T. Patel, G. Petersen, F. Que, M. Rivera, L. Roberts, R. Smallridge, T. Smyrk, M. Stanton, R.H. Thompson, M. Torbenson, J.D. Yang, L. Zhang, F. Brimo, J.A. Ajani, A.M. Angulo Gonzalez, C. Behrens, J. Bondaruk, R. Broaddus, B. Czerniak, B. Esmaeli, J. Fujimoto, J. Gershenwald, C. Guo, C. Logothetis, F. Meric-Bernstam, C. Moran, L. Ramondetta, D. Rice, A. Sood, P. Tamboli, T. Thompson, P. Troncoso, A. Tsao, I. Wistuba, C. Carter, L. Haydu, P. Hersey, V. Jakrot, H. Kakavand, R. Kefford, K. Lee, G. Long, G. Mann, M. Quinn, R. Saw, R. Scolyer, K. Shannon, A. Spillane, J. Stretch, M. Synott, J. Thompson, J. Wilmott, H. Al-Ahmadie, T.A. Chan, R. Ghossein, A. Gopalan, D. A. Levine, V. Reuter, S. Singer, B. Singh, N.V. Tien, T. Broudy, C. Mirsaidi, P. Nair, P. Drwiega, J. Miller, J. Smith, H. Zaren, J.W. Park, N.P. Hung, E. Kebebew, W. M. Linehan, A.R. Metwalli, K. Pacak, P.A. Pinto, M. Schiffman, L.S. Schmidt, C. D. Vocke, R. Worrell, H. Yang, M. Moncrieff, C. Goparaju, J. Melamed, H. Pass, N. Botnariuc, I. Caraman, M. Cernat, I. Chemencedji, A. Clipca, S. Doruc, G. Gorincioi, S. Mura, M. Pirtac, I. Stancul, D. Tcaciuc, M. Albert, I. Alexopoulou, A. Arnaout, J. Bartlett, J. Engel, S. Gilbert, J. Parfitt, H. Sekhon, G. Thomas, D. M. Rassl, R.C. Rintoul, C. Bifulco, R. Tamakawa, W. Urba, N. Hayward, H. Timmers, A. Antenucci, F. Facciolo, G. Grazi, M. Marino, R. Merola, R. de Krijger, A.P. Gimenez-Roqueplo, A. Piché, S. Chevalier, G. McKercher, K. Birsoy, G. Barnett, C. Brewer, C. Farver, T. Naska, N.A. Pennell, D. Raymond, C. Schilero, K. Smolenski, F. Williams, C. Morrison, J.A. Borgia, M.J. Liptay, M. Pool, C. W. Seder, K. Junker, L. Omberg, M. Dinkin, G. Manikhas, D. Alvaro, M. C. Bragazzi, V. Cardinale, G. Carpino, E. Gaudio, D. Chesla, S. Cottingham, M. Dubina, F. Moiseenko, R. Dhanasekaran, K.F. Becker, K.P. Janssen, J. Slotta-Huspenina, M.H. Abdel-Rahman, D. Aziz, S. Bell, C.M. Cebulla, A. Davis, R. Duell, J.B. Elder, J. Hilty, B. Kumar, J. Lang, N.L. Lehman, R. Mandt, P. Nguyen, R. Pilarski, K. Rai, L. Schoenfield, K. Senecal, P. Wakely, P. Hansen, R. Lechan, J. Powers, A. Tischler, W.E. Grizzle, K.C. Sexton, A. Kastl, J. Henderson, S. Porten, J. Waldmann, M. Fassnacht, S.L. Asa, D. Schadendorf, M. Couce, M. Graefen, H. Huland, G. Sauter, T. Schlomm, R. Simon, P. Tennstedt, O. Olabode, M. Nelson, O. Bathe, P.R. Carroll, J.M. Chan, P. Disaia, P. Glenn, R.K. Kelley, C.N. Landen, J. Phillips, M. Prados, J. Simko, K. Smith-McCune, S. VandenBerg, K. Roggin, A. Fehrenbach, A. Kendler, S. Sifri, R. Steele, A. Jimeno, F. Carey, I. Forgie, M. Mannelli, M. Carney, B. Hernandez, B. Campos, C. Herold-Mende, C. Jungk, A. Unterberg, A. von Deimling, A. Bossler, J. Galbraith, L. Jacobus, M. Knudson,

T. Knutson, D. Ma, M. Milhem, R. Sigmund, R. Madan, H.G. Rosenthal, A. Boussioutas, D. Beer, T. Giordano, A.M. Mes-Masson, F. Saad, T. Bocklage, L. Landrum, R. Mannel, K. Moore, K. Moxley, R. Postier, J. Walker, R. Zuna, M. Feldman, F. Valdivieso, R. Dhir, J. Luketich, E.M. Mora Pinero, M. Quintero-Aguilo, C.G. Carlotti, J.S. Dos Santos, R. Kemp, A. Sankarankuty, D. Tirapelli, J. Catto, K. Agnew, E. Swisher, J. Creaney, B. Robinson, E.M. Godwin, S. Kendall, C. Shipman, C. Bradford, T. Carey, A. Haddad, J. Moyer, L. Peterson, M. Prince, L. Rozek, G. Wolf, R. Bowman, K.M. Fong, I. Yang, R. Korst, W.K. Rathmell, J. L. Fantacone-Campbell, J.A. Hooke, A.J. Kovatich, C.D. Shriver, J. DiPersio, B. Drake, R. Govindan, S. Heath, T. Ley, B. Van Tine, P. Westervelt, M.A. Rubin, J. Il Lee, N.D. Aredes, A. Mariamidze, A comprehensive pan-cancer molecular study of gynecologic and breast cancers, Cancer Cell (2018), https://doi.org/10.1016/j.ccell.2018.03.014.

[453] E. Becht, L. McInnes, J. Healy, C.A. Dutertre, I.W.H. Kwok, L.G. Ng, F. Ginhoux, E. W. Newell, Dimensionality reduction for visualizing single-cell data using UMAP, Nat. Biotechnol. (2019), https://doi.org/10.1038/nbt.4314.

[454] M. Meylan, E. Becht, C. Sautès-Fridman, A. De Reyniès, W.H. Fridman, F. Petitprez, webMCP-counter: a web interface for transcriptomics-based quantification of immune and stromal cells in heterogeneous human or murine samples, 2020, https://doi.org/10.1101/2020.12.03.400754.

[455] N. Rusk, Expanded CIBERSORTx, Nat. Methods 16 (2019) 577, https://doi.org/10.1038/s41592-019-0486-8.

[456] C.B. Steen, C.L. Liu, A.A. Alizadeh, A.M. Newman, Profiling cell type abundance and expression in bulk tissues with CIBERSORTx, in: Methods Mol. Biol, Humana Press Inc., 2020, pp. 135–157, https://doi.org/10.1007/978-1-0716-0301-7_7.

[457] IgBlast tool. https://www.ncbi.nlm.nih.gov/igblast/, 2021 (accessed April 18, 2021).

[458] D.A. Bolotin, S. Poslavsky, I. Mitrophanov, M. Shugay, I.Z. Mamedov, E. V. Putintseva, D.M. Chudakov, MiXCR: software for comprehensive adaptive immunity profiling, Nat. Methods (2015), https://doi.org/10.1038/nmeth.3364.

[459] M.J.T. Stubbington, T. Lönnberg, V. Proserpio, S. Clare, A.O. Speak, G. Dougan, S. A. Teichmann, T cell fate and clonality inference from single-cell transcriptomes, Nat. Methods (2016), https://doi.org/10.1038/nmeth.3800.

[460] A. McKenna, M. Hanna, E. Banks, A. Sivachenko, K. Cibulskis, A. Kernytsky, K. Garimella, D. Altshuler, S. Gabriel, M. Daly, M.A. DePristo, The genome analysis toolkit: a MapReduce framework for analyzing next-generation DNA sequencing data, Genome Res. (2010), https://doi.org/10.1101/gr.107524.110.

[461] K. Cibulskis, M.S. Lawrence, S.L. Carter, A. Sivachenko, D. Jaffe, C. Sougnez, S. Gabriel, M. Meyerson, E.S. Lander, G. Getz, Sensitive detection of somatic point mutations in impure and heterogeneous cancer samples, Nat. Biotechnol. (2013), https://doi.org/10.1038/nbt.2514.

[462] S.A. Shukla, M.S. Rooney, M. Rajasagi, G. Tiao, P.M. Dixon, M.S. Lawrence, J. Stevens, W.J. Lane, J.L. Dellagatta, S. Steelman, C. Sougnez, K. Cibulskis, A. Kiezun, N. Hacohen, V. Brusic, C.J. Wu, G. Getz, Comprehensive analysis of cancer-associated somatic mutations in class i HLA genes, Nat. Biotechnol. (2015), https://doi.org/10.1038/nbt.3344.

[463] A. Szolek, B. Schubert, C. Mohr, M. Sturm, M. Feldhahn, O. Kohlbacher, OptiType: precision HLA typing from next-generation sequencing data, Bioinformatics (2014), https://doi.org/10.1093/bioinformatics/btu548.

[464] C. Lundegaard, K. Lamberth, M. Harndahl, S. Buus, O. Lund, M. Nielsen, NetMHC-3.0: accurate web accessible predictions of human, mouse and monkey MHC class I affinities for peptides of length 8-11, Nucleic Acids Res. (2008), https://doi.org/10.1093/nar/gkn202.

[465] T.J. O'Donnell, A. Rubinsteyn, M. Bonsack, A.B. Riemer, U. Laserson, J. Hammerbacher, MHCflurry: open-source class I MHC binding affinity prediction, Cell Syst (2018), https://doi.org/10.1016/j.cels.2018.05.014.

[466] B. Schubert, M. Walzer, H.P. Brachvogel, A. Szolek, C. Mohr, O. Kohlbacher, FRED 2: an immunoinformatics framework for Python, Bioinformatics (2016), https://doi.org/10.1093/bioinformatics/btw113.

[467] T. Trolle, M. Nielsen, NetTepi: an integrated method for the prediction of T cell epitopes, Immunogenetics (2014), https://doi.org/10.1007/s00251-014-0779-0.

[468] J. Hundal, B.M. Carreno, A.A. Petti, G.P. Linette, O.L. Griffith, E.R. Mardis, M. Griffith, pVAC-Seq: a genome-guided in silico approach to identifying tumor neoantigens, Genome Med. 8 (2016) 11, https://doi.org/10.1186/s13073-016-0264-5.

[469] J. Hundal, S. Kiwala, J. McMichael, C.A. Miller, A.T. Wollam, H. Xia, C.J. Liu, S. Zhao, Y.Y. Feng, A.P. Graubert, A.Z. Wollam, J. Neichin, M. Neveau, J. Walker, W.E. Gillanders, E.R. Mardis, O.L. Griffith, M. Griffith, PVACtools: a computational toolkit to identify and visualize cancer neoantigens, BioRxiv (2018) 501817, https://doi.org/10.1101/501817.

BBA - Reviews on Cancer 1878 (2023) 188913

Contents lists available at ScienceDirect

BBA - Reviews on Cancer

journal homepage: www.elsevier.com/locate/bbacan

Review

Multiple therapeutic approaches of glioblastoma multiforme: From terminal to therapy

Smita Kumari, Rohan Gupta, Rashmi K. Ambasta, Pravir Kumar *

Molecular Neuroscience and Functional Genomics Laboratory, Department of Biotechnology, Delhi Technological University, India

ARTICLE INFO

Keywords:
Glioblastoma multiforme
Combinatorial therapy
Nanotheranostic
Organoid models
Therapeutic strategies
Artificial intelligence
Personalized medicine

ABSTRACT

Glioblastoma multiforme (GBM) is an aggressive brain cancer showing poor prognosis. Currently, treatment methods of GBM are limited with adverse outcomes and low survival rate. Thus, advancements in the treatment of GBM are of utmost importance, which can be achieved in recent decades. However, despite aggressive initial treatment, most patients develop recurrent diseases, and the overall survival rate of patients is impossible to achieve. Currently, researchers across the globe target signaling events along with tumor microenvironment (TME) through different drug molecules to inhibit the progression of GBM, but clinically they failed to demonstrate much success. Herein, we discuss the therapeutic targets and signaling cascades along with the role of the organoids model in GBM research. Moreover, we systematically review the traditional and emerging therapeutic strategies in GBM. In addition, we discuss the implications of nanotechnologies, AI, and combinatorial approach to enhance GBM therapeutics.

1. Introduction

Glioblastoma multiforme (GBM) is defined as type IV brain cancer, which increases with the increase in age and exhibits a high prevalence rate in patients between 70 and 80 years old [1]. Mounting evidence highlighted the crucial role of various signaling pathways, such as the epidermal growth factor receptor (EGFR) pathway, Wnt/ β-catenin signaling event, fibroblast growth factor receptor (FGFR) pathway, PI3K/AKT/mTOR cascade, and other in the progression and pathogenesis of GBM [2]. For example, Boso et al., 2019 demonstrated the potential involvement of HIF-1α/Wnt signaling in neuronal differentiation of GBM stem cells, whereas Portela et al., 2019 concluded that the Wnt pathway activates JNK/MMP signaling loop that enhanced GBM progression [3,4]. Similarly, a study highlighted the importance of PI3K/AKT/mTOR as a putative therapeutic target in GBM, where the authors concluded that activation of the POU2F2-PDPK1 axis causes tumorigenesis through glycolysis and activation of PI3K/AKT/mTOR pathway [5]. Moreover, studying the mechanism and progression of GBM cells in the 2D culture model imposes various hurdles due to the absence of human microenvironment, and thus, the establishment of 3D model or organoid model was studied across the globe to extract the exact pathology of GBM [6]. For example, Weth et al., 2023 employed the

Abbreviation: GBM, Glioblastoma Multiforme; TME, Tumor Microenvironment; EGFR, Epidermal Growth Factor Receptor; FGFR, Fibroblast Growth Factor Receptor; LGG, Lower-Grade Glioma; RT, Radiotherapy; PDT, Photodynamic Therapy; AI, Artificial Intelligence; IDH, Isocitrate Dehydrogenase; GSCS, GBM Stem Cells; STAT1, Signal Transducer And Activator Of Transcription 1; SH2B3, SH2B Adaptor Protein 3; RECURRENT GBM, Recurrent GBM; HDAC, Histone Deacetylase; BET, Bromodomains And Extra-Terminal Motif; HH, Hedgehog; BBB, Blood-Brain Barrier; DOX, Doxorubicin; Tams, Tumor-Associated Macrophages; MDSCS, Myeloid-Derived Suppressor Cells; RB, Retinoblastoma; ROS, Reactive Oxygen Species; NP, Nanoparticle; DCS, Dendritic Cells; IPSC, Induced Pluripotent Stem Cells; TMZ, Temozolomide; PFS, Progression-Free Survival; OS, Overall Survival; IMRI, Intraoperative Magnetic Resonance Imaging; IOUS, Intraoperative Ultrasound; IORT, Intraoperative Radiotherapy; CIM, Confocal Intraoperative Microscope; IMS, Intraoperative Mass Spectrometry; OCT, Optical Coherence Tomography; ICIS, Immune Checkpoint Inhibitors; CAR, Chimeric Antigen Receptor; ACT, Adoptive T-Cell Transfer; Tils, Tumor-Infiltrate Lymphocyte; TAAS, Tumor-Associated Antigens; MSCs, Mesenchymal Stem Cells; TSCS, Therapeutic Stem Cells; 5-FC, 5-Fluorocytosine; HSV-TK, Herpes Simplex Virus Thymidine Kinase; CD, Cytosine Deaminase; ICG, Indocyanine Green; TTfields, Tumor-Treating Fields; LVS, Lentiviral Vectors; AVV, Adeno-Associated Virus; CRISPR, Clustered Regularly Interspaced Short Palindromic Repeats (CRISPR)/CRISPR Associated (Cas) Nuclease 9; RNAi, RNA Interference; SGT, Suicide Gene Therapy; DAMP, Damage-Associated Molecular Patterns; IGT, Immunostimulatory Gene Therapy; ICD, Immunogenic Cell Death.

* Corresponding author at: Department of Biotechnology, Molecular Neuroscience and Functional Genomics Laboratory, Delhi Technological University (Formerly Delhi College of Engineering), Room# FW4TF3, Mechanical Engineering Building, Shahbad Daulatpur, Bawana Road, Delhi 110042, India.
E-mail address: pravirkumar@dtu.ac.in (P. Kumar).

https://doi.org/10.1016/j.bbcan.2023.188913
Received 29 March 2023; Received in revised form 24 April 2023; Accepted 10 May 2023
Available online 12 May 2023
0304-419X/© 2023 Elsevier B.V. All rights reserved.

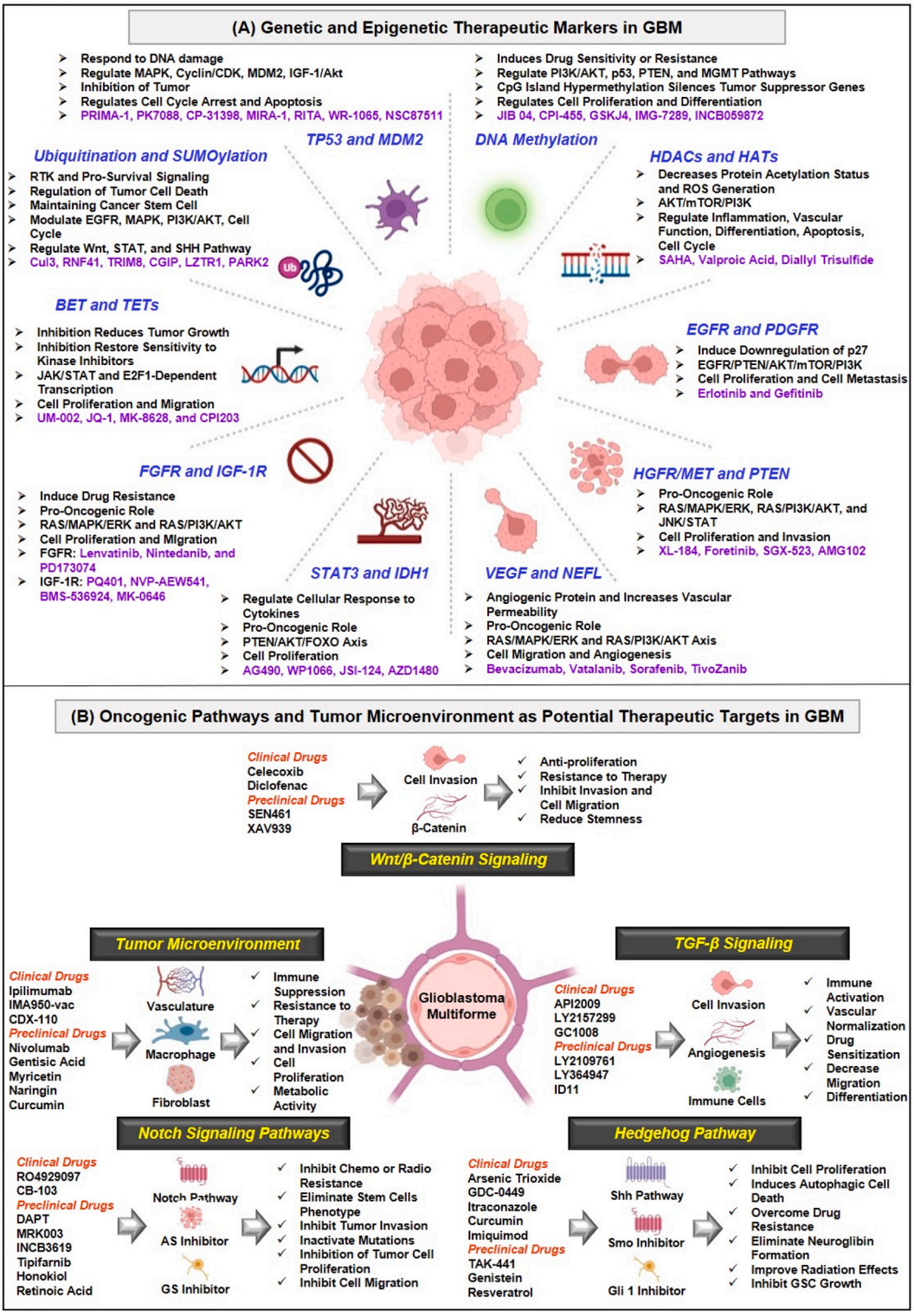

Fig. 1. (A) Genetic and epigenetic therapeutic markers in GBM: GBM is a multifactorial disease in which various genetic and epigenetic biomarkers have been implemented. For instance, STAT3, FGFR, PTEN, HGFR/MET, and IGF-1R are involved in cell proliferation, whereas, VEGF, NEFL, and BETs are involved in cell migration. Likewise, EGFR and PDGFR cause cell proliferation and cell metastasis, which can be inhibited by administering erlotinib and gefitinib. Ubiquitination and acetylation are two major lysine-induced post-translational modifications that regulate various signaling events in the pathogenesis and progression of GBM. Histone deacetylases and histone acetyltransferase modulate the cell cycle and apoptosis of GBM cells. DNA methylation is another epigenetic factor that regulates cell proliferation and differentiation by modulating PI3K/Akt and MGMT pathways. (B) Oncogenic pathways and tumor microenvironment as potential therapeutic targets in GBM: studies have confirmed the involvement of several signaling pathways, namely Wnt/β-catenin signaling, TGF-β signaling, Hedgehog pathway, and Notch signaling pathways in the pathogenesis and progression of GBM. Besides signaling pathways, tumor microenvironment plays a critical role in GBM etiology by modulating cell migration, proliferation, and differentiation.

cerebral organoid glioma 'GLICO' model for glioma screening applications, whereas Abdullah et al., 2022 established the patient-derived organoid model of lower-grade glioma (LGG) for identifying tumor immunology and identification of novel drug targets [7,8].

Standard treatment options involve chemotherapy, radiotherapy (RT), immunotherapy, and surgical resection, with low survival rates and high recurrence rates with adverse effects. Thus, there is utmost importance in developing novel therapeutic strategies to enhance the overall survival rate of GBM patients [9,10]. For instance, Yin et al., 2022 demonstrated that combined administration of ultrasmall Zirconium carbide nanodots and RT enhanced the therapeutic efficiency both *in vitro* and *in vivo* [11]. Herta et al., 2022 demonstrated that the Raman spectroscopy-enabled method effectively identifies tumor-infiltrated brains with higher sensitivity but lower specificity compared to the current standard of 5-aminolevulinic acid [12]. Recent studies emphasized the implementation of treatment strategies, such as adoptive cell therapy, gene therapy, viral and non-viral vectors-based therapy, RNA interference therapy, photodynamic therapy (PDT), photothermal therapy, stem-cell-based therapy, and vaccine therapy that exhibit promising primary outcomes in both experimental as well as clinical studies [13–16]. For example, Abbott et al., 2021 employed retained display antibody platform to develop single-chain variable fragments that have the potential to recognize epidermal growth factor receptor mutant variant III (EGFRvIII). The authors demonstrated that despite the higher affinity, GCT02 CAR T cells kill equivalently but secrete lower amounts of cytokine. In addition, GCT02-CAR T cells also mediate rapid and complete tumor elimination *in vivo* [17]. Likewise, Xu et al., 2022 concluded that targeted PDT of GBM cells induced by platelets marked the presence of DNA damage, reduced viability, and cell death [18]. Deciphering the mechanism of oncogenic signaling targets and TME biomarkers as therapeutic targets in GBM. Herein, we presented an overview of the therapeutic targets involved in the progression and pathogenesis of GBM, followed by the role of an organoid model in identifying therapeutic targets and enhancing the current knowledge of GBM pathology. Afterward, we discussed the current standard treatment options and emerging treatment options for reversing the GBM pathology. We also compelled the emerging status of artificial intelligence (AI) in the etiology of GBM through personalized medicine and drug repositioning methods. Lastly, we briefly explain the role of combination therapy and the clinical status of the drug molecules that can reverse or inhibit GBM progression and pathogenesis.

2. Mechanistic involvement of therapeutic targets in the progression and pathogenesis of GBM

GBM molecular patterns can partially predict clinical results and treatment outcomes. Recent discoveries related to genetic and epigenetics markers have been discussed in the current review article. For example, isocitrate dehydrogenase (IDH) mutation (R132 for IDH1, R140 or R172 for IDH2) is a crucial and defining factor in glioma formation and development, and it may be a critical target for treatments [19,20]. Another marker is signal transducer and activator of transcription 1 (STAT1), and research shows STAT1 transcribes SH2B adaptor protein 3 (SH2B3), predominantly expressed in GBM stem cells (GSCs), is significantly expressed in GBM and is associated with poor prognosis. The formation of xenograft tumors *in vivo* and the proliferation, migration, and self-renewal of GBM cells are all significantly hampered by targeting SH2B3 [21]. Studies showed gene therapy and vaccination are two methods to restore wild-type p53 into cells with mutant p53. Additional approaches include using p53-MDM2 targeted drugs (such as Nutlins or RITA) to stop the association between p53 and MDM2 and enable p53 to trigger cell senescence. Agents that connect to mutant p53 (such as PRIMA-1, PhiKan083, SCH529074, MIRA-3, and STIMA-1) and convert it to a wild-type form are included in a strategy that targets mutant p53 [22]. Another crucial factor is angiogenetic therapeutic indicators. Apart from VEGF, VEGFR, and neuronal markers NEFL, recently published studies have shown that human gliomas have significant levels of the novel angiogenic biomarker ELTD1. Anti-ELTD1 therapy dramatically improved survival, decreased tumor sizes, normalized the vasculature [23,24]. In addition, major receptor tyrosine kinases (RTK) targets include VEGFR as well as the hepatocyte growth factor receptor (HGFR/MET), FGFR, platelet-derived growth factor receptor (PDGFR), and EGFR. Following the FDA's approval of Bevacizumab to target the VEGFR2 in adult patients with recurrent GBM, targeted therapy against RTKs (Afatinib, Sunitinib, PLB-1001, and Osimertinib) has emerged as a novel treatment option [25]. Moreover, metastasis, chemo- and radio-resistance in GBM are connected to the loss of PTEN gene (therapeutic marker) activity. It is widely known that several epigenetic, transcriptional, and post-translational processes regulate PTEN's expression and function, pointing to the fact that PTEN is a crucial regulator of tumor sensitivity to various therapeutic modalities [26]. However, histone deacetylase inhibitors (HDACi) and DNA methyltransferase inhibitors have recently been utilized to treat malignancies, either separately or in combination, as part of epigenetic therapy. Many effective small drugs, such as 85P Mocetinostat (MGCD0103), Valproic Acid, SAHA, PXD101, and Beleodaq®, target HDAC, HATs enzymes, bromodomains and extra-terminal motif (BET) [27,28]. Currently, HDACi-based radiopharmaceuticals, such as [18F] TFAHA, can potentially treat GBM, and their use alongside other therapies is likely to bring advantages to GBM patients [29]. Studies demonstrated that epigenetic reader proteins with BET domains were promising therapeutic targets in GBM. Jermakowicz et al., 2021 developed the novel BET inhibitor UM-002 (targets BRD4 bromodomain), which entered the brain and suppressed genes associated with cell cycle and invasion [30]. DNA methylation is another interesting therapeutic target. In GBM, CpG promoter hypermethylation occurs at genes with diverse functions related to tumorigenesis and tumor progression, including cell cycle regulation (CDK2A-p16INK4a and CDK2B-p15INK4b), tumor suppression (RB1, VHL, EMP3, RASSF1A, and BLU), DNA repair (methylguanine DNA methyltransferase (MGMT) and MLH1), inhibition of apoptosis (DAPK1, TIMP3, CDH1), and genes associated with angiogenesis, regulation of tumor invasion, and chemoresistance. O^6-MGMT promoter methylation modulates sensitivity to drug Temozolomide (TMZ) and RT in GBM [31]. Babaeenezhad et al., 2022 showed that global DNA methylation provided a novel molecular mechanistic insight into the epigenetic silencing of peroxisome proliferator-activated receptor gamma (PPARγ) in GBM patients, suggesting that this tumor marker may be important for the GBM pathogenesis [32]. Li and colleagues further demonstrated that miR-148-3p suppressed proliferation, migration, and invasion of GBM by influencing the DNMT1-RUNX3 axis and the EMT (N-cadherin, vimentin, MMP-2, and MMP-9) in GBM [33]. However, Decitabine, a DNMT inhibitor, has been demonstrated to demethylate the STING promoter's cg16983159, turning on STING expression and activating the cGAS-STING signaling pathway, making GBM cells more susceptible to immunotherapies (converting 'cold' TME into 'hot' TME) [34]. Finally, ubiquitination governs apoptosis, GSCs, and the activation or inactivation of tumorigenic pathways in GBM. The ubiquitination pathways' molecular targets, Cul3, RNF41, TRIM8, CGIP, LZTR1, and PARK2, were intensively investigated in GBM. Several deubiquitinase, such as HAUSP, OTUB1, USP1, USP3–8, *etc.*, are implicated in the development of tumors. Bortezomib, MG132, and Saquinavir, drugs with anti-glioma action by UPS targeting [35]. Fox et al., 2019 underlined the important protein SUMOylation plays in the pathobiology of GBM. E1 (SAE1), E2 (Ubc9), and E3 (PIAS1 and 3) components as well as a SUMO-specific protease (SENP1) are potential therapeutic targets in GBM. Recently, it was discovered that topotecan inhibits global SUMOylation in GBM, which lowers levels of CDK6 and HIF-1 and causes substantial alterations to cell cycle progression and metabolic activity [36]. Focusing on the genetics and epigenetics of GBM and the effects of its mutations has thus brought attention to various therapy modalities targeting therapeutic markers in combating GBM (Fig. 1a).

3. Deciphering the mechanism of oncogenic signaling targets and tumor microenvironment biomarkers as therapeutic targets in GBM

3.1. Oncogenic signaling events

The Wnt signaling pathway is associated with different stages of GBM due to its being involved in glioma genesis, TMZ and radioresistance (feedback by DNA repair genes), maintenance of GSCs (due to PLAGL2, FoxM1, Evi/Gpr177, and ASCL1 regulators), migration and invasion (upregulation of ZEB1, SNAIL, TWIST, SLUG, MMPs, and N-cadherin). Studies using transcriptomics data showed that β-catenin, Dvl3, and cyclin D1 were significantly higher in glioma specimens compared to non-tumor brain tissue, while studies using proteomics data showed that β-catenin, TCF4, LEF1, c-MYC, n-MYC, and cyclin D1 were significantly higher in glioma samples [37,38]. Wnt's context-dependent activity and crucial part in maintaining the homeostasis of healthy tissues have led to the recognition of Wnt as a hallmark of therapeutic challenge [39]. Kouchi et al., 2017 have discovered (pro) renin receptor (PRR) plays a crucial part in the development of the GBM cell line (U251MG, U87MG, and T98G) by abnormal activation of the Wnt signaling pathway and has the ability to function as a therapeutic and prognostic marker [40]. Another small drug, SEN461, reduced the survival of cultured glioma cell lines and decreased the size of subcutaneously implanted xenograft tumors by inhibiting the WNT/β-catenin pathway involving Axin stabilization and a process partially sensitive to tankyrase (TNKS) enzymes [41]. In phase, I/II research for patients with advanced cancer, including TNBC, NSCLC, Colorectal, and GBM (NCT02038699), the dopamine receptor D2 (DRD2) antagonist ONC201 significantly suppressed CSCs and repressed the expression of CSC-related genes in GBM tumors by inhibiting the Wnt signaling pathway [42]. Moreover, Bagherian et al., 2020 discovered that Wnt signaling is the mechanism through which TMZ + curcumin or nano micellar-curcumin inhibits GBM [43]. Moreover, the phase II clinical trial of GBM tests different drugs, including isotretinoin and thalidomide (NCT00112502).

Hedgehog (HH) signaling induced the transcription of a group of oncogenic proteins, such as Bmi1, Myc, and VEGFA, which aided proliferation, invasion, and angiogenesis. Many cancers, including GBM, are driven by tumorigenesis, which is caused by abnormal HH pathway activation [44]. SMO inhibition was beneficial in glioma lines that overexpressed Gli, suggesting that HH signaling is probably a driver in a subset GBMs. Wu et al., 2021 demonstrated that SMO-193a.a., a novel protein encoded by circular SMO, is essential for HH signaling, promotes the growth of GBM tumors, and represents a new target for the treatment of GBM [45]. LDE225 (25 μM), Shh inhibitors alone or in combo with Rapamycin (100 nM, mTOR inhibitor) exhibit additive impact in lowering cell viability of $CD133^{+}$ GSCs by encouraging the transition of LC3-I to LC3-II and stimulates autophagy through mTOR independent pathway which could potentially conquer chemoresistance in GBM [46]. In the C6 cell line, a different drug called Naringenin (114 g/mL, flavonoid) increased the expression of Sufu at the protein level while decreasing the transcription of Gli-1 and SMO [47]. In addition, another study revels Chidamide (HDAC1, HDAC2, HDAC3, and HDAC10 inhibitor) inhibits the proliferation, migration, and invasion of U87MG and HS683 cell lines by induction of oxidative stress (increased expression of ROS and NOX2 expression) through the miRNA-338-5p regulation of HH signaling [48]. Vismodegib (GDC-0449, SMO inhibitor), when combined it Robotnikinin (PTCH1 transmembrane antagonist), was more efficient in reducing proliferation, invasion, and migration in the U87-MG cell line than when administered alone [49]. Similarly, Bureta et al., 2019 studied the synergistic effect of Vismodegib/ arsenic trioxide (HH pathway inhibitor) with TMZ to inhibit tumor growth in GBM pathogenesis [50]. For the first time, Linder et al., 2019 demonstrated that Arsenic Trioxide and (−)-Gossypol synergistically attack GSC-Like cells by suppressing both HH and Notch Signaling [51]. An ongoing phase I/II clinical trial (NCT03466450) included 75 participants undergoing combination therapy, including Glasdegib (PF-04449913, SMO inhibitor). Furthermore, it has been revealed that the organic chemical GANT-61, a hexahydropyrimidine derivative that selectively inhibits Gli transcription factors, can lower PD-L1 expression and tumor cell proliferation in both *in vivo* and *in vitro* setup of gastric cancer [52]. The HH route may also be a potential immunotherapy target for treating GBM. Nonetheless, it is still unclear how anti-PD-1 antibodies counteract GBM resistance by activating HH signaling. Despite the fact that the use of HH inhibitors in GBM hasn't been thoroughly studied, many studies have shown that using HH inhibitors in addition to standard therapies can significantly boost efficacy and lower the occurrence of drug resistance [44]. More clinical trials are also recommended to confirm whether HH inhibitors are advantageous to the therapeutic potential of GBM.

Increasing data indicate that Notch signaling is extremely active in GSCs, where it delays differentiation and preserves stem-like characteristics, promoting the development of tumors and resistance to standard therapies. Notch was inhibited with the γ-secretase inhibitors DAPT, MRK-003, GSI-18, LLN1eCHO, L-685,458, Dibenzazepine, γ-secretase inhibitor X. α-secretase ADAM17 inhibitor including GW280264X, INCB3619, ADAM17 short hairpin RNA [53]. Alternative treatment options targeting the notch pathway were Arsenic Trioxide [54] (decreases expression of Notch 1–4), Niclosamide [55] (reduces NOTCH 1), Retinoic Acid (inhibition of neurosphere growth, decreased clonogenicity, and decreased CSCs markers), Resveratrol [56]. In GBM, miRNAs that Notch governs include miR-34a, miR-34a-5p, miR-34c-3p, miR-34c-5p, miRNA-181c (downregulated in GBM) and miR-148a, miR-31, miRNA-33a, miRNA-18a (upregulated in GBM) which impede their translation or cause their instability and degradation [57]. Wan et al., 2013 have discovered that miR-125b inhibition/knockdown increases the susceptibility of human primary GBM cells to TMZ and inhibits migration and invasion through inhibiting the NOTCH 1 receptor [58]. Further knowledge of this signaling system is required since failures in clinical trials with Notch inhibitors may be attributed to their contradictory effects on the tumor *vs.* the tumor vasculature [59]. Herrera-Rios et al., 2020 compared first-in-human tested Brontictuzumab antibody against Notch1 with MRK003. They found that Brontictuzumab treatment affects the Notch pathway by inhibiting transcription of Hes1/Hey1 genes and considerably decreasing cleaved Notch1 receptor protein quantity, hindering cellular invasion in GSCs [60]. Indeed, Ma and colleagues found that farnesyltransferase inhibitors (FTIs, Tipifarnib) significantly increased sensitivity to γ-secretase inhibitors (RO4929097). Through suppressing two major pathways AKT and cell cycle progression, this combination revelled antineoplastic and radiosensitizing activities in GSCs [61]. Clinical investigations focusing on Notch pathways in GBM are still being conducted. For instance, the Phase II clinical trials of RO4929097 for recurrent GBM demonstrate a 6-month PFS as well as a 50% reduction in the growth of neurospheres in fresh tissue [62]. Moreover, Kumar et al., 2022 employed carbon ion radiation to minimize spheroid formation, suppress stemness and prevent glioma cells from migrating, perhaps by inhibiting the expression of the stable Notch1 intracellular domain [63]. Further, the multifunctional cytokine TGF-β is essential for immune responses, tissue wound healing, adult tissue homeostasis, and development. TGF-β signaling dysfunction has been linked to initiating and developing numerous tumor forms, including GBM, and maybe a therapeutic target [64]. For instance, Zhu et al., 2022 demonstrated that a biomimetic blood-brain barrier (BBB)-penetrating albumin nanosystem altered by a brain-targeting peptide was created for co-delivering a TGF-β receptor I inhibitor (LY2157299) and an mTOR inhibitor (Celastrol). The albumin nanosystem can suppress STAT3 signaling, which lowers TGF-1 production and triggers cell death, to target nAChRs that are overexpressed on both BBB and glioma cells and transform TAM to M1 phenotype [65]. (Fig. 1b)

3.2. Tumor microenvironment as therapeutics markers

The GBM microenvironment comprises immune cells, fibroblasts, endothelial cells, pericytes, GBM cells, GSCs, and ECM. The primary factor behind GBM's inadequate therapeutic impact is the TME [66]. Drug distribution *via* BBB crossing is one of the biggest challenges. In order to improve the effectiveness of drugs while minimizing their negative effects, cell-mediated drug delivery systems have been suggested as a potential technique in the cancer treatment process. Including the use of magnetic mesoporous silica NPs, liposomes, albumin NPs, and PLGA NPs, Hosseinalizadeh et al., 2022 employ neutrophils as Trojan horses for the delivery of drugs. Cytokines IL-8 activate neutrophils that show anticancer activity by developing neutrophil extracellular traps, allowing the concurrent release of NPs and delivery of chemotherapeutic drugs [67]. Besides, Li et al., 2021 constructed ZGO@TiO2@ALP-NEs, in which ZGO@TiO entraps paclitaxel and neutrophils to deliver anti-PD-1 antibodies. This can cross the BBB and move into tumor locations for enhanced and prolonged precision therapy, improving survival rates from 0% to 40% and providing long-term immuno-surveillance for tumor recurrence [68]. Similar to this, another team used a bioinspired neutrophil-exosome (NEs-Exos) delivery system to treat glioma using loaded doxorubicin (DOX) [69]. Another strategy is to use Tumor-associated macrophages (TAMs), which can be targeted in various ways, as possible therapeutic targets in the battle against GBM. By blocking the chemokine signaling that draws TAMs to the TME, one can interfere with the recruitment of TAMs to the tumor. A second approach is to boost anti-tumor immune responses by producing more TAMs with anti-tumor M1 characteristics. A third method minimizes the abundance of pro-tumor M2-like TAMs, which may enhance anti-tumor immune responses and ultimately slow tumor growth [70]. TAM expresses CSF1R, and BLZ-945, an inhibitor of this receptor, decreases M2 polarisation, improving radiation effectiveness and reducing immune suppression in GBM [71]. Additional TAM-expressed markers like CD39, CD73, CD163, and CD204 may be exploited as therapeutic targets [70]. Cancer-associated fibroblasts (CAFs), the most prevalent cells in the tumor stroma, are a major cellular component of the TME and play a crucial role in developing chemoresistance. CAFs also produce a significant tumor-promoting effect and physical barriers that prevent the delivery of nanomedicines by secreting pro-tumorigenic cytokines, increasing interstitial fluid pressure (IFP), and nonspecific internalization. Recent advancements in CAF-targeted nano-delivery methods increase the sensitivity of anti-tumor therapies by reversing malignancy, immunosuppression, or drug resistance in the TME [72,73]. It is well-established that Myeloid-derived suppressor cells (MDSCs) contribute significantly to the immunosuppressive TME [74]. Research showed that cell surface markers such as CD33, CD15, CD11b, and CD66b are not great for the differentiation of these populations. Hence, the identification of transcription factors, including CCAAT/enhancer-binding protein (C/EBP), retinoblastoma (RB), and Signal transducer and activator of transcription (STAT3), as well as immune-regulatory substances such as arginase1 (Arg1), Nitric oxide (NO), and Reactive oxygen species (ROS) should be taken into account [75]. The CCR2 antagonist, CCX872, reduced MDSCs and enhanced anti-PD-1 therapy in the GBM mouse model [76]. A promising therapeutic target is the macrophage inhibitory factor (MIF), also produced by glioma cells and regulates MDSC migration into the brain. Sulforaphane and Ibudilast, a MIF inhibitor, reduced the formation of MDSC and were toxic to glioma cells [74,77]. To increase the synergistic benefits of radiation for brain cancer, Wu et al., 2019 created a zinc-doped iron oxide nanoparticle (NP) with a cationic polymer surface that can attack both tumor cells and the immunosuppressive TME [78]. Further, the recruitment of Dendritic cells (DC) to the brain and spinal cord through either afferent lymphatics or high endothelial venules. Current studies reveal a complicated interaction between DCs, microglia and macrophages, T-cells, and tumor cells in the TME, while the precise involvement of DCs in the context of GBM is still being clarified [79]. According to a study by Wang et al., 2020 exosomal LGALS9, produced by GBM cells, inhibits DC antigen presentation and cytotoxic T-cell activation in the cerebrospinal fluid (CSF), and that loss of this inhibitory action can result in long-lasting systemic antitumor immunity [80]. Another study found that glioma-associated antigens, like the NY-ESO-1 peptide, can be combined with bioengineered recombinant vault nanoparticles to promote the maturation of native DC and trigger an anti-tumor response [81]. Active immunotherapy called DC vaccination (DCV) aims to trigger an anti-cancer immune response. Hundreds of GBM patients have been vaccinated in numerous DCV trials, which have confirmed the vaccine's viability and safety [82]. Until this moment, no Phase III clinical trial for DC vaccines in GBM has successfully met its goals and effectively implemented clinical development and transformation. Targeting combination therapy methods will be a breakthrough in treating GBM with the DC vaccination [83]. (Fig. 1b)

4. Technical approaches to study drug treatment and response in glioblastoma

In vitro and *in vivo* models of human GBM have significant promise for improving our knowledge of the pathophysiology of these tumors as well as for facilitating the creation of new therapeutic approaches. Glioma models, however, must adhere to particular and more stringent requirements than other cancer models, and these requirements are directly related to the confluence of genetic aberrations and the brain micro-environment gliomas grow in. The development of GBM therapies is hampered by the lack of acceptable and trustworthy *in vitro* models that should direct the selection of *in vivo* GBM animal models. Preclinical testing will move faster with 3D *in vitro* models, which will help design an efficient treatment for GBM [84,85].

4.1. 2D and 3D models of glioblastoma in drug discovery and development

Standard two-dimensional (2D) culture involves layering cells on an extremely rigid plastic substrate, which is subsequently kept alive with a solution that contains ECM proteins. The development of 2D cell cultures has facilitated the identification of numerous biological and pathological processes [86]. Immortalized cell lines are incapable of replicating key characteristics of primary tumors, including stemness, genetic heterogeneity, improper cell density, gradients of media ingredients, oxygen content, immune-mediated environment, and TME, in 2D culture. This platform is excellent for running functional experiments with commercially available and specialized test kits, examining cell morphology, several imaging techniques, and staining with antibodies [87]. Hence, it appears crucial to design new *in vitro* models that are more accurate and practical in order to get greater understanding about the molecular biology and treatment of GBM [88]. In contrast to the 3D model, where cells are in the centre of the (non-vascularized) organoid, cells in 2D culture are often immersed in the drug-containing culture medium that is readily available to all cells in culture, which may explain the higher efficacy of drug treatment evident in this model [89]. Lenin et al., 2021 executed a comprehensive examination of molecular processes that contribute to GBM growth by testing 65 drugs for their ability to eliminate patient derived GSCs in 2D culture and GBOs in 3D culture. Researchers identified a group of drugs from the evaluation that displayed various sensitivity on various patient-derived *in vitro* models. In addition, they discovered that the TERT inhibitor castanoside was successful in suppressing the cell viability of primary tumor models along with tumor models that have previously received chemotherapy and radiotherapy [90]. Researchers have developed and explored various multicellular 3D tumor models such as Cocultures, Spheroids, and Scaffolds. In an interesting study microglia were co-cultured with GBM cells in a 2D model, and it was discovered that their presence led to treatment resistance; however, this shielding effect was raised when the same cells were maintained in 3D model [88]. In addition, scaffolding-

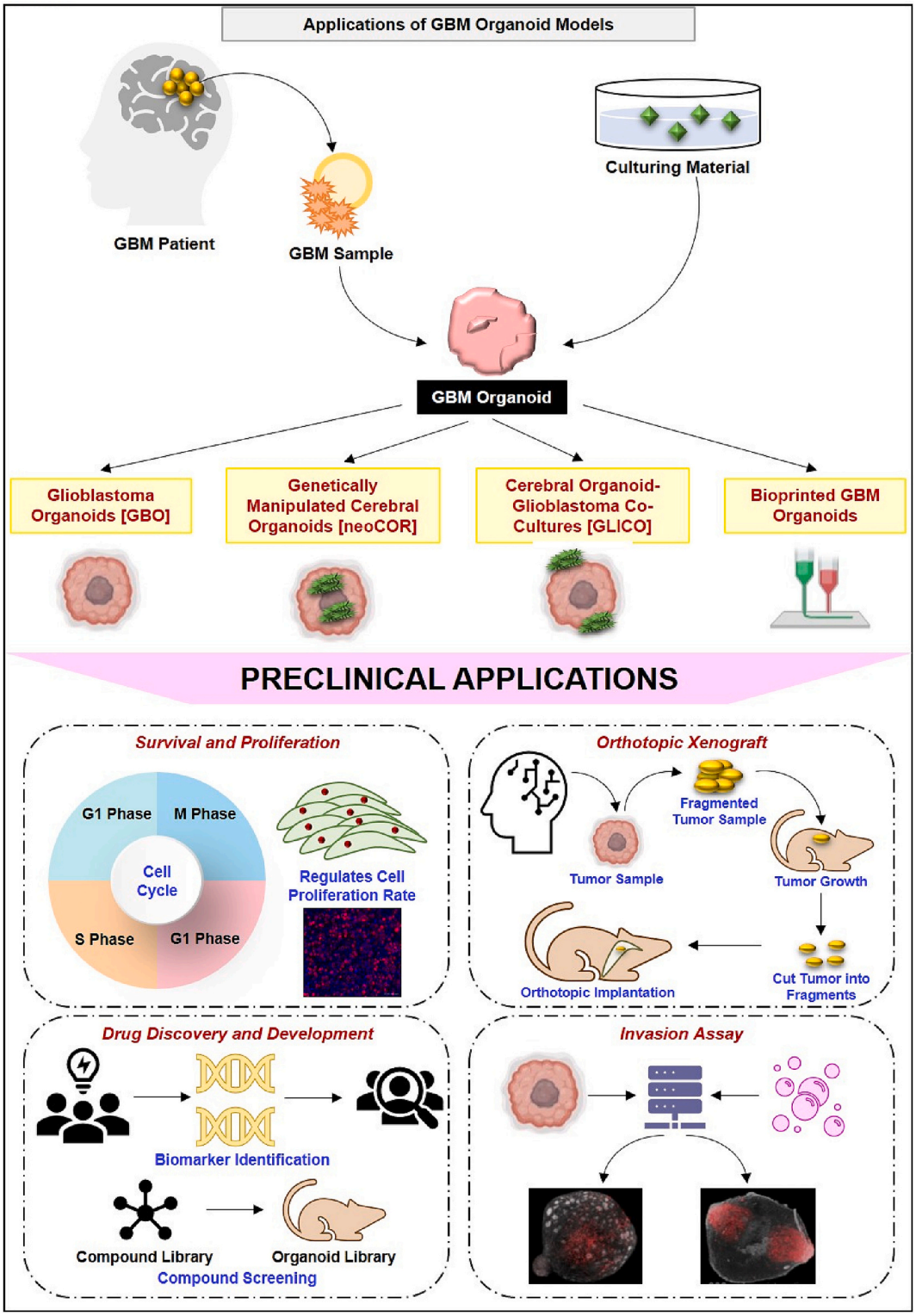

Fig. 2. Applications of GBM organoid models: Due to the limitations of the 2D culture models, researchers across the globe have developed 3D organoid models, namely glioblastoma organoids, genetically manipulated cerebral organoids, cerebral organoid glioblastoma co-culture, and bioprinted glioblastoma organoids to study the GBM etiology, which can be used in preclinical applications, such as survival and proliferation, orthotopic xenograft, drug discovery and development, and invasion assay.

supported models imitate the biochemical and mechanical properties of ECM. Various forms of scaffold, including hydrogels, fibrous materials, and porous materials [84]. A hydrogel called Matrigel, which combines mouse collagen, laminin, and ECM-associated growth factors, is frequently employed in GBM cultures to allow cells to develop while interacting across various sides [91]. Gelatin methacrylate hydrogels culture model and matrigel-coated 3D polystyrene scaffolds were previously employed extensively to investigate drug effectiveness, morphological structures in human cancer, and invasion [92]. Drawbacks of matrigel coating include its sarcoma tumor-derived origins,

predominant collagen and laminin composition, and lax quality control. It is challenging to guarantee that each batch comprises exactly the same amount of each component since it is isolated from mice tumors [92]. Florczyk et al., grown GBM cells over chitosan and hyaluronic acid (HA) polyelectrolyte complex 3D porous scaffold and discovered that it enhanced tumor spheroid formation and stem-like characteristics of GBM cells by increasing the expression of CD44, Nestin, Musashi-1, GFAP, and HIF-1α as compared with 2D cultures [93]. Additionally, the Neurospheres model, which grows GSCs in suspension and transfers them to a PEG and gelatin scaffold coated with geltrex to allow for 3D growth, assures that the cells being analyzed are tumorigenic and may be an important target for anti-glaucoma treatment [84,94]. In case of Spheroids culture Multicellular cell (cells from GBM patient resection) aggregates produced as spheres in a suitable culture medium, such as a polyethylene glycol/polyvinyl alcohol/polylactide-*co*-glycolide/polycaprolactone matrix. This will stimulate stemness marker expression, cell-to-cell and cell-matrix interaction, angiogenicity, and the release of cytokines and chemokines, with the main drawback being an increased spheroid size due to the diffusion gradient [95]. In addition to spheres, other 3D models are microfluidic system. Cells from a GBM patient's excision are cultivated in a microfluidic system using alginate hydrogel tubes that are filled with circulating medium. It serves as a highly helpful tool for analyzing GBM cell behavior, their relationship to tumor malignancy, and the effectiveness of various pharmacological treatment since it mimics the *in vivo* brain milieu [96]. The organ-on-a-chip model, commonly referred to as organ chips, is the result of recent developments in microfluidic chips. Organ chips are produced through computer microchip manufacture and filled with living cells that mimic the physiology and pathology of actual organ [97]. Through the use of a type 1 collagen hydrogel, a meticulous experiment was carried out to create a blood-brain barrier chip (BBBC) model that mirrored the *in vivo* configuration of micro blood arteries in the brain [98]. Glioma stem cell-derived 3D tumor sphere models are unable to communicate with the ECM elements and TME cells. Finally, when immunodeficient mice are used in animal models, they fall short of accurately simulating human anti-tumor immune responses. To create humanized GBM models, which were based on the 3D culture of GBM cells in a framework that replicated the microenvironment of human brain tumors, it was necessary to improve the *in vitro* techniques.

4.2. Contribution of organoid models of glioblastoma in drug discovery and development

The limitations of current preclinical GBM models (2D culture models) include the absence of a "normal" human microenvironment, which includes the absence of interactions between cancer cells, immune cells, GSCs, and their TME, as well as oxygen, nutrient, and pH microenvironment gradients. Additionally, tumor cell lines cannot accurately understand the pathogenesis and characteristics of GBM. Hence, to overcome the above limitation, 3D models of cancers, including tumor organoids, patient-derived xenografts (PDXs), and genetic mouse models, were developed, and they were superior in recapitulating the primary tumor characteristics. A novel 3D culture technique called the organoid model mimics the tumor conditions found in patients to help researchers better understand the biology of GBM [99] (Fig. 2). Induced pluripotent stem cells (iPSC) or patient-derived stem cells are embedded in a matrigel matrix and grown using a variety of growth factors to produce organoids. These cells divide and self-organize within a few days to form an organic structure that resembles the structure and function of an organ *in vivo* [100].Various possible organoid models were (a) *Patient-derived GBM organoid* was produced using enhanced cerebral organoid techniques that compromised sphere-forming CSCs in matrigel. Patient-derived organoids have the capacity to multiply while maintaining their tumorigenicity. Jacob et al., 2020 published a method that radically reduces the time required for creating Glioblastoma organoids (GBO) in a specific culture medium straight from fresh tumor specimens without single-cell separation (by microdissection of tissue into small pieces) [90]. GBO xenografts were highly invasive to neighboring tissue. Recently, Alicja et al., 2021 studied the efficacy and anti-GBM therapeutic potential of Monensin analog in GBM organoids as well as in host: tumor organoid model developed from iPSCs [101]. In the same year, Zhang et al., 2021 developed novel integrated systems encompassing patient-derived glioma cerebral organoids and xenografts for personalized treatment through drug screening and prediction of chemotherapeutic drug response [102]. (b) *Genetically engineered GBM organoids* are generated by genetically altering healthy tissue stem cells or cerebral organoids to facilitate tumor growth. This contains both tumor and healthy tissue, enabling the investigation of brain-tumor interactions. Bian et al., 2018 created a 3D *in vitro* model, termed neoplastic cerebral organoid (neoCOR), which recapitulates the development of brain tumors by incorporating oncogenic mutations in cerebral organoids derived from iPSCs by transposon and CRISPR/Cas9 based genome editing techniques [103]. They checked Afatinib concentration on different neoCOR models for 40 days and found a significantly lower number of GBM cells in neoCORs with EGFR overactivation because of the strong effect of the inhibitor. Hence, this model can be used to evaluate the drug mechanism and efficacy of all cancer caused by mutations [99]. NeoCOR tumors that develop within cerebral organoids made from iPSCs, which resemble a normally developing human brain, contrast with GBO, which is fully tumor and hence might be considered "tumoroids." This model is useful for simulating the glioblastoma start process, but it fails to adequately capture the genetic complexity of heterogeneous human tumors, limiting its applicability for drug discovery. To counteract this benefit, a new superior model was created that is (c) *Co-culture of iPSC/human embryonic stem cells organoids and GSC* [GLICO model]: this approach involves combined benefits of GBO and neoCOR model. Da Silva et al., 2018 and Linkous et al., 2019 established this model by showing that brain organoids could be co-culture with patient-derived cells, providing a great opportunity to study brain-tumor interaction (if GBM cells and organoids derived from the same patient source) [9]. Importantly, the research indicates that the GLICO model retains the parental tumor's important genetic traits and molecular signaling network. Moreover, because it is cultivated *in vitro*, the model is excellent for experimental manipulation, therapeutic interventions, efficient environmental and physiological parameters control, and high-throughput drug screening [106]. This model shows that patient-derived GBMs responded differently to different chemotherapeutics, such as patients' samples grown in 2D culture showed higher efficacy of TMZ drug as compared to bischloroethyl nitrosourea (BCNU) in contrast to GLICO models where BCNU treated samples was better than TMZ. As a result, the model is more scalable, allowing several patient-specific GLICOs to be generated for high-throughput drug screening [104]. Besides, these models have limitations as they lack vascularization, immune cells and lack of standardization and automated protocol [6]. It is therefore challenging to examine the effects of therapy (including immunotherapy), drug resistance, and angiogenesis. A different approach is to use an *in vitro* tumor model that resembles the *in vivo* TME for examining gliomagenesis and drugs resistance. In 2016, Dai et al. established a 3D bioprinted glioma stem cell model using an altered porous gelatin/alginate/fibrinogen hydrogel that imitates the ECM structure. This allowed GSCs to retain their intrinsic cancer stem cell and differentiation properties. However, TMZ drug sensitivity studies revealed that the 3D printed tumor model was less responsive to the drug than the 2D monolayer model at TMZ doses of 400–1600 g ml-1 [107]. (d) *Bioprinted GBM Organoids* are a more advanced technique that constructs volumetric, biomimetic microenvironments and can allow for improved mimicking molecular and clinical properties of the GBM microenvironment. It aids in angiogenesis and GSCs research [108]. Yi et al., 2019 developed an extrusion-based 3D-bio printed GBM model (GBM-on-a-chip) incorporating several cell types such as vascular endothelial cells, patient-derived tumor cells and decellularized porcine 'bio ink' brain consistent with ECM proteins.

Table 1
Various 3D models of glioblastoma involved in drug discovery and development.

Model	Drug	Target	Experimental Study	Outcomes	References
GBM spheroids	Temozolomide	HIF1A	GBM spheroids consisting of U87 or patient-derived GBM cells were encapsulated in soft (~1 kPa), stiff (~7 kPa), and dual-stiffness polyethylene glycol-based hydrogels and analyzed for viability, size, invasion, laminin expression, hypoxia, and proliferation	U87 spheroids were equally responsive to TMZ in the soft and stiff hydrogels, but cell viability in the spheroid periphery was higher than the core for stiff hydrogels. Patient-derived GBM spheroids did not show stiffness-dependent drug responses	[116]
GBM spheroids	Traditional Chinese medicine (TCM) musk	Transferrin receptor (TfR)	The drug penetrating ability into tumor spheroids were visualized using confocal laser scanning microscopy (CLSM). *In vivo* glioma-targeting ability of formulations was evaluated using whole-body fluorescent imaging system	The results showed that muscone and RI7217 co-modified DTX liposomes enhanced uptake into both hCMEC/D3 and U87-MG cells, increased penetration to the deep region of U87-MG tumor spheroids	[117]
GBM spheroids	Gemcitabine	Apoptosis markers	The vastly greater GBM cell-killing potency of Gem compared to the gold standard temozolomide is confirmed, moreover, it shows neuronal cells to be at least 104-fold less sensitive to Gem than GBM cells	Electrically-driven chemotherapy, here exemplified, has the potential to radically improve the efficacy of GBM adjuvant chemotherapy by enabling exquisitely-targeted and controllable delivery of drugs	[118]
GBM spheroids	21 compounds in combination with MEK or PI3K inhibitors	HDACs, BRD4, CHEK1, BMI-1, CDK1/2/5/9	*In vitro* drug combination screen on the only human NF1 patient derived HGG cell line available and on three mouse glioma cell lines derived from the NF1-P53 genetically engineered mouse model	Identified that six compounds targeting HDACs, BRD4, CHEK1, BMI-1, CDK1/2/5/9, and the proteasome that potently induced cell death in our NF1-associated HGG. Moreover, several of these inhibitors work synergistically with either MEK or PI3K inhibitors	[119]
GBM tumouroids	Zol	Rac1 and Rho prenylation	Investigated the role of FDPS in PDAC RR using the following methods: *in vitro* cell-based assay, immunohistochemistry, immunofluorescence, immunoblot, cell-based cholesterol assay, RNA sequencing, tumouroids	Improved failure-free survival (FFS), enhanced immune cell activation, and decreased microenvironment-related genes upon Zol + RT treatment	[120]
GBM tumouroids	–	Angiogenesis Markers	The model is used to recapitulate how individual components of the GBM's complex brain microenvironment such as hypoxia, vasculature-related stromal cells and growth factors support GBM angiogenesis	3D tumoroid *in vitro* model exhibits biomimetic attributes that may permit its use as a preclinical model in studying microenvironment cues of tumor angiogenesis	[121]
GBM tumouroids	Lapatinib and Nilotinib	DDR1/BCR-ABL	Transcriptomic correlations between gene DDR1, with an expression of genes for EGFR, ERBB2–4, mitogen-activated protein kinase (MAPK) pathway intermediates, BCR, and ABL and genes for cancer stem cell reactivation, cell polarity, and adhesion	Combinatorial targeting of DDR1/BCR-ABL with EGFR-ERBB2 signaling may offer a therapeutic strategy against stem-like KRAS-driven chemoradioresistant tumors of COAD and GBM	[122]
3D bioprinting model	Temozolomide	–	Biomimetic tri-regional GBM models with tumor regions, acellular ECM regions, and an endothelial region with regional stiffnesses patterned corresponding to the GBM stroma, pathological or normal brain parenchyma, and brain capillaries, are developed	Enables rapid, flexible, and reproducible patient-specific GBM modeling with biophysical heterogeneity that can be employed by future studies as a tunable system to interrogate GBM disease mechanisms and screen drug compounds	[123]
3D bioprinting model	—	GBM4, CD1, and C57BL	The use of complementary approaches, 3D bioprinting and scaffold-free 3D tissue culture, to examine the invasion of glioma cells into neural-like tissue with 3D confocal microscopy	Scaffold-free 3D approach has broad applicability, as we were easily able to examine invasion using different neural progenitor cell lines, thus mimicking differences that might be observed in patient brain tissue	[124]
3D bioprinting model	—	LOXP-STOP-LOXP-RFP	Self-assembled multicellular heterogeneous brain tumor fibers have been fabricated by a custom-made coaxial extrusion 3D bioprinting system, with high viability, proliferative activity and efficient tumor-stromal interactions	Coaxial 3D bioprinted multicellular self-assembled heterogeneous tumor tissue-like fibers provided preferable 3D models for studying tumor microenvironment *in vitro*	[125]
Brain organoid	Temozolomide	Cell viability markers	Established a model system whereby we can retro-engineer patient-specific GBMs using patient-derived glioma stem cells (GSCs) and human embryonic stem cell (hESC)-derived cerebral organoids	GLICO model provides a system for modeling primary human GBM *ex vivo* and for high-throughput drug screening	[104]
Brain organoid	Temozolomide	GBM signatures	Real-time integrated system by generating 3D *ex vivo* cerebral organoids and *in vivo* xenograft tumors based on glioma patient-derived tissues and cells	Developed an integrated system of parallel models from patient-derived glioma cerebral organoids and xenografts for understanding the glioma biology and prediction of response to chemotherapy drugs	[102]
Brain organoid	Tranylcypromine	BHC110/LSD1-targeted genes	Human pluripotent stem cell-derived cerebral organoids provide a valuable platform for investigating the human brain after different drugs treatments and for understanding the complex genetic background to human pathology	Tranylcypromine, which is used to treat refractory depression, caused human-induced pluripotent stem cell-derived brain organoids neurotoxicity, leading to decreased proliferation activity and apoptosis induction	[126]

(*continued on next page*)

Table 1 (*continued*)

Model	Drug	Target	Experimental Study	Outcomes	References
Brain organoid	CAR-T Therapy and Temozolomide	Cell death marker	Methods for generating and biobanking patient-derived glioblastoma organoids (GBOs) that recapitulate the histological features, cellular diversity, gene expression, and mutational profiles of their corresponding parental tumors	GBOs maintain many key features of glioblastomas and can be rapidly deployed to investigate patient-specific treatment strategies	[90]
Tumor spheroid co-culture with brain organoid	—	Netrin-1	The glioma cell invasion was investigated using *ex vivo* glioma tissue cultures and newly established primary cell cultures in 3D *in vitro* invasion assays. Intracranial mouse xenograft models were utilized to investigate the effects of netrin-1 on glioblastoma growth and invasion *in vivo*	Netrin-1 as an important regulator of glioblastoma cell stemness and motility. Netrin-1 activates Notch signaling in glioblastoma cells resulting in subsequent gain of stemness and enhanced invasiveness of these cells. Moreover, inhibition of netrin-1 signaling may offer a way to target stem-like cells	[127]

They used the same porcine bio-ink to bioprint a layer of human umbilical vein endothelial cells after bioprinting GBM cells. Imaging of fluorescently dyed GBM cells revealed signs of invasion into the neighboring endothelial cells. A bioprinting organoid revealed a hypoxic gradient when Pimonidazole, a hypoxia marker, was immunostained. These characteristics imply that key tumor characteristics are recapitulated by the bioprinted GBM organoid [89]. Maloney et al., 2020 employed bioprint model to perform a proof-of-concept experiment to determine the efficacy of combination therapy, including multiple concentrations of Dacomitinib (an EGFR inhibitor) and NSC59984 (p53 activator) along with the best methodology to quantify cell viability in complex systems [109]. Recently, Dai et al. produced "fused cells" of GSC and mesenchymal stem cells by method of Cre-LoxP switch gene and RFP/GFP dual-color fluorescence tracing in 3D-bioprinted tumor models namely low-temperature molding and coaxial bioprinting. These fused cells co-express GSCs and MSCs biomarkers and shows increased proliferation as compared to their parental cells, which enhances glioma progression [110]. Further. each organoid model has surmounted the limitations of traditional models and has several applications beyond drug development and screening, including studies on the importance of GBM TME, survival, proliferation, and invasion, personalized medicine, drug resistance, patient-derived orthotropic xenografts, biobanks, immunocompetent cancer organoids, and metabolomics and proteomics analysis [111,112]. Nevertheless, multiple groups have performed proof-of-concept experiments demonstrating the feasibility of this strategy in drug discovery (Table 1).

The accessibility of the drugs to the cells and the intricate microenvironment of the GBOs are two of the key elements that may have led to some treatments' decreased effectiveness in GBOs in contrast to 2D cells [113]. Additionally, it is well recognized that GBOs retain microglia, which significantly contribute to therapeutic resistance by inducing stemness [114,115]. Further, it is possible that the hypoxic gradients within the GBOs, which can cause the activation or expression of drug-resistant genes, as well as the medications' failure to completely enter the GBO, likely contributed to the drugs' ineffectiveness [89]. In conclusion, the unique benefits of patient-derived 2D and 3D models offer a novel approach for evaluating small groups of drugs with the possibility for a more customized strategy to the management of GBM.

5. Traditional and emerging therapeutic approaches targeting GBM pathogenesis

5.1. Surgical resection

GBM surgery aims to accomplish a "maximal safe resection" or remove the maximum amount of the tumor without permanently impairing brain function. Given that GBM can spread widely across several different brain regions, this strategy necessitates great neurosurgical competence [128]. To increase the survival and quality of life of patients, neurosurgeons used a variety of surgical adjuncts, including fluorescence-guided surgery, intraoperative magnetic resonance imaging (iMRI), brain mapping procedures, intraoperative ultrasound (IOUS), intraoperative radiotherapy (IORT), brain mapping strategies, confocal intraoperative microscope (CIM), intraoperative mass spectrometry (IMS), Raman spectrometry (RS), and optical coherence tomography (OCT) [129]. Following brain glioma surgery, the extend of resection (EOR) is the most crucial prognostic factor. Several studies revealed that OS and PFS for GBM patients are favorably correlated with rising EOR [130]. The first strategy involves performing fluorescence-guided surgery, which entails giving the patient 5-aminolevulinic acid (5-ALA), also known as a pink drink and a natural precursor of haemoglobin, 2–3 h prior to the procedure. Tumors metabolize it into porphyrin. In contrast to normal tissue, which does not exhibit any fluorescence and thus improves EOR, this accumulates in tumor tissue (very specific) and appears red when excited by blue light at 400–140 nm. An analysis of the effectiveness of 5-ALA-guided resection in 36 GBM patients found that 83% of cases saw full resection of the contrast-enhanced lesion, 100% of cases saw EOR $\geq$ 98%, and the mean EOR was 99.8% [131]. iMRI is another cutting-edge supplement technique to combat the brain shift phenomenon, which lowers the precision of traditional neuronavigation during surgery. In 2017, Marongiu et al., reported that the use of 1.5 T iMRI improved both EOR (total GTR: 88.5% *vs.* 44%) and 6-month PFS (73% *vs.* 38.9%) in 114 newly diagnosed patients with supratentorial GBM who had surgery with and without iMRI [132]. MR images that have been modified intraoperatively to improve EOR. There is insufficient data to show a meaningful improvement in patients' PFS and OS. Because iMRI requires more sophisticated surgical tools and extends the duration of the procedure, it may result in more expensive medical care. Additionally, IOUS is a widely used and affordable auxiliary surgical tool. Mahboob et al., 2016 conducted a meta-analysis of 15 trials involving 739 glioma patients, using IOUS was linked to improved EOR, primarily when the lesion was solitary and subcortical and there was no prior history of radiotherapy or surgery [133]. IOUS is a user-dependent tool, which must be acknowledged. Therefore, the effectiveness of this auxiliary tool in the operative procedure of GBM depends significantly on the neurosurgeon's knowledge, abilities, and experience [134]. IORT with low-energy X-rays may be more effective and safer for treating newly diagnosed GBM, based on a 51-patient international pooled analysis. Compared to traditional treatment, it increased the OS rate by 25% without causing serious side effects [135]. Additionally, CIM arises as a technique that offers microscopic views of tissues while being operated on, enhancing the resection of tumor margins. In a 2012 blinded investigation, 88 regions were investigated by Eschbacher et al., 2012, where the authors discovered that 26 (92.9%) of 28 lesions had the proper diagnosis [136]. Another important technique LIIT is the

cytoreduction of the tumor tissue by local thermocoagulation. Traylor et al. showed the outcomes of LITT in 69 patients with recurrent and newly diagnosed GBM. They claimed that LIIT could substitute for gross total resection (GTR) in treating brain tumors by reducing their burden and improving median PFS by up to 4 months over nonoperative treatment [137]. Further, the future of surgery may lie in RS and OCT. RS is an investigational technique that offers a biochemical profile of tissue and can identify tumor margins intraoperatively. Iturrioz-Rodrguez et al., 2022, used RS to distinguish between cancer and healthy cells with an overall accuracy of 92.5% [138]. Whereas the optical imaging method known as OCT serves as an optical biopsy and offers images of tissues in real-time without the requirement for sample processing or excision. Recently, researchers have used AI approaches to classify the acquired OCT images. This has the potential to simplify and enhance the accuracy of tumor diagnosis during excision. According to a study, AI may be used to automatically detect glioma invasion in living tissue with good sensitivity and specificity values (sensitivity >90%; specificity >82%) [139]. This has potential to work as theragnostic as well has scope in translation medicines in management of GBM [140]. The golden rule of this therapy option for GBM surgical resection is maximum safe resection. In order to increase these patients' chances of survival and quality of life, surgical adjuncts such fluorescence-guided surgery, iMRI, IOUS, IORT, brain mapping methods, CIM, IMS, LITT, RS, and OCT may be employed when appropriately recommended

5.2. Molecularly targeted therapies

Targeting cellular pathways commonly disrupted in GBM, for instance, the PI3K/Akt/mTOR, the p53 and the RB pathways, or EGFR gene amplification or mutation, epigenetics regulation, and angiogenesis, has not improved results, possibly because of redundant compensatory mechanisms, limited target coverage-connected in part to the BBB, or poor tolerability and safety. Most clinical trial strategies concentrating on intrinsic GBM targets address tyrosine receptor kinase (RTK)-mediated oncogenic signaling, cell cycle regulation, and vulnerability to apoptosis induction [141]. Therapeutic approaches targeting a) *EGFR pathway*: Rindopepimut is an EGFRvIII peptide vaccine demonstrating signs of activity in preclinical models of GBM and early phase trials [142]. In EGFRvIII-positive recurrent GBM the recently finished randomized phase II research ReACT assessed the association of Rindopepimut with Bevacizumab. Despite the trial's failure to achieve its primary aim, Rindopepimut treatment was beneficial across several endpoints, including the 2-year Overall survival (OS) rate and progression-free survival (PFS) [143]. An antibody-drug combination called ABT-414 combines an anti-EGFR mAb with the tubulin inhibitor Monomethylauristatin F. GBM patient-derived xenograft models expressing wildtype EGFR or EGFRvIII showed cytotoxicity when treated with ABT-414 [144]. b) *PDGF pathways*: Nearly 15% of GBM exhibit PDGFRA amplification. Dasatinib, a multikinase inhibitor that targets PDGFR, c-KIT, SRC, and EPHA2, was tested in a recently published phase II trial to assess its effectiveness [145]. c) *MET pathway*: Overexpression of c-MET or its ligand, the hepatocyte growth factor, and MET amplification or mutation have all been suggested as predictive biomarkers; however, their effectiveness and molecular underpinnings are still unexplored. Bevacizumab therapeutic resistance and the development of GBM have been linked to the MET pathway. Cabozantinib, a powerful multitarget inhibitor of MET and VEGFR2, was studied for its anti-GBM properties in an open-labeled Phase II trial with 70 patients [146]. d) *The PI3K/AKT/mTOR pathway had been dysregulated in GBM*: In a study by Langhans et al., 2017 the two drugs GDC-0941 and Rapamycin were compared, where *in vivo* GDC-0941 administration dramatically improved mouse survival, effectively slowed the growth of orthotopic human tumors transplanted into murine brains and appeared to have a greater impact on cellular motility than Rapamycin. They further proposed that the PI3K network may have unique, cell-specific roles within GBM tumors [147]. e) *Cell cycle regulation and apoptosis regulatory pathways*: The RB pathway is dysregulated mostly in IDH wildtype GBM due to homozygous CDKN2A/B deletion, CDK4 or CDK6 amplification, or RB1 gene alterations. PD033299, Cdk4/Cdk6 inhibitor suppressed tumor cell proliferation and demonstrated strong anti-tumor efficacy in RB-wildtype GBM models [148]. f) *The p53 pathway*: Glioma cells with TP53 mutation or deletion exhibit enhanced proliferation, clonal expansion, and impaired DNA repair, encouraging general genetic instability and transformation. In addition, MDM2 or MDM4 amplification can result in p53 inhibition (20% of patients overall) [149]. However, low potency and poor BBB penetration were two major drawbacks of the initial nutlin-based medications. Preclinical investigations in MDM2-amplified GBM models have shown remarkable anti-cancer effectiveness [150]. g) *TERT promoter mutation*: most common in GBM. The TERT promoter mutation has not yet developed into a significant pharmaceutical target for cancer treatment. Eribulin is a tubulin polymerization inhibitor linked to the TERT inhibitory effect in GBM models, which supports further clinical investigation of the drug [151]. h) *Epigenetic regulation*: Targeting IDH1 and HDAC also has the potential to address epigenetic dysregulation and tumor metabolism. Small chemical inhibitors of the IDH1 mutation, AG-120 (NCT02073994) and AG-881 (NCT02481154), were researched in clinical trials and demonstrated safety and tolerability profiles in GBM. A crucial NOA-16 experiment that targets the IDH1 R132H mutation is the first-in-man IDH1 peptide vaccination trial, which examines the patient population's immunological response to the vaccine and its safety and tolerability (NCT02454634) [152]. In addition, HDAC inhibitors are a new class of medications that have demonstrated efficacy in treating hematologic malignancies. Vorinostat, Panobinostat, and other HDAC inhibitors have been administered alone or in conjunction with TMZ, Bortezomib, or Bevacizumab in GBM patients to evaluate their potential to reduce tumor burden [153,154]. Another important class is targeting microenvironmental targets such as angiogenesis and integrins with monotherapy or combination. i) *Angiogenesis*: However, they have not demonstrated appreciable survival improvements in GBM despite being tested in various malignancies. Based on radiographic response rates of 28% to 59% reported in two single-arm trials, the FDA granted Bevacizumab clearance for treating recurrent GBM. Later trials failed to show that Bevacizumab or Lomustine alone or in combination with Lomustine was superior in terms of OS [155,156]. j) *Integrins*: cell surface molecules that integrate signals between cell-cell and cell-ECM. They play a key role in cellular functions like adhesion, motility, invasion, and angiogenesis. In GBM, αvβ3 and αvβ5 were first recognized as attractive therapeutic targets, expressed only on tumor-associated epithelial cells and GBM cells and not normal brain cells [157]. Cilengitide, a cyclic RGD pentapeptide, inhibits ligand binding and activation of αvβ3 and αvβ5 integrins and is used in combination with TMZ and RT against GBM [158]. Thus, better knowledge of the molecular mechanisms behind GBM malignancy has resulted in the development of several biomarkers and drugs that target particular molecular mechanisms in malignant cells.

5.3. Chemotherapy and radiotherapy

The development of chemotherapeutic drugs comes after determining the molecular targets and comprehending pathophysiology. Currently, GBM patients have access to four chemotherapy drugs: TMZ, Carmustine, Lomustine, and Cyclophosphamide (CPA) [159]. The therapeutic potential of TMZ is dependent on its capacity to alkylate or methylate DNA, which most frequently occurs at the N^{-7} or O^{-6} site of guanine residue. In a substantial randomized trial with 573 patients, TMZ combined with radiation dramatically increased median OS survival for GBM patients (27.2% *vs.* 10.9% in the radiotherapy alone at 2 years). Moreover, newly diagnosed patients found that the methylated MGMT gene acts as a positive prognostic biomarker for TMZ chemotherapy [160]. In 2002, the FDA approved BCNU (carmustine)-polymer wafers (Gliadel) as nitrosoureas where Carmustine acts as an alkylating

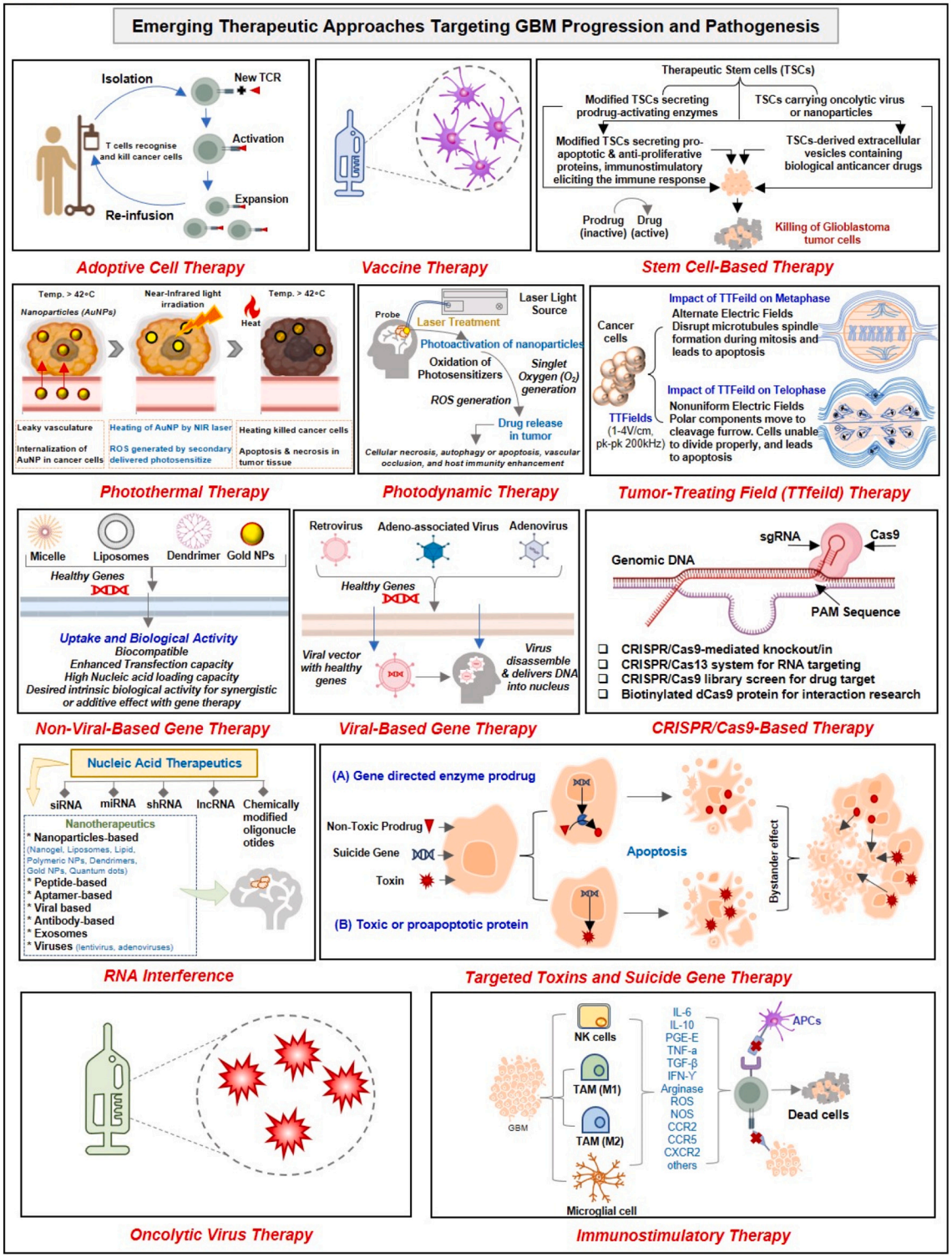

Fig. 3. Emerging therapeutic approaches targeting GBM progression and pathogenesis: Current treatment strategies in GBM includes chemotherapy, radiotherapy, immunotherapy, and surgical resection. However, despite the rigorous research, the survival rate still imposes an enormous challenge. Further, traditional therapeutic strategies come with a problem of adverse side effects. Thus, to overcome the obstacles and hurdles in conventional treatment strategies, scientists have developed various other treatment approaches, namely adoptive cell therapy, stem-cell therapy, viral and non-viral gene therapy, tumor treating field, vaccine therapy, and others, which enhance the survival rate and prognosis rate.

drug to create inter-strand cross-links in DNA, which impede transcription or replication of DNA. A meta-analysis comprising 513 patients revealed improved OS with toxicity, such as increased CSF leakage and elevated intracranial pressure from cerebral edema in newly diagnosed GBM [161], whereas recurrent GBM patients rarely experienced severe side effects, especially pulmonary toxicity, and had better outcomes [162]. Another important drug is Lomustine, an alkylating nitrosourea that affects DNA cross-linking and methylates amino groups. Similarly, a meta-analysis study was conducted to determine whether the combination therapy of Lomustine and Bevacizumab may significantly

Table 2
List of emerging and traditional therapies used to treat pathogenesis and progression of GBM.

Therapy 1	Therapy 2	Experimental Model	Dosage/IC_{50}	Target	Mechanism	Reference
			Immunotherapy-Based Combination			
Anti-PD-1	Anti-BTLA	C57BL/6 J mice were implanted with the murine glioma cell line GL261	Anti-PD-1: 600 μg Anti-BTLA: 1200 μg	CD4+ and CD8+ T cells	Combination of anti-BTLA and anti-PD-1 treatment increases the activation of CD4+ and CD8 + T cells and modulates the presence of Tregs in the brain and blood	[287]
Temozolomide	Interferon-gamma (IFN-γ)	Sprague-Dawley rats bearing intra-caudate nucleus (CN) culture medium	—	TLR-4, IL-10, and p-CREB	Combination therapy inhibited the growth of the tumor. Treatment groups alleviated tumor-induced anxiety-like behaviors and improved imbalance and memory impairment	[288]
PD-L1 antibody	LY2228820	C57BL/6 mice	LY2228820: 1 mg/kg/day PD-L1 antibody: 10 mg/kg/day	F4/80+/CD11b+	Combination therapy could be a treatment option for patients at the recurrence or chronic TMZ maintenance stages	[289]
IL-6	CD40	GL261 tumors	NA	Stat3/HIF-1α axis	Combination of IL-6 inhibition with CD40 stimulation reverses Mϕ-mediated tumor immunosuppression, sensitizes tumors to checkpoint blockade, and extends animal survival in two syngeneic GBM models	[179]
Varlilumab	Nivolumab	175 GBM patients	Varlilumab: 3 mg/kg once every 2 weeks Nivolumab: 240 mg once every 2 weeks	PD1 and CD27	Varlilumab and nivolumab were well tolerated, without significant toxicity beyond that expected for each agent alone	[290]
			Drug-Gene Therapy Combination			
Levetiracetam	Interferon-α	SKMG-4, U87, U373, and U251 cell line model	Interferon-α: 200 U/mL Levetiracetam: 40 μg/mL	NF-kB/p-NF-kB	Inhibited MGMT expression, activated pro-apoptosis molecules, and inhibit NF-kB phosphorylation	[291]
Temozolomide	IFN-ELP(V)	Female BALB/c nude mice	Temozolomide: 50 mg/kg/per mouse IFN-ELP(V): 53.47 pg/mL	IL-1β and IL-12	Resulting in dramatically improved pharmacokinetics and biodistribution, and thus inhibited GBM recurrence by stimulating antitumor immune response as compared to IFN	[292]
Bevacizumab	Ad-SGE-REIC	Human GBM cell lines U87ΔEGFR and U251MG	Bevacizumab: 0.1 mM Ad-SGE-REIC: MOI of 10	VEGF-A and Wnt signaling pathway	Cells treated with both bevacizumab and Ad-SGE-REIC and decreased β-catenin protein levels. Exerts anti-glioma effects by suppressing the angiogenesis and invasion of tumors	[293]
			Drug-Adoptive Cell Therapy			
Cold atmospheric plasma	Temozolomide	U87MG	Temozolomide: 50 μM CAP: 180 s, 1 treatment	αvβ3 and αvβ5 cell surface integrin	CAP, in conjunction TMZ, increased DNA damage measured by the phosphorylation of H2AX and induced G2/M cell cycle arrest	[294]
			Drug-Tumor Treating Fields			
Rapalink-1	Tumor treating fields	Glioblastoma neurospheres JHH520, SF188, BTSC233, NCH644, GBM1	NA	mTOR	Reduces cell growth	[295]
			Drug-Radiotherapy			
A-96649	Iodine-131 beta-particles	U87MG cell lines	A-966492: 1 μM	DNA repair pathway	The results demonstrated that iodine-131, in combination with A-966492 and TPT, had marked effects on radio-sensitizing and can be used as a targeted radionuclide for targeting radiotherapy in combination with topoisomerase I and PARP inhibitors to enhance radiotherapy in clinics	[296]
AZD6738	Radiotherapy	MES-GBM/GSCs	AZD6738: 1.531 μM	STAT3 pathway	ARPC1B promoted MES phenotype maintenance and radiotherapy resistance by inhibiting TRIM21-mediated degradation of IFI16 and HuR, thereby activating the NF-κB and STAT3 signaling pathways, respectively	[297]
			Drug-RNA Interference			
LB100	PRMT5 Depletion (siRNA)	Patient-derived primary GBM neurospheres (GBMNS)	LB100: 5 μM	MLKL	LB100 treatment combined with transient depletion of PRMT5 significantly decreased tumor size and prolonged survival	[298]

(*continued on next page*)

Table 2 (*continued*)

Therapy 1	Therapy 2	Experimental Model	Dosage/IC_{50}	Target	Mechanism	Reference
Fenofibrate	lncRNA HOTAIR	702 glioma patients' samples and human GBM cell lines U87 and U251	Fenofibrate: 100 μM	PPARα	Results suggest that HOTAIR can negatively regulate the expression of PPARα and that the combination of fenofibrate and si-HOTAIR treatment can significantly inhibit the progression of gliomas	[299]
Baicalin	Knockdown miR148a	Human glioblastoma multiforme T98G and U87MG cells	NA	Autophagy pathway	Significant reduction in cell viability and proliferation, the accumulation of subG1-phase cells and a reduced population of cells in the S and G2/M phases (only in the U87MG cell line), increased population of cells in the S phase in T98G cell line and apoptosis or necrosis induction and induction of autophagy for both cell lines	[300]
1-(3′,4′,5′-trimethoxyphenyl)-2-aryl-1H-imidazole	Anti-miR-10b-5p (lipofectamine RNAiMAX)	U251 GBM cell line	Anti-miR-10b-5p: 200 nM 1-(3′,4′,5′-trimethoxyphenyl)-2-aryl-1H-imidazole: 0.25 μM	Caspase-3/7	Induces apoptosis and inhibits cell growth. Caused the highest level of accumulation of the cells into the G2/M phase of the cell cycle	[301]
			Gene Therapy-Nanomaterial			
LPHNs-cRGD (CRISPR/Cas9)	FUS-MBs	NOD-SCID mice and T98G cells	NA	MGMT	LPHNs-cRGD could target GBM cells and mediate the transfection of pCas9/MGMT to downregulate the expression of MGMT, resulting in an increased sensitivity of GBM cells to TMZ. It inhibited tumor growth, and prolonged survival of tumor-bearing mice, with a high level of biosafety	[302]
			Drug-Radiotherapy			
PBI-05204	Radiotherapy	U251, A172, U87MG and T98G cell lines and Female CD1-nu/nu mice (Xenograft model)	PBI-05204: 5.0 μg/mL Radiotherapy: 4 Gy	γH2AX, Ku70, pDNA-PKc	Reduced tumor progression evidenced by both subcutaneous as well as orthotopic implanted GBM tumors	[303]
Voxtalisib	Low-intensity pulsed ultrasound	GBMCSCs isolated from the human glioblastoma U87 MG cell line		PI3K/AKT/mTOR pathway	High doses of Vox + LIPUS inhibited mTOR and decreased the viability in both cell groups. Inhibiting mTOR-activated autophagy and LIPUS increased autophagy in GBM cells	[304]

improve OS, PFS [163]. Next, CPA metabolite phosphoramide mustard can cross-link and alkylate DNA, affecting DNA function. Recent research suggested that CPA improves survival in orthotopic GL261 GBM in mice (administration every 6 days) compared to the control group [164]. Currently, several potential drugs, including Alisertib, Disulfiram, Regorafenib, Sorafenib, Vorinostat, *etc.*, are now being developed in various phases of clinical trials. Some clinical trials of major drugs and biologicals have been reviewed in articles [165]. Moreover, sonodynamic therapy is a glioma therapeutic strategy that eradicated tumors through activated sonosensitizers coupled with low-intensity ultrasound [166]. Recently, Ning et al., 2022 demonstrated that biomimetic drug delivery system (C-TiO2/TPZ@CM) was successfully synthesized for combined SDT and hypoxia-activated chemotherapy, which was composed of tirapazamine (TPZ)-loaded C-TiO2 hollow nanoshells (HNSs). C-TiO2@CM exhibited remarkable biocompatibility without manifest damage and toxicity to the blood and major organs of the mice, and thus, can be a potential agent in chemotherapy-sonodynamic therapy combination [167].

Another important technique is RT. For patients under 70 years old, standard radiotherapy or external beam radiation (EBRT) is used. It is delivered in 1.8–2 Gy fractions daily, 5 days a week, continuously for 6 weeks, to a total dose of 54–60 Gy [168]. However, hypofractionated radiotherapy (HFRT) is advised for patients over the age of 70 years and those with a constrained prognosis due to poor prognostic characteristics. It employs a biologically equivalent dose of 40 Gy divided into 15 fractions of 2.67 Gy. This enhanced OS with lower rates of toxicity [169,170]. Additionally, amino acid PET is being investigated to better define the target volume of radiation. This technique uses radiolabelled amino acids, primarily ^{11}C-methionine, ^{18}F-FDOPA, and ^{18}F-FET. Compared to conventionally fractionated RT, neither new methods of administering radiation therapy nor radiotherapy in conjunction with potential radiosensitizing drugs have demonstrated greater efficacy [171]. Recently for surgically targeted radiation therapy, Gessler et al., 2020 announced GammaTile® US FDA-cleared medical device, which includes ^{131}Cs radiation-emitting seeds in a resorbable collagen-based carrier tile for surgically targeted radiation to achieve highly conformal radiation while surgery. The technical obstacles related to conventional brachytherapy (means implantation of interstitial or intracavitary radioactive sources adjacent to the target tissue) are significantly reduced by embedding encapsulated ^{131}Cs radiation emitter seeds in collagen-based tiles [172]. In addition, RT has been explored in combination with chemotherapy (TMZ) [173], immunotherapy (Nivolumab) [174], biologics (Bevacizumab) [175], natural compounds (Resveratrol) [176] *etc.*, to improve efficacy and safety of GBM patients.

5.4. Immunotherapy, myeloid-targeted therapy and adoptive cell therapy

GBM is proficient at evading host immune surveillance. Using a patient's immune system as a tool, immunotherapies try to re-direct

immune cells away from a tumor. Numerous immunotherapies, including immune checkpoint inhibitors (ICIs) and chimeric antigen receptor (CAR) T cell therapy, are now being researched as potential treatments for GBM. Such treatment has great success against aggressive tumors and less in brain cancer. In order to restore T cell function and anti-cancer activity, ICIs target T cell depletion by blocking immunological checkpoints PD-1 and CTLA-4. However, the outcomes of numerous studies investigating the use of ICIs in glioma experimental models have been encouraging. Indeed, orthotopic GL261 tumors were eliminated by anti-PD-1 when administered in combination with TMZ and 44% when used alone. Tumor growth was not seen after rechallenge in mice treated with anti-PD-1 monotherapy, but it did occur in the combination group [177]. Wu A et al., 2019 investigated the synergistic effects of combining anti-PD-1 and anti-CXCR4 therapy. They found that these therapies improved OS reduced the number of suppressive myeloid cells, and boosted the amount of circulating inflammatory, anti-cancer cytokines [178]. Recently Yang et al., 2021 demonstrated that dual targeting of IL-6 and CD40-sensitized GBM to ICBs, inhibits tumor growth and that the subsequent triple combination (anti-PD-1/anti-CTLA-4 + CD40 antibody, IL-6 antibody) dramatically increased survival and TILs as well as in IFN-secreting CD8 T cells [179]. Although preclinical research has been encouraging, the limited efficacy of ICIs in treating patients with GBM may be due to their innate immunological "cool" nature, lack of T-cells, and predominance of pro-tumorigenic TAMs, especially in IDH-wild type tumors. They may also have a reduced mutational load rate, which affects their sensitivity to ICIs limited population likely to benefit [180]. As an illustration, the Checkmate 143 study was the first randomized trial evaluating ICIs for recurrent GBM cases. 40 patients with recurrent disease participated in the initial phase I research to evaluate the safety of Nivolumab (anti-PD-1) and Ipilimumab (anti-CTLA-4) drugs. The findings revealed that Nivolumab alone was more well tolerated than the dual therapy, with ipilimumab side effects [181]. Further, a recent phase II clinical trial evaluating Pembrolizumab (anti-PD-1) with or without Bevacizumab in patients with recurrent glioblastoma also failed to achieve the primary endpoint of 6 months PFS with either treatment strategy [182]. (Fig. 3) (Table 2).

Another effective immunotherapy is myeloid-targeted therapy, which involves reprogramming immunosuppressive microglia or monocyte-derived macrophages, which are pro-tumorigenic, to become more anti-tumorigenic. CSF-1R is a critical receptor for macrophage differentiation and survival. TAM promotes T-cell exhaustion *via* the PD-L1/PD-1 pathway, which mediates tumor growth [183]. It lacks CD80, CD86, and CD40, crucial costimulatory molecules for T-cell activation, which makes the tumor immunologically inert and contributes to its resistance to anti-angiogenesis therapy (Bevacizumab). Therefore, reversing active immunosuppression in the TME and halting tumor progression may be achieved with myeloid compartment-targeting treatment. Macrophages that have been re-educated to acquire an anti-tumor phenotype due to CSF-1R suppression exhibit tumor regression and improved survival. Despite the fact that CSF-1R inhibitors have had limited clinical success when used alone [184], emerging studies have revealed that radiation and TAM-targeted treatments may work in synergy to target the myeloid compartment more effectively [71]. Combining the reprogramming of macrophage morphologies with targeting particular TAM recruitment may result in a more robust method of disease control that has not yet been clinically tested. In addition to CSFs, other targets include CD40 activation, COX2 inhibition, several cytokines and chemokines, and insulin-like growth factor 1 (IGF1). Indeed, it has been discovered that myeloid immunosuppressive functions can be reversed using a variety of strategies, such as antibody-based therapy (blocking Periostin or CSF-1R), polarizing cytokine therapy, antisense oligonucleotide therapy (down-regulating pro-tumorigenic signals), and CAR Macrophages [185].

Adoptive T-cell transfer (ACT) includes tumor-infiltrate lymphocyte (TILs) transfer and genetically engineered T-cell transfer. It consists of re-infusing a patient of their own (autologous) or donor (allogenic) anti-tumor T-cells that are genetically modified to target tumor-associated antigens (TAAs) to attack receptors on the patient's cancer cells. This increases the amount of specific T-cells a tumor encounters and guarantees that they are properly activated, making them less vulnerable to the intra-tumoral immunosuppressive milieu [186]. There is no FDA-approved T-cell treatment for GBM, unlike hematologic cancers. In a preliminary trial, it was shown that giving GBM patients autologous TIL with IL-2 was successful. Six participants in this study underwent surgery, then received chemotherapy and an infusion of TILs and IL-2. Phase I clinical trial started in Feb 2022, (20 patients, NCT05333588) exploring the safety and efficacy of TIL therapy for malignant GBM. Anaplastic astrocytoma was identified in three of these individuals; one underwent a complete regression after 45 months, while the other underwent a partial regression. Two additional individuals with GBM showed a partial regression [64,65]. Recent studies on CAR T cells have been focused on targeting TAA, including EphA2, EGFRvIII, CD70, HER2, and IL-13Rα [189]. CAR T cell research for GBM is intense: ongoing CAR T cell clinical trials in GBM include EGFRvIII (NCT01454596, NCT05063682, NCT02209376, NCT02844062, and NCT03283631), ephrin type-A receptor 2 (EphA2) (NCT02575261, withdrawn), HER2 (NCT01109095, NCT03389230), IL-13Rα2 (NCT04510051, NCT05540873, NCT04003649, NCT02208362), and PD-L1 (NCT02937844) shown promising results. CAR T cell treatment is meant to be used in combination with other therapies because of the substantial tumor heterogeneity, immunoediting, and existence of a cold immunosuppressive microenvironment (with anti-PD-1 inhibitors, Pembrolizumab) [190] instead of a single therapy. However, other methods involve modifying T-cells to release stimulatory cytokines like IL-12 or CD40, improving T-cell proliferation and survival [191]. Research conducted by Bielamowicz et al., 2018 demonstrated enhanced survival in 15 GBM samples using trivalent T-cell products (UCAR T cells) equipped with three CAR molecules specific for EphA2, HER2, and IL-13Rα2 [192]. These advancements in ACT, together with other immunotherapy approaches, have the potential to be effective in the treatment of GBM.

5.5. *Vaccine therapy and stem cell therapy in glioblastoma*

Vaccines for GBM are an active immunotherapy method that can increase and modify immune responses against TAAs [193]. EGFRvIII, a mutant form of EGFR constitutively active and exclusively expressed in 50% of GBM, is the most thoroughly investigated TAAs [194]. In many clinical trials, the peptide vaccine Rindopepimut (CDX-110), which targets EGFRvIII, has been studied. For instance, 745 participants were enrolled in phase III randomized trial (NCT01480479, ACT IV) by Weller et al., 2017 to examine the effectiveness of Rindopepimut in newly diagnosed patients with EGFRvIII-positive GBM. Reardon et al., 2020 reported encouraging findings for the phase II ReACT trial (NCT01498328), which evaluated Bevacizumab with Rindopepimut for patients with relapsed EGFRvIII-positive GBM [195]. Additionally, the ICT-107 vaccine, which has also advanced to phase II randomized clinical trials (NCT01280552), consists of autologous DC primed with six synthetic peptide epitopes targeting GBM TAAs, including MAGE-1, HER-2, AIM-2, TRP-2, gp100, and IL13R2 [196]. The identification of tumor-specific neoantigens was also made possible by advancements in next-generation sequencing. Consequently, because it may successfully elicit *de novo* T-cell responses, these could possibly be employed in tailored neoantigen-based vaccines. Keskin et al., 2019 reported that 10 patients with newly diagnosed MGMT-unmethylated GBM underwent a phase Ib clinical trial to examine tailored neoantigen vaccinations after undergoing surgical resection and conventional radiation. However, they have demonstrated a rise in the number of T-cells that infiltrate tumors in patients who did not get dexamethasone, a potent corticosteroid, and polyfunctional neoantigen-specific CD4+ and $CD8^+$ T cell responses that are enriched in memory phenotypes [197]. Combining

vaccination with other treatments, such as immune checkpoint inhibition, may be advantageous because neoantigen-targeting vaccines can favorably change the immunological environment of GBM. (Fig. 3) (Table 2).

Many studies demonstrate that GBM tumors initiated from GSCs are the root cause of cancer patients' resistance to treatments. GSC characteristics are upheld by the expression of the CSCs markers CD133, CD44, Oct4, Sox2, Nanog, and ALDH1A1, as well as by the signaling pathways mTOR, AKT, NOTCH1, and Wnt/β-catenin [198]. Also, given the potential for regenerative medicine applications, the migration or homing of supplied Mesenchymal stem cells (MSCs) in a therapeutic environment is undoubted of great interest [199]. To enhance their anticancer efficacy against GBM, GSCs can be altered in various ways or delivered with diverse payloads targeting tumor cells and other TME components. *a) Utilizing both viral and non-viral techniques,* the Therapeutic Stem cells (TSCs) can be altered to secrete particular anti-cancer proteins, including pro-apoptotic (S-TRAIL) and antiproliferative proteins (Bcl2). For instance, Knock et al., 2007 used the lentivirus delivery method to investigate the therapeutic effects of combining the secretable form of (S) TRAIL-induced apoptosis with the downregulation of Bcl-2 for the total eradication of gliomas [200]. b) *TSC-secreting prodrug-activating enzymes:* Engineered TSCs are used in TSC-mediated suicide therapy to secrete an enzyme that catalyzes the conversion of a harmless prodrug into a cytotoxic drug, which promotes the bystander effect and triggers the death of the brain tumor cells. Examples of genes encoding enzymes that can transform prodrugs ganciclovir (GCV) and 5-fluorocytosine (5-FC) into medications that are cytotoxic for tumors include herpes simplex virus thymidine kinase (HSV-TK) and cytosine deaminase (CD) [201]. When they were expressed by MSCs and applied intravenously, the tumor growth was effectively suppressed by 86% compared to control groups, translating into significantly longer survival times [202]. c) *TSCs carrying oncolytic virus or NPs*: Huang et al., 2017 used adipose-derived stem cells to transport smart nanotherapeutics (SPION/PTX-loaded NPs (SPNPs)) for targeted delivery to GBM tumors. Therapy delivered across the BBB and, when paired with photo- or hyperthermia, exhibits enhanced therapeutic efficacy [203]. Further, The conditionally replication-competent oncolytic adenovirus (CRAd-S-pk7), which targets cells overexpressing survivin, a protein increased by radiation therapy and abundantly expressed in glioma cells, was also transfected into MSCs [204] d) *TSCs derived extracellular vesicles (EVs):* Two significant subtypes of EVs are microvesicles (MVs, 50–1000 nm) and exosomes (EXs, 30–100 nm). Researchers looked into the possibility of using MSCs designed to shed EVs that contain the miRNA miR-7, which regulates cell proliferation and apoptosis in tumors, to stimulate resistant tumor cells to induce apoptosis in GBM. Mainly when produced by MSCs that expressed S-TRAIL, miR-7 dramatically reduced the tumor's volume [205]. (Table 2)

5.6. Photodynamic therapy, photothermal therapy, and tumor-treating fields

A viable, focused therapeutic option for GBM has recently been identified as PDT. A photosensitizer molecule specifically integrated into cancerous cells gets photoactivated in this process. The photosensitizer (5-ALA, Porfimer sodium, Temoporfin, and Indocyanine green (ICG)) is activated by photoirradiation by transferring energy to the sensitizer, causing the excitation of molecular oxygen to a singlet or triplet state. Energy in the singlet state is either internally transformed to heat or released as light (fluorescence). ROS are produced in the triplet state, which is required to cause cell death. PDT has the ability to treat micro-invasive areas while safeguarding sensitive brain regions, in contrast to surgical resection and radiotherapy [206]. It is easier for 5-ALA (the most used photosensitizer) to diffuse into the tumor mass when the BBB is broken, which typically happens in the GBM microenvironment [14,207,208]. ICG photosensitive agents are subject to inherent limitations, including aggregation, instability, and photolytic destruction. For example, Kang et al., 2022 reported a nanoformulation (SIWV-pSiNP(ICG)), SIWV peptide-functionalized GBM homing, and ICG-incorporated porous silicon NPs (pSiNPs). With higher ICG incorporation stability, the nanoformulation showed superior photodynamic characteristics when exposed to NIR light. In the GBM xenograft mice, the SIWV-pSiNP (ICG) demonstrated higher therapeutic performance (anti-cancer efficiency) with outstanding biocompatibility [209]. Further, PDT is proven to successfully trigger an anti-cancer immune response. Shibata et al., 2019 created liposomal-formed, therapeutically applicable NPs, phospholipid-conjugated ICG (LP-iDOPE). These NPs accumulate in tumor tissues *via* the EPR effect and, when combined with NIR radiation, effectively elicits an immune response specific to GBM. This may be accomplished by increasing the production of HSP70, which is known to stimulate antigen-presenting cells *via* TLRs signaling [210]. Furthermore, research has concentrated on using different NPs to overcome the limitations of conventional photosensitizer delivery systems, such as hyaluronic acid-modified NPs, porphyrin-containing mesoporous silica NPs, gold NPs, and graphene quantum dots. Consequently, nanomedicine advancements can improve the clinical results of PDT-treated GBM [206]. (Fig. 3).

PTT is a non-invasive treatment using a photoabsorbing chemical (such as cyanine or porphyrin derivatives) that can accumulate at the tumor site in conjunction with an external NIR laser to irradiate the tumor topically or interstitially (*via* an optical fiber). After exposure to laser radiation, the PTA agent collects the light energy, transforms it, and then releases it as heat, producing localized HT that results in partial or total tumor ablation. Maziukiewicz et al., 2019 presented NDs@PDA@ICG (containing nanodiamonds conjugated with biomimetic polydopamine and ICG sensitizer) for PTT therapy in GBM with more than 40% photoconversion efficiency [211]. Similarly, Zhu Ge et al., 2019 created ICG-loaded Silk fibroin NPs (SFNP) cross-linked by proanthocyanidins to create stable ICG-CSFNPs for eliminating the remaining tumor niche after surgery using NIR. After surgical resection, PTT for gliomas using silk fibroin may be a potential treatment option [212]. In addition, a study shows that keratin-coated gold NPs (Ker-AuNPs) is a promising new approach in biocompatible photothermal agents for PPT therapies in GBM [213]. Sun et al., 2022 demonstrated a modified therapeutic agent against GBM based on SiNPs. Surfaces were altered using ICG and Glucosamine. This allows for BBB passage through GLUT1-mediated transcytosis pathways, is characterized by the EPR phenomenon, and is activated by 808 nm laser light [214]. Further, Guo et al., 2022 synthesized TA-Vox nano branches that demonstrated excellent photothermal conversion properties and causes HSP60 inhibition, whereas, Liu et al., 2023 developed ultrasmall zirconium carbide nanodots as non-inflammatory photosensitizers for PTT of gliomas that have the capability of performing CT imaging [215,216].

Thus, PTT may be a potential technique for treating GBM since it permits the tumor to be eliminated by employing heat as a non-chemical treatment for the disease, overcoming the constraints of GBM heterogeneity, conventional drug resistance mechanisms, and adverse effects on normal peripheral tissue.

The targeted administration of low-intensity (1–3 V/cm), intermediate-frequency (100–200 kHz), and alternating electrical fields to the tumor-bearing brain are known as tumor-treating fields (TTFields). These electrical fields are anticipated to block cell cycle progression through metaphase with little effect on the body's dormant and non-dividing cells [217]. The industrial illustration of TTFields is a product manufactured by Novocure called Optune®. In 2011 and 2015, the FDA authorized the management of recurrent and newly diagnosed supratentorial and histologically verified GBM [218]. Currently, there are several ongoing clinical trials in combination with chemotherapy (TMZ: NCT04474353, NCT03477110, NCT03705351, NCT04471844), biologics (NCT03223103), immunotherapy (NCT03430791) for new and recurrent GBM. In preclinical research and randomized phase III clinical studies, the benefits of TTFeilds in treating GBM have been shown to include non-invasive anti-tumor activity, enhanced

therapeutic efficacy when combined with chemotherapy, and reduced systematic toxicity [219]. A genuinely new cancer treatment approach has been created, and it will find numerous beneficial applications alone or in combination with other existing or novel treatments if those trials support the excellent benefits shown in GBM patients. (Table 2)

5.7. Viral and non-viral vectors-based gene therapy

To deliver the therapeutic payload in GBM and LGG, delivery vectors such as viral vectors, non-polymeric NPs, and polymeric NPs have been employed. Viral vectors are employed to transfer therapeutic genes into target cells, where they can operate specifically against tumors, play an oncolytic role in gene delivery, and trigger a host immune response. Viral vectors used in GBM therapy, including retrovirus (HSV-TK, TOCA511); Lentivirus (shRNA-lentivirus, sh-SirT1 lentivirus, miRNA-100 lentivirus, GAS1-PTEN lentivirus); Adenovirus (ONYX-015), Delta-24); Herpes simplex virus (HSV1716, C134, G2017); Oncolytic virus (Pelareorep/REOLYSIN, TG6002, H-1PV, PVS-RIPO) [220]. In suicide gene therapy, retroviruses are primarily used to deliver the desired gene to the tumor location. For instance, Vocimagene amiretrorepvec (Toca 511), an experimental γ-retroviral replicating vector utilized in a multicenter, randomized clinical trial, enhanced patient survival after tumor excision for the first or second recurrence of GBM [221]. Lentiviral vectors (LVs) were more dependable and less prone to insertion mutation than retroviral vectors. The distinct process of lentiviral vectors was the active transit of the pre-integration complex *via* the nucleopore [222]. Compared to other viral and non-viral gene delivery methods, LV has many benefits, including minimal immunogenicity, high delivering gene efficiency, the ability to transduce both proliferating and resting cells, and persistent gene transfer. Indeed, Wei et al., 2014 delivered a Rhomboid domain containing 1 (RHBDD1) shRNA by lentivirus to block the cell cycle in GBM *in vitro* [223]. Adenoviral vectors internalized adenovirus vectors through associations involving penton protein and host cell surface integrins and the coxsackie-adenovirus receptor, which mediates cell tropism. Adenoviruses did not integrate into the host genome after endocytosis into the tumor cells and remained episomal during gene expression [224]. In contrast, DNX-2401 (Delta-24-RGD; Tasadenoturev) is a tumor-selective, replication-competent oncolytic adenovirus that increases long-term survival in recurrent HGG. This improvement is likely attributable to the virus's direct oncolytic effects, which are followed by the induction of an immune-mediated anti-glioma response [225]. Another group has shown the addition of IFNγ along with DNX-2401 does not improve the survival of GBM patients in the phase Ib trial [226]. Adeno-associated virus (AAV)-mediated gene therapy has recently generated much interest due to its long-term stable transgene expression, broad tissue tropism, low cytotoxicity and low immunogenicity [227]. The neurotropic characteristic of HSV vectors makes them appealing for gene transduction in central nervous system malignancies. A phase I clinical trial (NCT03657576, C134-HSV-1) was carried out to evaluate the safety and tolerability of genetically modified C134 in recurrent GBM. Similarly to this, clinical investigations have shown that HSV-1716 can significantly increase patient survival [228]. Moreover, Mi et al., 2020 demonstrated the synergistic effectiveness of recombinant HSV-1 in combination with CD suicide gene therapy and lentivirus-mediated VP22 (HSV-1 tegument protein is necessary for virus cell-to-cell transmission and cell cycle regulation) [229]. In addition to directly destroying tumor cells, oncolytic viruses stimulate the immune system's reaction to the tumor. In order to combine a direct oncolysis action with a prodrug conversion activity, the vaccinia virus was modified to create TG6002 [230]. However, TG6002 and 5-FC began clinical development in patients with recurrent GBM (NCT03294486) [231]. In addition to viral vectors, non-viral vectors have also been examined for the delivery of glioma gene therapy and have looked impressive in both preclinical and clinical research as gene vectors for glioma treatment. These non-viral vectors include both non-polymeric and polymeric delivery methods. Dendrimers, Dendrigrafts, Polymeric Micelles, Poly(−amino ester), Gold NPs, and Liposomes, are some of the more well-known non-viral vectors [232]. Lipid NPs are quickly produced, have minimal immunogenicity, transport larger genes, incorporate ligands into specific target cells, and pass the BBB [233]. Gregory et al., 2020 created designed albumin-based NPs with cell-penetrating iRGD peptide and siRNA targeting signal transducer and activation of transcription 3 factors (STAT3i) and proved that when given in combination with ionizing radiation, these NPs stimulate anti-GBM immunologic memory, which leads in tumor remission and long-term survival of GBM bearing mice [234]. Transfected glioma cells underwent apoptosis after exposure to a poly (β-amino ester) library of PBAE-based NPs containing HSV-TK DNA. Further, when administered intracranially, this resulted in an increase in the median survival of glioma-bearing mice [235]. Similarly, Kim et al., 2020 created modified poly(ethylene glycol)-modified poly (beta-amino ester) (PEG-PBAE) polymers to improve the efficacy of gene therapy, raising the median survival time from 53.5 to 67 days in the human GBM orthotopic xenograft model [236]. Furthermore, dendrimers can be employed to deliver biologics that trigger specific gene knockdown and genes that promote apoptosis [237]. IFNβ is an immune gene with anti-tumor activity, and intratumoral injection of arginine-modified G4 PAMAM dendrimers successfully decreased the tumor size in U87MG tumor-bearing mice [238]. Moreover, a CX3CR-1GFP mouse orthotopic GL261 GBM model was used in a subsequent study to demonstrate the ability of dendrimer-siRNA conjugates to concurrently lengthen the half-life of siRNA in plasma and drastically reduce GFP expression *in-vivo* [239]. Furthermore, The RGD functionalized dendrimer-entrapped gold NPs (Au DENPs) have also been created by Kong et al., 2016 for the delivery of VEGF and BCL2 siRNA into GBM cells [240]. The above research demonstrated that targeting gene delivery systems through viral and non-viral had promising applications for treating GBM. (Fig. 3) (Table 2)

5.8. CRISPR/Cas9 genome editing system

A prominent gene editing technique utilized in cancer research is the Clustered Regularly Interspaced Short Palindromic Repeats (CRISPR)/CRISPR associated (Cas) nuclease 9 (CRISPR/Cas9) system. It contributes to identifying new oncogenes that govern autophagy, angiogenesis, and invasion and are significant in developing GBM [241,242]. CRISPR/Cas9 has been used as a therapeutic approach such as a) *to identify and modify the genetic regulators* of the hallmark of GBM; b) *to find the novel biomarkers*, oncogenic drivers, mechanisms of chemotherapy resistance, and markers that enhance the responsiveness of tumor cells to conventional or synergistic therapy. c) *identifying genetic regulators of autophagy in GBM*. Many studies have linked autophagy activation in GBM with severe disease and treatment resistance, although autophagy's involvement in the development and progression of GBM is debatable [243]. For instance, an essential autophagy-related protein involved in tumor development and spread is vacuole membrane protein 1 (VMP1). VMP1 was eliminated through gene editing using CRISPR/Cas9, drastically reducing cell proliferation, enhancing cell death, and causing cell cycle arrest. Hence, Glioma cells became more susceptible to RT and chemotherapy due to the knockout of VMP1, which restricted the autophagic flux [244]. d) *identifying genetic regulators of apoptosis in GBM*. Rodvolt et al., 2020, knockout the Unfolded Protein Response (UPR) genes ERN1, IGFBP3, and IGFBP5 in U251 cells using CRISPR/Cas9, which made the cells more vulnerable to cell death in response to 12 ADT, an ER stress-inducing drug [245]; e) *identifying genetic regulators of angiogenesis in GBM*. Angiogenesis-related factors' expression was shown to be downregulated after CRISPR/Cas9 was utilized to suppress the DDX39B (DExD-box helicase 39B) gene in the U87MG cell line [246]. f) *gene editing decreases cell invasion and migration in GBM*. In a study using the human GBM cell lines A172, U251, and LN229, the ability of cell invasion, stemness, and migration was reduced by CRISPR/Cas9-mediated reduction of the germline-related protein Dazl

(deleted in azoospermia like) gene [247]. Moreover, the significance of cell surface receptors or associated proteins in controlling GBM invasiveness was also determined using CRISPR/Cas9. Further, in GBM U251 cells, Pu et al., 2020 demonstrated that caveolin-1 and cavin knockdown (caveolin-1 expression and cavin stability govern caveolae dynamics) suppressed the production of matrix metalloproteinases (MMPs), epithelial-mesenchymal biomarkers, and epithelial-mesenchymal transition (EMT) markers and decreased cell invasion [248]; g) *editing of the inflammatory and immune response genes in GBM.* CRISPR/Cas9 mediated gene knockdown in GBM cells discovered OPN, DDX39B, and AIM2, important genes responsible for aberrant immune response, improved drug sensitivity to TMZ, suppressed NF-κB pathway signaling, decreased cell proliferation in GBM [249]. The immune checkpoint mediated by PD-1/PD-L1 is one potential therapeutic target in GBM. In an another study, CRISPR/Cas9-mediated T cell immunoglobulin mucin family member 3 (TIM3), knockout in human NK cells increased the NK cells' ability to kill GBM cells (T98G and LN-18) [250]; h) *Editing the genes in GBM that control self-renewal capacity*. An investigation showed the expression of the cancer stem cell markers Oct4 and Sox2 was decreased by the CRISPR-Cas9 FOXO3 gene deletion in U87MG cells [251]. Alternative treatment strategies utilizing CRISPR/CAS9. Ruan et al., 2022 developed a brain-targeted CRISPR/Cas9 based nanomedicine by fabricating an angiopep-2 decorated, guanidinium and fluorine functionalized polymeric NPs with loading Cas9/gRNA RNP for the treatment of GBM by knockout of proto-oncogene polo-like kinase 1 (PLK1). The CRISPR/Cas9 technology is so fantastic that it might represent a technical breakthrough in genome editing for biomedical research and drug discovery that has never been possible. In the future, it is anticipated that research on the application of CRISPR technology to the treatment of glioma will advance and have a wide range of potential applications. (Fig. 3) (Table 2)

5.9. Application of RNA interference

Even though several targeted therapies, gene therapies, and immunotherapies are currently available or being tested in clinical settings, the OS of GBM patients has not changed much over the past 20 years. Thus, innovative multitarget modalities like RNA interference (RNAi) are urgently needed. Small RNA oligonucleotides are used in RNAi-based therapeutics to control expression levels at the post-transcriptional mechanism [13]. Synthetic RNA oligonucleotides like siRNA, miRNA, shRNA and lncRNA have demonstrated potential as cutting-edge therapies. Even while RNAi therapy can be a valuable tool in the fight against cancer, especially for untreatable tumors like GBM, certain obstacles still stand in the way of realizing its full potential. To overcome this drawback, herein Liu et al., 2020 developed intelligent biomimetic nanotechnology-based RNAi that uses Angiopep-2 peptide-modified, immune-free RBCm and charge conversational components to solve this disadvantage. This increased orthopedic GBM RNAi therapy's therapeutic effectiveness, increased patient survival rates, and reduced systemic adverse effects [252]. In addition, due to its anti-inflammatory, anti-oxidative, and neuroprotective properties, a novel nanomaterial called *DNA tetrahedron* has recently become a multipurpose treatment [253]. Likewise, Zohu et al., 2021 designed a tetrahedral DNA nanostructure packed with survivin interfering RNA (As-TDN-R) 2021 to specifically identify tumor cells overexpressing nucleolin protein and inhibit glioma apoptotic pathways [254]. Another major clinical challenge is radiotherapy-resistant GBM (rrGBM). Tang et al., 2023 reported that radiation-triggered RNAi nanocapsule has more excellent physiological stability, favorable BBB transcytosis, and powerful and effective rrGBM accumulation, making them encouraging radiosensitizers that could significantly enhance the performance of rrecurrent GBM-patients following low-dose X-ray irradiation [255]. Moreover, Wang et al., 2023 synthesized cancer cell membrane (CCM)-disguised hypoxia-triggered RNAi nanomedicine (a biomimetic intelligent RNAi nanomedicine, poly (MIs)/PTX@PEI/siPGK1@CCM) which demonstrated extended blood circulation, increased BBB transcytosis and precise deposition at GBM sites through homotypic recognition. Impairing PGK1-driven GBM progression makes chemotherapy and radiation therapy more effective [256]. However, to overcome the chemoresistance challenge, a study showed the presence of positively overexpressed Glectin-1 gene causes resistance. According to research by Danhier and colleagues, mice with orthotropic U87MG glioma cells had a higher median survival rate after receiving a local injection of anti-galectin-1 and anti-EGFR siRNA administered by chitosan lipid nanocapsules with TMZ. [257]. Through miRNAs that bind to complementary target mRNA sequences to cause translational repression, several oncogenic pathways, *viz.* regulation of PTEN, p53, MMP, EGFR, *etc.*, can be manipulated. Moreover. Moller and co-workers reported that in the GBM microenvironment, 256 miRNAs (miR-21, miR-10b, miR-93, miR-17, miR18, miR20, miR21, miR-30a, miR-130b) were found to be over-expressed, whereas 95 miRNAs (miR-7, miR-34a, miR-95, miR-137, miR-153, miR-128) were found to be under-expressed [258]. Recently, Lopez-Bertoni created poly (β-amino ester) NPs carrying miR-148a and miR-296-5p (nano-miRs). These nano-miRs demonstrated efficient intracellular uptake, minimal side effects, efficient endosomal escape, and release of cargo to the particular site of action, which suppressed the *in vitro* phenotype of human GBM 1A stem cells [259]. Oncogenic long non-coding RNA such as Maternally expressed gene 3 (MEG3), *Homo sapiens* HOX transcript antisense RNA (HOTAIR), H19, NEAT1, XIST and tumor suppressor LncRNA including RAMP2-AS1, Cancer Susceptibility Candidate 2 (CASC2). Others were involved in the predictor of survival in GBM patients, such as GAS5, CRNDE and TP73-AS1 [260]. The distribution of nucleic acids, which is complicated and involves several factors, is one of the main difficulties with RNAi therapies. These factors include quick renal clearance, opsonization, interaction with serum proteins, enzymatic degradation, and intracellular trafficking. These restrictions could be overcome without impairing the efficacy of the nucleic acids by using specific delivery systems such as nanogel-based, peptide-based, aptamer chimaeras, spherical nucleic acid-based, exosomes, dendriplexes, micelleplexes, liposomes, and others [261]. (Fig. 3).

5.10. Targeted toxins and suicide gene therapy

The goal of suicide gene therapy (SGT) is to introduce a gene that either code for a toxin or an enzyme that will make the target cell more susceptible to chemotherapy. SGT stands for an alternate strategy to treat diseases when standard therapies are ineffective [262]. Solid tumors can be treated with SGT in two steps. A suicide gene, such as cytosine deaminase (CD), Herpes simplex virus 1 (HSV), or TKHSV-thymidine kinase (TK), is transduced into cancer cells in the first phase. This enzyme can catalyze the conversion of a prodrug into a harmful metabolite. The second stage entails administering the relevant prodrug, which, when catalyzed by the prodrug-converting enzyme, causes cell death. The nontoxic prodrug is changed through viral vectors into a toxic metabolite that kills tumor cells once the suicide gene is introduced into glioma cells [263]. It should be emphasized that the toxin (or intermediate byproducts) can spread from the transduced tumor cells to the untransduced tumor cells through either gap junctions or diffusion, ultimately resulting in the death of both transduced and untransduced cells. The bystander effects the term used to describe this phenomenon. Depending on the characteristics of the harmful drug, bystander effect has a specific mechanism. Stem cells reprogrammed to commit suicide only use bystander effects to kill tumor cells [264]. Some major systems and their combination with prodrugs used in SGT in GBM were HSVtk/GCV system, CD/5-FC system, rabbit carboxylesterase (rCE)/irinotecan system, deoxycytidine kinase (dCK)/cytosine arabinoside (AraC) system [265]. For instance, CD changes the prodrug 5-FC into a harmful 5-FU metabolite, whereas HSV-TK changes GCV into GCV monophosphate, which is then changed into a harmful GCV triphosphate by the enzymes of tumor cells [266]. In a study by Villatoro et al., 2022, GCV prodrug was combined with canine adipose mesenchymal stem cells (cAd-MSCs)

expressing HSV-TK TK-cAd-MSCs as an alternative to GBM therapy. TK-cAd-MSCs have a significantly large secretory profile of certain cytokines and exosomes engaged in the antitumor immune response [263]. According to a study by Jubayer et al., 2019 long-term valganciclovir (valGCV) administration should be taken into account as an alternative to short-term GCV treatment in clinical trials of HSV-TK-mediated SGT in recurrent GBM [267]. To further improvement HSV-TK therapy, clenbuterol hydrochloride (Cln) as a β2-adrenergic receptor agonist was used. The findings show that Cln could increase the bystander effect of HSVTK-GCV gene therapy in human GBM cells by upregulating Cx43 expression (connexin 43 (Cx43) levels are downregulated in GBM cells, and its upregulation improves the efficacy of the gene therapy) [268]. Similarly, another group used cell-based suicide therapy and showed that by encouraging the overexpression of Cx43 in MSCs and gap junction intercellular communication (GJIC) formation between MSCs and tumor cells, iron oxide NPs have the potential to improve the suicide gene expression levels of transfected MSCs and increase the sensitivity of glioma cells to HSV-TK/GCV suicide gene therapy [269]. Other stems cells used as other cell-based delivery were such as Neural stem cells (NSCs), hematopoietic progenitor cells, induced pluripotent stem cell (iPSC)–derived NSCs, embryonic stemcell–derived astrocytes [265]. Further, in accordance with recent research, SGT may trigger the production of chemical compounds known as damage-associated molecular patterns (DAMP) and/or the presentation of neo-antigens (neoAgs), both of which can result in immunogenic cell death (ICD). The subsequent anticancer immune response is mostly mediated by lymphocytes and myeloid antigen-presenting cells [264]. Indeed, Toca 511 (vocimagene amiretrorepvec), developed by Mitchell and colleagues, is a retroviral replicating vector expressing an improved yeast CD (CD transforms the prodrug 5-FC into the active chemotherapeutic 5-FU). In randomized phase II/III trials, 5-FC produces direct tumor cell killing and changes in immune cell infiltrate, leading to a permissive TME (T cell-mediated anti-tumor immune response) in GBM [270]. Furthermore, lately, researchers have crossed the critical era of antibody-mediated toxin delivery (Immunotoxins) *via* vesicles, NPs, peptides or lipidic co-adjuvants and move towards using genes coding for toxic proteins or non-human enzymes. Research on genes having bacterial or plant origins has been extensive (*it may decrease some of the undesirable side effects that have already been noted with these important therapies.*). Some examples of bacterial toxins are Diphtheria Toxin, Pseudomonas Exotoxin A/PE38, *Clostridium perfringens* enterotoxin (CPE), Streptolysin O (SLO), Enterotoxin H (she). Plant genes such as plant ribosome-inactivating proteins (RIPs) are toxic weapons [271]. Overall, these studies hopefully move towards novel clinical investigation studies. (Fig. 3) (Table 2)

5.11. Immunostimulatory gene therapy and oncolytic virotherapy

Immunostimulatory gene therapy (IGT) aims to trigger tumor-specific lymphocyte death by stimulating DCs, T helper (Th-1) cells, and cytotoxic T lymphocytes (CTLs), shifting the continuing immunosuppression towards Th1 immunity. IGT aims to introduce genes that code for immunostimulatory proteins into the tumor site to promote tumor immunity. Drugs that block MDSCs, Tregs, or M2 macrophages should be combined with IGT. Preconditioning chemotherapy is frequently provided to reduce Tregs and MDSCs in patients receiving immunotherapy [272]. The tyrosine kinase inhibitor (TKI) sunitinib was created to target signaling in tumor cells, however, it was found that one of its modes of action was a direct inhibitory effect on MDSCs [273]. According to research by Hooren et al., 2021, systemic administration of immune-stimulatory agonistic CD40 antibodies in a glioma model causes the development of tertiary lymphoid structures related to T-cells with impaired function and compromises the response to ICIs [274]. Recently, Wei Gu and colleagues created a ROS-degradable therapeutic hydrogel (ADU-AAV-PD1@Gel) that contains AVVs and can release soluble PD-1 (sPD-1) and the STING agonist ADU-S100 locally for an extended period of time. Additionally, using gel in combination with RT therapy can encourage prolonged T-cell infiltration, restore T-cell effector function, and create a long-lasting immunological memory to prevent the recurrence of GBM [275]. Further studies demonstrate that small compounds can stimulate myeloid cells to provide anti-tumor effector activities. For instance, when administered alone or in combination with anti-PD-1 therapy, synthetic cyclodextrin-adjuvant nanoconstructs (CANDI) loaded with R848 (TLR7,8 agonist) and LCL-161 (cIAP inhibitor) activate myeloid cells and effectively induce anti-tumor immunity in GBM [276]. Similar findings were noted for IL-12 and other cytokines [277]. A phase I clinical trial (NCT03636477, NCT04006119) has 21 recurrent GBM patients showed Veledimex regulatable IL-12 gene therapy dose-dependent efficacy in combination with Nivolumab and showed improved OS was 16.9 months [278]. Further, a few studies revealed that RT causes changes in the tumor environment by releasing various factors, ultimately changing the tumor's immunogenicity and ensuring tumor cell death during GBM relapses [279]. In contrast to Tregs, MDSC migration to irradiated TME led to RT immunosuppressive characteristics by releasing numerous immunosuppressive cytokines, including IL-10, TGF-β, and IL-35 [280]. However, this effect is constrained by time and space and depends on RT modalities. It was demonstrated in various preclinical investigations that RT (FLASH-RT, Proton treatment) can reactivate anti-tumor immune responses by generating the abscopal effect, induce ICD, and transform "cold" tumors into "hot" tumors by activating the cGAS-STING pathway [279]. (Fig. 3).

Oncolytic virus (OVs) therapy is a very effective type of cancer immunotherapy that uses genetically altered viruses to attack and destroy cancerous cells preferentially while sparing healthy cells. Lysis of tumor cells releases TAA, viral pathogen-associated molecular patterns (PAMPs), and DAMPs, which can be used by DCs and NK cells to quickly clear virus-infected cells, activating innate immunity, as well as uninfected tumor cells through bystander effects [281]. In addition, cytokines and proinflammatory cytokines activate APCs and enhance CTL infiltration, thus resulting in an adaptative immune response [282]. OVs are used in numerous clinical investigations. Clinical trials were being conducted for newcastle disease virus, reovirus, parvovirus, adenovirus, poliovirus, vaccinia virus, and HSV concerning malignant gliomas In June 2021, DELYTACT® (teserpaturev/G47Δ), a genetically modified OV based on HSV-1, received conditional and temporary authorization in Japan for the treatment of malignant gliomas [283]. In a recent phase II single-arm experiment, Todo et al., 2022 mainly evaluated the effectiveness of G47Δ, a triple-mutated, third-generation oncolytic, in 19 patients with residual or recurrent supratentorial GBM following RT and TMZ. The primary endpoint of 1-year survival was 84.2%, OS was 20.2 months after G47Δ initiation and 28.8 months after the initial operation, and there were more TIL infiltrates [284]. An additional phase I/II trial was conducted in 13 Japanese patients with progressive/recurrent GBM despite receiving RT and TMZ treatments. The 1-year survival rate was 38.5%, and the median OS was 7.3 months from the most recent G47Δ injection [285]. In 2022, chimeric OncoViron was investigated and tested in solid tumors. It is a novel, broad-spectrum anticancer drug that, when used with immunotherapy, can have several synergistic effects. In GBM, this also has to be explored [286]. Due to their efficacy and specificity, OVs are potentially intriguing therapeutic strategies for GBM. The preliminary findings are encouraging, and new recombinant OVs are being developed. Additionally, methods are combined with OV therapy to greatly expand the therapeutic possibilities while minimizing their invasiveness and improving their accuracy.

6. Advent of nanotechnology in glioblastoma-targeted theranostic applications

6.1. Exosomes and liposomes-based targeted therapies

Exosomes help in enhancing drug life and hence increase the drugs' bioavailability. For instance, Yong-Wu et al., 2021 developed exosome-

Table 3
Nanomaterial-based drug combinations implemented in GBM therapeutics.

Therapy 1	Therapy 2	Experimental Model	Dosage/IC_{50}	Target	Mechanism	Reference
Temozolomide	Depatux-m	Xenograft models of GBM, U-87MG and U-87MG EGFRvIII	Depatux-m: 1 mg/kg once every 4 days Temozolomide: 1.5 mg/kg daily for 14 days	EGFR	Adding depatux-m enhances the efficacy of standard-of-care therapy in preclinical models of GBM. The durability of response to depatux-m + TMZ *in vivo* and synergy of the drug-drug interaction correlates with the amount of antigen expressed by the tumor cells	[347]
Silver nanoparticle	Cisplatin	DBTRG-05MG cells	Silver nanoparticle: 100 μg/mL Cisplatin: 25 μM	TRPM2	The combination of AgNPs and CiSP was synergistic *via* the stimulation of TRPM2 to treat DBTRG-05MG cells. The combination of AgNPs and CiSP showed a favorable action *via* the stimulation of TRPM2 in the treatment of glioblastoma tumor cells	[348]
DOX@PO-ANG-AuNPs	Radiotherapy	U87-MG cells	ANG-conjugated polymersomes: 400 μg/mL	LRP1	The inhibition of tumor cell growth was significantly increased through the combined effects of DOX and radiotherapy	[349]
Nanomicelle-curcumin	Erlotinib	U87 cell line	Nanomicelle-curcumin: 50 μM Erlotinib: 50 μM	Wnt pathway and NF-κB (p65)	Regulated autophagy and apoptosis-associated proteins. Total phospho-NF-κB (p65) and total NF-κB (p65) declined in each treatment at the protein levels	[350]
mApoE-DOXO-LIPs	Radiotherapy	Human cerebral microvascular endothelial cells were cocultured with U87-MG, A172 cells	mApoE-DOXO-LIPs: 25 μg/mL	Apoptosis pathway and immune activation	Radiotherapy and adjuvant administration of drug-loaded, mApoE-targeted nanovectors as an effective strategy to deliver cytotoxic molecules to GSCs at the surgical tumor margins, the forefront of GBM recurrence, circumventing BBB hurdles	[314]
Naringenin-loaded solid lipid nanoparticles	Paclitaxel	U87 glioma cells	NA	Apoptosis pathway	*In vitro* drug release and *in vivo* pharmacokinetic studies revealed significant improvement in the release rate and drug absorption performance from the prepared SLN formulations. The surface functionalization of SLNs with cRGD also exhibited better cellular uptake and cytotoxicity ability	[351]
Doxorubicin lauroyl hydrazone	α-tocopherol succinate micelles	GL261 cells and U87 cell line	Doxorubicin lauroyl hydrazone: 5 μM	Necroptotic cell death	The higher cytotoxicity of DOXC12-TOS-TPGS2000 micelles was mainly caused by necrosis	[352]
PEGylated liposomal doxorubicin	PEGylated liposomal carboplatin	Rat glioma C6 cells	PEGylated liposomal doxorubicin: 8.7 μM PEGylated liposomal carboplatin: 12.9 μM	ROS pathway	EG-Lip-DOX/CB, compared to DOX + CB and Lip-DOX/CB, caused less severe acute tubular necrosis and liver cell necrosis	[353]
ApoE-ARTPC	Temozolomide	U251-TR GBM *in vivo*	NA	Wnt/β-catenin signaling cascade	The combination liposomes reduced systemic TMZ-induced toxicity, highlighting the preclinical potential of this novel integrative strategy to deliver combination therapies to brain tumors	[354]
CPI444	PEGylated graphene oxide loaded vatalanib	U87MG cell lines	CPI444 + vatalanib@GO-PEG: 14 μM	VEGFR, PDGFR, A2AR, and c-KIT	Cellular assays confirmed inhibition of cell proliferation, migration, and angiogenic potential of GBM treated with GO-PEG–Drug conjugates	[355]
Oncolytic Newcastle disease virus	PLGA nanoparticles encapsulating temozolomide	AMGM5 cell lines	NDV and TMZ-PLGA-NPs: 0.1 + 6.25, 0.5 + 12.5, and at 1 + 25 MOI and μgmL−1	Cell growth and apoptosis pathway	TMZ-PLGA-NPs exerted the synergistic enhancements of the antitumor activity on the AMGM5 cell lines	[356]
MNPs@ Temozolomide	Cisplatin	Mice-bearing orthotopic U87MG or drug-resistant U251R GBM tumor	NA	Blood-brain barrier	nanoparticle formulation overcomes multiple challenges currently limiting the efficacy of combined TMZ and CDDP GBM drug therapy	[357]

mimetics coated with angiopep-2 to enhance GBM drug-delivery through manipulating protein corona. The authors also demonstrated that DOX-loaded exosome-mimetic with anngiopep-2 modification shows enhanced BBB permeability and increased concentration of DOX in the tumor area [305]. Likewise, siRNA-loaded exosomes, namely Exo-angiopep-2-siRNA, demonstrated high blood stability, efficient cellular uptake, and high BBB permeability through targeting STAT3 [306]. Valipour et al., 2022 demonstrated the anti-angiogenic effect of atorvastatin-loaded exosomes in GBM. The authors concluded that atorvastatin-loaded exosomes significantly inhibit proliferation, migration, and tube formation [307]. Mounting evidence has highlighted that GBM released myriads of exosomes in the blood vesicles, which is a potential biomarker in treating and diagnosing GBM [308]. Recently, Manterola et al., 2014 found that a snRNA and mi-RNA, namely RNU6–1, miR-320, and miR-574-3p, were significantly expressed in GBM patients and considered as a predictor of a GBM diagnosis [309].

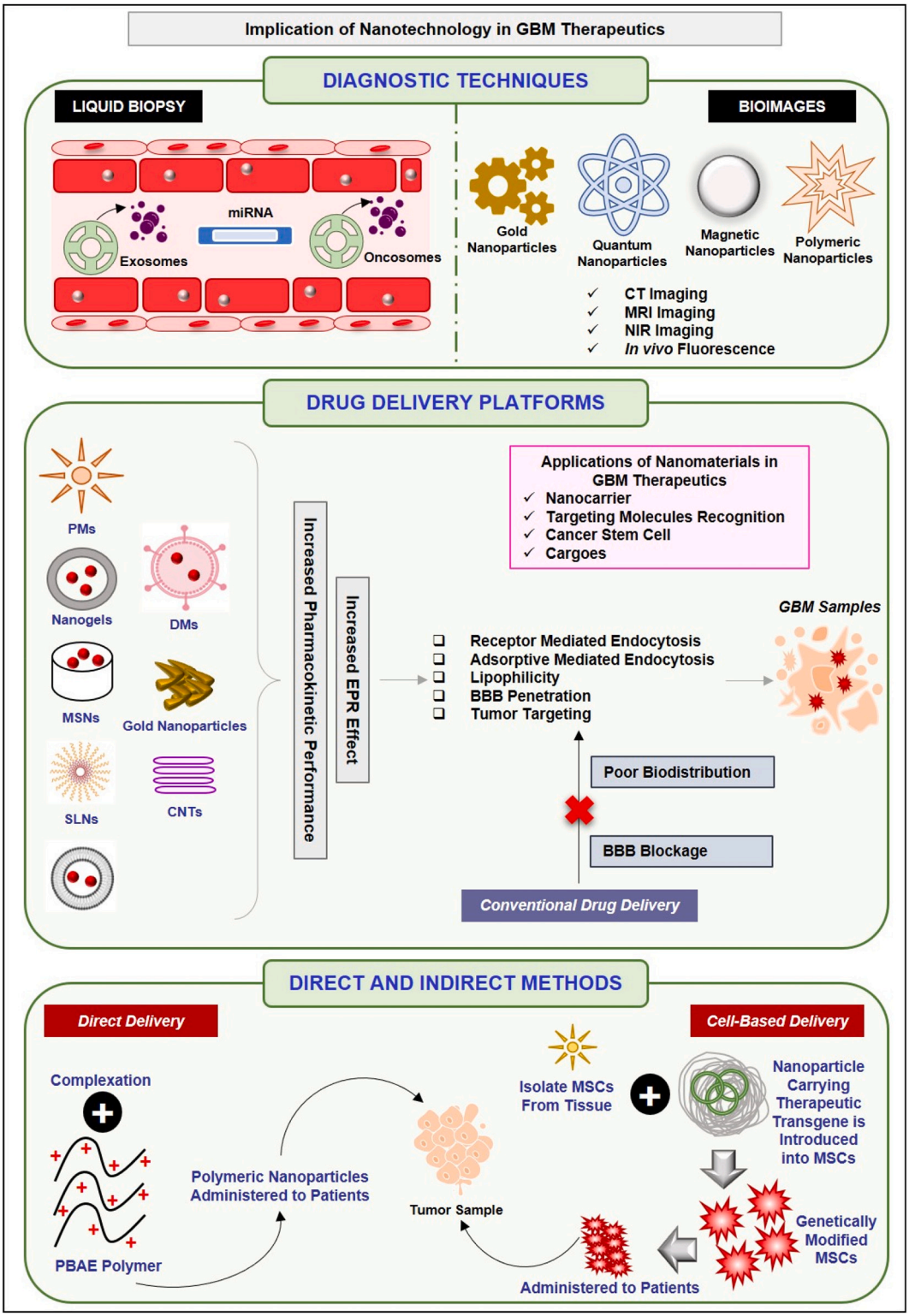

Fig. 4. Implication of Nanotechnology in GBM Therapeutics: Emerging studies have demonstrated the role of nano theranostics in GBM therapeutics through advanced drug delivery methods and diagnostic techniques. Nanoparticles, such as exosomes and oncosomes, have been involved in diagnostic procedures through liquid biopsy, whereas, nanoparticles, namely gold nanomaterials, quantum materials, magnetic nanoparticles, and polymeric nanomaterials are used for diagnostic purposes through imaging techniques, namely CT, MRI, and NIR imaging. Further, nanomaterials enhanced the drug delivery methods through increased EPR effect and pharmacokinetic properties involved in BBB penetration and tumor targeting. Compared to conventional drug delivery, nano delivery has improved bio-distribution and BBB penetration properties. As discussed in the figure, nanomaterial-based drug delivery is of two types, namely direct delivery and cell-based delivery. (For interpretation of the references to color in this figure legend, the reader is referred to the web version of this article.)

Further, it has been demonstrated that a single GBM cell secretes approximately 10,000 exosomes over a period of 48 h that carry different signaling molecules compared to GBM exosomes [310,311]. Exosomes also facilitate chemoresistance, which protects cancer cells against different drugs. However, GSCs possess several properties that make them resistance to pharmacological treatment and radiotherapy [312]. Recent studies have described a novel test, namely liquid biopsy, that allows the identification of GBM-specific exosomes in blood or CSF to facilitate the specific characterization of tumor cells.

Liposomes are highly biocompatible and biodegradable substances with a specialized compartment for hydrophobic and hydrophilic drug molecules. In GBM etiology, liposomes facilitate the desired cellular uptake through binding with the targeted ligand [313]. For instance, liposomes surfaced with apolipoprotein *E*-modified peptide were loaded with doxorubicin to enhance BBB permeability and promote liposome specificity. The results highlighted that combining doxorubicin-apolipoprotein E-liposomes significantly reduced tumor growth due to glioma stem cell apoptosis [314]. Further, drug resistance is another feature adopted by GBM cells that have shown limited efficacy by administration of a single drug through NPs. For example, smart chlorotoxin-functionalized liposomes LS for sunitinib formulation showed enhanced biocompatibility and high yield. The results also concluded that the desired formulation upregulated BAX, CASP3 and BCLN1 expression levels, whereas it downregulated Ki67, VEGFR2, PECAM1 and BCL2 expressions [315]. Similarly, the formulation of liposomes encapsulated Givinostat with or without a surface decorated with apolipoprotein E causes a reduction in cell viability, the receptors involved in cholesterol metabolism, and the reduction in HDAC activity [316]. Further, substrate-mediated, liposome-based therapeutic platforms are ideal for drug delivery because of their controlled drug release and excellent drug encapsulation. For example, hyaluronic acid (HA)-functionalized liposomes by embedding these in polyelectrolyte multilayer (PEM) to achieve sustainable delivery [317]. Additionally, in order to achieve optimal theranostic applications, nanocarriers, namely liposomes, should guide high imaging and therapeutic activities through loading suitable agents. Zhang et al., 2015 demonstrated that manganese enhanced the nano-capsulation of arsenic trioxide [318]. Table 3 discusses the nanomaterial-based drug combinations implemented in GBM therapeutics.

6.2. Carbon dots and carbon-based quantum dots

Carbon-based nanomaterials exhibit several properties, such as ultrasmall size, consistent dispersion, and high reactivity. However, fullerenes struggle with solubility issues due to their excessive hydrophobicity, which limits their biomedical applications. To normalize this issue, researchers across the globe discovered the C_{60} form that showed excellent results against GBM through inhibiting cell growth. Later, the scientists developed C_{60} conjugates that are loaded with ^{64}Cu and functionalized with cRGD peptide and 4,7-triazacyclononane-1,4,7-triacetic acid (NOTA) for targeting αvβ3 integrins in GBM pathogenesis [319,320]. Further, carbon-based nanomaterials are associated with the issue of uncontrollable toxicity, which should be resolved through modifications in physical properties. Additionally, functionalized fullerenes, such as carboxy fullerenes, metallofullerenes, and radio fullerenes, act as a potential nanocarrier to conjugate with IL-13, which is a significant receptor on the GBM cells [321–323]. Moreover, surface-modified quantum dots open new doors for treating GBM due to their excellent biocompatibility and synergistic effect with other drugs [324]. For instance, Filho et al., 2016 demonstrated the efficient conjugation between quantum dots and transferrin receptors, where the authors presented specific transferrin receptor labeling using nanotechnology [325]. Likewise, Perini et al., 2020 demonstrated enhanced chemotherapy for GBM by applying functionalized graphene quantum dots. The authors demonstrated that combining graphene quantum dots and a chemotherapeutic agent, namely doxorubicin, have a synergistic effect that enhances the treatment efficiency [326]. Carbon nanotubes are other nanomaterials that demonstrated outstanding therapeutic, imaging, drug-carrier and targeting abilities that make them suitable as theragnostic material in GBM. For example, a study on mice bearing intracranial GL261 gliomas have demonstrated that conjugation of carbon nanotubes with CpG oligodeoxynucleotides does not confers toxicity to the cells and enhanced the CpG uptake. The carbon nanotubes and CpG conjugate also potentiated the pro-inflammatory cytokine production through primary monocytes [327]. However, carbon nanotubes are associated with several disadvantages, such as agglomeration, thrombosis, inflammatory actions, and others. (Fig. 4)

6.3. Magnetic and metal-based therapies

Magnetic NPs are highly attractive nanomaterials that can be easily monitored with the help of imaging techniques. For example, iron oxide-based magnetic NPs, such as Fe_3O_4 and Fe_2O_3, demonstrate high biodegradability, biocompatibility, non-toxicity, and supramagnetic features, enhancing tumor imaging and targeting applications [328]. Pulvirenti et al., 2022 demonstrated that combined treatment of iron oxide-based NPs with temozolomide suppressed cell viability by targeting brain tumors [329]. Likewise, Swietek et al., 2022 concluded that tannic acid-coated silica magnetic nanoparticles exhibit high antioxidant properties and have high potential as nanocarriers [330]. However, setting up specific boundaries for GBM is still challenging; thus, the developed NPs should have high imaging contrast. To achieve this, several studies have been performed to enhance the contrast of magnetic NPs, for example, angiopep-2-conjugated PEGylated-ultrasmall NPs with high BBB permeability and stability [331]. Recently, lipid-based magnetic NPs have been developed for targeting GBM. Tapeinos et al., 2019 demonstrated that lipid-based magnetic NPs enhance the release in response to the magnetic field and increase the hydrogen peroxide concentration. The authors concluded that lipid-based magnetic nano vectors enhanced apoptosis in GBM cells through synergistic chemotherapy and hyperthermia [332]. In addition to magnetic NPs, metal-based NPs have been developed to target GBM cells. Tumor ablation and hyperthermia are the two widely used applications of metal-based NPs. Gold NPs, especially gold nanorods, have been used to solve the issues related to metal-based NPs for their excellent tunable optical properties [333]. For example, Coluccia et al., 2018 demonstrated that cisplatin-gold NPs conjugates combined with MR-guided focused ultrasound intensify GBM treatment through increased DNA damage and enhanced BBB permeability [334]. Recently, Yu et al., 2022 concluded that TMZ-conjugated Gold NPs increase cell apoptosis by regulating signaling molecules and cell cycle [335]. Further, gold nanorods have high biocompatibility, and they also possess the ability to interact with tumor biomarkers. A study observed that PEGylated conjugated nestin combined with gold nanorods have low cytotoxicity and are efficiently taken up by multicellular tumor spheroids [336]. However, incorporating gold NPs in GBM treatment faces several questions, such as non-selective heating and uneven distribution within GBM cells. Table 3 discusses the nanomaterial-based drug combinations implemented in GBM therapeutics.

6.4. Polymer-based nanomaterials

Polymer-based NPs, such as chitosan, cellulose, polyethylene glycol, and alginates, possess several physiochemical properties: high biodegradability, long-term stability, drug-loading capacity, and targeting ability that makes them ideal nanocarrier. Polymer-based NPs can easily cross BBB permeability through different mechanisms, such as carrier-mediated transport and adsorption-mediated transcytosis [337]. For example, miR-219-chitosan NPs reduced cell viability and suppressed tumor growth [338]. Similarly, n-butylidenephthalide-polyethylene glycol-gold NPs significantly inhibit brain cancer cell proliferation and regulate the cell cycle [339]. Moreover, polymer-based NPs have

Table 4
List of combinatorial drugs administrated in GBM therapeutics.

Therapy 1	Therapy 2	Experimental Model	Dosage/IC_{50}	Target	Mechanism	Reference
			Drug-Drug Combination			
Temozolomide	AZD3463	T98G GBM cells	Temozolomide: 1.54 mM AZD3463: 529 nM	PI3K/AKT signaling pathway	Causes the cell cycle arrest in distinct phases and induces apoptosis	[421]
Temozolomide	Resveratrol	Human LN-18 and LN-428 cell lines	Temozolomide: 750 μM Resveratrol: 75 μM	STAT3 signaling event	The combination significantly reduced the expression of the STAT3/Bcl-2/survivin signaling pathway	[422]
Temozolomide	Cedrol	DBTRG-05MG, RG2 cell lines, and CTX TNA2 rat astrocytes	Temozolomide: 206 μM and 5 mg/kg Cedrol: 112.4 μM and 75 mg/kg	MGMT, MDR1, and CD33	Resulted in consistently higher suppression of cell proliferation *via* regulation of the AKT and MAPK signaling pathways in GBM cells. Combination treatment induced cell cycle arrest at the G0/G1 phase	[423]
Dutasteride	Androgen receptor antagonists	U87 cell culture model	Dutasteride: 5 μM Cyproterone: 25 μM Flutamide: 50 μM	Androgen regulation	A combination of these drugs enhanced their inhibitory effects. The combination of dutasteride with flutamide was most effective at decreasing GB cell proliferation	[424]
Polish propolis	*Bacopa monnieri*	T98G, LN-18, U87MG cell lines	NA	Necrosis and apoptosis pathway	The inhibitory effects on the viability and proliferation of the tested glioma cells observed after incubation with the combination of PPE and BcH were significantly stronger	[425]
Temozolomide	KC7F2	U87MG glioma cell line	Temozolomide: 100–500 μM KC7F2: 1–30 μM	HIF-α and HIF-1β	Combined effect of the reduced effective dose of the TMZ alkylating agent and the effect was increased, and the effect of the combined therapy is assessed from a metabolic point of view and that it suppresses aerobic glycolysis	[426]
Gossypol	Phenformin	Sphere-cultured U87 and GBM TS (TS13–64)	Gossypol: 10 μM Phenformin: 10 μM	Autophagy pathway	Combination therapy with gossypol, phenformin, and TMZ induced a significant reduction in ATP levels, cell viability, stemness, and invasiveness compared to TMZ monotherapy and dual therapy with gossypol and phenformin	[427]
Dichloroacetate	Metformin	C57BL/6 mice GL-261 allograft model, Human U-87 MG (U-87) and murine GL-261 glioblastoma cell lines	Dichloroacetate: 20 mM Metformin: 10 mM	Apoptosis and necroptosis pathway	DCA and MET synergistically suppress the growth of glioblastoma cells *in vivo*	[428]
AZD6482	URMC-099	U-87 MG, U-118 MG, U-138 MG, U-343 MG, U-373 MG, U-251 MG, A-172, LN-Z308 and SK-MG3 cell line model, normal human astrocytes cell line	AZD6482: 34.56 μM URMC-099: 4.57 μM	MLK3 and PI3Kβ	Combination of AZD6482 and URMC-099 effectively decreased glioblastoma xenograft growth in nude mice. Glioblastoma cells treated with this drug combination showed reduced phosphorylation of Akt and ERK and decreased protein expression of ROCK2 and Zyxin	[429]
MS-275	TAK-733/Trametinib	Human GB cell lines U87 and U251	MS-275: 1 μM TAK-733: 1 μM Trametinib: 1 μM	Histone H3, MAPK, p-MAPK	HDACi and MEKi alone at 1 μM significantly reduced the number of spheres formed	[430]
Cordycepin	Doxorubicin	LN-229, U251 and T98G cells	Cordycepin: 80 μM Doxorubicin: 1 μM	EMT-related genes	Inhibits the growth and proliferation of LN-229 cells through various pathways. Combination inhibits cell invasion and migration by regulating the EMT switch of tumor cells	[431]
Temozolomide	Onalespib	Patient-derived glioma stem cell lines	Temozolomide: 10 μM Onalespib: 0.4 μM	HSP90 and GSCs	The combination of onalespib with radiation and TMZ extended survival in a zebra fish and a mouse xenograft model of GBM compared to the standard of care	[432]

(*continued on next page*)

Table 4 (*continued*)

Therapy 1	Therapy 2	Experimental Model	Dosage/IC_{50}	Target	Mechanism	Reference
Temozolomide	Anlotinib	A172, U87, and U251 human glioblastoma cell lines	Temozolomide: 100 μM Anlotinib: 2 μM	JAK2/STAT3 signaling pathway	Exerts anti-glioblastoma activity, possibly through the JAK2/STAT3/VEGFA signaling pathway.	[433]
Temozolomide	Taurine	U-251 MG cell lines	Temozolomide: 375 μM Taurine: 12 mM	Cell cycle pathway	Exerts anticancer properties against U-251 MG manifested by the induction of G2/M arrest and apoptosis	[434]
Temozolomide	Menadione/ascorbate	GS9L cell transplants - intracranial model	NA	Mitochondrial superoxide	Causing redox alterations and oxidative stress only in the tumor.	[435]
Temozolomide	Bortezomib	T98G cells of human GBM	NA	MGMT	Combination of TMZ and CCNU with a proteasome inhibitor-bortezomib-significantly increases their ability to eradicate cells of a radioresistant GBM	[436]
Temozolomide	Valproic acid	GBM cell lines U87, DBTRG-05MG, U118MG, and LN229	Temozolomide: 3 mM Valproic acid: 2.5 mM	p53-PUMA apoptosis pathway	Survival benefit of a combined TMZ and VPA treatment in GBM patients is dependent on their p53 gene status	[437]
Acalabrutinib	Rapamycin	U87MG and LN229 cell lines	Acalabrutinib: 5 μM Rapamycin: 0.1 μM	SOX2, OCT4, CD133, KLF4, and NANOG	Rapamycin and Acalabrutinib effectively reduced the viability of gbm cell lines and exerted a synergistic antiproliferation effect, and reduced the tumorsphere-formation potential	[438]
Temozolomide	Celecoxib	LN229 and LN18 cell lines	Temozolomide: 250uM Celecoxib: 30uM	Cyclooxygenase-2	Combination therapy may inhibit cell proliferation, increases apoptosis, and increases the autophagy on LN229 and LN18	[439]
THTMP	T0510.3657	Mesenchymal cell lines derived from patients' tumors	THTMP: 50 μM T0510.3657: 10 μM	HSP27 and p53	Combination of THTMP + T0 profoundly increased the $[Ca2^{+}]$ i, reactive oxygen species in a time-dependent manner, thus affecting MMP and leading to apoptosis	[440]
Temozolomide	Gefitinib	U87MG cell lines	Gefitinib: 11 μM Temozolomide: 100 μM	VEGF, MMP9, and MMP2	Indicates synergistic effects of GFI plus TMZ against glioma are mediated by the potentiated anti-angiogenesis	[441]
LY294002	Sorafenib	MOGGCCM and T98G cell lines	LY294002: 10 μM Sorafenib: 1 μM	PI3K and Raf	Combination of LY294002 and sorafenib was very efficient in apoptosis induction in glioma cells	[442]
Bevacizumab	Temsirolimus	Ex ovo CAM, Rat 9 L or human U87 glioblastoma cells	Bevacizumab: 17 μg/mL Temsirolimus: 100 ng/mL	Angiogenesis and hypoxia signaling pathway	Combination therapy is effective even at concentrations further reduced 10-fold with a CI value of 2.42E-5, demonstrating high levels of synergy	[443]
Perampanel	Temozolomide	U87, U138, and A172 glioma cell lines	Perampanel: 150 μM Temozolomide: 300 μM	GluR2/3 receptor	Synergic effect causes apoptosis that inhibits the growth of the cells.	[444]
Arsenite	Gamabufotalin	Human glioblastoma cell lines U-87 and U-251	Arsenite: 3.3, 5, and 7.5 μM Gamabufotalin: 40, 60, and 90 nM	p38 MAPK	The results observed a synergistic cytotoxic effect of ASCII and gamabufotalin in glioblastoma cell line u-87 but not u-251	[445]
Ciclopirox	Bortezomib	Human glioblastoma cell lines U251, SF126, A172, and U118	Ciclopirox: 20 μM Bortezomib: 24 nM	JNK/p38 MAPK and NF-κB signaling	The combination of CPX and BTZ promotes apoptosis of GBM cells and inhibits GBM tumor growth *in vivo*	[446]
Temozolomide	ZSTK474	human GBM cells *in vitro* and *in vivo*	ZSTK474: 0.4 μM for SF295, 1.2 μM for U87 Temozolomide: 120 μM for SF295, 180 μM for U87	PI3K	The combination treatment led to significantly increased cell apoptosis and DNA double-strand breaks (DSBs)	[447]
Temozolomide	SB225002	Human umbilical vein endothelial cells (HUVECs)	SB225002: 0.03 μM Temozolomide: 10 μM	CXCR2 and VEGFR	Combination therapy induces downregulation of anti-apoptotic BCL2 and CXCR2 gene, and protein expression is altered differently by the combination therapy	[448]

(*continued on next page*)

Table 4 (*continued*)

Therapy 1	Therapy 2	Experimental Model	Dosage/IC_{50}	Target	Mechanism	Reference
Eicosapentaenoic acid	Cisplatin	DBTRG cells	Cisplatin: 25 μM Eicosapentaenoic acid: 30 μM	TRPM2 channel	Anticancer, apoptotic, and oxidant actions of CiSP were further increased *via* the activation of the TRPM2 channel in the DBTRGs by the treatment of EPA	[449]
Ascorbic acid	Menadione	U251 human glioblastoma cells	Ascorbic acid: 1 mM Menadione: 20 μM	AMPK/mTORC1/ULK1 pathway	Combined treatment induced strong cytoplasmic vacuolization and a significant decrease in cell density. Induces ROS- and mitochondrial depolarization-mediated necrotic cell death	[450]
Temozolomide	Metformin	LN229 cells	Temozolomide: 100 μM Metformin: 50 mM	MGMT and EMT pathway	The sensitivity of the TMZ-resistant GBM cell line to metformin might be mediated *via* the suppression of mitochondrial biogenesis, EMT, and MGMT expression	[451]
Melittin	Cisplatin	DBTRG-05MG cells	Cisplatin: 25 μM Melittin: 2.5 μg/mL	TRPM2	The treatment of MLT increased the anticancer, tumor cell death, apoptotic, and oxidant effects of CSP in the glioblastoma tumor cells *via* activating the TRPM2	[452]
NBM-BMX	Temozolomide	GBM cell lines, U87, U87R, A172, and A172R	NBM-BMX: 10 μM Temozolomide: 50 μM	β-catenin/c-Myc/SOX2 Pathway and p53-Mediated MGMT pathway	BMX overcomes TMZ resistance by enhancing TMZ-mediated cytotoxic effect by downregulating the β-catenin/c-Myc/SOX2 signaling pathway and upregulating WT-p53 mediated MGMT inhibition	[453]
BH3-mimetics (ABT-263, WEHI-539, and S63845)	Chemotherapeutic drugs (Temozolomide, CCNU, and VCR)	GSC-ECLs	S63845: 0.1 μM WEHI-539: 1 μM Temozolomide: 250 μM CCNU: 20 μM VCR: 0.5 μM	NOXA pathway	Combination of BH3-mimetics targeting Bcl-xL with chemotherapeutic agents caused a marked increase in cell death and this sensitivity to Bcl-xL inhibition correlated with Noxa expression levels	[454]
Ruxolitinib	Temozolomide	U87MG, BCSC, and HBMEC cell lines	Ruxolitinib: 89.75 μM Temozolomide: 391.48 μM	WNT signaling pathway	The BBB-crossing agent ruxolitinib promises the potential to increase the efficacy of temozolomide in glioblastoma	[455]
Temozolomide	Etoposide	U87 MG cells	Temozolomide: Etoposide:	Oxidative stress, cell cycle, apoptosis, and autophagy signaling	Combined high-dose treatments of classical antineoplastic agents to sensitize tumors may trigger multi-drug resistance and inhibit maintenance treatment	[456]
Berbamine	Arcyriaflavin A	U87MG- and C6-derived GSCs	Arcyriaflavin A: 20 μM Berbamine: 10 μM	CaMKIIγ and CDK4	Promotes GSC apoptosis, downregulates CaMKIIγ-mediated growth signaling pathway	[457]
Matteucinol	Temozolomide	U-251 cell line	Matteucinol: 28 μg/mL Temozolomide: 9.71 μg/mL	TNFR1	This combination selectively reduced cell viability in the tumor cell line (U-251 MG)	[458]
Letrozole	Temozolomide	patient-derived G76, BT142, G43, and G75 GBM lines	Letrozole: 40 nM Temozolomide: reduced by 8, 37, 240 and 640 folds in G76, BT-142, G43 and G75 cells, respectively	Apoptotic signaling pathways	LTZ increases DNA damage and synergistically enhances TMZ activity in TMZ-sensitive and TMZ-resistant GBM lines	[459]
Mebendazole	Temozolomide	U87 and U373 cells	Mebendazole: 0.2 μM Temozolomide: 50 μM	Cell cycle arrest	The combination of MBZ and CQ also showed an enhanced effect in TMZ-resistant glioblastoma cells	[460]
Cannabigerol (CBG)	Cannabidiol (CBD)	Human GB cell lines U87 and U373	CBG: 1.5 μM CBD: 5 μM	Apoptosis pathway	CBG similarly inhibited GBM invasion to CBD, and the TMZ	[461]
Osimertinib	Bevacizumab	GBM Patients	Osimertinib: 80 mg/day Bevacizumab: 15 mg/kg	STAT3 and PTEN	EGFR amplification plus EGFRvIII mutation	[462]
Temozolomide	Lonafarnib	GBM cells in multicellular tumor spheroid (MCTS) models	Lonafarnib: 5 μM Temozolomide: 100 μM	NESTIN, SOX2, CD133, NANOG, and OCT4	Expression of most of the stemness markers significantly increased in the LNF + TMZ treated condition as compared to the untreated condition	[463]

excellent self-assembling properties, allowing them to encapsulate DNA molecules that involve modifying biological entities easily. For example, Ren et al., 2022 developed a reduction-sensitive heterodimer prodrug of doxorubicin and dihydroartemisinin NPs that demonstrated anti-tumor activity. The authors demonstrated that *in vitro* DOX-dihydroartemisinin-disulfide bonds NPs proved to be a tumor suppressor that increases survival time [340]. Similarly, An et al., 2015 concluded that artificially synthesized polycation with redox-sensitive disulfides in RNAi nanospheres enhanced the survival time and decreased the glioma proliferation rate [341]. Moreover, BBB is a significant problem in GBM therapeutics. In order to overcome this problem, polymer-based NPs can be used for the controlled and sustainable delivery of chemotherapeutic agents [342]. Mounting evidence suggests that polymer-based NPs can be highly stable and induce selective toxicity. Ibarra et al., 2020 developed a conjugated polymer NP-loaded monocyte to improve PDT in GBM. The authors demonstrated that conjugated polymer NP-loaded monocyte did not affect the monocyte viability in the absence of light and did not exhibit nonspecific release after the drug loading [343]. Recent studies have focused on polymer-based NPs in diagnosing GBM, associated with high-resolution imaging modalities. Polymer-based NPs, with their superparamagnetic properties, have been implemented as imaging agents in MRI techniques [344]. For example, Ganipineni et al., 2018 developed paclitaxel and superparamagnetic iron oxide-loaded PEGylated poly (lactic-*co*-glycolic acid)-based NPs through emulsion-diffusion-evaporation method and identified that the developed NPs have potential to disrupt BBB with enhanced accumulation in GBM site. Further, the developed NPs can enhance the survival rate with less toxicity effects [345]. Likewise, Wang et al., 2018 constructed poly lactic-*co*-glycolic acid-superparamagnetic-polyethyleneimine-conjugated fluorescein isothiocyanate loaded with paclitaxel and concluded that the developed NPs inhibit cell proliferation and cell migration through the accumulation of autophagosomes [346]. Despite having the several advantages of polymer-based NPs, many more experimental and clinical studies should be performed for an effective anti-GBM therapy that leads to more patient-specific and targeted anti-cancer therapies. (Fig. 4).

7. The emergence of combination therapies: Fosters innovation and hope

With recent development in molecular biology approaches and due to the lack of significant overall survival benefits, there is an utmost need for combinatorial strategies in GBM therapeutics. Mounting evidence has demonstrated that combining TMZ with other therapeutic drugs increases the therapeutic efficiency in patients with malignant glioma. For instance, the combination of TMZ either with Lomustine (100 mg/m^2), Ralimetinib (100 mg/kg), and Mebendazole (200 mg/kg) improves survival in patients with glioma with methylated MGMT promoter as compared to standard therapy of TMZ [400–402]. Table 4 encompasses the list of combinatorial drugs administrated in GBM therapeutics. A clinical trial on 38 patients with recurrent GBM was administered with Macitentan (300 mg once a day) and Levetiracetam (2000 mg/day) that concluded the protective effect of repurposed drugs in combination with TMZ [403,404]. Recently, Wang et al., 2021 demonstrated that treating GBM patients with Carelizumab, Anlotinib, and Oxitinib during RT increases the OS and PFS [405]. Likewise, Lustig et al., 2022 concluded that the combination of TMZ with Ko143, a non-toxic analog of fumitremorgin C, decreases IC_{50} of TMZ by 41.07% in the resistant phenotype and enhanced the inhibition rate of P-glycoprotein as compared to the treatment of TMZ alone [406]. Drug administration of a single drug is a crucial focus in GBM therapeutics, however, the combination of the drug with other therapies, such as radiotherapy and immunotherapy, increases its efficiency and overall survival rate. For instance, treatment of GBM patients with TMZ in combination with immunotherapy significantly enhanced the OS rate of patients at about 22 months [407]. A study conducted by Serra et al., 2022 reported that a combination of acriflavine, TMZ, and radiation significantly improved the OS rate in an intracranial rat gliosarcoma model [408]. Similarly, Momeny et al., 2021 concluded that cediranib, a pan-inhibitor of VEGFR, inhibits cell proliferation rate and enhances therapeutic sensitivity in GBM [409]. Recently, the focus has been shifted towards identifying novel therapies for GBM, where a combination of drug-siRNA and drug-miRNA was the most promising approach. For example, a study conducted by Amini et al., 2021 showed that siRNA-mediated suppression of PIK3R3 activity inhibited cell proliferation and activated apoptosis by decreasing the IC_{50} value of Erlotinib [410]. Likewise, the combination of Sulforaphane and PNA-a15b increases the pro-apoptotic effects and inhibited cell proliferation through increasing the expression of caspase 3 and caspase 7 [411]. Setdi et al., 2022 tested a combination of fatty acids omega-3, 6, and 9 on mitochondria isolated from U87MG human glioma cells, where they reported that the combination significantly reduced the activity of succinate dehydrogenase and enhanced toxicity effects through mitochondria [412]. Likewise, a combination of Ulipristal-TMZ-hydroxyurea administration in the human U251 GBM cell line significantly reduced the cell proliferation and total antioxidant capacity. The study also concluded that the combination of three drugs reduced the expression of immunosuppressive and/or GBM-growth stimulating cytokines TGFβ, IL-10 and IL-17 while increasing the expression of GBM-growth suppressing cytokine IL-23 [413]. The combination of Chloroquine, Naringenin and Phloroglucinol synergistically potentiated the efficacy of TMZ on glioma *in vitro* and *in vivo* through downregulation of Bcl-2 and VEGF [414]. On the same trend, the combination of epigenetic modifiers, namely BIX01294, DZNep, and Trichostatin A at low concentrations exhibited a synergistic effect on cell viability and cell proliferation [415]. Guo et al., 2022 reported the protective function of micheliolide- L-buthionine sulfoximine combination in GBM therapeutics through targeting redox and metabolic pathway [416]. BET proteins have been considered crucial epigenetic markers in GBM pathogenesis, where inhibition of BET through BETi in combination with TMZ induces increased levels of γ-H2AX, a proxy for DNA double-strand breaks [417]. Different other studies have demonstrated the positive effect of drug combinations, namely dabrafenib-trametinib, irinotecan-bevacizumab, and acridone derivatives-TMZ to overcome drug sensitivity and inhibit cell proliferation in GBM therapeutics [418–420]. Thus, the studies mentioned above have concluded the positive effect of combinatorial therapy against GBM pathogenesis and progression by inhibiting cell proliferation and migration.

8. The journey so far: ongoing clinical trials in GBM therapeutics

Therapeutic advancements to combat GBM have occurred in the last 2 decades. However, the failure of phase III clinical trials to meet their end-goals led to the development of novel therapeutic approaches, namely nanomaterials-based treatment, combination therapy, stem-cell-based therapy, and others [464]. Herein, we presented the data that provides the real-world scenario of clinical trials to raise the key questions. Till date, more than 160 clinical trials have been performed on different drug molecules and therapies to reverse the progression of GBM. The majority of phase I, phase II, and phase III clinical trials were associated with adverse effects, such as toxicity, safety, and dosage. Among those phases, I, II, and III clinical trials, more than 87% of studies were nonrandomized and had no control. Further, only 40% of studies have enhanced OS, 27% have PFS, and 22% have an objective response rate as the primary outcome [465,466]. Additionally, the major drawback associated with clinical trials in GBM is the preliminary phase II study design because of their lack of historical records. Thus, single-arm phase II clinical trials are associated with a high risk of leading to the incorrect decision for phase III clinical trials [467,468]. Immune checkpoint inhibitors have changed the landscape of GBM therapeutics. For instance, PD-1/PD-L1 monotherapy treatments have been investigated in GBM progression. A phase II study demonstrated that the

Table 5
Ongoing clinical trials of different therapies against GBM progression.

S. No	Intervention	Treatment	Status	Phase	NCT Number	Study Start Date	Primary Outcome
1	B7-H3 CAR-T + TMZ	**B7-H3 CAR-T**: B7-H3 (overexpressed in cancer cells) targeted CAR-T	Recruiting	I/III I	NCT04077866 NCT05241392	01.06.2023 27.01.2022	Safety and tolerability intratumoral/ intracerebroventricular injection of B7-H3 CAR-T
2	LITT surgery + TMZ	**LIIT:** minimally invasive and cytoreductive neurosurgical technique	Active, not recruiting	I/II	NCT05663125	01.12.2022	Safety of MRI-guided LITT techniques
3	Pembrolizumab + Olaparib + TMZ	**Olaparib**: PARP inhibitor	Recruiting	II	NCT05463848	21.10.2022	TIL Density and PFS for 6 months
4	Atezolizumab + fractionated stereotactic RT	**Atezolizumab**: anti-PDL1 monoclonal therapy	Recruiting	I	NCT05423210	21.09.2022	Efficacy of combination
5	Retifanlimab + TMZ + RT	**Retifanlimab**: anti-PD-1 monoclonal Therapy	Recruiting	I	NCT05083754	31.08.2022	Safety of combination retifanlimab and RT with and without TMZ upto 2 years
6	CYNK-001 + Recombinant Human IL-2	**CYNK-001** is a CD56 + CD3- enriched, off-the-shelf, allogeneic natural killer cell product expanded from placental CD34 cells	Recruiting	I/II	NCT05218408	08.03.2022	Maximum tolerated dose and Dose-limiting toxicity
7	M032 + Pembrolizumab	**M032**: Genetically Engineered HSV-1 Expressing IL-12	Active, not recruiting	I/II	NCT05084430	25.02.2022	OS and PFS for 12 and 6 months
8	Tamoxifen + Etoposide	**Tamoxifen**: competitively inhibits estrogen binding to its receptor Etoposide: inhibits DNA synthesis by forming a complex with topoisomerase II and DNA	Recruiting	II	NCT04765098	28.01.2022	PFS for 3 months
9	GX-17 + Bevacizumab	**GX-I7**: a long-acting interleukin-7	Active, not recruiting	II	NCT05191784	26.01.2022	OS upto 24 months
10	Pembrolizumab + Stereotactic RT + Surgery	**Pembrolizumab:** anti-PD-1 monoclonal Therapy	Recruiting	I/II	NCT04977375	09.12.2021	Safety and tolerability and OS upto 2 years
11	NMS-03305293 + TMZ	**NMS-03305293:** orally bioavailable nuclear enzyme PARP inhibitor	Recruiting	I/II	NCT04910022	01.12.2021	Safety, efficacy, and dose-limiting toxicity of the combination
12	Camrelizumab + GSC-DCV	**Camrelizumab:** humanized IgG4-kappa anti-PD-1 monoclonal antibody **GSC-DCV:** Vaccine containing DCs pulsed with glioblastoma stem-like cell (GSC) antigens	Recruiting	II	NCT04888611	26.10.2021	Safety and efficacy of combination; OS and PFS for 24 and 12 months, respectively
13	ACT001 + Pembrolizumab	**ACT001:** Plasminogen activator inhibitor-1 protease inhibitor; **Pembrolizumab:** anti-PD-1 monoclonal Therapy	Recruiting	I/II	NCT05053880	22.09.2021	Dose-limiting toxicities
14	Dendritic Cells (DC) vaccine + TMZ	**DC vaccine:** contains 2–10 million DC cells, loaded with 5–20 tumor neoantigen peptides	Recruiting	I	NCT04968366	30.07.2021	An incident of Treatment-Emergent Adverse Events
15	Berubicin + Lomustine	**Berubicin:** cytotoxic anthracycline topoisomerase II inhibitor **Lomustine:** alkylating agent	Recruiting	II	NCT04762069	18.05.2021	OS upto 4 years
16	Camrelizumab + Bevacizumab	**Camrelizumab:** humanized IgG4-kappa anti-PD-1 monoclonal antibody; **Bevacizumab:** selectively binding circulating VEGF, inhibiting the binding of VEGF to its cell surface receptors	Recruiting	II	NCT04952571	01.05.2021	PFA upto 6 months; Drug safety and tolerability of the combination
17	Stereotactical PDT + 5-aminolevulinic acid (Gliolan)	**5-aminolevulinic acid:** a Porphyrin Precursor and Optical Imaging Agent. Stereotactic biopsy followed by stereotactical photodynamic therapy	Recruiting	II	NCT04469699	12.04.2021	PFS for 1.5 years
18	Onfekafusp alfa + TMZ (GLIOSUN)	**Onfekafusp alfa:** anti-(human fibronectin ed-b domain) (synthetic human clone l19 scfv fragment) fusion protein with human TNF-alpha.,	Recruiting	I/II	NCT04443010	20.01.2021	Dose finding; Safety and Efficacy of combination
19	TTFields + SRS	**SRS:** Stereotactic radiosurgery TTFields: uses alternating electric fields of intermediate frequency (~100–500 kHz) and low intensity (1–3 V/cm) to disrupt cell division	Recruiting	II	NCT04671459	26.12.2020	1-year survival analysis
20	Enzastaurin Hydrochloride + TMZ followed by PT	**Enzastaurin Hydrochloride:** serine/ threonine kinase inhibitor, inhibits protein kinase C activity and phosphorylation and activation of AKT, GSK3, and S6K, leading to inhibition of tumor cell proliferation	Active, not recruiting	III	NCT03776071	16.12.2020	OS upto 3 years
21	CC-90010 + TMZ/RT	**CC-90010:** an oral, reversible, small-molecule inhibitor of BET proteins	Recruiting	I	NCT04324840	10.07.2020	Incidence of adverse events, Safety and tolerability
22	Selinexor + RT/TMZ/ bevacizumab/TTField/ Lomustine	**Selinexor:** a first-in-class selective inhibitor of nuclear transport (SINE) compound **Lomustine:** alkylating nitrosourea compound (cross-linking of DNA (at the O6 position of guanine-containing bases)	Active, not recruiting	I/II	NCT04421378	08.06.2020	Maximum Tolerated Dose, OS for 24 months and PFS for 3 months

(*continued on next page*)

Table 5 (*continued*)

S. No	Intervention	Treatment	Status	Phase	NCT Number	Study Start Date	Primary Outcome
23	2-OHOA + TMZ	**2-OHOA:** 2-hydroxyoleic acid induces cell cycle arrest	Recruiting	II/III	NCT04250922	01.12.2019	Efficacy and PFS of combination
24	Valganciclovir + TMZ + RT	**Valganciclovir:** antiviral medication used to treat cytomegalovirus infections	Recruiting	II	NCT04116411	04.09.2019	Efficacy upto 30 months
25	Nivolumab/BMS-986205/Radiation Therapy + TMZ	**BMS-986205:** IDO1 Inhibitor Nivolumab: humanized IgG4-kappa anti- PD-1 monoclonal antibody	Recruiting	I	NCT04047706	13.08.2019	Drug safety and tolerability

administration of durvalumab in combination with bevacizumab increases CD8 + Ki67 + T cells [469]. Duerinck et al., 2021 demonstrated that in the phase I clinical trial (NCT03233152), intracerebral administration of CTLA-4 and PD-1 immune checkpoint blocking monoclonal antibodies in patients maximized safe resection of recurrent GBM [470]. Similarly, a phase III randomized clinical study highlighted the synergistic effect of Veliparib-chemotherapy and Depatuxizumab-mafodotin combination in GBM patients to increase overall survival rate and decrease cell proliferation [471,472]. Likewise, a phase III clinical trial on 369 GBM patients demonstrated that administration of nivolumab in combination with radiotherapy improved survival rate [473]. Table 5 discusses the ongoing clinical trials in GBM progression and pathogenesis.

9. Conclusion and future perspectives

Despite having enormous amount of research on cancer therapeutics across multiple tumor types, treatment, and management of GBM is still a huge challenge that requires the development and execution of advanced therapeutic approaches. Currently, approximately more than 500 clinical trials have been registered at clinicaltrial.gov. However, they fail to show promising results in phase III randomized clinical trials despite having the hopeful results at early phases. Moreover, the recurrence rate is incredible high in GBM with lower survival rate [474]. Tumor microenvironment and GBM heterogeneity are two other crucial factors that makes the therapeutic management of GBM difficult. Thus, all these mentioned challenges highlighted the importance of identifying novel therapeutic biomarkers, biomolecules, and strategies. Mounting evidence suggests the involvement of several signaling pathways (MAPK, RTKs, JNK, PI3K, and others) and signaling molecules (EphA3, EGFR, VEGF, PDGFR, and MET) that can be used as crucial therapeutic targets in GBM etiology [475]. Although, there has been varied and minimal clinical success in the use of specific target inhibitors as anti-cancer therapies. Thus, there is utmost importance of identifying novel signaling pathways and molecules that shows promising clinical effects. For instance, WNTs and their downstream molecules regulates cell proliferation and migration that might be associated with GBM etiology, whereas, hedgehog pathway inhibition or inactivation regulates the death of cancer stem cells in GBM [38,476].

Moreover, the traditional treatment option includes chemotherapy, immunotherapy, radiotherapy, and surgical resection that enhanced the survival rate of the patient but imposes various side effects, such as toxicity [477]. To overcome the problems associated with conventional therapies, the scientists have developed emerging methods for the treatment of GBM, namely adoptive cell therapy, tumor treating fields, photodynamic therapy, targeted toxins and suicide gene therapy, vaccine therapy, photothermal therapy, and others that demonstrated the high survival rate and low recurrence rate. For instance, Adhikari et al., 2022 developed human cytomegalovirus-based multi-antigen vaccine for GBM, where they demonstrated that administration of vaccine causes increased in survival rate up to 56% through upregulation of T cells expression [478]. Likewise, Chen et al., 2019 demonstrated that MSH6-CXCR4-TGFB1 feedback loop accelerated the GBM etiology, which can be targeted by Cu2(OH)PO4@PAA + near infrared (NIR) irradiation, and leads to its inactivation that rescue cell proliferation and migration [479]. Additionally, CAR T-based therapy exhibited a promising therapeutic solution, but antigenic heterogeneity and post-therapy restoration of immunosuppressive paradigm limits the responses of CAR T-based therapy [480]. Recent studies have demonstrated the potential role of nanomaterials in GBM. The most challenging task in GBM therapeutics is crossing the BBB by drug molecules. In respond to limited and damaged lymphatic system in the GBM etiology, nanoparticles have potential to retain in GBM tissues and elicit antitumor effects that make nanotheranostic, a potential therapeutic strategy to reverse GBM progression [481].

Furthermore, combinatorial therapies are currently being explored for their antitumor response and exhibits positive response. Several combinatorial therapies, such as chemotherapy + adoptive cell therapy, chemotherapy + stem cell therapy, radiotherapy + vaccine therapy, radiotherapy + photothermal therapy, chemotherapy + gene therapy, nanomaterial + immunotherapy, and others have been successfully tested and administered, which showed enhanced survival rate and high prognosis rate [482–484]. However, there are various limitations that are associated with combinatorial therapy that should be understand before using combination therapy in GBM therapeutics [485]. First, understanding of signaling pathways and their downstream molecules is crucial to achieve maximum success. Secondly, drug combination might induce unwanted side effects on patient's health that lower the success rate of combinatorial therapy. Third, tumor heterogeneity and unique immunological landscape imparts a huge challenge in designing effective drug combination [486]. To overcome these challenges artificial intelligence and machine learning algorithms plays an important role. Mathematical modeling of synergism of drugs and associated pathways are effective in predicting drug combinations and doses. Additionally, mathematical modeling enables in visualizing drug dose response matrix that can be validated *in vitro* and *in vivo* [487]. Moreover, drug repurposing to target altered signaling events and targets in GBM etiology is an alternative strategy to combat GBM. There are several drugs that exhibited positive results and make them effective drug molecule, whereas, some drugs unable to cross BBB permeability that make them ineffective. Overall, awareness of cancer cell interactions and tumor microenvironment is essential for developing effective therapeutic strategies against GBM [488].

Funding

S·K has received Senior Research Fellowship (SRF) from the Department of Biotechnology (DBT), Govt. of India (Fellow ID: DBT/2019/DTU/1308).

Author's contribution

Conceived and designed by P.K. Materials collected and art work done by S.K. and R.G. Critical evaluation and analysis of data done by R. K.A and PK. Manuscript written by S.K., R.G., R.K.A., and P.K. All authors read the manuscript and agreed to submit.

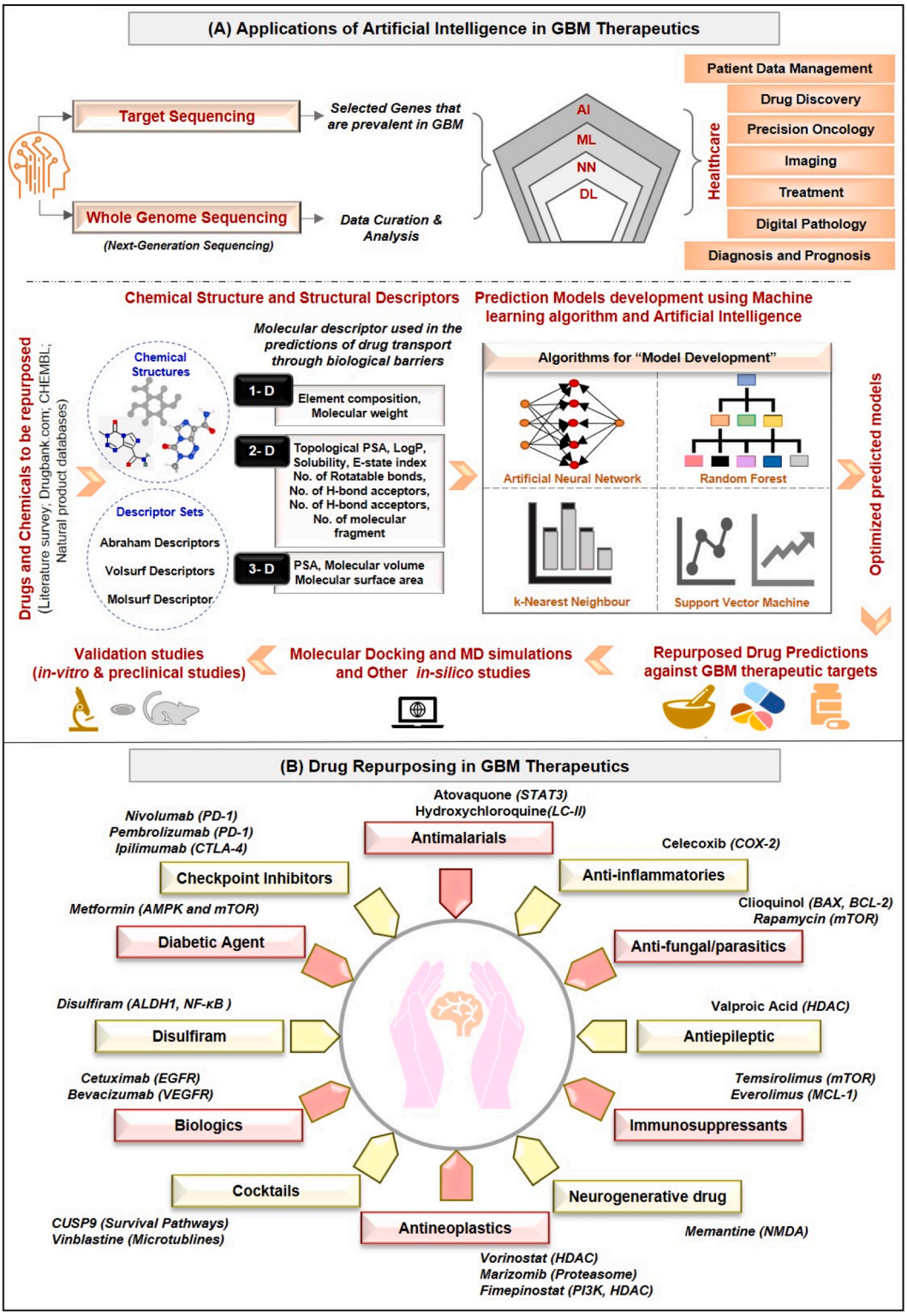

Fig. 5. (A) Applications of Artificial Intelligence in GBM Therapeutics: mounting evidence have demonstrated that artificial intelligence changes the paradigm of GBM therapeutics through drug discovery, precision medicine, imaging methods, treatment strategies, digital pathology, and data management. Further, in drug discovery and development, machine learning and artificial intelligence algorithms have analyzed the chemical data and molecular descriptors associated with chemical structures to develop a novel algorithm that predicts optimal repurposed drugs in GBM therapeutics. (B) Drug Repurposing in GBM Therapeutics: Several drugs have been repurposed for GBM, namely antimalarials, anti-inflammatory drugs, anti-fungal, anti-epileptic, neuro regenerative drugs, antineoplastics, anti-diabetic compounds, and others.

Artificial intelligence and machine learning change the perspective of GBM therapeutics

Era of personalized medicine in the management of GBM

AI provides novel doors in treating various diseases, including GBM, for effective and personalized treatment. Collaboration between computer scientists and medical researchers enables the utilization of transformative technology directly for patients with GBM [358]. AI serves several applications, such as grading prediction, glioma genomics, pre-operative planning, intra-operative treatment planning, and others in treating and managing glioma to encourage personalized medicine [359,360]. In this section, we have discussed all the applications of AI in glioma management for personalized medicine in detail. The differentiation between LGG and HGG is critical for treatment planning and prognosis, and using the AI approach for differentiation may play an essential role in this task. For this purpose, different AI/ML algorithms, namely logistic regression, support vector machine, artificial neural networks, and random forest, have been developed based on imaging modalities with an accuracy of above 90% [359,361–364]. Additionally, two deep learning-based software, namely GoogLeNet and AlexNet have been constructed to predict glioma grading before surgery in 113 GBM patients with an accuracy rate of 0.867 and 0.866, respectively. (Fig. 5a).

Compared to humans, AI-based algorithms can detect glioma grading through many imaging features that improve the glioma grading predicting capability [365]. Zhang et al., 2017 compared 25 different ML algorithms on 120 glioma patients with 8 independent attribute selection methods for differentiating grade II, III, and IV gliomas-based on MRI images [366]. Additionally, the advancements in imaging modalities led to the prediction of genetic mutations-based on radiological features using AI/ML methods [367,368]. For instance, prediction of the IDH mutations and MGMT promoter methylation using AI algorithms were associated with enhanced treatment response and survival rates [369–372]. Further, deep-learning algorithms, namely convolutional neural networks, residual convolutional neural networks, and random forest classifiers, have been constructed to predict genetic mutations associated with GBM [373–376]. Besides predicting genetic information, scientists have been rigorously involved in extracting massive data from genetic databases, which are used for predicting prognosis and treatment response [377]. Moreover, AI plays an important role in pre-operative and intra-operative treatment planning in GBM therapeutics. For example, support vector machines, random forest methods, and convolutional neural networks have been implemented in tumor segmentation [378,379]. In a study, a multi-pathway convolutional neural network and conditional random field were implemented for 3D FLAIR images to segment a low-grade glioma [380]. Similarly, AI has been implemented in resecting the maximum amount of tumor and the minimum amount of normal tissue during oncological surgery [381]. Recently, scientists have discovered the potential benefits of AI in histopathologic diagnosis, which can reduce the time from tissue preparation to diagnosis. Slide scanners have used AI methods to convert microscopic slides to high-quality image files. AI models, namely support vector machines, decision trees, random forests, and convolutional neural networks, have been used for diagnostic purposes and glioma grading [382–385]. In neuroradiology, differentiation between post-treatment changes becomes a considerable challenge, which can be resolved by applying anatomic images using AI methods. For instance, support vector machine (SVM) classifiers have been used to diagnose pseudo-progression *versus* recurrence in GBM patients, whereas convolutional neural networks have been trained to differentiate true *versus* pseudo-progression in GBM patients after RT and resection [386,387]. However, there are many challenges and unanswered questions that may be resolved before the adaptation of AI in oncological centers. For example, no such study demonstrates the cost-benefits or confirms that AI can improve patient outcomes. Likewise, the interaction between clinicals and engineers is still a significant challenge in adapting AI to glioma treatment [388]. Thus, the role of AI in GBM management and treatment acts like a sword with edges on both sides.

Application of drug repurposing in GBM therapeutics

The development and prosecution of novel anti-GBM drugs from bench to bedside can incur significant time and cost implications, and thus, drug-repurposing helps to overcome the obstacles imparted by *de novo* drug designing and development. Till now, various drug molecules, namely memantine, captopril (NCT02770378), metformin (NCT02780024), imipramine (NCT04863950), sertraline (NCT02770378), and others have been approved in clinical trials that target GBM-associated signaling pathways and molecules to treat GBM [389]. For example, the administration of Amitriptyline, Clomipramine, and Doxepin reduces cell proliferation and induces the autophagy pathway by inhibiting PI3K/Akt/mTOR signaling cascade. It also reduced cell stemness and invasive capacity, enhancing immunotherapy efficiency [390,391]. Likewise, Aprepitant, an antiemetic drug, is used for chemotherapy through blocking substance-P activity and neurokinin-1 activation. A study demonstrated that the administration of Aprepitant inhibited GBM growth in a dose-dependent manner [392,393]. Disulfiram, a drug used to treat alcohol abuse, has been demonstrated to have efficacy against GBM cells. For instance, inhibition of acetaldehyde dehydrogenase through disulfiram administration inhibits GBM growth through downregulating proteasomes activity [394]. Antibiotics, such as tetracyclines, macrolides, and anti-mycobacterial, were examined as potential antineoplastics in GBM therapeutics through the regulation of mitochondrial biogenesis, oxidative stress, and energy requirements [395–397]. Recently, the potential of antiparasitic, antihypertensives and anti-inflammatory substances have been examined as potential antineoplastic agents against GBM. For instance, mebendazole inhibits VEGF2, which causes a decrease in tumor angiogenesis, microtubule formation, and microvascular density [398]. Applications of AI in drug repurposing for GBM therapeutics enhance the treatment facilities. For instance, Vargas-Toscano et al., 2020 demonstrated that a robotic workstation was programmed to perform a drug concentration to cell-growth analysis, which identified 22 potential therapeutic substances, and suggests the implication of neurotransmitter signal-modulating agents in GBM therapeutics [399]. Thus, further studies are required to extract the potential of AI/ML algorithms in drug repurposing for GBM therapeutics. (Fig. 5b)

Declaration of Competing Interest

The authors declare that there is no conflict of interest.

Data availability

No data was used for the research described in the article.

Acknowledgment

We would like to thank the senior management of Delhi Technological University for their constant support and guidance and the Department of Biotechnology (DBT), Government of India, for their constant support and financial assistance.

References

[1] F. Hanif, K. Muzaffar, K. Perveen, S.M. Malhi, S.U. Simjee, Glioblastoma multiforme: a review of its epidemiology and pathogenesis through clinical presentation and treatment, Asian Pac. J. Cancer Prev. 18 (2017) 3, https://doi.org/10.22034/APJCP.2017.18.1.3.

[2] M. Khabibov, A. Garifullin, Y. Boumber, K. Khaddour, M. Fernandez, F. Khamitov, L. Khalikova, N. Kuznetsova, O. Kit, L. Kharin, Signaling pathways

and therapeutic approaches in glioblastoma multiforme (review), Int. J. Oncol. 60 (2022) 1–18, https://doi.org/10.3892/IJO.2022.5359/HTML.
[3] M. Portela, V. Venkataramani, N. Fahey-Lozano, E. Seco, M. Losada-Perez, F. Winkler, S. Casas-Tintó, Glioblastoma cells vampirize WNT from neurons and trigger a JNK/MMP signaling loop that enhances glioblastoma progression and neurodegeneration, PLoS Biol. 17 (2019), e3000545, https://doi.org/10.1371/JOURNAL.PBIO.3000545.
[4] D. Boso, E. Rampazzo, C. Zanon, S. Bresolin, F. Maule, E. Porcù, A. Cani, A. Della Puppa, L. Trentin, G. Basso, L. Persano, HIF-1α/Wnt signaling-dependent control of gene transcription regulates neuronal differentiation of glioblastoma stem cells, Theranostics. 9 (2019) 4860, https://doi.org/10.7150/THNO.35882.
[5] R. Yang, M. Wang, G. Zhang, Y. Li, L. Wang, H. Cui, POU2F2 regulates glycolytic reprogramming and glioblastoma progression via PDPK1-dependent activation of PI3K/AKT/mTOR pathway, Cell Death Dis. 125 (12) (2021) 1–14, https://doi.org/10.1038/s41419-021-03719-3.
[6] E. Klein, A.C. Hau, A. Oudin, A. Golebiewska, S.P. Niclou, Glioblastoma organoids: pre-clinical applications and challenges in the context of immunotherapy, Front. Oncol. 10 (2020) 1–18, https://doi.org/10.3389/fonc.2020.604121.
[7] K.G. Abdullah, C.E. Bird, J.D. Buehler, L.C. Gattie, M.R. Savani, A.C. Sternisha, Y. Xiao, M.M. Levitt, W.H. Hicks, W. Li, D.M.O. Ramirez, T. Patel, T. Garzon-Muvdi, S. Barnett, G. Zhang, D.M. Ashley, K.J. Hatanpaa, T.E. Richardson, S. K. McBrayer, Establishment of patient-derived organoid models of lower-grade glioma, Neuro-Oncology 24 (2022) 612–623, https://doi.org/10.1093/NEUONC/NOAB273.
[8] F.R. Weth, L. Peng, E. Paterson, S.T. Tan, C. Gray, Utility of the cerebral organoid glioma 'GLICO' model for screening applications, Cells 12 (2022) 153, https://doi.org/10.3390/CELLS12010153.
[9] E.N. Mathew, B.C. Berry, H.W. Yang, R.S. Carroll, M.D. Johnson, Delivering therapeutics to glioblastoma: overcoming biological constraints, Int. J. Mol. Sci. 23 (2022), https://doi.org/10.3390/IJMS23031711.
[10] C. Fernandes, A. Costa, L. Osório, R.C. Lago, P. Linhares, B. Carvalho, C. Caeiro, Current standards of care in glioblastoma therapy, Glioblastoma (2017) 197–241, https://doi.org/10.15586/CODON.GLIOBLASTOMA.2017.CH11.
[11] M. Yin, X. Chen, Q. Guo, L. Xiao, P. Gao, D. Zang, J. Dong, Z. Zha, X. Dai, X. Wang, Ultrasmall zirconium carbide nanodots for synergistic photothermal-radiotherapy of glioma, Nanoscale. 14 (2022) 14935–14949, https://doi.org/10.1039/D2NR04239H.
[12] J. Herta, A. Cho, T. Roetzer-Pejrimovsky, R. Höftberger, W. Marik, G. Kronreif, T. Peilnsteiner, K. Rössler, S. Wolfsberger, Optimizing maximum resection of glioblastoma: Raman spectroscopy versus 5-aminolevulinic acid, J. Neurosurg. 1 (2022) 1–10, https://doi.org/10.3171/2022.11.JNS22693.
[13] E.L. Lozada-Delgado, N. Grafals-Ruiz, P.E. Vivas-Mejía, RNA interference for glioblastoma therapy: innovation ladder from the bench to clinical trials, Life Sci. 188 (2017) 26–36, https://doi.org/10.1016/J.LFS.2017.08.027.
[14] S.W. Cramer, C.C. Chen, Photodynamic therapy for the treatment of glioblastoma, Front. Surg. 6 (2020) 1–11, https://doi.org/10.3389/fsurg.2019.00081.
[15] L. Wu, W. Zhou, L. Lin, A. Chen, J. Feng, X. Qu, H. Zhang, J. Yue, Delivery of therapeutic oligonucleotides in nanoscale, Bioact. Mater. 7 (2022) 292–323, https://doi.org/10.1016/J.BIOACTMAT.2021.05.038.
[16] L. Chen, W. Hong, W. Ren, T. Xu, Z. Qian, Z. He, Recent progress in targeted delivery vectors based on biomimetic nanoparticles, Signal Transduct. Target. Ther. 61 (6) (2021) 1–25, https://doi.org/10.1038/s41392-021-00631-2.
[17] R.C. Abbott, D.J. Verdon, F.M. Gracey, H.E. Hughes-Parry, M. Iliopoulos, K. A. Watson, M. Mulazzani, K. Luong, C. D'Arcy, L.C. Sullivan, B.R. Kiefel, R. S. Cross, M.R. Jenkins, Novel high-affinity EGFRvIII-specific chimeric antigen receptor T cells effectively eliminate human glioblastoma, Clin. Transl. Immunol. 10 (2021), e1283, https://doi.org/10.1002/CTI2.1283.
[18] H.Z. Xu, T.F. Li, Y. Ma, K. Li, Q. Zhang, Y.H. Xu, Y.C. Zhang, L. Zhao, X. Chen, Targeted photodynamic therapy of glioblastoma mediated by platelets with photo-controlled release property, Biomaterials. 290 (2022), 121833, https://doi.org/10.1016/J.BIOMATERIALS.2022.121833.
[19] Z. Turkalp, J. Karamchandani, S. Das, S. Labatt Brain, K. Research Centre, L. Ka Shing, IDH mutation in glioma: new insights and promises for the future, JAMA Neurol. 71 (2014) 1319–1325, https://doi.org/10.1001/JAMANEUROL.2014.1205.
[20] S. Han, Y. Liu, S.J. Cai, M. Qian, J. Ding, M. Larion, M.R. Gilbert, C. Yang, IDH mutation in glioma: molecular mechanisms and potential therapeutic targets, Br. J. Cancer 122 (2020) 1580–1589, https://doi.org/10.1038/s41416-020-0814-x.
[21] S. Cai, J.X. Lu, Y.P. Wang, C.J. Shi, T. Yuan, X.P. Wang, SH2B3, transcribed by STAT1, promotes glioblastoma progression through transducing IL-6/gp130 signaling to activate STAT3 signaling, Front. Cell Dev. Biol. 9 (2021) 1–14, https://doi.org/10.3389/fcell.2021.606527.
[22] M. Muir, S. Gopakumar, J. Traylor, S. Lee, M. Muir, S. Gopakumar, J. Traylor, S. Lee, G. Rao, Expert opinion on therapeutic targets glioblastoma multiforme : novel therapeutic targets, Expert Opin. Ther. Targets 00 (2020) 1–10, https://doi.org/10.1080/14728222.2020.1762568.
[23] M. Zalles, N. Smith, J. Ziegler, D. Saunders, S. Remerowski, L. Thomas, R. Gulej, N. Mamedova, M. Lerner, K.M. Fung, J. Chung, K. Hwang, J. Jin, G. Wiley, C. Brown, J. Battiste, J.D. Wren, R.A. Towner, Optimized monoclonal antibody treatment against ELTD1 for GBM in a G55 xenograft mouse model, J. Cell. Mol. Med. 24 (2020) 1738–1749, https://doi.org/10.1111/JCMM.14867.
[24] J. Ziegler, M. Zalles, N. Smith, D. Saunders, M. Lerner, K.-M. Fung, M. Patel, J. D. Wren, F. Lupu, J. Battiste, R.A. Towner, Targeting ELTD1, an angiogenesis marker for glioblastoma (GBM), also affects VEGFR2: molecular-targeted MRI assessment, Am. J. Nucl. Med. Mol. Imaging 9 (2019) 93.
[25] A. Qin, A. Musket, P.R. Musich, J.B. Schweitzer, Q. Xie, Receptor tyrosine kinases as druggable targets in glioblastoma: do signaling pathways matter? Neuro-Oncol. Adv. 3 (2021) 1–12, https://doi.org/10.1093/noajnl/vdab133.
[26] J.A. Benitez, J. Ma, M. D'Antonio, A. Boyer, M.F. Camargo, C. Zanca, S. Kelly, A. Khodadadi-Jamayran, N.M. Jameson, M. Andersen, H. Miletic, S. Saberi, K. A. Frazer, W.K. Cavenee, F.B. Furnari, PTEN regulates glioblastoma oncogenesis through chromatin-associated complexes of DAXX and histone H3.3, Nat. Commun. 8 (2017) 1–14, https://doi.org/10.1038/ncomms15223.
[27] D. Wu, Y. Qiu, Y. Jiao, Z. Qiu, D. Liu, Small molecules targeting HATs, HDACs, and BRDs in cancer therapy, Front. Oncol. 10 (2020) 1–14, https://doi.org/10.3389/fonc.2020.560487.
[28] F. Khathayer, 85P Mocetinostat (MGCD0103) or MG0103 is an isotype-selective histone deacetylase (HDAC) inhibitor induce apoptosis and suppress tumor in glioblastoma cell lines C6 and T98G, Ann. Oncol. 33 (2022) S1409, https://doi.org/10.1016/j.annonc.2022.09.086.
[29] L. Everix, E.N. Seane, T. Ebenhan, I. Goethals, J. Bolcaen, Introducing HDAC-targeting radiopharmaceuticals for glioblastoma imaging and therapy, Pharmaceuticals. 16 (2023) 1–21, https://doi.org/10.3390/ph16020227.
[30] A.M. Jermakowicz, M.J. Rybin, R.K. Suter, J.N. Sarkaria, Z. Zeier, Y. Feng, N. G. Ayad, The novel BET inhibitor UM-002 reduces glioblastoma cell proliferation and invasion, Sci. Rep. 11 (2021) 1–14, https://doi.org/10.1038/s41598-021-02584-6.
[31] A. Liu, C. Hou, H. Chen, X. Zong, P. Zong, Genetics and epigenetics of glioblastoma: applications and overall incidence of IDH1 mutation, Front. Oncol. 6 (2016) 1, https://doi.org/10.3389/FONC.2016.00016.
[32] E. Babaeenezhad, M. Moradi Sarabi, M. Rajabibazl, S. Oraee-Yazdani, S. Karima, Global and regional DNA methylation silencing of PPARγ associated with glioblastoma multiforme pathogenesis, Mol. Biol. Rep. 50 (2022) 589–597, https://doi.org/10.1007/S11033-022-08051-3/FIGURES/5.
[33] Y. Li, F. Chen, J. Chu, C. Wu, Y. Li, H. Li, H. Ma, miR-148-3p inhibits growth of glioblastoma targeting DNA methyltransferase-1 (DNMT1), Oncol. Res. 27 (2019) 911, https://doi.org/10.3727/096504019X15516966905337.
[34] L. Qiu, Y. Meng, J. Han, STING cg16983159 methylation: a key factor for glioblastoma immunosuppression, Signal Transduct. Target. Ther. 71 (7) (2022) 1–3, https://doi.org/10.1038/s41392-022-01093-w.
[35] S. Maksoud, The role of the ubiquitin proteasome system in glioma: analysis emphasizing the main molecular players and therapeutic strategies identified in glioblastoma multiforme, Mol. Neurobiol. 58 (2021) 3252, https://doi.org/10.1007/S12035-021-02339-4.
[36] B.M. Fox, A. Janssen, D. Estevez-Ordonez, F. Gessler, N. Vicario, G. Chagoya, G. Elsayed, H. Sotoudeh, W. Stetler, G.K. Friedman, J.D. Bernstock, SUMOylation in glioblastoma: a novel therapeutic target, Int. J. Mol. Sci. 20 (2019), https://doi.org/10.3390/ijms20081853.
[37] C. Liu, Y. Tu, X. Sun, J. Jiang, X. Jin, X. Bo, Z. Li, A. Bian, X. Wang, D. Liu, Z. Wang, L. Ding, Wnt/beta-catenin pathway in human glioma: expression pattern and clinical/prognostic correlations, Clin. Exp. Med. 11 (2011) 105–112, https://doi.org/10.1007/S10238-010-0110-9.
[38] Y. Lee, J.K. Lee, S.H. Ahn, J. Lee, D.H. Nam, WNT signaling in glioblastoma and therapeutic opportunities, Lab. Investig. 962 (96) (2015) 137–150, https://doi.org/10.1038/labinvest.2015.140.
[39] M. Latour, N.G. Her, S. Kesari, E. Nurmemmedov, WNT Signaling as a therapeutic target for glioblastoma, Int. J. Mol. Sci. 22 (2021), https://doi.org/10.3390/IJMS22168428.
[40] M. Kouchi, Y. Shibayama, D. Ogawa, K. Miyake, A. Nishiyama, T. Tamiya, (Pro) renin receptor is crucial for glioma development via the Wnt/b-catenin signaling pathway, J. Neurosurg. 127 (2017) 819–828, https://doi.org/10.3171/2016.9.JNS16431.
[41] A. De Robertis, S. Valensin, M. Rossi, P. Tunici, M. Verani, A. De Rosa, C. Giordano, M. Varrone, A. Nencini, C. Pratelli, T. Benicchi, A. Bakker, J. Hill, K. Sangthongpitag, V. Pendharkar, B. Liu, F.M. Ng, S.W. Then, S.J. Tai, S. M. Cheong, X. He, A. Caricasole, M. Salerno, Identification and characterization of a small-molecule inhibitor of Wnt signaling in glioblastoma cells, Mol. Cancer Ther. 12 (2013) 1180–1189, https://doi.org/10.1158/1535-7163.MCT-12-1176-T.
[42] I. Arrillaga-Romany, Y. Odia, V.V. Prabhu, R.S. Tarapore, K. Merdinger, M. Stogniew, W. Oster, J.E. Allen, M. Mehta, T.T. Batchelor, P.Y. Wen, et al., Neuro-Oncology 22 (2020) 94–102, https://doi.org/10.1093/NEUONC/NOZ164.
[43] A. Bagherian, R. Mardani, B. Roudi, M. Taghizadeh, H.R. Banfshe, A. Ghaderi, A. Davoodvandi, S. Shamollaghamsari, M.R. Hamblin, H. Mirzaei, Combination therapy with nanomicellar-curcumin and temozolomide for in vitro therapy of glioblastoma multiforme via Wnt signaling pathways, J. Mol. Neurosci. 70 (2020) 1471–1483, https://doi.org/10.1007/s12031-020-01639-z.
[44] H. Wang, Q. Lai, D. Wang, J. Pei, B. Tian, Y. Gao, Z. Gao, X. Xu, Hedgehog signaling regulates the development and treatment of glioblastoma (review), Oncol. Lett. 24 (2022) 1–15, https://doi.org/10.3892/ol.2022.13414.
[45] X. Wu, S. Xiao, M. Zhang, L. Yang, J. Zhong, B. Li, F. Li, X. Xia, X. Li, H. Zhou, D. Liu, N. Huang, X. Yang, F. Xiao, N. Zhang, A novel protein encoded by circular SMO RNA is essential for hedgehog signaling activation and glioblastoma tumorigenicity, Genome Biol. 22 (2021) 1–29, https://doi.org/10.1186/S13059-020-02250-6/FIGURES/6.
[46] H.C. Hung, C.C. Liu, J.Y. Chuang, C.L. Su, P.W. Gean, Inhibition of sonic hedgehog signaling suppresses glioma stem-like cells likely through inducing autophagic cell death, Front. Oncol. 10 (2020) 1–15, https://doi.org/10.3389/fonc.2020.01233.
[47] M.L. Sargazi, K.B. Juybari, M.E. Tarzi, A. Amirkhosravi, M.H. Nematollahi, S. Mirzamohammdi, M. Mehrbani, M. Mehrabani, M. Mehrabani, Naringenin

attenuates cell viability and migration of C6 glioblastoma cell line: a possible role of hedgehog signaling pathway, Mol. Biol. Rep. 48 (2021) 6413–6421, https://doi.org/10.1007/s11033-021-06641-1.
[48] H. Zhou, L. Han, H. Wang, J. Wei, Z. Guo, Z. Li, N.K. Kaushik, Chidamide inhibits glioma cells by increasing oxidative stress via the miRNA-338-5p regulation of hedgehog signaling, Oxidative Med. Cell. Longev. 2020 (2020), https://doi.org/10.1155/2020/7126976.
[49] A. Karadağ, Y. Başbinar, Novel approach to the hedgehog signaling pathway: combined treatment of SMO and PTCH inhibitors, J. Basic Clin. Heal. Sci. 1 (2022) 492–500, https://doi.org/10.30621/jbachs.1193720.
[50] C. Bureta, Y. Saitoh, H. Tokumoto, H. Sasaki, S. Maeda, S. Nagano, S. Komiya, N. Taniguchi, T. Setoguchi, Synergistic effect of arsenic trioxide, vismodegib and temozolomide on glioblastoma, Oncol. Rep. 41 (2019) 3404–3412, https://doi.org/10.3892/or.2019.7100.
[51] B. Linder, A. Wehle, S. Hehlgans, F. Bonn, I. Dikic, F. Rödel, V. Seifert, D. Kögel, Arsenic trioxide and (−)-gossypol synergistically target glioma stem-like cells via inhibition of hedgehog and notch signaling, Cancers (Basel) 11 (2019), https://doi.org/10.3390/cancers11030350.
[52] J. Chakrabarti, L. Holokai, L.J. Syu, N.G. Steele, J. Chang, J. Wang, S. Ahmed, A. Dlugosz, Y. Zavros, Hedgehog signaling induces PD-L1 expression and tumor cell proliferation in gastric cancer, Oncotarget. 9 (2018) 37439–37457, https://doi.org/10.18632/oncotarget.26473.
[53] Z. Gersey, A.D. Osiason, L. Bloom, S. Shah, J.W. Thompson, A. Bregy, N. Agarwal, R.J. Komotar, Therapeutic targeting of the notch pathway in glioblastoma multiforme, World Neurosurg. 131 (2019) 252–263.e2, https://doi.org/10.1016/j.wneu.2019.07.180.
[54] Y. Fang, Z. Zhang, Arsenic trioxide as a novel anti-glioma drug: a review, Cell. Mol. Biol. Lett. 25 (2020) 44, https://doi.org/10.1186/s11658-020-00236-7.
[55] H.C. Oh, J.K. Shim, J. Park, J.H. Lee, R.J. Choi, N.H. Kim, H.S. Kim, J.H. Moon, E. H. Kim, J.H. Chang, J.I. Yook, S.G. Kang, Combined effects of niclosamide and temozolomide against human glioblastoma tumorspheres, J. Cancer Res. Clin. Oncol. 146 (2020) 2817–2828, https://doi.org/10.1007/s00432-020-03330-7.
[56] F. Giordano, F.I. Montalto, M.L. Panno, S. Andò, F. De Amicis, A notch inhibitor plus resveratrol induced blockade of autophagy drives glioblastoma cell death by promoting a switch to apoptosis, Am. J. Cancer Res. 11 (2021) 5933–5950.
[57] R. Bazzoni, A. Bentivegna, Role of notch signaling pathway in glioblastoma, Pathogenesis (2019) 1–25, https://doi.org/10.3390/cancers11030292.
[58] Y. Wan, G. Sun, S. Zhang, Z. Wang, L. Shi, MicroRNA-125b inhibitor sensitizes human primary glioblastoma cells to chemotherapeutic drug temozolomide on invasion, In Vitro Cell. Dev. Biol. Anim. 49 (2013) 599–607, https://doi.org/10.1007/s11626-013-9644-y.
[59] F.C. Kipper, M.W. Kieran, A. Thomas, D. Panigrahy, Notch signaling in malignant gliomas : supporting tumor growth and the vascular environment, Cancer Metastasis Rev. (2022) 737–747, https://doi.org/10.1007/s10555-022-10041-7.
[60] D. Herrera-Rios, G. Li, D. Khan, J. Tsiampali, A.C. Nickel, P. Aretz, M. Hewera, A. K. Suwala, T. Jiang, H.J. Steiger, M.A. Kamp, S. Muhammad, D. Hänggi, J. Maciaczyk, W. Zhang, U.D. Kahlert, A computational guided, functional validation of a novel therapeutic antibody proposes notch signaling as a clinical relevant and druggable target in glioma, Sci. Rep. 10 (2020) 1–12, https://doi.org/10.1038/s41598-020-72480-y.
[61] Y. Ma, Z. Cheng, J. Liu, L. Torre-Healy, J.D. Lathia, I. Nakano, Y. Guo, R. C. Thompson, M.L. Freeman, J. Wang, Inhibition of farnesyltransferase potentiates NOTCH-targeted therapy against glioblastoma stem cells, Stem Cell. Report 9 (2017) 1948–1960, https://doi.org/10.1016/j.stemcr.2017.10.028.
[62] D.M. Peereboom, X. Ye, T. Mikkelsen, G.J. Lesser, F.S. Lieberman, H.I. Robins, M. S. Ahluwalia, A.E. Sloan, S.A. Grossman, A phase II and pharmacodynamic trial of RO4929097 for patients with recurrent/progressive glioblastoma, Neurosurgery. 88 (2021) 246–251, https://doi.org/10.1093/neuros/nyaa412.
[63] V. Kumar, M. Vashishta, L. Kong, J.J. Lu, X. Wu, B.S. Dwarakanath, C. Guha, Carbon ion irradiation downregulates notch signaling in glioma cell lines, impacting cell migration and spheroid formation, Cells. 11 (2022), https://doi.org/10.3390/cells11213354.
[64] J.L. Birch, B.J. Coull, L.C. Spender, C. Watt, A. Willison, N. Syed, A.J. Chalmers, M.K. Hossain-Ibrahim, G.J. Inman, Multifaceted transforming growth factor-beta (TGFβ) signalling in glioblastoma, Cell. Signal. 72 (2020), 109638, https://doi.org/10.1016/J.CELLSIG.2020.109638.
[65] S. Zhu, F. Sun, P. Zhao, G. Liang, X. Sun, L. Zeng, Y. Huang, Brain-targeting biomimetic nanoparticles for codelivery of celastrol and LY2157299 for reversing glioma immunosuppression, Int. J. Pharm. 619 (2022), 121709, https://doi.org/10.1016/J.IJPHARM.2022.121709.
[66] D.F. Quail, J.A. Joyce, The microenvironmental landscape of brain tumors, Cancer Cell 31 (2017) 326–341, https://doi.org/10.1016/j.ccell.2017.02.009.
[67] H. Hosseinalizadeh, M. Mahmoodpour, Z. Razaghi Bahabadi, M.R. Hamblin, H. Mirzaei, Neutrophil mediated drug delivery for targeted glioblastoma therapy: a comprehensive review, Biomed. Pharmacother. 156 (2022), 113841, https://doi.org/10.1016/j.biopha.2022.113841.
[68] Y. Li, X. Teng, Y. Wang, C. Yang, X. Yan, J. Li, Neutrophil delivered hollow titania covered persistent luminescent nanosensitizer for ultrosound augmented chemo/immuno glioblastoma therapy, Adv. Sci. 8 (2021) 1–7, https://doi.org/10.1002/advs.202004381.
[69] J. Wang, W. Tang, M. Yang, Y. Yin, H. Li, F. Hu, L. Tang, X. Ma, Y. Zhang, Y. Wang, Inflammatory tumor microenvironment responsive neutrophil exosomes-based drug delivery system for targeted glioma therapy, Biomaterials. 273 (2021), 120784, https://doi.org/10.1016/J.BIOMATERIALS.2021.120784.
[70] R.S. Andersen, A. Anand, D.S.L. Harwood, B.W. Kristensen, Tumor-associated microglia and macrophages in the glioblastoma microenvironment and their implications for therapy, Cancers (Basel) 13 (2021) 1–26, https://doi.org/10.3390/cancers13174255.
[71] M.F. Almahariq, T.J. Quinn, P. Kesarwani, S. Kant, C.R. Miller, P. Chinnaiyan, Inhibition of colony-stimulating factor-1 receptor enhances the efficacy of radiotherapy and reduces immune suppression in glioblastoma, In Vivo (Brooklyn). 35 (2021) 119–129, https://doi.org/10.21873/INVIVO.12239.
[72] B.C. Jena, C.K. Das, D. Bharadwaj, M. Mandal, Cancer associated fibroblast mediated chemoresistance: a paradigm shift in understanding the mechanism of tumor progression, Biochim. Biophys. Acta - Rev. Cancer 1874 (2020), 188416, https://doi.org/10.1016/j.bbcan.2020.188416.
[73] J. Guo, H. Zeng, Y. Chen, Emerging nano drug delivery systems targeting cancer-associated fibroblasts for improved antitumor effect and tumor drug penetration, Mol. Pharm. 17 (2020) 1028–1048, https://doi.org/10.1021/ACS.MOLPHARMACEUT.0C00014/ASSET/IMAGES/MEDIUM/MP0C00014_0010.GIF.
[74] Y. Mi, N. Guo, J. Luan, J. Cheng, Z. Hu, P. Jiang, W. Jin, X. Gao, The emerging role of myeloid-derived suppressor cells in the glioma immune suppressive microenvironment, Front. Immunol. 11 (2020) 1–11, https://doi.org/10.3389/fimmu.2020.00737.
[75] M. Salemizadeh Parizi, F. Salemizadeh Parizi, S. Abdolhosseini, S. Vanaei, A. Manzouri, F. Ebrahimzadeh, Myeloid-derived suppressor cells (MDSCs) in brain cancer: challenges and therapeutic strategies, Inflammopharmacology. 29 (2021) 1613–1624, https://doi.org/10.1007/s10787-021-00878-9.
[76] J.A. Flores-Toro, D. Luo, A. Gopinath, M.R. Sarkisian, J.J. Campbell, I.F. Charo, R. Singh, T.J. Schall, M. Datta, R.K. Jain, D.A. Mitchell, J.K. Harrison, CCR2 inhibition reduces tumor myeloid cells and unmasks a checkpoint inhibitor effect to slow progression of resistant murine gliomas, Proc. Natl. Acad. Sci. U. S. A. 117 (2020) 1129–1138, https://doi.org/10.1073/pnas.1910856117.
[77] K. Bijangi-Vishehsaraei, M.R. Saadatzadeh, H. Wang, A. Nguyen, M.M. Kamocka, W. Cai, A.A. Cohen-Gadol, S.L. Halum, J.N. Sarkaria, K.E. Pollok, A.R. Safa, Sulforaphane suppresses the growth of glioblastoma cells, glioblastoma stem cell-like spheroids, and tumor xenografts through multiple cell signaling pathways, J. Neurosurg. 127 (2017) 1219–1230, https://doi.org/10.3171/2016.8.JNS161197.
[78] C. Wu, M.E. Muroski, J. Miska, C. Lee-Chang, Y. Shen, A. Rashidi, P. Zhang, T. Xiao, Y. Han, A. Lopez-Rosas, Y. Cheng, M.S. Lesniak, Repolarization of myeloid derived suppressor cells via magnetic nanoparticles to promote radiotherapy for glioma treatment, Nanomedicine 16 (2019) 126–137, https://doi.org/10.1016/J.NANO.2018.11.015.
[79] S. Srivastava, C. Jackson, T. Kim, J. Choi, M. Lim, A characterization of dendritic cells and their role in immunotherapy in glioblastoma: from preclinical studies to clinical trials, Cancers 11 (2019) 537, https://doi.org/10.3390/CANCERS11040537.
[80] M. Wang, Y. Cai, Y. Peng, B. Xu, W. Hui, Y. Jiang, Exosomal LGALS9 in the cerebrospinal fluid of glioblastoma patients suppressed dendritic cell antigen presentation and cytotoxic T-cell immunity, Cell Death Dis. 11 (2020), https://doi.org/10.1038/s41419-020-03042-3.
[81] D.T. Nagasawa, J. Yang, P. Romiyo, C. Lagman, L.K. Chung, B.L. Voth, C. Duong, V.A. Kickhoefer, L.H. Rome, I. Yang, Bioengineered recombinant vault nanoparticles coupled with NY-ESO-1 glioma-associated antigens induce maturation of native dendritic cells, J. Neuro-Oncol. 148 (2020) 1–7, https://doi.org/10.1007/s11060-020-03472-1.
[82] A. Datsi, R.V. Sorg, Dendritic cell vaccination of glioblastoma: road to success or dead end, Front. Immunol. 12 (2021) 1–28, https://doi.org/10.3389/fimmu.2021.770390.
[83] L. Li, J. Zhou, X. Dong, Q. Liao, D. Zhou, Y. Zhou, Dendritic cell vaccines for glioblastoma fail to complete clinical translation: bottlenecks and potential countermeasures, Int. Immunopharmacol. 109 (2022), 108929, https://doi.org/10.1016/J.INTIMP.2022.108929.
[84] T. Ahmed, Biomaterial-based in vitro 3D modeling of glioblastoma multiforme, Cancer Pathog. Ther. (2023), https://doi.org/10.1016/J.CPT.2023.01.002.
[85] J.D.R. Aguilera-Márquez, G.T. de Dios-Figueroa, E.E. Reza-Saldivar, T. A. Camacho-Villegas, A.A. Canales-Aguirre, P.H. Lugo-Fabres, Biomaterials: emerging systems for study and treatment of glioblastoma, Neurol. Perspect. 2 (2022) S31–S42, https://doi.org/10.1016/J.NEUROP.2021.12.001.
[86] M. Kapałczyńska, T. Kolenda, W. Przybyła, M. Zajączkowska, A. Teresiak, V. Filas, M. Ibbs, R. Bliźniak, Ł. Łuczewski, K. Lamperska, 2D and 3D cell cultures - a comparison of different types of cancer cell cultures, Arch. Med. Sci. 14 (2018) 910–919, https://doi.org/10.5114/AOMS.2016.63743.
[87] K. Lenting, R. Verhaak, M. ter Laan, P. Wesseling, W. Leenders, Glioma: experimental models and reality, Acta Neuropathol. 133 (2017) 263–282, https://doi.org/10.1007/S00401-017-1671-4.
[88] M. Paolillo, S. Comincini, S. Schinelli, In vitro glioblastoma models: a journey into the third dimension, Cancers (Basel) 13 (2021), https://doi.org/10.3390/CANCERS13102449.
[89] H.G. Yi, Y.H. Jeong, Y. Kim, Y.J. Choi, H.E. Moon, S.H. Park, K.S. Kang, M. Bae, J. Jang, H. Youn, S.H. Paek, D.W. Cho, A bioprinted human-glioblastoma-on-a-chip for the identification of patient-specific responses to chemoradiotherapy, Nat. Biomed. Eng. 3 (2019) 509–519, https://doi.org/10.1038/S41551-019-0363-X.
[90] F. Jacob, R.D. Salinas, D.Y. Zhang, P.T.T. Nguyen, J.G. Schnoll, S.Z.H. Wong, R. Thokala, S. Sheikh, D. Saxena, S. Prokop, D. Ao Liu, X. Qian, D. Petrov, T. Lucas, H.I. Chen, J.F. Dorsey, K.M. Christian, Z.A. Binder, M. Nasrallah, S. Brem, D.M. O'Rourke, G. Li Ming, H. Song, A patient-derived glioblastoma organoid model and biobank recapitulates inter- and intra-tumoral heterogeneity, Cell. 180 (2020) 188, https://doi.org/10.1016/J.CELL.2019.11.036.

[91] S. Caragher, A.J. Chalmers, N. Gomez-Roman, Glioblastoma's next top model: novel culture systems for brain cancer radiotherapy research, Cancers (Basel) 11 (2019), https://doi.org/10.3390/CANCERS11010044.
[92] N. Gomez-Roman, K. Stevenson, L. Gilmour, G. Hamilton, A.J. Chalmers, A novel 3D human glioblastoma cell culture system for modeling drug and radiation responses, Neuro-Oncology 19 (2017) 229–241, https://doi.org/10.1093/NEUONC/NOW164.
[93] S.J. Florczyk, K. Wang, S. Jana, D.L. Wood, S.K. Sytsma, J.G. Sham, F.M. Kievit, M. Zhang, Porous chitosan-hyaluronic acid scaffolds as a mimic of glioblastoma microenvironment ECM, Biomaterials. 34 (2013) 10143–10150, https://doi.org/10.1016/J.BIOMATERIALS.2013.09.034.
[94] K. Ganser, F. Eckert, A. Riedel, N. Stransky, F. Paulsen, S. Noell, M. Krueger, J. Schittenhelm, S. Beck-Wödl, D. Zips, P. Ruth, S.M. Huber, L. Klumpp, Patient-individual phenotypes of glioblastoma stem cells are conserved in culture and associate with radioresistance, brain infiltration and patient prognosis, Int. J. Cancer 150 (2022) 1722–1733, https://doi.org/10.1002/IJC.33950.
[95] A. Soubéran, A. Tchoghandjian, Practical review on preclinical human 3D glioblastoma models: advances and challenges for clinical translation, Cancers (Basel) 12 (2020) 1–21, https://doi.org/10.3390/CANCERS12092347.
[96] X. Cai, R.G. Briggs, H.B. Homburg, I.M. Young, E.J. Davis, Y.H. Lin, J.D. Battiste, M.E. Sughrue, Application of microfluidic devices for glioblastoma study: current status and future directions, Biomed. Microdevices 22 (2020), https://doi.org/10.1007/S10544-020-00516-1.
[97] A. Sontheimer-Phelps, B.A. Hassell, D.E. Ingber, Modelling cancer in microfluidic human organs-on-chips, Nat. Rev. Cancer 192 (19) (2019) 65–81, https://doi.org/10.1038/s41568-018-0104-6.
[98] F. Yu, S.K. Nivasini, L.C. Foo, S.H. Ng, W. Hunziker, D. Choudhury, A pump-free tricellular blood–brain barrier on-a-chip model to understand barrier property and evaluate drug response, Biotechnol. Bioeng. 117 (2020) 1127–1136, https://doi.org/10.1002/BIT.27260.
[99] D.C.R. Batara, S. Zhou, M.-C. Choi, S.-H. Kim, Glioblastoma organoid technology: an emerging preclinical models for drug discovery, Organoid. 2 (2022), e7, https://doi.org/10.51335/organoid.2022.2.e7.
[100] M.J. Rybin, M.E. Ivan, N.G. Ayad, Z. Zeier, Organoid models of glioblastoma and their role in drug discovery, Front. Cell. Neurosci. 15 (2021) 1–11, https://doi.org/10.3389/fncel.2021.605255.
[101] A. Urbaniak, M.R. Reed, B. Heflin, J. Gaydos, S. Piña-Oviedo, M. Jędrzejczyk, G. Klejborowska, N. Stępczyńska, T.C. Chambers, A.J. Tackett, A. Rodriguez, A. Huczyński, R.L. Eoff, A.M. MacNicol, Anti-glioblastoma activity of monensin and its analogs in an organoid model of cancer, Biomed. Pharmacother. 153 (2022), https://doi.org/10.1016/j.biopha.2022.113440.
[102] L. Zhang, F. Liu, N. Weygant, J. Zhang, P. Hu, Z. Qin, J. Yang, Q. Cheng, F. Fan, Y. Zeng, Y. Tang, Y. Li, A. Tang, F. He, J. Peng, W. Liao, Z. Hu, M. Li, Z. Liu, A novel integrated system using patient-derived glioma cerebral organoids and xenografts for disease modeling and drug screening, Cancer Lett. 500 (2021) 87–97, https://doi.org/10.1016/j.canlet.2020.12.013.
[103] S. Bian, M. Repic, Z. Guo, A. Kavirayani, T. Burkard, J.A. Bagley, C. Krauditsch, J. A. Knoblich, Genetically engineered cerebral organoids model brain tumour formation, Nat. Methods 15 (2018) 631, https://doi.org/10.1038/S41592-018-0070-7.
[104] A. Linkous, D. Balamatsias, M. Snuderl, L. Edwards, K. Miyaguchi, T. Milner, B. Reich, L. Cohen-Gould, A. Storaska, Y. Nakayama, E. Schenkein, R. Singhania, S. Cirigliano, T. Magdeldin, Y. Lin, G. Nanjangud, K. Chadalavada, D. Pisapia, C. Liston, H.A. Fine, Modeling patient-derived glioblastoma with cerebral organoids, Cell Rep. 26 (2019) 3203–3211.e5, https://doi.org/10.1016/j.celrep.2019.02.063.
[106] X. Xu, L. Li, L. Luo, L. Shu, X. Si, Z. Chen, W. Xia, J. Huang, Y. Liu, A. Shao, Y. Ke, Opportunities and challenges of glioma organoids, Cell Commun. Signal. 19 (2021) 1–13, https://doi.org/10.1186/s12964-021-00777-0.
[107] X. Dai, C. Ma, Q. Lan, T. Xu, 3D bioprinted glioma stem cells for brain tumor model and applications of drug susceptibility, Biofabrication. 8 (2016), https://doi.org/10.1088/1758-5090/8/4/045005.
[108] L. Neufeld, E. Yeini, N. Reisman, Y. Shtilerman, D. Ben-Shushan, S. Pozzi, A. Madi, G. Tiram, A. Eldar-Boock, S. Ferber, R. Grossman, Z. Ram, R. Satchi-Fainaro, Microengineered perfusable 3D-bioprinted glioblastoma model for in vivo mimicry of tumor microenvironment, Sci. Adv. 7 (2021) 1–20, https://doi.org/10.1126/sciadv.abi9119.
[109] E. Maloney, C. Clark, H. Sivakumar, K. Yoo, J. Aleman, S.A.P. Rajan, S. Forsythe, A. Mazzocchi, A.W. Laxton, S.B. Tatter, R.E. Strowd, K.I. Votanopoulos, A. Skardal, Immersion bioprinting of tumor organoids in multi-well plates for increasing chemotherapy screening throughput, Micromachines. 11 (2020), https://doi.org/10.3390/MI11020208.
[110] X. Dai, Y. Shao, X. Tian, X. Cao, L. Ye, P. Gao, H. Cheng, X. Wang, Fusion between glioma stem cells and mesenchymal stem cells promotes malignant progression in 3D-bioprinted models, ACS Appl. Mater. Interfaces 14 (2022) 35344–35356, https://doi.org/10.1021/ACSAMI.2C06658/ASSET/IMAGES/MEDIUM/AM2C06658_0013.GIF.
[111] F. Andreatta, G. Beccaceci, N. Fortuna, M. Celotti, D. De Felice, M. Lorenzoni, V. Foletto, S. Genovesi, J. Rubert, A. Alaimo, The organoid era permits the development of new applications to study glioblastoma, Cancers (Basel) 12 (2020) 1–16, https://doi.org/10.3390/cancers12113303.
[112] C. Gray, Screening Applications, 2023.
[113] S. Lenin, E. Ponthier, K.G. Scheer, E.C.F. Yeo, M.N. Tea, L.M. Ebert, M. O. Mansilla, S. Poonnoose, U. Baumgartner, B.W. Day, R.J. Ormsby, S.M. Pitson, G.A. Gomez, A drug screening pipeline using 2D and 3D patient-derived in vitro models for pre-clinical analysis of therapy response in glioblastoma, Int. J. Mol. Sci. 22 (2021), https://doi.org/10.3390/IJMS22094322.
[114] M. Martinez-Lage, T.M. Lynch, Y. Bi, C. Cocito, G.P. Way, S. Pal, J. Haller, R. E. Yan, A. Ziober, A. Nguyen, M. Kandpal, D.M. O'Rourke, J.P. Greenfield, C. S. Greene, R.V. Davuluri, N. Dahmane, Immune landscapes associated with different glioblastoma molecular subtypes, Acta Neuropathol. Commun. 7 (2019), https://doi.org/10.1186/S40478-019-0803-6.
[115] Q. Wang, B. Hu, X. Hu, H. Kim, M. Squatrito, L. Scarpace, A.C. de Carvalho, S. Lyu, P. Li, Y. Li, F. Barthel, H.J. Cho, Y.H. Lin, N. Satani, E. Martinez-Ledesma, S. Zheng, E. Chang, C.E.G. Sauvé, A. Olar, Z.D. Lan, G. Finocchiaro, J.J. Phillips, M.S. Berger, K.R. Gabrusiewicz, G. Wang, E. Eskilsson, J. Hu, T. Mikkelsen, R. A. DePinho, F. Muller, A.B. Heimberger, E.P. Sulman, D.H. Nam, R.G.W. Verhaak, Tumor evolution of glioma-intrinsic gene expression subtypes associates with immunological changes in the microenvironment, Cancer Cell 32 (2017) 42–56, e6, https://doi.org/10.1016/J.CCELL.2017.06.003.
[116] J. Bruns, T. Egan, P. Mercier, S.P. Zustiak, Glioblastoma spheroid growth and chemotherapeutic responses in single and dual-stiffness hydrogels, Acta Biomater. (2022), https://doi.org/10.1016/J.ACTBIO.2022.05.048.
[117] S. Kang, W. Duan, S. Zhang, D. Chen, J. Feng, N. Qi, Muscone/RI7217 co-modified upward messenger DTX liposomes enhanced permeability of blood-brain barrier and targeting glioma, Theranostics. 10 (2020) 4308, https://doi.org/10.7150/THNO.41322.
[118] L. Waldherr, M. Seitanidou, M. Jakešová, V. Handl, S. Honeder, M. Nowakowska, T. Tomin, M. Karami Rad, T. Schmidt, J. Distl, R. Birner-Gruenberger, G. von Campe, U. Schäfer, M. Berggren, B. Rinner, M. Asslaber, N. Ghaffari-Tabrizi-Wizsy, S. Patz, D.T. Simon, R. Schindl, Targeted chemotherapy of glioblastoma spheroids with an iontronic pump, Adv. Mater. Technol. 6 (2021) 2001302, https://doi.org/10.1002/ADMT.202001302.
[119] J. Dougherty, K. Harvey, A. Liou, K. Labella, D. Moran, S. Brosius, T. De Raedt, Identification of therapeutic sensitivities in a spheroid drug combination screen of neurofibromatosis type I associated high grade gliomas, PLoS One 18 (2023), e0277305, https://doi.org/10.1371/JOURNAL.PONE.0277305.
[120] P. Seshacharyulu, S. Halder, R. Nimmakayala, S. Rachagani, S. Chaudhary, P. Atri, R. Chirravuri-Venkata, M.M. Ouellette, J. Carmicheal, S.K. Gautam, R. Vengoji, S. Wang, S. Li, L. Smith, G.A. Talmon, K. Klute, Q. Ly, B.N. Reames, J. L. Grem, L. Berim, J.C. Padussis, S. Kaur, S. Kumar, M.P. Ponnusamy, M. Jain, C. Lin, S.K. Batra, Disruption of FDPS/Rac1 axis radiosensitizes pancreatic ductal adenocarcinoma by attenuating DNA damage response and immunosuppressive signalling, EBioMedicine. 75 (2022), 103772, https://doi.org/10.1016/J.EBIOM.2021.103772.
[121] A.S. Tatla, A.W. Justin, C. Watts, A.E. Markaki, A vascularized tumoroid model for human glioblastoma angiogenesis, Sci. Report. 111 (11) (2021) 1–9, https://doi.org/10.1038/s41598-021-98911-y.
[122] K. Gupta, J.C. Jones, V.D.A. Farias, Y. Mackeyev, P.K. Singh, A. Quiñones-Hinojosa, S. Krishnan, Identification of synergistic drug combinations to target KRAS-driven chemoradioresistant cancers utilizing tumoroid models of colorectal adenocarcinoma and recurrent glioblastoma, Front. Oncol. 12 (2022) 1, https://doi.org/10.3389/FONC.2022.840241/FULL.
[123] M. Tang, S.K. Tiwari, K. Agrawal, M. Tan, J. Dang, T. Tam, J. Tian, X. Wan, J. Schimelman, S. You, Q. Xia, T.M. Rana, S. Chen, Rapid 3D bioprinting of glioblastoma model mimicking native biophysical heterogeneity, Small. 17 (2021) 2006050, https://doi.org/10.1002/SMLL.202006050.
[124] D.M. van Pel, K. Harada, D. Song, C.C. Naus, W.C. Sin, Modelling glioma invasion using 3D bioprinting and scaffold-free 3D culture, J. Cell Commun. Signal. 12 (2018) 723–730, https://doi.org/10.1007/S12079-018-0469-Z/FIGURES/5.
[125] X. Dai, L. Liu, J. Ouyang, X. Li, X. Zhang, Q. Lan, T. Xu, Coaxial 3D bioprinting of self-assembled multicellular heterogeneous tumor fibers, Sci. Report. 71 (7) (2017) 1–11, https://doi.org/10.1038/s41598-017-01581-y.
[126] J. Huang, F. Liu, H. Tang, H. Wu, L. Li, R. Wu, J. Zhao, Y. Wu, Z. Liu, J. Chen, Tranylcypromine causes neurotoxicity and represses BHC110/LSD1 in human-induced pluripotent stem cell-derived cerebral organoids model, Front. Neurol. 8 (2017) 626, https://doi.org/10.3389/FNEUR.2017.00626/BIBTEX.
[127] I. Ylivinkka, H. Sihto, O. Tynninen, Y. Hu, A. Laakso, R. Kivisaari, P. Laakkonen, J. Keski-Oja, M. Hyytiäinen, Motility of glioblastoma cells is driven by netrin-1 induced gain of stemness, J. Exp. Clin. Cancer Res. 36 (2017) 1–18, https://doi.org/10.1186/S13046-016-0482-0/FIGURES/7.
[128] M. Lara-Velazquez, R. Al-Kharboosh, S. Jeanneret, C. Vazquez-Ramos, D. Mahato, D. Tavanaiepour, G. Rahmathulla, A. Quinone-Hinojosa, Advances in brain tumor surgery for glioblastoma in adults, Brain Sci. 7 (2017) 1–16, https://doi.org/10.3390/brainsci7120166.
[129] A.H.A. Sales, J. Beck, O. Schnell, C. Fung, B. Meyer, J. Gempt, Surgical treatment of glioblastoma: state-of-the-art and future trends, J. Clin. Med. 11 (2022), https://doi.org/10.3390/jcm11185354.
[130] D. Laurent, R. Freedman, L. Cope, P. Sacks, J. Abbatematteo, P. Kubilis, F. Bova, M. Rahman, Impact of extent of resection on incidence of postoperative complications in patients with glioblastoma, Neurosurgery. 86 (2020) 625–630, https://doi.org/10.1093/NEUROS/NYZ313.
[131] R. Díez Valle, S. Tejada Solis, M.A. Idoate Gastearena, R. García De Eulate, P. Domínguez Echávarri, J. Aristu Mendiroz, Surgery guided by 5-aminolevulinic fluorescence in glioblastoma: volumetric analysis of extent of resection in single-center experience, J. Neuro-Oncol. 102 (2011) 105–113, https://doi.org/10.1007/S11060-010-0296-4/FIGURES/5.
[132] A. Marongiu, G. D'Andrea, A. Raco, 1.5-T field intraoperative magnetic resonance imaging improves extent of resection and survival in glioblastoma removal, World Neurosurg. 98 (2017) 578–586, https://doi.org/10.1016/J.WNEU.2016.11.013.

[133] S. Mahboob, R. McPhillips, Z. Qiu, Y. Jiang, C. Meggs, G. Schiavone, T. Button, M. Desmulliez, C. Demore, S. Cochran, S. Eljamel, Intraoperative ultrasound-guided resection of gliomas: a meta-analysis and review of the literature, World Neurosurg. 92 (2016) 255–263, https://doi.org/10.1016/J.WNEU.2016.05.007.
[134] M. Ganau, G.K. Ligarotti, V. Apostolopoulos, Real-time intraoperative ultrasound in brain surgery: neuronavigation and use of contrast-enhanced image fusion, Quant. Imaging Med. Surg. 9 (2019) 350–358, https://doi.org/10.21037/qims.2019.03.06.
[135] G.R. Sarria, E. Sperk, X. Han, G.J. Sarria, F. Wenz, S. Brehmer, B. Fu, S. Min, H. Zhang, S. Qin, X. Qiu, D. Hänggi, Y. Abo-Madyan, D. Martinez, C. Cabrera, F. A. Giordano, Intraoperative radiotherapy for glioblastoma: an international pooled analysis, Radiother. Oncol. 142 (2020) 162–167, https://doi.org/10.1016/j.radonc.2019.09.023.
[136] J. Eschbacher, N.L. Martirosyan, P. Nakaji, N. Sanai, M.C. Preul, K.A. Smith, S. W. Coons, R.F. Spetzler, In vivo intraoperative confocal microscopy for real-time histopathological imaging of brain tumors, J. Neurosurg. 116 (2012) 854–860, https://doi.org/10.3171/2011.12.JNS11696.
[137] J.I. Traylor, R. Patel, M. Muir, D.C. de Almeida Bastos, V. Ravikumar, C. Kamiya-Matsuoka, G. Rao, J.G. Thomas, Y. Kew, S.S. Prabhu, Laser interstitial thermal therapy for glioblastoma: a single-center experience, World Neurosurg. 149 (2021) e244–e252, https://doi.org/10.1016/J.WNEU.2021.02.044.
[138] N. Iturrioz-Rodríguez, D. De Pasquale, P. Fiaschi, G. Ciofani, Discrimination of glioma patient-derived cells from healthy astrocytes by exploiting Raman spectroscopy, Spectrochim. Acta - Part A Mol. Biomol. Spectrosc. 269 (2022), https://doi.org/10.1016/j.saa.2021.120773.
[139] R.M. Juarez-Chambi, C. Kut, J.J. Rico-Jimenez, K.L. Chaichana, J. Xi, D. U. Campos-Delgado, F.J. Rodriguez, A. Quinones-Hinojosa, X. Li, J.A. Jo, AI-assisted in situ detection of human glioma infiltration using a novel computational method for optical coherence tomography, Clin. Cancer Res. 25 (2019) 6329–6338, https://doi.org/10.1158/1078-0432.CCR-19-0854.
[140] K. Yashin, M.M. Bonsanto, K. Achkasova, A. Zolotova, A.M. Wael, E. Kiseleva, A. Moiseev, I. Medyanik, L. Kravets, R. Huber, R. Brinkmann, N. Gladkova, OCT-guided surgery for gliomas: current concept and future perspectives, Diagnostics (Basel, Switzerland) 12 (2022), https://doi.org/10.3390/DIAGNOSTICS12020335.
[141] M. Touat, A. Idbaih, M. Sanson, K.L. Ligon, Glioblastoma targeted therapy: updated approaches from recent biological insights, Ann. Oncol. 28 (2017) 1457–1472, https://doi.org/10.1093/annonc/mdx106.
[142] E. Le Rhun, M. Preusser, P. Roth, D.A. Reardon, M. van den Bent, P. Wen, G. Reifenberger, M. Weller, Molecular targeted therapy of glioblastoma, Cancer Treat. Rev. 80 (2019), 101896, https://doi.org/10.1016/j.ctrv.2019.101896.
[143] D.C. Binder, E. Ladomersky, A. Lenzen, L. Zhai, K.L. Lauing, S.D. Otto-Meyer, R. V. Lukas, D.A. Wainwright, Lessons learned from rindopepimut treatment in patients with EGFRvIII-expressing glioblastoma, Transl. Cancer Res. 7 (2018) S510, https://doi.org/10.21037/tcr.2018.03.36.
[144] A.C. Phillips, E.R. Boghaert, K.S. Vaidya, M.J. Mitten, S. Norvell, H.D. Falls, P. J. Devries, D. Cheng, J.A. Meulbroek, F.G. Buchanan, L.M. McKay, N.C. Goodwin, E.B. Reilly, ABT-414, an antibody-drug conjugate targeting a tumor-selective EGFR epitope, Mol. Cancer Ther. 15 (2016) 661–669, https://doi.org/10.1158/1535-7163.MCT-15-0901.
[145] A.B. Lassman, S.L. Pugh, M.R. Gilbert, K.D. Aldape, S. Geinoz, J.H. Beumer, S. M. Christner, R. Komaki, L.M. Deangelis, R. Gaur, E. Youssef, H. Wagner, M. Won, M.P. Mehta, Phase 2 trial of dasatinib in target-selected patients with recurrent glioblastoma (RTOG 0627), Neuro-Oncology 17 (2015) 992–998, https://doi.org/10.1093/neuonc/nov011.
[146] P.Y. Wen, J. Drappatz, J. De Groot, M.D. Prados, D.A. Reardon, D. Schiff, M. Chamberlain, T. Mikkelsen, A. Desjardins, J. Holland, J. Ping, R. Weitzman, T. F. Cloughesy, Phase II study of cabozantinib in patients with progressive glioblastoma: subset analysis of patients naive to antiangiogenic therapy, Neuro-Oncology 20 (2018) 249–258, https://doi.org/10.1093/neuonc/nox154.
[147] J. Langhans, L. Schneele, N. Trenkler, H. Von Bandemer, L. Nonnenmacher, G. Karpel-Massler, M.D. Siegelin, S. Zhou, M.-E. Halatsch, K.-M. Debatin, M.-A. Westhoff, The effects of PI3K-mediated signalling on glioblastoma cell behaviour 6, 2017, p. 398, https://doi.org/10.1038/s41389-017-0004-8.
[148] L. Cen, B.L. Carlson, M.A. Schroeder, J.L. Ostrem, G.J. Kitange, A.C. Mladek, S. R. Fink, P.A. Decker, W. Wu, J.S. Kim, T. Waldman, R.B. Jenkins, J.N. Sarkaria, P16-Cdk4-Rb axis controls sensitivity to a cyclin-dependent kinase inhibitor PD0332991 in glioblastoma xenograft cells, Neuro-Oncology 14 (2012) 870–881, https://doi.org/10.1093/neuonc/nos114.
[149] C.W. Brennan, R.G.W. Verhaak, A. McKenna, B. Campos, H. Noushmehr, S. R. Salama, S. Zheng, D. Chakravarty, J.Z. Sanborn, S.H. Berman, R. Beroukhim, B. Bernard, C.J. Wu, G. Genovese, I. Shmulevich, J. Barnholtz-Sloan, L. Zou, R. Vegesna, S.A. Shukla, G. Ciriello, W.K.A. Yung, W. Zhang, C. Sougnez, T. Mikkelsen, K. Aldape, D.D. Bigner, E.G. Van Meir, M. Prados, A.E. Sloan, K. L. Black, J. Eschbacher, G. Finocchiaro, W. Friedman, D.W. Andrews, A. Guha, M. Iacocca, B.P. O'Neill, G. Foltz, J. Myers, D.J. Weisenberger, R. Penny, R. Kucherlapati, C.M. Perou, D.N. Hayes, R. Gibbs, M. Marra, G.B. Mills, E. S. Lander, P. Spellman, R. Wilson, C. Sander, J. Weinstein, M. Meyerson, S. Gabriel, P.W. Laird, D. Haussler, G. Getz, L. Chin, C. Benz, W. Barrett, Q. Ostrom, Y. Wolinsky, B. Bose, P.T. Boulos, M. Boulos, J. Brown, C. Czerinski, M. Eppley, T. Kempista, T. Kitko, Y. Koyfman, B. Rabeno, P. Rastogi, M. Sugarman, P. Swanson, K. Yalamanchii, I.P. Otey, Y.S. Liu, Y. Xiao, J. T. Auman, P.C. Chen, A. Hadjipanayis, E. Lee, S. Lee, P.J. Park, J. Seidman, L. Yang, S. Kalkanis, L.M. Poisson, A. Raghunathan, L. Scarpace, R. Bressler, A. Eakin, L. Iype, R.B. Kreisberg, K. Leinonen, S. Reynolds, H. Rovira, V. Thorsson, M.J. Annala, J. Paulauskis, E. Curley, M. Hatfield, D. Mallery, S. Morris, T. Shelton, C. Shelton, M. Sherman, P. Yena, L. Cuppini, F. DiMeco, M. Eoli, E. Maderna, B. Pollo, M. Saini, S. Balu, K.A. Hoadley, L. Li, C.R. Miller, Y. Shi, M. D. Topal, J. Wu, G. Dunn, C. Giannini, B.A. Aksoy, Y. Antipin, L. Borsu, E. Cerami, J. Gao, B. Gross, A. Jacobsen, M. Ladanyi, A. Lash, Y. Liang, B. Reva, N. Schultz, R. Shen, N.D. Socci, A. Viale, M.L. Ferguson, Q.R. Chen, J.A. Demchok, L.A. L. Dillon, K.R. Mills Shaw, M. Sheth, R. Tarnuzzer, Z. Wang, L. Yang, T. Davidsen, M.S. Guyer, B.A. Ozenberger, H.J. Sofia, J. Bergsten, J. Eckman, J. Harr, C. Smith, K. Tucker, C. Winemiller, L.A. Zach, J.Y. Ljubimova, G. Eley, B. Ayala, M. A. Jensen, A. Kahn, T.D. Pihl, D.A. Pot, Y. Wan, N. Hansen, P. Hothi, B. Lin, N. Shah, J.G. Yoon, C. Lau, M. Berens, K. Ardlie, S.L. Carter, A.D. Cherniack, M. Noble, J. Cho, K. Cibulskis, D. DiCara, S. Frazer, S.B. Gabriel, N. Gehlenborg, J. Gentry, D. Heiman, J. Kim, R. Jing, M. Lawrence, P. Lin, W. Mallard, R. C. Onofrio, G. Saksena, S. Schumacher, P. Stojanov, B. Tabak, D. Voet, H. Zhang, N.N. Dees, L. Ding, L.L. Fulton, R.S. Fulton, K.L. Kanchi, E.R. Mardis, R.K. Wilson, S.B. Baylin, L. Harshyne, M.L. Cohen, K. Devine, S.R. Van Den Berg, M.S. Berger, D. Carlin, B. Craft, K. Ellrott, M. Goldman, T. Goldstein, M. Grifford, S. Ma, S. Ng, J. Stuart, T. Swatloski, P. Waltman, J. Zhu, R. Foss, B. Frentzen, R. McTiernan, A. Yachnis, Y. Mao, R. Akbani, O. Bogler, G.N. Fuller, W. Liu, Y. Liu, Y. Lu, A. Protopopov, X. Ren, Y. Sun, J. Zhang, K. Chen, J.N. Weinstein, M.S. Bootwalla, P.H. Lai, T.J. Triche, D.J. Van Den Berg, D.H. Gutmann, N.L. Lehman, D. Brat, J. J. Olson, G.M. Mastrogianakis, N.S. Devi, Z. Zhang, E. Lipp, R. McLendon, The somatic genomic landscape of glioblastoma, Cell 155 (2013) 462, https://doi.org/10.1016/j.cell.2013.09.034.
[150] M. Verreault, C. Schmitt, L. Goldwirt, K. Pelton, S. Haidar, C. Levasseur, J. Guehennec, D. Knoff, M. Labussière, Y. Marie, A.H. Ligon, K. Mokhtari, K. Hoang-Xuan, M. Sanson, B.M. Alexander, P.Y. Wen, J.Y. Delattre, K.L. Ligon, A. Idbaih, Preclinical efficacy of the MDM2 inhibitor RG7112 in MDM2-amplified and TP53 wild-type glioblastomas, Clin. Cancer Res. 22 (2016) 1185–1196, https://doi.org/10.1158/1078-0432.CCR-15-1015.
[151] M. Takahashi, S. Miki, K. Fujimoto, K. Fukuoka, Y. Matsushita, Y. Maida, M. Yasukawa, M. Hayashi, R. Shinkyo, K. Kikuchi, A. Mukasa, R. Nishikawa, K. Tamura, Y. Narita, A. Hamada, K. Masutomi, K. Ichimura, Eribulin penetrates brain tumor tissue and prolongs survival of mice harboring intracerebral glioblastoma xenografts, Cancer Sci. 110 (2019) 2247–2257, https://doi.org/10.1111/cas.14067.
[152] S. Pellegatta, L. Valletta, C. Corbetta, M. Patanè, I. Zucca, F. Riccardi Sirtori, M. G. Bruzzone, G. Fogliatto, A. Isacchi, B. Pollo, G. Finocchiaro, Effective immuno-targeting of the IDH1 mutation R132H in a murine model of intracranial glioma, Acta Neuropathol. Commun. 3 (2015) 4, https://doi.org/10.1186/s40478-014-0180-0.
[153] E.Q. Lee, D.A. Reardon, D. Schiff, J. Drappatz, A. Muzikansky, S.A. Grimm, A. D. Norden, L. Nayak, R. Beroukhim, M.L. Rinne, A.S. Chi, T.T. Batchelor, K. Hempfling, C. McCluskey, K.H. Smith, S.C. Gaffey, B. Wrigley, K.L. Ligon, J. J. Raizer, P.Y. Wen, Phase II study of panobinostat in combination with bevacizumab for recurrent glioblastoma and anaplastic glioma, Neuro-Oncology 17 (2015) 862–867, https://doi.org/10.1093/neuonc/nou350.
[154] B.B. Friday, S.K. Anderson, J. Buckner, C. Yu, C. Giannini, F. Geoffroy, J. Schwerkoske, M. Mazurczak, H. Gross, E. Pajon, K. Jaeckle, E. Galanis, Phase II trial of vorinostat in combination with bortezomib in recurrent glioblastoma: a north central cancer treatment group study, Neuro-Oncology 14 (2012) 215–221, https://doi.org/10.1093/NEUONC/NOR198.
[155] W. Wick, M. Platten, A. Wick, A. Hertenstein, A. Radbruch, M. Bendszus, F. Winkler, Current status and future directions of anti-angiogenic therapy for gliomas, Neuro-Oncology 18 (2016) 315–328, https://doi.org/10.1093/neuonc/nov180.
[156] W. Wick, T. Gorlia, M. Bendszus, M. Taphoorn, F. Sahm, I. Harting, A.A. Brandes, W. Taal, J. Domont, A. Idbaih, M. Campone, P.M. Clement, R. Stupp, M. Fabbro, E. Le Rhun, F. Dubois, M. Weller, A. von Deimling, V. Golfinopoulos, J. C. Bromberg, M. Platten, M. Klein, M.J. van den Bent, Lomustine and bevacizumab in progressive glioblastoma, N. Engl. J. Med. 377 (2017) 1954–1963, https://doi.org/10.1056/nejmoa1707358.
[157] L. Malric, S. Monferran, J. Gilhodes, S. Boyrie, P. Dahan, N. Skuli, J. Sesen, T. Filleron, A. Kowalski-Chauvel, E.C.J. Moyal, C. Toulas, A. Lemarié, Interest of integrins targeting in glioblastoma according to tumor heterogeneity and cancer stem cell paradigm: an update, Oncotarget. 8 (2017) 86947–86968, https://doi.org/10.18632/ONCOTARGET.20372.
[158] D.A. Reardon, B. Neyns, M. Weller, J.C. Tonn, L.B. Nabors, R. Stupp, Cilengitide: an RGD pentapeptide αvβ3 and αvβ5 integrin inhibitor in development for glioblastoma and other malignancies, Future Oncol. 7 (2011) 339–354, https://doi.org/10.2217/FON.11.8.
[159] H. Zhang, R. Wang, Y. Yu, J. Liu, T. Luo, F. Fan, Glioblastoma treatment modalities besides surgery, J. Cancer 10 (2019) 4793–4806, https://doi.org/10.7150/jca.32475.
[160] R. Stupp, M.E. Hegi, W.P. Mason, M.J. van den Bent, M.J. Taphoorn, R.C. Janzer, S.K. Ludwin, A. Allgeier, B. Fisher, K. Belanger, P. Hau, A.A. Brandes, J. Gijtenbeek, C. Marosi, C.J. Vecht, K. Mokhtari, P. Wesseling, S. Villa, E. Eisenhauer, T. Gorlia, M. Weller, D. Lacombe, J.G. Cairncross, R.O. Mirimanoff, Effects of radiotherapy with concomitant and adjuvant temozolomide versus radiotherapy alone on survival in glioblastoma in a randomised phase III study: 5-year analysis of the EORTC-NCIC trial, Lancet Oncol. 10 (2009) 459–466, https://doi.org/10.1016/S1470-2045(09)70025-7.
[161] W.K. Xing, C. Shao, Z.Y. Qi, C. Yang, Z. Wang, The role of Gliadel wafers in the treatment of newly diagnosed GBM: a meta-analysis, Drug Des. Dev. Ther. 9 (2015) 3341–3348, https://doi.org/10.2147/DDDT.S85943.
[162] C. Jungk, D. Chatziaslanidou, R. Ahmadi, D. Capper, J.L. Bermejo, J. Exner, A. von Deimling, C. Herold-Mende, A. Unterberg, Chemotherapy with BCNU in

recurrent glioma: analysis of clinical outcome and side effects in chemotherapy-naïve patients, BMC Cancer 16 (2016), https://doi.org/10.1186/S12885-016-2131-6.
[163] X. Ren, D. Ai, T. Li, L. Xia, L. Sun, Effectiveness of lomustine combined with bevacizumab in glioblastoma: a meta-analysis, Front. Neurol. 11 (2021) 1–8, https://doi.org/10.3389/fneur.2020.603947.
[164] L. Ferrer-Font, N. Arias-Ramos, S. Lope-Piedrafita, M. Julià-Sapé, M. Pumarola, C. Arús, A.P. Candiota, Metronomic treatment in immunocompetent preclinical GL261 glioblastoma: effects of cyclophosphamide and temozolomide, NMR Biomed. 30 (2017), https://doi.org/10.1002/NBM.3748.
[165] V. Rajaratnam, M.M. Islam, M. Yang, R. Slaby, H.M. Ramirez, S.P. Mirza, Glioblastoma : pathogenesis and current status of, Cancers (Basel) 12 (2020) 1–28.
[166] Q.L. Guo, X.L. Dai, M.Y. Yin, H.W. Cheng, H.S. Qian, H. Wang, D.M. Zhu, X. W. Wang, Nanosensitizers for sonodynamic therapy for glioblastoma multiforme: current progress and future perspectives, Mil. Med. Res. 9 (2022), https://doi.org/10.1186/S40779-022-00386-Z.
[167] S. Ning, X. Dai, W. Tang, Q. Guo, M. Lyu, D. Zhu, W. Zhang, H. Qian, X. Yao, X. Wang, Cancer cell membrane-coated C-TiO2 hollow nanoshells for combined sonodynamic and hypoxia-activated chemotherapy, Acta Biomater. 152 (2022) 562–574, https://doi.org/10.1016/J.ACTBIO.2022.08.067.
[168] E.P. Sulman, N. Ismaila, T.S. Armstrong, C. Tsien, T.T. Batchelor, T. Cloughesy, E. Galanis, M. Gilbert, V. Gondi, M. Lovely, M. Mehta, M.P. Mumber, A. Sloan, S. M. Chang, Radiation therapy for glioblastoma: American Society of Clinical Oncology clinical practice guideline endorsement of the American Society for Radiation Oncology guideline, J. Clin. Oncol. 35 (2017) 361–369, https://doi.org/10.1200/JCO.2016.70.7562.
[169] P. Ciammella, M. Galeandro, N. D'Abbiero, A. Podgornii, A. Pisanello, A. Botti, E. Cagni, M. Iori, C. Iotti, Hypo-fractionated IMRT for patients with newly diagnosed glioblastoma multiforme: a 6 year single institutional experience, Clin. Neurol. Neurosurg. 115 (2013) 1609–1614, https://doi.org/10.1016/j.clineuro.2013.02.001.
[170] N.S. Floyd, S.Y. Woo, B.S. Teh, C. Prado, W.Y. Mai, T. Trask, P.L. Gildenberg, P. Holoye, M.E. Augspurger, L.S. Carpenter, H.H. Lu, J.K. Chiu, W.H. Grant, E. B. Butler, Hypofractionated intensity-modulated radiotherapy for primary glioblastoma multiforme, Int. J. Radiat. Oncol. Biol. Phys. 58 (2004) 721–726, https://doi.org/10.1016/S0360-3016(03)01623-7.
[171] A. Moreau, O. Febvey, T. Mognetti, D. Frappaz, D. Kryza, Contribution of different positron emission tomography tracers in glioma management: focus on glioblastoma, Front. Oncol. 9 (2019) 1–20, https://doi.org/10.3389/fonc.2019.01134.
[172] D.J. Gessler, C. Ferreira, K. Dusenbery, C.C. Chen, GammaTile®: surgically targeted radiation therapy for glioblastomas, Future Oncol. 16 (2020) 2445–2455, https://doi.org/10.2217/fon-2020-0558.
[173] V.M. Lu, P. Kerezoudis, D.A. Brown, T.C. Burns, A. Quinones-Hinojosa, K. L. Chaichana, Hypofractionated versus standard radiation therapy in combination with temozolomide for glioblastoma in the elderly: a meta-analysis, J. Neuro-Oncol. 143 (2019) 177–185, https://doi.org/10.1007/s11060-019-03155-6.
[174] A. Omuro, A.A. Brandes, A.F. Carpentier, A. Idbaih, D.A. Reardon, T. Cloughesy, A. Sumrall, J. Baehring, M. van den Bent, O. Bähr, G. Lombardi, P. Mulholland, G. Tabatabai, U. Lassen, J.M. Sepulveda, M. Khasraw, E. Vauleon, Y. Muragaki, A. M. Di Giacomo, N. Butowski, P. Roth, X. Qian, A.Z. Fu, Y. Liu, V. Potter, A. G. Chalamandaris, K. Tatsuoka, M. Lim, M. Weller, Radiotherapy combined with nivolumab or temozolomide for newly diagnosed glioblastoma with unmethylated MGMT promoter: an international randomized phase III trial, Neuro-Oncology 25 (2023) 123–134, https://doi.org/10.1093/neuonc/noac099.
[175] D.P. Kulinich, J.P. Sheppard, T. Nguyen, A.M. Kondajji, A. Unterberger, C. Duong, A. Enomoto, K. Patel, I. Yang, Radiotherapy versus combination radiotherapy-bevacizumab for the treatment of recurrent high-grade glioma: a systematic review, Acta Neurochir. 163 (2021) 1921–1934, https://doi.org/10.1007/s00701-021-04794-3.
[176] A.A. Arabzadeh, T. Mortezazadeh, T. Aryafar, E. Gharepapagh, M. Majdaeen, B. Farhood, Therapeutic potentials of resveratrol in combination with radiotherapy and chemotherapy during glioblastoma treatment: a mechanistic review, Cancer Cell Int. 21 (2021) 1–15, https://doi.org/10.1186/s12935-021-02099-0.
[177] J. Park, C.G. Kim, J.K. Shim, J.H. Kim, H. Lee, J.E. Lee, M.H. Kim, K. Haam, I. Jung, S.H. Park, J.H. Chang, E.C. Shin, S.G. Kang, Effect of combined anti-PD-1 and temozolomide therapy in glioblastoma, Oncoimmunology. 8 (2018), https://doi.org/10.1080/2162402X.2018.1525243.
[178] A. Wu, R. Maxwell, Y. Xia, P. Cardarelli, M. Oyasu, Z. Belcaid, E. Kim, A. Hung, A. S. Luksik, T. Garzon-Muvdi, C.M. Jackson, D. Mathios, D. Theodros, J. Cogswell, H. Brem, D.M. Pardoll, M. Lim, Combination anti-CXCR4 and anti-PD-1 immunotherapy provides survival benefit in glioblastoma through immune cell modulation of tumor microenvironment, J. Neuro-Oncol. 143 (2019) 241–249, https://doi.org/10.1007/s11060-019-03172-5.
[179] F. Yang, Z. He, H. Duan, D. Zhang, J. Li, H. Yang, J.F. Dorsey, W. Zou, S. Ali Nabavizadeh, S.J. Bagley, K. Abdullah, S. Brem, L. Zhang, X. Xu, K.T. Byrne, R. H. Vonderheide, Y. Gong, Y. Fan, Synergistic immunotherapy of glioblastoma by dual targeting of IL-6 and CD40, Nat. Commun. 12 (2021), https://doi.org/10.1038/S41467-021-23832-3.
[180] T.R. Hodges, M. Ott, J. Xiu, Z. Gatalica, J. Swensen, S. Zhou, J.T. Huse, J. De Groot, S. Li, W.W. Overwijk, D. Spetzler, A.B. Heimberger, Mutational burden, immune checkpoint expression, and mismatch repair in glioma: implications for immune checkpoint immunotherapy, Neuro-Oncology 19 (2017) 1047–1057, https://doi.org/10.1093/NEUONC/NOX026.
[181] A. Omuro, G. Vlahovic, M. Lim, S. Sahebjam, J. Baehring, T. Cloughesy, A. Voloschin, S.H. Ramkissoon, K.L. Ligon, R. Latek, R. Zwirtes, L. Strauss, P. Paliwal, C.T. Harbison, D.A. Reardon, J.H. Sampson, Nivolumab with or without ipilimumab in patients with recurrent glioblastoma: results from exploratory phase I cohorts of CheckMate 143, Neuro-Oncology 20 (2018) 674–686, https://doi.org/10.1093/NEUONC/NOX208.
[182] L. Nayak, A.M. Molinaro, K. Peters, J.L. Clarke, J.T. Jordan, J. de Groot, L. Nghiemphu, T. Kaley, H. Colman, C. McCluskey, S. Gaffey, T.R. Smith, D. J. Cote, M. Severgnini, J.H. Yearley, Q. Zhao, W.M. Blumenschein, D.G. Duda, A. Muzikansky, R.K. Jain, P.Y. Wen, D.A. Reardon, Randomized phase II and biomarker study of pembrolizumab plus bevacizumab versus pembrolizumab alone for patients with recurrent glioblastoma, Clin. Cancer Res. 27 (2021) 1048–1057, https://doi.org/10.1158/1078-0432.CCR-20-2500.
[183] S. Goswami, S. Anandhan, D. Raychaudhuri, P. Sharma, Myeloid cell-targeted therapies for solid tumours, Nat. Rev. Immunol. 232 (23) (2022) 106–120, https://doi.org/10.1038/s41577-022-00737-w.
[184] N. Butowski, H. Colman, J.F. De Groot, A.M. Omuro, L. Nayak, P.Y. Wen, T. F. Cloughesy, A. Marimuthu, S. Haidar, A. Perry, J. Huse, J. Phillips, B.L. West, K. B. Nolop, H.H. Hsu, K.L. Ligon, A.M. Molinaro, M. Prados, Orally administered colony stimulating factor 1 receptor inhibitor PLX3397 in recurrent glioblastoma: an ivy foundation early phase clinical trials consortium phase II study, Neuro-Oncology 18 (2016) 557–564, https://doi.org/10.1093/NEUONC/NOV245.
[185] M.A. Exley, S. Garcia, A. Zellander, J. Zilberberg, D.W. Andrews, Challenges and opportunities for immunotherapeutic intervention against myeloid immunosuppression in glioblastoma, J. Clin. Med. 11 (2022), https://doi.org/10.3390/jcm11041069.
[186] B.D. Choi, M.V. Maus, C.H. June, H. John, I. Program, M.G. Hospital, M. G. Hospital, M.G. Hospital, B. Tumor, I. Program, Immunotherapy for Glioblastoma: Adoptive T-cell Strategies 25, 2019, pp. 2042–2048, https://doi.org/10.1158/1078-0432.CCR-18-1625.Immunotherapy.
[189] S.J. Bagley, A.S. Desai, G.P. Linette, C.H. June, D.M. O'Rourke, CAR T-cell therapy for glioblastoma: recent clinical advances and future challenges, Neuro-Oncology 20 (2018) 1429–1438, https://doi.org/10.1093/neuonc/noy032.
[190] E.A. Chong, J.J. Melenhorst, S.F. Lacey, D.E. Ambrose, V. Gonzalez, B.L. Levine, C.H. June, S.J. Schuster, PD-1 blockade modulates chimeric antigen receptor (CAR)-modified T cells: refueling the CAR, Blood. 129 (2017) 1039–1041, https://doi.org/10.1182/BLOOD-2016-09-738245.
[191] K.J. Curran, B.A. Seinstra, Y. Nikhamin, R. Yeh, Y. Usachenko, D.G. Van Leeuwen, T. Purdon, H.J. Pegram, R.J. Brentjens, Enhancing antitumor efficacy of chimeric antigen receptor T cells through constitutive CD40L expression, Mol. Ther. 23 (2015) 769–778, https://doi.org/10.1038/MT.2015.4.
[192] K. Bielamowicz, K. Fousek, T.T. Byrd, H. Samaha, M. Mukherjee, N. Aware, M. F. Wu, J.S. Orange, P. Sumazin, T.K. Man, S.K. Joseph, M. Hegde, N. Ahmed, Trivalent CAR T cells overcome interpatient antigenic variability in glioblastoma, Neuro-Oncology 20 (2018) 506, https://doi.org/10.1093/NEUONC/NOX182.
[193] M. Saxena, S.H. van der Burg, C.J.M. Melief, N. Bhardwaj, Therapeutic cancer vaccines, Nat. Rev. Cancer 21 (2021) 360–378, https://doi.org/10.1038/S41568-021-00346-0.
[194] M. Weller, K. Kaulich, B. Hentschel, J. Felsberg, D. Gramatzki, T. Pietsch, M. Simon, M. Westphal, G. Schackert, J.C. Tonn, A. Von Deimling, T. Davis, W. A. Weiss, M. Loeffler, G. Reifenberger, Assessment and prognostic significance of the epidermal growth factor receptor vIII mutation in glioblastoma patients treated with concurrent and adjuvant temozolomide radiochemotherapy, Int. J. Cancer 134 (2014) 2437–2447, https://doi.org/10.1002/IJC.28576.
[195] D.A. Reardon, A. Desjardins, J.J. Vredenburgh, D.M. O'Rourke, D.D. Tran, K. L. Fink, L.B. Nabors, G. Li, D.A. Bota, R.V. Lukas, L.S. Ashby, J. Paul Duic, M. M. Mrugala, S. Cruickshank, L. Vitale, Y. He, J.A. Green, M.J. Yellin, C.D. Turner, T. Keler, T.A. Davis, J.H. Sampson, Rindopepimut with bevacizumab for patients with relapsed EGFRvIII-expressing glioblastoma (ReACT): results of a double-blind randomized phase II trial, Clin. Cancer Res. 26 (2020) 1586–1594, https://doi.org/10.1158/1078-0432.CCR-18-1140.
[196] P.Y. Wen, D.A. Reardon, T.S. Armstrong, S. Phuphanich, R.D. Aiken, J.C. Landolfi, W.T. Curry, J.J. Zhu, M. Glantz, D.M. Peereboom, J.M. Markert, R. LaRocca, D. M. O'Rourke, K. Fink, L. Kim, M. Gruber, G.J. Lesser, E. Pan, S. Kesari, A. Muzikansky, C. Pinilla, R.G. Santos, J.S. Yu, A randomized double-blind placebo-controlled phase II trial of dendritic cell vaccine ICT-107 in newly diagnosed patients with glioblastoma, Clin. Cancer Res. 25 (2019) 5799, https://doi.org/10.1158/1078-0432.CCR-19-0261.
[197] D.B. Keskin, A.J. Anandappa, J. Sun, I. Tirosh, N.D. Mathewson, S. Li, G. Oliveira, A. Giobbie-Hurder, K. Felt, E. Gjini, S.A. Shukla, Z. Hu, L. Li, P.M. Le, R.L. Allesøe, A.R. Richman, M.S. Kowalczyk, S. Abdelrahman, J.E. Geduldig, S. Charbonneau, K. Pelton, J.B. Iorgulescu, L. Elagina, W. Zhang, O. Olive, C. McCluskey, L. R. Olsen, J. Stevens, W.J. Lane, A.M. Salazar, H. Daley, P.Y. Wen, E.A. Chiocca, M. Harden, N.J. Lennon, S. Gabriel, G. Getz, E.S. Lander, A. Regev, J. Ritz, D. Neuberg, S.J. Rodig, K.L. Ligon, M.L. Suvà, K.W. Wucherpfennig, N. Hacohen, E.F. Fritsch, K.J. Livak, P.A. Ott, C.J. Wu, D.A. Reardon, Neoantigen vaccine generates intratumoral T cell responses in phase Ib glioblastoma trial, Nature. 565 (2019) 234–239, https://doi.org/10.1038/S41586-018-0792-9.
[198] A.R. Safa, M.R. Saadatzadeh, A.A. Cohen-Gadol, K.E. Pollok, K. Bijangi-Vishehsaraei, Emerging targets for glioblastoma stem cell therapy, J. Biomed. Res. 30 (2016) 19, https://doi.org/10.7555/JBR.30.20150100.
[199] B. de Lucas, L.M. Pérez, B.G. Gálvez, Importance and regulation of adult stem cell migration, J. Cell. Mol. Med. 22 (2018) 746–754, https://doi.org/10.1111/JCMM.13422.

[200] N. Kock, R. Kasmieh, R. Weissledery, K. Shah, Tumor therapy mediated by lentiviral expression of shBcl-2 and S-TRAIL, Neoplasia. 9 (2007) 435–442, https://doi.org/10.1593/NEO.07223.
[201] N.G. Rainov, A Phase III Clinical Evaluation of Herpes Simplex Virus Type 1 Thymidine Kinase and Ganciclovir Gene Therapy as an Adjuvant to Surgical Resection and Radiation in Adults with Previously Untreated Glioblastoma Multiforme. Https://Home.Liebertpub.Com/Hum 11, 2004, pp. 2389–2401, https://doi.org/10.1089/104303400750038499.
[202] L. Dührsen, S. Hartfuß, D. Hirsch, S. Geiger, C.L. Mair, J. Sedlacik, C. Guenther, M. Westphal, K. Lamszus, F.G. Hermann, N.O. Schmidt, Preclinical analysis of human mesenchymal stem cells: Tumor tropism and therapeutic efficiency of local HSV-TK suicide gene therapy in glioblastoma, Oncotarget. 10 (2019) 6049–6061, https://doi.org/10.18632/oncotarget.27071.
[203] W.C. Huang, I.L. Lu, W.H. Chiang, Y.W. Lin, Y.C. Tsai, H.H. Chen, C.W. Chang, C. S. Chiang, H.C. Chiu, Tumortropic adipose-derived stem cells carrying smart nanotherapeutics for targeted delivery and dual-modality therapy of orthotopic glioblastoma, J. Control. Release 254 (2017) 119–130, https://doi.org/10.1016/J.JCONREL.2017.03.035.
[204] B. Thaci, A.U. Ahmed, I.V. Ulasov, A.L. Tobias, Y. Han, K.S. Aboody, M.S. Lesniak, Pharmacokinetic study of neural stem cell-based cell carrier for oncolytic virotherapy: targeted delivery of the therapeutic payload in an orthotopic brain tumor model, Cancer Gene Ther. 19 (2012) 431–442, https://doi.org/10.1038/cgt.2012.21.
[205] D. Bhere, K. Tamura, B. Purow, J. Debatisse, K. Shah, Mesenchymal stem cells shuttle micrornas via extracellular vesicles and prime resistant GBM to caspase mediated apoptosis, Cytotherapy. 19 (2017) e4–e5, https://doi.org/10.1016/j.jcyt.2017.03.017.
[206] H.S. Kim, D.Y. Lee, Nanomedicine in clinical photodynamic therapy for the treatment of brain tumors, Biomedicines. 10 (2022) 1–26, https://doi.org/10.3390/biomedicines10010096.
[207] A.P. Michael, N. Nordmann, M.S. Zaghloul, R.E. Kast, 5-aminolevulinic acid radiodynamic therapy for treatment of high-grade gliomas, Horizons Cancer Res. 80 (80) (2021) 155–194, https://doi.org/10.1007/s11060-019-03103-4.5-Aminolevulinic.
[208] E.S. Ara, A.V. Noghreiyan, A. Sazgarnia, Evaluation of photodynamic effect of indocyanine green (ICG) on the colon and glioblastoma cancer cell lines pretreated by cold atmospheric plasma, Photodiagn. Photodyn. Ther. 35 (2021), 102408, https://doi.org/10.1016/J.PDPDT.2021.102408.
[209] R.H. Kang, Y. Kim, H.J. Um, J. Kim, E.K. Bang, S.G. Yeo, D. Kim, Glioblastoma homing photodynamic therapy based on multifunctionalized porous silicon nanoparticles, ACS Appl. Nano Mater. 5 (2022) 5387–5397, https://doi.org/10.1021/ACSANM.2C00368/SUPPL_FILE/AN2C00368_SI_001.PDF.
[210] S. Shibata, N. Shinozaki, A. Suganami, S. Ikegami, Y. Kinoshita, R. Hasegawa, H. Kentaro, Y. Okamoto, I. Aoki, Y. Tamura, Y. Iwadate, Photo-immune therapy with liposomally formulated phospholipid-conjugated indocyanine green induces specific antitumor responses with heat shock protein-70 expression in a glioblastoma model, Oncotarget. 10 (2019) 175–183, https://doi.org/10.18632/ONCOTARGET.26544.
[211] D. Maziukiewicz, B.F. Grześkowiak, E. Coy, S. Jurga, R. Mrówczýnski, NDs@PDA@ICG conjugates for photothermal therapy of glioblastoma multiforme, Biomimetics 4 (2019) 3, https://doi.org/10.3390/BIOMIMETICS4010003.
[212] D.L. ZhuGe, L.F. Wang, R. Chen, X.Z. Li, Z.W. Huang, Q. Yao, B. Chen, Y.Z. Zhao, H.L. Xu, J.D. Yuan, Cross-linked nanoparticles of silk fibroin with proanthocyanidins as a promising vehicle of indocyanine green for photo-thermal therapy of glioma, Artif. Cells Nanomed. Biotechnol. 47 (2019) 4293–4304, https://doi.org/10.1080/21691401.2019.1699819.
[213] A. Guglielmelli, P. Rosa, M. Contardi, M. Prato, G. Mangino, S. Miglietta, V. Petrozza, R. Pani, A. Calogero, A. Athanassiou, G. Perotto, L. De Sio, Biomimetic keratin gold nanoparticle-mediated in vitro photothermal therapy on glioblastoma multiforme 16, 2021, pp. 121–138, https://doi.org/10.2217/NNM-2020-0349.
[214] R. Sun, M. Liu, Z. Xu, B. Song, Y. He, U. Jo, B.U. Qsftfou, U.I.F. Qsfwbmfou, D. Usfbunfou, S. Cmppe, D. Boe, J. Qipupuifsnbm, Q. Uifsbqfvujd, Q. Jo, D. Uifsbqz, Silicon-based nanospores crosses the blood-brain barrier for photothermal therapy of glioblastoma 15, 2022, pp. 7392–7401.
[215] Q. Guo, M. Yin, J. Fan, Y. Yang, T. Liu, H. Qian, X. Dai, X. Wang, Peroxidase-mimicking TA-VOx nanobranches for enhanced photothermal/chemodynamic therapy of glioma by inhibiting the expression of HSP60, Mater. Des. 224 (2022), 111366, https://doi.org/10.1016/J.MATDES.2022.111366.
[216] D. Liu, X. Dai, W. Zhang, X. Zhu, Z. Zha, H. Qian, L. Cheng, X. Wang, Liquid exfoliation of ultrasmall zirconium carbide nanodots as a noninflammatory photothermal agent in the treatment of glioma, Biomaterials. 292 (2023), 121917, https://doi.org/10.1016/J.BIOMATERIALS.2022.121917.
[217] J. Rick, A. Chandra, M.K. Aghi, Tumor treating fields: a new approach to glioblastoma therapy, J. Neuro-Oncol. 137 (2018) 447–453, https://doi.org/10.1007/s11060-018-2768-x.
[218] J.J. Zhu, S.A. Goldlust, L.R. Kleinberg, J. Honnorat, N.A. Oberheim Bush, Z. Ram, Tumor treating fields (TTFields) therapy vs physicians' choice standard-of-care treatment in patients with recurrent glioblastoma: a post-approval registry study (EF-19), Discov. Oncol. 13 (2022), https://doi.org/10.1007/s12672-022-00555-5.
[219] P. Zhu, J.J. Zhu, Tumor treating fields: a novel and effective therapy for glioblastoma: mechanism, efficacy, safety and future perspectives, Chin. Clin. Oncol. 6 (2017) 1–15, https://doi.org/10.21037/cco.2017.06.29.
[220] J. Li, W. Wang, J. Wang, Y. Cao, S. Wang, J. Zhao, Viral gene therapy for glioblastoma multiforme: a promising hope for the current dilemma, Front. Oncol. 11 (2021) 1819, https://doi.org/10.3389/FONC.2021.678226/XML/NLM.
[221] T.F. Cloughesy, K. Petrecca, T. Walbert, N. Butowski, M. Salacz, J. Perry, D. Damek, D. Bota, C. Bettegowda, J.J. Zhu, F. Iwamoto, D. Placantonakis, L. Kim, B. Elder, G. Kaptain, D. Cachia, Y. Moshel, S. Brem, D. Piccioni, J. Landolfi, C. C. Chen, H. Gruber, A.R. Rao, D. Hogan, W. Accomando, D. Ostertag, T. T. Montellano, T. Kheoh, F. Kabbinavar, M.A. Vogelbaum, Effect of Vocimagene Amiretrorepvec in combination with flucytosine vs standard of care on survival following Tumor resection in patients with recurrent high-grade glioma: a randomized clinical trial, JAMA Oncol. 6 (2020) 1939–1946, https://doi.org/10.1001/JAMAONCOL.2020.3161.
[222] C. Manikandan, A. Kaushik, D. Sen, Viral vector: potential therapeutic for glioblastoma multiforme, Cancer Gene Ther. 27 (2020) 270–279, https://doi.org/10.1038/S41417-019-0124-8.
[223] X. Wei, T. Lv, D. Chen, J. Guan, Lentiviral vector mediated delivery of RHBDD1 shRNA down regulated the proliferation of human glioblastoma cells, Technol. Cancer Res. Treat. 13 (2014) 87–93, https://doi.org/10.7785/tcrt.2012.500362.
[224] O. Mozhei, A.G. Teschemacher, S. Kasparov, Viral vectors as gene therapy agents for treatment of glioblastoma, Cancers (Basel) 12 (2020) 1–23, https://doi.org/10.3390/cancers12123724.
[225] F.F. Lang, C. Conrad, C. Gomez-Manzano, W.K. Alfred Yung, R. Sawaya, J. S. Weinberg, S.S. Prabhu, G. Rao, G.N. Fuller, K.D. Aldape, J. Gumin, L.M. Vence, I. Wistuba, J. Rodriguez-Canales, P.A. Villalobos, C.M.F. Dirven, S. Tejada, R. D. Valle, M.M. Alonso, B. Ewald, J.J. Peterkin, F. Tufaro, J. Fueyo, Phase I study of DNX-2401 (delta-24-RGD) oncolytic adenovirus: replication and immunotherapeutic effects in recurrent malignant glioma, J. Clin. Oncol. 36 (2018) 1419–1427, https://doi.org/10.1200/JCO.2017.75.8219.
[226] F.F. Lang, N.D. Tran, V.K. Puduvalli, J.B. Elder, K.L. Fink, C.A. Conrad, W.K. A. Yung, M. Penas-Prado, C. Gomez-Manzano, J. Peterkin, J. Fueyo, Phase 1b open-label randomized study of the oncolytic adenovirus DNX-2401 administered with or without interferon gamma for recurrent glioblastoma 35, 2017, https://doi.org/10.1200/JCO.2017.35.15_SUPPL.2002, 2002–2002.
[227] X. Xu, W. Chen, W. Zhu, J. Chen, B. Ma, J. Ding, Z. Wang, Y. Li, Y. Wang, X. Zhang, Adeno-associated virus (AAV)-based gene therapy for glioblastoma, Cancer Cell Int. 21 (2021) 1–10, https://doi.org/10.1186/s12935-021-01776-4.
[228] S. Harrow, V. Papanastassiou, J. Harland, R. Mabbs, R. Petty, M. Fraser, D. Hadley, J. Patterson, S.M. Brown, R. Rampling, HSV1716 injection into the brain adjacent to tumour following surgical resection of high-grade glioma: safety data and long-term survival, Gene Ther. 11 (2004) 1648–1658, https://doi.org/10.1038/SJ.GT.3302289.
[229] R. Mi, W. Fan, J. Ji, C. Dong, G. Jin, F. Liu, The enhanced efficacy of herpes simplex virus by lentivirus mediated VP22 and cytosine deaminase gene therapy against glioma, Brain Res. 1743 (2020), 146898, https://doi.org/10.1016/J.BRAINRES.2020.146898.
[230] S. Rius-Rocabert, N. García-Romero, A. García, A. Ayuso-Sacido, E. Nistal-Villan, Oncolytic virotherapy in glioma tumors, Int. J. Mol. Sci. 21 (2020) 1–32, https://doi.org/10.3390/ijms21207604.
[231] J. Foloppe, J. Kempf, N. Futin, J. Kintz, P. Cordier, C. Pichon, A. Findeli, F. Vorburger, E. Quemeneur, P. Erbs, The enhanced tumor specificity of TG6002, an armed oncolytic vaccinia virus deleted in two genes involved in nucleotide metabolism, Mol. Ther. - Oncol. 14 (2019) 1–14, https://doi.org/10.1016/j.omto.2019.03.005.
[232] B. Caffery, J.S. Lee, A.A. Alexander-Bryant, Vectors for glioblastoma gene therapy: viral & non-viral delivery strategies, Nanomaterials. 9 (2019), https://doi.org/10.3390/nano9010105.
[233] M.T. Luiz, L.B. Tofani, V.H.S. Araújo, L.D. Di Filippo, J.L. Duarte, J.M. Marchetti, M. Chorilli, Gene therapy based on lipid nanoparticles as non-viral vectors for glioma treatment, Curr. Gene Ther. 21 (2021) 452–463, https://doi.org/10.2174/1566523220999201230205126.
[234] J.V. Gregory, P. Kadiyala, R. Doherty, M. Cadena, S. Habeel, E. Ruoslahti, P. R. Lowenstein, M.G. Castro, J. Lahann, Systemic brain tumor delivery of synthetic protein nanoparticles for glioblastoma therapy, Nat. Commun. 11 (2020), https://doi.org/10.1038/S41467-020-19225-7.
[235] J. Choi, Y. Rui, J. Kim, N. Gorelick, D.R. Wilson, K. Kozielski, A. Mangraviti, E. Sankey, H. Brem, B. Tyler, J.J. Green, E.M. Jackson, Nonviral polymeric nanoparticles for gene therapy in pediatric CNS malignancies, Nanomedicine. 23 (2020), https://doi.org/10.1016/J.NANO.2019.102115.
[236] J. Kim, S.K. Mondal, S.Y. Tzeng, Y. Rui, R. Al-Kharboosh, K.K. Kozielski, A. G. Bhargav, C.A. Garcia, A. Quiñones-Hinojosa, J.J. Green, Poly(ethylene glycol)-poly(beta-amino ester)-based nanoparticles for suicide gene therapy enhance brain penetration and extend survival in a preclinical human glioblastoma orthotopic xenograft model, ACS Biomater. Sci. Eng. 6 (2020) 2943–2955, https://doi.org/10.1021/ACSBIOMATERIALS.0C00116.
[237] B.M. Tyler, Dendrimer Technology in Glioma : Functional Design and Potential Applications, 2023.
[238] C.Z. Bai, S. Choi, K. Nam, S. An, J.S. Park, Arginine modified PAMAM dendrimer for interferon beta gene delivery to malignant glioma, Int. J. Pharm. 445 (2013) 79–87, https://doi.org/10.1016/J.IJPHARM.2013.01.057.
[239] W. Liyanage, T. Wu, S. Kannan, R.M. Kannan, Dendrimer–siRNA conjugates for targeted intracellular delivery in glioblastoma animal models, ACS Appl. Mater. Interfaces (2022), https://doi.org/10.1021/ACSAMI.2C13129.
[240] L. Kong, Y. Wu, C.S. Alves, X. Shi, Efficient delivery of therapeutic siRNA into glioblastoma cells using multifunctional dendrimer-entrapped gold nanoparticles 12, 2016, pp. 3103–3115, https://doi.org/10.2217/NNM-2016-0240.

[241] H. Yin, W. Xue, D.G. Anderson, CRISPR–Cas: a tool for cancer research and therapeutics, Nat. Rev. Clin. Oncol. 165 (16) (2019) 281–295, https://doi.org/10.1038/s41571-019-0166-8.
[242] X. Kang, Y. Wang, P. Liu, B. Huang, B. Zhou, S. Lu, W. Geng, H. Tang, Progresses, challenges, and prospects of CRISPR/Cas9 gene-editing in glioma, Studies (2023) 1–15.
[243] M.A. Taylor, B.C. Das, S.K. Ray, Targeting autophagy for combating chemoresistance and radioresistance in glioblastoma, Apoptosis. 23 (2018) 563–575, https://doi.org/10.1007/s10495-018-1480-9.
[244] W. Lin, Y. Sun, X. Qiu, Q. Huang, L. Kong, J.J. Lu, VMP1, a novel prognostic biomarker, contributes to glioma development by regulating autophagy, J. Neuroinflammation 18 (2021) 1–15, https://doi.org/10.1186/s12974-021-02213-z.
[245] J.J. Rodvold, S. Xian, J. Nussbacher, B. Tsui, T. Cameron Waller, S.C. Searles, A. Lew, P. Jiang, I. Babic, N. Nomura, J.H. Lin, S. Kesari, H. Carter, M. Zanetti, IRE1α and IGF signaling predict resistance to an endoplasmic reticulum stress-inducing drug in glioblastoma cells, Sci. Rep. 10 (2020) 1–12, https://doi.org/10.1038/s41598-020-65320-6.
[246] S.J. Szymura, G.M. Bernal, L. Wu, Z. Zhang, C.D. Crawley, D.J. Voce, P. A. Campbell, D.E. Ranoa, R.R. Weichselbaum, B. Yamini, DDX39B interacts with the pattern recognition receptor pathway to inhibit NF-κB and sensitize to alkylating chemotherapy, BMC Biol. 18 (2020) 1–17, https://doi.org/10.1186/s12915-020-0764-z.
[247] F. Zhang, R. Liu, H. Zhang, C. Liu, C. Liu, Y. Lu, Suppressing Dazl modulates tumorigenicity and stemness in human glioblastoma cells, BMC Cancer 20 (2020) 1–13, https://doi.org/10.1186/s12885-020-07155-y.
[248] W. Pu, J. Qiu, Z.D. Nassar, P.N. Shaw, K.A. McMahon, C. Ferguson, R.G. Parton, G.J. Riggins, J.M. Harris, M.O. Parat, A role for caveola-forming proteins caveolin-1 and CAVIN1 in the pro-invasive response of glioblastoma to osmotic and hydrostatic pressure, J. Cell. Mol. Med. 24 (2020) 3724–3738, https://doi.org/10.1111/jcmm.15076.
[249] N. Al-Sammarraie, S.K. Ray, Applications of CRISPR-Cas9 technology to genome editing in glioblastoma multiforme, Cells 10 (2021) 2342, https://doi.org/10.3390/CELLS10092342.
[250] T. Morimoto, T. Nakazawa, R. Matsuda, F. Nishimura, M. Nakamura, S. Yamada, I. Nakagawa, Y.S. Park, T. Tsujimura, H. Nakase, CRISPR-Cas9–mediated TIM3 knockout in human natural killer cells enhances growth inhibitory effects on human glioma cells, Int. J. Mol. Sci. 22 (2021), https://doi.org/10.3390/ijms22073489.
[251] E. Martinez, N. Vazquez, A. Lopez, V. Fanniel, L. Sanchez, R. Marks, L. Hinojosa, V. Cuello, M. Cuevas, A. Rodriguez, C. Tomson, A. Salinas, M. Abad, M. Holguin, N. Garza, A. Arenas, K. Abraham, L. Maldonado, V. Rojas, A. Basdeo, E. Schuenzel, M. Persans, W. Innis-Whitehouse, M. Keniry, The PI3K pathway impacts stem gene expression in a set of glioblastoma cell lines, J. Cancer Res. Clin. Oncol. 146 (2020) 593–604, https://doi.org/10.1007/s00432-020-03133-w.
[252] Y. Liu, Y. Zou, C. Feng, A. Lee, J. Yin, R. Chung, J.B. Park, H. Rizos, W. Tao, M. Zheng, O.C. Farokhzad, B. Shi, Charge conversional biomimetic nanocomplexes as a multifunctional platform for boosting orthotopic glioblastoma RNAi therapy, Nano Lett. 20 (2020) 1637–1646, https://doi.org/10.1021/ACS.NANOLETT.9B04683/SUPPL_FILE/NL9B04683_SI_001.PDF.
[253] Q. Zhang, S. Lin, S. Shi, T. Zhang, Q. Ma, T. Tian, T. Zhou, X. Cai, Y. Lin, Anti-inflammatory and antioxidative effects of tetrahedral DNA nanostructures via the modulation of macrophage responses, ACS Appl. Mater. Interfaces 10 (2018) 3421–3430, https://doi.org/10.1021/ACSAMI.7B17928.
[254] Y. Zhou, Q. Yang, F. Wang, Z. Zhou, J. Xu, S. Cheng, Y. Cheng, Self-assembled DNA nanostructure as a carrier for targeted siRNA delivery in glioma cells, Int. J. Nanomedicine 16 (2021) 1805–1817, https://doi.org/10.2147/IJN.S295598.
[255] X. Tang, Z. Wang, Y. Xie, Y. Liu, K. Yang, T. Li, H. Shen, M. Zhao, J. Jin, H. Xiao, H. Liu, N. Gu, Radiation-triggered selenium-engineered mesoporous silica nanocapsules for RNAi therapy in radiotherapy-resistant glioblastoma, ACS Nano (2023), https://doi.org/10.1021/ACSNANO.3C00269.
[256] Z. Wang, Biomimetic hypoxia-triggered RNAi nanomedicine for synergistically mediating chemo / radiotherapy of glioblastoma (n.d.), 2023, pp. 1–26.
[257] F. Danhier, K. Messaoudi, L. Lemaire, J.P. Benoit, F. Lagarce, Combined anti-Galectin-1 and anti-EGFR siRNA-loaded chitosan-lipid nanocapsules decrease temozolomide resistance in glioblastoma: in vivo evaluation, Int. J. Pharm. 481 (2015) 154–161, https://doi.org/10.1016/J.IJPHARM.2015.01.051.
[258] H.G. Møller, A.P. Rasmussen, H.H. Andersen, K.B. Johnsen, M. Henriksen, M. Duroux, A systematic review of MicroRNA in glioblastoma multiforme: micro-modulators in the mesenchymal mode of migration and invasion, Mol. Neurobiol. 47 (2013) 131, https://doi.org/10.1007/S12035-012-8349-7.
[259] H. Lopez-Bertoni, K.L. Kozielski, Y. Rui, B. Lal, H. Vaughan, D.R. Wilson, N. Mihelson, C.G. Eberhart, J. Laterra, J.J. Green, Bioreducible polymeric nanoparticles containing multiplexed cancer stem cell-regulating miRNAs inhibit glioblastoma growth and prolong survival, Nano Lett. 18 (2018) 4086, https://doi.org/10.1021/ACS.NANOLETT.8B00390.
[260] C. DeOcesano-Pereira, R.A.C. Machado, A.M. Chudzinski-Tavassi, M.C. Sogayar, Emerging roles and potential applications of non-coding RNAs in glioblastoma, Int. J. Mol. Sci. 21 (2020) 2611, https://doi.org/10.3390/IJMS21072611.
[261] P. Singh, A. Singh, S. Shah, J. Vataliya, A. Mittal, D. Chitkara, RNA interference nanotherapeutics for treatment of glioblastoma multiforme, Mol. Pharm. 17 (2020) 4040–4066, https://doi.org/10.1021/acs.molpharmaceut.0c00709.
[262] S. Saeb, J. Van Assche, T. Loustau, O. Rohr, C. Wallet, C. Schwartz, Suicide gene therapy in cancer and HIV-1 infection: an alternative to conventional treatments, Biochem. Pharmacol. 197 (2022), 114893, https://doi.org/10.1016/J.BCP.2021.114893.
[263] A.J. Villatoro, C. Alcoholado, M. del Carmen Martín-Astorga, N. Rubio, J. Blanco, C.P. Garrido, J. Becerra, Suicide gene therapy by canine mesenchymal stem cell transduced with thymidine kinase in a u-87 glioblastoma murine model: secretory profile and antitumor activity, PLoS One 17 (2022) 1–16, https://doi.org/10.1371/journal.pone.0264001.
[264] J.A. Hossain, A. Marchini, B. Fehse, R. Bjerkvig, H. Miletic, Suicide gene therapy for the treatment of high-grade glioma: past lessons, present trends, and future prospects, Neuro-Oncol. Adv. 2 (2020) 1–12, https://doi.org/10.1093/NOAJNL/VDAA013.
[265] R. Tamura, H. Miyoshi, K. Yoshida, H. Okano, M. Toda, Recent progress in the research of suicide gene therapy for malignant glioma, Neurosurg. Rev. 441 (44) (2019) 29–49, https://doi.org/10.1007/S10143-019-01203-3.
[266] S.A. Kaliberov, J.M. Market, G.Y. Gillespie, V. Krendelchtchikova, D. Della Manna, J.C. Sellers, L.N. Kaliberova, M.E. Black, D.J. Buchsbaum, Mutation of *Escherichia coli* cytosine deaminase significantly enhances molecular chemotherapy of human glioma, Gene Ther. 1414 (14) (2007) 1111–1119, https://doi.org/10.1038/sj.gt.3302965.
[267] J.A. Hossain, M.A. Latif, L.A.R. Ystaas, S. Ninzima, K. Riecken, A. Muller, F. Azuaje, J.V. Joseph, K.M. Talasila, J. Ghimire, B. Fehse, R. Bjerkvig, H. Miletic, Long-term treatment with valganciclovir improves lentiviral suicide gene therapy of glioblastoma, Neuro-Oncology 21 (2019) 890–900, https://doi.org/10.1093/NEUONC/NOZ060.
[268] S. Hosseindoost, S.M. Mousavi, A.R. Dehpour, S.A. Javadi, B. Arjmand, A. Fallah, M. Hadjighassem, b 2-Adrenergic receptor agonist enhances the bystander effect of HSV-TK / GCV gene therapy in glioblastoma multiforme via upregulation of connexin 43 expression, Mol. Ther. Oncol. 26 (2022) 76–87, https://doi.org/10.1016/j.omto.2022.05.010.
[269] A. Li, T. Zhang, T. Huang, R. Lin, J. Mu, Y. Su, H. Sun, X. Jiang, Theranostics Iron Oxide Nanoparticles Promote Cx43-Overexpression of Mesenchymal Stem Cells for Efficient Suicide Gene Therapy during Glioma Treatment 11, 2021, https://doi.org/10.7150/thno.60160.
[270] L.A. Mitchell, F. Lopez Espinoza, D. Mendoza, Y. Kato, A. Inagaki, K. Hiraoka, N. Kasahara, H.E. Gruber, D.J. Jolly, J.M. Robbins, Toca 511 gene transfer and treatment with the prodrug, 5-fluorocytosine, promotes durable antitumor immunity in a mouse glioma model, Neuro-Oncology 19 (2017) 930–939, https://doi.org/10.1093/NEUONC/NOX037.
[271] M. Ardini, R. Vago, M.S. Fabbrini, R. Ippoliti, From immunotoxins to suicide toxin delivery approaches: is there a clinical opportunity? Toxins (Basel) 14 (2022) 1–21, https://doi.org/10.3390/toxins14090579.
[272] A. Loskog, Immunostimulatory gene therapy using oncolytic viruses as vehicles, Viruses. 7 (2015) 5780, https://doi.org/10.3390/V7112899.
[273] O. Draghiciu, H.W. Nijman, B.N. Hoogeboom, T. Meijerhof, T. Daemen, Sunitinib depletes myeloid-derived suppressor cells and synergizes with a cancer vaccine to enhance antigen-specific immune responses and tumor eradication, Oncoimmunology. 4 (2015) 1–11, https://doi.org/10.4161/2162402X.2014.989764.
[274] L. van Hooren, A. Vaccaro, M. Ramachandran, K. Vazaios, S. Libard, T. van de Walle, M. Georganaki, H. Huang, I. Pietilä, J. Lau, M.H. Ulvmar, M.C.I. Karlsson, M. Zetterling, S.M. Mangsbo, A.S. Jakola, T. Olsson Bontell, A. Smits, M. Essand, A. Dimberg, Agonistic CD40 therapy induces tertiary lymphoid structures but impairs responses to checkpoint blockade in glioma, Nat. Commun. 12 (2021), https://doi.org/10.1038/s41467-021-24347-7.
[275] S. Sun, W. Gu, H. Wu, Q. Zhao, S. Qian, H. Xiao, K. Yang, J. Liu, Y. Jin, C. Hu, Y. Gao, H. Xu, H. Liu, J. Ji, Y. Chen, Immunostimulant in situ hydrogel improves synergetic radioimmunotherapy of malignant glioblastoma relapse post-resection, Adv. Funct. Mater. 32 (2022), https://doi.org/10.1002/adfm.202205038.
[276] S. Lugani, E.A. Halabi, J. Oh, R.H. Kohler, H.M. Peterson, X.O. Breakefield, E.A. A. Chiocca, M.A. Miller, C.S. Garris, R. Weissleder, Dual Immunostimulatory pathway agonism through a synthetic nanocarrier triggers robust anti-tumor immunity in murine glioblastoma, Adv. Mater. 2208782 (2022), https://doi.org/10.1002/adma.202208782.
[277] K.G. Nguyen, M.R. Vrabel, S.M. Mantooth, J.J. Hopkins, E.S. Wagner, T. A. Gabaldon, D.A. Zaharoff, Localized Interleukin-12 for cancer immunotherapy, Front. Immunol. 11 (2020) 1–36, https://doi.org/10.3389/fimmu.2020.575597.
[278] E.A. Chiocca, A.B. Gelb, C.C. Chen, G. Rao, D.A. Reardon, P.Y. Wen, W.L. Bi, P. Peruzzi, C. Amidei, D. Triggs, L. Seften, G. Park, J. Grant, K. Truman, J.Y. Buck, N. Hadar, N. Demars, J. Miao, T. Estupinan, J. Loewy, K. Chadha, J. Tringali, L. Cooper, R.V. Lukas, Combined immunotherapy with controlled interleukin-12 gene therapy and immune checkpoint blockade in recurrent glioblastoma: an open-label, multi-institutional phase I trial, Neuro-Oncology 24 (2022) 951, https://doi.org/10.1093/NEUONC/NOAB271.
[279] H. Awada, F. Paris, C. Pecqueur, Exploiting radiation immunostimulatory effects to improve glioblastoma outcome, Neuro-Oncology (2022), https://doi.org/10.1093/NEUONC/NOAC239.
[280] Y. Li, Y. Liu, Y.J. Chiang, F. Huang, Y. Li, X. Li, Y. Ning, W. Zhang, H. Deng, Y. G. Chen, DNA damage activates TGF-β signaling via ATM-c-Cbl-mediated stabilization of the type II receptor TβRII, Cell Rep. 28 (2019) 735–745.e4, https://doi.org/10.1016/J.CELREP.2019.06.045.
[281] T. Shi, X. Song, Y. Wang, F. Liu, J. Wei, Combining oncolytic viruses with cancer immunotherapy: establishing a new generation of cancer treatment, Front. Immunol. 11 (2020), https://doi.org/10.3389/FIMMU.2020.00683.
[282] J. Zeng, X. Li, M. Sander, H. Zhang, G. Yan, Y. Lin, Oncolytic viro-immunotherapy: an emerging option in the treatment of gliomas, Front. Immunol. 12 (2021), https://doi.org/10.3389/FIMMU.2021.721830.

[283] H.-M. Nguyen, D. Saha, O. Virotherapy, The current state of oncolytic herpes simplex virus for glioblastoma treatment, Oncol. Virother. 10 (2021) 1–27, https://doi.org/10.2147/OV.S268426.
[284] T. Todo, H. Ito, Y. Ino, H. Ohtsu, Y. Ota, J. Shibahara, M. Tanaka, Intratumoral oncolytic herpes virus G47Δ for residual or recurrent glioblastoma: a phase 2 trial, Nat. Med. 28 (2022) 1630–1639, https://doi.org/10.1038/s41591-022-01897-x.
[285] T. Todo, Y. Ino, H. Ohtsu, J. Shibahara, M. Tanaka, A phase I/II study of triple-mutated oncolytic herpes virus G47Δ in patients with progressive glioblastoma, Nat. Commun. 13 (2022) 1–13, https://doi.org/10.1038/s41467-022-31262-y.
[286] Y. Su, J. Li, W. Ji, G. Wang, L. Fang, Q. Zhang, L. Ang, M. Zhao, Y. Sen, L. Chen, J. Zheng, C. Su, L. Qin, Triple-serotype chimeric oncolytic adenovirus exerts multiple synergistic mechanisms against solid tumors, J. Immunother. Cancer 10 (2022) 1–15, https://doi.org/10.1136/jitc-2022-004691.
[287] J. Choi, R. Medikonda, L. Saleh, T. Kim, A. Pant, S. Srivastava, Y.H. Kim, C. Jackson, L. Tong, D. Routkevitch, C. Jackson, D. Mathios, T. Zhao, H. Cho, H. Brem, M. Lim, Combination checkpoint therapy with anti-PD-1 and anti-BTLA results in a synergistic therapeutic effect against murine glioblastoma, Oncoimmunology. 10 (2021), https://doi.org/10.1080/2162402X.2021.1956142.
[288] A. Moslemizadeh, M.H. Nematollahi, S. Amiresmaili, S. Faramarz, E. Jafari, M. Khaksari, N. Rezaei, H. Bashiri, R. Kheirandish, Combination therapy with interferon-gamma as a potential therapeutic medicine in rat's glioblastoma: a multi-mechanism evaluation, Life Sci. 305 (2022), 120744, https://doi.org/10.1016/J.LFS.2022.120744.
[289] W. Dang, J. Xiao, Q. Ma, J. Miao, M. Cao, L. Chen, Y. Shi, X. Yao, S. Yu, X. Liu, Y. Cui, X. Zhang, X. Bian, Combination of p38 MAPK inhibitor with PD-L1 antibody effectively prolongs survivals of temozolomide-resistant glioma-bearing mice via reduction of infiltrating glioma-associated macrophages and PD-L1 expression on resident glioma-associated microglia, Brain Tumor Pathol. 38 (2021) 189–200, https://doi.org/10.1007/S10014-021-00404-3/FIGURES/5.
[290] R.E. Sanborn, M.J. Pishvaian, M.K. Callahan, A. Weise, B.I. Sikic, O. Rahma, D. C. Cho, N.A. Rizvi, M. Sznol, J. Lutzky, J.E. Bauman, R.L. Bitting, A. Starodub, A. Jimeno, D.A. Reardon, T. Kaley, F. Iwamoto, J.M. Baehring, D. S. Subramaniam, J.B. Aragon-Ching, T.R. Hawthorne, T. Rawls, M. Yellin, T. Keler, Original research: safety, tolerability and efficacy of agonist anti-CD27 antibody (varlilumab) administered in combination with anti-PD-1 (nivolumab) in advanced solid tumors, J. Immunother. Cancer 10 (2022) 5147, https://doi.org/10.1136/JITC-2022-005147.
[291] X.R. Ni, C.C. Guo, Y.J. Yu, Z.H. Yu, H.P. Cai, W.C. Wu, J.X. Ma, F.R. Chen, J. Wang, Z.P. Chen, Combination of levetiracetam and IFN-α increased temozolomide efficacy in MGMT-positive glioma, Cancer Chemother. Pharmacol. 86 (2020) 773–782, https://doi.org/10.1007/S00280-020-04169-Y/FIGURES/5.
[292] P. Liang, G. Wang, X. Liu, Z. Wang, J. Wang, W. Gao, Spatiotemporal combination of thermosensitive polypeptide fused interferon and temozolomide for post-surgical glioblastoma immunochemotherapy, Biomaterials. 264 (2021), 120447, https://doi.org/10.1016/J.BIOMATERIALS.2020.120447.
[293] Y. Hattori, K. Kurozumi, Y. Otani, A. Uneda, N. Tsuboi, K. Makino, S. Hirano, K. Fujii, Y. Tomita, T. Oka, Y. Matsumoto, Y. Shimazu, H. Michiue, H. Kumon, I. Date, Combination of Ad-SGE-REIC and bevacizumab modulates glioma progression by suppressing tumor invasion and angiogenesis, PLoS One 17 (2022), https://doi.org/10.1371/JOURNAL.PONE.0273242.
[294] E. Gjika, S. Pal-Ghosh, M.E. Kirschner, L. Lin, J.H. Sherman, M.A. Stepp, M. Keidar, Combination therapy of cold atmospheric plasma (CAP) with temozolomide in the treatment of U87MG glioblastoma cells, Sci. Rep. 10 (2020) 16495, https://doi.org/10.1038/S41598-020-73457-7.
[295] A. Vargas-Toscano, A.C. Nickel, G. Li, M.A. Kamp, S. Muhammad, G. Leprivier, E. Fritsche, R.A. Barker, M. Sabel, H.J. Steiger, W. Zhang, D. Hänggi, U.D. Kahlert, Rapalink-1 targets glioblastoma stem cells and acts synergistically with tumor treating fields to reduce resistance against temozolomide, Cancers (Basel) 12 (2020) 1–19, https://doi.org/10.3390/CANCERS12123859.
[296] F. Koosha, S. Eynali, N. Eyvazzadeh, M.A. Kamalabadi, The effect of iodine-131 beta-particles in combination with A-966492 and Topotecan on radio-sensitization of glioblastoma: an in-vitro study, Appl. Radiat. Isot. 177 (2021), 109904, https://doi.org/10.1016/J.APRADISO.2021.109904.
[297] Z. Gao, J. Xu, Y. Fan, Z. Zhang, H. Wang, M. Qian, P. Zhang, L. Deng, J. Shen, H. Xue, R. Zhao, T. Zhou, X. Guo, G. Li, ARPC1B promotes mesenchymal phenotype maintenance and radiotherapy resistance by blocking TRIM21-mediated degradation of IFI16 and HuR in glioma stem cells, J. Exp. Clin. Cancer Res. 41 (2022) 323, https://doi.org/10.1186/S13046-022-02526-8.
[298] Y. Otani, H.P. Sur, G. Rachaiah, S. Namagiri, A. Chowdhury, C.T. Lewis, T. Shimizu, A. Gangaplara, X. Wang, A. Vézina, D. Maric, S. Jackson, Y. Yan, Z. Zhengping, A. Ray-Chaudhury, S. Kumar, L.Y. Ballester, P. Chittiboina, J. Y. Yoo, J. Heiss, B. Kaur, Y.K. Banasavadi-Siddegowda, Inhibiting protein phosphatase 2A increases the antitumor effect of protein arginine methyltransferase 5 inhibition in models of glioblastoma, Neuro-Oncology 23 (2021) 1481, https://doi.org/10.1093/NEUONC/NOAB014.
[299] W. Zhu, H. Zhao, F. Xu, B. Huang, X. Dai, J. Sun, A.M.K. Nyalali, K. Zhang, S. Ni, The lipid-lowering drug fenofibrate combined with si-HOTAIR can effectively inhibit the proliferation of gliomas, BMC Cancer 21 (2021), https://doi.org/10.1186/S12885-021-08417-Z.
[300] M. Paul-Samojedny, E. Liduk, M. Kowalczyk, P. Borkowska, A. Zielińska, R. Suchanek-Raif, J. Kowalski, The combination of baicalin with knockdown of miR148a gene suppresses cell viability and proliferation and induces the apoptosis and autophagy of human glioblastoma multiforme T98G and U87MG cells, Curr. Pharm. Biotechnol. 23 (2022), https://doi.org/10.2174/1389201023666220627144100.
[301] M. Zurlo, R. Romagnoli, P. Oliva, J. Gasparello, A. Finotti, R. Gambari, Synergistic effects of a combined treatment of glioblastoma U251 cells with An anti-miR-10b-5p molecule and An AntiCancer agent based on 1-(3′,4′,5′-trimethoxyphenyl)-2-aryl-1H-imidazole scaffold, Int. J. Mol. Sci. 23 (2022), https://doi.org/10.3390/IJMS23115991/S1.
[302] Q. Yang, Y. Zhou, J. Chen, N. Huang, Z. Wang, Y. Cheng, Gene therapy for drug-resistant glioblastoma via lipid-polymer hybrid nanoparticles combined with focused ultrasound, Int. J. Nanomedicine 16 (2021) 185, https://doi.org/10.2147/IJN.S286221.
[303] A. Colapietro, P. Yang, A. Rossetti, A. Mancini, F. Vitale, S. Chakraborty, S. Martelluci, F. Marampon, V. Mattei, G.L. Gravina, R. Iorio, R.A. Newman, C. Festuccia, The botanical drug PBI-05204, a supercritical CO2 extract of Nerium Oleander, is synergistic with radiotherapy in models of human glioblastoma, Front. Pharmacol. 13 (2022) 23, https://doi.org/10.3389/FPHAR.2022.852941/FULL.
[304] I. Tutak, B. Ozdil, A. Uysal, Voxtalisib and low intensity pulsed ultrasound combinatorial effect on glioblastoma multiforme cancer stem cells via PI3K/AKT/mTOR, Pathol. Res. Pract. 239 (2022), 154145, https://doi.org/10.1016/J.PRP.2022.154145.
[305] J.Y. Wu, Y.J. Li, J. Wang, X. Bin Hu, S. Huang, S. Luo, D.X. Xiang, Multifunctional exosome-mimetics for targeted anti-glioblastoma therapy by manipulating protein corona, J. Nanobiotechnol. 19 (2021) 1–15, https://doi.org/10.1186/S12951-021-01153-3/FIGURES/6.
[306] S.F. Liang, F.F. Zuo, B.C. Yin, B.C. Ye, Delivery of siRNA based on engineered exosomes for glioblastoma therapy by targeting STAT3, Biomater. Sci. 10 (2022) 1582–1590, https://doi.org/10.1039/D1BM01723C.
[307] E. Valipour, F.E. Ranjbar, M. Mousavi, J. Ai, Z.V. Malekshahi, N. Mokhberian, Z. Taghdiri-Nooshabadi, M. Khanmohammadi, V.T. Nooshabadi, The anti-angiogenic effect of atorvastatin loaded exosomes on glioblastoma tumor cells: an in vitro 3D culture model, Microvasc. Res. 143 (2022), 104385, https://doi.org/10.1016/J.MVR.2022.104385.
[308] Y. Chen, Y. Jin, N. Wu, Role of tumor-derived extracellular vesicles in glioblastoma, Cells. 10 (2021) 1–14, https://doi.org/10.3390/CELLS10030512.
[309] L. Manterola, E. Guruceaga, J.G. Pérez-Larraya, M. González-Huarriz, P. Jauregui, S. Tejada, R. Diez-Valle, V. Segura, N. Samprón, C. Barrena, I. Ruiz, A. Agirre, Á. Ayuso, J. Rodríguez, Á. González, E. Xipell, A. Matheu, A. López De Munain, T. Tuñón, I. Zazpe, J. García-Foncillas, S. Paris, J.Y. Delattre, M.M. Alonso, A small noncoding RNA signature found in exosomes of GBM patient serum as a diagnostic tool, Neuro-Oncology 16 (2014) 520–527, https://doi.org/10.1093/NEUONC/NOT218.
[310] A. Yekula, A. Yekula, K. Muralidharan, K. Kang, B.S. Carter, L. Balaj, Extracellular vesicles in glioblastoma tumor microenvironment, Front. Immunol. 10 (2020) 3137, https://doi.org/10.3389/FIMMU.2019.03137/BIBTEX.
[311] B. Basu, M.K. Ghosh, Extracellular vesicles in glioma: from diagnosis to therapy, BioEssays. 41 (2019) 1800245, https://doi.org/10.1002/BIES.201800245.
[312] R. Kalkan, Glioblastoma stem cells as a new therapeutic target for glioblastoma, Clin. Med. Insights. Oncol. 9 (2015) 95, https://doi.org/10.4137/CMO.S30271.
[313] Y. Chen, L. Liu, Modern methods for delivery of drugs across the blood–brain barrier, Adv. Drug Deliv. Rev. 64 (2012) 640–665, https://doi.org/10.1016/J.ADDR.2011.11.010.
[314] M. Pizzocri, F. Re, E. Stanzani, B. Formicola, M. Tamborini, E. Lauranzano, F. Ungaro, S. Rodighiero, M. Francolini, M. Gregori, A. Perin, F. Dimeco, M. Masserini, M. Matteoli, L. Passoni, Radiation and adjuvant drug-loaded liposomes target glioblastoma stem cells and trigger in-situ immune response, Neuro-Oncol. Adv. 3 (2021) 1–13, https://doi.org/10.1093/NOAJNL/VDAB076.
[315] E.A. Charkhat Gorgich, H. Kasbiyan, R. Shabani, M. Mehdizadeh, F. Hajiahmadi, M. Ajdary, M. Barati, F. Moradi, D. Ahmadvand, Smart chlorotoxin-functionalized liposomes for sunitinib targeted delivery into glioblastoma cells, J. Drug Deliv. Sci. Technol. 77 (2022), 103908, https://doi.org/10.1016/J.JDDST.2022.103908.
[316] L. Taiarol, C. Bigogno, S. Sesana, M. Kravicz, F. Viale, E. Pozzi, L. Monza, V. A. Carozzi, C. Meregalli, S. Valtorta, R.M. Moresco, M. Koch, F. Barbugian, L. Russo, G. Dondio, C. Steinkühler, F. Re, Givinostat-liposomes: anti-tumor effect on 2D and 3D glioblastoma models and pharmacokinetics, Cancers (Basel) 14 (2022) 2978, https://doi.org/10.3390/CANCERS14122978/S1.
[317] S.L. Hayward, D.M. Francis, M.J. Sis, S. Kidambi, Ionic driven embedment of hyaluronic acid coated liposomes in polyelectrolyte multilayer films for local therapeutic delivery, Sci. Report. 51 (5) (2015) 1–13, https://doi.org/10.1038/srep14683.
[318] L. Zhang, Z. Zhang, R.P. Mason, J.N. Sarkaria, D. Zhao, Convertible MRI contrast: Sensing the delivery and release of anti-glioma nano-drugs OPEN, 2015, https://doi.org/10.1038/srep09874.
[319] F.Y. Hsieh, A.V. Zhilenkov, I.I. Voronov, E.A. Khakina, D.V. Mischenko, P. A. Troshin, S.H. Hsu, Water-soluble fullerene derivatives as brain medicine: surface chemistry determines if they are neuroprotective and antitumor, ACS Appl. Mater. Interfaces 9 (2017) 11482–11492, https://doi.org/10.1021/ACSAMI.7B01077/ASSET/IMAGES/LARGE/AM-2017-01077F_0006.JPEG.
[320] Y. Peng, D. Yang, W. Lu, X. Hu, H. Hong, T. Cai, Positron emission tomography (PET) guided glioblastoma targeting by a fullerene-based nanoplatform with fast renal clearance, Acta Biomater. 61 (2017) 193–203, https://doi.org/10.1016/J.ACTBIO.2017.08.011.
[321] M.D. Shultz, J.C. Duchamp, J.D. Wilson, C.Y. Shu, J. Ge, J. Zhang, H.W. Gibson, H.L. Fillmore, J.I. Hirsch, H.C. Dorn, P.P. Fatouros, Encapsulation of a radiolabeled cluster inside a fullerene cage, 177LuxLu(3- x)N@C80: an

interleukin-13-conjugated radiolabeled metallofullerene platform, J. Am. Chem. Soc. 132 (2010) 4980–4981, https://doi.org/10.1021/JA9093617/SUPPL_FILE/JA9093617_SI_001.PDF.
[322] H.L. Fillmore, M.D. Shultz, S.C. Henderson, P. Cooper, W.C. Broaddus, Z.J. Chen, C.Y. Shu, J. Zhang, J. Ge, H.C. Dorn, F. Corwin, J.I. Hirsch, J. Wilson, P. P. Fatouros, Conjugation of functionalized gadolinium metallofullerenes with IL-13 peptides for targeting and imaging glial tumors 6, 2011, pp. 449–458, https://doi.org/10.2217/NNM.10.134.
[323] Q. Liu, X. Zhang, X. Zhang, G. Zhang, J. Zheng, M. Guan, X. Fang, C. Wang, C. Shu, C70-carboxyfullerenes as efficient antioxidants to protect cells against oxidative-induced stress, ACS Appl. Mater. Interfaces 5 (2013) 11101–11107, https://doi.org/10.1021/AM4033372/SUPPL_FILE/AM4033372_SI_001.PDF.
[324] G. Perini, V. Palmieri, G. Ciasca, M. D'ascenzo, J. Gervasoni, A. Primiano, M. Rinaldi, D. Fioretti, C. Prampolini, F. Tiberio, W. Lattanzi, O. Parolini, M. De Spirito, M. Papi, Graphene quantum dots' surface chemistry modulates the sensitivity of glioblastoma cells to chemotherapeutics, Int. J. Mol. Sci. 21 (2020) 6301, https://doi.org/10.3390/IJMS21176301.
[325] P.E. Cabral Filho, A.L.C. Cardoso, M.I.A. Pereira, A.P.M. Ramos, F. Hallwas, M.M. C.A. Castro, C.F.G.C. Geraldes, B.S. Santos, M.C. Pedroso De Lima, G.A.L. Pereira, A. Fontes, CdTe quantum dots as fluorescent probes to study transferrin receptors in glioblastoma cells, Biochim. Biophys. Acta, Gen. Subj. 1860 (2016) 28–35, https://doi.org/10.1016/J.BBAGEN.2015.09.021.
[326] G. Perini, V. Palmieri, G. Ciasca, M. D'Ascenzo, A. Primiano, J. Gervasoni, F. De Maio, M. De Spirito, M. Papi, Enhanced chemotherapy for glioblastoma multiforme mediated by functionalized graphene quantum dots, Mater 13 (2020) 4139, https://doi.org/10.3390/MA13184139.
[327] D. Zhao, D. Alizadeh, L. Zhang, W. Liu, O. Farrukh, E. Manuel, D.J. Diamond, B. Badie, Carbon nanotubes enhance CpG uptake and potentiate anti-glioma immunity, Clin. Cancer Res. 17 (2011) 771, https://doi.org/10.1158/1078-0432.CCR-10-2444.
[328] J. Winsett, A. Moilanen, K. Paudel, S. Kamali, K. Ding, W. Cribb, D. Seifu, S. Neupane, Quantitative determination of magnetite and maghemite in iron oxide nanoparticles using Mössbauer spectroscopy, SN Appl. Sci. 1 (2019) 1–8, https://doi.org/10.1007/S42452-019-1699-2/TABLES/1.
[329] L. Pulvirenti, F. Monforte, F. Lo Presti, G. Li Volti, G. Carota, F. Sinatra, C. Bongiorno, G. Mannino, M.T. Cambria, G.G. Condorelli, Synthesis of MIL-modified Fe3O4 magnetic nanoparticles for enhancing uptake and efficiency of temozolomide in glioblastoma treatment, Int. J. Mol. Sci. 23 (2022) 2874, https://doi.org/10.3390/IJMS23052874.
[330] M. Świętek, Y.H. Ma, N.P. Wu, A. Paruzel, W. Tokarz, D. Horák, Tannic acid coating augments glioblastoma cellular uptake of magnetic nanoparticles with antioxidant effects, Nanomater 12 (2022) 1310, https://doi.org/10.3390/NANO12081310.
[331] C. Du, X. Liu, H. Hu, H. Li, L. Yu, D. Geng, Y. Chen, J. Zhang, Dual-targeting and excretable ultrasmall SPIONs for T1-weighted positive MR imaging of intracranial glioblastoma cells by targeting the lipoprotein receptor-related protein, J. Mater. Chem. B 8 (2020) 2296–2306, https://doi.org/10.1039/C9TB02391G.
[332] C. Tapeinos, A. Marino, M. Battaglini, S. Migliorin, R. Brescia, A. Scarpellini, C. De Julián Fernández, M. Prato, F. Drago, G. Ciofani, Stimuli-responsive lipid-based magnetic nanovectors increase apoptosis in glioblastoma cells through synergic intracellular hyperthermia and chemotherapy, Nanoscale. 11 (2018) 72–88, https://doi.org/10.1039/C8NR05520C.
[333] E.C. Leuthardt, C. Duan, M.J. Kim, J.L. Campian, A.H. Kim, M.M. Miller-Thomas, J.S. Shimony, D.D. Tran, Hyperthermic laser ablation of recurrent glioblastoma leads to temporary disruption of the peritumoral blood brain barrier, PLoS One 11 (2016), e0148613, https://doi.org/10.1371/JOURNAL.PONE.0148613.
[334] D. Coluccia, C.A. Figueiredo, M.Y.J. Wu, A.N. Riemenschneider, R. Diaz, A. Luck, C. Smith, S. Das, C. Ackerley, M. O'Reilly, K. Hynynen, J.T. Rutka, Enhancing glioblastoma treatment using cisplatin-gold-nanoparticle conjugates and targeted delivery with magnetic resonance-guided focused ultrasound, Nanomedicine 14 (2018) 1137–1148, https://doi.org/10.1016/J.NANO.2018.01.021.
[335] Y. Yu, A. Wang, S. Wang, Y. Sun, L. Chu, L. Zhou, X. Yang, X. Liu, C. Sha, K. Sun, L. Xu, Efficacy of temozolomide-conjugated gold nanoparticle photothermal therapy of drug-resistant glioblastoma and its mechanism study, Mol. Pharm. 19 (2022) 1219–1229, https://doi.org/10.1021/ACS.MOLPHARMACEUT.2C00083/SUPPL_FILE/MP2C00083_SI_001.PDF.
[336] D.P.N. Gonçalves, D.M. Park, T.L. Schmidt, C. Werner, Modular peptide-functionalized gold nanorods for effective glioblastoma multicellular tumor spheroid targeting, Biomater. Sci. 6 (2018) 1140–1146, https://doi.org/10.1039/C7BM01107E.
[337] K. Zhi, B. Raji, A.R. Nookala, M.M. Khan, X.H. Nguyen, S. Sakshi, T. Pourmotabbed, M.M. Yallapu, H. Kochat, E. Tadrous, S. Pernell, S. Kumar, PLGA nanoparticle-based formulations to cross the blood–brain barrier for drug delivery: from R&D to cGMP, Pharm 13 (2021) 500, https://doi.org/10.3390/PHARMACEUTICS13040500.
[338] R. Alswailem, F.Y. Alqahtani, F.S. Aleanizy, B.M. Alrfaei, M. Badran, Q. H. Alqahtani, H.G. Abdelhady, I. Alsarra, MicroRNA-219 loaded chitosan nanoparticles for treatment of glioblastoma, Artif. Cells Nanomed. Biotechnol. 50 (2022) 198–207, https://doi.org/10.1080/21691401.2022.2092123.
[339] M.T. Hsing, H.T. Hsu, C.H. Chang, K.B. Chang, C.Y. Cheng, J.H. Lee, C.L. Huang, M.Y. Yang, Y.C. Yang, S.Y. Liu, C.M. Yen, S.F. Yang, H.S. Hung, Improved delivery performance of n-butylidenephthalide-polyethylene glycol-gold nanoparticles efficient for enhanced anti-cancer activity in brain tumor, Cells. 11 (2022) 2172, https://doi.org/10.3390/CELLS11142172/S1.
[340] G. Ren, D. Duan, G. Wang, R. Wang, Y. Li, H. Zuo, Q. Zhang, G. Zhang, Y. Zhao, R. Wang, S. Zhang, Construction of reduction-sensitive heterodimer prodrugs of doxorubicin and dihydroartemisinin self-assembled nanoparticles with antitumor activity, Colloids Surf. B: Biointerfaces 217 (2022), 112614, https://doi.org/10.1016/J.COLSURFB.2022.112614.
[341] S. An, X. Jiang, J. Shi, X. He, J. Li, Y. Guo, Y. Zhang, H. Ma, Y. Lu, C. Jiang, Single-component self-assembled RNAi nanoparticles functionalized with tumor-targeting iNGR delivering abundant siRNA for efficient glioma therapy, Biomaterials. 53 (2015) 330–340, https://doi.org/10.1016/J.BIOMATERIALS.2015.02.084.
[342] B.S. Mahmoud, A.H. Alamri, C. McConville, Polymeric nanoparticles for the treatment of malignant gliomas, Cancers (Basel) 12 (2020), https://doi.org/10.3390/CANCERS12010175.
[343] L.E. Ibarra, L. Beaugé, N. Arias-Ramos, V.A. Rivarola, C.A. Chesta, P. López-Larrubia, R.E. Palacios, Trojan horse monocyte-mediated delivery of conjugated polymer nanoparticles for improved photodynamic therapy of glioblastoma 15, 2020, pp. 1687–1707, https://doi.org/10.2217/NNM-2020-0106.
[344] B.T. Luk, L. Zhang, Current advances in polymer-based nanotheranostics for cancer treatment and diagnosis, ACS Appl. Mater. Interfaces 6 (2014) 21859–21873, https://doi.org/10.1021/AM5036225/ASSET/IMAGES/LARGE/AM-2014-036225_0010.JPEG.
[345] L.P. Ganipineni, B. Ucakar, N. Joudiou, J. Bianco, P. Danhier, M. Zhao, C. Bastiancich, B. Gallez, F. Danhier, V. Préat, Magnetic targeting of paclitaxel-loaded poly(lactic- co-glycolic acid)-based nanoparticles for the treatment of glioblastoma, Int. J. Nanomedicine 13 (2018) 4509–4521, https://doi.org/10.2147/IJN.S165184.
[346] X. Wang, L. Yang, H. Zhang, B. Tian, R. Li, X. Hou, F. Wei, Fluorescent magnetic PEI-PLGA nanoparticles loaded with paclitaxel for concurrent cell imaging, enhanced apoptosis and autophagy in human brain cancer, Colloids Surf. B: Biointerfaces 172 (2018) 708–717, https://doi.org/10.1016/J.COLSURFB.2018.09.033.
[347] K.S. Vaidya, M.J. Mitten, A.L. Zelaya-Lazo, A. Oleksijew, C. Alvey, H.D. Falls, S. Mishra, J. Palma, P. Ansell, A.C. Phillips, E.B. Reilly, M. Anderson, E. R. Boghaert, Synergistic therapeutic benefit by combining the antibody drug conjugate, depatux-m with temozolomide in pre-clinical models of glioblastoma with overexpression of EGFR, J. Neuro-Oncol. 152 (2021) 233–243, https://doi.org/10.1007/S11060-021-03703-Z/METRICS.
[348] Y. Akyuva, M. Nazıroğlu, Silver nanoparticles potentiate antitumor and oxidant actions of cisplatin via the stimulation of TRPM2 channel in glioblastoma tumor cells, Chem. Biol. Interact. 369 (2023), 110261, https://doi.org/10.1016/J.CBI.2022.110261.
[349] C. He, Z. Zhang, Y. Ding, K. Xue, X. Wang, R. Yang, Y. An, D. Liu, C. Hu, Q. Tang, LRP1-mediated pH-sensitive polymersomes facilitate combination therapy of glioblastoma in vitro and in vivo, J. Nanobiotechnol. 19 (2021) 29, https://doi.org/10.1186/S12951-020-00751-X.
[350] A. Bagherian, B. Roudi, N. Masoudian, H. Mirzaei, Anti-glioblastoma effects of nanomicelle-curcumin plus erlotinib, Food Funct. 12 (2021) 10926–10937, https://doi.org/10.1039/D1FO01611C.
[351] L. Wang, X. Wang, L. Shen, M. Alrobaian, S.K. Panda, H.A. Almasmoum, M. M. Ghaith, R.A. Almaimani, I.A.A. Ibrahim, T. Singh, A.A. Baothman, H. Choudhry, S. Beg, Paclitaxel and naringenin-loaded solid lipid nanoparticles surface modified with cyclic peptides with improved tumor targeting ability in glioblastoma multiforme, Biomed. Pharmacother. 138 (2021), https://doi.org/10.1016/J.BIOPHA.2021.111461.
[352] M. Wang, A. Malfanti, C. Bastiancich, V. Préat, Synergistic effect of doxorubicin lauroyl hydrazone derivative delivered by α-tocopherol succinate micelles for the treatment of glioblastoma, Int. J. Pharm. X 5 (2023), 100147, https://doi.org/10.1016/J.IJPX.2022.100147.
[353] M. Ghaferi, A. Raza, M. Koohi, W. Zahra, A. Akbarzadeh, H. Ebrahimi Shahmabadi, S.E. Alavi, Impact of PEGylated liposomal doxorubicin and carboplatin combination on glioblastoma, Pharmaceutics. 14 (2022), https://doi.org/10.3390/PHARMACEUTICS14102183/S1.
[354] M. Ismail, W. Yang, Y. Li, T. Chai, D. Zhang, Q. Du, P. Muhammad, S. Hanif, M. Zheng, B. Shi, Targeted liposomes for combined delivery of artesunate and temozolomide to resistant glioblastoma, Biomaterials. 287 (2022), 121608, https://doi.org/10.1016/J.BIOMATERIALS.2022.121608.
[355] V.S. Mishra, S. Patil, P.C. Reddy, B. Lochab, Combinatorial delivery of CPI444 and vatalanib loaded on PEGylated graphene oxide as an effective nanoformulation to target glioblastoma multiforme: in vitro evaluation, Front. Oncol. 12 (2022), https://doi.org/10.3389/FONC.2022.953098/FULL.
[356] Z.A. Kadhim, G.M. Sulaiman, A.M. Al-Shammari, R.A. Khan, O. Al Rugaie, H. A. Mohammed, Oncolytic Newcastle disease virus co-delivered with modified PLGA nanoparticles encapsulating temozolomide against glioblastoma cells: developing an effective treatment strategy, Molecules. 27 (2022) 5757, https://doi.org/10.3390/MOLECULES27185757.
[357] Y. Zou, Y. Wang, S. Xu, Y. Liu, J. Yin, D.B. Lovejoy, M. Zheng, X.J. Liang, J. B. Park, Y.M. Efremov, I. Ulasov, B. Shi, Brain co-delivery of temozolomide and cisplatin for combinatorial glioblastoma chemotherapy, Adv. Mater. 34 (2022) 2203958, https://doi.org/10.1002/ADMA.202203958.
[358] H. Sotoudeh, O. Shafaat, J.D. Bernstock, M.D. Brooks, G.A. Elsayed, J.A. Chen, P. Szerip, G. Chagoya, F. Gessler, E. Sotoudeh, A. Shafaat, G.K. Friedman, Artificial intelligence in the management of glioma: era of personalized medicine, Front. Oncol. 9 (2019) 768, https://doi.org/10.3389/FONC.2019.00768/BIBTEX.
[359] K. Li-Chun Hsieh, C.Y. Chen, C.M. Lo, Quantitative glioma grading using transformed gray-scale invariant textures of MRI, Comput. Biol. Med. 83 (2017) 102–108, https://doi.org/10.1016/J.COMPBIOMED.2017.02.012.
[360] D.N. Louis, A. Perry, P. Wesseling, D.J. Brat, I.A. Cree, D. Figarella-Branger, C. Hawkins, H.K. Ng, S.M. Pfister, G. Reifenberger, R. Soffietti, A. Von Deimling,

D.W. Ellison, The 2021 WHO classification of tumors of the central nervous system: a summary, Neuro-Oncology 23 (2021) 1231, https://doi.org/10.1093/NEUONC/NOAB106.
[361] J. Wu, Z. Qian, L. Tao, J. Yin, S. Ding, Y. Zhang, Z. Yu, Resting state fMRI feature-based cerebral glioma grading by support vector machine, Int. J. Comput. Assist. Radiol. Surg. 10 (2015) 1167–1174, https://doi.org/10.1007/S11548-014-1111-Z/FIGURES/4.
[362] Q. Tian, L.F. Yan, X. Zhang, X. Zhang, Y.C. Hu, Y. Han, Z.C. Liu, H.Y. Nan, Q. Sun, Y.Z. Sun, Y. Yang, Y. Yu, J. Zhang, B. Hu, G. Xiao, P. Chen, S. Tian, J. Xu, W. Wang, G. Bin Cui, Radiomics strategy for glioma grading using texture features from multiparametric MRI, J. Magn. Reson. Imaging 48 (2018) 1518–1528, https://doi.org/10.1002/JMRI.26010.
[363] G. Ranjith, R. Parvathy, V. Vikas, K. Chandrasekharan, S. Nair, Machine learning methods for the classification of gliomas: initial results using features extracted from MR spectroscopy, Neuroradiol. J. 28 (2015) 106, https://doi.org/10.1177/1971400915576637.
[364] Y. Mao, W. Liao, D. Cao, L. Zhao, X. Wu, L. Kong, G. Zhou, Y. Zhao, D. Wang, An artificial neural network model for glioma grading using image information, Zhong Nan Da Xue Xue Bao Yi Xue Ban 43 (2018) 1315–1322, https://doi.org/10.11817/J.ISSN.1672-7347.2018.12.006.
[365] Y. Yang, L.F. Yan, X. Zhang, Y. Han, H.Y. Nan, Y.C. Hu, B. Hu, S.L. Yan, J. Zhang, D.L. Cheng, X.W. Ge, G. Bin Cui, D. Zhao, W. Wang, Glioma grading on conventional MR images: a deep learning study with transfer learning, Front. Neurosci. 12 (2018) 804, https://doi.org/10.3389/FNINS.2018.00804.
[366] X. Zhang, L.F. Yan, Y.C. Hu, G. Li, Y. Yang, Y. Han, Y.Z. Sun, Z.C. Liu, Q. Tian, Z. Y. Han, L. De Liu, B.Q. Hu, Z.Y. Qiu, W. Wang, G. Bin Cui, Optimizing a machine learning based glioma grading system using multi-parametric MRI histogram and texture features, Oncotarget. 8 (2017) 47816, https://doi.org/10.18632/ONCOTARGET.18001.
[367] Y. Sonoda, I. Shibahara, T. Kawaguchi, R. Saito, M. Kanamori, M. Watanabe, H. Suzuki, T. Kumabe, T. Tominaga, Association between molecular alterations and tumor location and MRI characteristics in anaplastic gliomas, Brain Tumor Pathol. 32 (2015) 99–104, https://doi.org/10.1007/S10014-014-0211-3/FIGURES/3.
[368] E. Lotan, R. Jain, N. Razavian, G.M. Fatterpekar, Y.W. Lui, State of the Art: Machine Learning Applications in Glioma Imaging 212, 2018, pp. 26–37, https://doi.org/10.2214/AJR.18.20218.
[369] C. Houillier, X. Wang, G. Kaloshi, K. Mokhtari, R. Guillevin, J. Laffaire, S. Paris, B. Boisselier, A. Idbaih, F. Laigle-Donadey, K. Hoang-Xuan, M. Sanson, J. Y. Delattre, IDH1 or IDH2 mutations predict longer survival and response to temozolomide in low-grade gliomas, Neurology. 75 (2010) 1560–1566, https://doi.org/10.1212/WNL.0B013E3181F96282.
[370] N.L. Jansen, C. Schwartz, V. Graute, S. Eigenbrod, J. Lutz, R. Egensperger, G. Pöpperl, H.A. Kretzschmar, P. Cumming, P. Bartenstein, J.C. Tonn, F.W. Kreth, C. La Fougère, N. Thon, Prediction of oligodendroglial histology and LOH 1p/19q using dynamic [18F]FET-PET imaging in intracranial WHO grade II and III gliomas, Neuro-Oncology 14 (2012) 1473, https://doi.org/10.1093/NEUONC/NOS259.
[371] P. Bourdillon, C. Hlaihel, J. Guyotat, L. Guillotton, J. Honnorat, F. Ducray, F. Cotton, Prediction of anaplastic transformation in low-grade oligodendrogliomas based on magnetic resonance spectroscopy and 1p/19q codeletion status, J. Neuro-Oncol. 122 (2015) 529–537, https://doi.org/10.1007/S11060-015-1737-X/FIGURES/3.
[372] Y. Iwadate, N. Shinozaki, T. Matsutani, Y. Uchino, N. Saeki, Research paper: molecular imaging of 1p/19q deletion in oligodendroglial tumours with 11C-methionine positron emission tomography, J. Neurol. Neurosurg. Psychiatry 87 (2016) 1016, https://doi.org/10.1136/JNNP-2015-311516.
[373] Z. Akkus, I. Ali, J. Sedlář, J.P. Agrawal, I.F. Parney, C. Giannini, B.J. Erickson, Predicting deletion of chromosomal arms 1p/19q in low-grade gliomas from MR images using machine intelligence, J. Digit. Imaging 30 (2017) 469–476, https://doi.org/10.1007/S10278-017-9984-3.
[374] K. Chang, H.X. Bai, H. Zhou, C. Su, W.L. Bi, E. Agbodza, V.K. Kavouridis, J. T. Senders, A. Boaro, A. Beers, B. Zhang, A. Capellini, W. Liao, Q. Shen, X. Li, B. Xiao, J. Cryan, S. Ramkissoon, L. Ramkissoon, K. Ligon, P.Y. Wen, R.S. Bindra, J. Woo, O. Arnaout, E.R. Gerstner, P.J. Zhang, B.R. Rosen, L. Yang, R.Y. Huang, J. Kalpathy-Cramer, Residual convolutional neural network for determination of IDH status in low- and high-grade gliomas from MR imaging, Clin. Cancer Res. 24 (2018) 1073, https://doi.org/10.1158/1078-0432.CCR-17-2236.
[375] B. Zhang, K. Chang, S. Ramkissoon, S. Tanguturi, W.L. Bi, D.A. Reardon, K. L. Ligon, B.M. Alexander, P.Y. Wen, R.Y. Huang, Multimodal MRI features predict isocitrate dehydrogenase genotype in high-grade gliomas, Neuro-Oncology 19 (2017) 109, https://doi.org/10.1093/NEUONC/NOW121.
[376] Z. Li, Y. Wang, J. Yu, Y. Guo, W. Cao, Deep learning based radiomics (DLR) and its usage in noninvasive IDH1 prediction for low grade glioma, Sci. Rep. 7 (2017), https://doi.org/10.1038/S41598-017-05848-2.
[377] J.D. Young, C. Cai, X. Lu, Unsupervised deep learning reveals prognostically relevant subtypes of glioblastoma, BMC Bioinforma. 18 (2017), https://doi.org/10.1186/S12859-017-1798-2.
[378] S. Pereira, A. Pinto, V. Alves, C.A. Silva, Brain tumor segmentation using convolutional neural networks in MRI images, IEEE Trans. Med. Imaging 35 (2016) 1240–1251, https://doi.org/10.1109/TMI.2016.2538465.
[379] K. Kamnitsas, C. Ledig, V.F.J. Newcombe, J.P. Simpson, A.D. Kane, D.K. Menon, D. Rueckert, B. Glocker, Efficient multi-scale 3D CNN with fully connected CRF for accurate brain lesion segmentation, Med. Image Anal. 36 (2017) 61–78, https://doi.org/10.1016/J.MEDIA.2016.10.004.
[380] Z. Li, Y. Wang, J. Yu, Z. Shi, Y. Guo, L. Chen, Y. Mao, Low-grade glioma segmentation based on CNN with fully connected CRF, J. Healthc. Eng. 2017 (2017), https://doi.org/10.1155/2017/9283480.
[381] H. Fabelo, M. Halicek, S. Ortega, M. Shahedi, A. Szolna, J.F. Piñeiro, C. Sosa, A. J. O'Shanahan, S. Bisshopp, C. Espino, M. Márquez, M. Hernández, D. Carrera, J. Morera, G.M. Callico, R. Sarmiento, B. Fei, Deep learning-based framework for in vivo identification of glioblastoma tumor using hyperspectral images of human brain, Sensors 19 (2019) 920, https://doi.org/10.3390/S19040920.
[382] F.S. Abas, H.N. Gokozan, B. Goksel, J.J. Otero, M.N. Gurcan, Intraoperative neuropathology of glioma recurrence: cell detection and classification 9791, 2016, pp. 59–68, https://doi.org/10.1117/12.2216448.
[383] K. Fukuma, V.B.S. Prasath, H. Kawanaka, B.J. Aronow, H. Takase, A study on nuclei segmentation, feature extraction and disease stage classification for human brain histopathological images, Procedia Comput. Sci. 96 (2016) 1202–1210, https://doi.org/10.1016/J.PROCS.2016.08.164.
[384] A. Yonekura, H. Kawanaka, V.B.S. Prasath, B.J. Aronow, H. Takase, Automatic disease stage classification of glioblastoma multiforme histopathological images using deep convolutional neural network, Biomed. Eng. Lett. 8 (2018) 321–327, https://doi.org/10.1007/S13534-018-0077-0.
[385] X. Wang, D. Wang, Z. Yao, B. Xin, B. Wang, C. Lan, Y. Qin, S. Xu, D. He, Y. Liu, Machine learning models for multiparametric glioma grading with quantitative result interpretations, Front. Neurosci. 13 (2019) 1046, https://doi.org/10.3389/FNINS.2018.01046/BIBTEX.
[386] X. Hu, K.K. Wong, G.S. Young, L. Guo, S.T. Wong, Support vector machine (SVM) multi-parametric MRI identification of pseudoprogression from tumor recurrence in patients with resected glioblastoma, J. Magn. Reson. Imaging 33 (2011) 296, https://doi.org/10.1002/JMRI.22432.
[387] B.S. Jang, S.H. Jeon, I.H. Kim, I.A. Kim, Prediction of pseudoprogression versus progression using machine learning algorithm in glioblastoma, Sci. Report. 81 (8) (2018) 1–9, https://doi.org/10.1038/s41598-018-31007-2.
[388] C. Luchini, A. Pea, A. Scarpa, Artificial intelligence in oncology: current applications and future perspectives, Br. J. Cancer 1261 (126) (2021) 4–9, https://doi.org/10.1038/s41416-021-01633-1.
[389] S. Alomari, B. Tyler, I. Zhang, A. Hernandez, C.Y. Kraft, D. Raj, J. Kedda, Drug repurposing for glioblastoma and current advances in drug delivery—a comprehensive review of the literature, Biomolecules. 11 (2021) 1870, https://doi.org/10.3390/BIOM11121870.
[390] S.C. Higgins, G.J. Pilkington, The in vitro effects of tricyclic drugs and dexamethasone on cellular respiration of malignant glioma, Anticancer Res. 30 (2010).
[391] Y. Levkovitz, I. Gil-Ad, E. Zeldich, M. Dayag, A. Weizman, Differential induction of apoptosis by antidepressants in glioma and neuroblastoma cell lines: evidence for p-c-Jun, cytochrome c, and caspase-3 involvement, J. Mol. Neurosci. 27 (2005) 029–042, https://doi.org/10.1385/JMN:27:1:029.
[392] L. Patel, C. Lindley, Aprepitant–a novel NK1-receptor antagonist, Expert. Opin. Pharmacother. 4 (2003) 2279–2296, https://doi.org/10.1517/14656566.4.12.2279.
[393] M. Muñoz, R. Coveñas, The Neurokinin-1 receptor antagonist aprepitant: an intelligent bullet against cancer? Cancers (Basel) 12 (2020) 1–22, https://doi.org/10.3390/CANCERS12092682.
[394] D. Chen, Q.C. Cui, H. Yang, Q.P. Dou, Disulfiram, a clinically used anti-alcoholism drug and copper-binding agent, induces apoptotic cell death in breast cancer cultures and xenografts via inhibition of the proteasome activity, Cancer Res. 66 (2006) 10425–10433, https://doi.org/10.1158/0008-5472.CAN-06-2126.
[395] Q. Tan, X. Yan, L. Song, H. Yi, P. Li, G. Sun, D. Yu, L. Li, Z. Zeng, Z. Guo, Induction of mitochondrial dysfunction and oxidative damage by antibiotic drug doxycycline enhances the responsiveness of glioblastoma to chemotherapy, Med. Sci. Monit. 23 (2017) 4117–4125, https://doi.org/10.12659/MSM.903245.
[396] R. Lamb, B. Ozsvari, C.L. Lisanti, H.B. Tanowitz, A. Howell, U.E. Martinez-Outschoorn, F. Sotgia, M.P. Lisanti, Antibiotics that target mitochondria effectively eradicate cancer stem cells, across multiple tumor types: treating cancer like an infectious disease, Oncotarget. 6 (2015) 4569–4584, https://doi.org/10.18632/ONCOTARGET.3174.
[397] G. Karpel-Massler, R.E. Kast, M.D. Siegelin, A. Dwucet, E. Schneider, M. A. Westhoff, C.R. Wirtz, X.Y. Chen, M.E. Halatsch, C. Bolm, Anti-glioma activity of dapsone and its enhancement by synthetic chemical modification, Neurochem. Res. 42 (2017) 3382–3389, https://doi.org/10.1007/S11064-017-2378-6.
[398] A.R. Larsen, R.Y. Bai, J.H. Chung, A. Borodovsky, C.M. Rudin, G.J. Riggins, F. Bunz, Repurposing the antihelmintic mebendazole as a hedgehog inhibitor, Mol. Cancer Ther. 14 (2015) 3, https://doi.org/10.1158/1535-7163.MCT-14-0755-T.
[399] A. Vargas-Toscano, D. Khan, A.-C. Nickel, M. Hewera, M.A. Kamp, I. Fischer, H.-J. Steiger, W. Zhang, S. Muhammad, D. Hänggi, U.D. Kahlert, Robot technology identifies a parkinsonian therapeutics repurpose to target stem cells of glioblastoma, CNS Oncol. 9 (2020), https://doi.org/10.2217/CNS-2020-0004.
[400] U. Herrlinger, T. Tzaridis, F. Mack, J.P. Steinbach, U. Schlegel, M. Sabel, P. Hau, R.D. Kortmann, D. Krex, O. Grauer, R. Goldbrunner, O. Schnell, O. Bähr, M. Uhl, C. Seidel, G. Tabatabai, T. Kowalski, F. Ringel, F. Schmidt-Graf, B. Suchorska, S. Brehmer, A. Weyerbrock, M. Renovanz, L. Bullinger, N. Galldiks, P. Vajkoczy, M. Misch, H. Vatter, M. Stuplich, N. Schäfer, S. Kebir, J. Weller, C. Schaub, W. Stummer, J.C. Tonn, M. Simon, V.C. Keil, M. Nelles, H. Urbach, M. Coenen, W. Wick, M. Weller, R. Fimmers, M. Schmid, E. Hattingen, T. Pietsch, C. Coch, M. Glas, Lomustine-temozolomide combination therapy versus standard temozolomide therapy in patients with newly diagnosed glioblastoma with methylated MGMT promoter (CeTeG/NOA–09): a randomised, open-label, phase

3 trial, Lancet. 393 (2019) 678–688, https://doi.org/10.1016/S0140-6736(18)31791-4.
[401] J. Biau, E. Thivat, E. Chautard, D. Stefan, M. Boone, B. Chauffert, C. Bourgne, D. Richard, I. Molna, S. Levesque, R. Bellini, F. Kwiatkowski, L. Karayan-Tapon, P. Verrelle, C. Godfraind, X. Durando, Phase 1 trial of ralimetinib (LY2228820) with radiotherapy plus concomitant temozolomide in the treatment of newly diagnosed glioblastoma, Radiother. Oncol. 154 (2021) 227–234, https://doi.org/10.1016/J.RADONC.2020.09.036.
[402] G.L. Gallia, M. Holdhoff, H. Brem, A.D. Joshi, C.L. Hann, R.Y. Bai, V. Staedtke, J. O. Blakeley, S. Sengupta, T.C. Jarrell, J. Wollett, K. Szajna, N. Helie, A.K. Mattox, X. Ye, M.A. Rudek, G.J. Riggins, Mebendazole and temozolomide in patients with newly diagnosed high-grade gliomas: results of a phase 1 clinical trial, Neuro-Oncol. Adv. 3 (2021) 1–8, https://doi.org/10.1093/NOAJNL/VDAA154.
[403] S.P. Weathers, J. Rood-Breithaupt, J. De Groot, G. Thomas, M. Manfrini, M. Penas-Prado, V.K. Puduvalli, C. Zwingelstein, W.K.A. Yung, Results of a phase I trial to assess the safety of macitentan in combination with temozolomide for the treatment of recurrent glioblastoma, Neuro-Oncol. Adv. 3 (2021) 1–12, https://doi.org/10.1093/NOAJNL/VDAB141.
[404] M. Sun, N. Huang, Y. Tao, R. Wen, G. Zhao, X. Zhang, Z. Xie, Y. Cheng, J. Mao, G. Liu, The efficacy of temozolomide combined with levetiracetam for glioblastoma (GBM) after surgery: a study protocol for a double-blinded and randomized controlled trial, Trials. 23 (2022), https://doi.org/10.1186/S13063-022-06168-1.
[405] Z. Wang, F. Du, Y. Ren, W. Jiang, Treatment of MGMT promoter unmethylated glioblastoma with PD-1 inhibitor combined with anti-angiogenesis and epidermal growth factor receptor tyrosine kinase inhibitor: a case report, Ann. Transl. Med. 9 (19) (2021) 1508, https://doi.org/10.21037/ATM-21-4625.
[406] S.D. Lustig, S.K. Kodali, S.L. Longo, S. Kundu, M.S. Viapiano, Ko143 reverses MDR in glioblastoma via deactivating P-glycoprotein, sensitizing a resistant phenotype to TMZ treatment, Anticancer Res. 42 (2022) 723–730, https://doi.org/10.21873/ANTICANRES.15530.
[407] S.W. Van Gool, J. Makalowski, M. Bitar, P. Van de Vliet, V. Schirrmacher, W. Stuecker, Synergy between TMZ and individualized multimodal immunotherapy to improve overall survival of IDH1 wild-type MGMT promoter-unmethylated GBM patients, Genes Immun. 23 (2022) 255, https://doi.org/10.1038/S41435-022-00162-Y.
[408] R. Serra, A. Mangraviti, N.L. Gorelick, T. Shapira-Furman, S. Alomari, A. Cecia, N. Darjee, H. Brem, Y. Rottenberg, A.J. Domb, B. Tyler, Combined intracranial Acriflavine, temozolomide and radiation extends survival in a rat glioma model, Eur. J. Pharm. Biopharm. 170 (2022) 179–186, https://doi.org/10.1016/J.EJPB.2021.12.011.
[409] M. Momeny, S. Shamsaiegahkani, B. Kashani, S. Hamzehlou, F. Esmaeili, H. Yousefi, S. Irani, S.A. Mousavi, S.H. Ghaffari, Cediranib, a pan-inhibitor of vascular endothelial growth factor receptors, inhibits proliferation and enhances therapeutic sensitivity in glioblastoma cells, Life Sci. 287 (2021), 120100, https://doi.org/10.1016/J.LFS.2021.120100.
[410] R. Amini, H. Karami, M. Bayat, Combination therapy with PIK3R3-siRNA and EGFR-TKI Erlotinib synergistically suppresses glioblastoma cell growth in vitro, Asian Pac. J. Cancer Prev. 22 (2021) 3993, https://doi.org/10.31557/APJCP.2021.22.12.3993.
[411] J. Gasparello, C. Papi, M. Zurlo, L. Gambari, A. Rozzi, A. Manicardi, R. Corradini, R. Gambari, A. Finotti, Treatment of human glioblastoma U251 cells with sulforaphane and a peptide nucleic acid (PNA) targeting miR-15b-5p: synergistic effects on induction of apoptosis, Molecules. 27 (2022), https://doi.org/10.3390/MOLECULES27041299.
[412] E. Seydi, H. Sadeghi, M. Ramezani, L. Mehrpouya, J. Pourahmad, Selective toxicity effect of fatty acids Omega-3, 6 and 9 combination on glioblastoma neurons through their mitochondria, Drug Res. (Stuttg) 72 (2022) 94–99, https://doi.org/10.1055/A-1640-8561/ID/R2021-08-2345-0036.
[413] M.A. Altinoz, A. Yilmaz, A. Taghizadehghalehjoughi, S. Genc, Y. Yeni, I. Gecili, A. Hacimuftuoglu, Ulipristal-temozolomide-hydroxyurea combination for glioblastoma: in-vitro studies, J. Neurosurg. Sci. (2022), https://doi.org/10.23736/S0390-5616.22.05718-6.
[414] S. Daisy Precilla, S.S. Kuduvalli, E. Angeline Praveena, S. Thangavel, T.S. Anitha, Integration of synthetic and natural derivatives revives the therapeutic potential of temozolomide against glioma- an in vitro and in vivo perspective, Life Sci. 301 (2022), 120609, https://doi.org/10.1016/J.LFS.2022.120609.
[415] A.R. Alexanian, A. Brannon, Unique combinations of epigenetic modifiers synergistically impair the viability of the U87 glioblastoma cell line while exhibiting minor or moderate effects on normal stem cell growth, Med. Oncol. 39 (2022) 1–5, https://doi.org/10.1007/S12032-022-01683-2/FIGURES/2.
[416] J. Guo, K. Liu, J. Wang, H. Jiang, M. Zhang, Y. Liu, C. Shan, F. Hu, W. Fu, C. Zhang, J. Li, Y. Chen, A rational foundation for micheliolide-based combination strategy by targeting redox and metabolic circuit in cancer cells, Biochem. Pharmacol. 200 (2022), 115037, https://doi.org/10.1016/J.BCP.2022.115037.
[417] A. Tancredi, O. Gusyatiner, P. Bady, M.C. Buri, R. Lomazzi, D. Chiesi, M. Messerer, M.E. Hegi, BET protein inhibition sensitizes glioblastoma cells to temozolomide treatment by attenuating MGMT expression, Cell Death Dis. 13 (2022), https://doi.org/10.1038/S41419-022-05497-Y.
[418] G. Lu, P. Zhu, M. Rao, N. Linendoll, L.M. Buja, M.B. Bhattacharjee, R.E. Brown, L. Y. Ballester, X. Tian, M. Pilichowska, J.K. Wu, G.W. Hergenroeder, W.F. Glass, L. Chen, R. Zhang, A.K. Pillai, R.L. Hunter, J.J. Zhu, Postmortem study of organ-specific toxicity in glioblastoma patients treated with a combination of temozolomide, irinotecan and bevacizumab, J. Neuro-Oncol. 160 (2022) 221–231, https://doi.org/10.1007/S11060-022-04144-Y/TABLES/3.
[419] G. Cerretti, D. Cecchin, L. Denaro, M. Caccese, M. Padovan, V. Zagonel, G. Lombardi, Impressive response to dabrafenib and trametinib plus silybin in a heavily pretreated IDH wild-type glioblastoma patient with BRAFV600E -mutant and SOX2 amplification, Anti-Cancer Drugs 34 (2023) 190–193, https://doi.org/10.1097/CAD.0000000000001376.
[420] M. Chakravarty, P. Ganguli, M. Murahari, R.R. Sarkar, G.J. Peters, Y.C. Mayur, Study of combinatorial drug synergy of novel acridone derivatives with temozolomide using in-silico and in-vitro methods in the treatment of drug-resistant glioma, Front. Oncol. 11 (2021), 625899, https://doi.org/10.3389/FONC.2021.625899/FULL.
[421] B. Goker Bagca, N.P. Ozates, A. Asik, H.O. Caglar, C. Gunduz, C. Biray Avci, Temozolomide treatment combined with AZD3463 shows synergistic effect in glioblastoma cells, Biochem. Biophys. Res. Commun. 533 (2020) 1497–1504, https://doi.org/10.1016/J.BBRC.2020.10.058.
[422] Y. Liu, X. Song, M. Wu, J. Wu, J. Liu, synergistic effects of resveratrol and temozolomide against glioblastoma cells: underlying mechanism and therapeutic implications , Cancer Manag. Res. 12 (2020) 8341–8354, https://doi.org/10.2147/CMAR.S258584.
[423] K.F. Chang, X.F. Huang, J.T. Chang, Y.C. Huang, W.S. Lo, C.Y. Hsiao, N.M. Tsai, Cedrol, a Sesquiterpene alcohol, enhances the anticancer efficacy of temozolomide in attenuating drug resistance via regulation of the DNA damage response and MGMT expression, J. Nat. Prod. 83 (2020) 3021–3029, https://doi.org/10.1021/ACS.JNATPROD.0C00580/ASSET/IMAGES/LARGE/NP0C00580_0007.JPEG.
[424] M. Orozco, R.A. Valdez, L. Ramos, M. Cabeza, J. Segovia, M.C. Romano, Dutasteride combined with androgen receptor antagonists inhibit glioblastoma U87 cell metabolism, proliferation, and invasion capacity: androgen regulation, Steroids. 164 (2020), 108733, https://doi.org/10.1016/J.STEROIDS.2020.108733.
[425] J. Moskwa, S.K. Naliwajko, R. Markiewicz-Żukowska, K.J. Gromkowska-Kępka, P. Nowakowski, J.W. Strawa, M.H. Borawska, M. Tomczyk, K. Socha, Chemical composition of polish propolis and its antiproliferative effect in combination with Bacopa monnieri on glioblastoma cell lines, Sci. Rep. 10 (2020) 21127, https://doi.org/10.1038/S41598-020-78014-W.
[426] Z. Abbaszade, B.G. Bagca, C.B. Avci, Molecular biological investigation of temozolomide and KC7F2 combination in U87MG glioma cell line, Gene. 776 (2021), 145445, https://doi.org/10.1016/J.GENE.2021.145445.
[427] H.H. Park, J. Park, H.J. Cho, J.K. Shim, J.H. Moon, E.H. Kim, J.H. Chang, S. Y. Kim, S.G. Kang, Combinatorial therapeutic effect of inhibitors of aldehyde dehydrogenase and mitochondrial complex I, and the chemotherapeutic drug, temozolomide against glioblastoma tumorspheres, Molecules. 26 (2021), https://doi.org/10.3390/MOLECULES26020282.
[428] L. Korsakova, J.A. Krasko, E. Stankevicius, Metabolic-targeted combination therapy with dichloroacetate and metformin suppresses glioblastoma cell line growth in vitro and in vivo, In Vivo (Brooklyn). 35 (2021) 341, https://doi.org/10.21873/INVIVO.12265.
[429] H. Fu Zhao, C. Peng Wu, X. Ming Zhou, P. Yu Diao, Y. Wen Xu, J. Liu, J. Wang, X. Jian Huang, W. Lan Liu, Z. Ping Chen, G. Dong Huang, W. Ping Li, Synergism between the phosphatidylinositol 3-kinase p110β isoform inhibitor AZD6482 and the mixed lineage kinase 3 inhibitor URMC-099 on the blockade of glioblastoma cell motility and focal adhesion formation, Cancer Cell Int. 21 (2021), https://doi.org/10.1186/S12935-020-01728-4.
[430] E.I. Essien, T.P. Hofer, M.J. Atkinson, N. Anastasov, Combining HDAC and MEK inhibitors with radiation against glioblastoma-derived spheres, Cells. 11 (2022), https://doi.org/10.3390/CELLS11050775/S1.
[431] J. Chen, Y.D. Zhuang, Q. Zhang, S. Liu, B.B. Zhuang, C.H. Wang, R.S. Liang, Exploring the mechanism of cordycepin combined with doxorubicin in treating glioblastoma based on network pharmacology and biological verification, PeerJ. 10 (2022), https://doi.org/10.7717/PEERJ.12942/SUPP-15.
[432] J. Xu, P.J. Wu, T.H. Lai, P. Sharma, A. Canella, A.M. Welker, C.E. Beattie, J. B. Elder, M. Easley, R. Lonser, N.K. Jacob, M. Pietrzak, C.M. Timmers, F. Lang, D. Sampath, V.K. Puduvalli, Disruption of DNA repair and survival pathways through heat shock protein inhibition by Onalespib to sensitize malignant gliomas to chemoradiation therapy, Clin. Cancer Res. 28 (2022) 1979, https://doi.org/10.1158/1078-0432.CCR-20-0468.
[433] P. Xu, H. Wang, H. Pan, J. Chen, C. Deng, Anlotinib combined with temozolomide suppresses glioblastoma growth via mediation of JAK2/STAT3 signaling pathway, Cancer Chemother. Pharmacol. 89 (2022) 183, https://doi.org/10.1007/S00280-021-04380-5.
[434] T. Surarak, P. Chantree, K. Sangpairoj, Synergistic effects of taurine and temozolomide via cell proliferation inhibition and apoptotic induction on U-251 MG human glioblastoma cells, Asian Pac. J. Cancer Prev. 22 (2021) 4001, https://doi.org/10.31557/APJCP.2021.22.12.4001.
[435] A. Sumiyoshi, S. Shibata, Z. Zhelev, T. Miller, D. Lazarova, G. Zlateva, I. Aoki, R. Bakalova, Pharmacological strategy for selective targeting of glioblastoma by redox-active combination drug – comparison with the chemotherapeutic standard-of-care temozolomide, Anticancer Res. 41 (2021) 6067–6076, https://doi.org/10.21873/ANTICANRES.15426.
[436] O. Pak, S. Zaitsev, V. Shevchenko, A. Sharma, H.S. Sharma, I. Bryukhovetskiy, Effectiveness of bortezomib and temozolomide for eradication of recurrent human glioblastoma cells, resistant to radiation, Prog. Brain Res. 266 (2021) 195–209, https://doi.org/10.1016/BS.PBR.2021.06.010.
[437] H.C. Tsai, K.C. Wei, P.Y. Chen, C.Y. Huang, K.T. Chen, Y.J. Lin, H.W. Cheng, Y. R. Chen, H.T. Wang, Valproic acid enhanced temozolomide-induced anticancer activity in human glioma through the p53–PUMA apoptosis pathway, Front. Oncol. 11 (2021), https://doi.org/10.3389/FONC.2021.722754/FULL.

[438] Y.K. Su, O.A. Bamodu, I.C. Su, N.W. Pikatan, I.H. Fong, W.H. Lee, C.T. Yeh, H. Y. Chiu, C.M. Lin, Combined treatment with acalabrutinib and rapamycin inhibits glioma stem cells and promotes vascular normalization by downregulating btk/mtor/vegf signaling, Pharmaceuticals. 14 (2021), https://doi.org/10.3390/PH14090876/S1.
[439] D. Yin, G. Jin, H. He, W. Zhou, Z. Fan, C. Gong, J. Zhao, H. Xiong, Celecoxib reverses the glioblastoma chemo-resistance to temozolomide through mitochondrial metabolism, Aging (Albany NY) 13 (2021) 21268, https://doi.org/10.18632/AGING.203443.
[440] P. Doan, P. Nguyen, A. Murugesan, N.R. Candeias, O. Yli-Harja, M. Kandhavelu, Alkylaminophenol and GPR17 agonist for glioblastoma therapy: a combinational approach for enhanced cell death activity, Cells. 10 (2021), https://doi.org/10.3390/CELLS10081975/S1.
[441] A. Karami, M. Hossienpour, E. Mohammadi Noori, M. Rahpyma, K. Najafi, A. Kiani, Synergistic Effect of Gefitinib and Temozolomide on U87MG Glioblastoma Angiogenesis 74, 2021, pp. 1299–1307, https://doi.org/10.1080/01635581.2021.1952441.
[442] A. Zając, J. Sumorek-Wiadro, A. Maciejczyk, E. Langner, I. Wertel, W. Rzeski, J. Jakubowicz-Gil, LY294002 and sorafenib as inhibitors of intracellular survival pathways in the elimination of human glioma cells by programmed cell death, Cell Tissue Res. 386 (2021) 17, https://doi.org/10.1007/S00441-021-03481-0.
[443] M.I. Dorrell, R.K.W. Heidi, R.T. Botts, S.A. Bravo, J.R. Tremblay, S. Giles, J. F. Wada, E. MaryAnn Alexander, G. Garcia, C.B. Villegas, K.J. Booth, H. M. Purington, E.N. Everett, M. Siles, J.A. Wheelock, B.M. Silva, C.A. Fortin, A. L. Lowey, T.L. Hale, J.C. Kurz, D.M. Rusing, P. Goral, A.M. Thompson, D. J. Johnson, R. Elson, C.E. Tadros, C. Gillette, A.L. Coopwood, J.M. Snowbarger Rausch, A novel method of screening combinations of angiostatics identifies bevacizumab and temsirolimus as synergistic inhibitors of glioma-induced angiogenesis, PLoS One 16 (2021), https://doi.org/10.1371/JOURNAL.PONE.0252233.
[444] A. Salmaggi, C. Corno, M. Maschio, S. Donzelli, A. D'urso, P. Perego, E. Ciusani, Synergistic effect of perampanel and temozolomide in human glioma cell lines, J. Pers. Med. 11 (2021) 390, https://doi.org/10.3390/JPM11050390/S1.
[445] B. Yuan, K. Xu, R. Shimada, J.Z. Li, H. Hayashi, M. Okazaki, N. Takagi, Cytotoxic effects of arsenite in combination with gamabufotalin against human glioblastoma cell lines, Front. Oncol. 11 (2021), 628914, https://doi.org/10.3389/FONC.2021.628914/FULL.
[446] Z. Su, S. Han, Q. Jin, N. Zhou, J. Lu, F. Shangguan, S. Yu, Y. Liu, L. Wang, J. Lu, Q. Li, L. Cai, C. Wang, X. Tian, L. Chen, W. Zheng, B. Lu, Ciclopirox and bortezomib synergistically inhibits glioblastoma multiforme growth via simultaneously enhancing JNK/p38 MAPK and NF-κB signaling, Cell Death Dis. 12 (2021), https://doi.org/10.1038/S41419-021-03535-9.
[447] W. Jiao, S. Zhu, J. Shao, X. Zhang, Y. Xu, Y. Zhang, R. Wang, Y. Zhong, D. Kong, ZSTK474 sensitizes glioblastoma to temozolomide by blocking homologous recombination repair, Biomed. Res. Int. 2022 (2022), https://doi.org/10.1155/2022/8568528.
[448] R.M. Urbantat, C. Jelgersma, P. Vajkoczy, S. Brandenburg, G. Acker, Combining TMZ and SB225002 induces changes of CXCR2 and VEGFR signalling in primary human endothelial cells in vitro, Oncol. Rep. 48 (2022), https://doi.org/10.3892/OR.2022.8373.
[449] Ö. Öcal, M. Nazıroğlu, Eicosapentaenoic acid enhanced apoptotic and oxidant effects of cisplatin via activation of TRPM2 channel in brain tumor cells, Chem. Biol. Interact. 359 (2022), 109914, https://doi.org/10.1016/J.CBI.2022.109914.
[450] A. Despotović, A. Mirčić, S. Misirlić-Denčić, L. Harhaji-Trajković, V. Trajković, N. Zogović, G. Tovilović-Kovačević, Combination of ascorbic acid and menadione induces cytotoxic autophagy in human glioblastoma cells, Oxidative Med. Cell. Longev. 2022 (2022), https://doi.org/10.1155/2022/2998132.
[451] S.W. Feng, P.C. Chang, H.Y. Chen, D.Y. Hueng, Y.F. Li, S.M. Huang, Exploring the mechanism of adjuvant treatment of glioblastoma using temozolomide and metformin, Int. J. Mol. Sci. 23 (2022), https://doi.org/10.3390/IJMS23158171.
[452] K. Ertilav, M. Nazıroğlu, Honey bee venom melittin increases the oxidant activity of cisplatin and kills human glioblastoma cells by stimulating the TRPM2 channel, Toxicon. 222 (2023), 106993, https://doi.org/10.1016/J.TOXICON.2022.106993.
[453] C.Y. Tsai, H.J. Ko, S.J. Chiou, Y.L. Lai, C.C. Hou, T. Javaria, Z.Y. Huang, T. S. Cheng, T.I. Hsu, J.Y. Chuang, A.L. Kwan, T.H. Chuang, C.Y.F. Huang, J.K. Loh, Y.R. Hong, Nbm-bmx, an hdac8 inhibitor, overcomes temozolomide resistance in glioblastoma multiforme by downregulating the β-catenin/c-myc/sox2 pathway and upregulating p53-mediated mgmt inhibition, Int. J. Mol. Sci. 22 (2021) 5907, https://doi.org/10.3390/IJMS22115907/S1.
[454] M.B. Vera, O. Morris-Hanon, G.I. Nogueiras, L.B. Ripari, M.I. Esquivel, C. Perez-Castro, L. Romorini, G.E. Sevlever, M.E. Scassa, G.A. Videla-Richardson, Noxa and Mcl-1 expression influence the sensitivity to BH3-mimetics that target Bcl-xL in patient-derived glioma stem cells, Sci. Rep. 12 (2022), https://doi.org/10.1038/S41598-022-20910-4.
[455] B. Goker Bagca, N.P. Ozates, C. Biray Avci, Ruxolitinib enhances cytotoxic and apoptotic effects of temozolomide on glioblastoma cells by regulating WNT signaling pathway-related genes, Med. Oncol. 40 (2022), https://doi.org/10.1007/S12032-022-01897-4.
[456] O. Doğanlar, Z.B. Doğanlar, S. Erdoğan, E. Delen, Antineoplastic multi-drug chemotherapy to sensitize tumors triggers multi-drug resistance and inhibits efficiency of maintenance treatment inglioblastoma cells, EXCLI J. 22 (2023) 35, https://doi.org/10.17179/EXCLI2022-5556.
[457] J.M. Han, H.J. Jung, Synergistic anticancer effect of a combination of berbamine and arcyriaflavin a against glioblastoma stem-like cells, Molecules. 27 (2022), https://doi.org/10.3390/MOLECULES27227968/S1.
[458] J.B. Netto, E.S.A. Melo, A.G.S. Oliveira, L.R. Sousa, L.R. Santiago, D.M. Santos, R. C.R. Chagas, A.S. Gonçalves, R.G. Thomé, H.B. Santos, R.M. Reis, R.I.M. A. Ribeiro, Matteucinol combined with temozolomide inhibits glioblastoma proliferation, invasion, and progression: an in vitro, in silico, and in vivo study, Braz. J. Med. Biol. Res. 55 (2022), https://doi.org/10.1590/1414-431X2022E12076.
[459] A.S. Karve, J.M. Desai, N. Dave, T.M. Wise-Draper, G.A. Gudelsky, T.N. Phoenix, B. DasGupta, S. Sengupta, D.R. Plas, P.B. Desai, Potentiation of temozolomide activity against glioblastoma cells by aromatase inhibitor letrozole, Cancer Chemother. Pharmacol. 90 (2022) 345–356, https://doi.org/10.1007/S00280-022-04469-5/METRICS.
[460] S. Bin Jo, S.J. Sung, H.S. Choi, J.S. Park, Y.K. Hong, Y.A. Joe, Modulation of autophagy is a potential strategy for enhancing the anti-tumor effect of mebendazole in glioblastoma cells, Biomol. Ther. (Seoul) 30 (2022) 616, https://doi.org/10.4062/BIOMOLTHER.2022.122.
[461] T.T. Lah, M. Novak, M.A. Pena Almidon, O. Marinelli, B.Ž. Baškovič, B. Majc, M. Mlinar, R. Bošnjak, B. Breznik, R. Zomer, M. Nabissi, Cannabigerol is a potential therapeutic agent in a novel combined therapy for glioblastoma, Cells. 10 (2021) 1–22, https://doi.org/10.3390/CELLS10020340.
[462] A.F. Cardona, D. Jaramillo-Velásquez, A. Ruiz-Patiño, C. Polo, E. Jiménez, F. Hakim, D. Gómez, J. Fernando Ramón, H. Cifuentes, J. Armando Mejía, F. Salguero, C. Ordoñez, Á. Muñoz, S. Bermúdez, N. Useche, D. Pineda, L. Ricaurte, Z. Lucia Zatarain-Barrón, J. Rodríguez, J. Avila, L. Rojas, E. Jaller, C. Sotelo, J. Esteban Garcia-Robledo, N. Santoyo, C. Rolfo, R. Rosell, O. Arrieta, Efficacy of osimertinib plus bevacizumab in glioblastoma patients with simultaneous EGFR amplification and EGFRvIII mutation, J. Neuro-Oncol. 154 (2021) 353–364, https://doi.org/10.1007/s11060-021-03834-3.
[463] P.S. Nakod, R.V. Kondapaneni, B. Edney, Y. Kim, S.S. Rao, The impact of temozolomide and lonafarnib on the stemness marker expression of glioblastoma cells in multicellular spheroids, Biotechnol. Prog. 38 (2022), e3284, https://doi.org/10.1002/BTPR.3284.
[464] S.J. Bagley, S. Kothari, R. Rahman, E.Q. Lee, G.P. Dunn, E. Galanis, S.M. Chang, L. B. Nabors, M.S. Ahluwalia, R. Stupp, M.P. Mehta, D.A. Reardon, S.A. Grossman, E. P. Sulman, J.H. Sampson, S. Khagi, M. Weller, T.F. Cloughesy, P.Y. Wen, M. Khasraw, Glioblastoma clinical trials: current landscape and opportunities for improvement, Clin. Cancer Res. 28 (2022) 594, https://doi.org/10.1158/1078-0432.CCR-21-2750.
[465] N. Cihoric, A. Tsikkinis, G. Minniti, F.J. Lagerwaard, U. Herrlinger, E. Mathier, I. Soldatovic, B. Jeremic, P. Ghadjar, O. Elicin, K. Lössl, D.M. Aebersold, C. Belka, E. Herrmann, M. Niyazi, Current status and perspectives of interventional clinical trials for glioblastoma - analysis of ClinicalTrials.gov, Radiat. Oncol. 12 (2017), https://doi.org/10.1186/S13014-016-0740-5.
[466] A.M. Vanderbeek, R. Rahman, G. Fell, S. Ventz, T. Chen, R. Redd, G. Parmigiani, T.F. Cloughesy, P.Y. Wen, L. Trippa, B.M. Alexander, The clinical trials landscape for glioblastoma: is it adequate to develop new treatments? Neuro-Oncology 20 (2018) 1034–1043, https://doi.org/10.1093/NEUONC/NOY027.
[467] J.J. Mandel, M. Youssef, E. Ludmir, S. Yust-Katz, A.J. Patel, J.F. De Groot, Highlighting the need for reliable clinical trials in glioblastoma, Expert. Rev. Anticancer. Ther. 18 (2018) 1031–1040, https://doi.org/10.1080/14737140.2018.1496824.
[468] A.M. Vanderbeek, S. Ventz, R. Rahman, G. Fell, T.F. Cloughesy, P.Y. Wen, L. Trippa, B.M. Alexander, To randomize, or not to randomize, that is the question: using data from prior clinical trials to guide future designs, Neuro-Oncology 21 (2019) 1239–1249, https://doi.org/10.1093/NEUONC/NOZ097.
[469] L. Nayak, N. Standifer, J. Dietrich, J.L. Clarke, G.P. Dunn, M. Lim, T. Cloughesy, H.K. Gan, E. Flagg, E. George, S. Gaffey, J. Hayden, C. Holcroft, P.Y. Wen, M. MacRi, A.J. Park, T. Ricciardi, A. Ryan, P. Schwarzenberger, R. Venhaus, M. De Los Reyes, N.M. Durham, T. Creasy, R.Y. Huang, T. Kaley, D.A. Reardon, Circulating immune cell and outcome analysis from the phase II study of PD-L1 blockade with durvalumab for newly diagnosed and recurrent glioblastoma, Clin. Cancer Res. 28 (2022) 2567–2578, https://doi.org/10.1158/1078-0432.CCR-21-4064.
[470] J. Duerinck, J.K. Schwarze, G. Awada, J. Tijtgat, F. Vaeyens, C. Bertels, W. Geens, S. Klein, L. Seynaeve, L. Cras, N. D'Haene, A. Michotte, B. Caljon, I. Salmon, M. Bruneau, M. Kockx, S. Van Dooren, A.M. Vanbinst, H. Everaert, R. Forsyth, B. Neyns, Original research: intracerebral administration of CTLA-4 and PD-1 immune checkpoint blocking monoclonal antibodies in patients with recurrent glioblastoma: a phase I clinical trial, J. Immunother. Cancer 9 (2021) 2296, https://doi.org/10.1136/JITC-2020-002296.
[471] S.S. Ramalingam, S. Novello, S.Z. Guclu, D. Bentsion, Z. Zvirbule, M. Szilasi, R. Bernabe, K. Syrigos, L.A. Byers, P. Clingan, J. Bar, E.E. Vokes, R. Govindan, M. Dunbar, P. Ansell, L. He, X. Huang, V. Sehgal, J. Glasgow, B.A. Bach, J. Mazieres, Veliparib in combination with platinum-based chemotherapy for first-line treatment of advanced squamous cell lung cancer: a randomized, multicenter phase III study, J. Clin. Oncol. 39 (2021) 3633, https://doi.org/10.1200/JCO.20.03318.
[472] A.B. Lassman, S.L. Pugh, T.J.C. Wang, K. Aldape, H.K. Gan, M. Preusser, M. A. Vogelbaum, E.P. Sulman, M. Won, P. Zhang, G. Moazami, M.S. Macsai, M. R. Gilbert, E.E. Bain, V. Blot, P.J. Ansell, S. Samanta, M.G. Kundu, T.S. Armstrong, J.S. Wefel, C. Seidel, F.Y. de Vos, S. Hsu, A.F. Cardona, G. Lombardi, D. Bentsion, R.A. Peterson, C. Gedye, V. Bourg, A. Wick, W.J. Curran, M.P. Mehta, Depatuxizumab mafodotin in EGFR-amplified newly diagnosed glioblastoma: a phase III randomized clinical trial, Neuro-Oncology (2022), https://doi.org/10.1093/NEUONC/NOAC173.
[473] D.A. Reardon, A.A. Brandes, A. Omuro, P. Mulholland, M. Lim, A. Wick, J. Baehring, M.S. Ahluwalia, P. Roth, O. Bähr, S. Phuphanich, J.M. Sepulveda,

P. De Souza, S. Sahebjam, M. Carleton, K. Tatsuoka, C. Taitt, R. Zwirtes, J. Sampson, M. Weller, Effect of nivolumab vs bevacizumab in patients with recurrent glioblastoma: the CheckMate 143 phase 3 randomized clinical trial, JAMA Oncol. 6 (2020) 1003–1010, https://doi.org/10.1001/JAMAONCOL.2020.1024.

[474] A. Shergalis, A. Bankhead, U. Luesakul, N. Muangsin, N. Neamati, Current challenges and opportunities in treating glioblastomas, Pharmacol. Rev. 70 (2018) 412–445, https://doi.org/10.1124/PR.117.014944/-/DC1.

[475] H. Mao, D.G. Lebrun, J. Yang, V.F. Zhu, M. Li, Deregulated Signaling pathways in glioblastoma multiforme: molecular mechanisms and therapeutic targets, Cancer Investig. 30 (2012) 48, https://doi.org/10.3109/07357907.2011.630050.

[476] E.E. Bar, A. Chaudhry, A. Lin, X. Fan, K. Schreck, W. Matsui, S. Piccirillo, A. L. Vescovi, F. DiMeco, A. Olivi, C.G. Eberhart, Cyclopamine-mediated hedgehog pathway inhibition depletes stem-like cancer cells in glioblastoma, Stem Cells 25 (2007) 2524–2533, https://doi.org/10.1634/STEMCELLS.2007-0166.

[477] J.B. Stone, L.M. DeAngelis, Cancer treatment-induced neurotoxicity: a focus on newer treatments, Nat. Rev. Clin. Oncol. 13 (2016) 92, https://doi.org/10.1038/NRCLINONC.2015.152.

[478] A.S. Adhikari, J. Macauley, Y. Johnson, M. Connolly, T. Coleman, T. Heiland, Development and characterization of an HCMV multi-antigen therapeutic vaccine for glioblastoma using the UNITE platform, Front. Oncol. 12 (2022), https://doi.org/10.3389/FONC.2022.850546/FULL.

[479] Y. Chen, P. Liu, P. Sun, J. Jiang, Y. Zhu, T. Dong, Y. Cui, Y. Tian, T. An, J. Zhang, Z. Li, X. Yang, Oncogenic MSH6-CXCR4-TGFB1 feedback loop: a novel therapeutic target of photothermal therapy in glioblastoma multiforme, Theranostics. 9 (2019) 1453, https://doi.org/10.7150/THNO.29987.

[480] M.C. Milone, J. Xu, S.J. Chen, M.K.A. Collins, J. Zhou, D.J. Powell, J. J. Melenhorst, Engineering enhanced CAR T-cells for improved cancer therapy, Nat. Can. 2 (2021) 780, https://doi.org/10.1038/S43018-021-00241-5.

[481] J.S. Michael, B.-S. Lee, M. Zhang, D.J.S. Yu, Nanotechnology for treatment of glioblastoma multiforme, J. Transl. Intern. Med. 6 (2018) 128, https://doi.org/10.2478/JTIM-2018-0025.

[482] M. Arruebo, N. Vilaboa, B. Sáez-Gutierrez, J. Lambea, A. Tres, M. Valladares, Á. González-Fernández, Assessment of the evolution of cancer treatment therapies, Cancers (Basel) 3 (2011) 3279, https://doi.org/10.3390/CANCERS3033279.

[483] Y. Hao, C.K. Chung, Z. Yu, R.V. Huis In, T. Veld, F.A. Ossendorp, P. Ten Dijke, L. J. Cruz, Combinatorial therapeutic approaches with nanomaterial-based photodynamic cancer therapy, Pharm 14 (2022) 120, https://doi.org/10.3390/PHARMACEUTICS14010120.

[484] J. Nam, S. Son, L.J. Ochyl, R. Kuai, A. Schwendeman, J.J. Moon, Chemo-photothermal therapy combination elicits anti-tumor immunity against advanced metastatic cancer, Nat. Commun. 91 (9) (2018) 1–13, https://doi.org/10.1038/s41467-018-03473-9.

[485] X. Wang, C. Wu, S. Liu, D. Peng, Combinatorial therapeutic strategies for enhanced delivery of therapeutics to brain cancer cells through nanocarriers: Current trends and future perspectives 29, 2022, pp. 1370–1383, https://doi.org/10.1080/10717544.2022.2069881.

[486] D. Ghosh, S. Nandi, S. Bhattacharjee, Combination therapy to checkmate glioblastoma: clinical challenges and advances, Clin. Transl. Med. 7 (2018) 33, https://doi.org/10.1186/S40169-018-0211-8.

[487] L.A. Mathews Griner, R. Guha, P. Shinn, R.M. Young, J.M. Keller, D. Liu, I. S. Goldlust, A. Yasgar, C. McKnight, M.B. Boxer, D.Y. Duveau, J.K. Jiang, S. Michael, T. Mierzwa, W. Huang, M.J. Walsh, B.T. Mott, P. Patel, W. Leister, D. J. Maloney, C.A. Leclair, G. Rai, A. Jadhav, B.D. Peyser, C.P. Austin, S.E. Martin, A. Simeonov, M. Ferrer, L.M. Staudt, C.J. Thomas, High-throughput combinatorial screening identifies drugs that cooperate with ibrutinib to kill activated B-cell-like diffuse large B-cell lymphoma cells, Proc. Natl. Acad. Sci. U. S. A. 111 (2014) 2349–2354, https://doi.org/10.1073/PNAS.1311846111/-/DCSUPPLEMENTAL.

[488] S.K. Tan, A. Jermakowicz, A.K. Mookhtiar, C.B. Nemeroff, S.C. Schürer, N. G. Ayad, Drug repositioning in glioblastoma: a pathway perspective, Front. Pharmacol. 9 (2018) 218, https://doi.org/10.3389/FPHAR.2018.00218.